

ACS SYMPOSIUM SERIES **399**

# Plant Cell Wall Polymers

## Biogenesis and Biodegradation

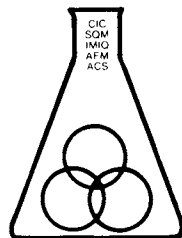
**Norman G. Lewis**, EDITOR

*Virginia Polytechnic Institute and State University*

**Michael G. Paice**, EDITOR

*Pulp and Paper Research Institute of Canada*

Developed from a symposium sponsored  
by the Cellulose, Paper, and Textile Division  
of the American Chemical Society  
at the Third Chemical Congress of North America  
(195th National Meeting  
of the American Chemical Society),  
Toronto, Ontario, Canada,  
June 5-11, 1988



American Chemical Society, Washington, DC 1989



**Library of Congress Cataloging-in-Publication Data**

Plant cell wall polymers.

(ACS symposium series, ISSN 0097-6156; 399)

"Developed from a symposium sponsored by the Cellulose, Paper, and Textile Division at the Third Chemical Congress of North America (195th National Meeting of the American Chemical Society), Toronto, Ontario, Canada, June 5-11, 1988."

Includes bibliographical references.

1. Plant polymers—Synthesis—Congresses. 2. Plant polymers—Biodegradation—Congresses. 3. Plant Cell Walls—Congresses.

I. Lewis, Norman G., 1949— . II. Paice, Michael G., 1949— . III. Chemical Congress of North America (3rd: 1988: Toronto, Ont.) IV. American Chemical Society Meeting (195th: 1988: Toronto, Ont.) V. American Chemical Society. Cellulose, Paper, and Textile Division. VI. Series.

QK898.P76P53 1989 581.87'5  
ISBN 0-8412-1658-4

89-17541

Copyright © 1989

American Chemical Society

All Rights Reserved. The appearance of the code at the bottom of the first page of each chapter in this volume indicates the copyright owner's consent that reprographic copies of the chapter may be made for personal or internal use or for the personal or internal use of specific clients. This consent is given on the condition, however, that the copier pay the stated per-copy fee through the Copyright Clearance Center, Inc., 27 Congress Street, Salem, MA 01970, for copying beyond that permitted by Sections 107 or 108 of the U.S. Copyright Law. This consent does not extend to copying or transmission by any means—graphic or electronic—for any other purpose, such as for general distribution, for advertising or promotional purposes, for creating a new collective work, for resale, or for information storage and retrieval systems. The copying fee for each chapter is indicated in the code at the bottom of the first page of the chapter.

The citation of trade names and/or names of manufacturers in this publication is not to be construed as an endorsement or as approval by ACS of the commercial products or services referenced herein; nor should the mere reference herein to any drawing, specification, chemical process, or other data be regarded as a license or as a conveyance of any right or permission to the holder, reader, or any other person or corporation, to manufacture, reproduce, use, or sell any patented invention or copyrighted work that may in any way be related thereto. Registered names, trademarks, etc., used in this publication, even without specific indication thereof, are not to be considered unprotected by law.

PRINTED IN THE UNITED STATES OF AMERICA

**American Chemical Society**  
**Library**

1155 16th St., N.W.

In Plant Cell Wall Polymers; Lewis, N. et al.;

ACS Symposium Series; American Chemical Society: Washington, DC, 1989.

# ACS Symposium Series

**M. Joan Comstock, *Series Editor***

## *1989 ACS Books Advisory Board*

**Paul S. Anderson**  
Merck Sharp & Dohme Research  
Laboratories

**Alexis T. Bell**  
University of California—Berkeley

**Harvey W. Blanch**  
University of California—Berkeley

**Malcolm H. Chisholm**  
Indiana University

**Alan Elzerman**  
Clemson University

**John W. Finley**  
Nabisco Brands, Inc.

**Natalie Foster**  
Lehigh University

**Marye Anne Fox**  
The University of Texas—Austin

**G. Wayne Ivie**  
U.S. Department of Agriculture,  
Agricultural Research Service

**Mary A. Kaiser**  
E. I. du Pont de Nemours and  
Company

**Michael R. Ladisch**  
Purdue University

**John L. Massingill**  
Dow Chemical Company

**Daniel M. Quinn**  
University of Iowa

**James C. Randall**  
Exxon Chemical Company

**Elsa Reichmanis**  
AT&T Bell Laboratories

**C. M. Roland**  
U.S. Naval Research Laboratory

**Stephen A. Szabo**  
Conoco Inc.

**Wendy A. Warr**  
Imperial Chemical Industries

**Robert A. Weiss**  
University of Connecticut

## Foreword

The ACS SYMPOSIUM SERIES was founded in 1974 to provide a medium for publishing symposia quickly in book form. The format of the Series parallels that of the continuing ADVANCES IN CHEMISTRY SERIES except that, in order to save time, the papers are not typeset but are reproduced as they are submitted by the authors in camera-ready form. Papers are reviewed under the supervision of the Editors with the assistance of the Series Advisory Board and are selected to maintain the integrity of the symposia; however, verbatim reproductions of previously published papers are not accepted. Both reviews and reports of research are acceptable, because symposia may embrace both types of presentation.

## Preface

**P**LANT CELL WALLS ARE COMPLEX, HETEROGENEOUS STRUCTURES composed mainly of polymers, such as cellulose, hemicelluloses, and lignins. In spite of several decades of research, cell wall assembly and the biosynthesis and ultimate biodegradative pathways of individual polymers are still far from being fully understood. One simple example will suffice: Even today, no enzyme capable of catalyzing cellulose formation *in vitro* has been obtained.

The objective of the symposium on which this book is based was to bring together scientists from different plant-related disciplines, who do not often interact with each other, to discuss the subjects of cell wall polymer biogenesis and biodegradation. These individuals, linked by a common interest in plant polymers, exchanged, promoted, and at times discarded ideas, often in spirited discussions. This book attempts to place current and emerging concepts that were discussed into a common perspective. This approach is timely because within the past five years several subject areas have advanced rapidly. For example, an increased understanding of lignin biogenesis and structure has been achieved by *in situ* labeling, and new techniques for structural analysis of other plant polymers (e.g., cutin, suberin, and hemicelluloses) have been developed. Additionally, scientists have made substantial progress in localizing the enzymes associated with cell wall polymer formation and have an improved understanding of the temporal and spatial distribution of polymer constituents within the plant cell wall. This progress leads to the conclusion that we can make an optimistic prognosis for the eventual understanding of the mechanism of cell wall assembly.

The same facts apply to biodegradative processes: Five years ago, little was known about the enzymology of lignin biodegradation, and the molecular biology of cellulases was in its infancy. Advances have since been made in leaps and bounds; these advances are fully discussed within this volume.

This book is divided into eight sections, spanning cell wall development, biogenesis, plant-microbe interactions, and biodegradation. Each section contains informative, up-to-date reviews and original reports by some of the leading researchers in their fields.

We are indebted to a number of individuals and organizations for their contributions to this book. The symposium itself was sponsored by the Cellulose, Paper, and Textile Division of the American Chemical Society, Phillip Morris Tobacco Company, the U.S. Department of Energy (the Energy Conversion and Utilization Technology Biobased Materials project through the Solar Energy Research Institute), Weyerhaeuser, Abitibi-Price, and the Chemical Institute of Canada. Virginia Polytechnic Institute and State University and the Pulp and Paper Research Institute of Canada provided valuable assistance with correspondence, and Kathryn Hollandsworth and Janice Baker-Briand were particularly helpful in preparing many of the manuscripts. Cheryl Shanks of the ACS Books Department provided much-needed support during the editing and publication process. We would be remiss not to mention Helena Li Chum, who tirelessly and selflessly contributed much to the overall success of the symposium on which this book is based. However, most of all, to the authors and referees who invested their time and effort in writing and refining the manuscripts, we extend our sincerest thanks.

NORMAN G. LEWIS  
Virginia Polytechnic Institute and State University  
Blacksburg, VA 24061-0323

MICHAEL G. PAICE  
Pulp and Paper Research Institute of Canada  
Pointe Claire, Quebec H9R 3J9, Canada

March 30, 1989

# Chapter 1

## Control of Plant Cell Wall Biogenesis

### An Overview

D. H. Northcote

Department of Biochemistry, University of Cambridge, Tennis Court  
Road, Cambridge CB2 1QW, England

All the polysaccharides of the cell wall are synthesized in association with phospholipid membranes. The hemicelluloses and pectin polysaccharides are formed at the membranes of the Golgi apparatus, cellulose at the plasma membrane. Control of the rate of polysaccharide synthesized and the type of polymer formed is exerted by the transport of donor nucleoside diphosphate sugar molecules across the membranes, the amount, type, and activity of the synthases (glycosyltransferases) and fusion and targetting of vesicles containing the polysaccharides at specific sites at the plasma membrane. The formation of a polysaccharide typically depends on an enzyme complex organized on a membrane. The complex consists of transporters, glycosyltransferases, epimerases and binding proteins to hold the acceptor molecules. In addition to these, subsidiary proteins may also be present which may act to bring about and control the assembly of the complex and its location on the membrane. They may also act as modulators of the polysaccharide synthesis in conjunction with smaller molecules or ions. During xylem formation, lignin is deposited as well as polysaccharides. Part of the control mechanism for the formation of lignin is the level of phenylalanine ammonia lyase activity. Proteins and lipids are also deposited in the wall and although these constituents are not present in large amounts, they are very important for the function of the wall and the cell during growth.

0097-6156/89/0399-0001\$06.00/0

© 1989 American Chemical Society

The cell wall is formed from materials within the cytoplasm which are subsequently transported either as monomers or polymers to the outside of the cell. During growth and differentiation of the cell its composition and structure changes, and it can also alter in response to environmental factors. There is therefore a dialogue between the outside of the cell and the synthetic and transport systems at the inside of the cell so that the changes in the wall are brought about in an ordered manner at particular stages of its development (1).

The major polymers that make up the wall are polysaccharides and lignin. These occur together with more minor but very important constituents such as protein and lipid. Water constitutes a major and very important material of young, primary walls (2). The lignin is transported in the form of its building units (these may be present as glucosides) and is polymerized within the wall. Those polysaccharides which make up the matrix of the wall (hemicelluloses and pectin material) are polymerized in the endomembrane system and are secreted in a preformed condition to the outside of the cell. Further modifications of the polysaccharides (such as acetylation) may occur within the wall after deposition. Cellulose is polymerized at the cell surface by a complex enzyme system transported to the plasma membrane (3).

The control of the development of the cell wall must be regulated at the various processes which make the constituents and which deposits them to the outside of the cell. These may be summarized as follows: (1) regulation of synthesis by the amounts of the synthase; this is directly controlled by gene regulation; (2) biochemical feed-back control mechanisms which regulate the level of the precursors of the polymers or the activities of the synthases which form them; (3) regulation of the segregation and targeting of material formed within the endoplasmic reticulum and Golgi apparatus; (4) control of transport of monomers to the synthases of the polymers; (5) control of vesicle fusion and targeting of the membrane bound material to specific sites at the cell surface; (6) receptors for plant growth substances and mechanisms for cell signalling at the cytoplasmic surface and other cell membranes. This chapter reviews some of these topics in more detail for the polysaccharides, lignin, protein and lipid of the wall.

## Polysaccharides

This section describes a detailed hypothesis for the control of polysaccharide synthesis and deposition in the wall during growth.

Most of the biochemical studies on polysaccharide synthesis to date have been concerned with the formation of homopolymers even when it is known that the synthesis of the homopolymer chain occurs *in vivo* as part of a heteropolysaccharide (4-6). Cytochemical investigations have made no such distinctions and the polymers located by these studies have nearly always been sites at which heteropolymers were present and where deposition in the wall occurred. The bulk of the polysaccharides that occur in the wall, with the exception of cellulose and callose, are heteropolymers. Generally the polysaccharides of the hemicelluloses and pectins are composed of poly-



mers containing different monosaccharides combined by different linkages (2, 7-10). Usually there is a backbone made up of a single chain, built of the same monosaccharide (two in the case of glucomannans, see below) usually combined by a specific linkage, onto which short branches are attached which may be just a single monosaccharide different from that of the units of the main chain, e.g., glucuronoxylan, arabinoglucuronoxylans, xyloglucans. In addition more complicated polymers such as the arabinogalactans occur but even in these polymers there is a central core onto which the branches are constructed (2). The influence of the incorporation of the side branches on the synthesis of the main chain and vice versa is of some significance for the control of the polysaccharide synthesis and introduces the idea of an enzyme complex at the site for the polymer synthesis.

The backbone chain can in most cases be synthesized separately when an *in vitro* system is used. These investigations have shown that the synthase activities which transfer the sugar from a nucleoside diphosphate sugar donor to the growing polysaccharide chain are related to the amount of polysaccharide which is formed at any stage of the growth and development of the wall (5, 6, 11, 12). There is also strong circumstantial evidence which indicates that these variations in activity are due to changes in the amounts of the synthases which are available at the particular sites at a particular time (13). Thus the development of the wall has some control mechanisms directly related to the regulation of the genome during differentiation; this controls the amounts of the synthases which are formed, probably at the level of transcription rather than translation.

*Synthesis.* The synthases are present at the endomembrane system of the cell and have been isolated on membrane fractions prepared from the cells (5, 6). The nucleoside diphosphate sugars which are used by the synthases are formed in the cytoplasm, and usually the epimerases and the other enzymes (e.g., dehydrogenases and decarboxylases) which interconvert them are also soluble and probably occur in the cytoplasm (14). Nevertheless some epimerases are membrane bound and this may be important for the regulation of the synthases which use the different epimers in a heteropolysaccharide. This is especially significant because the availability of the donor compounds at the site of the transglycosylases (the synthases) is of obvious importance for control of the synthesis. The synthases are located at the lumen side of the membrane and the nucleoside diphosphate sugars must therefore cross the membrane in order to take part in the reaction. Modulation of this transport mechanism is an obvious point for the control not only for the rate of synthesis but for the type of synthesis which occurs in the particular lumen of the membrane system. Obviously the synthase cannot function unless the donor molecule is transported to its active site and the transporters may only be present at certain regions within the endomembrane system. It has been observed that when intact cells are fed radioactive monosaccharides which will form and label polysaccharides, these cannot always be found at all the membrane sites within the cell where the synthase activities are known to occur (15). A possible reason for this difference may be the selection of precursors by the transport mechanism.

The preformed polysaccharides before they are deposited in the wall can be detected in the Golgi apparatus either by radioactive labelling techniques and direct analysis of the isolated organelle, or by cytochemical stains, the most specific of which are identifications using antibodies. Figure 1 shows a section of a developing secondary wall from the hypocotyl cells of bean. The antibody was raised in rabbits against oligosaccharides prepared from walnut  $\beta$  1  $\rightarrow$  4 xylan (5) and conjugated to bovine serum albumin. The antibody to the protein was removed by affinity chromatography and the resultant purified antibody was specific to antigens carrying  $\beta$  1  $\rightarrow$  4 xylose units. It did not cross-react with xyloglucan,  $\beta$  1  $\rightarrow$  4 glucan, arabinan or mannan. The section shown in Figure 1 was treated with the antibody and stained with gold-labelled goat-antirabbit serum. The xylan is present at the secondary wall (st) and in the vesicles of the Golgi apparatus (v). Figure 2 shows a meristematic cell from the root of bean, treated with an antibody specific for L-arabinofuranose and stained with gold-labelled goat-antirabbit serum. The label was present at the cell wall (cw) and the developing cell-plate (cp) where pectin was being laid down.

*Glucomannan Synthesis.* Although the heteropolymers are usually similar to the glucuronoarabinoxylans, there are heteropolymers in which two different monosaccharides occur in the main chain, e.g., glucomannans and galactoglucomannans. For a discussion of the construction and control of the synthesis of a heteropolymer the synthesis of glucomannan in the hemicellulose of gymnosperms serves as a good example (16, 17).

A membrane preparation isolated from pine stem tissues incorporated glucose into glucans from both UDPGlc and GDPGlc. These were mixed polymers containing  $\beta$  1  $\rightarrow$  3 and  $\beta$  1  $\rightarrow$  4 linked glucose. It also carried an epimerase which interconverted GDPGlc and GDPMan (18). The membrane preparation formed a glucomannan in the presence of added GDPMan and in the presence of GDPMan the formation of glucan containing  $\beta$  1  $\rightarrow$  3 links from GDPGlc was repressed and the  $\beta$  1  $\rightarrow$  4 glucomannan was formed (whether a separate  $\beta$  1  $\rightarrow$  4 glucan was synthesized in addition was difficult to determine) (Table I) (18). The activity of the glucan synthase which used UDPGlc was unaffected by the presence of GDPMan. These observations can best be explained in terms of an enzyme complex carried on the membrane. This complex has a minimum of three activities: (1) an epimerase for the interconversion of GDPMan and GDPGlc; (2) a synthase which used UDPGlc; (3) a synthase which used both GDPGlc and GDPMan. This latter synthase had a greater affinity for GDPGlc than GDPMan and, *in vitro*, in the presence of GDPGlc but in the absence of added GDPMan, it formed a glucan in spite of the presence of the epimerase. Since the influence of the presence of the GDPMan on the incorporation from GDPGlc into a different type of polymer is so direct, the two activities, one for the transfer of glucose and the other for the transfer of mannose from the GDP sugars, must either be carried out by the same transglycosylase or the two transglycosylases must be very close together so that they can influence one another.

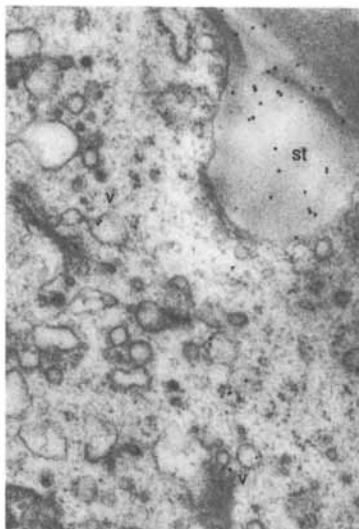


Figure 1. Developing secondary thickened wall of the hypocotyl of *Phaseolus vulgaris*. The section was treated with an antibody specific for  $\beta$  1  $\rightarrow$  4 linked D-xylose units and stained with gold-labelled goat-antirabbit serum. The label is seen at the secondary thickening (st) and the vesicles of the Golgi apparatus (v).

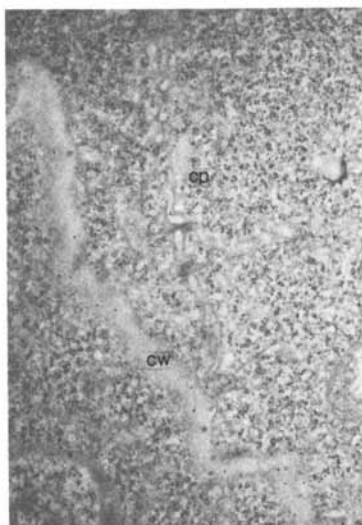


Figure 2. Meristematic cell of the root-tip of *Phaseolus vulgaris*. The section was treated with an antibody specific for L-arabinofuranose and stained with gold-labelled goat-antirabbit serum. The label is seen at the developing cell plate (cp) and the young wall (cw) of the mother cell.

Table I. The influence of the presence of exogenous GDPMan on the synthesis of a mixed  $\beta 1 \rightarrow 3, 1 \rightarrow 4$  glucan from GDPGlc by a membrane preparation from pine stem tissue. Measurements were made from the incorporation of radioactive glucose from GDP[U- $^{14}\text{C}$ ]Glc (18). (- indicates that no glucan carrying a  $\beta 1 \rightarrow 3$  linkage was formed.)

GDP[U- $^{14}\text{C}$ ]Glc as the Primary Substrate (1.0 nmol)		
GDPMan Additions nmol	$\beta 1 \rightarrow 3, 1 \rightarrow 4$ glucan formed nmol. min $^{-1}$ (mg protein) $^{-1}$	$\beta 1 \rightarrow 4$ glucomannan formed nmol. min $^{-1}$ (mg protein) $^{-1}$
0.0	0.28	0.0
0.5	-	0.57
1.0	-	0.56
2.5	-	1.0
5.0	-	0.70
10.0	-	0.39

It is likely that in addition to the synthases and epimerases there is also present at the membrane in close proximity to these, transporter systems for the transfer of the nucleoside diphosphate donor compounds to the transglycosylases situated on the lumen side of the membrane.

The polymer which formed was either a mixed  $\beta 1 \rightarrow 3, \beta 1 \rightarrow 4$  glucan or a  $\beta 1 \rightarrow 4$  glucomannan and runs of  $\beta 1 \rightarrow 4$  linked glucose occurred in the glucomannan (18). The glucosyl transferase that used GDPGlc added glucose either at the 3 position of the receiving sugar, or at the 4 position. It was also shown that the transglycosylase added the glucosyl radical to water to form free glucose (18). In this system, therefore, the transglycosylase using GDPGlc was not specific for the receptor molecule since this may be water, glucose at the 3 position, glucose at the 4 position, or mannose at the 4 position. When a glucomannan was formed, the linkage was always made at the 4 position. The acceptor molecule, although it was not specific in the transglycosyl reaction, influenced how the transfer occurred.

These diverse actions of the transglycosylase can be most easily explained by postulating the existence of a binding protein which holds the acceptor molecules. Then during the transglycosylase reaction that forms the glucomannan chain, a glucosyl radical could first be transferred to water within an associated binding protein and the resultant sugar could then be extended by subsequent transfers to the non-reducing end of the growing chain, either from GDPMan or GDPGlc. It is possible to have the acceptor sugar precisely orientated by such a binding protein, in order to receive the new glycosyl residue by the transglycosylase at the particular hydroxyl which is presented to the donor molecule. The transglycosylase itself could have a domain at which the acceptor oligosaccharide was held but since the

orientation of the acceptor molecule is altered independently of the transglycosylase there are probably at least two proteins involved: one used for transfer and holding the donor and another necessary for holding the acceptor. The transglycosylase protein is not therefore specific for the acceptor molecule. This is in contrast to the way in which the glycosylation of certain glycoproteins is thought to occur (19). Definite sequences of sugars are built on the protein because the various transglycosylases involved are specific for the acceptor oligosaccharide which changes in a stepwise manner. At each stage a definite glycosyltransferase can act to form a definite sequence of sugars.

*Binding Protein and Enzyme Complex.* That sugars and oligosaccharides can specifically bind to protein is well known. Hexokinase is known to hold glucose within a cleft of the enzyme by hydrogen bonds; indeed, the presence of glucose causes a movement in the conformational structure of the protein so that it folds around the glucose and the hydroxyl group at the 6 position is presented to the kinase for the transfer of the phosphate group from the ATP (20). Specific associations between proteins and oligosaccharides and polysaccharides are also well documented. Lysozyme and takamylase are known to hold oligosaccharides in a ribbon-like configuration by hydrogen bonding and van der Waals forces within a binding-site groove (21). Precise and stereospecific interactions are formed and maintained by the orientation of hydrogen-bonding residues which are in turn fixed by complex hydrogen bond networks to other residues within the binding sites. During binding, conformational changes may occur which allow the carbohydrates to be oriented for the binding to progress and specific interaction between protein and carbohydrate results (22).

During the synthesis of a mixed polysaccharide such as a glucuronoxylan or a xyloglucan, at least two transglycosylases are involved which work in conjunction with one another (23-27). It is possible to envisage the main chain of either glucose or xylose being held by a binding protein and the side chains being guided onto the backbone which is held in such a way as to present the appropriate hydroxyl to the substituent sugar and the appropriate transglycosylase.

Whatever the mechanism, the coordinated synthesis of a polysaccharide, such as glucomannan or glucuronoxylan or the arabinogalactans of the pectins or even a homopolymer such as single cellulose chains (3), needs the cooperation of a set of proteins. These must be organized close to one another in correct orientation for the synthesis to occur in an economical and rapid manner. There is thus a multienzyme system organized on the membrane and held in a coordinated way. The membrane on and in which the proteins are held becomes an important part of the synthetic process. Disruption of the membrane will bring about loss of organization and the *in vitro* preparations made from intact cells may form polysaccharides different from those formed *in vivo* (e.g., callose instead of cellulose) (28) or for a heteropolysaccharide the dependence of one transglycosylase on the action of another will become less precise (24, 29) in the *in vitro* preparation than in the intact cell.

It seems likely that the enzyme complexes for hemicelluloses, pectins and cellulose are constructed, at least in part, on the endoplasmic reticulum and then transferred to the Golgi apparatus, where they are modified and sorted so that they can be segregated within the compartments of the Golgi cisternae (30, 31). The complex for cellulose synthesis is not normally active within the Golgi apparatus and it is transported to active sites at the plasma membrane (1). The hemicelluloses and pectins are formed within vesicles and cisternae of the Golgi apparatus and the vesicles are transported to the plasma membrane, where fusion occurs and the polysaccharides are packed into the wall (1). It is not known whether particular polysaccharides such as the xylans of the hemicellulose and the arabinogalactans of the pectins are transported in separate vesicles or together in one vesicle. Nor is it known if the complex for cellulose synthesis is transported by vesicles which carry hemicellulose and pectin polysaccharides.

*Deposition of Wall Polysaccharides.* Whatever the distribution of the polysaccharides and synthase systems in the vesicles, the movement of the vesicles to particular sites and the rate of fusion with the plasmamembrane constitute important control points for the deposition of the material into the wall. It is known that at sites of active wall deposition vesicles are directed to the plasmamembrane by microtubules (32). However, it is possible that other signals and receptors at the membrane surface may be involved in recognition of the sites for incorporation. Part of the control for vesicle fusion at the surface is mediated by the ionic atmosphere at the membrane, and  $\text{Ca}^{2+}$  is necessary for the fusion to occur. The rate of vesicle fusion can be a limiting process for the rate of cell wall formation, since at any one time the number of vesicles ready for fusion exceeds the number that are fusing and depositing material into the wall. In this way the composition and amount of wall material deposited may respond very quickly to a stimulus at the cell surface which allows the rate of vesicle fusion to vary. For instance, the material deposited in the cell wall, especially the pectin, changes very quickly at the initial stages of plasmolysis when the wall is just separated from the plasmamembrane. A new steady state would then be achieved that produced the requisite number of vesicles from the Golgi apparatus to maintain the altered rate of fusion (32-34).

### Lignin Precursors and Lignin Formation

*Phenylalanine Ammonia-Lyase.* The building units of lignin are formed from carbohydrate via the shikimic acid pathway to give aromatic amino acids. Once the aromatic amino acids are formed, a key enzyme for the control of lignin precursor synthesis is phenylalanine ammonia-lyase (PAL) (1). This enzyme catalyzes the production of cinnamic acid from phenylalanine. It is very active in those tissues of the plant that become lignified and it is also a central enzyme for the production of other phenylpropanoid-derived compounds such as flavonoids and coumarins, which can occur in many parts of the plant and in many different organs (35). Radioactive phenylalanine and cinnamic acid are directly incorporated into lignin in vascular tissue (36).

The induction of PAL activity at the onset of vascular differentiation can be shown by the use of plant tissue cultures (37-39). Xylem cells with secondary and lignified walls are differentiated over a time course of 3-14 days by the application of the plant growth factors naphthylene acetic acid (NAA) and kinetin in the ratio 5: 1 (1.0 mg/liter NAA, 0.2 mg/liter kinetin) to tissue cultures of bean cells (*Phaseolus vulgaris*) (37, 40). The time for differentiation varies with the type of culture, solid or suspension, and with the frequency and duration of subculture, but for any one culture it is relatively constant (37, 41, 42). At the time of differentiation when the xylem vessels form, the activity of PAL rises to a maximum. The rising phase of the enzyme activity was inhibited by actinomycin D and by D-2,4-(4-methyl-2,6-dinitroanilino)-N-methylpropionamide (MDMP) applied under carefully controlled conditions (42). This indicated that both transcription and translation were necessary for the response to the hormones. Experiments using an antibody for PAL and a cDNA probe for the PAL-mRNA have also shown that there is an increase in the amount of transcript for PAL during the formation of lignin when *Zinnia mesophyll* cells are induced to form xylem elements in culture (Lin and Northcote, unpublished work).

The induction of PAL activity by the two growth factors can be separated in time so that they may act at different sites within the cell to bring about the response (40). Auxin added at the time of subculture of the tissue changes the pattern of protein synthesis of the cells by changing the transcription pattern of the mRNA after two hours (43). Kinetin does not have this effect (44).

*Hydroxylation and Methylation.* The pathway for the production of the lignin building units involves hydroxylation of the aromatic ring and methylation of the hydroxyl groups. It has been demonstrated that the methylations are brought about by S-adenosylmethionine:caffeic acid, 3-O-methyl transferase. This transferase is meta specific and can also methylate 5-hydroxyferulic acid and 3,4,5-trihydroxycinnamic acid to sinapic acid (45). The induction of this enzyme in bean cultures during differentiation is coincident with the rise in PAL activity (46). The hydroxylation of the aromatic ring of cinnamic acid is brought about by cinnamic acid 4-hydroxylase, and a further hydroxylase, p-coumaric acid 3-hydroxylase, also occurs to give caffeic acid (47). The 4-hydroxylase activity, in some tissue, is induced at the same time as the PAL activity (48, 49). Therefore, some coordinated induction of gene expression for the production of lignin precursors during differentiation is possible.

The PAL activity that is necessary for lignin formation occurs in the cytoplasm or bound to the cytoplasmic surface of the endoplasmic reticulum membranes. The cinnamic acid produced is probably carried on the lipid surface of the membranes, since it is lipophilic, and it is sequentially hydroxylated by the membrane-bound hydroxylases (47, 50). In this way there is the possibility of at least a two-step channeling route from phenylalanine to p-coumaric acid. The transmethylnases then direct the methyl groups to the meta positions. There is a difference between the transmethylnases from angiosperms and those from gymnosperms, since with the latter

preparations the enzyme is relative inactive on 5-hydroxyferulate. Thus it is possible that these transmethylases may have some part in the control of the type of lignin formed. The guaiacyl type (3-methoxy-4-hydroxy) is found in gymnosperms and the syringyl-guaiacyl type (3,5-dimethoxy-4-hydroxy) in dicotyledons (51).

*Formation and Polymerization of the Building Units of Lignin.* The acid building units are reduced to the corresponding alcohols before polymerization to lignin. This reduction occurs as a two-step process involving the CoA ester of the acid and using NADPH as cofactor. The enzymes CoA ligase, cinnamoyl-CoA:NADPH oxidoreductase, and cinnamyl alcohol dehydrogenase are involved, and they give finally the three building units of lignin: p-coumaryl alcohol, coniferyl alcohol, and sinapyl alcohol (51). Various isoenzymes of the CoA ligases may also control the type of lignin that is formed, since the isoenzymes have different affinities and activities for p-coumaric, ferulic and sinapic acid and these isoenzymes occur in different proportions in different plants and in different tissues of the same plant (51).

The activation of the phenylpropionic acids and their subsequent reduction may occur in vesicles that fuse with the plasma membrane and empty the precursors of lignin into the wall (52). The NADPH for the reduction is provided by the pentose phosphate pathway (53,54). The control for the final steps that produce the cinnamyl alcohols, which are the immediate building units of the lignin, is therefore dependent on the energy status of the cell, since ATP is necessary for the ligase activity, and it is also dependent on the distribution of carbohydrate metabolism between the pentose phosphate pathway and glycolysis. It is within the wall that the polymerization process to form a complex lignin cage occurs.

The cinnamyl alcohols may reach the wall as the free alcohols or as  $\beta$ -glucosides formed by glucosyltransferases with UDPGlc (55). For polymerization, the free alcohol is necessary, and  $\beta$ -glucosidases occur in the walls of tissues that are lignified (56). Glucosides may be important for the transport of the alcohols to the walls, but they are not obligatory for lignin synthesis. They may act as reservoirs of the lignin precursors. The precursors arise in cells that are undergoing lignification, or they may arise from neighboring cells of young differentiating xylem, which themselves are not at the stage of massive lignification (36). Lignification is brought about by the oxidation of the alcohols to yield mesomeric phenoxy radicals with half-lives of about 45 sec, so that rapid polymerization occurs. At the same time, linkages of these radicals, and hence the lignin, to carbohydrate can take place (56,57). It is probable that the final oxidation of the phenolic hydroxy group to give the free radicals is brought about by a specific isoenzyme of peroxidase that occurs in the walls of plant cells (58-60). This isoenzyme, on electrophoresis, is an anodic-migrating component. In *Zinnia elegans*, the activity of wall-bound peroxidase increases during the onset of lignification, although the total soluble peroxidase activity of the cell may decrease (39,46). Another isoenzyme of peroxidase might be required to produce the hydrogen peroxide on which the oxidative polymerization process de-



pendes (61). The synthesis and activity of some isoenzymes of peroxidase are therefore possible control sites for lignification.

### Establishment of Cross Linkages in the Wall

In the rigid secondary wall of woody tissue, the lignin replaces the water of the growing cell wall and forms a hydrophobic matrix around the microfibrils. Strong hydrogen bonds occur between the polysaccharides at the microfibrillar-matrix interface and between components of the matrix. These, together with the covalent bonds formed between carbohydrate and lignin, make the wall a composite in which the linear polysaccharide polymers are enclosed in a cross-linked polymer cage. The wall has great tensile strength because of the microfibrils and a rigid structure because of the lignified matrix (2).

The peroxidase of the wall may also establish other covalent linkages between wall polymers. The wall contains protein and the tyrosine residues of the proteins may be oxidized by peroxidase to give cross-linkages of isodityrosine between the polypeptides (62,63). Ferulic acid occurs in the cell walls of some herbaceous plants and grasses and this may be oxidized to give diferulic acid ester linkages joining polysaccharide chains (64,65). The possible formation of these covalent cross linkages between the polymers of the primary wall is believed by some workers to limit plant cell wall extensibility and have some part in the mechanisms for the control of cell growth and extension by plant growth factors (66).

### Protein in the Wall

Most of the proteins found in the cell wall are glycoproteins. These can be enzymes such as isoenzymes of peroxidase, phosphatase and amylase or the hydroxyproline-rich glycoproteins (67) and glycine-rich proteins (68). The hydroxyproline-rich glycoproteins may be classified on the basis of the size of their sugar prosthetic groups. The soluble lectins and agglutinins and the insoluble wall glycoproteins have small oligosaccharides of arabinose ( $\alpha$ -L-Araf(1  $\rightarrow$  3)-0- $\beta$ -L-Araf (1  $\rightarrow$  2)-0- $\beta$ -L-Araf(1  $\rightarrow$  2)-0- $\beta$ -L-Araf-1 Hyp) linked to the hydroxyproline (Hyp) and also single galactose units attached to serine (69-71), while the arabinogalactan proteins are mainly large molecular weight polysaccharides attached to protein, the resultant molecule being about 80-90% carbohydrate (72,73). Hydroxylation of peptidyl proline occurs as a post-translational process in the endoplasmic reticulum (74-76), and the addition of the small arabinosyl oligosaccharides probably occurs within the Golgi apparatus without the necessity for assembly on a lipid intermediate (77). However, with the large molecular weight arabinogalactan protein a lipid carrier might be involved, especially as repeating subunits within the arabinogalactan portion of the molecule have been detected. Oligosaccharides linked to polyisoprenyl-pyrophosphate have been found to contain arabinose (78) and galactose (79); the galactose was linked by 1  $\rightarrow$  6, 1  $\rightarrow$  4 and 1  $\rightarrow$  3 bonds and the arabinose was 1  $\rightarrow$  5 linked. These isoprenyl diphosphate oligosaccharides were formed by membranes of pea

cells when they were incubated with the appropriate radioactive UDP sugar compounds, and they could serve as precursors of the arabinogalactan-glycoproteins.

The possible inclusion of lipid-linked intermediates in the transglycosylations involved in glycoprotein and polysaccharide formation provides a further step at which control of the synthase system can be exercised. However, although lipid intermediates are well established for the formation of N-linked glycoproteins and, in some instances, for polysaccharides where glycoproteins can function as intermediates during the formation of these polysaccharides (80-82), there is, at present, no evidence for the direct transfer from lipid-oligosaccharide onto polysaccharide. One of the important consequences of the participation of lipid-oligosaccharide intermediates is that the sequence of sugars formed on the lipid can be successively transferred so that a repeating ordered sequence of the mixed sugars in the oligosaccharide could occur in the synthesized polymer (83-85).

### Formation of Lipid and Transport to the Wall

Many cell walls have layers in the outer regions of the wall that carry lipid material. These are cutin, suberin, and waxes (67). How these are transported to the outside of the cell wall is not known. Pores have not been found, nor has a volatile lipid solvent been detected that would carry the lipid through the hydrophilic wall.

The fatty acids are synthesized in chloroplasts or proplastids and moved into the cytoplasm and the endomembrane system for further modification and synthesis of neutral fats, phospholipids, and other compounds (86). The fatty acids could be carried by proteins by a process similar to the way in which serum albumin binds fatty acid in the bloodstream of mammals. Other types of lipid might be formed into complexes analogous to low-density lipoproteins of the type found in animal tissues, where the lipid core of the lipoprotein is surrounded by a hydrophilic cortex made up of protein, phospholipid, and cholesterol (87). This allows the lipid to be moved in an aqueous environment. The protein of the lipoprotein shell could also act as possible ligands for particular receptors at the membrane of the cell at which the export occurs. The lipoproteins, if they are present, would probably be formed within the endomembrane lumen and would receive the proteins at the endoplasmic reticulum.

### Summary

This chapter has attempted to suggest how the synthesis of the main constituents of the wall (polysaccharides, lignin, protein and lipid) are controlled during their deposition into the wall. A hypothesis is developed for the synthesis of polysaccharides. It arises from the evidence for glucomanan synthesis (18), and also for cellulose and callose synthesis (28). Different glycosidic linkages are formed from the same membrane preparation under different conditions. This is most easily explained by postulating the existence of a binding protein to hold the acceptor molecules of the

transglycosylase reaction. The hypothesis suggests that there is a complex of proteins, with different functions, organized close together at the membrane of the cell. A transglycosylase, nucleoside diphosphate sugar transporters, and the binding protein are all necessary. The latter protein, since it holds the growing polysaccharide chain, can modulate the transglycosylase reaction by orientating the receptor molecule. In this way the same transglycosylase may transfer the glycosyl group to different hydroxyls of the acceptor, e.g., to give  $1 \rightarrow 3$  or  $1 \rightarrow 4$  linkages.

### Literature Cited

1. Northcote, D. H. In *Biosynthesis and Biodegradation of Wood Components*; Academic Press: London, 1985; Ch. 5.
2. Northcote, D. H. *Ann. Rev. Plant Physiol.* 1972, **23**, 113-132.
3. Northcote, D. H. In *Biosynthesis and Biodegradation of Cellulose and Cellulose Materials*; Marcel Dekker Inc.: New York, 1988; Ch. 3.
4. Bailey, R. W.; Hassid, W. Z. *Proc. Natl. Acad. Sci.* 1966, **56**, 1586-93.
5. Dalessandro, G.; Northcote, D. H. *Planta* 1981, **151**, 53-60.
6. Dalessandro, G.; Northcote, D. H. *Planta* 1981, **151**, 61-67.
7. Timell, T. E. *Adv. Carbohydr. Chem.* 1964, **19**, 247-302.
8. Timell, T. E. *Adv. Carbohydr. Chem.* 1965, **20**, 409-483.
9. O'Neill, M. A.; Selvendran, R. R. *Carb. Res.* 1983, **111**, 239-255.
10. Aspinall, G. O.; Molloy, J. A.; Craig, J. W. T. *Can. J. Biochem. Physiol.* 1969, **47**, 1063-70.
11. Bolwell, G. P.; Northcote, D. H. *Planta* 1981, **152**, 225-33.
12. Bolwell, G. P.; Dalessandro, G.; Northcote, D. H. *Phytochem.* 1985, **24**, 699-702.
13. Bolwell, G. P.; Northcote, D. H. *Planta* 1984, **162**, 139-46.
14. Dalessandro, G.; Northcote, D. H. *Biochem. J.* 1977, **162**, 139-46.
15. Bolwell, G. P.; Northcote, D. H. *Biochem. J.* 1983, **210**, 497-507.
16. Ramsden, L.; Northcote, D. H. *Phytochem.* 1987, **26**, 2679-83.
17. Dalessandro, G.; Piro, G.; Northcote, D. H. *Planta* 1986, **169**, 564-74.
18. Dalessandro, G.; Piro, G.; Northcote, D. H. *Planta* 1988, **175**, 60-70.
19. Watkins, W. M. *Carbohydr. Res.* 1986, **149**, 1-12.
20. Steitz, T. A.; Shoham, M.; Bennett, W. S. *Phil. Trans. R. Soc. London* 1981, **B293**, 43-52.
21. Matura, Y.; Kusunoki, M.; Harada, W.; Kakudo, M. *J. Biochem.* 1984, **95**, 697-702.
22. Quijcho, F. A. *Ann. Rev. Biochem.* 1986, **55**, 287-315.
23. Waldron, K. W.; Brett, C. T. *Biochem. J.* 1983, **213**, 115-22.
24. Waldron, K. W.; Brett, C. T. In *Biochemistry of Plant Cell Walls*; SEB Seminar Series 1985; **28**, 79-97.
25. Ray, P. M. *Biochim. Biophys. Acta* 1980, **629**, 431-44.
26. Hayashi, T.; Matsuda, K. *J. Biol. Chem.* 1981, **256**, 11117-22.
27. Hayashi, T.; Matsuda, K. *Plant and Cell Physiol.* 1981, **22**, 1571-84.
28. Jacob, S. R.; Northcote, D. H. *J. Cell Sci.* 1985 **Suppl.2**, 1-11.
29. Campbell, R. E.; Brett, C. T.; Hillman, J. R. *Biochem. J.* 1988, in press.

30. von Figura, K.; Hasilik, A. *Ann. Rev. Biochem.* 1986, **55**, 167-93.
31. Pfeffer, S. R.; Rothmann, J. E. *Ann. Rev. Biochem.* 1987, **56**, 829-52.
32. Northcote, D. H. *Encyclopedia of Plant Physiology* 1982, **New Series 14A**, 637-55.
33. Boffey, S. A.; Northcote, D. H. *Biochem. J.* 1975, **150**, 433-40.
34. Northcote, D. H. In *The Synthesis, Assembly and Turnover of Cell Surface Components*; Elsevier/North-Holland Biomedical Press, 1977; **4**, 717-39.
35. Jahnen, W.; Hahlbrock, K. *Planta* 1988, **173**, 453-8.
36. Rubery, P. H.; Northcote, D. H. *Nature* 1968, **219**, 1230-34.
37. Haddon, L. E.; Northcote, D. H. *J. Cell Sci.* 1975, **17**, 11-26.
38. Kuboi, T.; Yamada, Y. *Biochim. Biophys. Acta* 1978, **542**, 181-90.
39. Fukuda, H.; Komamine, A. *Planta* 1982, **155**, 423-30.
40. Bevan, M.; Northcote, D. H. *Planta* 1979, **147**, 77-81.
41. Bevan, M.; Northcote, D. H. *J. Cell Sci.* 1979, **39**, 339-53.
42. Jones, D. H.; Northcote, D. H. *Eur. J. Biochem.* 1981, **116**, 117-25.
43. Bevan, M.; Northcote, D. H. *Planta* 1981, **152**, 32-35.
44. Bevan, M.; Northcote, D. H. *Planta* 1981, **152**, 24-31.
45. Poulton, J. E. In *The Biochemistry of Plants: Secondary Plant Products*; Academic Press: London, 1981; **7**, 667-723.
46. Haddon, L.; Northcote, D. H. *Planta* 1976, **128**, 255-62.
47. Butt, V. S.; Lamb, C. J. In *The Biochemistry of Plants: Secondary Plant Products*; Academic Press: London, 1981; **7**, 627-65.
48. Amrhein, N.; Zenk, M. H. *Naturwiss.* 1970, **57**, 312.
49. Hahlbrock, K.; Wellman, E. *Biochim. Biophys. Acta* 1973, **304**, 702-6.
50. Hanson, K. R.; Havir, E. A. In *The Biochemistry of Plants: Secondary Plant Products*; Academic Press: London, 1981; **7**, 577-625.
51. Grisebach, H. In *The Biochemistry of Plant Products: Secondary Plant Products*; Academic Press: London, 1981; **7**, 457-78.
52. Alibert, G.; Ranjera, R.; Boudet, A. M. *Physiol. Veg.* 1977, **15**, 279-301.
53. Pryke, J. A.; ap Rees, T. *Planta* 1976, **132**, 279-89.
54. Pryke, J. A.; ap Rees, T. *Phytochem.* 1977, **16**, 557-60.
55. Ibrahim, R. K.; Grisebach, H. *Arch. Biochem. Biophys.* 1976, **176**, 700-8.
56. Freudenberg, K. *Science* 1965, **148**, 595-600.
57. Freudenberg, K. In *Constitution and Biosynthesis of Lignin*; Springer-Verlag: Berlin, 1968; **2**, 45-122.
58. Yung, K.-H.; Northcote, D. H. *Biochem. J.* 1975, **151**, 141-4.
59. Mader, M. *Planta* 1976, **131**, 11-15.
60. Mader, M.; Nessel, A.; Bopp, M. *Z. Pflanzenphysiol.* 1977, **82**, 247-60.
61. Mader, M.; Amberg-Fisher, V. *Pl. Physiol.* 1982, **70**, 1128-31.
62. Fry, S. C. *Biochem. J.* 1982, **204**, 449-55.
63. Cooper, J. B.; Varner, J. E. *Biochem. Biophys. Res. Commun.* 1983, **112**, 161-7.
64. Fry, S. C. *Planta* 1983, **157**, 111-23.
65. Tanner, G. R.; Morrison, I. M. *Phytochem.* 1983, **22**, 1433-39.

66. Fry, S. C. *Ann. Rev. Pl. Physiol.* 1986, **37**, 165-86.
67. Gould, J.; Northcote, D. H. In *Bacterial Adhesion: Mechanisms and Physiological Significance*; Plenum: New York, 1984; 89-110.
68. Cassab, G. I.; Varner, J. E. *Nature* 1986, **323**, 110.
69. Lamport, D. T. A. In *The Biochemistry of Plants: Carbohydrates*; Academic Press: London, 1980; **3**, 501-41.
70. Allen, A. K.; Dsai, N. N.; Neuberger, A.; Creeth, J. M. *Biochem. J.* 1978, **171**, 665-74.
71. Muray, R. H. A.; Northcote, D. H. *Phytochem.* 1978, **17**, 623-9.
72. Fincher, G. B.; Stone, B. A.; Clarke, A. E. *Ann. Rev. Pl. Physiol.* 1983, **34**, 47-70.
73. Cassab, G. I. *Planta* 1986, **168**, 441-46.
74. Wienecke, K.; Glas, R.; Robinson, D. G. *Planta* 1982, **155**, 58-63.
75. Blankenstein, P.; Lang, W. C.; Robinson, D. G. *Planta* 1986, **169**, 238-44.
76. Sauer, A.; Robinson, D. G. *Planta* 1985, **164**, 287-94.
77. Owens, R. J.; Northcote, D. H. *Biochem. J.* 1981, **195**, 661-7.
78. Hayashi, T.; Maclachlan, G. *Biochem. J.* 1984, **217**, 791-803.
79. Hayashi, T.; Maclachlan, G. *Phytochem.* 1984, **23**, 487-92.
80. Green, J. R.; Northcote, D. H. *Biochem. J.* 1978, **170**, 599-608.
81. Green, J. R.; Northcote, D. H. *Biochem. J.* 1979, **178**, 661-71.
82. Green, J. R.; Northcote, D. H. *J. Cell Sci.* 1979, **40**, 235-44.
83. Ielpi, L.; Couso, R.; Dankert, R. *FEBS Lett.* 1981, **130**, 253-56.
84. Ielpi, L.; Couso, R.; Dankert, R. *Biochem. Biophys. Res. Comm.* 1981, **102**, 1400-8.
85. Couso, R. O.; Ielpi, L.; Garcia, R. C.; Dankert, R. *Eur. J. Biochem.* 1982, **123**, 617-27.
86. Stumpf, P. K.; Shimakata, T. In *Biosynthesis and Function of Plant Lipids Proc 6 University of California*; Amer. Soc. Pl. Physiologists: Maryland, 1983; 1-27.
87. Nilsson-Ehle, P.; Garfinkel, A. S.; Schotz, M. C. *Ann. Rev. Biochem.* 1980, **49**, 667-92.

RECEIVED May 19, 1989

## Chapter 2

# Formation and Functions of Xyloglucan and Derivatives

David A. Brummell and Gordon A. MacLachlan

Biology Department, McGill University, 1205 Avenue Dr Penfield,  
Montreal, Quebec H3A 1B1, Canada

Xyloglucan is a matrix polysaccharide which in primary cell walls associates with cellulose microfibrils by hydrogen bonding to form a relatively rigid structure. Its synthesis by Golgi membranes requires the activity of at least four enzymes: 1,4- $\beta$ -glucosyl-, 1,6- $\alpha$ -xylosyl-, 1,2- $\beta$ -galactosyl-, and 1,2- $\alpha$ -fucosyl-transferases. Continued chain elongation by the  $\beta$ -glucosyltransferase is dependent upon concurrent  $\alpha$ -xylosyl transfer. The xyloglucan backbone is substituted with galactosyl and fucosyl residues at very specific xylosyl side groups to complete a polysaccharide with regular alternating subunits of Glc<sub>4</sub>·Xyl<sub>3</sub> and Glc<sub>4</sub>·Xyl<sub>3</sub>·Gal·Fuc. Auxin treatment of young dicot tissues induces both growth and the production of an endo-1,4- $\beta$ -glucanase, the main substrate of which appears to be cell wall xyloglucan. Auxin evokes a net increase in xyloglucan levels, but depolymerization and turnover also take place during growth. Although oligosaccharide products of xyloglucan hydrolysis inhibit auxin-stimulated growth, at the same time they stimulate endo-1,4- $\beta$ -glucanase activity versus xyloglucan *in vitro*.

The primary cell walls of growing tissues in higher plants are composed of highly hydrated polymeric materials consisting mainly of complex polysaccharides, with smaller amounts of glycoprotein. Generally 20-30% of the dry weight of the wall is cellulose, with the balance of the polysaccharides being made up of pectins and hemicelluloses. In dicots, the predominant hemicellulose is xyloglucan, which forms about 20% of the wall (1). In the typical growing region of pea stems, for example, the ratio of xyloglucan to cellulose is about 0.7:1 on a weight basis (2). In monocots, the main

0097-6156/89/0399-0018\$06.00/0

© 1989 American Chemical Society

hemicelluloses are glucans and arabinoxylans, with xyloglucan apparently forming only a minor fraction of the wall. However, in monocots the glucan backbone of xyloglucan is much less substituted than in dicots (3), which may result in their under-estimation. Arabinoxylans in monocots appear to exhibit many of the same properties as do xyloglucans in dicots (4, 5).

The extraprotoplasmic wall defines the cell shape, and metabolic regulation of cell wall structure is believed to control the direction and rate of cell expansion. Xyloglucan, unlike cellulose, is clearly subject to turnover during growth. Decreases in xyloglucan average molecular weight during development have been noted, particularly after auxin treatment, as well as the release of small quantities of solubilized material including xyloglucan oligosaccharide subunits of characteristic structure (6). This review examines the synthesis of xyloglucan and its functions in the cell walls of young growing regions of dicot stems. The roles in growth of xyloglucan turnover and of oligosaccharide fragments derived by partial hydrolysis of xyloglucan are also considered.

### Structure of Xyloglucan

Mature xyloglucans of dicot plants possess a very regular structure composed of a 1,4- $\beta$ -D-glucan backbone with D-xylosyl residues 1,6- $\alpha$ -linked to three (in growing tissue) or an average of two (in seeds) out of four sequential glucosyl residues (1,7). The addition either of L-fucosyl-1,2- $\alpha$ -D-galactose (in growing tissue) or D-galactose alone (in seeds) linked 1,2- $\beta$  to specific xylosyl residues further extends the side chains at selected intervals (Fig. 1). In some species terminal L-arabinosyl residues are found instead of fucose (1). Xyloglucan from growing monocot tissue is less substituted with xylose and galactose than in dicots (3) and appears to lack fucose (8), whereas that from gymnosperms resembles dicot xyloglucan (9).

The structure of xyloglucan has been determined through examination of digestion products after hydrolysis with specific endo-1,4- $\beta$ -glucanases and analysis of the linkages present in the resulting fragments after methylation. Partial hydrolysis of pea xyloglucan (Fig. 1) results in a nonasaccharide (Glc<sub>4</sub>·Xyl<sub>3</sub>·Gal·Fuc) and a heptasaccharide (Glc<sub>4</sub>·Xyl<sub>3</sub>) (2). Identical structures have been determined for sycamore (10), soybean (11), and mung bean (12) xyloglucan. In mung bean small amounts of a decasaccharide (Glc<sub>4</sub>·Xyl<sub>3</sub>·Gal<sub>2</sub>·Fuc) were also found.

When xyloglucan from pea epicotyl cell walls was hydrolyzed *in vitro* with purified endo-1,4- $\beta$ -glucanase from *Streptomyces*, reducing sugar was produced at a linear rate for at least 48 h (2). Fractionation of the hydrolysate on Bio-Gel P6 columns showed that endo-1,4- $\beta$ -glucanase cleaved the 1,4- $\beta$ -glucan backbone at unsubstituted glucosyl residues to generate equal amounts of heptasaccharide and nonasaccharide (Fig. 1). These units accumulated with time of hydrolysis until they were essentially the only end products. Transient amounts of higher molecular weight products were also found, identified as dimers of the resulting oligosaccharides. These were mainly composed of the 16 saccharide unit (a nonasaccharide plus a

heptasaccharide, Fig. 1), with smaller amounts of 18 (two nona-) and 14 (two hepta-) saccharides.

Since the nonasaccharide and the heptasaccharide were present in approximately a 1:1 molar ratio and the main dimer contained the two oligosaccharides, it appears that pea xyloglucan is composed of these two subunits arranged primarily in alternating sequence. However, the presence of the 14 and 18 saccharide dimers showed that this distribution is not perfect. The molecular weight of xyloglucan varies with species and stage of growth. In young cell walls, xyloglucan has a molecular weight of 250 kD to 350 kD, which represents a degree of polymerization (DP) of the glucan backbone of 800 to 1200, suggesting that 100 or more of each oligosaccharide subunit are present (2).

Treatment of xyloglucan with fungal mixed endo- and exo-glycosidase preparations, such as from *Aspergillus*, degraded the molecule to monosaccharides and isoprimeverose (6-O- $\alpha$ -D-xylopyranosyl-D-glucopyranose) (13, 14). The presence of this disaccharide in such digests is uniquely characteristic of xyloglucan, and the incorporation of UDP-[ $^{14}$ C]xylose into isoprimeverose has been used as an unambiguous assay for xyloglucan biosynthesis (14).

### Biosynthesis of the Xyloglucan Backbone

Xyloglucan, like the other non-cellulosic wall polysaccharides, is synthesized and secreted by membranes of the Golgi apparatus. The transferases responsible for xyloglucan biosynthesis co-sedimented with markers for Golgi membranes in density gradients (13, 15), and immunogold localization studies using a polyclonal antibody to xyloglucan found the polysaccharide to be present in Golgi cisternae and vesicles (16). No label was seen over the endoplasmic reticulum, indicating that synthesis of xyloglucan occurs in the Golgi. The very regular structure of the final polymer implies a precise coordination of the enzymes responsible for xyloglucan biosynthesis.

The glucose-xylose backbone of xyloglucan is synthesized by coordinated activity of a specific glucosyltransferase and a xylosyltransferase which appear to function independently to only a very limited extent. Early studies on pea membranes suggested that some glucosyl transfer could occur in the absence of xylosyl transfer, and it was concluded that xylosyl transfer took place onto a preformed glucan chain (13). However, with membranes from soybean cultured cells, incorporation of glucose from UDP-glucose into xyloglucan was almost completely dependent on the concentration of UDP-xylose in the incubation mixture (14). Conversely, membranes incorporated only a small amount of labelled material when incubated with UDP-[ $^{14}$ C]xylose alone, but substantial incorporation ensued in the presence of UDP-glucose and UDP-[ $^{14}$ C]xylose together (14). The products formed *in vitro* were composed mainly of two subunits, a pentasaccharide (Glc<sub>3</sub>-Xyl<sub>2</sub>) and a heptasaccharide (Glc<sub>4</sub>-Xyl<sub>3</sub>). Pulse-chase experiments indicated that the pentasaccharide was converted to the heptasaccharide, and that this process was dependent upon and regulated by the concentration of UDP-xylose (17).



Recently, the molecular size of water-insoluble 1,4- $\beta$ -linked polysaccharides newly synthesized by pea membranes from UDP-[ $^{14}\text{C}$ ]glucose has been determined (18). Reaction products were first exhaustively hydrolyzed with purified 1,3- $\beta$ -glucanase to remove 1,3- $\beta$ -linked products. The 1,4- $\beta$ -linked polymers so obtained were dissolved in anhydrous paraformaldehyde:dimethylsulfoxide (40-45%, w/v) and fractionated by exclusion chromatography on columns of controlled pore glass beads. The 1,4- $\beta$ -linked products formed from 1 mM UDP-[ $^{14}\text{C}$ ]glucose alone displayed a peak of molecular size equivalent to the elution volume of commercial  $\alpha$ -dextran with a molecular weight of 70 kD (Fig. 2). This product contained only a few [ $^{14}\text{C}$ ]glucose units added with 1,4- $\beta$ -linkages to the non-reducing end of an unknown endogenous acceptor. It was clearly unable to elongate further in this reaction system since its size remained the same even in the presence of higher substrate concentrations and after longer incubation periods (19).

However, when UDP-xylose was present in the reaction medium in addition to UDP-[ $^{14}\text{C}$ ]glucose, incorporation of label proceeded over a longer period and the elution peak from glass bead columns increased in apparent size with time to approach that of authentic xyloglucan (Fig. 2, cf. 20). Enzymic hydrolysis confirmed that the product contained isoprimeverose, thereby establishing unambiguously that a xyloglucan backbone had been formed. Pulse-chase experiments provided unequivocal evidence that the truncated product formed from UDP-glucose alone was a precursor for the xyloglucan formed when UDP-xylose was also present (18). These studies suggested that formation of the glucan backbone of xyloglucan was restricted in the absence of xylosyl transfer, and that both glucose and xylose must be incorporated in a concerted manner for the complete xyloglucan backbone to form. Synthesis of the glucose-xylose backbone *in vitro* did not require the presence of UDP-galactose or GDP-fucose, and the glucosyl- and xylosyltransferases appeared to act together independently of the addition of terminal sugars.

### Additions to the Xyloglucan Backbone

Pea membrane preparations incorporated [ $^{14}\text{C}$ ]fucose from GDP-[ $^{14}\text{C}$ ]fucose into large pre-made primer chains which did not undergo detectable elongation with time (20). Incorporation of fucose occurred only onto high molecular weight (up to 300 kD) acceptors, even with very short incubation times (Fig. 3), and these products hydrolyzed to the nonasaccharide subunit of xyloglucan. The transfer of fucose from GDP-[ $^{14}\text{C}$ ]fucose to these products was promoted by, but not dependent on, the presence of UDP-glucose, UDP-xylose or UDP-galactose in the reaction mixture. This suggests that fucosyl transfer is independent of glucose and xylose transfer (and thus chain elongation), and that the pre-made primers were already partially galactosylated. Nevertheless, when double-labelling experiments were performed in the presence of all four nucleotide sugars needed for xyloglucan biosynthesis, including UDP-[ $^3\text{H}$ ]xylose and GDP-[ $^{14}\text{C}$ ]fucose, nonasaccharide containing both labels could be isolated from the reaction products (20). This indicates that the xyloglucan backbone can be decorated with galactose and fucose even while elongation occurs.

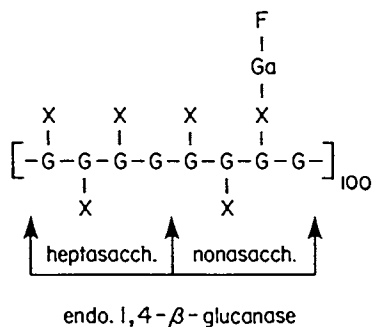


Figure 1. Repeating subunits of pea epicotyl xyloglucan. The molecule is composed of a nonasaccharide ( $\text{Glc}_4\cdot\text{Xyl}_3\cdot\text{Gal}\cdot\text{Fuc}$ ) and a heptasaccharide ( $\text{Glc}_4\cdot\text{Xyl}_3$ ) arranged primarily in alternating sequence. This 16-saccharide dimer is repeated about 100 times in the average molecule. Arrows show where hydrolysis by purified pea or fungal endo-1,4- $\beta$ -glucanase occurs (2). Identical structures have been determined for sycamore (10), soybean (11) and mung bean (12) xyloglucan.

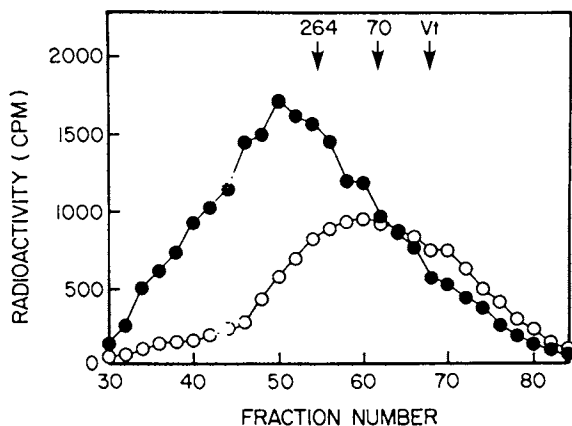


Figure 2. Elution profile from columns ( $100 \times 1.0$  cm) of controlled pore glass beads of 1,4- $\beta$ -linked products formed *in vitro* by pea membranes in 30 min. Products were dissolved in hot paraformaldehyde:DMSO and eluted with DMSO in 1 ml fractions. Open circles, 1 mM UDP- $^{14}\text{C}$ glucose alone; closed circles, 1 mM UDP- $^{14}\text{C}$ glucose plus 50  $\mu\text{M}$  UDP-xylose. Size markers show the molecular weight of peak elution volumes of standard dextrans, 264 = 264000 D; 70 = 70000 D. (Taken with permission from Ref. 18. ©1988 J. Wiley & Sons.)

Fucosyltransferase in pea microsomal preparations also fucosylated exogenously-added xyloglucan acceptors in addition to endogenous primers (21). Extracts of pea cell wall xyloglucan were found to be a poor fucosyl acceptor, presumably because they were almost completely fucosylated already. Tamarind seed xyloglucan, however, which is galactosylated but contains no fucose, strongly promoted fucosyl transfer from GDP- $[^{14}\text{C}]$ fucose, giving rise to typical xyloglucan nonasaccharides upon endoglucanase digestion. Xyloglucan oligosaccharides up to the octasaccharide did not act as fucosyl acceptors but instead inhibited fucosyl transfer to both endogenous and exogenous acceptors, showing that the active site of the fucosyltransferase recognized a fragment longer than the galactosylated octasaccharide. This work confirmed that fucosylation of xyloglucan proceeds independently of the elaboration of the glucose-xylose backbone. Note, however, that complete *in vitro* synthesis of the xyloglucan molecule from the four nucleotide sugars without the involvement of pre-made primers has so far not been achieved.

### Localization of Xyloglucan in Cell Walls

Xyloglucan is believed to play a key role in the architecture of dicot cell walls by linking together cellulose microfibrils and possibly other components of the wall in order to achieve structural rigidity (1). Most cell wall components can be solubilized by hot water, chelating agents or dilute alkali (4% KOH). However, the association between xyloglucan and cellulose is so strong that it requires concentrated alkali (24% KOH) to dissolve xyloglucan from the xyloglucan-cellulose macromolecular complex (2). Xyloglucan binds to cellulose *in vitro* in a pH-dependent manner (22), suggesting that the polymers are associated by hydrogen bonds. The 1,4- $\beta$ -linkage of the glucan backbone of xyloglucan creates a linear molecule, and the galactosyl-fucose side chain may curl around one side of the backbone, thus allowing unimpeded hydrogen bonding between the other side of the backbone and cellulose microfibrils (10). The presence of the galactosyl-fucose side chain may also prevent further hydrogen bonding of xyloglucan with other xyloglucan molecules, creating cellulose microfibrils coated with a single layer of xyloglucan (10). Enzymic and chemical fractionation of cell walls from sycamore (*Acer*) and *Rosa* indicated hydrogen bonding between xyloglucan and cellulose *in vivo*, and implied the presence of glycosidic linkages between xyloglucan and pectic polymers (10, 23). Subsequent work, however, suggested that the bonding between xyloglucan and pectins was principally noncovalent (24).

Autoradiography of cell walls from living tissue previously incubated with  $[^3\text{H}]$ fucose (2) and immunogold localization using polyclonal antibodies to xyloglucan (16) suggested that xyloglucan was distributed throughout the cellulose-containing part of the wall, and was absent only in the middle lamella (16). When cell wall "ghosts" (the cell wall xyloglucan-cellulose complex, which retained the shape of the cell) were prepared by extraction of pea stem tissue with hot 70% ethanol, 0.1 M EDTA and 4% KOH, the

residues contained only xyloglucan and cellulose (2). Treatment of these "ghosts" with a fluorescent fucose-binding lectin clearly showed xyloglucan distributed over the entire surface (Fig. 4).

Electron microscopical observations of shadowed "ghost" preparations showed xyloglucan to be distributed both on and between cellulose microfibrils (2). Even in the cell walls of maturing tissues, as the content of xyloglucan in the wall substantially declined, cellulose was still almost completely coated with xyloglucan (22). Thus, xyloglucan exists *in situ* in intimate association with cellulose throughout the wall at all stages of growth.

### Metabolism of Xyloglucan

*Structural Function of Xyloglucan.* The cell wall has sufficient rigidity to counteract the forces of turgor generated by the protoplasm, and breakdown of key components may be necessary in order to allow the inelastic cellulose microfibrils to move relative to one another and the cell to expand. That cell wall "ghosts", essentially consisting only of xyloglucan and cellulose, retained the shape of the cell suggests that xyloglucan not only coats individual cellulose microfibrils but also bonds the microfibrils together (2). Endohydrolysis of xyloglucan may be essential in order to permit the movement of cellulose microfibrils relative to one another, and consequently cell wall extension. A requirement for exposed xyloglucan in growth has been demonstrated in studies using fucose-binding lectins (25). The lectins bound to the cell wall of azuki bean epicotyl segments, and inhibited both auxin-induced cell wall loosening and growth, presumably by protecting xyloglucan from turnover.

*Deposition of Xyloglucan.* In dicot stem segments, auxin rapidly (after about 1 h) promoted an increase in the rate of deposition of cellulosic and non-cellulosic cell wall materials, even if growth were inhibited (26, 27). In pea epicotyl apices, auxin treatment for 48 h resulted in a small increase in cellulose content but more than a doubling of xyloglucan as the cells expanded (Table I). The synthesis and incorporation of xyloglucan into the wall may thus be hormonally controlled. The activity of "xyloglucan synthase" (xyloglucan xylosyltransferase was actually measured) declined in the growing region of the stem of whole pea plants as this zone matured, but treatment of the plants with auxin prevented the decline (28). Auxin treatment of decapitated whole plants and of isolated stem segments also maintained the activity of  $\beta$ -glucan synthase (29, 30), an enzyme which may be responsible for the synthesis of the 1, 4- $\beta$ -glucan backbone of xyloglucan (18).

*Degradation of Xyloglucan.* In addition to promoting xyloglucan deposition, auxin treatment brings about a massive induction (up to 30-fold after 72 h) of endo-1, 4- $\beta$ -glucanase activity (31). Concomitant with this induction, a marked decline in the average molecular weight of xyloglucan, but not cellulose, was observed (Table I). These changes occurred despite the increases in net deposits of xyloglucan and cellulose. *In vitro* incubation

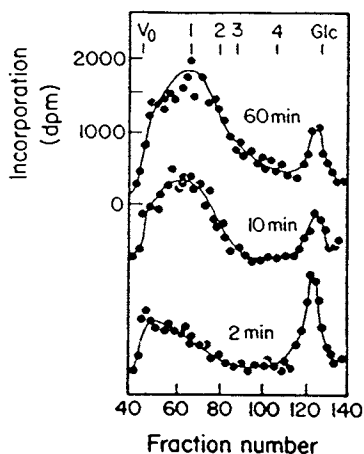


Figure 3. Gel filtration of alkali-soluble xyloglucan on columns ( $95 \times 1.5$  cm) of Sepharose CL-6B. Pea microsomal membranes were incubated for various periods with GDP- $[^{14}\text{C}]$ fucose and unlabelled sugar nucleotides. Products were eluted with 0.1 M NaOH in 1 ml fractions. Molecular weights of dextran markers, 1 = 264000 D; 2 = 70000 D; 3 = 40000 D; 4 = 10600 D; Glc=glucose. Redrawn from Camirand and Maclachlan (20).

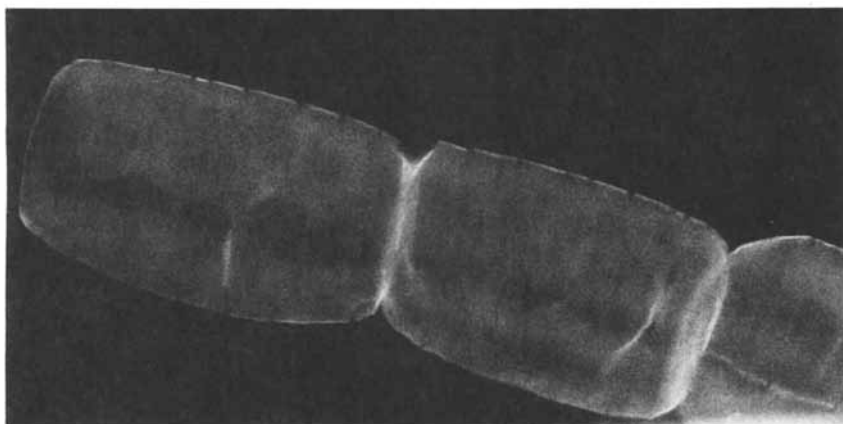


Figure 4. Pea stem material was sequentially extracted with hot 70% ethanol, 0.1 M EDTA and 4% KOH-0.1%  $\text{NaBH}_4$  to leave xyloglucan-cellulose cell wall "ghosts". Binding of fluorescent fucose-binding lectin from *Ulex europaeus* as visualized by fluorescence microscopy shows xyloglucan distributed over the whole wall surface. Photograph courtesy of Dr. T. Hayashi.

of pea cell wall "ghosts" with purified endo-1,4- $\beta$ -glucanase dramatically increased the number of residual reducing ends and brought about solubilization of xyloglucan before any hydrolysis of cellulose took place (32). The localization of xyloglucan in the wall, where cellulose microfibrils are sheathed by a layer of xyloglucan, may make xyloglucan more accessible to the enzyme than is cellulose. This study confirmed that in cell walls auxin-induced endo-1,4- $\beta$ -glucanase (commonly called "cellulase") preferentially hydrolyzes xyloglucan over cellulose.

Table I. Effects of auxin treatment on pea epicotyl apices. Apical 5 mm regions of etiolated epicotyls were delineated, seedlings sprayed once at zero time with or without 4.5 mM 2,4-D and marked regions examined after 48 h. Data compiled from refs. 28 and 32

Parameter	Zero Time	48 h	
		Untreated	Auxin
Length (mm/seg)	5	25	7.5
Fresh weight (mg/seg)	12	56	44
Weight/Length (mg/mm)	2.4	2.2	5.9
Xyloglucan ( $\mu\text{g}/\text{seg}$ )	28	59	137
Cellulose ( $\mu\text{g}/\text{seg}$ )	40	515	615
Xyloglucan ( $\text{DP} \times 10^{-3}$ )	1.1	0.8	0.2
Cellulose ( $\text{DP} \times 10^{-3}$ )	8.4	11.0	9.2
Endo-1,4- $\beta$ -glucanase activity (units/seg)	13	40	234

In soybean hypocotyl, the activity of cell wall endo-1,4- $\beta$ -glucanase was higher in regions of the stem actively undergoing cell expansion, and this increased activity was correlated with a reduced average molecular weight of cell wall xyloglucan (33). In azuki bean epicotyl cell walls, auxin treatment reduced the average molecular weight of xyloglucan within 2 h, although a decrease in the average molecular weight of the total hemicellulose fraction was observed after only 30 min (34). Auxin also rapidly evoked a reduction in average molecular weight of the xyloglucan component of *Avena* coleoptile cell walls (35). These changes were not a result of cell expansion, since they occurred even when growth was osmotically suppressed by mannitol.

When pea epicotyl segments were pulse-chased with [ $^{14}\text{C}$ ]glucose, subsequent incubation with auxin brought about a loss of cell wall glucose and xylose and the appearance in the incubation medium of soluble polymeric material containing xylose and glucose (36). The apparent solubilization of cell wall xyloglucan was detectable after only 15 min of auxin treatment and thus occurred as quickly as the increased growth rate (37). Moreover, solubilization increased as growth rate increased, and was not prevented

when growth was inhibited by mannitol (37), suggesting that xyloglucan hydrolysis reflected the wall-loosening process. Subsequent work confirmed a decrease in cell wall xyloglucan upon auxin treatment (38). Collection of cell wall free space solutions using a low-speed centrifugation technique also found an auxin-induced production of water-soluble materials possessing the properties of xyloglucan (39). Xyloglucan subunits have been detected in the bathing medium of cultured cells during growth (6).

Enzymes capable of hydrolyzing xyloglucan to monosaccharides have been detected in extracts from soybean cell walls (33,40). High levels of endo-1,4- $\beta$ -glucanase activity were found in elongating regions of the stem, where xyloglucan appeared to be cleaved into comparatively large fragments. Other enzymes, however, presumably including an  $\alpha$ -xylosidase, a  $\beta$ -glucosidase, a  $\beta$ -galactosidase and an  $\alpha$ -fucosidase, showed higher activity in non-elongating regions. These findings suggest that partly degraded xyloglucan eventually will become completely broken down and that oligosaccharides will not accumulate in the cell wall space. In pea stems auxin treatment enhanced the activity of enzymes cleaving glucosidic, xylosidic and galactosidic bonds (41), although it was not shown that these enzymes were localized in the cell wall.

The full induction of endo-1,4- $\beta$ -glucanase by auxin treatment required a period of many hours or even days (31) rather than minutes, precluding the appearance of new endo-1,4- $\beta$ -glucanase as mediating the "rapid action" of auxin on growth. Changes in the activity of pre-existing endo-1,4- $\beta$ -glucanase seem more likely, perhaps related to the suggestion that auxin promotes growth by causing the acidification of the cell wall space by the protoplasm (42). Consistent with this are the findings that buffer of pH 7 prevented both growth and the release of soluble xyloglucan from the wall induced by auxin, and that buffer of pH 4 caused a similar release of xyloglucan as did auxin, and in the short-term also caused a similar promotion of growth (43). Acid treatment at 0°C did not result in xyloglucan release, suggesting that xyloglucan degradation was enzyme mediated (39). The activities of a  $\beta$ -glucosidase and a  $\beta$ -galactosidase in *Avena* coleoptile cell walls were promoted by changing the pH from 7 to around 5 (44), but it is not known if these enzymes act on xyloglucan in the wall. Endo-1,4- $\beta$ -glucanase, which does act on xyloglucan in the wall, has a broad pH optimum of 6.0-6.5 (45). Furthermore, the occurrence in the whole plant of changes in cell wall pH of the magnitude of those described above has been questioned (46). Thus, the mechanism by which auxin regulates the very rapid changes observed in xyloglucan DP is not yet fully clarified.

The continued incorporation of matrix wall polymers into the wall also seems to be essential for long-term growth (27), implying that incorporation as well as breakdown of xyloglucan may be important in the wall-expansion process. Further study of how synthesis and breakdown of wall components are coordinated to regulate cell wall loosening is required.

### Xyloglucan Subunits as Oligosaccharins

Fragments of cell wall polysaccharides of specific structure can bring about

regulatory effects on plant cells. Oligoglucosides from fungal cell walls and fragments of homogalacturonan, released from the plant's own cell wall by enzymes in pathogens, can induce the *de novo* production of mRNA's and enzymes responsible for the synthesis of phytoalexins, natural plant antibiotics (47). Fragments of pectic polysaccharides can also induce the formation of protease inhibitors which protect plants from digestive attack by insects and microbes. Cell wall polysaccharide fragments have several other morphogenetic effects on plants, for they may modify such processes as flowering and vegetative growth (48). Biologically active cell wall polysaccharide fragments have been termed oligosaccharins (48).

The endo-1,4- $\beta$ -glucanase whose formation was induced by auxin ultimately hydrolyzed xyloglucan to characteristic oligosaccharides. The nonasaccharide derived from cultured sycamore xyloglucan, when added in very low concentrations to pea stem segments, inhibited auxin-stimulated growth (49). This report was recently confirmed using nonasaccharides derived from *Rosa* cell walls (50). In both cases the nonasaccharide showed an optimum for growth-inhibitory action, being less effective or totally ineffective at higher concentrations (Table II). The optimum was around 10 nM (49) or 1 nM (50) in the two studies, and concentrations above about 100 nM were ineffective. Considerable variability in the degree of inhibition by the nonasaccharide was observed, ranging from 70 to almost 100% in the experiments reported by York *et al.* (49), and from about 30 to 70% in those shown by McDougall and Fry (50). In both reports the heptasaccharide was found to be without growth-inhibitory effect.

Table II. Effects of xyloglucan oligosaccharide subunits on auxin-stimulated growth of pea epicotyl segments *in vivo* and pea endo-1,4- $\beta$ -glucanase activity *in vitro*. Growth of segments in 1  $\mu$ M 2,4-D was measured after 18 h. Endo-1,4- $\beta$ -glucanase activity was determined viscometrically after 30 min using tamarind xyloglucan as substrate. Data calculated from refs. 50 and 51

Oligosaccharide concentration	Xyloglucan	
	Heptasaccharide	Nonasaccharide
	Inhibition of auxin-stimulated growth (%)	
0.1nM	3	0
1.0	4	65
10.0	0	50
100.0	0	20
	Stimulation of $\beta$ -glucanase activity (%)	
50 $\mu$ M	210	430
100	280	550
150	350	640
200	410	700



Effects of xyloglucan oligosaccharides on endo-1,4- $\beta$ -glucanase activity *in vitro* have also been observed (51). Pea nona- and heptasaccharide both dramatically stimulated pea endo-1,4- $\beta$ -glucanase activity as determined viscometrically using tamarind xyloglucan as substrate (Table II). Stimulation was concentration-dependent, and approached saturation at 200  $\mu$ M. Nonasaccharide was the more effective, causing over 700% stimulation at 200  $\mu$ M, a concentration at which the heptasaccharide caused 400% activation. Even xyloglucan pentasaccharide caused a doubling of activity. The stimulation was both substrate- and enzyme-specific. Activation by oligosaccharides was not detected using carboxymethylcellulose as substrate, nor with endo-1,4- $\beta$ -glucanase from *Trichoderma* using xyloglucan as substrate.

Thus, at nM concentrations *in vivo*, nonasaccharide produced by the metabolism of cell wall xyloglucan appears to act as a negative feedback modulator of auxin-stimulated growth. But, if oligosaccharides also stimulate endo-1,4- $\beta$ -glucanase action *in vivo*, this would act by positive feedback to magnify the decay rate of cell wall xyloglucan further, and lead to the production of more oligosaccharide. This could perhaps raise the concentration of nonasaccharide *in vivo* to above that which was inhibitory towards growth. In cultured spinach cells, a fucose-containing nonasaccharide accumulated in the culture medium to a steady-state concentration of about 430 nM (6). However, the levels of nonasaccharide existing *in vivo* at the load-bearing region of the innermost wall layers of cells in the expansion zone of the stem, where regulation of growth presumably occurs, are not known.

Of course, in a given tissue nonasaccharide may inhibit growth and stimulate endo-1,4- $\beta$ -glucanase activity independently of one another. The observation that heptasaccharide was inactive in one system but active in the other suggested that the effects were mediated by different mechanisms. The heptasaccharide was not itself inhibitory to growth, nor did it interfere with the nonasaccharide effect (50), suggesting great specificity in the perception of nonasaccharide for growth inhibition. The existence of two independent mechanisms may explain the loss of inhibitory effect of xyloglucan nonasaccharides on auxin-stimulated growth when concentrations exceeded 10 nM. At higher concentrations oligosaccharides may act directly on cell wall endo-1,4- $\beta$ -glucanase, increasing its activity and promoting xyloglucan hydrolysis and cell wall loosening. This may then override the mechanism producing the growth-inhibitory effect at lower concentrations of nonasaccharide. Another alternative is that the two mechanisms are spatially separated and occur in different regions of the stem. Perhaps low concentrations of nonasaccharide are found only near cells approaching full size, where they act to inhibit auxin-stimulated growth, whereas higher concentrations are found in regions where cells are already fully expanded. Here the oligosaccharides may stimulate the activities of various glycosidases in the wall, resulting in the complete hydrolysis of the comparatively large xyloglucan pieces and oligosaccharides to monosaccharides. This would remove any biological activity of the fragments, and the monosaccharides could be absorbed by the cell and reused.

## Conclusions

The picture that emerges is that xyloglucan functions in the walls of growing tissues as a binding polysaccharide which contributes to the rigidity of the cellulose framework. During the stimulation of growth evoked by auxin, endo-1,4- $\beta$ -glucanase is induced which hydrolyzes xyloglucan preferentially. Such a hydrolysis is correlated with the wall-loosening process. Presumably new synthesis is required in order to preserve the strength of the wall, and to maintain it in a state capable of further loosening during long-term growth. The relationship between new wall synthesis and the degradation of existing wall polymers in wall loosening is poorly understood at present.

The role played in growth by xyloglucan oligosaccharide fragments is just beginning to be investigated. Xyloglucan nonasaccharide specifically inhibited auxin-evoked growth at certain concentrations in the nM range, but nona-, hepta- and pentasaccharide all stimulated endo-1,4- $\beta$ -glucanase activity *in vitro* in the  $\mu$ M range. This latter effect, if it occurs *in vivo* at concentrations of oligosaccharides likely to be present in the cell wall space, would be expected to enhance xyloglucan depolymerization, wall loosening and growth. These apparently opposite effects of nonasaccharide on growth and the putative wall-loosening process constitute a challenging problem for future work to resolve.

## Acknowledgments

This review was prepared with support by grants from the Natural Sciences and Engineering Research Council of Canada. We thank Drs. Anne Camirand, Ruth Gordon, and Vladimir Farkas for useful discussions.

## Literature Cited

1. McNeil, M.; Darvill, A. G.; Fry, S. C.; Albersheim, P. *Ann. Rev. Biochem.* 1984, **53**, 625-63.
2. Hayashi, T.; Maclachlan, G. A. *Plant Physiol.* 1984, **75**, 596-604.
3. Kato, Y.; Iki, K.; Matsuda, K. *Agric. Biol. Chem.* 1981, **45**, 2745-53.
4. Carpita, N. C. *Plant Physiol.* 1983, **72**, 515-21.
5. Carpita, N. C. *Plant Physiol.* 1984, **76**, 205-12.
6. Fry, S. C. *Planta* 1986, **169**, 443-53.
7. Reid, J. S. G. *Adv. Bot. Res.* 1985, **11**, 125-55.
8. Kato, Y.; Matsuda, K. *Plant Cell Physiol.* 1985, **26**, 437-45.
9. Thomas, J. R.; McNeil, M.; Darvill, A. G.; Albersheim, P. *Plant Physiol.* 1987, **83**, 659-71.
10. Bauer, W. D.; Talmadge, K. W.; Keegstra, K.; Albersheim, P. *Plant Physiol.* 1973, **51**, 174-87.
11. Hayashi, T.; Kato, Y.; Matsuda, K. *Plant Cell Physiol.* 1980, **21**, 1405-18.
12. Kato, Y.; Matsuda, K. *Agric. Biol. Chem.* 1980, **44**, 1759-66.
13. Ray, P. M. *Biochim. Biophys. Acta* 1980, **629**, 431-4.

14. Hayashi, T.; Matsuda, K. *J. Biol. Chem.* 1981, **256**, 11117-22.
15. Camirand, A.; Brummell, D. A.; Maclachlan, G. A. *Plant Physiol.* 1987, **84**, 753-6.
16. Moore, P. J.; Staehelin, L. A. *Planta* 1988, **174**, 433-45.
17. Hayashi, T.; Nakajima, T.; Matsuda, K. *Agric. Biol. Chem.* 1984, **48**, 1023-7.
18. Gordon, R.; Maclachlan, G. A. *J. Appl. Polym. Sci. Symp.* 1988, **43**, in press.
19. Gordon, R. Ph.D. Thesis, McGill Univ., Montreal, 1988.
20. Camirand, A.; Maclachlan, G. A. *Plant Physiol.* 1986, **82**, 379-83.
21. Farkas, V.; Maclachlan, G. A. *Arch. Biochem. Biophys.* 1988, **264**, 48-53.
22. Hayashi, T.; Marsden, M. P. F.; Delmer, D. P. *Plant Physiol.* 1987, **83**, 384-9.
23. Chambat, G.; Barnoud, F.; Joseleau, J.-P. *Plant Physiol.* 1984, **74**, 687-93.
24. Fry, S. C. *Ann. Rev. Plant Physiol.* 1986, **37**, 165-86.
25. Hoson, T.; Masuda, Y. *Physiol. Plant.* 1987, **71**, 1-8.
26. Abdul-Baki, A. A.; Ray, P. M. *Plant Physiol.* 1971, **47**, 537-44.
27. Brummell, D. A.; Hall, J. L. *Physiol. Plant.* 1985, **63**, 406-12.
28. Hayashi, T.; Maclachlan, G. A. *Plant Physiol.* 1984, **76**, 739-42.
29. Spencer, F. S.; Ziola, B.; Maclachlan, G. A. *Can. J. Biochem.* 1971, **49**, 1326-32.
30. Ray, P. M. *Plant Physiol.* 1973, **51**, 601-8.
31. Datko, A. H.; Maclachlan, G. A. *Plant Physiol.* 1968, **43**, 735-42.
32. Hayashi, T.; Wong, Y.-S.; Maclachlan, G. A. *Plant Physiol.* 1984, **75**, 605-10.
33. Koyama, T.; Hayashi, T.; Kato, Y.; Matsuda, K. *Plant Cell Physiol.* 1981, **22**, 1191-8.
34. Nishitani, K.; Masuda, Y. *Physiol. Plant.* 1981, **52**, 482-94.
35. Inouhe, M.; Yamamoto, R.; Masuda, Y. *Plant Cell Physiol.* 1984, **25**, 1341-51.
36. Labavitch, J. M.; Ray, P. M. *Plant Physiol.* 1974, **53**, 669-73.
37. Labavitch, J. M.; Ray, P. M. *Plant Physiol.* 1974, **54**, 499-502.
38. Gilkes, N. R.; Hall, M. A. *New Phytol.* 1977, **78**, 1-15.
39. Terry, M. E.; Jones, R. L.; Bonner, B. A. *Plant Physiol.* 1981, **68**, 531-7.
40. Koyama, T.; Hayashi, T.; Kato, Y.; Matsuda, K. *Plant Cell Physiol.* 1983, **24**, 155-62.
41. O'Neill, R. A.; White, A. R.; York, W. S.; Darvill, A. G.; Albersheim, P. *Phytochemistry* 1988, **27**, 329-33.
42. Rayle, D. L.; Cleland, R. E. *Curr. Top. Dev. Biol.* 1977, **11**, 187-214.
43. Jacobs, M.; Ray, P. M. *Plant Physiol.* 1975, **56**, 373-6.
44. Johnson, K. D.; Daniels, D.; Dowler, M. J.; Rayle, D. L. *Plant Physiol.* 1974, **53**, 224-8.
45. Maclachlan, G. A. *Methods Enzymol.* 1988, **160**, 382-91.
46. Brummell, D. A.; Hall, J. L. *Plant Cell Environ.* 1987, **10**, 523-43.

47. Ryan, C. A. *Ann. Rev. Cell Biol.* 1987, **3**, 295-317.
48. Tran Thanh Van, K.; Toubart, P.; Cousson, A.; Darvill, A. G.; Gollin, D. J.; Albersheim, P. *Nature* 1985, **314**, 615-7.
49. York, W. S.; Darvill, A. G.; Albersheim, P. *Plant Physiol.* 1984, **75**, 295-7.
50. McDougall, G. J.; Fry, S. C. *Planta* 1988, **175**, 412-6.
51. Farkas, V.; Maclachlan, G. A. *Carbohydr. Res.* 1988, in press.

RECEIVED March 10, 1989

## Chapter 3

# Toward a Working Model of the Growing Plant Cell Wall

## Phenolic Cross-Linking Reactions in the Primary Cell Walls of Dicotyledons

Stephen C. Fry and Janice G. Miller

Department of Botany, University of Edinburgh, The King's Buildings,  
Mayfield Road, Edinburgh EH9 3JH, Scotland

The efficient formation of inter-polymeric cross-links by oxidative coupling of the small number of polymer-bound phenolic side-chains present in the non-lignified, growing plant cell wall requires considerable specificity in the reactions concerned. In this paper we summarize some of the evidence that such specificity exists. We suggest that the cell wall is initially assembled by non-covalent interactions, especially involving the hydrogen-bonding of neutral xyloglucan chains to several microfibrils, thereby tethering these microfibrils. Oxidative coupling of other matrix polymers [acidic polysaccharides and/or basic glycoproteins] via their phenolic side-chains is seen as a subsequent wall-modification reaction whereby xyloglucan chains may be strapped to their current microfibrils so that the existing architecture is rendered more nearly permanent. Efficient strapping (i.e., fastening the maximum amount of material with fewest "buckles") requires chemical specificity—the formation of cross-links at appropriate sites. There is great specificity both in the biosynthetic reactions by which phenolic side-chains become attached to the wall polymers and also in the choice of phenolic partners and orientation during coupling.

The growing plant cell wall contains polymers which bear a small proportion of phenolic side-chains. These side-chains appear to be subject *in vivo* to oxidative phenolic coupling and thus to participate in cross-linking reactions that may be highly significant in the control of wall extensibility (and therefore in cell growth) and of enzymic digestibility (1,2). For phenolic cross-linking to be biologically effective, despite the presence of only low levels of phenolic compounds in the primary cell wall, the reactions

0097-6156/89/0399-0033\$06.00/0

© 1989 American Chemical Society

must be accurately and efficiently steered: they must be specific. Here we summarize evidence that the necessary specificity exists.

## Hypothesis

In order to think about the nature and consequences of cell wall polymer phenolic cross-linking, we need a working model of the mode of assembly and the final structure of the primary cell wall. Unfortunately, there is no universally acceptable model: that proposed by Albersheim and co-workers (3) is not now widely accepted because the postulated inter-polysaccharide glycosidic bonds have not been demonstrated (4); and the 'warp-weft' model of Lamport (5) rests on the assumptions that extensin (i) forms a defined-porosity network (not proven); (ii) is orientated anticlinally to the cell surface [some evidence against (6)]; and (iii) is a major component of all primary cell walls (not true).

*Major Structural Polymers of the Cell Wall.* A wall model requires a description of the major polymers involved. The major polymers of the growing Dicotyledon cell wall are shown, approximately to scale, in Figure 1. They are described in more detail elsewhere (2); in brief, they are:

1. *The microfibrillar cellulose.* This forms the skeletal scaffolding of the cell wall. Microfibrils are about 4 nm in diameter (6) and are of indeterminate length.
2. *The neutral hemicelluloses.* These are xyloglucan in Dicotyledonous primary walls and principally mixed-linked  $\beta$ -(1 $\rightarrow$ 3), (1 $\rightarrow$ 4)-D-glucans in members of the Gramineae (grasses, including cereals). In isolation, xyloglucan is water-soluble, although the molecule is a relatively stiff rod approximately 150 to 1500 nm in total contour length (8). One xyloglucan had a measured axial ratio of about 100 (9). In the intact cell wall, the xyloglucan is firmly attached to the surface of the cellulosic microfibrils, principally by hydrogen-bonding (2,8,10-13), although some more secure bonds may also be present (2,10).
3. *The acidic polysaccharides.* In Dicotyledons, the major acidic polysaccharides are the pectins (partially methyl-esterified homogalacturonans and rhamnogalacturonans) and smaller amounts of arabinoglucuronoxylans (2). [In growing grass cell walls, the arabinoglucuronoxylans usually predominate over pectins.]
4. *The basic extensins.* These are hydroxyproline-, lysine- and tyrosine-rich glycoproteins consisting of rigid molecular rods about 80 nm long (14,15), bearing short mono- to tetrasaccharide side-chains (2,14). When newly secreted they bind ionically to the acidic polysaccharides of the cell wall and can be extracted with cold salt solutions; later they become much more resistant to salt-extraction and are said to be covalently bound, probably via dimerization of their tyrosine residues to form isodityrosine (15).

Some of the acidic and basic polymers of the cell wall bear phenolic side-chains. The acidic polysaccharides carry ferulic and *p*-coumaric acid and related cinnamate-derivatives, esterified to specific hydroxy groups

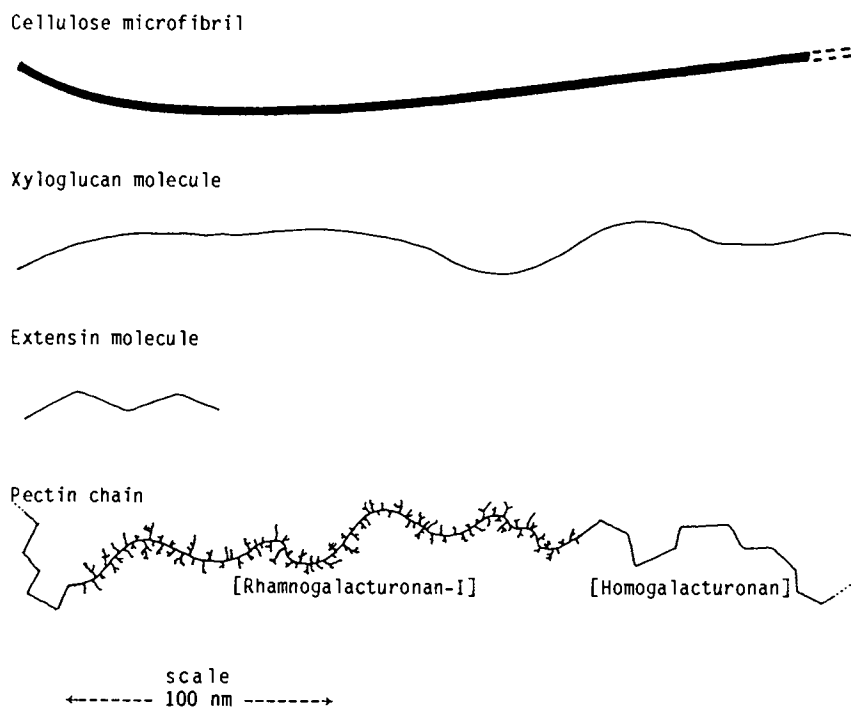


Figure 1. The principal structural components of the growing cell walls of a Dicotyledon. The drawings are approximately to scale.

(1,2,17-22). Feruloylated pectins have been found in the parenchymatous cell walls of many Dicotyledons (mainly in the Centrospermae and Solanaceae), but UV-fluorescence microscopy suggests that at least the *epidermal* cell walls of all Dicotyledons contain phenolic residues; it remains to be seen whether these phenolic residues are attached to polysaccharides or to cutin, but location of even a small quantity of, say, feruloyl-pectin in the epidermal wall would be particularly significant in the control of growth because the extensibility of the epidermis controls the expansion of whole stems (23) and leaves (Fry, unpublished observations). The extensins, as already mentioned, are rich in the phenolic amino acid tyrosine (2).

*Assembly of a Xyloglucan-Microfibril Framework to the Wall.* The initial assembly of the cell wall is likely to be via non-covalent bonding, especially hydrogen-bonding. These initial steps are believed to be non-enzymic. The microfibrils are synthesized by enzyme complexes which are mobile in the plasma membrane. The complexes churn out naked microfibrils, which come to lie in a plane—the innermost, accreting face of the cell wall. At the same time, Golgi-derived vesicles deposit the essentially soluble matrix polymers (Fig. 2a). Evidence suggesting that the matrix polymers are indeed water-soluble when newly secreted was provided by observation of the polysaccharides secreted by naked protoplasts directly into the culture medium (24). Of the various matrix polymers in this mixture (hemicelluloses, pectins and extensin), it is particularly the xyloglucan that will strongly hydrogen-bond to the microfibrils, clothing them with a molecular monolayer (10-12).

Since the total contour length of a xyloglucan molecule is 40 to 400 times greater than the diameter of a microfibril (8), it would seem inevitable that most of the newly deposited xyloglucan chains will have the opportunity to bind to the *several* microfibrils across which they are randomly laid down (Fig. 2b) (25).

Any tendency for a xyloglucan molecule to re-orientate and come to lie with its entire length along a single microfibril will be minimized by the presence in the space between the adjacent microfibrils of other matrix polymers which are not strongly hydrogen-bonding (pectins and extensins) and which will (a) retard the molecular motion of the xyloglucan and (b) [by some of them lying with their main-chains perpendicular to the microfibrils] physically prevent the xyloglucan chain from lining up along any favored microfibril. The consequence of this is that the individual xyloglucan molecules will come to be hydrogen-bonded along discrete segments of several microfibrils, tethering them, and the intervening lengths of xyloglucan will be suspended between the microfibrils (Fig. 2b).

It may be noted parenthetically that evidence that extensins are not strongly hydrogen-bonded in the cell wall is the ease with which they can be leached out of the wall with 25-50 mM  $\text{LaCl}_3$  or  $\text{AlCl}_3$  (20)—a treatment that effectively breaks ionic bonds but not hydrogen bonds—so long as the treatment is applied before the extensin has become covalently bonded in the cell wall. Evidence that at least one pectic polysaccharide (rhamnogalacturonan-I) is not strongly hydrogen-bonded in the cell



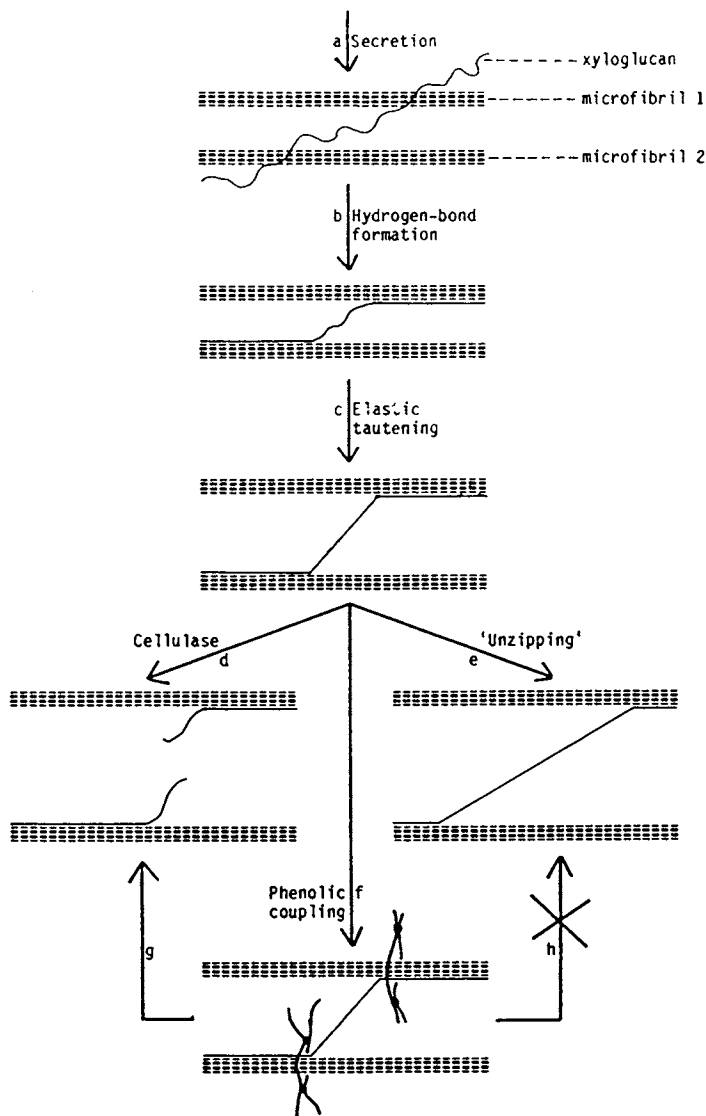


Figure 2. A speculative model for the assembly and growth of the Dicotyledonous cell wall. For clarity, the model shows two microfibrils (≡≡≡, ≡≡≡) and only one of the many xyloglucan molecules (—) that are proposed to interconnect them. The loops in the lower diagram represent other matrix polymers (extensin and/or pectins) whose phenolic side-chains have become oxidatively coupled. Steps (d) and (g) are proposed to be catalyzed by cellulase. For further details, see ref. (25).

wall is the fact that, despite its large size [DP 2,000 (27); similar to an average xyloglucan], it is released intact from the cell wall into cold neutral water following treatment with pure endo-polygalacturonase, an enzyme that hydrolyzes homogalacturonan (with which the backbone of the rhamnogalacturonan had presumably been contiguous) but does not affect the rhamnogalacturonan itself.

*An Important Requirement for Cell Growth.* With continued cell expansion, the intermicrofibrillar segments of xyloglucan will become stretched taut (Fig. 2c) and will eventually come to bear the burden of turgor. Further growth will then be impossible unless one or both of two things happens:

1. the inter-microfibrillar segments of xyloglucan are hydrolyzed (Fig. 2d) by an endo- $\beta$ -(1 $\rightarrow$ 4)-D-glucanase (cellulase), a well-established plant cell wall enzyme (28);
2. the xyloglucan-cellulose hydrogen-bonds are physically pulled open, unzipping the xyloglucan molecules from the microfibrils (Fig. 2e); hydrogen-bonds are considerably weaker than the covalent bonds of which the individual polysaccharide chains are constructed (13).

*Consequences and Requirements of Oxidative Phenolic Coupling in the Cell Wall.* If the phenolic side-chains present on pectins and/or extensins can cross-link in an appropriate manner and place, they could form loops that would encircle microfibrils and thereby strap particular xyloglucan molecules on to particular microfibrils (Fig. 2f). This would prevent the "unzipping" mode of growth, but would not affect the "hydrolytic" mode. Thus, while cross-linking could potentially decelerate growth very rapidly (Fig. 2h), such an effect *need not be irreversible* (Fig. 2g). The importance of this conclusion can be considered by reference to a physiological example: The rapidly-imposed inhibitory effect of blue light on the growth of stems has been hypothesized to be mediated by peroxidase-catalyzed cross-linking of wall polymer-bound phenolics (29); since the initial growth rate is rapidly restored when the blue light is switched off, the hypothesis only stands if the mechanism of growth inhibition is reversible.

Efficient cross-link formation by a small number of wall polymer-bound phenolics requires *great precision* in the metabolic reactions involved. It is not sufficient to form cross-links: the cross-links need to be formed in the proper place within the polymer molecule and within the cell wall. Evidence that cross-links form at all [albeit sometimes as a low percentage of the total wall phenolics] is presented elsewhere (1,2,13,16,30-32). Here we present evidence that sufficient molecular specificity exists to be compatible with *useful* cross-link formation.

### **Evidence for Specificity in the Reactions by which Phenolic Groups are Introduced into Wall Polymers**

*Background.* In order to maximize the efficiency of cross-linking based on a small number of phenolic groups, it is important that these groups should be sited on the wall polymers *at appropriate loci* rather than randomly. In the case of the phenolic side-chains of extensins this criterion is met since the siting of the tyrosines is genetically encoded (27).

*Siting of Ferulic Acid in the Wall Polysaccharides.* The origin of the feruloyl residues of the acidic wall polysaccharides is not so straightforward. However, there is good evidence that these phenolic side-chains are very specifically sited. The position of the feruloyl groups can most easily be explored by enzymic "dissection" of the polysaccharides with commercial mixtures of enzymes such as that known as Driselase (available from Sigma Chemical Co.). Driselase, which is widely used for the isolation of plant protoplasts because it possesses enzymes that hydrolyze most of the glycosidic linkages of the primary cell wall, lacks feruloyl-esterase activity and therefore leaves the feruloyl groups attached to the appropriate sugar unit of the polysaccharide. In addition, the endo- and exo-glycanases of Driselase cannot hydrolyze those glucose residues that bear feruloyl groups. The expected products of hydrolysis of a feruloyl-polysaccharide are thus mainly monosaccharides plus feruloyl-disaccharides (2). [Driselase lacks  $\alpha$ -xylosidase activity and therefore also yields large amounts of a simple disaccharide, D-xylopyranosyl- $\alpha$ -(1  $\rightarrow$  6)-D-glucose, from xyloglucan.]

The cell walls of Dicotyledons, especially in the Caryophyllales, yield upon Driselase digestion two major feruloyl-disaccharides, namely 3-*O*-(3-*O*-feruloyl- $\alpha$ -L-arabinopyranosyl)-L-arabinose (Fer-Ara<sub>2</sub>) and 4-*O*-(6-*O*-feruloyl- $\beta$ -D-galactopyranosyl)-D-galactose (Fer-Gal<sub>2</sub>) (17). These two compounds together account for 60-70% of the feruloyl residues of the primary walls of cultured spinach cells. In the grasses, the major feruloyl-disaccharide obtained with Driselase is 3-*O*-(5-*O*-feruloyl- $\alpha$ -L-arabinofuranosyl)-D-xylose (Fer-Ara-Xyl), but larger amounts of a feruloyl-trisaccharide, 4-*O*-[3-*O*-(5-*O*-feruloyl- $\alpha$ -L-arabinofuranosyl)- $\beta$ -D-xylopyranosyl]-D-xylose (Fer-Ara-Xyl<sub>2</sub>), usually predominate because Driselase is inefficient at hydrolyzing xylobiose (19,20).

The important conclusion is that much of the wall's ferulic acid is linked to specific hydroxy groups on specific sugars of specific polysaccharides. The specificity is particularly notable in the case of Fer-Ara<sub>2</sub>, since the feruloylated arabinose residues are in the rare pyranose ring-form (17). It is clear that the feruloylation reactions are not random, but are carefully steered biosynthetic steps.

*Evidence for Intracellular Feruloylation Reactions.* The reactions by which feruloyl residues are added to polysaccharides occur intracellularly. This was established for the Fer-Ara<sub>2</sub> units of the pectic polysaccharides of culture spinach cells by administration of [<sup>3</sup>H]arabinose so that the careers of polymer-bound pentose residues could be followed from their intracellular incorporation into nascent polysaccharides and glycoproteins, via their secretion through the plasma membrane, to their ultimate fate within the wall (28). The cells were fed [<sup>3</sup>H]arabinose for various defined periods of time, after which two distinct analyses were performed (Fig. 3):

- a. A sample of the cells was killed in ethanol and the alcohol-insoluble residue (containing the polysaccharides and glycoproteins) was digested exhaustively with Driselase. This converted the various pentose-containing units of the polymers to the following major breakdown products:

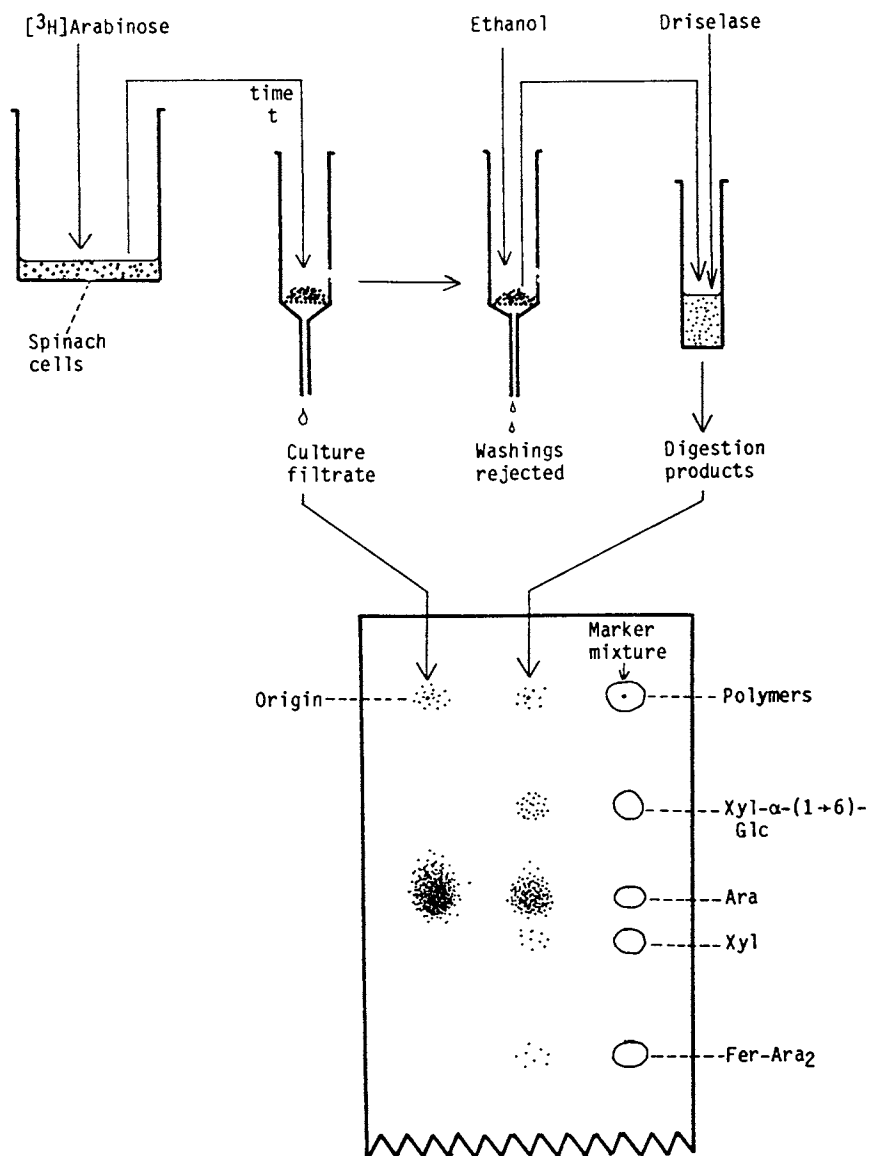
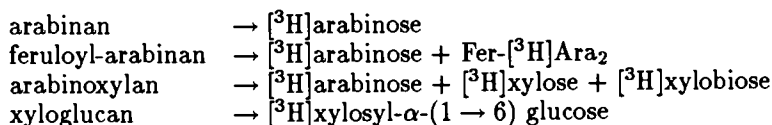


Figure 3. Scheme of an experiment to demonstrate the intracellular nature of polysaccharide-feruloylation.



—which were then separated by paper chromatography and assayed individually for <sup>3</sup>H by scintillation-counting.

- b. A sample of the culture filtrate was also analyzed by paper chromatography to separate the unchanged [<sup>3</sup>H]arabinose from any secreted polysaccharide present. The <sup>3</sup>H in the latter (R<sub>F</sub> = 0.00) was measured by scintillation-counting.

By step (a), a picture could be formed of the kinetics of the intracellular incorporation of <sup>3</sup>H from [<sup>3</sup>H]arabinose into the major polysaccharides of the cell wall. Radioactivity was incorporated into polymer-bound arabinose and xylosyl-glucose units after lag periods of about 3.5 min and 6.5 min, respectively. These lags are taken to be the time required for the [<sup>3</sup>H]arabinose to be taken up and activated to the appropriate donor for polysaccharide biosynthesis



(1,35) and possibly for the UDP-sugars to be transported into the endomembrane system where the polysaccharides are synthesized. After the lag, the rate of incorporation of <sup>3</sup>H into polymers remained fairly constant for several hours.

The incorporation of <sup>3</sup>H from [<sup>3</sup>H]arabinose into Fer-Ara<sub>2</sub> units showed a lag of about 4.2 min, after which it too became linear. This means that as little as 0.7 min after their incorporation into a (possibly still nascent) polysaccharide, [<sup>3</sup>H]arabinose residues were susceptible to feruloylation. The feruloylation reaction is thus likely to have been occurring in the endomembrane system, co-synthetically, as one of the highly regulated parts of the sophisticated polysaccharide-biosynthetic machinery. This can be compared to the co-translational modification known to occur in many proteins.

By step (b), further evidence was obtained that the feruloylation was intracellular. The extracellular polysaccharides and glycoproteins only started to acquire <sup>3</sup>H after a lag of about 25 min (34). This is interpreted to mean that before 25 min essentially all the [<sup>3</sup>H]polysaccharide was still intracellular, either in the Golgi bodies or packaged into Golgi-derived vesicles, but not yet passed through the plasma membrane. The fact that these sugar residues were being feruloylated, at the maximal rate, well before 25 min supports the conclusion that feruloylation was largely intracellular.

*Possible Extracellular Feruloylation.* It has been suggested (36) that feruloylation occurs extracellularly. Evidence in support of this contention was the observation that in maturing coleoptiles of barley the amount of polysaccharide-bound ferulate continued to increase for at least one day after total polysaccharide accumulation had ceased. However, this fact is open to the alternative explanation that relatively small amounts of a highly

feruloylated polysaccharide continued to be synthesized (intracellularly) in mature coleoptiles even after total wall polysaccharide synthesis had decelerated and been approximately equalled by polysaccharide breakdown so that the net rate of polysaccharide accumulation was zero.

Further evidence apparently in favor of some feruloylation being extracellular was the observation that [ $^{14}\text{C}$ ]feruloyl-CoA will bind covalently to coleoptile cell walls *in vitro* (37). It was suggested that this was due to the operation of an extracellular feruloyltransferase catalyzing a transesterification reaction whereby the feruloyl residue is transferred from the CoA donor to a polysaccharide acceptor. However, it remains to be seen (i) whether feruloyl-CoA, the proposed donor, occurs extracellularly; and (ii) whether, in the *in-vitro* system, the  $^{14}\text{C}$  remains as [ $^{14}\text{C}$ ]feruloyl residues or whether the [ $^{14}\text{C}$ ]feruloyl residues become bound to other wall-bound (non-radioactive) phenolic groups, perhaps by oxidative coupling. [Oxidative coupling in isolated cell walls in the absence of added  $\text{H}_2\text{O}_2$  has been observed (38).] Such a reaction would be inhibited by ascorbate, cyanide or possibly catalase (31). If [ $^{14}\text{C}$ ]feruloyl-CoA does indeed bind to cell walls *in vitro* via the formation of ester bonds, it will be of great interest to see whether the  $^{14}\text{C}$  can be recovered by Driselase digestion in the form of [ $^{14}\text{C}$ ]Fer-Ara-Xyl and [ $^{14}\text{C}$ ]Fer-Ara-Xyl<sub>2</sub> indicating that the highly specific feruloyl-sugar bond characteristic of grass cell walls had been synthesized by an extracellular enzyme system. Biosynthesis of ester bonds in the cell wall has a precedent in the proposed biosynthesis of cutin from fatty acyl-CoA thioesters in the epidermal cell wall (for a review, see 39). It is possible that Yamamoto *et al.* (37) have detected the biosynthetic system by which feruloyl residues are attached to the aliphatic core of cutin rather than to the wall polysaccharides. The current evidence seems to favor *intracellular* feruloylation of polysaccharides.

### Evidence for Specificity in the Oxidative Coupling of Phenolic Side-Chains in the Cell Wall

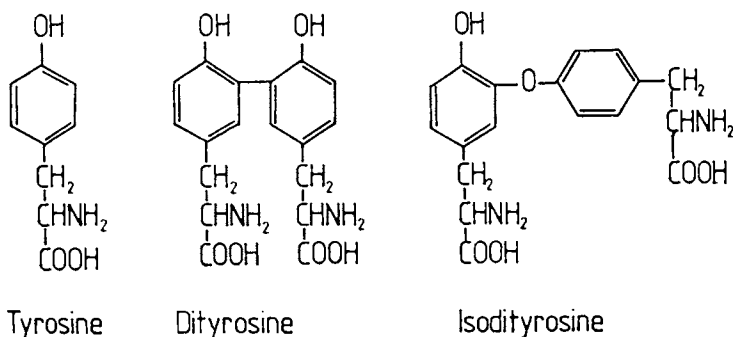
The previous section has presented evidence that phenolic units are carefully positioned within the wall polymers. When these units undergo oxidative phenolic coupling reactions in the cell wall, the coupling reactions themselves are also remarkably specific. This can be illustrated by reference to the tyrosine residues of extensin.

*Orientation of Coupling in Protein-Bound Tyrosine Residues.* Tyrosine can couple to form either of two isomeric dimers, dityrosine and isodityrosine (1,16) (Fig. 4). The choice between these two dimers is governed by the conditions under which the coupling is carried out; some examples are given in Table I.

In animal structural proteins *in vivo*, the only known dimer of tyrosine is dityrosine (40,41); in the extensin of plant cell walls, in contrast, the only dimer formed *in vivo* is isodityrosine (16). How is the coupling of tyrosine in plants confined to the formation of isodityrosine? There is nothing unique about the local environment of the tyrosine residues in (pure) extensin, since

Table I. Dimeric Products of the Oxidative Coupling of Protein-Bound Tyrosine Residues under Various Conditions

Substrate	System	pH	Products	Reference
Resilin <i>in vivo</i>	insect cuticle	> 7	DiT	(40)
Collagen <i>in vivo</i>	nematode cyst	> 7	DiT	(41)
Extensin <i>in vivo</i>	Dicot primary cell wall	< 7	Idt	(16)
Extensin <i>in vitro</i>	peroxidase + H <sub>2</sub> O <sub>2</sub>	9	DiT	(38)
Bovine serum albumin <i>in vitro</i>	peroxidase + H <sub>2</sub> O <sub>2</sub>	9	DiT	(42)
Extensin <i>in vitro</i>	isolated cell wall	6	Idt	(38)

Figure 4. Structures of tyrosine, dityrosine and isodityrosine. [Reproduced with permission from *Journal of Experimental Botany* 38, 853-62; © Oxford University Press, 1987.

these residues are quite capable of forming dityrosine (38) under the same optimal *in vitro* conditions as work for virtually any other protein (e.g., bovine serum albumin) (42). The only *in vitro* system in which isodityrosine production predominates is in extensin treated with isolated plant cell walls (38) at pH 6.

Two factors associated with the plant cell wall were considered which might direct exclusive isodityrosine formation:

- a. *The pH of the plant cell wall.* This pH is always likely to be below 7.0 *in vivo*, and therefore well below the optimum (pH *ca.* 9.0) for total dimerization of tyrosine; pH 9.0 was used in most *in vitro* assays other than those where cell walls were the source of peroxidase.
- b. *Specific isoperoxidases.* The cell wall contains a number of peroxidase isozymes, quite distinct from the major basic isozyme obtained from horseradish and used in most *in vitro* assays; it is possible that some of these other isozymes have a propensity to catalyze isodityrosine formation.

*Evidence Against Cell Wall pH and Isoperoxidase Specificity as Determinants of Isodityrosine Formation.* To test these possible explanations for the exclusive formation of isodityrosine in the plant cell wall, samples of [ $^{14}\text{C}$ ]tyrosine were oxidized by  $\text{H}_2\text{O}_2$  in the presence of three sharply contrasting horseradish-isoperoxidases [two low-pI (acidic) and one high-pI (basic)] at a wide range of pH values (37).

The two low-pI isozymes were considerably poorer than the high-pI isozyme at catalyzing total tyrosine-oxidation [the comparison was based on the use of a constant  $1.2 \mu\text{kat/ml}$  of each isozyme,  $1 \mu\text{kat}$  being the amount that will catalyze the oxidation of pyrogallol to purpurogallin at  $1 \mu\text{mol/s}$  at pH 6.0 and  $25^\circ\text{C}$ ]. The lower-pI isozyme oxidized tyrosine optimally at pH 6, and the high-pI isozyme had an optimum of pH 9. The rate of oxidation by the high-pI isozyme at pH 9 was about seven times greater than that of the lower-pI isozyme at pH 6. This confirms that the isozymes exhibited considerable differences in catalytic properties, as well as differing in pI.

When the dimers produced by these isozymes, at a wide range of pH values, were analyzed individually, no great difference was found (37). At high pH values (pH 8-10), both the low-pI and high-pI isozymes generated *ca.* 20 times more dityrosine than isodityrosine. As the pH was lowered, the yield of isodityrosine increased and that of dityrosine decreased until at pH 3 there was only about 2-3 times more dityrosine than isodityrosine; however, under no conditions did the yield of isodityrosine ever exceed that of dityrosine.

It may be concluded that neither pH nor isozyme-specificity is likely to direct the exclusive formation of isodityrosine in the plant cell wall *in vivo*. Indeed, it might be argued that isozyme-specificity is intrinsically unlikely to direct the orientation of coupling (dityrosine *vs.* isodityrosine) since the role of the enzyme is thought to be merely the production of tyrosine free radicals (44) which then *non-enzymically* pair off.

*Role of Neighboring Polysaccharide Molecules in Determining the Orientation of Tyrosine Residues During Coupling.* These considerations suggest a third possible explanation for the exclusive formation of isodityrosine in the plant cell wall *in vivo*: that the neighboring structural molecules of the wall constrain extensin to prevent dityrosine formation. This would mean that the biologically relevant substrate for peroxidase in the plant cell wall is not naked extensin but extensin complexed with another wall component, possibly an acidic polysaccharide to which the extensin would bind ionically.

## Conclusions

In conclusion, it seems fair to say that specificity exists in both the biosynthesis and in the oxidative coupling of polymer-bound phenols in the growing cell wall. (a) Tyrosine residues are placed at specific sites along the extensin molecule by genetically-encoded information. (b) Tyrosine cross-linking *in vivo* is a very specific, carefully steered process in that it occurs



only when the extensin is in a precise molecular environment, possibly as an ionic complex with an acidic polysaccharide. This is evidenced by the fact that cell walls couple their tyrosine residues to make isodityrosine rather than dityrosine, whereas the same residues in the absence of a cell wall generate mainly dityrosine. (c) The feruloylation and *p*-coumaroylation of acidic polysaccharides occurs on highly specific hydroxy groups. (d) It remains to be seen how precise or random the coupling of polysaccharide-bound phenolic side-chains is.

The significance of this precision is that it suggests that adequate specificity exists for the coupling reactions to take part *efficiently* in the "strapping" of hemicellulose molecules to microfibrils mentioned earlier. It will be of great interest in future research to explore whether and to what extent such "strapping" occurs.

### Acknowledgments

We are grateful to the Agricultural and Food Research Council for the award of a research grant in support of our work.

### Literature Cited

1. Fry, S. C. *Ann. Rev. Plant Physiol.* 1986, **37**, 165-86.
2. Fry, S. C. *The Growing Plant Cell Wall: Chemical and Metabolic Analysis*; Longman: London; and Wiley: New York, 1988.
3. Keegstra, K.; Talmadge, K. W.; Bauer, W. D.; Albersheim, P. *Plant Physiol.* 1973, **51**, 188-96.
4. Darvill, A. G.; McNeil, M.; Albersheim, P.; Delmer, D. P. In *The Biochemistry of Plants: A Comprehensive Treatise*; Vol. 1; Preiss, J., Ed.; Academic Press: New York, 1980; pp. 91-162.
5. Lamport, D. T. A. In *Cellulose: Structure, Modification and Hydrolysis*; Young, R. A.; Rowell, R. M., Eds.; Wiley: New York, 1986; pp. 77-90.
6. Stafstrom, J. P.; Staehelin, L. A. *Planta* 1988, **174**, 321-32.
7. Rubin, G. C. This volume.
8. Fry, S. C. *J. Exp. Bot.* 1989, **40**, 1-11.
9. O'Neill, R. A.; Selvendran, R. R. *Carbohydr. Res.* 1983, **111**, 239-55.
10. Hayashi, T.; Marsden, M. P. F.; Delmer, D. P. *Plant Physiol.* 1987, **83**, 384-9.
11. MacKay, A. L.; Wallace, J. C.; Sasaki, K.; Taylor, I. E. P. *Biochemistry* 1988, **27**, 1467-73.
12. MacKay, A. L.; Wallace, J. C.; Sasaki, K.; Taylor, I. E. P. This volume.
13. Fry, S. C. *Mod. Meth. Plant Analysis*, New Series, **10**, in press.
14. Heckman, J. W.; Terhune, B. T.; Lamport, D. T. A. *Plant Physiol.* 1988, **86**, 848-56.
15. Stafstrom, J. P.; Staehelin, L. A. *Plant Physiol.* 1986, **81**, 234-41.
16. Fry, S. C. *Biochem. J.* 1982, **204**, 449-55.
17. Fry, S. C. *Biochem. J.* 1982, **203**, 493-504.
18. Fry, S. C. *Planta* 1983, **157**, 111-23.

19. Kato, Y.; Nevins, D. J. *Carbohydr. Res.* 1985, **137**, 139-50.
20. Ahluwalia, B.; Fry, S. C. *J. Cer. Sci.* 1986, **4**, 287-95.
21. Smith, M. M.; Hartley, R. D. *Carbohydr. Res.* 1983, **118**, 65-80.
22. Gubler, F.; Ashford, A. E.; Bacic, A.; Blakeney, A. B.; Stone, B. A. *Aust. J. Plant Physiol.* 1985, **12**, 307-17.
23. Sachs, J. *Handbuch der Experimentalphysiologie der Pflanzen*; Engelmann: Leipzig, 1865.
24. Hanke, D. E.; Northcote, D. H. *J. Cell Sci.* 1974, **14**, 29-50.
25. Fry, S. C. *Physiol. Plant.* 1989, **75**, in press.
26. Smith, J. J.; Muldoon, E. P.; Lamport, D. T. A. *Phytochemistry* 1984, **23**, 1233-40.
27. McNeil, M.; Darvill, A. G.; Fry, S. C.; Albersheim, P. *Ann. Rev. Biochem.* 1984, **53**, 625-63.
28. Hayashi, T.; Wong, Y.; MacLachlan, G. *Plant Physiol.* 1984, **75**, 605-10.
29. Shinkle, J. R.; Jones, R. L. *Plant Physiol.* 1988, **86**, 960-6.
30. Fry, S. C. *Phytochemistry* 1984, **23**, 59-64.
31. Fry, S. C.; Miller, J. G. *Food Hydrocolloids* 1987, **1**, 395-7.
32. Biggs, K. J.; Fry, S. C. In *Physiology of Cell Expansion During Plant Growth*; Cosgrove, D. J.; Knievel, D. P., Eds.; Am. Soc. Plant Physiol.; 1987; pp. 46-57.
33. Chen, J.; Varner, J. E. *EMBO J.* 1985, **4**, 2145-51.
34. Fry, S. C. *Planta* 1987, **171**, 205-11.
35. Fry, S. C.; Northcote, D. H. *Plant Physiol.* 1983, **73**, 1055-61.
36. Yamamoto, E.; Towers, G. H. N. *J. Plant Physiol.* 1985, **117**, 441-9.
37. Yamamoto, E.; Bokelman, G. H.; Lewis, N. G., this volume.
38. Cooper, J. B.; Varner, J. E. *Plant Physiol.* 1984, **76**, 414-7.
39. Holloway, P. J. In *The Plant Cuticle*; Cutler, D. F.; Alvin, K. L.; Price, C. E., Eds.; Academic: London, 1982; pp. 45-85.
40. Andersen, S. O. *Biochim. Biophys. Acta* 1964, **93**, 213-5.
41. Lopez-Llorca, L. V.; Fry, S. C. *Nematologica* 1989, in press.
42. Aeschbach, R.; Amadò, R.; Neukom, H. *Biochim. Biophys. Acta* 1976, **439**, 292-301.
43. Fry, S. C. *J. Exp. Bot.* 1987, **38**, 853-62.
44. Ralston, I. M.; Dunford, H. B. *Can. J. Chem.* 1980, **58**, 1270-6.

RECEIVED May 19, 1989

## Chapter 4

# Deposition of Cell Wall Components in Conifer Tracheids

Keiji Takabe<sup>1</sup>, Kazumi Fukazawa<sup>1</sup>, and Hiroshi Harada<sup>2</sup>

<sup>1</sup>Faculty of Agriculture, Hokkaido University, Kita 9, Nishi 9, Kita-ku, Sapporo, Japan

<sup>2</sup>Rector Office, Kasetsart University, Bangkok, Bangkok, 10900, Thailand

The cell wall deposition processes, distribution of cell wall components, and cell organelles involved in the biosynthesis of polysaccharides and lignin in conifer tracheids were investigated using several chemical and microscopy techniques. The deposition process for cellulose was found to differ from that of hemicelluloses. Cellulose deposited actively between the S<sub>1</sub> and S<sub>3</sub> developmental stages, especially in the middle part of the S<sub>2</sub> stage. On the other hand, mannans and xylans were laid down between the latter part of S<sub>1</sub> and the early part of S<sub>2</sub> development, and between the latter part of the S<sub>2</sub> and S<sub>3</sub> stages. These results suggest that (i) the middle portion of S<sub>2</sub> is rich in cellulose, and (ii) hemicelluloses are abundant in S<sub>1</sub>, and the outer and inner portions of S<sub>2</sub> and S<sub>3</sub> tissue. Lignification was initiated at the outer surface of the primary wall cell corners, and proceeded into the intercellular layers, and the intercellular substances between cell corners. Lignification of the secondary walls was initiated at the S<sub>1</sub> cell corner, then proceeded to the unligified S<sub>1</sub> layer and toward the lumen, while lagging behind cell wall thickening. Cellulose synthesis occurred at the plasma membrane. The Golgi-body, and a small circular vesicle derived from the rough endoplasmic reticulum, were involved in the biosynthesis and/or transport of hemicelluloses, while the Golgi-body and smooth-endoplasmic reticulum were involved in the biosynthesis and/or transport of monolignols.

0097-6156/89/0399-0047\$06.00/0

© 1989 American Chemical Society

American Chemical Society

Library

1155 16th St., N.W.

In Plant Cell Wall Polymers: Lewis, N., et al.;

Washington, D.C., 20036

ACS Symposium Series; American Chemical Society: Washington, DC, 1989.

Cellulose, hemicelluloses, and lignin are the main components of cell walls in woody plants. For a long time, these plant polymers have stimulated the interest of many plant botanists and biochemists in terms of their biosynthetic pathways, functional interrelationships, and anatomical distribution.

The cell wall of conifer tracheids consists of both primary and secondary walls. The primary wall is formed during cell division and subsequent cell enlargement, whereas secondary wall formation only occurs after cell enlargement has been completed. Secondary walls are subdivided into three layers, named  $S_1$ ,  $S_2$ , and  $S_3$ , respectively. A large effort has been devoted to elucidating (i) structural and chemical properties of the polysaccharides and lignin in each cell wall layer and their functional interrelationships, and (ii) the role of cell organellae in cell wall biosynthesis. In spite of this, our knowledge of the entire process of cell wall construction and the interrelationships of cell wall components still remains incomplete.

### Deposition of Polysaccharides

Pioneering work on polysaccharide distribution in the cell wall was carried out by Meier and Wilkie (1) and Meier (2). They isolated radial sections from the differentiating xylem of *Pinus sylvestris*, *Picea abies*, and *Betula verrucosa*, separated each into subcellular fractions by a micromanipulator, and analyzed the monosaccharide composition of the different polysaccharide fractions by paper chromatography. From these studies it was concluded that, in softwood tracheids, the outer part of the  $S_2$  layer was richest in cellulose, whereas the  $S_3$  layer was richest in glucuronoarabinoxylan and the glucomannan content gradually increased towards the lumen. On the other hand, in hardwood fibers, the inner part of  $S_2$  and  $S_3$  were richest in cellulose, while  $S_1$  and the outer part of  $S_2$  showed a high glucuronoxylan content. Côté *et al.* (3) also investigated the polysaccharide distribution in *Abies balsamea* tracheids according to the method of Meier and obtained similar conclusions.

Larson (4,5) fed  $^{14}\text{CO}_2$  photosynthetically to *Pinus resinosa*, divided the differentiating xylem into several fractions, and counted the radioactivity of each cell wall component. From these studies, it was concluded that as tracheid maturation occurred, xylose deposition increased, whereas mannose remained relatively constant, and both arabinose and galactose decreased considerably.

In recent years, Hardell and Westermark (6) scratched *Picea abies* tracheids with tweezers, collected individual cell wall layers, and then analyzed the average monosaccharide composition. Surprisingly, among the individual cell wall layers no significant difference in the mannose:xylose:glucose ratio among individual cell wall layers was observed.

We have also studied polysaccharide deposition processes during cell wall formation (7), by gas-liquid chromatographic analysis of fractions sep-

arated by microfractionation and enriched in cells at different developmental stages. In that investigation, the differentiating system of *Cryptomeria japonica* was separated into twelve fractions and each had its neutral monosaccharide content and type determined (Figs. 1 and 2). (Note that glucose, mannose, and xylose are mainly derived from cellulose, mannans, and xylans, respectively.) Thus, it was concluded that cellulose was mainly deposited in the middle part of the S<sub>2</sub> layer, whereas hemicelluloses (mannans, xylan) were found mainly in the S<sub>1</sub> and the outer part of the S<sub>2</sub> and S<sub>3</sub> layers (Fig. 3). These results were further confirmed from our transmission electron microscopy (TEM) studies on differentiating xylem stained with PATAg. This technique, developed by Thiéry (8), is specific for hemicelluloses and showed heavy staining of the S<sub>1</sub>, outer S<sub>2</sub> and S<sub>3</sub> layers. Interestingly, the warty layer was also heavily stained by PATAg, indicating it to be mainly composed of hemicelluloses.

We next investigated the incorporation of U-<sup>14</sup>C glucose into the cell wall polymers during cell wall formation (9). After incorporation of the labelled sugar, the differentiating xylem of *Cryptomeria japonica* was separated into 8 fractions, each of which was subjected to mild acid hydrolysis. The monosaccharides, so released from the polysaccharides, were then separated by thin-layer chromatography (tlc) and the individual radioactivity content for each sugar was visualized by autoradiography and measured by scintillation counting. As can be seen from Figure 4, the distribution of radioactivity into the individual sugars was in good agreement with our previous analyses of the polymers, i.e., cellulose deposition mainly occurred in the middle part of the S<sub>2</sub> to S<sub>3</sub> developmental stage, whereas xylan deposition was in the S<sub>1</sub> to early S<sub>2</sub> and again in the S<sub>3</sub> developmental layers. Mannan deposition occurred mainly during secondary wall formation rather than during formation of the primary wall.

### Lignification of Tracheids

The first study on lignification of conifer tracheids was carried out by Wardrop (10). From examination of the differentiating xylem of *Pinus radiata* under an ultraviolet microscope, he observed that lignification was initiated at the cell corners of the primary wall, then extended to the middle lamella and secondary wall. Imagawa *et al.* (11) subsequently took UV-photomicrographs of the differentiating xylem of *Larix leptolepis* and demonstrated that lignification proceeded as follows: lignin accumulation begins in the intercellular layer at the cell corners and pit borders, then extends to both radial and tangential middle lamella, and then towards the lumen. Fujita *et al.* (12) investigated lignification of *Cryptomeria japonica* compression wood by the same method. These authors found that there are two types of lignin deposition processes: One was primary wall lignification which occurred from the early phase of S<sub>1</sub> deposition to the early phase of

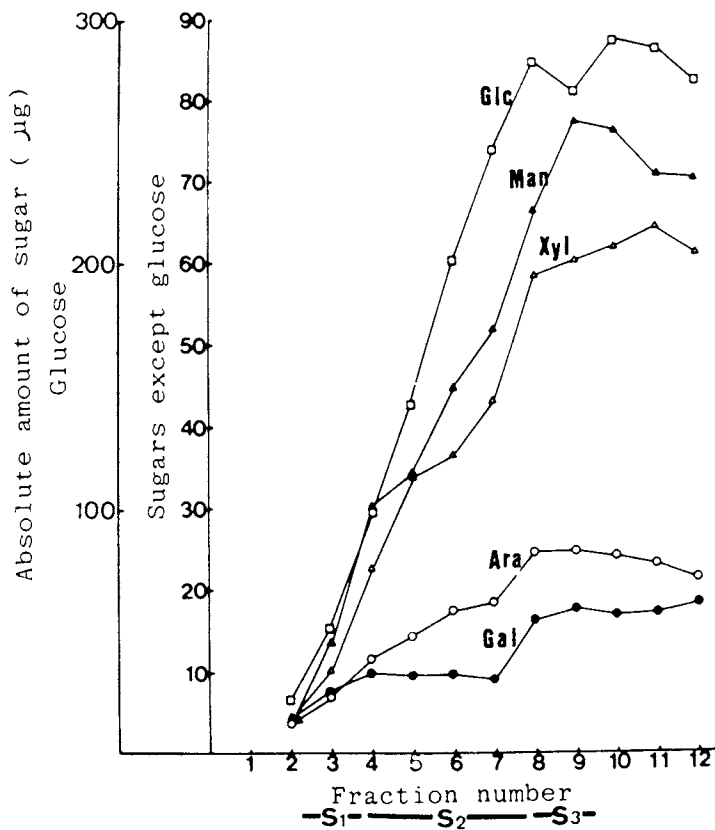


Figure 1. Changes in the absolute amount of sugars with tracheid maturation. The various components are designated as follows: glucose, □ ; mannose, ▲; xylose, △; arabinose, ○; and galactose, ●.

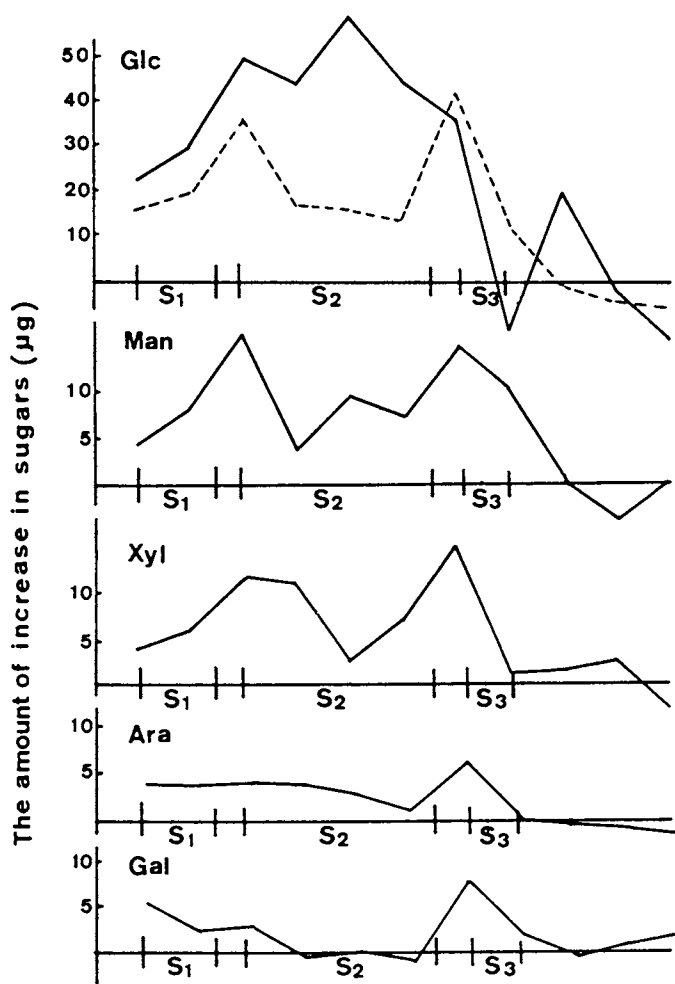


Figure 2. The amount of increase in sugars (the difference of the absolute amounts of sugar between the neighboring fractions). The dashed line shows the sum of arabinose, galactose, xylose, and mannose.

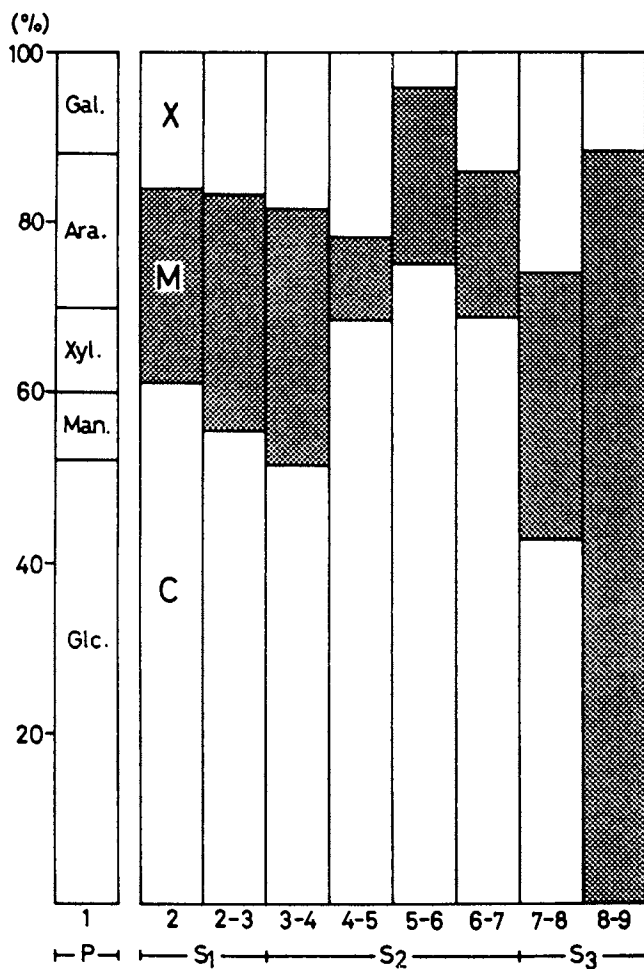


Figure 3. Distribution of polysaccharides through the cell wall. C, cellulose; M, galacto-glucomannan; X, arabino-4-O-methylglucuronoxylan.



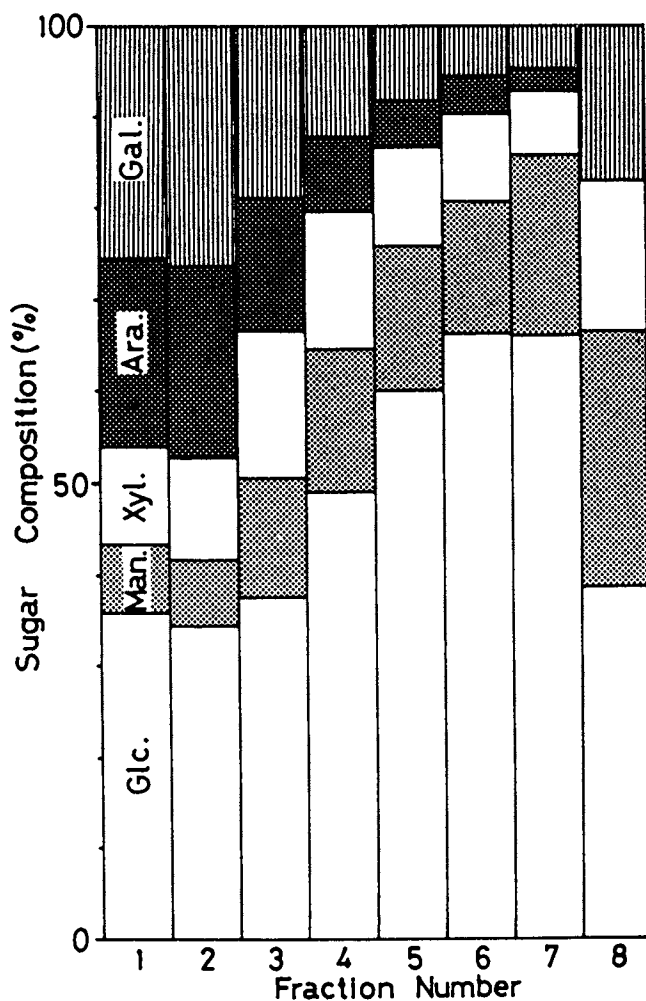


Figure 4. The composition of radioactivity in neutral sugars. Arabic numerals are the fraction numbers. The differentiating stages in each fraction are as follows: Fractions 1-2, primary wall stage; 3,  $S_1$  stage; 4-6,  $S_2$  stage; 7-8,  $S_3$  stage.

S<sub>2</sub> thickening; the other was secondary wall lignification which proceeded after S<sub>2</sub> thickening.

Although UV-microscopy has provided much information on the lignification process and lignin distribution through the cell wall, it has been of limited value because of its low resolving power as compared to electron microscopy. Consequently, some workers, using specimens fixed with potassium permanganate, studied lignification using TEM. In this way, Wardrop (13,14) found that with *Eucalyptus elaeophora*, lignin formation was initiated at the middle lamella of the cell corners, and subsequently at the outer part of the S<sub>1</sub> layer. It then proceeded along the middle lamella, through the primary wall, and ultimately to the secondary wall. Kutscha and Schwarzmann (15) also examined the lignification of *Abies balsamea* tracheids by TEM and showed that it was initiated in the middle lamella between pit borders of adjacent tracheids, and then extended into the pit borders and cell corners. In cell corners, it occurred at either the outer portion of the primary wall or the middle lamella. After that, lignification took place in the cell corner region of the S<sub>1</sub> layer, leaving the primary wall unligified, and then proceeded subsequently toward the lumen. This technique, using permanganate fixation, can, however, cause swelling of both the cell and the cell wall, and the extraction of many cell components. Indeed, Kishi *et al.* (16) reported that the staining intensity produced by permanganate does not reflect true lignin content, thus leaving the aforesaid results in some doubt.

Saka and Thomas (17) also investigated the lignification of *Pinus taeda* tracheids by the SEM-EDXA technique, and showed that it was initiated in the cell corner middle lamella and compound middle lamella regions during S<sub>1</sub> formation. Subsequently, rapid lignin deposition occurred in both regions. Secondary wall lignification was initiated when the middle lamella lignin concentration approached 50% of its maximum, and then proceeded towards the lumen.

We (18-20) have also investigated the lignification process using *Cryptomeria japonica* tracheids. Techniques employed were administration of tritiated phenylalanine as a lignin precursor, followed by a combination of UV-microscopy, light microscopic autoradiography, and TEM coupled with appropriate chemical treatments of ultra-thin sections. Figure 5 shows densitometer traces of UV-photonegatives of differentiating xylem. The UV-absorption of the compound middle lamella was first detected in the tracheid at the S<sub>1</sub> developmental stage, then increased during secondary wall thickening, becoming constant after the S<sub>3</sub> stage. On the other hand, UV-absorption at the secondary wall was first observed at the outer portion in the tracheid of the S<sub>2</sub> stage, then spread slowly towards the lumen in subsequent stages. The tracheid in the final part of cell wall formation showed uniform absorption through the secondary wall. From Figure 6,

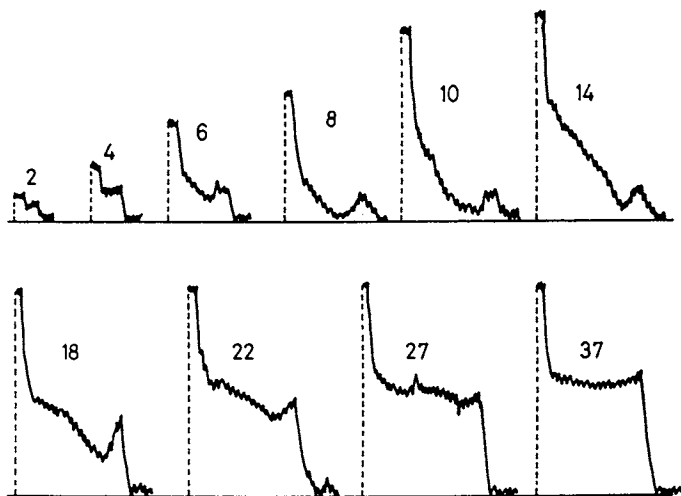


Figure 5. Densitometer traces of UV-photonegatives. Arabic numerals indicate the cell number which starts from the cell just before  $S_1$  formation.

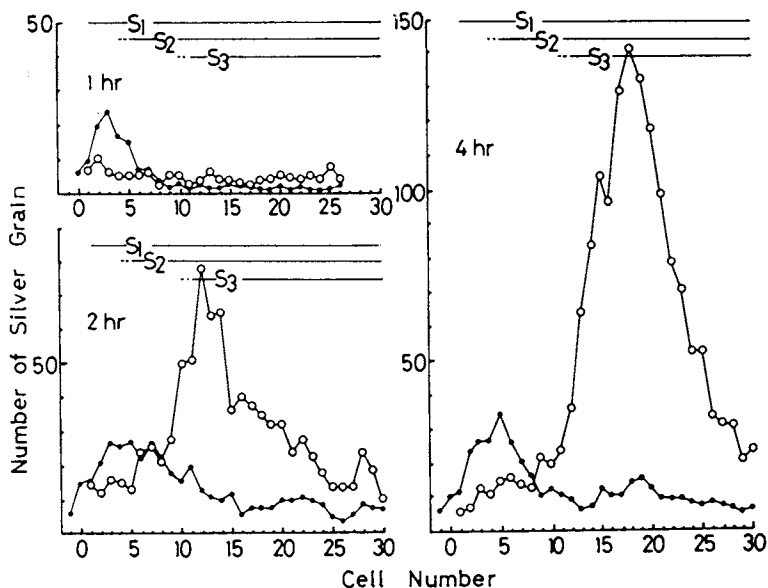


Figure 6. Incorporation of tritiated phenylalanine into the compound middle lamella lignin and the secondary wall lignin determined by counting the silver grains. Symbols are as follows: ●, compound middle lamella; ○, secondary wall.

it is evident that the labelled lignin precursor was rapidly incorporated into the compound middle lamella lignin, whereas it entered slowly into secondary wall lignin. Additionally, incorporation into compound middle lamella lignin took place during  $S_1$  and  $S_2$  developmental stages, while incorporation into secondary wall lignin occurred mainly after the  $S_3$  stage. In the latter case, radioactivity was distributed throughout the secondary wall. This indicated that monolignols were continuously supplied to all areas of the secondary wall. Thus, the lignin content in the secondary wall gradually increased by repeated linking of monolignol radicals.

These findings were also supported by analysis of the lignin skeleton of the differentiating xylem, obtained by treatment of ultra-thin sections with hydrofluoric acid after resin extraction (20). This removes polysaccharides effectively without any swelling of the cell wall. In this way, we found that lignification in the *Cryptomeria japonica* tracheid was initiated at the outer surface of the primary wall in the cell corners, just before  $S_1$  formation. Subsequently, it proceeded to the intercellular layer together with lignin deposition in the intercellular substances between the cell corners. When the tracheid was adjacent to a ray parenchyma, the cell corner region on the ray parenchyma side was lignified earlier than that on the opposite one. It was very interesting that secondary wall lignification was also initiated at the  $S_1$  cell corner region during the  $S_1$  developmental stage. It then proceeded to the unlignified  $S_1$  layer. When the tracheid was adjacent to a ray parenchyma, lignification of the  $S_1$  layer was also earlier on the ray side. After that, lignification gradually spread towards the lumen, lagging behind cell wall thickening. Lignin deposition then predominated after the  $S_3$  stage, while less active during the  $S_1$ ,  $S_2$ , and  $S_3$  developmental stages. The lignin content of the secondary wall became fairly constant in the final stage of cell wall formation, though the warty layer was more highly lignified.

### Changes in Cell Organelles During Cell Wall Formation

The cell organelles in woody plants are the nucleus, mitochondrion, rough-endoplasmic reticulum (r-ER), smooth endoplasmic reticulum (s-ER), Golgi-body, plastid, vacuole, microbody, etc. Their functions are very complicated, and some have definite roles in the biosynthesis of cell-wall components. Hence, changes in size of cell organelles are likely to occur, since cell-wall composition depends upon the stage of wall development.

We tried to estimate the size of the cell organelles in the cytoplasm, excluding the vacuolar compartment. To do this, we took at random a few hundred electron micrographs of cells in the differentiating xylem and measured the area of each cell organelle in the cytoplasm by a digitizer coupled to a microcomputer. We found not only changes in the area of cell organelles in the cytoplasm, but also in their structure during cell

wall formation. Figure 7 shows the results of semi-quantitative analysis of the areas for each cell organellae during cell wall formation. It was surprising that the Golgi-body, r-ER, and s-ER, showed appreciable changes in area during cell wall formation. The area of the Golgi-body was largest at the S<sub>1</sub> stage, and then gradually decreased in size with maturation of the tracheid, whereas the r-ER was largest in the primary wall stage, and then gradually decreased with cell wall formation. The s-ER, on the other hand, was a minor organelle from the primary wall stage to the early part of the S<sub>2</sub> stage, and then showed a gradual increase in area toward the S<sub>3</sub> developmental stage. The most striking fact was that the enlargement of the s-ER coincided with that of active lignification of the secondary wall.

Figure 8 shows the changes in the structure of cell organellae. The photographs are typical structures in each differentiating stage. Note that the Golgi-body consists of thin central cisternae and relatively small vesicles during the primary wall stage. The central cisternae then become thick, this being accompanied by the formation of many large vesicles containing fibrillar material during the S<sub>1</sub> and S<sub>2</sub> developmental stages. After that, the central cisternae became small in size, though the thickness was similar to that of previous stages. Interestingly, this stage appears to be accompanied by the formation of only a few vesicles, indicating depression of Golgi activity.

Several reticula of the r-ER show an ordered arrangement and many ribosomes are attached to their membrane during the primary wall development stage. As maturation proceeds, the r-ER's then gradually decrease not only in number and length of reticula, but also in the number of ribosomes. The s-ER's, on the other hand, become largest after the S<sub>3</sub> stage, and sometimes attach ribosomes at their terminals.

During primary wall formation the plastids contain starch and other materials which stain heavily with uranyl acetate and lead citrate. When the tracheid starts to form the S<sub>1</sub> layer, the plastid becomes surrounded by an endoplasmic reticulum. While the fate of these compounds is unknown, it can be envisaged that they are used for generation of energy and/or a source of cell wall materials.

### Cell Organellae Involved in Biosynthesis of Polysaccharides

Though cellulose is one of the most important biopolymers, it has not yet been possible to completely elucidate its biosynthetic pathway, or establish exactly the cell organellae involved in its synthesis. However, during the last decade, the freeze fracture technique has been applied to investigate cell wall formation, and this has produced much information on the site where cellulose synthesis occurs. It is now generally accepted that both terminal and rosette complexes are responsible for cellulose synthesis (21). Our results (19,22) support that view. In a TEM-autoradiographic investiga-

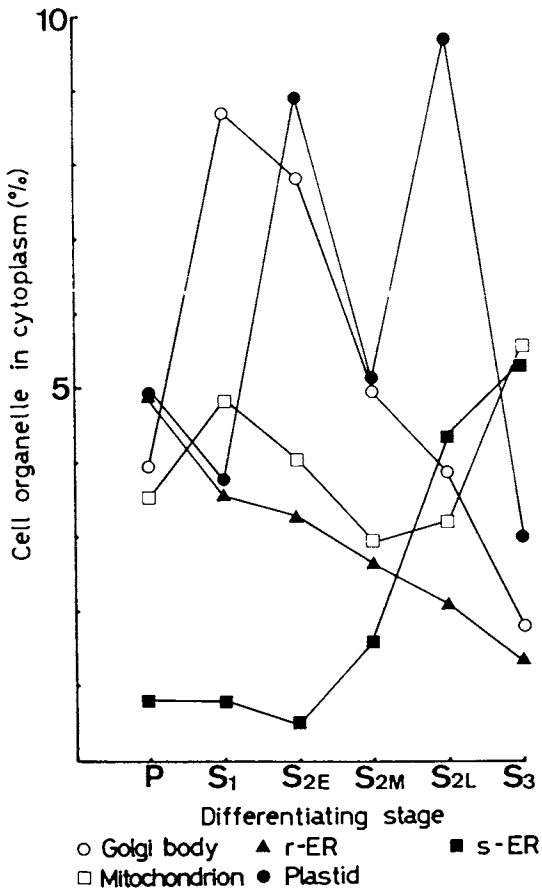


Figure 7. Semi-quantitative measurements of cell organelles in the cytoplasm.

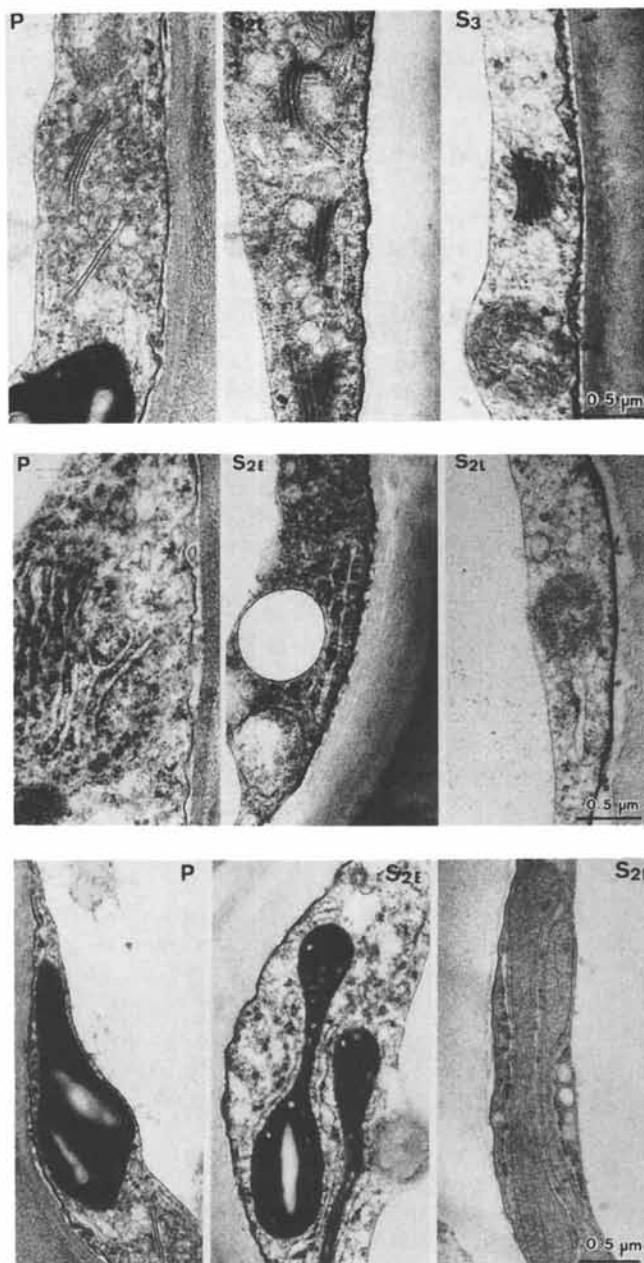


Figure 8. Changes in the structure of cell organelles during cell wall formation. Upper, middle, and lower photographs are Golgi-body, r-ER, and plastid, respectively. Abbreviations are as follows: P, primary wall stage;  $S_{2E}$ , early part of  $S_2$  stage;  $S_{2L}$ , later part of  $S_2$  stage.

tion of differentiating xylem, previously administered tritiated glucose, the radioactivity was concentrated at the boundary between the newly formed cell-wall and the cytoplasm in the middle and latter parts of the S<sub>2</sub> stage. A comparison with Figure 4 indicates that a major component of the labelled materials in these areas was in the cellulose polymer, and hence glucose derived. From a cytochemical investigation, fibrillar materials having a width of 6-7 nm were sometimes observed, these being generated from the plasma membrane (Fig. 9). They had similar dimensions to cellulose microfibrils from gelatinous layers of *Populus euramericana* as shown by Sugiyama *et al.* (23), thereby indicating the involvement of the plasma membrane in cellulose synthesis.

The biosynthesis of cell wall polysaccharides has also been studied by cytochemical staining methods. PATAg staining (8) resulted in establishing cell organelles involved in the biosynthesis of many polysaccharides. Pickett-Heaps (24) adapted this staining procedure to the root tips and coleoptiles of *Triticum vulgare* seedlings. In this way, he showed that Golgi-cisternae and their vesicles were stained positively, whereas ER cisternae stained negatively. This led to the conclusion that Golgi-bodies were involved in the biosynthesis and/or transport of polysaccharides. These results were confirmed again in later studies by Fowke and Pickett-Heaps (25) and Ryser (26). In recent years, Sugiyama *et al.* (27) observed the *Valonia macrophysa* cell-wall by means of selective visualization and chemical analysis of cell-wall components. The authors found that the materials stained positively with PATAg, or a combination of uranyl acetate and lead citrate, were non-cellulosic polysaccharides.

We have also applied the PATAg staining to the differentiating xylem of *Cryptomeria japonica* (22). While the contents in the Golgi-vesicles stained positively at all stages of cell wall formation, there were three main observations. During primary wall formation, the Golgi-vesicles were small and their contents only stained weakly. After that, the vesicles became larger and the components which showed fibrillar structures were strongly stained. Following the S<sub>3</sub> stage, the contents again stained weakly, and had a slimy appearance. This presumably (i) reflects changes in non-cellulosic polysaccharide composition and (ii) suggests that the Golgi-bodies are involved in the biosynthesis of non-cellulosic polysaccharides.

Figure 10 shows small circular vesicles which were distributed at the end of the r-ER cisternae and between the cisternae, and which were sometimes attached to the ER membrane. As the size and the shape of these vesicles (75 nm in mean diameter) were different from those of Golgi-vesicles (130 nm in mean diameter), the small circular vesicles were presumably derived from r-ER; they also stained positively with PATAg. These facts suggest that the small circular vesicles from the ER are involved in the biosynthesis and/or transport of non-cellulosic polysaccharides.



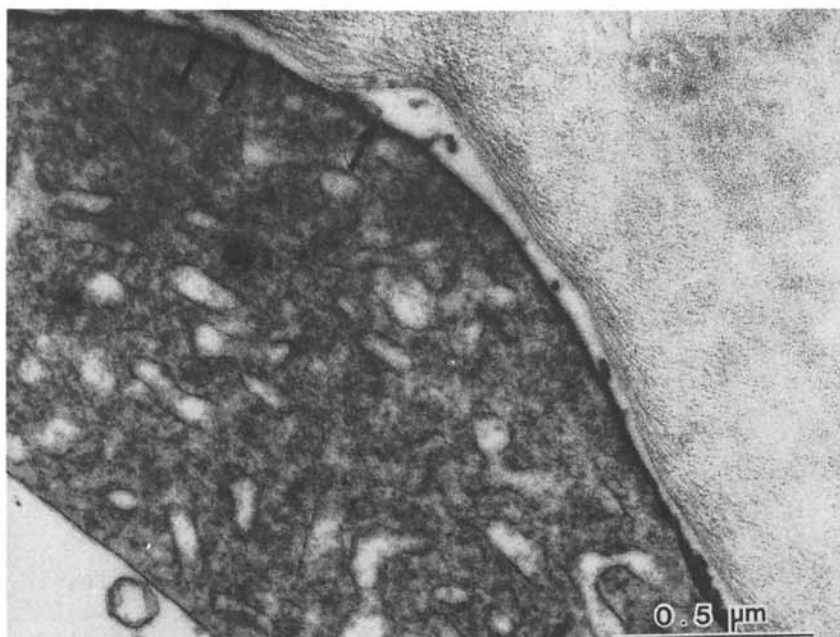


Figure 9. A tracheid in the S<sub>3</sub> stage. Fibrillar materials (arrows) are generated from the plasma membrane. (Reproduced with permission from Ref. 22. © 1986, Japan Wood Research Society.)

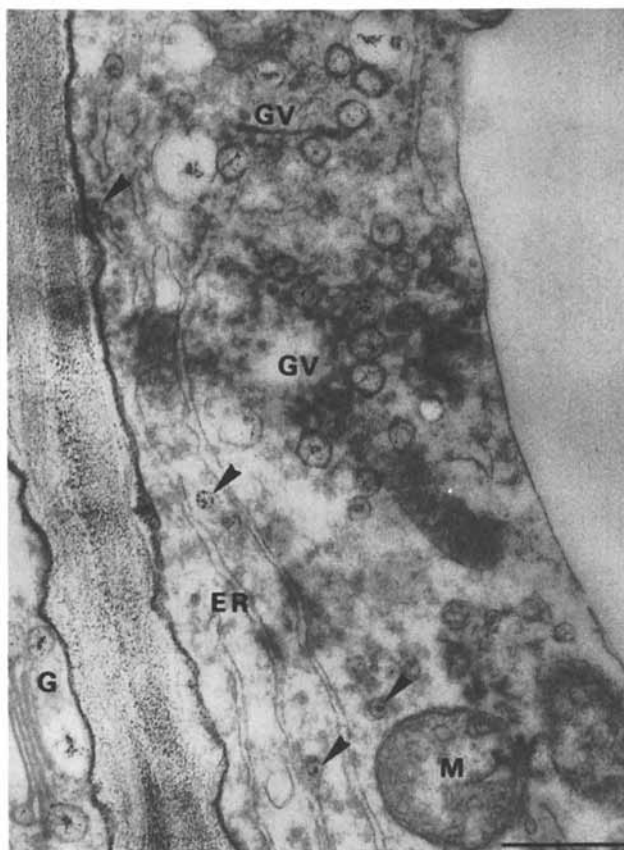


Figure 10. A differentiating tracheid stained with PATAg. Small circular vesicles (arrowheads), distributed near the ER are stained positively. The Golgi-vesicles are also stained positively. Abbreviations are as follows: GV, Golgi-vesicle; ER, endoplasmic reticulum. Scale bar is 500nm. (Reproduced with permission from Ref. 22. © 1986, Japan Wood Research Society.)

### Cell Organellae Involved in the Biosynthesis of Lignin

Only a few workers have attempted to identify the cell organellae involved in the biosynthesis of lignin. Pickett-Heaps (28) observed lignification in the xylem wall of wheat coleoptiles and suggested the involvement of both the Golgi-bodies and r-ER, since radioactivity was distributed on both organellae. More recently, Fujita *et al.* (29) studied lignification in compression wood cell walls of *Cryptomeria japonica* by TEM-autoradiography. Like Pickett-Heaps, they concluded that the Golgi-bodies participated in lignin biosynthesis.

Wardrop (13, 14) examined sclerenchyma fibers of *Liriodendron tulipifera* and sclereids of *Pyrus communis*, previously fixed with  $\text{KMnO}_4$ , and concluded that the vesicles supplied their contents to the cell wall, though the origin of the vesicles was not established. As discussed before, however, permanganate fixation is undesirable for these cytological observations.

Consequently, we administered tritiated phenylalanine, a lignin precursor, to the differentiating xylem of *Cryptomeria japonica*, and determined the location of the label by TEM-autoradiography (30). The radioactivity was located on the compound middle lamella, including the cell-corner regions from the final part of the primary wall stage to the early part of the  $S_2$  developmental stage. Corresponding to these stages, the radioactivity was distributed on Golgi-bodies which secreted many vesicles, and r-ER's (Fig. 11). Radioactivity was abundantly located on the secondary wall from the  $S_3$  stage to the completion of secondary wall lignification. Radioactivity was also located on s-ER's (Fig. 12). The radioactivity on the cell wall coincided with lignin deposition, as evidenced by UV-microscopy and TEM. These results therefore suggest that the Golgi-body, r-ER, and s-ER are all involved in the biosynthesis of lignin. However, since it is well known that the r-ER is a site of protein synthesis, some phenylalanine may be used for this purpose. On the other hand, the Golgi-bodies secrete many vesicles during active lignification of the compound middle lamella and secondary wall. The administered lignin precursor may, therefore, be incorporated into the Golgi-body directly or via other organellae, and then converted into monolignols via enzymatic conversion. The monolignols can then be secreted into the cell wall by exocytosis of the Golgi-vesicles. Many s-ER's also appear in the cytoplasm and these sometimes fuse to the plasma membrane at the  $S_3$  stage. Thus, lignin precursors may also be converted into monolignols at the lumen or the membrane of s-ER's, and then secreted into the cell wall by fusion of s-ER to the plasma membrane.

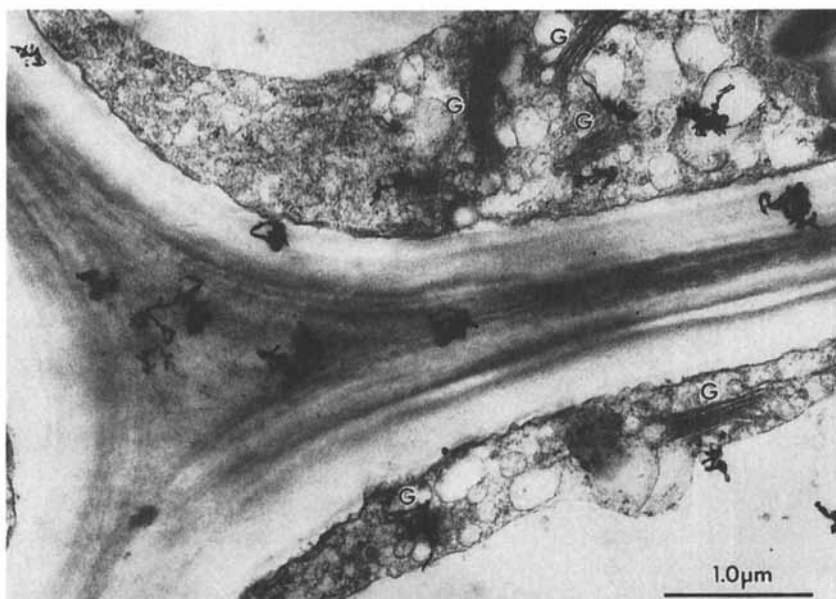


Figure 11. A tracheid in the early part of  $S_2$  stage. Radioactivities are observed on the Golgi-bodies and compound middle lamella.



Figure 12. A tracheid after  $S_3$  stage. Cytoplasm is filled with s-ER's. Radioactivity is distributed on the s-ER's and secondary wall.

### Concluding Remarks

It is evident that deposition processes for cellulose and hemicelluloses in conifer tracheids are quite different, i.e., cellulose is mainly deposited in the middle part of the  $S_2$  developmental stage, whereas hemicellulose deposition occurs from the  $S_1$  to the early part of the  $S_2$  stage, and then during the latter part of the  $S_2$  to  $S_3$  stages. As a result, the secondary wall shows a heterogeneous distribution of polysaccharides. Lignin deposition lags behind the polysaccharide formation. The most striking fact is that the monolignols, which are synthesized in the cytoplasm and secreted to the inner surface of the newly formed cell wall, pass through the pre-existing cell wall and reach the sites where lignification is proceeding. There is, however, no information as to how this transport actually occurs. Moreover, the intermolecular relationships between cellulose, hemicelluloses and lignin in the cell wall are still unclear.

Our electron microscopy observations have revealed some of the roles of cell organellae involved in biosynthesis of cell wall components: (i) the plasma membrane is the site of cellulose synthesis. This supports the proposal that terminal and rosette complexes at the plasma membrane are responsible for cellulose synthesis. (ii) The Golgi-bodies and small circular vesicles derived from the r-ER's are involved in the biosynthesis and/or transport of the hemicelluloses. Our investigations, however, could not distinguish between what type of cell organellae contained what kind of hemicelluloses, and how these polymers were processed in the organellae. (iii) The Golgi-bodies and s-ER's participate in the biosynthesis and/or transport of monolignols. It is expected that new techniques of both electron microscopy and biochemistry will improve our knowledge of the precise sites where enzymatic reactions leading to lignin formation occur.

### Literature Cited

1. Meier, H.; Wilkie, K. C. B. *Holzforschung* 1959, **13**, 177.
2. Meier, H. *J. Polym. Sci.* 1961, **51**, 11.
3. Côté, W. A., Jr.; Kutscha, N. P.; Simon, B. W.; Timell, T. E. *Tappi* 1968, **51**, 33.
4. Larson, P. R. *Holzforschung* 1969, **23**, 17.
5. Larson, P. R. *Tappi* 1969, **52**, 2170.
6. Hardell, H.-L.; Westermark, U. *Proc. 1st Int. Symp. Wood Pulping Chem.* 1981, I:32.
7. Takabe, K.; Fujita, M.; Harada, H.; Saiki, H. *Mokuzai Gakkaishi* 1983, **29**, 183.
8. Thiéry, J. *J. Microscopie* 1967, **6**, 987.
9. Takabe, K.; Fujita, M.; Harada, H.; Saiki, H. *Mokuzai Gakkaishi* 1984, **30**, 103.
10. Wardrop, A. B. *Tappi* 1957, **40**, 225.

11. Imagawa, H.; Fukazawa, K.; Ishida, S. *Res. Bull. Coll. Exp. Forests, Hokkaido Univ.* 1976, **33**, 127.
12. Fujita, M.; Saiki, H.; Harada, H. *Mokuzai Gakkaishi* 1978, **24**, 158.
13. Wardrop, A. B. In *Lignins*; Sarkanen, K. V.; Ludwig, C. H., Eds.; Wiley-Interscience: New York, 1971; p. 19.
14. Wardrop, A. B. *Appl. Poly. Symp.* 1976, **28**, 1041.
15. Kutscha, N. P.; Schwarzmann, J. M. *Holzforschung* 1975, **29**, 79.
16. Kishi, K.; Harada, H.; Saiki, H. *Bull. Kyoto Univ. Forests* 1982, **54**, 209.
17. Saka, S.; Thomas, R. J. *Wood Sci. Technol.* 1982, **16**, 167.
18. Takabe, K.; Fujita, M.; Harada, H.; Saiki, H. *Mokuzai Gakkaishi* 1981, **27**, 813.
19. Takabe, K. Ph.D. Thesis, Kyoto University, Kyoto, 1984.
20. Takabe, K.; Fujita, M.; Harada, H.; Saiki, H. *Res. Bull. Coll. Exp. Forests, Hokkaido Univ.* 1986, **43**, 783.
21. Brown, R. M., Jr.; Haigler, C. H.; Suttie, J.; White, A. R.; Roberts, E.; Smith, C.; Itoh, T.; Cooper, K. *J. Appl. Polym. Sci. (Appl. Polym. Symp.)* 1983, **37**, 33.
22. Takabe, K.; Harada, H. *Mokuzai Gakkaishi* 1986, **32**, 763.
23. Sugiyama, J.; Otsuka, Y.; Murase, H.; Harada, H. *Holzforschung* 1986, **40**(Suppl.), 31.
24. Pickett-Heaps, J. D. *J. Cell. Sci.* 1968, **3**, 55.
25. Fowke, L. C.; Pickett-Heaps, J. D. *Protoplasma* 1972, **74**, 19.
26. Ryser, U. *Protoplasma* 1979, **98**, 223.
27. Sugiyama, J.; Harada, H. *Mokuzai Gakkaishi* 1986, **32**, 770.
28. Pickett-Heaps, J. D. *Protoplasma* 1968, **65**, 181.
29. Fujita, M.; Harada, H. *Mokuzai Gakkaishi* 1979, **25**, 89.
30. Takabe, K.; Fujita, M.; Harada, H.; Saiki, H. *Mokuzai Gakkaishi* 1985, **31**, 613.

RECEIVED May 19, 1989

## Chapter 5

# Phenylpropanoid Metabolism in Cell Walls

### An Overview

Etsuo Yamamoto<sup>1</sup>, Gordon H. Bokelman<sup>2</sup>, and Norman G. Lewis<sup>1</sup>

<sup>1</sup>Departments of Wood Science and Biochemistry, Virginia Polytechnic Institute and State University, Blacksburg, VA 24061

<sup>2</sup>Philip Morris USA, Research Center, Richmond, VA 23261

Cell walls are major sites in which products of the phenylalanine-cinnamate pathway accumulate. These metabolites are found in cell walls in the form of (1) monomers, e.g., wall-esterified and ether-linked hydroxycinnamic acids, (2) dimers, e.g., didehydroferulic acid, 4,4'-dihydroxytruxillic acid, and (3) polymers, e.g., lignin, suberin. The distribution of these metabolites is characteristic of a particular group of plants, organs or tissues. There appear to be at least five types of reactions involved in the further conversion of phenylpropanoids in cell walls: (1) photochemical coupling, (2) E/Z isomerizations, (3) free-radical coupling reactions catalyzed by peroxidase, (4) hydrolysis of monolignol glucosides to their aglycone forms by  $\beta$ -glucosidases and (5) esterification of hydroxycinnamic acids. These reactions are reviewed in relation to cell wall structure.

A fascinating assortment of phenylpropanoids are contained within vascular plant cell walls and their vacuoles (1-6). In the cell walls, these substances (mainly lignins, suberins and covalently-linked hydroxycinnamic acids) are normally an integral part of the complex wall structure (7-9). In terms of function, lignins are required principally for mechanical support, but both they and suberins can also act as barriers to diffusion (9,10) and microbial invasion (11,12). On the other hand, the situation for wall-bound hydroxycinnamic acids remains unclear. Several roles have been suggested but not proven, e.g., in regulating cell-wall extension (3,5,7), as a defense mechanism against invading plant pathogens (5), and in lignification (13-15).

Surprisingly, little attention has been paid to (i) the mechanism of phenylpropanoid transport from the cytoplasm into the cell wall and (ii) subsequent chemical and biochemical modifications within the cell wall

0097-6156/89/0399-0068\$06.00/0

© 1989 American Chemical Society

structure. Studies of this type are urgently needed if we are to define the regulatory processes controlling cell-wall development; such investigations may, in turn, enhance our understanding of the structural and physiological functions of these metabolites.

Unfortunately, our knowledge of the transport mechanism is currently insufficient for a detailed discussion. The primary mechanism can probably be explained in terms of the "endomembrane theory" (16,17), i.e., phenylpropanoid monomers are transported via vesicles to the plasma membrane, and are then released into the cell wall following membrane fusion. However, more extensive experimental evidence is needed to unambiguously establish the detailed mechanism(s) involved.

As regards the second topic, namely that of phenylpropanoid reactions within plant cell walls, a more comprehensive discussion is possible and also timely, due to the recent increase in interest in this area. For the purpose of this review, the phenylpropanoids present in plant cell walls are first classified according to structural complexity (monomers, dimers, polymers, etc.), following which their main reactions are discussed.

### 1. Classification of Phenylpropanoids in Plant Cell Walls

The phenylpropanoids can be classified into two major groups, the first of which contribute to a broad class of compounds described as extractives. These compounds are non-structural entities of wood and bark tissue, and many originate in the vacuoles. As discussed in some detail by Hillis (18), some extractives (e.g., tannins) may diffuse into the cell wall matrix following rupture of the tonoplast. Another important group of phenylpropanoids are the normally dimeric lignans. Ubiquitous in nature and structurally very diverse, it is intriguing that within a given plant species the stereochemistry of most lignans is normally very well defined. (This suggests that the mechanism for their formation differs radically from that normally proposed for the closely-related polymeric material, lignin.)

The second group of phenylpropanoids, which is the main emphasis of this chapter, consists of those components which are integrated into the cell wall framework. This group can be subdivided into three categories; monomers, such as hydroxycinnamic acids, dimers, such as didehydroferulic and 4,4'-dihydroxytruxillic acids, and polymers, such as lignins and suberins. It is important to emphasize, at this juncture, that the dimers (4,5) and polymers (8,9) discussed in this chapter are considered to be formed within the cell walls from their corresponding monomers.

#### 1.1 Monomeric Phenylpropanoids

(a) *Hydroxycinnamic Acids*. Many angiosperms, particularly those belonging to the Gramineae of the monocotyledons (2-5,13), and the Caryophyllales of the dicotyledons (19), contain hydroxycinnamic acids linked to cell walls via ester-bonds. Recently, Harris and Hartley conducted a systematic histochemical survey of cell-bound hydroxycinnamic acids of over 350 angiosperm plant species, including some woody plants, and the reader is referred to these papers for more detailed information (20,21). Surprisingly, no published data for gymnosperms is yet available.



Hydroxycinnamic acids can be specifically visualized in plant tissue by their characteristic blue fluorescence when exposed to near ultraviolet light, and a green fluorescence following exposure of the tissue to ammonia (22-24). This fluorescence is particularly intense in the epidermal layers, vascular tissues and the stomata of grass leaves (24).

The most common hydroxycinnamic acids found in cell walls are ferulic **1** and *p*-coumaric **2** acids, and these are predominantly in their E-configurations. They can readily be released from the cell walls of grasses by saponification. While the amount of ferulic acid **1** liberated in this way normally ranges from 2-10 mg per gram dry cell walls (24-29), the amounts of *p*-coumaric acid **2** can vary even more markedly depending upon the tissue (see Table I) or the species under investigation (26). In addition to these acids, 5-hydroxyferulic acid **3** and trace amounts of sinapic acid **4** have also been isolated from the cell walls of corn and barley seedlings (29). Indeed, the recent isolation of 5-hydroxyferulic acid **3** (29), and the enzyme responsible for its formation (30), has confirmed the biosynthetic pathway to sinapic acid **4**, i.e., sinapate formation occurs via direct methylation of 5-hydroxyferulate **3**.

Table I. Wall-Esterified Hydroxycinnamic Acids in Various Tissues of 2-Week Old Maize (*Zea mays* cvs 259)

Tissue	Hydroxycinnamic Acids ( $\mu\text{mol/g}$ dry cell wall and their Z/E ratios)					
	Ferulic Acids			<i>p</i> -Coumaric Acids		
	E	Z	Z/E	E	Z	Z/E
Roots*	56.8	0.0	—	69.1	0.0	—
Mesocotyls	76.2	0.0	—	99.0	0.0	—
Nodes	45.3	1.3	0.03	70.2	0.2	0.003
Coleoptiles	31.9	5.4	0.17	3.4	0.3	0.09
Primary Leaves						
blade	20.9	9.7	0.46	6.5	1.5	0.23
sheath	21.6	4.8	0.22	25.7	1.9	0.07
Secondary Leaves						
blade	29.4	11.8	0.40	17.5	2.5	0.14
sheath	36.2	3.3	0.09	34.0	1.0	0.03
Tertiary Leaves	24.9	7.0	0.28	13.7	1.6	0.12

\* Crown roots are not included. Each value corresponds to the mean of duplicate experiments. Hydroxycinnamic acid determinations essentially followed the procedure of Yamamoto and Towers (25).

The cell wall polymers to which the hydroxycinnamic acids **1-4** are known to be covalently bound are the matrix polysaccharides (31-34), lignin (26,35), and suberin (10). As far as the polysaccharides are concerned, it is

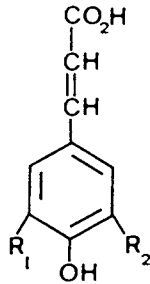
becoming recognized that these attachments are highly specific. This was established by enzymatic digestion of entire cell walls or purified matrix polysaccharides to yield either feruloylated or *p*-coumaroylated oligosaccharides. For instance, treatment of the cell walls of barley straw with *Oxyporus* cellulase afforded *O*-[5-*O*-(*trans-p*-coumaroyl)- $\alpha$ -L-arabinofuranosyl]-(1 $\rightarrow$ 3)-*O*- $\beta$ -D-xylopyranosyl-(1 $\rightarrow$ 4)-D-xylopyranose **5** (PAXX) and *O*-[5-*O*-*trans*-feruloyl- $\alpha$ -L-arabinofuranosyl]-(1 $\rightarrow$ 3)-*O*- $\beta$ -D-xylanopyranosyl-(1 $\rightarrow$ 4)-D-xylopyranose **6** (FAXX) (32). Similarly, FAXX was also isolated from bagasse (33) and from *Zea* shoots (34). Thus ferulic acid **1**, and probably some *p*-coumaric acid **2**, are specifically esterified to the arabinose residues of the matrix polysaccharides in plants of the Gramineae.

Not all hydroxycinnamic acids, however, are associated with the polysaccharides, since lignin (26,36) and suberin (10) have also been reported to be esterified with these acids. For lignin, this was established as follows: Higuchi and co-workers saponified isolated milled wood lignin preparations of *Miscanthus sacchariflooyus* (and other graminaceous plants) with cold alkali. This resulted in the release of *p*-coumaric acid **2**, corresponding to 3-10% by weight of lignin, together with small amounts of ferulic acid **1** (26). Interestingly, the ratio of *p*-coumaric acid **2** to ferulic acid **1** liberated in this way was 3-23 times higher than that released from the original plant material following cold alkaline treatment. This suggested that, at least for these plants, more *p*-coumaric acid **2** was linked to lignin than to the matrix polysaccharides.

The chemical nature of the ester-linkages of *p*-coumaric acid **2** to grass lignin has not yet been rigorously established. This is because (a) there is no known method to obtain identifiable oligomeric lignin fragments containing ester-linked hydroxycinnamic acids (e.g., by enzymic digestion) and (b) many grass lignin preparations are often contaminated with polysaccharides, which may also contain covalently-linked *p*-coumaric acid **2** (37-39).

Nevertheless, Nakamura and Higuchi (40,41) attempted to solve this problem by comparing the stability to acidolysis of *p*-coumarate linkages in isolated bamboo milled wood lignin, to those formed with veratryl alcohol **7** and 3,4-dimethoxypropen-2-ol **8**, respectively. Those model compounds were chosen since they were considered to adequately represent benzylic alcohol ( $C_\alpha$ ) and hydroxymethyl ( $C_\gamma$ ) environments within the lignin polymer. From this study, it was suggested that  $\sim 80\%$  of all *p*-coumarate linkages to lignin may involve esterification with terminal hydroxymethyl ( $C_\gamma$ ) groups, with the remainder attached to benzylic alcohol ( $C_\alpha$ ) functionalities. To account for the formation of these linkages to lignin, it has been proposed that either activated forms of hydroxycinnamic acids, such as *p*-coumaryl CoA, or preformed esters (such as **9**) are translocated from the cytoplasm into the cell wall. If so, such intermediates could be subsequently incorporated into lignin during polymerization (41).

In addition to ester-linkages, hydroxycinnamic acids can also be covalently linked to cell wall components via phenyl ether bonds. While this has only been demonstrated for wheat (*Triticum aestivum* L.) straw lignin (14), this finding is of importance since it clearly establishes the bifunc-

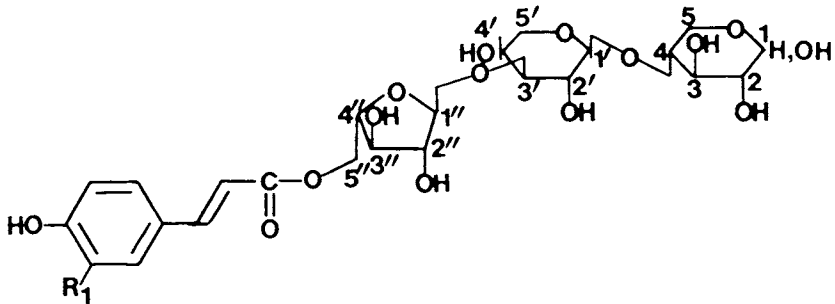


1,  $R_1 = H$ ,  $R_2 = OCH_3$

2,  $R_1, R_2 = H$

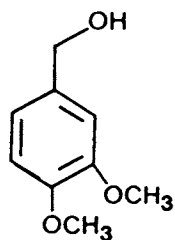
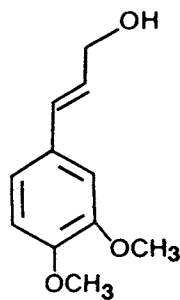
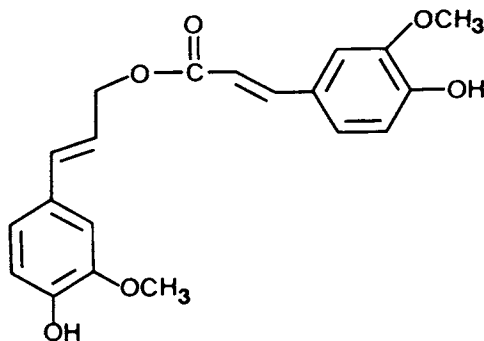
3,  $R_1 = OH$ ,  $R_2 = OCH_3$

4,  $R_1, R_2 = OCH_3$



5,  $R_1 = H$

6,  $R_1 = OCH_3$

789

tional nature of these molecules, and hence their potential as cross-linking agents.

(b) *Monolignols and their Glucosides*. Plants often contain minute quantities of the three monolignols, *p*-coumaryl, coniferyl and sinapyl alcohols. These are found mainly in the cambial sap, and hence, strictly speaking, are extractives. In general, they are assumed to have E-configurations (i.e., alcohols 10-12 respectively), although this has only rarely been verified.

Currently, the mechanism by which the monolignols are transported from the cytoplasm into the cell wall is not well understood. This is because there is still some confusion as to whether they are transported directly, or via their glucosidic conjugates (E-coniferin 13, E-syringin 14) or both (see Figure 1). Whatever the case may be, E-monolignols seldom accumulate in woody tissue, but are instead essentially incorporated completely into the lignin framework (42,43). Note also that the glucoside transportation hypothesis is enigmatic, since these substances apparently have limited distribution throughout woody plants. For example, (i) in gymnosperms, E-coniferin 13 only accumulates in a few species (8,9); and (ii) in the case of angiosperms, E-monolignol glucosides 13/14 appear to be mainly restricted to the *Magnoliceae* and *Oleacea* families (44). Consequently, at this point, we are unable to distinguish whether these glucosides are actively involved in monolignol transport, or whether they serve simply in a storage function (9,45-46).

Until recently (43), only E-monolignols were considered to be involved in the process of lignification. This concept of exclusivity presumably arose from the following observations: stereospecific deamination of phenylalanine, by phenylalanine ammonia lyase (PAL), affords E-cinnamic acid (45,47), and some of the enzymes involved in monolignol biosynthesis show a marked preference for the E-isomers (48,49). Such exclusivity may not exist, since in American beech (*Fagus grandifolia* Ehrh) bark only the Z-monolignols 17,18 and their glucosides 19-21 (50) are present. Interestingly, although Z-isoconiferin 20 was found in this plant, we have not yet detected Z-isosyringin 22. Additionally, the corresponding E-isomers 11-16 were not detected. One possible explanation for the absence of E-monolignols is that they are exclusively used for lignin formation, whereas the Z-isomers are not.

In order to address such questions, we are examining the formation and role of the Z-monolignols in beech bark (49). By means of appropriate radiotracer experiments, we established that the biosynthetic pathway to the Z-monolignols occurred as follows: phenylalanine first gave the E-monolignols, which then underwent isomerization to afford the corresponding Z-isomers. Note that while the E/Z isomerization of monolignols 10-12, 17-18 and their glucosides 13-15, 19-21 could be photochemically initiated under suitable conditions (51), no such conversions occurred during the radiotracer experiments carried out. These results suggest the mediation of a specific E/Z monolignol isomerase. At present, it is not known whether this isomerization occurs in the cytoplasm or in the cell wall, although the former situation is more likely.

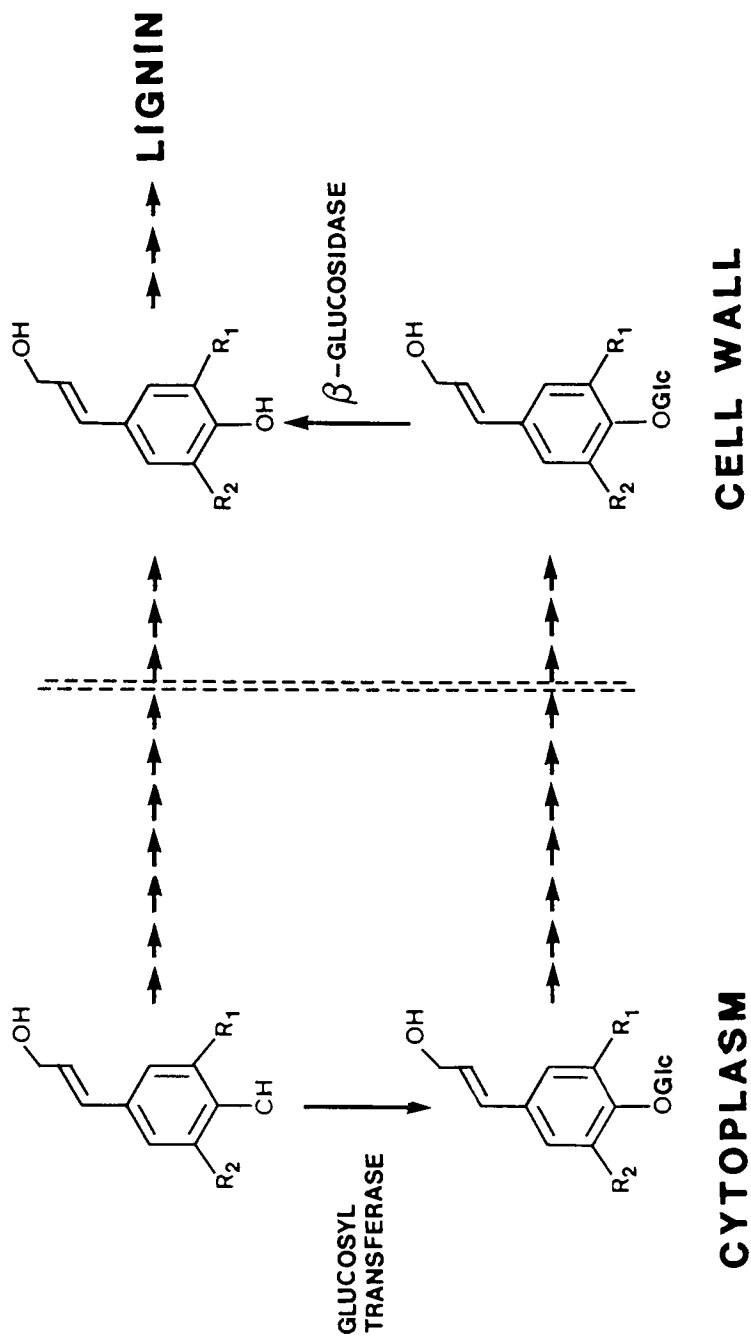
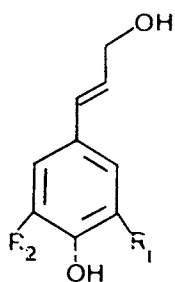


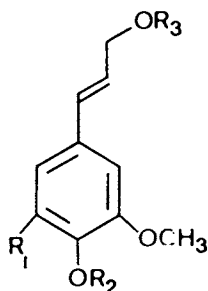
Figure 1. Proposed mechanisms of monolignol transport into the cell wall.



10,  $R_1, R_2 = H$

11,  $R_1 = OCH_3, R_2 = H$

12,  $R_1, R_2 = OCH_3$

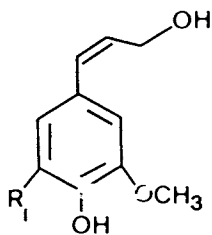


13,  $R_1, R_3 = H, R_2 = Glc$

14,  $R_1 = OCH_3, R_2 = Glc, R_3 = H$

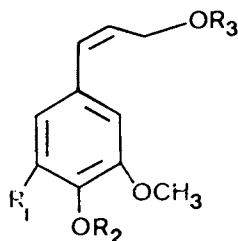
15,  $R_1, R_2 = H, R_3 = Glc$

16,  $R_1 = OCH_3, R_2 = H, R_3 = Glc$



17,  $R_1 = H$

18,  $R_1 = OCH_3$



19,  $R_1, R_3 = H, R_2 = Glc$

20,  $R_1, R_2 = H, R_3 = Glc$

21,  $R_1 = OCH_3, R_2 = Glc, R_3 = H$

22,  $R_1 = OCH_3, R_2 = H, R_3 = Glc$

Next, came the important finding (52) that a crude glucosyl transferase preparation from beech bark displayed a strong substrate specificity for *Z*-coniferyl alcohol **17** (i.e., only the *Z*-monolignol **17**, and not the corresponding *E*-isomer **11**, was glucosylated to give *Z*-coniferin **19**). Indeed, the *E*-monolignol **11** was not even converted into *E*-coniferin **13**. It will now be of interest to establish whether the *Z*-monolignols (or their glucosides) are transported into the cell wall of beech bark, and whether they are incorporated into the lignin polymer.

### 1.2 Dimeric Phenylpropanoids

Dimeric forms of ferulic and *p*-coumaric acids also occur in bound form within plant cell walls. The most common of these is didehydroferulic acid **23**, which has been isolated from some plants of the Gramineae (53,54) and spinach cell cultures (7). While no such *p*-coumaric acid **2** derived dimer (i.e., C<sub>5</sub>-C<sub>5</sub> linked) has ever been reported, cell walls of *Lolium multiflorum* contain another intriguing structural variation, namely 4,4'-dihydroxytruxillic acid **24** (5,55).

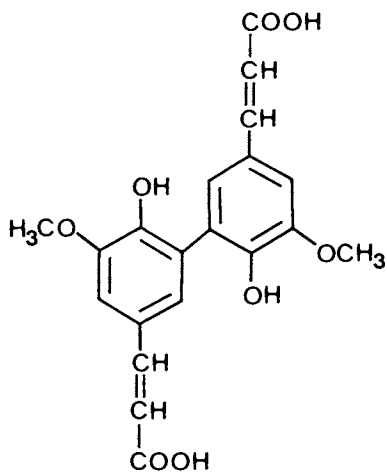
### 1.3 Polymeric Phenylpropanoids (Lignins, Suberins)

Lignins and suberins are complex phenylpropanoid polymers deposited in plant cell walls. Lignins are often described as dehydrogenative polymers of the three *E*-monolignols, i.e., *p*-coumaryl **10**, coniferyl **11**, and sinapyl **12** alcohols. Depending upon the plant species (or tissue) in question (8), the ratio of the monolignols in the lignin polymer can vary dramatically. For example, gymnosperm lignins are derived from ~ 80% of coniferyl alcohol **11** units, with the remainder consisting of *p*-coumaryl alcohol **10** derived moieties. With angiosperms, sinapyl alcohol **12** is also involved. Cereals and grasses have an additional complication due to the presence of covalently-linked hydroxycinnamic acids.

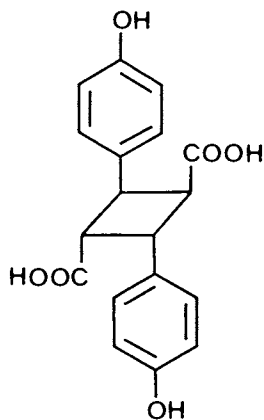
Suberin is a composite of polymeric phenylpropanoids and ester-linked long chain fatty acids and alcohols and consists of a hydrophobic layer attached to the cell walls of roots, bark and the vascular system (8,10). The phenylpropanoid portion of suberin purportedly has a lignin-like structure to which both aliphatic domains and hydroxycinnamic acids are esterified.

Because of their complexity, the structures of lignin and suberin can only be approximated. (Additionally, there is no known method of isolating lignin in its intact, or native, state.) We are currently overcoming such limitations by administering C-13 specifically labelled lignin precursors to intact growing plants, and subsequently monitoring the bonding patterns *in situ* by solid state C-13 nuclear magnetic resonance spectroscopy. To date, these experiments have enabled us to examine the bonding patterns of lignin *in situ* in *T. aestivum* (56), *L. leucocephala* (15,57,58) and *N. tabacum* (unpublished results). A similar strategy can potentially be developed for suberin.





23



24

## 2. Reactions of Phenylpropanoids in Plant Cell Walls

There are at least five types of phenylpropanoid related reactions which appear to occur in plant cell walls. Two are UV-mediated photochemical reactions, and hence may be restricted only to the first few layers of cells under the plant surface due to poor penetrability of the light (3). The other reactions appear to be enzymatically mediated, and result in the formation of dimers or polymers from the corresponding monomeric units.

### 2.1 Photochemical Reactions

(a) *E/Z Photoisomerization.* It is now well-established that cell walls of grasses (such as *Lolium* and *Phleum*), grown under normal lighting conditions, release both E- and Z-isomeric forms of hydroxycinnamic acids during alkaline hydrolysis (27). A similar observation has been noted for barley and corn seedlings (3,25). Interestingly, the Z-isomers were only present in the aerial parts of these plants (Table I) and were not detected in any tissue grown in the dark. However, subsequent exposure of etiolated barley seedlings to UV-A light (320-400 nm) resulted in the formation of Z-ferulic acid **1** in primary leaves and coleoptiles (25). It was also shown that the amount of the Z-isomer increased until the light was extinguished, or until the reaction had reached a photostationary state. Additionally, the Z-isomer content remained constant during the post-irradiation growth period, while the E-isomer continued to increase. These results strongly suggest that (i) E/Z isomerism of hydroxycinnamic acids is photochemically initiated, and (ii) that Z-ferulic acid, once formed, is metabolically stable. While the physiological significance of this photoisomerization remains unknown, its possible involvement in phototropic events was recently proposed (3).

(b) *Photochemical Coupling.* Recently dimers of *p*-coumaric acid, such as 4,4'-dihydroxytruxillic acid **24**, have been identified in the alkaline hydrolyzate of cell walls of *Lolium multiflorum* and are therefore presumably ester-bound (5,55). Since this compound can be readily photochemically synthesized from E-*p*-coumaric acid **2** (55,59), its formation *in vivo* presumably occurs via photocycloaddition of two *p*-coumaric acid moieties.

Such reactions may be of considerable significance. This is because, if two pendant *p*-coumarate linkages (or related molecules) are attached to two adjacent polysaccharide chains, an effective means of cross-linking via photochemical coupling could be achieved. However, there is no evidence at present to indicate that these dimers function as either intermolecular or intramolecular cross-linking reagents.

### 2.2 Enzymatic Reactions Involving Phenylpropanoids in Plant Cell Walls

This section describes reactions which are all presumably enzyme-mediated. These are (a) action of  $\beta$ -glucosidases to regenerate monolignols from their corresponding glucosides; (b) peroxidase-catalyzed polymerizations, in the presence of H<sub>2</sub>O<sub>2</sub>, to afford lignins and suberins; and (c) tentative evidence for the existence of an enzyme catalyzing the attachment of hydroxycinnamic acids to structural polysaccharides. As far

as  $\beta$ -glucosidases and peroxidase isozyme forms are concerned, it should be noted that these have rather broad substrate specificities. Hence it has been difficult to assign specific physiological functions to particular isozymes.

(a)  *$\beta$ -Glucosidases.* Originally, Freudenberg proposed that monolignol glucosides functioned as a means of monolignol transport from the cytoplasm into the cell wall (60). The monolignols would then be regenerated via action of a  $\beta$ -glucosidase. However, in a subsequent study using spruce (*P. abies*) hypocotyls, Marcinowski and Grisebach (9,61) reported that the rate of coniferin turnover was relatively slow compared to that of lignin deposition, i.e., the glucoside transport hypothesis could not account for all monomer transport.

Immunofluorescence techniques have been used to establish the sites of localization of  $\beta$ -glucosidases in spruce hypocotyls (9,61) and chickpea (*Cicer arietinum* L.) seedlings (46,62,63). In these investigations, the  $\beta$ -glucosidases were associated with lignified elements (tracheids and endodermis tissue), as well as those containing suberin and cutin.

Interestingly,  $\beta$ -glucosidase activity has also been observed in plant cell culture (62, 63), although no precise correlation with lignification could be made. For example, with chick pea cell cultures, substantial  $\beta$ -glucosidase activity was noted prior to the onset of lignification, and even under conditions where lignin deposition was inhibited by 2,4-dichlorophenol (2,4-D). This enzymic activity then essentially doubled during tracheid formation and lignin formation (as evidenced by a positive phloroglucinol-HCl test). The question remains though as to whether this  $\beta$ -glucosidase activity is essential for lignification to occur.

The substrate specificities of purified  $\beta$ -glucosidases from various sources have also been investigated, and the results obtained were also ambiguous (9). For chick pea cell cultures, the enzyme showed a strong preference for coniferin over syringin, with V/Km ratios of 125 and 6 respectively. On the other hand, the purified  $\beta$ -glucosidase from spruce hypocotyls was capable of hydrolyzing both coniferin and syringin (V/Km ratios of 111 and 67, respectively). These were unexpected findings since spruce, a gymnosperm, does not produce syringin, whereas chick pea presumably does. It will also be of interest to establish the  $\beta$ -glucosidase substrate specificities in beech bark for the Z-monolignol glucosides 19-21 previously described, and compare these with their E-counterparts.

(b) *Peroxidases.* Plant peroxidases are known to exist in multiple (isozyme) forms. Of these isozymes, some cell-wall bound peroxidases in the presence of H<sub>2</sub>O<sub>2</sub> are considered to initiate numerous free-radical coupling reactions (of plant phenolics) in cell walls, e.g., in the formation of didehydroferulic acid 23, the attachment of hydroxycinnamic acids to other cell-wall structural components, and in lignin/suberin formation.

*Didehydroferulic Acid 23 Formation.* It should be noted that no direct evidence has ever been obtained *in vivo* to prove that didehydroferulic acid 23 is formed via free radical coupling reactions. This mechanism is assumed, since *in vitro* incubation of ferulic acid 1 and wheat pentosan, with

horseradish peroxidase/H<sub>2</sub>O<sub>2</sub>, affords didehydroferulic acid **23** covalently linked to the polysaccharides (53). As before for 4,4'-dihydroxytruxillic acid **24**, the formation of these dimers has been envisaged as a mechanism for cross-linking polysaccharide chains to which adjacent ferulic acid **1** moieties are attached (5,7,19,64,65). However, this hypothesis still awaits experimental verification.

*Attachment of Hydroxycinnamic Acids to Structural Cell Wall Polymers.* Peroxidase mediation may also result in binding the hydroxycinnamic acids to the plant cell wall polymers (66,67). For example, it was reported that peroxidases isolated from the cell walls of *Pinus elliottii* catalyze the formation of alkali-stable linkages between [2-<sup>14</sup>C] ferulic acid **1** and pine cell walls (66). Presumably this is a consequence of free-radical coupling of the phenoxy radical species (from ferulic acid **1**) with other free-radical moieties on the lignin polymer. There is some additional indirect support for this hypothesis, since we have established that E-ferulic acid **1** is a good substrate for horseradish peroxidase with an apparent K<sub>m</sub> (77 μM), which is approximately one fifth of that for E-coniferyl alcohol (400 μM) (unpublished data).

A second mechanism is also possible for the introduction of covalent linkages between hydroxycinnamic acids and lignin. For example, during the free-radical coupling reactions of monolignols, the initial products are the transient quinone methides which can react subsequently with nucleophilic reagents such as ferulic **1** or *p*-coumaric **2** acid. Such reactions have been shown to occur *in vitro* (67), where transient quinone methides readily react with either phenolate anions (from the methyl esters of *p*-coumaric and ferulic acids), or the corresponding carboxylate anions. In such cases, this would lead to arylbenzyl ethers (so-called α-O-C) and benzylic esters respectively. This could account for some of the ester-bonding patterns reported for grass lignins at C<sub>α</sub> (40,41).

If such reactions between cell-wall bound hydroxycinnamic acids and monomers can indeed occur *in vivo*, this would provide an excellent mechanism for initiating lignin formation at specific points on polysaccharide chains. As shown in Figure 2, we propose that cell-wall bound hydroxycinnamic acids can undergo either free radical coupling (pathway A) or nucleophilic (pathway B) reactions. In such a way, the wall-bound hydroxycinnamic acids may function as "anchors" for lignification to occur. It is important to note that this mode of cross-linking differs substantially from conventional views on lignin-carbohydrate complex formation between the two preformed polymers (8).

*Lignin and Suberin Formation.* By far the most important peroxidase-mediated reaction involves that of the dehydrogenative polymerization of the monolignols (e.g., **10-12**) leading to lignin. However, not all peroxidase isozymes catalyze this polymerization equally well (68-70). Additionally, with *Populus euroamericana* xylem tissue, it has been reported that a specific peroxidase is produced, at or around the onset of lignification, for the purpose of lignin formation (71). This isozyme, readily visualized on either electrophoretic gels as a fast migrating band or in lignified plant

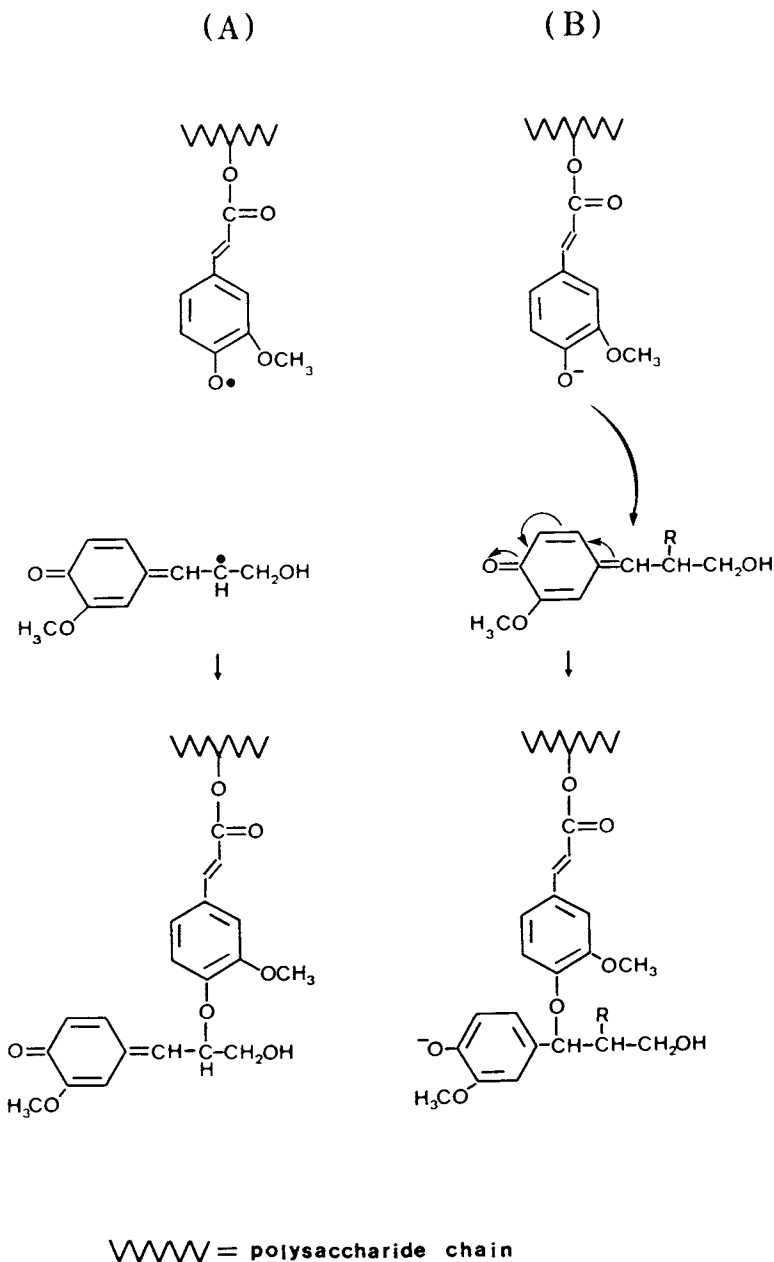


Figure 2. Hypothetical role of cell-wall bound hydroxycinnamic acids as "anchors" for lignification.

tissue, by the action of  $H_2O_2$ /syringaldazine (72), has been given the name syringaldazine oxidase (73). Interestingly, when syringaldazine was used for histochemical staining of cross-sections of wood-specimens, a more intense staining was observed with angiosperms than for gymnosperms. To account for these differences in staining intensity, it is conceivable that syringaldazine oxidase plays a more significant role in the polymerization of sinapyl alcohol **12** moieties into angiosperm lignin. Note also that specific lignin-catalyzing peroxidases have been reported for the gymnosperm, *Larix decidua* (74), and the annual plant, tobacco (*Nicotiana tabacum*) (75).

In order to prove that specific isozymes are, in fact, involved in lignin formation, each must first be purified to homogeneity and subjected to appropriate immunochemical and kinetic investigations. Some cautious optimism for the resolution of this problem can be hoped for, since an antibody of the isozyme from *Nicotiana tabacum* has been obtained and its cDNA cloned (75). It is to be hoped that the following can now be determined: (i) the precise location of the specific peroxidase isozyme in the cell wall; (ii) the timing of its appearance during the course of lignin formation; and (iii) its homology compared to other isozymes.

Another question that needs to be resolved is whether the Z-monolignols, previously mentioned, are involved in lignin formation in beech bark. In this regard, we have shown, in preliminary experiments *in vitro*, with horseradish peroxidase and  $H_2O_2$ , that a synthetic dehydrogenatively polymerized lignin can be formed from either Z or E-coniferyl alcohols (43). This suggests that the stereospecificity of the enzyme is not strict, with respect to E or Z configuration, and that either monolignol can be used. However, a more detailed investigation is needed to establish whether this is the case for peroxidase from beech bark. The suberization process in wounded potato tuber tissue (*Solanum tuberosum* L.) has also been investigated. In a similar manner to that for lignin, it was found that a temporal and spatial correlation could be made regarding suberization and the appearance of a specific isoperoxidase (76). More recently, indirect immunochemical staining (using a rabbit antiperoxidase and a goat antirabbit antibody, labelled with fluorescein or rhodamine), revealed that this suberin-specific peroxidase was localized on the innersides of actively suberizing walls (77). Other studies revealed some of the properties of this isozyme (78).

In short, the current body of evidence suggests that specific isozymes are involved in both lignin and suberin formation.

(c) *Evidence for Hydroxycinnamic Acid Transferases.* It is now well established that hydroxycinnamic acids are covalently linked to the matrix polysaccharides, and that such attachments are specific (19,32-34). At least two possibilities exist for the attachment of hydroxycinnamic acids to these polysaccharides. In the first case, feruloylation could occur intracellularly, with the preformed feruloylated polysaccharides then transported directly into the cell wall. This possibility is favored by Fry, for feruloylation of spinach cell walls in cell culture (19).

On the other hand, the current evidence accrued to date for feruloylation of the matrix polysaccharides in barley coleoptiles appears to fa-

vor an extracellular reaction. This working hypothesis is based on the following observations or arguments: if barley coleoptile matrix polysaccharides are feruloylated within the cytoplasmic membrane, then it might be expected that both ferulic acid and arabinose will display similar kinetics. This is not observed (25). In contrast, a temporal difference is observed between arabinose and ferulic acid deposition into the cell walls, i.e., an increased rate of arabinose deposition into the cell wall follows that of wall growth. On the other hand, feruloylation begins only when the cell wall weight increase is in an exponential phase, and continues even though no measurable gain in the dry weight of the walls occurs. This suggests, but does not prove, that feruloylation occurs within the cell wall. If esterification between ferulic acid and the arabinose residue of a preformed polysaccharide occurs within the cell wall, then a mechanism requiring a cell-wall enzyme to catalyze feruloylation would be required. From an energetics standpoint, transesterification of an activated feruloyl moiety to an arabinose residue would be a favored mechanism (Fig. 3). Activation of ferulic acid could presumably occur intracellularly, by either coenzyme A ligase (9), or a glucosyl transferase, to yield feruloyl CoA and feruloyl glucose, respectively. This activated form would then have to be discharged into the cell wall.

Preliminary radiotracer studies using isolated cell-walls from barley coleoptiles support extracellular feruloylation. For instance, when cell wall preparations were incubated with [2-<sup>14</sup>C] feruloyl CoA, a linear incorporation (up to 1%) of the radioactivity into the "cell wall" was observed by 3h. Subsequent treatment of the "cell wall" with Driselase released approximately 60% of the radioactivity incorporated into the cell wall as low molecular weight fragments. Note also that the Driselase, while containing some xylanase activity, had *no* esterase activity (45,80). Additionally, this incorporation rate was approximately four times higher than that of [2-<sup>14</sup>C] ferulic acid itself, and feruloyl glucose was only poorly incorporated. Thus, these *in vitro* experiments demonstrate that feruloylation of isolated cell-walls from barley coleoptiles can occur, and that the radioactivity incorporated can, in part, be removed by treatment with Driselase. It is now essential to establish the actual bonding patterns, in order to prove whether this binding is specific or not.

### Concluding Remarks

Vascular plant cell walls contain a wide variety of phenylpropanoids, such as monomers, dimers and polymers. Of these, the polymers (i.e., lignins and suberins) are the most abundant. According to our current knowledge, all cell-wall phenylpropanoids are derived from monomers synthesized in the cytoplasm. Following their excretion into the plant cell wall, these monomers can then be either photochemically or biochemically modified within the cell wall.

In this regard, several comments can be made:

(i) *p*-hydroxycinnamic acids ester-linked to cell wall polysaccharides are likely to be photochemically dimerized or isomerized under UV-A light (320-400 nm).

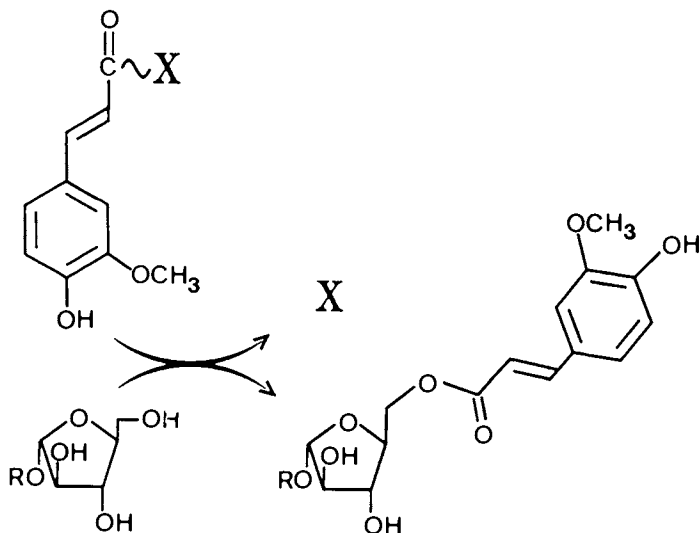


Figure 3. Hypothetical mechanisms for extracellular feruloylation of matrix polysaccharides. (X = SCoA or Glc; R = xylan or H)

(ii) The enzymatic mechanism leading to ester-linked cell-wall hydroxycinnamic acids bound to matrix polysaccharides needs to be established, since preliminary experiments suggest that both intra- and extracellular feruloylation reactions can occur.

(iii) The mechanism by which monolignols, or their glucosides, are transported into the cell wall needs to be more fully elucidated.

(iv) The presence of *Z*-monolignol glucosylation, and the strong substrate specificity for *Z*-monolignol glucosylation, may mean that beech bark lignin is formed from *Z*-, and not *E*-, monolignols.

(v) Cell-wall bound peroxidases apparently play a central role in catalyzing (a) polymerization processes yielding lignin and suberin, (b) formation of didehydroferulic acid, (c) the probable formation of ether linkages between *p*-hydroxycinnamic acids and lignin or suberin. Additionally, secondary reactions of intermediate transient quinone methides, formed after free-radical coupling, can occur. These can then react with nucleophiles, e.g., to afford lignin-carbohydrate complexes.

(vi) A strong correlation apparently exists between lignin formation and the appearance of particular isoperoxidases. However, the isolation of these isozymes and comparative enzymological studies, including structural analyses of the active center, are required before we can assign a specific function to them. Involvement of other isoperoxidases should not be dismissed at present, since peroxidases appear to have rather broad substrate specificities.



### Acknowledgments

The authors thank the U.S. Department of Energy (Grant DE-FG05-88-ER13883) and Philip Morris USA Research Center for financial assistance. The authors also thank Dr. R. G. Fulcher, Agriculture Canada, Ottawa Research Station, Ottawa, Canada, for the kind gift of *Zea mays* kernels.

### Literature Cited

1. Wiermann, R. In *The Biochemistry of Plants*; Vol. 7, Secondary Plant Products; Conn, E. E., Ed.; Academic Press: New York, 1981; p. 85-116.
2. Smith, D. C. C. *Nature* 1955, **176**, 267-68.
3. Towers, G. H. N.; Yamamoto, E. In *Ann Proc. Phytochemical Society of Europe*; Vol. 25, VanSumere, C. F.; Lea, P. J., Eds.; 1984, p. 271-89.
4. McNeil, M.; Darvill, A. G.; Fry, S. C.; Albersheim, P. *Ann. Rev. Biochem.* 1984, **53**, 625-63.
5. Hartley, R. D.; Ford, C. W. (this volume).
6. Strack, D.; Sharma, V. *Physiol. Plant.* 1985, **65**, 45-60.
7. Fry, S. C. *Ann. Rev. Plant Physiol.* 1986, **37**, 165-86.
8. Fengel, D.; Wegener, G. *Wood: Chemistry, Ultrastructure, Reactions*; Walter de Gruyter & Co.: Berlin, 1983.
9. Grisebach, H. In *The Biochemistry of Plants*; 7, Secondary Plant Products; Conn, E. E., Ed.; Academic Press: New York, 1981; p. 457-78.
10. Kolattukudy, P. E. In *Biosynthesis and Biodegradation of Wood Components*; Higuchi, T., Ed.; Academic Press: New York, 1985; p. 161-207.
11. Friend, J. In *Progress in Phytochemistry*; 7; Reinhold, L.; Harborne, J. B.; Swain, T., Eds.; Pergamon Press: New York, 1981; p. 197-261.
12. Asada, Y.; Matsumoto, I. Japan Sci. Soc. Press: Tokyo/Springer-Verlag: Berlin, 1987; p. 223-33.
13. El-Basyouni, S.; Towers, G. H. N. *Can. J. Biochem.* 1964, **42**, 203-10.
14. Scalbert, A.; Monties, B.; Lallemand, J.-Y.; Guittet, E.; Rolando, C. *Phytochemistry* 1985, **24**, 1359-62.
15. Lewis, N. G. *Bulletin de Liason Groupe Polyphenols* 1988, **14**, 398-410.
16. Northcote, D. H. 1989 (This volume).
17. Takabe, K.; Fukazawa, K.; Harada, H. 1989 (This volume).
18. Hillis, W. E. In *Biosynthesis and Biodegradation of Wood Components*; Higuchi, T. Ed.; Academic Press: New York, 1985; p. 209-28.
19. Fry, S. C.; Miller, J. G. 1989 (This volume).
20. Harris, P. J.; Hartley, R. D. *Biochem. Syst. Ecol.* 1980, **8**, 153-60.
21. Hartley, R. D.; Harris, P. J. *Biochem. Syst. Ecol.* 1981, **9**, 189-203.
22. Harris, P. J.; Hartley, R. D. *Nature* 1976, **259**, 508-10.
23. Fulcher, R. G.; O'Brien, T. P.; Lee, J. W. *Aust. J. Biol. Sci.* 1972, **25**, 23-34.
24. Knogge, W.; Weissenböck, G. *Planta* 1986, **167**, 196-205.
25. Yamamoto, E.; Towers, G. H. N. *J. Plant Physiol.* 1985, **117**, 441-49.
26. Higuchi, T.; Ito, Y.; Shimada, M.; Kawamura, I. *Phytochemistry* 1967, **6**, 1551-56.

27. Hartley, R. D.; Jones, E. C. *Phytochemistry* 1977, **16**, 1531-34.
28. Burritt, E. A.; Bittner, A. S.; Street, J. C.; Anderson, M. J. *Dairy Sci.* 1984, **67**, 1209-13.
29. Ohashi, H.; Yamamoto, E.; Lewis, N. G.; Towers, G. H. N. *Phytochemistry* 1987, **26**, 1915-16.
30. Grand, C. *FEBS Lett.* 1984, **169**, 7-11.
31. Fry, S. C. *Planta* 1983, **157**, 111-23.
32. Mueller-Harvey, I.; Hartley, R. D.; Harris, P. J.; Curzon, E. H. *Carbohydr. Res.* 1986, **148**, 71-85.
33. Kato, A.; Azuma, J.; Koshijima, T. *Chem. Lett.* 1983, 137-40.
34. Kato, Y.; Nevins, D. J. *Carbohydr. Res.* 1985, **137**, 139-50.
35. Hartley, R. D.; Jones, E. C. *J. Sci. Fd. Agric.* 1978, **29**, 777-82.
36. Nakano, J.; Ishizu, A.; Migita, N. *Mokuzai Gakkaishi* 1958, **4**, 1-5.
37. Himmelsbach, D. S.; Barton, F. E., II. *J. Agric. Food Chem.* 1980, **28**, 1203-08.
38. Morrison, I. M. *Biochem. J.* 1974, **139**, 197-204.
39. Nordkvist, E.; Salomonsson, A.-C.; Åman, P. *J. Sci. Food Agric.* 1984, **35**, 657-61.
40. Nakamura, Y.; Higuchi, T. *Holzforschung* 1976, **30**, 187-91.
41. Nakamura, Y.; Higuchi, T. *Cell. Chem. Technol.* 1978, **12**, 199-208.
42. Terazawa, M.; Miyake, M. *Mokuzai Gakkaishi* 1984, **30**, 329-34.
43. Morelli, E.; Rej, R. N.; Lewis, N. G.; Just, G.; Towers, G. H. N. *Phytochemistry* 1986, **25**, 1701-05.
44. Terazawa, M.; Okuyama, H.; Miyake, M. *Mokuzai Gakkaishi* 1984, **30**, 322-28.
45. Gross, G. G. In *Biosynthesis and Biodegradation of Wood Components*; Higuchi, T., Ed.; Academic Press: New York, 1985; p. 229-71.
46. Hösel, W. In *The Biochemistry of Plants*; 7, Secondary Plant Products; Conn, E. E., Ed.; Academic Press: New York, 1981; p. 725-53.
47. Higuchi, T. In *Biosynthesis and Biodegradation of Wood Components*; Higuchi, T., Ed.; Academic Press: New York, 1985; p. 141-60.
48. Knobloch, K.-H.; Hahlbrock, K. *Eur. J. Biochem.* 1975, **52**, 311-20.
49. Lewis, N. G.; Dubelsten, P.; Eberhardt, T. L.; Yamamoto, E.; Towers, G. H. N. *Phytochemistry* 1987, **26**, 2729-34.
50. Lewis, N. G.; Inciong, Ma. E. J.; Ohashi, H.; Towers, G. H. N.; Yamamoto, E. *Phytochemistry* 1988, **27**, 2119-21.
51. Lewis, N. G.; Inciong, Ma. E. J.; Dhara, K. P.; Yamamoto, E. (submitted for publication).
52. Lewis, N. G.; Inciong, E. Ma. J.; Yamamoto, E. (submitted for publication).
53. Hartley, R. D.; Jones, E. C. *Phytochemistry* 1976, **15**, 1157-60.
54. Shibuya, N. *Phytochemistry* 1984, **23**, 2233-37.
55. Hartley, R. D.; Whatley, R. F.; Harris, P. J. *Phytochemistry* 1988, **27**, 349-51.
56. Lewis, N. G.; Yamamoto, E.; Wooten, J. B.; Just, G.; Ohashi, H.; Towers, G. H. N. *Science* 1987; **237**, 1344-46.

57. Lewis, N. G.; Razal, R. A.; Yamamoto E.; Bokelman, G. H.; Wooten, J. B. 1989 (This volume).
58. Lewis, N. G.; Razal, R. A.; Dhara, K. P.; Yamamoto, E.; Bokelman G.; Wooten, J. B. *J.C.S. Chem. Commun.* 1988, 1626-28.
59. Cohen, M. D.; Schmidt, G. M. J.; Sanntag, F. I. *J. Chem. Soc.* 1964, 2000-13.
60. Freudenberg, K. *The Constitution and Biosynthesis of Lignin*; Freudenberg, K.; Neish, A. C., Eds.; Springer-Verlag: Berlin, 1968.
61. Marcinowski, S.; Grisebach, H. *Eur. J. Biochem.* 1978, **87**, 37-44.
62. Burmeister, G.; Hösel, W. *Planta* 1981, **152**, 578-86.
63. Hösel, W.; Fiedler-Preiss, A.; Borgmann, E. *Plant Cell Tissue Organ Cult.* 1982, **1**, 137-48.
64. Geissman, T.; Neukom, H. *Lebensm. Wiss. Technol.* 1973, **6**, 59-62.
65. Fry, S. C.; Miller, J. G. *Food Hydrocolloids* 1987, **1**, 395-97.
66. Whitmore, F. W. *Phytochemistry* 1976, **15**, 375-78.
67. Scalbert, A.; Monties, B.; Rolando, C.; Sierra-Escudero, A. *Holzforchung* 1986, **40**, 191-95.
68. Van Huystee, R. B. *Ann. Rev. Plant Physiol.* 1987, **38**, 205-19.
69. Gaspar, Th.; Penel, C.; Thorpe, T.; Greppin, H. *Peroxidases 1970-1980. A Survey of their Biochemical and Physiological Roles in Higher Plants*; Univ. Genève 1982; 324 pp.
70. Mäder, M.; Nessel, A.; Bopp, M. *Z. Pflanzenphysiol.* 1977, **82**, 247-60.
71. Imberty, A.; Goldberg, R.; Catesson, A. M. *Planta* 1985, **164**, 221-26.
72. Harkin, J. M.; Obst, J. R. *Science* 1973, **180**, 296-98.
73. Goldberg, R.; Catesson, A-M.; Czaninski, Y. *Z. Pflanzenphysiol.* 1983, **110**, 267-69.
74. Stich, K.; Ebermann R. *Holzforchung* 1988, **42**, 221-24.
75. Lagrimini, L. M.; Burkhart, W.; Moyer, M.; Rothstein, S. *Proc. Natl. Acad. Sci.* 1987, **84**, 7542-46.
76. Borchert, R. *Plant Physiol.* 1978, **62**, 789-93.
77. Espelie, K. E.; Francheschi, V. R.; Kolattukudy, P. E. *Plant Physiol.* 1986, **81**, 487-92.
78. Espelie, K. E.; Kolattukudy, P. E. *Arch. Biochem. Biophys.* 1985, **240**(1), 539-45.
79. Villegas, R. J. A.; Kojima, M. *Agric. Biol. Chem.* 1985, **49**, 263-65.
80. Fry, S. C. *Planta* 1987, **171**, 205-11.

RECEIVED May 19, 1989

## Chapter 6

# Biochemical Interface Between Aromatic Amino Acid Biosynthesis and Secondary Metabolism

Roy A. Jensen<sup>1</sup>, Paul Morris<sup>1</sup>, Carol Bonner<sup>1</sup>, and Lolita O. Zamir<sup>2</sup>

<sup>1</sup>Department of Microbiology and Cell Science, University of Florida, Gainesville, FL 32611

<sup>2</sup>Centre de Microbiologie Appliquée, Université du Québec, Institut Armand-Frappier, 531, Boulevard des Prairies, C.P. 100, Laval-des-Rapides, Laval, Quebec G1K 7P4, Canada

In higher plants aromatic amino acids are required not only for protein synthesis, but as precursors for hormones, and a vast diversity of phenylpropanoid or other secondary metabolites. Thus, the availability of aromatic amino acids in a number of the spatially separate compartments of the plant-cell microenvironment is essential. It is generally accepted that chloroplasts possess an intact pathway of aromatic amino acid biosynthesis that is tightly regulated. In addition, the subcellular location of some aromatic-pathway isozymes has been shown to be in the cytosol, but whether an intact pathway exists in the cytosol has not yet been proven. The evidence bearing on aromatic amino acid compartmentation and regulation is reviewed, with particular emphasis given to the relationship between primary biosynthesis and secondary metabolism in the cytosol.

Little is known about the relationship of regulated changes in enzyme levels of general phenylpropanoid biosynthesis (or of its divergent branches) with enzyme changes in the primary biosynthetic pathway (shikimate pathway) that generates precursor structures. This is understandable because the exact biochemical steps, regulation and compartmentation of aromatic amino acid biosynthesis in higher plants is only now being elucidated (1). A fairly complete picture of a tightly regulated pathway present in higher-plant chloroplasts is now established. A novel prephenate aminotransferase (2,3) transaminates prephenate to yield L-arogenate (4), an unstable amino acid precursor of both L-phenylalanine and L-tyrosine (Fig. 1). Arogenate

---

NOTE: Florida Agricultural Experiment Station Journal Series No. 9217.

0097-6156/89/0399-0089\$06.00/0  
© 1989 American Chemical Society

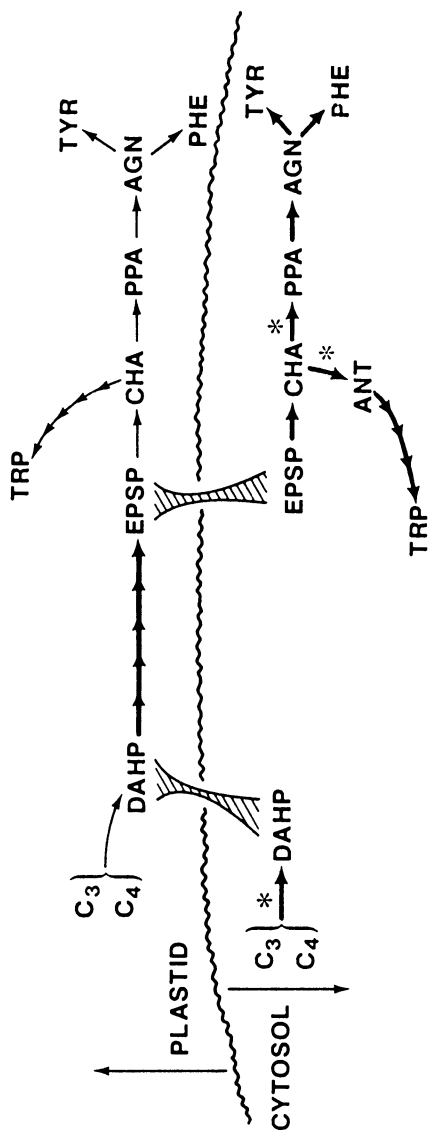


Figure 1. Hypothetical mechanism for shuttling of intermediates of the common aromatic pathway between plastidic and cytosolic compartments. Enzymes denoted with an asterisk (DAHP synthase-Co, chorismate mutase-2, and cytosolic anthranilate synthase) have been demonstrated to be isozymes located in the cytosol. DAHP molecules from the cytosol are shown to be shuttled into the plastid compartment in exchange for EPSP molecules synthesized within the plastid. Abbreviations: C<sub>3</sub>, phosphoenolpyruvate; C<sub>4</sub>, erythrose 4-P; DAHP, 3-deoxy-D-arabino-heptulosonate 7-phosphate; EPSP, 5-enolpyruvylshikimate 3-phosphate; CHA, chorismate; ANT, anthranilate; TRP, L-tryptophan; PPA, prephenate; AGN, L-arogenate; TYR, L-tyrosine; and PHE, L-phenylalanine.

dehydratase, arogenate dehydrogenase and anthranilate synthase are subject to feedback inhibition by L-phenylalanine (5,6), L-tyrosine (7,8) and L-tryptophan (5,9), respectively. Plastidic chorismate mutase is subject to feedback inhibition by L-phenylalanine or by L-tyrosine, and to allosteric activation by L-tryptophan (10-12). We have suggested that inhibition of plastidic chorismate mutase by L-phenylalanine or L-tyrosine occurs *in vivo* only under nutritional conditions of L-tryptophan starvation (1,13). With excess tryptophan, activation overwhelms the otherwise inhibitory effects of L-phenylalanine and L-tyrosine. Under conditions of total endproduct excess, L-arogenate would accumulate in the plastid. This would shut off the early-pathway step catalyzed by 3-deoxy-D-arabino-heptulosonate (DAHP) synthase, since the plastidic DAHP synthase is sensitive to feedback inhibition by L-arogenate (1,14). This allosteric pattern is a variation of sequential feedback inhibition, first described in *Bacillus subtilis* where prephenate feedback inhibits DAHP synthase (15), and later in *Xanthomonas campestris* where chorismate feedback inhibits DAHP synthase (16).

The tightly regulated pathway specifying aromatic amino acid biosynthesis within the plastid compartment implies maintenance of an amino acid pool to mediate regulation. Thus, we have concluded that loss to the cytoplasm of aromatic amino acids synthesized in the chloroplast compartment is unlikely (13). Yet a source of aromatic amino acids is needed in the cytosol to support protein synthesis. Furthermore, since the enzyme systems of the general phenylpropanoid pathway and its specialized branches of secondary metabolism are located in the cytosol (17), aromatic amino acids (especially L-phenylalanine) are also required in the cytosol as initial substrates for secondary metabolism. The simplest possibility would be that a second, complete pathway of aromatic amino acid biosynthesis exists in the cytosol. Ample precedent has been established for duplicate, major biochemical pathways (glycolysis and oxidative pentose phosphate cycle) of higher plants that are separated from one another in the plastid and cytosolic compartments (18). Evidence to support the hypothesis for a cytosolic pathway (1,13) and the various approaches underway to prove or disprove the dual-pathway hypothesis are summarized in this paper.

### The Existing Case for an Intact Cytosolic Pathway

- i. Proof that an intact pathway of aromatic amino acid biosynthesis is located within the chloroplast organelle was obtained by demonstration of the ability of isolated spinach chloroplasts to assimilate radioactive CO<sub>2</sub> or shikimate into aromatic amino acids (19,20). However, since the chloroplast-localized biosynthetic pathway did not account for total aromatic biosynthesis, a spatially separate pathway would explain the quantitative discrepancy.
- ii. A source of beginning substrates (PEP and erythrose 4-P) is available in the cytosol.
- iii. "Minor" cytosolic isozymes corresponding to most of the common-pathway reactions, although given little emphasis by the authors,

have in fact been demonstrated (21-22). HPLC chromatography of crude extracts has revealed previously unresolved isozymes of shikimate dehydrogenase (22) (plastidic and cytosolic species) and of 5-enolpyruvylshikimate-3-P synthase (23) (subcellular location not examined).

- iv. In one recent study (24) shikimate dehydrogenase has been reported to be located primarily in the cytosol.
- v. Detailed studies demonstrating cytosolic isozymes of both DAHP synthase (25) and chorismate mutase (12,26) have been carried out. There is steadily accumulating evidence that the separately compartmented isozyme pairs of DAHP synthase (DS-Mn and DS-Co) and chorismate mutase (CM-1 and CM-2) are generalized features of higher plants. Some apparent exceptions have been shown to be the result of technical problems. For example, potato tubers were reported to lack the cytosolic CM-2 (27) and the cytosolic DS-Co (28). However, we have shown recently that potato tuber possesses CM-2 and DS-Co isozymes that are in fact comparable to counterpart isozymes in other plant organisms (29).
- vi. The demonstration of a pair of anthranilate synthase isozymes in tobacco (9), the cytosolic isozyme being insensitive to allosteric control, adds substance to the emerging picture of dual aromatic pathways.

Of the separately compartmented isozyme pairs that exist for DAHP synthase, chorismate mutase, and anthranilate synthase, each isozyme member of a given pair has different properties of regulation and other distinctive characteristics (see Tables I and II). This suggests a high probability that each isozyme is the gene product of a different gene.

Table I. Differential Properties of DAHP Synthase Isozymes

Character	DAHP-Synthase-Mn	DAHP-Synthase-Co
Erythrose 4-P	Saturates at 0.6 mM	Saturates at 6.0 mM
Glyceraldehyde 3-P	Not used	Used as substrate
Dithiothreitol	Hysteretic activator	No activation
Effect of divalent cations	Activation ( $Mn^{++}$ )	Required ( $Mg^{++}$ , $Co^{++}$ , $Mn^{++}$ )
pH optimum <sup>a</sup>	pH 8.0	pH 8.8
Inhibitor	L-Arogenate	Caffeic acid

<sup>a</sup> Assay at low pH (7.0) can be used to increase the selectivity of assay conditions for DAHP synthase-Mn in isozyme mixtures.

The existence of the common-pathway isozymes, DS-Co and CM-2, in the cytosol appears improbable unless they are linked to the connecting sequence of enzymes. Yet a compelling demonstration of this enzyme succession in the cytosol has not been made. Since ample precedent exists for the shuttling of small molecules between spatial compartments in higher plant cells, one possibility is that the appropriate intermediates are shuttled

Table II. Differential Properties of Chorismate Mutase Isozymes

Character	Chorismate Mutase-1	Chorismate Mutase-2
Substrate saturation	0.9 mM	2.0 mM
pH optimum	7.0-8.0	7.0
Activators	L-Tryptophan	
Inhibitors	L-Phenylalanine, L-Tyrosine	Caffeic Acid

back and forth. Thus, according to the hypothetical model shown in Figure 1, DAHP formed in the cytosol is imported into the chloroplast where it connects with the second step of the plastidic pathway, ultimately being transformed to EPSP. A fraction of the plastidic EPSP is exported back into the cytosol. Although chorismate, rather than EPSP, could equally well be chosen in Figure 1 as the molecule exported, one might envision a measuring mechanism whereby the number of phosphorylated DAHP synthase molecules imported are matched by the number of phosphorylated EPSP molecules exported. A rationale for such a scheme might be that it provides a mechanism to utilize most of the pathway machinery of the chloroplast, while bypassing the allosterically controlled steps. Thus, events of carbohydrate metabolism that influence phosphoenolpyruvate and erythrose 4-P availability in the cytosol could impact directly upon aromatic amino acid production in the cytosol, independently of the tight allosteric control exercised in the plastid. This mechanism could tie carbohydrate levels to output of secondary metabolites.

### Approaches to Demonstrate an Intact Cytosolic Pathway

The scheme shown in Figure 1 is complicated, and simpler explanations to account for the difficulties encountered to date in demonstrating cytosolic isozymes are a logical first course of action. Possibilities currently under evaluation are: (i) Most cytosolic isozymes may be particulate; (ii) Different enzymatic routes may be employed in the cytosol; (iii) Detection of cytosolic isozymes may require conditions of secondary metabolism (e.g., after wounding) that maximize expression levels of enzyme; and (iv) Detection of cytosolic isozymes may require conditions of normal growth physiology that maximize expression levels of enzyme.

### Materials and Methods

*Solubilization of Membrane Proteins.* A modification of the procedure of Hjelmeland *et al.* (30) was employed. A 300-g portion of liquid-nitrogen frozen, 6-day *Nicotiana glauca* cultured cells was suspended in 200 ml of 50 mM N-(2-hydroxyethyl)-piperazine-N'-3-propanesulfonic acid (EPPS-KOH) buffer, 1 mM dithiothreitol (DTT), and 0.1 mM EDTA extraction buffer with constant stirring until completely suspended (20 min). The slurry was centrifuged in a Sorvall SS 34 rotor at 9,000g for 20 min at 4°C. The supernatant was passed through miracloth (Calbiochem). An aliquot



was removed, desalted on a PD10 column (Pharmacia), and designated Supernatant I. The remaining extract was ultracentrifuged at 160,000g at 4°C for 30 min in a 70.1 Ti rotor. The supernatant was removed, desalted as above, and labeled Supernatant II. Pellets were resuspended in 0.5-2.0 ml of buffer, pooled, and ultracentrifuged as above. The supernatant, desalted as above, was designated Pellet Wash. The pellets were resuspended in extraction buffer and homogenized with three strokes of a tissue homogenizer. After protein determination, aliquots of the extract were diluted with extraction buffer and the designated detergent to give a final protein concentration of 5 mg/ml and the critical micelle concentration of detergent. We used octyl glucoside, CHAPS (3-[(3-cholamidopropyl)-dimethylammonio]-1-propanesulfonate), deoxycholate, Triton X-100, and NP-40 (Sigma non-ionic detergent p-40) detergents (29). An aliquot of extract to which no detergent was added was included as an unsolubilized control. The sample mixtures were stirred for 60 min at 4°C in 5-ml beakers and then ultracentrifuged for 30 min (4°C) at 160,000g.

Three preliminary experiments were carried out: the first done as described above, the second utilized a modified buffer containing protectants, and the third utilized both the modified buffer and a hemoglobin gel step to remove proteases. The modified buffer had the following recipe: 50 mM EPPS-KOH buffer at pH 8.6, 20% (v/v) glycerol, 1.0 mM EDTA, 1.0 mM DTT, 0.5 mM phenylmethylsulfonyl fluoride (PMSF), 0.05 mM leupeptin, and 0.05%  $\beta$ -mercaptoethanol.

*Removal of Proteases.* Proteases pose a fundamental obstacle in the isolation and purification of enzymes from higher plants. Although we routinely include protease inhibitors such as PMSF or leupeptin in extraction and column chromatography buffers, considerable protease activity persists. We successfully utilized hemoglobin-bound Sepharose, based on the column method of Chua and Bushuk (31), to remove the bulk of proteases from crude extracts of *N. silvestris*. Substrate (protease) grade bovine hemoglobin (Sigma) was coupled to CNBr-activated Sepharose 4B (Pharmacia), according to manufacturer recommendations. Glycine (0.2 M) was used to block remaining active groups. Alternate washes with high- and low-pH buffer solutions were used to remove excess adsorbed protein. After equilibration with extraction buffer, the hemoglobin-bound Sepharose was ready for use. We added 25 ml of hemoglobin-Sepharose conjugate per 200 ml of crude extract contained in a polypropylene centrifuge bottle, and this mixture was rotated end-over-end for 30 min at 4°C. The hemoglobin-bound Sepharose was then removed by centrifugation (2,000g for 10 min at 4°C), and the supernatant was carefully removed.

*Enzyme Assays.* Procedures for the HPLC assay of prephenate aminotransferase (32), the spectrophotometric assay of shikimate dehydrogenase (33), the spectrophotometric assay of arogenate dehydrogenase (34), and the thiobarbituric acid assay of DAHP synthase (29) were carried out as referenced. When the DS-Co isozyme was assayed with glyceraldehyde-3-P, 6mM DL-glyceraldehyde-3-phosphate (Sigma) was used.

## Results and Discussion

*Particulate Enzymes?* One of the greatest challenges in the field of enzymology and metabolic regulation is the analysis of enzyme organization *in vivo*. It is becoming increasingly apparent that "most so-called soluble enzymes do not exist as such *in vivo*" (35,36). Recent studies have provided evidence for the membrane association of "soluble" enzymes of the glycolytic pathway (37,38), Calvin cycle (39), and flavonoid metabolism (17,40). Metabolic pathways or biochemical segments are not merely the summed properties of individual enzyme steps—although this has been the essential approach for progress in the past. The subtleties of the organization of the enzymes of the glycolytic network, a previously classical example of "soluble" enzymes, exemplify this point. Aside from instances of obvious organization of multiple catalytic domains in the form of multifunctional proteins, enzymes may be membrane-bound as integral or peripheral proteins. These, in turn, may be associated with other enzyme proteins. The state of association or dissociation may have regulatory or developmental significance in a metabolic system that possesses a highly integrated arrangement of interlocking enzymic components. The rapid expansion in this topic area is illustrated by a recent flurry of publications describing covalent and noncovalent interactions between lipids and proteins with respect to association of proteins with membranes (41). Proteins able to interact specifically with lipids and directly with hydrophobic domains of membrane in a reversibly associating fashion have been termed amphitropic proteins (36). Recognition and preservation of such organizational features of enzyme networks is obviously of great relevance to the current sophistication of modern science goals of manipulating metabolic pathways for beneficial advances in medicine and agriculture.

Chalcone synthase, the first enzyme committed to flavonoid biosynthesis, is a membrane-bound protein (40). Since it is readily solubilized, it had previously been regarded as a soluble enzyme. Likewise, DS-Co and CM-2 may prove to be membrane-organized proteins that are readily solubilized.

High priority is being given to assessment of the extent to which aromatic-pathway isozyme species may be not at all (or only partially) solubilized with routine procedures typically used for extract preparation in our laboratories. For preliminary experimentation, we selected prephenate aminotransferase, arogenate dehydrogenase, and shikimate dehydrogenase. With the former two enzymes, minor peaks have been resolved following chromatographic procedures. With shikimate dehydrogenase, only a single large peak has been found in numerous chromatographic separations. However, a systematic purification/resolution using high-efficiency HPLC columns has not been attempted. For each enzyme, the following data obtained are consistent with the possibility that detergent-solubilized isozymes may indeed exist.

*Prephenate aminotransferase:* The specific activity of this enzyme in Supernatant I was 19.2 nmol/min/mg, and the total activity was retained in Supernatant II following centrifugation at 60,000g. The homogenized pellet (about 300 mg of protein) exhibited enzyme activity (specific activity of

0.53). A similar activity level was obtained in the deoxycholate, Triton X-100, and NP-40 extract preparations. Octyl glucoside and CHAPS extract preparations showed no detectable prephenate aminotransferase activity. When the hemoglobin step was used, there was no increase in the soluble activity recovered in the initial supernatant fraction, but the specific activity of the deoxycholate (the only detergent tried in this experiment) extract increased about tenfold. We would anticipate equally good results with use of Triton X-100 or NP-40 in combination with the hemoglobin step.

*Shikimate dehydrogenase:* The use of modified buffer increased the specific activities (S.A.) of this enzyme in the soluble supernatant preparations about sixfold (from 3.0 to 20.3). In addition, activity not otherwise measured in the homogenized pellet was found there with the use of modified buffer. In modified buffer shikimate dehydrogenase activity (e.g., S.A. = 0.67 in octyl glucoside buffer) could be found in all of the detergent-extract preparations. As above, the hemoglobin step increased dramatically the S.A. of shikimate dehydrogenase assayed in detergent-extract preparations.

*Arogenate dehydrogenase:* The use of modified buffer was essential for detection of arogenate dehydrogenase in either the soluble supernatant or in any of the particulate-derived fractions. (Glycerol is known to be critical for stability of the soluble plastidic enzyme). In modified buffer the soluble supernatant S.A. was 3.4 nmol/min/mg. The homogenized pellet exhibited excellent activity (S.A. = 0.89), but only marginal activity was detected when attempts were made to solubilize this via detergent extraction. Interestingly, a simple high-salt extraction (0.3 M KCl) of the homogenized-pellet sample solubilized a significant portion of the activity (S.A. = 0.44).

*A Different Pathway?* Prior to the discovery of L-arogenate (42), the post-prephenate pathway of aromatic amino acid biosynthesis was thought to be universal. This post-prephenate pathway now exemplifies the biochemical diversity that can exist in nature for even major metabolic pathways (43-45). With this precedent, perhaps the common-pathway sequence of reactions in early aromatic biosynthesis should not be taken for granted. Figure 2 shows the alternative phenylpyruvate and arogenate routes to phenylalanine now known to exist in nature. The difference is a simple matter of the order of the two enzymic steps: sidechain transamination, or decarboxylation/dehydration/aromatization. The order of catalytic steps dictates whether phenylpyruvate or arogenate will be unique molecules in the system. By analogy, a hypothetical possibility is shown in Figure 3, in consideration of catalytic steps 3 and 4 of the common shikimate pathway. There is no reason *a priori* why the two steps of the classical pathway shown (forming dehydroshikimate) could not occur in the opposite order. This would replace dehydroshikimate with quinate as a unique intermediate. As far as we know, existing tracer studies would not have revealed this in view of the complications imposed by the coexisting, highly active plastidic pathway. In *Zea mays* a bifunctional dehydroquinase/quinatase:NAD dehydrogenase has been reported (46). This protein could possibly cat-

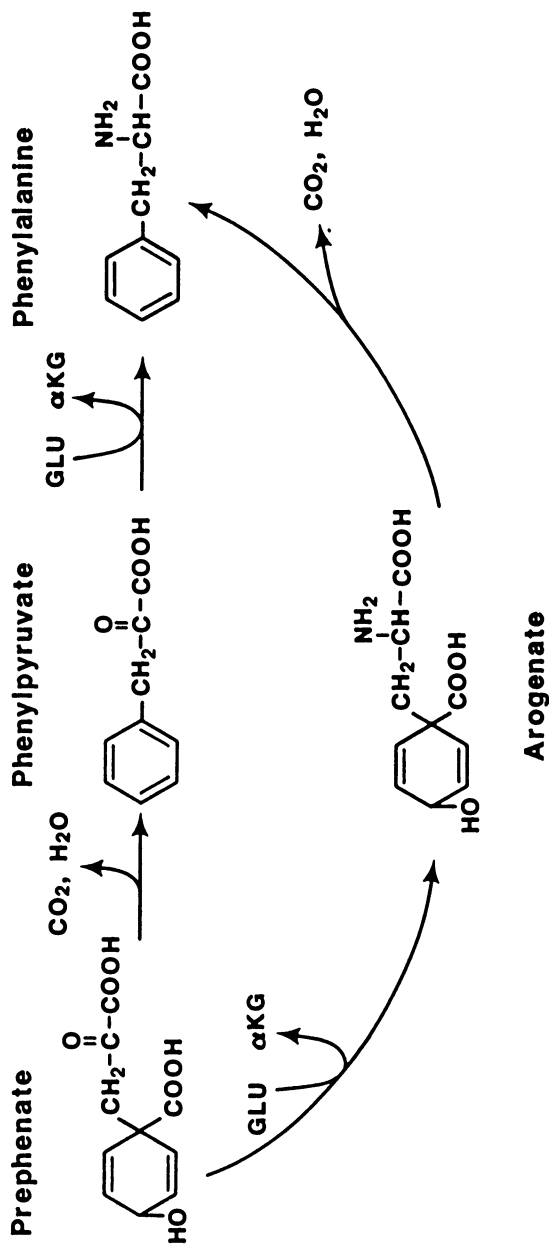


Figure 2. Alternative enzymatic routing for L-phenylalanine biosynthesis. Dehydration followed by transamination defines the phenylpyruvate route, whereas the reverse order of reactions defines the arogenate route. Abbreviations: GLU, L-glutamate; αKG, 2-ketoglutarate.

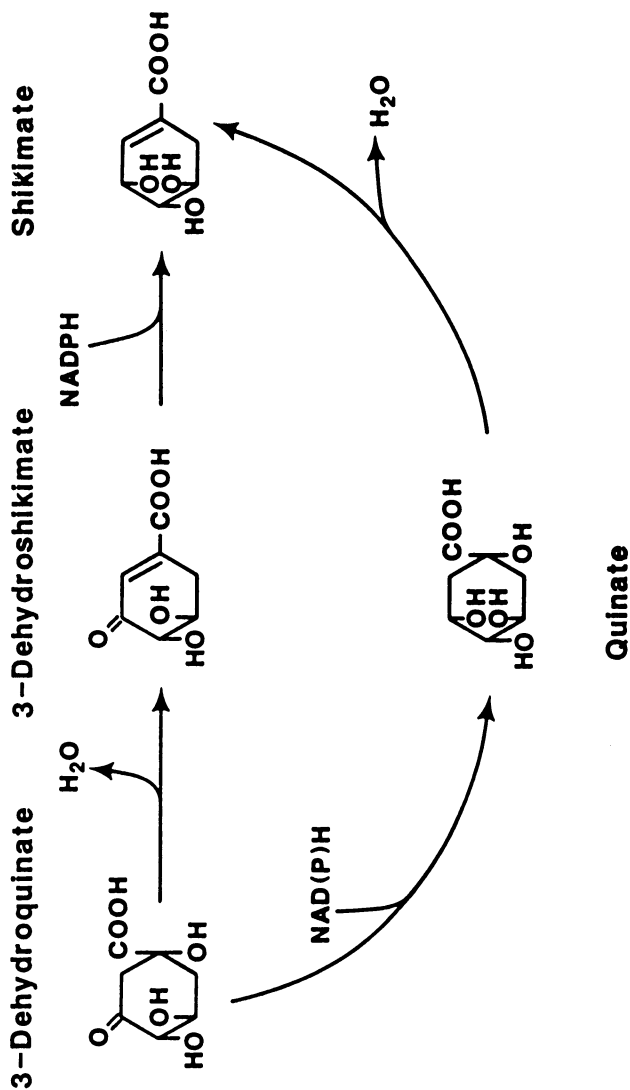


Figure 3. Hypothetical alternative enzyme path between 3-dehydroquininate and shikimate. A reversed order of the dehydratase and dehydrogenase steps of the classical pathway (top) would produce the quinate route (bottom).

alyze the sequence of steps shown in the bottom path of Figure 3. It is of further interest that the existence of a quinate dehydratase reaction was also suggested (46), albeit within the context of a different overall pathway scheme.

A far more drastic possibility is suggested (Figure 4) by the observation that DS-Co is catalytically active when erythrose 4-P is replaced with glyceraldehyde 3-P as substrate. The glyceraldehyde 3-P/PEP combination is in fact several-fold better than the erythrose 4-P/PEP combination. DS-Mn does not exhibit this breadth of substrate recognition, nor do any of a number of microbial DAHP synthase enzymes available in our laboratories. Broad substrate specificity of enzymes is not unusual, but recognition of non-substrate molecules is almost always of minor magnitude compared to the normal substrate. Could 2-keto-3-deoxy-D-threo-hexulose-6-phosphate, a new metabolite similar to 3-deoxy-6-phosphogluconate of the microbial Entner-Doudoroff pathway, in fact be an intermediate of aromatic amino acid biosynthesis in the cytosol? A possible scheme is outlined in Figure 5. Although the pathway shown is more expensive than is the classical pathway (by virtue of the utilization of an additional ATP), this may be offset by the plentiful availability of triose-phosphate exported to the cytosol as output from operation of both the reductive and oxidative pentose phosphate pathways in the plastid.

*Manipulation of Isozyme Expression by Environmental Treatments.* An impressive battery of diverse environmental or biochemical manipulations are known that cause elevation of general phenylpropanoid-pathway or flavonoid-pathway enzymes. These include mechanical wounding, illumination, administration of fungal elicitors, presence of ethylene, and dilution of cell cultures in water. Since increased aromatic amino acid biosynthesis is needed to supply initial precursor molecules of secondary metabolism, one might anticipate that overall response to environmental treatment may include elevation of some or all enzymes of aromatic amino acid biosynthesis. Scattered information indicates this to be so. Shikimate dehydrogenase has been shown to increase in level upon wounding (47). In a clever experiment with buckwheat (48), shikimate accumulation caused by glyphosate (inhibitor of EPSP synthase, see Figure 1) treatment was found to be much greater in the light than in the dark, indicating that illumination enhances early-pathway activity levels.

To what extent is the response of cytosolic and plastidic isozymes of the shikimate pathway coordinated or coupled with one another and to alterations in expression of enzymes of the flavonoid and phenylpropanoid-pathway segments? Some of the emerging information is given in Figure 6. Thus, light induction, well known to induce PAL and enzymes of the flavonoid pathway, also induces both DS-Mn and DS-Co in parsley cell cultures (49). However, only the cytosolic CM-2 (and not the plastidic CM-1) was induced. Fungal elicitor was reported to induce only DS-Mn—not DS-Co or either of the chorismate mutase isozymes (49). Previous studies (50) had indicated an absence of elicitor effects upon overall DAHP synthase and shikimate dehydrogenase activities, but these experiments were

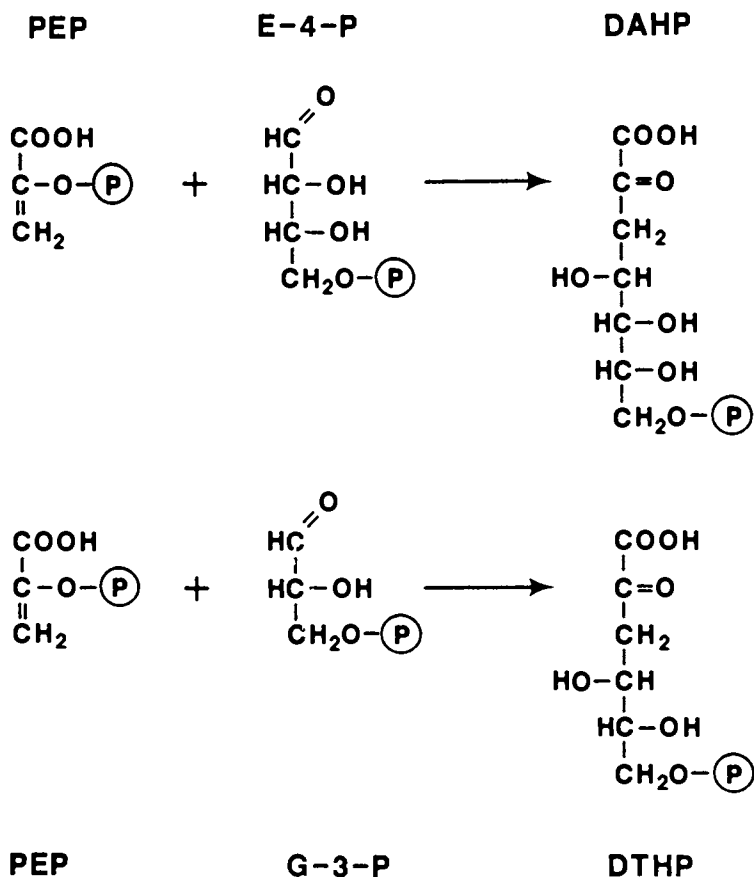


Figure 4. Reactions catalyzed by the broad-specificity DAHP synthase-Co of higher plant cytosol. Condensation of PEP and erythrose 4-P (top) yields 3-deoxy-D-arabino-heptulosonate 7-P (DAHP), whereas condensation of PEP and D-glyceraldehyde 3-P (G-3-P) yields 2-keto-3-deoxy-D-threo-hexulosonate 6-P (DTHP).

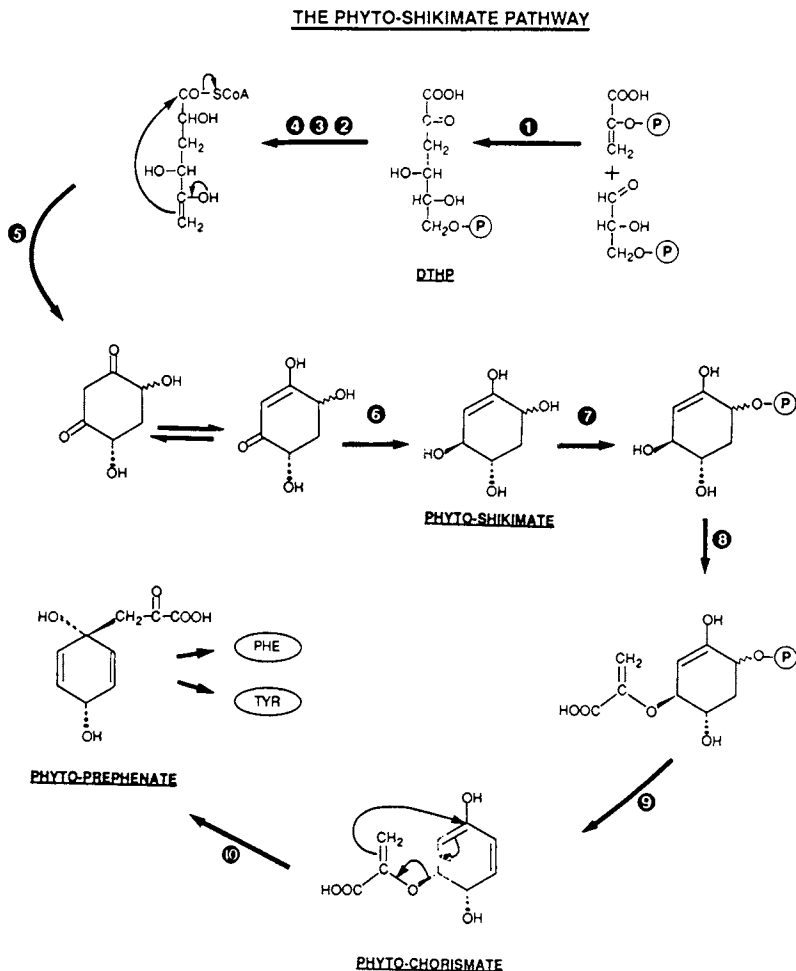


Figure 5. Hypothetical scheme based on condensation of two  $C_3$  substrate species (instead of  $C_3 + C_4$ ), where glyceraldehyde 3-phosphate replaces erythrose 4-phosphate. The enzymes involved are: (1) a synthase (analogous to DAHP synthase), (2) a NAD(P)H-dependent dehydrogenase, (3) an acyl coenzyme A synthase requiring ATP and coenzyme A, (4) a phosphoric acid elimination, and (5) an enzyme catalyzing the Claisen condensation and producing a product in keto-enol equilibrium. The subsequent reactions are reminiscent of the shikimate pathway: (6) a NAD(P)H-dependent dehydrogenase leading to the shikimate analog denoted phyto-shikimate, (7) a kinase, (8) condensation with phosphoenolpyruvate, (9) elimination of phosphoric acid leading to a hypothetical chorismate analog denoted phyto-chorismate, and (10) a Claisen rearrangement catalyzed by a mutase to yield the prephenate analog, denoted phyto-prephenate.



Treatment	Cytosolic Enzyme			Plastid Enzyme	
	[PAL]	[CHS]	[DS-Co]	[DS-Mn]	[CM-1]
Mechanical wounding	↑	↑	↑	↑	↑
Illumination	↑	↑	↑	↑	↑
Fungal elicitors	↑	↑	→	↑	↑
Ethylene	↑	↑			
Cell-culture starvation	↑	→			
Cell-culture stationary phase			↑		↑

Figure 6. Effects of various treatments or manipulations upon levels of phenylalanine ammonia-lyase (PAL), chalcone synthase (CHS), and the separately compartmented isozymes of DAHP synthase and chorismate mutase. Upwardly pointed arrows indicate a positive response (enzyme elevation) to the indicated treatment, whereas horizontal arrows indicate no change in enzyme level. References documenting the results shown are: line 1 (54); our results with DAHP synthase and chorismate mutase isozymes); line 2 (49,55); line 3 (49,50,56); line 4 (57); line 5 (51); line 6 (52).

limited to the 24-h period following elicitor treatment. Hahlbrock and Schroder (51), using *Petroselinum hortense* cell cultures, found that effects of dilution (nutrient starvation) were limited to enzymes of general phenylpropanoid metabolism—whereas irradiation with light additionally induced the flavonoid glycoside pathway. A concerted, coordinated effort in which key enzymes of secondary metabolism (e.g., PAL and chalcone synthase) are examined in relationship to the differently compartmented isozymes of aromatic biosynthesis (e.g., DS-Mn/DS-Co and CM-1/CM-2), following the variety of environmental treatments available will be of obvious value.

We have examined the time course of changes induced in isozymes of chorismate mutase and DAHP synthase in potato tubers following mechanical wounding (Table III). In each case both isozymes responded—the plastidic isozyme responding sooner and to a greater extent than the cytosolic isozyme. All five of the other pathway enzymes so far examined were induced by mechanical wounding.

Table III. Response of aromatic-pathway enzymes to mechanical wounding

Enzyme <sup>a</sup>	Fold <sup>b</sup>	Peak Activity <sup>c</sup>	Peak Day <sup>d</sup>
DAHP synthase-Mn	2	21	1.5
Chorismate mutase-1	8	46	4
DAHP synthase-Co	1.5	51	2
Chorismate mutase-2	3	7	4
Shikimate dehydrogenase	5	220	6
Shikimate kinase	3	35	5
EPSP synthase	4	70	5
Prephenate aminotransferase	2	34	2
Arogenate dehydrogenase	2	1.5	5

<sup>a</sup> Enzymes are grouped (from top to bottom) as plastidic isozymes, cytosolic isozymes, or total activities of unknown mixtures.

<sup>b</sup> Approximate factor of specific activity increase, comparing values obtained on the day of peak activity following wounding, with unwounded controls.

<sup>c</sup> Expressed as  $\text{nmol min}^{-1}\text{mg}^{-1}$ .

<sup>d</sup> Approximate post-wounding day when maximal activity was observed throughout a 6-day interval.

Although the plastidic isozymes of DAHP synthase and chorismate mutase respond to wounding to a greater extent than do the cytosolic isozymes, wounding offers good prospects as a manipulation that may help unmask cytosolic isozymes by increasing their levels. For example, suggestive data were obtained with arogenate dehydrogenase and shikimate dehydrogenase, where a second rise in activity between days 4 and 5 after wounding might reflect the relatively slow elevation response of a cytosolic isozyme. A fuller account of these results has been given by Morris *et al.* (*Life Sci. Advances - Plant Physiol.* 1988, 7, in press).

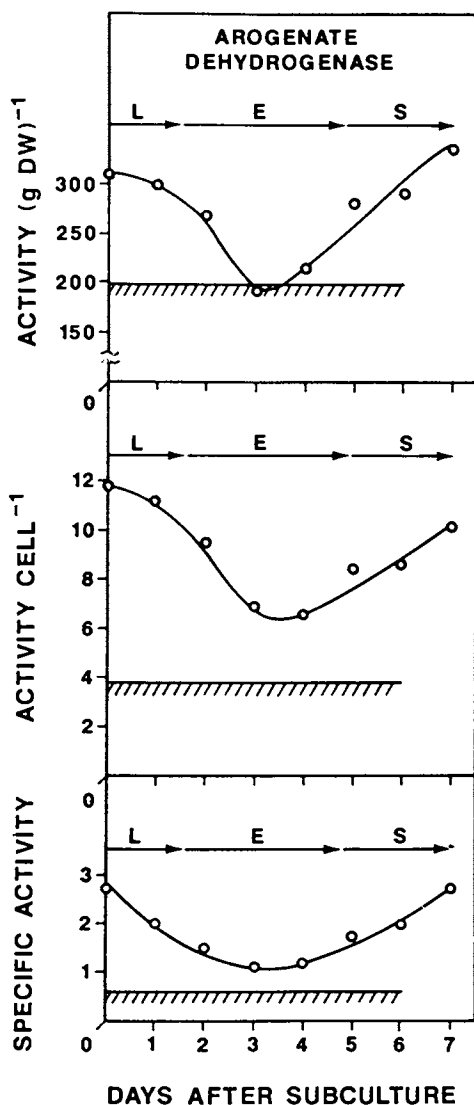


Figure 7. Variation of aroenate dehydrogenase levels as a function of the physiological phase of growth in suspension cultures of *Nicotiana silvestris*. A stationary-phase inoculum was diluted into fresh medium and followed throughout the lag (L), exponential (E), and stationary (S) phases of growth. The hatched bar indicates the activity levels of EE cells, i.e., cells maintained continuously in exponential growth for 10 or more generations (53). Profiles are shown in which activity is related to soluble protein (specific activity), to cell number, or to dry weight.

Since the presumed cytosolic pathway interfaces directly with the network of secondary metabolism, the observed induction of DS-Co and CM-2 isozymes in response to wounding was expected. However, the even greater response of plastidic isozymes was unexpected. Perhaps the increased "pull" on carbohydrate metabolism in the cytosol affects the balance of substrates feeding into the aromatic pathway of the plastid. If so, a tendency to starvation for pathway endproducts may trigger derepression of the plastidic-pathway isozymes.

*Physiological Manipulation of Isozyme Expression.* Recent studies in our laboratory have indicated that enzymes of the aromatic amino acid pathway change with the growth phase in cultured cells of *N. silvestris* (33). The cytosolic enzyme Ds-Co reaches its highest level of expression in the stationary phase of growth (52). The cytosolic CM-2 is highest in leaf tissue compared to exponentially growing cells in suspension culture (1)—indicating a wide range of expression, depending upon the physiological conditions. The overall elevation of enzymes in stationary-phase cells may reflect an increase in secondary metabolism and an increased complement of cytosolic enzymes.

Data obtained for arogenate dehydrogenase, in which activity was followed throughout a growth curve initiated by the subculture of stationary-phase cells, are shown in Figure 7. Activity levels characteristic of cells maintained indefinitely in exponential phase (EE cells) (53) are increased when cultures are allowed to progress into the stationary phase of growth. When cell cultures were harvested in late exponential-phase growth (day 4) as the source of extract for DEAE-cellulose chromatography, a major and a minor peak of arogenate dehydrogenase were resolved (Bonner, unpublished data). Perhaps the minor peak of activity will be enhanced when stationary-phase cells are used—the implication being that it is an isozyme located in the cytosol.

## Conclusion

Aromatic amino acids interface with a diverse and vast network of connecting secondary metabolism in the cytosol, but not in other major compartments such as the chloroplast. A strong rationale and emerging lines of experimental evidence support the probable existence of an intact cytosolic pathway of aromatic amino acid biosynthesis which links carbohydrate metabolism (via PEP and erythrose-4-P, or possibly glyceraldehyde-3-P) and secondary metabolism.

## Acknowledgments

This research was supported by Department of Energy contract DE-FG05-86ER13581.

## Literature Cited

1. Jensen, R. A. *Rec. Adv. Phytochem.* 1986, **20**, 57-82.

2. Bonner, C. A.; Jensen, R. A. *Arch. Biochem. Biophys.* 1985, **238**, 237-46.
3. Bonner, C. A.; Jensen, R. A. *Planta* 1987, **172**, 417-23.
4. Zamir, L. O.; Jensen, R. A.; Arison, B.; Douglas, A.; Bowen, J. R. *J. Am. Chem. Soc.* 1980, **102**, 4499-504.
5. Jung, E.; Zamir, L. O.; Jensen, R. A. *Proc. Natl. Acad. Sci. USA* 1986, **83**, 7231-35.
6. Siehl, D. L.; Conn, E. E. *Arch. Biochem. Biophys.* 1988, **260**, 822-29.
7. Gaines, C. G.; Byng, G. S.; Whitaker, R. J.; Jensen, R. A. *Planta* 1982, **156**, 233-40.
8. Connelly, J. A.; Conn, E. E. *Z. Naturforsch.* 1986, **41c**, 69-78.
9. Brotherton, J. E.; Hauptmann, R. M.; Widholm, J. M. *Planta* 1986, **168**, 214-21.
10. Gilchrist, D. G.; Kosuge, T. *Arch. Biochem. Biophys.* 1974, **164**, 95-105.
11. Goers, S. K.; Jensen, R. A. *Planta* 1984, **162**, 117-24.
12. Singh, B. K.; Connelly, J. A.; Conn, E. E. *Arch. Biochem. Biophys.* 1985, **243**, 374-84.
13. Jensen, R. A. *Physiol. Plant.* 1986, **66**, 164-68.
14. Rubin, J. L.; Jensen, R. A. *Plant Physiol.* 1985, **79**, 711-18.
15. Nester, E. W.; Jensen, R. A. *J. Bacteriol.* 1966, **91**, 1594-98.
16. Whitaker, R. J.; Berry, A.; Byng, G. S.; Fiske, M. J.; Jensen, R. A. *J. Mol. Evol.* 1985, **21**, 139-49.
17. Hrazdina, G.; Wagner, G. J. *Arch. Biochem. Biophys.* 1985, **237**, 88-100.
18. Gottlieb, L. D. *Science* 1982, **216**, 373-80.
19. Bickel, H.; Palme, L.; Schultz, G. *Phytochemistry* 1978, **17**, 119-24.
20. Buchholz, B.; Reupke, B.; Bickel, H.; Schultz, G. *Phytochemistry* 1979, **18**, 1109-11.
21. Mousdale, D. M.; Coggins, J. R. *Planta* 1985, **163**, 241-49.
22. Mousdale, D. M.; Campbell, M. S.; Coggins, J. R. *Phytochemistry* 1987, **26**, 2665-70.
23. Ream, J. E.; Steinrücken, H. C.; Porter, C. A.; Sikorski, J. A. *Plant Physiol.* 1988, **87**, 232-38.
24. Wendel, J. F.; Goodman, M. M.; Stuber, C. W.; Beckett, J. B. *Biochem. Gen.* 1988, **26**, 421-45.
25. Ganson, R. J.; d'Amato, T. A.; Jensen, R. A. *Plant Physiol.* 1986, **82**, 203-10.
26. d'Amato, T. A.; Ganson, R.; Jensen, R. A. *Planta* 1984, **162**, 104-08.
27. Kuroki, G. W.; Conn, E. E. *Arch. Biochem. Biophys.* 1988, **260**, 616-21.
28. Pinto, J.; Suzich, J. A.; Herrmann, K. M. *Plant Physiol.* 1986, **82**, 1040-44.
29. Morris, P. F.; Doong, R.-L.; Jensen, R. A. *Plant Physiol.* 1989, **89**, 10-14.
30. Hjelaland, L. M.; Chrumbach, A. *Methods Enzymol.* 1984, **104**, 305-18.

31. Chua, G. K.; Bushuk, W. *Biochem. Biophys. Res. Commun.* 1969, **37**, 545-50.
32. Bonner, C. A.; Jensen, R. A. *Meth. Enzymol.* 1987, **142**, 479-87.
33. Bonner, C. A.; Vrba, J.; Jensen, R. A. *Physiol. Plant.* 1988, **73**, 451-56.
34. Bonner, C. A.; Jensen, R. A. *Meth. Enzymol.* 1987, **142**, 488-94.
35. Wombacher, H. *Mol. Cell. Biochem.* 1983, **56**, 155-64.
36. Keleti, T.; Vertessy, B.; Welch, G. R. *J. Theor. Biol.* 1988, **135**, 75-83.
37. Moorehead, G. B. G.; Plaxton, W. C. *Plant Physiol.* 1988, **86**, 348-51.
38. Andres, A. R.; Lazaro, J. J.; Chueca, A.; Hermoso, R.; Lopez-George, J. *Plant Sci.* 1987, **52**, 41-8.
39. Gontero, B.; Cardenas, M. L.; Ricard, J. *Eur. J. Biochem.* 1988, **173**, 437-43.
40. Hrazdina, G.; Zobel, A. M.; Hoch, H. C. *Proc. Natl. Acad. Sci. USA* 1987, **84**, 8966-70.
41. Burn, P. *Trends Biochem. Sci.* 1988, **13**, 79-83.
42. Stenmark, S. L.; Pierson, D. L.; Glover, G. I.; Jensen, R. A. *Nature* 1974, **247**, 290-92.
43. Byng, G. S.; Kane, J. F.; Jensen, R. A. *Crit. Rev. Microbiol.* 1982, **9**, 227-52.
44. Jensen, R. A. *Mol. Biol. Evol.* 1985, **2**, 92-108.
45. Ahmad, S.; Jensen, R. A. *Origins of Life* 1988, **18**, 41-57.
46. Graziana, A.; Boudet, A.; Boudet, A. M. *Plant Cell Physiol.* 1980, **21**, 1163-74.
47. Kojima, M.; Minamikawa, T.; Uritani, I. *Plant Cell Physiol.* 1969, **10**, 245-57.
48. Amrhein, N.; Holländer, H. *Naturwissenschaften* 1981, **68**, 43.
49. McCue, K. F.; Conn, E. E. *Amer. Soc. Plant Physiol. Abstr.* 1988, **86**, #642, 107.
53. Robbins, M. P.; Bolwell, G. P.; Dixon, R. A. *Eur. J. Biochem.* 1985, **148**, 563-69.
51. Hahlbrock, K.; Schroder, J. *Arch. Biochem. Biophys.* 1985, **171**, 500-06.
52. Ganson, R. J.; Jensen, R. A. *Plant Physiol.* 1987, **83**, 479-82.
53. Bonner, C. A.; Kenyon, C.; Jensen, R. A. *Physiol. Plant.* 1988, **74**, 1-10.
54. Whitehead, I. M.; Dey, P. M.; Dixon, R. A. *Planta* 1982, **154**, 156-64.
55. Hrazdina, G.; Parsons, G. F. *Plant Physiol.* 1982, **70**, 506-10.
56. Cramer, C. L.; Bell, J. N.; Ryder, T. B.; Bailey, J. A.; Schuch, W.; Bolwell, G. P.; Robbins, M. P.; Dixon, R. A.; Lamb, C. J. *EMBO J.* 1985, **4**, 285-89.
57. Ecker, J. R.; Davis, R. W. In *Molecular Biology of Plant Growth Control*; Fox, J.E.; Jacobs, M., Eds.; Alan R. Liss: New York, 1987; pp. 133-43.

RECEIVED March 10, 1989

## Chapter 7

# Enzymology of Gallotannin Biosynthesis

Georg G. Gross

Universität Ulm, Abteilung Allgemeine Botanik, Oberer Eselsberg,  
D-7900 Ulm, Federal Republic of Germany

Ample knowledge available to date of the chemistry and natural distribution of a wide variety of galloylglucose esters has led to the view that both gallotannins and the structurally related ellagitannins are derived from one common precursor, 1,2,3,4,6-*O*-pentagalloyl- $\beta$ -D-glucose. Recent investigations with enzymes from oak or sumach leaves have shown that the biosynthesis of this polyphenolic ester is initiated by the formation of  $\beta$ -glucogallin (1-*O*-galloyl- $\beta$ -D-glucose) from UDP-glucose and free gallic acid. This monoester, in turn, was found to serve as the activated acyl-donor in a series of subsequent transacylation steps, yielding specifically substituted di-, tri-, tetra-, and finally pentagalloylated glucose derivatives. In contrast, the biosynthesis of gallic acid itself is still largely obscure, and this applies also to the final steps of the entire biogenetic sequence, i.e., the mechanisms involved in the formation of meta-depside linkages and hexahydroxydiphenyl residues characterizing gallotannins and ellagitannins, respectively.

Vegetable tannins are commonly classified into condensed tannins (or proanthocyanidins), which are of flavonoid origin, and hydrolyzable tannins, which are characterized by a central polyol moiety (mostly  $\beta$ -D-glucose) whose hydroxyl groups are esterified with gallic acid. These polyphenolic compounds can be further substituted with additional galloyl residues attached via meta-depside linkages, giving rise to the formation of the gallotannins proper (Figure 1). Alternatively, dimerization of adjacent galloyl groups can occur, yielding the hexahydroxydiphenyl residues characteristic of the related ellagitannins (Figure 2); after hydrolytic release, these biphenyl derivatives rearrange spontaneously to give the stable name-giving dilactone, ellagic acid.

0097-6156/89/0399-0108\$06.00/0

© 1989 American Chemical Society

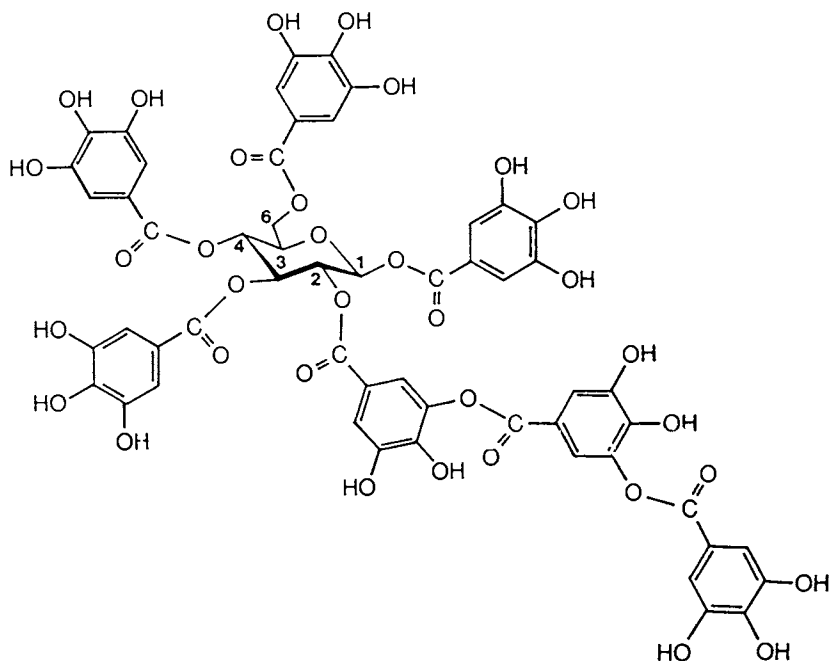


Figure 1. Structure of a gallotannin typical of chinese gallotannin, found, e.g., in galls of *Rhus semialata*. Note the characteristic meta-depside linkages of the galloyl residues at C-2.

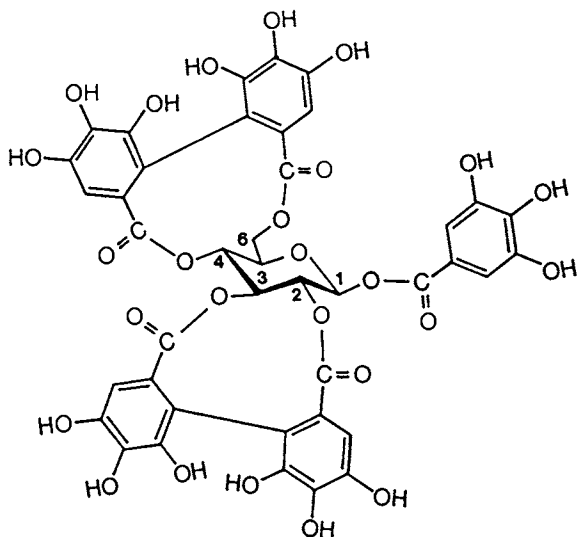


Figure 2. Structure of an ellagitannin, 1-*O*-galloyl-2,3:4,6-di-*O*-hexahydroxydiphenoyl- $\beta$ -D-glucose (casuarictin).



Innumerable variations of these fundamental structural principles have been detected in higher plants; discussion of which, however, lies beyond the scope of this article [for recent relevant reviews see, e.g., (1-7)]. This well documented detailed knowledge of the chemical configuration and natural distribution of hydrolyzable tannins stimulated thoughts on their biosynthesis (cf. 5-9). It was proposed that glucose and gallic acid initially combined to give  $\beta$ -glucogallin (1-*O*-galloyl- $\beta$ -D-glucose) which, in turn, underwent a series of further acylation reactions leading to pentagalloyl- $\beta$ -D-glucose. This latter ester was thought to function as the common precursor both of the gallotannins and the related ellagitannins. This plausible pathway was until a few years ago totally unproven. It now comprises several important aspects, namely (1) the formation of gallic acid, (2) the nature of the energy-rich intermediates required for the synthesis of  $\beta$ -glucogallin, (3) the transacylation mechanisms leading to pentagalloylglucose, and (4) the secondary transformations involved in the synthesis of gallotannins and ellagitannins.

As reported below, recent enzymatic studies have provided insight into several of these problems; in particular, many of the questions concerning the formation of  $\beta$ -glucogallin and its subsequent conversion to pentagalloylglucose have been answered by this technique. Other aspects outlined above remain rather obscure, but starting points for their eventual clarification will be discussed.

### Biosynthesis of Gallic Acid

In spite of numerous investigations during the past decades, the biosynthesis of gallic acid remained one of the major enigmas of plant phenolics metabolism. Based on feeding experiments with putative precursors, three different pathways, as depicted in Figure 3, were proposed [references in (2, 10, 11)]. Evidence was presented that gallic acid was produced by direct aromatization of dehydroshikimic acid (or shikimic acid). Alternatively, two routes via the phenylalanine-cinnamate pathway were postulated along which gallic acid was formed, either by  $\beta$ -oxidation of 3,4,5-trihydroxycinnamic acid (never detected in plants) or by the sequence caffeic  $\rightarrow$  protocatechuic  $\rightarrow$  gallic acid. Later, two short reports (12, 13) on work with cell-free systems were published suggesting a sequence dehydroshikimic  $\rightarrow$  protocatechuic  $\rightarrow$  gallic acid; unfortunately, these observations still await confirmation by more detailed studies.

Theoretically, many of the above discrepancies could be settled by experiments with carboxyl-labeled shikimic acid because this functional group would be lost in the formation of phenylalanine, but retained in the case of a direct conversion to gallic acid. Only ambiguous evidence was obtained, however, from such efforts (10), and it was concluded that at least two pathways for gallic acid biosynthesis must exist (14), with the preferential route depending on leaf age and plant species investigated (15, 16).

A different approach to discriminate between the two principal routes to gallic acid, i.e., via  $C_6C_3$ -intermediates *vs.* a direct conversion was de-

veloped. This uses glyphosate [N-(phosphonomethyl)glycine, an inhibitor of shikimic acid utilization] and L-2-aminooxy-3-phenylpropionic acid (L-AOPP, an inhibitor of phenylalanine deamination) in feeding experiments with labeled shikimic acid. While AOPP had no effect, glyphosate greatly enhanced the amount and radioactivity of the isolated gallic acid (17), indicating that the direct conversion of shikimic to gallic acid represented at least a significant, if not the major, route.

### Biosynthesis of $\beta$ -Glucogallin

The naturally occurring depside  $\beta$ -glucogallin (1-*O*-galloyl- $\beta$ -D-glucose) was considered the primary metabolite in the biosynthesis of hydrolyzable tannins (5, 7, 8). For thermodynamic reasons, the participation of an activated intermediate has to be postulated in the formation of such an ester. This requirement can be met in two ways, either by reaction of an energy-rich galloyl derivative with free glucose, or by using a nucleoside diphosphate-activated glucose (most likely UDPG) and the free acid. The results of our recent work on these aspects are presented below.

*Galloyl-Coenzyme A.* Numerous enzymatic studies on the formation of the ubiquitous plant phenolic chlorogenic acid (3-*O*-caffeoyl-D-quinic acid) and related depsides have showed that cinnamoyl-CoA thioesters were utilized as activated intermediates in these esterification reactions (Table I). By analogy, it appeared conceivable that galloyl-CoA might be involved in the biosynthesis of gallotannins. To test this hypothesis, this then unknown thioester was synthesized (26), via the *N*-succinimidyl derivative of 4-*O*- $\beta$ -D-glucosidogallic acid (cf. Figure 4), and characterized by spectrophotometric methods; the UV-spectrum was perhaps the most prominent property (Figure 5).

Table I. Phenolic Acid Esters Formed via Intermediate Acyl-Coenzyme A Esters

Donor	Acceptor	Product	Ref.
Caffeoyl-CoA	Quinate	Chlorogenate	18, 20
<i>p</i> -Coumaroyl-CoA	Quinate	3- <i>p</i> -Coumaroyl- quinate	19, 21
<i>p</i> -Coumaroyl-CoA	Shikimate	3- <i>p</i> -Coumaroyl- shikimate	22
<i>p</i> -Coumaroyl-CoA	Tartronate	<i>p</i> -Coumaroyl- tartronate	23
Caffeoyl-CoA	Isocitrate	Caffeoyliso- citrate	24
Hydroxycinnamoyl- CoAs	Sugar acids (glucuronate, glucarate, galactarate)	Monoesters; exact position of the <i>O</i> -ester group unclear	25

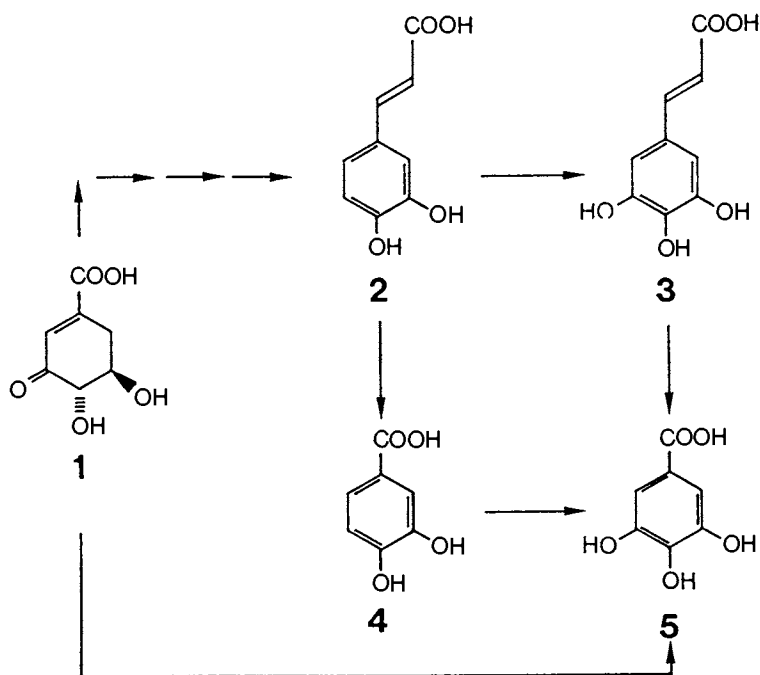


Figure 3. Proposed biosynthetic pathways to gallic acid (5). (1) Dehydroshikimic acid; (2) caffeic acid; (3) 3,4,5-trihydroxycinnamic acid; (4) protocatechuic acid.

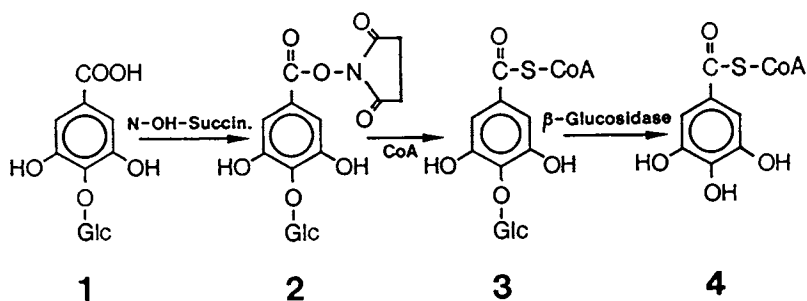
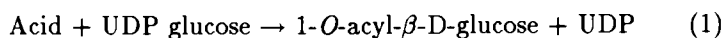


Figure 4. Chemical synthesis of galloyl coenzyme A thioester (4). (1) 4-O-β-D-glucosidogallic acid; (2) *N*-succinimidyl 4-O-β-D-glucosidogallate; (3) 4-O-β-D-glucosidogalloyl-CoA.

In enzymatic studies with cell-free extracts from higher plants, however, no evidence has been found to date for galloyl-CoA's involvement in the biosynthesis of  $\beta$ -glucogallin, or its higher galloylated derivatives; an eventual role in the formation of the chemically different meta-depside bonds of gallotannins has not been investigated.

*Formation of  $\beta$ -Glucogallin.* About the time as the above mentioned studies with galloyl-CoA were carried out, it became evident that glucose esters of phenolic acids could be formed by an alternate mechanism, i.e., by reaction of the free acid with UDP-glucose serving as the energy-rich component. This was because of a number of findings (27), where it was demonstrated that the conjugation of glucose with numerous benzoic and cinnamic acids (28-33), and indole-3-acetic acid (34,35), occurred according to the general mechanism shown below (Equation 1):



It therefore appeared that a general mechanism for enzymatic esterification of phenolic acids with glucose was operative, whereas the reaction with other alcoholic moieties proceeded via carboxyl-activated acyl derivatives. [In this context it should be emphasized that glucose esters must not be confused with glucosides; different enzymes are involved in the biosynthesis of these two types of phenolic glucose derivatives (36)].

It was thus not surprising to establish that  $\beta$ -glucogallin was also synthesized according to this mechanism (Figure 6) by enzyme preparations from tannin-producing oak leaves (37,38). Substrate specificity studies revealed that this glucosyl transferase depended exclusively on UDP-glucose as donor substrate, and that it exhibited activity toward a great variety of benzoic and cinnamic acids as acceptor molecules. Considering the growing importance of such esters within the area of general plant secondary metabolism, this latter property has recently been utilized for the convenient preparation and spectroscopic characterization (UV, IR,  $^1\text{H-NMR}$ ) of differently substituted 1-*O*-benzoyl- $\beta$ -D-glucoses (39), thus providing a convenient alternative to chemical syntheses [cf., e.g., (40)].

### $\beta$ -Glucogallin to Pentagalloylglucose

According to recent suggestions,  $\beta$ -glucogallin should undergo a series of position-specific galloylation steps to yield pentagalloylglucose (5-9). Elucidation of this hitherto unknown biogenetic sequence was established with enzyme preparations from young oak leaves (41); it was thus demonstrated that, by analogy with the preceding synthesis of  $\beta$ -glucogallin, galloyl-CoA was not required. Instead, both di- and trigalloylglucose were formed in the presence of  $\beta$ -glucogallin as the sole substrate, proving that this ester served also as an acyl donor (41). Supporting evidence from several laboratories also indicated that phenolic acid esters were not necessarily metabolically inert compounds but could be employed as activated intermediates for secondary transacylation reactions. As summarized in Table II, this new view was corroborated by many detailed enzyme studies.

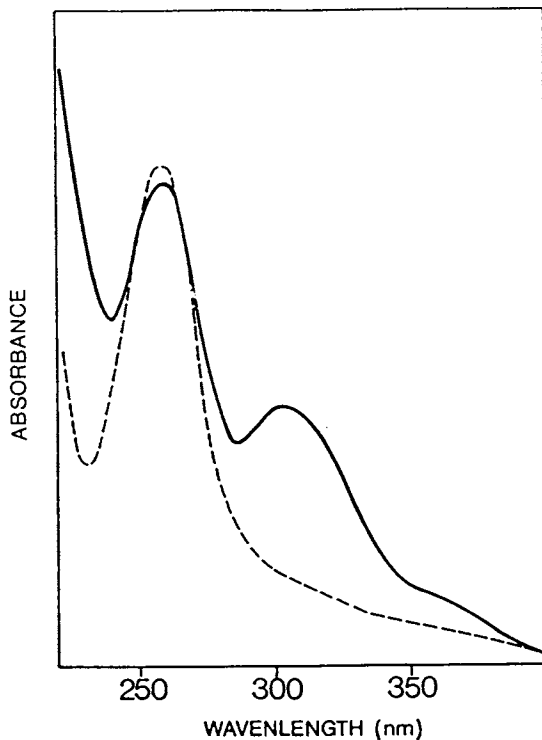


Figure 5. UV spectrum of galloyl coenzyme A. ( — ) Spectrum of the thioester; ( - - - ) spectrum after hydrolysis in 0.1N NaOH or hydroxylaminolysis in 1M  $\text{NH}_2\text{OH}$ , pH 6. Both spectra were recorded in 0.1M potassium phosphate buffer, pH 7.0.

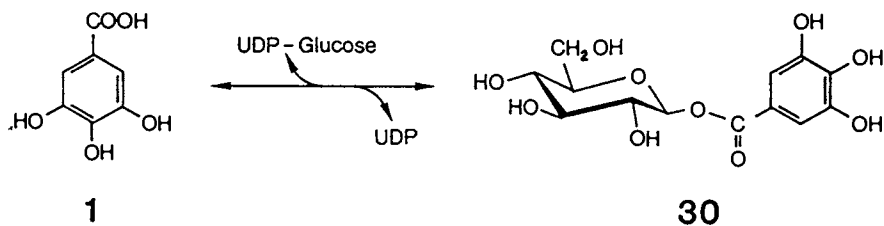


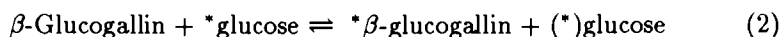
Figure 6. Enzymatic synthesis of  $\beta$ -glucogallin.

Table II. Biosynthesis of Aromatic Monoacyl Esters by Acyltransferases from Higher Plants

Donor	Acceptor	Product	Ref.
1- <i>O</i> -Sinapoylglucose	L-Malate	Sinapoyl-L-malate	42,43
1- <i>O</i> -Sinapoylglucose	Choline	Sinapoylcholine (Sinapine)	44-46
1- <i>O</i> -Indolylacetylglucose	myo-Inositol	Indolylacetylmyo-inositol	35
1- <i>O</i> -Caffeoylglucose	D-Quinate	Chlorogenate	47,48
1- <i>O-p</i> -Coumaroylglucose	D-Quinate	<i>p</i> -Coumaroylquininate	49
1- <i>O-p</i> -Coumaroylglucose	meso-Tartarate	<i>p</i> -Coumaroylmeso-tartarate	50
Chlorogenate	Glucarate	Caffeoylglucarate	51

With respect to gallotannins, substantial evidence indicated that  $\beta$ -glucogallin was also metabolically active, as the acyl donor for galloyltransferase reactions; some details related to this aspect are described below.

*Galloyl-Exchange between  $\beta$ -Glucogallin and Glucose.* Cell-free extracts from oak leaves produced labeled  $\beta$ -glucogallin when incubated with unlabeled glucogallin and [ $^{14}\text{C}$ ]glucose (41). This unexpected result was explained by the existence of an acyltransferase catalyzing the exchange reaction shown below:



where the asterisk indicates an appropriate label (e.g.,  $^{14}\text{C}$ ) to allow measurement of the reaction. Studies with the purified enzyme showed that it was active with various 1-*O*-benzoylglucose esters as donor substrates, while D-glucose functioned very specifically as the acceptor molecule. The physiological significance of this reaction is still unknown; however, it was successfully employed for the facile and rather economic preparation of labeled glucogallin and related esters, thus avoiding many problems involved in the chemical synthesis of such compounds (52,53).

*Biosynthesis of Digalloylglucose.* Besides the above mentioned acyltransferase, oak leaves also contained a completely different type of acyltransferase that catalyzed the formation of digalloylglucose (41). It became evident that this ester was synthesized by a new reaction mechanism in which  $\beta$ -glucogallin was utilized as both acyl donor and acceptor; this conclusion was supported by the isolation of analogous acyltransferases related to other metabolic pathways (cf. Table III). Recent studies (54) have shown, in accordance with previous proposals (5, 7, 8), that 1,6-*O*-digalloylglucose was produced by the enzyme, and that the stoichiometry of the reaction

was fully consistent with the assumed mechanism (cf. Figure 7). Substrate specificity studies with numerous 1-*O*-benzoylglucoses revealed that the enzyme was most active with its natural substrate,  $\beta$ -glucogallin (Gross, G. G.; Denzel, K.; Schilling, G., unpublished data).

Table III. Biosynthesis of Multiple-substituted Phenolic Acid Esters by Acyltransferases from Higher Plants

Donor	Acceptor	Product	Ref.
1- <i>O</i> -Galloylglucose ( $\beta$ -glucogallin)	1- <i>O</i> -Galloyl- glucose	1,6- <i>O</i> -Digalloyl- glucose	54
1- <i>O</i> -Galloylglucose	1,6- <i>O</i> -Digalloyl- glucose	1,2,6- <i>O</i> -Tri- galloylglucose	55
1- <i>O</i> -Galloylglucose	1,2,3,6- <i>O</i> - Tetragalloyl- glucose	1,2,3,4,6- <i>O</i> - Pentagalloyl- glucose	<sup>a</sup>
1- <i>O</i> -Sinapoylglucose	1- <i>O</i> -Sinapoyl- glucose	1,2- <i>O</i> -Disinapoyl- glucose	56-58
Chlorogenate	Chlorogenate	3,5-Dicaffeoyl- quinate (Isochlorogenate)	59,60

<sup>a</sup> Camman, J.; Denzel, K.; Schilling, G.; Gross, G. G., unpublished data.

*Higher Galloylated Glucose Derivatives.* As summarized in Table III, the formation of higher galloylated derivatives occurs by the same sort of mechanism as above, i.e., by the transfer of the galloyl moiety of  $\beta$ -glucogallin to the acceptor substrate. Thus, the biosynthesis of 1,2,6-trigalloylglucose from the 1,6-disubstituted precursor was proven unequivocally with an enzyme from sumach leaves (55), and recently an enzyme from oak leaves that catalyzed the galloylation of 1,2,3,6-tetragalloylglucose to 1,2,3,4,6-pentagalloylglucose was characterized (Cammann, J.; Denzel, K.; Schilling, G.; Gross, G. G., unpublished data). Only the conversion of tri- to tetragalloylglucose has not yet been verified by detailed enzyme studies, due to insufficient amounts of available substrate. The expected ester, 1,2,3,6-tetragalloylglucose, has, however, been isolated as a by-product from scaled-up enzyme assays designed for the preparation of 1,6-digalloylglucose [cf. (54)].

Thus, the entire sequence of reactions from  $\beta$ -glucogallin to pentagalloylglucose is summarized in Figure 7. Preliminary evidence suggests that the individual steps are catalyzed by different enzymes, but this question has to be answered by future detailed investigations. Concerning the substitution pattern of the metabolites, the scheme presented here is in accord with recent results obtained by analyzing the galloylglucoses produced in callus cultures from oak (61).

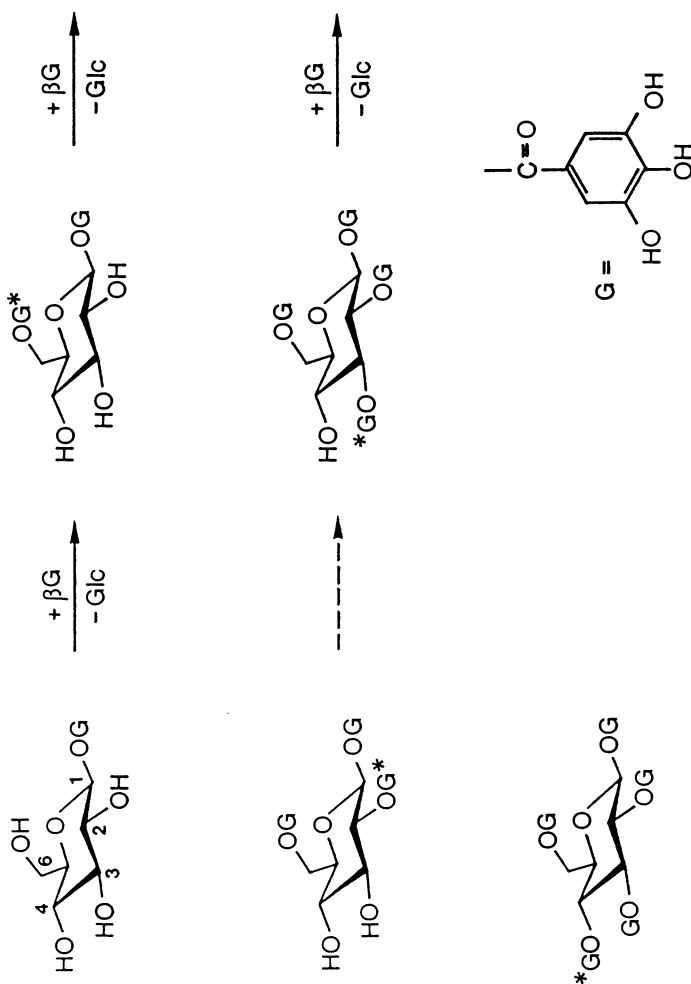


Figure 7. Biosynthetic pathway from  $\beta$ -glucogallin to pentagalloylglucose. The galloyl residue introduced in each individual step is marked by an asterisk; as indicated by the dashed arrow, the enzyme catalyzing the step from tri- to tetragalloylglucose has not yet been isolated.  $\beta$ G,  $\beta$ -Glucogallin; Glc, glucose.



### Biosynthesis of Gallotannins and Ellagitannins

As mentioned, recent biogenetic schemes suggest 1,2,3,4,6-pentagalloylglucose to be the principal common precursor of gallotannins and ellagitannins. However, there are many compounds of these two classes of natural products that contain one, or occasionally more than one, free OH-group on the glucose moiety, particularly at the C-1 position. No evidence is currently available as to whether such tannins are derived from partially galloylated precursors of pentagalloylglucose, or from the result of secondary deacylation reactions. The latter could be caused by a very active esterase encountered in cell-free extracts from oak or sumach leaves (Gross, G.G.; Denzel, K., unpublished results).

Little knowledge also exists on the mechanisms involved in the biosynthesis of the characteristic structures of gallotannins and ellagitannins, as will be briefly discussed below.

*Gallotannins.* Virtually nothing is known about the formation of the characteristic meta-depside bond of these compounds. For thermodynamic reasons one has to postulate an activated galloyl derivative in this reaction. The only speculations possible at present are whether  $\beta$ -glucogallin serves as an acyl donor, or whether, due to the markedly differing nature of the phenolic OH-group, other intermediates with a much higher group-transfer potential (e.g. galloyl-CoA) are required.

*Ellagitannins.* More than 50 years ago it was postulated (62) that the characteristic hexahydroxydiphenoyl residues of ellagitannins originated from the dehydration of gallic acid esters, e.g., depsidic tannins, and this widely accepted view has been supported by recent feeding experiments (16). Such oxidation reactions [reviewed, e.g., in (63)] were carried out by chemical means [e.g. (64)], or by *in vitro* studies with the fungal enzyme laccase (65, 66) or with peroxidases from higher plants (64, 67, 68), using gallic acid, methyl gallate,  $\beta$ -glucogallin, 3,6-digalloylglucose and pentagalloylglucose as substrates. In all cases, ellagic acid was formed as a typical product, indicating the expected intermediate synthesis of hexahydroxydiphenic acid. Unfortunately, this latter compound has never been isolated in its esterified form in these experiments, and thus it remains questionable whether these enzyme systems (i.e., laccase or some other polyphenol oxidase + O<sub>2</sub>, or peroxidase + H<sub>2</sub>O<sub>2</sub>) really reflect natural conditions. These doubts are supported by recent studies with cell-free extracts from oak leaves (Hofmann, A.; Gross, G. G., unpublished results). In the presence of suitable electron acceptors, the substrate, 1,2,3,4,6-pentagalloylglucose, was converted to a not yet fully characterized new product (and eventually 1,4,6-tri-*O*-galloyl-2,3-*O*-hexahydroxydiphenoylglucose), together with minor quantities of a compound that cochromatographed with pedunculagin (2,3:4,6-di-*O*-hexahydroxydiphenoylglucose). These preliminary results indicate that rather specific oxidoreductases, and not the abovementioned very unspecific oxidases, are involved in the biosynthesis of ellagitannins.

### Conclusion

As documented in a review article (9), no experimental data was available to support hypothetical mechanisms for the biosynthesis of hydrolyzable tannins until recently. Enzymatic studies have now changed this unsatisfactory situation, at least as far as the formation of pentagalloylglucose is concerned. Future work will provide insight into those other challenges discussed in this contribution and that still require clarification.

### Acknowledgments

I am indebted to the coworkers of my laboratory who contributed to the research reported in this article, and to the Deutsche Forschungsgemeinschaft and the Fonds der Chemischen Industrie for financial support.

### Literature Cited

1. Haslam, E. *Rec. Adv. Phytochem.* 1979, **12**, 475-523.
2. Haslam, E. In *The Biochemistry of Plants. Vol. 7. Secondary Plant Products*; Conn, E. E., Ed.; Academic: New York, 1981; pp. 527-56.
3. Haddock, E. A.; Gupta, R. K.; Al-Shafi, S. M. K.; Haslam, E. *J. Chem. Soc. Perkin Trans. I* 1982, 2515-24.
4. Gupta, R. K.; Al-Shafi, S. M. K.; Layden, K.; Haslam, E. *J. Chem. Soc. Perkin Trans. I* 1982, 2525-34.
5. Haddock, E. A.; Gupta, R. K.; Haslam, E. *J. Chem. Soc. Perkin Trans. I* 1982, 2535-45.
6. Haslam, E. *Fortschr. Chem. Org. Naturst.* 1982, **41**, 1-46.
7. Haslam, E. *Rec. Adv. Phytochem.* 1986, **20**, 163-200.
8. Haddock, E. A.; Gupta, R. K.; Al-Shafi, S. M. K.; Layden, K.; Haslam, E.; Magnolato, D. *Phytochemistry* 1982, **21**, 1049-62.
9. Hillis, W. E. In *Biosynthesis and Biodegradation of Wood Components*; Higuchi, T., Ed.; Academic: Orlando, 1985; pp. 325-47.
10. Billek, G.; Schmook, F. P. *Österr. Chem. Ztg.* 1966, **67**, 401-9.
11. Zenk, M. H. In *Pharmacognosy and Phytochemistry*; Wagner, H.; Hörhammer, L., Eds.; Springer: Berlin, 1971; pp. 314-46.
12. Tateoka, T. N. *Bot. Mag. Tokyo* 1968, **81**, 103-4.
13. Kato, N.; Shiroya, M.; Yoshida, S.; Hasegawa, M. *Bot. Mag. Tokyo* 1968, **81**, 506-7.
14. Saijo, R. *Agric. Biol. Chem.* 1983, **47**, 455-60.
15. Ishikura, N. *Experientia* 1975, **31**, 1407-8.
16. Ishikura, N.; Hayashida, S.; Tazaki, K. *Bot. Mag. Tokyo* 1984, **97**, 355-67.
17. Amrhein, N.; Topp, H.; Joop, O. *Plant Physiol.* 1984, **75**, supplement, p. 18.
18. Stöckigt, J.; Zenk, M. H. *FEBS Letters* 1974, **42**, 131-4.
19. Ulbrich, B.; Zenk, M. H. *Phytochemistry* 1979, **18**, 929-33.
20. Rhodes, M. J. C.; Wooltorton, L. S. C. *Phytochemistry* 1976, **15**, 947-51.

21. Rhodes, M. J. C.; Woollorton, L. S. C.; Lourenço, E. J. *Phytochemistry* 1979, **18**, 1125-9.
22. Ulbrich, B.; Zenk, M. H. *Phytochemistry* 1980, **19**, 1625-9.
23. Strack, D.; Ruhoff, R.; Gräwe, W. *Phytochemistry* 1986, **25**, 833-7.
24. Strack, D.; Leicht, P.; Bokern, M.; Wray, V.; Grotjahn, L. *Phytochemistry* 1987, **26**, 2919-22.
25. Strack, D.; Keller, H.; Weissenböck, G. *J. Plant Physiol.* 1987, **131**, 61-73.
26. Gross, G. G. *Z. Naturforsch.* 1982, **37c**, 778-83.
27. Corner, J. J.; Swain, T. *Nature* 1965, **207**, 634-5.
28. Macheix, J. J. *Compt. Rend. Acad. Sci. Ser. D* 1977, **284**, 33-36.
29. Fleuriet, A.; Macheix, J. J.; Suen, R.; Ibrahim, R. K. *Z. Naturforsch.* 1980, **35c**, 967-72.
30. Strack, D. *Z. Naturforsch.* 1980, **35c**, 204-8.
31. Nurmman, G.; Strack, D. *Z. Pflanzenphysiol.* 1981, **102**, 11-7.
32. Nagels, L.; Molderez, M.; Parmentier, F. *Phytochemistry* 1981, **20**, 965-7.
33. Shimizu, T.; Kojima, M. *J. Biochem.* 1984, **95**, 205-12.
34. Michalczuk, L.; Bandurski, R. S. *Biochem. Biophys. Res. Commun.* 1980, **93**, 588-92.
35. Michalczuk, L.; Bandurski, R. S. *Biochem. J.* 1982, **207**, 273-81.
36. Bäumker, P. A.; Jütte, M.; Wierman, R. *Z. Naturforsch.* 1987, **42c**, 1223-30.
37. Gross, G. G. *FEBS Letters* 1982, **148**, 67-70.
38. Gross, G. G. *Phytochemistry* 1983, **22**, 2179-82.
39. Weisemann, S.; Denzel, K.; Schilling, G.; Gross, G. G. *Bioorg. Chem.* 1988, **16**, 29-37.
40. Klick, S.; Herrmann, K. *Phytochemistry* 1988, **27**, 2177-80.
41. Gross, G. G. *Z. Naturforsch.* 1983, **38c**, 519-23.
42. Tkotz, N.; Strack, D. *Z. Naturforsch.* 1980, **35c**, 835-7.
43. Strack, D. *Planta* 1982, **155**, 31-6.
44. Strack, D.; Knogge, W.; Dahlbender, B. *Z. Naturforsch.* 1983, **38c**, 21-7.
45. Regenbrecht, J.; Strack, D. *Phytochemistry* 1985, **24**, 407-10.
46. Gräwe, W.; Strack, D. *Z. Naturforsch.* 1986, **41c**, 28-33.
47. Villegas, R. J. A.; Kojima, M. *Agric. Biol. Chem.* 1985, **49**, 263-5.
48. Villegas, R. J. A.; Kojima, M. *J. Biol. Chem.* 1986, **261**, 8729-33.
49. Kojima, M.; Villegas, R. J. A. *Agric. Biol. Chem.* 1984, **48**, 2397-9.
50. Strack, D.; Hellemann, J.; Boehner, B.; Grotjahn, L.; Wray, V. *Phytochemistry* 1987, **26**, 107-11.
51. Strack, D.; Gross, W.; Wray, V.; Grotjahn, L. *Plant Physiol.* 1987, **83**, 475-8.
52. Gross, G. G.; Schmidt, S. W.; Denzel, K. *J. Plant Physiol.* 1986, **126**, 173-9.
53. Denzel, K.; Weisemann, S.; Gross, G. G. *J. Plant Physiol.* 1988, **133**, 113-5.

54. Schmidt, S. W.; Denzel, K.; Schilling, G.; Gross, G. G. *Z. Naturforsch.* 1987, **42c**, 87-92.
55. Denzel, K.; Schilling, G.; Gross, G. G. *Planta* 1988, **176**, 135-7.
56. Dahlbender, B.; Strack, D. *J. Plant Physiol.* 1984, **116**, 375-9.
57. Strack, D.; Dahlbender, B.; Grotjahn, L.; Wray, V. *Phytochemistry* 1984, **23**, 657-9.
58. Dahlbender, B.; Strack, D. *Phytochemistry* 1986, **25**, 1043-6.
59. Kojima, M.; Kondo, T. *Agric. Biol. Chem.* 1985, **49**, 2467-9.
60. Villegas, R. J. A.; Shimokawa, T.; Okuyama, H.; Kojima, M. *Phytochemistry* 1987, **26**, 1577-81.
61. Krajci, I.; Gross, G. G. *Phytochemistry* 1987, **26**, 141-3.
62. Erdtman, H. *Svensk. Kem. Tidskr.* 1935, **47**, 223-30.
63. Taylor, W. I.; Battersby, A. R.; Eds.; *Oxidative Coupling of Phenols*; Marcel Dekker: New York, 1967.
64. Mayer, W.; Hoffmann, E. H.; Lösch, N.; Wolf, H.; Wolter, B.; Schilling, G. *Liebigs Ann. Chem.* 1984, 929-38.
65. Hathway, D. E. *Biochem. J.* 1957, **67**, 445-50.
66. Flaig, W.; Haider, K. *Planta Med.* 1961, **9**, 123-39.
67. Kamel, M. Y.; Saleh, N. A.; Ghazy, A. M. *Phytochemistry* 1977, **16**, 521-4.
68. Pospíšil, F.; Cvikrová, M.; Hrubcová, M. *Biol. Plantarum* 1983, **25**, 373-7.

RECEIVED April 10, 1989

## Chapter 8

# Biogenesis and Localization of Polymethylated Flavonoids in Cell Walls of *Chrysosplenium americanum*

Ragai Ibrahim, Lillian Latchinian, and Louise Brisson

Plant Biochemistry Laboratory, Department of Biology, Concordia University, Montreal, Quebec H3G 1M8, Canada

The semiaquatic species, *Chrysosplenium americanum* (Saxifragaceae), which lacks lignin, accumulates a number of tri- to penta-*O*-methylated flavonol glucosides instead. Their enzymatic synthesis is catalyzed by five position-specific methyltransferases, which exhibited distinct pH optima, pI values, cation requirements and preference for flavonol aglycones or glucosides as substrates. *O*-Glucosylation of methylated flavonols at 2'- and 5'-positions is mediated by two distinct glucosyltransferases, which were resolved by affinity chromatography on UDP-glucuronic acid agarose and Brown 10X dye ligand. Kinetic analysis of both groups of enzymes indicates that this multistep pathway is subject to tight control, and that the kinetic constants regulate the rate of synthesis of the final products. The use of electron microscopy, immunofluorescence and immunocytochemical techniques unequivocally indicate that these highly lipophilic metabolites are associated with the walls of epidermal and mesophyll cells.

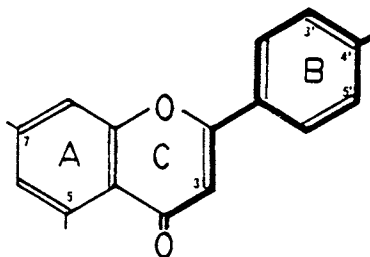
It was more than 20 years ago that hydroxycinnamic acids were reported (1) to be esterified in appreciable amount with the un lignified cell walls of grasses and other plant species. Monocot arabinoxylans (a hemicellulose fraction) have been reported to be substituted with *p*-coumarate, ferulate and *p*-hydroxybenzoate (2,3), and yielded on enzymatic hydrolysis feruloylarabinosylxylose. Alkaline hydrolysis of grass cell walls gave diferulic acid (2,4-6), the oxidative coupling product of feruloyl residues. Pectins from spinach culture cell walls contain ferulate and *p*-coumarate (7,8), which on partial hydrolysis give two feruloyl disaccharides, 4-*O*-(6-feruloyl- $\beta$ -D-galactosyl)-D-galactose and 3-*O*-(3-feruloyl- $\alpha$ -L-arabinosyl)-L-arabinose

0097-6156/89/0399-0122\$06.00/0  
© 1989 American Chemical Society

(9) and a small amount of diferulate. The common occurrence of phenolic acid sugar esters in association with cell walls is not surprising, since these are known natural plant constituents (10). On the other hand, the cell wall glycoprotein, extensin contains the oxidatively coupled dimer, isodityrosine (11) and a trimer of tyrosine (12) which have been proposed (13) to crosslink with two or three polypeptide chains of extensin.

In contrast with the above mentioned phenolic residues, which may be H-bonded or covalently linked with different cell wall fractions, another group of phenolic compounds—the simple flavonoids—may be secreted on plant surfaces as gummy or farinose exudates. These were first reported in poplar (14) and are now known to occur in many woody and herbaceous species, including ferns (15). On the other hand, the semi-aquatic species, *Chrysosplenium americanum* (Saxifragaceae) which lacks lignin, synthesizes instead a variety of tri- to penta-*O*-methylated flavonol glucosides. These highly lipophilic metabolites were found associated with the plant cell walls, although the nature of this association is yet to be determined.

Flavonoid compounds are natural plant constituents of wide distribution in nature; among which are the flower and fruit pigments (anthocyanins) and the yellow pigments (flavones and flavonols), found in all plant parts. These compounds share a common biosynthetic origin; being formed of two phenolic ring systems A and B, which are derived from acetate and cinnamate, respectively, although they differ in the oxidation level of the heterocyclic ring C (see structure below). Flavones and flavonols, which occur naturally as glycosides, may be *O*-methylated or *O*-glucosylated at one or several positions on the flavonoid ring system. Partially and fully methylated flavonoids are now considered to be widely distributed in the plant kingdom (16, 17). Both enzymatic reactions are believed to play an important role in the detoxification of reactive hydroxyl groups and hence, their compartmentation within plant cells and tissues (18).



Enzymatic *O*-methylation of flavonoids, which is catalyzed by *O*-methyltransferases (E.C. 2.1.1.6-) involves the transfer of the methyl group of an activated methyl donor, *S*-adenosyl-*L*-methionine, to the hydroxyl group of a flavonoid acceptor with the formation of the corresponding methylether and *S*-adenosyl-*L*-homocysteine. The latter product is, in

most cases, a competitive inhibitor of the enzyme reaction (19). A number of flavonoid-specific *O*-methyltransferases has recently been characterized; among which are those which attack positions 3' of flavones and flavonols (20-22), 3'/5' of anthocyanins (23), 4' of isoflavones (24) and flavones (25), 5 of isoflavones (26), 7 of flavonols (27, 28) and C-glycoflavones (29) and 8 of flavonols (30, 31).

It should be noted, however, that these enzymes catalyzed single methylation steps, and did not accept partially methylated substrates for further *O*-methylation. The common occurrence of partially methylated flavonoids (16, 17), such as those of *C. americanum* (Figure 1), raised the question as to whether multiple methyl transfers were catalyzed by one or several position-specific *O*-methyltransferases!

Enzymatic glucosylation, on the other hand, is mediated by *O*-glucosyltransferases (E.C. 2.4.1-) and involves the transfer of the glucosyl moiety of a nucleotide diphosphate sugar to the hydroxyl groups of a phenol/flavonoid acceptor with the formation of the corresponding glucoside and the nucleotide diphosphate. The latter may also act as competitive inhibitor of the enzyme reaction (32). Although glucosyltransferases are known to be substrate-specific and position-oriented (33), it is not known whether glucosylation of the less common 2' and 5' positions of flavonoids (e.g., compounds I and III, respectively, Figure 1) is catalyzed by one or two distinct enzymes.

The present work describes the multienzyme system which is involved in the methylation-glucosylation sequence of *Chrysosplenium* flavonoids. The latter tissue is an ideal experimental system since it accumulates six, tri- to penta-*O*-methylated flavonol glucosides. Two of these, I and II, are derivatives of 2'-substituted quercetin (3, 5, 7, 4', 5'-penta-hydroxyflavone); two others, III and IV, are 6-substituted quercetin (quercetagenin) derivatives; whereas the remaining two compounds, V and VI, are 2'-substituted quercetagenin (Figure 1). Whereas the first pair of flavonoids is glucosylated at the less common 2'-position, all the others are 5'-*O*-glucosides. None of the lower methylated intermediates of the pathway accumulate in this tissue, although they can be synthesized enzymatically *in vitro* (34). Due to the highly lipophilic, and partially hydrophilic, nature of these metabolites it was considered of interest to study their intracellular localization in this tissue.

*Biogenesis of Chrysosplenium Flavonoids.* Tracer experiments using [2-<sup>14</sup>C]cinnamate administered to young shoots resulted in labeling of the six methylated flavonol glucosides within 5 to 10 min pulse (Figure 2), but none of the low methylated intermediates. Furthermore, the partially purified enzyme preparations catalyzed the methylation of quercetin, but not quercetagenin, to its 3-mono-, 3, 7-di- and 3, 7, 4'-trimethyl derivatives (34-36), as well as the glucosylation of partially methylated intermediates to their corresponding glucosides (37). These results suggested the existence, in this tissue, of the enzyme complement involved in the biosynthesis of these metabolites and prompted the characterization of the individual enzymes of the pathway.

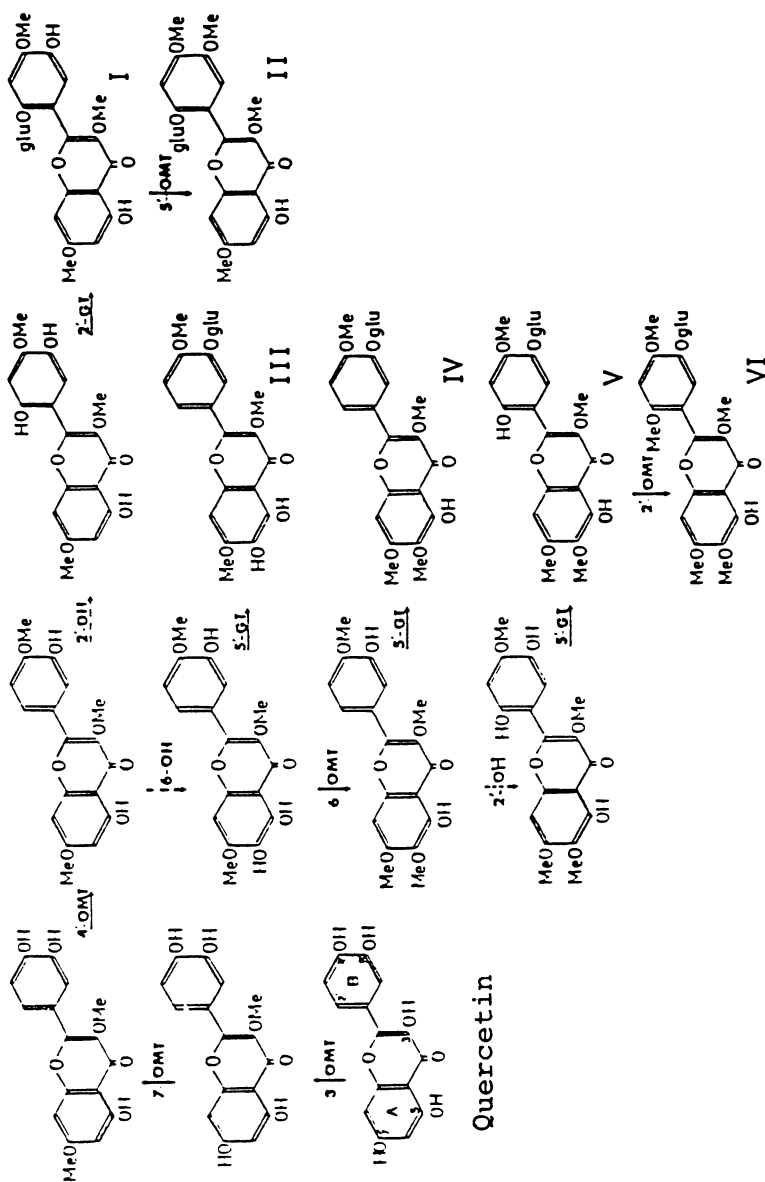


Figure 1. Postulated pathway for the enzymatic synthesis of polymethylated flavonol glucosides in *Chrysosplenium americanum*: GT, O-glucosyltransferase; OH, hydroxylase; OMT, O-methyltransferase.



### The Multistep Methylation Sequence

**Purification of O-Methyltransferases.** Using conventional, open-column chromatography alternatively with a fast protein liquid chromatography (FPLC) system, we were able to purify five distinct, position-specific methyltransferases (38,39). The last step of purification was achieved by chromatofocusing on a Mono P analytical column (40) using a gradient between pH 6 and pH 4 (Figure 3). The extent of purification of these enzymes varied between 85 to 164-fold using conventional column and 400 to 650-fold using the FPLC system (Table I).

Table I. Properties of *Chrysosplenium* Methyltransferases

Property	3-	6-	7-	4'-	2'/5'
Purification (-fold)					
Open column	85	92	6	164	123
HPLC	650	400	460	460	420
pH optimum	4.8	9.0	8.2	8.8	7.0
pI value	4.0	5.2	4.8	5.0	4.6
Mol. Wt. (Kd)	57	57	57	57	57
Km (SAM), $\mu\text{M}$	114	51	65	130	100
Km (Flav), $\mu\text{M}$	12	18	7	15	2
Ki (SAH), $\mu\text{M}$	4.5	16	10	4.4	
Ki (Me-Flav), $\mu\text{M}$	128	167	15	10	

**Substrate Specificity of O-Methyltransferases.** A flavonol with 4',5'-hydroxylation pattern, such as quercetin but not quercetagenin, is believed to be the first methyl acceptor in this pathway. The highly purified enzymes (Figure 3) exhibited strict position specificity for positions 3 of quercetin (3-methyltransferase), 7 of 3-methylquercetin (7-methyltransferase), 4' of 3,7-dimethylquercetin (4'-methyltransferase), 6 of 3,7,4'-trimethylquercetagenin (6-methyltransferase), 5' of 5,2',5'-trihydroxy-3,7,4'-trimethoxyflavone-2'-glucoside and 2'-position of 5,2',5'-trihydroxy-3,6,7,4'-tetramethoxyflavone-5'-glucoside (2'-/5'-methyltransferase). It is interesting to note that, in contrast with the earlier enzymes of the pathway which utilized aglycones as substrates, the two later methylation steps (2'- and 5'-positions) took place at the glucoside level (Fig. 1), and were catalyzed equally well by the same protein preparation (39,40). However, in view of the strict position specificity of the former enzymes (3-, 6-, 7- and 4'-methyltransferases), it can be assumed that the two later methylation steps of the pathway may be mediated by two distinct enzymes which remain to be resolved. None of these enzymes accepted phenylpropanoids, flavones, dihydroflavonols, or any of their glucosides. Both substrate and position specificities of these enzymes indicate a coordinated sequence of methyl transfers to quercetin  $\rightarrow$  3-methylquercetin  $\rightarrow$  3,7-dimethyl-quercetin  $\rightarrow$  3,7,4'-trimethylquercetin. After hydroxylation of

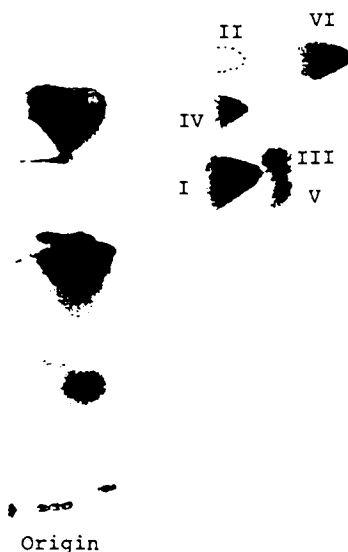


Figure 2. Photograph of an autoradiogram of the chromatographed leaves administered [ $^{14}\text{C}$ ]cinnamate for 10 min. Compounds I to VI (Figure 1) are the final flavonoid metabolites which accumulate in this tissue.

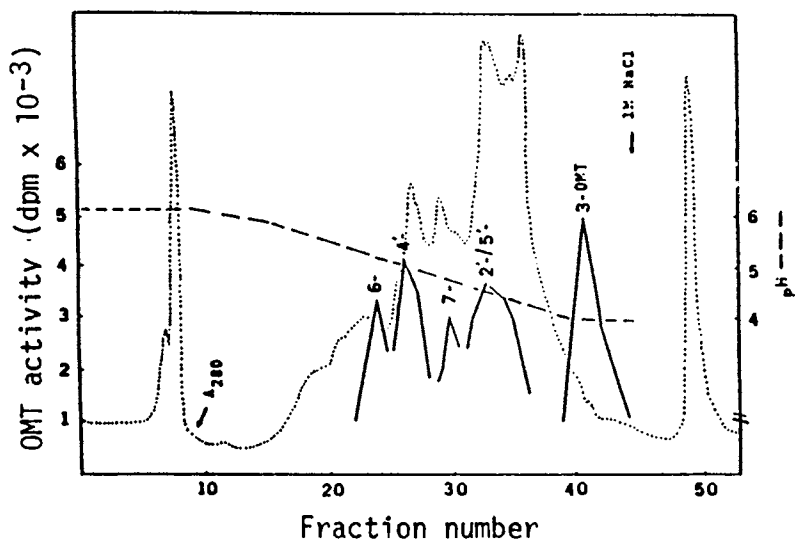


Figure 3. Elution profile of five *O*-methyltransferases after chromatofocusing on an analytical Mono-P column, using a gradient between pH 6 and pH 4.

the latter at position 2' and its subsequent glucosylation, it is further methylated to its 5'-methyl derivative (compound II). 3,7,4'-trimethylquercetin may also be hydroxylated at position 6, further methylated at that position (compound III), then glucosylated at 5' (compound IV). The latter, after further hydroxylation at the 2'-position (compound V) is finally methylated to compound VI (Figure 1).

*Properties of O-Methyltransferases.* The different enzymes exhibited distinct pI values and pH optima (Table I), although they had similar molecular weights. Unlike the other enzymes of the methylation sequence, the 6-methyltransferase exhibited absolute requirement for Mg ions, whose activation was saturable and was inhibited by EDTA. The different O-methyltransferases were inhibited by 1 mM of the SH group reagents, *p*-chloromercuri-benzoate and N-ethylmaleimide to various extent. The addition of 14 mM 2-mercaptoethanol partially prevented this inhibition (38).

*Kinetics of O-Methylation.* The steady state kinetic analysis of these enzymes (41,42) was consistent with a sequential ordered reaction mechanism, in which *S*-adenosyl-L-methionine and *S*-adenosyl-L-homocysteine were leading reaction partners and included an abortive EQB complex. Furthermore, all the methyltransferases studied exhibited competitive patterns between *S*-adenosyl-L-methionine and its product, whereas the other patterns were either noncompetitive or uncompetitive. Whereas the 6-methylating enzyme was severely inhibited by its respective flavonoid substrate at concentrations close to  $K_m$ , the other enzymes were less affected. The low inhibition constants of *S*-adenosyl-L-homocysteine (Table I) suggests that earlier enzymes of the pathway may regulate the rate of synthesis of the final products.

### Glucosylation of Partially Methylated Flavonols

The fact that *Chrysosplenium* flavonoids are glucosylated at the less common 2'- and 5'-positions prompted an investigation as to whether both glucosylation steps are mediated by one or two distinct enzymes.

*Purification of 2'-/5'-O-Glucosyltransferase.* Previous studies in this laboratory (37) have demonstrated the existence, in this tissue, of a novel ring B-specific O-glucosyltransferase. This enzyme attacked either 2'- or 5'-position of partially methylated flavonols and required two, *para*-oriented substituents on ring B for optimum activity (e.g., aglycones of II and VI, Figure 1). The fact that the 2'- and 5'-glucosylating activities could not be separated by either conventional chromatography on several columns (37) or by FPLC (43), seemed to indicate that both glucosylations may be catalyzed by one enzyme. However, unlike other glucosyltransferases (32) the *Chrysosplenium* enzyme binds UDP (44), the second product of the reaction. This kinetic property allowed binding the enzyme to a UDP-glucuronic acid agarose affinity support (43), although it did not bind to UDP-agarose. The glucosyltransferase activity was eluted at approximately 60 mM KCl, then desalted before being applied to Brown 10X dye ligand at pH 6.5. Elution of the enzyme protein from the latter column was performed using a linear pH-salt gradient, and resulted in the separation of

the 2'- and 5'-activities at pH values of 7.8 and 7.3, respectively (Figure 4). The combined purification steps resulted in an increase in specific activity of 1200-fold (43). Each of the purified fractions gave a single flavonoid glucoside when assayed against the respective aglycone, as shown by autoradiography of the reaction products (Figure 4, insert). These results indicate that glucosylation of the 2'- and 5'-positions of flavonoids is catalyzed by two distinct enzymes.

It should be pointed out that, in contrast with the enzymes of primary metabolism (e.g., photosynthesis, respiration, etc.), those catalyzing the synthesis of secondary metabolites usually occur in very low abundance, and are therefore, very difficult to purify to homogeneity especially for the purpose of raising antibodies. However, the recent advances in immunization and selection techniques made it possible to overcome the need for homogeneous protein in order to raise monoclonal antibodies.

*Immunological Evidence for 2'-O-Glucosyltransferase.* Murine monoclonal antibody to the partially purified enzyme was produced by an *in vitro* immunization technique (45) of Balb/c mice spleen cells, followed by fusion with mouse myeloma cells. Screening culture supernatants of the resulting hybridomas by an enzyme-linked immunosorbent assay (ELISA) revealed the presence of two highly immunoreactive IgM-secreting clones, C3-2 and C7-1 (Table II) (46). Only the former clone displayed > 50% inhibition of the 2'-glucosyltransferase activity, whereas neither antibodies C3-2 nor C7-1 inhibited the 5'-activity (Figure 5). These results clearly demonstrate the existence of an immunologically distinct flavonol 2'-O-glucosyltransferase. Furthermore, the native form of this enzyme was essential for recognition by the C3-2 antibody, hence, immunoreactive bands on Western blots (Figure 5, insert) could only be visualized following native-PAGE, and not SDS-PAGE. Further work is aimed at selecting a 5'-specific antibody in order to demonstrate, unequivocally, the involvement of two distinct 2'- and 5'-glucosyltransferases.

Table II. Specific Fusion Efficiency

Fusion	Ig-Producing Wells (% of total)		Specific Immunoreactive Wells (% of IgM-Secretors)
	IgM	IgG	
Day 5	50.5	3.6	22.2
Day 7	45.9	0.5	18.6

*Properties of the Glucosyltransferase.* Except for its strict substrate specificity, the properties of this enzyme were similar to those of other flavonoid glucosyltransferases (32,33) and are listed in Table III.

*Kinetics of Glucosylation.* The detailed kinetic analysis of the partially purified enzyme (44) was consistent with an ordered bi bi mechanism, where UDP-glucose binds to the enzyme first, followed by the flavonoid aglycone

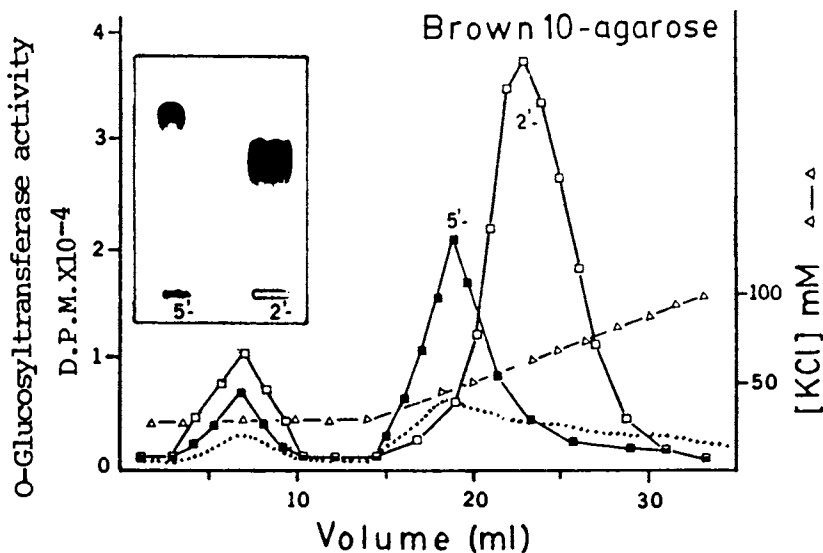


Figure 4. Elution profile of the 2'- and 5'-*O*-glucosyltransferases after chromatography on Brown 10X agarose column using pH-salt gradient. Insert: autoradiographed enzyme reaction products.

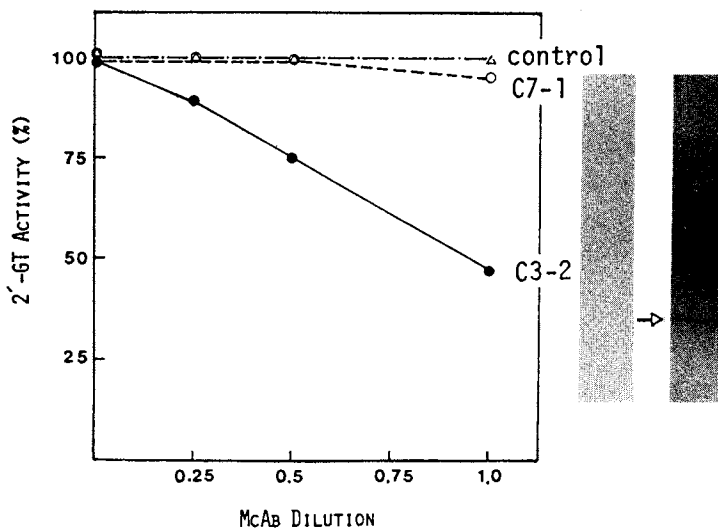


Figure 5. Immunoremoval (inhibition) of 2'-glucosyltransferase activity by different concentrations of monoclonal antibody C3-2. Insert: Western blot of the native enzyme after PAGE (left, control; right, blot with C3-2 antibody).

Table III. Properties of *Chrysosplenium* Glucosyltransferases

Property	2'-	5'
Purification (-fold)	1200	1200
pH optimum	8.0	8.0
pI value	5.2	5.2
Mol. Wt. (Kd)	42	42
Km (UDPglc) $\mu$ M	250	250
Km (Flav.) $\mu$ M	5	10
Ki (UDP) $\mu$ M	25	20
Ki (Flav. gluc.) $\mu$ M	1000	1000

and the release of the glucoside followed by UDP. The latter was a competitive inhibitor with respect to UDP-glucose and noncompetitive with respect to both UDP-glucose and the flavonoid substrate. The high inhibition constant of the glucosylated product, as compared with those of the substrate and co-substrate (Table III) indicates that glucosylation of the partially methylated flavonoids is not inhibited by the products formed (44), and is consistent with the accumulation of compounds I, II, V and VI (Figure 1) as the major flavonoid constituents of this tissue.

*Regulation of Flavonoid Synthesis in C. americanum.* Biosynthesis of methylated flavonol glucosides seems to be under tight regulation, not only by the substrate specificity of the enzymes involved, but also by other factors, among which are: (a) the strict position specificity of these enzymes towards their hydroxylated or partially methylated substrates; (b) the apparent difference in microenvironment of the different methyl-transferases, whereby those earlier in the pathway utilized aglycones whereas later enzymes accepted only glucosides as substrates; (c) the subtle characteristic differences in methyl-transferases with respect to their pH optima, pI values and requirement for Mg ions, despite their similar molecular size; (d) the sequential ordered mechanism of all the enzymes involved in the methylation-glucosylation sequence of this pathway. Another important aspect of regulation derives from the kinetic analysis of the enzymes studied. This is demonstrated by the similarity of their kinetic mechanisms and their regulation by a specific range of substrate and product concentrations (41,42). Despite the fact that the methylating enzymes had Km values in the same range as those of glucosylation, however, the Ki values for the latter reaction were in the mM range as compared with the  $\mu$ M values for methylation (Tables I and III), and are consistent with glucoside accumulation as the final products. Another means of regulation of the methylation sequence involves the differential affinities of the different enzymes for *S*-adenosyl-L-methionine and *S*-adenosyl-L-homocysteine (41,42). Whereas the four methyltransferases studied exhibited similar affinities for their respective flavonoid substrates (Table I), the affinity for the methyl donor *S*-adenosyl-L-methionine was similar for the 3- and 4'-*O*-methyltransferases, while those attacking positions 6 and 7 were two times greater. Further-

more, the former enzymes were subject to inhibition by low concentrations of *S*-adenosyl-L-homocysteine, since the apparent  $K_i$  for the latter two enzymes was 25 times smaller than the  $K_m$  for *S*-adenosyl-L-methionine, as compared with 3 and 6 times for the 6- and 7-methyltransferases, respectively (Table I). These characteristics suggest that the enzymes earlier in the methylation sequence may regulate the rate of synthesis of the final products.

*Localization Studies.* Localization of flavonoid compounds has usually been studied using cytochemical methods, including the formation of precipitates with suitable reagents for nonfluorescent compounds (18, 33 and refs. therein), as well as ultraviolet fluorescence microscopy for fluorescent compounds. Despite the variety of techniques used in the separation of plant tissues for localization of metabolites, it is difficult to interpret the data due to the varying degree of purity of the isolated tissue/organelle, or its possible contamination with the metabolites released during isolation. Such problems have been compounded by the lack of specific histochemical tests for the detection of phenolic/flavonoid compounds, and their solubility in the organic solvents normally used for microscopic preparations. Therefore, we have used three different strategies for the localization, *in situ*, of *Chrysozplenium* polymethylated flavonol glucosides.

*Electron Microscopy.* Using caffeine as prefix and visualizing agent (47 and refs. cited therein) allowed us to study the ultrastructural features of flavonoid accumulation in this tissue. These studies (48) revealed the presence of electron-dense deposits within the walls of leaf epidermal and mesophyll cells (Figure 6A). Various membrane profiles and associated vesicles in the periplasmic area were also filled with darkly stained material. The fact that most of these vesicles were fused with the plasmalemma (Figure 6A) suggested the secretory nature of these cells (47). There was no evidence to indicate that the Golgi apparatus was involved in packaging or channeling of flavonoids. Furthermore, the cell wall flavonoid deposits (Figure 6A) could be leached out by dipping leaf segments in organic solvents for 1-2 second intervals (48). HPLC analysis of these effusates indicated the recovery of the major flavonoid constituents. These observations are consistent with the lipophilic nature of the highly methylated flavonol glucosides and their localization within the walls of epidermal and mesophyll cells of this tissue.

*Immunofluorescence.* This is a sensitive, highly specific technique which has recently been used for the localization of large molecules, such as storage proteins or enzymes. To our knowledge, there has been no information on the use of this technique for flavonoid localization. This may be due to the difficulty in raising antibodies against relatively small molecules (ca. < 5000 dalton). Compound I (Figure 1) was conjugated to bovine serum albumin by the diazo reaction (49) and was used to raise antibody in rabbits (50). This antibody was found to be specific for the 2'-glucosides of tri- and tetramethoxyflavones I and II. However, there was some cross reactivity against the pentamethoxyflavone-5'-glucoside (compound VI), but none with quercetin or any of its tri- or tetramethyl derivatives (50). This

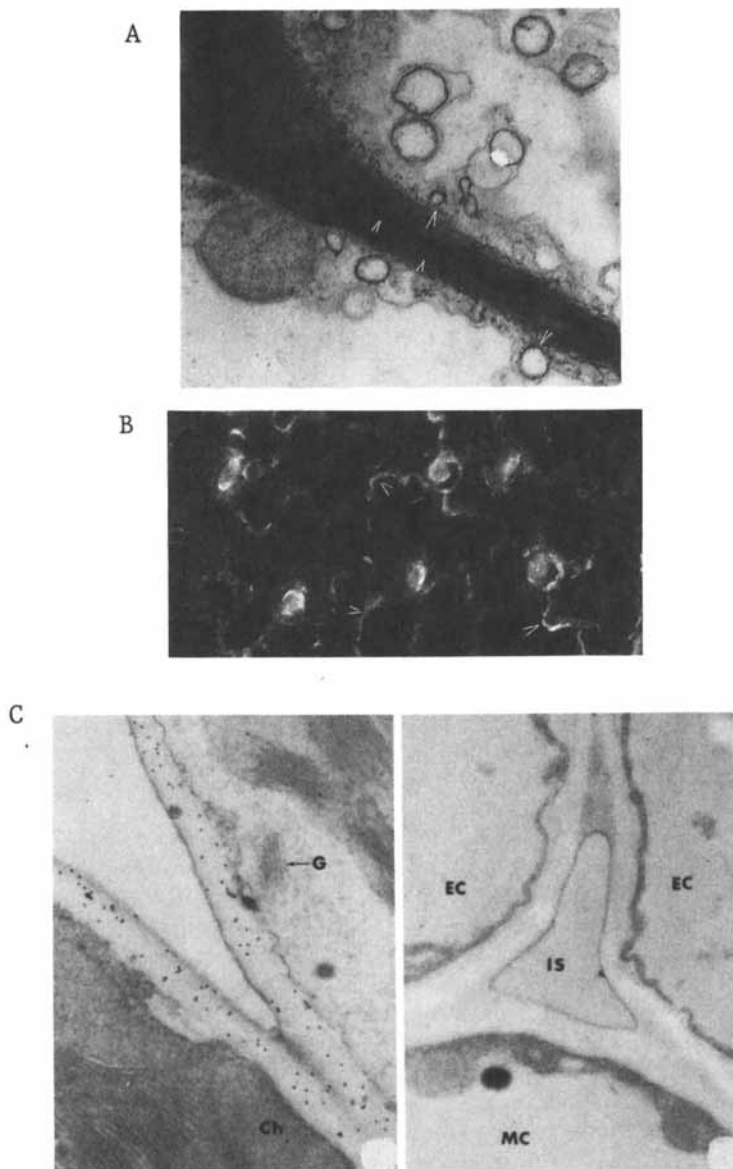


Figure 6. A: Photomicrograph ( $\times 51,000$ ) of caffeine treated leaf epidermal cell showing electron-dense deposits on cell wall and membrane vesicles fusing with the plasmalemma (arrows). B: Immunofluorescence labeling of flavonoids in cell walls of leaf epidermal strips (arrows) and autofluorescent stomata ( $\times 62.5$ ). C: Immunogold labeling of the walls of a mesophyll cell (left,  $\times 41,000$ ). Ch, chloroplast; EC, epidermal cell; G, Golgi; IS, intercellular space; MC, mesophyll cell; (right, control  $\times 19,500$ ).



antibody was applied with an indirect immunofluorescence technique (51) utilizing fluorescein isothiocyanate-labeled goat antirabbit antibody with leaf epidermis, cross sections and protoplasts. The results (Figure 6B) indicated that flavonoid accumulation occurred mainly in the walls of epidermal cells and, to a much lesser extent, in mesophyll cell walls. The weak fluorescence observed in the vacuoles of protoplasts suggested a minor role of this compartment in the accumulation process (51).

*Immunocytochemistry.* Further unequivocal evidence for the site of flavonoid accumulation was obtained using the proteinA-gold post-embedding technique (52), coupled with transmission electron microscopy (53). Antibody-specific labeling was observed mainly on the walls of epidermal and mesophyll cells (Figure 6C). Furthermore, there was significant amount of labeling associated with the plasmalemma, but none with other organelles such as the endoplasmic reticulum, Golgi or chloroplasts. These results provide strong evidence for the localization of partially methylated flavonol glucosides in the cell walls of this tissue.

### Significance of Flavonoid Accumulation in Cell Walls

Whereas the accumulation of flavonoids in plant cell walls may be difficult to explain, however, it may be considered as a means of eliminating such cytotoxic agents from the cell symplast. Such site for flavonoid accumulation may also be considered as a means of protection against pathogens, predators and ultraviolet radiation (54), especially in the absence of lignified tissues, as in the case of *Chrysosplenium*.

### Conclusions

To our knowledge, this is the first reported instance where flavonoid compounds have been found in association with plant cell walls. Whereas the enzymes involved in the biosynthesis of these wall constituents have always been recovered in the cytosolic fraction, it is not known whether they are actually soluble, or easily solubilized enzymes. It is tempting to postulate that flavonoid synthesis in *Chrysosplenium* takes place on the surface of an aggregated, membrane associated (e.g. the ER) multienzyme system (55), where the component enzymes may be loosely associated or held together by non-covalent bonds. Despite the unsuccessful attempts to isolate such an aggregate, however, several lines of evidence (biosynthetic, enzymatic and kinetic), mentioned above, tend to support this concept. Due to their cytotoxicity and highly lipophilic nature, these metabolites may be sequestered in the form of 'flavonoid vesicles,' which have been observed (48) to fuse with the plasmalemma for the discharge of their contents within the cell walls. The fact that these metabolites were readily recovered from leaf effusates suggests that they may be adsorbed on cell wall proteins. Subcellular localization of the enzymes catalyzing this pathway should provide supporting evidence for this proposed model. We are working along these lines.

### Acknowledgments

Work cited from the senior author's laboratory has been supported by operating and equipment grants from the Natural Sciences and Engineering

Council of Canada and Quebec Department of Higher Education, for which we are grateful. We wish to acknowledge the collaboration of Dr. P. M. Charest, Laval University, in the immunocytochemical work.

### Literature Cited

1. El-Basyouni, S. Z.; Neish, A. C.; Towers, G. H. N. *Phytochemistry* 1964, **3**, 627-639.
2. Harris, P. J.; Hartley, R. D. *Biochem. Syst. Ecol.* 1980, **8**, 153-160.
3. Tanner, G. R.; Morrison, I. M. *Phytochemistry* 1983, **22**, 1433-1439.
4. Hartley, R. D.; Jones, E. C. *Phytochemistry* 1976, **15**, 1157-1160.
5. Markwalder, H.-U.; Neukom, H. *Phytochemistry* 1976 **15**, 836-837.
6. Shibuya, N. *Phytochemistry* 1984, **23**, 2233-2237.
7. Fry, S. C. *Planta* 1979, **146**, 343-351.
8. Fry, S. C. *Phytochemistry* 1980, **19**, 735-740.
9. Fry, S. C. *Biochem. J.* 1982, **203**, 493-504.
10. Ibrahim, R. K. In *Methods in Plant Biochemistry*; Vol. 5; Harborne, J. B., Ed.; Academic Press: New York, 1988 (in press).
11. Fry, S. C. *Biochem. J.* 1982, **204**, 449-455.
12. Fry, S. C. In *Current Topics in Plant Biochemistry and Physiology*; Rendall, D. D.; Blevins, D. G.; Larson, R. I.; Rapp, B. J., Eds.; Vol. 2, Univ. Missouri Press, 1983, pp. 59-72.
13. Fry, S. C. *Annu. Rev. Plant Physiol.* 1986, **37**, 165-186.
14. Wollenweber, E. *Biochem. Syst. Ecol.* 1975, **3**, 35-45.
15. Wollenweber, E. In *Biology and Chemistry of Plant Trichomes*; Rodriguez, E.; Healy, P.; I. Mehta, Eds.; Plenum Press: New York, 1984, pp. 53-69.
16. Wollenweber, E.; Dietz, V. H. *Phytochemistry* 1981, **20**, 869-932.
17. Wollenweber, E.; Jay, M. In *The Flavonoids, Advances in Research*; Vol. 2, Harborne, J. B., Ed.; Chapman & Hall: London, 1988 (in press).
18. Luckner, M.; Bietrich, B.; Lerbs, W. In *Progress in Phytochemistry*; Vol. 6, Reinhold, L.; Harborne, J. B.; Swain, T., Eds. Pergamon Press: London, 1982, pp. 103-142.
19. Poulton, J. E. In *The Biochemistry of Plants*; Vol. 7, Conn, E. E., Ed., Academic Press: New York 1981, pp. 667-722.
20. Ebel, J.; Hahlbrock, K.; Grisebach, H. *Biochim. Biophys. Acta* 1972, **268**, 313-326.
21. Poulton, J. E.; Hahlbrock, K.; Grisebach, H. *Arch. Biochem. Biophys.* 1977, **180**, 543-549.
22. Sutfeld, R.; Wiermann, R. *Biochem. Physiol. Pflanzen* 1978, **172**, 111-123.
23. Jonsson, L. M.; Aarsman, M.; Scram, A. W.; Bennink, G.J. *Phytochemistry* 1982, **21**, 2457-2459.
24. Wengenmayer, H.; Ebel, J.; Grisebach, H. *Eur. J. Biochem.* 1974, **50**, 135-143.
25. Kuroki, G.; Poulton, J. E. *Z. Naturforsch.* 1981, **36c**, 916-920.
26. Khouri, H. E.; Tahara, S.; Ibrahim, R. K. *Arch. Biochem. Biophys.* 1988, **262**, 592-98.
27. Tsang, Y. F.; Ibrahim, R. K. *Phytochemistry* 1979, **18**, 1131-1136.

28. Tsang, Y. F.; Ibrahim, R. K. *Z. Naturforsch.* **34c**, 46-50.
29. Knogge, W.; Weissenbock, G. *Eur. J. Biochem.* 1984, **140**, 113-118.
30. Jay, M.; De Luca, V.; Ibrahim, R. K. *Z. Naturforsch.* **38c**, 414-417.
31. Jay, M.; De Luca, V.; Ibrahim, R. K. *Eur. J. Biochem.* **153**, 321-325.
32. Hosel, W. In *The Biochemistry of Plants*; Vol. 7, Conn, E. E., Ed., Academic Press: New York, 1981, pp. 725-753.
33. Ibrahim, R. K.; Khouri, H. E.; Brisson, L.; Barron, D.; Latchinian, L.; Varin, L. *Bull. Liaison Groupe Polyphenols* 1986, **13**, 3-14.
34. Collins, F. W.; De Luca, V.; Voirin, B.; Jay, M. *Z. Naturforsch.* 1981, **36c**, 730-736.
35. Ibrahim, R. K.; De Luca, V.; Jay, M.; Voirin, B. *Naturwissenschaften* 1982, **69**, 41-42.
36. De Luca, V.; Ibrahim, R. K. *Phytochemistry* **21**, 1537-1540.
37. Bajaj, K. L.; De Luca, V.; Khouri, H. E.; Ibrahim, R. K. *Plant Physiol.* 1983, **72**, 891-896.
38. De Luca, V.; Ibrahim, R. K. *Arch. Biochem. Biophys.* 1985, **238**, 596-605.
39. Khouri, H. E.; Ishikura, N.; Ibrahim, R. K. *Phytochemistry* 1986, **25**, 2475-2479.
40. Khouri, H. E.; Ibrahim, R. K. *J. Chromatogr.* 1987, **407**, 291-297.
41. De Luca, V.; Ibrahim, R. K. *Arch. Biochem. Biophys.* 1985, **238**, 606-618.
42. Khouri, H. E.; De Luca, V.; Ibrahim, R. K. *Arch. Biochem. Biophys.* 1988, **265**, 1-7.
43. Latchinian, L.; Khouri, H. E.; Ibrahim, R. K. *J. Chromatogr.* 1987, **338**, 235-242.
44. Khouri, H. E.; Ibrahim, R. K. *Eur. J. Biochem.* 1984, **142**, 559-564.
45. Boss, B. *Methods Enzymol.* 1986, **121**, 27-33.
46. Latchinian, L.; Ibrahim, R. K. *Biochem. Cell Biol.* 1988 (in press).
47. Charest, P. M.; Brisson, L.; Ibrahim, R. K. *Protoplasma* 1986, **134**, 95-101.
48. Brisson, L.; Ibrahim, R. K.; Rideau, M. *Plant Cell Rep.* 1988, **7**, 130-133.
49. Erlanger, B. F. *Methods in Enzymol.* 1980, **70**, 85-104.
50. Lamoureux, S.; Vacha, W.; Ibrahim, R. K. *Plant Sci.* 1986, **44**, 169-173.
51. Brisson, L.; Vacha, W.; Ibrahim, R. K. *Plant Sci.* 1986, **44**, 175-181.
52. Roth, J.; Bendayan, M.; Orci, L. J. *Histochem. Cytochem.* 1978, **28**, 1074-1081.
53. Marchand, L.; Charest, P. M.; Ibrahim, R. K. *J. Plant Physiol.* 1987, **131**, 339-348.
54. Harborne, J.B. *Introduction to Ecological Biochemistry* 1982.
55. Stafford, H. A. In *The Biochemistry of Plants*; Conn, E. E., Ed.; Vol. 7; Academic Press: New York, 1981, pp. 117-137.

RECEIVED March 17, 1989

## Chapter 9

# Phenolic Constituents of Plant Cell Walls and Wall Biodegradability

Roy D. Hartley<sup>1</sup> and Clive W. Ford<sup>2</sup>

<sup>1</sup>Richard B. Russell Agricultural Research Center, Agricultural Research Service, U.S. Department of Agriculture, Athens, GA 30613

<sup>2</sup>Division of Tropical Crops and Pastures, Commonwealth Scientific and Industrial Research Organisation, Cunningham Laboratory, St. Lucia, Queensland 4067, Australia

The nature and amounts of low molecular weight phenolic constituents in cell walls of graminaceous plants (grasses and cereals) are reviewed and relationships discussed between these constituents and wall biodegradability. The formation in cell walls of 4,4'-dihydroxytruxillic acid and other cyclodimers of *p*-coumaric and ferulic acid is suggested as an important mechanism for limiting the biodegradability of wall polysaccharides.

An understanding of relationships between cell wall constituents and wall biodegradation is of particular importance to the economics of animal production since low digestibility of forages is associated with reduced intake. Such an understanding is also important in elucidating the role of fiber in human nutrition and of the decomposition of organic matter in soil.

Various components of cell walls including silica, highly ordered cellulose structure and acetyl groups linked to hemicellulose have been suggested as possible detrimental factors causing low biodegradability of the wall polysaccharides, but there is an increasing body of evidence suggesting that the phenolic constituents (including lignin) are an important factor (e.g., see reviews 1-3). Many studies in animal nutrition have shown that as the lignin content of graminaceous cell walls increases, their digestibility in the rumen of cattle or sheep decreases. A major problem of relating chemical structure to digestibility from this work is that the compounds comprising forage lignins are ill-defined. For example, Klason lignin of forages can contain cutins, carbohydrate degradation products and nitrogenous material (1). When considering mechanisms of wall biodegradation, account must also be taken of the accessibility of the various wall types to wall degrading enzymes (4).

In recent years, positive relationships have been found between phenolic constituents of cell walls liberated by alkali and biodegradability of the

0097-6156/89/0399-0137\$06.00/0

© 1989 American Chemical Society

walls measured *in vitro* with rumen liquor from sheep or cattle, or with a commercial cellulase preparation having hemicellulase activity ("cellulase") (1). For example, when cell walls of maize stem were treated with sodium hydroxide (0.1M) at 20°C for various times to release different amounts of phenolics, a highly significant correlation ( $r = 0.98$ ) was found between the amount of phenolics released and wall biodegradability (measured by "cellulase") (5). It is of interest to note that alkali treatment of poor quality graminaceous forages (e.g., cereal straw) is used commercially to increase their biodegradability, and thus their feed value for the animal (1).

This paper examines the nature and amounts of monomeric and dimeric phenolic constituents of the walls of graminaceous plants and the relationships of these constituents to wall biodegradability.

### Monomeric Phenolic Acids, Aldehydes and Dehydrodiferulic Acid of Cell Walls

Phenolic acids and aldehydes released from graminaceous cell walls by treatment with alkali are shown in Figure 1. Examples of the amounts released from various cell walls are listed in Table I.

Table I. Amounts of Phenolic Acids and Phenolic Aldehydes Released from Graminaceous Cell Walls by Treatment with Sodium Hydroxide

Phenolic Acid or Aldehyde (mg g <sup>-1</sup> cell walls)	Maize Stem(6)	Barley Stem(6)	Wheat Bran(6)	Italian Ryegrass Shoot(7)
<i>Trans</i> + <i>cis</i> - <i>p</i> -coumaric acid	33.05	3.42	0.07	0.90
<i>Trans</i> + <i>cis</i> -ferulic acid	3.78	2.26	5.60	6.50
<i>Trans</i> , <i>trans</i> + <i>cis</i> , <i>trans</i> - dehydrodiferulic acid	0.11	0.13	0.18	0.20
<i>p</i> -Hydroxybenzaldehyde	0.26	0.02	0.06	n.d.
Vanillin	0.22	0.23	0.10	n.d.
Syringaldehyde	0.22	0.10	zero	n.d.

n.d. - not determined.

The amounts of the *trans* isomers of *p*-coumaric and ferulic acids were approximately ten times those of the corresponding *cis* isomers: dehydrodiferulic acid occurred mainly as the *trans*, *trans* isomer. A major difference between cell walls of temperate (e.g., ryegrass, wheat) and sub-tropical (e.g., maize, Coastal bermudagrass) graminaceous plants is that the latter group contain comparatively large amounts of *trans*-*p*-coumaric acid (1, 3, 8, 9). Several other families of monocotyledons and some species of dicotyledons have similar contents of *p*-coumaric and ferulic acids to those of graminaceous plants (10, 11).

At least some ferulic acid units in the cell walls of vegetative parts of sugar cane, maize and barley are esterified via the carboxyl group to arabinose units (12-14). This was established by treatment of these

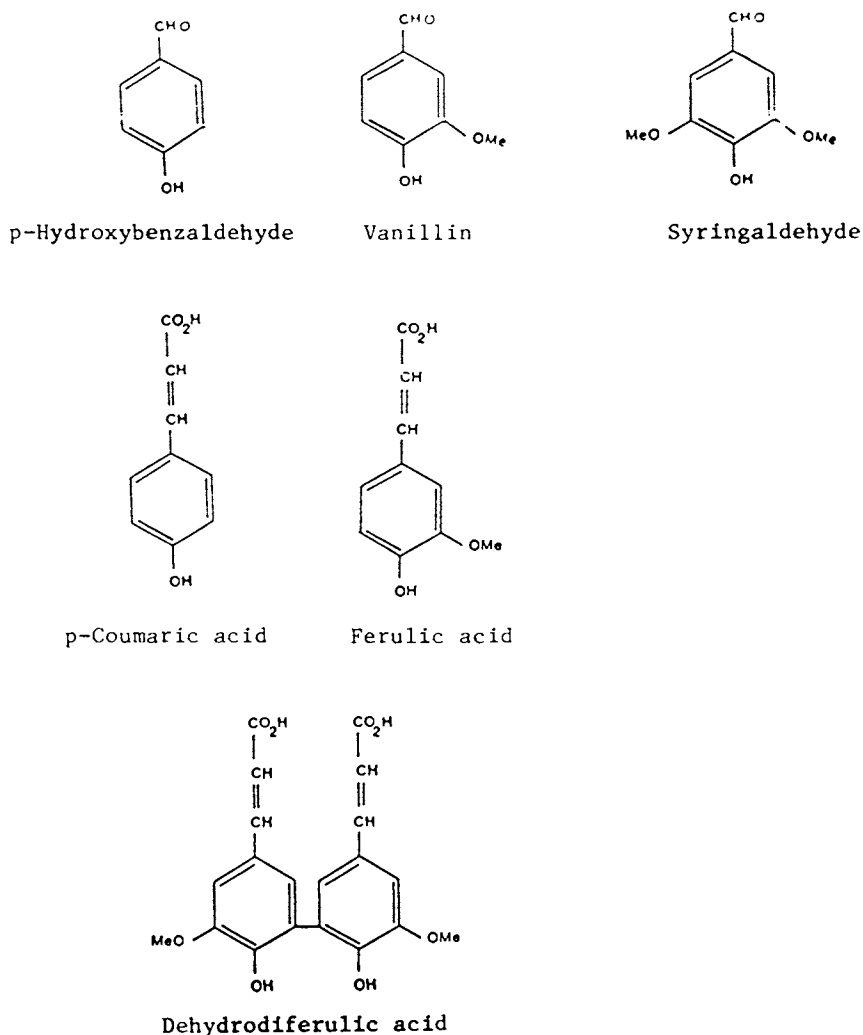


Figure 1. Compounds released from graminaceous cell walls by treatment with sodium hydroxide.

walls with "cellulase," leading to the release of water-soluble O-[5-O-(*trans*-feruloyl)- $\alpha$ -L-arabinofuranosyl]-(1  $\rightarrow$  3)-O- $\beta$ -D-xylopyranosyl-(1  $\rightarrow$  4)-D-xylopyranose (FAXX, Ia). A similar method led to the release of O-[5-O-(*trans-p*-coumaroyl)- $\alpha$ -L-arabinofuranosyl]-(1  $\rightarrow$  3)-O- $\beta$ -D-xylopyranaosyl-(1  $\rightarrow$  4)-D-xylopyranose (PAXX, Ib) from cell walls of barley straw showing that some *trans-p*-coumaric acid units are similarly linked to the walls (14): approximately 17% of the *trans-p*-coumaric acid that could be released from the walls by treatment with cold sodium hydroxide solution was recovered as PAXX and 50% of the *trans*-ferulic acid was recovered as FAXX. These recoveries should be seen as minimum values as grinding small amounts of the cell walls to a smaller particle size before treatment with "cellulase" increased the yields of PAXX and FAXX. It was estimated that one in every 31 arabinose residues was esterified with *trans-p*-coumaric acid and one in every 15 with *trans*-ferulic acid (14).

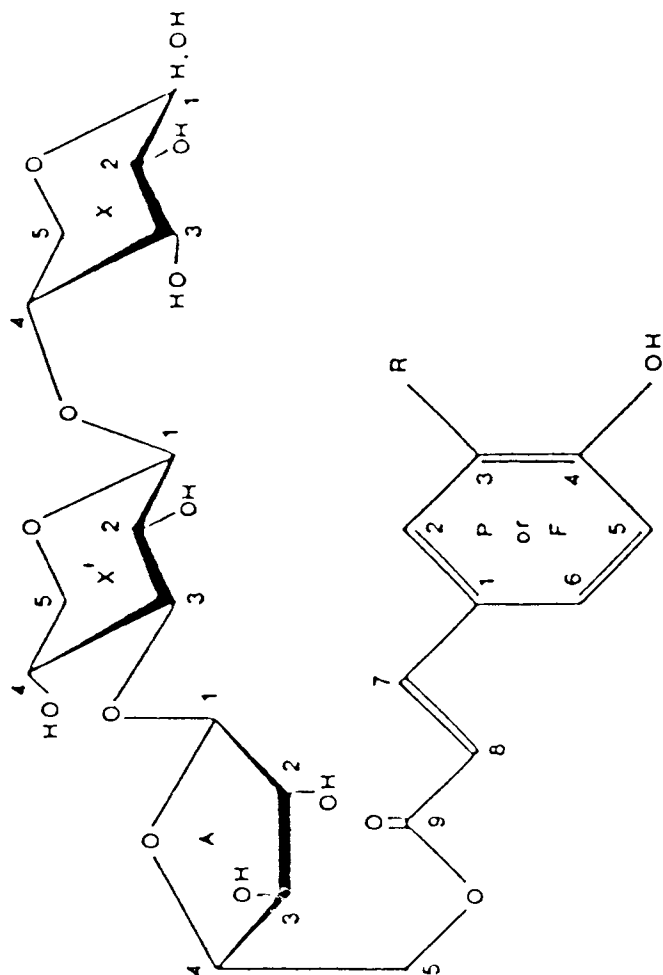
There is also evidence that at least some of the phenolic aldehydes and dehydrodiferulic acid (Figure 1) are linked covalently to cell wall polysaccharides. When ryegrass cell walls were treated with "cellulase," the aldehydes and the acid were released as water-soluble carbohydrate-aromatic compounds from which the aromatics were released by cold sodium hydroxide treatment (6,7). This suggests that these compounds are either ether-linked or, in the case of the acid, ester-linked to the polysaccharides.

It has been proposed that dehydrodiferulic acid units are formed by enzymic dehydrogenation of two ferulic acid units ester-linked to the cell wall (15). As can be seen from Table I, only very small amounts of the acid were found in cell walls: it seems unlikely that such amounts are sufficient to have a large effect on limiting the biodegradation of the walls.

Several workers have suggested that some, and possibly most, of the *p*-coumaric acid in graminaceous cell walls is ester-linked to lignin (16-19). Others have provided evidence that a small proportion of the ferulic acid units of cell walls are ether-linked via their phenolic groups to lignin (20).

*Relationships with Biodegradability.* As grasses mature and wall biodegradability decreases, the lignin content of their cell walls increases and the ratio of ferulic to *p*-coumaric acid in the walls decreases (2,21,22). Ruminant digestion of such walls leads to a preferential loss of ferulic acid, probably due to the degradation of mesophyll and other cell types that contain relatively high proportions of this acid compared with *p*-coumaric acid (21-25). It is also of interest to note that esterification of cell walls of orchard grass with *p*-coumaric and ferulic acids led to a decrease in wall biodegradability: a linear relationship was found between the rate of esterification and biodegradability (26).

The toxicity of monomeric phenolic acids and aldehydes of graminaceous cell walls to microflora in the rumen has been examined by several workers (3,27-32). In general, *trans-p*-coumaric acid was found to be the most toxic of the phenolic acids and decreased the rate of digestion of the cell walls. An important effect of the acid is that it limits the attachment of wall-degrading bacteria (32). The toxicity of *p*-hydroxybenzaldehyde was similar to *p*-coumaric acid but only very small amounts of the aldehyde

Ia R = OCH<sub>3</sub> (FAXX)

Ib R = H (PAXX)



have been found in cell walls. As yet there are no reports in the literature of the effects of dimeric phenolic acids on microorganisms.

### Dimeric Phenolic Acid Constituents (Substituted Cyclobutanes) of Cell Walls

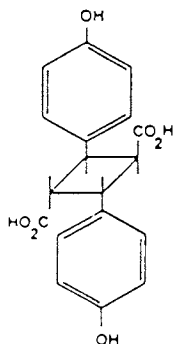
Recent work has shown that a dimer of *p*-coumaric acid, 4,4'-dihydroxytruxillic acid, is released from the cell walls of a temperate grass (*Lolium multiflorum*) by alkali treatment. The dimer was identified by gas chromatography/mass spectrometry of its tetra-trimethylsilyl (TMSi) derivative (33) and, from comparative studies, appeared to be identical to the synthetic isomer (II) prepared by the method of Cohen *et al.* (34). This compound, designated as a *p*-coumaric acid-*p*-coumaric acid (PCA-PCA) dimer, was also identified in the cell walls of tropical grasses (*Setaria anceps*, *Digitaria decumbens*, *Heteropogon contortus*). Cell walls of *Lolium multiflorum* and the tropical grasses also contained other PCA-PCA type isomeric dimers as well as analogous substituted cyclobutane dimers of ferulic acid [ferulic acid-ferulic acid (FA-FA) type] and "mixed" dimers [*p*-coumaric acid-ferulic acid (PCA-FA) type] (35: Ford, C. W.; Hartley, R. D., unpublished).

The total amount of PCA-PCA, FA-FA and PCA-FA dimers released from leaf and stem cell walls of the tropical grasses ranged from 0.5 to 4.4 mg g<sup>-1</sup> dry walls. These values compare with the total amount of *p*-coumaric plus ferulic acids ranging from 14 to 21 mg g<sup>-1</sup> dry walls; only traces of dehydrodiferulic acid were detected (Ford, C. W.; Hartley, R. D., unpublished).

It is well established that cinnamic acid and some substituted cinnamic acids (including *trans-p*-coumaric acid but not ferulic acid) can be dimerized *in vitro* by sunlight to truxillic and truxinic acids and their derivatives (34, 36, 37). Theoretically, *trans-p*-coumaric acid can produce 12 isomers depending on whether head-to-tail (4,4'-dihydroxytruxillic acid) or head-to-head (4,4'-dihydroxytruxinic acid) dimerizations occur with *syn* or *anti* and with *cis* or *trans* ring junctions (37). Mass spectrometric analysis of the tetra-TMSi derivatives showed that head-to-tail dimers split symmetrically on electron impact, whereas head-to-head dimers fragment asymmetrically (Figures 2 and 3) (33, 35, 38, 39). Thus the tetra-TMSi derivative of 4,4'-dihydroxytruxillic acid has a mass spectrum similar to that of the bis-TMSi derivative of *p*-coumaric acid (33).

Further examination of the mass spectra of the cyclodimers (PCA-PCA, FA-FA and PCA-FA types) from tropical grasses indicated that head-to-tail dimerization was most common; head-to-head dimerization was only found in PCA-PCA type dimers (Ford, C. W.; Hartley, R. D., unpublished).

It therefore seems probable that, in the cell walls of the growing plant, dimerization of *p*-coumaric and ferulic acid units linked to arabinoxylan occurs under the influence of sunlight. Earlier work (34) showed that *trans-p*-coumaric acid converts readily in sunlight to 4,4'-dihydroxytruxillic acid. It has recently been shown (40) that FA-FA and PCA-FA type cyclodimers can be obtained in low yield (less than 10%) by irradiating mixtures of the



11

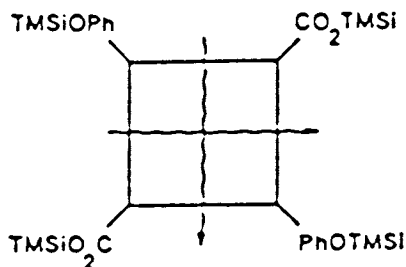


Figure 2. Symmetrical splitting (mass spectrometry) of the tetra-TMSi derivative of 4,4'-dihydroxytruxillic acid.

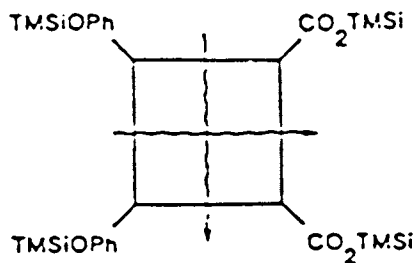


Figure 3. Asymmetrical splitting (mass spectrometry) of the tetra-TMSi derivative of 4,4'-dihydroxytruxinic acid.

monomers in plant growth cabinets in which the lighting approximately simulates low intensity sunlight.

The only stem materials examined were from the *Setaria anceps* and *Digitaria decumbens* grasses. The major substituted cyclobutane dimers in these walls appeared, from the mass spectral data, to be mixed dimers of ferulic acid and coniferyl alcohol (FA-ConAlc type). Further examination of the aromatics of stems is required but if such dimers are present then they may well be involved in the biosynthesis of lignin (41, 42).

Formation of phenolic dimers in plant cell walls during growth could cause the cross-linking of polysaccharide chains leading to increased wall rigidity as well as limiting biodegradability by microorganisms in the animal or in soil. As yet it is not understood how this cross-linking process relates to that of lignification. The relationships of the amounts of low molecular weight phenolics, particularly *p*-coumaric acid, of graminaceous cell walls with wall biodegradability could be utilized by the plant breeder as one of the selection criteria for the production of forages with increased digestibility for ruminant feeds.

### Literature Cited

1. Hartley, R. D. *Agric. Environm.* 1981, **6**, 91-113.
2. Hartley, R. D. In *Improved Utilization of Lignocellulosic Materials in Animal Feed*; OECD: Paris, 1985; pp. 10-30.
3. Akin, D. E. *J. Anim. Sci.* 1986, **63**, 962-77.
4. Akin, D. E. *Agron. J.*, in press.
5. Hartley, R. D.; Jones, E. C. *J. Sci. Food Agric.* 1978, **29**, 777-89.
6. Hartley, R. D.; Keene, A. S. *Phytochemistry* 1984, **23**, 1305-07.
7. Hartley, R. D.; Jones, E. C. *Phytochemistry* 1976, **15**, 1157-60.
8. El-basyouni, S. Z., Neish, A. C., Towers, G. H. N. *Phytochemistry* 1964, **3**, 627-39.
9. Higuchi, T.; Ito, Y., Kawamura, I. *Phytochemistry* 1967, **6**, 875-81.
10. Harris, P. J.; Hartley, R. D. *Biochem. Syst. Ecol.* 1980, **8**, 153-60.
11. Hartley, R. D.; Harris, P. J. *Biochem. Syst. Ecol.* 1981, **9**, 189-203.
12. Kato, A.; Azuma, J.; Koshijima, T. *Chem. Lett.* (Japan) 1983, 137-140.
13. Kato, Y.; Nevins, D. J. *Carbohydr. Res.* 1985, **137**, 139-50.
14. Mueller-Harvey, I.; Hartley, R. D.; Harris, P. J.; Curzon, E. H. *Carbohydr. Res.* 1986, **148**, 71-85.
15. Markwalder, H. U.; Neukom, H. *Phytochemistry* 1976, **15**, 836-37.
16. Nakamura, Y.; Higuchi, T. *Holzforschung* 1976, **30**, 187-91.
17. Himmelsbach, D. S.; Barton, F. E. *J. Agric. Food Chem.* 1980, **28**, 1203-08.
18. Atsushi, K.; Azuma, J.; Koshijima, T. *Holzforschung* 1984, **38**, 141-49.
19. Azuma, J.; Nomura, T.; Koshijima, T. *Agric. Biol. Chem.* 1985, **449**, 2661-69.
20. Scalbert, A.; Monties, B.; Lallemand, J.-Y.; Guittet, E.; Rolando, C. *Phytochemistry* 1985, **24**, 1359-62.
21. Hartley, R. D. *J. Sci. Food Agric.* 1972, **23**, 1347-54.
22. Aman, P.; Nordkvist, E. *Swedish J. Agric. Res.* 1983, **13**, 61-67.

23. Harris, P. J.; Hartley, R. D.; Lowry, K. H. *J. Sci. Food Agric.* 1980, **31**, 959-62.
24. Chesson, A. *J. Sci. Food Agric.* 1981, **32**, 745-58.
25. Lindberg, J. E.; Ternrud, I. E.; Theander, O. *J. Sci. Food Agric.* 1984, **35**, 500-06.
26. Sawai, A.; Kondo, T.; Ara, S. *J. Jap. Grassl. Sci.* 1983, **29**, 175-79.
27. Akin, D. E. *Agron. J.* 1982, **74**, 424-28.
28. Chesson, A.; Stewart, C. S.; Wallace, R. J. *Appl. Environ. Microbiol.* 1982, **44**, 597-603.
29. Borneman, W. S.; Akin, D. E.; Van Eseltine, W. P. *Appl. Environ. Microbiol.* 1986, **52**, 1331-39.
30. Akin, D. E.; Rigsby, L. L. *Appl. Environ. Microbiol.* 1987, **53**, 1987-95.
31. Theodorou, M. K.; Gascoyne, D. J.; Akin, D. E.; Hartley, R. D. *Appl. Environ. Microbiol.* 1986, **53**, 1046-50.
32. Akin, D. E.; Rigsby, L. L.; Theodorou, M. K.; Hartley, R. D. *Anim. Feed Sci. Technol.* 1988, **19**, 261-75.
33. Hartley, R. D.; Whatley, F. R.; Harris, P. J. *Phytochemistry* 1988, **27**, 349-51.
34. Cohen, M. D.; Schmidt, G. M. J.; Sonntag, F. I. *J. Chem. Soc.* 1964, 2000-2013.
35. Ford, C. W.; Hartley, R. D. *J. Chromatogr.* 1988, **436**, 484-89.
36. Schmidt, G. M. J. *J. Chem. Soc.* 1964, 2014-2021.
37. Khan, R. O. *Organic Photochemistry*; McGraw-Hill: New York, 1971; p. 157.
38. Caccamese, S.; Montaudo, G.; Przbylski, M. *Org. Mass Spec.* 1974, **9**, 1114-23.
39. Egerton, P. L.; Hyde, E. M.; Trigg, J.; Payne, A.; Beynon, P.; Mijovic, M. V.; Reiser, A. *J. Am. Chem. Soc.* 1981, **103**, 3859-63.
40. Ford, C. W.; Hartley, R. D. *J. Sci. Food Agric.* 1989, **46**, 301-310.
41. Nakamura, Y.; Higuchi, T. *Cell. Chem. Technol.* 1978, **12**, 209-21.
42. Katayama, Y.; Morohoshi, N.; Haraguchi, T. *Mokuzai Gakkaishi* 1980, **26**, 358-62.

RECEIVED May 19, 1989

## Chapter 10

# An Improved Radiotracer Method for Studying Formation and Structure of Lignin

Noritsugu Terashima

Faculty of Agriculture, Nagoya University, Nagoya 464-01, Japan

Since it is impossible to isolate lignin in its unaltered state, or to depolymerize it quantitatively into known structural entities, it has been difficult to determine lignin structure in the cell wall directly. Among attempts to circumvent these difficulties, the improved radiotracer method has provided useful information unobtainable by other methods. In this approach, specific dual-labeling of structural units in protolignin in intact plant tissue was achieved by administration of  $^3\text{H}$  and  $^{14}\text{C}$  labeled lignin precursors to differentiating tree xylem. Subsequent analysis of the resulting tissue (or lignin isolated from the tissue) was then carried out. These double-labeling experiments provided quantitative information on the structure of protolignin, as well as the changes occurring during its removal. Extension of this improved technique to the dehydrogenative polymerization of monolignols *in vitro* provided a method of more closely simulating lignin biogenesis in the cell wall.

Many approaches have been employed to attempt to elucidate the structure of lignin. However, most studies dealt with isolated lignins and utilized a number of different physical and chemical methods. These have included  $^1\text{H}$ -NMR,  $^{13}\text{C}$ -NMR, UV and IR spectroscopy, and the analysis of degradation products from acidolysis, thioacidolysis, alkaline nitrobenzene oxidation, permanganate oxidation, hydrogenolysis, and pyrolysis. While these methods provided important basic information on the structure of isolated lignins, its structure within the cell wall still remains an open question. This is because (i) in its native state, lignin is heterogeneous with respect to its macromolecular structure, morphological location and association with carbohydrates; this information is lost during its isolation from the

0097-6156/89/0399-0148\$06.00/0  
© 1989 American Chemical Society

cell wall; and (ii) it is impossible to obtain a lignin sample which can be unambiguously considered to represent whole protolignin; moreover, (iii) it is very difficult to depolymerize lignin quantitatively into known monomeric or oligomeric building units by established degradative methods.

In attempts to circumvent these difficulties, protolignin within cell walls has been examined by means of non-degradative methods such as UV, IR, Raman and NMR spectroscopy, SEM-EDXA and histochemical analysis. In addition to these techniques, administration of radio-labeled lignin precursors to actively lignifying plant tissue *in vivo*, followed by appropriate analyses of the lignin, has contributed greatly to our current understanding of lignin structure.

The specific labeling of lignin in plant tissue is usually achieved by administration of an appropriate precursor when lignification is actively occurring. Suitable precursors include L-phenylalanine, *p*-coumaric acid, ferulic acid, sinapic acid, *p*-glucocoumaryl alcohol, coniferin and syringin. For graminaceous plants, L-tyrosine is also effective. Labelled precursors can be prepared by replacement of either a specific hydrogen or carbon of the precursor with  $^3\text{H}$  or  $^{14}\text{C}$  respectively. Of these precursors, the monolignol glucosides, which occur naturally in the cambial sap of gymnosperms (1) and some angiosperms (2), have been shown to be the most suitable precursors for specific labeling of lignin in many plants (3,4). For example, monolignol glucosides were efficient precursors of lignin in both poplar (5) and rice plants (6), even though these glucosides were not detected in the lignifying tissues of these plants. Further, since cinnamyl alcohol-glucosyl transferases are widely distributed in the plant kingdom (7,8), this suggests that these glucosides may function as universal precursors for lignin biosynthesis.

In this chapter, improvements in the application of the radiotracer methods are discussed, using as an example, the *in vivo* formation of "condensed" substructures in the lignin macromolecule. Additionally, (i) the structural changes that the lignin macromolecule undergoes during its removal by chemical means; (ii) the use of labeled synthetic lignin preparations; and (iii) the importance of carbohydrates in lignification, are discussed.

## Materials and Methods

*Selective Labeling of a Specific Structural Unit in Protolignin.* In the experiments described, two to five year old shoots of approximately the same size were cut from trees grown under similar conditions. To each shoot, the labeled precursor was administered through the cut end. After a predetermined period for uptake and metabolism, the bark tissue was removed. The newly formed xylem tissue containing cell walls at the same stage of differentiation was collected mechanically by cutting 100  $\mu\text{M}$  tangential sections from the cambium toward the inner part of the xylem tissue by means of a sliding microtome.

For radioassays, sections were milled to about 40 mesh, and then extracted successively with ethanol, benzene-ethanol and hot water. The

resulting tissue was then subjected to combustion to give, depending upon the precursor administered, either  $^3\text{H}_2\text{O}$ ,  $^{14}\text{CO}_2$ , or both. Radioactivity contents were then determined by liquid scintillation counting. The standard deviation of the assay was 2%.

*Synthesis of DHP (Dehydrogenative Polymer) from Coniferyl Alcohol- $[\text{}^3\text{H}$ ,  $^{14}\text{C}]$  in the Presence of Carbohydrates.* Coniferyl alcohol-[ring  $^3\text{H}$ , U- $^{14}\text{C}$ ] (10 mg,  $^3\text{H}$ , 8300 dpm;  $^{14}\text{C}$ , 3630 dpm) was dissolved in Britton Robinson buffer (2.0 ml) containing the appropriate polysaccharide (30 mg) and peroxidase (10  $\mu\text{g}$ , Horseradish Type II, Sigma Co., USA) to afford a gel. Hydrogen peroxide (0.5 mL, 0.5%) was slowly added by permeation through a cellulose dialysis membrane, spread over the end of a glass tube (diameter: 1.5 cm) and inserted just below the surface of the gel. Following polymerization at 25°C for 53h, the water was removed slowly in a desiccator under slightly reduced pressure. The reaction mixture was then macerated in ethanol (0.5 mL  $\times 3$ ), to dissolve the soluble DHP fraction and any low molecular weight entities, thereby leaving an insoluble lignin-carbohydrate complex (LCC). The DHP polymer was then obtained by combining the ethanol fractions, removing the solvent under reduced pressure, and then redissolving the residue in  $\text{CH}_2\text{Cl}_2$ -EtOH (0.5 mL, 2:1 v/v). This solution was then poured into dry ether (10 mL), following which the precipitated DHP was collected by centrifugation (8000 $\times$  g, 10 min).

## Results and Discussion

*Specific Labeling of Protolignin.* The major part of softwood lignin is constituted of guaiacyl lignin. Consequently, ferulic acid is efficiently and intactly incorporated into guaiacyl lignin in pine (9). However, when hardwoods are administered radiolabeled ferulic or sinapic acids in the light, considerable methoxylation or demethoxylation of guaiacyl or syringyl residues can occur, thereby interconverting said precursors. To some extent, such interconversions can be reduced by administering these precursors in the dark, e.g., when [ring-2- $^3\text{H}$ ] ferulic or sinapic acids were individually administered to poplar shoots, the distribution of label into guaiacyl and syringyl components was 80:20 and 27:73, respectively (10). This distribution was established by subjecting the lignin to nitrobenzene oxidation, and determining the radioactivity of the liberated aldehydes, vanillin and syringaldehyde.

These precursor scrambling problems were essentially overcome by administering labeled coniferin and syringin to *Magnolia kobus* DC (3). The lignin so obtained was then subjected to oxidation as before, where it was found that 90 and 99% of the activity of total aldehydes was present in vanillin and syringaldehyde, respectively (3), i.e., the glucosides were incorporated selectively into the lignin polymer. [Note that the monolignols themselves are not normally used in labeling experiments, even though they are the immediate precursors of lignin. This is because they can be polymerized without any biochemical control, as soon as they are in contact with tissue containing peroxidase and hydrogen peroxide, and could thus potentially give erroneous results.]

*Analysis of the Structure and Reactions of Lignin by the Double-Labeling Technique.* Table I shows the type of information that can be obtained by means of double-radiolabeling experiments, using as an example gymnosperm tissue. That is, by judicious use of doubly-labeled precursors, it is possible to ascertain the extent of substitution/condensation reactions at selected aromatic ring positions, as well as demethylation and (propanoid) side-chain elimination reactions. Such strategies are described in greater detail below, using both gymnosperms and angiosperms.

Table I. Use of Doubly labeled Guaiacyl Lignin Precursors in Lignin Biosynthesis Studies

Position of Label in Precursor		
<sup>3</sup> H	<sup>14</sup> C	Information Attainable
Arom. ring 5	Arom. ring	Degree of substitution at the position of aromatic ring labeled with <sup>3</sup> H
Arom. ring 2	Arom. ring	
Arom. ring 6	Arom. ring	
Methoxyl	Arom. ring	Demethylation, demethoxylation
Arom. ring 2	Side-chain C <sub>α</sub>	Elimination of side-chain carbon (C <sub>α</sub> , C <sub>β</sub> and C <sub>γ</sub> ) and formation of β-1 structure
Arom. ring 5	Side-chain C <sub>β</sub>	
Arom. ring 6	Side-chain C <sub>γ</sub>	

*Degree of Substitution at the Aromatic Ring.* This method is based on the fact that when a lignin precursor, tritiated at a specific position in the aromatic ring, is incorporated into the lignin polymer and then undergoes a substitution reaction at that position, the corresponding tritium label is eliminated. For example, if [arom. ring-5-<sup>3</sup>H, U-<sup>14</sup>C] coniferyl alcohol (I) is incorporated into lignin, the degree of formation of substructures V-VII (Fig. 1) can be estimated from the degree of substitution (D.S.%). This is calculated as follows:

$$\text{D.S.\%} = \frac{{}^3\text{H}/{}^{14}\text{C} \text{ ratio of monolignol} - {}^3\text{H}/{}^{14}\text{C} \text{ ratio of polymer}}{{}^3\text{H}/{}^{14}\text{C} \text{ ratio of monolignol}} \times 100$$

However, since the frequency of aromatic 4-O-5 diaryl ether substructure (V) in lignin is low (11-13), the D.S.% really provides an estimate of the amount of "condensed" structures (VI, VII). This is illustrated in the following example: When [ring-5-<sup>3</sup>H, U-<sup>14</sup>C] ferulic acid, a precursor of I, was administered to Japanese black pine (*Pinus thunbergii* Parl.), an average D.S. value of 56% was obtained. However, this value varied widely from 30-80% depending upon the stage of cell wall formation examined. (The different xylem sections were obtained by means of a microtome) (14,15). These results can be explained as follows: during initial lignification, lignin is deposited in the middle lamella and has a high D.S. (75-80%), thereby establishing that significant "condensation" has occurred (14). On the other



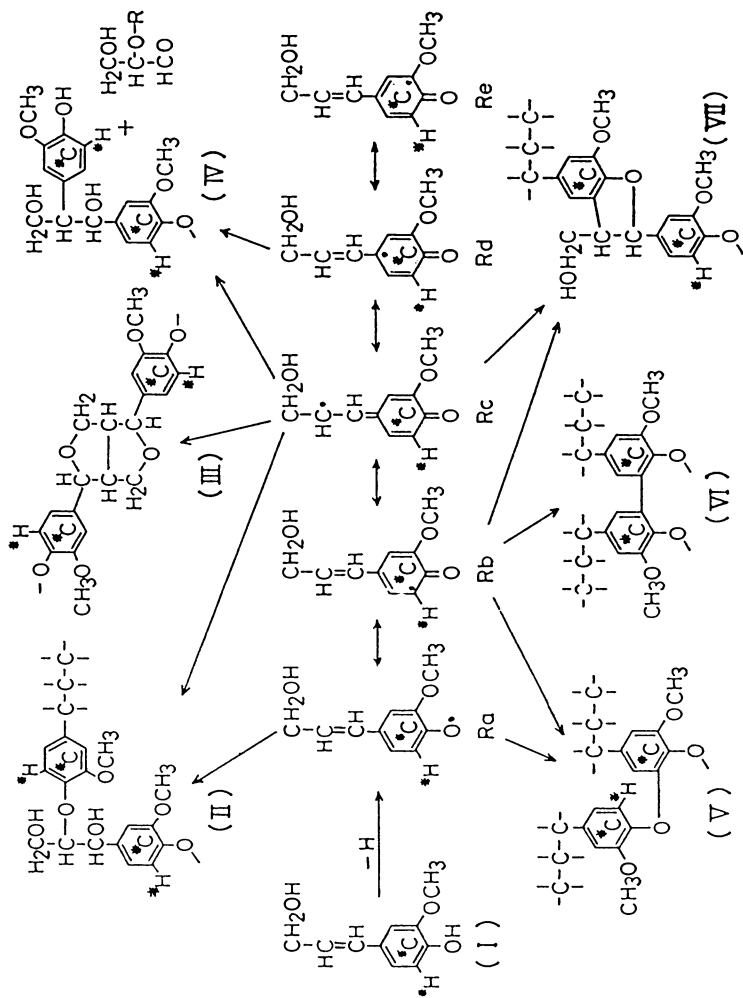


Figure 1. Removal of  $^3\text{H}$  at position 5 of the guaiacyl ring of coniferyl alcohol (I) by formation of ring substituted structures (V, VI, VII) during dehydrogenative polymerization.

hand, the lignin deposited in the secondary walls had a much lower D.S. value (30-75%), indicating that this reaction was not as prevalent in that tissue.

Other factors such as temperature (15), plant hormone addition (16), light (17), gravity (14), and pH of the precursor solution (15), also have an effect on the D.S. value. This can best be illustrated by examples: (i) growth of *P. thunbergii* at room temperature (25-30°C) gave a lignin with more condensed units (48-73%) than that obtained at 10°C (33-57%) (11); (ii) when [ring-5-<sup>3</sup>H, U-<sup>14</sup>C] ferulic acid was administered in a solution containing the plant hormone, auxin (IAA, 10<sup>-6</sup>M), the degree of condensation increased (59-87%), whereas with abscisic acid (ABA, 10<sup>-6</sup>M) it was reduced (24-64%); (iii) when the precursor solutions were administered at pH 5.2 and 8.0, the D.S. was higher in the former case (54-79%) than in the latter (54-71%). In all cases, higher and lower D.S. values were found for lignins in tissue sections nearest to the cambium and in the tissue furthest from the cambium (1000 μm) respectively. (iv) When a pine shoot growing at an angle of 45° was administered [ring-5-<sup>3</sup>H, U-<sup>14</sup>C] ferulic acid, the <sup>3</sup>H/<sup>14</sup>C ratio was lower in the underside tissue than in the upperside, as indicated in the D.S. (%) values shown in Table II (14,15). This indicated that the lignin in compression wood of gymnosperms had more condensed guaiacyl units (at C-5) than the lignin present in the upperside wood, which more closely resembled normal wood. Note, though, that the gymnosperm ginkgo showed a much smaller response; however, this result was in agreement with other analyses establishing ginkgo to be an exception to most gymnosperms (18). In the case of angiosperms (poplar, locust and oleander), however, the situation was very different than that of pine (Table II). No significant differences in D.S. (%) values were observed at position C-5 of the guaiacyl component of angiosperm lignin between the upper and lower tissues. The DS values obtained for C-2 and C-6 also provided valuable information: and these are shown for both gymnosperms and angiosperms (16). As can be seen from Table II, these values were low in all cases (≤ 3.9%) and no discernible differences between upper and lower tissues were observable.

Thus, these results are in agreement with other studies (19,20), (e.g., by degradative analysis) where it was found that (i) gymnosperm compression wood lignin differs from "normal wood" lignin by virtue of its high content of condensed units, and (ii) tension wood lignin in angiosperms contains only slightly more condensed units than normal wood lignin.

*Retention of Propanoid Side-Chains During Lignin Formation.* As noted previously from Table II, the degree of substitution at C-2 of the guaiacyl ring of lignin was low (0-2%). This finding can be used to determine the extent of side-chain elimination as a result of formation of β-1 structures (Fig. 1, Structure IV). In order to determine this, labeling of the appropriate lignin precursor with <sup>3</sup>H at C-2 of the aromatic ring, and <sup>14</sup>C in the side-chain, was carried out. Obviously, if little or no elimination of the side-chain took place during its incorporation into the lignin polymer, then the <sup>3</sup>H/<sup>14</sup>C ratio would remain essentially unchanged. On the

Table II. Degree of Substitution (%) of the Guaiacyl Ring of Lignin in the Upper and Lower Portions of Various Tree Shoots Grown at a 45° Angle

	Position 5		Position 6		Position 2	
	Upper (DS %) <sup>g</sup>	Lower (DS %) <sup>g</sup>	Upper (DS %) <sup>g</sup>	Lower (DS %) <sup>g</sup>	Upper (DS %) <sup>g</sup>	Lower (DS %) <sup>g</sup>
Pine <sup>a</sup>	52.1	62.2	3.9	3.9	2.0	2.0
Ginkgo <sup>b</sup>	49.9	51.8	0.0	0.0	0.0	0.0
Italian Poplar <sup>c</sup>	49.9	49.9	3.0	3.0	1.9	0.0
Kamabuchi Poplar <sup>d</sup>	54.1	51.1	2.0	2.0	2.0	2.0
Locust <sup>e</sup>	46.2	44.0	3.0	3.0	1.9	1.9
Oleander <sup>f</sup>	47.9	47.3	0.0	0.0	0.0	0.0

<sup>a</sup> *Pinus thunbergii* Parl.

<sup>b</sup> *Ginkgo biloba* L.

<sup>c</sup> *Populus euramericana* cv. 'I-214'.

<sup>d</sup> *Populus nigra* L. X *Populus maximowiczii* A. Henry.

<sup>e</sup> *Robinia pseudoacacia* L.

<sup>f</sup> *Nerium indicum* Mill.

<sup>g</sup> DS % = degree of substitution (%).

other hand, an increase would signify the involvement of side-chain elimination. These labeling studies showed, however, that little or no elimination occurred (21). In agreement with this finding, <sup>1</sup>H-NMR examination of milled wood lignin from spruce and birch also revealed that the β-1 content was very low (22,23).

*Retention of Methoxyl Groups During the Formation of Lignin in vivo.* Following uptake of [ring-2-<sup>3</sup>H, O<sup>14</sup>CH<sub>3</sub>] ferulic acid to growing stems of pine and locust, and subsequent analysis of the resulting lignin, it was found that no significant demethylation or demethoxylation of the guaiacyl nucleus occurs during lignin formation (15).

*Changes to the Macromolecule during Delignification.* As discussed beforehand, there is no method currently available for the isolation of protolignin in its unaltered state. On the other hand, while there are many techniques used to isolate lignin, the effect of these chemical treatments on the structure of the macromolecule is poorly understood. As previously mentioned, since the elimination of side-chain and methoxyl groups scarcely occurs during gymnosperm lignin formation, the carbon skeleton of guaiacyl-rich protolignin can be considered to be mainly C<sub>6</sub>-C<sub>3</sub>-OCH<sub>3</sub>. Thus, specifically labeled guaiacyl lignin can be used to determine some of the changes that it undergoes during various chemical treatments. The labeled guaiacyl lignin used in these studies was either present in intact tissue of pine, or in an isolated milled wood lignin preparation (24). Table III summarizes the results obtained. As can be seen, the lignins isolated by solvolysis with ethanol, dimethoxypropane, benzyl ethyl ether or dioxane had very similar <sup>3</sup>H/<sup>14</sup>C ratios to that of the original protolignin (24). On

the other hand, and as can be seen from the  $^3\text{H}/^{14}\text{C}$  ratios obtained, substantial structural changes occurred during the isolation of Klason (24) and kraft (25) lignins, with appreciable amounts of both methoxy groups and side-chain carbons being lost. From these investigations, it can thus be concluded that the average repeating unit in kraft lignin is  $\text{C}_6\text{-C}_{2.32}(\text{OCH}_3)_{0.76}$ , i.e., significant modifications to the carbon skeleton have occurred (25). Estimation by  $^{13}\text{C}$  NMR gave similar results for loss of side-chain carbons for pine kraft lignin (26).

Table III. Relative Numbers of Methoxyl and Side-Chain Carbons to Guaiacyl Ring Carbons in Various Lignin Derivatives Isolated from *Pinus thunbergii* (25,26)

Lignin Type	Arom. Ring	Methoxy	$\text{C}_\alpha$	$\text{C}_\beta$	$\text{C}_\gamma$	Side- Chain
Protolignin in cell wall	6.00	1.00	1.00	1.00	1.00	3.00
Benzyl ethyl ether lignin <sup>a</sup>	6.00	1.04	0.97	0.99	0.95	2.91
Dimethoxypropane lignin <sup>b</sup>	6.00	0.92	0.98	1.00	1.05	3.03
Ethanolysis lignin	6.00	0.99	0.95	0.95	0.96	2.86
Dioxane lignin	6.00	0.92	1.08	0.95	1.07	3.10
Klason lignin	6.00	0.87	0.92	0.92	0.84	2.68
Kraft lignin <sup>c</sup>	6.00	0.76	0.79	0.84	0.69	2.32

<sup>a</sup> Solvolysis lignin prepared by transesterification (24).

<sup>b</sup> Solvolysis lignin prepared with 2,2-dimethoxypropane (24).

<sup>c</sup> Wood meal singly labeled with  $^{14}\text{C}$  was employed. This estimation was made on the basis of radioactivity and UV absorbance (25).

*Dehydrogenative Polymerization of Monolignols* in vitro. As observed from the microautoradiograms of newly formed xylem of pine (*P. thunbergii*), the early stages of cell wall development lignin deposition are always preceded by deposition of pectic substances (27), and then by hemicelluloses in the later stages (27). Interestingly, the lignin macromolecule in the compound middle lamella deposited during these early stages of cell wall differentiation contains more "condensed" units than that formed later in the secondary wall (14,15). This could be due to the influence of several factors, such as (i) pectic substances and mannans affecting the process of dehydrogenative polymerization of the monolignols (28); (ii) the concentration of peroxidase being higher in the cell corner and middle lamella regions (29). This could result in the formation of a more "condensed" lignin (28); (iii) *p*-hydroxyphenylpropane units participating more extensively during the formation of middle lamella lignin (4,30). Such influences can be examined, at least in a crude way, by synthesizing labeled dehydrogenative polymer (DHP) from [ring-5- $^3\text{H}$ , U- $^{14}\text{C}$ ] coniferyl alcohol under conditions approximating these situations.

Effect of Carbohydrate: Table IV shows the effect of carbohydrates on the D.S. (%) of both lignin-carbohydrate complexes (LCC's) and DHP's

produced from [ring-5-<sup>3</sup>H, U-<sup>14</sup>C] coniferyl alcohol at pH 5.5, 6.5 and 7.5, respectively. As can be seen, the D.S.(%) of DHP's formed in the presence of xylan was greater than that observed for the DHP's formed in the absence of polysaccharides. As far as the LCC's were concerned, the D.S. (%) values with xylan and pectin were also higher than that for DHP's produced solely from coniferyl alcohol.

Table IV. The Effect of Carbohydrates on the Degree of Substitution at Position 5 of Guaiacyl Ring in DHP and LCC Fractions

Carbohydrate	pH	D.S.% of DHP	Yield (%)	D.S.% of LCC	Yield (%)
None	5.5	42.7	47.6	—	n.d. <sup>e</sup>
None	6.5	39.5	41.8	—	—
None	7.5	35.0	44.4	—	—
Xylan <sup>a</sup>	5.5	51.3	46.7	45.2	22.9
Xylan	6.5	43.3	45.3	45.5	21.0
Xylan	7.5	44.3	43.2	35.1	18.0
Mannan <sup>b</sup>	5.5	40.0	44.5	28.0	18.0
Mannan	6.5	35.6	45.3	25.5	15.6
Mannan	7.5	35.6	40.9	36.4	19.9
Pectin <sup>c</sup>	5.0	—	—	45.1	n.d.
Pectin	6.5	41.4	29.5	41.8	27.8
Pectin	6.5d	37.9	37.4	35.1	28.6
Pectin	7.5d	26.2	—	36.6	n.d.

<sup>a</sup> Isolated from cotton seed hulls by delignification with chlorous acid followed by extraction with sodium hydroxide.

<sup>b</sup> Obtained from manufacturer of konnyaku, a type of food made from the tuber of the konyak plant (*Amorphophallus konjac* C. Koch).

<sup>c</sup> Citrus pectin purchased from Tokyo Kasei Co., Tokyo.

<sup>d</sup> 3 mg of calcium hydroxide was added.

<sup>e</sup> n.d. = not determined.

Effect of pH: The effect of pH was also interesting. As can be seen (Table IV), the D.S.(%) values for the polymers formed at low pH were higher than those at high pH. Next we examined the effect of calcium cations, since calcium is supposed to participate in the lignification process (31). Direct addition of calcium hydroxide to the reaction mixture lowered the D.S, but this was probably only a consequence of increased pH. The effects noted for pectin and xylan can be partly ascribed to their acidic properties. These results may therefore explain the observation that when a pine shoot is administered [ring-5-<sup>3</sup>H, ring-U-<sup>14</sup>C] ferulic acid, dissolved in phosphate buffer at pH 5.2 and 8.0, the D.S.(%) value due to condensation at C-5 of the lignin was higher in the shoot administered at low pH (15). This pH effect can potentially be explained as follows: Freudenberg *et al.* established that coniferyl alcohol is first dehydrogenated by mushroom laccase/O<sub>2</sub> or peroxidase/H<sub>2</sub>O<sub>2</sub> to yield the transient phenoxy radical species, shown in

Figure 1. Among the five resonance structures shown, Ra, Rb and Rc will undergo random coupling reactions more readily than Rd and Re, since the radicals Rd and Re are sterically hindered. Indeed, this is what is found experimentally, since only minor amounts of  $\beta$ -1 structures (derived from Rd) have been found in milled wood lignin (22,23), and demethoxylation does not occur to any appreciable extent during lignin formation (21). The reactivity of the phenoxy radical, Ra, will be affected greatly by pH since it can be masked by protons under acidic conditions, and its reactivity will thus be diminished. On the other hand, the reactivity of Rb and Rc will not be affected appreciably by pH. Thus more frequent coupling of Rb-Rc, Rb-Rb and Rc-Rc can be expected at low pH, and more of Ra-Rb and Ra-Rc coupling at high pH.

For some time now, it has been proposed that the structural variations observed in DHP's are caused by the mode of polymerization, with bulk polymerization containing more condensed units than end-wise polymerization (32,33). However, in these experiments, DHP's prepared under the same conditions gave different D.S. values depending upon the pH at which the reaction took place. This result suggests that the molecular structure of lignin in the cell wall can also be controlled by factors other than the mode of polymerization.

*Condensed Structures in p-Hydroxyphenyl-Guaiacyl Type DHP.* It has been difficult to determine the exact amount of *p*-hydroxyphenylpropane units in lignin. This can best be illustrated by an example; nitrobenzene oxidation of a DHP prepared by the Zutropfverfahren method from a mixture of *p*-coumaryl alcohol, coniferyl alcohol and sinapyl alcohol, gave no detectable *p*-hydroxybenzaldehyde on alkaline nitrobenzene oxidation (34). To determine the reasons for this, DHP's were prepared from a mixture of [ring-2-<sup>3</sup>H] *p*-coumaryl alcohol and [ $\alpha$ -<sup>14</sup>C] coniferyl alcohol in the presence of carbohydrates by the procedure described above (35). The "LCC" fraction so obtained was subjected to combustion, and the exact *p*-hydroxyphenylpropane:guaiacylpropane ratio was determined from the activity of <sup>3</sup>H<sub>2</sub>O and <sup>14</sup>CO<sub>2</sub> released (Figure 2). A portion of the same LCC fraction was also oxidized with nitrobenzene and alkali, and the resulting liberated aromatic aldehydes were then analyzed by HPLC. Results are shown in Table V.

Table V. Molar Ratios of *p*-Hydroxyphenyl (H) to Guaiacyl (G) Units in DHP's and their Nitrobenzene Oxidation Products

	H:G	H:G	H:G
Starting monolignol mixtures <sup>a</sup>	2.00:1.00	1.00:1.00	0.50:1.00
"LCC" fraction of polymers <sup>a</sup>	1.88:1.00	0.90:1.00	0.47:1.00
Oxidation products <sup>b</sup>	1.21:1.00	0.72:1.00	0.41:1.00

<sup>a</sup> Estimated from the radioactivities of <sup>3</sup>H<sub>2</sub>O and <sup>14</sup>CO<sub>2</sub> produced by combustion.

<sup>b</sup> Molar ratios of *p*-hydroxybenzaldehyde to vanillin were determined by HPLC.

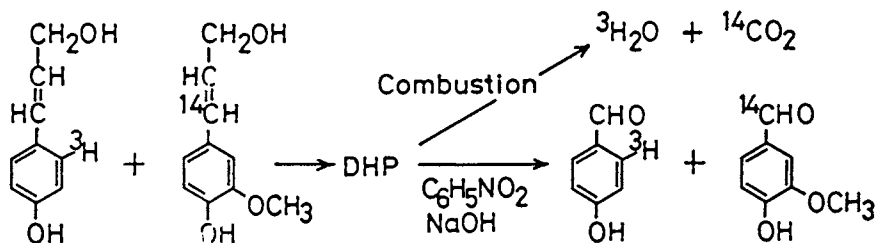


Figure 2. Dehydrogenative polymerization of a mixture of *p*-coumaryl alcohol-[ring-2- $^3\text{H}$ ] and coniferyl alcohol-[U- $^{14}\text{C}$ ], and nitrobenzene oxidation of the DHP to give *p*-hydroxybenzaldehyde-[ring-2- $^3\text{H}$ ] and vanillin-[formyl- $^{14}\text{C}$ ].

As can be seen, the molar ratios of *p*-hydroxyphenyl to guaiacyl units were slightly lower for the DHP's when compared to the original mixtures. This implies that coniferyl alcohol tends to be incorporated into the polymer slightly more readily than *p*-coumaryl alcohol. On the other hand, the much-reduced ratio of *p*-hydroxybenzaldehyde to vanillin, liberated during alkaline nitrobenzene oxidation, proved that this DHP contained a larger amount of condensed *p*-hydroxyphenylpropane units than condensed guaiacyl units.

Finally, it should be noted that the structure of the DIHP varies greatly depending on the polymerization conditions employed. Additionally, the yield and chemical and physical properties of these DHP preparations differ substantially from protolignin. Further improvements in simulation of the lignification process are therefore needed, and the radiotracer method can be employed as one approach to solve such problems.

### Concluding Remarks

1. The specific labeling of specific moieties in protolignin can be achieved by administration of an appropriate labeled precursor to a growing plant.
2. Double labeling with  $^3\text{H}$  and  $^{14}\text{C}$  at specific positions of an appropriate structural moiety in lignin, combined with accurate determination of  $^3\text{H}/^{14}\text{C}$  ratios, provides reliable information concerning protolignin structure and structural changes that occur during delignification.
3. The double labeling technique, combined with the technique of collection of xylem tissue at different stages of differentiation, provides additional information on the distribution of specific lignin substructures such as "condensed units" in different morphological regions.
4. The double-labeling technique is also useful for *in vitro* studies on the mechanism of dehydrogenative polymerization of monolignols.
5. This improved radiotracer method can be employed as a non-degradative method for examining the distribution, structure and reactions of lignin within the cell wall.

### Literature Cited

1. Freudenberg, K.; Harkin, J. M. *Phytochemistry* 1963, **2**, 322.
2. Terazawa, M.; Okuyama, H.; Miyake, M. *Mokuzai Gakkaishi* 1984, **30**, 322.

3. Terashima, N.; Fukushima, K.; Takabe, K. *Holzforschung* 1986, **40**, Suppl., 101.
5. Fukushima, K.; Terashjima, N. *Proc. 32nd Lignin Symp. at Fukuoka* 1987, p. 13.
6. He, L-F.; Terashima, N. *Mokuzai Gakkaishi* 1988, **35**, 117.
7. Ibrahim, R. K.; Grisebach, H. *Arch. Biochem. Biophys.* 1976, **176**, 100.
8. Ibrahim, R. K. *Z. Pflanzenphysiol.* 1977, **85**, 253.
9. Terashima, N.; Suganuma, N.; Araki, H.; Kanda, T. *Mokuzai Gakkaishi* 1976, **22**, 450.
10. Terashima, N.; Fukushima, K.; Tsuchiya, S.; Takabe, K. *J. Wood Chem. Technol.* 1986, **6**, 495.
11. Erickson, M.; Larsson, S.; Miksche, G. E. *Acta Chem. Scand.* 1973, **B27**, 903.
12. Nimz, H. *Angew. Chem. Int. Engl. Ed.* 1974, **13**, 313.
13. Glasser, W. G.; Glasser, H. R. *Pap. Puu* 1981, **63**, 71.
14. Terashima, N.; Tomimura, Y.; Araki, H. *Mokuzai Gakkaishi* 1979, **25**, 595.
15. Tomimura, Y.; Yokoi, T.; Terashima, N. *Mokuzai Gakkaishi* 1979, **25**, 743.
16. Tomimura, Y.; Yokoi, T.; Terashima, N. *Mokuzai Gakkaishi* 1980, **26**, 37.
17. Terashima, N. *Proc. 32nd Ann. Mtg. Jap. Wood Res. Soc.* 1982, p. 238.
18. Timell, T. E. *Wood Sci. Technol.* 1978, **12**, 89.
19. Morohoshi, N.; Sakakibara, A. *Mokuzai Gakkaishi* 1971, **17**, 393.
20. Yasuda, S.; Sakakibara, A. *Mokuzai Gakkaishi* 1975, **21**, 363.
21. Tomimura, Y.; Terashima, N. *Mokuzai Gakkaishi* 1979, **25**, 427.
22. Lundquist, K. *Acta Chem. Scand.* 1980, **B34**, 21.
23. Lundquist, K. *Acta Chem. Scand.* 1981, **B35**, 497.
24. Kachi, S.; Araki, H.; Terashima, N.; Kanda, T. *Mokuzai Gakkaishi* 1975, **21**, 669.
25. Terashima, N.; Araki, H.; Suganuma, N. *Mokuzai Gakkaishi* 1977, **23**, 343.
26. Robert, D. R.; Bardet, M.; Gellerstedt, G.; Lindfors, E. L. *J. Wood Chem. Technol.* 1984, **4**, 239.
27. Terashima, N.; Fukushima, K.; Takabe, K. *Holzforschung* 1988, **42**, 347.
28. Terashima, N.; Seguchi, Y. *Cell. Chem. Technol.* 1988, **22**, 147.
29. Takabe, K.; Harada, H. *Proc. 30th Lignin Symp. at Kochi* 1985, p. 1.
30. Whiting, P.; Goring, D. A. I. *Wood Sci. Technol.* 1982, **16**, 261.
31. Wardrop, A. B. *Appl. Polym. Symp.* 1976, **28**, 1041.
32. Sarkanen, K. V. In *Lignins: Occurrence, Formation, Structure and Reactions*; Sarkanen, K. V.; Ludwig, C. H., Eds.; Wiley-Interscience: New York, 1971, p. 150.
33. Lai, Y-Z.; Sarkanen, K. V. *Cell. Chem. Technol.* 1975, **9**, 239.
34. Faix, V. O.; Schweers, W. *Holzforschung* 1975, **29**, 48.
35. Terashima, N.; *Proc. 38th Ann. Mtg. Jap. Wood Res. Soc.* 1988, p. 368.

RECEIVED March 27, 1989



## Chapter 11

# Biogenesis and Structure of Macromolecular Lignin in the Cell Wall of Tree Xylem as Studied by Microautoradiography

Noritsugu Terashima and K. Fukushima

Faculty of Agriculture, Nagoya University, Nagoya 464-01, Japan

Specific labeling of the protolignin of various trees was achieved by administration of appropriate  $^3\text{H}$ -labeled monolignol glucosides to differentiating tree xylem. The process of deposition of each labeled precursor in the developing cell wall was visualized by means of high resolution microautoradiography. It was found that the monolignol (and polysaccharide which affects polymerization) changed with both type and age of the individual cell. The incorporation of monolignols into the protolignin macromolecule occurred in the order of increasing complexity, i.e., *p*-hydroxyphenyl-, guaiacyl- and syringylpropane units were deposited successively. It was noted that the lignin deposited in the early stages of cell wall development in the compound middle lamella region contained more condensed structures than that formed in the later stages in secondary wall. It was concluded that lignin formation occurs under definite biochemical regulation to give a macromolecule which is heterogeneous in structure and specific in its morphological location.

It is well known that the structure, distribution and properties of protolignin in cell walls vary according to cell type and morphological location. This is based upon extensive studies on topochemical properties of lignin using various methods such as ultraviolet microscopic photometry (1,2), bromination-SEM-EDXA (3) and other physical or chemical analyses of isolated tissue fractions (4).

In woody gymnosperms, there are significant differences in the distribution, reactivity and physical properties of protolignins found in the compound middle lamella and the secondary wall (1-3). Additionally, variations between lignins in vessels and fibers have also been noted (3). All of these

0097-6156/89/0399-0160\$06.00/0  
© 1989 American Chemical Society

observations are potentially explicable by factors such as (i) differences in monomeric composition, (ii) differences in interunit linkages between individual lignin monomers, (iii) linkages between lignin and carbohydrates, and (iv) variations in distribution (frequency and localization) of structural moieties in the lignin macromolecule. Many approaches have been tried to solve these problems, particularly degradation analyses such as acidolysis and oxidation. However, these have afforded only limited information on the topochemical nature of lignin. Hence, more detailed information about the macromolecular structure of protolignin can only be obtained by suitable non-degradative analyses.

In this chapter, the results obtained from the combined use of specific radiolabeling of lignin in plant tissue and microautoradiography are discussed.

### Materials and Methods

*Radioactive Precursors for Microautoradiography.* Several lignin precursors were labeled with  $^3\text{H}$  or  $^{14}\text{C}$  at specific points. These precursors included *p*-coumaric, ferulic, and sinapic acids, and the  $\beta$ -D-glucosides of the three monolignols, *p*-coumaryl, coniferyl, and sinapyl alcohols.  $^3\text{H}$ -labeled precursors were usually prepared by replacement of the hydrogen at position 2 of the aromatic ring with  $^3\text{H}$ , since essentially all (> 98%) of the  $^3\text{H}$  at this position is retained during lignin formation (5). Precursors labeled at C-5 or C-6 of the aromatic rings can also be employed for determination of the extent of substitution reactions at these positions (Terashima, this volume). After incorporation of precursors into growing plants, microautoradiograms of radiolabeled tissue sections were prepared, and these gave semiquantitative information regarding their deposition within the cell wall. This was obtained by determination of their activities using the technique of silver grain counting (6). Generally, the  $^3\text{H}$ -labeled precursors are more suitable for such semiquantitative estimations than their C-14 counterparts, because low energy  $\beta$ -emitter  $^3\text{H}$  can afford a high resolution autoradiogram. The specific radioactivity of the precursors must, however, be high enough (>  $1\mu\text{Ci}/\mu\text{mol}$ ) to obtain a good microautoradiogram in a reasonable period of time (< 3 weeks). On the other hand, precursors labeled with  $^{14}\text{C}$  at positions in the aromatic ring are more desirable for tracing the fate of particular structural units during various reactions. Precursors labeled at side-chain carbons with C-14 could also be used since side-chain cleavage reactions from the lignin macromolecule rarely occur during lignin formation (5).

*Administration of Precursor.* Precursors were administered to plants according to previously described procedures (6). Shoots of 2-3 year old trees were obtained during June or July, when the rate of thickening growth was highest. A V-shaped groove, 2 mm wide and 5 mm long, was made with a razor blade in a circumferential direction on the shoot, so that the bottom of the groove reached the differentiating xylem. Fine glass wool was packed into the groove, and a solution of the precursor (8-10  $\mu\text{Ci}$ , 1 mg in 100

$\mu\text{l}$  phosphate buffer, pH 7.0) was added dropwise to the fine glass wool, and allowed to metabolize for 3 h. A drop of 3% glutaraldehyde in phosphate buffer (pH 7.0) was then added to the groove, and a small block of xylem tissue near the groove was cut and fixed again in 3% glutaraldehyde overnight in the refrigerator. Part of the xylem tissue was dehydrated by means of a graded ethanol series and embedded in epoxy resin prepared by mixing Quetol 812 (100 g, Nissin EM Co. Ltd., Tokyo), methyl nadic anhydride (89 g) and 2,4,6-tri-[dimethylaminomethyl]-phenol (1.7 g).

*Preparation of Microautoradiogram.* Microautoradiograms were prepared according to the procedure described earlier (10). Two  $\mu\text{m}$  thick transverse sections were cut from the embedded xylem tissue using a Reichert-Jung Supercut 2050 microtome equipped with a glass knife. These were then mounted on glass slides and covered with Kodak AR-10 stripping film. The glass slides were stored in a refrigerator from 3 weeks to 1 year as required, following which they were developed with Kodak D-19 and fixed with Fuji-Fix. The sections were stained with toluidine blue O, and photomicrographs were made using a Zeiss IBAS 1 image analyzer. A polarization microscope, Olympus POS, was used to observe the deposition of cellulose microfibrils during secondary wall formation.

## Results and Discussion

*Selectivity of Labeling.* The degree of selectivity of labeling of a specific lignin monomer was estimated from the incorporation of radioactivity into the aromatic aldehydes, obtained by nitrobenzene oxidation of labeled wood tissue. Among many compounds tested, labeled ferulic acid and coniferin were suitable precursors for labeling of pine lignin (5,7). Indeed, it was recently shown that exogeneously applied ferulic acid was utilized by cucumber seedlings as an effective precursor for endogeneous lignification (8). Additionally, under special feeding conditions, labeled sinapic acid can be employed to predominantly label the syringyl moiety of poplar lignin (9). However, highest selectivity in labeling is normally achieved by administration of *p*-glucocoumaryl alcohol, coniferin or syringin (6,10).

*Biogenesis of Lignin in Woody Angiosperms.* While the lignin precursors, coniferin and syringin have been found in the cambial sap of a few angiosperms belonging to the Magnoliaceae and Oleaceae families (11), the glucoside of *p*-coumaryl alcohol has never been detected. Nevertheless, these three glucosides were prepared in radiolabeled form as candidate monolignol precursors. Thus, when coniferin and syringin, labeled with  $^3\text{H}$  at position 2 of the aromatic ring, were administered to *Magnolia kobus* DC., each was efficiently incorporated into its lignin during all phases of lignification (10). On the other hand, the incorporation of *p*-glucocoumaryl alcohol was only observed during early stages of cell wall formation (12).

Additional experiments revealed the following: when a growing stem of lilac (*Syringa vulgaris* L.) was administered the same  $^3\text{H}$ -labeled monolignol glucosides, each was efficiently incorporated into the newly formed

xylem, although at different stages of cell wall formation as revealed by microautoradiography (Fig. 1). Again, *p*-coumaryl alcohol was incorporated only during the earliest stages of cell wall development. Figure 2 shows an enlarged photograph of a part of this autoradiogram. As can be seen, the distribution of silver grains indicates that the *p*-hydroxyphenyl lignin components were deposited mainly in the middle lamella regions, and were not present in the secondary wall. On the other hand, guaiacyl lignin formed continuously from the early to the later stages, and in both the vessels and fiber walls. Interestingly, syringyl lignin was deposited mostly in the secondary wall of fibers, although a small amount was also used for formation of middle lamella lignin (Figs. 1 and 3).

Similar trends were observed in magnolia (10) and poplar (9).

*Biogenesis of Lignin in Woody Gymnosperms.* Figure 4 shows the distribution of silver grains in the newly formed xylem of the gymnosperm, Japanese black pine (*Pinus thunbergii* Parl.) administered the three <sup>3</sup>H-labeled monolignol glucosides as before, and UDP-glucuronic acid-[glucuronyl-U-<sup>14</sup>C] and GDP-mannose-[mannose-1-<sup>3</sup>H]. These nucleotides are considered to be precursors of pectin and hemicellulose (13).

Finally, when the labeled UDP-glucuronic acid was administered, a large part of the silver grains was localized mainly on the cell walls formed during the earliest stage of xylem differentiation and partly on those formed during the next stage. This can be ascribed to the initial deposition of pectic substances and hemicelluloses derived from UDP-glucuronic acid. On the other hand, the activity from GDP-mannose was incorporated largely during secondary wall formation. As previously discussed, the lignin formed during the early stages of cell wall development in the middle lamella and cell corner region contains more condensed units than that formed during later stages in the secondary wall (Terashima, this volume, and ref. 6). This finding can now be rationalized by the fact that when coniferyl alcohol was polymerized in pectin and mannan gel *in vitro*, the "LCC" fraction formed in pectin contains more condensed units than that formed in mannan (Terashima, this volume, and ref. 14); i.e., the type of polysaccharide influences product formation.

All three monolignols were incorporated into lignin at different stages of cell wall formation. Autoradiograms revealed that 62, 38 and 24% of the silver grains, assigned to *p*-hydroxyphenyl, guaiacyl and syringyl units respectively, were in the compound middle lamella (Fig. 4). This is in good agreement with the observation made on black spruce wood that middle lamella lignin contains a reduced methoxyl content when compared with secondary wall lignin (15). Syringaldehyde has been reported to be one of the minor components of the aldehyde mixture obtained by nitrobenzene oxidation of lignin in various conifers (16). A small syringyl content has also been detected during the thioacidolysis of pine (*Pinus pinaster*) compression wood (17). In a related study, when Japanese black pine (*P. thunbergii*) wood was subjected to nitrobenzene oxidation, syringaldehyde was obtained in a considerable amount, and represented about 5 mol% of the total aldehyde mixture (18). Interestingly, in the cell wall of this

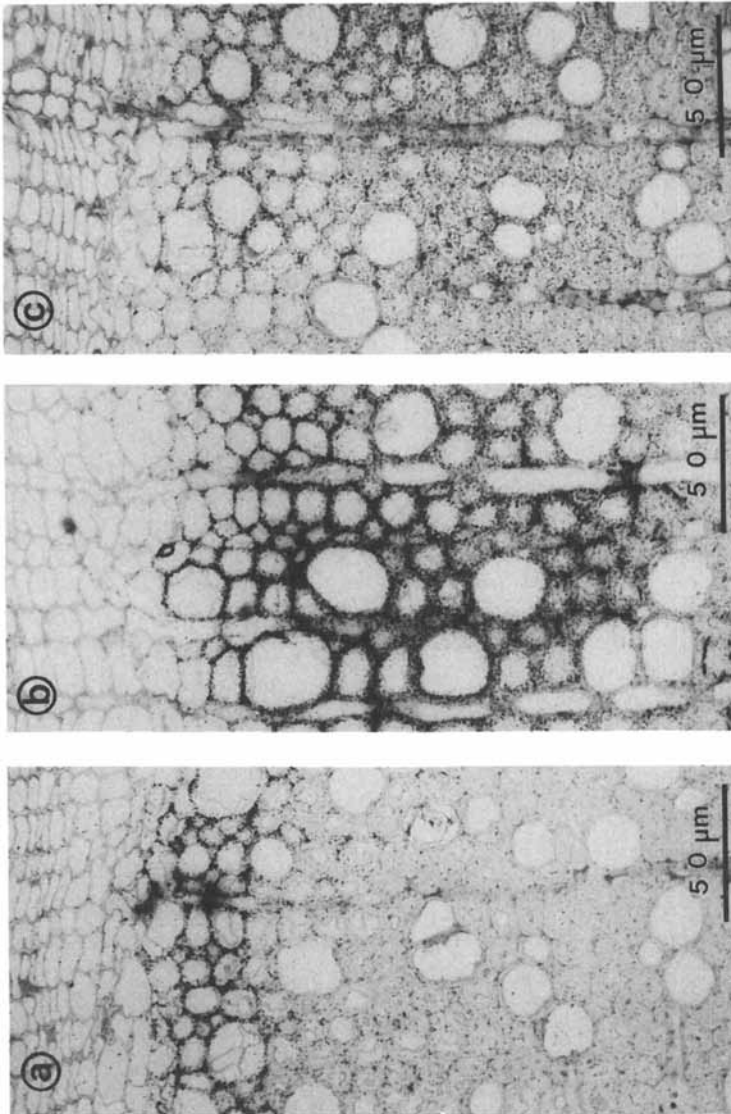


Figure 1. Microautoradiograms of differentiating xylem of *Syringa vulgaris* L. administered with [arom. ring-2-<sup>3</sup>H] *p*-glucocoumaryl alcohol (a); [arom. ring-2-<sup>3</sup>H] coniferin (b); and [arom. ring-2-<sup>3</sup>H] syringin (c).

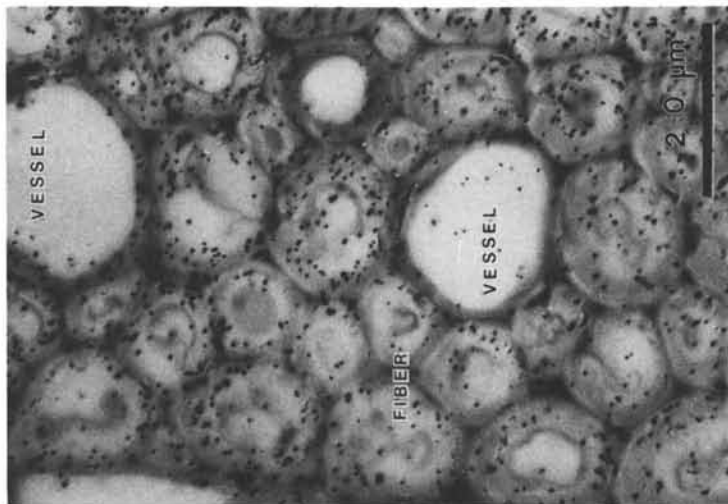


Figure 3. A part of microautoradiogram of differentiating xylem of *Syringa vulgaris* L. administered [arom. ring-2-<sup>3</sup>H] syringin.

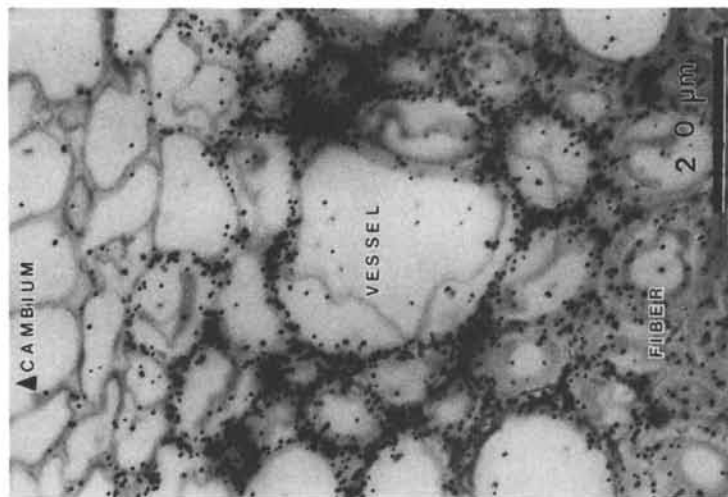


Figure 2. A part of microautoradiogram of differentiating xylem of *Syringa vulgaris* L. administered [arom. ring-2-<sup>3</sup>H] *p*-glucocoumaryl alcohol.

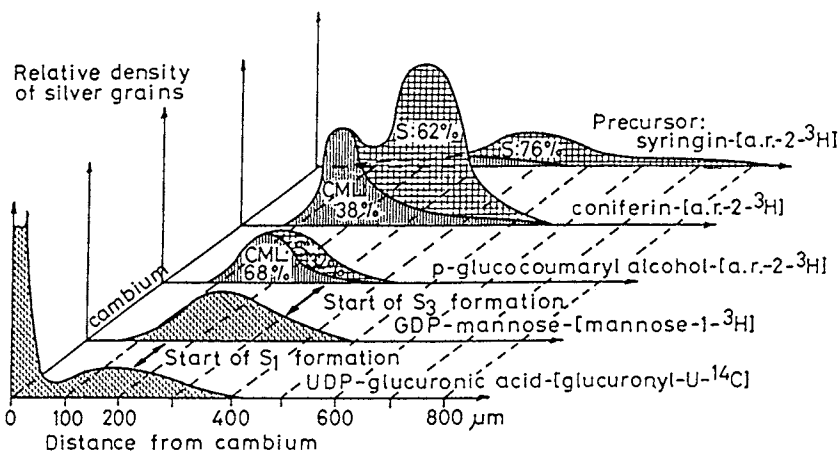


Figure 4. Distribution of silver grains in microautoradiograms of differentiating xylem of pine administered with precursors of lignin and hemicellulose.

pine, the syringyl moieties are distributed mainly in the inner layer of the secondary wall, even though its content is very low.

### Concluding Remarks

The results obtained by autoradiography and other studies (6,7,10, and Terashima, this volume), indicated that the structure of the protolignin macromolecule is heterogeneous with respect to monomer composition, distribution of interunit linkages (to form condensed substructures), and association with carbohydrates. However, protolignin is not a disordered copolymer of various monolignols. Instead, macromolecular formation occurs in a biochemically regulated manner, and the heterogeneous nature of protolignin is a natural and inevitable consequence of its unique mechanism of biogenesis. Figure 5 summarizes the successive deposition of cell wall components and their irreversible assembly to form a lignified cell wall in tree xylem. The causes of protolignin heterogeneity can be explained as follows.

1. The process of lignification is fundamentally controlled by each individual cell.
2. Lignification is preceded always by deposition of cell wall polysaccharides, and monolignol polymerization occurs within the carbohydrate gel, resulting in the structure of the polyignol. However, the type of carbohydrate changes with cell wall development stages, i.e., formation of cell wall layers, as shown in Figure 5. As discussed, the polymerization of monolignols in pectic substances in early stages may be one of the reasons why the middle lamella and cell corner lignin contains more condensed substructures than secondary wall lignin.
3. The monolignol utilized varies with type and age of the cell. Indeed, incorporation of monolignols into protolignin occurs in order of in-

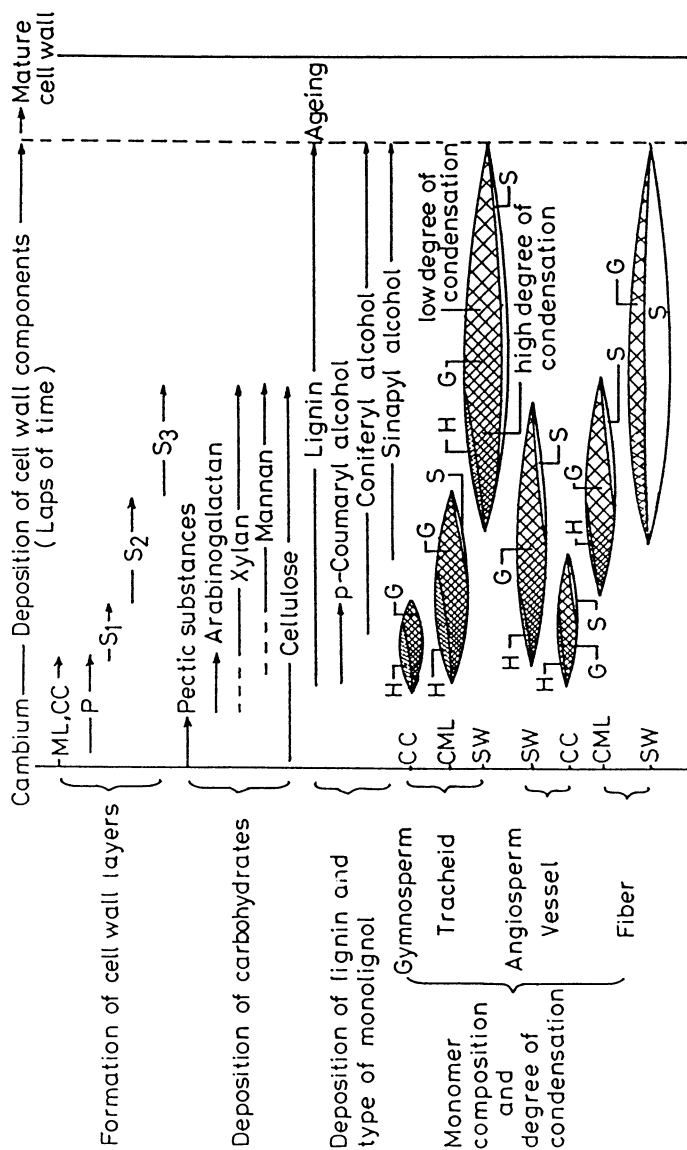


Figure 5. A schematic representation of the process of deposition of cell wall components and the heterogeneous formation of protolignin macromolecule. ML, middle lamella; CC, cell corner; P, primary wall; CML, compound middle lamella; S<sub>1</sub>, S<sub>2</sub>, and S<sub>3</sub>, outer, middle, and inner layer of secondary wall; H, G, and S, *p*-hydroxy-, guaiacyl-, and syringylpropane units.



creasing complexity, namely *p*-coumaryl, coniferyl and finally sinapyl alcohols are deposited successively (Fig. 5). Moreover, since the *p*-hydroxyphenylpropane unit is able to form interunit linkages at both C-3 and C-5 of the aromatic rings, the participation of *p*-coumaryl alcohol in early stages is another reason why the middle lamella lignin is more condensed.

4. Polymerization conditions will determine the structure and properties of protolignin. In this respect, the following factors are considered to be important (Terashima, this volume, and ref. 14): (a) activity of peroxidase, (b) generation of hydrogen peroxide, (c) type and nature of carbohydrate gel in which the polymerization proceeds, (d) pH of the reaction site, (e) effect of inorganic constituents such as calcium. These factors are presumably closely coordinated with each other.

Finally, it is to be noted that there is a common feature in biogenesis between gymnosperm and angiosperm lignins. The differences in properties between softwood and hardwood lignin will be better understood by more comprehensive studies on the biosynthesis of cell wall polymers and formation of the lignified cell wall.

#### Literature Cited

1. Fergus, B. J.; Procter, A. R.; Scott, J. N.; Goring, D. A. I. *Wood Sci. Technol.* 1969, **3**, 117.
2. Fergus, B. J.; Goring, D. A. I. *Holzforschung* 1970, **24**, 118.
3. Saka, S.; Goring, D. A. I. In *Biosynthesis and Biodegradation of Wood Components*; Higuchi, T., Ed.; Academic: New York, 1985; p. 51.
4. Hardell, H-L.; Leary, G. J.; Stoll, M.; Westermark, U. *Svensk Papperstidn.* 1980, **83**, 71.
5. Tomimura, Y.; Terashima, N. *Mokuzai Gakkaishi* 1979, **25**, 427.
6. Terashima, N.; Fukushima, K. *Wood Sci. Technol.* 1988, **22**, 259.
7. Terashima, N.; Fukushima, K.; Takabe, K. *Holzforschung* 1988, **42**, 347.
8. Shann, J. R.; Blum, U. *Phytochemistry* 1987, **26**, 2977.
9. Terashima, N.; Fukushima, K.; Tsuchiya, S.; Takabe, K. *J. Wood Sci. Technol.* 1986, **6**, 495.
10. Terashima, N.; Fukushima, K.; Takabe, K. *Holzforschung* 1986, **40**, Suppl., 101.
11. Terazawa, M.; Okuyama, H.; Miyake, M. *Mokuzai Gakkaishi* 1984, **30**, 322.
12. Fukushima, K.; Terashima, N. *Proc. 32nd Lignin Symposium at Fukuoka*, 1987, p. 13.
13. Dalessandro, G.; Northcote, D. H. *Planta* 1981, **151**, 53.
14. Terashima, N.; Seguchi, Y. *Cell Chem. Technol.* 1988, **22**, 147.
15. Whiting, P.; Goring, D. A. I. *Wood Sci. Technol.* 1982, **16**, 261.
16. Leopold, B.; Malstrom, I. L. *Acta Chem. Scand.* 1952, **6**, 49.
17. Lapiere, C.; Rolando, C. *Holzforschung* 1988, **42**, 1.
18. Fukushima, K.; Terashima, N. *Proc. 5th Intl. Symp. Wood Pulp. Chem.* 1989.

RECEIVED March 27, 1989

## Chapter 12

### <sup>13</sup>C Specific Labeling of Lignin in Intact Plants

Norman G. Lewis<sup>1</sup>, Ramon A. Razal<sup>1</sup>, Etsuo Yamamoto<sup>1</sup>, Gordon H. Bokelman<sup>2</sup>, and Jan B. Wooten<sup>1</sup>

<sup>1</sup>Departments of Wood Science and Biochemistry, Virginia Polytechnic Institute and State University, Blacksburg, VA 24061

<sup>2</sup>Philip Morris USA, Research Center, Richmond, VA 23261

Lignin deposition processes in *Leucaena leucocephala* and *Triticum aestivum* L. have been monitored *in situ*, following administration to the growing plants of various specifically-labelled C-13 lignin precursors and analysis of the resulting plant tissue by solid state carbon-13 nuclear magnetic resonance spectroscopy. The results obtained were compared to those obtained with artificial dehydrogenatively polymerized (DHP) lignins, long thought to more or less represent lignin structure. For *L. leucocephala* plant tissue, it was found that the dominant bonding environment of lignin corresponded to 2-O-4' (so-called  $\beta$ -O-4) linkages. Importantly, bond frequencies were very different when compared to artificial synthetic preparations. Surprisingly, lignified *T. aestivum* tissue provided very different results, and no significant contribution due to  $\beta$ -O-4 bonding was evident. This underscored the point that lignins vary greatly in structure depending upon the plant species under investigation. It was also found that significant bonding occurred at C<sub>3</sub> (so-called C $\alpha$ ) to other constituents, presumed to be mainly of carbohydrate origin. These results again showed the limitation of DHP polymers as adequate representation of lignin structure *in situ*.

Lignins and suberins are complex, structural cell wall polymers of terrestrial vascular plants. Their roles include imparting rigidity and strength to cell walls, as well as providing barriers to diffusion and infection (1,2). All current evidence suggests that lignins are exclusively metabolic products of the phenylpropanoid pathway, whereas suberins are composites having both phenylpropanoid and aliphatic (fatty acid, fatty alcohol derived) domains.

0097-6156/89/0399-0169\$06.00/0

© 1989 American Chemical Society

Of the two polymer classes, lignins are the more abundant and can often account for as much as 20-30% of dry plant tissue. In gymnosperms, lignins are thought to be formed from two monolignols, E-*p*-coumaryl 1 and E-coniferyl 2 alcohols, whereas in angiosperms sinapyl alcohol 3 is also involved (1). Grasses and cereals also contain covalently-bound hydroxycinnamic acids (e.g., *p*-coumaric 4, ferulic 5), a portion of which are considered to be part of the lignin framework (3-5). In the case of suberins, the exact chemical identity of the precursors undergoing polymerization has not yet been unambiguously established (2).

Following precursor transportation from the cytoplasm into the cell wall, the polymerization reactions leading to lignin and suberin are believed to be catalyzed by peroxidase(s) and H<sub>2</sub>O<sub>2</sub> (1,2). Interestingly, specific isoperoxidases are thought to be involved (6-12), although this still awaits rigorous experimental verification (13).

Unfortunately, there still remain massive gaps in our knowledge of the processes of deposition of lignin and suberization, and their ultimate structures in plant tissue. For instance, although it is well documented that lignin formation begins in the cell corners (14), our knowledge of how this is initiated and regulated is essentially unknown. Further, as regards lignin structure within plant cell walls, this is poorly understood for two main reasons: firstly, there is no known method whereby lignins can be isolated in their native, or intact, state. Consequently, current representations proposed for lignin structure are based upon analyses of isolated derivatives. This tends to be misleading since these have undergone extensive structural modification, the severity of which depends upon the method employed for isolation. Thus, lignins are currently classified according to plant tissue and isolation method (15). Secondly, there is a growing body of evidence suggesting that lignin polymers can vary, in terms of monomer composition and bonding patterns, with respect to morphological region (16). However, this has been a most difficult point to prove, since individual cell wall layers are not readily obtainable in amounts sufficient for detailed, reproducible chemical analyses.

It therefore follows that when isolated lignins (and suberins) are examined and subsequent structural representations are proposed, critical information on native structure has already been lost, e.g., as regards the extent of polymer modification during removal from the cell wall, and the effect of "mixing" polymers from the various cell wall layers from which they originated. For these reasons, all current representations of native lignin (and suberin) structure should be viewed with caution until such questions are satisfactorily resolved.

In this chapter, we review our recent progress in establishing the exact bonding patterns of lignin *in situ* in intact plants. Presumably, similar strategies can be employed to study suberin structure.

### Lignin Structure *in situ* in Vascular Plant Cell Walls

*Biosynthesis of E-Monolignols and Lignins.* Over the past forty years or so, a fairly detailed knowledge of the metabolic pathways leading to

the E-monolignols 1-3, from phenylalanine 7 (and in some cases, tyrosine 8) has been obtained (1,17,18) (Fig. 1). As can be seen, stereospecific deamination, hydroxylation and methylation as required then affords the E-hydroxycinnamic acids 4-6, which can be converted into their monolignols via the corresponding aldehydes 12-14. These pathways were determined by short-term radiolabelling experiments (normally < 24h), together with isolation of the appropriate enzymes involved. However, polymerization studies have suffered from two major drawbacks: (i) all investigations used wounded tissue (1,17,18), which can lead to *de novo* synthesis of an altered lignin, particularly if the tissue is infected (19), and (ii) newly-synthesized lignin (formed within 24-48h) is more alkali-labile than that of more mature tissue (20), suggesting significant differences in structure.

*Solid State Carbon-13 Nuclear Magnetic Resonance Spectroscopy of Intact Plant Tissue.* Carbon-13 nuclear magnetic resonance (nmr) spectroscopy has found considerable application for direct solid-state analysis of plant tissue (21), and isolated polymers such as cellulose (22,23). In the case of plant tissue, the carbohydrate resonances tend to mask important lignin inter-unit linkages, and hence key structural information is lost. Thus, with respect to lignin structure, C-13 nmr analysis of natural abundance plant tissue is of limited usefulness. An alternate strategy was therefore required if we were to observe resonances due to specific inter-unit linkages in the lignin polymer in its native state. This was achieved by administering appropriate specifically-labelled C-13 lignin precursors to intact growing plants over extended durations of time (weeks, months) and then examining the resulting lignified plant tissue by solid state C-13 nmr (5,24,25). The plants treated in this way were the hardwood, *Leucaena leucocephala* (25) and wheat, *Triticum aestivum* L. (24). These were grown either hydroponically or on agar from germinated seeds under aseptic conditions, and on media containing the appropriate precursor and inorganic nutrients. For methods development, the lignin precursor used was ferulic acid 5, labelled at the [1-<sup>13</sup>C], [2-<sup>13</sup>C] and [3-<sup>13</sup>C] positions, respectively, i.e., structures 5a-c.

At this point, it must be emphasized that, based on previous structural analysis of isolated lignins (27), appropriate lignin model compounds and synthetic dehydrogenatively polymerized (DHP) lignin preparations (28-30), it was concluded that the main bonding environments in native lignin were the substructures A-E as shown. Thus, these C-13 labelling experiments using plant tissue as described should provide information essential to verify, one way or the other, the validity of these proposed structural representations. The results obtained are discussed below:

*Incorporation of [1-<sup>13</sup>C] Ferulic Acid.* [1-<sup>13</sup>C] ferulic acid 5a, synthesized as previously described (26), was administered for 21-28 days to seedlings of *L. leucocephala* and *T. aestivum* following germination. The solid state C-13 spectra so obtained are shown in Figs. 2a and 2b, respectively. Note that these are difference spectra, obtained by subtraction of natural abundance resonances from that of the C-13 enriched samples, i.e., only C-13 enhanced resonances are evident.

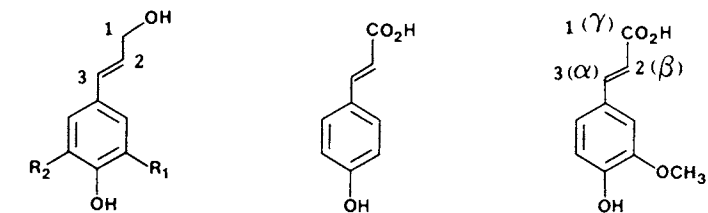
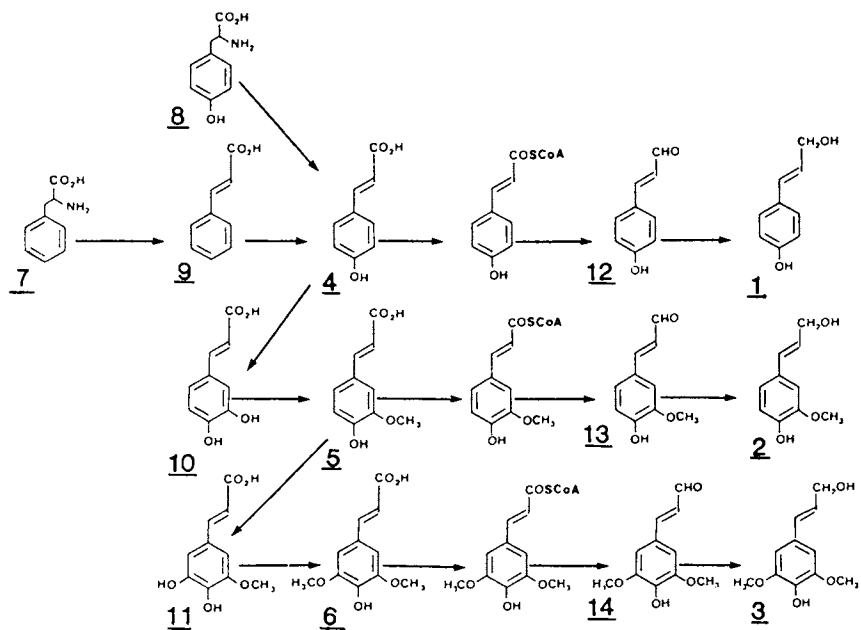
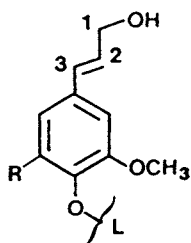
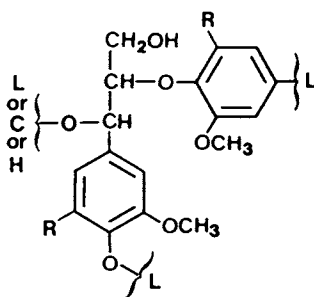
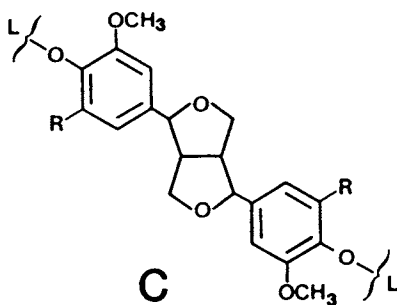
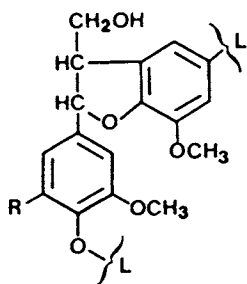
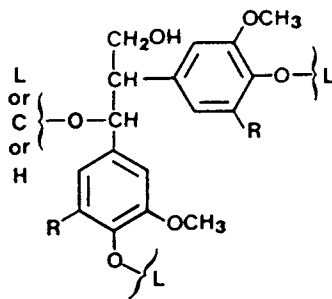
1,  $R_1, R_2 = H$ 45 a, 1 =  $^{13}C$ 2,  $R_1 = OCH_3, R_2 = H$ b, 2 =  $^{13}C$ a, 1 =  $^{13}C$ c, 3 =  $^{13}C$ b, 2 =  $^{13}C$ c, 3 =  $^{13}C$ 3,  $R_1, R_2 = OCH_3$ 

Figure 1. Biosynthetic pathways to E-monomignols 1-3 from Phe 7 (or Tyr 8).

**A****B****C****D****E**

L = Lignin

C = Carbohydrate

H = Hydrogen

R = H, guacyl substructures

R = OCH<sub>3</sub>, syringyl substructures

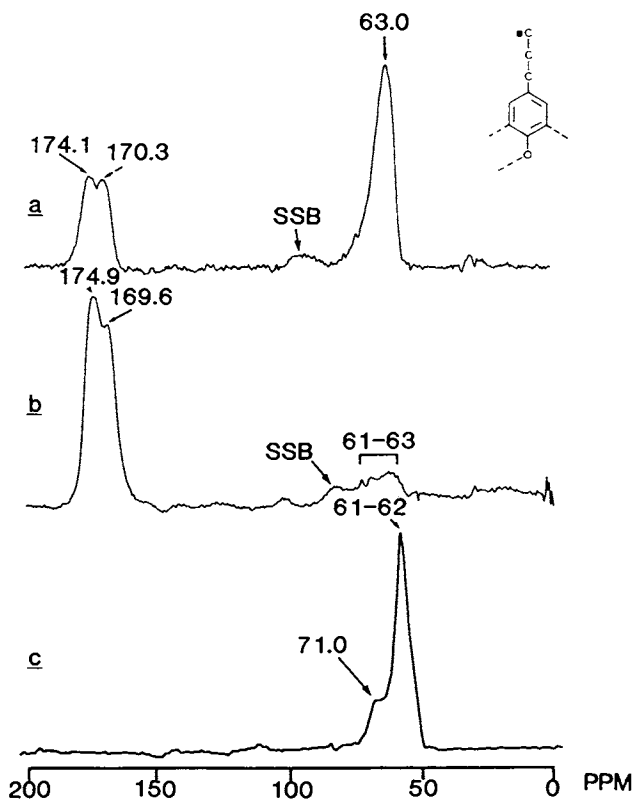


Figure 2.  $^{13}\text{C}$  NMR solid state difference spectra of (a) *L. leucocephala* and (b) *T. aestivum* (24) root tissue previously administered  $[1-^{13}\text{C}]$  ferulic acid **5a**. Fig. 2c shows the difference spectrum of a DHP polymer, derived from  $[1-^{13}\text{C}]$  coniferyl alcohol **2a** (29). CP/MAS spectra were obtained at 50 MHz on a Varian XL-200 Spectrophotometer equipped with a Doty Scientific MAS Probe. SSB = spinning side band.

For *L. leucocephala* tissue, one major signal is observed at 63 ppm, as well as two overlapping resonances ranging from 170-174 ppm (Fig. 2a). In agreement with previous results from appropriate radiolabelling studies, this large resonance at 63 ppm provided unequivocal proof that reduction to the monolignols, and then incorporation into lignin, had occurred. The chemical shift at 63 ppm is coincident to those of substructures **A**, **B**, **D** and **E**. Note though that while it is possible to distinguish between these individual possible substructures in solution state spectra (29), severe line-broadening prevents this possibility in the solid state at present. The smaller signals at 170.3 and 174.1 ppm can be considered due to hydroxycinnamic acids or esters, respectively. We are currently establishing whether these latter resonances are an integral part of the lignified tissue of *L. leucocephala*, or some transient species involved in lignification. If it is the latter, this may explain Higuchi's observation (20) that newly-synthesized lignin is more alkali-labile. This question will be resolved in the near future.

As can be seen from Fig 2b, the solid state C-13 nmr spectrum of *T. aestivum* also shows sets of enhanced resonances at 61 ppm and 169.6-174.9 ppm respectively (24). However, their relative intensities are very different from that observed for *L. leucocephala*. Indeed, it can immediately be seen that very little reduction of the administered precursor to hydroxymethyl analogues (at 61 ppm) has occurred. On the other hand, the dominant resonances at 169.6 and 174.9 ppm are coincident with bound hydroxycinnamic acids (e.g. ferulic **5a**) and its esters (31). Subsequent analysis of its isolated acetal lignin derivative (32) indicated that much of the lignin contained hydroxycinnamate residues (33).

For comparative purposes, a synthetic dehydrogenative polymer was prepared from [1-<sup>13</sup>C] coniferyl alcohol **2a** by the action of horseradish peroxidase/H<sub>2</sub>O<sub>2</sub> (29). Such polymers have long been viewed to closely resemble native lignin structure (17). The resulting spectrum is shown in Fig. 2c (24,29). The large resonance at 61 ppm corresponds to guaiacyl substructures **A**, **B**, **D** and **E**, whereas the smaller resonance at 71 ppm is attributed to substructure **C**. While the DHP polymer showed closest resemblance to *L. leucocephala* root tissue, it is not possible to draw any conclusions regarding relative bond frequencies or type. This is because virtually all of the hydroxymethyl resonances for the different substructures overlap in the solid state C-13 spectrum.

*Incorporation of [2-<sup>13</sup>C] Ferulic Acid.* Figs. 3a and 3b show the results obtained when [2-<sup>13</sup>C] ferulic acid **5b** was administered to *L. leucocephala* (25) and *T. aestivum* L. (24), respectively. In the case of *L. leucocephala*, the dominant resonance observed at 82.7 ppm was coincident to that of 2-O-4' bonding (substructure **B**) (25). We consider this to represent the first definitive proof that this is the major bonding pattern of that carbon in lignified woody tissue. The smaller resonances centered at ~ 54 and 127.5 ppm can tentatively be assigned to substructures **C-E** and **A**, respectively, based on similar chemical shifts. The small signal at 117.4 ppm was attributed to those corresponding to hydroxycinnamic acids and es-



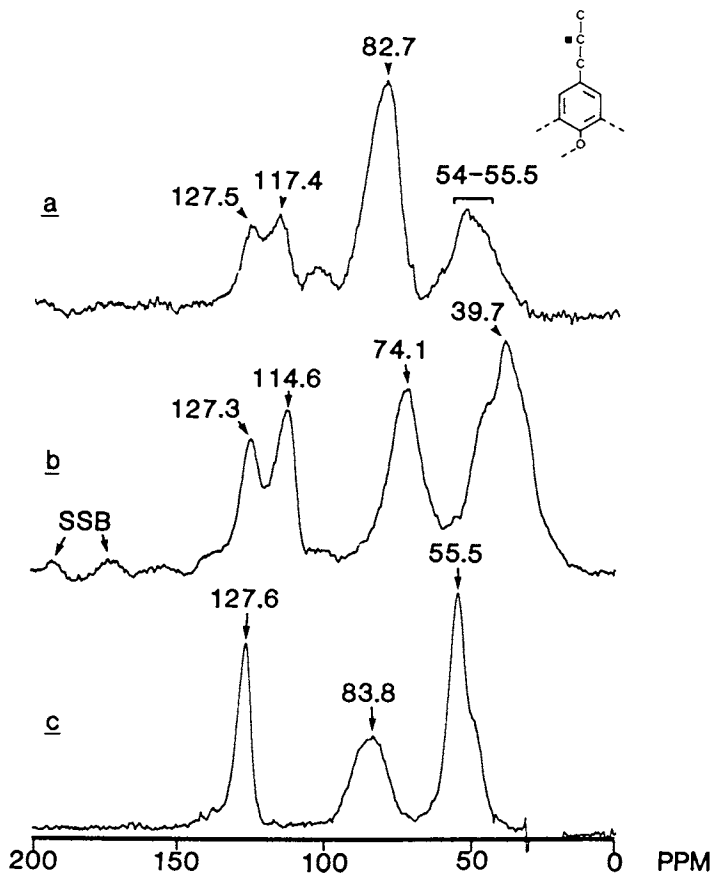


Figure 3.  $^{13}\text{C}$  NMR solid state difference spectra of a, *L. leucocephala* (25) and b, *T. aestivum* (24, 25) root tissue previously administered  $[2-^{13}\text{C}]$  ferulic acid **5b**. c shows the difference spectrum of a DHP polymer, derived from  $[2-^{13}\text{C}]$  coniferyl alcohol **2b** (29). SSB, spinning side band. (Reproduced with permission from ref. 25. Copyright 1988.)

ters, although, as stated above, no evidence for their involvement in lignin formation in this plant has been demonstrated.

For *T. aestivum* (see Fig. 3b), enhanced resonances were observed at 127.3 (substructure A), 114.6 (hydroxycinnamic acid or esters), 74.1 and 39.7 ppm (24). While the latter two resonances are currently unassigned, neither is consistent with a 2-*O*-4' bonding pattern. This was a most unexpected result, and more work is required to establish the exact chemical identity of these bonding environments.

For comparative purposes, the spectrum for the DHP polymer from [2-<sup>13</sup>C] coniferyl alcohol **2b** is also included (Fig. 3c) (24,29). As readily noted, the guaiacyl resonances at 127.6 (substructure A), 83.8 (substructure B) and 55.5 ppm (substructures C-E) show some similarity to *L. leucocephala* tissue. However, even in this case, the DHP polymer is not an adequate representation since relative intensities are essentially inverted between both spectra (Fig. 3b and 3c).

*Incorporation of [3-<sup>13</sup>C] Ferulic Acid 5c.* Figs. 4a and 4b show the results obtained following uptake of [3-<sup>13</sup>C] ferulic acid **5c** to *L. leucocephala* and *T. aestivum* L., respectively; the spectrum shown in Fig. 4c corresponds to a synthetic DHP polymer from [2-<sup>13</sup>C] coniferyl alcohol **2c**.

As regards *L. leucocephala* (Fig. 4a), large resonances were observed at 74.7 and 83.2 ppm with minor signals at 132 (hydroxycinnamyl alcohol), 146 (hydroxycinnamic acids/esters), 170.1 and 174.3 ppm. The small signals at 170.1 and 174.3 ppm presumably provide evidence that low levels of C<sub>2</sub>-C<sub>3</sub> cleavage have occurred to give substituted benzoic acids, such as vanillic or syringic acids. However, since most of the lignin in *L. leucocephala* was apparently involved in 2-*O*-4' linkages (see Fig. 3a and substructure B), the dominant resonances at 74.7 and 83.2 ppm must be explained on that basis. Thus, the large signal at 74.7 is attributed to 2-*O*-4' substructures (i.e. substructure B), having free benzylic alcohol (C<sub>3</sub>) functionalities. Note also that resonances due to substructure E would also be expected in this region, but at relatively reduced levels as was evident from Fig. 3a. The resonance at 83.2 ppm is important since, based on model compounds, it is coincident with benzyl ether linkages to both carbohydrates (34), or lignin in 2-*O*-4' (substructure B) (4) bonding environments. Such bonding environments have long been proposed. Finally, the relative frequency of substructures C and D is difficult to assess, since these are essentially concealed by the large resonance at 83 ppm.

In the case of *T. aestivum*, four major resonances were evident at 83 and 73 ppm, with minor signals at 132-137.1 and 146.5 ppm (24). These latter two signals correspond to hydroxycinnamyl alcohol and hydroxycinnamate functionalities as before. However, the large signals at 83 and 73 ppm cannot be explained on the same basis as for *L. leucocephala*. This is because substructure B (2-*O*-4' bonding) was found to be only a minor constituent in the lignified tissue. Nevertheless, while current evidence again points to lignin-carbohydrate bonding as before, the precise nature of the bonding environments present for C<sub>3</sub> in this tissue needs to be unambiguously determined.

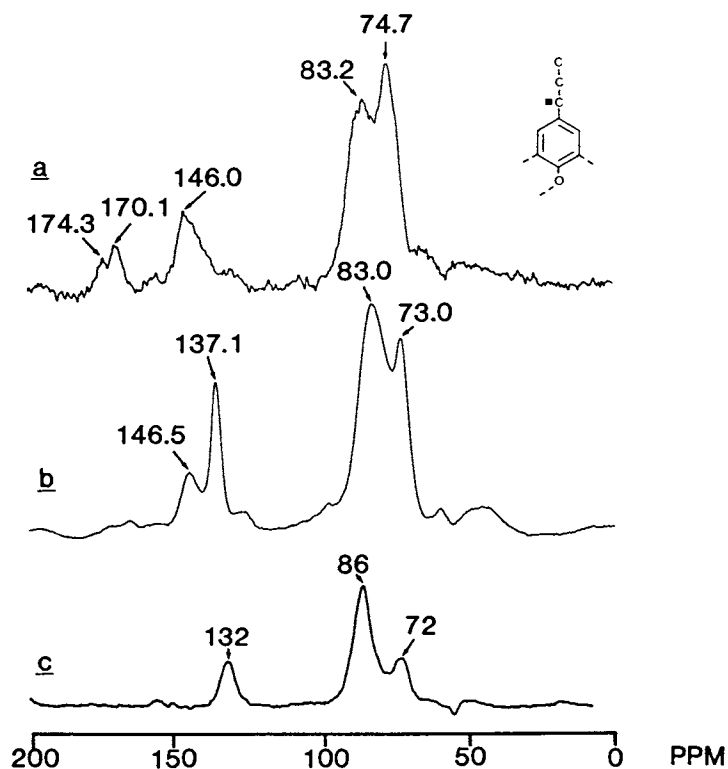


Figure 4.  $^{13}\text{C}$  NMR solid state difference spectra of (a) *L. leucocephala* and (b) *T. aestivum* (25) previously administered  $[3-^{13}\text{C}]$  ferulic acid 5c. Fig. 4c shows the difference spectrum of a DHP polymer, derived from  $[3-^{13}\text{C}]$  coniferyl alcohol 2c (29).

Comparison with the synthetic DHP polymer from [3-<sup>13</sup>C] coniferyl alcohol **2c** was also carried out (24,29). Resonances were observed at 132 (substructure **A**), 86 (substructures **C** and **D**) and 72 (substructures **B** and **E**) ppm, respectively. No precise correlation with either lignified tissue was possible.

### Concluding Remarks

It should now be self-evident that substantial progress has been made in developing methodology to probe lignin structure *in situ*. Obviously similar strategies for suberin also could be developed. The following points can now be made:

- i. Following incorporation of [1-<sup>13</sup>C] ferulic acid **5a** into the lignin of *L. leucocephala* root tissue, substantial conversion of the precursor into the corresponding monolignols, coniferyl (and sinapyl?) alcohols, had occurred. These monolignols were then subsequently converted into lignin as evidenced by the large signal at ~ 63 ppm. While smaller resonances corresponding to hydroxycinnamic acids and their esters were evident, these may represent some transient species involved in lignification. An answer to this question needs to be obtained. On the other hand, the incorporation of [1-<sup>13</sup>C] ferulic acid **5a** into *T. aestivum* provided products with very different bonding patterns/environments to that observed for *L. leucocephala*. The reasons for these differences need to be identified. However, it clearly emphasizes that phenylpropanoid bonding patterns vary markedly between different plant tissues.
- ii. Administration of [2-<sup>13</sup>C] ferulic acid **5b** to *L. leucocephala* revealed that the prevalent bonding environment in that tissue corresponded to 2-*O*-4' (so-called  $\beta$ -*O*-4) linkages. Interestingly, the *T. aestivum* tissue did not give a similar result.
- iii. The spectra obtained for *L. leucocephala* and *T. aestivum* tissue, previously administered [3-<sup>13</sup>C] ferulic acid **5c**, provided convincing evidence for the existence of benzylic linkages to carbohydrate (and perhaps lignin) polymers.
- iv. DHP polymers did not adequately represent lignin structure *in situ*, when compared to the results obtained for *T. aestivum* and *L. leucocephala*. This should not be unexpected, since it is generally thought that lignification in plant tissue is a highly coordinated and tightly controlled process occurring within a carbohydrate matrix.
- v. It is also important to recall that significant variations in lignin structure have been reported which can vary depending upon the cell wall layer under investigation. Hence, methodology needs to be developed to obtain carbon-13 enhanced spectra of lignin in the individual cell wall layers (i.e., middle lamella, secondary cell walls) of (woody) plant tissue.

### Acknowledgments

The authors thank the U.S. Department of Energy (DE-FGO5-88-ER-13883) and Philip Morris, USA, for financial assistance. An expression

of gratitude is also given to Dr. J. L. Brewbaker, Nitrogen Fixing Tree Association, Waimanalo, Hawaii, for the very kind gift of *L. leucocephala* seeds.

### Literature Cited

1. Grisebach, H. In *The Biochemistry of Plants*; 7, Secondary Plant Products; Conn, E. E., Ed.; Academic Press: New York, 1981; pp. 457-78.
2. Kolattukudy, P. E.; Espelie, K. E. "Biosynthesis of Cutin, Suberin and Associated Waxes"; In *Biosynthesis and Biodegradation of Wood Components*; Higuchi, T., Ed; Academic Press: New York, 1985; pp. 161-207.
3. El-Basyouni, S.; Towers, G. H. N. *Can. J. Biochem.* 1964, **42**, 203-10.
4. Scalbert, A.; Monties, B.; Lallemand, J.-Y.; Guittet, E.; Rolando, C. *Phytochemistry* 1985, **24**, 1359-62.
5. Lewis, N. G. *Bulletin de Liason Groupe Polyphenols* 1988, **14**, 398-410.
6. Imberty, A.; Goldberg, R.; Catesson, A. M. *Planta* 1985, **164**, 221-26.
7. Goldberg, R.; Catesson, A.-M.; Czaninski, Y. *Z. Pflanzen-Physiol.* 1983, **110**, 267-79.
8. Stich, K.; Ebermann, R. *Holzforschung* 1988, **42**, 221-24.
9. Lagrimini, L. M.; Burkhart, W.; Moyer, M.; Rothstein, S. *Proc. Natl. Acad. Sci.* 1987, **84**, 7542-46.
10. Borchert, R. *Plant Physiol.* 1978, **62**, 789-93.
11. Espelie, K. E.; Francheschi, V. R.; Kolattukudy, P. E. *Plant Physiol.* 1986, **81**, 487-92.
12. Villegas, R. J. A.; Kojima, M. *Agric. Biol. Chem.* 1985, **49**, 263-65.
13. Yamamoto, E.; Bokelman, G. H.; Lewis, N. G. 1989, This volume.
14. Takabe, K.; Fukazawa, K.; Harada, H. 1989, This volume.
15. Fengel, D.; Wegener, G. In *Wood: Chemistry, Ultrastructure, Reactions*; Walter de Gruyter: Berlin, New York, 1984.
16. Saka, S.; Goring, D. A. I. "Localization of Lignins in Wood Cell Walls"; In *Biosynthesis and Biodegradation of Wood Components*; Higuchi, T., Ed.; Academic Press: New York, 1985; pp. 51-62.
17. Freudenberg, K.; Neish, A. C. In *Constitution and Biosynthesis of Lignin*; Springer-Verlag: Berlin, 1968 (and references therein).
18. Higuchi, T. "Biosynthesis of Lignin." In *Biosynthesis and Biodegradation of Wood Components*; Higuchi, T., Ed.; Academic Press: New York, 1985; pp. 141-60.
19. Ride, J. P. *Physiol. Pl. Path.* 1975, **5**, 125-34.
20. Higuchi, T.; Ito, Y.; Kawamura, I. *Phytochemistry* 1967, **6**, 875-81.
21. Bartuska, V. J.; Maciel, G. E.; Bolker, H. I.; Fleming, B. I. *Holzforschung* 1980, **34**, 214-217.
22. Atalla, R. M.; Gast, J. C.; Sindorf, D. W.; Bartuska, V. J.; Maciel, G. E. *J. Am. Chem. Soc.* 1980, **102**, 3249-51.
23. Earl, W. L., VanderHart, D. L., *J. Am. Chem. Soc.* 1980, **102**, 3251-52.
24. Lewis, N. G.; Yamamoto, E.; Wooten, J. B.; Just, G.; Ohashi, H.; Towers, G. H. N. *Science* 1987, **237**, 1344-46.

25. Lewis, N. G.; Razal, R. A.; Dhara, K. P.; Yamamoto, E.; Bokelman, G. H.; Wooten, J. B. *J. Chem. Soc. Chem. Commun.* 1988, 1626-28.
26. Newman, J.; Rej, R. N.; Just, G.; Lewis, N. G. *Holzforschung* 1986, 40 (Supp.), 369-73.
27. Ludemann, H. D.; Nimz, H. H. *Makromol. Chem.* 1974, 175, 2409-22.
28. Nimz, H. H.; Mogharab, I.; Ludemann, H.-D. *Makromol. Chem.* 1974, 175, 2563-75.
29. Lewis, N. G.; Newman, J.; Just, G.; Ripmeister, *Macromolecules* 1987, 20, 1752-56.
30. Gagnaire, D.; Robert, D. *Makromol. Chem.* 1977, 178, 1477-95.
31. Kato, A.; Azuma, J.; Koshijima, T. *Chem. Lett.* 1983, 137-40.
32. Bolker, H. E.; Terashima, N. *Adv. in Chem. Ser.* 59; American Chemical Society: Washington, DC, 1966; p. 110-24.
33. Eberhardt, T. L. M.S. Thesis, Virginia Polytechnic Institute and State University, 1988.
34. Taneda, H.; Hosoya, S.; Nakano, J.; Chang, H-M. *Proc. Intl. Symp. on Wood and Pulping Chemistry*; Poster Sessions; Canadian Pulp and Paper Association: Montreal, 1985, pp. 117-20.

RECEIVED May 19, 1989

## Chapter 13

# Biochemical and Biosynthetic Studies on Lignification of Gramineae

Monique Gaudillere and Bernard Monties

Laboratoire de Chimie Biologique, INRA, Institut National Agronomique  
Paris-Grignon, Centre de Grignon, 78850 Thiverval-Grignon, France

Differences in lignification of forage crops were examined in terms of genetic, biosynthetic and environmental factors. This was achieved by comparison of brittle ecotypes of fescue (*Festuca arundinacea*), and brown-midrib (b.m.3)-mutants of maize (*Zea mays*) with the corresponding "normal" plants. For each plant type, Klason, acid-insoluble and acetyl bromide lignin contents, and monomeric compositions, were determined and compared. While only weak differences in lignification were found in the case of fescue, significant differences in both lignin content, and its monomeric composition, were found for maize between its upper and lower internodes. These differences were due to genetic and/or environmental factors. Heterogeneity in lignification, brittle organ character, and other biosynthetic aspects of stem formation in Gramineae are discussed, in relation to results previously obtained with rice and wheat.

Forages such as hay and straws of the Gramineae are produced for ruminant feed on an enormous scale. In France, annual production is  $12.8 \times 10^6$  T (1) which approaches that for wood-harvesting operations ( $23 \times 10^6$  T) (2). As described in preceding chapters, lignins (and related aromatics) appear to bind physically and/or chemically to the cell wall polysaccharides of forages. These aromatic substances have a profound effect on animal nutrition (3-10). Differences between forage digestibility have also been correlated with environmental and nutritional factors (11), as well as species and genetic variabilities (12,13). As regards lignin (14) and cell-wall-bound hydroxycinnamic acids (15) (i.e., p-coumaric, ferulic acids), it is now generally accepted that any increase in their content results in decreased digestibility. Ruminant digestibility of plant material can be improved by either mild acid (16)

0097-6156/89/0399-0182\$06.00/0

© 1989 American Chemical Society

or, more usually, alkali (17-18) treatment to remove labile phenolics and lignin-carbohydrate fractions, thus leaving behind a more readily-accessible polysaccharide feed. Interestingly, differences in digestibility between cultivars can be higher than differences resulting from chemical treatment (19), thus underscoring the importance of biological variability. To date, most conclusions made regarding digestibility differences of maize, sorghum and rice, have been explained on the basis of variations in lignin contents. In the case of maize (*Zea mays* L.), a family of ten single- or double-mutants was first observed by Kuc *et al.* (20,21). Such mutants were distinguished by a browning of the mid-ribs of the leaves (brown-midrib: b.m-mutant), by a lower lignin content and higher digestibility. In these mutants, differences in both lignin monomer composition (following nitrobenzene oxidation) and in the relative content of cell-wall-ester linked p-coumaric and ferulic acids were observed. Brown-midrib mutants of sorghum (*Sorghum bicolor* L. Moensch) were the second family of mutants studied, and were also characterized by a lower lignin content (22-23). A mutant of rice (*Oriza sativa* L.) was also found, and was readily distinguishable by a brittleness of the culm which appeared only after maturity of the plant. This mutant had a lower cellulose content, and this difference was assumed to be related to the brittleness of the culm (24). Significant differences were also found in the extractability of the lignin fractions and associated phenolic acids (25-26), suggesting that lignin formation was also affected.

In this work, our main objective was to explore the underlying reasons for such variations in graminaceous lignins. As before for rice (26), phenolic-ester and lignin analyses (content and monomer composition) were carried out, although only lignin data are shown here.

Firstly, we studied possible relationships between lignin variation and brittleness of plant organs, using two ecotypes of tall fescue grass (*Festuca arundinacea* Schreb). Thus, both "normal" fescue and a brittle ecotype (discovered by Jadas-Hecart (27)), characterized by a brittleness of leaves, sheath and stem, were compared. Possible environmental effects on the biochemistry of lignin formation were estimated by comparison of several parallel crops from two locations.

Secondly, a biosynthetic investigation on lignin variation was undertaken using maize internodes. Maize internodes were examined in this study since: (a) fewer plants were required for analysis (greater biomass); and (b) possible variations between normal and b.m-mutants (21) could be studied. Lignin contents and monomer composition were compared between internodes, both being collected at the top and the bottom of the maize stem. These plant parts were chosen because of differences in the digestibility of different internodes as documented for Timothy (*Phleum pratense*) (28) and, in lignification, for wheat (*Triticum aestivum* L.) (29-30).

## Materials and Methods

*Material.* Plants were grown under field or greenhouse conditions at Grignon, and harvested before heading for Fescue (27), and at grain maturity in the case of maize (31). In each case, plants were harvested at the



same stage of maturity, as shown by the development of inflorescence, and the relative ratio of leaves and stalk.

*Methods.* Whole plants were harvested in the case of fescue leaves, whereas for maize stalks, sheaths and nodes were removed, leaving internodes which were wholly analyzed. Samples (6 to 10 plants) were freeze dried, finely ground and exhaustively extracted, in a Soxhlet, with toluene-ethanol (2/1:v/v), ethanol, then water, leaving an insoluble "parietal residue" (PR) which was freeze dried before storage and analysis. Lignin determinations used three different methods; Klason lignin (KL) (72% H<sub>2</sub>SO<sub>4</sub>); acid-insoluble lignin (AIL) (5% H<sub>2</sub>SO<sub>4</sub> prehydrolysis followed by Klason determination); and acetyl bromide lignin (ABL), using ferulic acid as a reference material (26). Cell-wall-esters of p-coumaric-(PC) and ferulic-(FA) acids were hydrolyzed with 2M NaOH and estimated after HPLC (26,32). Monomeric compositions were obtained following nitrobenzene oxidation (32), or thioacidolysis, with gas chromatography-mass spectrometry (GC-MS) determination of thioacidolysis products (33). Lignocellulose (LC), recovered after 5% H<sub>2</sub>SO<sub>4</sub> pretreatment (34), and saponification residues (SR), obtained after NaOH hydrolysis of phenolic esters (26), were characterized according to the procedures previously adopted for characterization of parietal residue (32,33). Phenolic acids (p-coumaric, caffeic, ferulic and sinapic) were obtained from FLUKA and used without purification; 5-hydroxyferulic acid was a gift from N. G. Lewis (Virginia Polytechnic Institute and State University, Blacksburg, VA 24061, USA).

## Results and Discussion

*Lignification of Fescue.* Results shown in all Tables are the mean of three determinations. Tables I and II show lignin contents and monomer compositions for both normal and brittle fescue grass ecotypes. These were harvested at two locations: Grignon and Lusignan. Data shown were only for one of two crops grown at Grignon, and one of three at Lusignan. No visible differences between the same crops from either location were discernible. In all cases, though, lignin contents were significantly higher at Grignon than at Lusignan. As plants were harvested at the same stage of development, differences can be ascribed to environmental effects. Table I also shows the differences in overall lignin contents of both ecotypes from the same origin. Interestingly, only acetylbromide lignin (ABL) contents were significantly different between fescues grown at Grignon, while only sulfuric acid lignins (KL and AIL) contents were different at Lusignan; such variations are difficult to explain at present. Furthermore, in each case, acid-insoluble lignin contents were lower than Klason lignin contents confirming the importance, in the AIL procedure, of the 5% sulfuric acid prehydrolysis step required in the case of green plants, which are usually rich in protein as discussed previously (34).

ABL contents, expressed in ferulic acid equivalents, were of the same order of magnitude as Klason and acid-insoluble lignin contents. However, this agreement was fortuitous as the ABL determination provided only

Table I. Klason, Acid-insoluble, and Acetylbromide Lignin Contents of Normal and Brittle Fescue Ecotypes Grown at Grignon and Lusignan (standard deviation less than 10%)

Type of Lignin	Lignin Content (%)			
	Grignon Harvest		Lusignan Harvest	
	Normal (%)	Brittle (%)	Normal (%)	Brittle (%)
KL	20.4	19.4	17.2	15.1
AIL	14.0	14.4	11.2	7.7
ABL	18.0	15.5	12.0	13.0

Where KL = Klason lignin  
 AIL = Acid Insoluble Lignin  
 ABL = Acetyl Bromide Lignin

Table II. Lignin Monomer Composition, Obtained by Nitrobenzene Oxidation of Lignin from Normal and Brittle Fescue Grown at Lusignan (Same as in Table I)

Mass %	Normal		Brittle	
	PR	LC	PR	LC
V	1.2	0.8	1.3	0.8
S	0.4	0.5	0.4	0.4
V + S	1.6	1.3	1.7	1.2
S/V	0.3	0.6	0.3	0.5

Where V = Vanillin  
 S = Syringaldehyde  
 PR = Parietal residue  
 LC = Lignocellulose

amounts relative to ferulic acid absorptivity. Differences between ABL values of normal and brittle fescue must be related to variations in lignin content, since no significant differences in the total content of *p*-coumaric and ferulic esters were found between samples from the same origin (data not shown).

The monomeric composition of lignin in parietal residues (PR), and the corresponding lignocellulose (LC) of normal and brittle fescue, harvested at Lusignan are shown in Table II. As differences between KL and AIL contents had previously only been found between fescues grown at Lusignan (Table I), the lignin composition of PR and the corresponding LC fractions were compared. As can be seen from Table II, no significant differences between normal and brittle ecotypes were observed. However, significant differences in monomeric composition of lignin from LC and PR are clearly

discernible for each ecotype. These differences may be due to acid pre-treatment, resulting in differences in condensation reactions and loss of acid-soluble lignin fractions (34). As similar trends were observed for both ecotypes, the results suggest a great similarity between the reactivity of the lignins of both plants. Thus, comparisons of lignin of both ecotypes revealed that differences were mainly related to environmental factors, and not genetic variability.

*Lignification of Maize Internodes.* Lignin variability in maize was studied by comparison of the lignin contents and monomeric composition of its internodes.

Table III shows a weak trend in KL and AIL contents between the upper and lower internodes of both ecotypes. Lignin contents are slightly higher in the lower internode, in agreement with previous results (4). This conclusion was further strengthened by comparison of the ABL (SR) data. As alkaline hydrolysis, used for the SR preparation, had previously only solubilized phenolic esters and a fraction of the lignin, this data confirmed not only a higher lignin content, but also a lower reactivity (delignification) of the lignin core in the lower internodes of both types. ABL data for parietal residues (PR) are more difficult to interpret because they include both lignin and phenolic esters. These bound esters differ for both ecotypes. In agreement with Kuc *et al.* (20,21), only ferulic and p-coumaric acids were found as the two main phenolic esters linked to the cell walls of normal and mutant maize. In each case, the PC/FE ratio for normal maize was about twice that of the b.m. mutant (data not shown); these results are in agreement with previous studies on bm-1, but not bm-3, mutants (20,21).

Table III. Klason (KL), Acid-insoluble (AIL) and Acetylbromide (ABL) Lignin Contents in Upper and Lower Internodes from Normal and b.m.-Mutant of Maize. (PR = parietal residue, SR = NaOH saponification residue, standard deviation less than 10%)

	Lignin contents (%)			
	Normal		Mutant	
	Upper	Lower	Upper	Lower
KL (PR)	17.6	18.5	14	14.5
AIL (PR)	10.7	11.2	6.4	7.5
ABL (PR)	12.5	12.3	9.8	10.3
ABL (SR)	1.8	4.6	1.5	2.3

Tables IV and V show the monomer composition of lignins for both parietal and saponification residues. In this regard, comparison between PR and SR values allows the characterization of the lignin core, which is not solubilized after alkaline treatment (20,21). Instead of using nitrobenzene oxidation, thioacidolysis was used to characterize the non-condensed

monomeric units linked by aryl-alkyl ether linkages in the lignin polymers. Thioacidolysis allows a more specific characterization of lignin (35); in the case of woods, it provides a good correlation with nitrobenzene oxidation data (36) and, in the case of gramineae, it allows an unambiguous discrimination between lignin monomeric units and associated phenolic acids. This is not possible by direct nitrobenzene oxidation of parietal residues (37). As shown in Figure 1, the two main thioacidolysis products of non-condensed guaiacyl (G) and syringyl (S) units are clearly separable by gas chromatography with relative retention times ( $R_t$ ) of  $R_t^G = 1.14$ ,  $1.15$  and  $R_t^S = 1.24$ ,  $1.25$  with reference to tetracosane as an internal standard. Under these conditions, the  $R_t$ 's of p-coumaric acid (PC), ferulic acid (FA) and their addition products with ethanethiol, were  $R^{PC} = 0.69$ ,  $R^{PCA} = 0.85$ ,  $R^{FE} = 0.77$  and  $R^{FEA} = 0.81$ , respectively. Thus, thioacidolysis products of phenolic acids and lignin monomeric units can be clearly separated; this is not the case for nitrobenzene oxidation products where, for example, vanillin can originate from either lignin monomers or ferulic acid.

Table IV. Monomeric Composition of Lignin in the Parietal Residue (PR) of the Upper and Lower Internode from Stem or Normal and b.m.-Mutant of Maize shown by Thioacidolysis (G = guaiacyl and S =syringyl-trithioethylethers: Fig. 1). (Yields are expressed as micromoles per gram of ABL in each sample of PR; standard deviation less than 10%)

	Normal		Mutant	
	Upper	Lower	Upper	Lower
G	126	168	184	234
S	109	289	11	69
S + G	234	457	193	303
S/G	0.86	1.71	0.06	0.29

Table V. Monomeric Composition of Lignin in the Saponification Residue (SR) of the Upper and Lower Internode from Stem of Normal and b.m.-Mutant of Maize as shown by Thioacidolysis (abbreviations and data as in Table IV)

	Normal		Mutant	
	Upper	Lower	Upper	Lower
G	72	202	73	217
S	56	224	n.c.	30
S + G	122	426	73	248
S/V	0.74	1.10	n.c.	0.14

n.c.: not calculated.

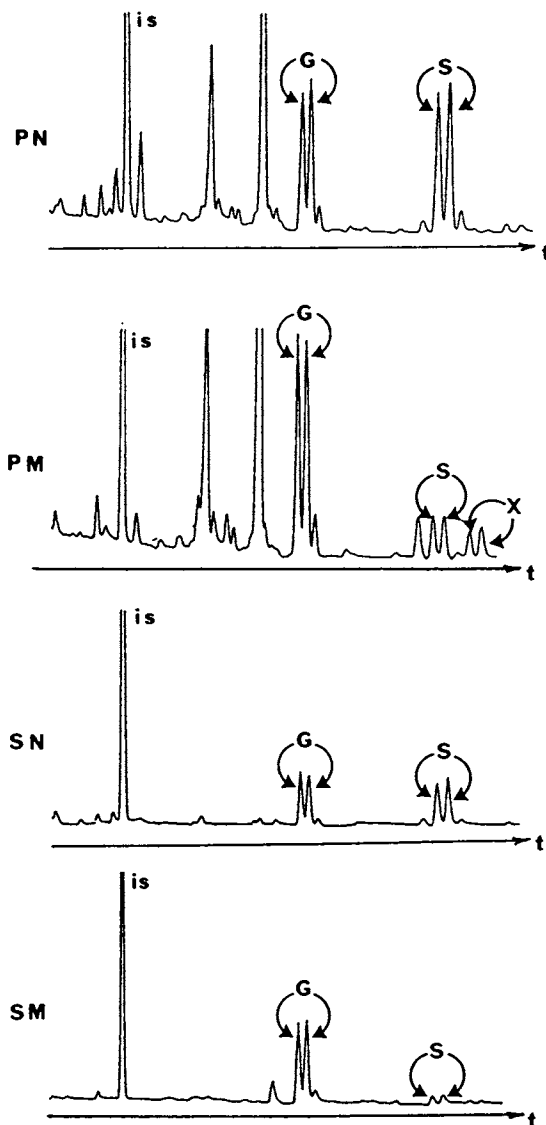


Figure 1. Partial GC chromatogram showing the peaks of the main thioacidolysis products, separated as TMS derivatives in function of time (t), from parietal residue of normal (PN) and mutant (PM) maize and, from corresponding saponification residue SN and SM. For each type of monomer: guaiacyl (G) and syringyl (S), two *erythro* and *threo* TMS-glycerol-trithioethylether isomers were observed with similar mass spectra. The case of X isomers, with similar fragmentation patterns to those of G and S, has been discussed elsewhere (45).

Table IV shows that, in both ecotypes, the yields of non-condensed guaiacyl and syringyl units were higher in the lower internode. Thus, lignin was apparently less condensed in lower, rather than upper, internodes. From the syringyl to guaiacyl ratio it was also evident that more syringyl units were deposited in the lower internode. Interestingly, the mutants had slightly higher guaiacyl contents and much reduced syringyl contents, in comparison to the normal plant. Using nitrobenzene oxidation, Kuc *et al.* had reported exactly the opposite for normal and b.m.3-mutants of maize (21). Using their nitrobenzene oxidation method for comparison, the monomeric composition of the lower internodes from mutant and normal maize were again determined. In agreement with thioacidolysis data, the mutant showed the same trends as before. Thus, the discrepancy between these results and data from Kuc *et al.* (21) cannot be attributed to differences in the analytical procedures used, and an alternate explanation is required.

In the case of saponification residues (Table V), these trends were even more pronounced for the upper internode. Total yields of thioacidolysis products, (S + G), were slightly higher for the case of PR (Table IV), than that of SR (Table V). However, the residual lignin from the SR of the lower internodes was relatively unchanged when compared with PR, with the difference between SR and PR being nearly negligible in the case of normal maize but significant in the case of the mutant.

Comparison of qualitative and quantitative data on lignification of the upper and the lower internodes of maize stems shown in Tables III to V, indicated only weak quantitative differences in lignin contents. However, there were significant differences in lignin monomeric composition and reactivity (delignification) between internodes in the maize stalk.

The lignin contents and monomeric compositions were also compared between fractions of internodes as follows: Each of the upper and lower internodes previously studied was divided into three parts of equal length. Comparison of lignin contents and monomeric compositions of upper and lower parts of each internode revealed only weak differences (data not shown).

## Conclusions

Results from this study suggest several differences in lignification between ecotypes of fescue and mutants of maize. While weak differences in total lignin contents were observed between brittle fescue and normal plant ecotypes, no significant variations in lignin monomeric composition and reactivity were evident, even after 5% H<sub>2</sub>SO<sub>4</sub> pretreatment. Environmental effects on lignification of fescues were minor and mainly changed only lignin contents; thus, in contrast to rice, the brittle character of fescue was not due to direct variations in lignin content or monomeric composition. Even though brittleness of plant organs was not measured and quantitatively related to lignification parameters, it seems likely that organ brittleness and lignin content are not related. On the other hand, a relationship between brittleness and structure of fibers and polysaccharide content has been re-

peatedly suggested (24,38,39,40). Likely the brittle properties rely upon the formation of molecular associations and networks, whose properties depend more on mutual association of components than on their intrinsic chemical composition. This topic was discussed recently (41) and would require reevaluation in the case of brittle rice and fescue.

Unlike the cases of rice and fescue, differences in both lignin content and monomeric composition were found between normal plants and the b.m.3-type mutant of maize. In agreement with Kuc *et al.* (20,21), lignin contents were always lower in these mutants. However, the syringyl/guaiacyl ratios were significantly lower than those described previously for the b.m.3-type (21). A similar discrepancy was also noted for the PC/FE ratios. In both cases, the ratios found for the b.m.3-type were similar to values reported for the b.m.1-type by these authors (20,21). These differences cannot be explained at present, but may be related to the fact that the b.m. genes, or genetic blocks, were expressed in a different epigenetic environment in the case of Kuc's experiments and in the case reported here. Differences in lignification between the maize internodes may be related to the biosynthesis and elongation of the stem (4); to our knowledge, no data have been published concerning the mutants of maize in this respect. In addition to environmental effects on lignin contents, significant differences were found between internodes in terms of both lignin content and monomeric composition. Weak differences were also found within internodes. Such differences may be explained by the biosynthetic model of growth of gramineae stems in which intercalating meristems subtend the development of a series of separated internodes. The biosynthetic heterogeneity of lignin in the apical internode of wheat (reported previously (20,30)) are in agreement with this model; these differences are related not only to lignin properties, but also to associated cell-wall-phenolics in their relation to cell wall reticulation (41,42).

It should be evident that an unequivocal estimation of the relative effects of genetic and environmental factors on gramineae lignification requires more biosynthetic studies in relation to organs, tissues and cell differentiation, and less global biochemical analysis. In particular heterogeneity of lignin (43) should be emphasized. Anatomical examination of b.m.-mutant of maize, for example, has already indicated that, possibly, several kinds of lignins are found within the same plant in different tissues (44). Very recently, during the editing of the manuscript, thioacidolysis of lignin from internodes of b.m.-mutant has shown that additional 5-hydroxyguaiacyl monomeric units, compound X (Fig. 1) were incorporated into the lignin of this mutant (45), confirming the possibility of qualitative variations in lignin which may be of great interest for biotechnological manipulation of lignins.

### Acknowledgments

The authors are grateful to Elisabeth Grenet and J. Jadas-Hecart (INRA) for providing samples of respectively b.m.3 maize, brittle fescue and corresponding normal plants; thanks are also due to Dr. Catherine Lapiere

for helpful discussions and critical review of manuscript and to F. Jagic for plant cultivation at Grignon.

### Literature Cited

1. Jouany, J. P.; Besle, J. M. In *Production et Utilisation des Biomasses Lignocellulosiques*; Monties, B., Ed.; Apria-Lavoisier: Paris, 1988 (in press).
2. Anonyme. In *Informations-Bois*; AFOCEL: Paris, 1988, p. 7, 15.
3. Akin, D. E. In *Nutritional Limits to Animal Production from Pastures*; Hacker, J. B. Ed.; CSIRO Pub., Comm. Agric. Bur., Farnham Royal (UK), 1981; p. 201-223.
4. Hacker, J. B.; Minson, D. J. *Herbage Abstr.* 1981, **51**, 459-482.
5. S-Thiago, L. R. L.; Kellaway, R. C. *Anim. Feed. Sci. Technol.* 1982, **7**, 71-81.
6. Aman, P.; Nordkvist, E. *Swedish J. Agric. Res.* 1983, **13**, 61-67.
7. Sullivan, J. T. *J. Anim. Sci.* 1959, **18**, 1292-1298.
8. Lindberg, J. E.; Ternrud, I. E.; Theander, O. *J. Sci. Food Agric.* 1984, **35**, 500-506.
9. Jung, H. J.; Fahey, G. C. Jr. *J. Anim. Sci.* 1983, **57**, 206-219.
10. Reeves, J. B., Jr. *J. Anim. Sci.* 1985, **60**, 316-322.
11. Wilson, J. R. In *Nutritional Limits to Animal Production from Pastures*; Hacker, J. B., Ed.; CSIRO pub., Comm. Agr. Bur., Farnham Royal (UK), 1981; p. 112-131.
12. Norton, B. W. In *Nutritional Limits to Animal Production from Pastures*; Hacker, J. B., Ed.; CSIRO pub., Comm. Agr. Bur., Farnham Royal (UK), 1981; p. 89-110.
13. Hacker, J. B. In *Nutritional Limits to Animal Production from Pastures*; Hacker, J. B., Ed.; CSIRO pub., Comm. Agr. Bur., Farnham Royal (UK), 1981; p. 305-326.
14. Morrisson, I. M. *Grass Forage Sci.* 1980, **35**, 287-293.
15. Hartley, R. D. *J. Sci. Food Agric.* 1971, **23**, 1347-1354.
16. Crosthwaite, C.; Ishimara, M.; Richards, G. N. *J. Sci. Food Agric.* 1984, **35**, 1041-1050.
17. Jackson, M. G. *Anim. Feed Sci. Technol.* 1977, **2**, 105-130.
18. Morrisson, I. M. *J. Sci. Food Agric.* 1988, **42**, 295-304.
19. White, L. M.; Hartman, G. P.; Bergman, J. W. *Agron. J.* 1981, **73**, 117-121.
20. Kuc, J.; Nelson, O. E. *Arch. Biochem. Biophys.* 1964, **105**, 103-113.
21. Kuc, J.; Nelson, O. E.; Flanagan, P. *Phytochem.* 1968, **7**, 1435-1436.
22. Porter, K. S.; Axtell, J. D.; Lechtenberg, V. L.; Colenbrander, V. F. *Crop Science* 1978, **18**, 205-208.
23. Bulcholtz, D. L.; Cantrell, R. P.; Axtell, J. D.; Lechtenberg, V. L. *J. Agric. Food Chem.* 1980, **28**, 1239-1241.
24. Doat, J.; Marie, R. *Ann. Amelior. Plantes* 1977, **27**, 705-715.
25. Monties, B.; Mestres, C.; Bagdhadi, K. In *Proc. First Intl. Symp. Wood & Pulp. Chem. (ISWPC)*; S.T.F.I. Pub.: Stockholm, 1981; **5**, 40-43.



26. Sharma, U.; Brillouet, J. M.; Scalbert, A.; Monties, B. *Agronomie* 1986, **6**, 265-271.
27. Jadas-Hecart, J. *Agronomie* 1985, **5**, 459-462.
28. Davies, I. *Welsh Plant Breed. Stat. Tech. Bull.* 1969, **3**, 61-76.
29. Agossin, E.; Odier, E.; Gaudillere, M.; Monties, B. *Bull. Groupe Polyphenols* 1982, **11**, 187-195.
30. Gaudillere, M.; Monties, B. *Proc. Fourth Cell Wall Meet. (Cell Wall 86)*; Paris, 1986, 284-287.
31. Grenet, E.; Barry, P. *Reprod. Nut. Dev.* 1988, **28**, 125-129.
32. Scalbert, A.; Monties, B.; Rolando, C. B. *Holzforchung* 1986, **40**, 119-127.
33. Lapiere, C.; Monties, B.; Rolando, C. *Holzforchung* 1986, **40**, 113-118.
34. Monties, B. *Agronomie* 1981, **4**, 317-321.
35. Rolando, C.; Lapiere, C.; Monties, B. In *Methods in Lignin Chemistry*; Lin, S. Y.; Dence, C. W., Eds.; Springer, in press.
36. Tollier, M.-T.; Monties, B.; Lapiere, C.; Herve du Penhoat, C.; Rolando, C. *Holzforchung* 1986, **40**(supp.), 75-79.
37. Lapiere, C.; Scalbert, A.; Monties, B.; Rolando, C. *Bull. Groupe Polyphenols* 1986, **13**, 128-135.
38. Kneebone, W. R. *Agron. J.* 1960, **52**, 539-542.
39. Wilson, D. *J. Agric. Sci.* 1965, **65**, 285-292.
40. Coley, P. D. *Ecolog. Monog.* 1983, **53**, 209-233.
41. Monties, B. In *Production et Utilisation des Biomasses Lignocellulosiques*; Monties, B., Ed.; Apria-Lavoisier: Paris, in press.
42. Ranner, G. R.; Morrisson, J. M. *J. Sci. Food Agric.* 1983, **34**, 137-144.
43. Monties, B. In *The Biochemistry of Plant Phenolics (Ann. Proc. Phytochem. Soc. Europ.)*; Van Sumere, C. F.; Lea, P. J., Eds.; Clarendon: Oxford, 1985; **25**, 161-181.
44. Wardrop, A. B. In *Proc. Int. Symp. Wood & Pulping Chem. (ISWPC)*; S.T.F.I. Pub.: Stockholm, 1981; **I**, 44-51.
45. Lapiere, C.; Tollier, M.-T.; Monties, B. *C. R. Acad. Sci. Paris* 1988, **307**, 723-728.

RECEIVED May 19, 1989

## Chapter 14

# Inhibition of Cell Wall Peroxidases with Ferulic Salts and Fluorinated Analogues

Anne-Marie Catesson<sup>1</sup>, An Pang<sup>1</sup>, Charlette Francesch<sup>2</sup>, Christian Rolando<sup>2</sup>, and Renée Goldberg<sup>1</sup>

<sup>1</sup>Biomembranes et Surfaces Cellulaires Végétales, ENS, 46 rue d'Ulm, 75230 Paris Cedex 05, France

<sup>2</sup>Laboratoire de l'Activation Moléculaire, ENS, 24 rue Lhomond, 75231 Paris Cedex 05, France

The extent of inhibition of the oxidation of peroxidase substrates by ferulic salts was quite variable, from no inhibition to total inhibition. Total inhibition occurred when the substrate (e.g., syringaldazine) was closely related to ferulic acid. The presence of a fluorine atom in ferulic acid slightly reduced the inhibitory effect. Oxidation of ferulic compounds was restricted to lignifying cell walls *in situ*. Cell wall peroxidases from bark and xylem were fractionated into their component isozymes. Two main anionic groups were present in the xylem and their activity towards ferulic salts and their fluorinated analogues was determined. Whether the two isozymes represent enzymes specifically involved in lignin biosynthesis is discussed.

Peroxidases are widely distributed enzymes in the plant kingdom. Despite their ubiquity and the ever-increasing number of functions ascribed to them, the precise role and localization of the many isozymes remain uncertain (1,2). One of the difficulties of peroxidase studies is that the enzymes can react with a number of synthetic or natural substrates and that even the use of purified isozymes in assays for substrate specificity does not identify any definitive roles. A search for specific inhibitors represents another approach which is still poorly developed despite its potential utility.

The only biological function which has been repeatedly confirmed is the role of peroxidases in lignin monomer polymerization (1). But even in this case, the role of the various isozymes is not yet clear, although anionic, cell wall bound peroxidases generally seem to be involved in lignification (1,2). In plant cell walls, lignin monomers seem to be present *in vivo* in the form of cinnamyl alcohols. *In vitro*, their acid precursors can also be oxidized by peroxidases (3). In order to gain further insight into the possible

0097-6156/89/0399-0193\$06.00/0  
© 1989 American Chemical Society

role of each isoperoxidase in lignin biosynthesis, we decided to check the potential inhibitory effects of cinnamyl compounds and their fluorinated analogues. The exchange of hydrogen for a fluorine atom in the 2 position of the propane chain ( $\beta$ -carbon) should interact with the site of coupling of lignin monomers. In this regard, a preliminary survey (4) showed that fluorinated cinnamyl alcohols and acids had similar effects to unfluorinated compounds. However, although alcohols are natural lignin precursors, they are difficult to use as inhibitors since they are water insoluble. Hence, a detailed study was undertaken on the action of the acids. The present paper reports comparative results obtained with ferulic and fluoroferulic acids on cell wall peroxidases.

### Materials and Methods

Five- to six-month-old tobacco plants (*Nicotiana tabacum* var. Samsun) grown in a glasshouse at 20°C were used for this study. Commercial synthetic substrates employed both for histochemical and biochemical assays were guaiacol, p-phenylenediamine-pyrocatechol (PPD-PC), 3-3' diaminobenzidine (DAB), tetramethylbenzidine (TMB) and syringaldazine. Isopropylamine and monosodium salts of ferulic acid were also used as substrates as well as their " $\beta$ -fluorinated analogues" substituted with a fluorine atom on the  $\beta$ -carbon (Fig. 1). Histochemical observations were done on hand-made transverse sections of fresh tobacco stems. Biochemical assays were performed separately on bark (inner cortical parenchyma, phloem and fibres) and xylem fractions. Technical data of incubation, enzyme extraction, spectrophotometric and electrophoretic assays were given elsewhere (5-7). Synthesis of fluorinated compounds was performed as previously described (4).

### Results and Discussion

*Oxidation of Salts from Ferulic and  $\beta$ -Fluoroferulic Acids.* When stem sections were incubated with ferulic acid, isopropylamine or sodium salts, the cell walls of the youngest xylem or sclerenchyma elements were stained a light pink color. No reaction was observed in other cell walls (Table I). The same result was obtained with fluorinated analogues. The fact that only peroxidases from lignifying cell walls are able to oxidize ferulic compounds and syringaldazine must be emphasized. Absorption spectra of the pink oxidation products of ferulic acid and  $\beta$ -fluoroferulic acid in the presence of hydrogen peroxide and peroxidases extracted from tobacco cell walls ("covalently bound" fraction) showed a peak at 520 nm.

Thus ferulic acid, which is not *in vivo* a natural substrate for peroxidases involved in lignification processes, can be oxidized not only *in vitro* but also *in situ*, i.e., in the normal, biological environment of the enzyme. Furthermore, the oxidation seems to be limited to the walls of lignifying cells. This restricted localization has been described only in the case of syringaldazine, a synthetic substrate closely related to cinnamic compounds (8,9). It is interesting to note that the presence of a fluorine atom on the

Table I. Staining Relative Intensity Observed in Tobacco Stem Sections Incubated with Different Peroxidase Substrates. Transverse sections were incubated with H<sub>2</sub>O<sub>2</sub> and a peroxidase substrate. The oxidation of routinely used commercial substrates was checked in the presence or the absence of ferulic acid salts. Variations of staining intensity in cell walls (- to ++) were judged by observation with a light microscope

Substrate	Bark			
	Parenchyma	Fibres	Phloem	Young Xylem
Ferulic Salt	-	+	-	+
$\beta$ -Fluoroferulic Salt	-	+	-	+
Syringaldazine	-	++	-	++
+Ferulic Salt	-	-	-	-
+ $\beta$ -Fluoroferulic Salt	-	-/+	-	-/+
TMB	+	++	++	++
+Ferulic Salt	-	-/+	-	-/+
+ $\beta$ -Fluoroferulic Salt	-	-/+	-	-/+
DAB	++	++	++	++
+Ferulic Salt	+	+	+ / ++	+
+ $\beta$ -Fluoroferulic Salt	+	-/+	-/+	+
Guaiacol	++	++	++	++
+Ferulic Salt	+	+	-/+	-/+
+ $\beta$ -Fluoroferulic Salt	-/+	+	-/+	+
PPD-PC	-/+	++	-/+	++
+Ferulic Salt	-/+	+ / ++	-/+	+ / ++
+ $\beta$ -Fluoroferulic Salt	-/+	+ / ++	-/+	+ / ++

$\beta$ -carbon does not alter the results. This suggests that the red color may be due to reactions occurring on the aromatic ring since the fluorine atom is present on the side chain.

These data agree with the idea that lignifying walls contain specific isozymes, each possessing different affinities towards given substrates. In order to check this hypothesis, an analysis of cell wall peroxidase fractions was undertaken.

*Oxidative Activities of Cell Wall Isozymes.* Previous electrophoretic studies (4) have revealed the presence of several isozymes in all enzyme extracts. We attempted therefore to fractionate them by anion exchange chromatography. We began our study with the most active enzymes, i.e., the lightly-bound ("ionically-bound") peroxidases from bark tissues and the strongly bound ("covalently-bound") enzymes from the xylem. Chromatograms obtained with bark ionically bound peroxidases are shown in Figure 2. Enzyme activities were estimated with isopropylamine salt from  $\beta$ -fluoroferulic acid, syringaldazine and TMB, respectively. Two main peaks

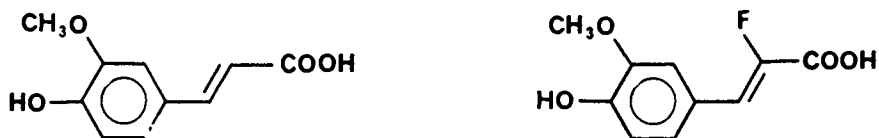


Figure 1. Chemical structure of ferulic acid (left) and  $\beta$ -fluoroferulic acid (right).

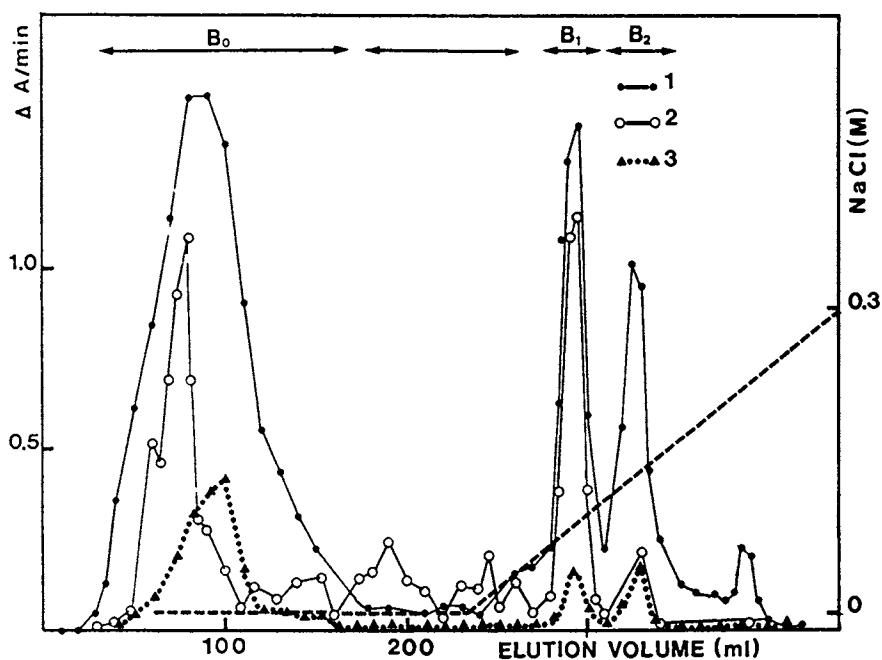


Figure 2. Anion exchange chromatogram of ionically bound phloem peroxidases on DEAE-Sepharose. Collected fractions were analyzed for their oxidase activity towards TMB (1), syringaldazine (2) and isopropylamine salt from  $\beta$ -fluoroferulic acid (3).  $B_0$ : cationic peroxidases;  $B_1$  and  $B_2$ : anionic peroxidases. Column was equilibrated with 0.01 M phosphate buffer (pH 7.1). Fractions were eluted with a NaCl gradient (0-0.5 M) in the same buffer (0.01 M phosphate, pH 7.1).

(B<sub>1</sub> and B<sub>2</sub>) of anionic isozymes were separated and their purity checked by polyacrylamide gel electrophoresis. They probably represented the two anionic groups reported in crude extracts of tobacco tissues (2). Both peaks oxidized the three tested substrates but reactions were markedly weaker with the fluorinated salt. Large amounts of cationic peroxidases (B<sub>0</sub>) were present in the extract. They were also able to oxidize the three substrates. According to Mader (2), basic isozymes would represent cytoplasmic enzymes binding to the wall during cell breakage. Ion exchange chromatography of xylem extracts allowed the separation of two anionic peaks (X<sub>1</sub> and X<sub>2</sub>) of peroxidase activity when TMB was used as substrate (Fig. 3).

Once the four anionic fractions were isolated (B<sub>1</sub>, B<sub>2</sub>, X<sub>1</sub>, X<sub>2</sub>), their activities were investigated using ferulic or  $\beta$ -fluoroferulic isopropylamine salts as substrates. Rates were plotted as a function of substrate concentration. The Lineweaver-Burk plots obtained (Fig. 4) were not always strictly linear as already reported in the case of ferulic acid and scolopetin oxidation (10,11). An estimation was made of the apparent  $K_m$  using the linear part of the plots and results were compared with those obtained for TMB. The values found in this case were in the same order of magnitude, about  $0.5 \times 10^{-3}$  to  $1 \times 10^{-3}$  M. In all extracts,  $\beta$ -fluoroferulic salt inhibited enzyme activity for concentrations higher than  $0.25 \times 10^{-2}$  M.

*Inhibition of Commercial Synthetic Substrates with Salts from Ferulic and  $\beta$ -Fluoroferulic Acids.* Table I summarizes the results obtained on stem sections incubated in a medium containing one of the usual commercial substrates and a salt of ferulic or  $\beta$ -fluoroferulic acid. Three types of interactions could be observed:

1. No inhibition, or only a very slight one, could be seen on sections incubated in a PPD-PC medium. Absorption spectra did not show much difference when ferulic or  $\beta$ -fluoroferulic acid were added to the assay mixture.
2. A rather weak inhibition was observed when sections were incubated in DAB and guaiacol.
3. A strong inhibition occurred with TMB and syringaldazine. For instance, syringaldazine oxidation could be completely inhibited with ferulic acid either *in situ* (Table I) or *in vitro*. Inhibition of syringaldazine and TMB oxidations was noticeably weaker when  $\beta$ -fluoroferulic salt was used instead of ferulic salt.

Consequently, at a given concentration an inhibition can develop between ferulic acid (or their fluorinated analogues) and some of the currently used synthetic substrates but there is no interaction with others, e.g., PPD-PC. The same differences in inhibitory ability were previously observed with  $\beta$ -fluoroconiferyl alcohol (4). These differences might be related to the configuration of substrate molecules. The strongest inhibition was observed when the three-dimensional structure of the substrate was closely related to cinnamyl compounds. This suggests that lignifying cell walls contain at least one distinctive isoperoxidase specifically able to recognize this type

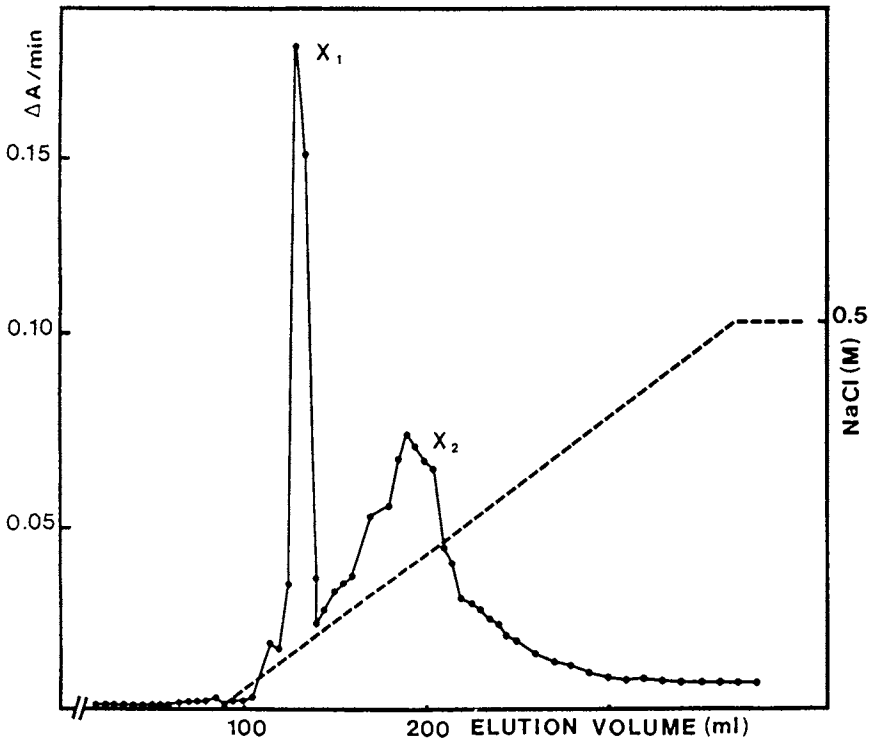


Figure 3. Anion exchange chromatogram of covalently bound xylem peroxidases. Collected fractions were analysed for their activity towards TMB. X<sub>1</sub> and X<sub>2</sub>: anionic peroxidases. For elution details, see Figure 2.

of molecule. Experiments with  $\beta$ -fluoroferulic salts corroborate this interpretation since the fluorinated analogue is less readily oxidized with the specific isoperoxidase(s).

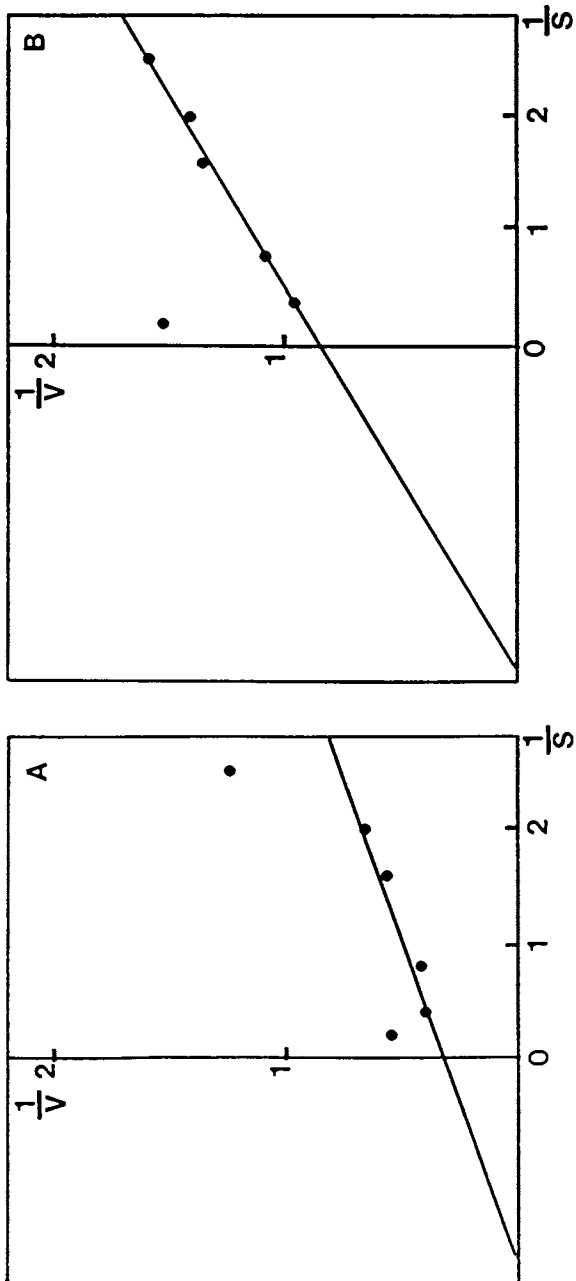
The activity of isoperoxidases able to oxidize ferulic acid is not restricted to a few similar substrates such as syringaldazine or TMB. A wider range of substrates are involved (3). Syringaldazine-oxidases from poplar and sycamore are known to react at least with TMB, PPD-PC and guaiacol, but their affinity towards the last substrate is 100 to 1000 times lower than for syringaldazine (5,7,9). Similar results were obtained with other materials (12-14). However, other isozymes are not able to react with ferulic acid or syringaldazine (5,7,12,13).

Several hypotheses could be given to explain our results. The first one postulates the simultaneous existence of at least two active sites on isozymes. One of them would exclusively recognize cinnamic compounds and would be restricted to isozymes involved in lignification processes. At the present time, we are not aware of any experimental arguments supporting this interpretation. According to a second hypothesis, all isozymes would be able to oxidize a wide range of substrates but their specificity towards a given substrate would be modulated by cellular events probably through conformational changes. This interpretation agrees with the hypothesis of a polyfunctionality of peroxidase protein modulated by metal ions (14). Phenols were also proposed as inducers of conformational changes (15). Differences in redox potential between peroxidase isozymes might also explain their specificity. Interactions between isozymes might also play a role (16).

## Conclusions

It is often stated that the last step of lignin biosynthesis requires the simultaneous presence in the cell wall of a specific isoperoxidase and its two substrates, i.e., hydrogen peroxide and lignin monomers. Xylem and sclerenchyma cells are programmed to synthesize these substances in the course of their differentiation. In fact, the presence of  $H_2O_2$  in the cell wall was demonstrated only in two instances, during cell wall lignification (5,8) and during primary cell wall reticulation through phenolic bonds (17). Thus  $H_2O_2$  production and lignin monomer supply are two limiting factors in cell wall lignification. But peroxidase availability might not be in itself a limiting factor since the enzyme is present in most cell walls. For instance, if the hypothesis of peroxidase polyfunctionality was proved to be true, limiting factors would be the molecules controlling the conformational changes necessary to induce specific recognition of cinnamyl alcohols. Alternatively, cytoplasmic compartments, especially the vacuoles, contain peroxidases with a wide range of affinities. Some of them are even able to oxidize syringaldazine (7,9). They could constitute a storage pool of enzyme, allowing rapid responses to metabolic or environmental changes.





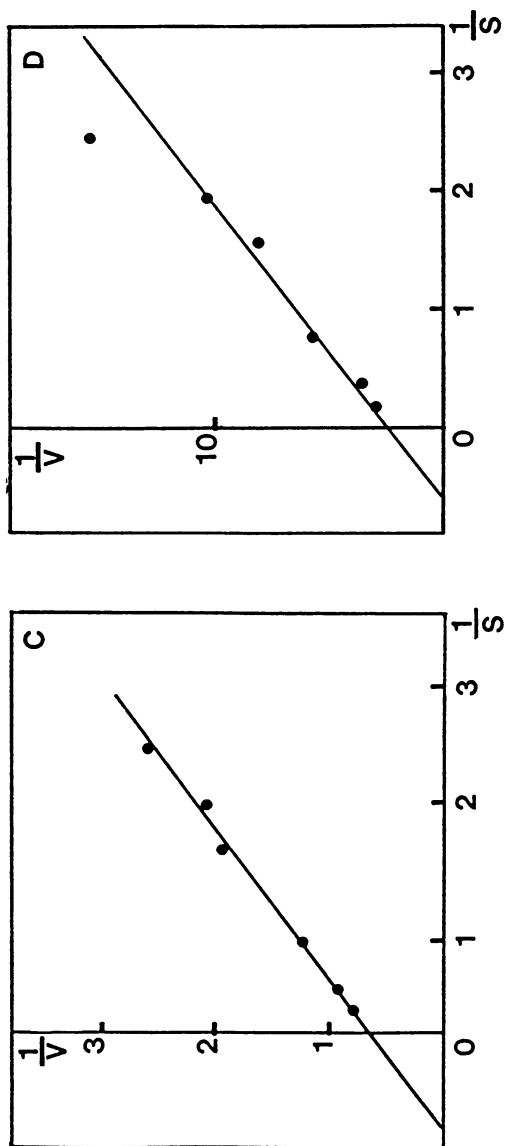


Figure 4. Double reciprocal plots of the relation between oxidation rate ( $V$ ) and substrate concentration ( $S$ ). The substrates were isopropylamine salts from  $\beta$ -fluoroferulic acid (A and B) and ferulic acid (C and D). A and C: xylem isoperoxidase  $X_1$ , B and D: xylem isoperoxidase  $X_2$ .

## Literature Cited

1. Gaspar, T.; Penel, C.; Thorpe, T.; Greppin, H. *Peroxidases 1970-1980*; Université de Genève, Centre de Botanique Publ., 1982, 324p.
2. Mäder, M.; Nessel, A.; Schloss, P. In *Molecular and Physiological Aspects of Plant Peroxidases*; Greppin, H.; Penel, C.; Gaspar, Th. Eds.; Université de Genève, Centre de Botanique Publ., 1986, pp. 247-60.
3. Pickering, J. W.; Powell, B. L.; Wender, S. H.; Smith, E. C.; *Phytochemistry* 1973, **12**, 2639-43.
4. Goldberg, R.; Pang, A.; Pierron, M.; Catesson, A. M.; Czaninski, Y.; Francesch, C.; Rolando, C. *Phytochemistry* 1988, **27**, 1647-51.
5. Goldberg, R.; Catesson, A.-M.; Czaninski, Y. *Zeit. Pflanzenphysiol.* 1983, **110**, 267-79.
6. Imberty, A.; Goldberg, R.; Catesson, A. M. *Pl. Sci. Lett.* 1984, **35**, 103-08.
7. Imberty, A.; Goldberg, R.; Catesson, A.M. *Planta* 1985, **164**, 221-26.
8. Catesson, A. M.; Czaninski, Y.; Monties, B. *C. R. Acad. Sci., Paris* 1978, **286D**, 1787-90.
9. Catesson, A. M.; Imberty, A.; Goldberg, R.; Czaninski, Y. In *Molecular and Physiological Aspects of Plant Peroxidases*; Greppin, H.; Penel, C.; Gaspar, Th., Eds.; Université de Genève, Centre de Botanique Publ., 1986, 189-98.
10. Reigh, D. L.; Wender, S. H.; Smith, E. C. *Physiol. Plant.* 1975, **34**, 44-46.
11. Kim, S. S.; Wender, S. H.; Smith, E. C. *Phytochemistry* 1980, **19**, 165-68.
12. Fleuriet, A.; Deloire, A. *Zeit. f. Pflanzenphysiol.* 1982, **107**, 259-68.
13. Quessada, M. P.; Macheix, J. J. *Physiol. Veg.* 1984, **22**, 533-40.
14. Bakardjieva, N. T. In *Molecular and Physiological Aspects of Plant Peroxidases*; Greppin, H.; Penel, C.; Gaspar, Th., Eds.; Université de Genève, Centre de Botanique Publ., 1986, pp. 189-98.
15. Ros Barcelo, A.; Munoz, R.; Sabatier, F. *Physiol. Pl.* 1987, **71**, 448-54.
16. Asada, A. Y.; Ohguchi, T.; Matsumoto, I. *Rev. Plant Prot. Res.* 1975, **8**, 104-13.
17. Goldberg, R.; Liberman, M.; Mathieu, C.; Pierron, M.; Catesson, A. *M. J. Exp. Bot.* 1987, **38**, 1378-90.

RECEIVED May 19, 1989

## Chapter 15

# Lignification in Young Plant Seedlings Grown on Earth and Aboard the Space Shuttle

Joe R. Cowles, R. LeMay, G. Jahns, W. H. Scheld, and C. Peterson

Department of Biology, University of Houston, Houston, TX 77204-5513

The space shuttle era has provided an opportunity for investigators to conduct experiments in a microgravity environment. Two shuttle flights, STS-3 and STS-51F, each contained an experiment designed principally to determine whether young plant seedlings exposed to microgravity had reduced lignin content in comparison to seedlings grown at one gravity. Three different plant species, pine, oats, and mung beans, were exposed for eight days to the microgravity environment of the shuttle. The lignin content of in-flight seedlings was less than the control seedlings in all seven sets of seedlings included in these two experiments. In five sets of seedlings, the reduction in lignin content in flight seedlings ranged from 6 to 24% and was statistically significant. In addition, the activity of two enzymes involved in lignin synthesis, phenylalanine ammonia lyase and peroxidase, were significantly reduced in pine seedlings. It was therefore concluded that microgravity, as perceived by young plant seedlings, results in reduced lignin synthesis.

The stems of most higher plants grow upward in an antigravitational direction, and are supported by the structural polymers synthesized and deposited in the cell walls. The principal structural components of plant cell walls are lignin, cellulose and hemicelluloses. The biosynthesis of at least one of these polymers, lignin, is believed to be effected by gravity (1-4). The evidence that gravity is an important factor in lignin synthesis has accumulated from a number of different experiments over several years (2-5). Until recently, however, investigators were unable to determine directly whether gravity was required for lignification because a zero or micro gravity was not available for an extended period of time. This has changed

0097-6156/89/0399-0203\$06.00/0  
© 1989 American Chemical Society

with the advent of the space shuttle where scientific experiments can be exposed to at least the microgravity environment of the space shuttle. We were provided an opportunity to fly two plant experiments on the shuttle. The first experiment was on Space Transport System-3 (STS-3), which was launched on March 21, 1982. The second experiment was part of Spacelab II, which was flown aboard STS-51F that was launched on July 29, 1985. Both of these flights were for eight days duration. The principal experimental objective was to establish the effect of microgravity on lignification in higher plant seedlings, and was part of an overall goal to understand the effect of gravity on lignification in higher plants.

This paper reports a summary of lignification values and phenylalanine ammonia lyase (PAL) and peroxidase activity from the STS-3 and STS-51F experiments. The results show a reduction in both lignification and enzyme activity in flight seedlings as compared to one gravity control seedlings.

### Materials, Procedures and Methods

**Flight Hardware.** The experiments were contained in minigrowth units referred to as Plant Growth Units (PGU's). Basically the PGU's consisted of a cavity for growing plants, a light source, a passive temperature control system and an automated recording system (6) (Fig. 1). The seedlings were grown in small plant growth chambers (PGC's) that fitted within the cavity of the PGU's (Fig. 2). Each PGU accommodated up to 6 PGC's. Two flight-qualified PGU's were built by Lockheed Missiles and Space Co. and NASA Ames Research Center, respectively. In the STS-3 experiment, one PGU was flown and the other was used to grow control seedlings in real time at NASA Kennedy Space Center (KSC). In the STS-51F experiment both PGU's were flown and subsequently used for the post-flight control experiment at NASA KSC.

**Pre-flight Activities.** The pre-flight activities at NASA KSC were initiated 10 and 15 days ahead of the scheduled STS-3 and STS-51F launches, respectively. In both experiments mung bean and oat seeds were planted within 16 hours of scheduled launch. In addition to planted seeds, the experiments included 4-day-old pine (*Pinus elliotti* Engelm) seedlings in the STS-3 experiment and 4- and 10-day-old pine seedlings in the STS-51F experiment. In the STS-3 experiment 2 PGC's were devoted to each plant species (16 seeds or seedlings each). In the STS-51F experiment 3 PGC's were committed to each age group of pine seedlings and 2 and 4 PGC's were devoted to oats (*Avena sativa* L. cv. Garry) and mung beans (*Vigna radiata*), respectively. Pre-launch activities included planting mung bean and oat seeds, assembling PGC's, exchanging atmospheric gas in the sealed PGC's with a defined gas (21% O<sub>2</sub>, 300 ppm CO<sub>2</sub> and balance N<sub>2</sub>), PGC photography, and loading PGC's into PGU. The loaded PGU's were transported to the launch pad and placed into the shuttle mid-deck.

**Flight Activities.** The PGU's were designed to require minimal in-flight attendance. Shuttle crew time, however, was requested to read and record PGC temperatures and to check flight equipment 2 to 3 times daily. On the STS-3 mission, the temperature data were routinely voiced down and used

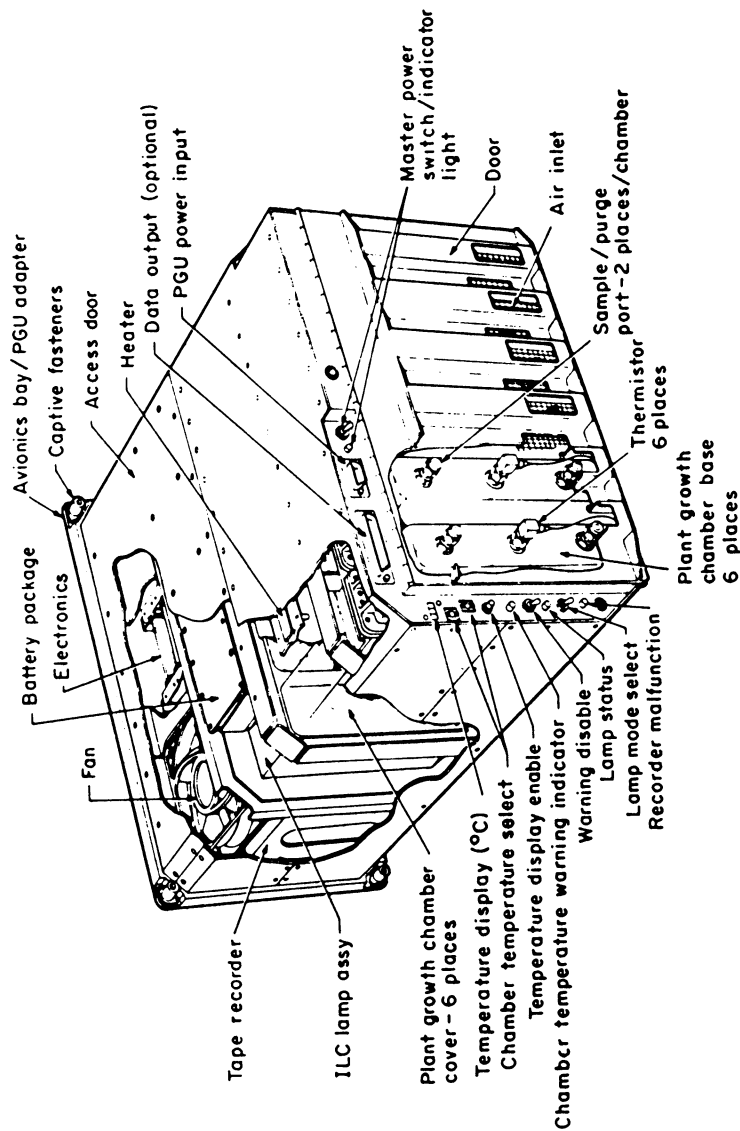


Figure 1. A diagrammatic sketch of the PGU.

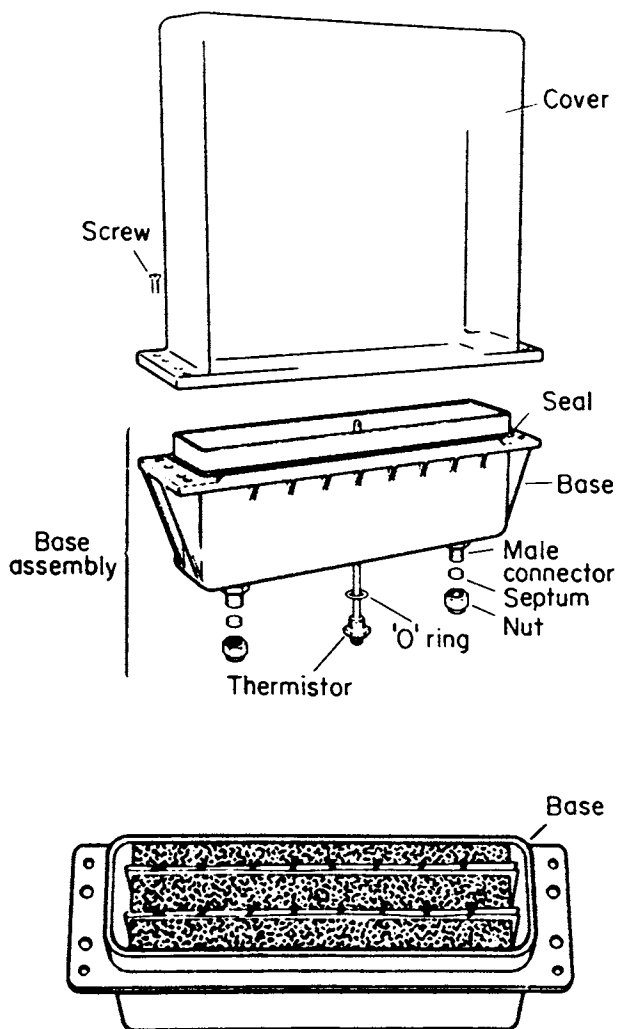


Figure 2. A diagrammatic sketch of the PGC.

in conducting the control experiment. In addition to reading temperatures and checking hardware, the STS-51F flight crew also took photographs of the plant seedlings and sampled atmospheric air in the PGC's.

*Post-Flight Activities.* The STS-3 flight landed at an alternate landing site near White Sands, New Mexico, where a temporary laboratory was established in a motor home. The PGU arrived to the laboratory about 75 min post-landing, where observations, PGC air sampling and analysis, photography, and plant measuring and packaging was conducted. About 4 hr after landing the seedlings were packed in insulated containers surrounded by cold packs for return to the PI laboratory for analysis. Upon arrival (about 13 hr post-landing), seedlings selected for lignin and enzyme analysis were further processed. The stem sections used for enzyme analysis were frozen for later analysis. All stems were measured and cut into sections. The stem sections used for lignin analysis were treated with 1.5 ml acetone/1% HCl to begin a 24 hr digestion. This phase of processing was completed about 18 hr post-landing.

The STS-51F flight landed at NASA Dryden, Edwards Air Force Base, California, where a temporary laboratory had been established. The amount of experimental tissue was twice that of the STS-3 experiment and the measuring and sectioning were conducted at the landing site. The two PGU's were received at the landing site laboratory 2 hrs after touchdown. Gas samples were taken from the PGC's and the plants were observed and photographed. The seedlings were removed, measured, weighed, sectioned, and placed in labeled containers. The tissues designated for lignin analysis were chilled while those to be used for enzyme analysis were frozen on dry ice. The tissues either chilled or frozen were returned to the PI laboratory where the lignin samples were immediately treated with 1.5 ml acetone/1% HCl as before.

*Control Experiments.* The one gravity (1g) control for the STS-3 experiment was conducted during the flight mission. The control PGC's were prepared at the same time as those designated for flight. In fact, the control PGU was transported to the launch pad as a backup experimental package but was returned to the operations building when the flight PGU was declared functional. The control PGU was connected to ground support equipment for power and monitoring.

The 1g control for the STS-51F experiment was conducted post-flight at NASA KSC Life Support Facilities. The loaded PGU's were connected to ground support equipment located in a computer-controlled environmental room. The temperature of the room was maintained such that the PGU's were able to maintain PGC temperature profiles similar to those of flight. The flight time profile also was simulated in the control experiment.

### Lignin Analysis

Lignin quantitation was based upon a modified procedure of Johnson, Moore, and Zank (7) and van Zyl (8). In the STS-3 experiment eight seedlings from each PGC (every other seedling) were selected for lignin analysis. In the STS-51F experiment, five seedlings from each PGC were



selected for lignin analysis. The pine hypocotyls were cut into six equal sections and oat stems into two equal sections in both experiments. In the STS-3 experiment only three 1 cm mung bean stems were analyzed. These were the sections located just below the needles and cotyledons and just above the root collar. In the STS-51F experiment, mung beans were first cut into hypocotyl and epicotyl regions and each region was further divided into three equal sections. The lower oat stem was cut into two 3 cm sections. Each stem section constituted a sample. Before digestion each section was cut into approximate 2 mm subsections. The subsections were extracted in a series of steps: 1.5 ml absolute acetone/1% HCl for 24 hr at  $-10^{\circ}\text{C}$ , 1.5 ml 2N NaOH for 48 hr at room temperature, and 7 ml deionized water for 24 hr at room temperature. The samples were dehydrated with 0.5 ml acetone and oven-dried for 1 hr at  $70^{\circ}\text{C}$ . The samples were digested in 0.4 ml 25% acetyl bromide/glacial acetic acid for 1 hr at  $70^{\circ}\text{C}$ , and diluted with 2.7 ml glacial acetic acid/NaOH (15:2.7) and  $20\ \mu\text{l}$  7.5 M hydroxylamine-HCl. After solubilization the samples were quantitated spectrophotometrically ( $A_{280}$ ) and compared to a wood lignin standard.

### Enzyme and Protein Analysis

Six pine seedlings from each PGC were selected for enzyme and protein analysis in the STS-3 and STS-51F experiments. The pine seedlings were sectioned as described previously for lignin analysis. All six sections from each region were pooled for analysis. The samples were frozen at this point. Later the samples were homogenized 30 to 60 sec at  $4^{\circ}\text{C}$  using a Polytron homogenizer. The tissues were homogenized in 1.5 ml of buffer containing 0.1 M Na-borate buffer (pH 8.8) containing 0.1 M KCl and soluble polyvinylpyrrolidone (PVP) (20% mg/ml). After centrifugation for 10 min at 15,000 rpm the supernatants were transferred to ice-cold test tubes.

Phenylalanine ammonia lyase (PAL) activity was determined as previously described (9). The reaction mixture contained 0.25 ml 0.4 M sodium borate buffer (pH 8.8) containing 0.4 M KCl, 0.1 ml 100 mM phenylalanine, 0.1 ml  $2\ \mu\text{Ci/ml}$  ( $\text{U-}^{14}\text{C}$ )-phenylalanine, 0.1 ml tissue homogenate and deionized  $\text{H}_2\text{O}$  to a volume of 1.0 ml. The mixture was incubated 1 hr at  $37^{\circ}\text{C}$  and the reaction stopped by addition of 0.4 ml 50% trichloroacetic acid (TCA).

Peroxidase activity was based on the polymerization rate of guaiacol in the presence of hydrogen peroxide (10). The reaction mixture contained 2.0 ml 13 mM potassium phosphate buffer (pH 7.0) containing 5 mM  $\text{H}_2\text{O}_2$ , 0.7 ml 15 mM guaiacol, and 0.1 ml of tissue extract. The reaction rates were monitored continuously in a spectrophotometer. Changes in absorbance ( $A_{470}$ ) were recorded at 15 sec intervals for 2 to 3 min.

Protein concentration was determined by use of Coomassie Blue reagent (11).

### Results

The principal experimental objective of the STS-3 and STS-51F flight experiments was to determine whether young plant seedlings grown predom-

inantly in a microgravity environment would respond by synthesizing less lignin. The STS-3 experiment was designed to be a preliminary experiment that would provide useful results in planning the Spacelab II experiment to be flown on STS-51F. It was important, however, that at least some of the STS-51F experiment be a repeat of the STS-3 experiment.

This was accomplished in principle in that (1) the same three plant species were flown on both missions; (2) durations of the missions were similar (194 hr for STS-3 and 190.5 hr for STS-51F); and (3) the same regions of oats and pine were analyzed in the two experiments, while more of the mung bean stem was analyzed in the STS-51F experiment. It is important, however, to note certain major differences in the two experiments. Firstly, the lamps remained on continuously in the STS-51F experiment rather than being on a 14/10 hr day/night cycle as with the STS-3 experiment. Secondly, the temperature in the PGC's remained just above 26°C in the STS-51F experiment rather than cycling between 23°C and 26°C with the day/night cycling of the STS-3 experiment. Finally, there were twice as many seedlings in the STS-51F experiment.

Pine seedlings that were 4 days old at launch and 12 days old at landing were analyzed for lignin in both flight experiments. In both cases, flight seedlings contained less lignin than control seedlings (Table I). The average decrease in lignin in flight seedlings over controls was 4.4% and 5.5% for the STS-3 and STS-51F experiments, respectively. This small difference in lignin content between flight and control seedlings was statistically significant at the 0.5% level in the STS-51F experiment but not in the STS-3 experiment. In both experiments the largest reduction in pine seedling lignin occurred in the upper hypocotyl region.

Table I. Lignin Content in 12-day-old Pine Seedlings

Section Number	Flight Number					
	STS-3			STS-51F		
	Flight ( $\mu\text{g}/\text{stem section}$ )	Control ( $\mu\text{g}/\text{stem section}$ )	Difference (%)	Flight ( $\mu\text{g}/\text{stem section}$ )	Control ( $\mu\text{g}/\text{stem section}$ )	Difference (%)
1	157.3	162.1	- 2.9	208.2	198.7	+ 4.8
2	137.8	139.6	- 1.3	188.3	187.5	+ 0.4
3	112.7	117.9	- 4.4	155.5	166.0	- 6.3
4	85.2	88.0	- 3.1	133.8	146.4	- 8.6
5	55.8	58.4	- 4.6	107.5	123.6	-13.0
6	28.5	37.6	-24.2	62.5	72.7	-14.0
		Av:	- 4.4		Av:	- 5.5

The STS-51F experiment also included pine seedlings that were 10 days old at launch and 18 days old at landing. The lignin content in flight seedlings was reduced 13.0% in comparison to controls (Table II). In this

set of seedlings the reduction in lignin content was significant at the 0.1% level. The reduction in lignin content in older flight seedlings was more evenly distributed over the hypocotyl than in the younger pine seedlings.

Table II. Lignin Content in 18-day-old Pine Seedlings Flown on STS-51F

Section Number	Flight ( $\mu\text{g}/\text{stem section}$ )	Control	Difference (%)
1	162.7	205.5	-20.8
2	173.3	197.9	-12.4
3	154.9	179.2	-13.6
4	141.5	153.5	- 7.8
5	118.8	128.9	- 7.8
6	79.4	89.5	-11.3
		Av:	-13.0

Mung beans were started as seeds in the STS-3 and STS-51F experiments and germinated and grown to an average height of about 12 cm within the 8-day experimental periods. In the STS-3 experiment only three 1 cm sections of mung bean stems were analyzed for lignin. These would be equivalent to a portion of sections 3, 4 and 6 in the STS-51F experiment (Table III). Flight mung bean seedlings in the STS-3 experiment contained 16% less lignin than control seedlings. This relatively large and statistically significant difference in lignin content between flight and control mung beans led to a more extensive analysis of mung beans in the STS-51F experiment. The results from the latter experiment showed an even greater reduction (37%) in lignin in flight as compared to control seedlings. The largest change in lignin content in the microgravity environment was in the younger stem region.

Table III. Lignin Content in Mung Bean Seedlings

Section Number	Flight Number					
	STS-3			STS-51F		
	Flight ( $\mu\text{g}/\text{stem section}$ )	Control	Difference (%)	Flight ( $\mu\text{g}/\text{stem section}$ )	Control	Difference (%)
1	50.6	59.6	-15.1	138.6	186.2	-25.6
2	—	—	—	116.1	160.4	-27.6
3	32.6	41.9	-22.2	109.3	167.7	-34.8
4	—	—	—	131.0	235.4	-44.4
5	—	—	—	77.3	162.6	-52.5
6	17.2	21.0	-18.2	42.5	69.9	-39.2
		Av:	-16.1		Av:	-37.4

Six 12-day-old pine seedlings per PGC were utilized to determine protein content and PAL and peroxidase activity in both the STS-3 and STS-51F experiments. In both experiments, flight seedlings contained significantly less PAL activity than control seedlings (Table IV). The average reduction in PAL activity was 22.2% for the STS-3 experiment and 18.3% for the STS-51F experiment. The change in PAL activity was more or less evenly distributed along the pine hypocotyl.

Table IV. PAL Activity in 12-day-old Pine Seedlings

Section Number	Flight Number					
	STS-3			STS-51F		
	Flight ( $\mu\text{g}/\text{stem section}$ )	Control ( $\mu\text{g}/\text{stem section}$ )	Difference (%)	Flight ( $\mu\text{g}/\text{stem section}$ )	Control ( $\mu\text{g}/\text{stem section}$ )	Difference (%)
1	3.78	5.25	-28.0	3.27	4.67	-30.0
2	5.44	6.30	-13.6	3.62	4.07	-11.1
3	5.88	7.28	-19.3	4.16	5.73	-27.4
4	6.58	7.51	-12.4	4.45	5.17	-13.9
5	6.15	8.62	-28.7	4.51	5.62	-19.8
6	3.67	5.53	-33.6	3.05	2.95	+ 3.4
		AV:	-22.2		AV:	-18.3

Peroxidase activity in flight seedlings was reduced to essentially the same extent as PAL activity. Again, the average difference in the STS-3 (-19.0%) and STS-51F (-20.2%) experiments were similar (Table V). As with PAL activity the reduction in peroxidase activity in flight seedlings was similar along the pine hypocotyl.

Table V. Peroxidase Activity in 12-day-old Pine Seedlings

Section Number	Flight Number					
	STS-3			STS-51F		
	Flight ( $\mu\text{g}/\text{stem section}$ )	Control ( $\mu\text{g}/\text{stem section}$ )	Difference (%)	Flight ( $\mu\text{g}/\text{stem section}$ )	Control ( $\mu\text{g}/\text{stem section}$ )	Difference (%)
1	47.96	59.16	-18.9	68.61	107.75	-36.3
2	42.56	57.06	-25.4	60.95	72.12	-15.5
3	45.56	53.91	-15.5	55.27	61.29	- 9.8
4	41.76	50.06	-16.6	47.36	56.85	-16.7
5	42.91	52.86	-18.8	49.13	55.26	-11.1
6	56.41	68.96	-18.2	42.68	52.81	-19.2
		Av:	-19.0		Av:	-20.2

## Discussion

Our conclusion is that young higher plant seedlings perceive microgravity and respond by synthesizing significantly less lignin. Lignin content was reduced in all seven sets of flight and control seedlings compared in the two experiments. In five sets of seedlings, two mung beans, two pines and one oat, the difference in lignin between flight and control experiments ranged from 6 to 24% and all were statistically significant. The two sets of seedlings, oats and 4-day-old pines that exhibited smaller and statistically insignificant differences in lignin were part of the STS-3 experiment where the total amount of light received was considerably less than in the STS-51F experiment. Both of these seedling types exhibited a significant difference in lignin in the STS-51F experiment.

The magnitude of the reduction in lignin content due to microgravity was especially significant considering that (1) lignification is a developmental process; (2) the experimental period was relatively short for demonstrating differences in lignification; (3) the experimental tissue was not appreciably weight-bearing; and (4) the microgravity environment of the shuttle was in the  $1 \times 10^{-3}g$  range, which is not near weightlessness.

The results on PAL and peroxidase activity also support the hypothesis that young seedlings perceive microgravity and synthesize less lignin. The activity of both enzymes was reduced about 20% in flight seedlings over controls in both experiments. These results were very consistent and were statistically significant. Whether reduced activity of these enzymes was principally responsible for reduced lignin content remains to be determined. The experimental procedures and assays were designed to measure total PAL and peroxidase activity and not just that associated with lignification. These same procedures and assays, however, have been used to demonstrate a positive correlation between the activity of these enzymes and lignification during elongation in young pine seedlings (increased enzyme activity at the time of increased lignification, unpublished results).

The results between the two flight experiments were positively related or could be accounted for by known experimental differences. The difference between lignin content of 12-day-old flight and control pine seedlings was similar between the two experiments, as were PAL and peroxidase activity. The significant reduction in lignin content in flight mung beans and oats in the STS-51F experiment, as compared to the STS-3 experiment, was probably due to the positive response of these plant species to the additional amount of light and to the slightly higher temperatures of the STS-51F experiment. The amount of lignin in both flight and control seedlings was higher in the STS-51F experiment (Tables I and III). Again, this was probably a positive response to the increased amount of light in the STS-51F experiment. The difference in light also helped explain the data shown in Table III where the amount of lignin in the STS-51F experiment was 2 to 4 times that of the STS-3 experiment. Another important difference in the mung bean data was that the STS-3 values for both the flight and control seedlings were for 1 cm sections and the STS-51F values were one-sixth of the stem length, which averaged more than 2 cm.

It is important that these flight experiments be followed by exposure of plants to longer experimental periods in microgravity. While results reported here suggest a significant reduction in lignification as a result of microgravity, other experiments are needed to establish (1) the extent of reduction over time; (2) how different levels of microgravity effect lignification; and (3) how reduction in lignification is brought about at the biochemical and cellular level.

### Acknowledgments

We wish to thank Dr. Thora Halstead, NASA headquarters, for her extraordinary support for the overall project, Drs. Ed Merck and John Tremor, NASA-Ames, for their assistance as project scientists, and Mr. Ronald Mancini, NASA-Ames, for hardware engineering. We also acknowledge the capable assistance of astronauts Gordon Fullerton and Story Musgrave, flight payload manager Mr. Marty Eiband, NASA-Goddard, and the 50 or more individuals at the NASA centers who contributed to the project. We also thank Dr. Reff Omen and Marilyn Stevens for their valuable technical and clerical assistance. The project was supported in part by NASA grant NSG 9042 and NAS 2-11165.

### Literature Cited

1. Scott, D. R. M.; Preston, S. B. *For. Sci.* 1955, **1**, 179-82.
2. Siegel, S. M.; Carrol, P.; Umeus, I.; Carre, C. *Rec. Adv. Phytochem.* 1972, **4**, 223-38.
3. Scarfield, G. *Science* 1973, **179**, 647-55.
4. Siegel, S.; Siegel, B.; Chen, J. In *Life in the Universe*; Billingham, J., Ed.; MIT: Boston, 1981; pp. 307-16.
5. Westing, A. H. *Bot. Rev.* 1968, **34**, 51-78.
6. Cowles, J. R.; Scheld, H. W.; LeMay, R.; Peterson, C. *Ann. Bot. Suppl.* 1984, **3**, 33-48.
7. Johnson, D. B.; Moore, W. E.; Zank, L. C. *Tappi* 1961, **44**, 793-98.
8. van Zyl, J. D. *Wood Sci. Technol.* 1978, **12**, 251-59.
9. Lau, Y. L.; Scheld, H. W.; Cowles, J. R. *Physiol. Plant.* 1980, **49**, 299-303.
10. Chance, B.; Machly, A. C. In *Methods in Enzymology*; Colowick, S. P.; Kaplan, N. O., Eds.; Academic: New York, 1955; Vol. II, pp. 764-73.
11. Bradford, M. M. *Anal. Biochem.* 1976, **72**, 248-54.

RECEIVED May 19, 1989

## Chapter 16

# Molecular Structure and Dynamics of Intact Plant Polyesters

### Solid-State NMR Studies

Ruth E. Stark<sup>1</sup>, Tatyana Zlotnik-Mazori<sup>1</sup>, Lisa M. Ferrantello<sup>1</sup>, and Joel R. Garbow<sup>2</sup>

<sup>1</sup>Department of Chemistry, College of Staten Island, City University of New York, Staten Island, NY 10301

<sup>2</sup>Monsanto Company, St. Louis, MO 63198

High-resolution <sup>13</sup>C NMR studies have been conducted on intact cuticles from limes, suberized cell walls from potatoes, and insoluble residues that remain after chemical depolymerization treatments of these materials. Identification and quantitation of the major functional moieties in cutin and suberin have been accomplished with cross-polarization magic-angle spinning as well as direct polarization methods. Evidence for polyester crosslinks and details of the interactions among polyester, wax, and cell-wall components have come from a variety of spin-relaxation measurements. Structural models for these protective plant biopolymers have been evaluated in light of the NMR results.

Cutin is the structural polymer of plant cuticle (Fig. 1, top), functioning along with surface waxes as a barrier against loss of moisture from aerial organs (1). Suberin plays a related role for underground organs and periderms (Fig. 1, bottom); it also forms within wound-healing tissues to prevent fungal penetration (1). Both materials are biopolyesters with many known fatty-acid constituents, but their insolubility has hampered investigations of how the monomeric units are linked together in functionally useful ways. The agricultural importance of cutin and suberin has prompted us to examine their molecular structure and dynamic properties using modern solid-state nuclear magnetic resonance (NMR) methods.

During the last 15 years, the cross-polarization magic-angle spinning (CPMAS) technique (2) has been used with increasing frequency to provide detailed structural information about solid polymers and biopolymers (3). For example, the dynamic state of backbone sites in synthetic block copolyesters, as well as the chemical bonding patterns in plant lignins, have been elucidated (4-6).

0097-6156/89/0399-0214\$06.00/0

© 1989 American Chemical Society

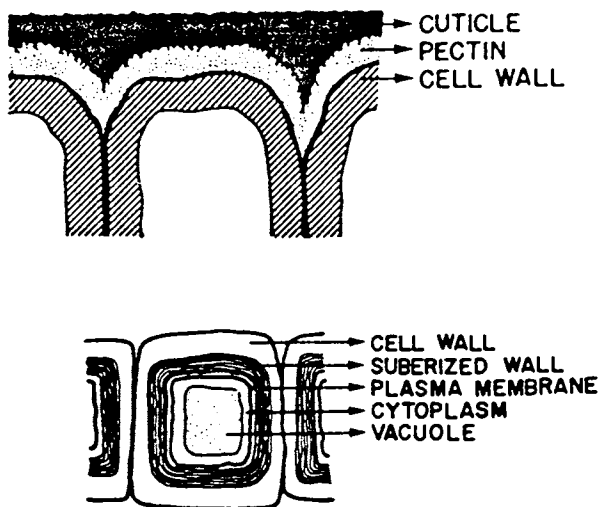


Figure 1. The location of plant polyesters: cutin attached to the epidermal wall (top); and suberin within the cell wall of a plant periderm (bottom). Reproduced by permission of the National Research Council of Canada, from Ref. 1.



We report herein on high-resolution NMR studies of cuticles from limes (7) and of suberized cell walls from potatoes. Measurements include identification and quantitation of magnetically distinct carbon moieties, determination of site-specific polymer dynamics on both MHz and kHz timescales, and delineation of the interactions among polyester, wax, and cell-wall components.

## Materials and Methods

*Isolation of the Biopolyesters.* Cutin was obtained from the skin of limes using published methods (8,9). The final solvent extractions were omitted in studies of cutin-wax interactions. Typically, 20 limes provided 800 mg of powdered polymer. Suberized cell walls were isolated from wound-healing potatoes after seven days of growth (10), with a yield of 4.5 g from 22 kg of potatoes. Chemical depolymerization of both polyesters was accomplished via transesterification with  $\text{BF}_3/\text{CH}_3\text{OH}$  (11).

Preliminary structural characterization was carried out on the soluble products of treatment with  $\text{BF}_3/\text{CH}_3\text{OH}$  (or  $\text{LiAlH}_4$ ) (8), in order to verify the similarity of our samples to materials studied previously (8-11). Gas chromatography-mass spectrometry (GC-MS) (Finnigan 3300 spectrometer) was used to establish the molecular ion and fragmentation patterns; solution-state  $^{13}\text{C}$  NMR (IBM Instruments WP-200 spectrometer) was employed for quantitation of  $\text{CH}_2$ ,  $\text{CH}_2\text{OH}$ , and  $\text{CHOH}$  moieties.

Samples for solid-state NMR (175-300 mg) were ground with a mortar and pestle and packed into either  $\text{Al}_2\text{O}_3$  or boron nitride rotors of cylindrical design. Independent polyester preparations gave identical spectral results.

*NMR Spectra.*  $^{13}\text{C}$  NMR spectra of the polymers and depolymerization residues were obtained on two instruments: an IBM Instruments WP-200 (operating at a  $^{13}\text{C}$  resonance frequency of 50.33 MHz, equipped with high-power amplifiers and a Doty Scientific probe for MAS at 5.0 kHz) and a homebuilt solid-state NMR spectrometer operating at 31.94 MHz and a spinning speed of 3.0 kHz.

CPMAS experiments were run at ambient temperature (300 K) and with a  $^1\text{H}$  decoupling field of 48-60 kHz (dipolar decoupling). Proton spin-temperature alternation and quadrature phase cycling were employed to avoid baseline distortions and other spectral artifacts (12). Recycle delays of 1-3 s were inserted between acquisitions to permit repolarization of the proton spin reservoir. Variation of the  $^1\text{H}$ - $^{13}\text{C}$  contact time served to determine the relative number of each carbon type and rotating-frame relaxation times  $T_{1\rho}(\text{H})$  (2). Two spectral editing sequences were also employed: (a) CP with delayed decoupling (50-100  $\mu\text{s}$ ) to allow dephasing and suppression of signals from rigid protonated carbons (13, 14) and (b) CP followed by delayed decoupling and a 0.6 s longitudinal relaxation period to additionally suppress signals from mobile CH and  $\text{CH}_2$  carbons (15).

For direct polarization experiments (DPMAS), data were acquired from the Bloch decay following a single  $^{13}\text{C}$  pulse. Alternatively, FT spectra and spin-lattice relaxation times were measured in a high-resolution probe

with conventional z-axis spinning (20 Hz). Both measurements employed a 6 kHz decoupling field (scalar decoupling). Recycle delays of 0.2-2.0 s were used in these experiments.

*Quantitation of Carbon Types* (2,7). Two measurements were made on a single cutin sample in the MAS probe: (a)  $^{13}\text{C}$  integrated intensities from CPMAS spectra acquired with  $^1\text{H}$ - $^{13}\text{C}$  contact times of 0.75-12.0 ms and a recycle delay of  $\geq 6 T_1(\text{H})$ 's; (b)  $^{13}\text{C}$  integrated intensities in a DPMAS spectrum acquired with a recycle delay of  $\simeq 5 T_1(\text{C})$ 's. Because the transfer times  $T_{\text{CH}}$  were short with respect to the contact time, the decay of  $^{13}\text{C}$  signal intensities in CP experiments was governed by  $T_1\rho(\text{H})$ . A linear extrapolation of CPMAS intensities to zero contact time provided quantitative estimates of the magnetically distinct rigid carbons (7); DPMAS intensities provided similar estimates for the mobile carbons. Corrections for double-counting of signal intensity, CP efficiency, and nuclear Overhauser effects are described elsewhere (7).

*Polymer Dynamics.*  $^{13}\text{C}$  spin-lattice relaxation times ( $T_1$ ) were determined with either an inversion-recovery sequence (16) (for carbons observed by direct polarization) or with a modified cross-polarization experiment (17).  $^{13}\text{C}$  rotating-frame relaxation times ( $T_1\rho(\text{C})$ ) were derived from measurements of the carbon signal that remained after a  $T_1\rho(\text{C})$  hold time of 0.05-12.0 ms following spin locking and cross polarization. Average values ( $\langle T_1\rho(\text{C}) \rangle$ ) were derived from the initial decay of carbon signal as a function of delay time (2,4).  $\langle T_1\rho(\text{C}) \rangle$ 's were measured for  $B_1(\text{C})$  values ranging from 37 to 60 kHz. As is customary for amorphous polymers, these relaxation parameters were interpreted in terms of molecular motion (4,18).

## Results and Discussion

*Intact Cutin.* Figure 2 shows a typical  $^{13}\text{C}$  CPMAS spectrum of lime cutin, and chemical-shift assignments for this material are summarized in Table I. As expected for a polyester derived from hydroxylated fatty acids, signals were observed from bulk methylenes (29, 42 ppm), aliphatic carbons bound to oxygen (64, 72 ppm), and carboxyl groups (168, 173 ppm). Evidence for  $\omega$ -hydroxy-oxo-palmitic acid constituents came from the observation of a keto peak (209 ppm). Finally, the presence of *p*-coumaric or related moieties was suggested by aromatic and olefinic peaks at 105-150 ppm (21,22). Environmentally similar groupings, probably part of an irregular polymer or a mixture of materials, gave rise to rather broad  $^{13}\text{C}$  lines.

Table II highlights the  $^{13}\text{C}$  NMR relaxation times that reflect molecular motions and help define the physical properties of the cutin polymer. For those "solid-like" carbons that cross polarized, considerable motional freedom was evidenced for  $\underline{\text{C}}\text{H}_2$  groups and  $\underline{\text{C}}\text{H}_2\text{OCOR}$  groups, on both MHz and kHz timescales, by the short values of  $T_1(\text{C})$  and  $T_1\rho(\text{C})$ , respectively. By contrast, the  $\underline{\text{C}}\text{HOCOR}$  moiety was more restricted dynamically as judged from its long value of  $T_1(\text{C})$ ; low-frequency motions in particular were implicated by the strong dependence of  $T_1\rho(\text{C})$  on  $B_1$ . These latter groups

Table I.  $^{13}\text{C}$  Chemical Shifts for Intact Lime Cutin<sup>a</sup>

Carbon Type <sup>a</sup>	Shielding (ppm) <sup>b</sup>
$-(\text{CH}_2)_n-$	29 (has two shoulders)
$-\text{CH}_2\text{CH}_2-\text{O}-\overset{\text{O}}{\parallel}{\text{C}}-\text{R}$	42
$-\text{CH}_2-\text{O}-\overset{\text{O}}{\parallel}{\text{C}}-\text{R}$	64 <sup>c</sup>
$\text{>CH}-\text{O}-\overset{\text{O}}{\parallel}{\text{C}}-\text{R}$ , $\text{>CH}-\text{OH}$	72 <sup>c</sup> <sup>d</sup> (may be two peaks)
$\text{RO}-\overset{\text{O}}{\parallel}{\text{C}}-\text{CH}=\text{CH}-\text{C}_6\text{H}_2(\text{OCH}_3)_2$	105 <sup>d</sup>
$\text{RO}-\overset{\text{O}}{\parallel}{\text{C}}-\text{CH}=\text{CH}-\text{C}_6\text{H}_2(\text{OCH}_3)_2$ , $\text{RO}-\overset{\text{O}}{\parallel}{\text{C}}-\text{CH}=\text{CH}-\text{C}_6\text{H}_2(\text{OCH}_3)_2$	115
$\text{RO}-\overset{\text{O}}{\parallel}{\text{C}}-\text{CH}=\text{CH}-\text{C}_6\text{H}_2(\text{OCH}_3)_2$ , $\text{RO}-\overset{\text{O}}{\parallel}{\text{C}}-\text{CH}=\text{CH}-\text{C}_6\text{H}_2(\text{OCH}_3)_2$	120 - 135 (broad, contribution from nonprotonated carbons) <sup>e</sup>
$\overset{\text{O}}{\parallel}{\text{C}}-\text{R}$ , $\text{RO}-\overset{\text{O}}{\parallel}{\text{C}}-\text{CH}=\text{CH}-\text{C}_6\text{H}_2(\text{OCH}_3)_2$	147 (nonprotonated) <sup>e</sup>
$\text{RO}-\overset{\text{O}}{\parallel}{\text{C}}-\text{CH}=\text{CH}-\text{C}_6\text{H}_4(\text{OH})$	156 (nonprotonated) <sup>e</sup>
$-\text{CH}_2-\text{O}-\overset{\text{O}}{\parallel}{\text{C}}-\text{R}$	168 (nonprotonated) <sup>e</sup>
$\text{>CH}-\text{O}-\overset{\text{O}}{\parallel}{\text{C}}-\text{R}$	173 (nonprotonated) <sup>e</sup>
$\text{>C}=\text{O}$	209 (nonprotonated) <sup>e</sup>

<sup>a</sup> Assigned from data for model compounds (19-21).

<sup>b</sup> From  $^{13}\text{C}$  CPDAS spectra, obtained as described in Figure 2 and referenced to external TMS.

<sup>c</sup> Ether or peroxide linkages are also possible (1).

<sup>d</sup> May include contributions from residual polysaccharide. After extended treatment with cellulase, pectinase, and hemicellulase enzymes, an additional reduction in signal intensity occurs at 105 ppm and, to a minor extent, at 72 ppm (Zlotnik-Mazori, T.; Stark, R. E., unpublished results).

<sup>e</sup> Determined from spectral editing experiments.

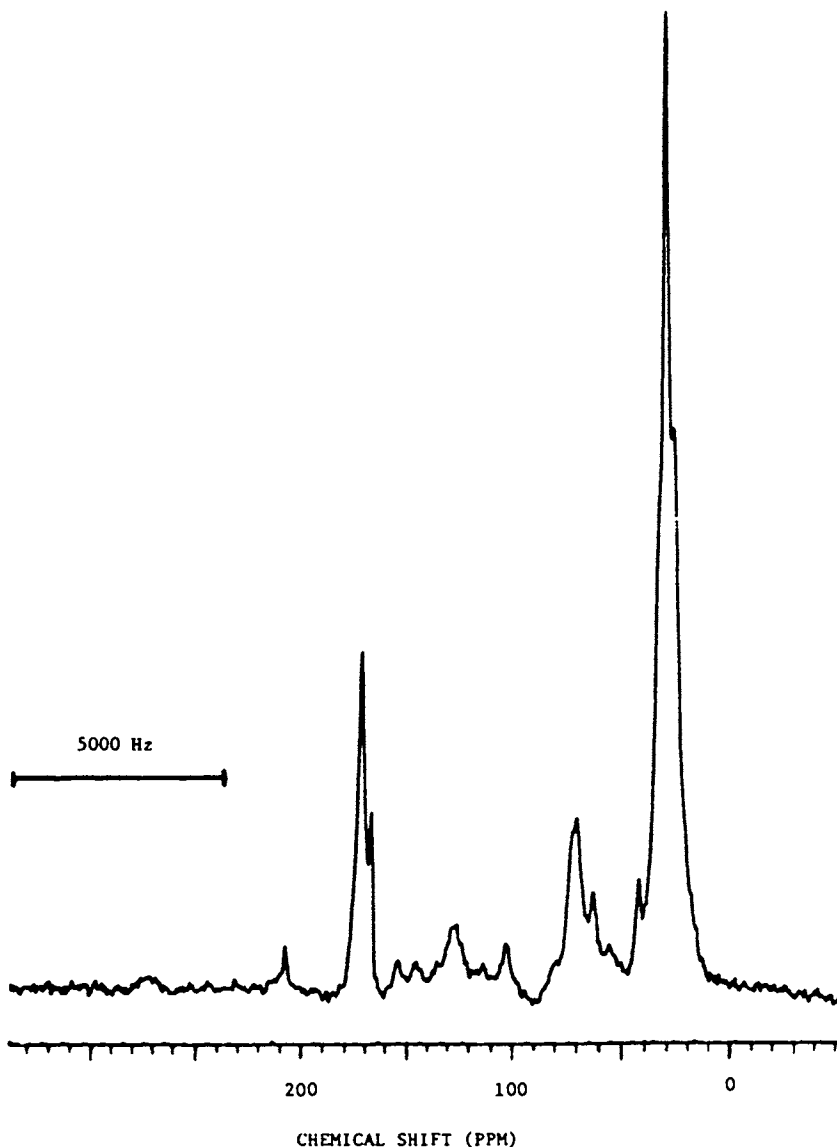


Figure 2. 50.33 MHz <sup>13</sup>C NMR spectrum of lime cutin, obtained with cross polarization (contact time 1.5 ms, repetition rate 1.0 s), magic-angle spinning (5.0 kHz), and dipolar decoupling ( $\gamma B_2/2\pi = 48$  kHz). This spectrum was the result of 6000 accumulations and was processed with a digital line broadening of 20 Hz. Chemical-shift assignments are summarized in Table I. Reproduced from Ref. 7 of the American Chemical Society.

may well correspond to the postulated crosslinks in the cutin structure (1,23).

Table II. Spin-Relaxation Times for Intact Lime Cutin

Carbon Type	$\langle T_1\rho(C) \rangle$ (ms) <sup>a</sup>			$T_1(C)$ (ms)
	37 kHz	44 kHz	50 kHz	
				225 <sup>b</sup>
( $\underline{C}H_2$ ) <sub>n</sub> , DP				420 <sup>b</sup>
( $\underline{C}H_2$ ) <sub>n</sub> , CP	2.4	2.8	3.3	145 <sup>c</sup>
$\underline{C}H_2OCOR$	3.4	4.0	5.3	122 <sup>c</sup>
$\underline{C}HOCOR, \underline{C}HOH$	6.7	8.7	12.4	>7000 <sup>c</sup>
aromatics, alkenes				~1000 <sup>c</sup>
$\underline{C}H_2OCOR$				~100 <sup>c</sup>
$\underline{C}HOCOR$				~1700 <sup>c</sup>

<sup>a</sup> From a straight-line fit of <sup>13</sup>C signal heights vs.  $T_1\rho(C)$  hold times of 0.05-1.00 ms. Values of  $B_1(C)$  were as noted. Accuracy of the measurements was 10%.

<sup>b</sup> From direct-polarization inversion-recovery experiments at 305 and 356 K, respectively. Accuracy of the measurements was 10% (7).

<sup>c</sup> From cross-polarization inversion-recovery experiments at 300 K and 50.33 MHz. Accuracy of the measurements was 15-20% (7).

Also displayed in Table II are spin-lattice relaxation data for "liquid-like" ( $\underline{C}H_2$ )<sub>n</sub> groups that were observable in DPMAS experiments. Both the dependence on temperature and the particular  $T_1$  values suggested rapid segmental motions within long runs of methylene groups, quite similar to the dynamic behavior reported for soft-segment  $\underline{C}H_2$ 's in synthetic polyesters (19).

Finally, CPMAS and DPMAS results were combined to estimate the numbers of each chemically distinct carbon type, as presented in Table III. Despite some uncertainties (7), this quantitative information served to augment prior hypotheses regarding cutin structure (1). Our determinations of methylenes, carbonyls, and aliphatics bonded to oxygen were consistent with a  $C_{16}$  polyester framework, and aromatic moieties could be present additionally as sidechains (Figure 3). A substantial degree of crosslinking was suggested by the large number of rigid secondary-alcohol ester carbons and the high proportion of immobilized methylene groups (Tables II and III).

*Cutin Depolymerization Residue.* Figure 4 compares the <sup>13</sup>C CPMAS spectra obtained for intact cutin and for the insoluble residue remaining after transesterification with  $BF_3/CH_3OH$ . The narrowing of most spectral lines suggested that the depolymerization-resistant material was a less heterogeneous polymer; delayed-coupling experiments confirmed that, among those



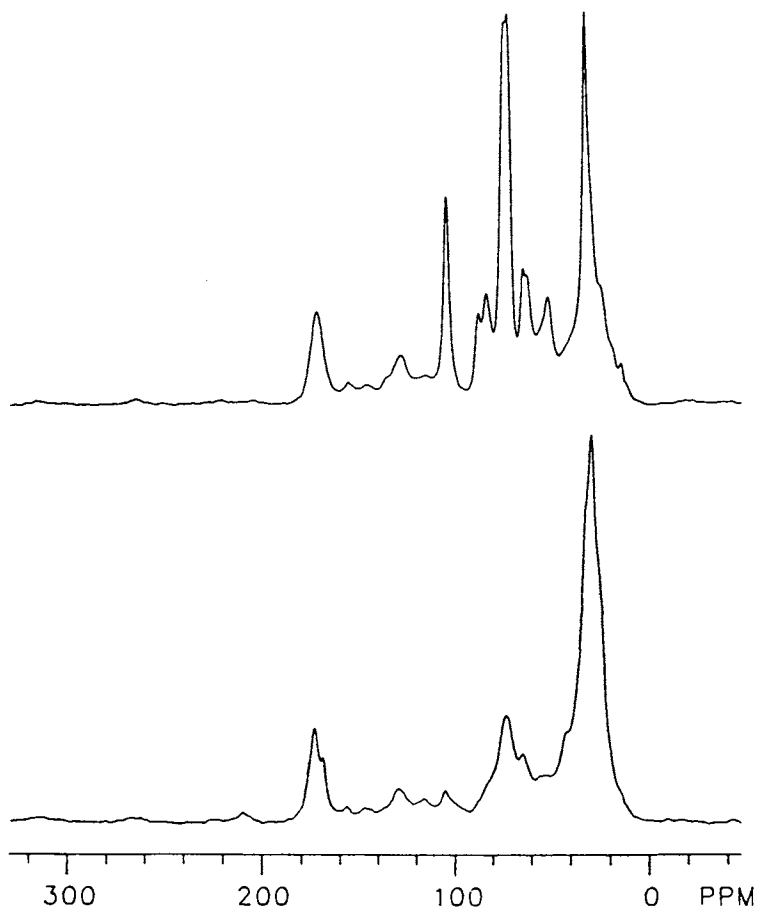


Figure 4. 31.94 MHz  $^{13}\text{C}$  NMR data for intact lime cutin (bottom) and the solid residue of a depolymerization treatment (top). Both spectra were obtained with a  $^1\text{H}$ - $^{13}\text{C}$  contact time of 1.0 ms, repetition rate of 1.0 s, spinning rate of 3.0 kHz, a  $^1\text{H}$  decoupling field of 60 kHz, and a line broadening of 20 Hz. (For the chosen contact time, peak intensities *within* each spectrum reflect the approximate numbers of each carbon type.) Only the intact cutin spectrum retained signal intensity near 30 ppm when decoupling was delayed before acquisition (13, 14).

Table III. Composition of Carbon Types in Intact Lime Cutin

Carbon Type	Rigid Moieties <sup>a</sup>	Mobile Moieties <sup>b</sup>
(CH <sub>2</sub> ) <sub>n</sub> <sup>c</sup>	51	72 <sup>d</sup>
CH <sub>2</sub> OCOR	1.9; 5.0 <sup>e</sup>	f
CHOCOR, CHOH	8.1	f
aromatics, alkenes <sup>g</sup>	4.3	
CH <sub>2</sub> OCOR	(1) <sup>h</sup>	
CHOCOR	5.5	
CO	0.8	

<sup>a</sup> From extrapolation to zero contact time of cross-polarization signal intensities.

<sup>b</sup> From comparison of integrated intensities for DPMAS and CPMAS experiments (see Materials and Methods section).

<sup>c</sup> Includes signals that span the chemical shift range of 25-33 ppm.

<sup>d</sup> Reported (incorrectly) as 36 in Ref. 7.

<sup>e</sup> Derived from slopes of a biphasic decay.

<sup>f</sup> Some signal intensity appeared at elevated temperatures.

<sup>g</sup> Sum of extrapolated intensities for peaks at 105, 128, and 156 ppm.

<sup>h</sup> Arbitrarily set to 1.

carbons that cross polarize, immobile (CH<sub>2</sub>)<sub>n</sub> groups were retained preferentially by the BF<sub>3</sub>/CH<sub>3</sub>OH treatment. The appearance of prominent resonances between 60 and 105 ppm was attributed to residual polysaccharides and to CHOCOR crosslinks, both of which are likely to resist this chemical depolymerization treatment.

*Cutin-Wax Interactions.* In order to obtain a more complete structural picture of plant cuticle, <sup>13</sup>C CPMAS data were also obtained for the polymeric assembly prior to removal of waxes (Figure 5). A second (CH<sub>2</sub>)<sub>n</sub> peak appeared in the spectrum, and additional signal intensity in the carboxyl region produced a single broadened peak. Bulk methylene carbons from cutin and wax components exhibited identical values of T<sub>1ρ</sub>(H), indicating that they were mixed intimately and shared a common <sup>1</sup>H spin reservoir (2,4). Assessments of the impact of waxes on cutin flexibility are currently in progress (Garbow, J. R.; Stark, R. E., unpublished results).

*Suberized Cell Walls.* An analogous set of CPMAS experiments is presented for suberin in Figure 6. Because this polymer is an integral part of the plant cell wall, the <sup>13</sup>C NMR spectrum had contributions from both polysaccharide and polyester components. Chemical-shift assignments, summarized in Table IV, demonstrated the feasibility of identifying major polyester and sugar moieties despite serious spectral overlap. Semiquantitative estimates for the various carbon types indicated that, as compared with cutin, the suberin polyester had dramatically fewer aliphatic and more aromatic residues. A similar observation was made previously for the soluble depolymerization products of these plant polymers (1,8,11).



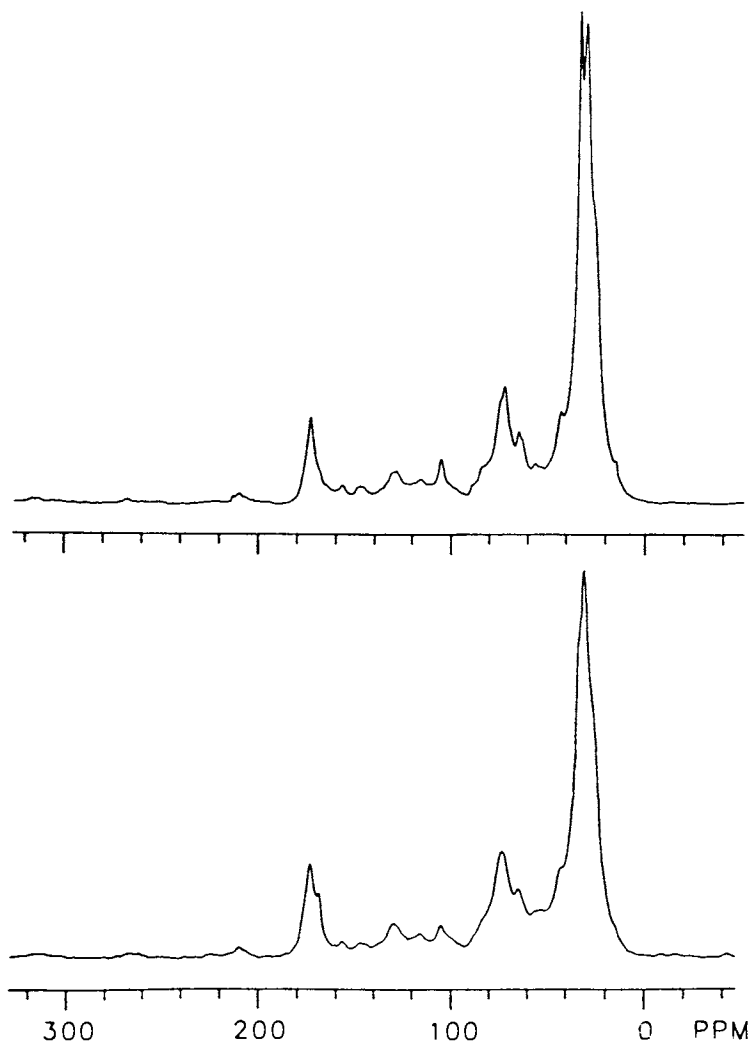


Figure 5. 31.94 MHz  $^{13}\text{C}$  NMR data for the lime cutin polyester (bottom) and a cutin-wax mixture (top). The experimental conditions were as described in Figure 4. For contact times that exceeded 3 ms, the cutin-wax assembly displayed two resolved carboxyl peaks near 170 ppm.

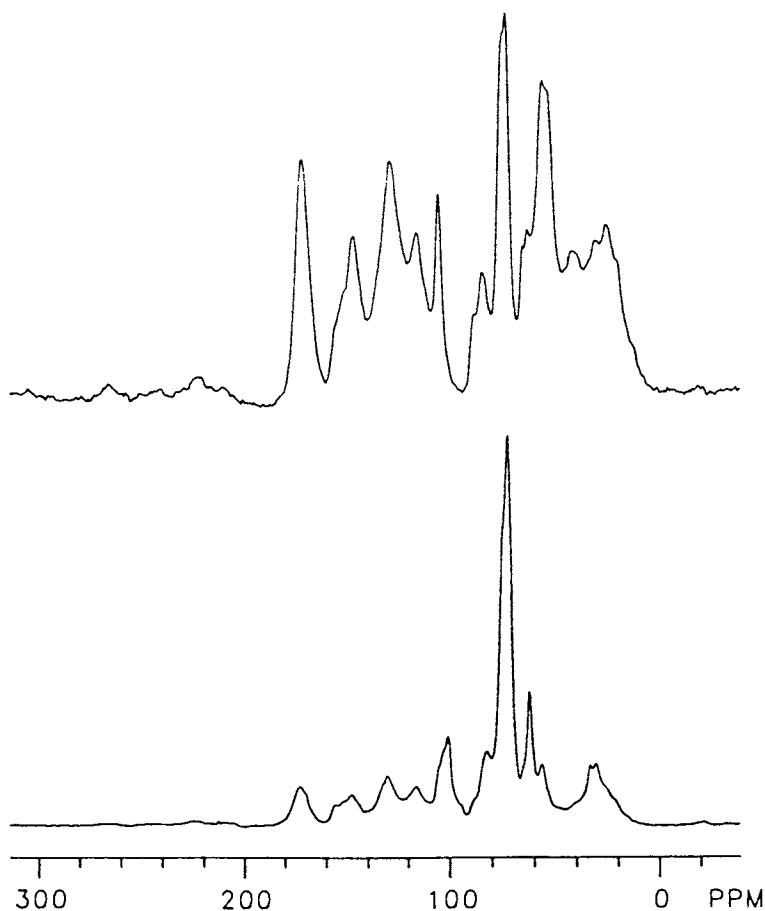


Figure 6. 31.94 MHz  $^{13}\text{C}$  NMR spectra for suberized cell walls from potatoes, before (bottom) and after (top) depolymerization treatment. The experimental parameters were as in Figure 4. Chemical-shift assignments and relative numbers of carbons for the untreated material are found in Table IV. Delayed-decoupling experiments left some  $(\text{CH}_2)_n$  signal intensity in the spectrum of intact suberin, but the analogous signals were drastically attenuated in the NMR spectrum of the depolymerization residue.

Table IV. Carbon Types in Suberized Cell Walls

Carbon Type <sup>a</sup>	Shielding <sup>b</sup> (ppm)	Relative Number <sup>c</sup>
<i>(CH<sub>2</sub>)<sub>n</sub></i>	30	1.8
<i>6</i>	62	
<i>2,3,5</i>	72	
<i>4</i>	82	
<i>1</i>	101	
aromatics, alkenes	110-160	3.6
<u>COOR</u>	172	(1)

<sup>a</sup> Assigned from data for model compounds (19-21; 24, 25). Cell-wall resonances are noted in *italics*.

<sup>b</sup> From <sup>13</sup>C CPMAS spectra, obtained as described in Figure 6 (bottom) and referenced externally to TMS.

<sup>c</sup> From extrapolation to zero contact time of cross-polarization signal intensities, omitting consideration of DPMAS spectra. For these estimates, *(CH<sub>2</sub>)<sub>n</sub>*, aromatics/alkenes, and COOR were taken as the chemical-shift regions 20-40, 110-160, and 165-180 ppm, respectively.

Intact suberized tissue yielded fairly sharp signals from the cell-wall component, but, as with cutin, broad spectral features characterized the polyester material in Figure 6 (bottom). This situation was altered after depolymerization with BF<sub>3</sub>/CH<sub>3</sub>OH: suberin lines were narrowed (Figure 6, top), suggesting selective removal of particular polymeric moieties. Again, the relatively immobile *(CH<sub>2</sub>)<sub>n</sub>*'s of Figure 6 (top) were retained preferentially. No substantial change in aliphatic-to-aromatic carbon ratio was observed, but the cell-wall signals between 40 and 110 ppm were now a much smaller proportion of the total signal intensity.

Important structural inferences may be made from the dynamic characteristics of suberin-cell wall assemblies, which are summarized in Table V. First, the unequal T<sub>1</sub>ρ(H) values derived from suberin and polysaccharide carbon signals indicated that the two components formed separate structural domains (2,4). This could result if, for example, suberin extended away from its cell-wall attachment site. Secondly, the unequal T<sub>1</sub>ρ(C) values and B<sub>1</sub> dependences suggested differing degrees of motional freedom for the polyester and polysaccharide carbon moieties. Bulk methylene carbons of the former component were similar dynamically (on the kHz timescale) to corresponding cutin moieties: low-frequency motions were facile in both cases, particularly in comparison with synthetic poly(butylene terephthalate) (4). The polysaccharide component had more restricted motions on this timescale, and the presence of such low-frequency motions was further indicated by the strong dependence of <T<sub>1</sub>ρ(C)> values on the field strength B<sub>1</sub>(C) for these carbons. Again, these spin-relaxation results were consistent with a structural model in which the suberin polymer was attached to (rather than embedded in) a relatively rigid cell wall.

Table V. Spin-Relaxation Parameters for Suberized Cell Walls

Carbon Type	$\langle T_1\rho(H)\rangle$ (ms) <sup>a</sup>	$\langle T_1\rho(C)\rangle$ (ms) <sup>b</sup>			
		37 kHz	44 kHz	50 kHz	60 kHz
( $\underline{C}H_2$ ) <sub>n</sub>	5.7	2.7	3.1	3.8	4.4
6	6.8	3.3	6.3	7.8	9.8
2,3,5	6.8	9.9	17.7	21.4	28.0
1	6.7	11.9	—	19.1	25.9
aromatics <sup>c</sup>	5.3	6.4	6.5	6.2	7.7

<sup>a</sup> From a straight-line fit of <sup>13</sup>C signal heights vs. contact times of 1.5-12.0 ms. Accuracy of the measurements was 10%.

<sup>b</sup> From a straight-line fit of <sup>13</sup>C signal heights vs.  $T_1\rho(C)$  hold times of 0.05-1.00 ms. Values of  $B_1(C)$  were as noted. Accuracy of the measurements was 10%.

<sup>c</sup> Resonance at 116 ppm.

## Conclusions

Solid-state <sup>13</sup>C NMR was employed to characterize intact samples of cutin and suberin biopolyesters. Although a considerable degree of structural heterogeneity was observed for both materials, it was possible nonetheless to resolve and assign many NMR peaks, even when the polyesters were accompanied by waxes or cell walls. Quantitative estimates for the various aliphatic, aromatic, and carbonyl carbon types indicated that cutin was primarily aliphatic in composition, whereas suberin had more aromatic and olefinic moieties. Additional analysis should be facilitated by the biosynthetic incorporation of selectively <sup>13</sup>C-enriched precursors (26,27).

Key features of molecular structure were also deduced from the dynamic characteristics of these plant polymers: (a) long runs of methylene groups in cutin were flexible enough to display NMR spectra under direct-polarization/scalar-decoupling conditions; (b) other methylenes formed shorter molecular segments (in cutin) or were associated with cell walls (in suberin) and must be observed with cross-polarization/dipolar-decoupling NMR methods; (c) many of the moieties described in (b) had spin-relaxation parameters that suggested considerable motion on MHz and kHz timescales; (d) esters of secondary alcohols probably constituted rigid crosslinks and contributed to the integrity of these biopolymers, as indicated by their  $T_1(C)$  and  $\langle T_1\rho(C)\rangle$  values. Thus, cutin appears to be a resilient crosslinked netting, whereas suberin is rendered somewhat more rigid by the cell-wall matrix in which it grows.

For the study of complex cuticular mixtures, measurements of cross-polarization dynamics proved to be especially informative. The equality of  $T_1\rho(H)$  values in cutin-wax assemblies demonstrated that these cuticular materials were mixed intimately. By contrast,  $T_1\rho(H)$  measurements showed that the polymeric components of suberized cell walls were present in distinct domains, suggesting that suberin was attached at a few structural sites rather than being embedded in the polysaccharide wall.

Preliminary structural studies of cutin and suberin breakdown involved examination of  $^{13}\text{C}$  NMR spectra for insoluble residues that were resistant to chemical depolymerization. In cutin samples, flexible  $\text{CH}_2$  moieties in particular were removed by such treatments, but CHOCOR crosslinks and polysaccharide impurities were retained preferentially. A concomitant narrowing of NMR spectral lines suggested that the treatments produced more homogeneous polyester structures in both cases. Our current studies of cuticular breakdown also employ selective depolymerization strategies with appropriate enzymes (1,28).

These results demonstrated the usefulness of  $^{13}\text{C}$  NMR in studies of molecular structure and dynamics for the polymeric constituents of plant cuticle. Although these materials are insoluble and sometimes present as interpenetrating phases, CPMAS and spin relaxation techniques helped identify important carbon types and provided structural clues to the protective functions of cutin and suberin in terrestrial plants.

### Acknowledgments

We wish to thank Dr. Y. Y. Lin for assistance with the GC-MS experiments. We are also indebted to Drs. L. W. Jelinski, J. B. Wooten, and G. Odian for helpful discussions during the course of this work. Partial support for this research was provided by grants (to R.E.S.) from the National Science Foundation (DMR-8617595), the Professional Staff Congress-City University of New York, and the College of Staten Island.

### Literature Cited

1. Kolattukudy, P. E. *Can. J. Bot.* 1984, **62**, 2918-33.
2. Schaefer, J.; Stejskal, E. O. *Top. Carbon-13 NMR Spectrosc.* 1979, **3**, 283-324.
3. Fyfe, C. A. *Solid State NMR for Chemists*; CFC Press: Guelph, Ontario, 1983.
4. Bovey, F. A.; Jelinski, L. W. *J. Phys. Chem.* 1985, **89**, 571-583.
5. Maciel, G. E.; Haw, J. F.; Smith, D. H.; Gabrielson, B. C.; Hatfield, G. R. *J. Agric. Food Chem.* 1985, **33**, 185-91.
6. Lewis, N. G.; Yamamoto, E.; Wooten, J. B.; Just, G.; Ohashi, H.; Towers, G. H. N. *Science* 1987, **237**, 1344-46.
7. Zlotnik-Mazori, T.; Stark, R. E. *Macromolecules* 1988, **21**, 2412-17.
8. Walton, T. J.; Kolattukudy, P. E. *Biochemistry* 1972, **11**, 1885-97.
9. Deas, A. H. B.; Baker, E. A.; Holloway, P. J. *Phytochemistry* 1974, **13**, 1901-05.
10. Kolattukudy, P. E.; Dean, B. B. *Plant Physiol.* 1974, **54**, 116-21.
11. Kolattukudy, P. E.; Kronman, K.; Poulouse, A. J. *Plant Physiol.* 1975, **55**, 567-73.
12. Stejskal, E. O.; Schaefer, J. *J. Magn. Reson.* 1975, **18**, 560-63.
13. Alla, M.; Lippmaa, E. *Chem. Phys. Lett.* 1976, **37**, 260-64.
14. Opella, S. J.; Frey, M. H. *J. Am. Chem. Soc.* 1979, **101**, 5854-56.

15. Murphy, P. D. *J. Magn. Reson.* 1985, **62**, 303-08.
16. Vold, R. L.; Waugh, J. S.; Klein, M. P.; Phelps, D. E. *J. Chem. Phys.* 1968, **48**, 3831-32.
17. Torchia, D. A. *J. Magn. Reson.* 1978, **30**, 613-16.
18. Schaefer, J.; Stejskal, E. O.; Steger, T. R.; Sefcik, M. D.; McKay, R. A. *Macromolecules* 1980, **13**, 1121-26.
19. Jelinski, L. W.; Schilling, F. C.; Bovey, F. A. *Macromolecules* 1981, **14**, 581-86.
20. Sohar, P. *Nuclear Magnetic Resonance Spectroscopy*; CRC Press: Boca Raton, FL, 1983; Vol. II.
21. Ludemann, H. D.; Nimz, H. *Biochem. Biophys. Res. Comm.* 1973, **52**, 1162-69.
22. Riley, R.; Kolattukudy, P. E. *Plant Physiol.* 1975, **56**, 650-54.
23. Deas, A. H. B.; Holloway, P. J. In *Lipids and Lipid Polymers in Higher Plants*; Tevini, M.; Lichtenthaler, H. K., Eds.; Springer-Verlag: New York, 1977; pp. 293-300.
24. Atalla, R. H.; Gast, J. C.; Sindorf, D. W.; Bartuska, V. J.; Maciel, G. E. *J. Am. Chem. Soc.* 1980, **102**, 3249-51.
25. Earl, W. L.; VanderHart, D. L. *J. Am. Chem. Soc.* 1980, **102**, 3251-52.
26. Dean, B. B.; Kolattukudy, P. E. *Plant Physiol.* 1977, **59**, 48-54.
27. Cottle, W.; Kolattukudy, P. E. *Plant Physiol.* 1982, **69**, 393-99.
28. Brown, A. J.; Kolattukudy, P. E. *Arch. Biochem. Biophys.* 1978, **190**, 17-26.

RECEIVED March 10, 1989

## Chapter 17

### Cellulose Biosynthesis

#### The Terminal Complex Hypothesis and Its Relationship to Other Contemporary Research Topics

Arland T. Hotchkiss, Jr.

U.S. Department of Agriculture, Agricultural Research Service, Eastern Regional Research Center, 600 East Mermaid Lane, Philadelphia, PA 19118

Cellulose biosynthesis is a complex, sensitive, and not fully characterized process that occurs in organisms ranging from plants to bacteria to animals. Two fundamental approaches have been used to investigate cellulose biosynthesis; one structural and the other biochemical. The terminal complex hypothesis proposes that the cellulose synthesizing enzyme complex can be visualized with electron microscopy. Terminal complex is the name given to collections of plasma membrane particles thought to represent the cellulose synthase. While direct evidence is still not available to support this hypothesis, the amount of indirect supporting evidence has grown dramatically in the past few years. The relationship between terminal complexes, cellulose physical structure and the biochemical events of cellulose biosynthesis will be discussed.

Cellulose, a polysaccharide consisting of linear 1,4- $\beta$ -D-anhydroglucopyranose chains laterally associated by hydrogen bonds, is the most abundant and commercially important plant cell wall polymer (1). Consequently, cellulose is also one of the most thoroughly investigated plant cell wall polymers. However, it is enigmatic in the sense that significant elements of cellulose physical structure and the mechanism of cellulose biosynthesis still are not well understood. Since these subjects have been reviewed recently (2-10), this review will update topics covered previously and provide a new analysis of selected topics of contemporary interest.

#### Cellulose Assembly

The terminal complex hypothesis proposes that structural manifestations of the cellulose synthase enzyme complex can be visualized with the freeze fracture specimen preparation technique for electron microscopy. These

This chapter not subject to U.S. copyright  
Published 1989 American Chemical Society

structures, consisting of collections of intramembranous particles observed on the internal fracture faces of the plasma membrane, are frequently associated with the ends of cellulose microfibril impressions. Furthermore, since biochemical evidence has demonstrated that cellulose biosynthesis occurs at the plasma membrane and terminal complexes are located at the site of cellulose microfibril assembly, the hypothesis proposes that terminal complexes are the cellulose synthase protein complexes.

Since Roelofsen (11) and Preston (12) first provided the conceptual basis for the terminal complex hypothesis, these structures have been reported in a variety of organisms reviewed by Brown (6). The rosette/globule terminal complex consists of a collection of six particles arranged hexagonally on the protoplasmic face (PF) with a complementary globule on the exoplasmic face (EF) of the plasma membrane. Since the last review (6), rosette terminal complexes have been observed in the vascular plants *Lepidium sativum* L. (13) and *Zinnia elegans* (14), as well as in the green algae *Chara globularis* var. *capillacea* (15), *Nitella translucens* var. *axillaris* (16), and *Mougeotia* sp. (17,18). The linear terminal complex consists of particle rows (single, triple, or diagonal) and have been reported on the EF, PF, or both faces of the plasma membrane. Linear terminal complexes consisting of diagonal rows of PF intramembranous particles have been reported recently in *Vaucheria* of the Xanthophyceae (19). The remarkable dichotomy between the taxonomic distribution of the rosette/globule and linear types of terminal complexes continues to exist (18). Rosette/globule terminal complexes have been observed throughout the evolutionary spectrum of organisms from primitive plants such as green algae (Charophyceae) to advanced vascular plants. However, linear terminal complexes are only found in certain algal groups; the Chlorophyceae and Ulvophyceae classes in the green algae, the Xanthophyceae (yellow-green algae) and the Phaeophyceae (brown algae, *Pelvetia*, 20).

Direct microscopic evidence demonstrating that terminal complex particles are cellulose synthesizing enzymes is not currently available and will await the production of antibodies against cellulose synthase following its isolation and purification. However, the proposal that terminal complexes are part of the cellulose synthase complex is increasingly becoming accepted (2) due to the accumulation of indirect evidence supporting this hypothesis. Some of the most convincing data correlates high densities of terminal complexes with localized deposition of cellulose microfibrils during certain stages of plant cellular development. Rosette/globule terminal complex density values up to 191 per  $\mu\text{m}^2$  were observed under the secondary cell wall thickenings of xylem tracheary elements of *Lepidium sativum* (13) and of *Zinnia elegans* (14). It has been known for quite some time that in tip-growing plant cells the density of rosette/globule terminal complexes increases dramatically at the tip (up to 48 rosettes per  $\mu\text{m}^2$ ), where the most active cellulose microfibril deposition occurs (21,22).

The identification of terminal complexes in the Gram-negative bacterium *Acetobacter xylinum* now appears to be in doubt. Previously, a single linear row of particles observed on the outer lipopolysaccharide membrane



PF had been proposed as the terminal complex (23) and associated pores were reported on the outer membrane EF (24). Due to their proximity to the site of cellulose ribbon extrusion from the cell surface, these structures were assumed to be responsible for cellulose synthesis. A model was advanced in which cellulose synthase was localized on the outer membrane, which invoked adhesion sites between the outer and plasma membranes as a mechanism to explain the transfer of uridine-diphosphoryl-glucose (UDPG) from the cytoplasm to the cellulose synthases (25,26). However, when the outer and plasma membranes of *Acetobacter* were isolated separately by density-gradient centrifugation, the cellulose synthase activity was localized only in the plasma membrane fraction (27). Therefore, the linear structures observed on the *Acetobacter* outer membrane, while they may be associated in some manner with cellulose biosynthesis, are probably not the cellulose synthase terminal complexes. Since no ultrastructural evidence for adhesion sites between the outer and plasma membranes has been presented, a thorough investigation of the mechanism of  $\beta$  (1-4) glucan chain translocation from the cytoplasmic membrane to the outer membrane in *Acetobacter xylinum* is now in order.

### Terminal Complex Structure and Phylogeny

Information derived from terminal complex structure has been used to probe phylogenetic relationships between cellulose producing organisms (6,17,18,26,28-30). As originally proposed (26), four characteristics of cellulose assembly (fixed vs. mobile sites of cellulose biosynthesis, linear vs. rosette terminal complexes, consolidated vs. unconsolidated terminal complexes, plasma membrane insertion of terminal complexes) were considered significant with regard to phylogenetic relationships. While most of these characteristics are still considered significant, their importance in determining phylogenetic relationships has been reinterpreted. Consequently, changes were made in the relative positions of organisms possessing terminal complexes in phylogenetic schemes which also reflect other ultrastructural and biochemical characteristics (18).

*Fixed vs. mobile sites of cellulose biosynthesis.* The phylogenetic utility of the fixed vs. mobile site characteristic of cellulose biosynthesis reflects basic structural differences between prokaryotic and eukaryotic organisms. In eukaryotic organisms, cellulose is produced from terminal complexes that move in the plane of the "fluid-mosaic" plasma membrane by the force generated from microfibril assembly (31), and deposit cellulose so that it envelops the cell. In contrast, most cellulose-producing prokaryotic organisms (including *Acetobacter*, *Achromobacter*, *Aerobacter*, *Agrobacterium*, *Alcaligenes*, *Azotobacter*, *Pseudomonas* and *Rhizobium*; 32) extrude cellulose as a ribbonlike extracellular product from a single fixed site on the cell surface. However, a cellulosic extracellular layer was reported in *Sarcina* (33). It would not be possible for the mobile site mechanism of cellulose biosynthesis to exist in prokaryotes due to the complication of cellulose extrusion through the peptidyl glycan cell wall and outer membrane.

*Consolidation of rosette/globule terminal complexes.* The strongly conserved nature of terminal complex morphology in certain eukaryotic taxonomic groups led to the reorganization of phylogenetic relationships, which were based on cellulose biosynthesis, along either a rosette terminal complex pathway or a linear terminal complex pathway (28). The significance of terminal complex consolidation is most obvious with zygnematalean algae in the rosette pathway. In this case, both solitary terminal complexes and terminal complex rows are associated with microfibril assembly during primary wall formation, whereas hexagonal arrays of terminal complexes are involved in secondary wall microfibril assembly. These examples represent three levels of terminal complex consolidation. First, the solitary rosette consists of six intramembranous particles consolidated in a pattern that contains six-fold rotational symmetry. Second- and third-order consolidation is observed in the linear translation of rosette/globule terminal complexes into rows or hexagonal arrays.

Terminal complex consolidation has also been reported in vascular plants as loosely aligned files of rosettes associated with secondary wall formation (13,14,34,35). Similar rosette files were also observed during primary wall formation in rapidly elongating regions of *Avena* coleoptiles (6,36). When coleoptiles were gravistimulated, terminal complex disaggregation occurred only on the lower coleoptile hemicylinder as evidenced by the observation of solitary globule terminal complexes (6,36). It was proposed that solitary terminal complexes produced microfibrils with less intermicrofibrillar hydrogen bonding than was present between microfibrils deposited by consolidated terminal complexes, allowing the lower hemicylinder to bend upward (36).

There appears to be a direct correlation between terminal complex length (linear consolidation) and the width of the microfibril produced. The best example of this correlation is in the deposition of secondary wall microfibrils in *Micrasterias* by hexagonal arrays of rosettes (37). In this example, the longest row of rosettes (up to 16 rosettes) located in the center of the array was associated with the widest microfibrils (up to 28.5 nm), while shorter rows were associated with narrower microfibrils. The relationship between the number of rosettes in a row and microfibril width is not proportional, however, since rows of 5 rosettes were associated with the deposition of 20 nm microfibrils in *Spirogyra* (38) and solitary rosettes were associated with 8 nm microfibrils in *Mougeotia* (17). The loosely associated files of rosettes involved in secondary wall formation in vascular plants have less linear order than the rosette rows found in zygnematalean hexagonal arrays. Correspondingly, the microfibril widths of the former were narrower than those in the latter. The consequence of the two types of secondary wall formation is that the zygnematalean secondary cell wall is more rigid than that typical of vascular plants (30), a characteristic that may be mutually advantageous for each organism in a functional sense.

*Consolidation of linear terminal complexes.* The correlation between linear consolidation of terminal complexes and microfibril width does not appear to be as consistent for linear terminal complexes, although this correlation

was previously reported (2,39). *Oocystis* and *Boergesenia* had the same average terminal complex length (510 nm), which was greater than that observed in *Valonia* (350 nm) and in *Vaucheria* (192 nm), while the *Oocystis*, *Valonia* and *Vaucheria* microfibril widths were similar (20 nm) but 10 nm less than that of *Boergesenia* (19,39,40). The structural development of the linear terminal complex has recently been reported during the regeneration of *Boergesenia* and *Valonia* protoplasts following wounding (41). In both genera terminal complex linear consolidation was reported to increase during primary wall formation, reaching a maximum length as secondary wall formation commenced. Similar results also were observed in *Boodlea* (Siphonocladales) during primary and secondary wall formation (42). Thus, linear terminal complex consolidation appears to be a manifestation of the stage of cell wall development rather than a significant factor in the determination of microfibril dimensions.

*Plasma membrane insertion of terminal complexes.* While the rosette/globule terminal complexes observed in the Zygnematales (*Micrasterias*, *Closterium*, *Spirogyra* and *Mougeotia*) were previously thought to be more transmembrane than those typical of vascular plants (26,37), the former terminal complexes are now considered to be more closely related to the latter than to the transmembrane linear terminal complexes characteristic of the Ulvophyceae (18). This statement does not imply disagreement with the observation that part of the rosette structure may be pulled away with the globule when the leaflets of the plasma membrane separate during the freeze fracture process. Rosette substructure appears to be a universal characteristic of globular terminal complexes, since it has been observed in vascular plants (30,43) and in the Zygnematales (37). It now appears that while the entire rosette/globule terminal complex spans the plasma membrane based on observations of complementary double replicas (37), neither the rosette nor the globule individually are transmembrane particles as suggested previously (37).

Herth (29) first reported that the rosette terminal complex was characteristic of those algae (Charophyceae) which represent the evolutionary line that gave rise to higher land plants. Several other taxonomic characteristics also are thought to support the proposal that the Charophyceae represents this phylogenetic line (44). Therefore, the insertion of the rosette/globule terminal complex in the plasma membrane does not appear to be phylogenetically significant, whereas this is the case for the linear terminal complex. Variation in linear terminal complex plasma membrane insertion exists in organisms representing distinctly different taxonomic groups. Only EF linear terminal complexes are observed in *Oocystis* (Chlorophyceae), while those in *Vaucheria* (Xanthophyceae) are observed only on the PF and those characteristic of *Valonia* and *Boergesenia* (Ulvophyceae) are found on both the EF and PF. The taxonomic groups represented by those organisms possessing linear terminal complexes are not considered to be closely related in a phylogenetic sense based on other ultrastructural and biochemical characteristics (44).

## Cellulose Structure

Variation in the physical structure of cellulose has been observed according to its source and developmental stage (2,5). This variation, which includes differences in microfibril crystallographic orientation, degree of polymerization (DP), transverse crystalline dimensions (crystallite size), patterns of glucan chain hydrogen bonding and glucan chain polarity, has made the basic crystalline structure of cellulose difficult to determine. X-ray diffraction studies have identified several crystalline polymorphs of cellulose (45). Cellulose isolated from plants and bacteria typically occurs in the form of cellulose I (native cellulose). The cellulose II polymorph is formed from cellulose I by treatment with alkali (mercerization) or by precipitation from solution. A reversal in glucan chain polarity from parallel to antiparallel is thought to result from the conversion from cellulose I to II. While cellulose I and II are the most common polymorphs, other forms (cellulose III, IV and X) have been reported (45).

The cellulosic microfibrils of *Acetobacter*, and those present in the primary and secondary walls of vascular plants are twisted and show no preferred crystallographic orientation relative to the cell surface. However, flat crystallographically oriented microfibrils are produced by siphonocladalean algae (*Valonia*, *Boergesenia*; Ulvophyceae; 46; Roberts and Hotchkiss, unpublished results), cladophoralean algae (*Cladophora*, *Chaetomorpha*; Ulvophyceae; 47,48), zygnematalean algae (*Mougeotia*; Charophyceae; 18) and xanthophycean algae (*Vaucheria*; 19) in which the 6.0Å lattice plane of cellulose is typically parallel to the cell surface (uniplanar orientation, 1). The flat *Spirogyra* (Zygnematales) microfibrils appear to have unusual uniplanar orientation, since either the 3.9Å or the 5.4Å lattice planes have been reported to parallel the cell surface (49). Unusual uniplanar orientation also has been reported in *Oedogonium* (Chlorophyceae), in which the 5.4Å lattice plane was observed to parallel the cell surface (1,50). Differences in cellulose microfibril crystallographic orientation within the Zygnematales are thought to result from the presence (*Spirogyra*) or absence (*Mougeotia*) of secondary wall formation (18). In this regard, it will be interesting to see if other zygnematalean algae with secondary wall formation (i.e., *Micrasterias*, *Closterium*) possess the same unusual uniplanar orientation.

Further cellulosic structural variation is displayed by DP and crystallite size parameters. *Acetobacter* and vascular plant primary wall celluloses are low in DP (2,000-6,000), while siphonocladalean and vascular plant secondary wall celluloses are relatively high in DP (> 10,000) (2). During cotton fiber development, the cellulose IV polymorph is produced during primary wall formation, while in secondary walls, cellulose I is observed (51). The cellulose crystallite size is highest in ulvophycean and certain chlorophycean algae (114-169Å), lowest in vascular plants (49-62Å) and intermediate in *Acetobacter* (70-84Å) (1). It appears that cellulose crystalline dimensions are independent of the type of terminal cellulose synthesizing complex. The idea that cellulose biosynthesis is not exclusively responsible for determining its crystalline dimensions has been proposed previously by Marx-Figini (52).

Raman spectroscopy and  $^{13}\text{C}$  CP-MAS NMR techniques have proved important in the investigation of cellulose crystalline structure (3). Based on the nonequivalence of alternate  $\beta$  (1-4) glucan chain glycosidic linkages as determined by Raman spectroscopy, it was concluded that the basic repeating unit was a disaccharide (53). The slight right and left-handed deviations from a two-fold screw axis were approximated by those observed in the crystal structures of cellobiose and methyl- $\beta$ -cellobioside model disaccharides. Cellulose computer models have also been generated based on the glycosidic oxygen bond rotational angles. These computer models were reported to better approximate the saddle position between the two major rotational angle energy of conversion minima (thought to be representative of native cellulose) than the cellobiose and methyl- $\beta$ -cellobiose crystallographic models (54).

Microscopic evidence confirming cellulose I glucan chain polarity was reported previously with *Valonia* cellulose (55,56). Recently, parallel chain polarity also was demonstrated by the asymmetrical arrangement of silver-labeled reducing ends at only one end of *Acetobacter* cellulose I fibrils (57). Two distinct crystalline forms of cellulose I ( $I_\alpha$  and  $I_\beta$ ) were reported by Atalla and VanderHart (58), based on CP-MAS  $^{13}\text{C}$  NMR evidence. Cellulose  $I_\alpha$  and  $I_\beta$  differed only in their patterns of hydrogen bonding, while their molecular conformations were otherwise identical (3). All cellulose microfibrils were thought to be mixtures of  $I_\alpha$  and  $I_\beta$  forms with the  $I_\alpha$  form predominant in cellulose from siphonocladalean algae and *Acetobacter*, whereas vascular plant cellulose primarily consisted of the  $I_\beta$  form. These conclusions were recently modified (59) following observations of the preferential  $I_\alpha$  susceptibility to acid hydrolysis and mechanical beating, as well as solid state  $^{13}\text{C}$  NMR methods which enhance the crystalline core resonances. It was determined that vascular plant cellulose consists almost exclusively of the  $I_\beta$  form, with far less (if any)  $I_\alpha$  content than reported earlier. The celluloses of *Mougeotia* and *Chara* were recently reported to be predominantly  $I_\beta$  (60). This evidence suggests that a correlation exists between the presence of solitary rosette/globule terminal cellulose synthesizing complexes and the assembly of  $I_\beta$  cellulose (60). Linear terminal complexes may be associated with the formation of a mixture of both  $I_\alpha$  and  $I_\beta$  crystalline forms.

It now appears that cellulose I is not exclusively the native polymorph present in all organisms. The results reported originally by Sisson (61), which provided evidence that cellulose II was the native polymorph present in *Halicystis* (Ulvophyceae) cell walls, were recently reinvestigated and confirmed (62). Additionally, cellulose II producing mutants of *Acetobacter* have been isolated and analyzed with x-ray and low-dose electron diffraction (63). When cellotetraose is induced to crystallize in solution it forms a structure which has been used as a model compound approximating the crystallographic nature of cellulose II based on x-ray diffraction, electron diffraction and CP-MAS  $^{13}\text{C}$  NMR evidence (64). Significantly, in all cases where *Acetobacter* cellulose synthase *in vitro* activity has been reported,

the product was cellulose II as determined by x-ray and low-dose electron diffraction (27,65). These observations indicate that cell-free synthesis of cellulose I is not known and that the spatial arrangement of components responsible for the biosynthesis of cellulose I may be easily disturbed. Therefore, the biosynthesis of cellulose II in nature may reflect alterations in the structures responsible for cellulose assembly in those organisms where it has been observed.

### *In Vitro* Cellulose Synthase Activity

While partial purification of UDPG:1,4- $\beta$ -D-glucan glucosyltransferase (cellulose synthase) from *Acetobacter* has been achieved (2,27,65), it has not been possible to demonstrate cellulose synthase activity in solubilized vascular plant membrane fractions. Instead, isolated vascular plant membranes produced  $\beta$  (1-3) glucan (callose) using UDPG as a substrate. Previously reported low levels of  $\beta$  (1-4) glucan *in vitro* synthesis in vascular plant solubilized membranes are now thought to represent xyloglucan biosynthesis (2,66). A possible candidate for the *Acetobacter* cellulose synthase has been purified as an 83 Kd concanavalin A-binding glycoprotein (65). An earlier report of *in vitro* cellulose biosynthesis by *Acetobacter* digitonin-solubilized membranes (67) is now considered to be in doubt since the product formed was reported as cellulose I and a correlation between the *in vitro* product formed and the observed electron diffraction pattern was not demonstrated (27). Cellulose synthase activity was localized on the plasma membrane of *Acetobacter* (27), and is known to be regulated by bis-(3'-5')-cyclic diguanylic acid, which is degraded by a membrane-bound  $\text{Ca}^{2+}$ -sensitive phosphodiesterase (2,68). However, vascular plant cellulose synthase does not appear to be under similar control. According to Delmer (2), the vascular plant cellulose synthase is a multifunctional  $\beta$ (1-3): $\beta$ (1-4) glucosyltransferase under the regulation of an 18 Kd 2,6-dichlorobenzonitrile (DCB) binding protein and  $\text{Ca}^{2+}$ . In order to test this hypothesis, antibodies raised against the DCB binding protein and callose synthase will be used to examine their affinity for rosette/globule terminal complexes (69). From the results of this research, it will be possible to determine whether cellulose synthase and callose synthase are the same enzyme complexes and if the terminal complex structure is actually associated with cellulose biosynthesis.

It also should be noted that Northcote (70; see chapter 1, this volume) has proposed a mechanism to explain the production of callose when vascular plant cells are damaged (including during membrane isolation for *in vitro* cellulose synthase activity). In this model, the cellulose synthase complex includes a binding protein which controls the orientation of the growing glucan chain non-reducing end. Under normal conditions, the C-4 hydroxyl at the non-reducing end is oriented so that it is the most favored site for transfer of the next glucose from UDPG. When cell damage occurs, the orientation of the binding protein is disrupted so that the C-3 hydroxyl is the most favored site for acceptance of glucose. However, this model fails to explain how the transfer of glucose to the glucan chain non-reducing end

is coordinated so that each successive glucose is rotated  $180^\circ$  relative to the adjacent one. No experimental evidence is currently available to determine the possible correlation between the Northcote model and electron microscopic observations of terminal complex structure.

Progress comparable to that made in understanding the  $\beta$  (1-4) glucan polymerization event has not been achieved with the cellulose crystallization process, since no evidence demonstrating the *in vitro* production of cellulose I has been reported. Haigler's cell-directed self-assembly model comes closest to explaining cellulose crystallization in *Acetobacter* (25,26). This model proposes that linear rows of outer membrane particle pores maintain nascent  $\beta$  (1-4) glucan chains in 1.5 nm nondissociable fibrils as they are extruded. Outside of the cell, glucan chains in register (established by the outer membrane pores) spontaneously self-assemble into 3.5 nm cellulose I microfibrils.

How the self-assembly of 1.5 nm fibrils occurs is the source of current debate. Ruben and Bokelman (71; see chapter, this volume) have observed 1.78 nm submicrofibrils arranged in a left-hand-twisted, triple-stranded pattern within 3.68 nm microfibrils by platinum-carbon shadowing for electron microscopy. They concluded that this type of construction was incompatible with the proposal (5,26) that microfibrils were formed by the lateral fasciation of 1.5-1.8 nm fibrils along crystal lattice planes. A helicoidal association of submicrofibrils mediated by the hydrogen-bond forces of xylose-containing hemicellulosic polysaccharides was suggested as the mechanism of self-assembly in *Acetobacter* (71). However, the recent evidence that crystal lattices of *Acetobacter* cellulose up to 25 nm wide were imaged by electron microscopy (72), suggests that continuous, uninterrupted crystalline domains of cellulose exist, which intrinsically follow crystal lattice planes. Furthermore, no evidence for the presence of xylose-containing polysaccharides in *Acetobacter* pellicles was confirmed (Gretz and Hotchkiss, unpublished data). Therefore, the self-assembly of 1.5 nm fibrils into microfibrils probably occurs in a helical fashion, but by a mechanism which maintains the symmetry of congruent lattice planes. More evidence is needed to prove that the self-assembly process is helicoidal.

### Alteration of Cellulose Biosynthesis

Attempts to examine the process of cellulose crystallization have frequently involved culturing *Acetobacter* in the presence of fluorescent brighteners, direct dyes, carboxy-methyl-cellulose, or other agents which compete for interchain hydrogen bond sites, thereby disrupting microfibril formation (5,26). The sheet-like structure of the altered *Acetobacter* cellulose is now better understood following x-ray and electron diffraction analysis (73). The results of this study indicated that fluorescent brightening agents, such as Calcofluor, stack transverse to the glucan chain long axis and assume a helical orientation due to glucan chain twisting. The primary forces involved in the stacking of dyes to the nascent glucan chains were reported to be hydrophobic interactions. Helically twisted fibrils of cellulose I could be regenerated from the noncrystalline altered cellulose following water

washing. However, a reduction in crystallite size relative to that typical of *Acetobacter* cellulose was observed. Kai (74) reported that dye-altered cellulose was not totally amorphous, observing reflections at 6.0Å. In contrast, the only reflections Haigler and Chanzy (73) observed (3.99Å) with similar material were attributed to the helical stacking of the dye.

These results suggest that if the events of cell-directed extrusion and nascent glucan chain self-assembly become uncoupled (as in the case of cellulose regeneration from dye-altered cellulose), the native crystalline cellulose dimensions will not be achieved. The cell-directed self-assembly model is strengthened by this information, with the corollary that the cellulose synthase is localized on the plasma membrane as suggested by Bureau and Brown (27). It appears obvious that, regardless of how the nascent glucan chains traverse the peptidyl glycan cell wall and outer membrane, the critical structural components responsible for cell-directed extrusion are localized on the outer membrane. Absence of the linear row of outer membrane particles in cellulose II producing mutants (63) suggests that the cell-directed extrusion mechanism was altered, leading to the crystallization of cellulose II. Future research examining the self-assembly of extruded  $\beta$  (1-4) glucan chains in the presence of compounds that undergo cholesteric liquid crystal formation should also yield valuable information that will address the possibility of a helicoidal mechanism for microfibril construction.

Since the events of glucan chain polymerization and cellulose crystallization are not spatially separated in eukaryotic organisms as they are in prokaryotic organisms, the observation of cellulose II in the former (62,63) raises interesting questions concerning the structure of a terminal complex that could assemble antiparallel cellulose. One possibility is that the PF component contains the cellulose synthase activity and the EF component either is missing or lacks the ability to align nascent glucan chains in a parallel orientation. Alternatively, if cellulose II chain polarity is parallel instead of antiparallel, terminal complex mediated cellulose II assembly would be much more easily explained based on our present knowledge. A parallel crystal structure model for cellulose II has been described recently (75).

It is interesting to consider the effects of non-cellulosic cell wall polysaccharides on cellulose crystallization in eukaryotic organisms. The addition of purified pea xyloglucan (76) or mannodextrins (Atalla, personal communication) to *Acetobacter* cultures has been reported to prevent or alter cellulose microfibril crystallization. These results suggest that plant cell wall polysaccharides present during microfibril deposition may alter cellulose biosynthesis. Based on  $^1\text{H-NMR}$  evidence (second moment and solid echo analysis), a model was proposed which suggests that cellulose microfibrils form a highly ordered complex with an immobile-population of xyloglucan in the primary cell walls of bean hypocotyls (77). While this model is preliminary, it appears to imply that the intimate association with xyloglucan may be due to crystallization of cellulose in the presence of xyloglucan at the plasma membrane. These proposals represent a possible explanation for the observed variation in cellulose crystallite sizes that would be open to developmental regulation based on changes in cell wall composition.



Cell wall components also have been reported to influence the pattern of microfibril deposition. Glucuronoxylan has been affinity-labeled (xylanase-gold complex) preferentially at the points of helicoidal microfibril orientation shifts between  $S_1$  and  $S_2$  lamellae in *Tilia platyphyllos* wood (78). It was proposed that the structural attributes of the hemicellulosic glucuronoxylan (elongated stiff backbone with short, flexible side chains) were favorable for cholesteric liquid crystal formation. Therefore, through close association with the cellulose, the glucuronoxylan could induce a helicoidal transition between  $S_1$  and  $S_2$  microfibril orientations. The turnover of xyloglucan in dicots and  $\beta$ -glucan (mixed 1-3, 1-4 linkages) in monocots catalyzed by specific cell wall localized glucanohydrolyases in addition to  $Ca^{2+}/H^+$  ion exchange by acidic cell wall carbohydrates, are thought to allow the slippage reorientation of cellulose microfibrils to occur during cell elongation (79). Cell wall glycoproteins may also influence the spatial arrangement of cellulose microfibrils. The distribution of isodityrosine cross-links between adjacent hydroxyproline-rich glycoproteins has been proposed to establish a cell wall matrix mesh which restricts the deposition of cellulose microfibrils in vascular plants (80).

### Molecular Genetics of Cellulose Biosynthesis

Biochemical knowledge of biosynthetic metabolism has often been aided by genetic studies of mutants defective in key enzymes in various anabolic pathways. It is hoped that this research approach will also be helpful in investigations of cellulose biosynthesis. Currently *Acetobacter* mutants deficient in cellulosic pellicle production ( $Pel^-$ ) have been produced (81,82). However, the  $Pel^-$  mutants produced in one study (82) still made small quantities of cellulose II *in vivo*, possessed normal UDPG:1,4- $\beta$ -D-glucan glucosyltransferase activity *in vitro* and had no detectable galactose in lipopolysaccharides (LPS). These observations were interpreted to mean that the  $Pel^-$  defect was not in the cellulose polymerization event but that the defect may have been in the preceding step catalyzed by UDPG pyrophosphorylase (83). However, an additional mutation affecting the structures responsible for nascent glucan chain translocation through the peptidyl glucan and outer membrane may also be present since cellulose II is produced *in vivo*. The alteration in lipopolysaccharide structure may be a manifestation of the latter type of defect in  $Pel^-$  mutants. Further investigation of these mutants should provide valuable information about the mechanism of cellulose II formation and glucan chain translocation in *Acetobacter*.

Isolation and sequencing of the cellulose synthase gene(s) has not been accomplished yet; however, DNA from *Acetobacter xylinum* containing this gene(s) was cloned into broad host-range plasmid vectors (82). These vectors were mobilized into  $Pel^-$  mutants to test for complementation. To date, this approach has not produced a pellicle-forming transconjugant from a  $Pel^-$  mutant of *Acetobacter* (82). The direct correlation between cellulose production and presence of plasmid DNA in *Acetobacter* has been reported

(84), suggesting that the cellulose synthase gene(s) was localized on one or more plasmids. However, some *Acetobacter* strains lacking plasmids or cured of plasmids were recently reported to produce cellulose (82). Therefore, plasmids cannot be regarded as the exclusive site for cellulose synthase genes.

### Conclusions

Much progress has been made in the field of cellulose biosynthesis in the past few years. The distribution of terminal complexes in plants has been more fully described. The gap between ultrastructural observations of terminal complexes and biochemical evidence for their function in cellulose biosynthesis has been narrowed, leading to a growing acceptance of the terminal complex hypothesis in the scientific community. In *Acetobacter*, the cellulose synthase has been localized on the plasma membrane and significant progress has been made toward its isolation. High resolution evidence has been presented to describe the process of cell-directed self-assembly of *Acetobacter* cellulose ribbons. Future examination of the role of cholesteric liquid crystallization in cell-directed self-assembly may help to resolve differences between this model and the triple-stranded, left-hand-twisted cellulose microfibril model for cellulose crystallization. The diversity of cellulose physical structure in nature has been further defined. Especially significant in this regard have been the observations of the correlation of terminal complex type with cellulose  $I_\alpha$  and  $I_\beta$  structure and the occurrence of native cellulose II.

Due to the abundance of literature concerning cellulose structure and biogenesis, this review was not intended to be comprehensive in nature. Instead, interpretation, speculation and analysis of recent progress in various areas of cellulose biosynthesis research have been offered in an attempt to stimulate new ideas and discussion. Many of the recent investigations enumerated can potentially make significant contributions toward a better understanding of cellulose structure and its biosynthesis in the future. The author agrees with Delmer (2,85) that there is ample opportunity for new contributors and novel approaches in this enigmatic field.

### Acknowledgments

I would like to thank Eric Roberts, R. Malcolm Brown, Jr., Kevin Hicks and Julia Goplerud for many helpful suggestions during the preparation of this manuscript.

### Literature Cited

1. Preston, R. D. *Physical Biology of Plant Cell Walls*; Chapman and Hall: London, 1974; 491 pp.
2. Delmer, D. P. *Ann. Rev. Plant Physiol.* 1987, **38**, 259.
3. Atalla, R. H. In *The Structures of Cellulose*; Atalla, R. H., Ed.; ACS Symposium Series No. 340; American Chemical Society: Washington, DC, 1987; p. 1.

4. Preston, R. D. In *Cellulose: Structure, Modification and Hydrolysis*; Young, R. A.; Powell, R. M., Eds.; John Wiley and Sons: New York, 1986; p. 3.
5. Haigler, C. H. In *Cellulose Chemistry and its Applications*; Nevell, R. P.; Zeronian, S. H., Eds.; John Wiley and Sons: New York, 1985; p. 30.
6. Brown, R. M., Jr. *J. Cell Sci. Suppl.* 1985, **2**, 13.
7. Bikales, N.; Segal, L., Eds. *Cellulose and Cellulose Derivatives*; Wiley-Interscience: New York, 1981.
8. Brown, R. M., Jr., Ed. *Cellulose and Other Natural Polymer Systems*; Plenum Press: New York, 1982.
9. Sarko, A., Ed. Ninth Cellulose Conference, *J. Appl. Polymer Sci.: Appl. Polymer Symp.* 1983, **37**.
10. Schuerch, C., Ed. *Cellulose and Wood—Chemistry and Technology*; John Wiley and Sons: New York, 1989, in press.
11. Roelofsen, P. A. *Acta Bot. Néerl.* 1958, **7**, 77.
12. Preston, R. D. In *Formation of Wood in Forest Trees*; Zimmermann, M. H., Ed.; Academic Press: London, 1964, p. 169.
13. Herth, W. *Planta* 1985, **164**, 12.
14. Haigler, C. H.; Brown, R. M., Jr. *Protoplasma* 1986, **134**, 111.
15. McLean, B.; Juniper, B. E. *Planta* 1986, **169**, 153.
16. Hotchkiss, A. T., Jr.; Brown, R. M., Jr. *J. Phycol.* 1987, **23**, 229.
17. Hotchkiss, A. T., Jr. Ph.D. dissertation, The University of Texas at Austin, 1987, 196 pp.
18. Hotchkiss, A. T., Jr.; Brown, R. M., Jr. In *Cellulose and Wood—Chemistry and Technology*; Schuerch, C., Ed.; John Wiley and Sons: New York, 1989, in press.
19. Mizuta, S.; Roberts, E. M.; Brown, R. M., Jr. In *Cellulose and Wood—Chemistry and Technology*; Schuerch, C., Ed.; John Wiley and Sons: New York, 1989, in press.
20. Peng, H. B.; Jaffee, L. F. *Planta* 1976, **133**, 57.
21. Wada, M.; Staehelin, L. A. *Planta* 1981, **151**, 462.
22. Reiss, H.-D.; Schnepf, E.; Herth, W. *Planta* 1984, **160**, 428.
23. Brown, R. M., Jr.; Willison, J. H. M.; Richardson, C. L. *Proc. Natl. Acad. Sci. USA* 1976, **73**, 4565.
24. Zaar, K. *J. Cell Biol.* 1979, **80**, 773.
25. Haigler, C. H.; Benziman, M. In *Cellulose and Other Natural Polymer Systems*; Brown, R. M., Jr., Ed.; Plenum Press: New York, 1982; p. 273.
26. Brown, R. M., Jr.; Haigler, C. H.; Suttie, J.; White, A. R.; Roberts, E. M.; Smith, C.; Itoh, T.; Cooper, K. *J. Appl. Polymer Sci.: Appl. Polymer Symp.* 1983, **37**, 33.
27. Bureau, T. E.; Brown, R. M., Jr. *Proc. Natl. Acad. Sci. USA* 1987, **84**, 6985.
28. Hotchkiss, A. T., Jr.; Roberts, E. M.; Itoh, T.; Brown, R. M., Jr. *J. Cell Biol.* 1983, **97**, 415a.
29. Herth, W. In *Botanical Microscopy 1985*; Robards, A. W., Ed.; Oxford University Press: Oxford, 1985; p. 285.

30. Herth, W. In *Cellulose and Wood—Chemistry and Technology*; Schuerch, C., Ed.; John Wiley and Sons: New York, 1989; in press.
31. Mueller, S. C.; Brown, R. M., Jr. *Planta* 1982, **154**, 489.
32. Deinema, M. H.; Zevenhuizen, L. P. T. M. *Arch. Mikrobiol.* 1971, **78**, 42.
33. Canale-Parola; Borasky, R.; Wolfe, R. S. *J. Bacteriol.* 1961, **81**, 311.
34. Herth, W. *Naturwissenschaften* 1984, **71**, 216.
35. Schneider, B.; Herth, W. *Protoplasma* 1986, **131**, 142.
36. Folsom, D. S.; Brown, R. M., Jr. In *Physiology of Cell Expansion During Plant Growth*; Cosgrove, D. J.; Knievel, D. P., Eds.; American Society of Plant Physiologists: Rockville, MD, 1987; p. 58.
37. Giddings, T. H., Jr.; Brower, D. L.; Staehelin, L. A. *J. Cell Biol.* 1980, **84**, 327.
38. Herth, W. *Planta* 1983, **159**, 347.
39. Itoh, T.; O'Neil, R. M.; Brown, R. M., Jr. *Protoplasma* 1984, **123**, 174.
40. Itoh, T.; Brown, R. M., Jr. *Planta* 1984, **160**, 372.
41. Itoh, T.; Brown, R. M., Jr. *Protoplasma* 1988, **144**, 160.
42. Mizuta, S. *Plant Cell Physiol.* 1985, **26**, 1443.
43. Mueller, S. C.; Brown, R. M., Jr. *J. Cell Biol.* 1980, **84**, 315.
44. Mattox, K. R.; Stewart, K. D. In *Systematics of the Green Algae*; Irvine, D. E. G.; John, D. M., Eds.; Academic Press: Orlando, FL, 1984; p. 29.
45. Sarko, A. *TAPPI* 1978, **61**, 59.
46. Preston, R. D.; Astbury, W. T. *Proc. Roy. Soc.* 1937, **B122**, 76.
47. Astbury, W. T.; Preston, R. D. *Proc. Roy. Soc.* 1940, **B129**, 54.
48. Nicolai, M. F. E.; Frey-Wyssling, A. *Protoplasma* 1938, **30**, 401.
49. Kreger, D. R. *Nature* 1957, **180**, 914.
50. Parker, B. C. *Phycologia* 1964, **4**, 63.
51. Chanzy, H. C.; Imada, K.; Vuong, R. *Protoplasma* 1978, **94**, 299.
52. Marx-Figini, M. *J. Polymer Sci.: Part C* 1969, **28**, 57.
53. Atalla, R. H. *Adv. Chem. Ser.* 1979, **181**, 55.
54. French, A. D. In *Cellulose and Wood—Chemistry and Technology*; Schuerch, C., Ed.; John Wiley and Sons: New York, 1989; in press.
55. Hieta, K.; Kuga, S.; Usuda, M. *Biopolymers* 1984, **23**, 1807.
56. Chanzy, H. C.; Henrissat, B. *FEBS Lett.* 1985, **184**, 285.
57. Kuga, S.; Brown, R. M., Jr. *Carbohydr. Res.* 1988, **180**, 345.
58. Atalla, R. H.; VanderHart, D. L. *Science* 1984, **223**, 283.
59. VanderHart, D. L.; Atalla, R. H. In *The Structures of Cellulose*; Atalla, R. H., Ed.; ACS Symposium Series No. 340, American Chemical Society: Washington, DC, 1987; p. 88.
60. Atalla, R. H.; VanderHart, D. L. In *Cellulose and Wood—Chemistry and Technology*; Schuerch, C., Ed.; John Wiley and Sons: New York, 1989; in press.
61. Sisson, W. *Science* 1938, **87**, 350.
62. Roberts, E. M. Ph.D. dissertation, The University of Texas at Austin, 1989.

63. Roberts, E. M.; Saxena, I. M.; Brown, R. M., Jr. In *Cellulose and Wood—Chemistry and Technology*; Schuerch, C., Ed.; John Wiley and Sons: New York, 1989; in press.
64. Henrissat, B.; Perez, S.; Tvaroska, I.; Winter, W. T. In *The Structures of Cellulose*; Atalla, R. H., Ed.; ACS Symposium Series No. 340, American Chemical Society: Washington, DC, 1987; p. 38.
65. Lin, F. C.; Brown, R. M., Jr. In *Cellulose and Wood—Chemistry and Technology*; Schuerch, C., Ed.; John Wiley and Sons: New York, 1989; in press.
66. Gordon, R.; Maclachlan, G. In *Cellulose and Wood—Chemistry and Technology*; Schuerch, C., Ed.; John Wiley and Sons: New York, 1989; in press.
67. Lin, F. C.; Brown, R. M., Jr.; Cooper, J. B.; Delmer, D. P. *Science* 1985, **230**, 822.
68. Ross, P.; Aloni, Y.; Michaeli, D.; Weinberger-Ohana, P.; Meyer, R.; Benziman, M. *FEBS Lett.* 1985, **186**, 191.
69. Delmer, D. P. In *Cellulose and Wood—Chemistry and Technology*; Schuerch, C., Ed.; John Wiley and Sons: New York, 1989; in press.
70. Northcote, D. H. In *Biochemistry of Plant Cell Walls*; Brett, C. T.; Hillman, J. R., Ed.; Cambridge University Press: Cambridge, UK, 1985; p. 177.
71. Ruben, G. C.; Bokelman, G. H. *Carbohydr. Res.* 1987, **160**, 434.
72. Kuga, S.; Brown, R. M., Jr. *J. Electron Microsc. Tech.* 1987, **6**, 349.
73. Haigler, C. H.; Chanzy, H. In *Cellulose and Wood—Chemistry and Technology*; Schuerch, C., Ed.; John Wiley and Sons: New York, 1989; in press.
74. Kai, A. In *Cellulose and Wood—Chemistry and Technology*; Schuerch, C., Ed.; John Wiley and Sons: New York, 1989; in press.
75. Sakthivel, A.; Turbak, A. F.; Young, R. A. In *Cellulose and Wood—Chemistry and Technology*; Schuerch, C., Ed.; John Wiley and Sons: New York, 1989; in press.
76. Hayashi, T.; Marsden, M. P. F.; Delmer, D. P. *Plant Physiol.* 1987, **83**, 384.
77. Taylor, I. E. P.; MacKay, A. L.; Wallace, J. In *Cellulose and Wood—Chemistry and Technology*; Schuerch, C., Ed.; John Wiley and Sons: New York, 1989; in press.
78. Vian, B.; Reis, D.; Mosiniak, M.; Roland, J. C. *Protoplasma* 1986, **131**, 185.
79. Carpita, N. C. In *Physiology of Cell Expansion During Plant Growth*; Cosgrove, D. J.; Knievel, D. P., Eds.; American Society of Plant Physiologists: Rockville, MD, 1987; p. 28.
80. Lamport, D. T. A.; Epstein, L. In *Current Topics in Plant Biochemistry*; Vol. 2; Randall, D. D., Ed.; University of Missouri Press: Columbia, MO, 1983; p. 73.
81. Swissa, M.; Aloni, Y.; Weinhouse, H.; Benziman, M. *J. Bacteriol.* 1980, **143**, 1142.

82. Saxena, I. M.; Brown, R. M., Jr. In *Cellulose and Wood—Chemistry and Technology*; Schuerch, C., Ed.; John Wiley and Sons: New York, 1989; in press.
83. Fukasawa, T.; Jokura, K.; Kurahashi, K. *Biochim. Biophys. Acta* 1963, **74**, 608.
84. Valla, S.; Coucheron, D. H.; Kjosbakken, J. *Arch. Microbiol.* 1983, **134**, 9.
85. Delmer, D. P. *Adv. Carbohydr. Chem. Biochem.* 1983, **41**, 105.

RECEIVED March 13, 1989

American Chemical Society  
Library

1155 16th St., N.W.

Washington, D.C. 20036

In Plant Cell Wall Polymers; Lewis, N., et al.;  
ACS Symposium Series; American Chemical Society: Washington, DC, 1989.

## Chapter 18

### (1,3)- $\beta$ -Glucan Synthase

#### Subunit Identification Studies

B. P. Wasserman<sup>1</sup>, T. L. Mason<sup>1</sup>, D. J. Frost<sup>1</sup>, S. M. Read<sup>1,3</sup>, R. M. Slay<sup>2</sup>,  
and A. E. Watada<sup>2</sup>

<sup>1</sup>Department of Food Science, New Jersey Agricultural Experiment Station, Cook College, Rutgers University, New Brunswick, NJ 08903

<sup>2</sup>Horticultural Crops Quality Laboratory, U.S. Department of Agriculture, Agricultural Research Service, Beltsville Agricultural Research Center, Beltsville, MD 20705

Tools have recently been developed that should enable identification of the catalytic subunits of the plasma membrane  $\beta$ -(1,3)-glucan synthase from red beet storage tissue and other plant sources. These include: an efficient procedure for solubilization and enrichment of this enzyme using the detergent CHAPS, generation of antibodies, and use of affinity labels such as UDP-pyridoxal. In addition, it is shown that partially purified preparations are enriched in several polypeptides including a 54 kD polypeptide that becomes phosphorylated in the presence of ATP and protein kinase. Preliminary results of these studies are described.

Cell wall polysaccharides in fungi and higher plants are thought to be biosynthesized from their appropriate monomeric precursors by membrane-bound glycosyl transferases (1,2). Glycosyl transferases from a variety of sources have been characterized in crude form, but have proven difficult to purify (3-7). This has hindered generation of the genetic and immunological probes necessary to study the regulation of polysaccharide formation during growth and development.

Our laboratory has been focusing on purifying and identifying the catalytic subunits of the plasma membrane  $\beta$ -(1,3)-glucan synthase from red beet storage tissue. This source of glucan synthase possesses good stability (8). Recently an effective procedure for partial purification consisting of two-step solubilization and gel filtration with phospholipid (functional reconstitution) using the detergent 3-[[3-cholamidopropyl]dimethylammonio]-1-propanesulfonate (CHAPS) was developed (4). In this

<sup>3</sup>Current address: Plant Cell Biology Research Centre, School of Botany, University of Melbourne, Parkville, Victoria 3052, Australia

way, the specific activity of the enzyme could be increased from 50 U/mg in microsomal membranes to over 1,000 in the functionally reconstituted form.

Efforts to purify the enzyme beyond the reconstituted form have proven difficult thus far due to activity losses occurring during resolubilization. Therefore, we have focused our efforts on identification of subunits using methods that may be applied to partially pure preparations (3). Approaches that show promise are: (i) generation of antibodies to partially pure fractions; (ii) use of affinity labels such as UDP-pyridoxal; and (iii) studying the possible regulation of activity by phosphorylation and showing the existence of subunits that are phosphorylated by ATP in the presence of added or endogenous protein kinases. Our preliminary results are presented here.

### Materials and Methods

*Preparation of Glucan Synthase Fractions.* Microsomal and plasma membranes were isolated by differential and density-gradient centrifugation. CHAPS-solubilized glucan synthase (CSGS) was prepared by the two-step procedure (4,9). In step 1, contaminating proteins were extracted with 0.3% CHAPS in the presence of divalent cations and in step 2 enzyme was solubilized with 0.6% CHAPS in the presence of chelators. Reconstituted glucan synthase (RCGS) fractions were prepared by passage of CSGS through a Sephacryl S-400 gel filtration column eluted with 50 mM Tris-HCl, pH 7.5, containing 0.1% CHAPS, 0.15 mg/ml alectin, 1 mM dithioerythritol (DTE) and 5% glycerol. Enzyme was assayed in the presence of 5 mM MgCl<sub>2</sub>, 2 mM CaCl<sub>2</sub>, 5 mM cellobiose or sucrose, 0.01% digitonin, 1 mM UDPG and 50 mM N-2-hydroxyethylpiperazine-N'-2-ethanesulfonic acid (HEPES)-NaOH or Tris-HCl, pH 7.5. The specific activity of CSGS preparations ranged between 300-500 nmol/min/mg and RCGS between 900 and 1,500 nmol/min/mg. Details of each of these procedures with current modifications are described in a recent review (9). Plasma membranes from celery were isolated by two-phase partitioning essentially as described (10).

*Electrophoresis.* Electrophoresis was conducted on 9 to 18% gradient gels under denaturing conditions as described (11,12). For detection, proteins were electrotransferred to nitrocellulose paper (13) and stained using colloidal gold with a silver overlay (14).

*Chemical Modification.* Inhibitor screening was conducted by preincubating CSGS in 50 mM HEPES-NaOH with each inhibitor as follows: N-ethylmaleimide, 30 min, on ice, pH 8.0; phenylglyoxal, 15 min, 30°C, pH 7.5; formaldehyde, 90 min, 23°C, pH 7.5, in the presence of 10 mM NaCNBH<sub>3</sub>. UDP-pyridoxal was preincubated with CSGS on ice with 5 mM MgCl<sub>2</sub>, 2 mM CaCl<sub>2</sub>, 5 mM cellobiose, 0.01% digitonin, and 125 mM HEPES-NaOH, pH 7.5. After 1 hr, mixtures were brought to 50  $\mu$ M NaBH<sub>4</sub>.

Effector dependence studies with UDP-pyridoxal were conducted as follows: Red beet plasma membranes (10  $\mu$ g protein) were preincubated in



80  $\mu\text{l}$  of 50 mM HEPES/NaOH, pH 7.5, containing 100 mM sucrose, 0.01% digitonin and effectors at the following concentrations:  $\text{MgCl}_2$ , 5 mM;  $\text{CaCl}_2$ , 2 mM; EGTA and EDTA, 1 mM each; and UDPG, 2.5 mM. This was followed by addition of UDP-pyridoxal to 5  $\mu\text{M}$ . After 30 min at 0°C, the reaction was stopped by addition of  $\text{NaBH}_4$  to 200  $\mu\text{M}$ . Samples were incubated a further 10 min and triplicate 20  $\mu\text{l}$  aliquots removed for assay. UDP-Pyridoxal was synthesized essentially as described (15).

**Phosphorylation.** To study regulation of enzyme activity, fractions were preincubated with 150  $\mu\text{M}$  ATP, 5 U protein kinase catalytic subunit from bovine heart, 5 mM  $\text{MgCl}_2$ , 60 mM dithiothreitol, 120  $\mu\text{M}$  ATP, 5-80  $\mu\text{g}$  protein depending on source and 50 mM Tris-HCl, pH 8. Samples were held 5 min at 35°C and assayed.

For labeling studies, samples were first concentrated to 8.5  $\mu\text{g}$  of protein and then phosphorylated in a volume of 100  $\mu\text{l}$  as above with 2  $\mu\text{Ci}$  [ $\gamma$ - $^{32}\text{P}$ ] ATP. Incubations were for 10 min at 37°C. Electrophoresis was conducted on 10% polyacrylamide gels as described above.

## Results

**Electrophoretic Analysis.** Electrophoretic profiles of glucan synthase fractions purified from red beet are shown in Figure 1. To visualize protein subunits it was necessary to utilize a highly sensitive staining method. For this system, colloidal gold staining followed by a silver overlay (Figure 1) gave excellent visualization (14).

Three major polypeptide bands of 72, 68 and 54 kD, all of which cofractionated with the distribution of enzyme activity on RCGS columns, were seen upon reconstitution in all preparations examined to date (Figure 1). Other polypeptides, whose presence and intensity seemed to vary between preparations, were seen at 45, 42 and 30 and 28 kDa.

The fact that the 72, 68 and 54 kD polypeptides are invariably present in purified fractions raised speculation that these bands represented glucan synthase subunits. A number of recent findings suggest that the 54 kD band might be of particular interest. These are: (1) a 54 kD band was greatly enriched in a reconstituted fraction from another plant source, celery (Fig. 2); (2) a 54 kD band had weak  $\text{Ca}^{2+}$  binding activity in the denatured state; (3) a 54 kD band became phosphorylated by both endogenous and added kinases (see below); and (4) in mung bean, a 54 kD band reacted with a monoclonal antibody directed against glucan synthase activity (16).

**Antibody Generation and Immunoprecipitation.** Obtaining antibodies that specifically bound to a catalytic or regulatory subunit of glucan synthase would represent a major step towards understanding the regulation and function of this enzyme system. As a first effort towards reaching this goal, polyclonal antibodies were generated against CSGS and RCGS fractions. RCGS antisera was tested for its ability to immunoprecipitate activity. RCGS antibodies immunoprecipitated approximately 74% of the activity relative to preimmune sera (Table I). This confirmed the presence of antibodies directed against the enzyme.

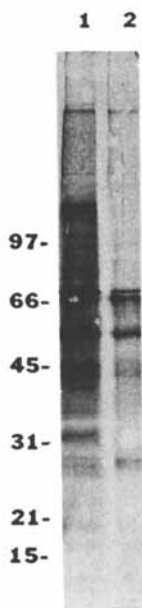


Figure 1. Electrophoretic profiles of glucan synthase fractions purified from red beet. Proteins were transferred to nitrocellulose and stained by colloidal gold followed by silver overlay. Lane 1, solubilized enzyme (CSGS); Lane 2, reconstituted glucan synthase (RCGS).

Table I. Immunoprecipitation of CHAPS-Solubilized Glucan Synthase <sup>1</sup>

Sera	Activity (nmol/min/ml)	Percent Retained
Preimmune	3.5	100.0
Reconstituted	0.9	26.3

<sup>1</sup> Equal volumes of antigen and sera were combined in 0.85% (w/v) NaCl. Each mixture was incubated on ice for 7 hr. Protein A agarose was added followed by an additional 1 hr incubation on ice. Protein A was pelleted by centrifugation and the supernatants assayed for activity.

Immunoblots showed that antibodies were produced against many of the bands present in both preparations. The important question remains whether antibodies for specific bands can be obtained and used to immunoprecipitate the enzyme. We are pursuing this question further by isolating specific antibodies by affinity purification (17, 18) and by generating antibodies to specific subunits excised from gels. The antibodies will be raised against both native and deglycosylated forms of these antigens (19, 20).

*Affinity Labeling with UDP-pyridoxal.* Read and Delmer (21) utilized the substrate analog UDP-pyridoxal to inhibit mung bean glucan synthase. This affinity label inhibited glucan synthase at micromolar levels and inhibition was protected against with UDP-glucose. A 42 kD polypeptide could be labelled with [<sup>3</sup>H]UDP-pyridoxal.

Table II shows that UDP-pyridoxal had a similar inhibitory effect on red beet glucan synthase. It inhibited activity at much lower concentrations than other covalent modification reagents, such as N-ethylmaleimide (cysteine), phenylglyoxal (arginine) and formaldehyde (lysine). UDP-pyridoxal had an I<sub>50</sub> that is 62-fold lower than formaldehyde.

Table II. Chemical Modification of CHAPS Solubilized Glucan Synthase

Inhibitor	I <sub>50</sub> (μM)
Phenylglyoxal	2,000
n-Ethylmaleimide	1,600
Formaldehyde	250
UDP Pyridoxal	4.5

The chemistry of UDP-pyridoxal binding was consistent with the pattern observed in mung bean. Table III shows that inactivation was Ca<sup>2+</sup>-dependent and did not occur when the aldehyde group was reduced. In addition, inactivation was protected against by UDPG (Table III). Thus, it appears that UDP-pyridoxal is targeted towards a lysine located at the

Table III. Inhibition of Plasma Membrane Glucan Synthase by UDP-pyridoxal

Preincubation Conditions	Spec. Act. (nmol/min/mg)	Activity Remaining (%)
No Inhibitors (Control)	119	100
UDP-pyridoxine, Mg <sup>2+</sup> , Ca <sup>2+</sup>	115	97
UDP-pyridoxal, Mg <sup>2+</sup> , Ca <sup>2+</sup>	16	14
UDP-pyridoxal, Mg <sup>2+</sup> , EGTA	70	59
UDP-pyridoxal, EDTA	98	82
UDP-pyridoxal, UDPG, Mg <sup>2+</sup> , Ca <sup>2+</sup>	127	107

active site. Experiments to determine which polypeptides in CSGS and RCGS label with UDP-[<sup>3</sup>H]-pyridoxal are underway.

*Phosphorylation Studies.* It is becoming increasingly evident that phosphorylation is an important mechanism for the regulation of membrane-bound plant enzymes (22, 23). A recent report offered evidence that glucan synthase I from corn coleoptile was stimulated by phosphorylation (24). Preliminary experiments with beet suggested that the phosphorylation state may modulate glucan synthase activity; however, the extent to which this occurs needs to be clarified. In the presence of protein kinase and ATP, activity was reduced in membranes and solubilized fractions. ATP alone was slightly inhibitory in microsomes, suggesting the presence of endogenous protein kinase activity which was known previously to be present in beet membranes (25).

Figure 3 shows an autoradiogram of CSGS and RCGS after phosphorylation with [ $\gamma$ -<sup>32</sup>P]-ATP in the presence and absence of protein kinase. With CSGS subunits of 92, 54 and 38 kD became phosphorylated. The 62 kD band is protein kinase, which is self-phosphorylating. Since phosphorylation occurred in the absence of kinase, CSGS appeared to contain an endogenous kinase activity. This kinase was probably that described by Bidwai and Takemoto (25). In the RCGS fraction the 54 kD band was preferentially phosphorylated, paralleling the enrichment seen on the SDS gel (Fig. 1). Phosphorylation in RCGS fractions without exogenous kinase was weak. Endogenous kinase activity was completely removed along with other contaminants during the reconstitution step.

### Concluding Remarks

Development of the CHAPS-based solubilization and reconstitution procedure has provided fractions of glucan synthase that are significantly more purified than the membrane-bound forms. Although homogeneous preparations of glucan synthase are not yet available, it was of sufficient purity to probe subunit composition. The current data point suggestively to a 54 kD polypeptide as being a catalytic or regulatory subunit of the enzyme complex. It was enriched in RCGS and may be regulated by phos-

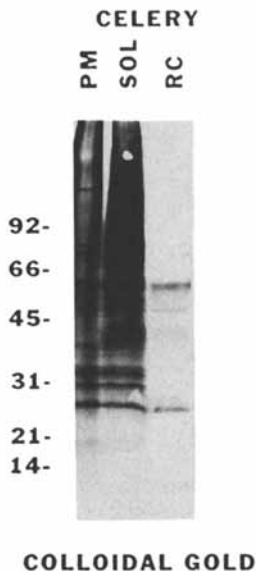


Figure 2. Electrophoretic profiles of glucan synthase fractions purified from celery. Proteins were transferred to nitrocellulose and stained by colloidal gold. Symbols: PM, plasma membranes; SOL, CHAPS-solubilized; RC, reconstituted glucan synthase preparations. Plasma membranes were isolated by two-phase partitioning. Specific activities of the three membrane preparations were 398, 1355, and 626 nmol/min/mg, respectively. The low specific activity of RC relative to SOL may be a reflection of enzyme instability following the gel filtration step.

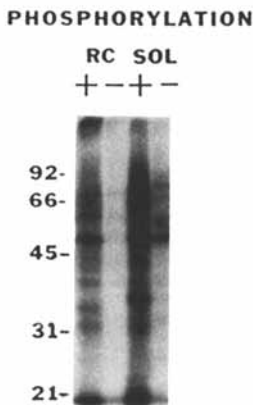


Figure 3. Autoradiograph of phosphorylated polypeptides. RCGS and CSGS were incubated with  $[\gamma\text{-}^{32}\text{P}]\text{-ATP}$  in the presence (+) and absence (-) of protein kinase as described in Materials and Methods.

phorylation. Caution must be exercised in interpreting these results. On one-dimensional gels, several polypeptides may migrate close together at 54 kD. Two-dimensional gels must be run to be certain that phosphorylation,  $\text{Ca}^{2+}$ -binding and affinity label-binding sites reside on the same polypeptide. Other subunits such as the 68 kD polypeptide were present in RCGS preparations and cannot be ruled out as functional subunits. Work is continuing on the development of additional probes such as antibodies and photoaffinity labels. Confirming the subunit composition of the  $\beta$ -(1,3)-glucan synthase should enable development of genetic probes and hopefully provide cogent answers to some of the many longstanding questions surrounding the enzymatic mechanism of callose and cellulose biosynthesis.

### Acknowledgments

This research was supported in part by grants from the U.S. Department of Agriculture (87-CRCR-1-2414), the Charles and Johanna Busch Foundation, and the New Jersey Agricultural Experiment Station with State and Hatch Act funds. New Jersey Agricultural Experiment Station, Publication No. F-10546-1-88. We thank Mrs. Marianne Bianco for assisting with manuscript preparation.

### Literature Cited

1. Delmer, D. P. *Ann. Rev. Plant Physiol.* 1987, **38**, 259-90.
2. Wasserman, B. P.; Eiberger, L. L.; McCarthy, K. J. *Food Technol.* 1986, **40**, 90-98.
3. Wasserman, B. P.; Sloan, M. E. In *Biosynthesis and Biodegradation of Cellulose and Cellulosic Materials*; Weimer, P.; Haigler, C., Eds.; Marcel Dekker: New York, 1988; in press.
4. Sloan, M. E.; Rodis, P.; Wasserman, B. P. *Plant Physiol.* 1987, **85**, 516-522.
5. Eiberger, L. L.; Wasserman, B. P. *Plant Physiol.* 1987, **83**, 982-987.
6. Hayashi, T.; Read, S. M.; Bussell, J.; Thelen, M.; Lin, F.-C.; Brown, R. M.; Delmer, D. P. *Plant Physiol.* 1987, **83**, 1054-1062.
7. Kauss, H.; Jeblick, E. *Plant Sci.* 1987, **48**, 63-69.
8. Eiberger, L. L.; Ventola, C. L.; Wasserman, B. P. *Plant Sci. Lett.* 1985, **37**, 195-198.
9. Wasserman, B. P.; Frost, D. J.; Lawson, S. G.; Mason, T. L.; Rodis, P.; Sabin, R. D.; Sloan, M. E. In *Mod. Meth. Pl. Anal.*; Linskens, H. F.; Jackson, J. F., Eds.; Springer: Berlin, 1989; in press.
10. Yoshida, S.; Uemura, M.; Niki, T.; Sakai, A.; Gusta, L. V. *Plant Physiol.* 1983, **72**, 105-144.
11. Laemmli, U. K. *Nature* 1970, **227**, 680-685.
12. Porzio, M. A.; Pearson, A. M. *Biochim. Biophys. Acta* 1976, **490**, 27-34.
13. Towbin, H.; Staehelin, T.; Gordon, J. *Proc. Natl. Acad. Sci.* 1979, **76**, 4350-4354.

14. Moeremans, M.; Daneels, G.; De Mey, J. *Anal. Biochem.* 1985, **145**, 315-321.
15. Tagaya, M.; Nakamo, K.; Fukui, T. *J. Biol. Chem.* **260**, 6670-6676.
16. Delmer, D. P. *J. Appl. Polym. Sci. Symp.* 1989, in press.
17. Olmsted, J. B. *J. Biol. Chem.* 1981, **256**, 11955-11957.
18. Mishkind, M. L.; Plumley, F. G.; Raikheil, N. V. In *Handbook of Plant Cytochemistry*; Vaughn, K. C., Ed.; CRC Press: Boca Raton, FL, 1987; Vol. 2, p. 65.
19. Desai, N. N.; Allen, A. K.; Neuberger, A. *Biochem. J.* 1983, **211**, 273-276.
20. Sojar, H. T.; Bahl, O. P. *Arch. Biochem. Biophys.* 1987, **259**, 52-57.
21. Read, S. M.; Delmer, D. P. *Plant Physiol.* 1987, **85**, 1008-1015.
22. Ranjeva, R.; Boudet, A. M. *Ann. Rev. Plant Physiol.* 1987, **38**, 73-93.
23. Poovaiah, B. W.; Reddy, A. S. N. *CRC Crit. Rev. Plant Sci.* 1987, **6**, 47-103.
24. Paliyath, G.; Poovaiah, B. W. *Plant Cell Physiol.* 1988, **29**, 67-73.
25. Bidwai, A. P.; Takemoto, J. Y. *Proc. Natl. Acad. Sci.* 1987, **84**, 6755-6759.

RECEIVED March 10, 1989

## Chapter 19

# Biogenesis of Cellulose Microfibrils and the Role of Microtubules in Green Algae

Takao Itoh

Wood Research Institute, Kyoto University, Uji, Kyoto 611, Japan

This chapter reviews our knowledge of factors controlling cellulose deposition in green algae. Firstly, the types of cellulose synthesizing particle complexes in green algae are discussed. Secondly, new evidence on the orientation of microtubules in selected giant marine algae and their relationship to the orientation of cellulose microfibrils is presented. Based on this information, a mechanism for the assembly of cellulose microfibrils in giant marine algae is proposed.

Our current understanding of cellulose microfibril biogenesis and assembly comes from (a) freeze-fracture studies of the plasma membrane of cells actively producing cellulose microfibrils; (b) observations of microtubules by immunofluorescence microscopy; (c) direct imaging of cellulose microfibrils (1-5); and (d) *in vitro* synthesis of cellulose using bacterial cell membrane preparations (6). This chapter examines recent progress in freeze-fracture and immunofluorescence studies on the biogenesis of cellulose microfibrils, as well as addressing the role of microtubules in several green algae.

For the last decade, much of our knowledge of the structure and function of cellulose forming enzyme complexes (so-called Terminal Complexes or TC's) has been based on results obtained from freeze-fracture studies. The main discoveries from these studies were (a) the existence of linear TC's by Brown and Montezinos (7) in *Oocystis apiculata*, and (b) the occurrence of rosette TC's by Giddings *et al.* (8) in *Micrasterias denticulata*. As will be discussed later, the occurrence of these two types of cellulose synthesizing complexes has some evolutionary significance as regards current phylogenetic relationships within the plant kingdom. This is because all land plants, including higher plants, mosses and ferns, have rosettes (9-11), whereas some algae have linear TC's and others do not. It has been

0097-6156/89/0399-0257\$06.00/0

© 1989 American Chemical Society



proposed that the TC's move on the fluid plasma membrane by forces generated during crystallization of cellulose microfibrils (12,13). In green algae, the newly synthesized microfibrils first have a random orientation during the synthesis of the primary wall and then an ordered orientation during secondary wall formation. It is thus conceivable that the factors controlling the orientation of TC's in green algae may also be responsible for the orientation of microfibrils; this could be achieved, for example, by channelling cytoplasmic microtubules. This view is presented because in higher plants, and some algal cells, rosette particles are apparently channelled by cytoplasmic microtubules which run parallel to one another (14-16). However, as a counter to this argument, some green algae have linear TC's which do not appear to have microfibrillar orientation controlled by microtubules during secondary wall synthesis (17). This evidence suggests therefore that there may be different mechanisms controlling microfibrillar orientation between higher and lower plants.

### Structure of TC's in Green Algae

The green algae include both Chlorophyta and Charophyta. The TC's of Chlorophyta have been observed in four orders of Chlorellales, Cladophorales, Siphonocladales, and Zygnematales, and those of Charophyta in one order of Charales (Table I). Recent investigations show that 17 genera and 23 species out of three orders of Chlorellales, Cladophorales and Siphonocladales all have linear TC's, as shown in Table I. While linear TC's have been observed in some freshwater algae such as *Oocystis* (7,18), *Eremosphaera* (19), and *Glaucocystis* (20) species, most are found in marine-type algae such as *Boergesenia* (21,22), *Boodlea* (Fig. 1) (23,24), *Dictyosphaeria* (Fig. 2), *Ernodesmis* (Fig. 3), *Microdictyon* (19), *Siphonocladus* (Fig. 4), *Struvea* (Fig. 5), *Valonia* (Fig. 6) (17,24,25), *Valoniopsis* (Fig. 7), and *Chaetomorpha* (Fig. 8) (19,25) species; these eight genera belong to the Siphonocladales. Although Chlorellales, Cladophorales and Siphonocladales have linear TC's, there are significant differences in their locations; that is, Chlorellales have TC's only on the E-fracture face, while both Cladophorales and Siphonocladales have TC's on both E- and P-fracture faces, thereby making transmembrane particles.

Additionally, the TC structure of Zygnematales is quite different from those of the other three orders in Chlorophyta. Four genera of the Zygnematales, including *Closterium* (16,26), *Micrasterias* (8,27,28), *Mougeotia* (29), and *Spirogyra* (19,30) species have been investigated so far. All have rosettes only on the P-fracture face. The cells can have either random and/or unidirectional rosette distributions during active synthesis of the primary wall, and hexagonal arrays during the synthesis of the secondary wall.

More recently, rosettes have been observed in *Chara* sp. (31) and *Nitella translucens* (32), which belong to another subdivision, Charophyta. The rosettes in this species occur separately without making any polygonal arrays as found in Zygnematales. This suggests that Charales are closer to vascular plants than the other algae, if plant phylogenetic classifications

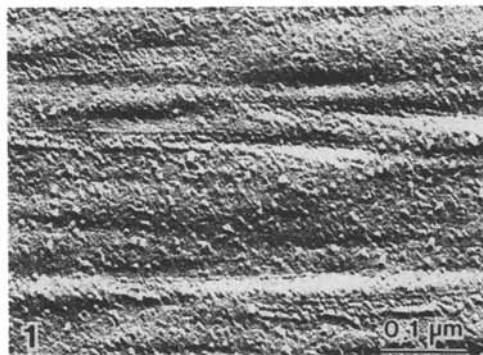


Figure 1. TC's of *Boodlea composita* on P-fracture face.

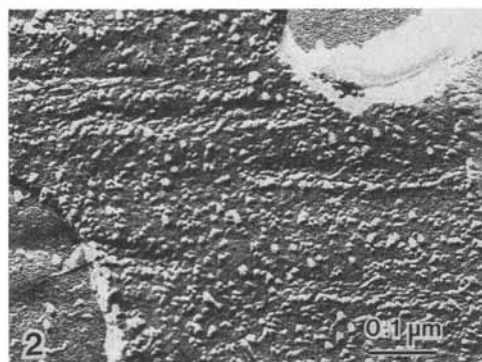


Figure 2. TC's of *Dictyosphaeria cavernosa* on P-fracture face.

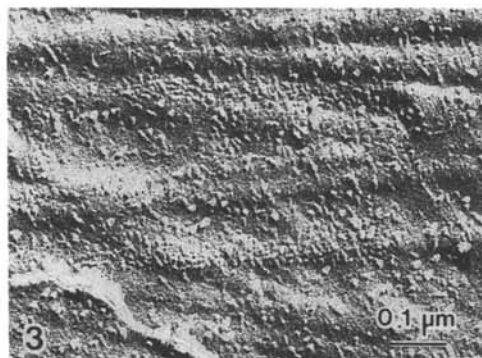


Figure 3. TC's of *Ernodesmis verticillata* on E-fracture face.

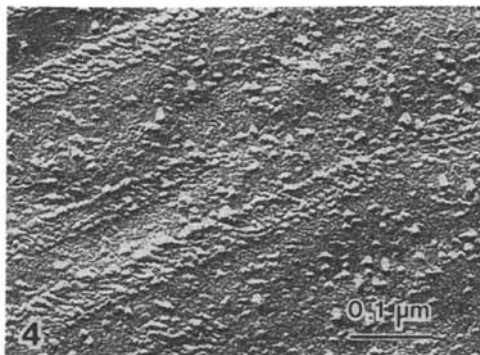


Figure 4. TC's of *Siphonocladus tropicus* on P-fracture face.

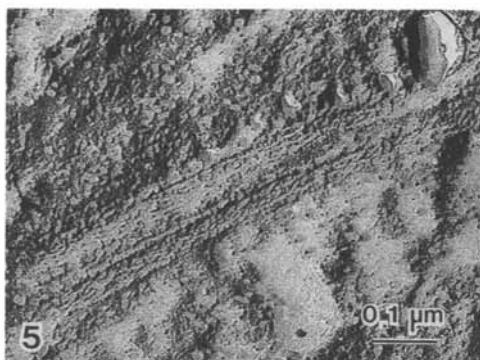


Figure 5. TC's of *Struvea elegans* on P-fracture face.

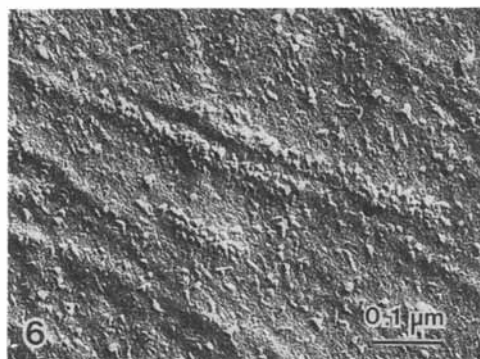


Figure 6. TC's of *Valonia ventricosa* on E-fracture face.

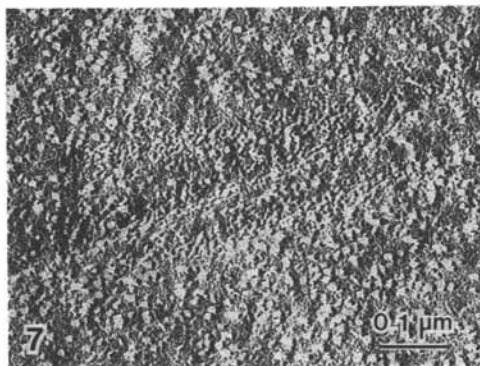


Figure 7. TC's of *Valoniopsis pachynema* on P-fracture face.

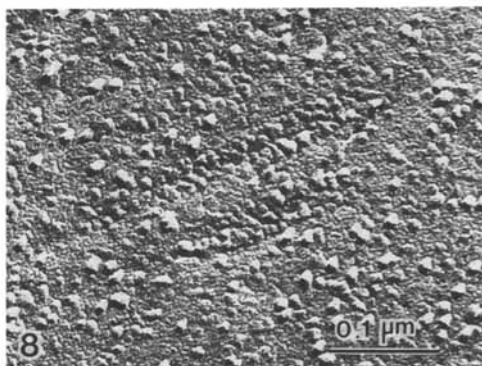


Figure 8. TC's of *Chaetomorpha auricoma* on P-fracture face.

Table I. Current Summary of the Structure and Location of TCs among Green Algae

Subdivision, Order, Species	TC Structure	TC Location	Reference
Chlorophyta			
Chlorellales			
<i>Eremosphaera</i> sp.	Linear TC	EF only	19
<i>Glaucocystis nostochinearum</i>	Linear TC	EF only	20
<i>Oocystis apiculata</i>	Linear TC	EF only	7
<i>Oocystis solitaria</i>	Linear TC	EF only	18
Cladophorales			
<i>Chaetomorpha</i> sp.	Linear TC	EF & PF	19
<i>Chaetomorpha aerea</i>	Linear TC	EF & PF	24
<i>Chaetomorpha moniligera</i>	Linear TC	EF & PF	25
Siphonocladales			
<i>Boergesenia forbesii</i>	Linear TC	EF & PF	21,22
<i>Boodlea coacta</i>	Linear TC	EF & PF	23
<i>Boodlea composita</i>	Linear TC	EF & PF	24
<i>Dictyosphaeria cavernosa</i>	Linear TC	EF & PF	This chapter
<i>Ernodesmis verticillata</i>	Linear TC	EF & PF	This chapter
<i>Siphonocladus tropicus</i>	Linear TC	EF & PF	This chapter
<i>Struvea elegans</i>	Linear TC	EF & PF	This chapter
<i>Valonia macrophysa</i>	Linear TC	EF & PF	17
<i>Valonia ventricosa</i>	Linear TC	EF & PF	24,25
<i>Valonia ventricosa</i>	Linear TC	EF & PF	This chapter
Zygnematales			
<i>Closterium acerosum</i>	Rosettes	PF only	26
<i>Closterium</i> sp.	Rosettes	PF only	16
<i>Micrasterias cruzmelitensis</i>	Rosettes	PF only	28
<i>Micrasterias denticulata</i>	Rosettes	PF only	27,8
<i>Mougeotia</i> sp.	Rosettes	PF only	29
<i>Spirogyra</i> sp.	Rosettes	PF only	30,19
Charophyta			
Charales			
<i>Chara</i> sp.	Rosettes	PF only	31
<i>Nitella translucens</i>	Rosettes	PF only	32

can be made based upon cellulose synthesizing complexes. It could thus be argued from these data that the evolution of TC's will follow the lines envisaged in Fig. 9, which is a modification of a scheme proposed by Herth (11) for the hypothetical evolutionary lines of putative cellulose synthesizing complexes. Basically, this stems from the fact that both rosettes and linear TC's are composed of common particle subunits similar in size; rosettes consist of six particles, each having an 8 nm diameter of (8) and linear TC's consists of three rows with an average dimension of ca. 8 nm for each individual particle (25). However, TC's have only been found in a limited

number of species among the algae. Consequently, a further survey of TC's is necessary to develop a detailed phylogenic hypothesis.

TC's normally occur at the end of microfibril imprints on either E- or P-fracture faces of the plasma membrane. Each imprint does not necessarily correspond to a single microfibril, but often to bundles of them. During the deposition of random microfibrils of the primary wall, the imprints run along the plasma membrane, and often with curved trails. On the other hand, when ordered microfibrils of the secondary wall are synthesized, the imprints run straight and parallel to one another. In *Oocystis* species, each paired TC runs in an opposite direction (31). In most giant marine algae, some TC's appear to run in one direction, while others run in the opposite direction during the synthesis of ordered microfibrils. The latter case is illustrated in Figure 10 which shows the E-fracture face of newly formed cellulose microfibrils of ordered orientation. The TC numbered "1" is moving to the right whereas the TC numbered "2" is moving to the left. Clearly, if the individual TC synthesizes unidirectional glucan chains of  $\beta$ -1,4 linkages, the cell wall should have an anti-parallel glucan chain orientation.

### Development of Linear TC's in Selected Green Algae

The length of linear TC's is variable and depends on the developmental phase of cell growth. This was determined following wounding of the mother cells of *B. forbesii*, where the aplanospores were regenerated within 1.5 h, and the primary and the secondary walls were synthesized 2 to 4h and 4 to 5h after wounding, respectively (33). Figure 11 shows the effect of time on TC length following aplanospore induction in *Boergesenia forbesii*. As can be seen, the TC length increases only during formation of the primary wall; no further increase occurs after deposition of the secondary wall. However, when we look closer at the freeze-fracture replica of the aplanospores in *B. forbesii* just before, or at the time of, synthesis of cellulose microfibrils, many nascent TC's can be observed on the P-fracture face of the plasma membrane (Fig. 12). The smallest TC observed had only 10 particles. Most nascent TC's did not show a directional arrangement of particles, while some had already organized an elongated cluster (double arrows in Fig. 12). The mean length of the TC's in this phase was 114 nm. The nascent TC's increased in length during the synthesis of the primary wall, until the ordered microfibrils were assembled. The length of nascent TC's contrasted with that of fully elongated TC's, which had a maximum length of ca. 1  $\mu$ m (mean length: 665 nm) in 20h cells of *B. forbesii* (Fig. 13).

### Orientation of Cortical Microtubules

The cellulose synthesizing enzyme complexes in green algae can be divided into rosettes and linear TC's; the latter increases in size during circumferential expansion of the cells. The movement of both growing and mature TC's in the plasma membrane is controlled by forces generated by crystallization of microfibrils, leaving the highly crystalline microfibrils in their wake (7,34).

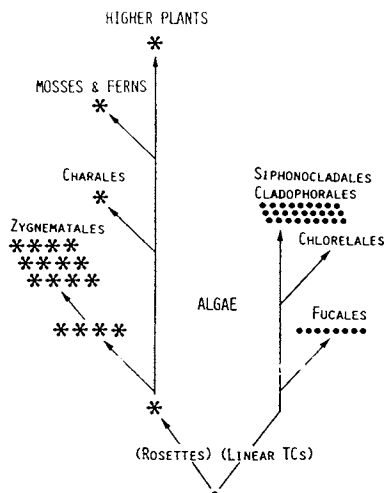


Figure 9. Hypothetical illustration for evolutionary trend of putative cellulose synthesizing enzyme complexes from algae to higher plants. Both rosettes and linear TC's originate from their common subunit of 8 nm particle. Asterisk (\*) represents a rosette.

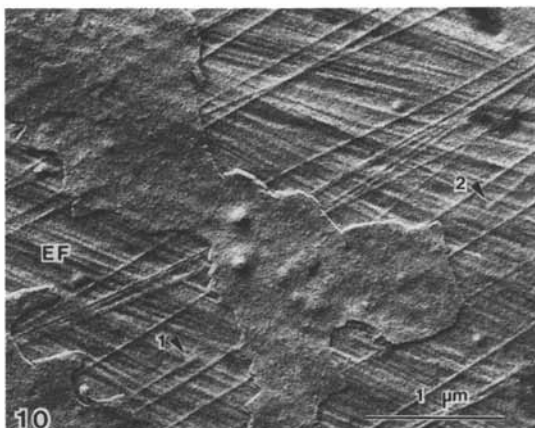


Figure 10. E-fracture face of the plasma membrane during active synthesis of ordered microfibrils in secondary wall of *Valonia macrophysa*. Imprints of microfibrils run parallel to one another. TC's numbered "1" and "2" direct opposite ways to one another.

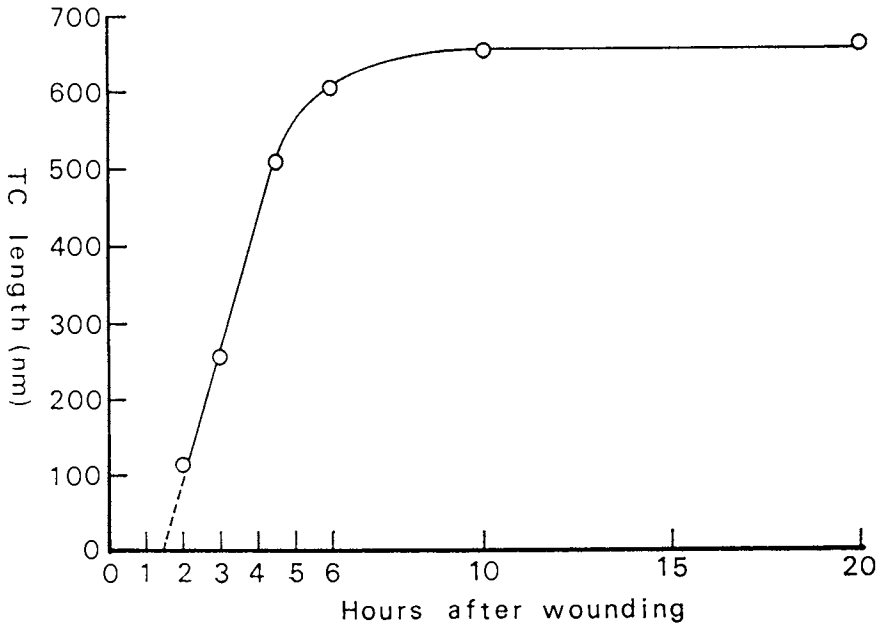


Figure 11. Time course of TC length in the aplanospores of *Boergesenia forbesii*.



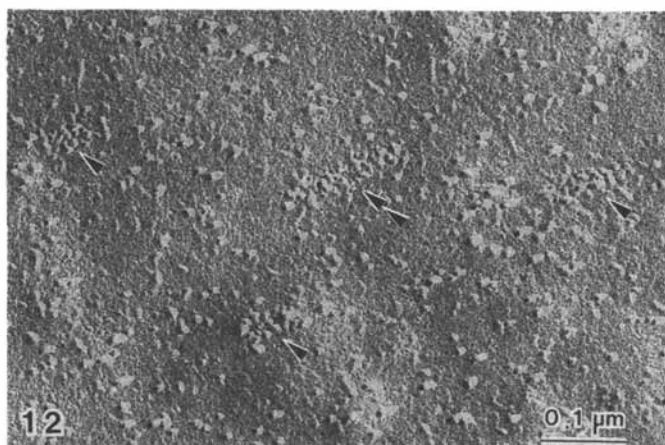


Figure 12. Four nascent TC's (arrowheads) are shown on P-fracture face of the plasma membrane in 2h aplanospore of *Boerghesia forbesii* after wounding.

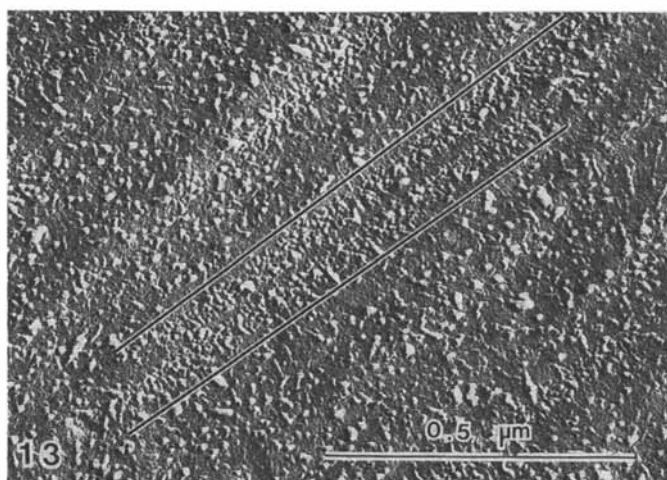


Figure 13. Two fully elongated TC's (ca. 1  $\mu$ m) are shown on P-fracture face of the plasma membrane in 20h cell of *Boerghesia forbesii*.

Since the mature walls of *Valonia* and *Boergesenia* have a crossed lamellate structure (17,35-37), the direction of TC movement must be controlled in some unknown manner. On the other hand, giant marine algae, which also have linear TC's, but of apparently random orientation, only synthesize microfibrils of random orientation on the innermost face of the plasma membrane during the synthesis of the primary wall. It was, therefore, timely to examine whether cortical microtubules were responsible for orientation of microfibrils, since recent investigations suggested that the direction of microfibril deposition in higher plant cells (38-40) and some algae (*Oocystis* and *Micrasterias* (8,16,33)), was controlled by cortical microtubules. However, in the alga *Closterium*, microtubules functioned only to limit cellulose synthesis to a localized region (41). Additionally, freeze-fracture studies suggested that newly synthesized microfibrils in the spherical cells of the giant marine algae *Valonia macrophysa* were not parallel to the underlying microtubules (17). In the light of these contradictory findings, the role of microtubular orientation in cellulose microfibrillar orientation among green algae was re-examined using immunofluorescence microscopy. Lloyd *et al.* (43) first used this technique to observe cortical microtubules, following the pioneering work on plant cells by Franke (42). Since then, it has been used many times to show microtubule orientation over whole cells (44).

The materials used for the immunofluorescent staining were aplanospores of *B. forbesii* and *V. ventricosa*, where cellulose microfibril orientation could easily be shown by staining with the fluorescent brightening agents Calcofluor and Tinopal LPW (34). As mentioned in the previous section, *Boergesenia* aplanospores synthesized random microfibrils between 2 and 4h after wounding of mother cells and ordered microfibrils after 4h. The *Boergesenia* aplanospores in which spheration had just been completed showed randomly oriented microtubules just under the plasma membrane (Fig. 14), and the aplanospores in 3h post-wounding did not differ from those at 1.5h. (Fig. 15). However, after 6h post-wounding, during which time the normally synthesized ordered microfibrils were deposited, only randomly oriented microtubules were observed under the thickened cell wall (Fig. 16). At a later phase of cell wall regeneration, immunofluorescent staining of microtubules by antigen-antibody reactions became more difficult because of the thickened wall surrounding the aplanospores. Nevertheless, we managed to observe the arrangement of microtubules even after 8, 10, and 20h post-wounding without having to resort to enzymatic cell wall digestion. In all cases, only random microtubular orientation patterns (Figs. 17, 18 and 19) were observed.

However, after successive culture of the spherical aplanospores for more than five days, germination occurred with a typical tip growth to make rhizoids (45); the orientation of microfibrils in a single elongating rhizoid of 10 days post-wounding, for example, has been described recently (13). In our study, the innermost wall lamellae in the rhizoid showed three different orientations of microfibrils, i.e., transverse, oblique, and longitudinal to the growing cell axis. Following immunofluorescent staining of the microtubules

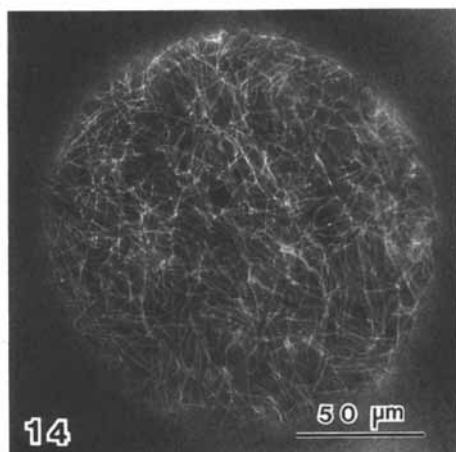


Figure 14. Immunofluorescence micrograph of microtubule orientation during cell regeneration in *Boergesenia forbesii* 1.5 h after wounding.

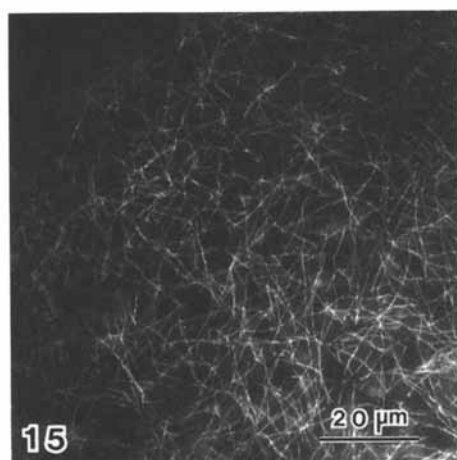


Figure 15. Immunofluorescence micrograph of microtubule orientation during cell regeneration in *Boergesenia forbesii* 3 h after wounding.

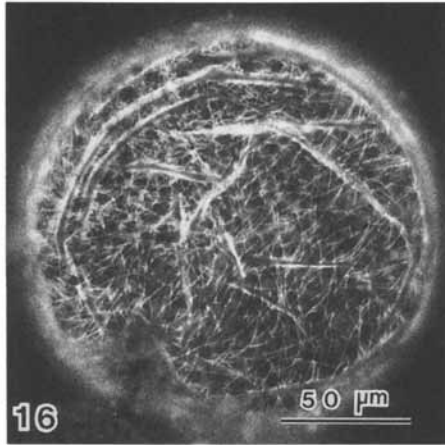


Figure 16. Immunofluorescence micrograph of microtubule orientation during cell regeneration in *Boergesenia forbesii* 6 h after wounding.

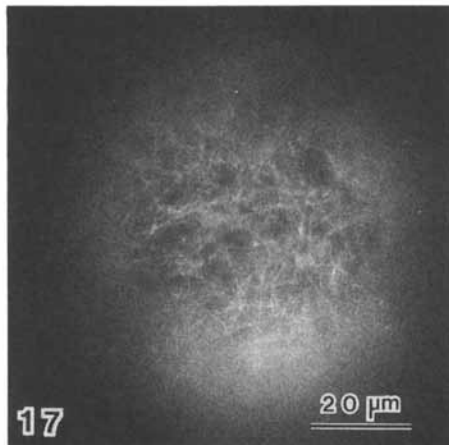


Figure 17. Immunofluorescence micrograph of microtubule orientation during cell regeneration in *Boergesenia forbesii* 8 h after wounding.

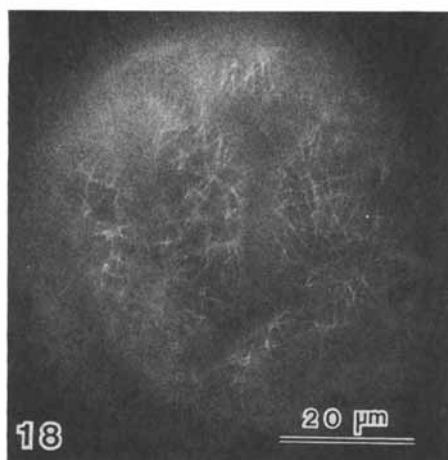


Figure 18. Immunofluorescence micrograph of microtubule orientation during cell regeneration in *Boergesenia forbesii* 10 h after wounding.

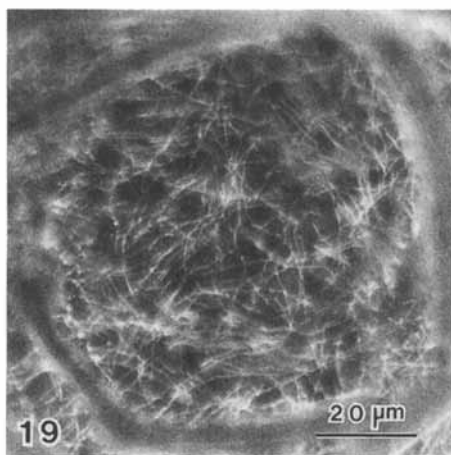


Figure 19. Immunofluorescence micrograph of microtubule orientation during cell regeneration in *Boergesenia forbesii* 20 h after wounding.

by the fluorescein isothiocyanate-conjugated antibody, an elongating rhizoid of 8 days post-wounding showed ordered microtubules oriented longitudinally to the growing cell axis, as well as parallel to one another (Fig. 20). It is noteworthy that longitudinal microtubules were also observed in the root hairs of some higher plants which show tip growth (46-48).

In the case of *V. ventricosa*, spheration was completed within 2h of wounding, following which random microfibrils were regenerated between 5 and 12h and ordered microfibrils within 12 to 15h. The time course of microtubule orientation in the aplanospores of *V. ventricosa* followed a trend similar to that observed for *B. forbesii*; that is, microtubules were always oriented randomly during the synthesis of both random and ordered microfibrils. It is worth noting the structural changes of microtubules in the early phase of cell regeneration; the aplanospores produced from *V. ventricosa* within 2 and 3h of post-wounding did not show cortical microtubules but instead perinuclear microtubule arrays (Fig. 21), and the aplanospores after 4h showed the initiation of wall microtubules (Fig. 22). Figures 23a and 23b show 3h aplanospores of actively synthesizing primary wall points. Both figures were taken from the same cell with different focusing. Figure 23a was focused on the nucleus; note that several microtubules radiate from the nucleus. Figure 23b was focused on the cortical microtubules, where some of the perinuclear microtubules appeared as part of the cortical microtubules. This evidence suggests that the nuclei may play a role as microtubule organizing centers (MTOC) during the regeneration of the cell wall in these green algae.

### Summary: Microtubule-Independent Control of Microfibril Orientation

From our immunofluorescence experiments, we have concluded that (1) only a random microtubular orientation occurs during regeneration of primary and secondary walls and (2) the growing rhizoids during tip growth only showed microtubules oriented longitudinally to the growing cell wall axis. However, since three different orientations of microfibrils in the innermost lamellae of the cell wall were observed, these findings suggest that the direction of movement of linear TC's was not controlled by cortical microtubules, at least not in the case of the two giant marine algae, *Boergesenia* and *Valonia*, studied.

LaClaire (49) recently described a highly ordered array of parallel and longitudinal microtubules in the coenocytic green algae *Ernodesmis verticillata*. However, with other filamentous green algae, *Boodlea coacta* (50) and *Chaetomorpha moniligera* (51), aligned microtubules and microfibrils were not always observed. It was thus suggested that microfibril orientation in Siphonocladales and probably Cladophorales may be independent of cytoplasmic microtubule orientation.

Once TC's are initiated in the plasma membrane, they distribute randomly with each TC running straight ahead. More recent investigations showed that the density of TC's was more or less constant (52), indicating that the number of TC's did not increase appreciably during primary wall

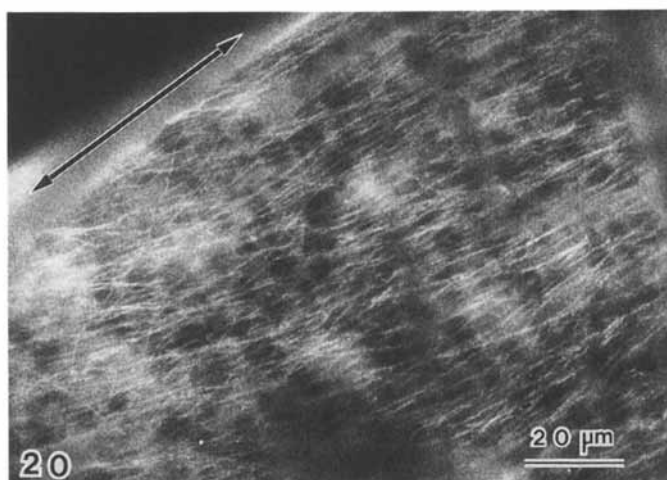


Figure 20. Immunofluorescence micrograph of microtubule orientation in 8 day old cells of *Boergesenia forbesii*. Highly ordered microtubules are oriented longitudinally to the cell axis (double-headed arrow).



Figure 21. Immunofluorescence micrograph of perinuclear microtubules in the aplanospore of 3h post-wounding of *Valonia ventricosa*.

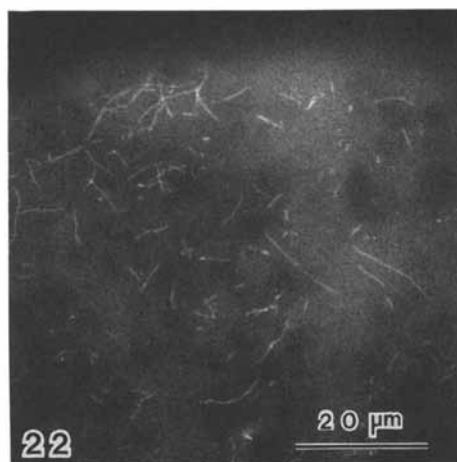


Figure 22. Immunofluorescence micrograph of cortical microtubules in the aplanospore of 4h post-wounding of *Valonia ventricosa*.

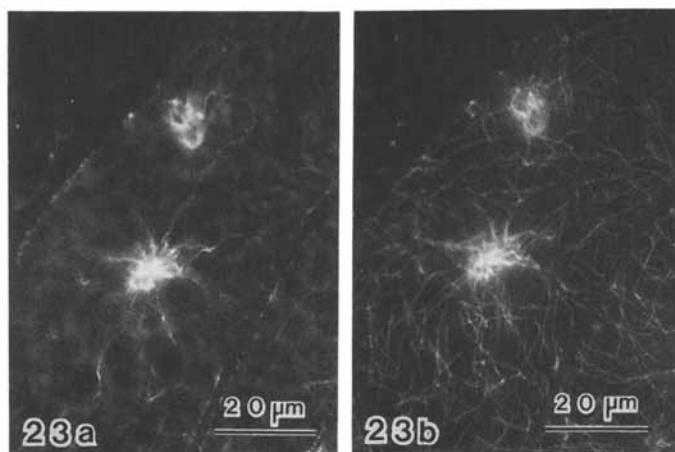


Figure 23. Immunofluorescence micrographs in the aplanospore of 3h post-wounding of *Boergesenia forbesii*. Figure 23a is focused on the perinuclear microtubules, while Figure 23b is focused on the cortical microtubules which are oriented randomly.



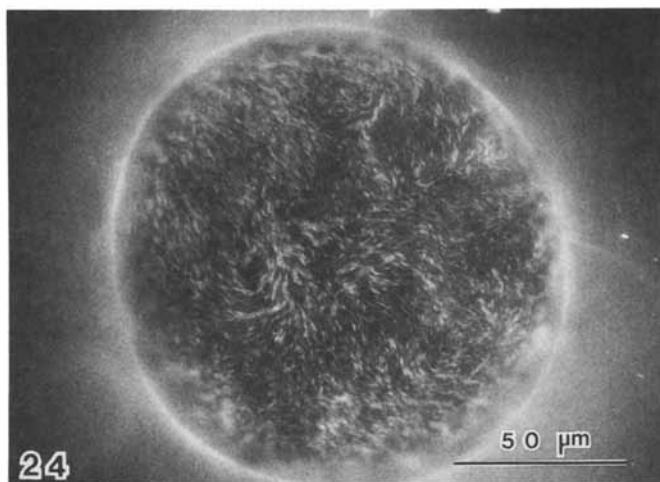


Figure 24. Orientation of microfibrils is shown in 4h aplanospore of *Boergeria forbesii*, stained with fluorescent brightening agent Tinopal LPW.

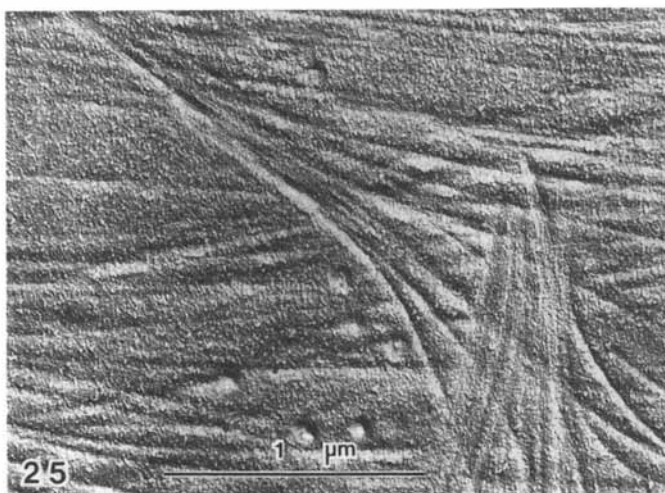


Figure 25. Freeze fractured replica. P-fracture face of the plasma membrane in 15h aplanospore of *Valonia ventricosa*. The clustered TC's are shown, suggesting the build-up of new axis for microfibril orientation.

synthesis, even though a high density of TC's was often localized in some areas of the plasma membrane. Figure 24 shows the orientation of microfibrils in aplanospores of *B. forbesii* 4h after wounding, and stained with the fluorescent brightening agent Tinopal LPW. In some areas, short striations of fluorescence merged into a center, suggesting a shift of microfibril orientation, probably by localized membrane flow. TC localization can often be observed in the transition from primary to secondary wall formation. Figure 25 is taken from such a phase in the aplanospore of *V. ventricosa*, and may correspond to an area in which clusters of TC's occur and move in a direction different from the former orientation of microfibrils. Linear TC's in giant marine algae may be stable, because (a) the TC's do not disappear following treatment with cycloheximide, a protein synthesis inhibitor (34), and (b) glutaraldehyde treatment in advance of freeze fracture did not destroy the TC's (unpublished data). Thus, linear TC's in giant marine algae may be involved in the synthesis of ordered microfibrils with much longer lifetimes than the rosettes (53).

Recently, more evidence for helicoidal arrangement of cellulose microfibrils has been reported for a variety of plant cells (54,55). In *Nitella*, the helicoidal orientation of cellulose microfibrils was shown to arise by a mechanism similar to self-assembly of a cholesteric liquid crystal (56). The control of microfibril orientation was primarily at the interface between the plasma membrane and the innermost lamellae of the newly formed wall. The helicoidal wall, characterized by a successive change of cellulose microfibrils, was supposed to be synthesized in the innermost surface of the new wall layer. If this is true, then the involvement of microtubules in higher plant cells is much less probable than previously believed. The self-assembly of cellulose microfibrils is related to those cells which have such a pattern of cell wall that show arced orientation of microfibrils in a transverse section (56). Both aplanospores and thallus cells of *B. forbesii* have an arced pattern of cellulose microfibrils. However, we showed that the microfibril orientation in both spherical cells and elongating rhizoids was independent of the orientation of microtubules. While this evidence does not contradict the self-assembly mechanism in helicoidal walls of green algae, both hypotheses need additional experimental verification.

### Acknowledgments

The author thanks Dr. R. Malcolm Brown, Jr., at the University of Texas at Austin, Texas, for the present part of the present study.

### Literature Cited

1. Sugiyama, J.; Harada, H.; Fujiyoshi, Y.; Uyeda, N. *Mokuzai Gakkaishi* 1984, **30**, 98-99.
2. Sugiyama, J.; Harada, H.; Fujiyoshi, Y.; Uyeda, N. *Mokuzai Gakkaishi* 1985, **31**, 61-67.
3. Sugiyama, J.; Harada, H.; Fujiyoshi, Y.; Uyeda, N. *Planta* 1985, **166**, 161-68.

4. Kuga, S.; Brown, R. M., Jr. *J. Electron Microscop. Tech.* 1987, **6**, 349-56.
5. Kuga, S.; Brown, R. M., Jr. *Polym. Commun.* 1987, **28**, 311-14.
6. Lin, F. C.; Cooper, J.; Delmer, D. P. *Science* 1985, **230**, 822-25.
7. Brown, R. M., Jr.; Montezinos, D. *Proc. Natl. Acad. Sci. USA* 1976, **73**, 143-47.
8. Giddings, T. H., Jr.; Brower, D. L.; Staehelin, L. A. *J. Cell Biol.* 1980, **84**, 327-39.
9. Wada, M.; Staehelin, L. A. *Planta* 1981, **151**, 462-68.
10. Reiss, H. *Planta* 1984, **160**, 428-35.
11. Herth, W. In *Botanical Microscopy*; Rolands, A. W., Ed.; 1985, 285-310.
12. Chafe, S. C. *Wood Sci. Technol.* 1978, **12**, 203-17.
13. Mueller, S. C.; Brown, R. M., Jr. *Planta* 1982, **154**, 489-500.
14. Roberts, K.; Burgess, J.; Roberts, I.; Linstead, P. In *Botanical Microscopy*; Robards, A. W., Ed.; 1985, 263-83.
15. Giddings, T. H., Jr.; Staehelin, L. A. *Planta* **173**, 22-30.
16. Staehelin, L. A.; Giddings, T. H., Jr. In *Developmental Order: Its Origin and Regulation*; Sabetly, S., and Green, P. B., Eds.; Liss: New York, 1982; p. 133-47.
17. Itoh, T.; Brown, R. M., Jr. *Planta* 1984, **160**, 372-81.
18. Quader and Robinson, *Ber. Deutsch. Bot. Ges.* 1981, **94**, 75-84.
19. Brown, R. M., Jr. *J. Cell Sci. Suppl.* 1985, **2**, 13-32.
20. Willison, J. H. M.; Brown, R. M., Jr. *J. Cell Biol.* 1978, **77**, 103-19.
21. Itoh, T.; O'Neil, R. M.; Brown, R. M., Jr. *Protoplasma* 1984, **123**, 174-83.
22. Mizuta, S. *Plant Cell Physiol.* 1985, **26**, 53-62.
23. Mizuta, S. *Plant Cell Physiol.* 1985, **26**, 1443-53.
24. Itoh, T. *Proc. Intern. Dissolv. Pulps Conf.* 1987, 117-20.
25. Mizuta, S.; Okuda, K. *Botanica Marina* 1987, **30**, 205-15.
26. Hogetsu, T. *Plant Cell Physiol.* 1983, **24**, 777-81.
27. Kiermayer, O.; Sleytr, U. B. *Protoplasma* 1979, **101**, 133-38.
28. Noguchi, T.; Tanaka, K.; Ueda, K. *Cell Struct. Funct.* 1981, **6**, 217-29.
29. Hotchkiss, A. T., personal communication.
30. Herth, W. *Planta* 1983, **159**, 347-56.
31. Brown, R. M., Jr. *The Third Philip Morris Science Symposium* 1978, 52-123.
32. Hotchkiss, A. T.; Brown, R. M., Jr. *J. Phycol.* 1987, **23**, 229-37.
33. Quader, H. *J. Cell Sci.* 1986, **83**, 223-34.
34. Itoh, T.; Legge, R. L.; Brown, R. M., Jr. *J. Phycol.* 1986, **22**, 224-32.
35. Steward, F. C.; Muhlethaler, K. *Ann. Bot. N.S.* 1953, **17**, 295-316.
36. Cranshaw, J.; Preston, R. D. *Proc. R. Soc. B London Ser.* 1958, **148**, 137-48.
37. Mizuta, S.; Wada, S. *Bot. Mag. Tokyo* 1981, **94**, 343-53.
38. Lloyd, C. W. *Intern. Rev. Cytol.* 1984, **86**, 1-51.
39. Haigler, C. H. In *Cellulose Chemistry and its Applications*; Nevell, T. P.; Zeronian, S. H., Eds.; Ellis Horwood; 1987, p. 30-83.

40. Delmer, D. P. *Adv. Carbohydr. Chem. & Biochem.* 1983, **41**, 105-53.
41. Hogetsu, T.; Takeuchi, Y. *Planta* 1982, **154**, 426-34.
42. Franke, W. W.; Seib, E.; Osborn, M.; Weber, K.; Herth, W.; Falk, H. *Cytobiol.* 1977, **15**, 24-48.
43. Lloyd, C. W. *Nature* 1979, **279**, 239-41.
44. Lloyd, C. W. *Ann. Rev. Plant Physiol.* 1987, **38**, 119-39.
45. Ishizawa, K.; Wada, S. *Plant Cell Physiol.* 1979, **20**, 973-82.
46. Emons, A. M. E.; Wolters-Arts, A. M. C. *Protoplasma* 1983, **117**, 68-81.
47. Emons, A. M. C. *Planta* 1985, **163**, 350-59.
48. Traas, J. A.; Braat, P.; Emons, A. M. C.; Meeks, M.; Derksen, J. *J. Cell Sci.* 1985, **76**, 303-20.
49. LaClaire, J. W., II. *Planta* 1987, **171**, 30-42.
50. Mizuta, S.; Okuda, K. *Bot. Gaz.* 1987, **148**, 297-307.
51. Okuda, K.; Mizuta, S. *Plant Cell Physiol.* 1987, **28**, 461-73.
52. Itoh, T.; Brown, R. M., Jr. *Protoplasma* 1988, **144**, 160-69.
53. Schneider, B.; Herth, W. *Protoplasma* 1986, **131**, 142-52.
54. Vian, B.; Roland, J. C. *New Phytol.* 1987, **105**, 345-57.
55. Roland, J. C.; Reis, D.; Vian, B.; Satiat-Jeunemaitre, B.; Mosiniak, M. *Protoplasma* 1987, **140**, 75-91.
56. Neville, A. C.; Levy, S. *Planta* 1984, **162**, 370-84.

RECEIVED March 27, 1989

## Chapter 20

# Triple-Stranded Left-Hand Helical Cellulose Microfibril in *Acetobacter xylinum* and in Tobacco Primary Cell Wall

George C. Ruben<sup>1</sup>, Gordon H. Bokelman<sup>2</sup>, and William Krakow<sup>3</sup>

<sup>1</sup>Department of Biological Sciences, Dartmouth College, Hanover, NH 03755

<sup>2</sup>Philip Morris Research Center, P.O. Box 26583, Richmond, VA 23261

<sup>3</sup>IBM, T. J. Watson Research Center, Box 218, Yorktown Heights, NY 10598

Tobacco primary cell wall and normal bacterial *Acetobacter xylinum* cellulose formation produced a  $36.8 \pm 3\text{\AA}$  triple-stranded left-hand helical microfibril in freeze-dried Pt-C replicas and in negatively stained preparations for transmission electron microscopy (TEM). *A. xylinum* growth in the presence of 0.25 mM Tinopal disrupted cellulose microfibril formation and produced a  $17.8 \pm 2.2\text{\AA}$  left-hand helical submicrofibril. Models of the triple-stranded left-hand helical microfibril and the left-hand helical submicrofibril were directly compared to TEM images. Computer generated optical diffraction patterns of the models and the images were complex and similar. The submicrofibril appears to have the dimensions of a nine (1-4)- $\beta$ -D-glucan parallel chain crystalline unit whose long,  $23\text{\AA}$ , and short,  $19\text{\AA}$ , diagonals form major and minor left-handed axial surface ridges every  $36\text{\AA}$ . Synthesis of the left-hand helical submicrofibril appears to be the driving force for self-assembly of a left-hand helical microfibril from three submicrofibrils.

The gram negative bacterium *Acetobacter xylinum* produces a ribbon of crystalline cellulose I whose neutral sugar content is 96.8% glucose and 3.2% xylose (1). Growth of *A. xylinum* in a medium containing 4,4'-bis(4-anilino-6-bis (2-hydroxyethyl) amino-1,3,5-triazin-2-ylamino) - 2,2'-stilbene-disulfonic acid, marketed under common names Calcofluor White ST or Tinopal LPW, can reversibly disrupt normal ribbon formation in concentrations greater than 0.1 mM and can increase the rate of cellulose synthesis up to four times in concentrations 1 mM or greater (2-5). This compound stoichiometrically binds to glucose residues of newly polymerized glucan chains and makes cellulose I crystallinity in the wet state, measured

0097-6156/89/0399-0278\$06.00/0

© 1989 American Chemical Society

by X-ray diffraction, undetectable. In the dry state cellulose I crystallinity is present and, depending on Calcofluor concentration, the crystallite sizes can be reduced from 65 and 74 Å to 28 Å (2, 3). Since microfibrils are assumed to crystallize from small filaments to larger ones by lateral fasciation, this enhanced growth rate and an undetectable wet state crystallinity have been interpreted as the separation of the primary cellulose I polymerization step from a sequential crystallization step (2-5) which is blocked. We have investigated *A. xylinum* cellulose production in the absence and presence of 0.25 mM Tinopal and report on the freeze-dried structure of the  $36.8 \pm 3 \text{ \AA}$  microfibril produced under normal conditions and the  $17.8 \pm 2.2 \text{ \AA}$  submicrofibril produced in the presence of Tinopal (1). We have also found submicrofibrils and microfibrils in tobacco primary cell wall similar to *A. xylinum*. We present models of the triple-stranded left-hand helical microfibril, the left-hand helical submicrofibril and the apparent relationship of the four sugar chain fiber diffraction unit cell to the submicrofibril (1, 6). Computer generated single molecule optical diffraction patterns of these models and of representative TEM micrographs reinforce our impression of congruency. The patterns suggest that the  $17.8 \text{ \AA}$  cellulose submicrofibril generated in the presence of 0.25 mM Tinopal is organized as a fibrillar unit with nine parallel sugar chains forming a left-handed helical structure (1). The prevalent assumption that the high rate of cellulose synthesis induced in *A. xylinum* by Tinopal or Calcofluor is due to a cellulose polymerization step uncoupled from a sequential rate-limiting crystallization step is not consistent with an ordered crystal-like submicrofibril.

### Methods and Materials

The *A. xylinum* (American Type Culture Collection 23769) was grown on 40 mM D-glucose and 0.5 M phosphate (pH 7, 20°C) until it formed a white, flocculent surface cap on the solution. Samples prepared in this way were then grown consecutively on 0.25 mM Tinopal for 1 h, on 0.25 mM Tinopal for 1.5 h, on .025 mM Tinopal for 1 h, and then on 40 mM D-glucose and 0.5 M phosphate (pH 7, 20°C) for 1 h. Each 1.25 cm pellicle of cellulose ribbons with cells growing and tethered by their ribbons at its periphery was rinsed sequentially, first in 5 separate dishes of water, then in 5 separate dishes of 1:3 ethanol-water. Each pellicle was then placed on a 1.25 cm Whatman 50 filter paper disc, blotted, and frozen in liquid propane. Pellicle from *A. xylinum* grown normally was freeze-dried for 1.5 h at -78°C, then replicated with  $17.3 \text{ \AA}$  Pt-C (at -178°C), and backed with  $90.2 \text{ \AA}$  carbon on a Wiltek Industries modified Balzer's 301 with cryopump and rebuilt cold stage (7). The Tinopal-treated sample was freeze-dried for 2.8 h at -70°C, replicated with  $16.4 \text{ \AA}$  Pt-C (at -178°C), and backed with  $156 \text{ \AA}$  of carbon. The tobacco lower epidermal peels were prepared from a Coker 319 leaf (No.13 on stalk). These peels were immersed in 1:3 ethanol-water, blotted to remove the excess solution and then frozen on 1.25 cm mica discs by rapid immersion in liquid propane (-190°C). This sample was freeze-dried for 3 h at -70°C, and then replicated with  $15.9 \text{ \AA}$  Pt-C (45° angle) at -178°C *in vacuo* ( $6.67 \mu\text{Pa}$ ) and backed with  $139 \text{ \AA}$  of

carbon. All of the samples were digested in 80% sulfuric acid. The replicas were rinsed in deionized water and then picked up with carbon-coated, 300 mesh grids from underneath and examined on a JEM 100CX instrument as described previously (8). Indirectly evaporated carbon films of  $\sim 80\text{\AA}$  thickness, suspended on 300-mesh grids, were used to support *A. xylinum* cellulose that had been treated with boiling trifluoroacetic acid to remove hemicellulose. This sample was negatively stained with 2% uranyl acetate at pH 3.8, as previously described (9).

To contrast-enhance unidirectional 15-18 $\text{\AA}$  thick Pt-C-coated cellulose specimens backed with 100-173 $\text{\AA}$  thick carbon films, micrographs were contrast-reversed on Kodak 7302 fine-grain, positive film (8). In addition to increasing the contrast of 10-20 $\text{\AA}$  features, the Pt-C coated surfaces became white, and the molecular details were modulated on this background in blacks and shades of grey for easy structural interpretation (10-14). Shooting a tilt series at  $10^\circ$  intervals at  $10^5\times$  magnification on a JEM 100CX at 80 kV with a 5 mm focal length and a  $40\mu\text{m}$  objective aperture achieved a 6.6 $\text{\AA}$  resolution and a 2625 $\text{\AA}$  depth of field in the picture series (8). The tilt series was generally viewed stereoscopically, and then a single image representing the 3-D structure was shown. In order to estimate the real size of a filament underneath its Pt-C coating (unidirectional at a  $45^\circ$  angle), the longitudinal axis of a filament had to be within  $10^\circ$  of the general shadow-direction on the replica surface, so that both sides of the filament were Pt-C coated. The filament should be roughly at a  $45^\circ$  angle with the Pt-C source (checked by stereo-viewing), although filaments which were Pt-C coated at approximately a  $90^\circ$  angle were only 1 $\text{\AA}$  smaller (12). Series of fiber width measurements, made at image magnifications of 2 to 5 million, and usually numbering fewer than 100, were averaged, and the Pt-C film thickness, measured on the quartz-crystal monitor, subtracted from the average width, to give an estimate of the real filament diameter (11). It was recently found that this width-correction method should be reduced by 1.5 $\text{\AA}$  (12, 13). In contrast, the center to center distance between either ridges or grooves along a Pt-C coated microfibril or submicrofibril were assumed to be unchanged.

Computer generated optical diffraction patterns of single cellulose microfibrils and submicrofibrils were obtained from large field micrographs printed at  $10^6\times$  magnification. The images were digitized via a television camera connected to an image frame store and controlled through an IBM 309D main frame computer (15, 16). Briefly, an area of the image containing a single molecule was selected by a circular electronic aperture defined by a graphics overlay cursor under operator control. When the image was shipped to the host CPU, the fast fourier transform (FFT) and subsequent power spectrum were computed from the region defined electronically, with an edge grading function to eliminate hard edge diffraction. The electronically sampled image region and its power spectrum (optical diffraction pattern) were then sent to a hard copy slide-making device. The diffraction pattern was calibrated using Keuffel & Esser (46 1513)  $10\times 10$  to cm graph paper with the same setup for digitizing the molecule. The optical

diffraction patterns were oriented in the same direction as the spacings appeared in the molecule (Figures 5, 6,7 and 10) and were generally scaled over 5-6 decades of intensity so that individual spot identity and position at lower intensities could be correctly identified at the higher intensity levels which enhanced fainter spots. The transparencies were all rephotographed with a low contrast film developer system and printed at the same magnification with 0-2 grade Ilford multigrade II print paper. The features of these diffraction patterns were recorded on overlaid tracing paper on a light table. The distance between centers of spots symmetric with the diffraction pattern center were measured with a vernier caliper and then divided by two to give the spot position in reciprocal space. The exact center of most elongated spots was estimated. The precision of the diffraction measurements was not better than 8%. The reciprocal space distance for the molecule was divided into the reciprocal distance for the 1 mm graph paper and multiplied by a magnification factor in Å/mm to compute optical diffraction spacings in Angstroms.

## Results

Imaging *A. xylinum*'s cellulose ribbon has previously been accomplished by adhering cells to a film coated grid, growing the cells on a nutrient buffer solution, and negative staining them for visibility and for transmission electron microscopy. Images show that *A. xylinum* produces a left-hand twisted ribbon normally, and in the presence of carboxymethylcellulose (CMC) (4, 5). When grown in the presence of 0.25 mM Calcofluor, this morphology is dramatically altered to a broad cellulose band composed of 15Å and larger filaments (2-5).

We have approached specimen preparation for TEM imaging differently. *A. xylinum* naturally forms a pellicle or gel of cellulose ribbons on the surface of a solution during growth with the cells tethered at the pellicle's periphery by ribbons. Since sequential growth conditions are recorded linearly along a ribbon, *A. xylinum* was grown normally, in 0.25 mM Tinopal, and normally again, then visualized after freeze-drying and Pt-C replication. Figure 1 shows a normally grown pellicle of *A. xylinum* cellulose ribbons that appear linear and untwisted. The small arrows point out left-hand twisted microfibrils within the ribbons. When *A. xylinum* was grown in the presence of 0.25 mM Tinopal, an altered cellulose was produced as shown in Figure 2. The same preparation shown at higher magnification in Figure 3 revealed 33Å Pt-C coated submicrofibrils (small arrows). These individual submicrofibrils averaged  $17.8 \pm 2.2\text{Å}$  after correction for the Pt-C coat (1), and frequently twisted together to form larger fibrils.

Submicrofibrils, previously imaged, have been correlated with the four glucan chain X-ray fiber diffraction unit cell as opposed to the two or eight chain unit cell by average diameter measurements (1). In the Figure 4 submicrofibril model the side and diagonal dimensions of the unit cell were estimated. By translating and rotating this parallel nine glucan chain cross section, the long diagonal of 23Å and the short diagonal of 19Å generated a major and minor surface ridge and also generate a submicrofibril with a



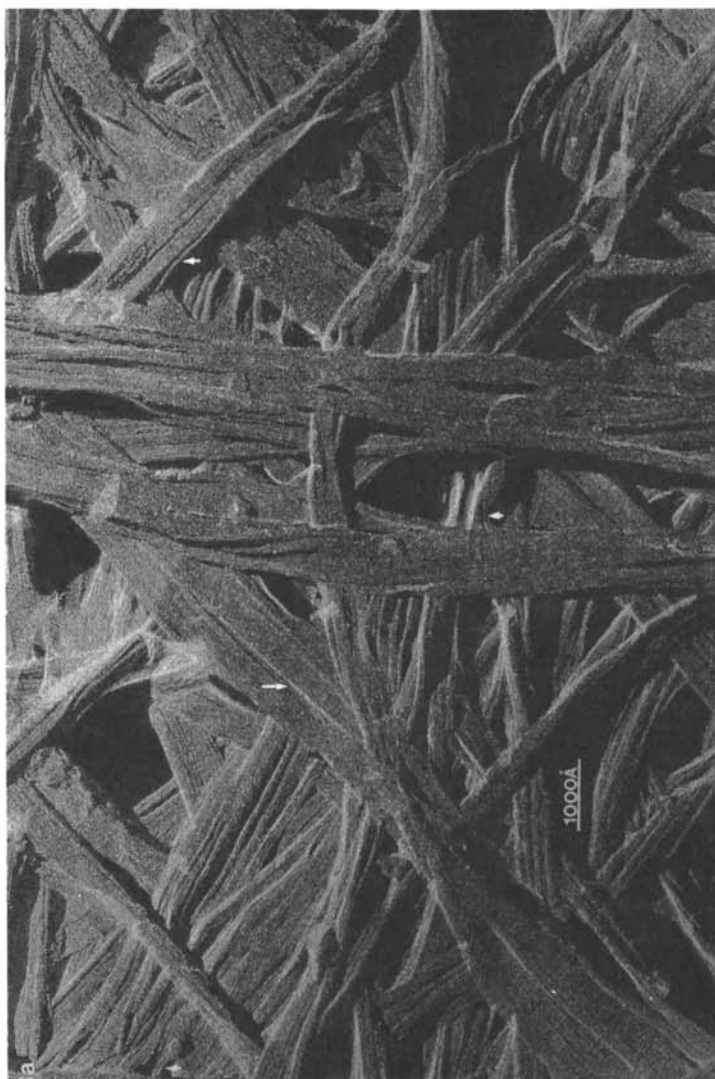


Figure 1. Freeze-dried gel of *A. xylinum* cellulose ribbons deposited during normal growth. The arrows point to triple-stranded left-hand helical microfibrils averaging  $36.8 \pm 3\text{Å}$  in diameter (1). The sample was replicated with  $17.3\text{Å}$  Pt-C and backed with  $90.2\text{Å}$  of carbon.

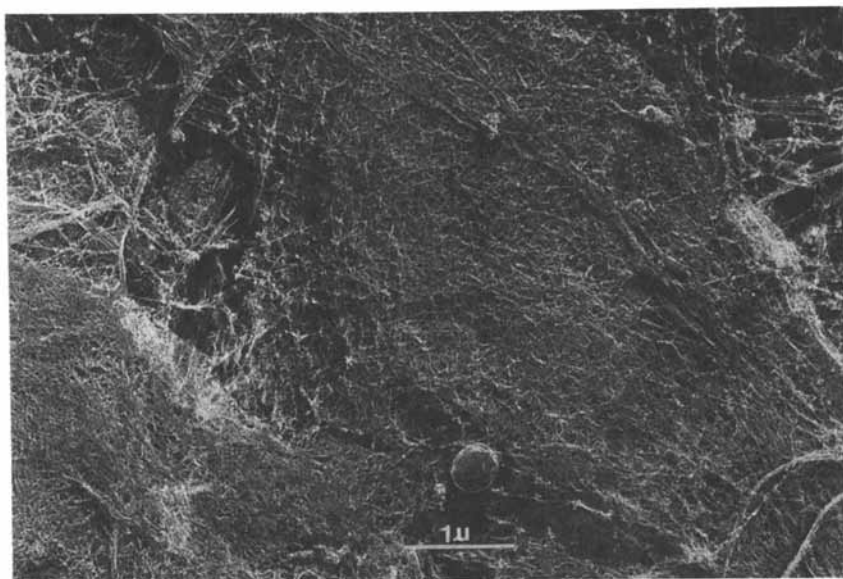


Figure 2. Freeze-dried *A. xylinum* cellulose grown in the presence of 0.25 mM Tinopal and replicated with 16.4Å Pt-C and backed with 156Å of carbon. A tangled mass of 33Å Pt-C coated submicrofibrils was formed instead of normal ribbon cellulose.

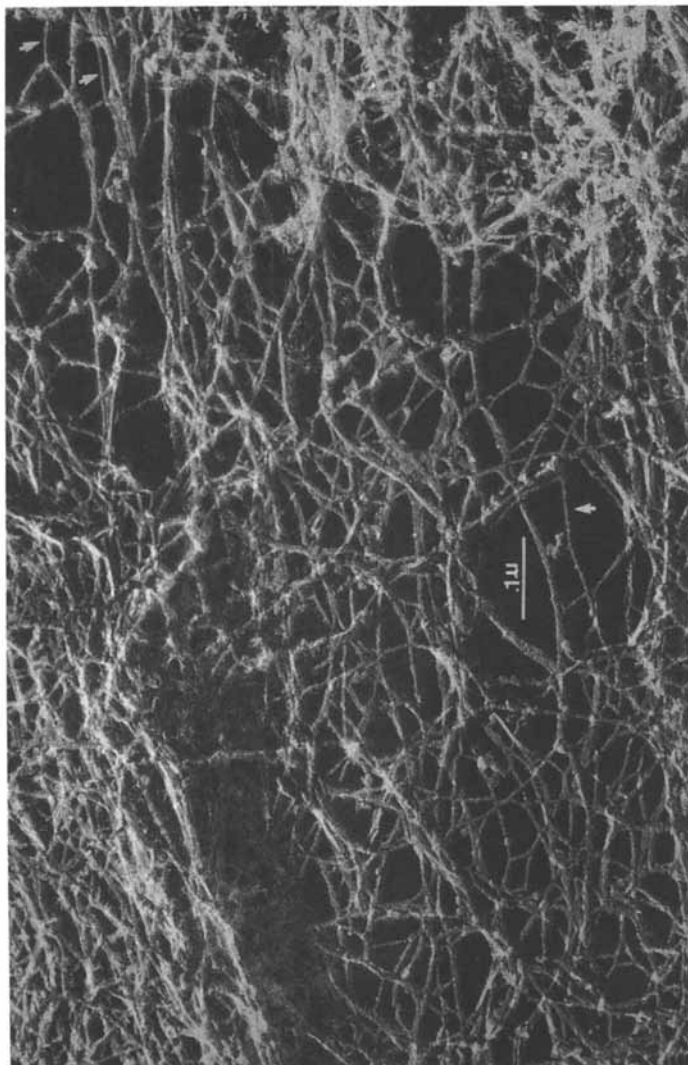


Figure 3. Higher magnification of *A. xylinum* cellulose grown in the presence of 0.25 mM Tinopal. The arrows point to single Pt-C coated submicrofibrils averaging  $33\text{\AA}$  in diameter ( $17.8 \pm 2.2\text{\AA}$  after correction for the  $16.4\text{\AA}$  Pt-C coating). Many of these submicrofibrils were twisted together forming thicker fibers.

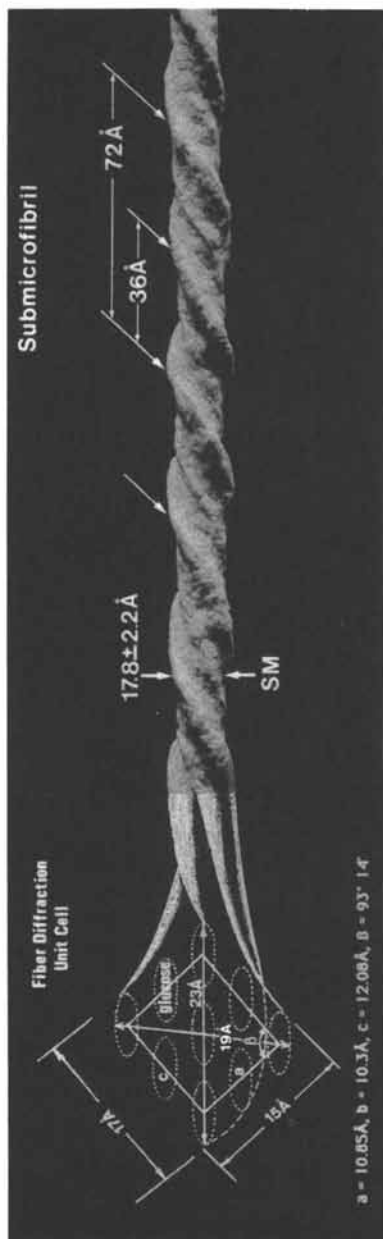


Figure 4. The model contains the four chain X-ray fiber diffraction unit cell dimensions, listed at the left of the figure, which were drawn as a cross section through the glucan chains. This unit cell has encompassed nine glucan chains with exterior side dimensions of 15 Å and 17 Å and diagonal dimensions of 19 Å and 23 Å as shown. By rotating and translating the unit cell we generated a submicrofibril (SM) geometry with a major ridge (23 Å diagonal) and an intermediate minor ridge (19 Å diagonal). Major ridges occur every 36 Å with a helical pitch of 72 Å. The original submicrofibril average measurement from micrographs was  $17.8 \pm 2.2$  Å, in agreement with the 18.5 Å found by averaging the exterior sides and diagonals. The average of these dimensions was slightly larger than originally reported (1) since the minor diagonal was increased from 16.5 Å to 19 Å. Generation of an ordered submicrofibril by this approach was consistent with the Ellis and Warwicker unit cell derivation which only assumed parallel glucan chain axes (6).

nonuniform diameter whose maximum dimension is  $23\text{\AA}$ . This submicrofibril had a helical pitch of  $72\text{\AA}$  with a major ridge crossing the axis every  $36\text{\AA}$  and a minor ridge crossing half-way between the major ridges. In Figure 5 the submicrofibril model (Fig. 5a) was compared at equivalent magnification to a TEM image of the submicrofibril (Fig. 5c). The Pt-C coated  $36\text{\AA}$  major ridge spacings and some of the minor ridges along the submicrofibril surface were preserved but the diameter increased by  $15.2\text{\AA}$  to  $33\text{\AA}$ . The image orientation with the computer generated optical diffraction patterns in Figures 5-7 were also preserved. The model's diffraction pattern (Fig. 5b) was generated from one side of a left-handed helix with prominent spacings ( $\pm 8\%$  precision) at  $25\text{\AA}$  and  $12\text{\AA}$ , with a vertical spacing at  $12\text{\AA}$  and with adjacent spots paralleling the  $25\text{\AA}$  and  $12\text{\AA}$  spot positions. The optical diffraction pattern generated from the TEM image of the submicrofibril (Fig. 5d) was similar to Fig. 5b with left-handed spacings ( $\pm 8\%$ ) of  $26\text{\AA}$  and  $12\text{\AA}$  or  $14\text{\AA}$  and with two spots below and above the larger spacing of  $26\text{\AA}$  (see horizontal arrows in Fig. 5d and 5b). The major ridges spaced  $26\text{\AA}$  apart traverse the submicrofibril axis at a  $45 \pm 15^\circ$  angle. This angle has geometrically determined the major ridge repeat along the fiber axis of  $36\text{\AA}$  ( $26\text{\AA} / \sin 45^\circ = 36.8\text{\AA}$ ). The Pt-C replica resolution in Figure 5d is  $9\text{\AA}$  was only slightly better than the  $12\text{\AA}$  or  $13\text{\AA}$  previously reported (10, 13).

The microfibril model composed of three submicrofibrils left-hand twisted together in Figure 6a was compared at the same magnification to the Pt-C coated microfibril image in Figure 6c. The major and minor ridges (thick and thin arrow heads) were visible along the submicrofibrils in the model and they could also be seen along the central submicrofibril in the TEM image. The computer generated optical diffraction patterns of the model shown in Figure 6b and of the Pt-C coated microfibril shown in Figure 6d were complex but similar. In the diffraction pattern in Figure 6b, we could assign the vertical spacing in the microfibril model at  $23\text{\AA}$  and one left-handed spacing at  $23\text{\AA}$  ( $-45^\circ \pm 15^\circ$  angle) to the long diagonal (see Fig. 4) or maximum diameter of the submicrofibril. The third  $23\text{\AA}$  spacing at  $-17^\circ \pm 15^\circ$  angle was probably related to a foreshortened projection of the major ridge center to center distance along the submicrofibril wrapped around the microfibril axis. The vertical spacing in Figure 6d of the TEM image was  $27\text{\AA}$  and there was also a left-handed spacing at  $27\text{\AA}$  at a  $-45^\circ \pm 15^\circ$  angle. This larger value may be due to the slightly greater separation between the submicrofibrils in the TEM image. A third spacing at  $23\text{\AA}$  or  $21\text{\AA}$  at a  $-17^\circ \pm 15^\circ$  angle was probably related to a foreshortened major ridge spacing along the submicrofibril.

The negatively stained microfibril shown in Figure 7a was first treated to remove hemicellulose before it was negatively stained. The computer generated optical diffraction pattern was only of the upper microfibril with the  $33\text{\AA}$  spacing. The diffraction pattern in Figure 7b showed a vertical spacing at  $24\text{\AA}$ , a left-handed spacing of  $23\text{\AA}$  at a  $-45^\circ \pm 5^\circ$  angle to the horizontal axis, and a spacing at  $25\text{\AA}$  similar to the major ridge spacing in Figure 6b. The  $33\text{\AA}$  left-handed axial microfibril spacing was geometrically related to the  $23\text{\AA}$  submicrofibril spacing ( $23\text{\AA} / \sin 45^\circ = 32.5\text{\AA}$ ).

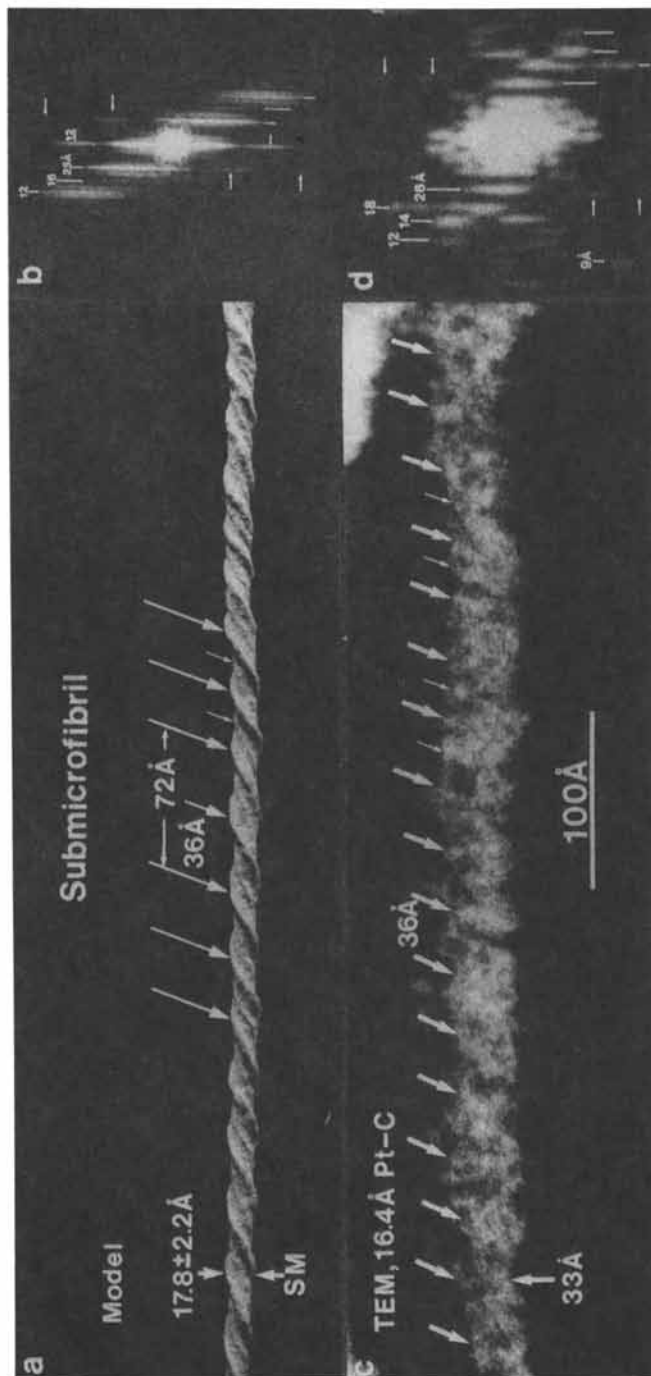


Figure 5. The submicrofibril model in a and the Pt-C coated submicrofibril image in c were compared at the same magnification. The optical diffraction of the model in b demonstrated a left-handed surface spacing of 25 Å and 12 Å with two spots (horizontal arrows) which appeared on layer lines below and above the 25 Å spot. The first layer line occurs at 12 Å and was the vertical separation of the minor ridge position between two major ridges 23 Å apart. The general features of this left-handed optical diffraction pattern occurred in the TEM image in d with spacings at 26 Å and 12 Å or 14 Å with similar spots indicated by horizontal arrows below and above the major ridge spacing of 26 Å. (c reproduced with permission from ref. 1. Copyright 1987 Elsevier.)

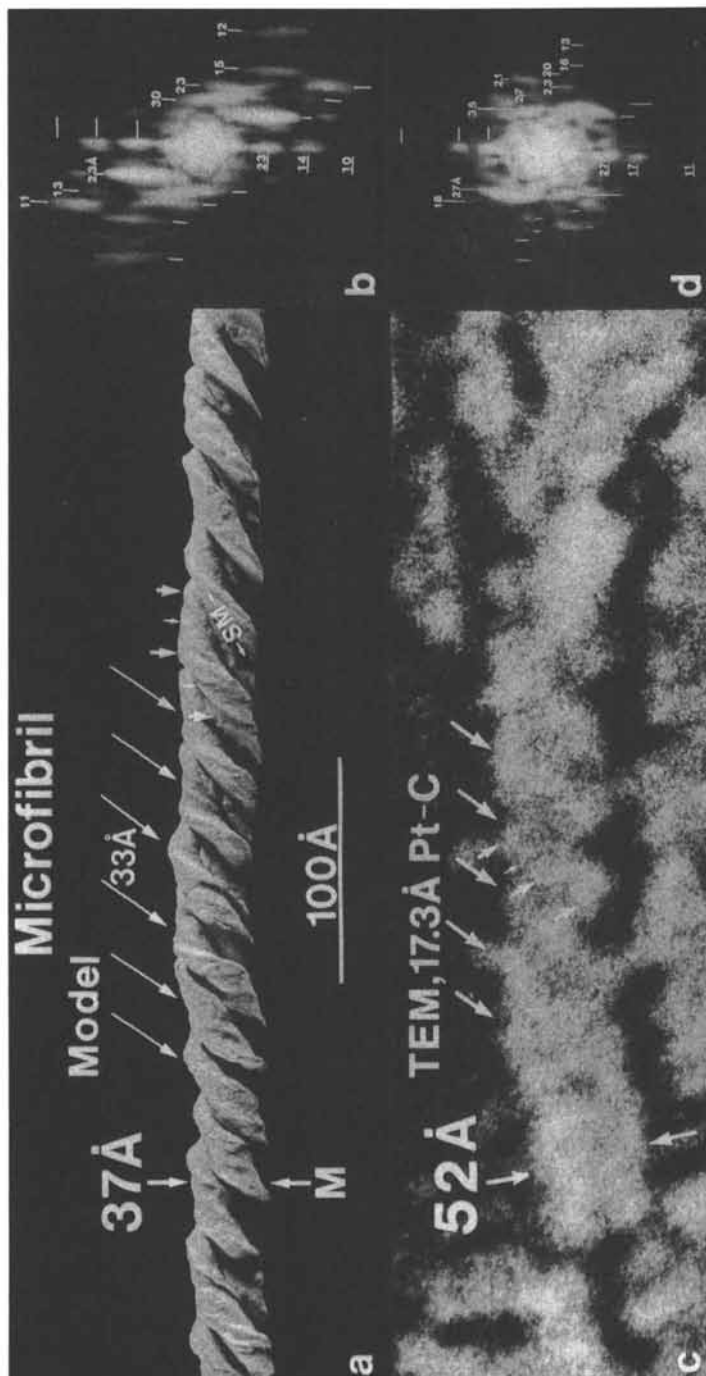


Figure 6. This model of the microfibril (M) composed of three submicrofibrils (SM) twisted together in a left-handed fashion (a) was compared at the same magnification to the Pt-C coated microfibril image in c. The major and minor ridges (thick and thin arrowheads) were visible along the submicrofibrils in the model and they could also be seen along a submicrofibril at the center of the TEM image. The optical diffraction pattern of the model shown in b and of the Pt-C coated microfibril shown in d were complex but similar. In d, the submicrofibrils cross the TEM microfibril axis at a  $45^\circ \pm 15^\circ$  angle. (c reproduced with permission from ref. 1. Copyright 1987 Elsevier.)

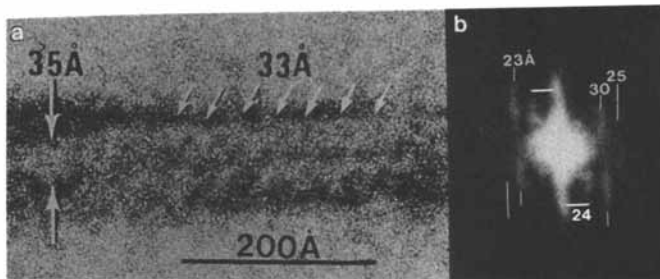


Figure 7. This microfibril was treated with hot trifluoroacetic acid to remove hemicellulose and was then negatively stained with 2% uranyl acetate in Figure 7a. The optical diffraction pattern in Figure 7b was only of the upper microfibril showing the 33 Å spacing. In Figure 7b the submicrofibrils cross the TEM microfibril axis at a  $45^{\circ} \pm 5^{\circ}$  angle. (7a reproduced with permission from Ref. 1. © 1987 Elsevier Science Publishers B. V.)



It was previously pointed out that filaments the size of submicrofibrils exit the cell wall of *A. xylinum* through pores (4). Figure 8 shows how a microfibril self-assembled from three submicrofibrils on the exterior of the cell (1). Arrows point to submicrofibrils 1 and 2 on the cell surface. At their junction submicrofibril 2 crosses 1 in a left-handed manner visible in stereo-micrographs (not shown). Submicrofibril 3 joins and then crosses the twisted pair of microfibrils in a left-handed manner near the bottom of the figure. The image of submicrofibril 3 also showed that it was not rod-like but was left-hand super-twisted. A model of this process in Figure 9 showed three left-hand helical submicrofibrils labelled SM 1, 2 and 3 emerging from the cell wall at the top of the figure. This model depicts three associated submicrofibrils being spun together to form a microfibril, although it was unclear how three submicrofibrils initially came together. This spinning process may be driven by the left-hand rotation and elongation of the submicrofibrils during cellulose synthesis. The left rotation of each submicrofibril drives the formation of a left-hand three-stranded microfibril which also left rotated as it grows longer. If any of the submicrofibrils elongated more rapidly than the other pair, it would become left-hand super-twisted as pointed out in Figure 8 for submicrofibril 3.

In tobacco primary cell wall the cellulose microfibrils observed individually or associated with bundles were also triple-stranded and left-hand helical. These observations are shown in Figure 10. Since cellulose is only 19% of the tobacco cell wall (17), the task of finding and identifying cellulose was complicated. For this reason *A. xylinum* which produces a pure ribbon of cellulose was used for studying cellulose structure.

## Discussion and Conclusions

Submicrofibril and triple-stranded left-hand helical microfibrils are found in tobacco primary cell wall and bacterial *A. xylinum* cellulose. We suspect from our results and the literature survey outlined in reference (1) that the triple stranded structures are prominent in the primary plant cell wall. The highly crystalline cellulose of plant and algae secondary cell wall appears by X-ray fiber diffraction (18,19) and TEM lattice imaging (20-23) to be largely crystalline arrays of planar straight chains of (1-4)- $\beta$ -D-glucan chains.

The submicrofibril in Figure 5c was clearly a left-handed helix with a major ridge repeat of 26Å and minor ridge half spacing at 12Å or 14Å evident in the optical diffraction pattern (Fig. 5d). The correspondence between the model and the Pt-C coated submicrofibril was stronger than expected since it was known that evaporated metal coatings do not just adhere where they land at ordinary replication temperatures (24-27). The specimen temperature used in this work (-178°C) was colder by 110°C than the temperature used previously (7). The greater metal sticking coefficient at lower temperatures preserved surface resolution to 9Å in Figure 5d.

The microfibril model in Figure 6a strongly resembled the Pt-C coated microfibril in Figure 6c, which also contained a major and minor ridge along a submicrofibril at the center of the image. The assignment of spots to molecular features in the complex optical diffraction pattern in Figure 6b

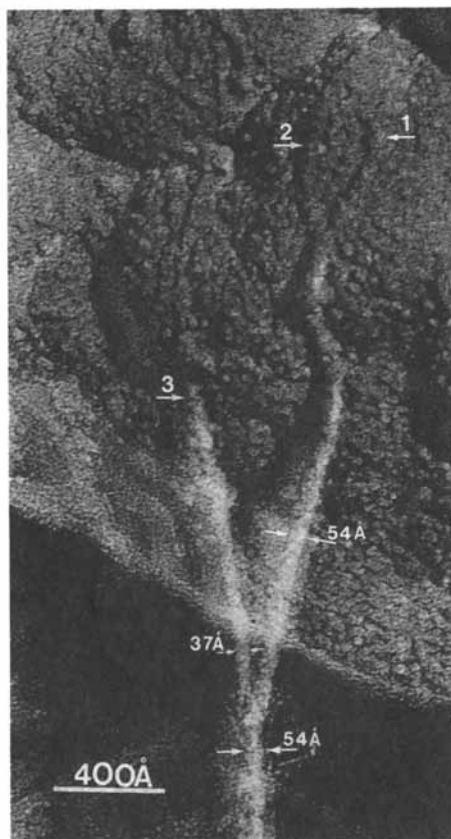


Figure 8. Since the submicrofibrils exit the cell wall of *A. xylinum* through pores (4), the self-assembly of a triple-stranded microfibril has occurred at the exterior surface of the cell (1). Submicrofibrils 1 and 2 appeared super-twisted on the cell surface. At their junction submicrofibril 2 crossed 1 in a left-handed manner which is only visible with stereo-micrographs (not shown). Submicrofibril 3, which was also left-hand super-twisted, joined and crossed the double fiber in a left-handed manner. This specimen was coated with 16.4 Å of Pt-C. (Reproduced with permission from Ref. 1. © Elsevier Science Publishers B. V.)

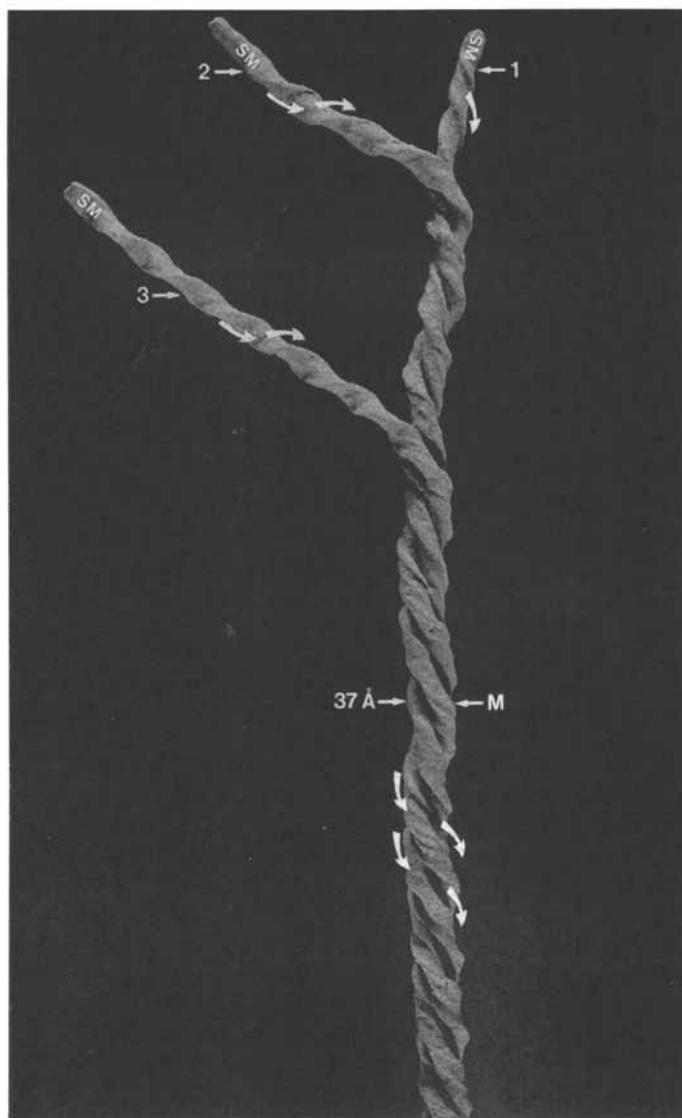


Figure 9. This model shows three left-handed helical submicrofibrils (SM) 1, 2 and 3 which emerged from the cell wall at their termini. It was not clear how the submicrofibrils first associated with other submicrofibrils but once associated they were spun together. This model assumed that cellulose synthesis provided the mechanical force that simultaneously extended and left-hand rotated the submicrofibrils, which in turn drove the secondary formation of three submicrofibrils into a left-hand helical microfibril (M).

could not be accomplished yet except at a rudimentary level. The vertical and left-handed spacing ( $-45^\circ \pm 15^\circ$ ) at  $23\text{\AA}$  represented the maximum width or long diagonal (Fig. 4) of the submicrofibril. The  $-17^\circ \pm 15^\circ$  spacing at  $23\text{\AA}$  probably represented a foreshortened major ridge spacing along a submicrofibril curving around the microfibril axis. The same spacings also appeared in the optical diffraction pattern (Fig. 7b) of the negatively stained microfibril in Figure 7a. The optical diffraction pattern of the freeze-dried Pt-C replicated microfibril (Fig. 6d) was far more complex, resolving more spots than its negatively stained counterpart in Figure 7b. The vertical and left-handed spacings at  $-45^\circ \pm 15^\circ$  in the Pt-C coated microfibril were  $27\text{\AA}$ , due either to a truly greater space between submicrofibrils in Figure 6c or merely to the 8% precision of measurement which made  $27\text{\AA}$  and  $23\text{\AA}$  of doubtful discriminability. A  $21\text{\AA}$  or  $23\text{\AA}$  spacing was also located at  $-17^\circ \pm 15^\circ$ , which could be attributed to the submicrofibril.

We believe that the TEM and model images of the cellulose helix in conjunction with the computer generated optical diffraction patterns provide strong evidence for a substructure that includes a left-hand helical microfibril composed of three submicrofibrils (Fig. 8) and a left-hand helical submicrofibril. Evidence that the four glucan chain fiber diffraction unit cell had the same size as the submicrofibril came from the correspondence between the unit cell's average diameter of  $18.5\text{\AA}$  and the measured submicrofibril diameter of  $17.8 \pm 2.2\text{\AA}$  (1), the major and minor ridges visible in TEM (Fig. 5c) and the maximum diameter of  $23\text{\AA}$  for the submicrofibril as determined from the microfibril's optical diffraction pattern. This strong correlation has supported the hypothesis that the parallel nine glucan chain unit represents the submicrofibril cross section.

The method we have advanced for generating the submicrofibril from the nine sugar unit cross section in Figure 4 provides a model for submicrofibril synthesis. After each nine glucan chain cross section has been assembled and moved to make room for the next, the submicrofibril elongates and simultaneously rotates. Microfibril self-assembly in Figure 8 was based on a cellulose synthesis-powered mechanism which extends and rotates each submicrofibril in the Figure 9 model. One obvious prediction of the model, besides the formation of a left-hand helical microfibril, was that the microfibril would also rotate in a left-handed direction as it elongated. We will return to this point in the last paragraph.

One important consequence of the nine parallel glucan chain unit, translated and rotated to generate a left-hand helical submicrofibril, was that all the (1-4)- $\beta$ -D-glucan chains were not conformationally equivalent in the Figure 4 submicrofibril model. For instance, the glucan chain at the center of this model would form a left-handed helix 7 cellobiose units long with a  $72\text{\AA}$  pitch, but all other glucan chains would require more cellobiose units to reach the same axial position. Recent theoretical calculations indicate that a family of left-hand helical (1-4)- $\beta$ -D-glucan chains 7-9 cellobiose units long with pitches of about  $72\text{\AA}$  to  $93\text{\AA}$  exist near a similar conformational energy minimum (28). The nine parallel glucan chain, twisted crystal model thus cannot be ruled out on either the basis of glucan

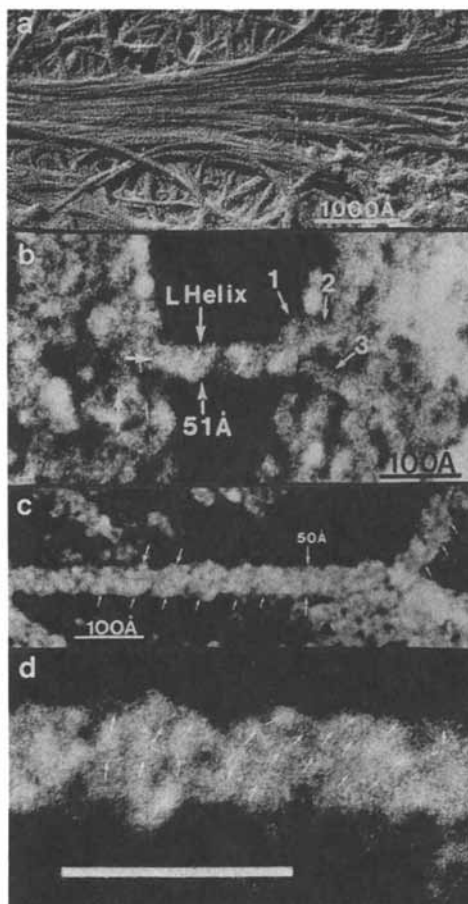


Figure 10. a, Bundled cellulose microfibrils in the lower epidermal cell wall (facing mesophyll cells) of Coker 319 tobacco leaves. This epidermal peel was freeze-dried, Pt-C replicated (15.9 Å thick) and carbon film backed (133 Å thick). b, A cellulose microfibril is seen connecting two bundles of microfibrils (similar to a). This Pt-C coated microfibril averages 51 Å in width, shows left-handed surface striations, and splits into three smaller submicrofibrils. c, Tobacco primary cell wall Pt-C coated microfibril averaging 50 Å shows left-handed surface striations. d, Three 16–18-Å submicrofibrils in adjacent ridges wrap (see arrows) in a left-handed fashion around the microfibril axis. Bar, 100 Å. (a–d reproduced with permission from ref. 1. Copyright 1987 Elsevier.)

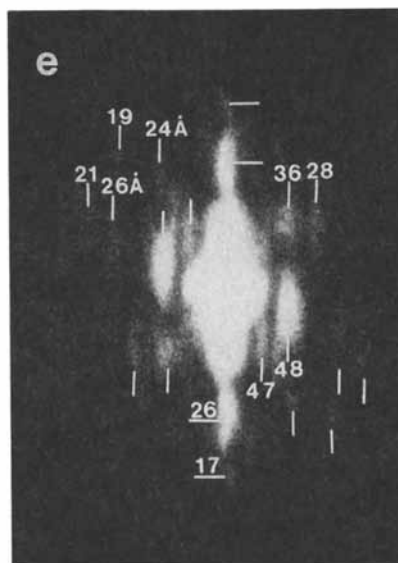


Figure 10. e, Optical diffraction pattern of c. Its important features were similar to those in the *A. xylinum* microfibril diffraction pattern in Figure 6d: left-handed spacings at roughly  $24 \pm 3 \text{ \AA}$ , a vertical spacing at  $26 \text{ \AA}$ , and right-handed spacings at  $36 \text{ \AA}$  and  $28 \text{ \AA}$ . The left-handed pattern at  $47 \text{ \AA}$  and  $48 \text{ \AA}$ , not previously seen, was probably caused by an artificial bunching of the submicrofibrils (d) when the microfibril was lifted above the cell wall surface by peeling the lower epidermal cell layer from the tobacco leaf.

chain energy considerations or the lack of left-handed glucan chain conformations. Others have also suggested that cellulose glucan chains form a left-handed helix of 72Å (29) and can also be left-handed helical in solution (30). The nonequivalence of glucan chains in a twisted crystal would limit its maximum lateral dimensions. Since chains farthest from the axis center are less twisted, it is not surprising that in larger secondary cell wall crystalline cellulose all the glucan chains can energetically assume a flat linear configuration with each cellobiose unit related to the next by a 180° rotation (18-23,31). Our observations suggest that the submicrofibril structure is a consequence of its small size and of (1-4)- $\beta$ -D-glucan chains' natural tendency to assume a left-handed helix (21). Larger cellulose crystals can untwist (1-4)- $\beta$ -D-glucan chains because of the favorable energetics of forming planar straight chain crystals (31).

The model in Figure 9 predicts that each microfibril would rotate in the process of cellulose ribbon formation. If the *A. xylinum* cell were held stationary, then the ribbon would be left-hand twisted (2-5); however, if the ribbon were held stationary, then the cell would rotate (32). The latter case explains why ribbons appear untwisted in the pellicle of ribbons shown in Figure 1. Moreover, it has been demonstrated that an *A. xylinum* cell ceased rotation when Calcofluor (> 0.1 mM) was added to the solution (32).

Previous work has shown that the presence of Calcofluor or Tinopal could dramatically increase *A. xylinum* cellulose synthesis. This observation was the basis for the hypothesis that cellulose polymerization can be uncoupled from a slower sequential crystallization step (2-5). We believe the hypothesis is not consistent with our observations. At the very least, the presence of an ordered and crystal-like submicrofibril produced in the presence of 0.25 mM Tinopal would relegate Tinopal's or Calcofluor's effects to an event occurring after the initial cellulose polymerization-crystallization step or steps.

The data we present show that *A. xylinum* cellulose microfibrils are formed by submicrofibrils being spun together, as shown in Figures 8 and 9, rather than associated through a mechanism of lateral fasciation (1, 4, 5). We have demonstrated that Tinopal disrupts ribbon formation and the microfibril formation process in Figures 2 and 3. Since the microfibril spinning process either rotates the ribbon or the cell, its disruption would uncouple a rate-limiting rotation, elongation process from cellulose synthesis. Thus, uncoupling of a cell's or a ribbon's mechanical rotation with Tinopal or Calcofluor would result in an increased rate of cellulose synthesis, an interpretation which is consistent both with our findings and with previous work (1-5, 32).

## Acknowledgments

We acknowledge Philip Morris' financial support for this work, N. J. Jacobs (Dartmouth Medical School) for culturing the *A. xylinum*, and the Dartmouth Rippel EM Facility for the use of their equipment.

## Literature Cited

1. Ruben, G. C.; Bokelman, G. H. *Carbohydr. Res.* 1987, **160**, 434-43.
2. Haigler, C. H.; Brown, R. M., Jr.; Benziman, M. *Science* 1980, **210**, 903.
3. Benziman, M.; Haigler, C. H.; Brown, R. M., Jr.; White, A. R.; Cooper, K. M. *Proc. Natl. Acad. Sci. U.S.A.* 1980, **77**, 6678-82.
4. Haigler, C. H.; Benziman, M. In *Cellulose and Other Natural Polymer Systems*; Brown, R. M., Jr., Ed.; Plenum Press: New York, 1982; Chap. 14; pp. 273-97.
5. Brown, R. M., Jr.; Haigler, C. H.; Suttie, J.; White, A. R.; Roberts, E.; Smith, C.; Itoh, T.; Cooper, K. M. *J. Appl. Polym. Sci., Appl. Polym. Symp.* 1983, **37**, 33-78.
6. Ellis, K. C.; Warwicker, J. O. *J. Polym. Sci.* 1962, **56**, 339-57.
7. Ruben, G. C. *J. Elect. Microsc. Tech.* 1985, **2**, 253-57.
8. Ruben, G. C.; Marx, K. A. *J. Elect. Microsc. Tech.* 1984, **1**, 373-85.
9. Ruben, G. C.; Harris, E. D.; Nagase, H. *J. Biol. Chem.* 1988, **263**, 2861-69.
10. Marx, K. A.; Ruben, G. C. *J. Biomol. Str. and Dynamics* 1984, **1**, 1109-32.
11. Ruben, G. C.; Marx, K. A. *Proc. 42nd Ann. Mtg. Elect. Microsc. Soc. Amer.*; 1984; p. 684.
12. Ruben, G. C.; Shafer, M. W. In *Better Ceramics through Chemistry II*; Brinker, C. J.; Clark, D. E.; Ulrich, D. R., Eds.; Materials Research Society: Pittsburgh, PA, 1986; V. 73, 207-12.
13. Ruben, G. C.; Bokelman, G. H. *Proc. 45th Ann. Mtg. Elect. Microsc. Soc. Amer.*; 1987, p. 966.
14. Yurchenco, P. D.; Ruben, G. C. *J. Cell Biol.* 1987, **105**, 2559-68.
15. Krakow, W. *Mat. Res. Soc. Symp. Proc.* 1984, **31**, 39-55.
16. Krakow, W. *Ultramicroscopy* 1985, **18**, 197-210.
17. Bokelman, G. H.; Ryan, W. S., Jr.; Oakley, E. *Agric. Food Chem.* 1983, **31**, 897-901.
18. Gardner, K. H.; Blackwell, J. *Biopolymers* 1974, **13**, 1975-2000.
19. Sarko, H.; Muggli, R. *Macromolecules* 1974, **7**, 486-94.
20. Knapek, E. *Ultramicroscopy* 1982, **10**, 71.
21. Sugiyama, J.; Harada, H.; Fujiyoshi, Y.; Uyeda, N. *Mokuzai Gakkaishi* 1984, **30**, 98.
22. Harada, H. *Mokuzai Gakkaishi* 1984, **30**, 513.
23. Revol, J.-F. *J. Mat. Sci. Let.* 1985, **4**, 1347.
24. Ruben, G. C.; Telford, J. N. *J. Microsc.* 1980, **118**, 191-216.
25. Ruben, G. C. *Proc. 39th Ann. Mtg. Elect. Microsc. Soc. Amer.* 1981, p. 566.
26. Ruben, G. C. *Proc. 39th Ann. Mtg. Elect. Microsc. Soc. Amer.* 1981, p. 568.
27. Ruben, G. C. *Proc. 39th Ann. Mtg. Elect. Microsc. Soc. Amer.* 1981, P. 570.
28. Simon, I.; Scheraga, H. A.; Manley, R. St.J. *Macromolecules* 1988, **21**, 983-90.



29. Viswanathan, A.; Shenouda, S. C. *J. Appl. Polymer Sci.* 1971, **15**, 519-35.
30. Zugenmaier, P. In *Wood and Cellulosics*; Kennedy, J. F.; Phillips, G. O.; Williams, P. A., Eds.; Ellis Harwood: Chichester, 1987; 231-38.
31. Simon, I.; Glasser, L.; Scheraga, H. A.; Manley, R. *St.J. Macromolecules* 1988, **21**, 990-98.
32. Roberts, E.; Legge, R.; Lin, F. C.; Brown, D.; Brown, R. M., Jr. Video Microscopy movie of Cellulose Synthesis shown at *24th Ann. Mtg. of Amer. Soc. Cell Biol.* 1984, 880a.

RECEIVED May 19, 1989

## Chapter 21

# Structural Characterization and Visualization In Situ and After Isolation of Tobacco Pectin

George C. Ruben<sup>1</sup> and Gordon H. Bokelman<sup>2</sup>

<sup>1</sup>Department of Biology, Dartmouth College, Hanover, NH 03755

<sup>2</sup>Philip Morris USA, Research Center, Richmond, VA 23234

Recently two different disciplines, chemical structural elucidation and transmission electron microscopy, were utilized in the study of pectin, with particular emphasis on tobacco pectin. The goal was to help bridge the gap between knowledge of their chemical structures to understanding the complex physical structures revealed by microscopy. To provide background on chemical structure, a study established that tobacco pectin was present as a series of related rhamnogalacturonans. All of these polysaccharides had a backbone consisting of 4-linked  $\alpha$ -D-galactopyranosyluronic acid residues interspersed with 2-linked L-rhamnopyranosyl residues. However, they varied in content of neutral sugars and extent of methyl-esterification. The presence of rhamnose in the backbone of pectin was believed to create "kinks" which probably disrupted helical stretches of the 4-linked  $\alpha$ -D-galactopyranosyluronic acid residues. In the present study pectin samples were gelled in deionized water, air-dried or freeze-dried, platinum-carbon replicated, carbon-backed and then examined by high resolution transmission electron microscopy. The pectin was found to be present as single chains of  $7 \pm 3\text{\AA}$  diameter that showed helical stretches with a  $13\text{\AA}$  left-handed surface striation.

Pectin is the major component found in the primary cell walls of dicots and may play a vital role in cell growth. During cell growth, loosening of the cell wall by acidification is an important process which enables the cell to elongate by its own turgor pressure. It has been suggested that the primary action of acidification is the loosening of a calcium pectate gel within the

0097-6156/89/0399-0300\$06.00/0

© 1989 American Chemical Society

cell wall (1). Pectin is also found in the middle lamella of land plant tissues where it is thought to function as an intercellular binding agent (2).

Pectin constitutes 11-12% of the total solids (3) or 34% of the cell wall materials (4) in tobacco lamina. By contrast, all of the following components are found to a lesser extent within the cell walls of tobacco lamina: protein (21.6%), cellulose (18.7%), hemicellulose (11.4%), and lignin (4.1%).

Galacturonic acid is the major constituent of all natural pectins. Pectins also contain varying quantities of neutral sugars, principally arabinose, galactose and rhamnose (5). The carboxyl function of the galacturonosyl residues may be present as a methyl ester, acid or salt.

Pectins are best known for their ability to form gels (6), a property which often involves intermolecular binding mediated by calcium cations (7). The principal commercial use of pectin is in the preparation of jelly and jam products (8). Pectins provide firmness in fresh fruits and vegetables (9-11). Historically, natural tobacco pectins also have been used as binders to prepare reconstituted sheets from tobacco by-products that are then incorporated into cigarette filler or cigar wrappers (12-14).

Pectins have been structurally characterized by a combination of chemical and spectroscopic methods.  $^{13}\text{C}$  NMR can be used to examine the purity, degree of esterification, and neutral sugar content of pectins (15). The monomeric composition of pectins may be determined directly by a combination of methanolysis (16) and silylation procedures to yield O-silylated methylglycosides that can be quantitated by GC (15). The linkage pattern of the monomeric sugars may be determined by methylation analysis. This procedure involves methylation of the starting pectin by the Hakomori method (17-19), reduction of the carboxylic acid functions (18), hydrolysis, reduction of the aldehyde functions and acetylation to yield partially methylated alditol acetates. The partially methylated alditol acetates then can be analyzed by GC/MS (20). In a variation of the procedures listed above, partial acid hydrolysis may be used to generate a series of di- and oligosaccharide derivatives (15). These derivatives can be identified by their electron impact mass spectral fragmentation (21). From all of the above information the chemical structure of the starting pectin then may be deduced.

The results from structural studies on pectins isolated from a number of different plant sources have been reported in several papers and review articles (10, 22-28). Chemical investigations of tobacco pectin (15, 29-31) have demonstrated that its structure is consistent with the basic structural elements found in pectins from other sources.

In one recent study (15), isolation and purification of tobacco pectin yielded a series of related rhamnogalacturonans. All of these polysaccharides were found to have a backbone consisting of 4-linked  $\alpha$ -D-galactopyranosyluronic acid residues interspersed with 2-linked L-rhamnopyranosyl residues in a ratio of  $\sim 16:1$  (see Fig. 1). The presence of rhamnose in the backbone of pectin is believed to create "kinks" which probably disrupt helical stretches of the 4-linked  $\alpha$ -D-galactopyranosyluronic acid



- Rha = L-rhamnopyranosyl residue  
 GalA = D-galactopyranosyluronic acid residue  
 6-Me-GalA = methyl-esterified D-galactopyranosyluronic acid residue  
 R = terminal  $\alpha$ -L-arabinofuranosyl residue  
       5-linked  $\alpha$ -L-arabinofuranosyl residue  
       terminal  $\beta$ -D-galactopyranosyl residue  
       4-linked  $\beta$ -D-galactopyranosyl residue

Figure 1. Model chemical structure of tobacco pectin.

residues (10). These tobacco rhamnogalacturonans varied in content of neutral sugars and extent of methyl-esterification. Their average degree of polymerization was estimated to be 400.

X-ray fiber diffraction studies have been performed on sodium and calcium pectate gels (32). From this research a working model for the helical portions of the pectin chain has emerged, which is important for comparison to the transmission electron microscopy (TEM) studies. The fiber diffraction gel models assume antiparallel  $\alpha$ -(1  $\rightarrow$  4) polygalacturonate chains which, when viewed down the c axis of the pectic acid unit cell, average about  $6.8 \times 7.2 \text{ \AA}$  along the a and b directions for a single sugar chain, respectively. One or two waters of hydration can increase this size by  $3 \text{ \AA}$  or  $6 \text{ \AA}$  (33, 34) in deep-etched preparations or an associated calcium ion can increase its cross-sectional dimensions by about  $2 \text{ \AA}$  (35).

Few previous attempts have been made to visualize pectin at the molecular level (36). In the present study, a Pt-C replication technique and TEM were used to characterize the uncutinized surface of lower epidermal cells (facing mesophyll cells) in both fresh, green and senescing Coker 319 tobacco leaves. These surfaces were compared to freeze-dried and air-dried calcium-free pectin gels. The surface textures and estimated diameters of single pectin chains in these preparations were compared. With high magnification imaging we were able to confirm the presence of the polygalacturonate chain helix in tobacco and citrus pectins.

### Methods and Materials

The tobacco pectin used in this study was obtained from a single grade of heavy or bodied, field-grown, flue-cured bright tobacco harvested at the upper midstalk position. Crude tobacco pectin was obtained by extraction with hot water of the tobacco lamina that previously had been treated with aqueous ethanol to remove waxes, nicotine, simple sugars and other low molecular weight components (15). This crude product was purified by tangential flow ultrafiltration, ion exchange chromatography and gel permeation chromatography (15). The purified tobacco pectin had a galacturonic acid content of  $\sim 80\%$ , a degree of esterification of  $\sim 22$  and a degree of polymerization of  $\sim 400$ . A separate sample of deesterified pectin was obtained by saponification (15) of the purified tobacco pectin.

Gels were obtained in the following manner from both the purified, starting tobacco pectin and the deesterified pectin obtained from it. First the sample of pectin was solubilized in deionized  $100^\circ\text{C}$  water ( $\sim 1\%$  solution). Then the pectin was gelled by ethanol vapor, introduced slowly (6 hrs) by surrounding the vessel containing aqueous pectin with  $100\%$  ethanol in a closed container at  $20^\circ\text{C}$ .

The gel from the purified tobacco pectin was formed on  $1.3 \text{ cm}$  ashless Whatman 50 filter paper discs which were frozen in propane at about  $-190^\circ\text{C}$ . These samples were then freeze-dried (90 min) at  $-70^\circ\text{C}$ , replicated with  $16.9 \text{ \AA}$  Pt/C at  $-178^\circ\text{C}$  in a  $5 \times 10^{-8}$  torr. vacuum and backed with  $146 \text{ \AA}$  of carbon. Finally, these samples were digested with  $80\%$  sulfuric acid, rinsed with deionized water, picked up from underneath with

carbon-coated 300 mesh grids (37) and examined by transmission electron microscopy. Unless specifically noted otherwise, the same general procedures were employed to prepare other samples for TEM examination. A more detailed discussion of the TEM procedures used, including micrograph reversals, has been published previously (37).

Citrus pectin ("Polygalacturonic Acid Methyl Ester from Citrus Fruits, Grade I") was obtained from the Sigma Chemical Company. It had a galacturonic acid content of ~ 89% and a degree of esterification of ~ 57. Separate aqueous solutions of citrus pectin were freeze-dried and air-dried in deionized water. These samples were replicated with 9.8Å Pt/C and backed with 148Å of carbon. The replicas for these samples were picked up without a carbon support film (38).

The following procedure was used to obtain images of the epidermal cell surfaces which face the mesophyll cells within the leaf interior. Both fresh green and senescing greenhouse-grown Coker 319 tobacco leaves were examined. The lower epidermal layer was peeled from the underside of each leaf, rinsed twice in a solution of 1:3/ethanol:water, and frozen on a  $\frac{1}{2}$ -in. mica disc. The senescing sample was freeze-dried at  $-80^{\circ}\text{C}$  for 105 min, replicated with 26.6Å Pt/C and backed with 215Å of carbon. The fresh, green sample was freeze-dried at  $-70^{\circ}\text{C}$  for 3 hr, replicated with 15.9Å Pt/C and backed with 139Å of carbon.

In a separate experiment a sample of the lower epidermal layer from a fresh, green Coker 319 tobacco leaf was treated with boiling water for 25 min. This sample was then rinsed, freeze-dried for 3.5 hr at  $-80^{\circ}\text{C}$ , replicated with 15.9Å Pt/C and backed with 133Å of carbon.

## Results and Discussion

Since it was known that pectin can be solubilized with hot water, a simple experiment was performed to help identify the location of pectin on the noncutinized surface of tobacco lower epidermal cells. The noncutinized surface of the lower epidermal cells is the side which faces the mesophyll cells. Figures 2A and 2B, respectively, show the control and treated samples for the noncutinized lower epidermal cell surface of a fresh, green Coker 319 tobacco leaf. Treatment consisted of immersing the lower epidermal peel in boiling water for 25 min. It may be seen in Figure 2A that the surface pectin coat was continuous, with numerous flat regions. This pectin coat disappeared following hot water extraction. Figure 2B shows the exterior surface of the lower epidermis for the boiling-water treated sample from which most of the pectin had been extracted. Some pectin-like material remained as smooth globs coating the filamentous primary cell wall cellulose. The contrast between Figures 2A and 2B indicated that a pectin gel permeates the cell wall.

Figures 3A and 3B show low and high magnification images of the noncutinized lower epidermal cell surfaces in a senescent Coker 319 tobacco leaf. The junctions between four different epidermal cells can be seen in Figure 3A. Also, multiple layers of pectin were evident on these lower epidermal cells, but were not present on the epidermal surface of

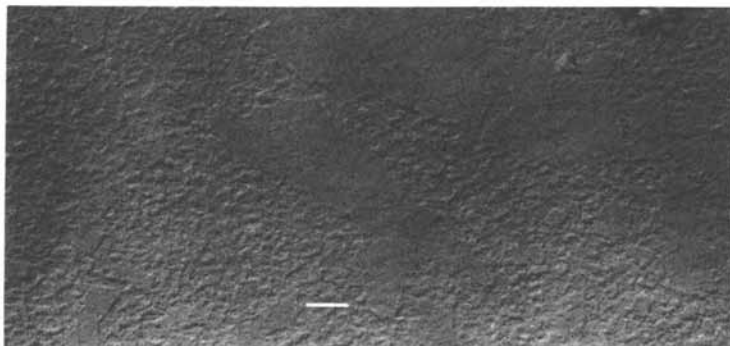


Figure 2A. Freeze-dried, Pt/C replicated, untreated noncutinized lower epidermal cell surface of a fresh, green Coker 319 tobacco leaf. (Bar = 1,000Å.)

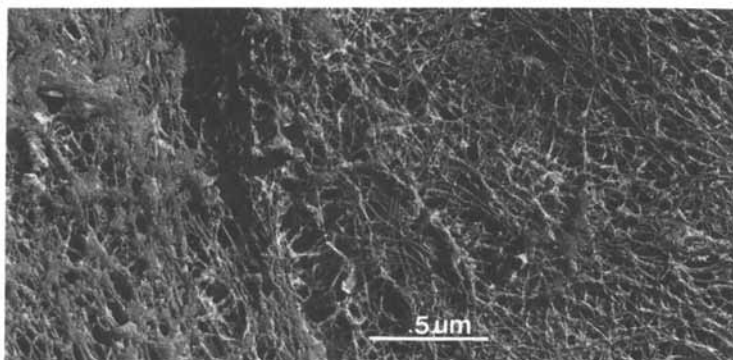


Figure 2B. Freeze-dried, Pt/C replicated, noncutinized lower epidermal cell surface of a fresh, green Coker 319 tobacco leaf treated with boiling water for 25 minutes. (Bar = 5,000Å.)

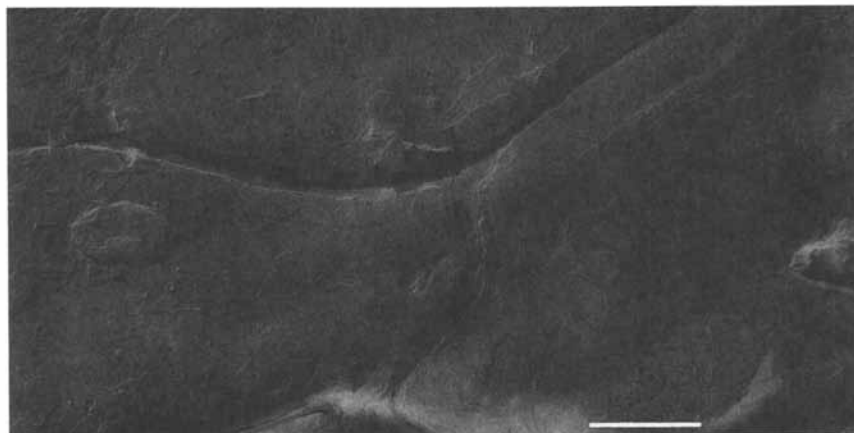


Figure 3A. Freeze-dried, Pt/C replicated, noncutinized lower epidermal cell surfaces in senescent Coker 319 tobacco leaf. (Bar = 5,000Å.)

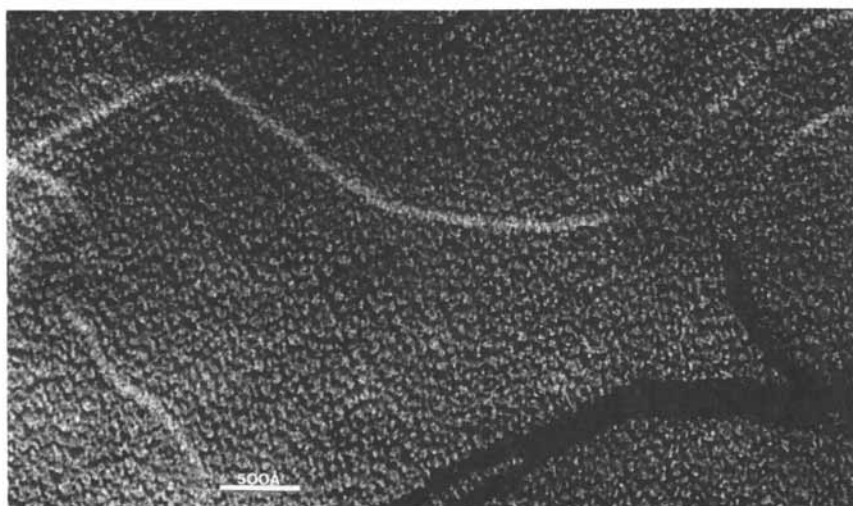


Figure 3B. Same as Figure 3A, except higher magnification. (Bar = 500Å.)



younger leaves (see Figure 2A). As many as 6 to 7 stacked surface layers were seen from which filaments protruded. The highly bent filaments with some linear stretches were even more evident in Figure 3B. The average filament width was measured at  $29.7\text{\AA}$  ( $n = 137$ , S.D. =  $4.8\text{\AA}$ ). Correction for the Pt/C film thickness (39) gave a real size of  $4.6 \pm 4.8\text{\AA}$ .

Figure 4A shows a relatively low magnification micrograph of a gel prepared from deesterified tobacco pectin. Unlike Figures 2A and 3A, its surface was smoother and did not show the layering effect seen on the lower epidermal cell surface.

Figure 4B is a high magnification micrograph of a gel of pectin filaments prepared from purified tobacco pectin. The average filament width with Pt/C coating was  $22.5\text{\AA}$ . After correcting for the added size due to the Pt/C coating (39), the pectin filament had a diameter of  $7.1 \pm 3\text{\AA}$  ( $n = 112$ , S.D. =  $3\text{\AA}$ ). Within the standard deviation of the measurements, the filament widths were the same for both the gel prepared from purified tobacco pectin and the tobacco epidermal cell surface. Both of these measurements also agreed very well with the x-ray fiber diffraction diameter,  $\sim 7\text{\AA}$ , which we estimated from the modeled gels of Walkinshaw and Arnott (32). On careful inspection, some of the pectin molecules in Figure 4B showed a left-handed surface striation occurring every  $13\text{\AA}$ . Walkinshaw and Arnott demonstrated that (citrus) pectin contained a  $13.3\text{\AA}$  3-fold helix in the polygalacturonate chain (32), but x-ray fiber diffraction did not give the helix handedness. We report here for the first time that it is a left-handed helix.

Since the x-ray fiber diffraction measurements based on citrus pectin (32) were consistent with the TEM measurements of tobacco pectin, we prepared a gel from citrus pectin similar to the previous x-ray sample. This gel was then examined by TEM. Air-dried samples of this gel, shown in Figure 5, demonstrated long stretches of helix in the molecules lying on the surface. (In the freeze-dried gels—not shown—only short stretches of helix were visible.) The average filament width in the air-dried gel was found to be  $14.2\text{\AA}$ . After correcting for the added size due to the Pt/C coating (39), the citrus pectin filament diameter was  $5.8 \pm 2\text{\AA}$  ( $n = 37$ , S.D. =  $2\text{\AA}$ ). In Figure 5 the citrus pectin molecules showed a left-handed surface striation occurring every  $13\text{\AA}$ . The surface helix period from both tobacco and citrus pectin samples was in agreement with the x-ray fiber diffraction measurements (32).

In conclusion, we have demonstrated that high resolution TEM is a valuable complement to x-ray fiber diffraction analysis and chemical structural elucidation. Its application provided information about the organization of pectin in cell walls and in calcium-free gels. Using freeze-dried samples that were Pt/C replicated, we demonstrated tobacco pectin filaments in a gel to be of the same diameter as the filaments on the noncutinized lower epidermal surface of senescing Coker 319 tobacco leaves. These filaments were  $7.1 \pm 3\text{\AA}$  and  $4.6 \pm 4.8\text{\AA}$ , respectively, and roughly the same diameter,  $\sim 7\text{\AA}$ , as fiber-diffraction modeled citrus pectin (32). Replicated

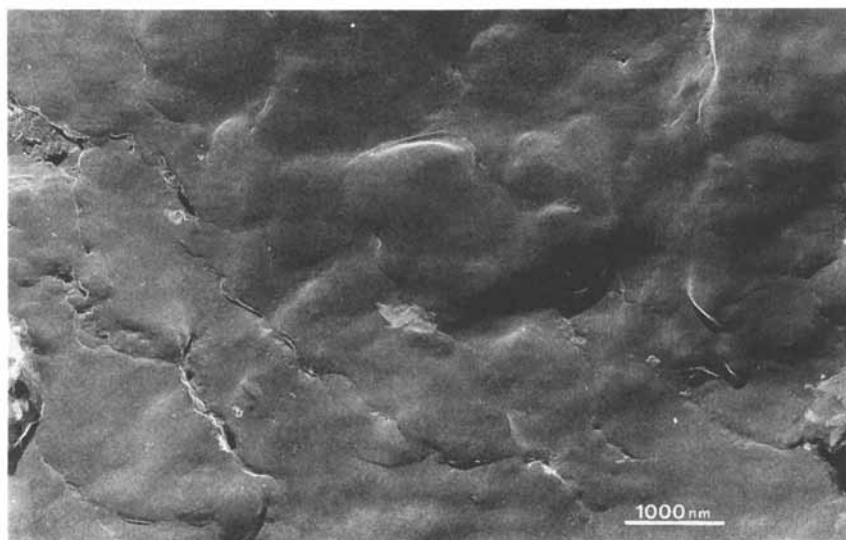


Figure 4A. Freeze-dried, Pt/C replicated gel prepared from deesterified tobacco pectin. (Bar = 10,000Å.)

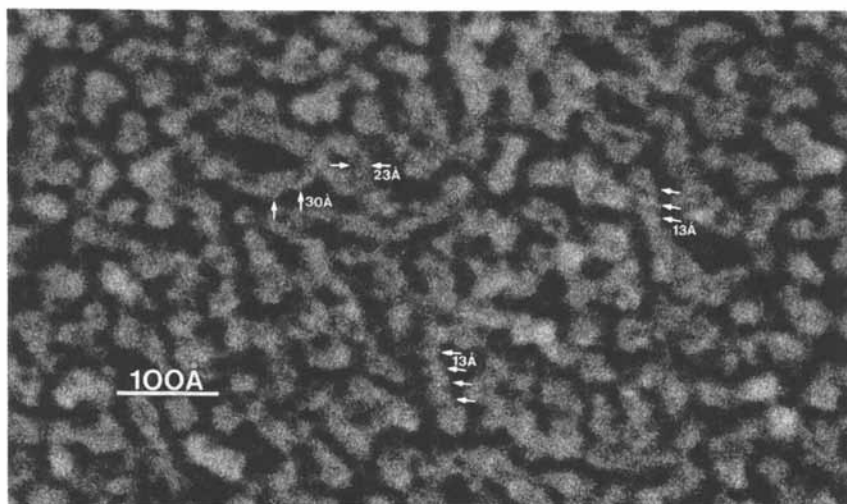


Figure 4B. Freeze-dried, Pt/C replicated gel prepared from tobacco pectin. This high magnification image shows two molecules with  $\sim 13\text{\AA}$  left-handed helical regions. (Bar = 100Å.)

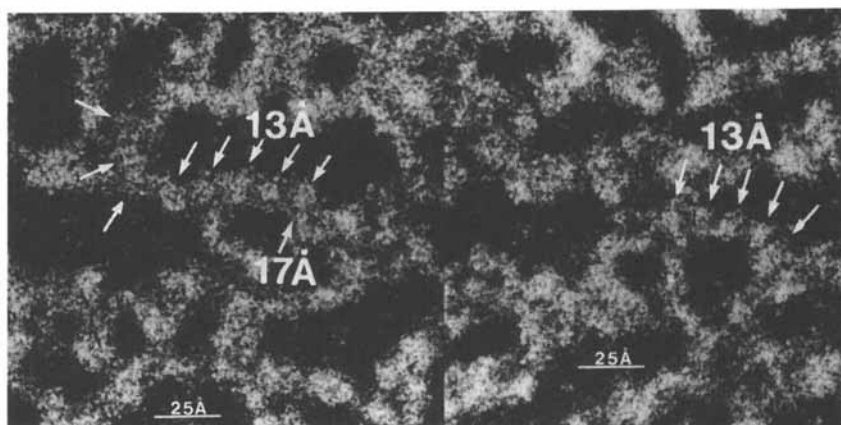


Figure 5. Air-dried, Pt/C replicated gel prepared from citrus pectin. This image features two pectin filaments with left-handed surface striations having  $\sim 13\text{\AA}$  spacings (Each bar =  $25\text{\AA}$ .)

citrus pectin filaments were also found to have similar diameters,  $5.8 \pm 2\text{\AA}$ . In addition, we demonstrated images, for the first time, of the left-handed surface spacings of  $\sim 13\text{\AA}$  in single pectin molecules, in both freeze-dried tobacco and air-dried citrus pectin.

We believe that single molecule imaging can contribute to a more thorough understanding of the role of pectin in the cell wall. Our future efforts will be focused on pectin gels formed in the presence of calcium. Eventually, it should be possible to visualize side chains on pectin and determine how rhamnose residues in the rhamnogalacturonan backbone of tobacco pectin disrupt the formation of helical regions.

### Literature Cited

1. Baydoun, E. A.-H.; Brett, C. T. *J. Exp. Bot.* 1984, **35**, 1820.
2. Dey, P. M.; Brinson, K. In *Advances in Carbohydrate Chemistry and Biochemistry*; Tipson, R. S.; Horton, D., Eds.; Academic Press: New York, 1984; Vol. 42, p. 265.
3. Bokelman, G. H.; Ryan, W. S., Jr.; Sun, H. H.; Ruben, G. C. *Recent Adv. Tob. Sci.* 1985, **11**, 71.
4. Bokelman, G. H.; Ryan, W. S., Jr.; Oakley, E. T. *J. Agric. Food Chem.* 1983, **31**, 897.
5. Aspinall, G. O.; Craig, J. W. T.; Whyte, J. L. *Carbohydr. Res.* 1968, **7**, 442.
6. Rees, D. A.; Welsh, E. J. *Angew. Chem. Int. Ed. Engl.* 1977, **16**, 214.
7. Whistler, R. L.; Smart, C. L. *Polysaccharide Chemistry*; Academic Press: New York, 1953.
8. Towle, G. A.; Christensen, O. In *Industrial Gums*, 2nd edn.; Whistler, R. L., Ed.; Academic Press: New York, 1973; p. 155.
9. Van Buren, J. P.; Peck, N. H. *J. Food Sci.* 1981, **47**, 311.
10. Jarvis, M. C. *Plant, Cell Environ.* 1984, **7**, 153.
11. McFeeters, R. F.; Fleming, H. P.; Thompson, R. L. *J. Food Sci.* 1985, **50**, 201.
12. Hind, J. D.; Seligman, R. B. U.S. Patent 3 353 541, 1967.
13. Hind, J. D.; Seligman, R. B. U.S. Patent 3 411 515, 1968.
14. Hind, J. D.; Seligman, R. B. U.S. Patent 3 420 241, 1969.
15. Sun, H. H.; Wooten, J. B.; Ryan, W. S., Jr.; Bokelman, G. H.; Åman, P. *Carbohydr. Polym.* 1987, **7**, 143.
16. Pritchard, D. G.; Todd, C. W. *J. Chromatogr.* 1977, **133**, 133.
17. Hakomori, S. *J. Biochem. (Tokyo)* 1964, **55**, 205.
18. Standford, P. A.; Conrad, H. E. *Biochemistry* 1966, **5**, 1508.
19. Phillips, L. R.; Fraser, B. A. *Carbohydr. Res.* 1981, **90**, 149.
20. Jansson, P. E.; Kenne, L.; Liedgren, H.; Lindberg, B.; Lonngren, J. *Chem. Commun. (Univ. of Stockholm)* 1976, No. 8.
21. Kochetkov, N. K.; Chizhov, O. S. In *Advances in Carbohydrate Chemistry*; Wolfson, M. L., Ed.; Academic Press: New York, 1966; Vol. 21, p. 39.
22. McNeil, M.; Darvill, A. G.; Albersheim, P. *Fortschr. Chem. Org. Naturst.* 1979, **37**, 191.

23. Aspinall, G. O. In *The Biochemistry of Plants*; Preiss, J., Ed.; Academic Press: New York, 1980; Vol. 3, p. 473.
24. Darvill, A. G.; McNeil, M.; Albersheim, P.; Delmer, D. P. In *The Biochemistry of Plants*; Tolbert, N. E., Ed.; Academic Press: New York, 1980; Vol. 1, p. 91.
25. Pilnik, W. *Proc. Eur. Symp. on Fiber in Human Nutrition, APRIA*, 1981, p. 91.
26. Selvendran, R. R. In *Dietary Fibre*; Birch, G. G.; Parker, K. J., Eds.; Applied Science Publishers: London, 1983; p. 95.
27. Pressey, R.; Himmelsbach, D. S. *Carbohydr. Res.* 1984, **127**, 356.
28. Keenan, M. H. J.; Belton, P. S.; Matthew, J. A.; Howson, S. J. *Carbohydr. Res.* 1985, **138**, 168.
29. Bourne, E. J.; Pridham, J. B.; Worth, H. G. J. *Phytochemistry* 1967, **6**, 423.
30. Eda, S.; Kato, K. *Agric. Biol. Chem.* 1980, **44**, 2793.
31. Siddiqui, I. R.; Rosa, N.; Woolard, G. R. *Tob. Sci.* 1984, **28**, 122.
32. Walkinshaw, M. D.; Arnott, S. J. *Mol. Biol.* 1981, **153**, 1055, 1075.
33. Marx, K. A.; Ruben, G. C. *J. Biomol. Struct. and Dynamics* 1984, **1**, 1109.
34. Ruben, G. C.; Telford, J. N. *J. Microsc.* 1980, **118**, 191.
35. Pauling, L. *The Nature of the Chemical Bond*; Cornell Univ. Press: Ithaca, NY, 1960; p. 518.
36. Hanke, D. E.; Northcote, D. H. *Biopolymers* 1975, **14**, 1.
37. Ruben, G. C.; Marx, K. A. *J. Elect. Microsc. Tech.* 1984, **1**, 373.
38. Ruben, G. C.; Bokelman, G. H. *Proc. 45th Ann. Meet. Elec. Microsc. Soc. Amer.*, 1987, p. 966.
39. Ruben, G. C.; Bokelman, G. H. *Carbohydr. Res.* 1987, **160**, 434.

RECEIVED March 10, 1989

## Chapter 22

# Control of Cell Wall Plasticity

## Relationship to Pectin Properties

**Renée Goldberg<sup>1</sup>, Paulette Devillers<sup>1</sup>, Roger Prat<sup>1</sup>, Claudine Morvan<sup>2</sup>,  
Véronique Michon<sup>3</sup>, and Catherine Hervé du Penhoat<sup>3</sup>**

**<sup>1</sup>Biomembranes et Surfaces Cellulaires Végétales, ENS, 46 rue d'Ulm,  
75230 Paris Cedex 05, France**

**<sup>2</sup>SCUEOR, Faculté des Sciences de Rouen, 76130 Mont-Saint Aignan,  
France**

**<sup>3</sup>Département de Chimie, Service RMN-ENS, 24 rue Lhomond 75231  
Paris Cedex, France**

Along the mung bean hypocotyl, the cell wall plasticity represents the limiting factor of cell growth potentials. Pectin molecules, known to control local cell wall pH's and to modulate phenolic cross-linking owing to the number of free acidic domains, were investigated. Young, plastic walls were characterized both by a high level of branched and methylated rhamnogalacturonans which leads to swollen cell walls and by a low level of linear galacturonans which induces a low Cation Exchange Capacity (CEC). In contrast, stiff, mature cell walls are characterized by a low water content and a high CEC which favors cross-linking.

The participation of pectins in controlling the extensibility of the primary cell walls has often been suggested. Most of the data described were obtained with dicots in which pectins account for 30 to 50% in the cell wall material, whereas monocots are known to be quite devoid of polyuronides. Correlations between cell wall plasticity and frequency of calcium bridges, degree of esterification or molecular size have been successively proposed. Recently new views about the manner in which pectins might participate in the control of cell wall extensibility have been expressed (1-3). On the one hand, pectins might intervene in cell wall stiffening processes as free acidic domains act as a template for cross-linking reactions (2). On the other hand, pectic molecules control local cell wall pH's and, consequently, positive or negative feedback systems (3). It is widely accepted that wall loosening as well as wall stiffening processes are enzymatically mediated. It may also be assumed that pectin properties will modulate the ability of cell walls to develop into more or less stretchable structures. We have therefore investigated the pectic material in fast and slow growing parts of Mung bean hypocotyls.

0097-6156/89/0399-0312\$06.00/0  
© 1989 American Chemical Society

## Materials and Methods

*Vigna radiata* (L. Wilczek) seedlings were raised as previously reported (4). Seedlings were grown 3 d at 26°C in the dark, and were used when the hypocotyls measured  $45 \pm 5.0$  mm.

**Growth Measurements.** Equidistant Indian ink marks were made along the hypocotyl and their displacements measured after 4 h. Displacement velocity was plotted as a function of the initial position of each mark, i.e., the distance from cotyledons. Relative elemental rates of elongation were then calculated as the derivatives of the displacement versus position (5). Growth measurements of excised segments were recorded with auxanometers using displacement transducers. The growth curves were then calculated with a microcomputer (TRS 80) as previously reported (6). Extensibility of the successive segments was estimated using two different methods. On the one hand, the segments (10 mm long) were pulled at a constant rate of deformation ( $60 \text{ mm min}^{-1}$ ) until a force (40 g) was reached, which required less than 1 sec. Irreversible deformation represents the immediate plasticity. On the other hand, the successive segments were subjected to a constant load (40 g) during 5 min and their length recorded during 10 min (5 min loading followed by 5 min unloading). Long term plasticity was then estimated by irreversible deformation. Strain values were calculated for both methods as irreversible deformations per mm.

Cell walls were isolated from 2 parts of the hypocotyl as previously described (7). Two pectic fractions, PF<sub>1</sub> and PF<sub>2</sub>, were sequentially extracted by boiling water and hot EDTA pH 6.0. As already reported, the residual cell walls were free of polygalacturonic acids (8). EDTA treatment did not significantly degrade the polyuronides since colorimetric estimations performed before and after dialysis gave similar results. The pectic fraction extracted by boiling water was submitted to ion-exchange chromatography on DEAE-Sephacrose CL6B (Pharmacia) equilibrated with 0.05 M sodium acetate buffer (pH 4.7). Neutral polysaccharides were not bound and acidic polysaccharides APF1 were eluted with 1 M buffer (9). Calcium contents of the pectic fractions were determined by atomic spectrophotometry with lanthanum as internal standard. Potentiometric measurements and estimations of selectivity coefficients were run according to ref. 8. Calcium activity was measured using a specific electrode (10). Galacturonic acids were estimated with m-diphenol (11). For estimation of cell wall water content, the diffusion film was eliminated from isolated cell walls on filter paper and the weight of the wet cell walls (MF) was estimated (10). The wall dry weight (MS) was measured after 1 h at 50°C. The cell wall water content (t) was obtained from the relation  $t = (MF - MS)/MS$ . The relative error was less than 10%.

A Bruker AM 400 spectrometer operating in the F.t. mode at 400.13 MHz for <sup>1</sup>H and 100.57 MHz for <sup>13</sup>C was used for NMR investigations. Samples were dissolved in D<sub>2</sub>O at 70°C. (CD<sub>3</sub>)<sub>2</sub>SO was the internal reference ( $\delta_c$  39.5,  $\delta_H$  2.72). Measurements were performed as described previously (9).

## Results and Discussion

*Growth Gradient Along the Mung Bean Hypocotyl.* Accurate estimation of growth potentials of cells *in situ* is difficult. Along an axis, indeed, data obtained by measuring mark displacements actually correspond to the cumulative cell growth at the successive levels crossed during the time of experiments. This difficulty had been overcome by estimating the derivatives of displacement velocities (5). These data give the instantaneous rate of elongation at each point on the axis. Along the Mung bean hypocotyl, this elongation rate decreases regularly from the hook (segment b) to the base (Fig. 1A). *In vitro* growth measurement using excised segments does not indicate the initial state of growth but the elongation of the sample after the excision. These measurements show the same growth gradient (Fig. 1A). In order to check whether wall properties were the growth limiting factor along the hypocotyl, wall plasticity of successive hypocotyl segments was measured using two different methods. As illustrated in Figure 1B, immediate plasticity as well as long term plasticity obviously decreased along the Mung bean hypocotyl. These data suggest that along this growing organ the plastic properties of the cell walls might control the growth potential of the cells.

*Composition of Pectin Fractions Extracted from Young and Mature Cell Walls (Table I).* Young cell-walls contained more polyuronides soluble in hot water and less polyuronides soluble in EDTA than mature cell walls. Calcium ions were mostly bound to water-insoluble pectins. In this fraction the galacturonic acid/ $\text{Ca}^{2+}$  ratio is identical for young and mature cell walls which indicates similar affinity for  $\text{Ca}^{2+}$  ions. Moreover, PF<sub>2</sub> polyuronides, in contrast to PF<sub>1</sub>, were not methylated. The activity of the calcium ions was estimated in each fraction. The mean distance between two free charges,  $b$ , could then be calculated (8). Extracts from young and mature cell walls gave close data. PF<sub>1</sub>  $b$  values were higher than  $b$  values of PF<sub>2</sub> but deesterified PF<sub>1</sub> was similar to PF<sub>2</sub>, the average distance between two free charges then being near 4.4 which corresponds to the value calculated for polygalacturonic acid. The principal chains of PF<sub>1</sub> and PF<sub>2</sub> molecules are then constituted by linked galacturonic acid molecules, 70% of which are methylated in PF<sub>1</sub> extracts. In PF<sub>1</sub>, the average distance between two free charges is nearly three times as great as the value obtained after deesterification. It is possible that PF<sub>1</sub> extracts contain orderly arranged molecules with a repeating unit constituted by two successive methylated molecules followed by an unmethylated one. Succession of extended sequences of methylated and unmethylated molecules would provide different values for  $\gamma\text{Ca}$ . Indeed, according to Kohn (12), occurrence of more than 8 successive unmethylated molecules inside a polygalacturonic chain entails low  $\gamma\text{Ca}$  values similar to those measured with polygalacturonic acid (i.e., nearly 0.18). However, a succession of short sequences (< 8 units) of methylated and unmethylated molecules cannot be excluded. Lastly, the high neutral/acidic sugars ratio noted for PF<sub>1</sub> might correspond to neutral sidechains.



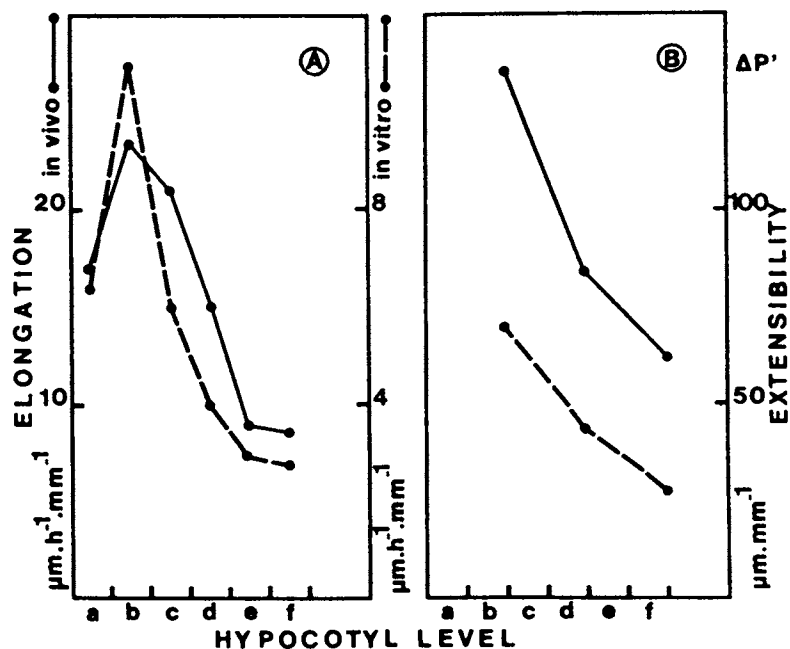


Figure 1. Development of growth potential and cell wall extensibility along the mung bean hypocotyl. A, elongation rates as  $\mu\text{m}/\text{h}^{-1}/\text{mm}^{-1}$ ;  $\bullet$ — $\bullet$  relative elemental elongation rate;  $\bullet$ — — — $\bullet$  spontaneous elongation of excised segments. B, cell wall extensibility as  $\mu\text{m}/\text{mm}^{-1}$ ;  $\bullet$ — $\bullet$  immediate plasticity;  $\bullet$ — — — $\bullet$  long term plasticity. Data correspond to irreversible deformations measured as described in Materials and Methods.

Table I. Composition of Pectic Fractions Extracted with Boiling Water (PF<sub>1</sub>) and Hot EDTA (PF<sub>2</sub>) from Young and Mature Cell Walls

	Young Cell Walls		Mature Cell Walls	
	PF <sub>1</sub>	PF <sub>2</sub>	PF <sub>1</sub>	PF <sub>2</sub>
Uronic acids (UA)	960	340	540	610
Calcium	50	10	45	200
Neutral/acidic sugars	1.05	0.35	0.90	0.12
UA/Calcium	19.2	3.10	12.0	3.05
DE (%)	70	0-10	70	0-10
$\gamma$ Ca				
intact pectins	0.57	0.18	0.58	0.15
demethylated pectins	0.22		0.20	
b	13.5	4.4	13.8	3.5

Uronic acids and Ca<sup>2+</sup> as  $\mu\text{eq.g}^{-1}$ .

DE, degree of esterification.

$\gamma$ Ca = activity coefficient of calcium ions.

b, average distances between two free charges, in Angströms, is calculated from the relations:  $\text{Ln } \gamma\text{Ca} = -0.5 - \text{Ln } 2\xi$  and  $\xi = 7.15 \text{ \AA}/b$ ;  $\xi$  is a dimensionless structural parameter, the charge density of the pectins.

We have also tried to investigate intact, unhydrolyzed pectic materials with NMR spectroscopy. Unfortunately, highly methylated PF<sub>1</sub> as well as PF<sub>2</sub> were unsuitable for high resolution NMR studies due to low solubility. Na<sup>+</sup> or Li<sup>+</sup> salt forms of the samples gave better results. <sup>13</sup>C spectra of the Na<sup>+</sup> form of PF<sub>1</sub> and PF<sub>2</sub> are given in Figure 2. On these spectra the major residues are (1 → 5) linked  $\alpha$ -arabinofuranose, (9,13,14), (1 → 4) linked  $\beta$ -galactopyranose (9,15,16), and (1 → 4) linked  $\alpha$ -galacturonic acid. The <sup>1</sup>H NMR spectra of these samples were compatible with the <sup>13</sup>C assignments and are in accord with literature data (9,17-19). Rhamnose could not be detected although GC performed after acid hydrolysis (8) revealed the presence of small amounts, nearly 4%, in all pectic fractions. The intensity of the C<sub>5</sub> signal of arabinofuranose at 68.3-68.5 ppm is consistently weaker, by about 80%, than that of the methine carbons 1-4. This C<sub>5</sub> signal was absent in the <sup>13</sup>C NMR spectrum of PF<sub>2</sub>. These data suggest either that arabino-furanose residues occupy terminal positions or that the furanosyl signals belong to another residue such as  $\beta$ -galacto-furanose. Galacturonic acid levels were much lower than the values obtained from m-diphenyl estimations. The very weak signals observed for galacturonic acid in the NMR spectra might be due to multichain aggregation processes which have already been described for very dilute solutions (17,20-22). Disappearance of NMR signals of pectins has already been reported for both solid (23) and liquid-state experiments (17). Ultrasonication did not improve the results. All these data show that PF<sub>1</sub> contains highly methylated, highly branched rhamnagalacturonans. Galactose and arabinose build sidechains

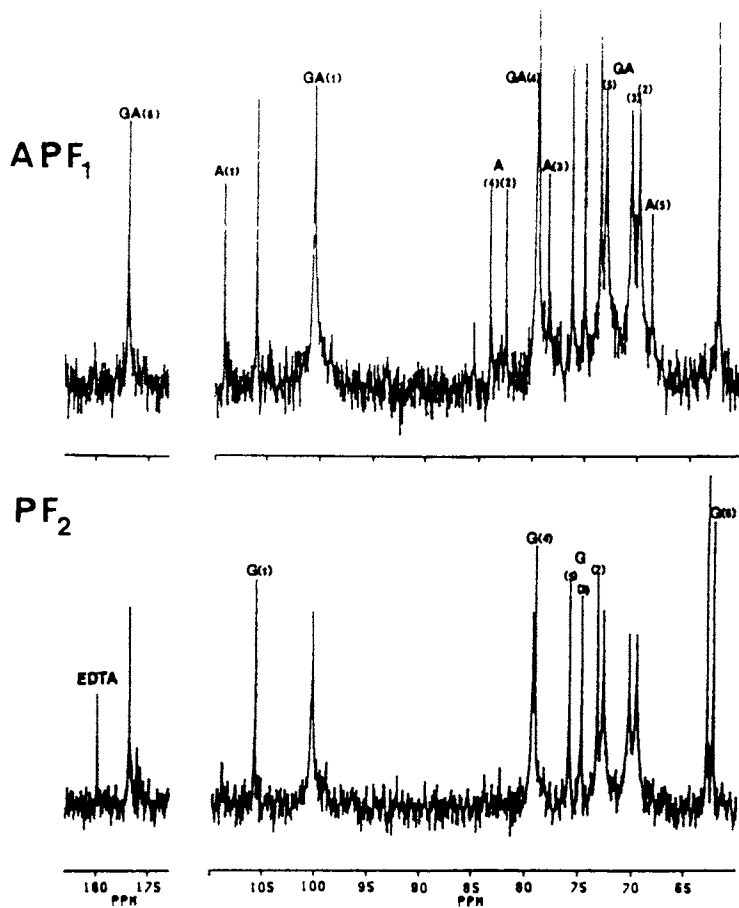


Figure 2. 100 MHz  $^{13}\text{C}$  spectra of pectic fractions. Internal  $\text{Me}_2\text{SO}$ ,  $\delta$  39.5—GA, galacturonic acid; G, galactose; A, arabinose.

(about 3 times more galactose than arabinose) which contain terminal arabinose. In contrast, PF<sub>2</sub> contains mostly homogalacturonans. The neutral sugars, from 10% to 30%, detected in this fraction might represent either contaminations with PF<sub>1</sub> or some short sidechains.

*Physicochemical Properties of Pectins. Solubilized Pectins.* Pectins solubilized by boiling water (PF<sub>1</sub>) and further extracted by EDTA (PF<sub>2</sub>) from young and mature cell walls were characterized by potentiometric measurements. Titrations were performed with different counterions: K<sup>+</sup>, Na<sup>+</sup>, Mg<sup>2+</sup>, Ca<sup>2+</sup>. In all cases the pH curves diverged for monovalent and divalent ions for neutralization degrees > 0.5 (Fig. 3A,C,D). This divergence is essentially due to valence differences. No differences could be detected when PF<sub>1</sub>'s were neutralized with Ca(OH)<sub>2</sub> or Mg(OH)<sub>2</sub>, whereas titration curves of PF<sub>2</sub>'s revealed a higher selectivity for calcium ions (Figs. 3B and 3D). However, saponification of PF<sub>1</sub>, which deesterifies the methylated polymers, induced a slight shift between Mg(OH)<sub>2</sub> and Ca(OH)<sub>2</sub> titration curves (Fig. 3C). With monovalent counterions, a difference in affinity for Na<sup>+</sup> and K<sup>+</sup> was noted (Fig. 3A). Curves obtained with pectic fractions isolated from young and mature cell walls were not significantly different.

*Pectins in situ.* After boiling water treatment, the residual cell walls contained only PF<sub>2</sub> pectins. Cation exchange capacity (CEC) of these cell walls was estimated for different pH's. In all cases, young cell walls exhibited a smaller CEC than the older ones (Fig. 4). Exchanges were then performed in order to compare the relative cell wall affinities for Ca<sup>2+</sup> and Mg<sup>2+</sup> ions. After hot water extraction, the selectivity coefficients  $K_{Mg}^{Ca}$  of young and mature cell walls were almost identical (Fig. 5C) for all pH values. The ionization of mature walls was higher than that of young ones (Fig. 5D). After EDTA treatment, the cell walls no longer behaved as cation exchangers, which reveals a complete solubilization of pectins.

Crude cell walls which contained both PF<sub>1</sub> and PF<sub>2</sub> fractions were also investigated. Their CEC values were higher than those measured for hot water extracted cell walls (Fig. 4) and young cell walls exhibited a smaller CEC than the older ones. The differences between the CEC's of crude and hot water extracted polymers can thus be attributed to the PF<sub>1</sub> polymers. Exchange experiments showed that, at constant ionic strength and equal ionic fractions of Ca<sup>2+</sup> and Mg<sup>2+</sup>, the selectivity coefficients were always higher for mature cell walls than for young ones. Whatever the value of the pH in the incubation medium (Fig. 5A), young crude cell walls exhibited a lower coefficient than young, hot water extracted ones. The PF<sub>1</sub> fraction, much more abundant in young cell walls (Table I), had a lower affinity for Ca<sup>2+</sup> ions than PF<sub>2</sub>. These data confirm the results obtained with pectins in solution. Physicochemical behavior of cell walls results then from the PF<sub>1</sub>/PF<sub>2</sub> ratios, the properties of the pectins embedded in the polysaccharide network being identical to those of solubilized pectins.

Water contents of intact and extracted cell walls were also estimated (Table II). The amount of absorbed water was the highest in young, intact cell walls. After boiling water treatment, the swelling of the cell walls was lower and quite similar for young and mature cell walls. The high water

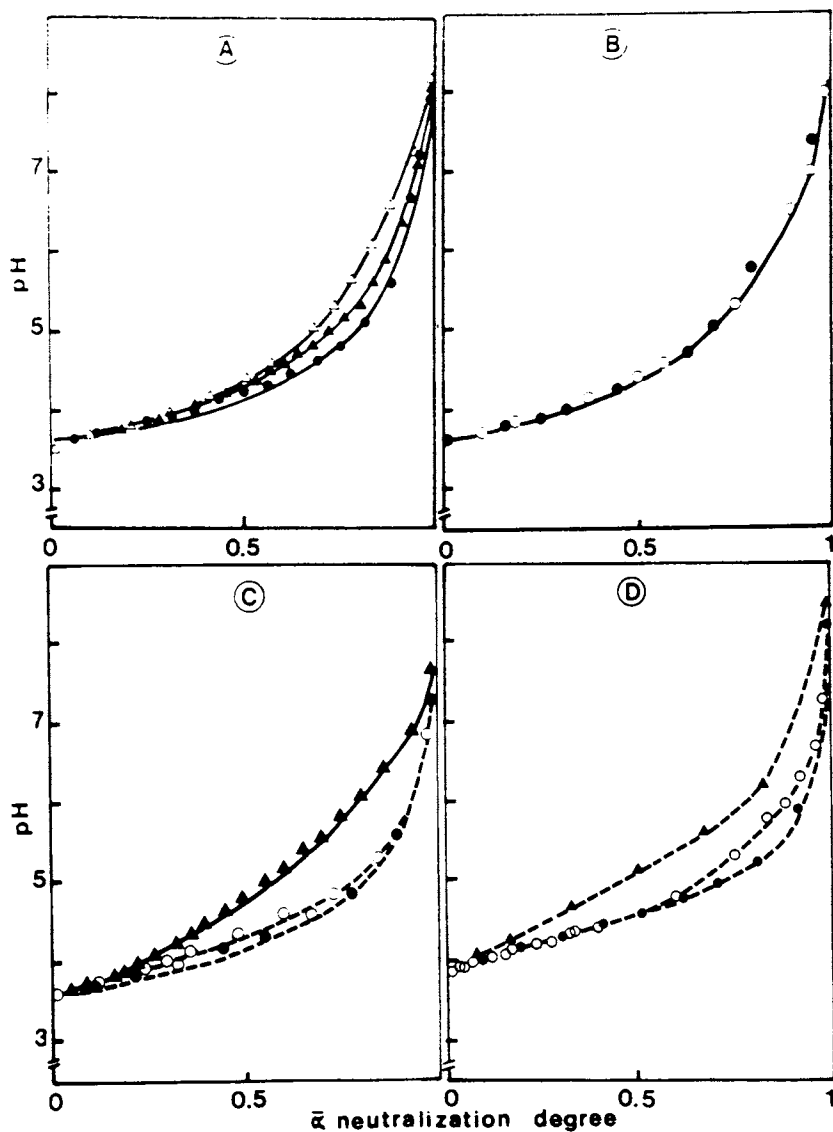


Figure 3. Titration of pectin fractions extracted from young cell walls. A, B, C, pectins extracted with boiling water; D, extracted with hot EDTA. A, B, intact PF<sub>1</sub>; C, demethylated PF<sub>1</sub>. Titrations were performed with KOH ( $\Delta$  —  $\Delta$ ), NaOH ( $\blacktriangle$  —  $\blacktriangle$ ), Ca(OH)<sub>2</sub> ( $\bullet$  —  $\bullet$ ), and Mg(OH)<sub>2</sub> ( $\circ$  —  $\circ$ ).

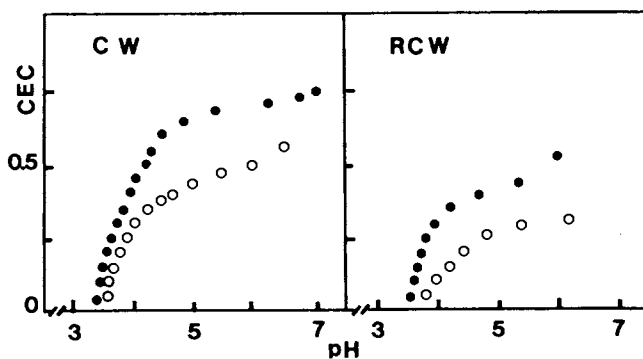


Figure 4. Cation exchange capacity (CEC) of isolated cell walls as a function of the pH of the incubation medium—CEC as meq per g cell walls. The titrations were run in  $\text{CaCl}_2$  solutions ( $I = 100 \text{ mM}$ ). CW, intact isolated cell walls; RCW, residual cell walls after boiling water treatment. ● — ● mature cell walls; ○ — ○ young cell walls.

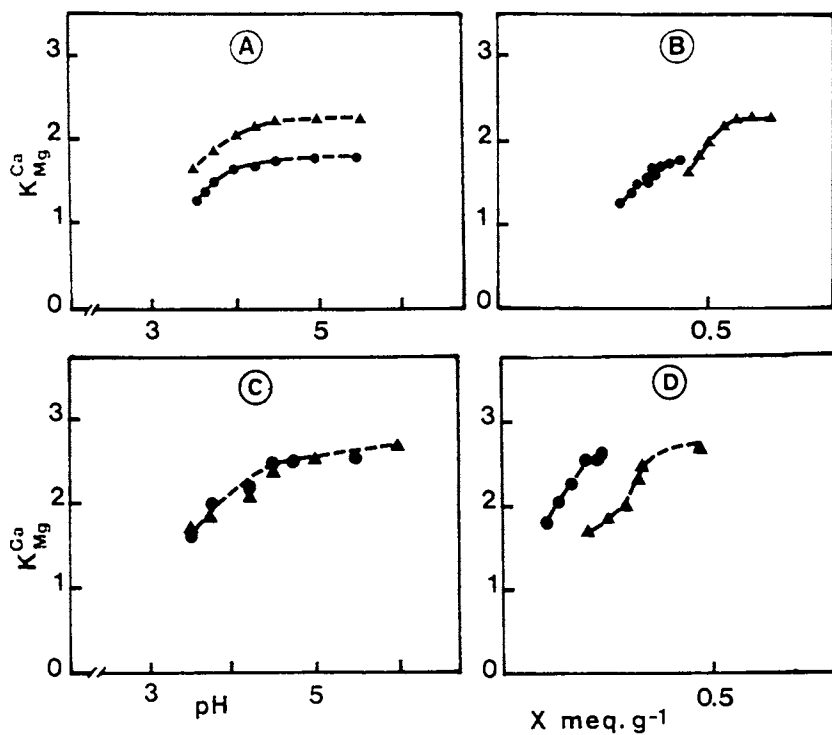


Figure 5. Selectivity coefficients  $K_{Mg}^{Ca}$  of young ( $\bullet$  —  $\bullet$ ) and mature ( $\blacktriangle$  —  $\blacktriangle$ ) cell walls. Values of  $K_{Mg}^{Ca}$  plotted as a function of pH (A, C) and of  $x$ , the number of ionized carboxyl groups (B, D). A and B, intact isolated cell walls; C and D, cell walls previously extracted by boiling water.

content of young cell walls results from the high amount of PF<sub>1</sub> in these walls. These data might explain the microscopic aspects of both kinds of cell walls, the young ones being more swollen than the mature ones (8).

Table II. Water content of intact (CW) and extracted cell walls (RCW) isolated from young and mature tissues of the hypocotyl as percent of cell wall dry matter

Young Tissues		Mature Tissues	
CW	RCW	CW	RCW
850	260	425	260

In conclusion, along the mung bean hypocotyl, the cell growth potential depends upon the wall extensibility. Young, plastic walls are characterized by a high level of branched and methylated rhamnogalacturonans which leads to swollen cell walls and a low level of linear galacturonans which induces a low CEC. In contrast, stiff, mature cell walls are characterized by a low water content and a high CEC. The low water content indicates stronger cohesion of the polysaccharide network. The high CEC is a possible factor for crosslinking and in turn for wall stiffening processes.

### Literature Cited

1. Lamport, D. T. A. In *Cellulose: Structure Modification and Hydrolysis*; Young, R. A.; Rowell, R. M., Eds.; John Wiley & Sons: New York, 1986; p. 77-90.
2. Fry, S. C. *Ann. Plant Physiol.* 1986, **37**, 165-86.
3. Nari, J.; Noat, G.; Diamantidis, G.; Woundstra, M.; Ricard, J. *Eur. J. Biochem.* 1986, **155**, 199-202.
4. Goldberg, R.; Prat, R. *Physiol. Veg.* 1981, **19**, 523-32.
5. Prat, R. *J. Exp. Bot.* 1985, **36**, 1150-58.
6. Bouchet, M. H.; Prat, R.; Goldberg, R. *Physiol. Plantarum* 1983, **57**, 95-100.
7. Goldberg, R. *Plant Sci. Lett.* 1977, **8**, 233-42.
8. Goldberg, R.; Morvan, C.; Roland, J. C. *Plant Cell Physiol.* 1986, **27**, 417-29.
9. Hervé du Penhoat, C.; Michon, V.; Goldberg, R. *Carbohydr. Res.* 1987, **165**, 31-42.
10. Morvan, C.; Demarty, M.; Thellier, M. *Physiol. Veg.* 1985, **23**, 333-44.
11. Blumenkrantz, N.; Asboe-Hansen, G. *Anal. Biochem.* 1973, **54**, 484-89.
12. Kohn, R. *Pure Appl. Chem.* 1975, **42**, 371-95.
13. Joseleau, J. P.; Chambat, G.; Lanvers, M. *Carbohydr. Res.* 1983, **122**, 107-13.
14. Capek, P.; Toman, R.; Kardosova, A.; Rosik, J. *Carbohydr. Res.* 1983, **117**, 133-40.



15. Eby, R.; Schuerch, C. *Carbohydr. Res.* 1981, **92**, 149-53.
16. Gorin, P. A. J.; *Carbohydr. Res.* 1982, **101**, 13-20.
17. Rinaudo, M.; Ravanat, G.; Vincendon, M. *Makromol. Chem.* 1980, **181**, 1059-70.
18. Joseleau, J. P.; Chambat, G. *Physiol. Vég.* 1984, **22**, 461-70.
19. Nakahara, Y.; Ogawa, T. *Carbohydr. Res.* 1987, **167**, C1-C7.
20. Jordan, R. C.; Brant, D. A. *Biopolymers* 1978, **17**, 2885-95.
21. Davies, M. A. F.; Gidley, M. J.; Morris, E. R.; Powzll, D. A.; Rees, D. A. *Int. J. Biol. Macromol.* 1980, **2**, 330-32.
22. Grasladeu, H.; Kvam, B. J. *Macromolecules* 1986, **19**, 1913-20.
23. Keenan, M. H. J.; Belton, P. S.; Matthew, J. A.; Howson, S. J. *Carbohydr. Res.* 1985, **138**, 168-77.

RECEIVED May 19, 1989

## Chapter 23

# Effect of Chemical Structure of Pectins on Their Interactions with Calcium

M. Rinaudo

University Joseph Fourier of Grenoble, Centre de Recherches  
sur les Macromolécules Végétales, Centre National de la Recherche  
Scientifique, B.P. 53X-38041, Grenoble Cedex, France

The interaction of  $\text{Ca}^{2+}$  with pectins is discussed. The role of carboxylic acid salt formation and the degree of polymerization are first considered in terms of electrostatic and/or cooperative specific interactions. Then the effect of the degree of esterification and that of the pattern of carboxylic group distribution are discussed; pectin esterase forms blocks which behave as fully hydrolyzed polymers and favor aggregation. Finally, the role of the calcium addition on the degree of aggregation was established. All the data show the important role of molecular structure of the pectins on calcium interactions.

Pectins are polysaccharides found in the primary cell walls of plants and in the middle lamella. They mainly consist of poly (1 → 4) $\alpha$ -D-galacturonic acids and their methyl esters. In addition, they also contain neutral sugars inserted into the main chain (L-rhamnose units) and in the side chain (nearly 10-15% of the neutral sugar by weight). Pectins are considered to have important structural roles (ion exchange and mechanical properties), and to be formed mainly of homogalacturonan blocks which play an important role in the mechanisms of interaction in the cell walls. The degree of esterification (DE) and the degree of polymerization (DP) of the pectic substances are directly controlled by enzymes and/or pH. This implies modification of their behavior with age, for example, and also indicates the necessity for control of conditions of extraction in order to isolate polymers representative of their native state.

The role of the structural properties of pectins was described recently (1) where it was shown that interactions of calcium with pectic substances were directly related to the existence of unbranched and non-esterified galacturonic blocks. Calcium was able to ionically bind two or more chains

0097-6156/89/0399-0324\$06.00/0  
© 1989 American Chemical Society

and to establish a three-dimensional network giving unique mechanical properties. In this chapter, we describe the behavior of pectins in aqueous solutions. Depending upon the experimental conditions employed, the calcium ions can induce a sol-gel transition.

### Materials and Methods

Polygalacturonic acid (Nutritional Biochemicals Corp., USA) was purified and isolated as the sodium salt (2,3) to give a preparation containing > 95% galacturonic acid. The oligogalacturonates were prepared by partial hydrolysis (4-6). Commercial apple pectin from Unipectine (France) was purified and partially deesterified (i) under alkaline conditions to produce randomly dispersed carboxylic acid functionalities along the chain and (ii) by an esterase to produce blockwise distribution of the carboxylic groups. These two series of samples allowed the demonstration of the effect of the distribution of carboxylic groups, and of the average level of carboxylic acid on the properties.

These ionic polymers can be considered as polyelectrolytes and their electrostatic properties can be predicted from the usual theories. In that respect, a polyelectrolyte is characterized by a structural charge parameter independent of the  $DP\lambda = \gamma e^2 / DhkT$  with  $\gamma$  equal to the number of ionized groups on a polymeric chain with length  $h$ ,  $D$ , the dielectric constant,  $e$ , the electronic charge and  $kT$ , the Boltzman term. Considering the structural length of the D-galacturonic unit in  ${}^4C_1$  conformation ( $b = 4.35\text{\AA}$  (7)), the poly  $\alpha$ -D-galacturonate is characterized by a  $\lambda$  value equal to 1.65. This parameter controls the thermodynamic properties as well as the activity coefficient of counterions or potentiometric titration. The interaction with calcium was determined from activity measurements of  $\text{Ca}^{2+}$  with a specific electrode (3,8); the apparent  $pK_a$  of the carboxylic acids was obtained from pH titration during neutralization. Conformational changes were monitored by circular dichroism (CD) (3,9). Interchain interactions were estimated by viscosity, gel permeation chromatography (10), light scattering measurements (11,12), and  ${}^{13}\text{C}$  NMR (2). All the data were obtained at a constant temperature ( $25^\circ\text{C} \pm 0.1$ ).

### Results and Discussion

*Role of DP and the Degree of Neutralization.* The role of the DP on the activity of calcium counterions in the presence of oligo- and polygalacturonates was first investigated by Kohn (13); the observed behavior was confirmed by Ravanat (10), who showed that when the DP is larger than 10, the activity coefficient of calcium decreases strongly due to interchain crosslinking interpreted in terms of the "egg-box" model (14,15). The geometry of the calcium-carbohydrate complex was more recently discussed by Dheu-Andries and Perez (16).

From Ravanat's and Kohn's data, the transition observed for calcium activity is in the range of DP 10 to 20, which means that at least 5 to 10  $\text{Ca}^{2+}$  cations are necessary to form a cooperative strong interchain binding. Until now, formation of chain dimers (as predicted in the "egg-box"

model) was only shown to exist with polymers taking into consideration the activity coefficient of  $\text{Ca}^{2+}$  counterions at infinite dilution (8). In fact, from thermodynamic considerations, it was concluded that polygalacturonate behavior up to  $\text{DP} = 5$  was in agreement with electrostatic theories considering a normal single molecule process (3). From CD measurements, this conclusion avoiding a specific interaction with calcium is confirmed (Fig. 1; curves (1) and (2)).

From circular dichroism, it appears that for pectins with a degree of neutralization ( $\alpha'$ ) of over 0.4, a specific interaction with calcium occurs (9). At the same time, the apparent pKa decreases corresponding to a specific binding (3). This critical value corresponds to a  $\lambda$  value of 0.64, which means that the  $\text{Ca}^{2+}$  must be associated with 24% of the carboxyl groups.

This result is directly proportional to the minimum number of carboxylic acid sites required to form a stable junction zone on polymers. The number of calcium cations bound must also be directly related to the stability of the junction and its thermoreversibility. Finally, it must be also pointed out that it is not the pH, but the degree of neutralization,  $\alpha'$ , which controls calcium binding.

*Effect of the Degree of Esterification and Carboxyl Group Distribution.* It is generally agreed that a transition in the behavior of pectins occurs around a degree of esterification of 50%. This is in fact the case for randomly dispersed carboxylic groups along the chain. The corresponding charge parameter is then the same as for a polygalacturonic acid with  $\alpha' = 0.5$ ; this value is in good agreement with our previous discussion.

The effect of the distribution of ionic sites on the aggregation process has also been elucidated (8,11,12). For these investigations, partial deesterification on apple pectins was performed, causing a random distribution of the carboxylic sites along the chain; on the other hand, action of a pectin esterase produced a blockwise distribution of the ionic groups. These two series of samples were tested allowing the comparison of thermodynamic properties for polymers having the same average charge parameter but different patterns of distribution of the carboxylic groups. It was then found that the pectin esterase produced blocks of free carboxylic group which behaved just as a fully hydrolyzed polymer, i.e., each attack produced a free zone on a chain which was able to be chelated in the presence of  $\text{Ca}^{2+}$ . Association of chains was clearly demonstrated by light scattering measurements (12).

*Effect of Calcium Content.* The application of gel permeation chromatography can also be used to answer the questions of interaction of calcium with sodium polygalacturonate.

Using a dilute aqueous solution of the polymer in the absence of external salt, a molecular weight distribution was obtained, although it was perturbed by electrostatic exclusion. When  $\text{CaCl}_2$  was added, a salt exclusion corresponding to NaCl was formed, i.e., an exchange process occurred up to at least 40% of the stoichiometry, where in each case one  $\text{Ca}^{2+}$  expelled two  $\text{Na}^+$  (10).

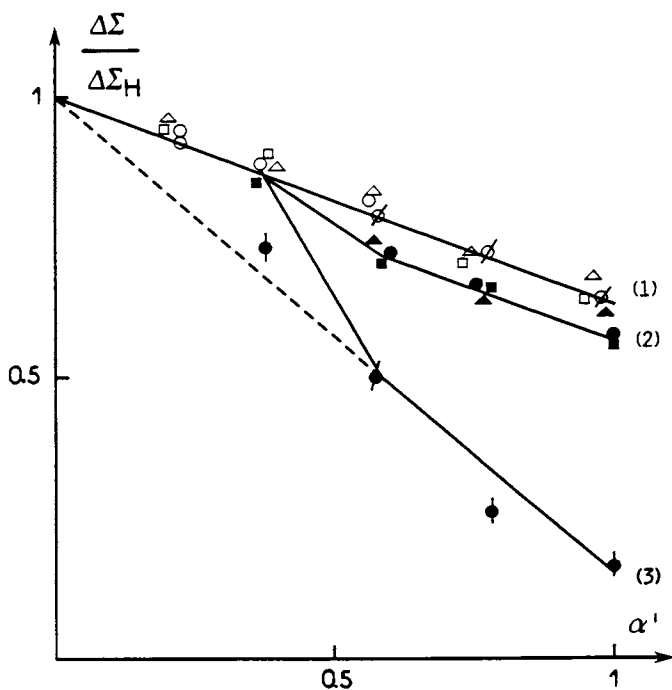


Figure 1. Normalized ellipticity at 210 nm as a function of the degree of neutralization ( $\alpha'$ ) for (1) sodium form of oligogalacturonates and polygalacturonate; (2) calcium form of galacturonates ( $\circ$  DP2,  $\triangle$  DP4,  $\square$  DP5), (3) calcium form of the polygalacturonate ( $\phi$ ). ( $\Delta\epsilon_H$  taken as reference is the ellipticity of acid forms for each product; open = sodium form; filled = calcium form.)

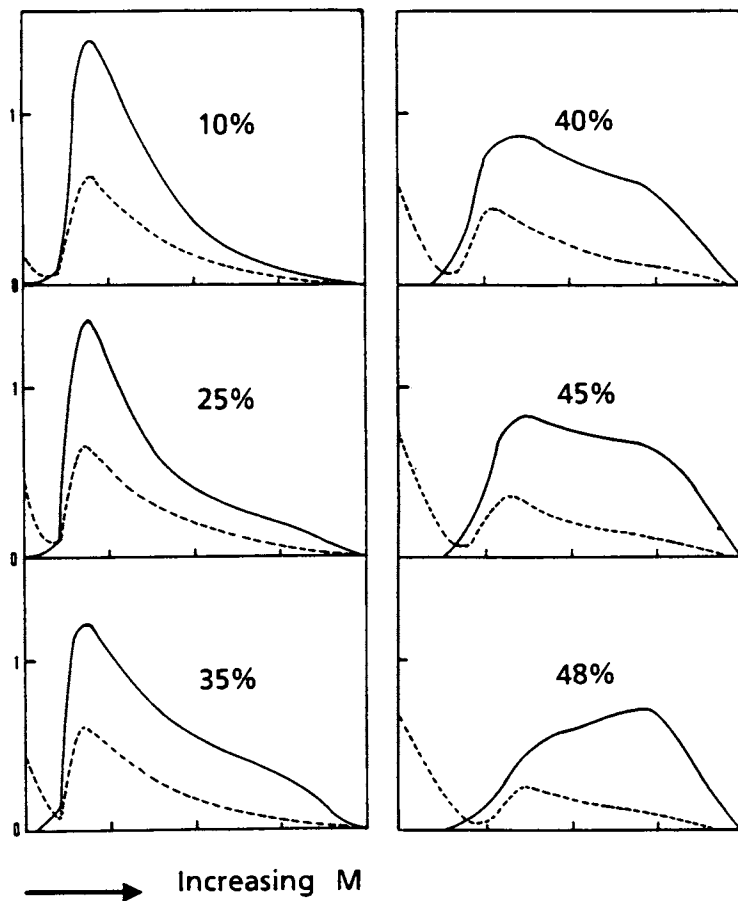


Figure 2. Refractometric (—) and conductimetric (---) traces for gel permeation chromatography of polygalacturonate sodium with progressive addition of  $\text{CaCl}_2$  expressed in equivalent percentage of  $\text{Ca}^{2+}$  added (polymer concentration 5 g/l; Spherosil porous materials with average pore diameter of 6000Å; elution  $\text{H}_2\text{O}$ ).

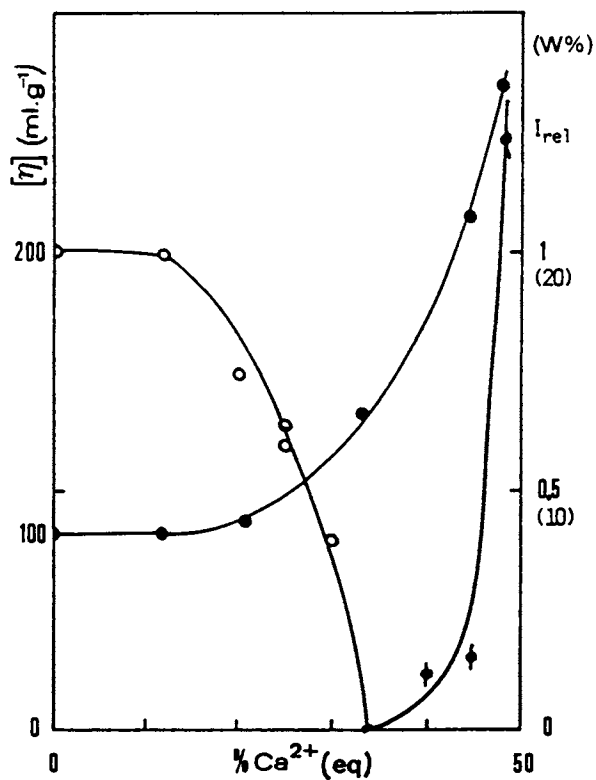


Figure 3. Dependence of the intrinsic viscosity ○ ( $[\eta]$ ), nmr signal ● (I), and gel fraction ◐ (wt. percent W%) as a function of equivalent percentage of Ca<sup>2+</sup> added. ( $[\eta]$  was determined by isoionic dilution of a 6 g/l solution of sodium polygalacturonate.)

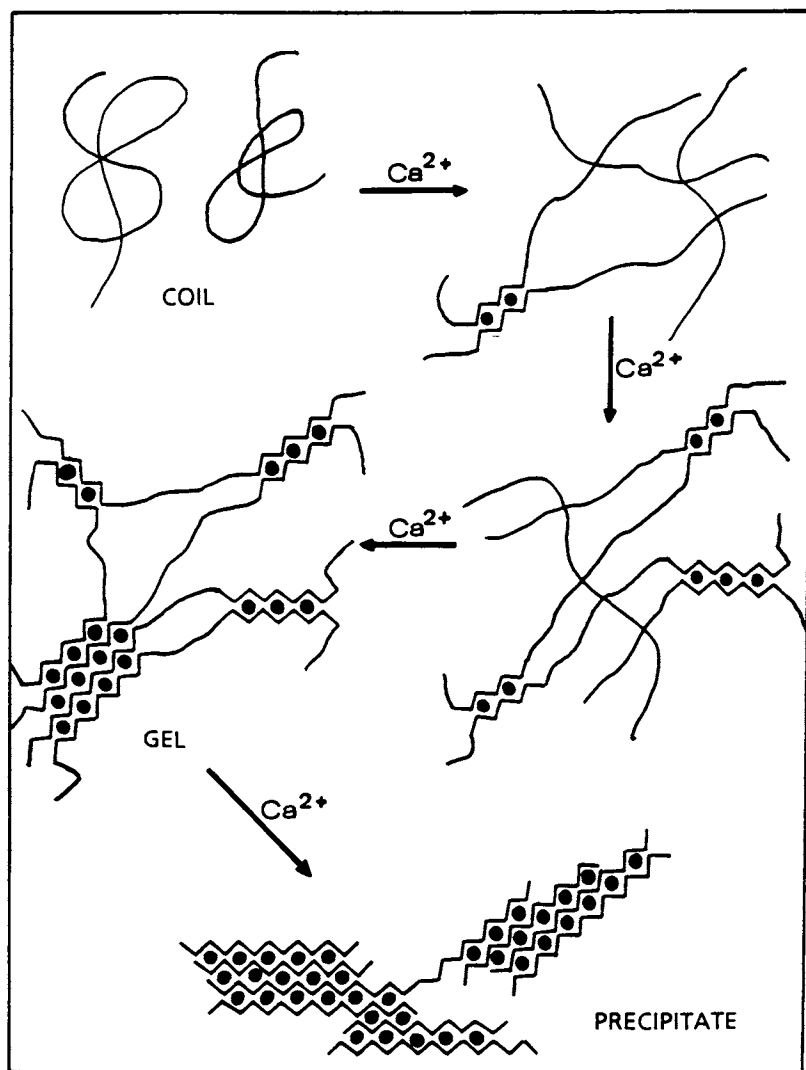


Figure 4. Crosslinking mechanism proposed for pectins in presence of  $\text{Ca}^{2+}$  (10). Black dots represent the calcium.



From Figure 2, it is clear that the apparent average molecular weight of the polymer increases progressively as soon as 25%  $\text{Ca}^{2+}$  equivalents are added and, at the same time, the intrinsic viscosity of the samples increased (Figure 3). The fraction of carboxylic groups bound with  $\text{Ca}^{2+}$  agrees with the value found in the discussion on the role of  $\alpha'$ .

From the refractometric trace on the chromatograms, it was possible to calculate the fraction of gel formed. When gel was formed in the system, the  $^{13}\text{C}$  NMR signals of the different carbon atoms disappear due to the decrease in their mobility (Fig. 3).

### Conclusions

The mechanism of interaction of calcium is directly related to the chemical structure of pectins. It also depends on the polymer concentration, the distribution of carboxylic groups and the amount of calcium present in the medium. To conclude, a mechanism of gelation can be given in Figure 4 which allows us to predict progressive aggregation, gelation or phase separation depending on experimental conditions.

From the different experimental results obtained, it can be concluded that the average number of  $\text{Ca}^{2+}$  ions bound is 1 per 8 carboxylic acid groups. However, from gel chromatography it is clear that this distribution is not homogeneous because aggregation is produced progressively; this also implies a degree of cooperativity in the interaction.

The following questions remain to be answered:

- What is the relationship between the observed behavior and that in the cell wall?
- What is the distribution of  $\text{Ca}^{2+}$  along the chains?
- How much  $\text{Ca}^{2+}$  is necessary to form a stable junction? This result is directly proportional to the minimum.

### Acknowledgments

The author wishes to thank J.-F. Thibault and G. Ravanat for their experimental contributions.

### Literature Cited

1. Jarvis, M. C. *Plant Cell Environ.* 1984, **7**, 163.
2. Rinaudo, M.; Ravanat, G.; Vincendon, M. *Makromol. Chem.* 1980, **181**, 1059.
3. Ravanat, G.; Rinaudo, M. *Biopolymers* 1980, **19**, 2209.
4. Kohn, R.; Larsen, B. *Acta Chem. Scand.* 1972, **26**, 2455.
5. Kohn, R.; Luknar, O. *Coll. Czech. Chem. Commun.* 1975, **40**, 959.
6. Kohn, R. *Carbohydr. Res.* 1971, **120**, 351.
7. Atkins, E. T. D.; Isaac, D. H.; Nieduszynski, I. A.; Philips, C. F.; Sheehan, J. K. *Polymers* 1974, **15**, 263.
8. Thibault, J.-F.; Rinaudo, M. *Biopolymers* 1985, **24**, 2131.

9. Thibault, J.-F.; Rinaudo, M. In *Chemistry and Function of Pectins*; ACS Symp. Ser. No. 310, 1986, p. 61.
10. Ravanat, G. Thesis, Grenoble, 1979.
11. Thibault, J.-F.; Rinaudo, M. *Biopolymers* 1986, **25**, 455.
12. Thibault, J.-F.; Rinaudo, M. *Brit. Polym.* 1985, **17**, 181.
13. Kohn, R.; Luknar, O. *Coll. Czech. Chem. Commun.* 1977, **42**, 731.
14. Grant, G. T.; Morris, E. R.; Rees, D. A.; Smith, P. J. C.; Thom, D. *FEBS Lett.* 1973, **32**, 195.
15. Powell, D. A.; Morris, E. R.; Gidley, M. J.; Rees, D. A. *J. Mol. Biol.* 1982, **15**, 517.
16. Dheu-Andries, M.-L.; Perez, S. *Carbohydr. Res.* 1983, **124**, 324.

RECEIVED April 28, 1989

## Chapter 24

# Comparative Studies on the Cell Wall Polymers Obtained from Different Parts of Rice Grains

Naoto Shibuya

National Food Research Institute, Ministry of Agriculture, Forestry, and  
Fisheries, Tsukuba, Ibaraki 305, Japan

Cell wall polymers from different parts of rice grain differed in both composition and detailed structure. Hemicellulosic polysaccharides of the cell wall preparations obtained from both outer and inner parts of the grain contained arabinoxylan and xyloglucan. The amount of  $\beta$ -1,3-1,4-glucan was negligible in the cell walls of the outer part of the grain when compared to that in the endosperm cell wall. The degree of lignification also differed from tissue to tissue. In addition, the arabinoxylan obtained from the outer part of the grain carried side-chains with more complicated structures than endospermic arabinoxylan. Similar differentiation on the molecular level is also suggested for other cell wall polymers.

In order to understand the process of differentiation and the properties of the resulting cell walls, it is necessary to identify the changes that occur in cell wall polymers. Several recent papers suggest that changes in cell surface carbohydrates in animals and plants may be both a cause and effect of differentiation (1-3). One possible approach to the study of differentiation is to compare the composition and chemical structure of cell-wall polymers during development. Cereal grains, such as rice and wheat, are composed of several tissues which appear at different stages of differentiation. Thus, starch endosperm originates from fertilized polar nuclei, while the thin cell walls are considered to be primary cell walls (4,5). The outer part of the endosperm is covered with several layers of aleuron cells, which are also derived from the same fertilized polar nucleus but which differentiate into a specific tissue during the maturation process. Cell walls of the aleuron cells are much thicker than those of the endosperm, and are considered to be secondary walls. The outermost part of the grain is a caryopsis coat consisting of several compressed cell layers with very thick ( $> 1 \mu\text{m}$ ) walls.

0097-6156/89/0399-0333\$06.00/0

© 1989 American Chemical Society

Germ, or embryo, is derived from the fertilized egg and consists of several different tissues.

In view of the practical importance of these grains, for example in dietary fibers, it is useful to study the cell wall polymers of their tissues during differentiation. In the present work, we used rice grains (brown rice without husk) as a starting material. They were fractionated into several distinct histological components, and the composition and detailed structure of cell wall polymers was compared.

### Materials and Methods

*Isolation of Cell Walls from Different Parts of Rice Grain.* Rice grains were gradually peeled using a conventional milling instrument (Satake Motor One-Pass Type Test Mill, Satake Engineering Co., Ltd., Tokyo), and the fractions rich in specific histological components were collected. The potassium content of these fractions was used as an index to identify the fraction enriched in aleuron tissue (6). The caryopsis coat fraction was obtained from the very first milling fraction. Starchy endosperm was obtained by thoroughly removing the outer part of the grain. The germ fraction was separated from the bran fraction by sieving with 10-20 mesh sieves. Cell walls were obtained by the successive extraction of the defatted tissues with SDS-mercaptoethanol and dimethylsulfoxide (7). An enzymatic method using a combination of protease and amylase (8) was also used to obtain cell walls from these tissues, and the analysis of the cell wall preparations so obtained showed that both methods gave basically the same preparations. The yield of the cell walls (w/w of defatted tissue) was 0.3% for the endosperm, 12% for the germ, 20% for the aleuron tissue, and 29% for the caryopsis coat. Scanning electron micrographs of these cell wall preparations (Fig. 1) showed that both of the cell wall preparations obtained from the caryopsis coat, and the aleuron tissue, were very thick and appeared of hard texture. On the other hand, the endosperm cell wall preparation was very thin and appeared to be of softer texture. The main part of the cell wall preparation from the germ looked similar to the endosperm cell wall but was somewhat thicker and harder. These preparations were free of other cellular particles such as starch or proteins.

### Results and Discussion

*Comparison of the Overall Composition of Cell Wall Preparations.* As can be seen from Table I, cell wall preparations showed a significant difference in their polymer composition. The endosperm cell walls resembled primary walls, since they were virtually free of lignin but rich in pectic substances. On the other hand, the cell wall preparations obtained from the caryopsis coat and the aleuron tissue were highly lignified, and their pectic content was very low. The germ cell wall showed a somewhat intermediate composition between these two types, probably reflecting the fact that it consists of several different tissues.

The monosaccharide composition of the hemicelluloses, which were a major fraction of all of these cell wall preparations, also showed significant differences, especially in the amounts of glucose and galactose (Table II).

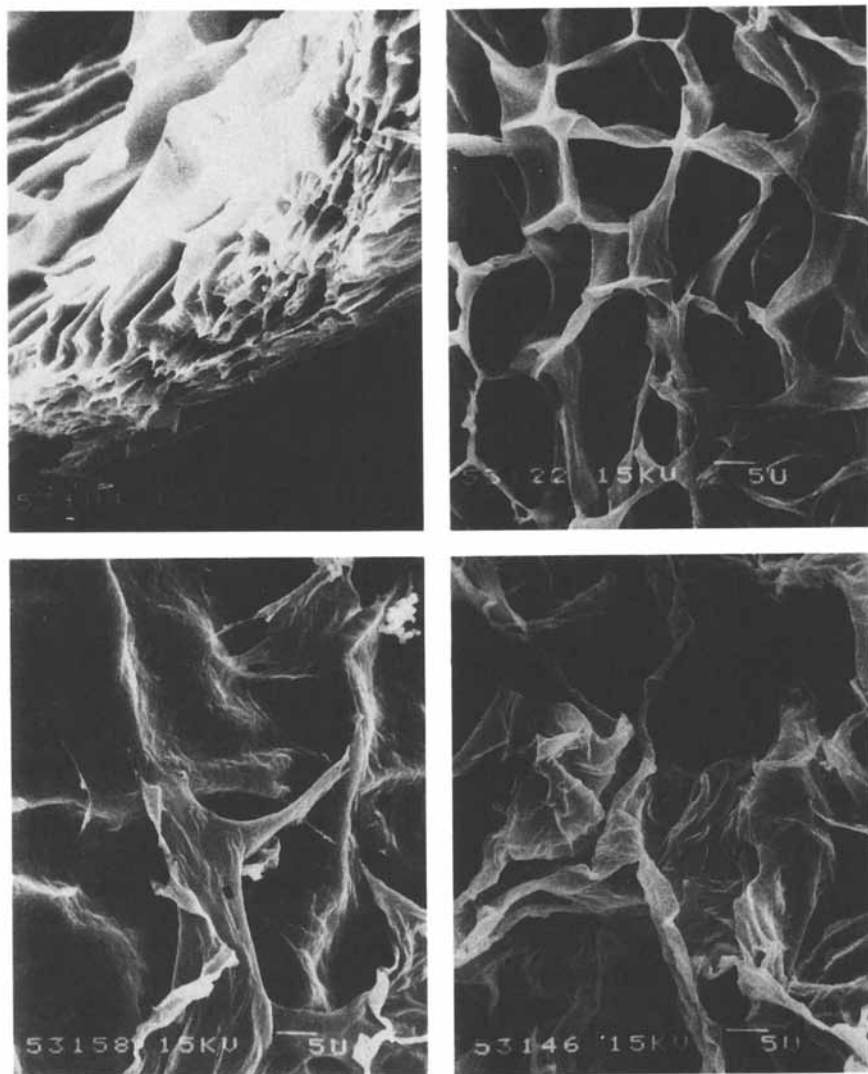


Figure 1. Scanning electron micrograph of the cell wall preparations obtained from the different parts of rice grain (7). Caryopsis coat (upper left), aleuron layer (upper right), germ (lower left) and starchy endosperm (lower right). Bars in the picture indicate 5  $\mu\text{m}$ .

Table I. Composition of the Cell Wall Preparations Obtained from Different Histological Fractions

Fraction	Pectic Substances	Hemicellulose	$\alpha$ -Cellulose	Lignin
Caryopsis coat	7	38	28	27
Aleuron tissue	11	42	31	16
Endosperm	27	49	23	1
Germ	23	47	21	9

While the hemicelluloses obtained from the germ, aleuron, and caryopsis coat cell walls all showed a similar monosaccharide composition, this was not the case for the endosperm tissue. Thus, a major difference in the structure of hemicellulosic polysaccharides exists between the preparations obtained from the endosperm cell walls and those from the cell walls of the other parts of the grain, i.e., rice bran. (Rice bran consists of the caryopsis coat, aleuron layer and germ.) Comparison of the detailed structural features of the hemicellulosic polysaccharides of endosperm and bran cell walls will be discussed in the following sections.

Table II. Monosaccharide Composition of Pectic Polysaccharides and Hemicellulose Obtained from Different Cell Wall Preparations

Fraction	Neutral Sugar Composition (mol %)						Uronic Acid Content (wt.%)
	Rhamn-ose	Fuc-ose	Ara- binose	Xyl-ose	Gal-actose	Glu-cose	
<i>Hemicellulose:</i>							
Caryopsis coat	1.0	0.4	35.6	43.6	7.4	12.0	13.5
Aleuron layer	1.0	0.4	36.7	43.5	7.4	11.1	12.8
Germ	1.2	0.5	36.7	38.1	8.8	14.7	13.8
Endosperm	0.9	0.5	26.4	41.1	1.9	29.1	12.1
<i>Pectic Polysaccharides:</i>							
Caryopsis coat	5.0	1.2	43.6	26.8	11.9	11.3	31.5
Aleuron layer	3.6	1.1	48.9	27.5	11.1	7.7	24.9
Germ	2.3	0.7	46.9	20.5	10.7	19.0	16.4
Endosperm	6.1	0.6	33.0	30.4	11.4	18.5	34.5

The sugar composition of the pectic polysaccharides obtained from these cell wall preparations (Table II) also suggested differences in the structural features of the different cell wall preparations. Detailed structural information is only available for the pectic polysaccharides obtained from the endosperm cell wall: The main fraction of endosperm pectic polysaccharide was separated into two fractions, a neutral sugar-rich fraction and a fraction with a very high content of D-galacturonic acid (8). Structural

analysis of the former fraction indicated a structure similar to the so-called rhamnogalacturonan-I structure (9), which consists of a backbone of 1,4-linked galacturonan chain interrupted by 1,2-linked L-rhamnosyl residues and side-chains rich in 1,5-linked L-arabinofuranosyl and 1,4-linked D-galactosyl residues (10). The yield of the pectic polysaccharide of the endosperm cell wall and the germ cell wall is similar, but the sugar composition is very different, as shown in Table II. The uronic acid content is much higher in the endosperm preparation. On the other hand, the amount of arabinose and rhamnose is much higher in the germ pectin. Note that these preparations are crude fractions and further structural studies on the purified fractions are necessary to reach any definitive conclusions. Nevertheless, these results suggest possible differences in their structural features, such as a difference in the ratio of the neutral sugar-rich domains and the galacturonan rich domains, length and structures of side-chains, etc.

Methylation analysis of whole cell wall preparation (7) also suggested differences in the composition and the structure of the component polysaccharides. For example, most of the arabinose residues in the endosperm cell wall were non-reducing. On the other hand, a large part of the arabinose residues in the germ cell wall were located in the inner chain portion with various types of linkages. Similar results were also obtained in the case of the aleuron cell wall. The 1,3-linked glucose residues were detected practically only in the endosperm cell wall preparation. These results suggest a significant difference in the composition and detailed structure of the component polysaccharides of these preparations.

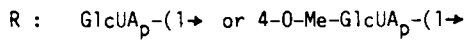
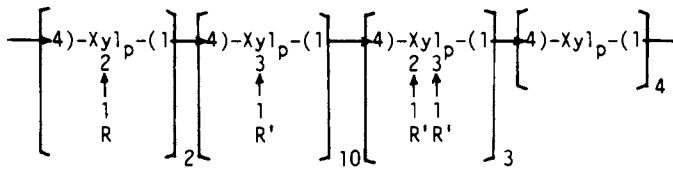
*Structure of the Hemicellulose Polysaccharides from Endosperm and Bran Cell Wall.* As suggested above, there is a major difference in the structure of hemicellulosic polysaccharides obtained from the endosperm and from the other parts of the grain. The hemicellulose preparations from both the endosperm and bran cell walls were further fractionated and subjected to structural analysis using chemical and enzymatic methods. Figure 2 summarizes the structure of the hemicellulosic polysaccharides obtained from the endosperm cell wall (11,12). Over two-thirds of the hemicellulose is composed of arabinoxylans, especially acidic arabinoxylans. They are highly branched, carrying mostly very short side chains of a single arabinofuranosyl or (4-O-methyl)-glucuronosyl residue. The endosperm hemicellulose also contained two other polysaccharides as minor components, namely, xyloglucan and  $\beta$ -1,3-,1,4-glucan. Both of these components were firmly associated with a small amount of arabinoxylan and could not be isolated from each other by conventional methods. The structure shown was derived from the analysis of the fragments obtained by the enzymatic degradation of this complex with the cellulase of *T. viride* (xyloglucan), and from the analysis of the insoluble polysaccharides obtained from the controlled Smith degradation of this fraction ( $\beta$ -1,3-,1,4-glucan).

Figure 3 shows the structure of the hemicellulosic polysaccharides obtained from the bran cell wall preparations. These structures were deduced from the results of the methylation analysis of purified fractions (13). In contrast to the endosperm cell wall, no  $\beta$ -1,3-,1,4-glucan was obtained from

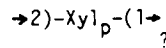




(1) arabinogalactoglucuronoxyylan<sup>a</sup>)



R':   periferal sugar           inner chain sugar  
       residue                       residue



(2) xyloglucan<sup>a</sup>)

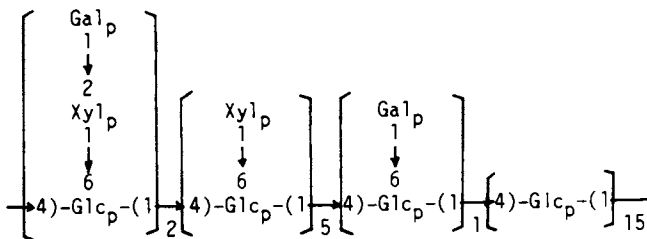


Figure 3. Structure of hemicellulosic polysaccharides obtained from rice bran. (a) Deduced from the results of methylation analysis described in ref. 13.

the bran cell wall. This result agreed well with the results of the methylation analysis of whole cell wall preparations in which we could not detect any significant amounts of 1,3-linked glucose residues. This is one of the characteristic features of bran hemicelluloses. Again, the acidic arabinoxylan was the main component of this preparation representing over 80% by weight. However, methylation analysis of this arabinoxylan indicated a difference in its detailed structure compared to the endospermic arabinoxylan. For example, the bran arabinoxylan contained a significant amount of doubly-branched xylose residues, but the endosperm arabinoxylan did not. Also, the bran arabinoxylan seemed to contain somewhat longer, and more complicated, side-chains than the endosperm arabinoxylan. This was based upon methylation analysis which showed the presence of appreciable amounts of inner chain arabinosyl residues together with terminal galactosyl and xylosyl residues of the bran preparation. Similar observations were made for the arabinoxylans isolated from the beeswing bran of wheat (14). Bran hemicellulose also contained xyloglucan as a minor component. It was associated with the arabinoxylan and could not be isolated by conventional methods. The xyloglucan-rich fraction was finally digested with a purified arabinofuranosidase and an endoxylanase to remove contaminating arabinoxylan, and the resulting pure xyloglucan was subjected to methylation analysis. Unfortunately, the structure of the xyloglucan so obtained (Figure 3) was not directly comparable with the structure of the endosperm xyloglucan. This was because the structure in Figure 3 was deduced from methylation analysis of the whole molecule, whereas the endosperm xyloglucan structure was based upon analysis of the fragments liberated by cellulase digestion.

*Detailed Structure of Side Chains of Bran Arabinoxylan.* In order to establish the chemical identity of the side-chains in the bran arabinoxylan, it was subjected to mild acid hydrolysis to liberate oligosaccharides originally attached to the xylan main chain through the acid-labile arabinofuranosyl residue (15). A mixture of the oligosaccharides so obtained was reduced and methylated to give the corresponding methylated oligosaccharide alditols. An aliquot of this methylated oligosaccharide alditol mixture was directly analyzed by GC-MS, and the remainder was hydrolyzed, reduced and acetylated. The products were analyzed by GC-MS. Chromatograms of the methylated oligosaccharide alditols showed the presence of di- and trisaccharides, in addition to monosaccharides which were mainly derived from the non-reducing end of arabinofuranosyl residues (Figure 4). The structure of each oligosaccharide was determined by combining the information obtained from their CI and EI mass spectra, and the linkage information was obtained from the analysis of their hydrolyzed products. In this way, the structure of the main peak in the trisaccharide region (peak 9 in Figure 4) was deduced as follows (Figure 5). From the pseudo-parent ion of this peak ( $QM^+ - MeOH$ ,  $m/z = 556$ ), it is clear that the original trisaccharide consists of one hexose and two pentose units. Also, from the fragment with  $m/z = 219$ , 379 and 192, the order of their arrangement must be hexose, pentose, pentose. Hence, the reducing end pentose must be substituted at

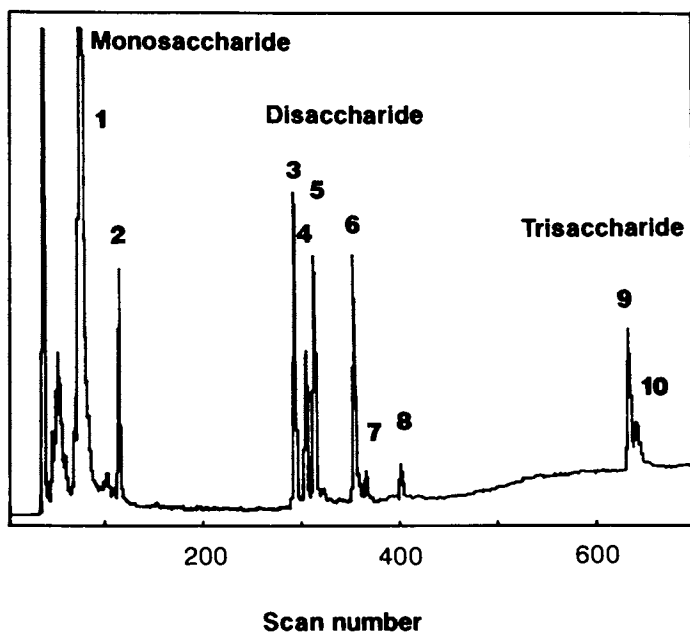


Figure 4. Total ion chromatogram of the methylated mono/oligosaccharide obtained by the partial acid hydrolysis of the bran arabinogalactogluconoxylan.

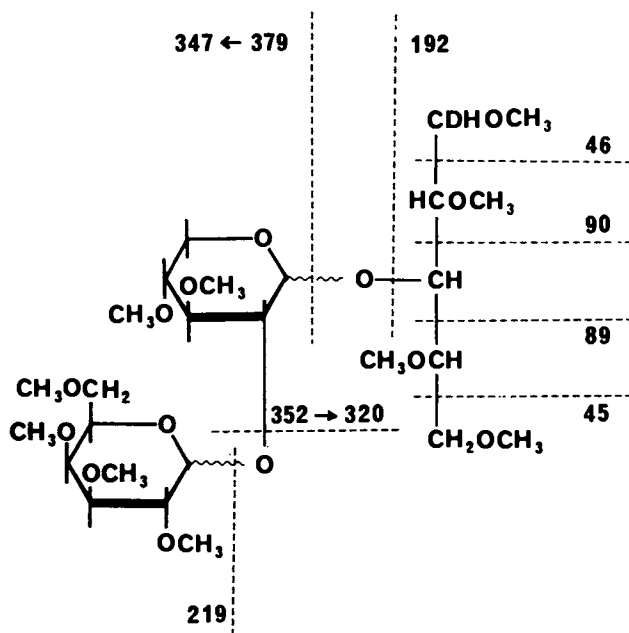


Figure 5. Proposed structure of peak 9 in Figure 4 and its fragmentation pattern. Deuterium at C-1 position was introduced during the reduction step with sodium borodeuteride.

the *O*-3 position, judging from the fragmentation at the reduced alditol portion ( $m/z = 45, 46, 89$  and  $90$ ). To further identify each sugar, and also the mode of linkage, the information obtained from the hydrolyzed products was used. Firstly, the only hexose with a non-reducing end in the mixture of methylated oligosaccharide alditols was galactose; that is, the first hexose unit must be galactose. In a similar way, the reducing end pentose must be arabinose, because the only reducing end pentose substituted at *O*-3 was arabinose. The pentose between these two sugar units should be xylose, because the only inner chain pentose residues detected were 4-linked and 2-linked xylose. At this point it is difficult to select any one of these two possibilities. However, an empirical rule reported by Karkkainen (16) was used to determine the linkage of this inner-chain xylose residue. In this case, fragments derived from the so-called bcA fragmentation ( $m/z = 379$  and  $347$ ) was much more extensive than those derived from baA fragmentation ( $m/z = 352$  and  $320$ ), thus suggesting a 1,2- rather than a 1,4-linkage. Thus, the structure of this oligosaccharide is proposed as the trisaccharide, Gal<sub>p</sub>1,2Xyl<sub>p</sub>1,3Ara<sub>f</sub>.

Based upon these studies, Table III summarizes the partially deduced structure of the mono-, di-, and trisaccharides, obtained by the partial degradation of the original arabinoxylan. These structures may not be completely accurate, because of some uncertainty in the theory used to speculate the mode of linkage. Consequently, each one needs to be isolated to unambiguously verify its structure. These results do, however, provide some indication of the complicated structure of the side-chains of bran arabinoxylan.

Table III. Possible Structure of Oligosaccharides Obtained by the Partial Acid Hydrolysis of Rice Bran Arabinogalactoglucuronoxylan

Oligosaccharides*	Proposed Structure**
1	Pentose (Mainly Ara)
2	Hexose (Gal)
3	Pen-Pen (Xyl-1, 3-Ara)
4	Pen-Pen (Xyl-1, 4-Ara)
5	Pen-Pen (Xyl-1, 2-Ara)
6	Hex-Pen (Gal-1, 2-Ara)
7	Hex-Pen
8	Hex-Pen
9	Hex-Pen-Pen (Gal-1, 2-Xyl-1, 2-Ara)
10	Pen-Hex-Pen (Xyl-1, 3-Gal-1, 5-Ara)

\* See Figure 4.

\*\* Pen = pentose; Hex = hexose.

### Concluding Remarks

The changes associated with the thickening of the cell walls in rice grain are summarized as follows: (1) a decrease or shutdown of the synthesis of pectic substances and  $\beta$ -1,3-,1,4-glucan; (2) initiation of lignin formation; and (3) synthesis or activation of the glycosyl transferases responsible for the elongation of the side chains of the arabinoxylan. Thus, the results described in this article give an example of how cell wall polymers change with differentiation of plant tissues, although an understanding of the physiological meaning of these changes requires further studies.

### Literature Cited

1. Van, K. T. T.; Toubart, P.; Cousson, A.; Darvil, A. G.; Gollin, D. J.; Chelf, P.; Albersheim, P. *Nature* 1985, **314**, 615-17.
2. Nojiri, H.; Takaku, F.; Terui, Y.; Miura, Y.; Saito, M. *Proc. Natl. Acad. Sci. U.S.A.* 1986, **83**, 782-86.
3. Albersheim, P.; Darvill, A. G. *Sci. Amer.* 1985, **253**, 44-50.
4. Mares, D. J.; Stone, B.A. *Aust. J. Biol. Sci.* 1973, **26**, 793-812.
5. Selvendran, R. R. *Dietary Fibre*; Birch, G. G.; Parker, K. J., Eds.; Applied Science: London, 1983; Ch. 7.
6. Tanaka, K.; Yoshida, T.; Asada, K.; Kasai, Z. *Arch. Biochem. Biophys.* 1973, **155**, 136-43.
7. Shibuya, N.; Nakane, R.; Yasui, A.; Tanaka, K.; Iwasaki, T. *Cereal Chem.* 1985, **62**, 252-58.
8. Shibuya, N.; Iwasaki, T. *Agric. Biol. Chem.* 1978, **42**, 2259-66.
9. McNeil, M.; Darvill, A. G.; Fry, S. C.; Albersheim, P. *Ann. Rev. Biochem.* 1984, **53**, 625-63.
10. Shibuya, N.; Nakane, R. *Phytochem.* 1984, **23**, 1425-29.
11. Shibuya, N.; Misaki, A. *Agric. Biol. Chem.* 1978, **42**, 2267-74.
12. Shibuya, N.; Misaki, A.; Iwasaki, T. *Agric. Biol. Chem.* 1983, **47**, 2223-30.
13. Shibuya, N.; Iwasaki, T. *Phytochem.* 1985, **24**, 285-89.
14. Brillouet, J. M.; Joseleau, J. P. *Carbohydr. Res.* 1987, **159**, 109-26.
15. Shibuya, N., unpublished.
16. Karkkainen, J. *Carbohydr. Res.* 1971, **17**, 11-18.

RECEIVED March 17, 1989

## Chapter 25

# Cell Wall Alterations and Antimicrobial Defense in Perennial Plants

R. B. Pearce

Oxford Forestry Institute, Department of Plant Sciences, University  
of Oxford, South Parks Road, Oxford OX1 3RB, England

Cell wall alterations, especially suberization responses, appear particularly important as disease resistance mechanisms in the perennial tissues of plants. Antimicrobial defence in such tissues may entail the durable operation of resistance mechanisms during prolonged host-parasite interactions: wall alterations are well suited to this requirement. In the bark of many trees, the suberized phellem forms a constitutive barrier to invasion, and suberization is an early and important part of the wound and defence responses restoring an intact periderm surface. This is exemplified by the response of Sitka spruce to attack by *Armillaria obscura*. Induced suberization responses also occur in sapwood, conferring enhanced resistance to degradation by decay fungi and contributing to the formation of barriers which limit the spread of pathogens in the living tree.

Antimicrobial defence in plants has been studied most extensively in annual, herbaceous species, a category including the majority of important agricultural crop plants. A range of different disease resistance mechanisms have been described for such plants, including both constitutive and induced antimicrobial compounds and cell wall alterations (1, 2). As the global emphasis in wood production, for timber, pulp, fuel and chemical products, shifts from the harvesting of natural or semi-natural forests to production in increasingly intensively managed plantations, the pathology of these woody perennials is attaining increasing importance. The adoption of such practices as the creation of highly uniform (physically and genetically) monoculture stands is likely to increase the potential for the development of disease epidemics, as commonly occur in agricultural crops (3, 4). In consequence increased attention has been given to disease resistance in woody species. Although our understanding of resistance in

0097-6156/89/0399-0346\$06.00/0  
© 1989 American Chemical Society

these woody perennials still lags behind that in annual plants, significant advances have been made during the past fifteen years. Sufficient studies have been carried out to indicate that the major defence mechanisms reported from herbaceous species occur also in woody plants. However, in the more extensively developed secondary tissues of these plants defence mechanisms may be organized to form clearly defined barriers (5). This chapter will concentrate on these structural barriers, which appear particularly important in the containment of pathogens or potential pathogens within these secondary tissues.

### Requirements for Defence in Perennial Plant Tissues

In annual plants the duration of the host-pathogen interaction is generally relatively brief; in perennial plants, however, these interactions may continue for greatly extended periods in the long-lived secondary tissues. Such long-term infections include perennial cankers and wood decaying pathogens, including many of the important root- and butt-rotting forest pathogens such as *Armillaria* spp. and *Heterobasidion annosum*. These perennial pathogens colonize (and frequently kill) a volume of host tissue, which provides a food base that can sustain the fungus during a prolonged interaction with the living tissues of the host. In the case of *Armillaria* spp. nutrients mobilized from one infected host may be translocated along rhizomorphs, supporting their growth and the infection process where they encounter a new potential host (6). In both perennial cankers and pathogenic wood decays there is an internal interface between the living host and the pathogen at the lesion margin. The advance of the pathogen at these interfaces is typically very slow.

Defences effective in limiting pathogen advance under these circumstances must be capable of maintaining their function for an extended time. Although this requirement for durability does not preclude the involvement of chemical defences, structural defence mechanisms are particularly well suited to the protection of the host under these circumstances. Whilst antimicrobial chemicals may be labile or diffusible, structural defences, comprising either wall alterations to pre-existing cells or tissues formed *de novo* by renewed cell division, are much more stable. Such barriers can protect the underlying tissues indefinitely against microorganisms lacking a specific ability to penetrate or circumvent them. Structural defences, particularly those requiring the production of new tissues by the plant may take some time to form (5, 7-9). Antimicrobial compounds may be important during the initial stages of the host-parasite interaction, before barrier development has occurred, or may occur concomitantly with cell wall alterations. In Sitka spruce (*Picea sitchensis*) the antifungal stilbenes astringenin and isorhapontigenin accumulate around bark wounds inoculated with potentially pathogenic fungi. These are released on infection from the corresponding stilbene glucosides astringin and rhaponticin which are constitutive in the bark tissues, and provide a rapid response to infection that may inhibit potential pathogens until more durable structural barriers have been formed (10).

American Chemical Society  
Library

1155 16th St., N.W.

Washington, D.C. 20036



### Structural Defence Mechanisms in Plants

Structures interpretable as having a defensive role may be either normal features of the plant, or their formation may be induced as a result of microbial challenge or wounding. In the case of induced structural defences the responses may comprise either changes in pre-existing cells, or may result in the formation of specific barrier tissues *de novo* by renewed or modified cell division. Occasionally non-cellular structural defences may operate. The resin flow that accompanies wounding or infection in many coniferous trees may act as a mechanical barrier, hardening to form an amorphous varnish impenetrable to fungal invasion (11). More commonly, however, structural defences are effected by cell wall alterations. These include lignification (12-14), suberization (14,15), callose deposition (16), and silicification (17,18).

Such wall alterations may operate in several ways. Probably the most obvious and widely suggested mechanism is by physical blockage of the pathogen. For a barrier to prevent the advance of a pathogen, it must be more resistant to the cell wall-degrading enzymes of the pathogen than unmodified walls. Such enhanced resistance to degradation has been demonstrated both for lignified papillae and halos in wheat leaf epidermal cells (19) and for suberized barriers in oak xylem (15). Alternatively, structural responses of a plant could establish a permeability barrier, isolating the pathogen from the living tissues of its host. Such a permeability barrier could protect healthy cells from fungal toxins or enzymes, it could reduce the rate of diffusion of host antifungal compounds from the infection court, perhaps enhancing the efficacy of these chemical defences, or it could reduce the flow of nutrients or water to the pathogen (20). A test for tissue permeability to ions, using ferric chloride and potassium ferricyanide, termed the F-F test (21), has demonstrated the impermeability of suberized barrier tissues at lesion margins in the bark of various woody species (7,14), although initially the suberization of these impervious tissues was not recognized (7). In addition, the processes leading to the formation of structural barriers may have a direct effect on the pathogen itself, either as a result of chemical inhibition by non-polymerized monomers of the wall-modifying material, or by deposition of this material onto the wall of the pathogen, with consequent interference with its growth (22).

Lignification responses have been implicated in disease resistance in perennial plants. In the leaves of oak species a lignified papilla response appears to be important in the resistance of older leaves to oak mildew, *Microsphaera alphitoides* (23). Leaves of a deciduous tree are, however, ephemeral organs, comparable to those of herbaceous species. As discussed in this paper, suberization of cell walls (sometimes accompanied by lignification also) is perhaps more typical of the barriers found in the secondary tissues of woody (8,14) and herbaceous (24) plants. Suberin, although still imperfectly characterized, is predominantly a polyester composed of long chain ( $C_{18}$ - $C_{30}$ ) hydroxy- and hydroxyepoxy-fatty acids. Lignin-like aromatic domains may also be associated with this polymer (25). It therefore differs markedly from the aromatic and carbohydrate polymers that com-

prise the bulk of the secondary plant tissues. Also, because of its hydrophobic properties it is highly effective as a permeability barrier to water. As water content has been implicated in the environmental exclusion of many wood-inhabiting fungi from the living secondary xylem (sapwood) of trees (26-28), this may be particularly significant in the protection of these tissues. While suberin can be degraded by some fungi, including *Armillaria* sp. (29) and *Rosellinia desmazieresii* (30), the rates of breakdown were not high.

### Constitutive Structural Defences

Although many structural features of a plant, such as form and arrangement of stomata, can be interpreted in terms of defence (31), only the secondary surface will be considered in detail here. This comprises a periderm, or series of sequent periderms forming a rhytidome. Periderms are sites of cambial activity, suberized phellem cells being produced externally by the phellogen. The thickness of phellem accumulating varies greatly between species.

Few pathogens are capable of penetrating the intact periderm surface of woody plants. Most, if not all, of the fungi that infect by this route (rather than by bypassing the surface barrier, infecting *via* wounds and natural discontinuities in the periderm) do so from established infections on a neighboring food base, permitting a prolonged attack. Commonly (e.g., with *Armillaria* spp., *Rosellinia* spp.) penetration is effected by mycelial aggregations, supported metabolically by mycelial cords or rhizomorphs (30, 32, 33). Without this capacity to mount a prolonged attack, in which both mechanical and enzymic activity may be involved, potential pathogens appear unable to overcome the periderm barrier. Perhaps because of its ubiquity, there have been few detailed studies of the role of surface periderms in defence: commonly the protection provided is assumed (e.g., 34), and is attributed to the resistance of the phellem cells to degradation. Periderm (or rhytidome) surfaces of some tree species persist without erosion for long periods, surface features remaining visible for several decades at least (35). The suberized phellem cells comprising an important component of these tissues are non-living and incapable of any active repair, but are clearly more durable than other plant tissues.

In certain instances, however, factors other than the cell wall polymers of the phellem may be important in the protection provided by the secondary surface. *Rosellinia desmazieresii* inoculated in a food base onto the underground stems of a resistant *Salix repens* hybrid (*S. x Friesiana*) exhibited greatly reduced epiphytic growth and cord formation compared with inoculations onto susceptible *S. repens* itself. Attempted penetration was not observed on the resistant hybrid (30). This behaviour suggests that diffusible chemical inhibitors at the stem surface may be important in resistance to this pathogen, which has a demonstrated ability to degrade suberin and penetrate the surface periderm (30).

Although in an unwounded, healthy, plant periderms are normally superficial, interxylary cork has been reported from at least 40 species of di-

cotyledonous plants (36). These interxylary periderms are associated with the fission of perennating axes and the dying back of annual organs such as aerial shoots. In *Epilobium angustifolium* an interxylary periderm is formed each year over the surface of the xylem connected with the previous year's aerial shoots. The older, redundant, vascular tissue is thus walled off from the functional tissues of the plant, which are then protected by both inner and outer suberized barriers. It has been suggested that such internal periderms may be important in affording protection against the ingress of microorganisms associated with the dying down of the annual aerial shoots (37), a function in accordance with the habit of many of the species from which they have been recorded.

### Defence in Bark Tissues

Should the barrier presented by the secondary plant surface be breached, defence mechanisms may operate in the bark (i.e., secondary cortex and phloem) of woody plants, limiting pathogen development. These include chemical defences and structural barriers resulting from cell wall alterations (5). Both probably act in concert, although in a non-woody plant (carrot) it has been concluded that the importance of cell wall alterations was secondary to that of chemical defence (24). Only the cell wall alterations involved in defence will be considered further here.

*Cell Wall Alterations in the Bark of Gymnosperms.* Non-specific defence responses to wounding, insect and fungal attack in the bark of conifers, leading to a restoration of the periderm surface, have been described. In essence, necrophylactic (wound) periderms are formed continuous with the normal structural surface periderm, walling off the lesion and effectively excluding it from the plant (7). Prior to the development of this periderm by dedifferentiation and renewed division of cells in the bark surrounding the lesion, cell wall alterations take place in pre-existing tissues bordering the lesion. Prominent among these alterations is the formation of an impervious zone immediately overlying the site of periderm restoration. This was initially described as non-suberized impervious tissue (NIT) (7). In a more recent study of defence responses following wounding and artificial inoculation of *Picea sitchensis* root bark with the weakly pathogenic butt rot fungus *Phaeolus schweinitzii*, use of improved histochemical techniques demonstrated that suberization of cell walls occurred in these tissues (9).

Cell walls in the necrotic tissue of these wounds were browned. Staining with diazotized *o*-toluidine and toluidine blue confirmed the polyphenolic nature of these brown depositions, which may have resulted from the polymerization of the stilbenes present in large quantities in spruce bark. Phenolic residues were deposited on the walls of certain cells internal to the necrotic tissues by 10 days after wounding. By 36 days these cells had become thick-walled. The precise nature of substances responsible for this thickening has not been determined, variable responses being obtained with histochemical tests for lignin (cf. Table I). Suberin was detectable in cells immediately underlying the thick walled cells, which corresponded to the

("non-") suberized impervious tissue, and in the thin walled phellem cells formed later by the developing necrophylactic periderm (9). These bark responses are illustrated diagrammatically in Figure 1.

Table I. Histochemical responses of cell walls associated with the necrophylactic periderm response in *Picea sitchensis* challenged with *Armillaria obscura*

Wall Polymer	Stain <sup>a</sup>	Reaction in Tissues			
		Healthy Bark Parenchyma	Necrophylactic Phellem	Thick Walled Tissue	Necrotic Tissues
Pectic Materials	Ruthenium red	+	-	±	+
Cellulose	Zinc-chlor-iodine	+	-	-	-
	Toluidine blue	+	-	-	-
Callose	Resorcinol blue	± (locally)	-	-	-
	Zinc-chlor-iodine	-	-	+	+
Lignin/ Wall-bound phenolics	Toluidine blue	-	±	+	+
	Phloroglucinol-HCl	-	+	+	-
	Maule test	-	-	-	-
	Lignin pink	-	-	-	±
Suberin	Sudan IV	-	+	-	-

<sup>a</sup> Specimen preparation and staining methods as described previously (15).

Essentially identical processes occur in unwounded spruce bark, challenged by, and resisting successfully, at least in the short term, the root- and butt-rot pathogen *Armillaria obscura* (Secretan) Herink. At rhizomorph contact and attempted infection sites on the bark of buttress roots of c 60-year-old trees of *Picea sitchensis* (Bong.) Carr., penetration of the surface periderm had occurred. Small (c 10 mm. diameter) necrotic regions resulted, confined to superficial bark tissues only. Mechanical attachment of these lesions (which had been initiated some time previously so that host responses to the challenge were essentially complete) was weak, and they were readily detached from the roots as bark scales. Cleavage occurred in the plane of a necrophylactic periderm, formed at the margin between tissue colonized by *A. obscura* and the healthy bark (Figure 2). Cell wall

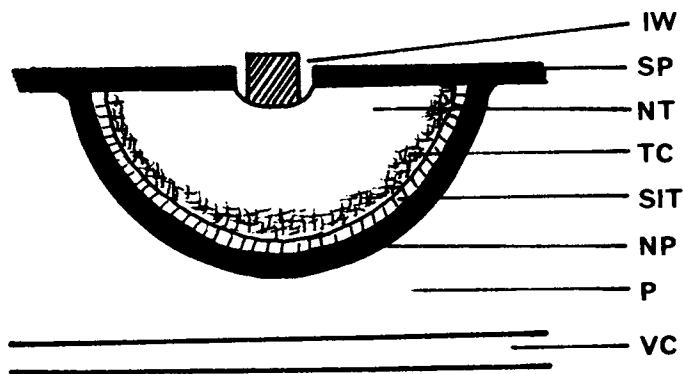


Figure 1. Structural responses of the bark of *Picea sitchensis* to wounding and inoculation with *Phaeolus schweinitzii*. IW, inoculated wound; SP, surface periderm; NT, necrotic tissue; TC, thickened cells; SIT, relic of suberized impervious tissue; NP, necrophylactic periderm; P, phloem; VC, vascular cambium.

alterations, identical to those associated with artificial wounds (9) were detectable in and around the lesion using a range of histochemical tests (Table I).

The underlying healthy bark was separated from the fungally colonized tissues by a necrophyllactic periderm, essentially similar to the normal root surface periderm. This comprised layers of thin walled, suberized phellem cells and thick walled cells staining positively with the phloroglucinol-HCl reagent. Outside the outermost phellem cells there existed a single layer of irregular suberized cells, corresponding to the cells forming the suberized impervious tissue prior to phellogen formation. The thickened, phloroglucinol-positive cells between these and the necrotic tissue were not suberized. Fungal hyphae were visible in these cells (Figure 3), indicating that this wall thickening did not itself pose a major impediment to the growth of the fungus, and were present also in the necrotic tissues, from which evidence of wall-bound phenolic compounds was also obtained. No hyphae were seen, however, in the suberized tissues, suggesting that these were crucial to the effectiveness of this barrier response.

*Cell Wall Alterations in the Bark of Woody Angiosperms.* Responses to wounding and infection closely similar to those found in Gymnosperms occur also in the bark of Angiosperms. These responses have been described in detail from a number of woody species (8, 14, 38, 39) and appear essentially similar in all. Formation of a suberized impervious tissue in undamaged tissues beneath the lesion is followed by the restoration of the plant surface by development of a necrophyllactic periderm. Where a rapidly spreading lesion results from poplar infections by *Cytospora chrysosperma*, there may be colonization of the host bark tissues without expression of these defensive responses. However, when slowly extending perennial cankers are formed by this pathogen a necrophyllactic periderm is produced by the plant, and advance of the fungus appears to take place only where there are discontinuities in this barrier, e.g., where it is traversed by bundles of phloem fibres (38).

*Responses in Non-woody Perennial Plants.* Although pathogens capable of mounting a prolonged attack from a colonized food base are less usual on non-woody species, such attacks can sometimes occur. In these instances periderm restoration responses comparable to those described from woody plants may operate to restrict pathogen ingress. This may be exemplified by the response of horseradish, *Armoracia rusticana* Gaertn, May & Scherb. to attack by an *Armillaria* species (probably *A. bulbosa* (Barla), Kile and Watling). Although not an important pathogen of this plant, *Armillaria* rhizomorphs may attempt to penetrate and colonize its large, fleshy roots.

Sections of infected roots show colonized, necrotic tissues bounded by suberized phellem cells. Penetration of these necrophyllactic periderms was effected by rhizomorph-like aggregations of hyphae (Figure 4). Cells in the necrotic zone stained green with toluidine blue and gave a positive response with the phloroglucinol-HCl reagent, but did not color with the Maule test, suggesting the presence of cell-wall bound phenolics in these tissues, al-

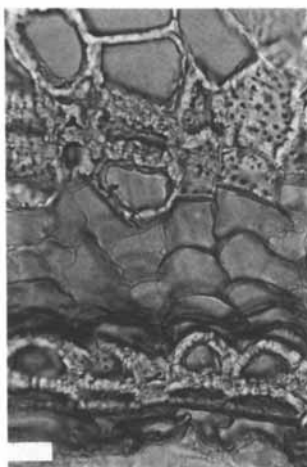


Figure 2. Necrophyllactic periderm in the bark of *Picea sitchensis* following attempted infection by *Armillaria obscura*. Bark sectioned and stained with Sudan IV, after extraction with chlorine dioxide to remove aromatic compounds, essentially as previously described (15). NT, necrotic tissue; TC, thickened cells; SIT, relic of suberized impervious tissue; NP, necrophyllactic periderm. Scale bar = 25  $\mu\text{m}$ .



Figure 3. Hyphae (arrowed) of *Armillaria obscura* in thick walled cells (TC) overlying the necrophyllactic periderm (NP) in *Picea sitchensis*. Bark sectioned and stained with toluidine blue as previously described (15). Scale bar = 25  $\mu\text{m}$ .

though lignin formation itself may not have occurred. Hyphae were present in these necrotic tissues but none were seen penetrating the suberized cells. Although the role of chemical defences in this interaction was not examined (cf. 24), it would appear that the suberized periderm barriers produced in response to infection posed a more effective defence against *Armillaria* than the wall-bound phenolics of the necrotic tissues. The periderms were, however, repeatedly breached by the aggregated mycelium of the fungus, resulting in a complex lesion containing many defeated periderm barriers extending into the root xylem.

### Defence in Living Wood

The sapwood of a living tree, comprising the xylem tissues functional in transport and storage, contains living cells and is capable of active responses to infection. In contrast the heartwood (in those species that form it) is non-living and incapable of further metabolic activity. Active defensive responses are thus impossible in heartwood, although antifungal compounds or cell wall alterations laid down when the wood was still living may continue to function. Indeed there are striking similarities between many of the defences induced in sapwood by fungal attack and the changes occurring during heartwood formation, suggesting that these processes may be related (5). Both antimicrobial chemical defences (40) and cell wall alterations have been reported from xylem of woody plants. As with defences in the bark, only cell wall alterations will be discussed. Two types of barrier can be identified—those comprising specialized tissues formed *de novo* in response to wounding and infection, and those formed in pre-existing xylem.

*Tissue Barriers Formed de novo.* Many woody perennials respond to wounds resulting in cambial damage, and concomitant fungal infection of underlying xylem, by the production of a distinctive barrier tissue. This barrier, which has been termed the compartmentalization wall 4 (41), comprises a sheet of traumatic axial parenchyma cells, formed by the cambium in the vicinity of the wound, and laid down as the first xylem tissue produced after wounding (15, 42). In conifers this parenchyma is commonly accompanied by resin ducts (43). In most, but not all, species so far examined the parenchyma cells of the wall 4 barrier zone are suberized, at least where they overlie fungally colonized wood (5, Pearce, R.B., unpublished data). Evidence has been obtained from oak (*Quercus robur*) to suggest that the suberization response of these tissues, but not necessarily their formation by the cambium, is fungally elicited (5).

Suberization of these cells renders them resistant to degradation by wood decaying fungi. Sections through the compartmentalization wall 4 barrier region in *Q. robur*, incubated for several weeks with the wood decay pathogen *Stereum gausapatum*, were extensively degraded by the fungus, except for the suberized cells which remained essentially intact (15). Suberized xylem cells are clearly able to resist degradation by wood decay fungi for prolonged periods: the relics of suberized cells and tyloses, formed as a



normal heartwood component in *Q. robur* (44), remained in wood otherwise more or less totally decayed by natural infection with the white-rot fungus *Ganoderma adspersum* (Figure 5).

In some species, however, e.g. ash, *Fraxinus excelsior*, cells of the traumatic axial parenchyma of the compartmentalization wall 4 may show no evidence of cell wall alterations, yet appear to act normally as a functional barrier to decay (Pearce, R.B., unpublished data). It is to be presumed that the spread of decay fungi is arrested either by chemical defences or by environmental constraints (cf. 26-28) in such species. Clearly, a contribution may be made by these defences in suberizing species also: phytoalexin-like antifungal compounds have been detected in association with a suberized wall 4 barrier in *Acer saccharinum* (42). More work will be required to elucidate the long-term effectiveness of the various mechanisms maintaining the function of these barrier walls.

*Cell Wall Alterations in Pre-existing Xylem.* Where xylem colonizing fungi interface with pre-existing sapwood, responses of the living parenchyma cells can result in the formation of a reaction zone (45-47). Reaction zones present a less well defined barrier to infection than the compartmentalization wall 4 and have been envisaged as a dynamic response, healthy sapwood being converted to reaction zone tissue ahead of the advancing fungus (45, 47). Evidence has recently been obtained that this is not a continuous process, but that reaction zones act as static boundaries to decay, which advance discontinuously within the tree, periods of rapid fungal advance eliciting little or no host response being followed by periods of stasis, accompanied by the formation of clearly defined reaction zones (5, Pearce, R.B., unpublished data).

The accumulation of phytoalexin-like antifungal compounds commonly occurs in reaction zone tissues (40, 42), and brown deposits, giving staining responses positive for phenolic compounds, are frequently present in cells in this region. Vessels may be occluded by these deposits (gummosis) or by the formation of tyloses, balloon-like outgrowths from the walls of vessel parenchyma cells (5). Cell wall suberization responses commonly occur in reaction zones (5, 48), although they are not always present, even in species having a demonstrable suberization response in the wall 4 barrier, e.g. *Acer saccharinum* (42). Tyloses are usually suberized (44, 49, Pearce, R.B., unpublished data). In those species in which abundant tylosis formation occurred in reaction zones, suberization of xylem parenchyma cells, including the ray parenchyma, was normally observed. In species in which vessel occlusion was predominantly by gummosis, suberization responses were often lacking (Pearce, R.B., unpublished data).

Unlike the compartmentalization wall 4, the suberized tissues in reaction zones do not form a continuous barrier, potentially impregnable by pathogens incapable of degrading suberized walls. However, suberized tyloses and parenchyma cell walls block the easiest routes of fungal spread in the xylem—axially along vessels and radially in the rays (50)—and may thus greatly hinder fungal spread. Undoubtedly these cell wall alterations normally act in concert with other defences—antifungal compounds and/or

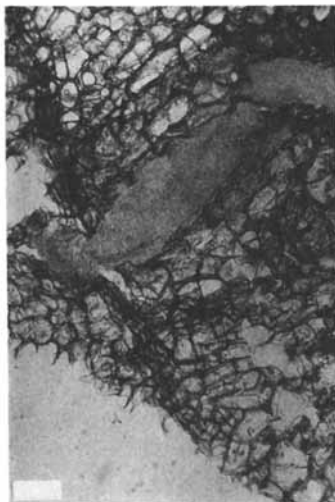


Figure 4. Penetration of necrophytactic periderms (NP) in the root of *Amoracia rusticana* by rhizomorph-like aggregations of hyphae (R). Scale bar = 100  $\mu\text{m}$ .

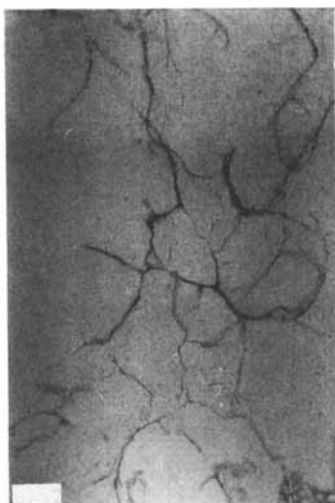


Figure 5. Heartwood of *Quercus robur* with advanced decay caused by *Ganoderma adspersum*. Although the wood has been extensively degraded, suberized tyloses and vessel linings remain recognizable. Wood sectioned and stained with Sudan IV as previously described (15). Scale bar = 100  $\mu\text{m}$ .

environmental constraints on pathogen growth (as with the wall 4 barrier also). Where cell wall alterations are not detectable it is to be presumed that adequate protection is afforded by these alternative mechanisms.

### Concluding Discussion

A common requirement for the successful protection of perennial plants against many of their pathogens is for defence to be durable. Secondary tissues may persist for decades or centuries, and pathogens supported by a substantial food base may be capable of mounting a prolonged assault on the potential host. Cell wall alterations, comprising either the deposition of new material on pre-existing cell walls, or the formation of new tissues with atypical or specialized cell walls, have been implicated as defence mechanisms in a wide range of circumstances in perennial plants. A role in antimicrobial defence can be ascribed to the suberized phellem forming the surface of the secondary tissues of such plants. Internal periderms which may have a defensive function occur in some species also. Wounding or infection of cortical and phloem (bark) tissues normally results in a sequence of cell wall alterations, commencing with changes to walls of pre-existing cells, and culminating with the restoration of the intact plant surface by means of the formation of a necrophylactic periderm. Wounds to the cambium and xylem result in the production of a traumatic barrier tissue, often with suberized walls, which prevents damage to the vital cambium and the youngest, metabolically most important, secondary tissues by pathogens becoming established in the exposed xylem. Suberization responses also often occur in the reaction zone margins of infection and decay in living wood.

As defence mechanisms in plants commonly act in concert, it would be wrong to ascribe a primary role to these various wall alterations without additional investigation: in virtually all cases evidence for the concomitant operation of chemical defences is also available. However, cell wall alterations are particularly well suited to long term defence, providing stable and durable barriers that are not dependant on the continuing metabolic activity of living cells to maintain them, and which are not subject to chemical instability or leaching.

In the cell wall alterations discussed suberization has played a prominent role. This is probably not coincidental. Both carbohydrate polymers and lignin are abundant in the secondary tissues of perennial plants, especially woody species. Pathogens adapted to inhabit this highly lignified environment are likely to possess effective enzyme systems for the metabolism of this phenolic polymer, which is therefore unlikely to present a serious impediment to these fungi. This is in marked contrast to the pathogens of primary plant tissues (leaves, etc.) in which lignin is not abundantly present, against which cell wall lignification may present an effective defence (51). Indeed, fungal colonization of cells with walls altered by lignification (or at least deposition of wall-bound phenolics) was seen in most of the interactions discussed here. The predominantly aliphatic polymer suberin is not a primary constituent of these secondary tissues and is

thus likely (as has been demonstrated) to present more of an impediment to such pathogens. Also, if as has been suggested (26-28), the maintenance of an appropriate moisture content in functional sapwood is important in limiting fungal colonization, suberin may provide the necessary permeability barrier to maintain this and minimize the extent of disruption to xylem transport resulting from wounding or microbial infection.

### Literature Cited

1. Callow, J.A. ., Ed. *Biochemical Plant Pathology*; John Wiley & Sons: Chichester, 1983.
2. Horsfall, J. G.; Cowling, E. B., Eds. *Plant Disease: An Advanced Treatise*; Vol. V; Academic Press: New York, 1980.
3. Gibson, I. A. S.; Burley, J.; Speight, M. R. *C.F.I Occasional Papers*, No. 18., 1980.
4. Woodward, S.; Pearce, R. *Biomass News International* 1986, **16**, 2-3.
5. Pearce, R. B. In *Fungal Infection of Plants*; Pegg, G.F.; Ayres, P.G., Eds.; Cambridge University Press: Cambridge, 1987; pp 219-238.
6. Sinclair, W. A.; Lyon, H. H.; Johnson, W. T. *Diseases of Trees and Shrubs*; Comstock Publ. Assoc.: Ithaca, 1987; pp 308-313.
7. Mullick, D. B. In *The Structure, Biosynthesis and Degradation of Wood*; Loewus, F. A.; Runeckles, V. C., Eds.; Plenum Press: New York, 1977; pp 395-442.
8. Biggs, A. R. *Phytopathology* 1985, **75**, 1191-1195.
9. Woodward, S.; Pearce, R. B. *Physiol. Mol. Plant Pathol.* 1988, **33**, 151-162.
10. Woodward, S.; Pearce, R. B. *Physiol. Mol. Plant Pathol.* 1988, **33**, 127-149.
11. Prior, C. *Ann. Bot.* 1976, **40**, 261-279.
12. Sherwood, R. T.; Vance, C. P. *Phytopathology* 1976, **66**, 503-510.
13. Ride, J. P.; Pearce, R. B. *Physiol. Plant Pathol.* 1979, **15**, 79-92.
14. Biggs, J.R. *Can. J. Bot.* 1984, **62**, 2814-2821.
15. Pearce, R. B.; Rutherford, J. *Physiol. Plant Pathol.* 1981, **19**, 359-369.
16. Aist, J. R. *Ann. Rev. Phytopathol.* 1976, **14**, 145-163.
17. Kunoh, H.; Ishizaki, H. *Physiol. Plant Pathol.* 1975, **5**, 283-287.
18. Heath, M. C. *Physiol. Plant Pathol.* 1979, **15**, 141-148.
19. Ride, J. P. *Physiol. Plant Pathol.* 1980, **16**, 187-196.
20. Aist, J. R. In *The Dynamics of Host Defence*; Bailey, J. A.; Deverall, B. J., Eds.; Academic Press: Sydney, 1983; pp.33-70.
21. Mullick, D. B. *Can. J. Bot.* 1975, **53**, 2443-2457.
22. Hammerschmidt, R.; Kuc, J. *Physiol. Plant Pathol.* 1982, **20**, 61-71.
23. Edwards, M. C.; Ayres, P. G. *New Phytol.* 1981, **89**, 411-418.
24. Garrod, B.; Lewis, B. G.; Brittain, M. J.; Davies, W. P. *New Phytol.* 1982, **90**, 99-108.
25. Kolattukudy, P. E. *Can. J. Bot.* 1984, **62**, 2918-2933.
26. Boddy, L.; Rayner, A. D. M. *New Phytol.* 1983, **94**, 623-641.
27. Cooke, R. C.; Rayner, A. D. M. *Ecology of Saprotrophic Fungi*; Longman: London, 1984; pp. 196-237.

28. Rayner, A. D. M. In *Water, Fungi and Plants*; Ayres, P.G.; Boddy, L., Eds.; Cambridge University Press: Cambridge, 1986; pp. 321-341.
29. Zimmermann, W.; Seemüller, E. *Phytopath. Z.* 1984, **110**, 192-199.
30. Ofong, A. U. Ph.D. Thesis, Oxford University, Oxford, UK, 1988.
31. Royle, D. J. In *Biochemical Aspects of Plant Parasite Relationships*; Friend, J.; Threlfall, D.R., Eds.; Academic Press: London, 1976; pp. 161-193.
32. Thomas, H. E. *J. Agric. Res.* 1934, **48**, 187-218.
33. Tourvieille de Labrouhe, D. *Agronomie* 1982, **2**, 553-560.
34. Campbell, C. L.; Huang, J. S.; Payne, G. A. In *Plant Disease: An Advanced Treatise*; Vol. V; Horsfall, J. G.; Cowling, E. B., Eds.; Academic Press: New York, 1980; pp. 103-120.
35. Hepper, F. N. *Arboricultural J.* 1981, **5**, 39-43.
36. Moss, E. H.; Gorham, A. L. *Phytomorphology* 1953, **3**, 285-294.
37. Moss, E. H. *Amer. J. Bot.* 1936, **23**, 114-120.
38. Biggs, A. R.; Davis, D. D.; Merrill, W. *Can. J. Bot.* 1983, **61**, 563-574.
39. Biggs, A. R.; Merrill, W.; Davis, D. D. *Can. J. For. Res.* 1984, **14**, 351-356.
40. Kemp, M. S.; Burden, R. S. *Phytochemistry* 1986, **25**, 1261-1269.
41. Shigo, A. L.; Marx, H. G. *USDA For. Serv. Agric. Inf. Bull. No. 405*, 1977.
42. Pearce, R. B.; Woodward, S. *Physiol. Mol. Plant Pathol.* 1986, **29**, 197-216.
43. Tippett, J. T.; Shigo, A. L. *Eur. J. For. Pathol.* 1981, **11**, 51-59.
44. Pearce, R. B.; Holloway, P. J. *Physiol. Plant Pathol.* 1984, **24**, 71-81.
45. Shain, L. *Phytopathology* 1967, **57**, 1034-1045.
46. Shain, L. *Phytopathology* 1971, **61**, 301-307.
47. Shain, L. *Phytopathology* 1979, **69**, 1143-1147.
48. Biggs, A.R. *Phytopathology* 1987, **77**, 718-725.
49. Parameswaran, N.; Knigge, H.; Liese, W. *IAWA Bull. N.S.* 1985, **6**, 269-271.
50. Greaves, H.; Levy, J. F. *J. Inst. Wood Sci.* 1965, **15**, 55-63.
51. Ride, J. P. In *Biochemical Plant Pathology*; Callow, J. A., Ed.; John Wiley & Sons: Chichester, 1983; pp. 215-236.

RECEIVED March 10, 1989

## Chapter 26

# Infection-Induced Lignification in Wheat

J. P. Ride, M. S. Barber, and R. E. Bertram

School of Biological Sciences, University of Birmingham, P.O. Box 363,  
Birmingham B15 2TT, England

Lignification occurs rapidly in wheat leaves in response to challenge by filamentous fungi. The response confers on the plant cell walls a high degree of resistance to degradation by plant-pathogenic fungi and may thus be important in disease resistance. Physical or chemical stresses which induce defence mechanisms in other plants do not generally elicit lignification in wheat; the response appears to be specific to filamentous fungi. Chitin, a key component of the cell walls of many fungi, has been identified as one elicitor of the response. The insolubility of this polymer suggests that soluble fragments are released by plant enzymes and then diffuse to the cells that respond. Chitin oligosaccharides (DP > 3) that elicit lignification have been identified and a model is proposed for the release, degradation and binding of these signal molecules in infected plants.

Cell wall alterations are now recognized as a common response of higher plants to attempted invasion by fungi. Many of the cell wall modifications may have a role to play in disease resistance. This is particularly true of lignification, which in relation to disease resistance has in the past been thought of as mainly a wound response, sealing off infected areas but not acting as a main line defence. However, the frequent rapidity of induced lignification, together with the high resistance it confers to microbial degradation, is leading to its acceptance as an important defensive response—one which may act alone or in concert with other mechanisms, such as phytoalexin production, to provide substantial resistance to fungal penetration (1-3).

0097-6156/89/0399-0361\$06.00/0  
© 1989 American Chemical Society

### Lignification as a Defence Mechanism in Wounded Wheat Leaves

The inoculation of wounds on wheat leaves with non-pathogenic fungi (i.e., pathogens of other plant species), such as *Botrytis cinerea* or *Mycosphaerella pinodes*, results in limitation of fungal growth to the wounds, despite heavy growth within the wounded tissue itself (4). This limitation is associated with cell wall alterations at the wound margins, giving a complete ring of tissue resistant to cell wall degrading enzymes being produced within 18 to 24 h after inoculation (4). Wounding alone does not induce such a response.

Histochemistry (4,5), autoradiography following precursor feeding (6), lignin thioglycolate extraction (5), ionization difference spectra following alkali extraction (4) and nitrobenzene oxidation products (4) all indicate the presence of lignin at the infected wound margins. Changes in the difference spectra, in the ratio of nitrobenzene oxidation products and in some histochemical reactions also indicate that the induced polymer is different from the polymer found in healthy leaves (4); in particular, the ratio of syringyl to guaiacyl moieties is increased.

The chemical and physical evidence for the presence of lignin in the material deposited at wound margins is supported by biochemical studies on the enzymes involved in phenylpropanoid metabolism. Thus, the extractable activities of phenylalanine ammonia-lyase, tyrosine ammonia-lyase, cinnamate-4-hydroxylase, caffeic acid O-methyltransferase, 5-hydroxyferulic acid O-methyltransferase, hydroxycinnamate:CoA ligase (4-coumarate ligase) and peroxidase all increase substantially following inoculation of wounds with *Botrytis cinerea* (7-9). Autoradiography following administration of labelled phenylalanine, cinnamate or sinapate indicates that the rapid induction of lignin deposition by fungi results in lignification not only of the cell walls but of all the cell contents, particularly in the cells undergoing the most prominent reaction at the very edge of the wound (6). Presumably the normal control mechanisms that prevent polymerisation of the monomers before they are exported to the wall are in some way defective in these rapidly degenerating cells.

The importance of lignification as a general resistance mechanism against fungi is supported by the rapidity of the response to non-pathogenic fungi (4), the slower rate of lignification in response to pathogenic *Septoria* (4), *Fusarium*, and *Penicillium* (10) species and the pronounced resistance to cell wall degrading enzymes that the response confers on the host tissue. Also, treatments which induce the response, such as non-pathogenic fungi or the fungal polysaccharide chitin, provide significant protection against subsequent inoculation with pathogens. Conversely, treatments such as cycloheximide or UV light which inhibit the response have been shown to make plants highly susceptible to many fungi—although it is plainly possible that many other unknown mechanisms may be also inhibited by these treatments (10).

## Lignification as a Defence Mechanism in Unwounded Wheat Leaves

Small quantities of lignin are deposited in unwounded wheat leaves when challenged by fungi. Attempted invasion of the epidermal cells of many plants, but particularly members of the Gramineae, results in the rapid formation of minute wall-like deposits called papillae, often accompanied by a modification to the adjacent epidermal wall called a halo (11). We have shown that in wheat these structures contain small, but probably significant, amounts of lignin (12) and that this confers on the structures a substantial degree of resistance to fungal degradation *in vitro*. Pathogens of wheat are no more capable of degrading the structures than fungi non-pathogenic on wheat (13). The success of pathogens is apparently dependent upon a slower response by the host.

Some pathogens, such as the stem rust pathogen *Puccinia graminis* f.sp. *tritici*, do not attempt to enter leaves via epidermal cells but instead use the natural openings provided by stomata. The reaction of resistant wheat varieties usually involves a "hypersensitive" response, where the invaded mesophyll cells undergo a rapid deterioration. Here again lignification has a potential significance (14). Fluorescence microscopy, histochemistry, and autoradiography all indicated that lignification occurred during the necrosis of the cells undergoing the hypersensitive response in near-isogenic wheat lines carrying the *Sr5* or *Sr6* (at 19°C) alleles for resistance to *P. graminis* f.sp. *tritici*. Lignification was not observed in the susceptible interactions between the fungus and the parent cultivar Marquis (*Sr5*, *Sr6*), or the *Sr6* line when tested at 26°C (14).

## Specificity of Induction of Lignification in Wounded Wheat Leaves

Lignification is one of many defensive responses that plants employ to counter potentially pathogenic fungi. Phytoalexin accumulation has received much attention and it is evident that this response is not restricted to occasions of fungal attack, but can usually be activated by a whole range of other stressful abiotic treatments, e.g., UV light, heavy metal salts, antimetabolites, oxidizing and reducing agents, physical damage, etc. (15). Phytoalexin production could therefore be viewed as a response to generalized damage to the plant, rather than a specific response to fungal invasion. By contrast, the induction of lignification in wheat appears to be highly specific to filamentous fungi (16). Thus, a range of abiotic treatments reported to induce phytoalexin accumulation in various plants failed to induce lignification in primary wheat leaves. Filamentous fungi were, however, usually potent inducers with yeasts and bacteria being less active (16).

## Elicitors of Lignification

The high specificity of induced lignification in wheat for filamentous fungi leads immediately to speculation as to the nature of the signals involved in the general recognition of fungi by wheat. Microbial molecules that trigger plant defence responses are usually termed "elicitors" (17).



In order to study elicitors of lignification in wheat leaves, a quantitative assay for induced lignification has recently been developed (5). The method involves locating lignin by staining leaves with *p*-nitrobenzene diazonium tetrafluoroborate after removal of soluble and wall-esterified phenolics by pre-extraction in ethanol and alkali. The local intensity of lignin is then determined by scanning the leaves with a gel-scanning densitometer. The method gives results which correlate well with those based on extraction with thioglycolic acid, but has the advantage that additional information on the location of the induced lignin is obtained.

Using this assay, a range of fungal and plant products has been screened for lignification-eliciting activity, including a number that were known elicitors of defence reactions in other plants (5). The majority of treatments were inactive. The major elicitors identified were chitin, chitosan, a commercial "cellulase" and "pectinase" of fungal origin, and a partial hydrolysate of the cell wall glucan of the fungus *Phytophthora megasperma* f.sp. *glycinea* containing oligo- $\beta$ -glucosides with a degree of polymerisation (DP) of 10-13. The "cellulase" was the most active and its activity was retained after heat-inactivation.

### Chitin as an Elicitor of Lignification

Although chitin, a  $\beta$ (1-4)-linked polymer of *N*-acetyl-D-glucosamine, was not the most active elicitor discovered, its widespread occurrence in fungi as a core component of the cell wall and its predominance at hyphal tips encouraged us to examine its elicitor activity in more detail. Although chitosan was also elicitor-active, its activity was thought to depend on the acetylated regions of the polysaccharide since fully deacetylated chitosan had negligible activity (5). Chitin is highly insoluble in water and in the inoculation procedure used it was unlikely to come into direct contact with the cells that lignify. It was therefore postulated that plant enzymes, presumably chitinases, release soluble fragments that are the signals that pass from pathogen to host.

To investigate this possibility, chitin oligosaccharides were first prepared by acid hydrolysis of chitin and separation of the products by HPLC (18). For comparison, the deacetylated counterparts were also prepared by ion-exchange chromatography of acid hydrolysates of chitosan. Tests on the prepared oligomers indicated that a minimum degree of polymerisation of 4 was necessary for elicitor activity, and that the presence of acetyl groups was essential since the deacetylated tetramer was inactive (18). Wheat leaf tissue has now been shown to contain several chitinases, all of which are endo in action and are capable of releasing the elicitor-active tetramer, and higher oligomers, from chitin (Ride & Barber, unpublished data).

The amount of chitin tetramer required to elicit the response, when administered as a single dose, was relatively high. One explanation for this phenomenon was that chitin oligomers are unstable in wheat leaf tissue, and that administration as a single dose did not properly mimic the low, but continual, levels that would be released from the polymer. This was supported by the observation that the tetramer, when administered

to wheat leaves at a dose which just failed to elicit a response, was reduced in concentration by approximately 70% within 8 hours. The loss was believed to be due not only to the action of the chitinases, which would generate only dimer, but possibly also to *N*-acetyl- $\beta$ -D-hexosaminidases, one of which has now been purified from leaves (Barber & Ride, unpublished data). The role of these enzymes in chitin-elicited lignification is currently being investigated.

### **Wheat Germ Agglutinin: a Possible Receptor for Chitin Oligomers?**

The identification of chitin oligomers as signals involved in the recognition of fungi by wheat leads to speculation on the nature of the presumed receptor for these molecules in plant cells. One candidate for the role is the lectin wheat germ agglutinin (WGA). This protein, isolated originally from wheat germ, carries binding sites that are highly specific for *N*-acetyl-D-glucosamine (GlcNAc), and particularly  $\beta$ (1-4) linked oligosaccharides of GlcNAc (19). Increasing the oligomer size results in increased binding affinity, at least up to the tetramer (19). Each binding site apparently has three subsites with different affinities for GlcNAc (19). Apart from sialyl lactose, where the *N*-acetylneuraminic acid residue mimics GlcNAc and binds to subsite 1, only chitin oligomers and other GlcNAc-containing molecules are known to bind to the lectin (20). It is thus possible that this lectin, whose natural function in wheat is currently unknown, is a receptor for elicitor-active chitin oligomers derived from fungal cell walls. If this is the case, it might be expected that the chitin trimer would be a good elicitor, rather than the weak one revealed in our tests (18), and that sialyl lactose would also elicit a response, which is not the case (Bertram & Ride, unpublished data). These apparent anomalies may be due to rapid degradation of the oligosaccharides in wheat leaves when administered as a single dose; this possibility is currently being assessed.

Despite its abundance in seeds, the lectin is present in much smaller quantities in seedlings and older plants (21), and reports indicate that only traces may occur in the leaves (22). Nevertheless, using specific antiserum raised against purified wheat germ agglutinin, we have now demonstrated the presence of a WGA-like chitin-binding protein in primary wheat leaves (Bertram & Ride, unpublished data). We are currently evaluating the possibility that this molecule is the receptor for elicitor-active chitin oligosaccharides.

### **A Model for the Recognition of Fungi by Wheat**

These results allow us to propose a hypothesis for the processes involved in the general recognition of filamentous fungi by wheat (Fig. 1). The model does not attempt to provide an explanation for the highly specific interactions between certain wheat cultivars and races of fungal pathogens, but deals with the much more general case of wheat resistance to non-pathogenic fungi, i.e., non-host resistance and resistance to saprophytes.

The hypothesis proposes that this basic incompatibility between fungi and wheat is governed by the recognition by the plant of soluble oligosac-

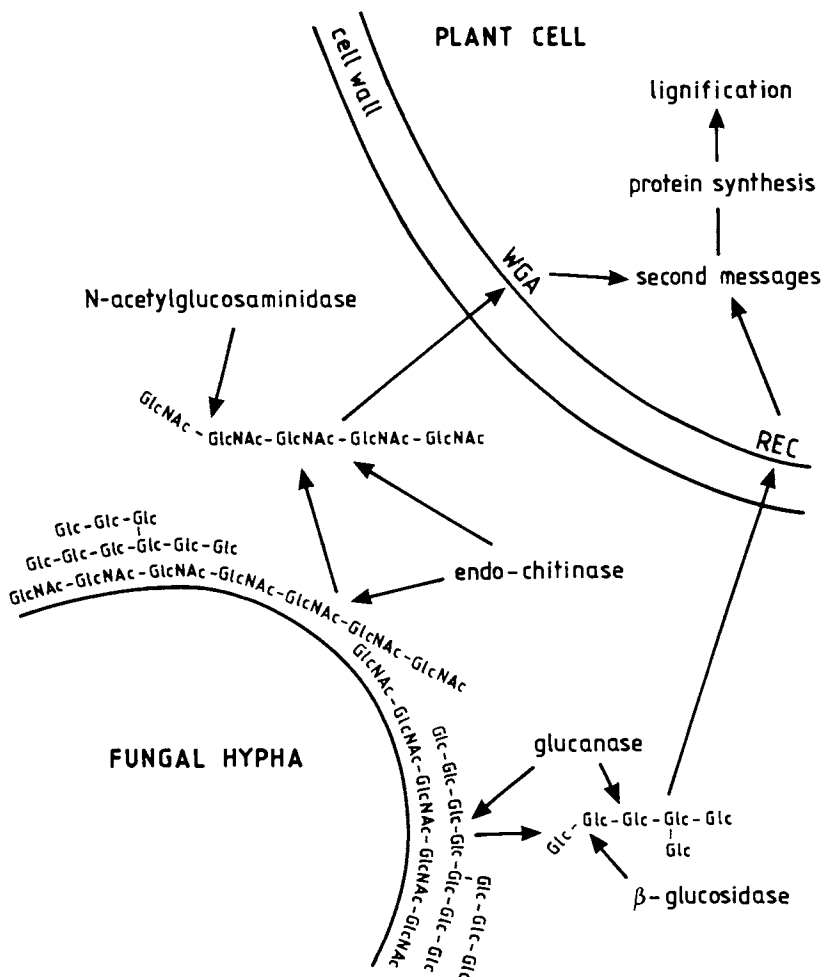


Figure 1. A proposed model for the general recognition of filamentous fungi by wheat resulting in lignification of the plant cells. Hydrolytic enzymes present constitutively in the apoplast of the plant, such as endo-chitinase and  $\beta(1-3)$  glucanase, release oligosaccharides of N-acetylglucosamine (GlcNAc) or glucose (Glc) from the chitin and glucan components of the fungal cell wall. Oligomers of sufficient size, such as the chitin tetramer, are the active signals that pass to the plant cells; the detailed structures of the putative glucose oligosaccharide signals are as yet unknown. Lectins, such as wheat germ agglutinin (WGA) and other unknown lectins (REC), may be the cell surface receptors for these oligosaccharides. The active oligomers are rapidly degraded both by the endo enzymes that liberated them and by glycosidases. Elicitation of defence responses thus depends on a continued but low level of oligosaccharides being liberated from the hyphal tip.

charide signals, which are released from the cell walls of the fungus by plant enzymes or perhaps are present on soluble glycoproteins. In the case of chitin oligosaccharides, these would be released from the hyphal tips by host chitinases. It is interesting in this context that wheat seed chitinase has been shown to release higher oligomers from freshly-synthesized "nascent" chitin, which is likely to be found at growing hyphal tips, than from colloidal or regenerated chitin (23).

The known instability of chitin oligomers in wheat leaves, presumed to be due primarily to the action of chitinases and *N*-acetyl- $\beta$ -D-hexosaminidases, suggests that the key oligosaccharide signals are rapidly turned over *in vivo* and that elicitation of the response probably depends on the presence of continued low levels of the active higher oligomers over a period of time. An obvious question that arises from such a proposed mechanism is why does wheat possess such a relatively insensitive system of recognition. The mechanism would be far more sensitive if there were no destruction of the elicitor-active oligomers; the oligomers would presumably be active at much lower doses and the plant might respond to attempted infection at an earlier stage. A possible answer to this question lies in the fact that lignification is an irreversible, energy-requiring process that frequently involves a certain amount of cell death; restriction of the response to genuine challenges by potential pathogens is therefore beneficial to the plant. Thus wheat only responds to the continued release of oligomers with a relatively high DP, such as that brought about by the presence of growing hyphal tips, and not to the passing presence of other stimuli, such as insect chitin.

Since not all fungi contain chitin, and even those that do have other wall components, it must be supposed that other general signals exist. The high elicitor activity of a partially hydrolysed glucan of fungal origin (5), together with the common occurrence of  $\beta(1-3)$  and  $\beta(1-6)$  linked glucans in fungal cell walls, leads us to propose that the action of glucanases liberates glucose oligosaccharides from fungal walls and that these are also elicitors of the lignification response. In this context it is interesting that  $\beta(1-3)$  glucanase activity has been detected in many plants (24). Lectins are proposed as the primary receptors for the oligosaccharide signals. The location of the WGA-like protein in wheat leaves has not yet been determined, but by analogy with other signal-receptor systems it seems likely that the receptor will be at the cell surface, presumably associated with the plasmalemma. Since analysis of the published amino-acid sequences of WGA isolectins 1 and 2 (25,26) does not immediately reveal any long hydrophobic, membrane-spanning regions, then if this protein is a surface receptor it must presumably be linked *in vivo* to a plasma membrane component.

Lectins have a high degree of specificity for the sugars they bind, and hence the proposal that more than one type of oligosaccharide signal is involved in elicitation necessarily dictates that more than one receptor is present at the cell surface. Since the different signals ultimately result in the same response, it is presumed that the signal transduction pathways

involved in the intracellular transmission of the different signals and their coupling to the response must meet at some point. Perhaps a common second messenger is activated by the interaction of the different signals with their corresponding receptors? An alternative hypothesis would be that the lectins are extracellular and act as transporters rather than membrane-bound receptors. The different elicitor-lectin complexes might then be recognized by a single receptor.

Induced lignification is blocked by treatments which inhibit protein synthesis (10), and it seems likely therefore that the increases in activities observed for enzymes involved in lignin biosynthesis (7,8) depend on enhanced translation, and probably enhanced transcription of the appropriate genes, as has been shown for the phytoalexin response of some plants (27). However, the molecular biology of the response in wheat awaits investigation.

### Literature Cited

1. Vance, C. P.; Kirk, T. K.; Sherwood, R. T. *Annu. Rev. Phytopath.* 1980, **18**, 259-88.
2. Ride, J. P. In *Biochemical Plant Pathology*; Callow, J. A., Ed.; John Wiley: Chichester, 1983; pp 215-36.
3. Ride, J. P. In *Natural Antimicrobial Systems, Part 1. Antimicrobial Systems in Plants and Animals*; Gould, G. W., Rhodes-Roberts, M. E.; Charnley, A. K.; Cooper, R. M.; Board, R. G., Eds.; Bath University Press: Bath, 1986; pp 159-75.
4. Ride, J. P. *Physiol. Pl. Path.* 1975, **5**, 125-34.
5. Barber, M. S.; Ride, J. P. *Physiol. Mol. Pl. Path.* 1988, **32**, 185-97.
6. Maule, A. J.; Ride, J. P. *Physiol. Pl. Path.* 1982, **20**, 235-41.
7. Maule, A. J.; Ride, J. P. *Phytochemistry* 1976, **15**, 1661-64.
8. Maule, A. J.; Ride, J. P. *Phytochemistry* 1983, **22**, 1113-16.
9. Thorpe, J. R.; Hall, J. L. *Physiol. Pl. Path.* 1984, **25**, 363-79.
10. Ride, J. P.; Barber, M. S. *Physiol. Mol. Pl. Path.* 1987, **31**, 349-60.
11. Aist, J. R. *Annu. Rev. Phytopath.* 1976, **14**, 145-63.
12. Ride, J. P.; Pearce, R. B. *Physiol. Pl. Path.* 1979, **15**, 79-92.
13. Ride, J. P. *Physiol. Pl. Path.* 1980, **16**, 187-96.
14. Beardmore, J.; Ride, J. P.; Granger, J. W. *Physiol. Pl. Path.* 1983, **22**, 209-20.
15. Bailey, J. A. In *Phytoalexins*; Bailey, J. A.; Mansfield, J. W., Eds; Halsted Wiley: New York, 1982; pp 289-318.
16. Pearce, R. B.; Ride, J. P. *Physiol. Pl. Path.* 1980, **16**, 197-204.
17. Keen, N. T. *Science* 1975, **187**, 74-5.
18. Barber, M. S.; Bertram, R. E.; Ride, J. P. *Physiol. Mol. Pl. Path.* 1988, in press.
19. Allen, A. K.; Neuberger, A.; Sharon, N. *Biochem. J.* 1973, **131**, 155-62.
20. Wright, C. S. *J. Mol. Biol.* 1984, **178**, 91-104.
21. Mishkind, M.; Keegstra, K.; Palevitz, B. A. *Pl. Physiol.* 1980, **66**, 950-55.

22. Raikhel, N. V.; Mishkind, M. L.; Palevitz, B. A. *Planta* 1984, **162**, 55-61.
23. Molano, J.; Polacheck, I.; Duran, A. ; Cabib, E. *J. Biol. Chem.* 1979, **254**, 4901-07.
24. Boller, T. In *Cellular and Molecular Biology of Plant Stress*; Key, J.L., Kosuge, T., Eds. Alan R. Liss: New York, 1985; pp 247-62.
25. Wright, C. S.; Gavilanes, F.; Peterson, D. L. *Biochemistry* 1984, **23**, 280-7.
26. Wright, C. S.; Olafsdottir, S. *J. Biol. Chem.* 1986, **261**, 7191-95.
27. Dixon, R. A. *Biological Reviews* 1986, **61**, 239-91.

RECEIVED March 10, 1989

## Chapter 27

# Lignin Biosynthesis in Stem Rust Infected Wheat

Bruno M. Moerschbacher

Institut für Biologie III (Pflanzenphysiologie) der RWTH Aachen,  
Worringerweg, D-5100 Aachen, Federal Republic of Germany

Highly resistant wheat varieties exhibit a typical hypersensitive response when infected with an avirulent race of the stem rust fungus. Host cells which are penetrated by a fungal haustorium undergo rapid necrotization, thus depriving the biotrophic parasite of its nutritional basis. This rapid cell death is correlated with the deposition of lignin or lignin-like material in the host cell walls and protoplasts. Inhibition of lignin biosynthesis delays necrotization of penetrated host cells and partially breaks resistance of wheat to stem rust. In resistant plants, an increase in the activities of the general phenylpropanoid pathway and of the specific branch pathway of lignin biosynthesis can be detected at the time of the hypersensitive cell death, contrasting to decreased activities in susceptible near-isogenic plants. The participation of both an elicitor and a suppressor in the signal exchange between host and parasite has been suggested. An elicitor of lignification could be isolated from fungal cell walls. An endogenous suppressor of the resistance reaction was found in wheat cell walls.

Lignin, the second most abundant organic compound on earth, is extremely resistant to microbial degradation (1,2) and thus constitutes one of the most effective mechanical barriers against pathogenic invasion (3,4). Consequently, the lignin content of higher plants has long been recognized as an important factor in the resistance against the attack by a myriad of potential pathogens.

In addition to its role as a preformed resistance factor, Hijwegen (5) has also proposed active induction of lignification as a defense mechanism of cucumber against *Cladosporium*. Subsequently, in a number of host-pathogen interactions, induced lignification has been proposed as the active

0097-6156/89/0399-0370\$06.00/0  
© 1989 American Chemical Society

mechanism for resistance. Some of the most intensely studied interactions are those of resistance of tobacco against tobacco mosaic virus (6-9), potato against *Phytophthora* (10-12) or non-pathogens (13), cucumber (14,15) and melons (16-18) against *Cladosporium* and *Colletotrichum* species.

In the family of the Gramineae, which includes some of man's most important crops, active lignification seems to be of special importance for induced resistance mechanisms (19,20). This may be correlated with the nearly complete absence of phytoalexins in this family (21). In spite of an intensive search for such infection-induced fungitoxic substances, no phytoalexins have been found in wheat to date (22). Nevertheless, induced lignification has been shown to play an important role in disease resistance of wheat against a variety of fungal pathogens (4):

The formation of a ring of lignified cells at wound margins prevents the spread of necrotrophic fungi (23-25). Lignified papillae produced in epidermal cells just below fungal appressoria prevent the ingress of fungal penetration pegs directly penetrating epidermal cells (26-29). Cellular lignification of penetrated epidermal and mesophyll cells and concomitant cell death arrest further growth of biotrophic parasites (22,30,31).

### Modes of Action of Lignification as a Resistance Mechanism

Several modes of action of lignification as a resistance mechanism have been proposed by Ride (32). Lignification enhances the resistance of plant cell walls against mechanical and enzymatic attack and may thus impede fungal invasion of host cells. Incrustation of cell walls with lignin may slow down diffusion and thus immobilize fungal toxins or decrease the flow of nutrients to the parasite. The phenolic precursors as well as the free radicals formed during the process of lignification may be fungitoxic and act as phytoalexins. Furthermore, lignification may spread to hyphal walls and thus impede further fungal growth.

One or several of these mechanisms may be involved in resistance responses when lignification takes place in the plant cell walls. In the case of biotrophic parasites which rely on functional mature haustoria within living host cells for their development (33-36), lignification of the whole cell contents leading to rapid host cell death may in itself be a decisive factor in the expression of resistance.

### Evidence for the Participation of Lignification in Resistance Reactions

Different approaches have been used to produce evidence for the participation of lignification in resistance reactions. We will confine the discussion to those techniques applied in investigations on resistance reactions of wheat, one of the best studied host plants to date (4).

The most convenient way of determining lignin is provided by a range of histochemical staining reactions (37): A positive outcome of the phloroglucinol/HCl or the chlorine/sulfite test, supposed to be the most specific stains for lignin (38,39), point to the participation of lignin in the investigated resistance phenomena (23-25,28-31).



Yellow autofluorescence of lignin in UV-light (40,41) has also been used as a criterion (28,30,31). However, in view of the countless autofluorescent substances in plants (40,42), even the recording of a typical emission spectrum for lignin (31) cannot be regarded as a specific proof for the presence of lignin.

The decreased enzymatic digestibility of plant cell walls upon incrustation with lignin (1,2,32) has also been used as an, albeit quite unspecific, demonstration of lignification (23,24,28-30).

The biochemical determination of newly synthesized lignin is difficult because of large amounts of preformed lignin in tracheary and supporting elements of healthy tissues. Nevertheless, it has been achieved in the case of non-host resistance reactions against wound infections by necrotrophic parasites (23).

When radioactive lignin precursors are applied to resistant host plants infected with an avirulent pathogen, the autoradiographic localization of radioactivity in resistant reacting host cells may help to corroborate the participation of lignification in the resistance response. Thorough extraction of non-polymerized precursor with organic solvents and the removal of esterified phenolics by alkaline hydrolysis are important steps in these experiments (25,28,30,31).

A different approach to investigate active lignification during resistance reactions is provided by the determination of enzyme activities involved in lignin biosynthesis. Resistant plants are expected to be more strongly activated during or immediately preceding the resistance reaction compared to susceptible plants. Thus, phenylalanine ammonia-lyase (PAL) (43-45), cinnamic acid 4-hydroxylase (46), O-methyltransferases (44), and 4-coumarate:CoA ligase (46) have been investigated in a number of studies. As these enzymes are part of the general phenylpropanoid pathway, and thus not just involved in lignin biosynthesis, their activation is only proof of overall participation of phenolic substances in the resistance reactions (47-49). In order to prove a specific induction of lignification, one or several enzymes of the specific branch pathway of lignin biosynthesis must be investigated. Although peroxidases catalyze the last enzymic step of this pathway (50), increased peroxidase activities cannot be regarded as a specific criterion for lignification, as these enzymes play a range of different roles in plant metabolism (51).

### Lignification in the Wheat-Stem Rust System

We will now consider the evidence that has accumulated to show the participation of lignification in the hypersensitive resistance of wheat to the wheat stem rust fungus, *Puccinia graminis* f. sp. *tritici*.

Beardmore *et al.* (30) and Tiburzy (31) showed that epidermal (31) and mesophyll (30,31) cells of resistant wheat plants, penetrated by haustoria of an avirulent race of the fungus, can be stained with phloroglucinol/HCl (31) and chlorine/sulfite (30,31). These cells show yellow autofluorescence under UV-light (30,31), the emission spectrum is identical to that of lignified tracheary elements (31).

The application of radioactive phenolic precursors—quinic acid and shikimic acid (52), phenylalanine (30,53), tyrosine (53), and cinnamic acid (30,31,53)—to infected wheat leaves led to a solvent- and alkali-resistant incorporation of radioactivity into hypersensitively reacting host cells suggesting lignin formation had occurred.

In a recent study (54), we showed increased activities of two enzymes of the general phenylpropanoid pathway, PAL and 4-coumarate:CoA ligase, as well as one enzyme of the specific pathway of lignin biosynthesis, cinnamyl-alcohol dehydrogenase (CAD), in resistant plants at the time of the hypersensitive host cell death. On the other hand, decreased activities were observed at the same time with susceptible host plants (54). Furthermore, we showed that the well known increase in peroxidase activities, which is strong in resistant and only weak in susceptible plants (55-58), is at least partly due to the increased activity of the lignin biosynthetic pathway (54,59).

When highly resistant wheat varieties are inoculated with an avirulent race of the stem rust fungus, fungal growth is arrested by the hypersensitive death of the first penetrated host cells (30,31.) Even in very densely inoculated leaves, the reaction of less than one percent of the host cells is sufficient to stop further development of the parasite. This small percentage may be the reason, why no increased content of biochemically determined lignin was measured in infected hypersensitive wheat leaves (60,61).

However, when an elicitor (see below), isolated from the stem rust fungus (62), is injected into the intercellular spaces of wheat leaves almost every cell in the infiltrated area exhibits a hypersensitive-like reaction (62-65). In the elicitor treated leaves, lignin content as determined by the thioglycolic acid procedure clearly increased (66).

### **Lignification as a Causal Factor in Resistance**

The above described studies strongly suggest a correlation between lignification and resistance. However, they do not allow any conclusion concerning a causal relationship between the two phenomena. The question remains as to whether lignification is indeed responsible for impaired fungal development. We have already briefly mentioned a possible chain of events during the incompatible interaction between highly resistant wheat leaves and avirulent strains of the stem rust fungus. Lignification of the whole cell contents may be regarded as an active mechanism for the penetrated host cell to commit "suicide" (30,31). This hypersensitive cell death in turn is thought to be responsible for the arrest of fungal growth, possibly by depriving the obligate parasite of its nutritional basis (67,68.)

The first step thus postulates lignification as the mechanism of active cell death. Cell death, a genetically programmed event associated with active processes (69,70), is closely correlated with lignification in a range of different developmental programs: firstly, senescence is often accompanied by increased lignification (71,72); secondly, lignification is one of the most prominent reactions during wound healing (73-79); and thirdly, lignification of dying cells invariably occurs during xylem differentiation (80). A direct

cause-effect relationship of lignification and cell death has been described recently (81).

The second step of the proposed chain of events, resistance as a direct consequence of cell death, is still controversial (82-86). In the wheat-stem rust system, evidence favouring the idea of hypersensitive cell death as the cause of resistance (30,31,87-90) contrasts to results suggesting cell collapse as being a mere consequence of a yet unknown preceding resistance mechanism (90-97).

Recently, Kogel *et al.* (98) showed that the injection of galactose-binding lectins or the enzyme galactose oxidase into resistant wheat leaves prevented the hypersensitive cell death of penetrated host cells and concomitantly led to increased fungal growth, suggesting a causal relationship between hypersensitive cell death and resistance.

Tiburzy (22,31) obtained similar results by application of the PAL inhibitor aminooxyacetic acid (AOA). However, AOA does not specifically inhibit PAL (99), and PAL is not only involved in lignin biosynthesis (100). Thus, AOA and the related inhibitor aminooxyphenyl propionic acid (AOPP) (101,102) inhibit the biosynthesis of lignin (103,104), anthocyanins (105), other flavonoids (106), and conjugates of cinnamic acids (107) via PAL, as well as ethylene (108-110) via a pyridoxal phosphate dependent enzyme (110,111). In view of the possible function of phenolic compounds as phytoalexins (21,112,113) and the well documented role of ethylene in some resistance reactions (114-116), the above cited experiments with AOA (22, 31) do not provide any conclusive evidence for a causal role of lignification in resistance.

Our recent observation (Moerschbacher & Noll, unpublished) that a different PAL inhibitor, (1-amino-2-phenylethyl) phosphonic acid (APEP), is equally active in preventing hypersensitive cell death and partially lowering resistance of wheat to stem rust strongly suggest that the effects of both inhibitors is via their inhibitory action against PAL.

Besides these well known PAL inhibitors, highly specific suicide inhibitors of CAD are now available (117,118). These inhibitors combine two important features: they act as substrate analogues and are able to specifically complex zinc ions. The combination of these properties guarantees the high specificity of these substances. Besides CAD, only cinnamoyl:CoA reductase is inhibited, both enzymes are only involved in lignin biosynthesis (119). The mechanism of inhibition is thought to be a pseudo-irreversible inactivation of the suicide type (120). Such inhibitors are ideally suited for *in-vivo* assays, as they are highly specific and generally slowly metabolized (121).

The application of two of these inhibitors, N(O-hydroxyphenyl) sulfenamoyl-tertiobutyl acetate and N(O-aminophenyl) sulfenamoyl-tertiobutyl acetate, to highly resistant wheat leaves infected with an avirulent strain of stem rust resulted in decreased lignification and decreased necrosis of penetrated host cells and concomitantly led to increased fungal development, occasionally even allowing some sporulation to occur (60).

The described inhibition of hypersensitive cell death by the CAD in-

hibitors strongly suggests a causal relationship between lignification and cell death. It can further be concluded from the increase of fungal growth upon CAD inhibition that the synthesis of the monomeric lignin precursors is causally related to resistance of wheat to stem rust. However, it remains speculative whether the polymerization of these monomers to the three-dimensional network of lignin itself is a prerequisite for resistance. Furthermore, the proposed causal relationship between cell death and resistance cannot be concluded from these experiments; both phenomena may be independent results of the lignification process.

### Elicitation of Lignification

The term elicitor, initially defined as a fungal metabolite capable of inducing phytoalexin production when applied to host plants (122, 123), has since been applied to parasite-derived molecules which induce any facet of resistance in appropriate host plants, including lignification (124).

The work of Ride and his coworkers (24,125,126) showed that products of filamentous fungi are able to elicit lignification at wound margins in wheat leaves. Chitin and some of its soluble derivatives have been shown to be elicitors of lignification in wheat (125), chitosan being more active than chitin (62,126). Most other  $\beta$ -glucans including laminarin did not exhibit elicitor activity (62, 126). A crude extract of *Phytophthora megasperma* f. sp. *glycinea* cell walls, capable of inducing glyceollin accumulation in soybeans, also elicited lignification in wheat (126), but purified elicitor from the same source (62) and the synthetic hepta- $\beta$ -glucoside elicitor (126) were ineffective.

We have previously reported the purification of an elicitor active fraction from cell walls of germinated stem rust uredospores which induces lignification when injected into the intercellular spaces of wheat leaves (62,63). Besides lignification, this elicitor induces other symptoms typical of the hypersensitive reaction, such as membrane degradation detected as increased activities of lipoxygenase (64) and phospholipase (65). The high molecular weight water-soluble elicitor has been characterized as a heat stable glycoprotein with the carbohydrate moiety bearing the active part(s) of the molecule(s) (62). Recent work identified a glycoprotein with about equal amounts of galactose and mannose and almost no glucose as the most active component (127).

Initially, a gene specific effect of this elicitor concerning the *Sr5*-gene for resistance of wheat to stem rust was reported (63). However, this was not confirmed in later work (66): Elicitors prepared from two races of the stem rust fungus differing in their spectrum of genes for avirulence were equally active, and near-isogenic wheat lines containing different genes for resistance reacted similar to both elicitors. The observed differences in reactivity to elicitors between different wheat cultivars turned out to be unrelated to any known resistance genes.

Similar results had been reported previously for an elicitor isolated from intercellular washing fluids of leaf rust infected wheat leaves which induced browning and chlorosis (128,129). The reactivity of wheat cultivars

to this elicitor was dependent on a gene on chromosome 5A which contains no known genes for seedling resistance to leaf or stem rust (129). It was shown that the same holds true for the stem rust elicitor (60, Sutherland & Moerschbacher, unpublished).

When injected into primary leaves of different cereals, the stem rust elicitor causes symptoms which closely resemble the respective resistance reactions of these species against the attack by stem rust of wheat, i.e., lignification in barley and rye, brown spots in oat, and no visible symptoms in maize (66).

The biochemical similarities of leaf and stem rust elicitors, the missing gene specificity of both elicitors, the fact that an equally active elicitor was isolated from germ tube cell walls of oat crown rust (60), together with the described reactions of different non-hosts to the stem rust elicitor led us to speculate that the isolated elicitors may play a role in the induction of general mechanisms of non-host resistance (130). Although they may be involved in the elicitation of race-cultivar specific resistance as well, race-cultivar specificity in the wheat-stem rust system clearly cannot be explained on the basis of the specificity of the isolated elicitors. One possible explanation would be the occurrence of race-cultivar specific suppressors of the resistance reaction (124,131,132).

Polygalacturonic acid has been shown to be a potent suppressor of the elicitor induced lignification response in wheat leaves (60). Moreover, pectic fragments were obtained from isolated wheat cell walls by pectolytic digestion (36,60) or HF-solvolysis (Moerschbacher, Ryan, Komalavilas, Mort, unpublished) which suppressed the activation of lignin biosynthesis when injected simultaneously with elicitor. Active components were tentatively classified as fragments of homogalacturonan and rhamnogalacturonan I. An in depth chemical characterization as well as an evaluation of possible race-cultivar specificity of these "endogenous suppressors" or their *in vivo* production during compatible and incompatible wheat-stem rust interactions is under way.

The injection of small amounts of pectolytic enzymes concomitantly with elicitors suppressed the induction of lignin biosynthetic enzyme activities as well (60). The investigation of pectic enzymes of the stem rust fungus (133) and the elucidation of their substrate specificities, combined with a detailed analysis of their natural substrates, the pectic components of primary wheat cell walls, are targets for future research. The highly developed race-cultivar specificity in the wheat-stem rust system may be based on the differential liberation of active suppressors during the penetration of the host cell wall by the haustorial neck of the fungus (Figure 1). Although speculative, a model can be drawn in which suppressors which potentially exist in the walls of all wheat varieties are set free only in compatible interactions. The failure of producing active suppressors during incompatible interactions would then lead to the elicitation of lignification as the mechanism of hypersensitive cell death and resistance of wheat to stem rust.

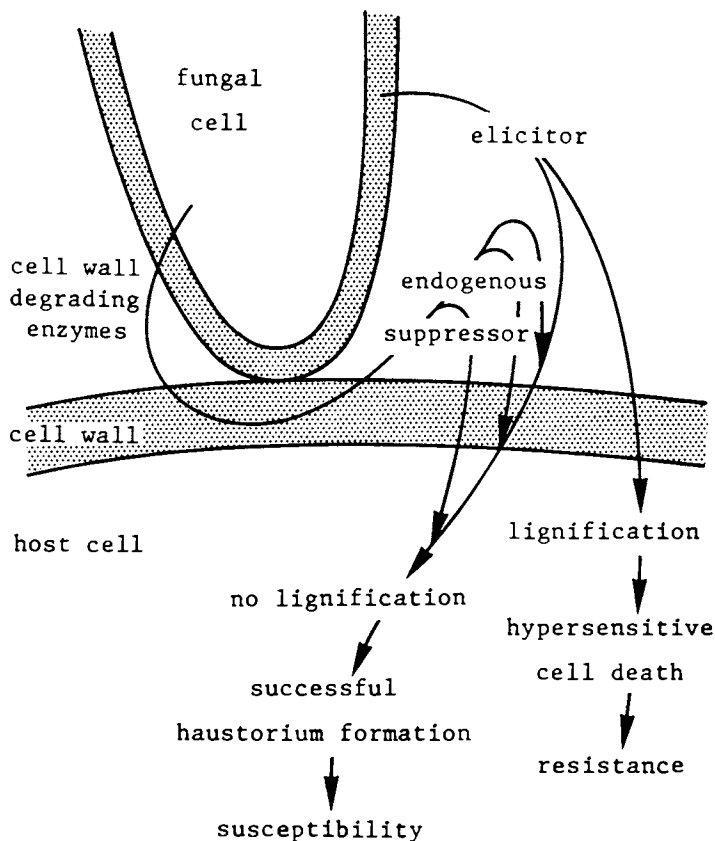


Figure 1. Hypothetical scheme of events leading to race-cultivar specific resistance or susceptibility in the rust system. If the substrate specificity of the fungal cell wall degrading enzymes (e.g., pectinases) is suitable for degradation of a specific host cell wall component (e.g., partly esterified pectin), endogenous suppressors will be produced which prevent the elicitor induced lignification response, thus leading to susceptibility.

### Acknowledgments

The author's work reported in this communication was carried out under the constant advice and encouragement from Prof. Dr. H. J. Reisener, in collaboration with U. Noll, B. E. Flott, U. Witte, D. Königs, A. Wüstefeld, U. Gotthardt, Dr. F. Schrenk, Dr. M. Sutherland, Dr. J. Ryan, Dr. P. Komalavilas and Prof. Dr. A. J. Mort. The PAL inhibitor APEP was generally provided by Prof. Dr. F. J. Schwinn, Ciba Geigy AG, Basel, Switzerland. Prof. Dr. L. Gorrichon, Université Paul Sabatier, Toulouse, France, kindly provided the CAD inhibitors. The work was supported in part by grants from the Land Nordrhein-Westfalen, the Deutsche Forschungsgemeinschaft, and the Deutscher Akademischer Austauschdienst.

### Literature Cited

1. Evans, C. S. *Process Biochem.* 1987, **22**, 102-105.
2. Kirk, T. K.; Farrell, G. L. *Ann. Rev. Microbiol.* 1987, **41**, 465-505.
3. Vance, C. P.; Kirk, T. M.; Sherwood, R. T. *Ann. Rev. Phytopathol.* 1980, **18**, 259-288.
4. Ride, J. P. In *Biochemical Plant Pathology*; Callow, J. A., Ed.; John Wiley: Chichester, 1983; pp. 215-236.
5. Hijwegen, T. *Neth. J. Plant Pathol.* 1963, **69**, 314-317.
6. Legrand, M.; Fritig, B.; Hirth, L. *Phytochem.* 1976, **15**, 1353-1359.
7. Legrand, M.; Fritig, B.; Hirth, L. *Planta* 1978, **144**, 101-108.
8. Massala, R.; Legrand, M.; Fritig, B. *Physiol. Plant Pathol.* 1980, **16**, 213-226.
9. Collendavello, J.; Legrand, M.; Fritig, B. *Plant Physiol.* 1983, **73**, 550-554.
10. Friend, J.; Reynolds, S. B.; Aveyard, M. A. *Physiol. Plant Pathol.* 1973, **3**, 495-507.
11. Friend, J.; Thornton, J. D. *Phytopathol. Z.* 1974, **81**, 56-64.
12. Henderson, S. J.; Friend, J. *Phytopathol. Z.* 1979, **94**, 323-334.
13. Hammerschmidt, R. *Physiol. Plant Pathol.* 1984, **24**, 33-42.
14. Hammerschmidt, R.; Kuc, J. *Physiol. Plant Pathol.* 1982, **20**, 61-71.
15. Hammerschmidt, R.; Boonen, A. M.; Bergstrom, G. C.; Baker, K. K. *Can. J. Bot.* 1985, **63**, 2393-2398.
16. Touze, A.; Rossignol, M. In *Biochemistry Related to Specificity in Host-Plant Pathogen Interactions*; Solheim, B., Raa, J., Eds.; Tromsø Universitets, 1977; pp 227-230.
17. Grand, C.; Rossignol, M. *Plant Sci. Lett.* 1982, **28**, 103-110.
18. Love, S. L.; Rhodes, B. B. *Hort. Sci.* 1982, **17**, 501.
19. Sherwood, R. T.; Vance, C. P. *Phytopathol.* 1980, **70**, 273-279.
20. Sherwood, R. T.; Vance, C. P. In *Plant Infection: The Physiological and Biochemical Basis*; Asada, Y., Bushnell, W. R., Ouchi, S., Vance, C. P., Eds.; Japan Scientific Societies: Tokyo, Springer: Berlin, 1982; pp 27-44.
21. Kuc, J. A. In *Encyclopedia of Plant Physiology*; Heitefuss, R., Williams, P. H., Eds.; Springer: Berlin, 1976; New Series Vol. 4, pp 632-652.

22. Reisener, H. J.; Tiburzy, R.; Kogel, K. H.; Moerschbacher, B.; Heck, B. In *Biology and Molecular Biology of Plant-Pathogen Interactions*; Bailey, J. A., Ed.; Springer: Berlin, 1986; NATO ASI Series Vol. H1, pp 141-148.
23. Ride, J. P. *Physiol. Plant Pathol.* 1975, **5**, 125-134.
24. Pearce, R. B.; Ride, J. P. *Physiol. Plant Pathol.* 1980, **16**, 197-204.
25. Maule, A. J.; Ride, J. P. *Physiol. Plant Pathol.* 1982, **20**, 235-241.
26. Young, P. A. *Bot. Gaz.* 1926, **81**, 258-279.
27. Robertson, H. T. *Sci. Agric.* 1932, **12**, 575-592.
28. Ride, J. P.; Pearce, R. B. *Physiol. Plant Pathol.* 1979, **15**, 79-92.
29. Bird, P. M.; Ride, J. P. *Physiol. Plant Pathol.* 1981, **19**, 289-299.
30. Beardmore, J.; Ride, J. P.; Granger, J. W. *Physiol. Plant Pathol.* 1983, **22**, 209-220.
31. Tiburzy, R. Ph.D. Thesis, RWTH Aachen, F.R.G., 1984.
32. Ride, J. P. *Physiol. Plant Pathol.* 1980, **16**, 187-196.
33. Mendgen, K. *Phytopathol.* 1981, **71**, 983-989.
34. Manners, J. M.; Gay, J. L. In *Biochemical Plant Pathology*; Callow, J. A., Ed.; John Wiley: Chichester, 1983, pp 163-195.
35. Niks, R. E. *Physiol. Molec. Plant Pathol.* 1986, **28**, 309-322.
36. Schrenk, F. Ph.D. Thesis, RWTH Aachen, F.R.G., 1988.
37. Jensen, W. A. *Botanical Histochemistry. Principles and Practice*; W. H. Freeman: San Francisco, 1962.
38. Sarkanen, K. V.; Ludwig, C. H. In *Lignins: Occurrence, Formation, Structure, and Reactions*; Sarkanen, K. V., Ludwig, C. H., Eds.; John Wiley: New York, 1971; pp 1-18.
39. Sherwood, R. T.; Vance, C. P. *Phytopathol.* 1976, **66**, 503-510.
40. Klein, G.; Linser, H. *Öster. Bot. Z.* 1930, **79**, 125-163.
41. Willemse, M. T. M. In *Cell Walls '81, Proc. 2nd Cell Wall Mtg.*; Robinson, D. G., Quader, H., Eds.; Wissenschaftliche: Stuttgart, 1981; pp 242-250.
42. Goodwin, R. H. *Ann. Rev. Plant Physiol.* 1953, **4**, 283-304.
43. Green, N. E.; Hadwiger, L. A.; Graham, S. O. *Phytopathol.* 1975, **65**, 1071-1074.
44. Maule, A. J.; Ride, J. P. *Phytochem.* 1976, **15**, 1661-1664.
45. Thorpe, J. R.; Hall, J. L. *Physiol. Plant Pathol.* 1984, **25**, 363-379.
46. Maule, A. J.; Ride, J. P. *Phytochem.* 1983, **22**, 1113-1116.
47. Friend, J. In *International Review of Biochemistry, Plant Biochemistry II*; Northcote, D. H., Ed.; University Park: Baltimore, 1977; Vol. 13, pp 141-182.
48. Friend, J. *Rec. Adv. Phytochem.* 1978, **12**, 557-588.
49. Legrand, M. In *Biochemical Plant Pathology*; Callow, J. A., Ed.; John Wiley: Chichester, 1983; pp 367-384.
50. Harkin, J. M.; Obst, J. R. *Science* 1973, **180**, 296-298.
51. Gaspar, T.; Penel, C.; Thorpe, T.; Greppin, H. *Peroxidases 1970-1980. A Survey of Their Biochemical and Physiological Roles in Higher Plants*; Université de Genève, Centre de Botanique: Genève, 1982; pp 103-106.



52. Rohringer, R.; Fuchs, A.; Lunderstädt, J.; Samborski, D. J. *Can. J. Bot.* 1967, **45**, 863-889.
53. Fuchs, A.; Rohringer, R.; Samborski, D. J. *Can. J. Bot.* 1967, **45**, 2137-2154.
54. Moerschbacher, B. M.; Noll, U. M.; Flott, B. E.; Reisener, H. J. *Physiol. Mol. Plant Pathol.* 1988, **33**, 33-46.
55. Macko, V.; Woodburg, W.; Stahmann, M. A. *Phytopathol.* 1968, **58**, 1250-1254.
56. Fric, F.; Fuchs, W. H. *Phytopathol. Z.* 1970, **67**, 161-174.
57. Daly, J. M.; Ludden, P.; Seevers, P. *Physiol. Plant Pathol.* 1971, **1**, 397-407.
58. Seevers, P. M.; Daly, J. M.; Catedral, F. F. *Plant Physiol.* 1971, **48**, 353-360.
59. Flott, B. E.; Moerschbacher, B. M.; Reisener, H. J. *New Phytol.* 1989, **111**, 000-000.
60. Moerschbacher, B. M. Ph.D. Thesis, RWTH Aachen, F.R.G., 1988.
61. Chigrin, V. V.; Rozum, L. V.; Zaprometov, M. N. *Fiziol. Rast.* 1973, **20**, 942-948.
62. Moerschbacher, B.; Kogel, K. H.; Noll, U.; Reisener, H. J. *Z. Naturforsch.* 1986, **41c**, 830-838.
63. Moerschbacher, B.; Heck, B.; Kogel, K. H.; Obst, O.; Reisener, H. J. *Z. Naturforsch.* 1986, **41c**, 839-844.
64. Ocampo, C. A.; Moerschbacher, B.; Grambow, H. J. *Z. Naturforsch.* 1986, **41c**, 559-563.
65. Ocampo, C. A.; Grambow, H. J. *New Phytol.* 1987, **107**, 709-714.
66. Moerschbacher, B. M.; Flott, B. E.; Noll, U.; Reisener, H. J. *Plant Physiol. Biochem.* 1989, **27**, 000-000.
67. Stakman, E. C. *J. Agric. Res.* 1915, **4**, 193-200.
68. Stakman, E. C.; Levine, M. N. *Univ. Minnesota Agric. Exp., 1922, Tech. Bull.* **8**, 3-10.
69. Leopold, A. C. *Science* 1961, **134**, 1727-1732.
70. Davies, I.; Sigeo, D. C. *Cell Ageing and Cell Death*; Soc. Exp. Biol. Sem. Ser. 25; Cambridge University: Cambridge, 1984.
71. Stone, J. E.; Blundell, M. J.; Tanner, K. G. *Can. J. Chem.* 1951, **29**, 734-745.
72. Faulkner, G.; Kimmins W. C. *Phytopathol.* 1975, **65**, 1396-1400.
73. Rhodes, J. M.; Wooltorton, L. S. C. In *Biochemistry of Wounded Plant Tissues*; Kahl, G., Ed.; Walter de Gruyter: Berlin, 1978; pp 243-286.
74. Fleuriet, A.; Deloire, A. *Z. Pflanzenphysiol.* 1982, **107**, 259-268.
75. Garrod, B.; Lewis, B. G.; Brittain, M. J.; Davies, W. P. *New Phytol.* 1982, **90**, 99-108.
76. Zimmermann, H. J.; Kahl, G. *BIUZ* 1982, **12**, 49-58.
77. Geballe, G. T.; Galston, A. W. *Phytopathol.* 1983, **73**, 619-623.
78. Biggs, A. R. *Can. J. Bot.* 1986, **64**, 2319-2321.
79. Hudler, G. W.; Banik, M. T. *Can. J. Bot.* 1986, **64**, 2406-2410.
80. Woolhouse, H. W. *Agric. Res.* 1915, **4**, 123-153.

81. Carceller, M.; Davey, M. D.; Fowler, M. W.; Street, H. E. *Protoplasma* 1971, **73**, 367-385.
82. Heath, M. C. *Phytopathol.* 1976, **66**, 935-936.
83. Ingram, D. S. *Ann. Appl. Biol.* 1978, **89**, 291-295.
84. Bushnell, W. R. In *Plant Infection, the Physiological and Biochemical Basis*; Asada, Y., Bushnell, W. R., Ouchi, S., Vance, C. P., Eds.; Japan Scientific Societies: Tokyo, Springer: Berlin, 1982; pp 97-116.
85. Doke, N.; Tomiyama, K.; Furuichi, N. In *Plant Infection, the Physiological and Biochemical Basis*; Asada, Y., Bushnell, W. R., Ouchi, S., Vance, C. P., Eds.; Japan Scientific Societies: Tokyo, Springer: Berlin, 1982; pp 79-96.
86. Tomiyama, K. In *Plant Infection, the Physiological and Biochemical Basis*; Asada, Y., Bushnell, W. R., Ouchi, S., Vance, C. P., Eds.; Japan Scientific Societies: Tokyo, Springer: Berlin, 1982; pp 329-344.
87. Skipp, R. A.; Samborski, D. J. *Can. J. Bot.* 1974, **52**, 1107-1115.
88. Samborski, D. J.; Kim, W. K.; Rohringer, R.; Howes, N. K.; Baker, R. J. *Can. J. Bot.* 1977, **55**, 1445-1452.
89. Harder, D. E.; Rohringer, R.; Samborski, D. J.; Rimmer, S. R.; Kim, W. K.; Chong, J. *Can. J. Bot.* 1979, **57**, 2617-2625.
90. Rohringer, R.; Kim, W. K.; Samborski, D. J. *Can. J. Bot.* 1979, **57**, 324-331.
91. Brown, J. F.; Shipton, W. A.; White, N. H. *Ann. Appl. Biol.* 1966, **58**, 279-290.
92. Ogle, H. J.; Brown, J. F. *Ann. Appl. Biol.* 1971, **67**, 309-319.
93. Kiraly, Z.; Barna, B.; Ersek, T. *Nature* 1972, **239**, 456-457.
94. Barna, B.; Ersek, T.; Mashaal, S. F. *Acta Phytopathol. Acad. Sci. Hung.* 1974, **9**, 293-300.
95. Mayama, S.; Daly, J. M.; Rehfeld, D. W.; Daly, C. R. *Physiol. Plant Pathol.* 1975, **7**, 35-47.
96. Mayama, S.; Rehfeld, D. W.; Daly, J. M. *Phytopathol.* 1975, **65**, 1139-1142.
97. Gousseau, H. D. M.; Deverall, B. J. *Can. J. Bot.* 1986, **64**, 626-631.
98. Kogel, K. H.; Schrenk, F.; Sharon, N.; Reisener, H. J. *J. Plant Physiol.* 1985, **118**, 343-352.
99. John, R. A.; Charteris, A.; Fowler, L. J. *Biochem. J.* 1978, **171**, 771-779.
100. Harborne, J. B. In *Encyclopedia of Plant Physiology*; Bell, E. A., Charlwood, B. V., Eds.; Springer: Berlin, 1980; New Series Vol. 8, pp 329-402.
101. Amrhein, N.; Gödeke, K. H.; Kefeli, V. I. *Ber. Deutsch. Bot. Ges.* 1976, **89**, 247-259.
102. Amrhein, N.; Gödeke, K. H. *Plant Sci. Lett.* 1977, **8**, 313-317.
103. Holländer, H.; Kiltz, H. H.; Amrhein, N. *Z. Naturforsch.* 1979, **34c**, 1162-1173.
104. Amrhein, N.; Frank, G.; Lemm, G.; Luhmann, H. B. *Eur. J. Cell Biol.* 1983, **29**, 139-144.
105. Amrhein, N.; Holländer, H. *Planta* 1979, **144**, 385-389.

106. Amrhein, N.; Diederich, E. *Naturwiss.* 1980, **67**, 40-41.
107. Amrhein, N.; Gerhardt, J. *Biochim. Biophys. Acta* 1979, **583**, 434-442.
108. Amrhein, N.; Wenker, D. *Plant Cell Physiol.* 1979, **20**, 1635-1642.
109. Yu, Y. B.; Adams, D. O.; Yang, S. F. *Plant Physiol.* 1979, **63**, 589-590.
110. Yu, Y. B.; Adams, D. O.; Yang, S. F. *Arch. Biochem. Biophys.* 1979, **198**, 280-286.
111. Yang, S. F.; Hoffman, N. E. *Ann. Rev. Plant Physiol.* 1984, **35**, 155-189.
112. Bailey, J. A.; Mansfield, J. W., Eds.; *Phytoalexins*; Blackie: Glasgow, 1982.
113. Kuc, J.; Rush, J. S. *Arch. Biochem. Biophys.* 1985, **236**, 455-472.
114. Pegg, G. F. In *Encyclopedia of Plant Physiology*; Heitefuss, R., Williams, P. H., Eds.; Springer: Berlin, 1976; New Series Vol. 4, pp 450-479.
115. Elstner, E. F. *BIUZ* 1978, **8**, 82-87.
116. Yang, S. F.; Pratt, H. K. In *Biochemistry of Wounded Plant Tissues*; Kahl, G., Ed.; Walter de Gruyter: Berlin, 1978; pp 595-622.
117. DeBlic, A.; Cazaux, L.; Gorrichon-Guigon, L.; Perry, M. *Synthesis* 1982, **281**, 281-282.
118. Baltas, M.; Bastide, J. D.; Cazaux, L.; Gorrichon-Guigon, L.; Maroni, P.; Tisnes, P. *Spectrochim. Acta* 1985, **41A**, 793-796.
119. Grand, C.; Sarni, F.; Boudet, A. M. *Planta* 1985, **163**, 232-237.
120. Baltas, M.; Cazaux, L.; Gorrichon-Guigon, L.; Maroni, P.; Tisnes, P. *Tetrahedron Lett.* 1985, **26**, 4447-4450.
121. Abeles, R. H.; Maycock, A. L. *Acc. Chem. Res.* 1976, **9**, 313-319.
122. Keen, N. T.; Partridge, J. E.; Zaki, A. *J. Phytopathol.* 1972, **62**, 768.
123. Keen, N. T. *Science* 1975, **187**, 74-75.
124. Callow, J. A. In *Encyclopedia of Plant Physiology*; Linskens, H. F., Heslop-Harrison, J., Eds.; Springer: Berlin, 1984; New Series Vol. 17, pp 212-237.
125. Pearce, R. B.; Ride, J. P. *Physiol. Plant Pathol.* 1982, **20**, 119-123.
126. Barber, M. S.; Ride, J. P. *Physiol. Molec. Plant Pathol.* 1988, **32**, 185-197.
127. Kogel, G.; Beißmann, B.; Reisener, H. J.; Kogel, K. H. *Physiol. Mol. Plant Pathol.* 1988, **33**, 173-185.
128. Deverall, B. J.; Deakin, A. L. *Physiol. Plant Pathol.* 1985, **27**, 99-107.
129. Deverall, B. J.; Deakin, A. L. *Physiol. Molec. Plant Pathol.* 1987, **30**, 225-232.
130. Day, P. R. *Genetics of Host-Parasite Interaction*; W. H. Freeman: San Francisco, 1974.
131. Heath, M. C. *Phytopathol.* 1981, **71**, 1121-1123.
132. Bushnell, W. R., Rowell, J. B. *Phytopathol.* 1981, **71**, 1012-1014.
133. VanSumere, C. F.; VanSumere-DePreter, C.; Ledingham, G. A. *Can. J. Microbiol.* 1957, **3**, 761-770.

RECEIVED March 10, 1989

## Chapter 28

# Virulence-Inducing Phenolic Compounds Detected by *Agrobacterium tumefaciens*

Paul A. Spencer and G. H. N. Towers

Department of Botany, University of British Columbia, Vancouver,  
British Columbia V6T 2B1, Canada

Construction of *vir::lacZ* fusion reporter genes and subsequent analysis of their expression in strains of *Agrobacterium tumefaciens* has permitted the discovery of a class of phytochemicals that this pathogen detects and which induce virulence. Preliminary screening of a variety of commercially available phenolics revealed that some were active as *vir* inducers. Two acetophenones were isolated from transformed tobacco root cultures. The results of a recent study by us indicate that there exists a range of virulence-inducing plant phenolics which are not limited to acetophenones but include chalcones as well as cinnamic acid derivatives. Among the latter are acids, alcohols and esters known to be associated with plant cell walls or implicated in lignin biosynthesis, a discovery which suggests that this wide host range pathogen likely responds to chemicals common to all susceptible hosts. We are currently studying signal compounds and natural inhibitors in relation to the host range of *Agrobacterium* strains. Activity was detected in extracts from a grapevine tissue culture, grapevine bark, and flavan-containing fractions obtained from grapes. In addition, as yet unidentified compounds inhibitory to *vir*-induction have been discovered.

It is now known that the initial interaction between plants and bacteria of the Rhizobiaceae is a chemical detection by the microbe of a susceptible host, i.e., the host produces compounds which act as signals for the microbial pathogen or symbiont. The microbe responds to these signals by expression of genes necessary in subsequent stages of the interaction. For a few of the Rhizobiaceae some signal compounds involved have been identified (1-7).

0097-6156/89/0399-0383\$06.00/0  
© 1989 American Chemical Society

The signal compounds of plant-*Agrobacterium tumefaciens* interactions have received much attention. This gram negative soil bacterium, which causes crown gall disease of a wide variety of dicotyledonous plants (8), is responsible for a neoplastic growth of the plant tissue by passing T-DNA, a part of its tumor inducing plasmid (pTi), into the host plant genome (9-14). This T-DNA includes genes which encode enzymes of auxin (15,16) and cytokinin (17,18) biosynthesis, which are expressed in the transformed plant cell (19,20). The microbe is a useful vector for genetic engineering in plants because certain of the normal T-DNA genes may be replaced with new genes of interest. Plant cells infected with the bacterium containing the modified Ti-plasmid are used to generate transgenic plants.

Detection of susceptible host cells and early stages of tumorigenesis are mainly controlled by a set of pTi genes known as the virulence (*vir*) genes (21,22). These genes are expressed upon cocultivation of the bacteria with host plant cells (23,24). Because of their role in the early stages of tumorigenesis, and therefore their central importance in transformation of plant genomes, research has been directed to understanding the mechanism involved in *vir* gene expression and identifying the *vir* gene products. Two of the *vir* genes (A and G) are regulatory in nature (25,26). *virA* is also a host range determinant and is thought to be the environmental sensor of the plant-derived inducer molecules (27). At least one more *vir* locus (*virC*) is connected with host range (28-30), and another (the *virD* operon) is now known to encode an endonuclease which recognizes and cleaves the left and right border sequences of T-DNA (31). The *virB* region encodes polypeptides similar to those involved in bacterial conjugation (32). Recently it was determined that *virE* encodes a single stranded DNA-binding protein (33). Activation of *vir* gene expression is known to result in the production of multiple single-stranded T-DNA molecules within the bacterium (34).

Bolton *et al.* (35) found that a mixture of simple, low molecular weight phenolic compounds could be used to induce expression of most of the *vir* genes. Stachel *et al.* (7) identified two active signal compounds, acetosyringone (AS) and  $\alpha$ -hydroxyacetosyringone (HO-AS), from tobacco tissues. In that report a few other related compounds were assayed at one or more concentrations for their *vir*-inducing activity. This comprised a very brief structure-activity study which presented some information about the structural features required to confer activity. At the concentrations tested, none of these compounds displayed the level of activity observed with acetosyringone. It was suggested that *Agrobacterium* is attracted to susceptible plant tissues by following a concentration gradient of these virulence inducing substances, and some results which support this idea were obtained by Ashby *et al.* (36,37).

The compounds AS and HO-AS have come to be regarded as the unique chemicals which *Agrobacterium* detects in nature and which trigger the initial events within the bacterium, resulting in tumor formation. However, it has yet to be shown that these acetophenones, which in fact have never previously been reported as naturally occurring phytochemicals, are the signal compounds produced by any other susceptible hosts. AS has been used to

boost the transformation efficiency (38). However, transformation of soybean cells was promoted by adding either AS or syringaldehyde [1b] to the inoculum (39). In addition, virulence inducing wound exudates obtained from a host plant extended the normal host range of *Agrobacterium* to include a monocot crop plant (40). We propose that other phytochemicals are involved in the induction of virulence in *Agrobacterium*.

We recently reported the *vir*-inducing activity over a range of concentrations of a variety of plant-derived phenolic compounds with structures related to that of acetosyringone and discussed the structural features necessary for the activation of *vir* genes (41). The activities of some cinnamic acid derivatives, chalcones, and of the lignin precursors sinapyl alcohol and coniferyl alcohol were examined. A number of these compounds are of widespread occurrence, and others such as the monolignols are ubiquitous in angiosperms and gymnosperms. In this report we review the results of our structure-activity analysis of *vir*-induction and discuss some preliminary results of our search for signal compounds for a grapevine isolate of *A. tumefaciens*.

Research has revealed that the *virA* gene product is located at the bacterial cell surface where it likely acts as the environmental sensor of plant derived signal compounds (27). The *virA* loci of limited host range (LHR) and wide host range (WHR) strains of *Agrobacterium* were sequenced and the predicted gene products compared. The gene products were found to have diverged most strongly in their putative periplasmic domain. Therefore we considered that differences in these gene products might correspond to differences in their specificity for signal compounds, and this in part may explain the differences observed in the host range of these two types of *Agrobacterium*. To prove this hypothesis, induction of other *vir* loci in the presence of LHR host plant cells, or by wound exudates thereof, had to be demonstrated. The signal compounds then had to be isolated and identified. Initially, however, only a *virB::lacZ* gene-fusion containing LHR strain of *Agrobacterium* (A856/pSM243cd) was available. In our preliminary experiments with this strain, *vir* expression was not greatly induced by cocultivation with host plant cells or by purified wound-induced phenolic compounds; therefore we wished to examine *vir*-induction in a different construct, namely, the LHR strain carrying a *lacZ* fusion to a different *vir* gene.

We have prepared a *virE::lacZ* gene fusion-containing LHR strain, A856/pSM358cd, by triparental mating and have used this strain, along with the strain A856/pSM243cd, to examine *vir* gene expression in the limited host range (grapevine) strain A856. Phenolic wound exudates from the leaves and stems of *Vitis lubrusca*, as well as exudates produced by two grapevine callus cultures (*Vitis* sp. cv. Seyval and *V. lubruscana* cv. Steuben) and extracts obtained from two varieties of grapes (red and green seedless) and grapevine bark (cv. Concord) were examined for *vir*-inducing compounds. We have established that the specificity of LHR signal compounds is unlike that previously described for WHR *A. tumefaciens* (41) in that *vir* gene expression is not as greatly induced by acetosyringone.

This indicates that, unlike the WHR strains of *Agrobacterium*, the LHR strains are less sensitive to phenylpropanoid metabolites. Preliminary results indicate that the virulence of grapevine isolates of *Agrobacterium* may be influenced by the presence of certain higher molecular weight phenolic esters of grape flavans in addition to less polar, chloroform soluble phenolics present in aqueous grapevine-stem wound exudates.

An understanding of the phytochemistry of *vir* gene expression in both WHR (7,35,41) and in LHR *Agrobacterium* should provide an interesting and potentially useful model system of host range control in plant-bacterial interactions. New insights into regulation of host range are of importance in plant biochemistry, biotechnology and pathology in that chemical clues are provided which could allow for extension of this pathogen's host range to include species which are refractory to transformation.

## Results and Discussion

In our analysis of the chemical structures which are active *vir*-inducers (41) it was found that the compounds fell into four groups: (1) acetophenones and related structures, (2) monolignols, (3) hydroxycinnamic acids and their esters, and (4) chalcone derivatives (Fig. 1). Each compound had either a guaiacyl or a syringyl nucleus, and with the exception of the monolignols, possessed a carbonyl group. Most were of common occurrence in vascular plants.

The activity curves with increasing concentration of a number of *vir*-inducing phenolic compounds are shown in Figures 2a (monolignols, chalcones and acetophenones) and 2b (phenolic acids and their methyl esters). Regarding the monolignols, we emphasized the bacterium's ability to respond to the presence of these lignin precursors. This result established that *Agrobacterium* may be capable of detecting cells which are undergoing lignin synthesis or cell wall repair and thereby target those cells for transformation. *Agrobacterium* responded equally well to the presence of lignin degradation products (7,35,41) and therefore the virulence of the microbe can be considered as sensitive to lignin metabolites in general. The unique activity curves of the chalcones [4a&4b] represent an interesting addition to the list of effective phenolics.

The methyl esters of ferulic [3d], syringic [1f], and sinapic acids [3f] exhibited significantly greater activity than the corresponding free acids (Fig. 2b). Some effects of esterification are discussed below. The ethyl esters tested were less active again (data not shown), perhaps due to altered hydrophilicity of the compound or some steric hindrance at the bacterial receptor site not evident with the methyl esters. In a plate assay for *vir*-induction we discovered that the glucose ester of ferulic acid was an effective inducer of *vir* gene expression. It is likely that such glucose esters, released upon wounding of the host plant, act as signal compounds. Phenolic glycosides, such as glucoferulaldehyde, were inactive.

We assayed a number of other phenolic compounds, including aurones, flavones, flavanones, flavanols, lignans and 5-hydroxycinnamic acid derivatives, but they all displayed little or no activity. The lack of activity of

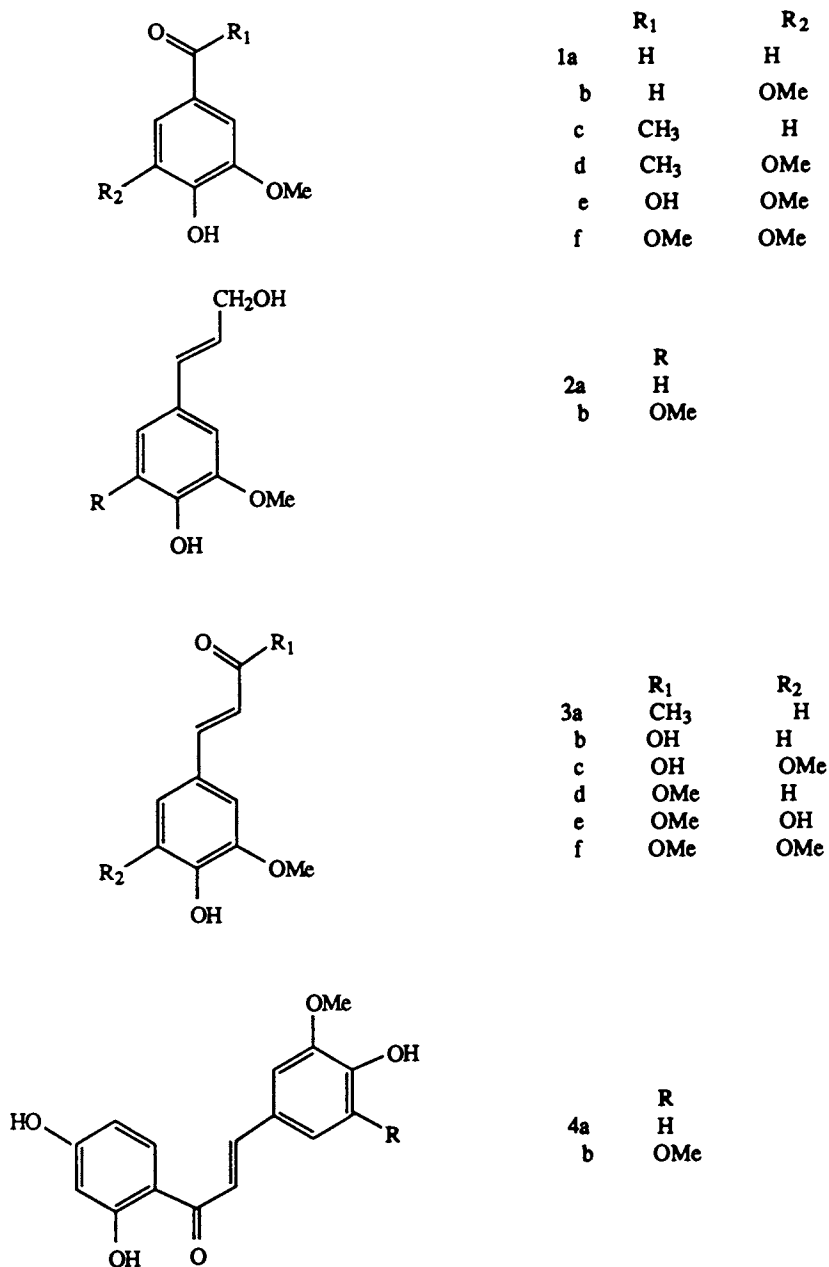


Figure 1. The structures of the *vir*-inducing phenolic compounds employed in our structure-activity analysis (41).



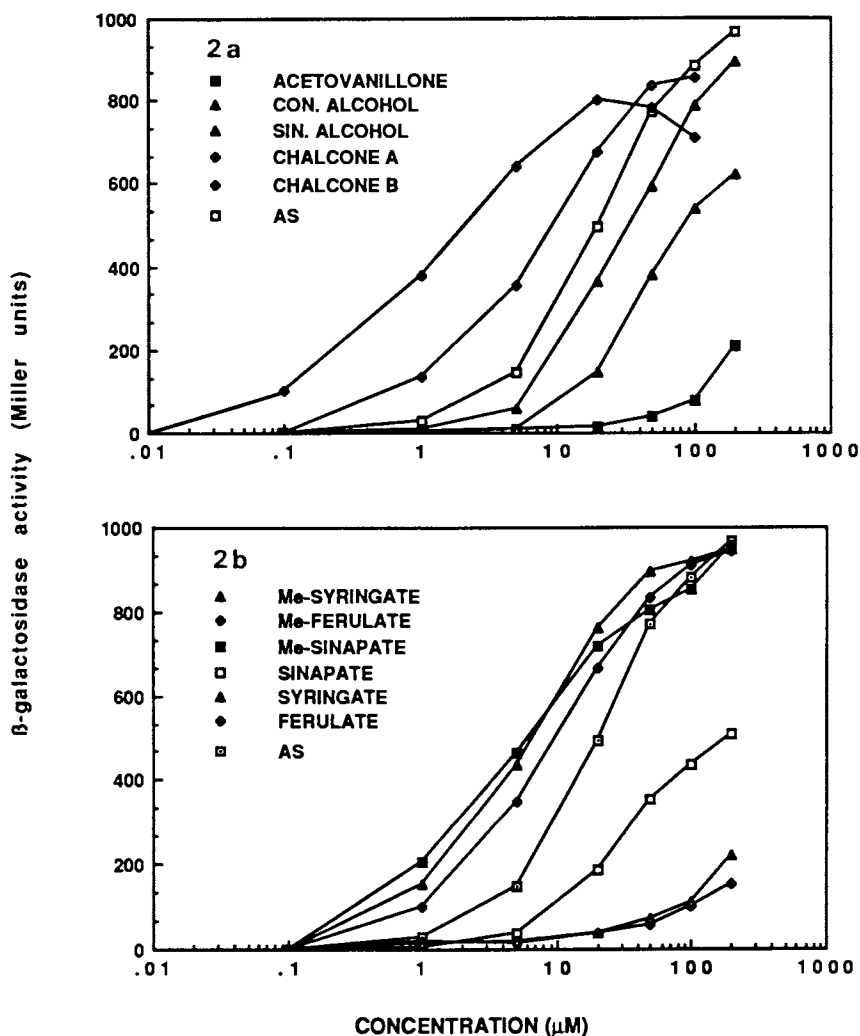


Figure 2. The virulence inducing activity of (a) monolignols, chalcones, and acetophenones, and (b) phenolic acids and their methyl esters. Following incubation with a compound in aqueous solution,  $\beta$ -galactosidase activity in a strain of *Agrobacterium* carrying a *virE:lacZ* fusion plasmid (A348/pSM358) was assayed as an indicator of *vir* gene induction. Abbreviations used: AS = acetosyringone; CON. ALCOHOL = coniferyl alcohol; SIN. ALCOHOL = sinapyl alcohol; CHALCONE A = 2',4',4-trihydroxy-3-methoxy chalcone; CHALCONE B = 2',4',4-trihydroxy-3,5 dimethoxy chalcone.

5-hydroxyferulic acid was of interest because it was recently identified as one of the cell wall bound acids in monocots (42). At that time we had not demonstrated inhibition of *vir*-induction by a phenolic compound, although we speculated about the occurrence of phenolic *vir*-inhibitors in monocots. Indeed, we have been informed of unidentified *vir*-inhibitors recently isolated from *Zea mays* (E.W. Nester, personal communication), and have initiated work on the identification of *vir*-inhibitors from *Vitis* species.

In addition to the inactive compounds listed above, each of the compounds used by Bolton *et al.* (35) was assayed individually, and of these only vanillin [1a] produced any significant *vir*-induction. Interestingly, at the concentrations examined by us the remaining compounds (gallic,  $\beta$ -resorcylic, pyrogalllic, p-hydroxybenzoic, and protocatechuic acids, and catechol) were essentially inactive. None of these inactive compounds has a guaiacyl or syringyl nucleus. We have observed low level induction by gallic acid at higher concentrations (e.g., 1mM, data not shown). The possible significance of this result with respect to *vir*-induction by grape flavans is discussed below.

The results indicated that two basic structural features were required to confer activity upon a compound: (1) guaiacyl or (usually conferring enhanced activity) syringyl substitution on a benzene ring, and (2) a carbonyl group on a substituent para to the hydroxy substituent on the ring. Monolignols, however, are active even though there is no carbonyl function in the side chain in the para position. When present, the carbonyl carbon may be one or three carbon atoms removed from the ring. However, to confer maximal activity, in the latter case there must be a double bond between the carbonyl carbon and the ring, as is present in the chalcones and cinnamic acid derivatives. Furthermore, the carbonyl group of a free acid is less effective than that of the corresponding ester. Esterification alters the solubility of the compound. In addition, esterification prevents one oxygen of the carboxyl group from forming a partial double bond, thereby rendering the carbonyl group more reactive. In these cases, and the case of the aldehydes and chalcones, this carbonyl group forms the terminus of a conjugated double bond system running from the hydroxyl group and through the ring. The presence of a C ring in the flavonoids tested virtually abolished activity, indicating that the more typical flavonoids are not active in this cell-cell signalling.

These structure-activity relationships are different from those reported for the activation of *nod* genes in *Rhizobium* species (1-6). Hydroxylated flavones, isoflavones or flavanones in nM to  $\mu$ M concentrations induce expression of *nod* genes. Each *Rhizobium* species is not only highly specific for its host plant species but also displays a high degree of specificity towards its signal compound. In contrast, the original strain of *A. tumefaciens*, from which the strain used in our study was derived, exhibited a wide host range (WHR) and, as we have seen, a comparatively lower degree of signal compound specificity. Furthermore, some of the very compounds which induce *vir* genes in *Agrobacterium* strongly inhibit *nod* gene activation by these flavonoids (1). At higher concentrations most of the *vir*-inducing phenolics

were bacteriostatic even against *Agrobacterium* (data not shown), and presumably they act in this way against *Rhizobium* species, or they may act more directly by competitive inhibition of *nod*-induction.

A number of these active compounds are of widespread occurrence dicotyledons. The lignin precursors are ubiquitous in susceptible hosts. It is tempting to conclude that the presence of any one of these compounds alone would determine whether a given plant is susceptible to infection by *Agrobacterium*. However, monocots also produce these compounds, even exuding them into the rhizosphere from intact roots (43) and yet, with few exceptions (44-47), they lie outside of the natural host range of any strain of *Agrobacterium*. This limitation of host range remains a significant problem in the use of this organism as a vector for genetic engineering in monocots. The attachment of *Agrobacterium* to monocot cells has been reported (48, and references therein). Therefore the underlying mechanism of host range determination appears to depend, at least in part, on the phytochemistry of the interaction. The recently established presence of *vir*-inhibitors in a monocot and, as will be discussed, LHR host exudates supports the concept of a phenolic milieu in which *vir*-inducers compete with *vir*-inhibitors. It may be that a sophisticated application of inducer compounds will permit the Ti-plasmid-mediated transformation of plant species normally resistant to infection.

Our initial experiments, using  $\beta$ -galactosidase activity in A856/pSM243cd as an indicator of *vir*-induction, suggested that wound-induced phenolics from the leaves of *V. lubrusca* did not include any LHR signal compounds. We considered the following possibilities: (1) that the source of the natural LHR signal compound might be tissue specific (e.g., limited to the roots or crown of the grapevine), (2) that unlike the WHR signal compounds, these unknown chemicals may not be low molecular weight phenolics (e.g., phenylpropanoids or acetophenones) extractable with the solvents used, and (3) that the signal compound could be a phytoalexin produced only after infection of the grapevine tissue.

In order to confirm our results with A856/pSM243cd we prepared the strain A856/pSM358cd as described. The plasmid pSM358cd contains a *virE::lacZ* gene fusion, and it was found that the higher levels of  $\beta$ -galactosidase activity which are inducible from this construct (35) permitted detection of even vanishingly small amounts of inducing compound. The results with this new strain confirmed our initial results; neither acetosyringone itself nor any of the isolated wound-induced phenolic compounds from grape leaves greatly induced the virulence genes of the LHR *A. tumefaciens*. Obviously either the techniques used to isolate compounds from the host material were not appropriate for the isolation of LHR inducers, or the LHR strain cannot efficiently detect the WHR signal compounds due to its different *virA* gene product.

Assuming the former to be the case, we considered that the LHR inducers might be more polar in nature and were therefore excluded by separatory techniques for compounds such as those known to induce WHR *A. tumefaciens*. Proanthocyanidin monomers (i.e., catechins, flavan-3-ols), oligomers,

and esters should be prevalent in the woody tissue of the grapevine. Such compounds have been studied in grapes with respect to wine quality (49) and recently reviewed with respect to their possible physiological role in connection with lignin (50). In view of the chemical specificity of virulence-induction in WHR *Agrobacterium* (41), a feature which in its sensitivity was not shared by the LHR strain used in this study, it was noteworthy that these flavans have been envisaged as functionally connected with lignin. Interestingly, in a review on proanthocyanidins and lignin chemistry, Stafford (50) mentioned the phenomenon of plant phenolic compounds as molecular signals for *Rhizobium* and *Agrobacterium*, and recognized the potential "informational" function of both types of compounds.

We analyzed the flavan-containing extracts obtained from two locally available varieties of grapes and detected activity in the fractions containing, among other phenolics, flavan monomers, dimers and esters. These components were separated by chromatography on Sephadex LH 20. Fractions with similar thin layer chromatographic (TLC) profiles were pooled and at least 3 out of 12 such pooled samples contained substances which resulted in *vir*-induction in the LHR strain. Similarly, grapevine bark flavans were examined, but only compounds inducing very low levels of *vir* gene expression were found. In fact, in addition to *vir*-inducers, a *vir*-inhibitory extract was obtained from grapevine bark. In plate assays, this LHR host-derived inhibitory substance completely prevented WHR *vir*-induction by acetosyringone.

Repeated TLC of active, pooled fractions from Red Flame grapes revealed major spots with  $R_f$ 's corresponding to those of catechin and epicatechin, identical color reaction with p-toluenesulfonic acid spray reagent, and coelution of trimethylsilane (TMS) derivatives by GC with reference samples of these flavans. However catechin and epicatechin were assayed with the bacterial strains described and no activity was detected. TMS-derivatized samples of active grape flavans were examined by GC-MS, but a search for the molecular ions of a number of known *vir*-inducing phenolics yielded negative results.

Isolated compounds were collected after separation by HPLC and assayed for *vir*-induction in the strains described. It became apparent that the limited host range strain responded to all the substances that induced *vir* expression in the wide host range strain, but the LHR strain was less sensitive to the same substances and as a result was considered a less sensitive bioassay organism. Therefore work on isolation of grapevine-derived signal compounds continued using the more sensitive WHR strain and plate assay system described.

Using A348/pSM358 as our bioassay organism with which to detect the *vir*-inducing substances, we isolated by HPLC the active compound present in a mixture obtained from gel filtration on Sephadex LH-20. Better resolution of the components of the grape flavan mixture was achieved by gel filtration with Sephadex G 25. In this way fractions enriched for the inducing compounds may be obtained. This may provide samples from which we can efficiently isolate new signal compounds in sufficient quan-

tity to permit structure elucidation. However, with the data at hand, we can make the following educated guess as to the nature of the active structure in the active grape flavan mixture. Considering the facts that gallic acid was reported to induce virulence (35), that epicatechin-gallate (Fig. 3) was previously reported from grapes (49), and that esters of phenolic acids exhibited enhanced activity, we suggest that a flavan ester such as epicatechin-gallate is the active component in our grape flavan fractions. Esters including phenolic acids with guaiacyl or syringyl nuclei should exhibit enhanced activity.

Two other sources of signal compounds from LHR host tissues were found. One source was the Seyval callus culture (see Experimental) and the other was the aqueous exudate produced in abundance upon cutting new grapevine stems in the spring, when the sap flow was great. Another grapevine callus culture (obtained from *V. lubrascana* cv. Steuben, a natural host of both LHR and WHR *Agrobacterium*), its exudates, and fractions partitioned therefrom, as well as exudates from mature *Nicotiana glauca* plants, were incapable of inducing *vir* gene expression in any of the strains used. Apparently not all callus cultures were equally capable of producing *vir*-inducing mixtures of substances. Perhaps the two cultures differed in the amounts of *vir*-inhibitory substances produced. Finally, in consideration of the natural setting in which the LHR strains infect their host, we felt it worthwhile to examine the copious aqueous exudates of cut grapevine stems. The chloroform soluble fraction of such an exudate from *V. lubrusca* was strongly active in a plate assay and is being further characterized.

## Conclusion

In conclusion, both *vir*-inducing and *vir*-inhibitory substances were produced from hosts and nonhosts of strains of *A. tumefaciens*. The compounds involved covered a range of polarity and molecular weight, and this likely reflects ester or other linkages between known lower molecular weight, *vir*-inducing, cinnamic acid derivatives and other organic compounds such as sugars and proanthocyanidin monomers (flavan-3-ols) or oligomers. It has been demonstrated (7,35,41) that *A. tumefaciens* is sensitive to the monomers involved in lignin biosynthesis. The data presented here suggest *Agrobacterium* may also be sensitive to compounds such as catechin- or epicatechin-gallate, which links *vir*-induction with the monomers of pro-cyanidin polymers.

We are continuing our efforts to identify both inducing and inhibitory compounds from grapevine cultivars and other hosts of *Agrobacterium*. With a more complete understanding of the chemical signals involved, it should be possible to induce Ti-mediated transformation in virtually any plant species. Clearly such a distant goal will also require a synthesis of data from a number of fields of research.

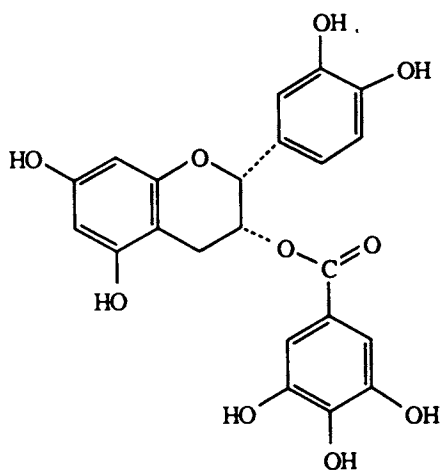


Figure 3. Epicatechin-gallate, a possible *vir*-inducer from grapes.

## Experimental

**Bacterial Strains.** In order to monitor *vir*-induction in the LHR strain A856 a *virE::lacZ* gene fusion-containing plasmid (pSM358cd) was introduced by triparental mating. This was done so that  $\beta$ -galactosidase activity in A856/pSM358cd could be assayed as an indicator of *vir*-induction. This plasmid contained the *virE* region of a WHR pTi in the absence of other *vir* loci, so only the LHR *virA* gene product acted as the environmental sensor of signal compounds. The donor strain of *E. coli* (JC2926/pS M358cd) was maintained on LB medium (51) containing 100  $\mu\text{g}/\text{mL}$  kanamycin. The strain of *E. coli* which contained the helper plasmid (JC2926/pRK2013) was maintained on LB medium containing 30  $\mu\text{g}/\text{mL}$  spectinomycin. A856 was resistant to chloramphenicol, rifampicin, and nalidixic acid (40  $\mu\text{g}/\text{mL}$ , 10  $\mu\text{g}/\text{mL}$ , and 20  $\mu\text{g}/\text{mL}$ , respectively). Resistance to these antibiotics were used in addition to kanamycin resistance to select for A856/pSM358cd. This strain was maintained on AB medium (51) containing 100  $\mu\text{g}/\text{mL}$  kanamycin. In addition, the LHR strain A856/pSM243cd (provided by Dr. Eugene Nester, University of Washington) was used to monitor *vir* gene induction and was also maintained on AB medium containing 100  $\mu\text{g}/\text{mL}$  kanamycin.

**Plant Materials.** The callus cultures used in this experiment (*Vitis* sp. cv. Seyval and *V. lubrascana* cv. Steuben) were also provided by Dr. Nester. Healthy, mature leaves of a number of *Vitis* cultivars were obtained from the University of British Columbia Botanical Gardens and also from local privately owned vines. Red seedless (Flame red) and Green seedless grapes, imported from Chile, were obtained from a local grocery store. *N. glauca* seedlings were obtained from the Agriculture Canada Research Station at U.B.C., and raised in our greenhouse.

**Isolation of LHR *vir*-Inducers.** Conditioned medium was obtained from 5 varieties of *Vitis* by cutting about 20 fresh leaves and stems into 1 cm pieces and placing them immediately into 1.5 L of sterile pH 5.7 Murashige and Skoog (MS) medium (52). Conditioned MS medium from callus cultures of the *Vitis* cultivar Steuben was obtained by breaking up healthy calli from 6-8 petri plates in 500 mL of sterile pH 5.7 MS medium. After 8-12 hours at room temperature, the plant material was removed and the conditioned medium was filtered, then processed immediately. Wound induced phenolic aglycones were partitioned from the conditioned medium using three volumes each of ethyl acetate or diethyl ether, and phenolic glycosides were partitioned from the conditioned medium using three volumes of n-butanol. The solvents were removed by rotary evaporation and each extract was re-suspended in a small volume of 100% methanol. Methanolic extracts were made directly from healthy, mature calli so that a comparison between the wound induced and naturally present compounds could be made.

The compounds present in these mixtures were separated either by column chromatography on polyamide (SC 6-AC) or by banding on preparative polyamide (AC 6) TLC plates. Each band was collected, the compound

eluted from the polyamide and then tested for *vir*-induction in the *Agrobacterium* strains A856/pSM358cd and A856/pSM243cd.

Grape flavans were isolated from the two varieties of commercially available grapes and from the bark of *Vitis* grapevine cultivar Concord according to the methods of Czochanska *et al.* (46). CHCl<sub>3</sub>, EtOAc, and aqueous fractions of both grape varieties were assayed for *vir*-inducing activity in both A854/pSM243cd and A856/pSM358cd. The EtOAc fractions from the flavan extractions of both varieties of grapes and bark were resuspended either in 100% ethanol or methanol for chromatography on Sephadex LH 20. The fractions were examined by TLC on cellulose (Merck, 0.1mm) developed with *sec*-BuOH:AcOH:H<sub>2</sub>O (14:1:5), and similar fractions were pooled and then assayed for activity or alternatively they were screened for activity and groups of active fractions were pooled. Grape flavan fractions were also separated on Sephadex G 25 using 10 mM NaCl as the developing solvent.

TLC on cellulose (*sec*-BuOH:AcOH:H<sub>2</sub>O; 14:1:5) of active, pooled fractions revealed at least 5 or more major compounds. GC showed that there were considerably more compounds also present.

HPLC of the active fractions was performed on a Varian model 502000-00 equipped with an analytical Waters C-18 column (0.5 × 30cm) and using solvent A: 5% acetic acid in H<sub>2</sub>O, and B: acetonitrile, under the following conditions 95% A:5% B, 10 min., changing to 25% B in 10 min., then 30% B in 10 min. and maintained for 10 min., and finally to 40% in 10 min. UV absorbance was monitored at 254 or 275 nm. The isolated compounds were tested for *vir*-induction as described below.

*vir*-Induction Assay. For the structure-activity study,  $\beta$ -galactosidase activity was assayed as a measure of *vir*-gene induction in a wide host range strain which carried a *virE::lacZ* gene fusion. The compounds tested were dissolved in DMSO and diluted in citrate-phosphate buffered pH 5.70 MS medium (52) to a final concentration of 0.1% DMSO. 100  $\mu$ L of bacterial cells from an overnight culture of A348/pSM358 (23) were inoculated into each 25 × 150mm culture tube and subjected to continuous shaking at 200 RPM and at 28°C for 8 hours to allow for induction of *virE::lacZ* expression. Cell density was determined by measuring absorbance at 600 nm and 1 ml aliquots were removed for  $\beta$ -galactosidase assay essentially as described by Miller (53).

Each point on the activity curve of a test compound represented the average of the results of each concentration tested in triplicate. *vir*-Induction was strongly pH dependent (24, our results, data not shown), so the buffer system was used to minimize variation in pH. Standard deviations rarely reached 10%, the average being 4.7% (n = 92) for results of 100 Miller units and above.

In the search for LHR *vir*-inducers, each phenolic aglycone or other fraction to be tested was dissolved in DMSO and diluted in pH 5.50 or 5.70 MS medium to a final concentration of 0.1% DMSO (phenolic glycosides and the grape flavan fractions were dissolved directly in pH 5.50 or 5.70 MS medium). Subsequent experiments revealed a more acidic pH optimum for



*vir*-induction in the LHR strain, so some experiments were conducted at pH 5.0. Standards of acetosyringone, catechin, epicatechin, and a proanthocyanidin polymer were assayed for LHR *vir*-induction. 100  $\mu$ L of cells from an overnight culture of A856/pSM358cd or A856/pSM243cd was inoculated into each 25  $\times$  150mm test tube containing 10 mL of MS or 0.1% DMSO-MS solution with various concentrations of the test substances, and all tubes were subjected to 200 rpm for 10-24 h and at 28°C to allow for induction of *vir* expression.  $\beta$ -Galactosidase activity was then assayed as described by Miller (53).

Alternatively, the following screening assay was used to identify *vir*-inducing fractions. HPLC fractions were collected, reduced to dryness under vacuum, resuspended in a small amount of MeOH and a few  $\mu$ L of each was applied to a filter paper disc. The discs were placed on a M9 (51) agar plate containing 0.1% 5-bromo-4-chloro-3-indolyl- $\beta$ -D-galactopyranoside (Xgal) with a lawn of A856/pSM358cd or A856/pSM243cd and the plates were incubated at 28°C for 24h or until blue zones (indicating  $\beta$ -galactosidase activity) developed surrounding any disc.

*Gas Chromatography.* In our GC analyses, N,O-bis-(Trimethylsilyl) Trifluoroacetamide (BSTFA)-derivatized standards of known *vir*-inducing phenolics failed to correspond in retention time to any of the derivatized samples of the most active grape flavan fractions. Catechin and epicatechin were tentatively identified by GC.

### Acknowledgments

We would like to give special thanks to Dr. Eugene W. Nester who provided the *Agrobacterium* strains A348/pSM358 and A856/pSM243cd, and the bacterial strains from which we prepared A856/pSM358cd. We also thank Don Champagne for useful discussions and Felipe Balza for conducting mass spectroscopy. We are grateful to Lacey Samuels for permission to use her SEM figures in our symposium presentation. P.A.S. was supported by a University Graduate Fellowship at the University of British Columbia. The research was funded by the Natural Sciences and Engineering Research Council of Canada.

### Literature Cited

1. Firmin, J. I.; Wilson, K. E.; Rossen, I.; Johnston, A. W. B. *Nature* 1986, **324**, 90.
2. Kosslak, R. M.; Bookland, R.; Barkei, J.; Paaren, H. E.; Appelbaum, E. R. *P.N.A.S.* 1987, **84**, 7428.
3. Peters, N. K.; Frost, J. W.; Long, S. R. *Science* 1986, **233**, 977.
4. Peters, N. K.; Long, S. R. *Plant Physiol.* 1988, **88**, 396.
5. Redmond, J. W.; Batley, M.; Djordjevic, M. A.; Innes, R. W.; Kuempel, P. L.; Rolfe, B. G. *Nature* 1986, **323**, 632.
6. Sadowsky, M. J.; Olson, E. R.; Foster, V. E.; Kosslak, R. M.; Verma, D. P. S. *J. Bact.* 1988, **170**, 171.

7. Stachel, S. E.; Messens, E.; Van Montagu, M.; Zambryski, P. *Nature* 1985, **318**, 624.
8. DeCleen, M.; Deley, J. *Bot. Rev.* 1976, **42**, 389.
9. Chilton, M. D.; Montoya, A. L.; Merlo, D. J.; Drummond, M. H.; Nutter, R.; Gordon, M. P.; Nester, E. W. *Cell* 1977, **11**, 263.
10. Thomashow, M. F.; Nuter, R.; Montoya, A. L.; Gordon, M. P.; Nester, E. W. *Cell* 1980, **19**, 729.
11. Yadav, N. S.; Postle, K.; Saiki, R. K.; Thomashow, M. F.; Chilton, M.-D. *Nature* 1980, **287**, 458.
12. Chilton, M.-D.; Saiki, R. K.; Yadav, N.; Gordon, M. P.; Quetier, F. *Proc. Natl. Acad. Sci. USA* 1980, **77**, 4060.
13. Willmitzer, L.; De Beuckeleer, M.; Lemmers, M.; Van Montagu, M.; Schell, J. *Nature* 1980, **287**, 359.
14. Zambryski, P.; Holsters, M.; Kruger, K.; Depicker, A.; Schell, J.; Van Montagu, M.; Goodman, H. M. *Science* 1980, **209**, 1385.
15. Schroder, G.; Waffenschmidt, S.; Weiler, F.W.; Schroder, J. *Eur. J. Biochem.* 1984, **138**, 387.
16. Thomashow, L. S.; Reeves, S.; Thomashow, M. F. *Proc. Natl. Acad. Sci.* 1984, **81**, 5071.
17. Akiyoshi, P. E.; Monis, R. O.; Hing, R.; Mischke, B. S.; Kosuge, T.; Garfinkel, D. J.; Gordon, M. P.; Nester, E. W. *Proc. Natl. Acad. Sci.* 1983, **80**, 407.
18. Akiyoshi, P. E.; Klee, H.; Amasino, R. M.; Nester, E. W.; Gordon, M. P. *Proc. Natl. Acad. Sci.* 1984, **81**, 5994.
19. Hille, J.; Hoekema, P.; Hoojkaas, P.; Shilperoort, R. In *Plant Gene Research. Genes Involved in Plant-Microbe Interactions*; Verman, D. P. S.; Hohn, T., Eds.; Springer-Verlag: New York, 1984.
20. Willmitzer, L.; Schmalenbach, W.; Schell, J. *Nucleic Acid Res.* 1981, **9**, 4801.
21. Horsch, R. B.; Klee, H. J.; Stachel, S.; Winans, S. C.; Nester, E. W.; Rogers, S. G.; Fraley, R. T. *Proc. Nat. Acad. Sci. USA* 1986, **83**, 2571.
22. Klee, H. J.; White, F. F.; Iyer, V. N.; Gordon, M. P.; Nester, E. W. *J. Bacteriol.* 1983, **153**, 878.
23. Stachel, S. E.; An, G.; Flores, C.; Nester, E. W. *EMBO J.* 1985, **4**, 891.
24. Stachel, S. E.; Nester, E. W.; Zambryski, P. C. *Proc. Natl. Acad. Sci.* 1986, **83**, 379.
25. Winans, S. C.; Ebert, P. R.; Stachel, S. E.; Gordon, M. P.; Nester, E. W. *Proc. Natl. Acad. Sci.* 1986, **83**, 8278.
26. Stachel, S. E.; Zambryski, P. *Cell* 1986, **46**, 325.
27. Leroux, B.; Yanofsky, M. F.; Winans, S. C.; Ward, J. E.; Ziegler, S. F.; Nester, E. W. *EMBO J.* 1987, **6**, 849.
28. Hille, J.; van Kan, J.; Shilperoort, R. J. *Bacteriol.* 1984, **158**, 754.
29. Hooykaas, P. J. J.; Hofker, M.; Den Dulk-Ras, H.; Shilperoort, R. A. *Plasmid* 1984, **11**, 195.
30. Yanofsky, M.; Lowe, B.; Montoya, A.; Rubin, R.; Krul, W.; Gordon, M.; Nester, E. W. *Molec. Gen. Genet.* 1985, **201**, 237.

31. Yanofsky, M. F.; Porter, S. G.; Young, C.; Albright, L. M.; Gordon, M. P.; Nester, E. W. *Cell* 1986, **47**, 471.
32. Engstrom, P.; Zambryski, P.; Van Montagu, M.; Stachel, S. *J. Mol. Biol.* 1987, **197**, 635.
33. Christie, P. J.; Ward, J. E.; Winans, S. C.; Nester, E. W. *J. Bact.* 1988, **170**, 2659.
34. Stachel, S. E.; Timmerman, B.; Zambryski, P. *EMBO J.* 1987, **6**, 857.
35. Bolton, G.; Nester, E. W.; Gordon, M. *Science* 1986, **232**, 983.
36. Ashby, A. M.; Watson, M. D.; Shaw, C. H. *Fed. Eur. Micro. Soc.* 1987, **41**, 189.
37. Ashby, A. M.; Watson, M. D.; Loake, G. L.; Shaw, C. H. *J. Bact.* 1988, **170**, 4181.
38. Sheikholleslam, S. N.; Weeks, D. P. *Plant Mol. Biol.* 1987, **8**, 291.
39. Owens, L. D.; Smigocki, A. C. *Plant Physiol.* 1988, **88**, 570.
40. Schafer, W.; Gorz, A.; Kahl, G. *Nature* 1987, **327**, 529.
41. Spencer, P. A.; Towers, G. H. N. *Phytochemistry* 1988, **27**, 2781.
42. Ohashi, H.; Yamamamoto, E.; Lewis, N.; Towers, G. H. N. *Phytochemistry* 1987, **26**, 915.
43. Tang, C.; Young, C. *Plant Physiol.* 1982, **69**, 155.
44. Hernalsteens, J. P.; Thia-Toong, L.; Schell J.; van Montagu, M. *EMBO J.* 1984, **3**, 3039.
45. Graves, A. C. F.; Goldman, S. L. *Plant Mol. Biol.* 1986, **7**, 43.
46. Graves, A. C. F.; Goldman, S. L. *J. Bacteriol.* 1987, **169**, 1745.
47. Hooykaas-van Slogteren, G. M. S.; Hooykaas, P. J. J.; Schilperoort, R. A. *Nature* 1984, **311**, 763.
48. Graves, A. E.; Goldman, S. L.; Banks, S. W.; Graves, A. C. F. *J. Bact.* 1988, **170**, 2395.
49. Czochanska, Z.; Foo, L. Y.; Porter, L. J. *Phytochemistry* 1979, **18**, 1819.
50. Stafford, H. A. *Phytochemistry* 1988, **27**, 1.
51. Maniatis, T.; Fritsch, E. F.; Sambrook, J. *Molecular Cloning*; Cold Spring Harbor Laboratory Press: New York, 1982.
52. Murashige, T.; Skoog, F. *Physiologia Pl.* 1962, **15**, 473.
53. Miller, J. H. *Experiments in Molecular Genetics*; Cold Spring Harbor Laboratory Press: New York, 1972.

RECEIVED May 19, 1989

## Chapter 29

# Properties of a Cutinase-Defective Mutant of *Fusarium solani*

Anne H. Dantzig

Lilly Research Laboratories, Eli Lilly and Company, Indianapolis,  
IN 46285

The fungal plant pathogen *Fusarium solani* produces an extracellular enzyme, cutinase, which catalyzes the degradation of the biopolymer, cutin, in the plant cuticle. The enzyme was repressed when the microorganism was grown on a medium containing glucose and induced to high levels by cutin or its hydrolysis products, the true inducers. In the present study, culture filtrates contained basal levels of cutinase when *Fusarium* was grown on 0.5% acetate as the sole carbon source and high levels of cutinase when grown on cutin. After mutagenesis, a cutinase-defective mutant of *Fusarium* was identified by screening acetate-grown colonies for a loss of enzyme activity. The mutant exhibited an 80-90% reduction in cutinase activity under several growth conditions due to a quantitative reduction in a qualitatively normal enzyme. The mutant also exhibited a reduction in virulence in the pea stem bioassay. Taken together, these data indicated that a growth condition exists where the cutinase enzyme was neither induced nor repressed and was present in basal levels. This condition may pose the pathogen for rapid enzyme induction when in the proximity of the plant cuticle. The cutinase-defective mutant was either a regulatory mutant with an altered expression of cutinase, or a mutant modified in its ability to excrete the enzyme.

The biopolymer cutin is a major constituent of the plant cuticle that provides a protective covering for plants (1,2). At the time of infection, a number of fungal pathogens secrete an extracellular hydrolytic enzyme, cutinase, which facilitates the degradation of cutin into its constituent C<sub>16</sub>- to C<sub>18</sub>-length hydroxy fatty acids (3,4). Since the enzyme is believed to

0097-6156/89/0399-0399\$06.00/0

© 1989 American Chemical Society

play an important role in virulence (5), many studies have been conducted to determine its biochemical properties and physiological role during pathogenesis.

To date the most comprehensive studies have been carried out by Kollattukudy and coworkers with a fungal plant pathogen of peas, *Fusarium solani* f. sp. *pisii*. When grown on cutin, the fungus produced two isozymes of cutinase of molecular weights 22,400 and 21,200, with the former being the precursor of the latter, mature form (6-8). The cDNA for the cutinase gene was isolated, sequenced, and the primary amino acid sequence deduced (9,10). DNA hybridization studies indicated that more than one gene was present in *Fusarium solani* (9).

Although details of the regulation of the expression of cutinase at the DNA level were not established, physiological studies indicated that the regulation of the enzyme was likely to be complex. The enzyme underwent catabolite repression and was induced to high levels when cutin, or its hydrolyzed products, were provided as the sole carbon source (11). Since cutin has a large molecular weight, it is not likely to penetrate the fungal cell wall; the degradation products are therefore believed to be the true inducers of the enzyme (11,12). Thus, the presence of the cutinase enzyme seemed to be required for its own induction in order to generate the small molecular weight inducers. Consequently, it seemed plausible that growth conditions might exist in which cutinase were present in basal quantities, thereby posing the pathogen for rapid enzyme induction when presented with the cutin biopolymer. The present study was undertaken to examine the regulation of cutinase by an alternate carbon source that might permit basal levels of the enzyme to be synthesized, and then to subsequently use this growth condition for the isolation of a cutinase-defective mutant. The details of this work have been previously published in Ref. 13.

## Results

Acetate is known to be a good carbon source for fungi and would be expected to be the ultimate degradation product of cutin (14). The effect of acetate on the production of cutinase by the T-8 strain of *F. solani* was examined and compared with that of glucose. Since previous studies showed that hydrolysis of the artificial substrate p-nitrophenylbutyrate, PNB, was specifically hydrolyzed by cutinase in the T-8 strain, this activity was used to measure cutinase levels (8). Figure 1 illustrates that basal levels of cutinase activity were detected in the growth medium when T-8 was grown on 0.5 and 1.5% acetate, but not 2.0% glucose, as the sole carbon source. As shown in Figure 2A, T-8 produced high levels of cutinase in the growth medium when grown on apple cutin as the sole carbon source, and was repressed by increasing concentrations of glucose; by contrast, Figure 2B showed that addition of increasing concentrations of acetate was less repressive than glucose. These data suggest that the enzyme was present at low concentrations when the organism was grown on acetate.

Since growth of *F. solani* on acetate medium permitted production of cutinase, this growth condition was used for the isolation of a mutant

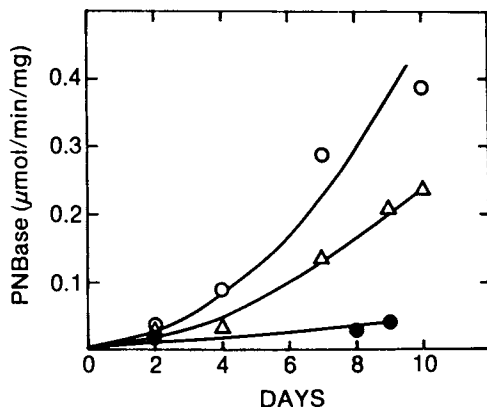


Figure 1. Specific activity of cutinase as a function of sole carbon source in the growth medium. The T-8 strain of *F. solani* was grown on 0.5% acetate (○), 1.5% acetate (△), or 1.5% glucose (●) as the sole carbon source. (Reproduced with permission from Ref. 13. © 1986, American Society for Microbiology.)

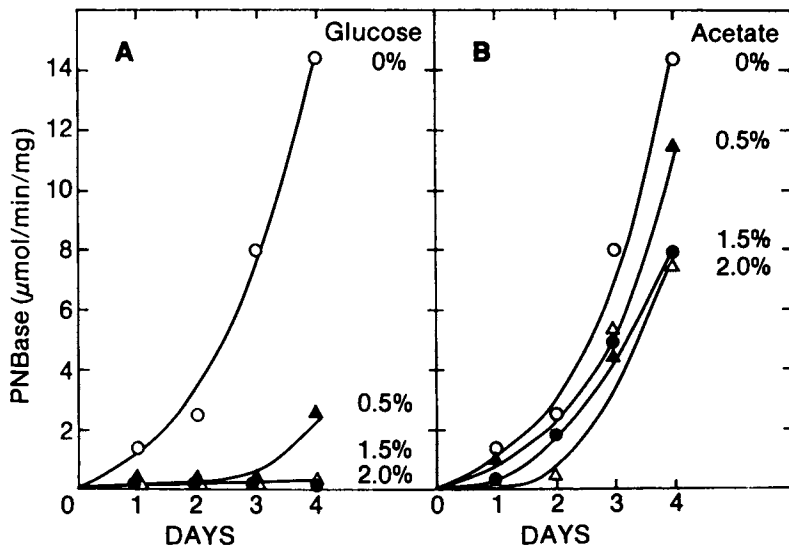


Figure 2. Specific activity of cutinase resulting from growth in cutin-containing medium with the addition of a second carbon source. The T-8 strain of *F. solani* was grown on medium containing 200 mg of apple cutin and glucose (A) or acetate (B). (Reproduced with permission from Ref. 13. © 1986, American Society for Microbiology.)

defective in cutinase; the procedure for mutant selection was described in Ref. 13 and is summarized in Figure 3. Initially, *Fusarium* was grown on medium containing peanut meal-peptone-Stadex II to produce microconidia needed for genetic studies (13). The conidia were *uv* irradiated to introduce mutations, regrown to permit expression of any mutation, and plated on growth medium containing agarose and 0.5% acetate as the sole carbon source. The resulting colonies were then overlaid with agarose containing PNB. Within 30 min the parental type hydrolyzed the substrate and turned yellow, and the presumptive mutants remained white. The resulting *PNB-1* mutant was one out of 4,300 colonies screened. The properties of this mutant were further characterized as described below.

Preliminary evaluation of the mutant indicated that it had produced low levels of the cutinase when grown on either acetate or cutin as the sole carbon source. A time course of the production of cutinase was examined for the T-8 parental strain and the *PNB-1* mutant strain when grown on cutin. As shown in Figure 4, the mutant exhibited a reduction in activity of 80-90% over the 15-day growth period, when enzyme activity was assayed using the artificial substrate PNB (Panel A) or when assayed using [ $^{14}\text{C}$ ]-labelled natural substrate cutin (Panel B). These data suggested that the mutant was defective in cutinase but not in general esterase.

Next the parent and mutant were compared for their ability to induce cutinase by cutin and hydrolyzed cutin (consisting of small molecular weight inducers) after growth on glucose. As shown in Figure 5, cutinase activity increased over the three-day induction period for both strains in the presence of cutin (Panel A) or hydrolyzed cutin (Panel B); however, cutinase was induced less effectively in the mutant strain, as evidenced by an 80-90% reduction. Hydrolyzed cutin was a 10-fold less effective inducer than cutin in both strains. These data indicated that lack of induction in the mutant was not related to its inability to hydrolyze cutin to small molecular weight inducers. Consequently the defect observed was not related to the inability of the mutant to produce the inducer.

To gain further insight into the nature of the defect in *PNB-1* mutant, the concentration dependence of the cutinase enzyme activity was examined over a wide substrate range and compared with that of the parental strain (Figure 6). In both strains, the enzyme activity was saturated with increasing substrate concentration, and gave simple Michaelis-Menten curves which were subsequently fitted by computer to a single Michaelis term. The  $K_m$  for PNB was determined to be  $0.97 \pm 0.20$  and  $0.64 \pm 0.07$  mM, respectively, in the parental and mutant strains, indicating that little change in the affinity for the substrate had occurred. By contrast, the  $V_{max}$  was reduced by 92% from  $38.86 \pm 2.68$  to  $2.62 \pm 0.09$   $\mu\text{mol}/\text{min}$  per mg protein in the parental and mutant strains, respectively. The large reduction in  $V_{max}$  might result from a quantitative reduction of a normal enzyme or from an aberrant enzyme being produced in normal quantities.

To find out if the mutant was making less enzyme, the two strains were induced to produce cutinase (as illustrated in Figure 5) in the presence of [ $^{35}\text{S}$ ]methionine, and the extracellular proteins were separated by

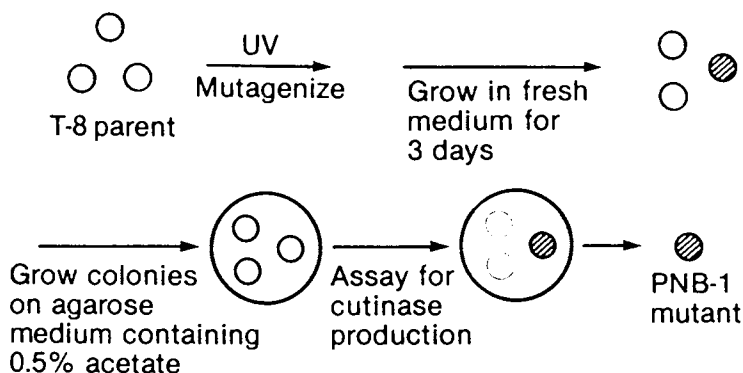


Figure 3. Summary of the selection procedure for cutinase-defective mutant. The T-8 strain of *F. solani* was mutagenized by ultraviolet irradiation, grown for 3 days, and plated on medium containing 0.5% acetate and agarose for 5-7 days to permit colony formation. Subsequently, the colonies were overlaid with an agarose solution containing 1.26 mM PNB. The parental colonies hydrolyzed the substrate and turned yellow while the presumptive mutant colonies remained white and were selected for analysis. Further details are given in Ref. 13.



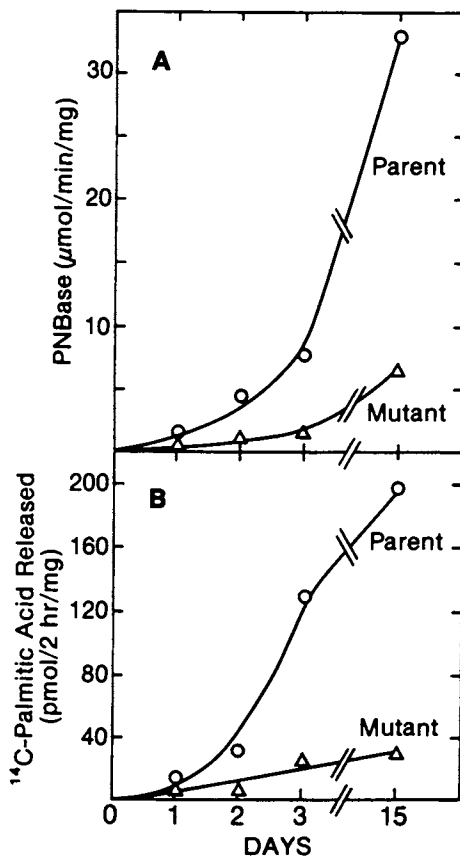


Figure 4. Specific activity of cutinase for the T-8 parental strain and *PNB-1* mutant strain after growth on medium containing 200 mg cutin. Enzyme activity was assayed with the artificial substrate PNB (Panel A) and with the natural substrate, [<sup>14</sup>C]-labelled cutin (Panel B). (Reproduced with permission from Ref. 13. © 1986, American Society for Microbiology.)

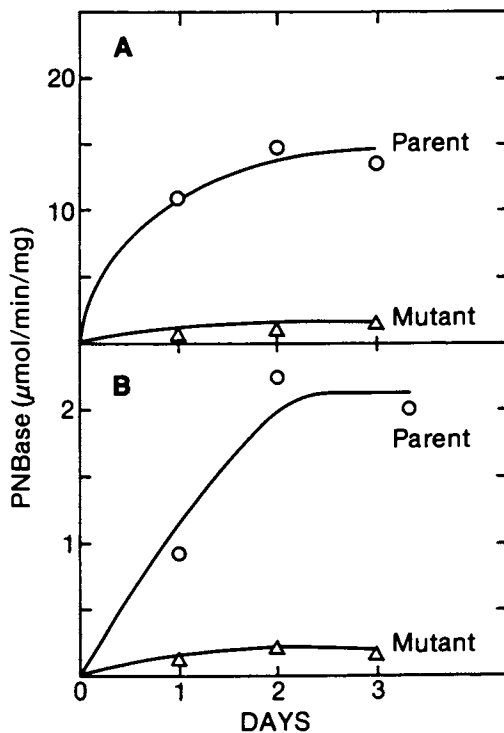


Figure 5. Comparison of effect of addition of cutin or hydrolyzed cutin on the induction of cutinase. The two strains were grown on medium containing 0.1% glucose for 3 days, and then 200 mg of cutin (A) or 8 mg of hydrolyzed cutin (B) was added to the growth medium on day zero. (Reproduced with permission from Ref. 13. © 1986, American Society for Microbiology.)

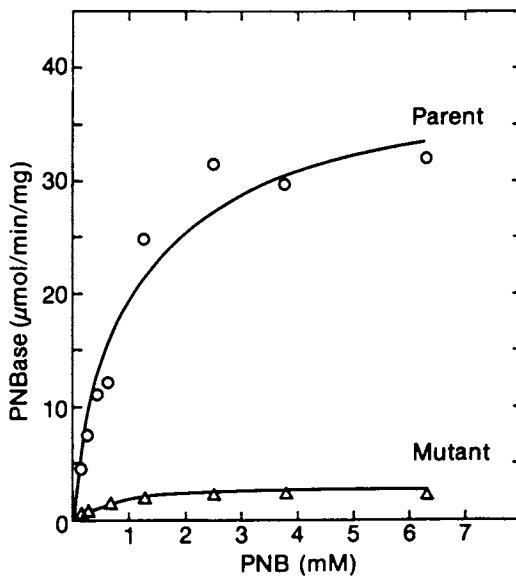


Figure 6. Kinetics of the specific activity of cutinase produced by the parental T-8 strain and the *PNB-1* mutant strain. The data were fitted to a Michaelis-Menten equation (13). (Reproduced with permission from Ref. 13. © 1986, American Society for Microbiology.)

electrophoresis on a 15% sodium dodecyl sulfate polyacrylamide gel. A fluorograph of the gel indicated that both strains possessed a protein band of about 22,000 in the same molecular weight range as the cutinase isozymes; however, by densitometer tracing the mutant exhibited about an 80% reduction in this band. Immunoblots were conducted with rabbit anticutinase serum which confirmed that this band corresponded to cutinase (Figure 7). Thus, the *PNB-1* mutant appeared to make less of a "normal" enzyme.

A reduction in cutinase production should result in the *PNB-1* mutant being less virulent. The pathogenesis of the two strains were evaluated in a pea stem bioassay developed by Kolattukudy and coworkers in which infection by *Fusarium solani* results in wound formation within three days on the epicotyl of pea seedlings (15). The virulence of T-8 had previously been shown to be reduced in this assay by the addition of inhibitors of cutinase or by rabbit anticutinase antibodies (15-18), indicating that cutinase played an important role in pathogenesis. When the cutinase-defective mutant was evaluated in the bioassay, the mutant exhibited a 55% reduction ( $p < 0.05$ ) in virulence compared with the T-8 parental strain and the addition of purified cutinase at 1 mg/ml to the mutant enhanced wound formation to 80% of that of the parent ( $p > 0.5$ ). These data further support the notion that the mutant was defective in cutinase.

## Discussion

Taken together, these data indicate that *Fusarium solani* produced low levels of cutinase when grown on acetate as the sole carbon source and that this carbon source was less repressive than glucose. The finding that a cutinase-defective mutant could be isolated using this growth condition provided additional support that cutinase was being produced when grown on acetate. Thus there were three discrete growth conditions which affected the synthesis of cutinase by the microorganism: one in which the enzyme was repressed (such as glucose); one in which the enzyme was induced to high levels (such as with cutin or its hydrolyzed products); and one in which it was neither induced nor repressed (such as acetate)—resulting in the production of basal levels of enzyme. Therefore, cutinase production by a fungus present in the field in the presence of a good carbon source would be expected to be repressed. Once that carbon source was depleted, then basal levels of the enzyme may be synthesized. If the fungus was in the proximity of the plant cuticle, then cutin may be hydrolyzed, resulting in inducer formation and rapid induction of cutinase synthesis aiding the fungus in the penetration of the plant (12).

The *PNB-1* mutant is a "leaky" mutant that is partially defective in cutinase production, and apparently produced 80 to 90% less "normal" enzyme. The regulation of the residual enzyme in the mutant was unchanged. The enzyme was repressed by glucose, and was induced by cutin or hydrolyzed cutin after depletion of glucose. Cutinase activity increased over a 15-day time period when the mutant was grown on cutin as the sole carbon source. The mutant was also less virulent than the parental strain. The nature of the *PNB-1* mutation remains to be elucidated and

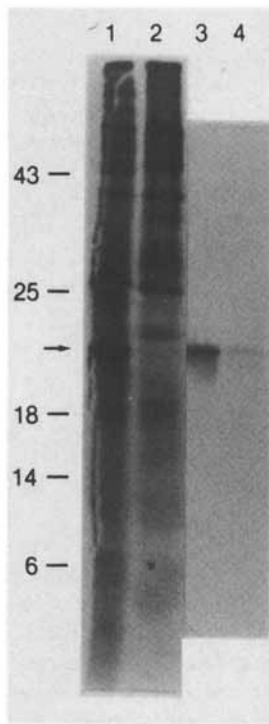


Figure 7. Comparison of separated [ $^{35}\text{S}$ ]-labelled extracellular proteins from the cutin induction medium of the parental and mutant strains on 15% sodium dodecyl sulfate-polyacrylamide gels by fluorography and Western blotting. Mycelia were grown and induced with cutin (as illustrated in Figure 5) with the addition of  $115\ \mu\text{Ci}$  of [ $^{35}\text{S}$ ]methionine. A 20-fold concentrated sample containing 100,000 cpm for the parent (lanes 1 and 3) or the mutant (lanes 2 and 4) was applied to parallel gels. Total protein synthesis was analyzed by fluorography of the gel containing lanes 1 and 2. Immunoreactive material in the gel containing lanes 3 and 4 was detected with rabbit anticutinase serum after electroblotting. Molecular weight standards ( $\times 10^3$ ) are indicated on the left. The band corresponding to the molecular weight of cutinase is indicated with the arrow. (Reproduced with permission from Ref. 13. © 1986, American Society for Microbiology.)

may reside in a promoter for the structural gene of cutinase or an as yet unidentified regulatory gene. Alternatively, the mutant may be defective in the secretion of cutinase. Further study of the *PNB-1* mutant should provide insight into the complex regulation or secretion of this biopolymer hydrolyzing enzyme. With a better understanding of these processes, it may be possible to design agents that can intervene in cutinase production resulting in the control of fungal pathogenesis in the field.

### Acknowledgments

Special thanks are given to Dr. Kolattukudy for providing the rabbit cutinase antiserum and purified cutinase used in this study.

### Literature Cited

1. Espelie, K. E.; Davis, R. W.; Kolattukudy, P. E. *Planta* 1980, **149**, 498-511.
2. Van den Erde, G.; Linskens, H. F. *Ann. Rev. Phytopathol.* 1974, **12**, 247-58.
3. Baker, C. J.; Bateman, D. F. *Phytopathology* 1978, **68**, 1577-84.
4. Dickman, M. B.; Patil, S. S.; Kolattukudy, P. E. *Physiol. Plant Pathol.* 1982, **20**, 333-47.
5. Lin, T. S.; Kolattukudy, P. E. *Physiol. Plant Pathol.* 1980, **17**, 1-15.
6. Purdy, R. E.; Kolattukudy, P. E. *Arch. Biochem. Biophys.* 1973, **159**, 61-9.
7. Purdy, R. E.; Kolattukudy, P. E. *Biochemistry* 1975, **14**, 2824-31.
8. Purdy, R. E.; Kolattukudy, P. E. *Biochemistry* 1975, **14**, 2832-40.
9. Soliday, C. L.; Flurkey, W. H.; Okita, T. W.; Kolattukudy, P. E. *Proc. Natl. Acad. Sci. USA* 1984, **81**, 3939-43.
10. Ettinger, W. G.; Thukral, S. K.; Kolattukudy, P. E. *Biochemistry* 1987, **26**, 7883-92.
11. Lin, T. S.; Kolattukudy, P. E. *J. Bacteriol.* 1978, **133**, 942-51.
12. Woloshuk, C. P.; Kolattukudy, P. E. *Proc. Natl. Acad. Sci. USA* 1986, **83**, 1704-8.
13. Dantzig, A. H.; Zuckerman, S. H.; Andonov-Roland, M. M. *J. Bacteriol.* 1986, **168**, 911-6.
14. Cochrane, V. W. In *Physiology of Fungi*; John Wiley & Sons: New York, 1958; pp. 55-98.
15. Maiti, I. B.; Kolattukudy, P. E. *Science* 1979, **205**, 507-8.
16. Koller, W.; Allan, C. R.; Kolattukudy, P. E. *Physiol. Plant Pathol.* 1982, **20**, 47-60.
17. Koller, W.; Allan, C. R.; Kolattukudy, P. E. *Pestic. Biochem. Physiol.* 1982, **18**, 15-25.
18. Shaykh, M.; Soliday, C.; Kolattukudy, P. E. *Plant Physiol.* 1977, **60**, 170-2.

RECEIVED March 10, 1989

## Chapter 30

# Roles of Secondary Metabolism of Wood Rotting Fungi in Biodegradation of Lignocellulosic Materials

Mikio Shimada<sup>1</sup>, Akira Ohta<sup>2</sup>, Hiroshi Kurosaka<sup>1</sup>, Takefumi Hattori<sup>1</sup>,  
Takayoshi Higuchi<sup>1</sup>, and Munezoh Takahashi<sup>1</sup>

<sup>1</sup>Wood Research Institute, Kyoto University, Uji, Kyoto 611, Japan

<sup>2</sup>Shiga Forest Research Center, Yasu, Shiga 520-23, Japan

The brown-rot fungus *Lentinus lepideus* produces 5 different phenylpropanoids and methyl *p*-anisate as secondary metabolites in both high and low nitrogen nutrient-containing cultures. A new metabolite, *p*-methoxyphenylpropanol, was also identified. The white-rot fungus *Phanerochaete chrysosporium* produces veratrylglycerol and veratryl alcohol as secondary metabolites in the extracellular culture fraction. The "ligninase" of this white-rot fungus catalyzes C $\alpha$ -C $\beta$  cleavage of veratrylglycerol, yielding glycolaldehyde and veratraldehyde. Both a synthetic lignin model substrate and the natural metabolites of the white-rot fungus were oxidized by this extracellular peroxidase. The possible roles of this nitrogen recycling system and the cinnamate pathway, which are involved in the secondary metabolism of L-phenylalanine in brown-rot and white-rot fungi, are discussed in relation to wood decay processes.

It is timely to attempt to forward an unifying hypothesis for the processes of: (i) lignin biosynthesis in higher plants and lignin biodegradation by white-rot fungi; (ii) cellulose and lignin degradation by white-rot fungi; (iii) the degradation of plant lignins and monomeric fungal metabolites during wood decay; and (iv) differences in L-phenylalanine-cinnamate pathways between white-rot and brown-rot fungi.

As Figure 1 depicts, phenylalanine ammonia-lyase (PAL), which occurs ubiquitously in higher plants and the wood-rotting Basidiomycetes (1-3), seems to play a common central role in the conversion of phenylalanine (by deamination) to a wide variety of secondary metabolites. These include lignins in higher plants (4), veratryl alcohol in the white-rot fungus *Phanerochaete chrysosporium* (4a), and methyl *p*-anisate in the brown-rot fungus

0097-6156/89/0399-0412\$06.00/0

© 1989 American Chemical Society

*Lentinus lepideus* (5). Interestingly, PAL is absent from both bacterial and animal kingdoms.

The true biochemical significance of this deamination, and the function of the secondary metabolic pathway originating from L-phenylalanine (6-9), are not fully understood. It is, though, noteworthy that wood-rotting Basidiomycetes preferentially attack nitrogen-poor wood substrates in their natural environments. [Note that the average C/N ratios for hardwoods and softwoods are 300 and 1000, respectively (10).] This preference is surprising since the availability of nitrogen is crucial for the growth of wood-destroying microorganisms. This fact, together with the abundant accumulation of nitrogen-free secondary metabolites in both plants and wood-rotting fungi, attracts our attention to the phenylalanine-cinnamate pathway in relation to carbon and nitrogen economy during growth.

Consequently, this review principally focuses on three points: (i) a possible function of nitrogen recycling, in which PAL plays a common role for L-phenylalanine-cinnamate pathways, in both the brown-rot (*L. lepideus*) and the white-rot (*P. chrysosporium*) fungi; (ii) possible metabolic connections between lignin biodegradation and veratryl alcohol biosynthesis carried out by the same white-rot fungi; and (iii) the means whereby secondary metabolic pathways function to support lignin degradation.

### Comparison of the Phenylalanine-Cinnamate Pathway in Brown-Rot and White-Rot Fungi

**Brown-Rot Fungi.** The brown-rot fungus *L. lepideus* was chosen as a model microorganism, since it has long received attention as a pine timber-degrader (11). From L-phenylalanine, it produces methyl *p*-methoxycinnamate and *p*-methoxybenzoate (*p*-anisate) esters as major metabolites (11-13). The phenylalanine-cinnamate pathway of this fungus has been established, as shown in Figure 2, by Shimazono *et al.* (13) and Towers (14).

The relationship, if any, between the secondary metabolism of L-phenylalanine and carbohydrate degradation during brown-rot wood decay processes has not yet been determined. However, we suspect that the secondary metabolism of this aromatic amino-acid plays an important role in converting monomeric sugars to nitrogen-free metabolites (Shimada, M., and Takahashi, M., In *Handbook of Wood and Cellulosic Materials*; Hon, D. N. S. and Shiraishi, N., Eds.; Marcel Dekker, in press).

Table I shows the amounts of secondary metabolites formed on days 11 and 33 (during an incubation of 63 days) for both nitrogen-poor (HC/LN) and nitrogen-rich (HC/HN) cultures (15). The initial C/N ratios of the two cultures were 240 and 24, respectively. Figure 3 shows the variations in the total amounts of the secondary metabolites produced, the weights of the fungal mycelium, and the nitrogen and glucose concentrations remaining in the HC-LN culture media during the incubation period shown.

The major metabolites formed in the HC/LN and HC/HN cultures were methyl *p*-methoxycinnamate (11), methyl *p*-methoxybenzoate (11),



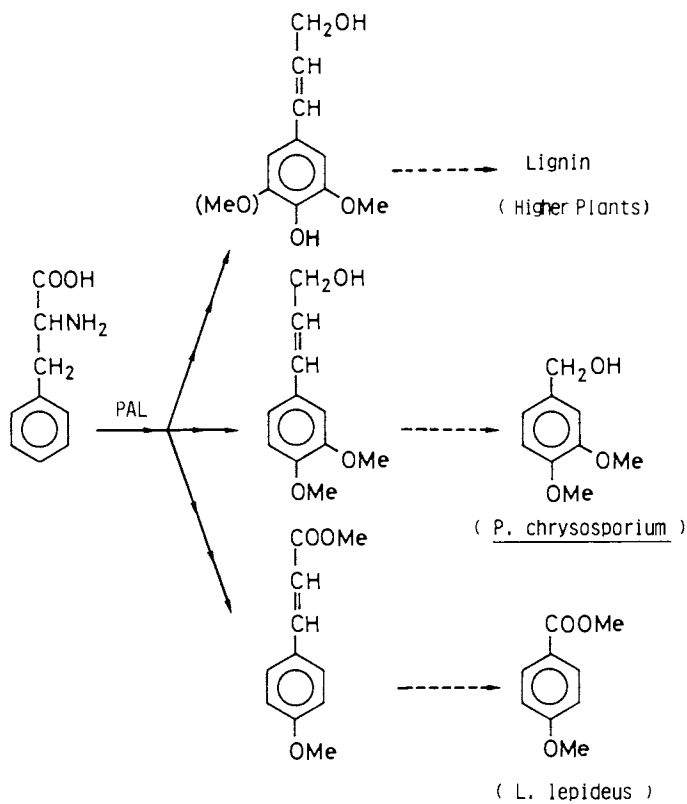


Figure 1. Phenylalanine ammonia-lyase (PAL) involvement in the biosynthesis of phenylpropanoid-derived secondary metabolites in plants and Basidiomycetes.

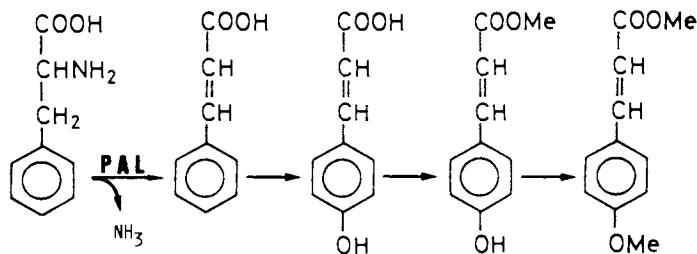


Figure 2. The phenylalanine-cinnamate pathway in the brown-rot fungus *Lentinus lepidus*.

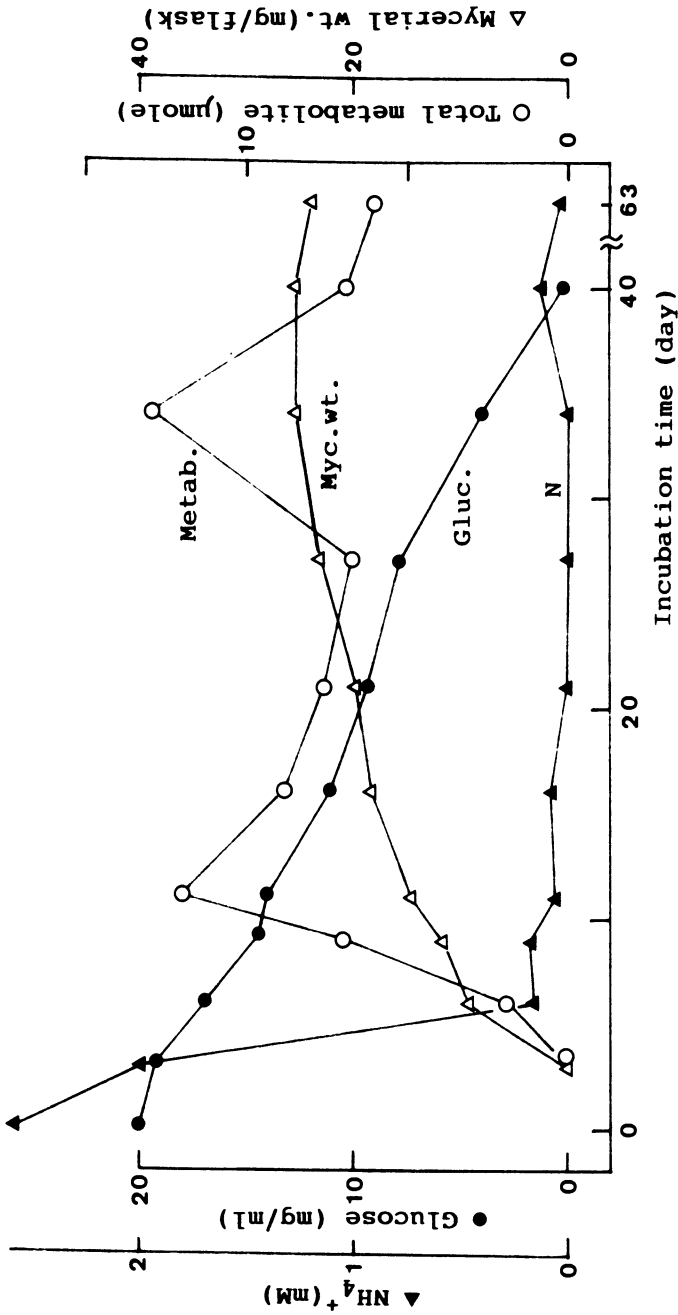


Figure 3. Relationship between secondary metabolite production, consumption of nitrogen and carbon sources, and growth of the brown-rot fungus *Lentinus lepideus* (HC-LN medium).

Table I. Secondary Metabolites Produced by the Brown-Rot Fungus *Lentinius lepideus* (15)

Metabolites	Amounts (mg/10 ml culture)			
	HC-LN		HC-HN	
	a	b	a	b
Methyl <i>p</i> -methoxybenzoate	0.72	0.23	1.38	0.18
trans-Methyl <i>p</i> -methoxycinnamate	0.98	1.98	0.93	0.00
cis-Methyl <i>p</i> -methoxycinnamate	0.40	0.20	0.05	0.03
Methyl iso-ferulate	0.00	0.03	0.15	0.00
Methyl <i>p</i> -coumarate	0.00	0.00	0.08	0.00
<i>p</i> -Methoxyphenylpropanol	0.00	0.01	0.51	0.00
Total amounts	2.20	2.45	3.10	0.21

a and b indicate the 11-day-old and 33-day-old cultures used, respectively, for analyses.

HC-LN = high carbon:low nitrogen ratio.

HC-HN = high carbon:high nitrogen ratio.

and *p*-methoxyphenylpropanol; the latter was a previously unknown secondary metabolite from this source, and was produced in even greater amounts in HC/HN culture. While the total amount of these secondary metabolites formed in HC/HN culture was slightly greater than that observed for the HC/LN culture, the relative amount per nitrogen unit in the HC/LN culture was 8-fold greater than that of the HC/HN culture.

The results (Figure 3) indicate that just before complete consumption of nitrogen, the quantity of secondary metabolites increases, reaching a first maximum on day 11. A second maximum then appears on day 33, at about the time of 60% glucose consumption. Although the reason for the appearance of two maxima is not clear, these results were reproducible. It is noteworthy, though, that nitrogen starvation accelerates the biosynthesis of metabolites derived from L-phenylalanine in HC/LN culture. Thus, PAL may contribute to secondary metabolite accumulation under nitrogen-limiting conditions, perhaps in an effort to economize the use of available nitrogen.

*White-Rot Fungi.* The white-rot fungus *P. chrysosporium* was chosen for comparison, since it has been extensively investigated for lignin biodegradation during this decade. Veratryl alcohol was first reported (16) to be biosynthesized from phenylalanine as a secondary metabolite in the ligninolytic culture of this white-rot fungus. Recently, other white-rot fungi have been reported to produce the same secondary metabolite (17). However, the biochemical significance of veratryl alcohol has remained unclear for some time (18).

The previously proposed metabolism of L-phenylalanine to veratryl alcohol (19-22) is now slightly modified, as shown in Figure 4. This pathway

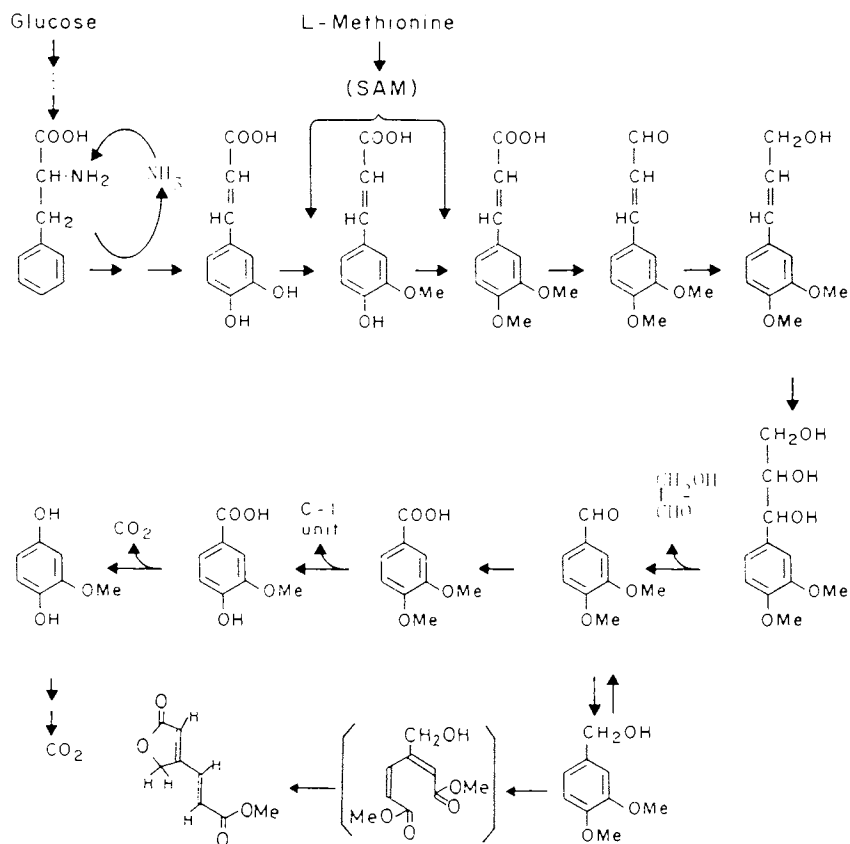


Figure 4. The L-phenylalanine-cinnamate pathway for biosynthesis and biodegradation of veratryl alcohol in the white-rot fungus *Phanerochaete chrysosporium*.

indicates that phenylalanine serves as a primary amino acid precursor, being converted to the accumulating metabolite veratryl alcohol via caffeic acid, ferulic acid, 3,4-dimethoxycinnamic acid, 3,4-dimethoxycinnamyl alcohol, and veratrylglycerol intermediates. Veratryl alcohol then seems to be degraded, via vanillic acid or ring cleavage products (23,24). The two methoxyl carbons of veratryl alcohol are probably derived from methionine via S-adenosylmethionine (SAM) (19), which is also involved in the biosynthesis of *p*-methoxycinnamate in *L. lepidus* (25,26). Interestingly, the fungal hydroxycinnamate pathways in both the brown-rot and white-rot fungi reminds us of the hydroxycinnamate pathways in the biosynthesis of plant lignins (27).

Table II shows (28) a correlation between the biosynthesis of veratryl alcohol and PAL activities, both of which are affected by initial glucose and ammonium salt levels. The HC-LN culture with a C/N ratio of 240, which is almost comparable to that of wood, shows the greatest amount of veratryl alcohol biosynthesis and, therefore, the highest PAL activity. As can be seen, depending upon the C:N balance of the media used, the amounts of secondary metabolites formed and PAL activities can vary greatly (Tables I and II).

Table II. PAL Activity of the White-Rot Fungus *P. chrysosporium* Grown in the Different Culture Media (28)

Culture <sup>a</sup>	C/N Ratio	Veratryl alcohol (nmoles/10 ml culture)		PAL Activity <sup>b</sup>	%
		7 days	14 days		
HC-LN	240	1786	7142	131,529	100
HC-HN	24	0	294	19,176	15
LC-HN	6	250	0	20,450	16
LC-LN	60	1595	857	35,496	27

<sup>a</sup> HC and LC indicate 2% and 0.5% glucose contained in the medium, respectively. HN and LN indicate 24 mM and 2.4 mM ammonium salt nitrogen, respectively, used for the cultures.

<sup>b</sup> PAL activities/6-day old culture (20 ml) are expressed as radioactivities (dpm) of cinnamate formed from L-phenylalanine-U-<sup>14</sup>C (2 nmoles/  $\mu$ Ci).

### Biochemical Significance of the Phenylalanine-Cinnamate Pathway in Plants and Fungi

Woody plants can synthesize anywhere from 15-30% of all biomass as lignin. Hence, equivalent amounts of phenylalanine are required at some point, i.e., during lignin formation, large amounts of ammonia are recycled as a consequence of PAL activity. While plants have no serious problems in obtaining glucose as a carbon source, supplied abundantly through photosynthesis,

the same cannot be said for nitrogen nutrient availability. This underscores the importance of ammonium recycling during lignin formation.

A similar analogy can be applied to the rationalization of the biosynthesis of secondary metabolites produced by wood-rotting fungi. The Basidiomycetes inhabiting wood hosts have no trouble obtaining glucose, but have problems in obtaining significant amounts of nitrogen-containing nutrients.

### Nitrogen Recycling with PAL

The total amount of metabolites synthesized by the brown-rot fungus after 33 days (Figure 3, second maximum) is about 10% of the dry weight of mycelia produced. However, the actual percentage is much higher, since metabolic turnover occurs during fungal growth. Cultures of *Phanerochaete chrysosporium* gave similar results, since the amount of veratryl alcohol produced was about 10% of the dry weight of the mycelia. This value must be higher, since veratryl alcohol turnover also occurs (4a). It can therefore be reasoned that the amounts of fungal metabolites produced approximate those of lignin in woody plants. Therefore, a similar level of nitrogen recycling (using PAL) operates in both plants and the wood-rotting Basidiomycetes (see Figure 1).

In contrast to lignins, the biological formation of the Basidiomycetes secondary metabolites is not clearly understood. However, we propose that there may be some biological significance in the conversion of nutritionally valuable glucose and amino acids to secondary metabolites with little nutritional value to other organisms sharing the same ecosystems. In other words, the accumulation of monomeric sugars, produced by the enzymatic hydrolysis of cellulose and hemicelluloses, would jeopardize their habitation by attracting intruders. Thus, the unique nutritional environment of wood substrates with high C/N ratios (i.e., nitrogen-poor) may have forced the Basidiomycetes to create a common cinnamate pathway. This is one possible explanation for the ubiquitous occurrence of PAL in the wood-destroying Basidiomycetes.

### Correlation between Veratryl Alcohol Synthesis and Lignin Degradation in White-rot Fungi

*Aromatic Ring and  $C\alpha$ - $C\beta$  Bond Cleavage.* Let us now turn our attention to aromatic ring cleavage of veratryl alcohol, and the  $C\alpha$ - $C\beta$  bond cleavage of veratrylglycerol, which are both formed from phenylalanine as shown in Figure 4. Both cleavage reactions may be related to the corresponding degradation reactions of lignin (29). Indeed, veratryl alcohol is commonly used as a substrate for an assay of "ligninase" activity (30), by measurement of the absorbance due to veratraldehyde formed. [However, small amounts of  $\gamma$ -(5-membered) (23) and  $\sigma$ -(6-membered) lactones (24) are also produced from veratryl alcohol as ring cleavage products (Figure 5).]

As can also be seen, veratrylglycerol undergoes  $C\alpha$ - $C\beta$  bond cleavage, yielding veratraldehyde and glycolaldehyde in the presence of "ligninase"

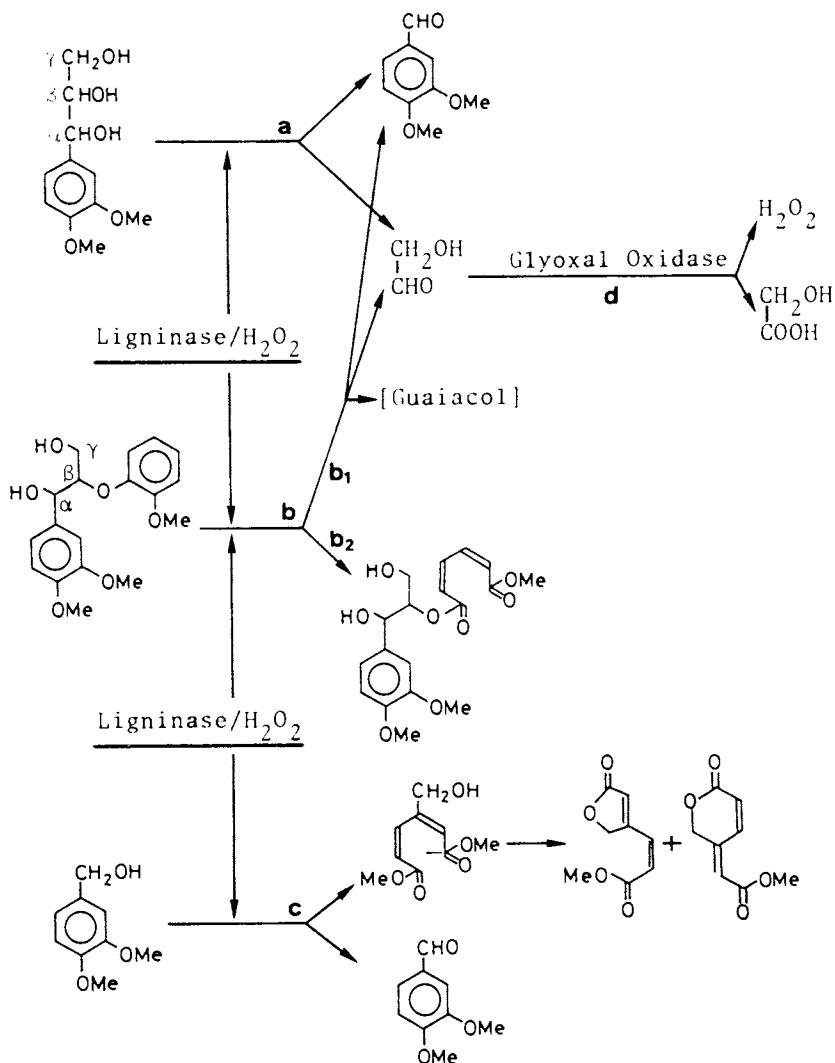


Figure 5. The enzymatic oxidation of a synthetic  $\beta$ -O-4 lignin model substrate and fungal secondary metabolites. Both undergo  $C\alpha$ - $C\beta$  bond and aromatic ring cleavages in reactions catalyzed by the same "ligninase" in the presence of H<sub>2</sub>O<sub>2</sub>.

and hydrogen peroxide (31). [Isolation of glycolaldehyde from the enzymic reaction mixture as its 2,4-dinitrophenylhydrazone derivative was achieved by treatment of the mixture with 2,4-dinitrophenylhydrazine at 30°C for 30 min.]

Oxidative degradation of the  $\beta$ -O-4 lignin substructure model compound (32), catalyzed by "ligninase"/H<sub>2</sub>O<sub>2</sub>, consists of two types of cleavage reactions (routes b1 and b2) (see Fig. 5). These correspond to C $\alpha$ -C $\beta$  bond cleavage (see route a) of veratrylglycerol and aromatic ring opening (see route c) of veratryl alcohol.

Thus, "ligninase" is shared by the three substrates of different origin: the synthetic lignin model substrate and the two natural metabolites of fungal origin. It can therefore be proposed that the biosynthetic pathway of veratryl alcohol (Figure 4) is linked to lignin degradation.

*Hydrogen Peroxide-Generating System.* Another important feature of this secondary metabolic pathway is the fact that glycolaldehyde is a required substrate for glyoxal oxidase (33), produced extracellularly by the same fungus to generate hydrogen peroxide required for lignin degradation (route d in Fig. 5). Interestingly, both veratrylglycerol and veratryl alcohol occur exclusively in the extracellular fluid of the fungal culture. Furthermore, formation of glyoxal, which is also found in the extracellular fraction of the culture, is a secondary metabolic event (33). We therefore suspect that glyoxal might be produced from glycolaldehyde, with the latter being formed by side-chain cleavage of both "endogenous" veratrylglycerol and "exogenous" lignin substrates.

Consequently, the extracellular oxidation of glycolaldehyde, derived from either the cinnamate pathway or side-chain cleavage of lignin, may function to support lignin degradation by producing H<sub>2</sub>O<sub>2</sub>, (route d in Fig. 5). This would then act in concert with other hydrogen peroxide-producing systems such as: (i) glyoxal/glyoxalase (33), (ii) glucose/glucose oxidase (34), (iii) NAD(P)H/peroxidase (35), and (iv) fatty acyl-coenzyme A oxidase (36).

### Physiological and Biochemical Relationships between Lignin Biodegradation and Veratryl Alcohol Biosynthesis

Parallel physiological and biochemical relationships between lignin biodegradation and veratryl alcohol biosynthesis are summarized below:

1. Both lignin biodegradation and veratryl alcohol biosynthesis are secondary metabolic events affected by several common physiological factors, such as oxygen tension, agitation, and nitrogen content (16,37-39). These C-, N-, and S-starvations are important triggers for in "ligninase" induction (37-39), since "ligninase" is produced constitutively regardless of the presence or absence of lignin as substrate.
2. Both processes are repressed by addition into the culture of nitrogen nutrients such as ammonium salts and L-glutamate (16, 37-39).
3. The level of cyclic AMP (cAMP) is increased by nitrogen starvation; this triggers expression of ligninolytic activity and veratryl alcohol biosynthesis (40).



4. Interestingly, peroxidase-less ( $PO^-$ ) mutants, which cannot decompose lignin nor biosynthesize veratryl alcohol (41,42), lack PAL activity (28).

However, there are two articles which report evidence against these relationships between biosynthesis of this secondary metabolite and lignin decomposition (43,44). For example, a mutant of *P. chrysosporium*, which does not produce veratryl alcohol, has ligninolytic activity (43). Another mutant, which lacks glucose oxidase, is unable to decompose lignin to  $CO_2$  and therefore is "ligninase"-less. It is, however, able to produce about 30% of the amount of veratryl alcohol normally found in the fungus (44).

These findings must be carefully interpreted. The veratryl alcohol negative mutant which has "ligninase" lacks PAL activity. Consequently, veratryl alcohol biosynthesis is shut down (Fig. 4). However, if veratryl alcohol or related aromatic compounds are added to the culture, they are decomposed to  $CO_2$  by the PAL-less mutant (42). For the glucose oxidase negative mutant, it may be that the mutant loses "ligninase" at the same time, and produces veratryl alcohol (to 30% of normal concentration) by an alternative pathway, e.g., by  $\beta$ -oxidation of 3,4-dimethoxycinnamic acid to veratric acid, which is then subsequently reduced to veratryl alcohol. Unfortunately, those authors did not examine the possibility of the absence of "ligninase" in the  $gox^-$  mutant. The "ligninase"-less and PAL-less mutant is, though, capable of converting exogenously added 3,4-dimethoxycinnamic acid and veratric acid to veratryl alcohol (28). This suggests that there is another route for the biosynthesis of veratryl alcohol, in addition to the veratryl-glycerol cleavage pathway already discussed (Fig. 4).

Taking these findings together, with the above-described parallelism and apparent contradictions, the following hypothesis is proposed. We suggest that the same key enzyme system, or "ligninase", couples the biosynthesis of veratryl alcohol and the biodegradation of lignin. It is also noteworthy that "ligninase" utilizes not only lignin, but a wide variety of xenobiotic compounds regardless of their chemical structures. Their ionization potentials are rather important for enzymatic oxidation (45). This is the reason why compounds such as benzo(a)pyrene (46), dioxin (47) and  $\alpha$ -keto- $\gamma$ -methylthiobutyric acid and dyes (48) are also oxidized by "ligninase."

### Concluding Remarks and Perspectives

In conclusion, focusing on the similarities and differences between white-rot and brown-rot fungi, these seemingly different biological processes can be explained as follows.

1. Both white-rot and brown-rot fungi have a common cinnamate pathway, initiated by PAL, which plays a key role in the biosynthesis of phenylpropanoids in basidiomycetous fungi. These fungi are able to convert glucose into "scavenged" metabolites under nitrogen-limiting conditions.
2. The phenylalanine-cinnamate pathway of the white-rot fungus *P. chrysosporium* is linked to lignin biodegradation by two reactions, i.e., by both  $C\alpha-C\beta$  bond and aromatic ring cleavages. These represent the

predominant features of lignin biodegradation, and therefore operate as part of the secondary metabolism of phenylalanine. Thus, during their biochemical evolution, the white-rot fungi have succeeded in adapting extracellular peroxidases to lignin breakdown, whereas the brown-rot fungi failed to develop such a biocatalyst or metabolic pathway. In contrast, higher plants might have created peroxidases for polymerizing hydroxycinnamyl alcohols to lignins during their biochemical evolution.

In closing, the recent advances in lignin biodegradation research are remarkable and are receiving widespread interest from many fields (49,50). At present, "ligninase" is known to catalyze a wide variety of one-electron oxidations, but it still cannot depolymerize the lignin *in vitro* (51,52). On the other hand, the white-rot fungi carry out an almost complete decomposition of lignin in wood in their natural environment. Thus, there may be another enzyme (or system) involved functioning as a depolymerizing factor coupled to lignin degradation. Further fundamental research is needed in order to elucidate the mechanism of whole wood decay processes, including the nitrogen recycling of amino acids involved in fungal secondary metabolism. Furthermore, biomimetic systems based on our understanding of the biochemistry of plants and fungi (53,54) may be more applicable for conversion of lignocellulosic materials.

### Literature Cited

1. Power, D. M.; Towers, G. H. N.; Neish, A. C. *Can. J. Biochem.* 1965, **43**, 1397.
2. Bandoni, R. J.; Moore, K.; Subba Rao, P. V.; Towers, G. H. N. *Phytochemistry* 1968, **7**, 205.
3. Vance, C. P.; Bandoni, R. J.; Towers, G. H. N. *Phytochemistry* 1975, **14**, 1513.
4. Hanson, K. R.; Havir, E. A. In *The Biochemistry of Plants*; Conn., E. E. Ed.; 1981, **7**, p. 577.
- 4a. Lundquist, K.; Kirk, T. K. *Phytochemistry* 1978, **17**, 1676.
5. Towers, G. H. N. *Phytochemistry*, 1973, **12**, 961.
6. Luckner, M. *Secondary Metabolism in Microorganisms, Plants, and Animals*; Springer-Verlag: Berlin, 1984, p. 407.
7. Wat, C.-K.; Towers, G. H. N. In *Recent Advances in Phytochemistry*; Swain, T.; Harborne, J. B.; Van Sumere, C. F., Eds.; Plenum: New York, 1979, **12**, 371.
8. Kirk, T. K.; Shimada, M. In *Biosynthesis and Biodegradation of Wood Components*; Higuchi, T., Ed.; Academic Press: Tokyo, 1985, p. 579.
9. Zahner, H.; Anke, H.; Anke, T. In *Secondary Metabolism and Differentiation in Fungi*; Bennet, J.; Ciegler, W., Eds.; Marcel Dekker: New York, 1983, p. 153.
10. Cowling, E. B.; Merrill, W. *Can. J. Bot.* 1966, **44**, 1539.
11. Birkinshaw, J. H.; Findlay, W. P. K. *Biochem. J.*; 1940, **34**, 82.
12. Wat, C. K.; Towers, G. H. N. *Phytochemistry* 1977, **16**, 290.
13. Shimazono, H.; Schmidt, W. J.; Nord, F. *J. Am. Chem. Soc.* 1958, **80**, 1992-94.

14. Towers, G. H. N. In *Perspectives in Phytochemistry*; Harborne, J. B.; Swain, T., Eds.; Academic: London, 1969; p. 179.
15. Ohta, A.; Shimada, M.; Hattori, T.; Higuchi, T.; Takahashi, M. *Proc. 38th Meet. J. Wood Res. Soc.* 1988; p. 200.
16. Shimada, M., Nakatsubo, F.; Kirk, T. K.; Higuchi, T. *Arch. Microbiol.* 1981, **129**, 321.
17. Kawai, S.; Umezawa, T.; Higuchi, T.; *Wood Research* 1984, **73**, 18.
18. Kirk, T. K. In *Lignin Biodegradation: Microbiology, Chemistry, and Potential Applications*; Kirk, T. K.; Higuchi, T. K.; Chang, H.-M., Eds.; CRC Press: Boca Raton, 1980; p. 51.
19. Shimada, M.; Nakatsubo, F.; Higuchi, T.; Kirk, T. K. *Proc. ISWPC (Ekman days)* 1981, p. 91.
20. Buswell, J. A.; Ander, P.; Petersson, B.; Eriksson, K.E. *FEBS Lett.* 1979, **103**, 98.
21. Yajima, Y.; Enoki, A.; Gold, M. H. *Arch. Microbiol.* 1979, **123**, 319.
22. Ander, P.; Hatakka, A.; Eriksson, K. E. *Arch. Microbiol.* 1980, **125**, 189.
23. Leisola, M. S. A.; Schmidt, B.; Thaney-Wyss, U.; Fiechter, A. *FEBS Lett.* 1985, **189**, 267.
24. Shimada, M.; Hattori, T.; Umezawa, T.; Higuchi, T.; Uzura, K. *FEBS Lett.* 1987, **221**, 327.
25. Shimazono, H. *Arch. Biochem. Biophys.* 1959, **83**, 206.
26. Wat, C.-H.; Towers, G. H. N. *Phytochemistry* 1975, **14**, 663.
27. Higuchi, T. *Biosynthesis and Biodegradation of Wood Components*; Academic: New York, 1985; p. 141.
28. Shimada, M. *Wood Res. Tech. Notes* 1983, **17**, 21.
29. Tai, D.; Terazawa, M.; Chen, C. L.; Chang, H. M.; Kirk, T. K. In *Recent Advances in Lignin Biodegradation*; Higuchi, T.; Chang, H.-M.; Kirk, T. K., Eds.; Uni: Tokyo, 1983; p. 44.
30. Tien, M.; Kirk, T. K.; Bull, C.; Fee, J. A. *J. Biol. Chem.* 1986, **261**, 1687.
31. Shimada, M.; Kurosaka, H.; Hattori, T.; Higuchi, T. *Proc. 38th Ann. Meet. Wood Res. Soc. Japan*; 1988, p. 100.
32. Umezawa, T.; Shimada, M.; Higuchi, T.; Kusai, K. *FEBS Lett.* 1986, **205**, 287.
33. Kersten, P. J.; Kirk, T. K. *J. Bacteriol.* 1987, **169**, 2195.
34. Kelley, R. L.; Reddy, C. A. *Arch. Microbiol.* 1986, **144**, 248.
35. Kuwahara, M.; Ishida, Y.; Miyagawa, Y.; Kawakami, C. F. *Ferment. Technol.* 1984, **62**, 237.
36. Green, R.; Gould, J. M. *Biochem. Biophys. Res. Commun.* 1984, **118**, 437.
37. Kirk, T. K. *Proc. ISWPC (Ekman Days)* 1981, **3**, 67.
38. Fenn, D.; Kirk, T. K. *Arch. Microbiol.* 1981, **130**, 59.
39. Fenn, D.; Kirk, T. K. *Arch. Microbiol.* 1981, **130**, 65.
40. MacDonald, M. J.; Paterson, A.; Broda, P. *J. Bacteriol.* 1984, **160**, 470.

41. Ander, P.; Hatakka, A.; Eriksson, K. E. *Arch. Microbiol.* 1980, **125**, 189.
42. Gold, M. H.; Mayfield, M. B.; Cheng, T. M.; Krisnangkura, K.; Shimada, M.; Enoki, A. *Arch. Microbiol.* 1982, **132**, 115.
43. Liwicki, R.; Patterson, A.; MacDonald, M. J.; Broda, P. *J. Bacteriol.* 1985, **162**, 641.
44. Ramasamy, K.; Kelley, R.L.; Reddy, C.A. *Biochem. Biophys. Res. Commun.* 1985, **131**, 436.
45. Kersten, P. J.; Kalyanaraman, B.; Hammel, K. E.; Kirk, T. K. In *Lignin Enzymic and Microbial Degradation*; Odier, E., Ed.; INRA Publ., 1987; p. 75.
46. Haemmerli, S. D.; Leisola, M. S. A.; Sanglard, D.; Fiechter, A. *J. Biol. Chem.* 1986, **261**, 6903.
47. Hammel, K. E.; Kalyanaraman, B.; Kirk, T. K. *J. Biol. Chem.* 1986, **261**, 16948.
48. Gold, M. H.; Glenn, J. K.; Mayfield, M. B.; Morgan, M. A.; Kutsuki, H. In *Recent Advances in Lignin Biodegradation*; Higuchi, T.; Kirk, T. K.; Chang, H.-M., Eds.; Uni: Tokyo, 1983; p. 219.
49. Odier, E. *Lignin Enzymic and Microbial Degradation*; INRA, 1987.
50. Buswell, J. A.; Odier, E. *CRC Crit. Rev. Biotechnol.* 1987, **6**, 1.
51. Haemmerli, S. D.; Leisola, M. S. A.; Fiechter, A. *FEMS Microbiol. Lett.* 1986, **35**, 33.
52. Kirk, T. K. *Proceedings Tappi Res. Dev.* 1986, p. 73.
53. Shimada, M.; Habe, T.; Higuchi, T.; Okamoto, T.; Panijpan, B. *Holz-forschung* 1987, **41**, 277.
54. Paszcynski, R.; Crawford, R. L.; Blanchette, R. A. *Appl. Environ. Microbiol.* 1988, **54**, 62.

RECEIVED May 19, 1989

## Chapter 31

# Ultrastructural Localization of Lignocellulose-Degrading Enzymes

I. M. Gallagher<sup>1</sup>, M. A. Fraser<sup>1</sup>, C. S. Evans<sup>1</sup>, P. T. Atkey<sup>2</sup>,  
and D. A. Wood<sup>2</sup>

<sup>1</sup>School of Biological Sciences, Thames Polytechnic, London SE18 6PF,  
England

<sup>2</sup>AFRC Institute of Horticultural Research, Littlehampton BN16 3PU,  
England

Transmission electron microscopy of immuno-gold labelled sections was used to show the localisation of the ligninolytic enzymes, lignin-peroxidase and laccase in ultrathin sections of hyphae of the white-rot fungus *Coriolum versicolor*. Both enzymes were localized in the fungal cell walls and mucilage layers of both generative and skeletal hyphae, whereas ligninase but not laccase was also evident adjacent to the plasma membrane. The localization of these enzymes was the same in hyphae grown in culture and in sections of beech heartwood infected with *C. versicolor*. Control experiments showed that no labelling was detected in the absence of primary antibodies, or when antibodies to animal or plant enzymes were substituted but antibodies to fungal proteins from different species were labelled in sections of *C. versicolor*. The source of antigenicity in these sections was investigated.

Basidiomycete fungi are the major organisms responsible for biodegradation of wood, with white-rot fungi able to degrade all components of the wood cell wall. Enzymes which partially degrade lignin, lignin-peroxidases, were first isolated from *Phanerochaete chrysosporium* (1-2) and more recently from other white-rot fungi including *Coriolum versicolor* (3). These enzymes appear to be similar in all white-rot fungi investigated, all containing a heme prosthetic group and requiring trace amounts of hydrogen peroxide to effect the breakdown of the lignin polymer (4-5). The polyphenol oxidase, laccase, produced as an extracellular enzyme by *C. versicolor*, has been well documented as a polymerizing enzyme but recent work has shown that under certain conditions it can also effect depolymerization of lignin (6-8).

0097-6156/89/0399-0426\$06.00/0

© 1989 American Chemical Society

Morphological data on the patterns of degradation of wood cell walls after infection by white-rot fungi showed that in addition to white-rots causing a localized degradation, characterized by a deep erosion trough in the secondary wall of the wood cell, a progressive thinning of the S2 layer of the secondary wall also occurred (9-12). Identification of osmiophilic particles in sections of decaying wood led to tentative suggestions that these were either enzyme molecules involved in wood decay or the products of lignocellulosic degradation (12-13). Studies of the biochemical mechanism of lignin-peroxidase have suggested that it is not always essential that the enzyme should be in direct contact with its substrate to effect lignin breakdown. The release of diffusible radical cations in phenolic substrates can enable degradation of the lignin polymer to proceed at some distance from the enzyme, and fungal hypha (14).

White-rot fungi secrete a polysaccharide mucilage around the hyphae which may function as a matrix for enzyme immobilization and enable products of reactions to be retained close to the hyphae for absorption (15; Evans, C. S., unpublished data). Recently, significant advances were made in the field of immuno-labelling with electron microscopy as a method of localizing proteins and other molecules within tissue sections, using colloidal gold as a marker of antibody-antigen interactions (16). In order to identify the site of action of lignin-degrading enzymes in wood decay, colloidal gold immunolocalization procedures were used to locate the extracellular enzymes, laccase and lignin-peroxidase, from the white-rot fungus *C. versicolor* cultured in beech heartwood and in malt agar.

## Methods

*Organism.* *Coriolus versicolor* strain 28A PRL (Building Research Establishment, Princes Risborough Laboratory, Aylesbury, Bucks., U.K.) was maintained on a solid medium of 3% (w/v) malt extract, 2% (w/v) agar at 20°C, or on nitrogen-limited nutrient medium (17) solidified with 2% agar.

*Growth of C. versicolor on Wood.* Samples of beech heartwood (*Fagus sylvatica*) were added to culture plates of *C. versicolor* after 7d. growth, using the Bravery miniature woodblock technique (12). Plate cultures were covered with a 1mm mesh 60mm diameter sterile nylon net. Sterile sections of beech (30 × 10 × 3mm) were placed aseptically onto the net and cultured at 20°C for 4 weeks. The external growth of mycelium was removed and the wood block cut into segments of approximately 3 × 1 × 1mm for preparation for electron microscopy. Uninfected wood samples were prepared in a similar manner.

*Immunogold Labelling.* Tissues were fixed in excess glutaraldehyde (2.5% w/v) in 100mM sodium cacodylate buffer (pH 7.2) for 3h, washed twice in the same buffer, followed by dehydration in a graded ethanol series. Samples were infiltrated with L. R. White hard grade resin (London Resin Co. Ltd). Thin sections were cut with an LKB Ultramicrotome II using a diamond knife and collected on copper grids (200 mesh). The immunogold labelling procedure followed the technique of Bergman (18). Sections were

etched in 5%  $H_2O_2$  for 5-10 min, washed twice in PBS (20mM phosphate buffer at pH 7.4 and 0.9% NaCl) containing 0.1% Tween 20, incubated for 1h in rabbit anti-laccase antiserum or rabbit anti-ligninase antiserum, diluted 1:100 (v/v) in PBS containing 0.1% Tween 20 and 1% bovine serum albumen (BSA), washed twice in PBS containing 0.1% Tween 20, incubated for 1h in goat anti-rabbit IgG conjugated to 10nm gold particles (Sigma), diluted 1:20 in PBS containing 1% BSA and 0.1% Tween 20, washed twice in distilled water and air dried.

*Post-staining Procedure.* Immunogold labelled sections were post-stained in saturated aqueous uranyl acetate for 15 min and lead citrate for 10 min (19).

*Transmission Electron Microscopy.* Transmission electron microscopy was performed on a Jeol 100S electron microscope operating at 80kV.

*Production of Antibodies.* Laccase A was isolated from cultures of *C. versicolor* and purified by a modified procedure of Fahraeus and Reinhammer (20). The criterion for purity was a single band on a heavily loaded SDS-polyacrylamide electrophoresis gel. Antibodies were raised in rabbits in response to three intravenous injections each of 2mg. of laccase A with Freund's adjuvant, at 2 weekly intervals. Blood was removed 7d after the last injection and serum collected after coagulation of the blood cells.

The antibody to laccase A was purified by affinity chromatography on CN-Br activated Sepharose 4B. Laccase (15mg) was bound to a column of 3.5ml volume in a coupling buffer of 0.1M  $NaHCO_3$  and 0.5M NaCl. The remaining active groups on the column were blocked with 0.2M glycine, before excess adsorbed protein was removed with the coupling buffer, resulting in 95% coupling of the laccase to the column. Crude antisera was bound to the laccase on the column, washed with buffer of 0.1M  $Na_2HPO_4$  and 0.5M NaCl, before elution with 0.2M glycine-HCl and 0.5M NaCl. The purified antibody was used as the primary antibody to laccase A.

Lignin-peroxidase, which oxidised veratryl alcohol to veratraldehyde, was isolated from cultures of *Phanerochaete chrysosporium* by the method of Tien and Kirk (1). It had a molecular weight of 44Kd on polyacrylamide gels, in the presence of sodium dodecyl sulphate. Antibodies to lignin-peroxidase were raised in rabbits as described for laccase A.

## Results

The titre of antibodies in laccase antisera was 1:16 as measured by the immunodiffusion technique of Ouchterlony (21). These antibodies were effective inhibitors of catechol oxidase activity, with 100 $\mu$ l of antisera reducing activity by 95%, in an assay mixture of 3ml of 0.1M catechol in 0.1M acetate buffer at pH 5 as described by Evans (7). Table I shows the effect of adding different volumes of antisera to the assay mixture.

Inhibition of enzyme activity was not used to assess the antibody-antigen reaction of lignin-peroxidase, as the addition of control serum to enzyme reaction mixtures increased the pH above the pH specificity of the

Table I. The effect of laccase antiserum on enzyme activity. The reaction mixture contained 3ml of 0.1M catechol in 0.1M acetate buffer at pH 5, 5 $\mu$ g laccase and 0-100 $\mu$ l of serum

Volume of antisera ( $\mu$ l) added:	0	10	20	50	100
Laccase activity (OD <sub>440</sub> catechol oxidation min <sup>-1</sup> )	0.21	0.18	0.15	0.04	0.02

enzyme, which has an optimum at pH 2.9 and is inhibited above pH 4 (4). Cross reactivity between antibody and antigen was measured by immunoprecipitation at a dilution of 1:16 of antiserum (21). Both antibodies showed specificity in reacting with their respective antigens as determined by Western blotting. The distribution of laccase in hyphae of *C. versicolor* grown in beech heartwood for 4 weeks was compared with that of hyphae cultured on malt agar. Both cultures gave positive tests for laccase when treated with guaiacol, producing yellow/brown colorations (22). Sections of hyphae from both agar and wood cultures of *C. versicolor* were treated with either laccase antiserum or purified laccase IgG. No difference in the pattern of labelling was observed when crude antisera was used compared with purified IgG. Figure 1 showed that hyphae grown on malt agar had labelling which was restricted to the hyphal cell wall and mucilage layer, with little cytoplasmic labelling and a very low level of background labelling. There was no label associated with the plasma membrane as seen in Figure 2, and the major site of labelling was the cell wall (in most sections the thickness of the mucilage was so small as to be indistinguishable from the cell wall). Hyphae in sections of infected wood showed similar morphology to that of hyphae grown on agar. A similar pattern of labelling was also observed, with most gold particles attached to the cell wall and mucilage layers and minimal labelling in the cytoplasm (Figures 3 and 4). At higher magnification it was seen that mucilage separated from the hyphal wall was also labelled, as was the secondary wall of the wood cell wall. There was a moderate level of label in the S2 wall layer whereas the middle lamella and decayed margins of the wall were not labelled. Sections of uninfected beech heartwood showed no background labelling of cell walls indicating that there was no non-specific binding of the laccase antibody to wood cell wall components (Fig. 5).

Sections of *C. versicolor* hyphae grown on N-limited nutrient agar were also treated with antibodies to lignin-peroxidase purified from *P. chrysosporium*. Cross reactive material was detected in the cell wall and mucilage of the hyphae as shown in Figure 6. There was a considerably lower level of labelling in the cytoplasm. The label within the wall of generative hyphae was localized into two distinct layers which was especially obvious in the thickened wall and mucilage layer, as shown in Figure 7. This double layer of lignin-peroxidase was situated adjacent to the plasma membrane and on the outer surface of the wall within the mucilage layer (Figure 8). In the skeletal hyphae there was intense labelling of the thicker cell wall



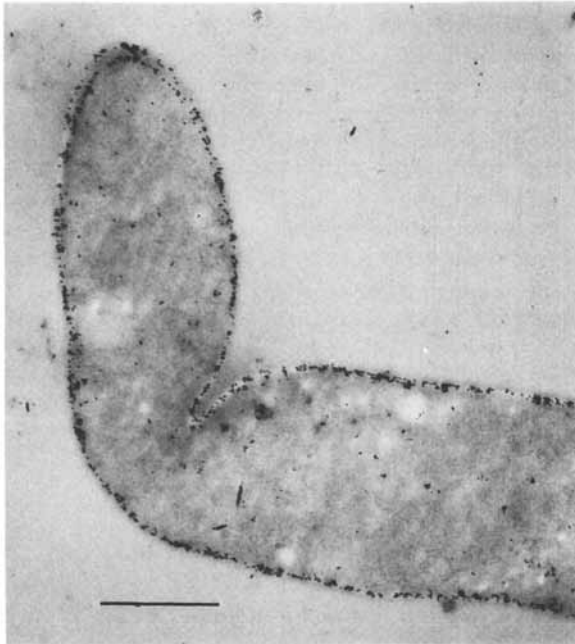


Figure 1. Single hypha of *C. versicolor* grown on malt agar, labelled with rabbit anti-laccase antibodies, localized with goat-antirabbit gold conjugate. The label is restricted to the hyphal wall, with little label in the cytoplasm. Magnification x 16,000.

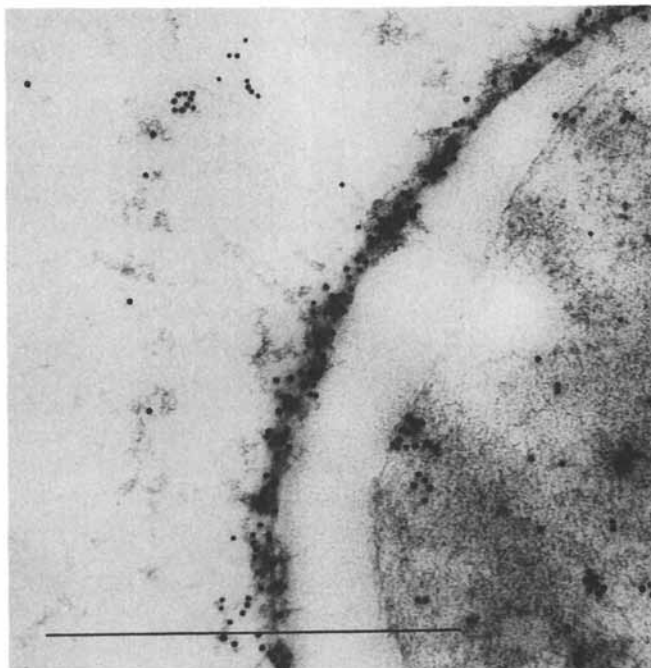


Figure 2. Higher magnification of laccase-labelling in the hyphal wall and mucilage layer. No label is seen on the plasma membrane or within the cytoplasm. Magnification x 59,500.

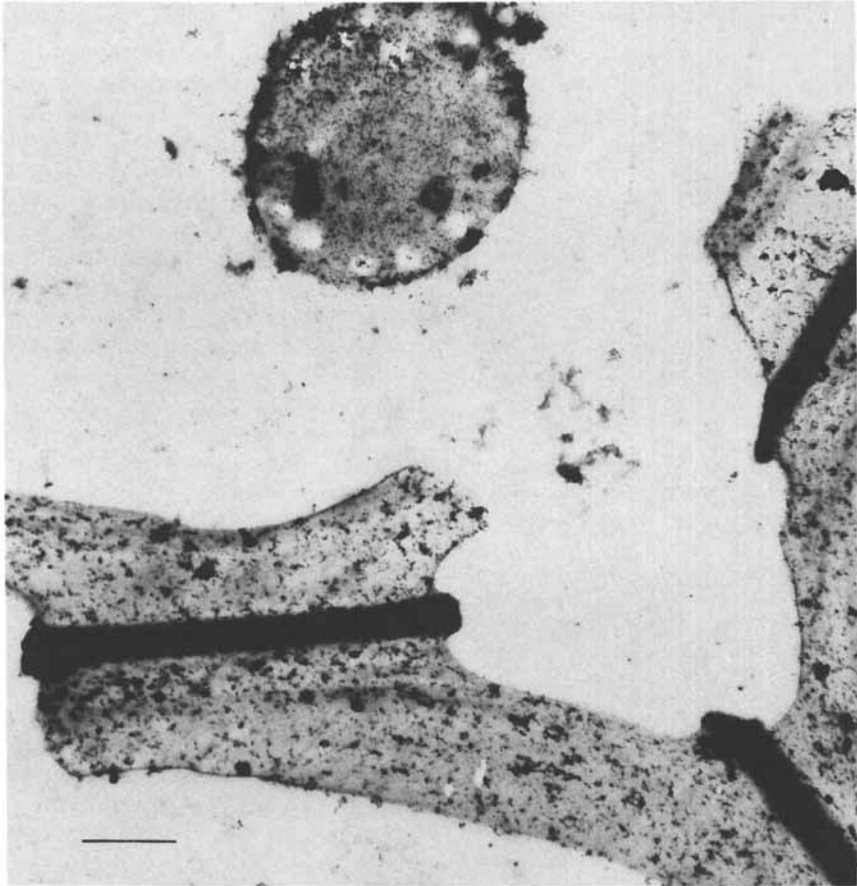


Figure 3. Beech heartwood, decayed for 4 weeks with *C. versicolor*, showing thinning of the secondary wall with enlargement of the cavity at the cell corner (the protruding ends of the middle lamella can be seen). A single hypha close to the wood cell wall shows where the secondary wall has been degraded. Label for laccase is seen uniformly distributed in the secondary wall. Magnification x 12,600.

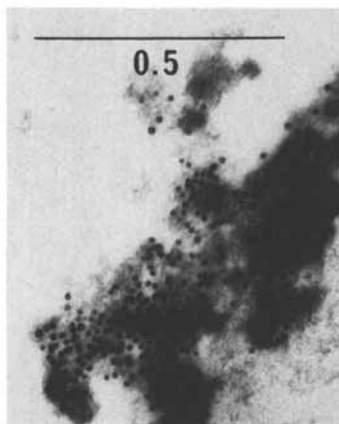


Figure 4. Higher magnification of hyphal wall in Figure 3 showing intense labelling of the wall and mucilage layer. Magnification x 66,500.



Figure 5. A single hypha from an agar grown culture of *C. versicolor* showing an absence of label after replacing primary antisera with rabbit IgG globulin. Magnification x 19,800.

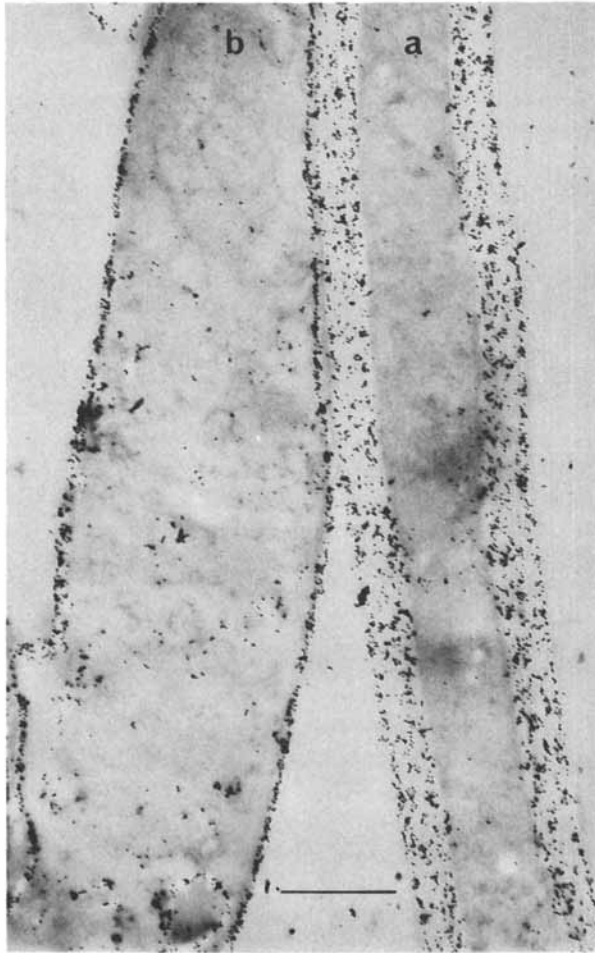


Figure 6. Hyphae from N-limited nutrient agar grown cultures of *C. versicolor* showing (a) a thick walled skeletal hypha and (b) a thin walled generative hypha labelled for lignin-peroxidase. Label is seen throughout the hyphal walls with little labelling in the cytoplasm. Magnification x 15,700.

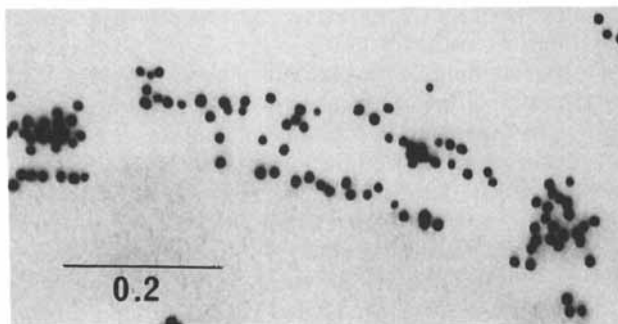


Figure 7. Higher magnification of generative hyphal walls from N-limited nutrient agar grown cultures labeled for lignin-peroxidase. Double layer of label on both margins of the hyphal wall. Magnification  $\times 11,000$ .

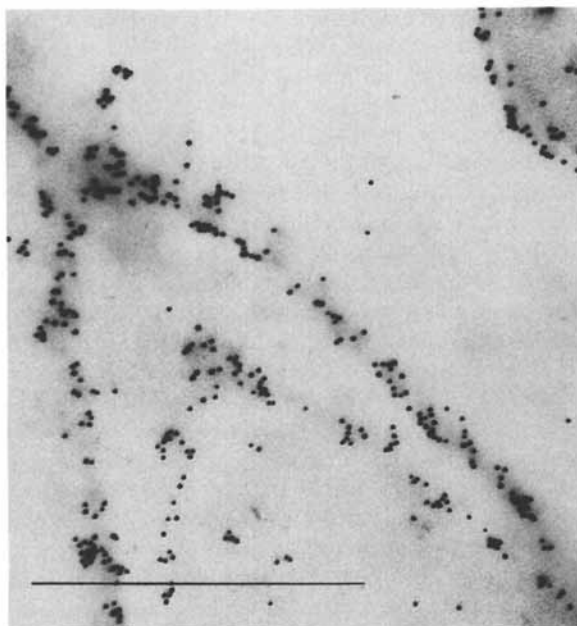


Figure 8. Higher magnification of generative hyphal walls from N-limited nutrient agar grown cultures labeled for lignin-peroxidase. Label on the hyphal tip where a thickening of the wall and mucilage form a "cap" at the tip. Magnification  $\times 44,000$ .

with virtually no labelling of the cytoplasm, or of the mucilage surrounding the wall. The difference in pattern, and in the degree of labelling of lignin-peroxidase in sections of generative and skeletal hyphae are presumably due to the difference in thickness of the wall. Hyphae grown on malt agar showed similar labelling of the plasma membrane with lignin-peroxidase antisera, though labelling of the cell wall was at a lower intensity than that seen in hyphae cultured on N-limited nutrient agar.

Sections of decayed and undecayed beech heartwood were also treated with lignin-peroxidase antibodies. Figure 9 shows that the labelling of decayed wood was far more intense than that seen in sections treated with laccase antibodies with the label uniformly distributed throughout the S2 cell wall layer. Little labelling of the S1 layer or middle lamella was observed. On sections of undecayed wood there was only a very slight amount of background label on the cell walls indicating that there was little non-specific binding to cell wall components, as seen in Figure 10. In preliminary experiments dilutions of 1/100 of both antisera were found to give the clearest results with minimum background labelling yet showing the highest intensity of specific labelling. Lower dilutions gave less specific labelling, whereas higher dilutions gave more non-specific labelling. Control experiments to assess the specificity of the labelling were performed by variations in the procedure. For example, when the primary antibody was omitted no labelling was observed, indicating that there was no non-specific binding of goat anti-rabbit IgG-gold conjugate to the sections. When rabbit IgG immunoglobulin was used to replace the primary antibody, again no labelling was seen indicating that non-specific binding of immunoglobulins to sections was not responsible for labelling in either hyphae or decayed wood cell walls. Similarly no labelling was observed when the primary antibody was replaced with antisera to plant phytochrome (Figure 11). When the primary antibody was replaced with antisera to laccase isolated from *Agaricus bisporus* grown in malt extract cultures, the labelling pattern observed was identical to that seen with the primary antibody to laccase from *C. versicolor* (Fig. 12). This suggests that laccase from *A. bisporus* has similar antigenic sites to laccase from *C. versicolor*. When the primary antibody was replaced with antisera raised against the enzyme mannitol dehydrogenase, a cytoplasmic enzyme from *Agaricus bisporus*, slight labelling was observed on sections of the hyphae, associated with both the wall and cytoplasm, an observation which is difficult to explain as mannitol dehydrogenase is a cytoplasmic enzyme in *A. bisporus*, not extracellular. When sections of beech wood were treated with antisera to mannitol dehydrogenase no labelling of the wood cell walls occurred. This indicated that non-specific binding was not taking place.

## Discussion

Transmission electron microscopy of immunogold labelled sections has shown that the extracellular lignin-degrading enzymes lignin-peroxidase and laccase were localized within the cell wall and mucilage of the hyphae of *C. versicolor*. Laccase was present in the cell wall layer whereas lignin-

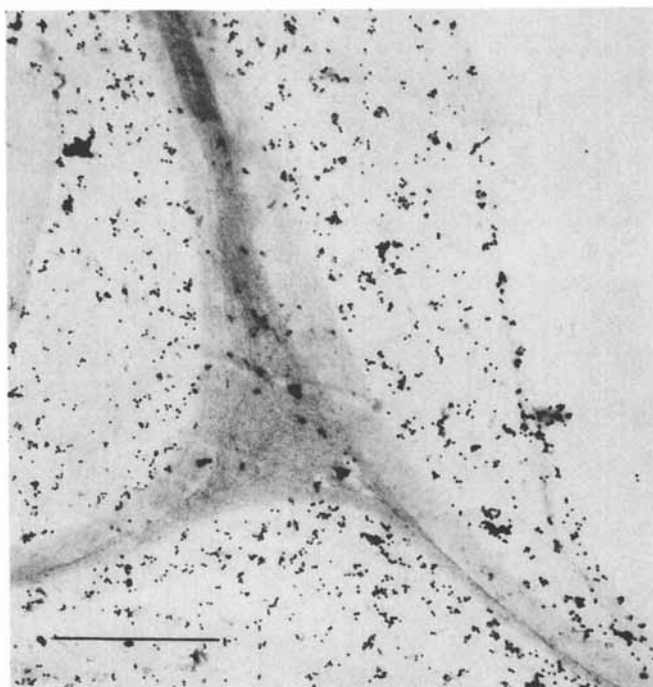


Figure 9. Beech heartwood decayed for 12 weeks with *C. versicolor* labelled for lignin-peroxidase. The label is distributed uniformly over the secondary wall which shows characteristic thinning and marked reduction in electron density. No label occurs in the middle lamella and cell corners. Magnification x 22,000.



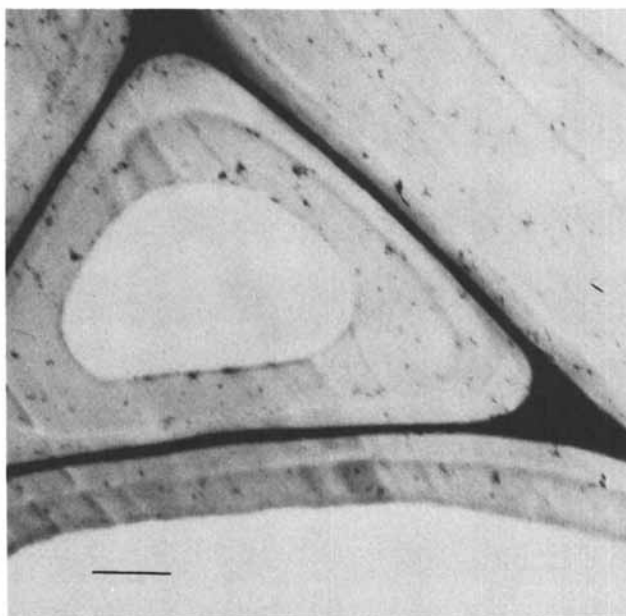


Figure 10. Undecayed beech heartwood labelled for lignin-peroxidase, with very little label on the secondary wall or middle lamella. Magnification x 9,800.

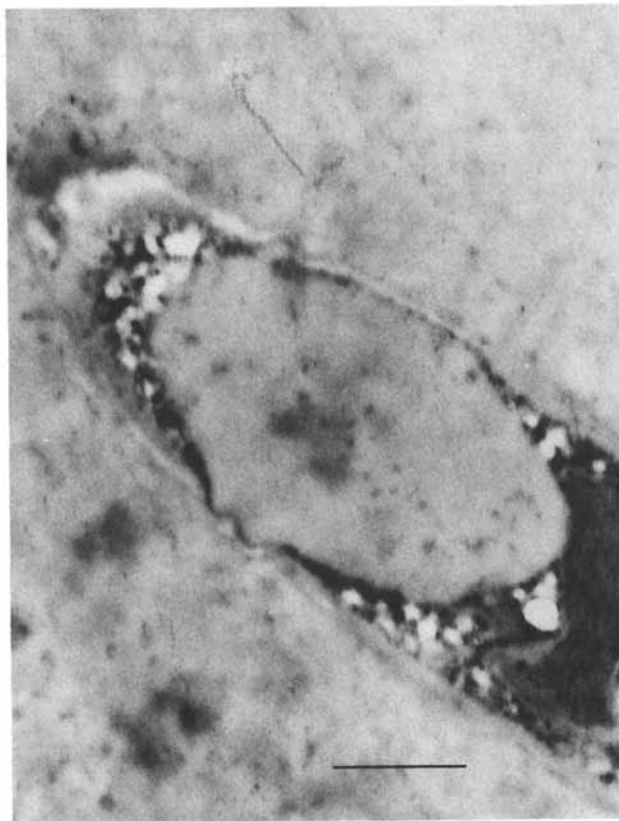


Figure 11. A single hypha from an agar grown culture of *C. versicolor* showing an absence of label after replacing primary antisera with antisera to plant phytochrome. Magnification x 17,400.

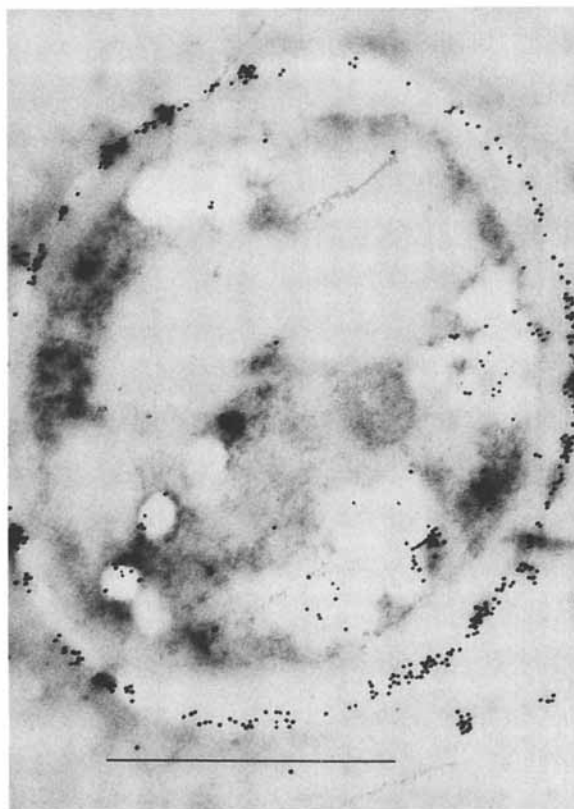


Figure 12. A single hypha from an agar grown culture of *C. versicolor* showing labeling when the primary antisera was replaced with antisera to laccase from malt agar cultures of *Agaricus bisporus*. Magnification  $\times 37,800$ . All bars, 1  $\mu\text{m}$ . All tissue was unstained and consequently of low contrast.

peroxidase was visualised as a double layer on the cell wall and adjacent to the plasma membrane. Both enzymes were localized within the S2 layer of the secondary wall of beech heartwood infected with *C. versicolor*. Penetration of the cell walls of wood was more pronounced for lignin-peroxidase than for laccase but neither enzyme had penetrated to the middle lamella or cell corners. The wood sections were significantly degraded and it is not known whether the diffusion of enzymes into the secondary wall occurred after widespread degradation of the lignocellulose or preceded secondary wall thinning. Other workers (23,24) have found that in *P. chrysosporium*, lignin-peroxidase was present as a cytoplasmic enzyme associated mainly with the plasma membrane in hyphae grown in sawdust and liquid culture. Garcia *et al.* (23) did not find the enzyme localised within the wood cell wall, whereas Srebotnik *et al.* (24) showed ligninase was detected extracellularly after fixation in picric acid. It is known that secretion of lignin-peroxidase only occurs during the secondary metabolic phase of growth in liquid cultures (25) and it is probable that this also occurs in wood. In our experiments, beechwood infected by *C. versicolor* showed decay patterns typical of advanced stages of fungal infection which would imply that the secondary metabolic phase had been reached. Further studies are required on the continuous degradation patterns resulting from fungal infections of wood to explain all these results.

The results of the control experiments with antisera to fungal proteins have led us to question the specificity of the antibodies to laccase and lignin-peroxidase. These enzymes are glycoproteins and both carbohydrate and protein moieties will provide antigenic sites for the polyclonal antibodies. However, using Western blotting techniques, the laccase antisera did not cross-react with lignin-peroxidase, nor did the lignin-peroxidase antisera cross-react with laccase. It is likely that as extracellular fungal proteins are secreted through the mucilage-polysaccharide layer around the hyphae the carbohydrate moieties of these glycoproteins have carbohydrate structures in common with the hyphal wall layer. This may explain why all the antibodies to fungal proteins which were tested produced labelling patterns in the wall, as some of the antigens would bind to carbohydrate characteristic of fungal cell walls. Unless deglycosylated proteins are used to raise antibodies the labelling patterns obtained do not indicate specifically the location of the protein moiety. However, this study has shown that all the fungal tissues tested have a common antigen which is not shared by the plant and animal tissues tested. In order to understand the labelling patterns of laccase and lignin-peroxidase more fully, it will be necessary to study the apoenzymes separated from carbohydrate before conclusions can be drawn about their distribution in hyphae during primary and secondary growth phases in natural substrates.

### Acknowledgments

We thank the following for gifts of antisera: Dr. B. Z. Chowdhry for IgG globulin, Dr. J. B. W. Hammond for mannitol dehydrogenase antisera, Dr. B. Thomas for plant phytochrome antisera. We thank SERC (UK) for the award of a postgraduate studentship.

## Literature Cited

1. Tien, M.; Kirk, T. K. *Science* 1983, **221**, 7-12.
2. Kuwahara, M.; Glenn, J. K.; Morgan, M. A.; Gold, M. H. *FEBS Letts.* 1984, **169**, 247-250.
3. Dodson, P. J.; Evans, C. S.; Harvey, P. J.; Palmer, J. M. *FEMS Micro. Letts.* 1987, **42**, 17-22.
4. Schoemaker, H. E.; Harvey, P. J.; Bowen, R. M.; Palmer, J. M. *FEBS Letts.* 1985, **183**, 7-12.
5. Kersten, P. J.; Tien, M.; Kalyanaran, B.; Kirk, T. K. *J. Biol. Chem.* 1985, **260**, 2609-2612.
6. Bollag, J. M.; Leonowicz, A. *Appl. Environ. Micro.* 1984, **48**, 647-653.
7. Evans, C.S. *FEMS Micro Letts.* 1985, **27**, 339-343.
8. Kawai, S.; Umezawa, T.; Higuchi, T. *FEBS Letts.* 1987, **210**, 61-65.
9. Blanchette, R.A. *Can. J. Bot.* 1980, 1496-1500.
10. Blanchette, R. A. *Appl. Environ. Micro.* 1984, **48**, 647-653.
11. Otjen, L.; Blanchette, R. *Appl. Environ. Micro.* 1985, **50**, 568-572.
12. Messner, K.; Stachelberger, H. *Trans. Brit. Mycol. Soc.* 1984, **83**, 209-216.
13. Messner, K.; Foisner, R.; Stachelberger, H.; Rohr, M. *Trans. Brit. Mycol. Soc.* 1985, **84**, 457-466.
14. Harvey, P. J.; Schoemaker, H. E.; Palmer, J. M. *FEBS Letts.* 1986, **195**, 242-246.
15. Montgomery, R. A. P. In *Decomposer Basidiomycetes*; Frankland; Hedger; Swift, Eds.; Cambridge Univ. Press: 1982; **3**, 51-65.
16. Horisberger, M. In *Scanning Electron Microscopy*; Johari, O., Ed.; 1981, **2**, 9-13.
17. Kirk, T. K.; Schultz, E.; Connors, W. J.; Lorenz, L.F.; Zeikus, J. G. *Arch. Micro.* 1978, **117**, 277-285.
18. Bergman, B.; Lindblad, P.; Pettersson, A.; Renstrom, E.; Tiberg, E. *Planta* 1985, **166**, 329-332.
19. Reynolds, E. S. *J. Cell Biol.* 1968, **17**, 208-212.
20. Fahraeus, G.; Reinhammer, B. *Acta Chem. Scand.* 1967, **21**, 2367-2378.
21. Ouchterlony, O. *Acta Path. Microbiol. Scand.* 1949, **26**, 507-515.
22. Westermarck, U.; Eriksson, K. E. *Acta Chem. Scand.* 1974, **B28**, 204-208.
23. Garcia, S.; Latge, J. P.; Prevost, M. C.; Leisola, M. *Appl. Environ. Micro.* 1987, **53**, 2384-2387.
24. Srebotnik, E.; Messner, K.; Foisner, R.; Pettersson, B. *Curr. Micro.* 1988, **16**, 221-227.
25. Keyser, P.; Kirk, T. K.; Zeikus, J. G. *J. Bact.* 1978, **135**, 790-797.

RECEIVED May 19, 1989

## Chapter 32

# Enzyme Excretion During Wood Cell Wall Degradation by *Phanerochaete chrysosporium*

Jean-Paul Joseleau and Katia Ruel

Centre de Recherches sur les Macromolécules Végétales,  
CERMAV—CNRS, B.P. 53X 38041, Grenoble Cedex, France

Wood degradation by *Phanerochaete chrysosporium*, with the hyphae in contact with, or at a distance from the host cell walls, was examined by electron microscopy with immunocytochemical techniques. An anti-ligninase antibody and antiserum raised against a mixture of cellulases and hemicellulases secreted from the fungus were used. The respective enzymes were localized in intracellular vesicles and seemed to be able to diffuse from the hyphae only when at a short distance from the site of degradation. When excreted from the hyphae the enzymes seemed to be associated with the 1-3, 1-6  $\beta$ -glucan which forms the sheath secreted during secondary growth of the fungus. The limited distance of migration of the enzymes suggested that a direct contact is needed between the wood and the fungal walls for degradation to occur. The propagation of the degradation might take place by an oxygen radical mechanism as revealed by the use of a specific cytochemical method.

Among wood-rotting fungi the basidiomycete *Phanerochaete chrysosporium* is able to degrade both lignin and polysaccharides from wood cell walls (1). Examination of white-rot decayed wood at the ultrastructural level reveals that several types of degradation can occur (2,3). In the case of *P. chrysosporium* and its anamorphous form (*Sporotrichum pulverulentum*), two patterns of attack were observed (4). In one, the hyphae were tightly associated with the degraded walls and this type of image can be said to be "in contact" (Fig. 1A). In the second case, the secondary wall was degraded but no hyphae could be observed in the nearby surroundings. This type of degradation can be described as "at a distance" (Fig. 1B) (4). These two extreme aspects of lysis of wood cell walls suggest that *P. chrysosporium* can degrade the lignocellulosic complex of the wall by at least two

0097-6156/89/0399-0443\$06.00/0

© 1989 American Chemical Society

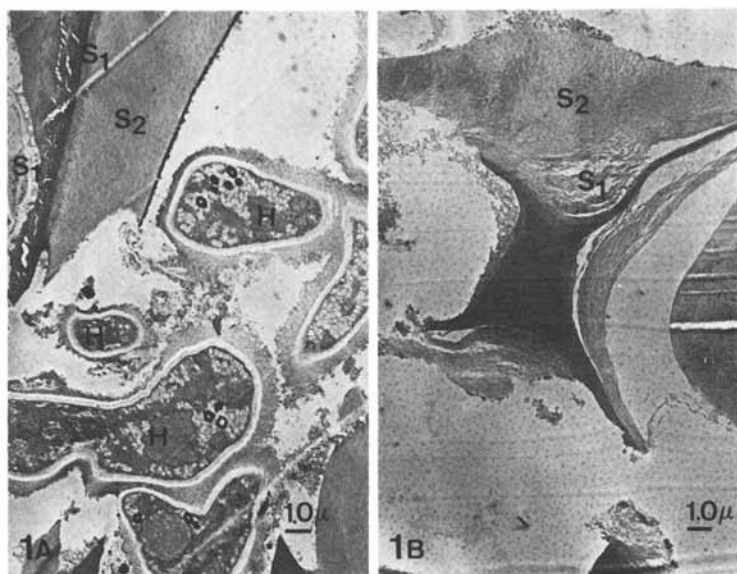


Figure 1. Two extreme aspects of *Populus* cell wall degradation by *P. chrysosporium*. 1A, "in contact;" 1B, "at a distance." (H = hypha; S<sub>1</sub>, S<sub>2</sub> = wood secondary wall layers.)

different biochemical mechanisms. Classically, biodegradation of cellulose and hemicellulose is ascribed to cellulolytic and hemicellulolytic enzymes of the fungus and lignin breakdown is attributed to the oxidative degradation by lignin-peroxidases (5,7). All these enzymes have been shown to be produced by *P. chrysosporium* in varying proportions, depending on growth conditions (8). Their release by the hyphae at the site of the attack should agree with the pattern of wood degradation said to be "in contact." However, it is far more difficult to explain the pattern described as "at a distance," since in this mode of degradation the lytic enzymes need to be first transported from the fungal hyphae to the wood cell walls. They must then diffuse within the wall, in order to effect a partial and local breakdown of the polysaccharides and of lignin. Such enzyme diffusion in the compact structure of the wood cell wall has never been demonstrated, and does not seem compatible with the relatively large size of these hydrolytic and oxidative enzymes. Another possibility which could explain the partial degradation of the wall would be the involvement of non-enzymatic diffusible agents of small size, which could be generated at a certain phase of the hyphal growth, or at a certain stage of biochemical attack. In this respect, activated oxygen species have been postulated as potent degradative extracellular agents, which could be produced by the fungus (9-11).

This chapter describes the use of electron microscopy, coupled with immunocytochemical techniques, to investigate the ability of lignolytic enzymes from *P. chrysosporium* to diffuse inside the wood cell wall.

## Materials and Methods

*Plant Material.* Wood samples were taken from a 20-year-old aspen tree (*Populus tremula*) harvested in France. Wood wafers (4 × 20 × 50 mm) were degraded by the wild type strain K3 of the white rot fungus *P. chrysosporium* at the STFI (Stockholm, Sweden) in the laboratory of Dr. K.-E. Eriksson.

*Preparation of Antisera.* Antisera directed against the crude enzymes mixture secreted by *P. chrysosporium* and cultivated in a fermentor on cellulose, were raised in rabbits. Immunoglobulins G (=IgG) were purified at the Institute Pasteur (Lyon) and used for immunolabeling. Secondary goat antirabbit gold marker was from Sigma. The anti-ligninase antiserum was raised in rabbit from a purified ligninase (gift of Dr. E. Odier, INA, Paris-Grignon, France).

*Tissue Preparation for Electron Microscopy.* Tissues were fixed in 2% paraformaldehyde, 2.5% glutaraldehyde in phosphate buffer (0.1 M, pH 7.4) and 0.02% picric acid. They were then dehydrated in glycol methacrylate monomer and embedded in glycol methacrylate (GMA) (24).

*Immunocytochemical Labeling.* Antibodies were used as post-embedding markers. Sections of decayed wood were first incubated on a drop of TBS (Tris-phosphate saline buffer 0.1 M, pH 7.4, NaCl 0.15 M or 0.5 M), glycine 0.15 M. After rinsing in TBS, they were floated on a drop of 1% TBS-BSA (bovine serum albumin) (or non-immune goat serum) before treating



either with IgG anti-crude enzymes (19 $\mu$ g/ml diluted in TBS-BSA) (or TBS/normal goat serum = TBS/NGS), or anti-ligninase antiserum diluted 1:250 in the same buffer, for 60 min at room temperature. The secondary antisera labeled with gold (10 nm in diameter) was a goat antirabbit antisera purchased from Janssen (Pharmaceutica, Beerse, Belgium). It was diluted 1:30 in TBS/NGS. The sections were examined on a Philips 400 T electron microscope without any counterstaining.

#### *Immunocytochemical Controls.*

- a. Substitution of the primary antibody with preimmune rabbit serum IgG fraction.
- b. Treatment of section with goat-antirabbit gold-labelled secondary antibody alone, omitting the primary antibody step.
- c. Labeling with antisera preadsorbed with their respective antigens. Equal volumes of anti-crude enzymes and of the enzymatic extract, or, anti-ligninase and pure ligninase, were incubated 1 h before use.

*Carbonyl Groups Labeling.* This was done under the usual conditions of PATAg staining (periodic acid, thiocarbohydrazide, silver proteinate) reactions (2) omitting the periodate oxidation step (= TAG), as described in (21). Fenton's reagent was prepared and applied as described in (18).

## Results and Discussion

*"Diffusion" of the Fungal Glycohydrolases.* A crude enzyme mixture from *P. chrysosporium* was obtained by ammonium sulfate precipitation from a culture grown on cellulose and maintained in primary growth conditions. This enzyme mixture, which was used for preparing a polyclonal antiserum, contained *inter alia* predominantly endo- and exoglucanases, with only traces of hemicellulases as evidenced by their action on the corresponding substrates. No lignin peroxidase activity could be detected (K.-E. Eriksson, personal communication). The immunoglobulins (IgG) raised in rabbit were first used to detect the site of secretion of the enzymes in the fungal cells. The primary antibodies were localized with a goat antirabbit secondary antibody adsorbed to colloidal gold. The diameter of gold particles was 10 nm.

Controls with the anti-glycohydrolases IgG, first incubated with the enzymic extract before being applied in thin sections, showed no labeling (Fig. 2B). Other controls performed, i.e., replacement of the primary antibody by normal rabbit serum or preimmune serum, suppression of the first step corresponding to the primary antibody, or labeling of uninfected wood specimen, were also negative.

The hyphae photographed in a highly decayed wood exhibited several aspects of their cytoplasmic content. The localization of the glycohydrolases varied accordingly as shown in Figure 2. In Figure 2A, they are localized intracellularly in small dense vesicles (arrows). In Figure 2C they appeared concentrated along the plasmalemma and dispersed through the cytoplasm (arrows). In Figure 3A, they have been secreted out of the hypha (arrows). These observations of the presence of an intracellular cellulolytic activity

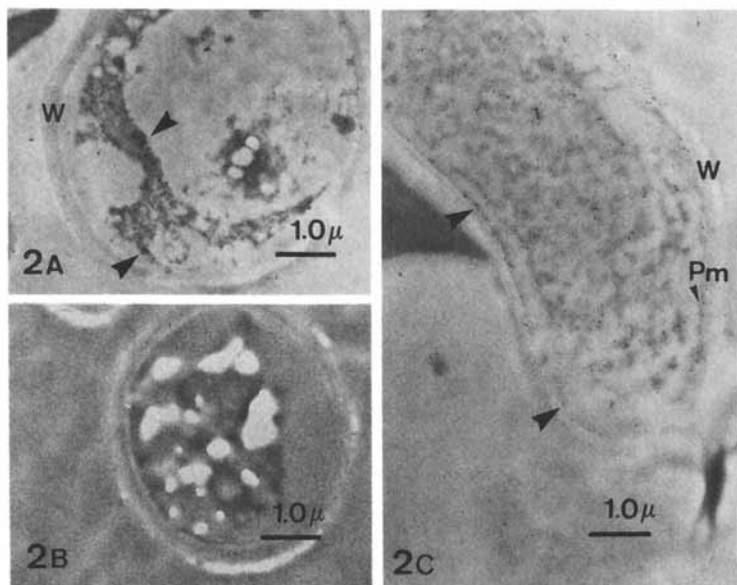


Figure 2. Labeling with anti-crude enzyme mixture. A and B show the specificity of the antibodies compared to the preimmune-treated control; C, plasmatic and cytoplasmic localization of the enzymes. No labeling in the fungal wall. (Pm, plasmalemma; W, hyphal wall.)

American Chemical Society  
Library

1155 16th St., N.W.

Washington, D.C. 20036

In Plant Cell and Tissue Culture, ed. by J. D. Bewley et al.;  
ACS Symposium Series; American Chemical Society: Washington, DC, 1989.

in the hypha agree with the results of Murmanis *et al.* (12). In zones of less advanced degradation (Fig. 3B), hyphae "in contact" with partially degraded wood cell walls had no enzymes in their own walls, but some glycohydrolases could be observed penetrating a short distance into the wood cell wall. The gold particles in wood are only seen in lightened areas where wood is already degraded. Nevertheless, this was an indication that some glycohydrolases could pass through the fungal cell wall and penetrate a short distance into wood cell walls. In areas of the degraded wood where no hyphae are visible in the surroundings (pattern "at a distance"), no gold particles were evident in the decayed wood cell walls. This suggested that in this case the enzymes remain associated with the hyphae (or the hyphal sheath).

*"Diffusion" of Lignin-peroxidase (Ligninase).* An anti-ligninase antiserum was raised in a rabbit using a purified ligninase fraction (13). In this study, the gold labeling was performed with the total antiserum. As can be seen in Figure 4, gold particles were localized in the cytoplasm, along the plasmalemma (Fig. 4A) and into the hyphal wall in Figure 4C. This localization of ligninase differs from that reported by Messner *et al.* (15). Some minor labeling was also present intracellularly in some cells (Fig. 4A) as described by Garcia *et al.* (16). Interestingly, some hyphae did not show any affinity for the ligninase antibody; these might correspond to those hyphae which did not secrete ligninase (14). [Fig. 4B corresponds to a control, where the antibody was preincubated with the ligninase before being applied on the section.]

In all cases examined, and regardless of the relative situation of the hypha to the wood cell wall, no extracellular accumulation of ligninase was detectable at the site of degradation. However, an oriented secretion of ligninase outwards, across the hyphae wall, was observed in Figure 4D. In this photograph the physiological state of the hypha could not be ascertained and it is therefore difficult to correlate the excretion of ligninase to a given state of the hypha. However, it could be possible that the excretion of ligninase could occur in sublethal hyphae in which the cytoplasmic membrane could have a modified permeability. In Figure 4E, there is a burst of lignin peroxidase outside a hypha which is obviously dead. From the above results, and in agreement with recent reports (15,16), it appears that *P. chrysosporium* does not secrete the bulk of its lignolytic enzymes during natural degradation of wood; this is in contrast to its secretion in batch cultures, which bears little resemblance to the natural degradation of wood tissues. These findings, however, provide no explanation for the degradation which takes place at some distance from the hyphae. If enzymes are not directly involved in this process, the diffusion of non-enzymatic agents, such as radical cations or activated oxygen species may be occurring (16,18). In this regard, it is known that oxygen species produced via hydrogen peroxide, e.g., the hydroxyl radical ( $\cdot\text{OH}$ ), are able to attack both the lignin and polysaccharides (9,19,20).

*Action of Hydroxyl Radicals on Wood Cell Walls.* In order to investigate

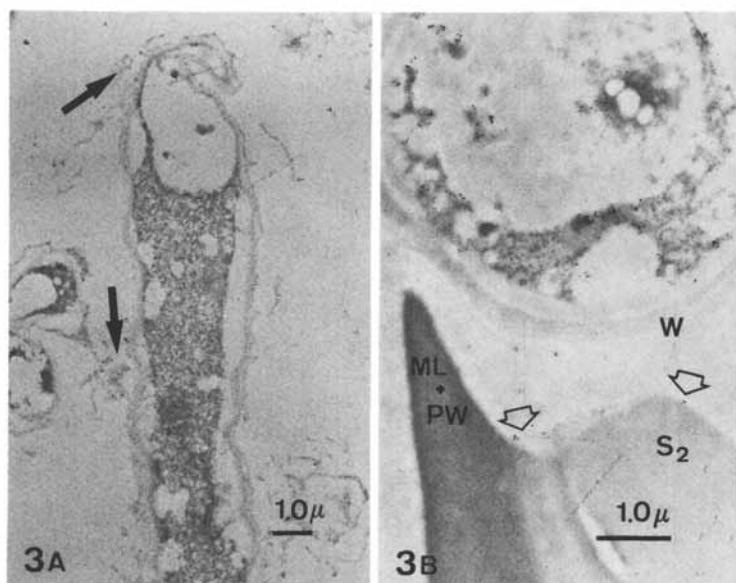


Figure 3. Labeling with anti-crude enzyme mixture. A, some labeling was observed on the electron-dense sheath (arrow). No post-staining. In B, some gold markers were localized on the outer part of the degraded S<sub>2</sub> layer. No labeling of the hyphal wall. (Pm, plasmalemma; W, hyphal wall.)

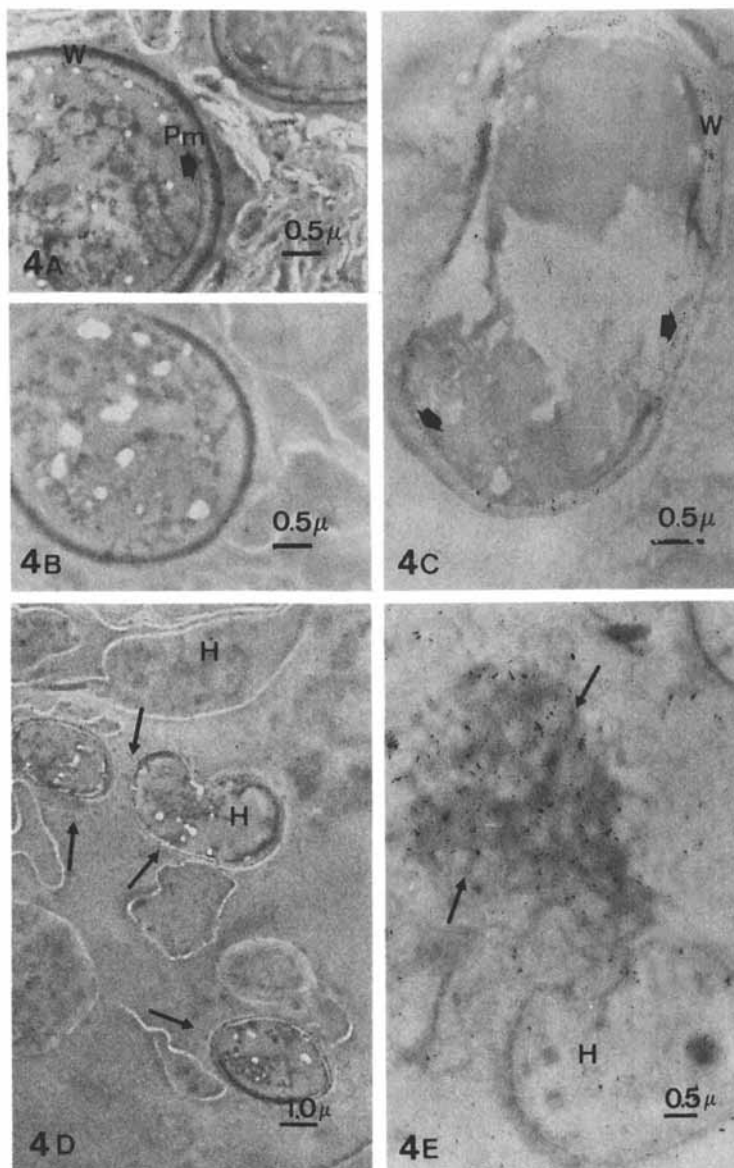


Figure 4. Labeling with anti-ligninase. 4A: Most of the labeling was evident in the plasmatic area and also in the wall. The labeling is still seen on the empty hyphae (4A and 4C). 4B corresponds to a control; the antibody was preincubated with the ligninase before being applied on the section. 4D: A group of hyphae at different physiological states. In some hyphae ligninase was clearly shown in the wall and crossing it outwards (arrows). 4E: An empty hypha is clearly excreting the bulk of its ligninase (arrows). (Pm = plasmalemma; W = hyphal wall; H = hypha.)

the possible degradation of wood components via  $\cdot\text{OH}$ , sound wood samples were submitted to the action of Fenton's reagent which is a good system for producing hydroxyl radicals. Previous results (18) showed that activated oxygen species generated *in situ* created patterns of degradation highly comparable with those created by the fungus. This oxidative action of the fungus can be visualized with electron microscopy in degraded wood samples, using a specific method designed to detect the carbonyl and carboxyl groups created in decayed wood by the fungus (21).

Following comparison to sound wood (Figs. 5A and 5B), it was clearly evident that degraded wood had undergone oxidation. This oxidative process could take place on both polysaccharides and lignin (22,23), and could therefore represent a general degradation mechanism of the wood cell wall polymers.

### Conclusion

Diffusion of enzymes from the fungal cells is complicated by the fact that hyphae behave differently depending upon their physiological state. Immunocytochemistry allowed the visualization of polysaccharide-degrading enzymes and lignin peroxidases during their secretion by the fungus. Penetration of cellulases, hemicellulases and ligninase was limited and no gold

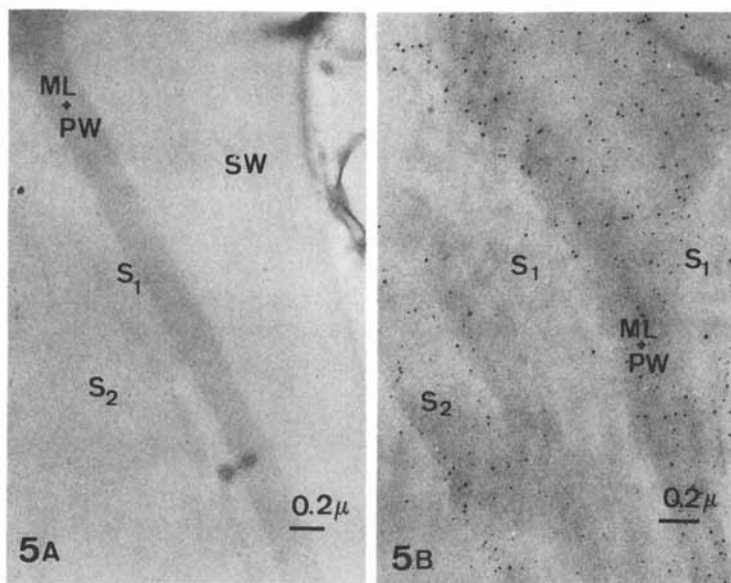


Figure 5. Carbonyl group labeling. Application of the TAg sequence. 5A: Control = TAg on sound wood. 5B: silver grain deposits correspond to the carbonyl groups created by the fungus. (ML + PW = middle lamella + primary wall; S<sub>1</sub> and S<sub>2</sub> = outer and middle layers of the secondary wall, respectively.)

labeling could be seen in sound wood. This means that enzymes invaded the wood cell walls only in places where a predegradation had already occurred. The oxidative action of Fenton's reagent which could be followed by specific cytochemistry suggested that activated oxygen species could participate in the propagation of the degradation initiated by lignin peroxidase. This might be an explanation of the type of decay "at a distance."

### Acknowledgments

Thanks are expressed to Dr. K.-E. Eriksson (STFI, Stockholm, Sweden) for the gift of the enzyme extract and inoculation of the wood samples; to Professor R. Guinet (Institut Pasteur, Lyon Lantilly, France) for the preparation of the IgG directed against the crude protein extracted; and to Dr. E. Odier (INA P.G., France) for providing the anti-ligninase antiserum.

### Literature Cited

1. Eriksson, K.-E. *Pure Appl. Chem.* 1981, **53**, 33-43.
2. Ruel, K.; Barnoud, F. In *Biosynthesis and Biodegradation of Wood Components*; Higuchi, T., Ed.; Academic: New York, 1985, p. 441.
3. Otjen, L.; Blanchette, R. A. *Can. J. Bot.* 1982, **60**, 2770-94.
4. Ruel, K.; Joseleau, J. P. *Symbiosis* 1986, **2**, 355-61.
5. Murmanis, L.; Highley, T.; Palmer, J. G. *Holzforschung* 1984, **38**, 11-18.
6. Tien, M.; Kirk, T. K. *Science* 1983, **221**, 661-63.
7. Eriksson, K.-E.; Wood, T. M. In *Biosynthesis and Biodegradation of Wood Components*; Higuchi, T., Ed.; Academic: New York, 1985; p. 469.
8. Ander, P.; Eriksson, K.-E. *Physiol. Plant.* 1977, **41**, 239-248.
9. Nakatsubo, F.; Reid, I. D.; Kirk, T. K. *Biochem. Biophys. Res. Commun.* 1981, **102**, 484-91.
10. Forney, L. J.; Reddy, A.; Tien, M.; Ausi, S. D. *J. Biol. Chem.* 1982, **257**, 11455-62.
11. Schoemaker, H. E.; Harvey, P. J.; Bowen, R. M.; Palmer, J. M. *FEBS Lett.* 1985, **183**, 7-12.
12. Murmanis, L.; Highley, T. L.; Palmer, J. G. *Sci. Technol.* 1987, **21**, 101-09.
13. Tonon, F.; Odier, E.; Asther, M.; Lesage, L.; Corrieu, G. In *Lignin Enzymic and Microbial Degradation*; E. Odier, Ed.; INRA Publications: 1987; pp. 165-70.
14. Keyser, P.; Kirk, T. K.; Zeikus, J. G. *J. Bact.* 1978, **135**, 3, 790-97.
15. Messner, K.; Strobotnik, E.; Erler, G.; Foisner, R.; Pettersson, B.; Stachelberger, H. In *Lignin Enzymic and Microbial Degradation*; Odier, E., Ed.; INRA Publications: 1987; 243-48.
16. Garcia, S.; Latgé, J. P.; Prevost, M. C.; Leisola, M. *Appl. Environ. Microbiol.* 1987, **53**, 2384-87.
17. Gupta, D. P.; Heale, J. B. *J. Gen. Microbiol.* 1971, **63**, 163-73.
18. Ruel, K.; Joseleau, J. P. *Food Hydrocolloids* 1987, **1**, 515-17.
19. Koenigs, J. W. *Wood Fibers* 1974, **6**, 66-79.

20. Weldock, D. J.; Parsons, B. J.; Phillips, G. O.; Thomas, B. In *Cellulose and its Derivatives*; Kennedy, J. F., Ed.; John Wiley and Sons: New York, 1985; **46**, pp. 503-10.
21. Joseleau, J. P.; Ruel, K. *Biol. Cell.* 1985, **53**, 61-66.
22. Isbell, H. S.; Frush, H. L. *Carbohydr. Res.* 1987, **161**, 181-93.
23. Gilbert, B. C.; King, D. M.; Thomas, C. B. *Carbohydr. Res.* 1984, **125**, 217-35.
24. Spaur, C. R.; Moriarty, G. C. *J. Histochem. Chem.* 1977, **25**, 163-74.

**RECEIVED March 17, 1989**



## Chapter 33

### Oxidation and Reduction in Lignin Biodegradation

Hans E. Schoemaker<sup>1</sup>, Emmo M. Meijer<sup>1</sup>, Matti S. A. Leisola<sup>2</sup>,  
Stephan D. Haemmerli<sup>2</sup>, Roland Waldner<sup>2</sup>, Dominique Sanglard<sup>2</sup>, and  
Harald W. H. Schmidt<sup>3</sup>

<sup>1</sup>DSM Research, Bio-organic Chemistry Section, P.O. Box 18, 6160 MD  
Geleen, Netherlands

<sup>2</sup>Department of Biotechnology, Swiss Federal Institute of Technology,  
ETH-Hönggerberg, 8093 Zürich, Switzerland

<sup>3</sup>Givaudan Forschungsgesellschaft AG, 8600 Dübendorf, Switzerland

Reductive activities of *Phanerochaete chrysosporium* were studied using monomeric aromatic acids, aldehydes and three different types of quinones as substrates. All of the tested substrates were rapidly reduced by ligninolytic cultures of *P. chrysosporium*. Reduction experiments carried out with intact fungal cells, cell extracts and partially purified enzymes gave evidence for the presence of at least three different types of reductases: *viz.* acid, aldehyde and quinone reductases. Further, comparison of relative quinone reduction rates indicated that possibly two or three different quinone reductases were operating. Based on these results and an extensive literature survey, it is postulated that lignin degradation by *P. chrysosporium* involves an array of oxidative and reductive conversions. Rapid metabolism of quinone type intermediates represents one possible way of shifting the polymerization-depolymerization equilibrium, induced by lignin peroxidases and phenoloxidases, towards degradation. Moreover, it is postulated that aldehyde and acid reductases play a role in the biodegradation of lignin by *P. chrysosporium*.

Lignin biodegradation research has extended over several decades, but the progress since the late 1970's has been remarkable. The discovery— independently by the groups of Kirk (1) and Gold (2)—of a ligninolytic enzyme, capable of oxidizing non-phenolic aromatic compounds, can be considered as a breakthrough in this area. The enzyme, isolated from ligninolytic cultures of the white-rot basidiomycete *Phanerochaete chrysosporium*, was originally described as a novel type of oxygenase. Subsequent research, however, showed that the enzyme should be classified as a peroxidase (3-6). Its discovery triggered a major worldwide research effort,

0097-6156/89/0399-0454\$06.00/0

© 1989 American Chemical Society

resulting in the formulation of a unifying theory rationalizing most of the reactions observed in lignin biodegradation (7-9).

Recently various review articles on lignin biodegradation have focused on the lignin peroxidases from *Phanerochaete chrysosporium*. In those articles the microbiology, physiology, (bio)chemistry, genetics and molecular biology of the system were discussed (10-12). Lignin biodegradation has been recognized as an extracellular, mainly oxidative process, characterized by cleavage of the aryl propyl side-chains, demethoxylation and other ether bond breaking reactions, aromatic ring cleavage, aromatic hydroxylation and aromatic carboxylic acid formation (13). With the possible exception of the latter reaction, most reactions are adequately rationalized by a lignin peroxidase-induced aromatic radical cation formation. However, a corollary of the latter process is the occurrence of phenol coupling reactions *in vitro*, resulting in lignin peroxidase catalyzed polymerization of milled wood lignin (14). *In vivo*, however, lignin is depolymerized by ligninolytic cultures of *P. chrysosporium*, a process stimulated by the addition of lignin peroxidase (15). Obviously, to degrade lignin the white-rot fungi have some currently unknown mechanism to prevent polymerization. We postulated (16) that since low molecular weight degradation products are rapidly metabolized by the fungus, this represents one mechanism to shift the equilibrium from spontaneous polymerization to degradation. In this paper, we propose that in addition to aromatic ring-cleaved products, quinones and hydroquinones are obvious candidates to function as those low molecular weight compounds. In this regard, Eriksson and coworkers (17,18) suggested that quinone reduction was an essential step. In recent reviews hardly any attention was given to the fact that the ligninolytic system of *P. chrysosporium* possessed a strong reducing activity. However, as pointed out by Eriksson (19) and Chen and Chang (20), lignin biodegradation by white-rot fungi is a combination of an array of oxidative and reductive reactions, rather than oxidative reactions alone. However, the nature and the role of this reducing activity is not clear at present. In addition to the quinone reductase system, this reducing activity is also manifested in the conversion of aromatic aldehydes and carboxylic acids to the corresponding benzylic alcohols.

Following a brief literature survey of some noteworthy (reductive) conversions of lignin model compounds by *P. chrysosporium*, including our own results on the metabolism of veratryl alcohol, we will focus on the different reducing properties of *P. chrysosporium*. Our preliminary results have led us to formulate a hypothetical scheme for lignin biodegradation based on both oxidative and reductive conversions, where the pivotal role of aromatic ring opened products and quinones/hydroquinones as lignin metabolites is discussed.

### Literature Survey

**Reduction.** The reductive capacity of *P. chrysosporium* has been known for a long time. For example, veratraldehyde, veratric acid, vanillin, vanillic acid and analogous structures were converted into the corresponding

benzylic alcohols (21,22). Also the initial products (mostly veratraldehyde analogs) in  $C\alpha$ - $C\beta$  cleavage studies on lignin models with *P. chrysosporium* are reduced to the corresponding alcohols(23).

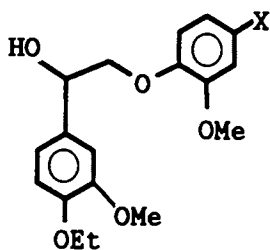
Additionally, studies by Eriksson and coworkers (17,18) showed that quinones produced were rapidly reduced to the corresponding hydroquinones and then further degraded.

Various authors have also described the reduction of dimeric lignin model structures; both aromatic aldehydes and aromatic acids were reduced by ligninolytic cultures of *P. chrysosporium*, as shown by the reduction of the  $\beta$ -O-4 model **1** (acid, lacking the  $C_\gamma$ -substituent) to the corresponding alcohol **2** (24) and the phenyl coumaran models **3** (acid) and **4** (aldehyde) to the corresponding alcohol **5** (25).

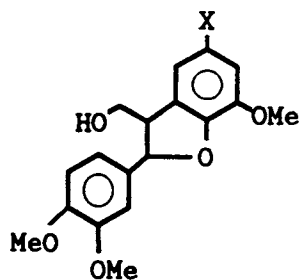
*Oxidation.* Most of the oxidative reactions observed in lignin biodegradation can be rationalized by one-electron oxidations of phenols (e.g., with laccase or peroxidase) to yield phenoxy-radicals and of non-phenolics by lignin peroxidase to yield radical cationic intermediates. As a consequence of these one-electron oxidations, phenolic lignin and lignin models frequently undergo  $C\alpha$ -arene cleavage resulting in quinone/hydroquinone formation (26). Supporting evidence for the radical cation mechanism was obtained for  $C\alpha$ - $C\beta$  cleavage, demethoxylation and other ether bond breaking reactions, aromatic hydroxylation, aromatic ring cleavage, benzylic oxidation, hydroxylation of benzylic methylene groups, styrene hydroxylation, specific oxygen incorporation, phenol coupling, etc. (7-12). So far, aromatic carboxylic acid formation, a rather characteristic reaction in lignin biodegradation (20,27), has not been demonstrated for lignin peroxidase catalyzed reactions. However, aromatic carboxylic acids were observed in hemin-catalyzed oxidation of lignin models (28). Recently, we obtained evidence for aromatic carboxylic ester formation in the lignin peroxidase catalyzed oxidation of the methyl ether of veratryl alcohol. The ester formation was more pronounced at higher (4-5) pH-values (Schmidt *et al.*, *Biochemistry*, in press). Higuchi and coworkers (27) have also shown that in ligninolytic cultures of *P. chrysosporium* dimeric lignin models of the  $\beta$ -O-4 and phenyl coumaran type with allyl alcohol side-chains (see structures **1** respectively **3**, X = CH=CH-CH<sub>2</sub>OH) were converted to carboxylic acids; due to the reducing capacity of *P. chrysosporium*, alcohols and aldehydes were also obtained.

*Quinone/Hydroquinone Formation.* In studies on biodegradation of lignin models with ligninolytic cultures of *P. chrysosporium* (and other fungi), a number of quinones and hydroquinones were isolated. In other studies their formation has been implied from the isolation of their structural counterparts (29,30), where rapid fungal degradation of the quinones prevented their isolation. Various routes to these metabolic intermediates exist, which have been extensively reviewed (26,27).

For the present discussion, a number of these conversions are of relevance. Phenolic dimeric model compounds of the  $\beta$ -1,  $\beta$ -O-4 and phenyl coumaran type are degraded via  $C\alpha$ -arene cleavage yielding methoxy-



- 1 X - COOH  
2 X - CH<sub>2</sub>OH



- 3 X - COOH  
4 X - CHO  
5 X - CH<sub>2</sub>OH

substituted quinones/hydroquinones. The monomeric lignin models vanillin, vanillic acid and vanillyl alcohol (22) and isovanillyl alcohol (16) were shown to be oxidized to methoxy-quinones/hydroquinones. More recently, it was shown that veratric acid, veratraldehyde and veratryl alcohol were degraded via quinone intermediates (15,31), with the aldehyde (15) and the acid (21) being first reduced to veratryl alcohol.

*Degradation of Non-Phenolic Lignin Models with a C $\alpha$ -Carbonyl Substituent.* Lignin peroxidase will oxidize a wide variety of lignin models. However, non-phenolic aromatic rings containing C $\alpha$ -carbonyl groups are not substrates for this enzyme; e.g., veratraldehyde and the  $\beta$ -O-4 dimeric model 6a are not substrates (32) and no cleavage of the B-ring in the latter compound occurs.

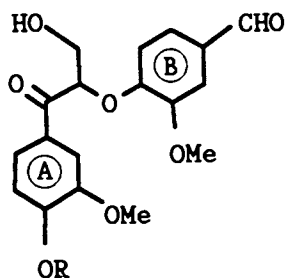
However, studies (33) with the analogous structure 7a, using ligninolytic cultures of *P. chrysosporium* as before, resulted in degradation products derived from oxidation of the B-ring being formed. Umezawa *et al.* (33) have suggested that the formyl substituent is first converted to a less electron-withdrawing group. Reduction to the alcohol or oxidation to the acid are two obvious possibilities. Kawai *et al.* (34) studied the lignin peroxidase catalyzed oxidation of the related dimeric acid 8 which contained an extra methoxy-substituent in the B-ring and found oxidation to the quinone-hemi-ketal 9.

Enoki and Gold (35) studied the degradation of a  $\beta$ -1 model with a C $\beta$ -hydroxy substituent. One of the products was the ketol 10. Enoki and Gold have postulated that 10 was further degraded to anisyl alcohol via reduction to the glycol 11, one-electron oxidation and C $\alpha$ -C $\beta$  cleavage followed by reduction of the initially formed anisaldehyde to the observed product anisyl alcohol. However, this view was countered again by Kirk and Nakatsubo (23). This reaction merits further investigation.

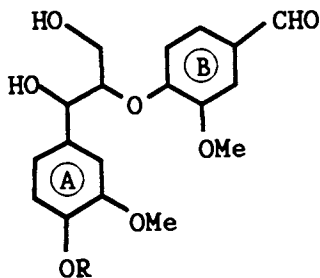
In our studies on the lignin peroxidase catalyzed oxidation of veratraldehyde and veratric acid no degradation was observed under the reaction conditions used. However, ligninolytic cultures of *P. chrysosporium* degraded veratraldehyde and veratric acid via reduction to veratryl alcohol (15,21). In Figure 1 the isolated reaction products of the veratryl alcohol oxidation are depicted.

### Aim of the Present Investigation

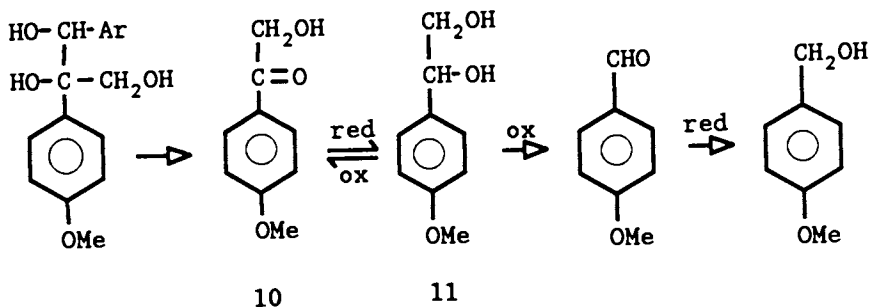
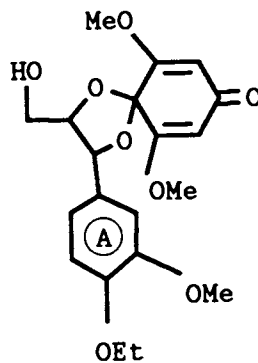
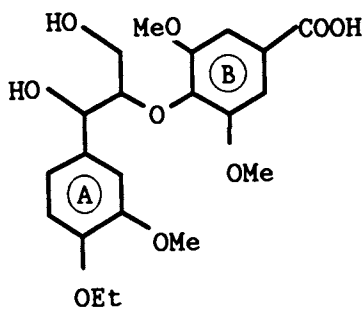
Lignin peroxidases, Mn(II)-dependent peroxidases and other active oxygen species will catalyze the oxidative depolymerization of lignin resulting in the formation of ring-opened products and small aromatic fragments. The latter fragments can polymerize again under those conditions. We propose that rapid metabolism of the small degradation products is one of the mechanisms by which the depolymerization-repolymerization equilibrium can be shifted towards degradation. Evidently, further metabolism of the ring-opened products constitutes a major degradation pathway. In this paper, however, we will focus on the metabolism of the aromatic fragments. We propose that these aromatic compounds are degraded via



6b R = H



7b R = H



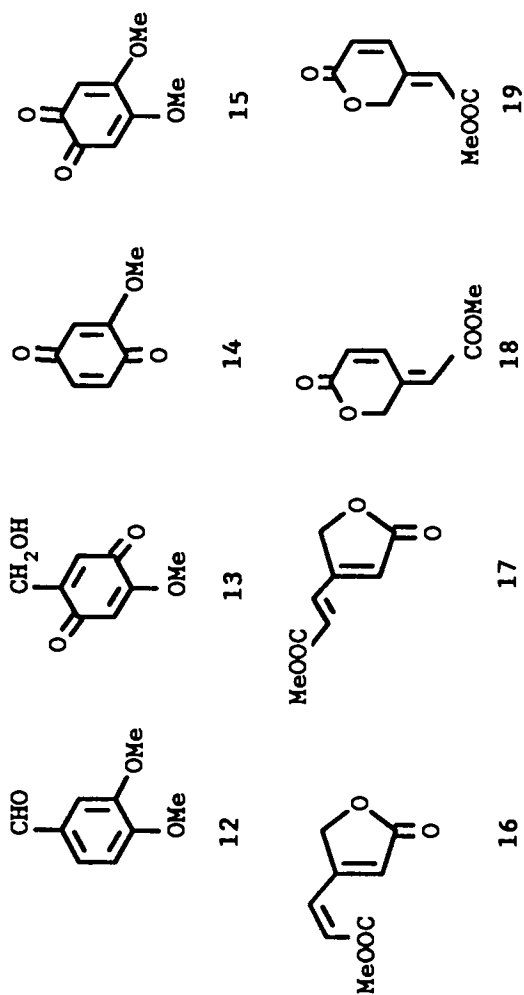


Figure 1. Products of veratryl alcohol oxidation by the lignin peroxidase of *P. chrysosporium*.

quinone/hydroquinone type intermediates. We also propose that reductive enzymes are involved in the degradation of the quinone type structures. In addition, we wish to propose that aromatic aldehyde reductases and aromatic acid reductases play a role also. The partial purification of these reductive enzymes is described and their relevance to the lignin biodegradation process is discussed.

### Materials and Methods

**Cell Growth.** Mycelial pellets of *P. chrysosporium* (ATCC 24725) were produced under nitrogen limited culture conditions at 37°C using a spore inoculum (36). The pellets were grown for 72 hr at 150 rpm after which they were concentrated fourfold by decanting excess medium. They were used for reduction experiments after a 24 hr activation period (37°C, 50 rpm, under 100% O<sub>2</sub> atmosphere).

**Reduction Experiments.** The reduction experiments were carried out with 50 ml of activated pellets. The cultures were agitated at 50 rpm and 37°C. Quinones were added at a concentration of 0.2 mM. Samples of the supernatant were taken at defined intervals and their absorption measured at 288 nm and 360 nm on a Perkin-Elmer 557 Photospectrometer.

High pressure liquid chromatography (HPLC) was used for the quantitative measurement of quinones and hydroquinones in the cultures. 20  $\mu$ l of supernatant were injected in a Merck-Hitachi HPLC system 655A-12 equipped with a 4.6  $\times$  250 mm Nucleosil C18 column (5  $\mu$ m, RP 18). The system was run at a flow rate of 1 ml min<sup>-1</sup> with a methanol/water gradient (10 to 20% methanol in 15 min, then 20 to 100% methanol in 5 min). The UV detector was operated at 281 nm or 275 nm to follow the reduction of quinones 13 and 14, respectively (37).

**Cell Disruption.** Fungal pellets from 5-6 d old, N-limited cultures were washed 3 times with 20 mM Tris/HCl buffer, pH 7.4, containing 20% glycerol and 1 mM EDTA and cooled on ice. 75 ml of wet pellets (equals the amount from two agitated flasks) and 125 ml glass beads (0.4 mm diameter; cooled to -18°C) were poured into the 150 ml glass vessel of Dynamill. Breaking of the cells was carried out at +1°C for 75 s at 2000 rpm. The glass beads were removed by filtration through a coarse sintered glass filter and washed twice with 50 ml of the Tris buffer. Cell fragments were removed by centrifugation at 30,000 g for 30 min.

**Partial Purification of the Reductases.** 4 M CaCl<sub>2</sub> was added to the crude extract to give a concentration of 16 mM. After mixing for 10 min the solution was centrifuged at 30,000 g for 30 min. The sediment was discarded. To the supernatant 4M ammonium sulfate was slowly added to give a final saturation of 40%. After centrifugation at 30,000 g for 30 min, 4M ammonium sulfate was added to the supernatant to a saturation of 55%. The sediment obtained by centrifugation at 30,000 g for 30 min was dissolved in 20 ml of 20 mM Tris/HCl buffer with 20% glycerol and 1 mM EDTA, pH 7.4 and dialysed over night against 2 l of this buffer.



**Reductase Activity Measurement.** Reductase activity was measured by the reduction of 200  $\mu\text{M}$  veratraldehyde to veratryl alcohol in the presence of 250  $\mu\text{M}$  NADPH. The reaction was carried out in 20 mM Tris buffer pH 7.4 (optimal pH = 6) with 20% glycerol and 1 mM EDTA. The decrease in absorbance of NADPH at 365 nm was measured. NADPH was slowly oxidized in those mixtures which were not purified by ion exchange even in the absence of veratraldehyde. This unspecific reaction was considered in the calculation of the reductase activity. One unit of reductase reduced 1  $\mu\text{mol min}^{-1}$  of veratraldehyde to veratryl alcohol at room temperature (25°C).

Reduction of the quinones was measured in the same way as that of veratraldehyde, at 365 nm. Substrate concentration was also 200  $\mu\text{M}$  and the concentration of NADPH or NADH was 250  $\mu\text{M}$ .

In some of the reductions of veratric acid or vanillic acid 250  $\mu\text{M}$  ATP was added to the reaction mixture.

## Results

Previously, the quantitative reduction of veratraldehyde and veratric acid to veratryl alcohol by active ligninolytic cultures of *P. chrysosporium* had been described by Leisola and Fiechter (21).

It has now been found that the quinones 13, 14 and 15 from the aerobic oxidation of veratryl alcohol by lignin peroxidase were also reduced by fungal mycelium to yield the corresponding hydroquinones. For quinone 14 this reduction had already been reported by Buswell *et al.* (17) in a study of vanillic acid metabolism.

The reduction of quinones 13 and 14 by intact cells of *P. chrysosporium* is shown in Figure 2. The concentrations of the quinones and hydroquinones were calculated from HPLC data and corrected for their specific absorbance at given wavelengths. Peaks were identified by comparison with retention times and UV spectra of reference compounds (37, see also Materials and Methods section). Figure 3 shows the change of absorption at 288 nm and 360 nm in culture supernatant during the reduction of quinone 13. This quinone had an absorbance maximum at 360 nm while the hydroquinone 13a had one at 288 nm. Quinone 15 was also reduced by whole cells as indicated by the change of absorption in culture supernatant (data not shown). However, the resulting hydroquinone was not detected by HPLC probably because it was autoxidized rapidly. Still, quinone 15 was metabolised by *P. chrysosporium* as can be seen in Figure 2. The rate of quinone reduction by the cells was highest just after addition of the compounds to the cultures. Hydroquinone formation was not quantitative (Fig. 2). Intracellular degradation of the hydroquinones is a possible explanation for this observation (18). From the data in Table I it can be concluded that the aldehyde-reducing enzyme (which has an absolute requirement for NADPH) differs from the acid reductase (no acid reductase present in the crude extracts) and the quinone reductases (both NADH and NADPH can be used as co-substrates at similar rates). Moreover, the data also indicated that more than one quinone reductase

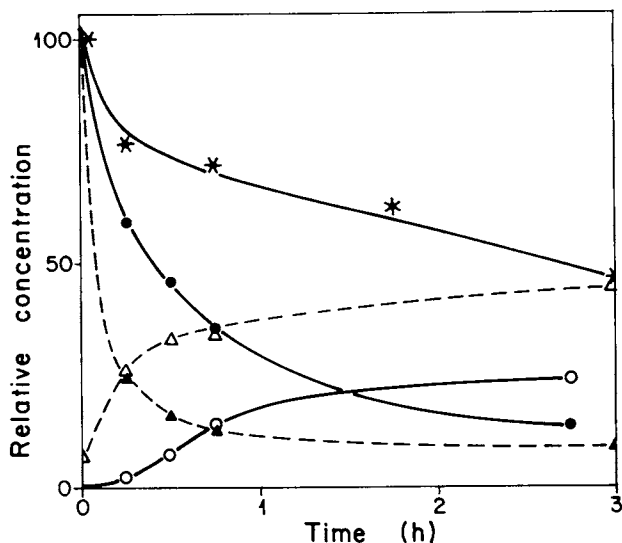


Figure 2. Relative concentrations of quinones **13** (●), **14** (▲), and **15** (\*) and hydroquinones **13a** (○) and **14a** (△) vs. time after addition of quinones to ligninolytic cultures of *P. chrysosporium*.

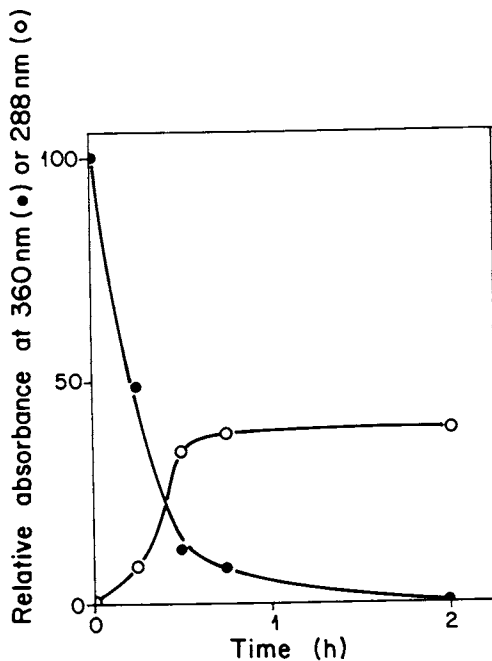


Figure 3. Relative absorbance of culture supernatant at 360 nm (●) and 288 nm (○) vs. time after addition of quinone **13** to ligninolytic cultures of *P. chrysosporium*.

was operating, as judged from differences in relative rates of quinone reduction for the different preparations. The ratio of the reduction rates for quinone 14/quinone 15 was 0.75 in both the crude extract and the 50% sediment fraction. In contrast, the ratio of the reduction rates for quinone 13/quinone 14 was approximately 1.0 in the crude extract and 0.27 in the dialyzed 50% sediment fraction, indicating that quinone 13 reductase differs from both quinone 14 reductase and from quinone 15 reductase. Quinone 14 reductase also appears to be different from quinone 15 reductase, as can be inferred from inhibition studies with 1 mM of DTT (dithiothreitol). DTT completely inhibited the reduction of quinone 13 and quinone 14, but DTT did not inhibit the reduction of veratraldehyde and quinone 15. Research is in progress to purify and characterize the reductive enzyme systems mentioned above.

Table I. Relative reduction rates ( $\Delta E_{365} \text{ min}^{-1}$ ) of veratraldehyde and the quinones 13-15 by partially purified reductases from *P. chrysosporium*

	Compound	$\Delta E_{365} \text{ min}^{-1}$	Cofactor-Dependence
crude extract	veratraldehyde 12	1.0	NADPH
	quinone 13	4.4	NAD(P)H
	quinone 14	4.5	NAD(P)H
	quinone 15	6.0	NAD(P)H
	veratric acid <sup>1</sup>	0.0	
	vanillic acid <sup>1</sup>	0.0	
CaCl <sub>2</sub> -supernatant	veratraldehyde 12	1.0	
	quinone 14	5.0	
50%-sediment (dialyzed)	veratraldehyde 12	1.0	
	quinone 13	0.4	
	quinone 14	1.5	
	quinone 15	2.0	

<sup>1</sup> With added ATP.

## Discussion

*Metabolism of Monomeric Lignin Models.* Leisola and coworkers (31,37) have reported on the products of the lignin peroxidase catalyzed oxidation of veratryl alcohol. Veratraldehyde was the major product (> 70% yield), together with a number of minor products, the quinones 13 and 14 and the ringopened lactones 16 and 17. In addition, Shimada *et al.* (38,39) showed that the  $\delta$ -lactone 18 was also formed. Recently we obtained evidence that the ortho-quinone 15 and the  $\delta$ -lactone 19 were also products of the lignin peroxidase catalyzed oxidation of veratryl alcohol (Schmidt *et al.*, *Biochemistry*, in press). Mechanisms for the formation of those compounds

have been discussed (16,31,38,39), although the reaction mechanisms for quinone formation require further investigation.

Leisola *et al.* (15) have studied the metabolism of veratryl alcohol by ligninolytic cultures of *P. chrysosporium*. From studies with  $^{14}\text{C}$  ring labeled compounds, the metabolic scheme depicted in Figure 4 was postulated.

In this scheme veratryl alcohol was viewed to be metabolized by the combined action of oxidative systems (the lignin peroxidase and possibly other active oxygen species) and reductive conversions (aldehyde and quinone reductions). A possible route via veratric acid was discounted because both veratraldehyde and veratric acid were not substrates for the lignin peroxidase under the condition studied. However, both veratraldehyde and veratric acid were rapidly and quantitatively reduced by ligninolytic cultures of *P. chrysosporium* (21).

Veratraldehyde was reduced by a NADPH dependent oxidoreductase, which most probably was also involved in the biosynthesis of veratryl alcohol (40), a secondary metabolite of *P. chrysosporium*. The  $^{14}\text{C}$  labeled quinones 13 and 14, prepared by lignin peroxidase catalyzed oxidation of [ $^{14}\text{C}$ ] veratryl alcohol, were also metabolized by ligninolytic cultures of *P. chrysosporium* (15). Eriksson and coworkers (17,18,22) studied the metabolism of ring labeled quinone 14, derived from  $^{14}\text{C}$  ring-labeled vanillic acid. From their work it could be inferred that quinone reductases played an important role. In addition, the data in Figures 2 and 3 indicate that the hydroquinones are further metabolized by the fungus. The present study indicated that the quinones obtained from lignin peroxidase catalyzed oxidation of veratryl alcohol indeed were first reduced to the corresponding hydroquinones. Note also that these quinone reductions can occur both extracellularly and intracellularly. The extracellular cellobiose-quinone oxidoreductase (41) was only involved if cellulose is present in the cultures. Quinone reduction appears to be mainly an intracellular process, involving a number of different enzymes which used NADPH or NADH as cosubstrates. In addition to the quinone reductase observed by Buswell *et al.* (17) in the study of vanillic acid metabolism, at least one and possibly two other quinone reductases with different catalytic properties were present.

*Metabolism of Lignin.* How can we relate the already complex results obtained in degradation studies of simple monomeric lignin models like veratryl alcohol, veratric acid, vanillic acid, quinones, etc., to the studies on the metabolism of the lignin polymer? As pointed out by Kirk (42), few monomeric compounds have been studied in detail because of the uncertainty of their relevance to lignin polymer degradation. Of these monomers, vanillic acid has been the best studied since it is a well known degradation product of fungal degraded wood. Veratryl alcohol is also being actively studied since it is a secondary metabolite of *P. chrysosporium*, and its role in lignin biodegradation is under active investigation. The degradation of veratryl alcohol seems to involve both oxidative and reductive conversions and metabolism via ring opened and quinone type structures (15). We believe that this metabolic pathway can serve in part as a model for lignin biodegradation.

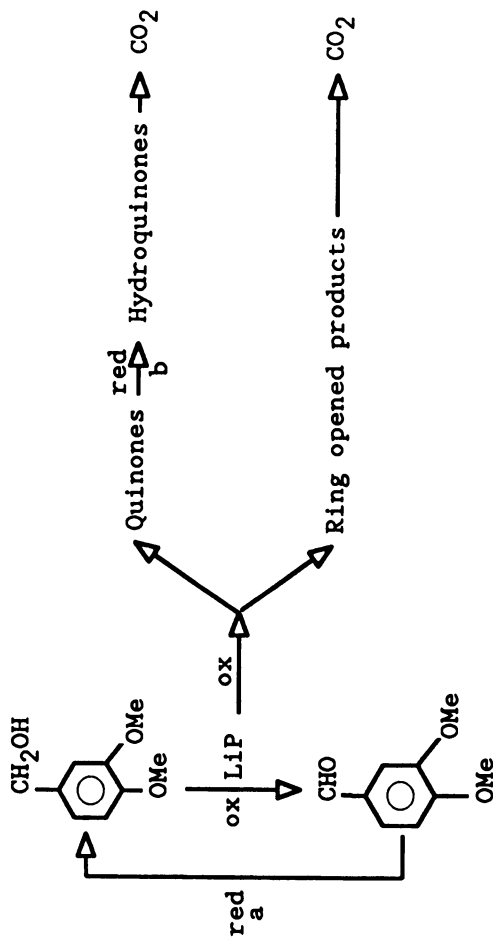


Figure 4. Hypothetical scheme for veratryl alcohol metabolism by ligninolytic cultures of *P. chrysosporium*:

ox = oxidation by LiP (lignin peroxidase)

red a = reduction by a NADPH dependent aldehyde reductase

red b = reduction by NAD(P)H dependent quinone reductases

Evidently, further metabolism of ring opened products (43-45) constitutes a major metabolic pathway for the degradation of the lignin polymer. In addition, we wish to postulate a pathway for the metabolism of small aromatic fragments, which are prone to undergo polymerization reactions under the oxidative conditions of the biodegradation process. We propose that rapid fungal metabolism of quinone/hydroquinone intermediates will shift the depolymerization-repolymerization equilibrium mentioned above towards degradation. This hypothesis is in part based on the fact that in numerous studies (17-19,22,29,30) on the enzymatic oxidation and the biodegradation of a wide variety of lignin model compounds quinones and hydroquinones were produced, or their formation was implied from the isolation of structural counterparts. Moreover, we wish to postulate that in the formation and the degradation of the quinones/hydroquinones both oxidative and reductive conversions play an important role.

In the lignin degradation scheme depicted in Figure 5 it is proposed that lignin peroxidase catalyzed oxidation significantly depolymerizes the lignin polymer. Then the quinones/hydroquinones formed, both as the result of C $\alpha$ -arene cleavage in the oxidation of phenolic lignin substructures by phenoloxidases (laccases, Mn(II)-dependent peroxidases), and lignin peroxidase catalyzed oxidation of non-phenolic lignin substructures, will be metabolized via the reductive system described.

Also depicted in Figure 5 are the aromatic ring cleavage pathway and the degradation of C<sub>1</sub>, C<sub>2</sub> and C<sub>3</sub> fragments derived from the phenylpropane side chain of the lignin building blocks.

In the depolymerization process, however, a complication can arise. Lignin peroxidase catalyzed oxidation will result in the formation of C $\alpha$ -carbonyl compounds (e.g., upon C $\alpha$ -C $\beta$  cleavage or C $\alpha$ -oxidation). If these degradation products are phenolics, they will be further degraded via the pathways discussed above. However, if these compounds are non-phenolics in which all of the aromatic rings have a C $\alpha$ -carbonyl substituent (most probably, these compounds will be either monomeric or dimeric, see for an example compound **6a**) they are not substrates for the lignin peroxidase. However, we postulate that *P. chrysosporium* uses its reductive system to convert these monomeric or dimeric substructures to the corresponding benzylic alcohols, which again are substrates for lignin peroxidase. In fact, both reduction of monomeric and of dimeric lignin substructures have been described (17,18,21-25,37). Subsequently, enzymatic oxidation either results in ring opening or quinone/hydroquinone formation and further metabolism of the products as discussed above.

It should be noted that if the non-phenolic C $\alpha$ -carbonyl compound contains an aromatic ring without C $\alpha$ -carbonyl group (i.e., the structure should contain at least two aromatic rings), then the compound will be a substrate for lignin peroxidase and will be degraded according to the mechanisms discussed above. Degradation of this type of compounds can result, for example, in the formation of vanillin and vanillic acid derivatives (see compounds **7a** and **8**). As has been shown by Eriksson and coworkers

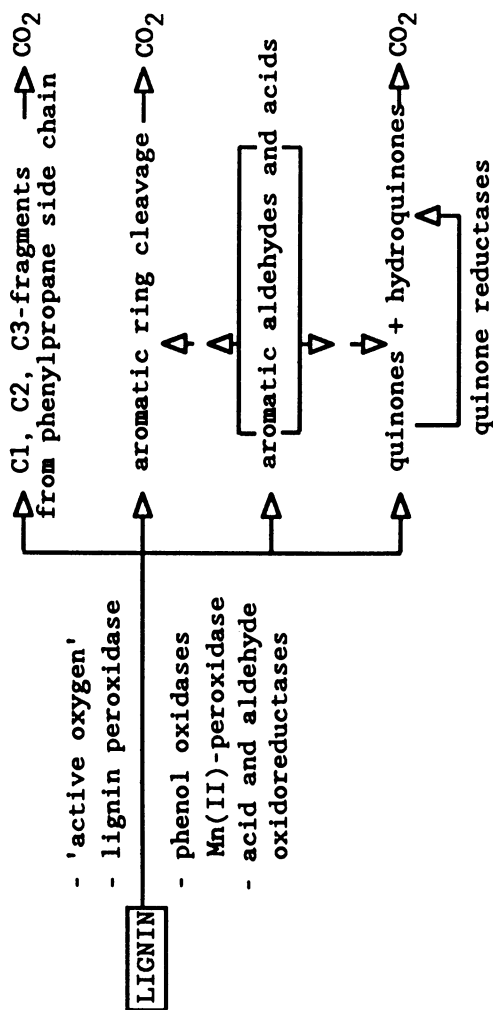


Figure 5. Hypothetical scheme for lignin degradation by ligninolytic cultures of *P. chrysosporium*.

(17-19), these structures are degraded via quinone/hydroquinone intermediates.

Thus, by a combination of oxidation by lignin peroxidases, Mn(II)-dependent peroxidases and other active oxygen species and reductions of some aromatic aldehydes, acids and ketones to the corresponding benzylic alcohols, all aromatic rings in the lignin polymer can be either converted to ring opened products or to quinones/hydroquinones. These products are then further metabolized to CO<sub>2</sub> by a currently unknown mechanism.

### Conclusion

In conclusion, we believe that lignin biodegradation by *P. chrysosporium* involves a combination of both oxidative and reductive conversions. Oxidative attack on the polymer is the predominant reaction. We postulate that rapid metabolism of ring opened products and quinone/hydroquinone type intermediates is one possible way of shifting the resulting polymerization-depolymerization equilibrium towards degradation. Reduction of the quinones to the hydroquinones appears to be the first step in this process. In addition, depending on specific conditions, the fungus can use the reduction of aromatic ketone, formyl and carboxyl groups in order to convert certain low molecular weight intermediates to compounds that are better substrates for the lignin peroxidase. Subsequent oxidation and degradation again can involve ring cleaved and quinone type intermediates. However, since this type of reduction has to be invoked only in the metabolism of non-phenolic compounds in which all aromatic rings have a C $\alpha$ -carbonyl substituent (most probably, monomeric and dimeric structures), its relevance to the overall process of lignin biodegradation has yet to be established. In this context also the relevance of reductive conversions in the metabolism of vanillin and vanillic acid requires further investigation. This working hypothesis now serves as the basis for future research. An important aspect to determine is what type of culture conditions influence the reductive system of *P. chrysosporium*. Is rapid metabolism of quinone type intermediates the only mechanism to prevent repolymerization, or do other factors play a role also? It has been suggested that binding of lignin fragments to the fungal mycelium is an important factor in lignin biodegradation (46,47). Additionally, are acids formed as intermediates on the metabolic pathway, or do they accumulate because their degradation is a relatively difficult process? In conjunction with this, the transport-mechanism of low molecular weight fragments through the cell membrane should be investigated.

In our opinion, the answers to these and related questions will help us in understanding the complicated mechanism of lignin biodegradation. Research is in progress in our laboratories which addresses those topics.

### Literature Cited

1. Tien, M.; Kirk, T. K. *Science* 1983, **221**, 661-663.
2. Glenn, J. K.; Morgan, M. A.; Mayfield, M. B.; Kuwahara, M.; Gold, M. H. *Biochem. Biophys. Res. Comm.* 1983, **114**, 1077-1083.



3. Harvey, P. J.; Schoemaker, H. E.; Bowen, R. M.; Palmer, J. M. *FEBS Lett.* 1985, **183**, 13-16.
4. Kuila, D.; Tien, M.; Fee, J. A.; Ondrias, M. R. *Biochemistry* 1985, **24**, 3394-3397.
5. Renganathan, V.; Gold, M. H. *Biochemistry* 1986, **25**, 1626-1631.
6. Hammel, K. E.; Kalyanaraman, B.; Kirk, T. K. *Proc. Natl. Acad. Sci. USA* 1986, **83**, 3708-3712.
7. Schoemaker, H. E.; Harvey, P. J.; Bowen, R. M.; Palmer, J. M. *FEBS Lett.* 1985, **183**, 7-12.
8. Kersten, P. J.; Tien, M.; Kalyanaraman, B.; Kirk, T. K. *J. Biol. Chem.* 1985, **260**, 2609-2612.
9. Hammel, K. E.; Tien, M.; Kalyanaraman, B.; Kirk, T. K. *J. Biol. Chem.* 1985, **260**, 8348-8353.
10. Tien, M. *CRC Crit. Rev. Microbiol.* 1987, **15**, 141-168.
11. Buswell, J. A.; Odier, E. *CRC Crit. Rev. Biotechnol.* 1987, **6**, 1-60.
12. Kirk, T. K.; Farrell, R. L. *Ann. Rev. Microbiol.* 1987, **41**, 465-505.
13. *Biosynthesis and Biodegradation of Wood Components*; Higuchi, T., Ed.; Academic Press: New York, 1985.
14. Haemmerli, S. D.; Leisola, M. S. A.; Fiechter, A. *FEMS Microbiol. Lett.* 1986, **35**, 33-36.
15. Leisola, M. S. A.; Haemmerli, S. D.; Waldner, R.; Schoemaker, H. E.; Schmidt, H. W. H.; Fiechter, A. *Cell. Chem. and Tech.* 1988, **22**, 267-277.
16. Schoemaker, H. E.; Leisola, M. S. A. *Proc. 31st IUPAC Congress of Pure and Appl. Chem.* 1987, Section 4, 267-280.
17. Buswell, J. A.; Hamp, S.; Eriksson, K. E. *FEBS Lett.* 1979, **108**, 229-232.
18. Ander, P.; Eriksson, K. E.; Yu, H.-S. *Arch. Microbiol.* 1983, **136**, 1-6.
19. Eriksson, K. E.; Ander, P.; Pettersson, B. *Proc. 3rd. Int. Conf. on Biotechn. in Pulp & Paper Ind.* 1986, 24-27.
20. Chen, C. H.; Chang, H. M. In *Biosynthesis and Biodegradation of Wood Components*; Higuchi, T., Ed.; Academic Press: New York, 1985; Chapter 19.
21. Leisola, M. S. A.; Fiechter, A. In *Advances in Biotechn. Processes 5*; Mizrahi, A.; Van Wezel, A. L., Eds.; Alan R. Liss: New York, 1985, 59-89.
22. Ander, P.; Hatakka, A.; Eriksson, K.E. *Arch. Microbiol.* 1980, **125**, 189-202.
23. Kirk, T. K.; Nakatsubo, F. *Biochem. Biophys. Acta* 1983, **756**, 376-384.
24. Enoki, A.; Goldsby, G. P.; Krisnangkura, K.; Gold, M. H. *FEMS Microbiol. Lett.* 1981, **10**, 373-377.
25. Nakatsubo, F.; Kirk, T. K.; Shimada, M.; Higuchi, T. *Arch. Microbiol.* 1981, **128**, 416-420.
26. Higuchi, T. *Wood Res.* 1986, **73**, 58-81.
27. Higuchi, T. In *Biosynthesis and Biodegradation of Wood Components*; Higuchi, T., Ed.; Academic Press: New York, 1985; Chapter 20.

28. Shimada, M.; Habe, T.; Higuchi, T.; Okamoto, T.; Panijpan, B. *Holz-forschung* 1987, **41**, 277-285.
29. Higuchi, T. *Wood Res.* 1981, **67**, 47-58.
30. Kamaya, Y.; Higuchi, T. *Wood Res.* 1984, **70**, 25-28.
31. Haemmerli, S. D.; Schoemaker, H. E.; Schmidt, H. W. H.; Leisola, M. S. A. *FEBS Lett.* 1987, **220**, 149-154.
32. Kirk, T. K.; Tien, M.; Kersten, P. J.; Mozuch, M. D.; Kalyanaraman, B. *Biochem. J.* 1986, **236**, 279-287.
33. Umezawa, T.; Kawai, S.; Yokota, S.; Higuchi, T. *Wood Res.* 1986, **73**, 8-17.
34. Kawai, S.; Umezawa, T.; Higuchi, T. *FEBS Lett.* 1987, **210**, 61-65.
35. Enoki, A.; Gold, M. H. *Arch. Microbiol.* 1982, **132**, 123-130.
36. Janshekar, H.; Haltmeier, T.; Brown, C. *Eur. J. Appl. Biotechn.* 1982, **14**, 174-181.
37. Haemmerli, S. D. Ph.D. Thesis ETH No. 8670, Swiss Federal Institute of Technology, Zürich, 1988.
38. Shimada, M.; Hattori, T.; Umezawa, T.; Higuchi, T.; Uzura, K. *FEBS Lett.* 1987, **221**, 327-331.
39. Hattori, T.; Shimada, M.; Umezawa, T.; Higuchi, T.; Leisola, M. S. A.; Fiechter, A. *Agric. Biol. Chem.* 1988, **52**, 879-880.
40. Shimada, M.; Nakatsubo, F.; Kirk, T. K.; Higuchi, T. *Arch. Microbiol.* 1981, **129**, 321-324.
41. Westermarck, U.; Eriksson, K. E. *Acta Chem. Scand.* 1974, **B28**, 209-214.
42. Kirk, T. K. In *Microbial Degradation of Organic Compounds*; Gibson D. T., Ed.; Marcel Dekker: New York, 1984; Chapter 14.
43. Leisola, M. S. A.; Schmidt, B.; Thanei-Wyss, U.; Fiechter, A. *FEBS Lett.* 1985, **189**, 267-270.
44. Umezawa, T.; Higuchi, T. *FEBS Lett.* 1985, **182**, 257-259.
45. Miki, K.; Renganathan, V.; Mayfield, M. B.; Gold, M. H. *FEBS Lett.* 1987, **210**, 199-203.
46. Janshekar, H.; Brown, C.; Haltmeier, T.; Leisola, M. S. A.; Fiechter, A. *Arch. Microbiol.* 1982, **132**, 14-21.
47. Chua, M. G. S.; Choi, S.; Kirk, T. K. *Holzforschung* 1983, **37**, 55-61.

RECEIVED March 10, 1989

## Chapter 34

# Oxidative Enzymes from the Lignin-Degrading Fungus *Pleurotus sajor-caju*

Robert Bourbonnais and Michael G. Paice

Pulp and Paper Research Institute of Canada, 570 St. John's Boulevard,  
Pointe Claire, Quebec H9R 3J9, Canada

Two extracellular oxidase enzymes proposed to play a role in lignin depolymerisation, laccase (polyphenol oxidase) and veratryl alcohol oxidase (VAO), were isolated from ligninolytic cultures of *Pleurotus sajor-caju*. The enzymes were produced in agitated, mycological broth cultures and were isolated after 12 days from supernatants by precipitation and chromatography. Two purified VAO enzymes had very similar physical and biochemical properties. They oxidised a variety of aromatic primary alcohols to aldehydes with reduction of oxygen to hydrogen peroxide. Sequential treatment of the laccase substrate ABTS with laccase and then VAO and veratryl alcohol produced first appearance and then disappearance of characteristic colors. A reduction-oxidation cycle is proposed for the two enzymes in depolymerisation of phenolic substructures of lignin.

White-rot fungi play a key role in biodegradation of woody materials. They are often the initial colonizers, and are probably the only microorganisms that extensively degrade lignin (1). The mechanism of lignin catabolism by *Phanerochaete chrysosporium* has been studied intensively, and a picture is now emerging of the enzymology involved. Lignin peroxidase, first recognized in 1983 (2,3), abstracts an electron from lignin substructures and subsequent free-radical transformations result in C $\alpha$ -C $\beta$ ,  $\beta$ -ether and aromatic ring cleavage (4,5). The reactions which are dependent on hydrogen peroxide can consume oxygen by addition of molecular oxygen to radical intermediates (6). Manganese peroxidase (7,8) is also produced by *P. chrysosporium* and abstracts electrons from lignin substructures with lower redox potentials such as phenolic units. The enzyme directly oxidised Mn II to Mn III as the initial step in lignin attack. Other enzymes

0097-6156/89/0399-0472\$06.00/0  
© 1989 American Chemical Society

implicated in lignin catabolism by *P. chrysosporium* are glucose oxidase (9,10) and glyoxal oxidase (11) for hydrogen peroxide production, and cellobiose quinone oxidoreductase (12) for quinone reduction. Since lignins can be both depolymerized and polymerized by lignin peroxidase (2,13), other enzymes are probably required for catabolism *in vivo*.

The question arises as to whether other white-rot fungi employ the same catabolic pathways as *P. chrysosporium*. Also, lignin degradation by *P. chrysosporium* occurs only during secondary metabolism, and employs veratryl alcohol, which is synthesized *de novo* by the fungus, as a mediator (14) or enzyme inducer (15). Are these conditions required by other fungi? It now appears that lignin peroxidase is produced by *Coriolus versicolor* (16) and perhaps by *Pleurotus ostreatus* (17). However these two white-rot fungi produce laccase isoenzymes which, like manganese peroxidase, can abstract electrons from phenolic substructures of lignin. Thus there appears to be no obvious requirement for manganese peroxidase in these fungi. In addition, it appears that *P. ostreatus* can degrade lignin effectively during primary metabolism, i.e. in a high nitrogen medium (18), although this has been disputed (19).

*Pleurotus sajor-caju* differs from *P. ostreatus* in not requiring cold-shock for fructification (20). *P. sajor-caju* selectively degrades lignin in wheat-straw under certain conditions (21,22), but this selectivity is lost when fruiting bodies form (23). Chlorolignin can be metabolised by *P. sajor-caju* (24). Waldner *et al.* (17) observed oxidation of veratryl alcohol to veratraldehyde by *P. ostreatus*. We have recently reported the discovery of a veratryl alcohol oxidase from *P. sajor-caju* (25). We now propose a role for the enzyme, in combination with laccase, in the depolymerization of phenolic moieties of lignin.

## Experimental

**Enzyme Production and Isolation.** The production and isolation of veratryl alcohol oxidase (VAO) was described earlier (25). Laccase produced from the same 12-day culture (8 litres) was isolated from the supernatant by precipitation at 0°C with ammonium sulfate (80% saturation). The precipitate was suspended in 0.05 M Na acetate buffer, pH 5.0 and dialysed overnight against 4 litres of buffer. The soluble material was concentrated by ultrafiltration (Amicon PM10) to about 60 mL and applied to a DEAE-Bio-gel A column (2.5 cm × 35 cm). The column was washed with 20 mL of the same buffer, then eluted with a linear gradient from 0 to 0.6 M NaCl (total volume 550 mL). Fractions were monitored for VAO and laccase activity as described below.

**Enzyme Assays.** Laccase activity was determined by oxidation of 2,2-azinobis-(3-ethylbenzthiazoline-6-sulfonate) (ABTS). The reaction of suitably diluted enzyme was determined at 420 nm in the presence of 0.03% ABTS and 100 mM sodium acetate buffer, pH 5.0. The extinction coefficient of ABTS is  $\epsilon_{420} = 3.6 \times 10^4 \text{ M}^{-1} \text{ cm}^{-1}$  (26).

VAO activity was measured with a mixture of 1 mM veratryl alcohol, 250 mM sodium tartrate buffer, pH 5.0 and enzyme. Oxidation to vera-

traldehyde was determined at 310 nm ( $\epsilon_{310} = 9300 \text{ M}^{-1} \text{ cm}^{-1}$ ). Lignin peroxidase was measured by veratryl alcohol oxidation at pH 3.0 in the presence of 0.4 mM  $\text{H}_2\text{O}_2$  (2). All enzyme units are  $\mu\text{mole}$  of product formed/min.

The combined effect of laccase and VAO on ABTS was determined as follows. The reagent (0.03%) was oxidised with purified laccase from *P. sajor-caju* (0.004 U/mL). After the appearance of the green (ABTS<sup>+</sup>) colour, VAO (0.07 U/mL) and veratryl alcohol (1 mM) was added and the decrease in colour was observed visually.

Oxygen uptake during substrate oxidation was measured with a Clark oxygen electrode (Rank Brothers, Cambridge, U.K.) at room temperature with 1 mM substrate in 0.25 mM sodium tartrate buffer, pH 3.0 (3 mL). Rates are expressed relative to veratryl alcohol oxidation.

## Results and Discussion

*Enzyme Production.* *P. sajor-caju*, when grown in a nutrient-rich medium under aerated, agitated conditions, was able to mineralize partially  $^{14}\text{C}$ -DHP lignin, as shown in Figure 1 (25).

Lignin peroxidase activity, (i.e., peroxide-dependent oxidation of veratryl alcohol at pH 3) was not detected over the 30 days tested, while laccase appeared at day 7. Culture medium from day 7 onwards could also oxidize veratryl alcohol to aldehyde with concomitant conversion of oxygen to hydrogen peroxide. This activity, which was optimal at pH 5.0, was named veratryl alcohol oxidase (VAO). The extracellular oxidative enzyme activities (laccase and veratryl alcohol oxidase) could be separated by ion-exchange chromatography (Figure 2). Further chromatography of the coincident laccase and veratryl alcohol oxidase (peak 2), as described elsewhere (25) resulted in the separation of two veratryl alcohol oxidases from the laccase.

*Enzyme Properties.* The two isolated veratryl alcohol oxidases had very similar properties (Table I). The difference in isoelectric points might be accounted for by aspartate content; all other amino acid contents except glycine were the same within experimental error (5%). The specific activities (veratryl alcohol as substrate) were significantly different, but both enzymes contained a flavin prosthetic group (25) and converted one molecule of oxygen to one molecule of hydrogen peroxide during alcohol oxidation.

Table I. Comparison of VAO I and II (Data summarized from ref. 25)

	VAO I	VAO II
Molecular weight	71,000	71,000
Isoelectric point	3.8	4.0
Glycosylated	yes	yes
Asp/mole	83	92
Gly/mole	77	66
Specific activity, IU/mg	35	31

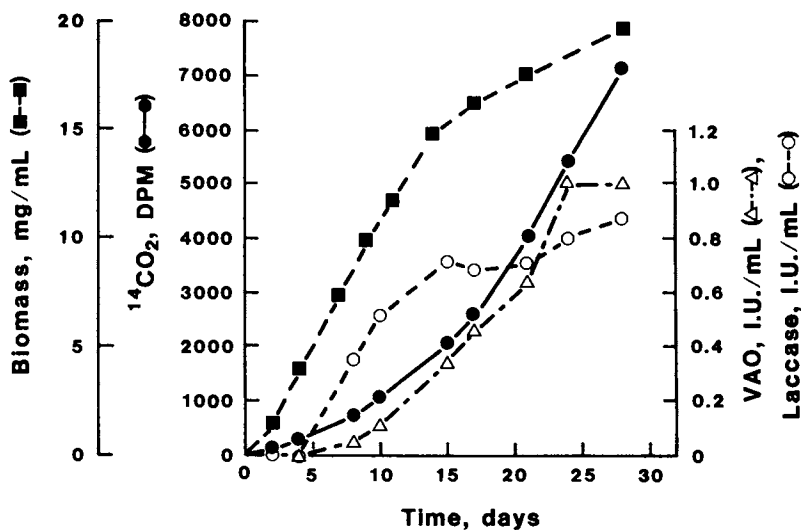


Figure 1. Time course of of ligninolytic activity (conversion of ring-labelled <sup>14</sup>C-DHP to <sup>14</sup>CO<sub>2</sub>), biomass concentration, VAO activity and laccase activity during growth of *Pleurotus sajor-caju* in agitated mycological broth cultures. (Reproduced with permission from Ref. 25, © 1988, Biochemical Society).

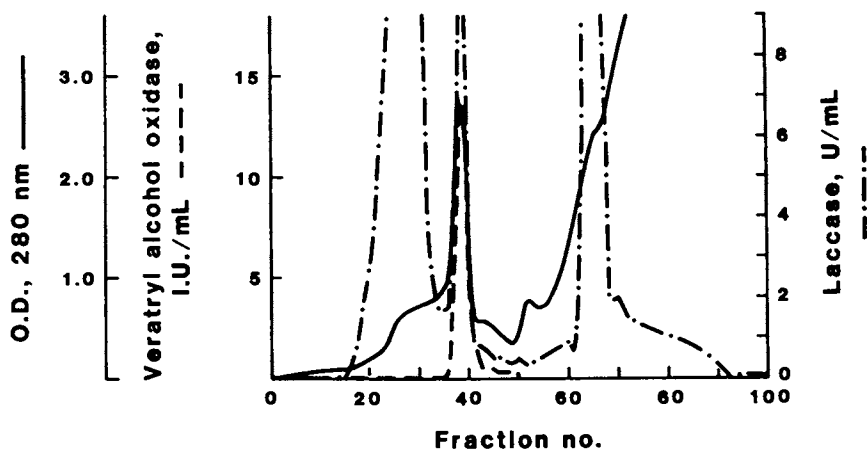


Figure 2. Elution profile of *P. sajor-caju* supernatant from DEAE-Bio-gel column, showing resolution of laccase and VAO peaks of activity.

p-Methoxybenzyl alcohol was oxidised fastest of the substrates tested. Some relative rates of oxidation, measured as oxygen consumption, are shown in Figures 3 and 4. Methoxy substituted benzyl alcohols showed wide variations in their relative rates of oxidation (Figure 3) which are not easily explained by electron availability. Para-hydroxyl substitution severely inhibited oxidation (Figure 4), even in  $\alpha, \beta$  unsubstituted aryl alcohols. Lignin model dimers, both phenolic and non-phenolic, and kraft lignin were not oxidised to any detectable extent.

The enzyme properties reported above are similar to those of an aromatic alcohol oxidase from *Polystictus versicolor* (27). However, the latter enzyme had a different substrate specificity and the cultures did not produce laccase.

**Possible Role in Lignin Biodegradation.** Oxidised products of veratryl alcohol have been proposed to play a key role in lignin peroxidase-mediated oxidation of lignin, either as one-electron carriers (14) or through further reaction which generates reactive oxygen species (28). Veratryl alcohol oxidases do not directly oxidize lignin, but they have a broad substrate range for monomeric aromatic alcohols and could therefore be involved in the final catabolic steps following depolymerization. It seems unlikely however, that the resulting aromatic aldehydes would *per se* oxidize lignin itself.

A possible reductive role for veratryl alcohol oxidase is proposed in Figure 5. Laccases from *C. versicolor* can produce both polymerization and depolymerization of lignin (29). In phenolic lignin model dimers, laccase can perform the same electron abstraction and subsequent bond cleavage as found for lignin peroxidase (30). The phenolic radical is however likely to polymerize unless the quinoid-type intermediates can be removed, for example by reduction back to the phenol. Veratryl alcohol oxidase, in

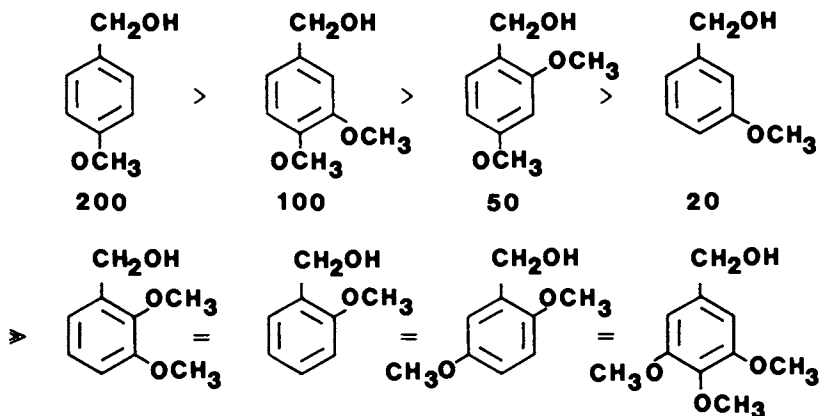


Figure 3. Relative oxidation rates of various methoxyl-substituted benzyl alcohols, measured by oxygen consumption/min. (veratryl alcohol = 100). No oxidation of the lower four alcohols was detected.



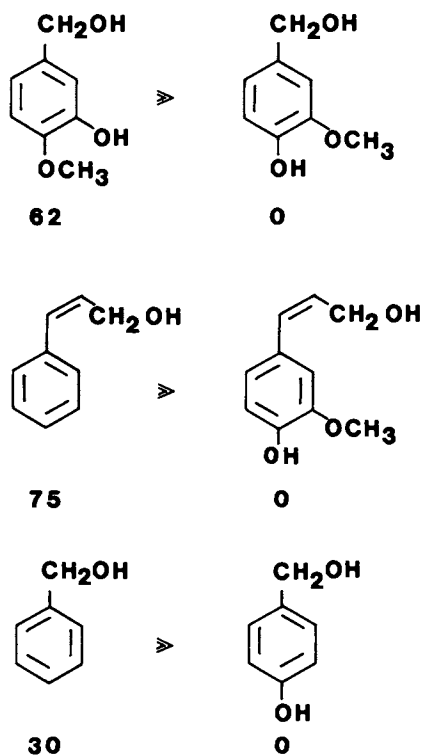


Figure 4. Relative oxidation rates of various aromatic alcohols. Para-hydroxyl substitution eliminates substrate oxidation.

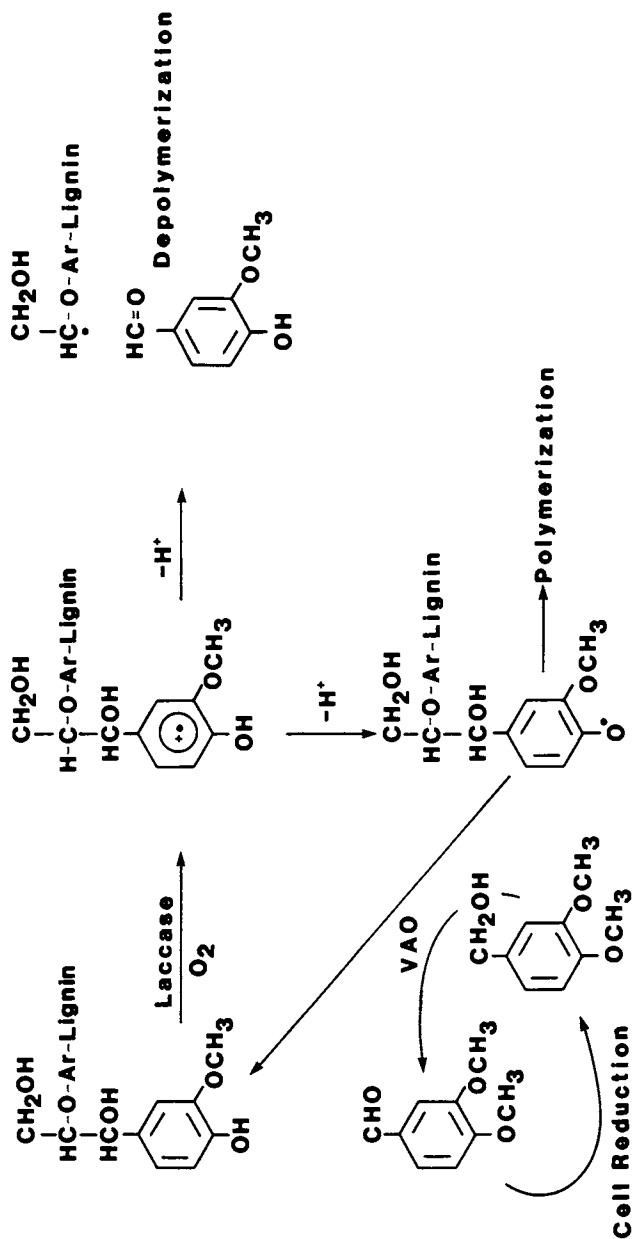


Figure 5. Proposed role of laccase and VAO in lignin depolymerisation.

the presence of veratryl alcohol or other cosubstrate, could provide this reducing power, as has been proposed previously for glucose oxidase (31) and cellobiose quinone oxidoreductase (12). In support of this hypothesis, we find that veratryl alcohol oxidase in the presence of veratryl alcohol will decolorize the oxidised products produced by laccase from ABTS.

### Acknowledgments

We thank F. Lafortune for excellent technical contribution. This work was supported in part with financial assistance from the National Research Council of Canada under Contribution number 949-6-0011.

### Literature Cited

1. Kirk, T. K.; Cowling, E. B. *The Chemistry of Solid Wood*; Amer. Chem. Soc.: Washington, D.C., 1984, p. 455-87.
2. Tien, M.; Kirk, T. K. *Science* 1983, **221**, 661-63.
3. Glenn, J.; Morgan, M. A.; Mayfield, M. B.; Kuwahara, M.; Gold, M. H. *Biochem. Biophys. Res. Commun.* 1983, **114**, 1077-83.
4. Schoemaker, H. E.; Harvey, P. J.; Bowen, R. M.; Palmer, J. M. *FEBS Lett.* 1985, **183**, 7-12.
5. Kersten, P. J.; Tien, M.; Kalyanaraman, B.; Kirk, T. K. *J. Biol. Chem.* 1985, **260**, 2609-12.
6. Miki, K.; Renganathan, V.; Gold, M. H. *Biochemistry* 1986, **26**, 4790-96.
7. Kuwahara, M.; Glenn, J. K.; Morgan, M. A.; Gold, M. H. *FEBS Lett.* 1984, **169**, 247-50.
8. Paszczynski, A.; Huynh, V. B.; Crawford, R. *Arch. Biochem. Biophys.* 1986, **244**, 750-65.
9. Ramasamy, K.; Kelley, R. L.; Reddy, C. A. *Biochem. Biophys. Res. Commun.* 1985, **131**, 436-41.
10. Eriksson, K. E.; Pettersson, B.; Vole, J.; Musilek, V. *Appl. Microbiol. Biotechnol.* 1986, **23**, 257-62.
11. Kersten, P. J.; Kirk, T. K. *J. Bacteriol.* 1987, **169**, 2195-2201.
12. Westermarck, U.; Eriksson, K. E. *Acta Chem. Scand.* 1987, **B29**, 419-24.
13. Haemmerli, S. D.; Leisola, M. S. A.; Fiechter, A. *FEMS Microbiol. Lett.* 1986, **35**, 33-36.
14. Harvey, P. J.; Schoemaker, H. E.; Palmer, J. M. *FEBS Lett.* 1986, **195**, 242-46.
15. Faison, B. D.; Kirk, T. K.; Farrell, R. L. *Appl. Environ. Microbiol.* 1986, **52**, 251-54.
16. Dodson, P. J.; Evans, C. S.; Harvey, P. J.; Palmer, J. M. *FEMS Microbiol. Lett.* 1987, **42**, 17-22.
17. Waldner, R.; Leisola, M.; Fiechter, A. *Proceeding Biotechnology in Pulp and Paper Industry*; 3rd Intl. Conf.; Stockholm 1986, 50-153.
18. Leatham, G. F.; Kirk, T. K. *FEMS Microbiol. Lett.* 1982, **16**, 65-67.
19. Commanday, F.; Macy, J. M. *Arch. Microbiol.* 1985, **142**, 61-65.
20. Mueller, J. C.; Gawley, J. R. *Mushroom Newsletter Tropics* 1983, **4**, 3-12.

21. Mueller, J. C.; Troesch, W. *Appl. Microbiol. Biotechnol.* 1986, **24**, 180-85.
22. Zadrazil, F. *Eur. J. Appl. Microbiol.* 1975, **1**, 327-335.
23. Tsang, L. J.; Reid, I. D.; Coxworth, E. C. *Appl. Environ. Microbiol.* 1987, **53**, 1304-06.
24. Bourbonnais, R.; Paice, M. G. *J. Wood Chem. Tech.* 1987, **7**, 51-64.
25. Bourbonnais, R.; Paice, M. G. *Biochem. J.* 1988, **255**, 445-50.
26. Wolfenden, B. S.; Willson, R. L. *J. Chem. Soc. Perkin Trans. II* 1982, 805-12.
27. Farmer, V.; Henderson, M. E. K.; Russell, J. D. *Biochem. J.* 1960, 257-62.
28. Haemmerli, S. D.; Schoemaker, H. E.; Schmidt, H. W. H.; Leisola, M. S. A. *FEBS Lett.* 1987, **220**, 279-87.
29. Morohoshi, N.; Nakamura, M.; Katayama, Y.; Haraguchi, T. *Pulping and Wood Chemistry Conf. Proceedings*; Paris, 1987, 305-15.
30. Kawai, S.; Umezawa, T.; Shimada, A. M.; Higuchi, T.; Koide, K.; Nishida, T.; Morohoshi, N.; Haraguchi, T. *Mokuzai Gakkaishi* 1987, **33**, 792-97.
31. Green, T. R. *Nature* 1977, **268**, 78-80.

RECEIVED March 17, 1989

## Chapter 35

# Mechanisms of Lignin Degradation by Lignin Peroxidase and Laccase of White-Rot Fungi

Takayoshi Higuchi

Wood Research Institute, Kyoto University, Uji, Kyoto 611, Japan

The main cleavage mechanisms of side-chains and aromatic rings of lignin model compounds and synthetic lignin (DHP) by lignin peroxidase and laccase of white-rot fungi have been elucidated. Tracer studies using  $^2\text{H}$ -,  $^{13}\text{C}$ - and  $^{18}\text{O}$ -labeled arylglycerol- $\beta$ -aryl ethers and diarylpropane-1,3-diols with  $^{18}\text{O}_2$  and  $\text{H}_2^{18}\text{O}$  indicated that side-chains and aromatic rings of these substrates were cleaved via aryl radical cation and phenoxy radical intermediates, in reactions mediated only by lignin peroxidase/ $\text{H}_2\text{O}_2$  and laccase/ $\text{O}_2$ .

The process of lignin biodegradation by microbes has evoked much interest in recent years (1-3). Several of these studies have been directed towards establishing the exact chemical mechanisms involved in lignin side-chain cleavage and aromatic ring-opening reactions, which are catalyzed by lignin peroxidase (4,5) and laccase (6). Almost all of these studies normally employ, as lignin-like substrates, various dimeric phenolic or nonphenolic model compounds which contain bonding patterns characteristic of substructures known to be present in isolated lignin preparations. For example, using  $\beta$ -1 and  $\beta$ -O-4 model compounds, it has been established that both lignin peroxidase and laccase catalyze one electron oxidations (5-7). In particular, lignin peroxidase converts both phenolic and nonphenolic moieties to their corresponding phenoxy radical and aryl radical cation intermediates, whereas laccase only catalyzes phenoxy radical formation from phenolic substrates; nonphenolic compounds are not oxidized (8). The aryl radical cations (formed from nonphenolic model compounds by lignin peroxidase/ $\text{H}_2\text{O}_2$ ) then undergo nucleophilic attack (e.g., by  $\text{H}_2\text{O}$ , or hydroxyl groups on adjacent functionalities) to generate aryl radical intermediates. Such reactive species, as well as the phenoxy radicals aforementioned, can then react with dioxygen radicals or alternatively they can

0097-6156/89/0399-0482\$06.00/0  
© 1989 American Chemical Society

undergo free radical coupling reactions. Thus two competing reactions can occur during lignin biodegradation: (1) reaction with dioxygen radicals resulting in lignin degradation and (2) free radical coupling leading to repolymerization. These findings help explain the current difficulties experienced in efficiently degrading the lignin polymer *in vitro* with isolated enzyme preparations (1).

At this juncture, it is pertinent to briefly describe our current understanding of lignin formation in xylem cell walls (9). Initially, free radical coupling of intermediates, formed from the corresponding monolignols via mediation of cell wall peroxidases and  $H_2O_2$ , affords dimeric quinone methides; subsequent nucleophilic attack (e.g., by  $H_2O$  or adjacent hydroxyl groups) results in rearomatization to afford dilignols, such as dehydrodiconiferyl alcohol, d,l-pinoresinol, guaiacylglycerol- $\beta$ -coniferyl ether, etc. These phenols can then be reconverted into their free radical forms, which then (in an analogous manner) undergo coupling and rearomatization to give the corresponding oligolignols. Repetition of these reactions results in lignin formation; this process is often described as dehydrogenative polymerization (Fig. 1). In our opinion, the reactions involved in lignin biodegradation (as catalyzed by lignin peroxidase and laccase) can be considered as an extension of the reactions encountered in lignin formation. We propose this idea since, as discussed later, it appears that degradation of the lignin polymer involves similar reactions.

In this chapter, some of the main reactions in lignin biodegradation (i.e., side-chain cleavage and aromatic ring-opening) are described, and the effects of both laccase and lignin peroxidase compared. The schemes proposed are all based on identified products from model compounds and supported wherever possible by appropriate labelling studies. Finally, the processes of lignin biosynthesis and biodegradation are compared.

## Results and Discussion

### *Side-Chain Cleavage Reactions of $\beta$ -1 and $\beta$ -O-4 Lignin Model Compounds Catalyzed by Lignin Peroxidase.*

**$\beta$ -1 Model Compounds.** These can be separated into two broad categories: nonphenolic and phenolic. As can be seen from Figure 2, the nonphenolic  $\beta$ -1 lignin model compound **1** is first converted into its aryl radical cation intermediate. This then undergoes  $C\alpha$ - $C\beta$  homolytic cleavage to afford 3,4,5-trimethoxybenzaldehyde **2**, and the diol **3**, with the latter trapping oxygen as shown by appropriate labelling experiments with  $^{18}O_2$  (Fig. 2) (4,10). The generality of this mechanism was demonstrated using a number of methoxybenzenes and diarylethane dimers as substrates (7,11). Reaction progress was monitored by ESR spectrometry (11); mechanisms were further established by using model compounds specifically deuterated at  $C\alpha$  and  $C\beta$  as required (12).

While the corresponding phenolic  $\beta$ -1 model compounds are also subject to  $C\alpha$ - $C\beta$  cleavage, other reactions can also occur (13). Figure 3 summarizes the main reactions identified to this point. These include (i)  $C\alpha$ - $C\beta$  cleavage of **4** to afford syringaldehyde **6** and the diol, **7**, (ii)  $C\alpha$  oxidation and dehydration to give the ketone **5** and (iii) alkyl-aryl cleavage to give the degradation products **8** and **9** respectively (13).

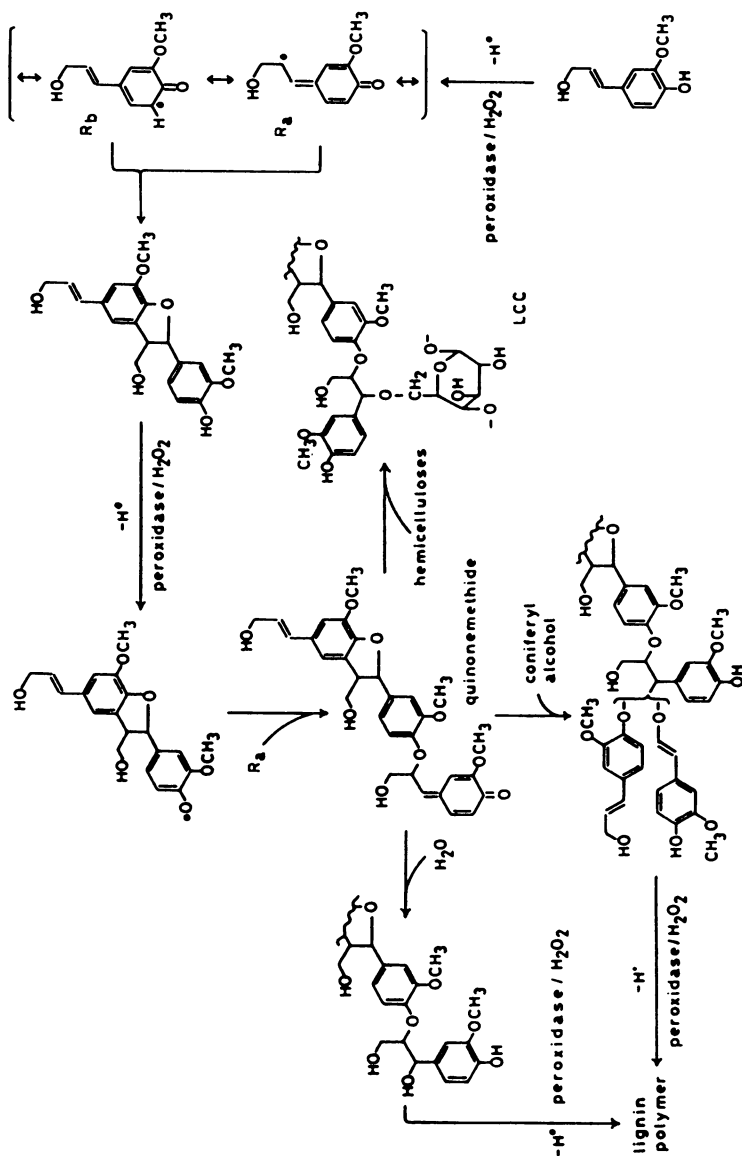


Figure 1. Formation of guaiacyl lignin and lignin-carbohydrate complexes (LCC) via dehydrogenative polymerization of coniferyl alcohol.

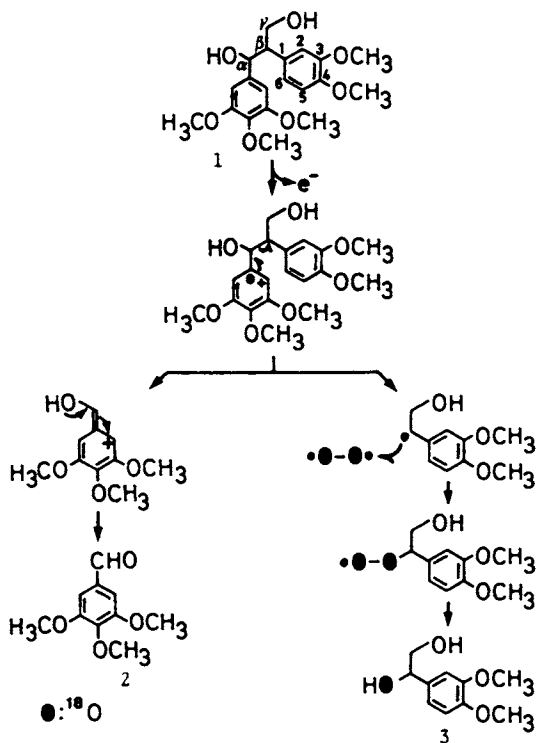


Figure 2. Side-chain cleavage of a nonphenolic  $\beta$ -1 model compound **1** by lignin peroxidase.



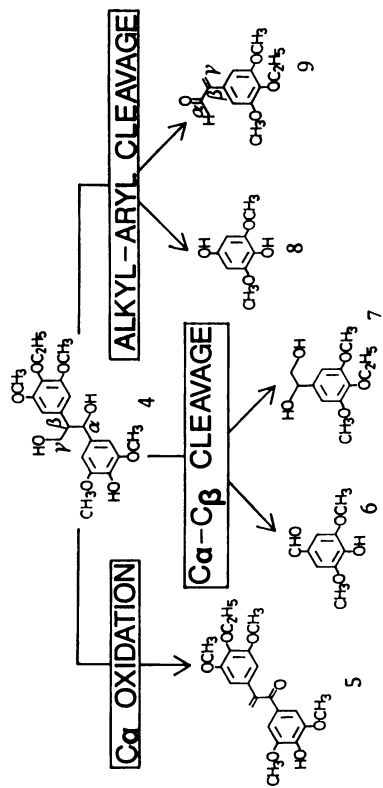


Figure 3. Possible degradation pathways of the phenolic  $\beta$ -1 model compound 4 by lignin peroxidase.

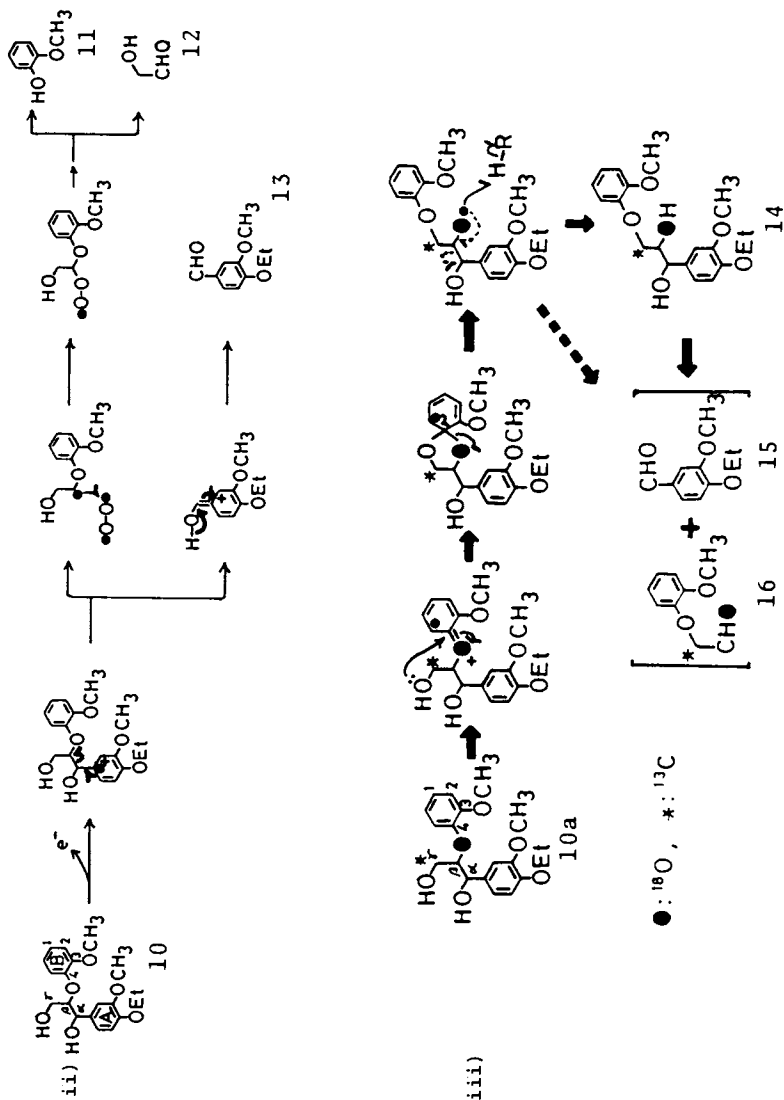
**$\beta$ -O-4 Model Compounds.** Investigations were conducted using both nonphenolic and phenolic lignin model substrates. Studies (12,14,15) with the nonphenolic dimer **10** revealed that four main reaction pathways were possible: (i) benzylic oxidation ( $C\alpha$ ) to give the corresponding ketone (not shown); (ii) formation of the aryl radical cation intermediate as before, followed by fragmentation to afford guaiacol **11**, the glycolic aldehyde **12** and 4-ethoxy-3-methoxybenzaldehyde **13** (Fig. 4, pathway ii); (iii) aryl radical cation formation, subsequent intermolecular nucleophilic attack by the  $\gamma$ -hydroxyl group and rearrangement, to give the isomeric diol **14** followed by homolytic cleavage to afford the aldehyde **15** and 2-(2'-methoxyphenol) acetaldehyde **16**. These unusual reactions were confirmed by labelling studies as shown (Fig. 4, pathway iii), and (iv) displacement and/or aromatic ring displacement to yield the triol **19** and *o*-quinone **20** (Fig. 4, pathway iv) (3).

Studies (16) employing phenolic  $\beta$ -O-4 model substrates revealed three major reactions, reminiscent of those previously described in Figure 3, i.e., (i) benzylic oxidation, (ii)  $C\alpha$ - $C\beta$  cleavage to give either the corresponding  $C\alpha$  aldehyde or acid; and (iii) alkyl-aryl bond rupture to give the hydroquinone (cf. 8, Fig. 3) and the corresponding glyceraldehyde-2-aryl ether.

*Side Chain Cleavage of  $\beta$ -1 and  $\beta$ -O-4 Model Compounds by Laccase.*

**$\beta$ -1 Model Compounds.** Only substrates with phenolic functionalities were examined, since nonphenolic substrates were unaffected. Thus, the two phenolic diols **4** and **21** were synthesized (6), and both were individually exposed to laccase from *Coriolus versicolor* (6). For diol **4**, alkyl-aryl cleavage gave 2,6-dimethoxyhydroquinone **8**, the corresponding benzoquinone **23** and the aldehyde **24** (Fig. 5, pathway B);  $C\alpha$  oxidation also afforded the ketone **22** (pathway A). Additionally, other reactions were also observed (Fig. 6), namely  $C\alpha$ - $C\beta$  cleavage to give syringaldehyde **6**, and the aryl keto-alcohol **25** (Fig. 6, pathway A). On the other hand, diol **21** only underwent  $C\alpha$ - $C\beta$  cleavage, generating the substituted benzaldehyde **27** and the phenylglycol **26** (Fig. 6, pathway B). Note that these mechanisms were based upon appropriate labelling studies using  $^{18}O_2$  (6). Thus, reactions involving phenolic substrates, and using both lignin peroxidase and laccase are similar; both encompass  $C\alpha$ - $C\beta$ , alkyl-aryl bond cleavages and oxidative reactions.

**$\beta$ -O-4 Model Compounds.** In this investigation, the substrate used for incubation with laccase was the model compound, syringylglycerol- $\beta$ -guaiacyl ether **28** (18). It was initially reported that this underwent conversion into glyceraldehyde-2-guaiacyl ether and 2,6-dimethoxybenzoquinone (17). Additionally, the hydroxyl group of the hydroquinone was labelled with  $^{18}O$ , when the experiment was carried out in the presence of  $H_2^{18}O$ . However, more comprehensive studies (18) have demonstrated that the dimer **28** also undergoes benzylic oxidation to give the ketone **29**, and  $C\alpha$ - $C\beta$  cleavage to afford guaiacol **11** and syringic acid **30** (Fig. 7). Thus, once again, the reactions catalyzed by laccase (for these phenolic substrates) show considerable resemblance to that already noted for lignin peroxidase.



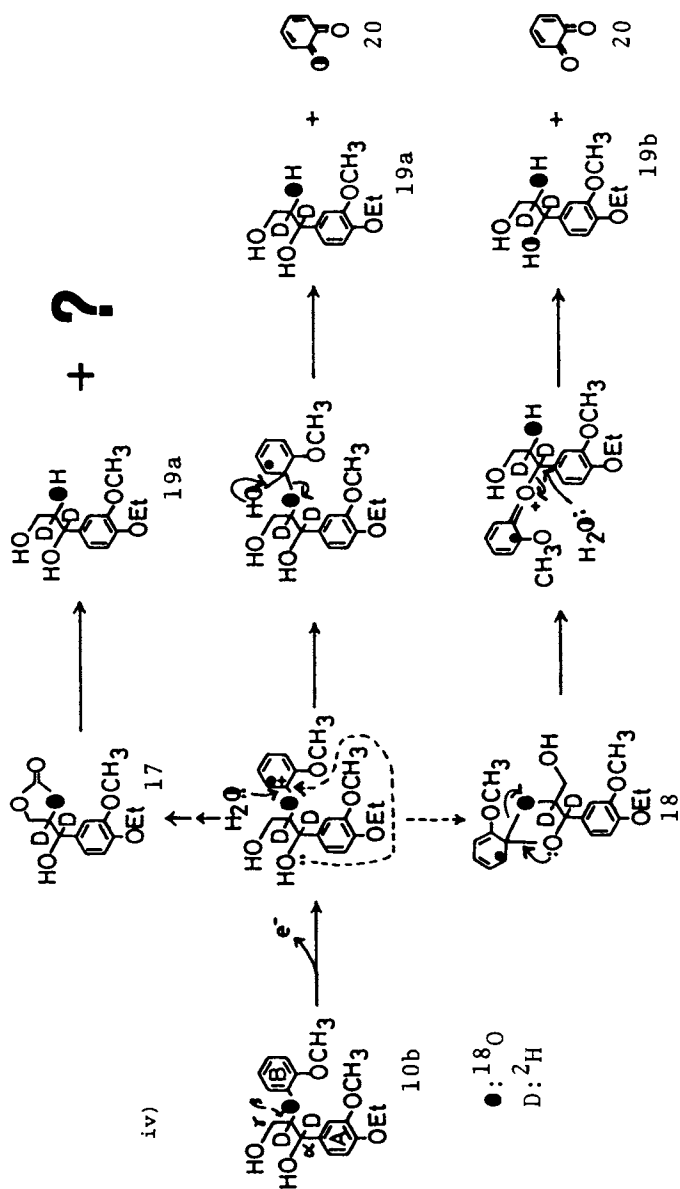


Figure 4. Side-chain cleavage of nonphenolic  $\beta$ -O-4 model compounds 10, 10a and 10b by lignin peroxidase.  $\circ = ^{18}\text{O}$ ;  $\square = ^2\text{H}$ .

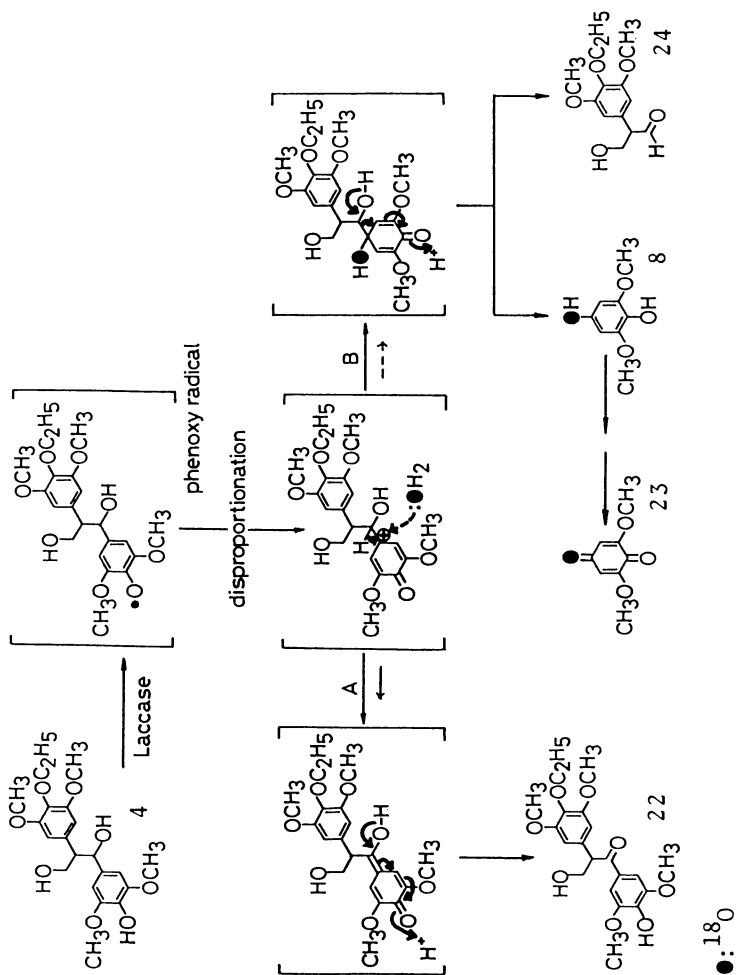


Figure 5. Possible mechanisms for C $\alpha$  oxidation (A) and alkyl-aryl cleavage (B) reactions of a phenolic  $\beta$ -1 model compound 4 by laccase.

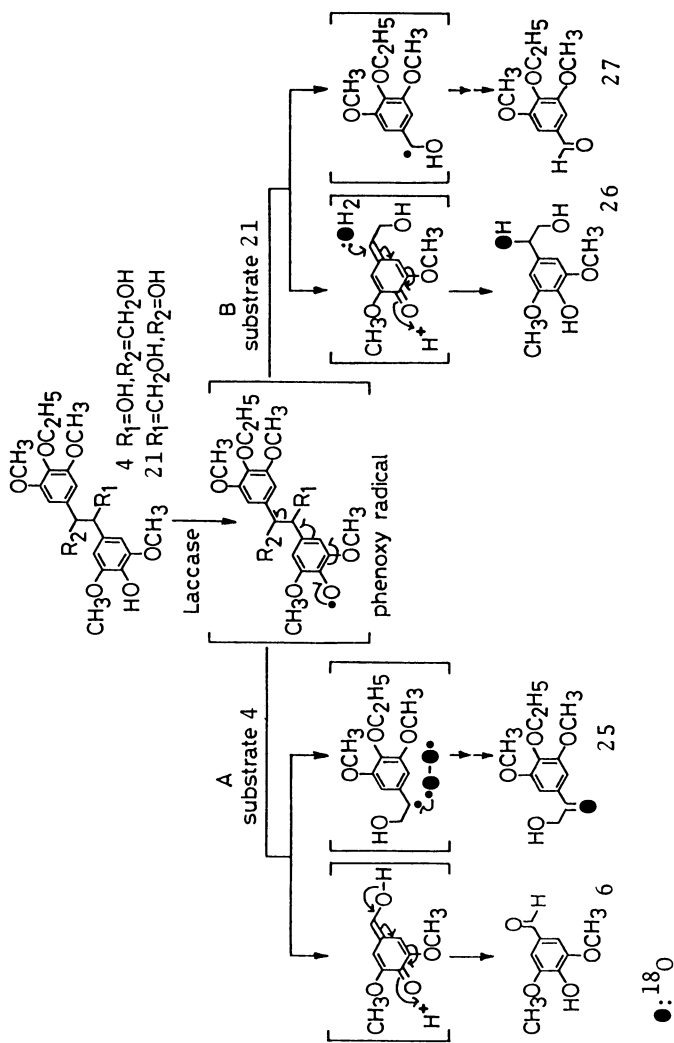


Figure 6. Possible mechanisms for  $\text{C}\alpha\text{-C}\beta$  cleavage of phenolic  $\beta\text{-1}$  model compounds **4** and **21** by laccase.

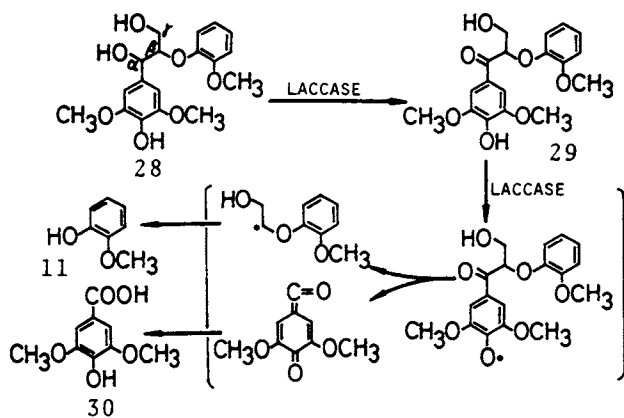


Figure 7. Side-chain cleavage of a phenolic  $\beta$ -O-4 model compound **28** by laccase.

*Aromatic Ring Cleavage of Nonphenolic  $\beta$ -O-4 Lignin Substructure Model Compounds and Veratryl Alcohol by Lignin Peroxidase.*

*$\beta$ -O-4 Model Compounds.* Three model compounds 31-33 were synthesized (19,20), and treated with lignin peroxidase as before. This resulted in their conversion into the arylglycerol cyclic carbonates 37-39, the O-formates 40,41, and the methyl oxalate derivatives 34-36. A fourth model compound 42 was also synthesized, and this underwent degradation to give the methyl oxalate derivative 44 and cis-cis muconate derivatives 43 (19,20). Labelling experiments, with  $^{18}\text{O}_2$  and  $\text{H}_2^{18}\text{O}$ , respectively, demonstrated that only one of the oxygens on the carbonyl groups of the methyl oxalate 34 and muconates 43 were  $^{18}\text{O}_2$  derived, with the other being formed from  $\text{H}_2^{18}\text{O}$  (Fig. 8) (19). To account for the formation of 43 as initial ring cleavage products, the hypothetical scheme shown in Figure 9 is proposed; initial formation of the aryl radical cation intermediate occurs which can then react with  $\text{H}_2\text{O}$ ,  $\text{O}_2$  and hydrogen radicals as shown. The mechanisms for the formation of other ring cleavage products 34-41 via aryl radical cation intermediates are shown in the chapter by Umezawa and Higuchi.

*Veratryl Alcohol.* Leisola *et al.* (21,22) recently reported that treatment of veratryl alcohol 45 with lignin peroxidase resulted mainly in the formation of veratryl aldehyde 49, the two  $\gamma$ -lactones 46 and 47 (Fig. 10) and several other quinones not shown. We (23,24) have established that the  $\delta$ -lactone 48 was also formed. When experiments were conducted in the presence of  $^{18}\text{O}_2$  and  $\text{H}_2^{18}\text{O}$ , regiospecific incorporation into products 46 and 47 was observed (Fig. 11). This regiospecificity did not occur during  $\delta$ -lactone 48 formation, although the reasons for this are not clear. [Note also that when vanillyl alcohol was used as substrate, the main products were the biphenyl  $\text{C}_5$ - $\text{C}_5$  adducts, together with small amounts of  $\delta$ -lactones (25).]

*Aromatic Ring Cleavage of Phenolic  $\beta$ -O-4 Substructure Model Compounds by Laccase.* When vanillyl alcohol was used as a substrate, only biphenyl formation ( $\text{C}_5$ - $\text{C}_5$  linked) occurred and no evidence for the formation of any ring-opened products was obtained (26). Hence, we also examined the effect of laccase on the sterically hindered 4,6-di-*t*-butylguaiaicol substrate 50, as it would be unlikely to undergo such free-radical coupling reactions (27). Treatment of the phenol 50 with laccase only afforded the muconolactone derivative 51 (Fig. 12). Interestingly, only oxygen from  $^{18}\text{O}_2$ , and not  $\text{H}_2^{18}\text{O}$ , was incorporated into this product (Fig. 13) (28).

*Aromatic Ring Cleavage of Artificial (DHP) Lignin by Lignin Peroxidase.* As discussed, our previous studies established that the aromatic rings of nonphenolic  $\beta$ -O-4 model compounds underwent opening to give cis,cis-muconate derivatives as their initial products (Fig. 9). However, these studies provided no information as to whether higher oligomers, or indeed, the lignin polymer itself, would undergo such reactions.

Since it is generally viewed that coniferous lignin has almost 40% of its linkages connected via  $\beta$ -O-4 bonds, these aforementioned results suggest that a lignin polymer connected primarily via such linkages should



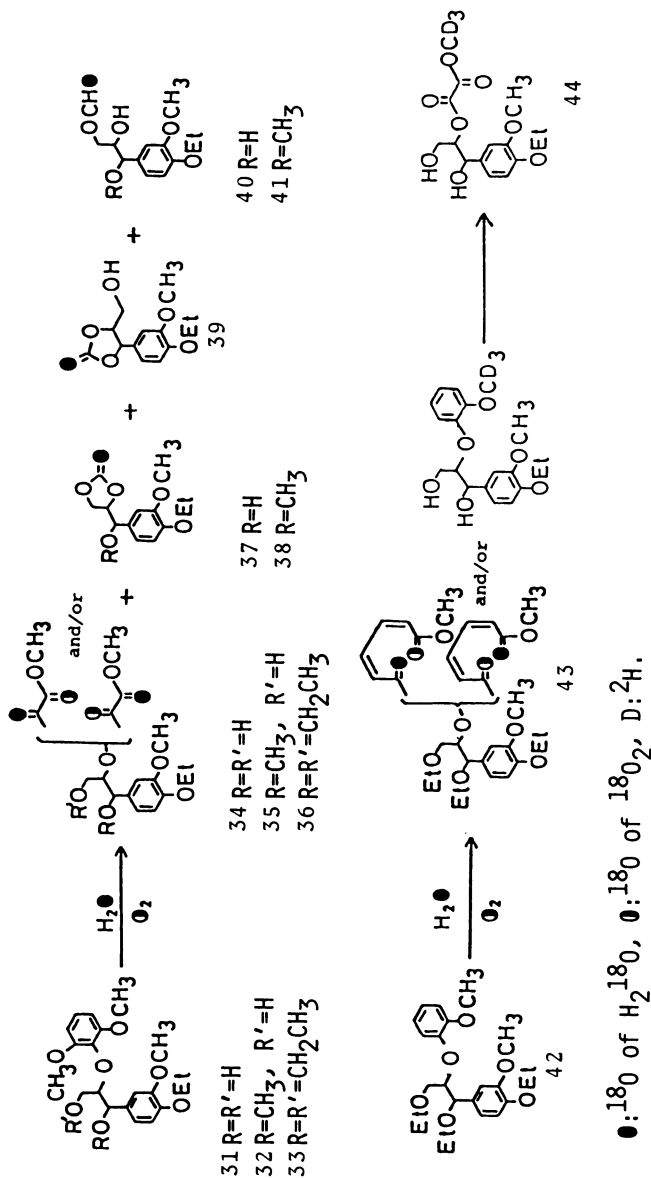


Figure 8. Aromatic ring cleavage of nonphenolic  $\beta$ -O-4 model compounds 31-33 by lignin peroxidase.

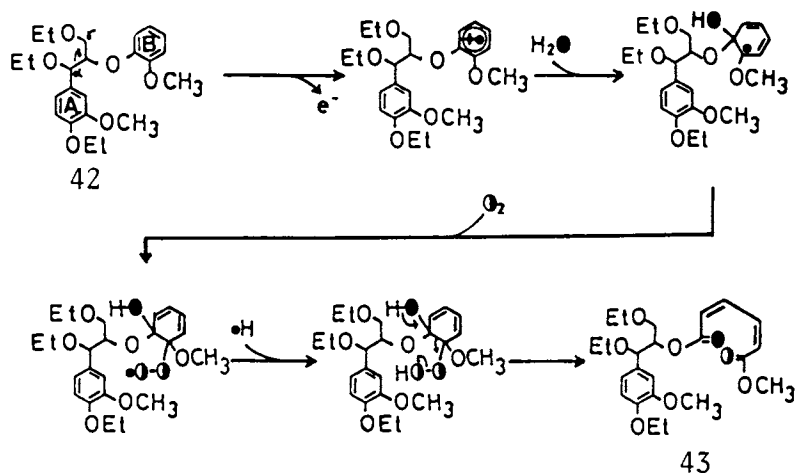


Figure 9. Mechanism for the formation of arylglycerol cis-cis muconate **43** by lignin peroxidase from the nonphenolic  $\beta$ -O-4 model compound **42**.

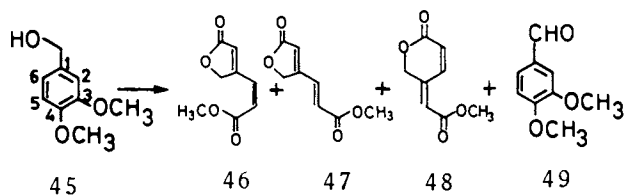


Figure 10. Degradation of veratryl alcohol **45** by lignin peroxidase.

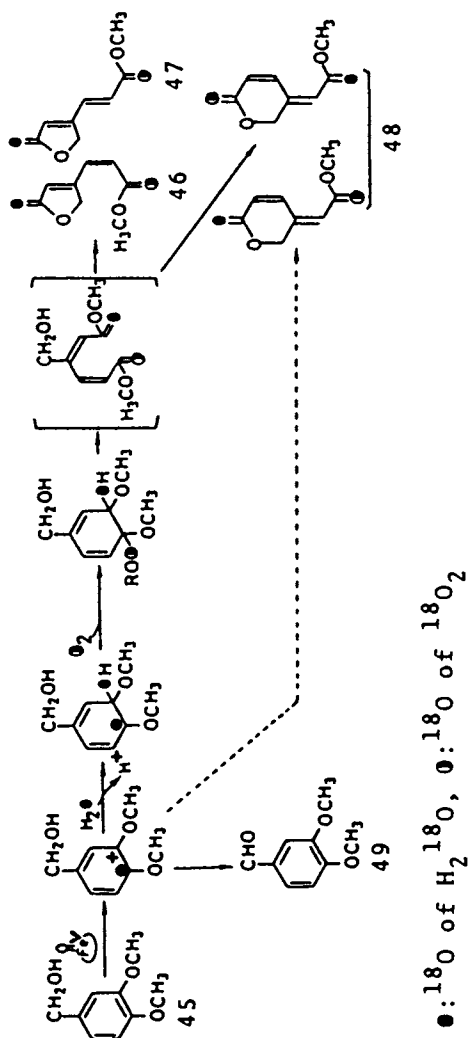


Figure 11. Mechanisms for the degradation of veratryl alcohol 45 by lignin peroxidase.

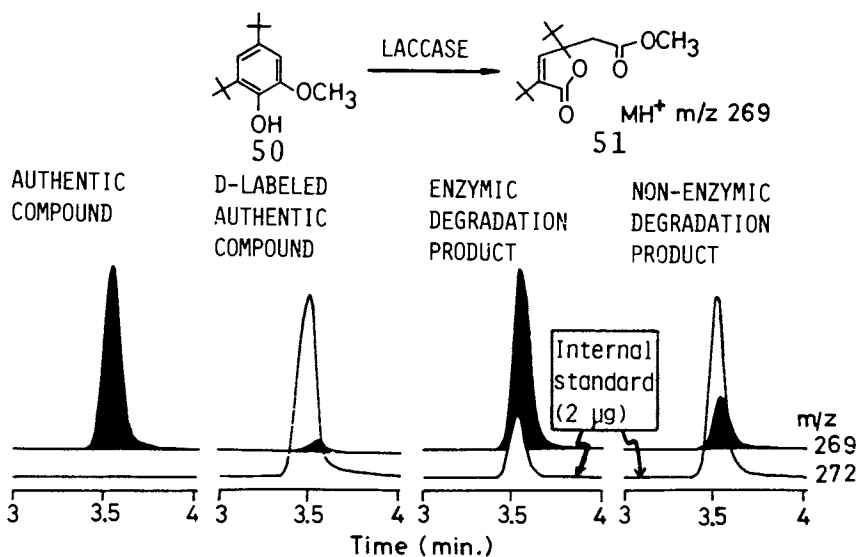


Figure 12. Mass chromatograms of degradation product **51** of 4,6-di-*t*-butylguaiacol **50** by laccase.

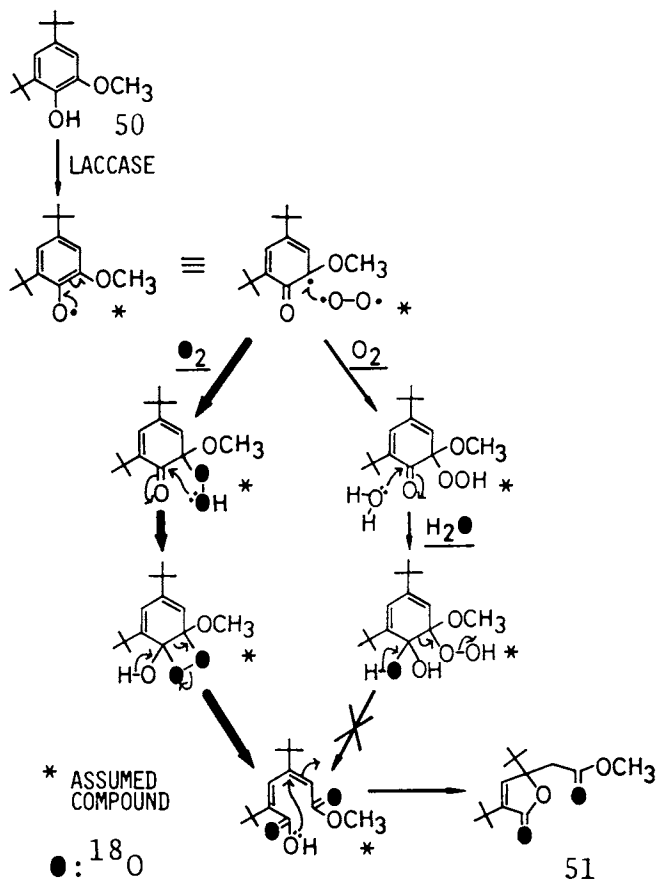


Figure 13. Proposed mechanisms for aromatic ring cleavage of 4,6-di-t-butylguaiacol 50 by laccase.

undergo similar degradative reactions. Lignin is often represented by various synthetic dehydrogenatively polymerized (DHP) preparations, produced via the peroxidase/H<sub>2</sub>O<sub>2</sub> induced polymerization of monolignol(s) (29). However, depending upon the polymerization process employed (Zulauf or Zutropf) the  $\beta$ -O-4 linkage frequency can vary from 10-40% (29). Consequently, we prepared a synthetic DHP lignin polymer from coniferyl alcohol via the Zutropf method, hence maximizing the  $\beta$ -O-4 linkage frequency. Following incubation of this synthetic polymer, with lignin peroxidase/H<sub>2</sub>O<sub>2</sub>, the degraded products were subjected to gel permeation chromatography using Sephadex LH20. The elution profile revealed that partial depolymerization had occurred (30). GC-MS analysis also revealed that a small amount of vanillin was formed via C $\alpha$ -C $\beta$  cleavage. Surprisingly, *no* aromatic ring cleavage products were observed.

Thus another DHP, prepared from a mixture of 4-ethoxy-3-methoxyphenylglycerol- $\beta$ -syringaresininol ether **51** and coniferyl alcohol **52** was synthesized (31). This polymer was of interest as it now contained the more readily cleavable  $\beta$ -O-4 syringyl linkages. Following DHP formation, the polymers were ethylated with diazoethane. The resulting ethylated polymer product **53** was then applied to a Sephadex LH20 column, with DMF as eluent. The higher molecular weight fraction eluted (MW > 2200) was then used as a substrate for lignin peroxidase/H<sub>2</sub>O<sub>2</sub> treatment. Following treatment with lignin peroxidase/H<sub>2</sub>O<sub>2</sub>, the degraded DHP polymer so obtained was acetylated and the resulting products partially purified by thin layer chromatography and analyzed by gas chromatography-mass spectroscopy (GC-MS). From this mixture, the arylglycerol cyclic carbonates **37**, **39**, and formate **40** were identified, together with 4-ethoxy-3-methoxyphenylglycerol (Fig. 14). These results therefore established that lignin peroxidase/H<sub>2</sub>O<sub>2</sub> catalyzes side-chain cleavage and aromatic ring-opening reactions of ethylated DHP lignin polymers, in agreement with the results previously obtained from the model systems.

### Conclusions

Over recent years, considerable progress has been made in elucidating the biochemical processes of lignin formation (biosynthesis) and lignin biodegradation. Table I summarizes, and compares, the main reactions involved in both processes. In our opinion, the overall chemical principles leading to both formation and degradation are similar.

Our investigations indicate that lignin can be degraded into smaller fragments via aryl radical cation and phenoxy radical intermediates, in a reaction mediated by only lignin peroxidase/H<sub>2</sub>O<sub>2</sub> and laccase/O<sub>2</sub>. However, it has been shown that *in vitro* some of the lignin is polymerized, probably via coupling reaction of phenoxy radicals of phenolic moieties of lignin, during treatment with lignin peroxidase (32) or laccase (33) in aqueous solution. Protolignin, on the other hand, which is present in the plant cell walls in association with polysaccharides, seems to be degraded smoothly to lower molecular weight fractions. Thus, the reaction conditions preventing repolymerization during *in vivo* lignin biodegradation need to be identified.

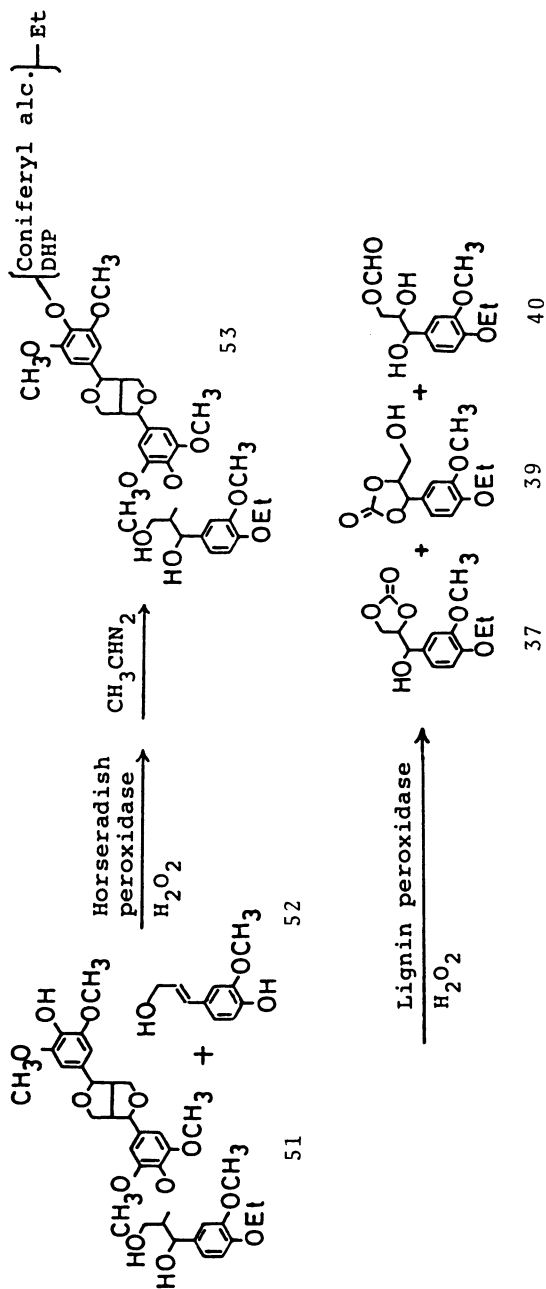


Figure 14. Aromatic ring-opening reactions of a DHP **53** by lignin peroxidase. (The DHP polymer **53** was prepared from 4-ethoxy-3-methoxyphenylglycerol- $\beta$ -syringaresinol ether **51** and coniferyl alcohol **52**.)

Table I. Comparison of Lignin Biosynthesis and Biodegradation Mechanisms

Biosynthesis	Biodegradation
<i>Enzymatic Reaction:</i>	<i>Enzymatic Reaction:</i>
1. Cell wall peroxidase/H <sub>2</sub> O <sub>2</sub> → Formation of phenoxy radicals of monolignols	1. Lignin peroxidase/H <sub>2</sub> O <sub>2</sub> → Formation of aryl radical cations of nonphenolic units
	2. Laccase/O <sub>2</sub> → Formation of phenoxy radicals of phenolic units
<i>Non-enzymatic Reaction:</i>	<i>Non-enzymatic Reaction:</i>
1. Coupling of phenoxy radicals to give dimeric quinone methides	1. Homolytic or heterolytic cleavage of side-chains (C $\alpha$ -C $\beta$ , alkyl-phenyl) and aromatic rings
2. Dioxygen radical attack on carbon-centered radicals	2. Dioxygen radical attack on carbon-centered radical intermediates
3. Nucleophilic attack on quinone methides by H <sub>2</sub> O and R-OH to give dilignols and higher oligomers	3. Nucleophilic attack on aryl cations and C $\alpha$ cations by H <sub>2</sub> O and R-OH to give degradation products

### Acknowledgments

This paper was prepared based on our recent work on lignin biodegradation in the Research Section of Lignin Chemistry. The author is indebted to Dr. M. Shimada, Dr. T. Umezawa, Messrs. S. Kawai, T. Habe, S. Yokota and T. Hattori in this section for their cooperation for this investigation.

### Literature Cited

1. Kirk, T. K.; Farrell, R. L. *Ann. Rev. Microbiol.* 1987, **41**, 465-505.
2. Higuchi, T. *Wood Res.* 1986, **73**, 58-81.
3. Buswell, J. A.; Odier, E. *CRC Rev. Biotechnol.* 1987, **6**, 1-60.
4. Tien, M.; Kirk, T. K. *Proc. Natl. Acad. Sci. USA* 1984, **81**, 2280-84.
5. Umezawa, T.; Higuchi, T. *FEBS Lett.* 1988, **218**, 255-60.
6. Kawai, S.; Umezawa, T.; Higuchi, T. *Arch. Biochem. Biophys.* 1988, **262**, 111-17.
7. Kersten, P. J.; Tien, M.; Kalyanarama, B.; Kirk, T. K. *J. Biol. Chem.* 1985, **260**, 2609-12.
8. Kawai, S.; Umezawa, T.; Shimada, M.; Higuchi, T.; Koide, K.; Nishida, T.; Morohoshi, N.; Haraguchi, T. *Mokuzai Gakkaishi* 1987, **33**, 792-97.
9. Higuchi, T. In *Biosynthesis and Biodegradation of Wood Components*; Higuchi, T., Ed.; Academic Press: Orlando, FL, 1985; Ch. 7.



10. Kuwahara, M.; Glenn, J. K.; Morgan, M. A.; Gold, M. H. *FEBS Lett.* 1984, **169**, 247-50.
11. Hammel, K. E.; Tien, M.; Kalyanarama, B.; Kirk, T. K. *J. Biol. Chem.* 1985, **260**, 8348-53.
12. Habe, T.; Shimada, M.; Umezawa, T.; Higuchi, T. *Agric. Biol. Chem.* 1985, **49**, 3505-10.
13. Yokota, S.; Umezawa, T.; Kawai, S.; Higuchi, T. *Abst. 38th Mtg. Japan Wood Res. Soc.* 1988, Asahikawa, Japan.
14. Umezawa, T.; Higuchi, T. *FEBS Lett.* 1985, **192**, 147-50.
15. Umezawa, T.; Higuchi, T. *FEMS Microbiol. Lett.* 1985, **26**, 123-26.
16. Yokota, S.; Umezawa, T.; Higuchi, T., unpublished.
17. Higuchi, T. In *Biosynthesis and Biodegradation of Wood Components*; Higuchi, T., Ed.; Academic Press: Orlando, FL, 1985; Ch. 20.
18. Kawai, S.; Umezawa, T.; Higuchi, T., unpublished.
19. Umezawa, T.; Higuchi, T. *FEBS Lett.* 1986, **205**, 293-98.
20. Umezawa, T.; Higuchi, T. *Agric. Biol. Chem.* 1987, **51**, 2281-84.
21. Leisola, M. S. A.; Schmidt, B.; Thanei-Wyss, U.; Fiechter, A. *FEBS Lett.* 1985, **189**, 267-90.
22. Leisola, M. S. A.; Haemmerli, S. D.; Smit, J. D. G.; Troller, J.; Waldner, R.; Schoemaker, H. E.; Schmidt, H. In *Lignin Enzymic and Microbial Degradation*, INRA Ed.; INRA: Paris, 1987; pp. 81-86.
23. Shimada, M.; Hattori, T.; Umezawa, T.; Higuchi, T.; Uzura, K. *FEBS Lett.* 1987, **221**, 327-31.
24. Hattori, T.; Shimada, M.; Umezawa, T.; Higuchi, T.; Uzura, K. *Agric. Biol. Chem.* 1988, **52**, 879-80.
25. Hattori, T., *et al.*, unpublished.
26. Kawai, S.; Umezawa, T.; Higuchi, T. *Abst. 38th Ann. Mtg. Japan Wood Res. Soc.* 1988, Asahikawa, Japan.
27. Gierer, J.; Imsgard, F. *Acta Chem. Scand.* 1977, **31**, 546-50.
28. Kawai, S.; Umezawa, T.; Shimada, M.; Higuchi, T. *FEBS Lett.* 1988, **236**, 309-11.
29. Sarkanen, K. V. In *Lignins: Occurrence, Formation, Structure and Reactions*; Sarkanen, K. V.; Ludwig, C. H., Eds.; Wiley-Interscience: New York, 1971; Ch. 4.
30. Umezawa, T.; Higuchi, T. *Abst. 38th Ann. Mtg. Japan Wood Res. Soc.* 1988, Asahikawa, Japan.
31. Umezawa, T.; Higuchi, T. *FEBS Lett.* 1989, **242**, 325-29.
32. Haemmerli, S. D.; Leisola, M. S. A.; Fiechter, A. *FEMS Microbiol. Lett.* 1986, **35**, 33-36.
33. Ishihara, T.; Miyazaki, M. *Mokuzai Gakkaishi* 1972, **18**, 416-19.

RECEIVED May 19, 1989

## Chapter 36

# Aromatic Ring Cleavage by Lignin Peroxidase

Toshiaki Umezawa and Takayoshi Higuchi

Research Section of Lignin Chemistry, Wood Research Institute, Kyoto University, Uji, Kyoto 611, Japan

Aromatic ring cleavages by white-rot fungi and by the enzyme lignin peroxidase are reviewed. Intact cells of white-rot fungi cleave aromatic rings of lignin substructure model compounds as well as polymeric lignin. Lignin peroxidase of *Phanerochaete chrysosporium* catalyzes the ring cleavage of  $\beta$ -0-4 lignin substructure model compounds and synthetic lignin (DHP). A mechanism for the ring cleavage by the enzyme is described.

Lignin biodegradation has been studied by two complementary approaches: (i) degradation of polymeric lignins (such as the dehydrogenation polymer of coniferyl alcohol (DHP), milled wood lignin, or wood *per se*) (1); and (ii) degradation of lignin substructure model compounds (2,3). In the early 1980's, analysis of lignin isolated from wood decayed by white-rot basidiomycetes had provided a general outline of lignin biodegradation. For example, cleavage of side chains and aromatic rings occurred during degradation of polymeric lignin by the fungi (1).

Lignin is a complex and heterogeneous polymer consisting of phenylpropane units connected via many C-C and C-O-C linkages. Thus, the elucidation of specific reactions involved in lignin biodegradation has been performed mainly with lignin substructure model compounds as substrate for fungal degradation. By the early 1980's, substructure model studies identified many of the degradative reactions suggested from polymeric lignin biodegradation such as C $\alpha$ -C $\beta$  cleavage of propyl side-chain and cleavage of  $\beta$ -0-4 bonds (2,3).

On the other hand, aromatic ring cleavage products of lignin substructure models by white-rot basidiomycetes were not identified until 1985, although earlier studies of the polymeric lignin degradation suggested the involvement of ring cleavage reactions (1). We identified for the first time aromatic ring cleavage products of a  $\beta$ -0-4 lignin substructure model dimer

0097-6156/89/0399-0503\$06.00/0

© 1989 American Chemical Society

produced by intact cells of the white-rot basidiomycete, *Phanerochaete chrysosporium* (4,5). Subsequently, we showed that the aromatic ring cleavage of the dimer was catalyzed by an extracellular enzyme of the fungus, lignin peroxidase (ligninase) (6-8), and proposed a mechanism of the ring cleavage by the enzyme (9).

The purpose of the present paper is to describe the aromatic ring cleavage of lignin substructure model compounds by white-rot basidiomycetes and by lignin peroxidase of *P. chrysosporium*. The aromatic ring cleavage of synthetic lignin (DHP) by the enzyme will also be described.

### Aromatic Ring Cleavage by Intact Cells of White-Rot Basidiomycetes

Earlier studies of fungus-degraded lignin isolated from decayed wood suggested cleavage of aromatic rings of lignin (1,10-15). However, the products of aromatic ring cleavage of lignin substructure model compounds by white-rot basidiomycetes were not identified until 1985 (4), while products of side-chain cleavage of lignin substructure model compounds by the fungi were identified earlier (2,3). During this study, we identified for the first time a product of aromatic ring cleavage of  $\beta$ -0-4 lignin substructure model compound **1** by *P. chrysosporium*, namely the  $\beta,\gamma$ -cyclic carbonate of arylglycerol **8** (4) (Fig. 1).

Subsequently, several esters of arylglycerol were identified as products of aromatic ring cleavage of  $\beta$ -0-4 lignin substructure model dimers **2** and **3** by the fungus:  $\alpha,\beta$ -cyclic carbonate of arylglycerol **9**,  $\gamma$ -formate of arylglycerol **11**, and methyl oxalate of arylglycerol **10** (Fig. 1) (5).

<sup>13</sup>C-tracer experiments with 1,3-dihydroxy-1-(4-ethoxy-3-methoxyphenyl)-2-[U-ring-<sup>13</sup>C](2-methoxyphenoxy)propane and 1,3-dihydroxy-1-(4-ethoxy-3-methoxyphenol)-2-[U-ring-<sup>13</sup>C](2,6-dimethoxyphenoxy)propane as substrates confirmed that the products were ring cleavage products.

Formation of these aromatic ring cleavage products was not limited to *P. chrysosporium*, but could be mediated by other white-rot basidiomycetes, *Coriolus versicolor* (16) and *Coriolus hirsutus* (17). In the degradation of **1**, **2** and **4** by *C. versicolor*, **8**, **9**, and **11** were identified as ring cleavage products. As for *C. hirsutus*, **8** and **9** were identified as ring cleavage products from degradation of **1** (Fig. 1).

### Aromatic Ring Cleavage of $\beta$ -0-4 Lignin Substructure Model Dimers by Lignin Peroxidase

Leisola *et al.* reported the aromatic ring cleavage of a monomeric aromatic compound, veratryl alcohol, by lignin peroxidase of *P. chrysosporium* (18), although they stated that the products were only tentatively identified. We showed, on the basis of firm identification of the products with synthetic authentic samples, that lignin peroxidase isolated from the fungus by a modification of the method of Tien and Kirk (19), catalyzed the aromatic ring cleavage of  $\beta$ -0-4 lignin substructure model dimers (6-8). Aromatic ring cleavage products formed in the intact culture of the fungus (Fig. 1)

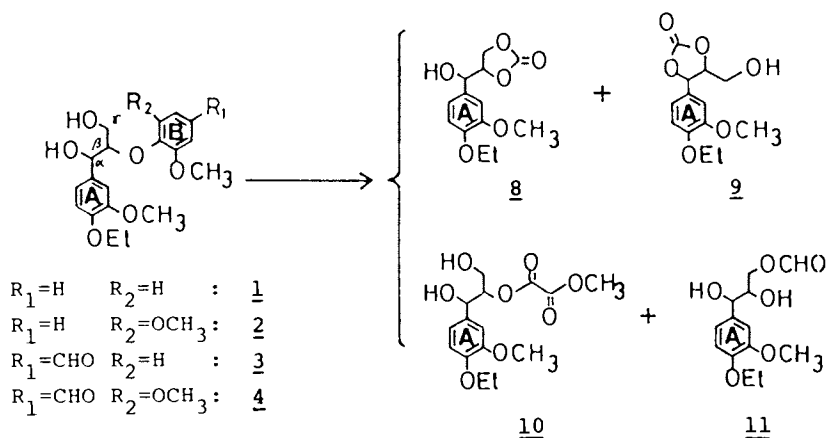


Figure 1.  $\beta$ -0-4 lignin substructure model dimers **1-4** and their degradation by white-rot fungi, *Phanerochaete chrysosporium*, *Coriolus versicolor*, and *Coriolus hirsutus*. The ether bond between the C $\beta$  and the B-aromatic nucleus is referred to as " $\beta$ -0-4 bond" in lignin chemistry.

were also produced by the enzyme. Aromatic ring cleavage products with the enzyme were cyclic carbonates of arylglycerols **8** and **9**, formate of arylglycerol **11**, methyl oxalates of arylglycerols **10** and **10-Et**, and a novel product, muconate of arylglycerol **12-Et** (Fig. 2). All the products were confirmed to be aromatic ring cleavage products by using ring-<sup>13</sup>C labeled substrates. Subsequently, Miki *et al.* reported formation of aromatic ring cleavage products involving cyclic carbonates similar to **8** and **9** in the degradation of a  $\beta$ -0-4 lignin model compound by the enzyme (20).

The muconate of arylglycerol **12-Et** retains all six carbon atoms of the B-ring of the substrate **1-Et**. Hence, this product seemed to be appropriate to examine mechanisms for the ring cleavage. Based on the results of tracer experiments, we proposed a ring cleavage mechanism for the enzyme (7,9), as now described. Degradation of 1,3-dihydroxyl-1-(4-ethoxy-3-methoxyphenyl)-2-(2-[OC<sup>2</sup>H<sub>3</sub>]methoxyphenoxy) propane **1-D** by the enzyme showed that the methyl group of methyl ester of oxalate **10-D** was derived from the methoxyl group of the B-ring of the substrate **1-D** (Fig. 3) (7). This result indicated that demethylation (or demethoxylation) which was previously postulated for the ring cleavage by the fungus (13) is not a prerequisite for the aromatic ring cleavage by the enzyme, and that the ring cleavage by the enzyme is completely different from the ring cleavage catalyzed by conventional dioxygenases (21).  $\beta$ -0-4 lignin model compounds **2**, **2-Me**, **2-Et** and **1-Et** were degraded under H<sub>2</sub><sup>18</sup>O or <sup>18</sup>O<sub>2</sub> (Fig. 4), and GC-MS analysis of the products showed that one of the carbonyl oxygen atoms of muconate **12-Et** and oxalates **10**, **10-Me** and **10-Et** was derived from H<sub>2</sub>O and the other from O<sub>2</sub>. As for cyclic carbonates **8**, **8-Me** and **9** and formates **11** and **11-Me**, the carbonyl oxygen atoms were derived from H<sub>2</sub>O (Fig. 4). Based on these results, we proposed a mechanism for aromatic ring cleavage by the enzyme which involves single electron oxidation of the B-ring to the corresponding cation radical, followed by nucleophilic attack of H<sub>2</sub>O and radical coupling with O<sub>2</sub> (or a radical species derived from O<sub>2</sub> (Fig. 5) (9)).

Similar mechanisms were also proposed for the ring cleavage of veratryl alcohol (22,23) and a  $\beta$ -0-4 lignin substructure model (24) by the enzyme.

As described in the previous section, the formation of the ring cleavage products **8**, **9** and **11** from  $\beta$ -0-4 lignin substructure models were also mediated by *C. versicolor* (16) and *C. hirsutus* (17). It is most likely that the aromatic ring cleavage by both fungi is mediated by an enzyme similar to lignin peroxidase of *P. chrysosporium*. Recently, it was shown that *C. versicolor* produces an enzyme similar to *P. chrysosporium* lignin peroxidase (25), although concrete evidence that the enzyme catalyzes the ring cleavage has not been shown.

### Aromatic Ring Cleavage of a ( $\beta$ -0-4)-( $\beta$ -0-4) Lignin Substructure Model Trimer by Lignin Peroxidase

Mechanisms which involve the cation radical intermediate were also proposed for the cleavage of C $\alpha$ -C $\beta$  and  $\beta$ -0-4 bonds of  $\beta$ -0-4 lignin substructure models by the enzyme (26,27). Thus, mechanisms for most of the



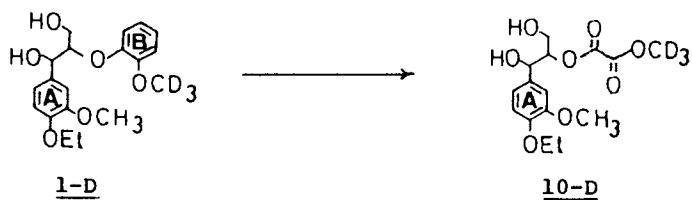


Figure 3. Methyl group of methyl oxalate was derived from methoxyl group of the B-ring of  $\beta$ -0-4 lignin model dimer **1-D**.





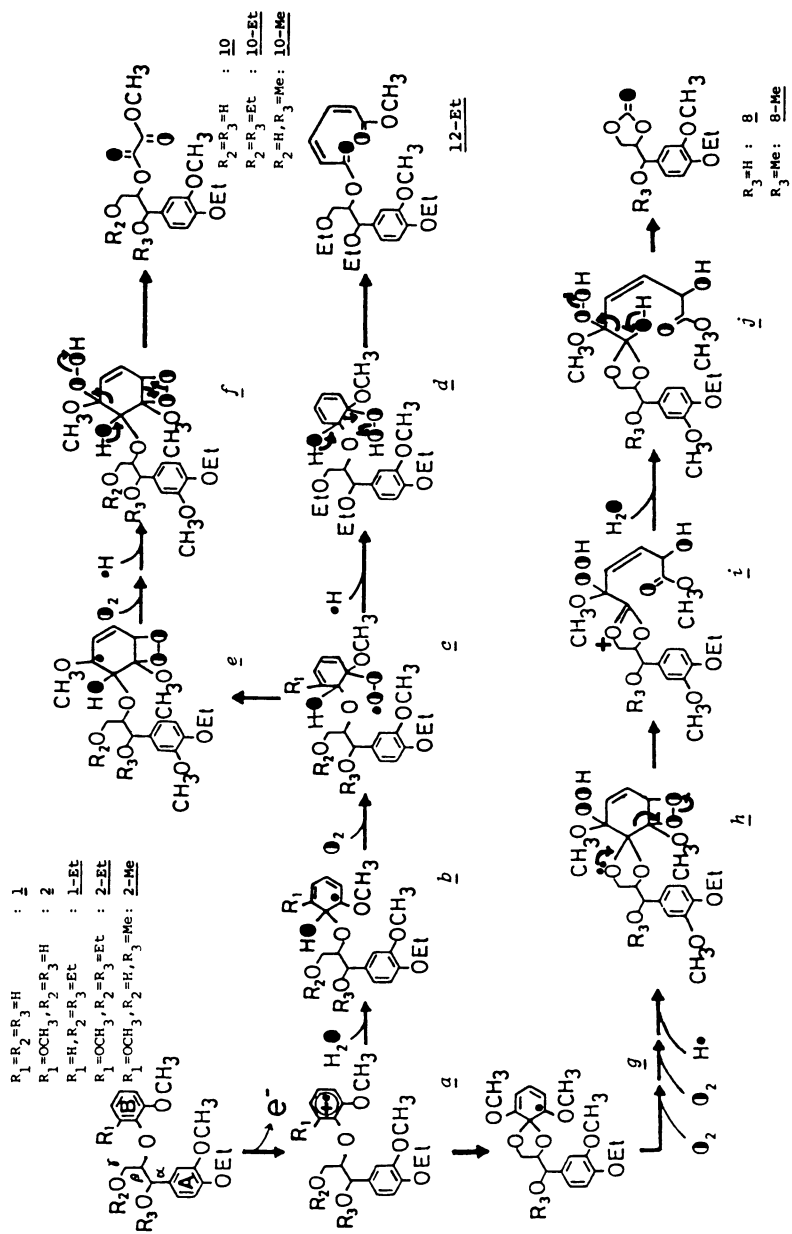


Figure 5. Proposed mechanisms for aromatic ring cleavage of  $\beta$ -O-4 lignin substructure model dimers by lignin peroxidases.

degradative reactions of  $\beta$ -0-4 lignin substructure models by the enzyme can be explained on the basis of single electron oxidation of aromatic rings.

On the other hand, aromatic ring cleavage of polymeric lignin by the enzyme has not been reported. The formation of B-ring cleavage products of  $\beta$ -0-4 lignin substructure models by the enzyme (Fig. 2) was expected to be an indicator of aromatic ring cleavage in polymeric lignin by the enzyme. However, the  $\beta$ -0-4 lignin model compounds used in the model studies have no propyl side-chain on the B-ring as shown in Figures 1 and 2, while the B-rings present in polymeric lignin have propyl side-chains. Furthermore, previous investigations showed that the aromatic substituents such as formyl or methoxyl groups influenced drastically the degradability of the  $\beta$ -0-4 lignin substructure models by the enzyme (6,26,27).

Hence, we examined the effect of the propyl side-chain of the B-ring on the B-ring cleavage by the enzyme using a lignin substructure model trimer composed of two  $\beta$ -0-4 substructures **5** (Fig. 6) (28). Identified degradation products by the enzyme were as follows (Fig. 6): Cyclic carbonates and formate of arylglycerol as B-ring cleavage products **8**, **9** and **11**; arylglycerol **13** and its  $\alpha$ -carbonyl derivative **14** as cleavage products of the  $\beta$ -0-4 bond between A- and B-rings; 4-ethoxy-3-methoxybenzaldehyde **15** as a  $\text{C}\alpha$ - $\text{C}\beta$  cleavage product between A- and B-rings; and 1,3-dihydroxy-1-(4-ethoxy-3-methoxyphenyl)-2-(4-formyl-2-methoxyphenoxy)propane **3** as a product of  $\text{C}\alpha$ - $\text{C}\beta$  cleavage between B- and C-rings. The results showed that the propyl side-chain of the B-ring of **5** did not influence, at least qualitatively, the aromatic ring cleavage by the enzyme.

The results suggested that polymeric lignin is degraded through the cleavage reaction of aromatic rings by the enzyme. In fact, aromatic ring cleavage of DHP (synthetic lignin) by the enzyme has now been proven as discussed in the following section.

### Aromatic Ring Cleavage of DHP by Lignin Peroxidase

Reaction mechanisms for degradation of  $\beta$ -0-4 lignin substructure model compounds by lignin peroxidase are being clarified rapidly, while the action of the enzyme on polymeric lignin is not fully elucidated. Tien and Kirk (29) reported degradation of methylated spruce lignin by the enzyme. They showed formation of low molecular weight degradation products on the basis of gel filtration with Sephadex LH-20, and detected a  $\text{C}\alpha$ - $\text{C}\beta$  cleavage product by an isotope trapping method (29). On the other hand, according to Haemmerli *et al.*, when polymeric lignin, phenolic hydroxyl groups of which are not alkylated, were treated by the enzyme, polymerization of the lignin occurred on the basis of gel filtration analysis of the degradation products (30). They monitored the chromatographic profile by a UV-detector. The results were confirmed by Odier *et al.* (31) by using  $^{14}\text{C}$ -labelled DHP as substrate.

Thus, for the degradation of polymeric lignin by the enzyme, two major questions were left: (i) Can lignin peroxidase, by itself, depolymerize polymeric lignin without repolymerization or not? (ii) Can lignin peroxidase cleave aromatic rings and  $\beta$ -0-4 bonds of polymeric lignin, or not?

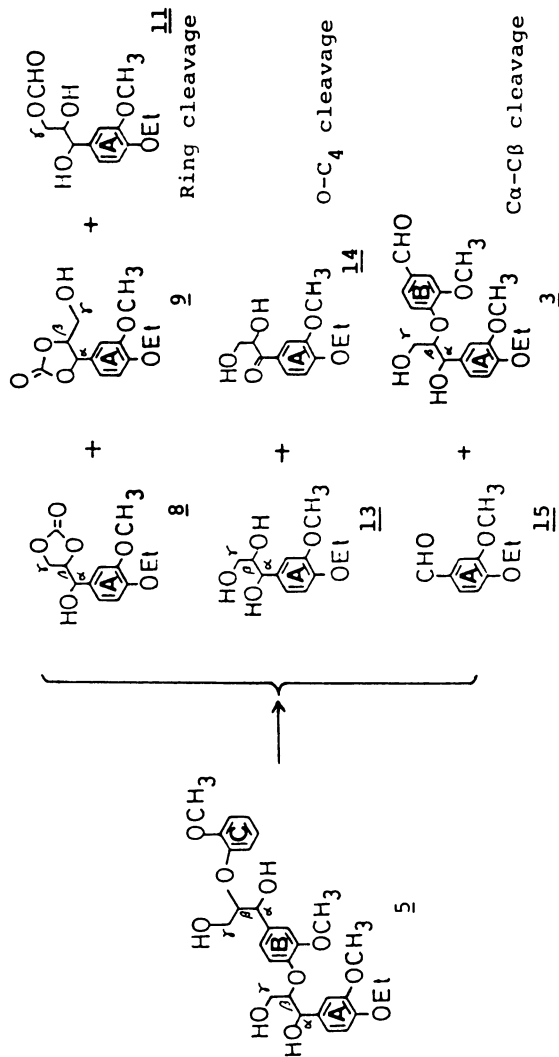


Figure 6.  $(\beta-0-4)$ - $(\beta-0-4)$  lignin substructure model trimer **6** and its degradation products by lignin peroxidase.

Since we have been investigating the aromatic ring cleavage of  $\beta$ -0-4 lignin substructure model compounds by intact cells of white-rot fungi and lignin peroxidase of *P. chrysosporium* as described above, we examined the aromatic ring cleavage and  $\beta$ -0-4 bond cleavage of polymeric lignin by lignin peroxidase.

We synthesized a copolymer of ( $\beta$ -0-4)-( $\beta$ - $\beta$ ) lignin substructure model trimer **6** and coniferyl alcohol **7**, which will be referred to as ( $\beta$ -0-4)-( $\beta$ - $\beta$ )-DHP in this review (Fig. 7). The ( $\beta$ -0-4)-( $\beta$ - $\beta$ )-DHP was ethylated with diazoethane and the ethylation product **16** was submitted to gel filtration (LH-20/DMF) to remove low molecular weight fractions. The high molecular weight fraction of the ethylated ( $\beta$ -0-4)-( $\beta$ - $\beta$ )-DHP **16** thus obtained (molecular weight > 2200, calibrated with polystyrene, Fig. 8) was degraded by lignin peroxidase. The degradation products were extracted with ethyl acetate, acetylated and partially purified by thin-layer chromatography (TLC). Gas chromatography mass spectroscopic (GC-MS) analysis of the TLC purified fraction showed the formation of cyclic carbonates of arylglycerol **8** and **9**, formate of arylglycerol **11**, arylglycerol **13**, and  $\alpha$ -carbonyl-aryl glycerol **14** (Fig. 9) (32). Since the compounds were previously identified as aromatic ring cleavage products and  $\beta$ -0-4 bond cleavage products of  $\beta$ -0-4 lignin substructure model compounds by the enzyme (Figs. 2 and 6), the results show that lignin peroxidase cleaves aromatic rings and  $\beta$ -0-4 bonds of the synthetic lignin (DHP).

Thus, most of the degradative reactions of polymeric lignins suggested previously by the analysis of decayed lignin isolated from decayed wood by white-rot fungi were catalyzed by lignin peroxidase.

### Aromatic Ring Cleavage of Monomeric Aromatic Compounds by White-Rot Basidiomycetes

Monomeric aromatic compounds such as vanillic acid and syringic acid are known to be produced in the degradation of polymeric lignin by white-rot basidiomycetes (13,14,33). It is still uncertain to what extent aromatic rings of polymeric lignin are cleaved by lignin peroxidase, as opposed to being degraded via sidechain cleavages to produce the monomeric C6-C1 intermediates such as vanillic acid and syringic acid. Furthermore, the fate of the monomeric degradation intermediates is not fully elucidated. Ander *et al.* (34) proposed a degradation pathway of vanillic acid via 1,2,4-trihydroxybenzene by intact cells of *Sporotrichum pulverulentum* (= *P. chrysosporium*). This pathway involves decarboxylation of vanillic acid catalyzed by vanillate hydroxylase to produce methoxyhydroquinone (35,36), followed by demethylation and subsequent aromatic ring cleavage of the demethylated product, 1,2,4-trihydroxybenzene, catalyzed by a dioxygenase of the fungus (37). On the other hand, the role of lignin peroxidase in the metabolism of these aromatic monomers remains uncertain, although a non-phenolic aromatic monomer, veratryl alcohol which is synthesized *de novo* by *P. chrysosporium*, is oxidized by lignin peroxidase to produce mainly veratraldehyde and trace amounts of aromatic ring cleavage products (18,22).

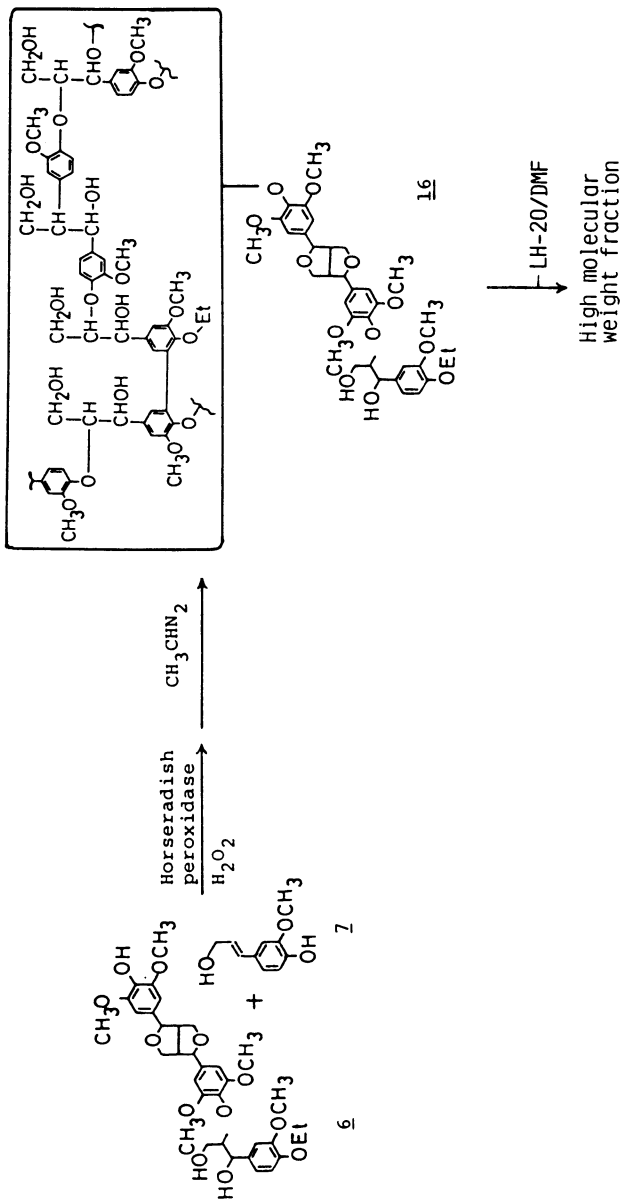


Figure 7. Preparation of synthetic lignin **16**, ethylated copolymer of the coniferyl alcohol **7** and arylglycerol- $\beta$ -syngaresinol ether **6**. In **16**, the rectangular enclosure represents an assumed structure of the moiety derived from **7**.

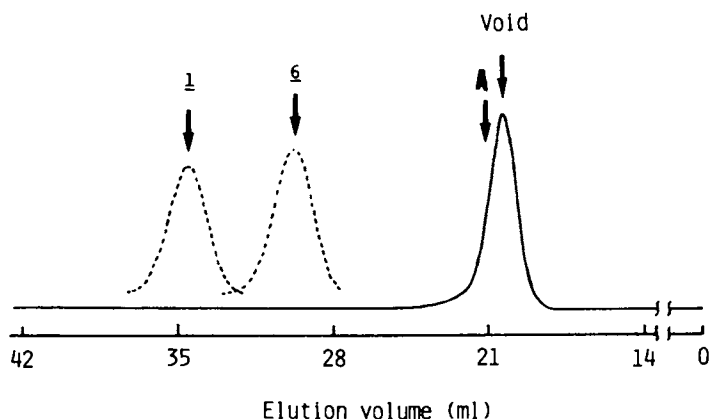


Figure 8. Gel filtration of ethylated ( $\beta$ -0-4)-( $\beta$ - $\beta$ )-DHP **16**. Solid line: Ethylated ( $\beta$ -0-4)-( $\beta$ - $\beta$ )-DHP **16** after removal of low molecular weight fractions. The column was calibrated with ( $\beta$ -0-4)-( $\beta$ - $\beta$ ) lignin substructure model trimer **6** (molecular weight 642);  $\beta$ -0-4 lignin model dimer **1** (molecular weight 348) and polystyrenes of molecular weight 9000, 4000 (void), 2200 (indicated by A). Column: Sephadex LH-20, 1.1  $\times$  48 cm. Eluent: DMF, 13.5-14.4 ml/hr. Detector: Refractive index detector RI-2 (Japan Analytical Industry Co., Ltd.).

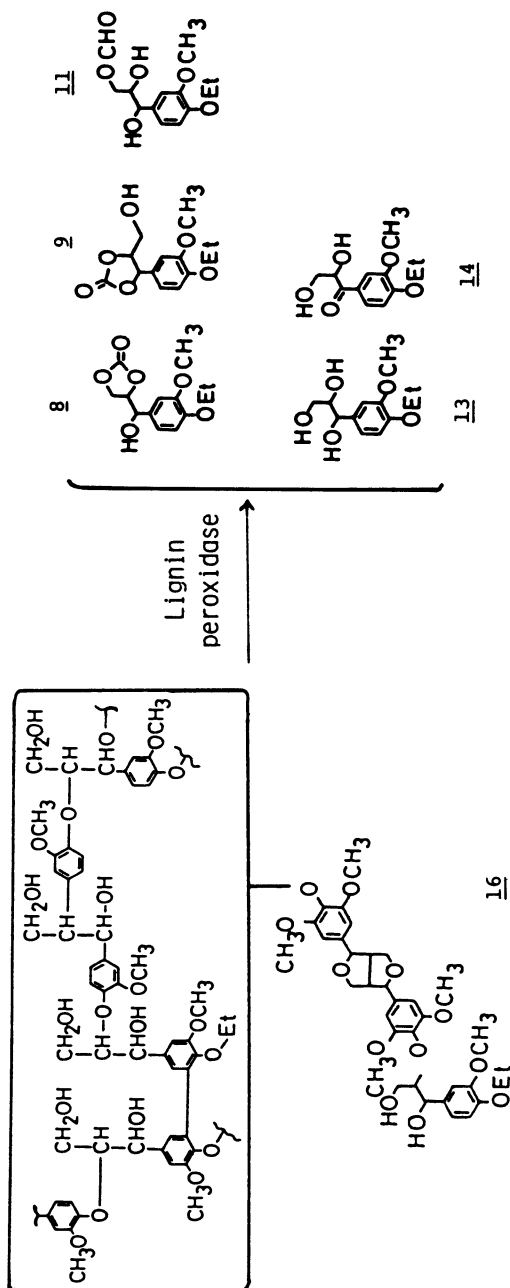


Figure 9. Degradation products of synthetic lignin (DHP) 16 by lignin peroxidase. 8, 9 and 11: Aromatic ring cleavage products; 13 and 14:  $\beta$ -0-4 bond cleavage products.

## Literature Cited

1. Chen, C.-L.; Chang, H.-m. In *Biosynthesis and Biodegradation of Wood Components*; Higuchi, T., Ed.; Academic: Orlando, FL, 1985; pp. 535-56.
2. Higuchi, T. In *Biosynthesis and Biodegradation of Wood Components*; Higuchi, T., Ed.; Academic: Orlando, FL, 1985; pp. 557-78.
3. Higuchi, T. *Wood Res.* 1986, **73**, 58.
4. Umezawa, T.; Higuchi, T. *FEBS Lett.* 1985, **182**, 257.
5. Umezawa, T.; Kawai, S.; Yokota, S.; Higuchi, T. *Wood Res.* 1986, **73**, 8.
6. Umezawa, T.; Shimada, M.; Higuchi, T.; Kusai, K. *FEBS Lett.* 1986, **205**, 287.
7. Umezawa, T.; Higuchi, T. *FEBS Lett.* 1986, **205**, 293.
8. Umezawa, T.; Higuchi, T. *Agric. Biol. Chem.* 1987, **51**, 2281.
9. Umezawa, T.; Higuchi, T. *FEBS Lett.* 1987, **218**, 255.
10. Kirk, T. K.; Chang, H.-m. *Holzforschung* 1975, **29**, 56.
11. von Ellwardt, P.-C.; Haider, K.; Ernst, L. *Holzforschung* 1981, **35**, 103.
12. Chua, M. G. S.; Chen, C.-L.; Chang, H.-m.; Kirk, T. K. *Holzforschung* 1982, **36**, 165.
13. Chen, C.-L.; Chang, H.-m.; Kirk, T. K. *J. Wood Chem. Technol.* 1983, **3**, 35.
14. Tai, D.; Terazawa, M.; Chen, C.-L.; Chang, H.-m.; Kirk, T. K. In *Recent Advances in Lignin Biodegradation Research*; Higuchi, T.; Chang, H.-m.; Kirk, T. K., Eds.; Uni Publishers: Tokyo, 1983; pp. 44-63.
15. Haider, K.; Kern, H. W.; Ernst, L. *Holzforschung* 1985, **39**.
16. Kawai, S.; Umezawa, T.; Higuchi, T. *Appl. Environ. Microbiol.* 1985, **50**, 1505.
17. Yoshihara, K.; Umezawa, T.; Higuchi, T.; Nishiyama, M. *Agric. Biol. Chem.* 1988, **52**, 2345.
18. Leisola, M. S. A.; Schmidt, B.; Thanei-Wyss, U.; Fiechter, A. *FEBS Lett.* 1985, **189**, 267.
19. Tien, M.; Kirk, T. K. *Proc. Natl. Acad. Sci. USA* 1984, **81**, 2280.
20. Miki, K.; Renganathan, V.; Mayfield, M. B.; Gold, M. H. *FEBS Lett.* 1987, **210**, 199.
21. Cain, R. B. In *Lignin Biodegradation: Microbiology, Chemistry, and Potential Applications*; Kirk, T. K.; Higuchi, T.; Chang, H.-m., Eds.; CRC Press: Boca Raton, FL, 1980; Vol. 1, pp. 21-60.
22. Shimada, M.; Hattori, T.; Umezawa, T.; Higuchi, T.; Uzura, K. *FEBS Lett.* 1987, **221**, 327.
23. Haemmerli, S. D.; Schoemaker, H. E.; Schmidt, H. W. H.; Leisola, M. S. A. *FEBS Lett.* 1987, **220**, 149.
24. Miki, K.; Kondo, R.; Renganathan, V.; Mayfield, M. B.; Gold, M. H. *Biochem.* 1988, **27**, 4787.
25. Dodson, P. J.; Evans, C. S.; Harvey, P. J.; Palmer, J. M. *FEMS Microbiol. Lett.* 1987, **42**, 17.
26. Kirk, T. K.; Tien, M.; Kersten, P. J.; Mozuch, M. D.; Kalyanaraman, B. *Biochem. J.* 1986, **236**, 279.



27. Miki, K.; Renganathan, V.; Gold, M. H. *Biochem.* 1986, **25**, 4790.
28. Umezawa, T.; Higuchi, T. *Mokuzai Gakkaishi* 1988, **34**, 929.
29. Tien, M.; Kirk, T. K. *Science* 1983, **221**, 661.
30. Haemmerli, S. D.; Leisola, M. S. A.; Fiechter, A. *FEMS Microbiol. Lett.* 1986, **35**, 33.
31. Odier, E.; Mozuch, M.; Kalyanaraman, B.; Kirk, T. K. In *Lignin Enzymic and Microbial Degradation*; Odier, E., Ed.; INRA: Paris, 1987; p. 131.
32. Umezawa, T.; Higuchi, T. *FEBS Lett.* 1989, **242**, 325.
33. Chen, C.-L.; Chang, H.-m.; Kirk, T. K. *Holzforschung* 1982, **36**, 3.
34. Ander, P.; Eriksson, K.-E.; Yu, H.-s. *Arch. Microbiol.* 1983, **136**, 1.
35. Buswell, J. A.; Ander, P.; Pettersson, B.; Eriksson, K.-E. *FEBS Lett.* 1979, **103**, 98.
36. Yajima, Y.; Enoki, A.; Mayfield, M. B.; Gold, M. H. *Arch. Microbiol.* 1979, **123**, 319.
37. Buswell, J. A.; Eriksson, K.-E. *FEBS Lett.* 1979, **104**, 258.

RECEIVED March 10, 1989

## Chapter 37

# Biomimetic Studies in Lignin Degradation

Futong Cui and David Dolphin

Department of Chemistry, University of British Columbia, 2036 Main  
Mall, Vancouver, British Columbia V6T 1Y6, Canada

A redox stable, water-soluble iron porphyrin has been used as a model ligninase. The reactions of lignin model compounds catalyzed by this biomimetic system were found to be dependent on pH and the solvent being used. Model studies showed that veratryl alcohol could mediate the oxidation of a polymeric lignin model compound under certain conditions but could not mediate the oxidation of small molecule model compounds.

Lignin is the second most abundant renewable organic compound on earth. It composes about 15-25% of the land-produced biomass. A considerable effort has been made to understand lignin biodegradation during the last 20 or 30 years, and since the discovery of lignin degrading enzymes (ligninases) in 1983 (1,2), progress has been made in understanding the mechanisms of lignin biodegradation. Model enzyme studies are important for both mechanistic elucidation and for practical applications. This is particularly true for the non-specific lignin degrading enzymes. Ligninase is synthesized by *P. chrysosporium* only under certain phases of growth and is difficult to obtain in quantity. It is a powerful oxidant which initiates lignin degradation by one electron oxidations, and a major role of the ligninase protein is to sterically protect the oxidized heme prosthetic group. It seems unlikely that ligninase will contain an "active site" to specifically bind the diverse structural components of lignin. Instead, electron transfer (either direct or mediated) will take place between the enzyme and polymeric lignin.

A sterically protected, water-soluble synthetic iron porphyrin could provide a readily available biomimetic catalyst for both basic research and potential industrial applications. Such a synthetic hemin might be superior to the enzyme, in that being a small molecule it could interact with the polymeric lignin molecule more readily than can ligninase.

Shimada *et al.* (3) first found that a synthetic porphyrin iron *meso*-tetraphenylporphyrin (FeTPP (I)) catalyzed C-C bond cleavage of  $\beta$ -1 type

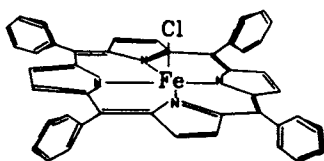
0097-6156/89/0399-0519\$06.00/0

© 1989 American Chemical Society

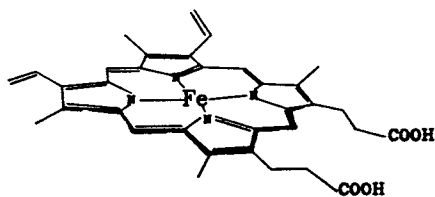
lignin model compounds, and further experiments (4) showed that the reaction had an optimal pH of 3.0 and was stimulated by the presence of imidazole. Isotope labeling experiments (5) showed that the iron porphyrin catalyzed reactions followed the same mechanistic routes as those of the ligninase catalyzed reactions (6). Protohemin (**II**) was also reported to be able to catalyze ring cleavage reactions of veratryl alcohol (7). Shimada *et al.* (8) recently reported that protohemin mimicked ligninase in most cases in degrading  $\beta$ -1,  $\beta$ -0-4, and  $\beta$ -5 model compounds. The simple iron porphyrins (**I,II**), however, suffer a great disadvantage in that they are rapidly destroyed by oxidants. Sterically protected water-soluble metalloporphyrins have been used in our laboratory as ligninase mimics and we discuss here some observations on our most promising catalyst iron meso-tetra-(2,6-dichloro-3-sulfonatophenyl)porphyrin chloride (TDC-SPPFeCl (**III**)).

## Experimental

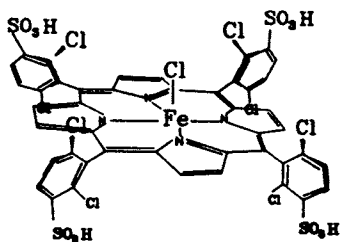
The oxidation of veratryl alcohol was carried out under air at room temperature. The reaction mixture contained 30  $\mu$ moles of veratryl alcohol, 0.05  $\mu$ moles of TDCSPPFeCl, 30  $\mu$ moles of *m*-chloroperbenzoic acid (*m*CPBA) made up to 6 ml using phosphate buffer or as otherwise indicated in Table I. 4-methoxyacetophenone (30  $\mu$ moles) was added as an internal standard. The reaction was stopped after 2 hours by partitioning the mixture between methylene chloride and saturated sodium bicarbonate solution. The aqueous layer was twice extracted with methylene chloride and the extracts combined. The products were analyzed by GC after acetylation with excess 1:1 acetic anhydride/pyridine for 24 hours at room temperature. The oxidations of anisyl alcohol, in the presence of veratryl alcohol or 1,4-dimethoxybenzene, were performed as indicated in Table III and IV in 6 ml of phosphate buffer (pH 3.0). Other conditions were the same as for the oxidation of veratryl alcohol described above. TDCSPPFeCl remaining after the reaction was estimated from its Soret band absorption before and after the reaction. For the decolorization of Poly B-411 (**IV**) by TDC-SPPFeCl and *m*CPBA, 25  $\mu$ moles of *m*CPBA were added to 25 ml 0.05% Poly B-411 containing 0.01  $\mu$ moles TDCSPPFeCl, 25  $\mu$ moles of manganese sulfate and 1.5 mmoles of lactic acid buffered at pH 4.5. The decolorization of Poly B-411 was followed by the decrease in absorption at 596 nm. For the electrochemical decolorization of Poly B-411 in the presence of veratryl alcohol, a two-compartment cell was used. A glassy carbon plate was used as the anode, a platinum plate as the auxiliary electrode, and a silver wire as the reference electrode. The potential was controlled at 0.900 V. Poly B-411 (50 ml, 0.005%) in pH 3 buffer was added to the anode compartment and pH 3 buffer was added to the cathode compartment to the same level. The decolorization of Poly B-411 was followed by the change in absorbance at 596 nm and the simultaneous oxidation of veratryl alcohol was followed at 310 nm. The same electrochemical apparatus was used for the decolorization of Poly B-411 adsorbed onto filter paper. Tetrabutylammonium perchlorate (TBAP) was used as supporting electrolyte when methylene chloride was the solvent.



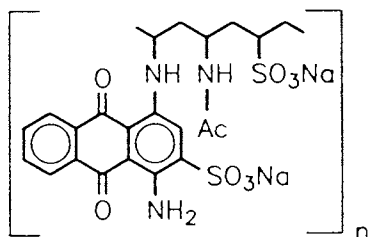
I



II



III



IV

## Results

Shimada *et al.* have carried out most of their studies on model ligninases in organic solvents (3-5,8). However, reactions in organic and aqueous solutions may take different routes and Dordick *et al.* (9) have reported that horseradish peroxidase and other peroxidases are able to depolymerize both natural and synthetic lignins in organic solvent but are unable to do so in aqueous solution, although these results have recently been reassessed (10). We have studied the solvent effect for TDCSPPFeCl catalyzed reactions using the simplest lignin model compound, veratryl alcohol. Table I shows that under the same concentrations of oxidant and catalyst the yield of veratraldehyde was higher in aqueous solution than in organic solvent. It was interesting to note that an additional product was formed at about the same yield as veratraldehyde when methanol was the solvent. Although the structure of this compound has not yet been elucidated, this result suggests that solvent can also change the product distribution. This was also dramatically demonstrated in the following example. The  $\beta$ -O-4 linkage is one of the most abundant substructures of lignin. In spruce lignin the  $\beta$ -O-4 bond was estimated to comprise 48% of the linkages connecting the phenylpropanoid units (11). While FeTPP (I) (8) cannot degrade 4-O-ethylguaiaacylglycerol- $\beta$ -guaiaacyl ether in organic solvents by the same pathway as the enzymic reactions (12), our initial results show that TDCSPPFeCl degraded this compound in water to give, among other products, 4-ethoxy-3-methoxybenzaldehyde and guaiacol (Fig. 1).

Table I. Oxidation of veratryl alcohol by TDCSPPFeCl and *m*CPBA in various solvents

Solvent	% Yield of Veratraldehyde <sup>a</sup>
6 ml pH 2 phosphate buffer	49.6
6 ml DMF	12.0
6 ml methanol	11.0 <sup>b</sup>

<sup>a</sup> Based on veratryl alcohol.

<sup>b</sup> A second product was obtained.

The optimal pH for TDCSPPFeCl catalysis was examined for the production of veratraldehyde from veratryl alcohol. The yield was highest at the lowest pH used (Table II). It can also be seen from Table II that TDCSPPFeCl was fairly stable over a wide range of pH. The pH of the medium is crucial for the natural degradation of lignin. Cation radicals are involved in both the biosynthesis and biodegradation of lignin. The biosynthesis occurs at around pH 7 which favors radical coupling of the *neutral* phenolate radical while biodegradation occurs under acidic condition which favors cation radical induced C-C bond cleavage.

Although no attempt was made to optimize the turnover of the catalyst, Table II shows that TDCSPPFeCl was stable under the extreme

oxidizing conditions, i.e., with a catalyst to oxidant ratio of 1:600. Other simple hemins are rapidly degraded under these conditions.

Table II. Oxidation of veratryl alcohol by TDCSPFeCl and *m*CPBA in aqueous solution as a function of pH

pH	% Yield of Veratraldehyde <sup>a</sup>	% TDCSPFeCl Left After Reaction
2	49.6	98
4	11.4	98
6	5.8	97
8	3.7	74
10	9.9	96

<sup>a</sup> Yield based on veratryl alcohol.

Palmer *et al.* (13) proposed that ligninase degrades lignin by single electron oxidations and that the cation radicals of small aromatic molecules could serve as diffusible redox mediators during lignin degradation. Veratryl alcohol was found to stimulate the oxidation of anisyl compounds (14) by ligninase and Harvey *et al.* suggested that the cation radical of veratryl alcohol functioned as a redox mediator in this reaction. Since the cation radical of veratryl alcohol has not so far been detected (15), the mediating role of veratryl alcohol is still an open question.

The oxidation of anisyl alcohol by TDCSPFeCl and *m*CPBA was carried out in the presence of varying amounts of veratryl alcohol. The results in Table III show that the presence of veratryl alcohol inhibited the oxidation of anisyl alcohol. These observations are readily rationalized on the basis of the oxidation potentials of the two compounds. Veratryl alcohol, which has a lower oxidation potential than anisyl alcohol, (1.52 V vs. 1.76 V as determined by cyclic voltametry in acetonitrile), is more easily oxidized thus decreasing the yield of anisyl alcohol by competing with it for the oxidant; the same will be true in the natural systems. The mediating role of a well known single-electron transfer agent, 1,4-dimethoxybenzene, was tested for comparison. It can be seen from Table IV that 1,4-dimethoxybenzene cannot stimulate the oxidation of anisyl alcohol either. Therefore, the increased yield of anisyl alcohol oxidation by ligninase cannot be attributed directly to the mediating role of veratryl alcohol. However the recent work of Harvey *et al.* (17) provides a good explanation of their early results (14) and confirms the speculation of Kirk *et al.* (16). Veratryl alcohol can protect ligninase from inactivation by preventing the formation of ligninase compound III (17) (Figure 2). Indeed, the low yield of veratraldehyde at high pH, coupled to the stability of the hemin (Table II, pH 10) was due to the facile formation of the compound III analog of TDCSPFeCl which is relatively long lived at high pH. Our inability to establish a mediating role for veratryl alcohol in the oxidation of anisyl alcohol does not exclude the possibility that it functions as a mediator in lignin degradation. The mediating role of veratryl alcohol might be difficult to observe for small molecule

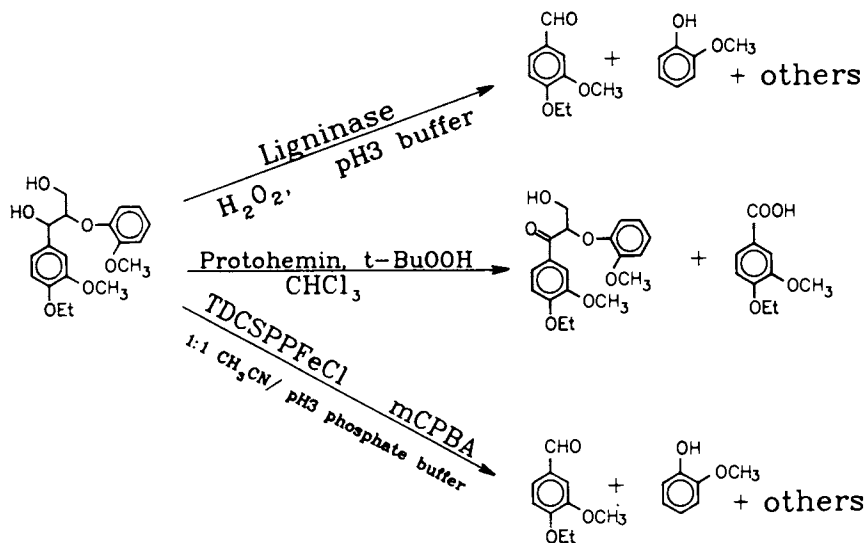


Figure 1. Comparison of the reactions of 4-O-ethylguaiacylglycerol- $\beta$ -guaiacyl ether catalyzed by FeTPP/ $t$ -BuOOH/ $\text{CHCl}_3$ , TDCSPPFeCl/ $m$ CPBA/ $\text{H}_2\text{O}$  and ligninase/hydrogen peroxide.

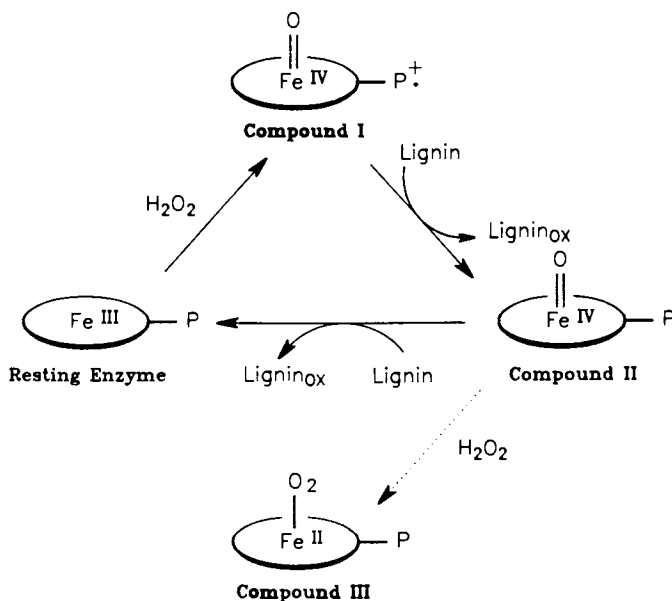


Figure 2. The catalytic cycles of ligninase.

interactions with the low molecular weight model compounds. Indeed, as described below, the results of electrochemical studies with a polymeric model compound shown in Figure 3 suggest such a mediating role.

Table III. Oxidation of anisyl alcohol by TDCSPPFeCl in aqueous solution in the presence of veratryl alcohol (pH 3)

Substrates		% yield of Anisaldehyde <sup>a</sup>	% TDCSPPFeCl Left After Reaction
Anisyl Alcohol ( $\mu$ moles)	Veratryl Alcohol ( $\mu$ moles)		
30	30	1.3	> 90
30	15	4.2	> 90
30	3	14.7	> 90
30	0.3	20.8	> 90
30	0	25.0	> 90

<sup>a</sup> Yield based on anisyl alcohol.

Table IV. Oxidation of Anisyl Alcohol by TDCSPPFeCl and *m*CPBA in Aqueous Solution in the Presence of 1,4-dimethoxybenzene (pH 3)

Substrates		% Yield of Anisaldehyde <sup>a</sup>	% TDCSPPFeCl Left After Reaction
Anisyl Alcohol ( $\mu$ moles)	1,4-dimethoxy Benzene ( $\mu$ moles)		
30	30	1.3	> 90
30	15	3.3	> 90
30	3	17.5	> 90
30	0.3	20.4	> 90
30	0	25.0	> 90

<sup>a</sup> Yield based on anisyl alcohol.

Poly B-411, a water-soluble, blue dye (IV) has been used as a lignin model by Glenn *et al.* (18). The dye was deposited onto a piece of filter paper, which was then attached directly to a glassy carbon anode. The anolyte contained 10 mM veratryl alcohol and 0.1 M tetrabutylammonium perchlorate (TBAP) in methylene chloride. The catholyte contained only 0.1 M TBAP in methylene chloride. After six hours controlled potential oxidation at 1.2 V, the blue color of filter paper on the side facing the anode turned to reddish brown. Complete oxidation of Poly B-411 in aqueous solution by TDCSPP FeCl and *m*CPBA gave the same color. The filter paper was not decolorized in a control experiment lacking veratryl alcohol. As Poly B-411 was not able to make direct contact with the electrode (since



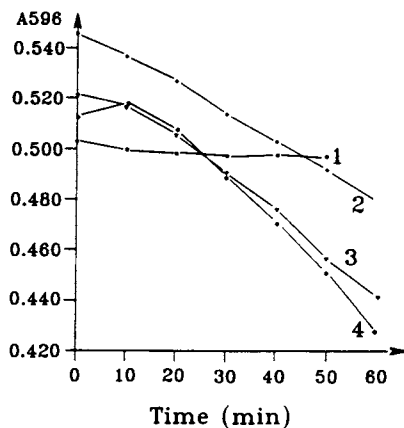


Figure 3. Electrochemical oxidation of Poly B-411 in the presence of veratryl alcohol at various concentrations (mM). 1, 0; 2, 0.1; 3, 1.0; 4, 10.

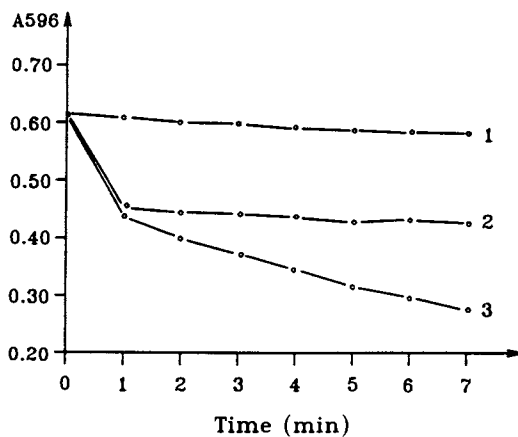


Figure 4. Decolorization of Poly B-411 by TDCSPFeCl and *m*CPBA in the presence of manganese sulfate and lactic acid (curve 3). Curves 1 and 2 show control experiments lacking TDCSPFeCl and manganese sulfate, respectively.

it is insoluble in methylene chloride) in the above experiment, veratryl alcohol (or one of its oxidation products) must have mediated its oxidation.

TDCSPPFeCl can also mimic the function of the Mn(II)-dependent peroxidase isolated from ligninolytic cultures of *P. chrysosporium* (19,20). The *m*CPBA-oxidized TDCSPPFeCl can oxidize Mn(II) to Mn(III) which in turn oxidizes Poly B-411 in the presence of various  $\alpha$ -hydroxycarboxylic acids. Figure 4 shows that TDCSPPFeCl can rapidly decolorize Poly B-411 in the presence of manganese sulfate, lactic acid, and *m*CPBA. Control experiments lacking either manganese sulfate or TDCSPPFeCl caused inefficient and very slow decolorization of Poly B-411 (Fig. 4). It has been suggested (23) that one function of manganese is that of a diffusible mediator for lignin degradation. The above observations support this mediating role and at the same time emphasize the role of the porphyrin (enzyme). Hydrogen peroxide, a two electron oxidant, cannot oxidize Mn(II) to Mn(III) (a one electron process), but at the same time manganese ions unlike iron do not initiate Fenton-like chemistry with peroxide. Peroxide can oxidize a ferric porphyrin to the compound I oxidation state ( $O = Fe(IV)Por^{+*}$ ) and this can bring about the one electron oxidation of Mn(II) leaving Compound II ( $O = Fe(IV)Por$ ). Compound II can then oxidize a second equivalent of Mn(II). Indeed this latter step is probably critically important in preventing Compound III formation in the manganese dependent peroxidase.

### Conclusions

We have shown that TDCSPPFeCl (III) is so far the most stable and efficient catalyst among the iron porphyrins used as model ligninases. All the known reactions catalyzed by this porphyrin mimic the ligninases quite well. TDCSPPFeCl can be used in both aqueous and polar organic solvent (such as methanol, DMF) so that solvent effects of lignin degradation can be studied. The catalyst is stable over a wide range of pH so the reactions at different pH can be compared.

Under carefully controlled conditions veratryl alcohol can act as a redox mediator but from the experiments described above, we expect that such a role must be of only minor importance in nature. The ability of veratryl alcohol (and Mn(II)) to reduce Compound II (preventing the formation of compound III) is probably of far more importance for the ligninases.

### Acknowledgment

This work was supported by the Natural Sciences and Engineering Research Council of Canada.

### Literature Cited

1. Tien, M.; Kirk, T. K. *Science* 1983, **221**, 661-63.
2. Glenn, J. K.; Morgan, M. A.; Mayfield, M. B.; Kuwahara, M.; Gold, M. H. *Biochem. Biophys. Res. Commun.* 1983, **114**, 1077-83.
3. Shimada, M.; Habe, T.; Umezawa, T.; Higuchi, T.; Okamoto, T. *Biochem. Biophys. Res. Commun.* 1984, **122**, 1247-52.

4. Habe, T.; Shimada, M.; Higuchi, T. *Mokuzai Gakkaishi* 1985, **31**, 54-55.
5. Habe, T.; Shimada, M.; Okamoto, T.; Panijpan, B.; Higuchi, T. *J. Chem. Soc., Chem. Commun.* 1985, 1323-24.
6. Tien, M.; Kirk, T. K. *Proc. Natl. Acad. Sci. USA* 1984, **81**, 2280-4.
7. Shimada, M.; Hattori, T.; Umezawa, T.; Higuchi, T.; Okamoto, T. *Proc. Intl. Symp. on Lignin Enzymic and Microbial Degradation*; Paris, France, April 23-24, 1987; p. 151.
8. Shimada, M.; Habe, T.; Higuchi, T.; Okamoto, T.; Panijpan, B.; *Holz-forschung* 1987, **41**, 277-85.
9. Dordick, J. S.; Marletta, M. A.; Klibanov, A. M. *Proc. Natl. Acad. Sci. USA* 1986, **83**, 6255-57.
10. Lewis, N. G.; Razal, R. A.; Yamamoto, E. *Proc. Natl. Acad. Sci. USA* 1987, **84**, 7925-27.
11. Adler, E. *Wood Sci. Technol.* 1977, **11**, 169-218.
12. Kirk, T. K.; Tien, M.; Kersten, P. J.; Mozuch, M. D. *Biochem. J.* 1986, **236**, 279-87.
13. Schoemaker, H. E.; Harvey, P. J.; Bowen, R. M.; Palmer, J. M. *FEBS Lett.* 1985, **183**, 7-12.
14. Harvey, P. J.; Schoemaker, H. E.; Palmer, J. M. *FEBS Lett.* 1986, **195**, 242-46.
15. Tien, M.; Kirk, T. K.; Bull, C.; Fee, J. A. *J. Biol. Chem.* 1986, **261**, 1687-93.
16. Kirk, T. K.; Farrell, R. L. *Ann. Rev. Microbiol.* 1987, **41**, 465-505.
17. Harvey, P. J.; Schoemaker, H. E.; Palmer, J. M.; *Proc. Intl. Symp. on Lignin Enzymic and Microbial Degradation*; Paris, France, April 23-24, 1987; p. 145.
18. Glenn, J. K.; Gold, M. H. *Appl. Environ. Microbiol.* 1983, **45**, 1741-47.
19. Kuwahara, M.; Glenn, J. K.; Morgan, M. A.; Gold, M. H. *FEBS Lett.* 1984, **169**, 247-50.
20. Paszczynski, A.; Huynh, Van-Ba; Crawford, R. *FEMS Microbiol. Lett.* 1985, **29**, 37-41.
21. Glenn, J. K.; Gold, M. H. *Arch. Biochem. Biophys.* 1985, **242**, 329-41.
22. Paszczynski, A.; Huynh, Van-Ba; Crawford, R. *Arch. Biochem. Biophys.* 1986, **244**, 750-65.
23. Glenn, J. K.; Akileswaran, L.; Gold, M. H. *Arch. Biochem. Biophys.* 1986, **251**, 688-96.

RECEIVED March 17, 1989

## Chapter 38

# Bacterial Degradation of Kraft Lignin

### Production and Characterization of Water-Soluble Intermediates Derived from *Streptomyces badius* and *Streptomyces viridosporus*

P. F. Vidal<sup>1</sup>, J. Bouchard<sup>1</sup>, R. P. Overend<sup>1,2</sup>, E. Chornet<sup>1</sup>, H. Giroux<sup>3</sup>, and F. Lamy<sup>3</sup>

<sup>1</sup>Department of Chemical Engineering, University of Sherbrooke, Sherbrooke, Quebec J1K 2R1, Canada

<sup>2</sup>National Research Council of Canada, Ottawa, Ontario K1A 0R6, Canada

<sup>3</sup>Department of Biochemistry, University of Sherbrooke, Sherbrooke, Quebec J1K 2R1, Canada

Two *Streptomyces* strains, *S. badius* and *S. viridosporus*, were found to be able to grow on kraft lignin (Indulin ATR) as sole carbon source. The resulting APPL (Acid Precipitable Polymeric Lignin) was characterized by FTIR and elemental analysis for C, H and N, and was found to contain proteins in addition to a relatively demethoxylated lignin component. The proteins were further characterized by amino acid analysis, while the lignin component was separated by solvent extraction and its molecular weight distribution determined by HPSEC.

In the last ten years, research on lignin biodegradation has followed two routes: fungi and bacterial delignification.

Crawford and co-workers were the first to study in detail the action of two streptomyces, *S. badius* 252 and *S. viridosporus* T7A, on lignocellulose from different sources. Their work led to the conclusion that the bacterial action on aqueous suspensions of these lignocellulosics resulted in the solubilization of lignin fragments which precipitate upon acidification: Acid Precipitable Polymeric Lignin (APPL) (1-10).

In this paper, we report on the bacterial growth of *S. badius* and *S. viridosporus* with Indulin ATR, a commercial kraft lignin practically free of sugars, as sole carbon source and on the characterization of the APPL derived from this degradation.

#### Materials and Methods

The materials and most of the methods used are described in previous papers (11,12). To summarize:

- Indulin ATR is a purified form (acidified water wash) of Indulin AT from Westvaco Corp., Charleston Heights, South Carolina.

0097-6156/89/0399-0529\$06.00/0

© 1989 American Chemical Society

- *S. badius* and *S. viridosporus* are obtained from the American Type Cultures Collection, ATCC #39115 and 39117, respectively.
- These strains are grown in Indulin ATR suspensions (0.5% w/v).  $\text{NH}_4\text{Cl}$ , yeast extract and glucose are used together or independently as nutrients.
- The DNA content is measured in order to determine the rate of bacterial growth according to Burton (13).
- APPL is determined by acid precipitation (12M HCl) using either turbidity measurements (nephelometry: abs. at 600 nm) or gravimetry according to Crawford *et al.* (4). All experiments reported in this paper were carried out with uninoculated controls whose values were always subtracted.
- Methoxyl content of the different samples were determined using a modified Zeisel procedure (14).
- Aqueous Size Exclusion Chromatography (ASEC): A Pharmacia system with superose TM12 gel as packing, TRIS-HCl 50 mM as eluent (flow rate  $0.4 \text{ ml min}^{-1}$ ), was used, detection being by UV at 280 nm.
- Fourier Transform Infrared (FTIR) Spectroscopy: A 5DXB Nicolet system with a TGDS detector was used at a resolution of  $4 \text{ cm}^{-1}$ . The samples were mixed with pure KBr at a concentration of 2% w/w and 64 scans were collected.
- High Performance Size Exclusion Chromatography (HPSEC): A Varian Model 5000 liquid chromatograph equipped with a variable wavelength UV detector, two columns in series (PL gel,  $300 \times 7.5 \text{ mm}$ , particle size  $5 \mu\text{m}$ , porosity of 50 and  $500 \text{ \AA}$ ), was used, THF being the eluent.

## Results and Discussion

**Bacterial Growth and APPL Production.** Glucose used as a secondary carbon source increases APPL production, though only after all glucose has been consumed. The increase is greater for *S. badius* than for *S. viridosporus* (Fig. 1). As previously shown by Crawford (2), we also observed that an organic source of nitrogen such as yeast extract was much better than an inorganic source such as  $\text{NH}_4\text{Cl}$ , the *Streptomyces* producing 7 to 9 times more APPL in the former case (Fig. 2). The increase of initial pH from 7.2 to 8.8 slightly increases APPL yield, while an addition of  $\text{Cu}^{++}$ ,  $\text{Fe}^{+++}$ ,  $\text{Mn}^{++}$  or  $\text{Zn}^{++}$  has no effect (data not shown).

The study of the DNA content, an indication of bacterial growth, shows that *S. badius* reaches its stationary phase after 5 days, 7 days prior to *S. viridosporus* (Fig. 3). In both cases, APPL production starts immediately ( $t = 0$ ) and increases linearly during incubation, *S. badius* producing more than *S. viridosporus*. After 35 days, the APPL yield represents 7% and 5% of the initial Indulin ATR weight for *S. badius* and *S. viridosporus*, respectively.

**Separation of Bacterial Extracellular, Membranous and Cytosolic Proteins and their Effect on Indulin ATR.** We first assume a lignin solubilization catalyzed by enzymes. In order to localize the enzymes responsible for the Indulin ATR degradation, the cells of each strain were fractionated: extra

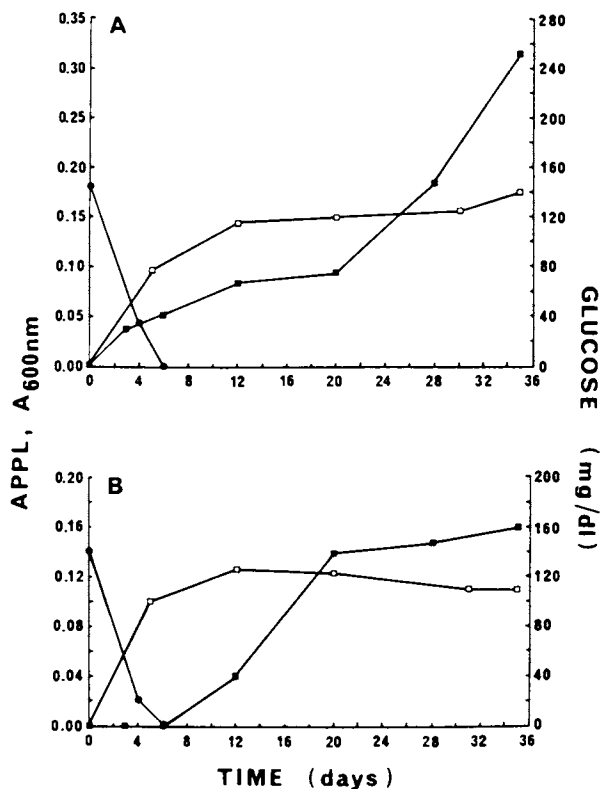


Figure 1. Influence of glucose on the production of APPL by cultures of *S. badius* (panel A) and *S. viridosporus* (panel B). The bacteria were grown in minimal culture media, adjusted at pH 7.8, with Indulin ATR (0.5%) as primary carbon source, glucose (0.2%) as secondary carbon source and  $\text{NH}_4\text{Cl}$  as nitrogen source. ●—● = glucose concentrations; ■—■ = APPL produced by bacteria grown in presence of Indulin and glucose; □—□ = APPL produced by bacteria grown in presence of Indulin alone. (Reproduced with permission from Ref. 11, © 1989 ASM.)

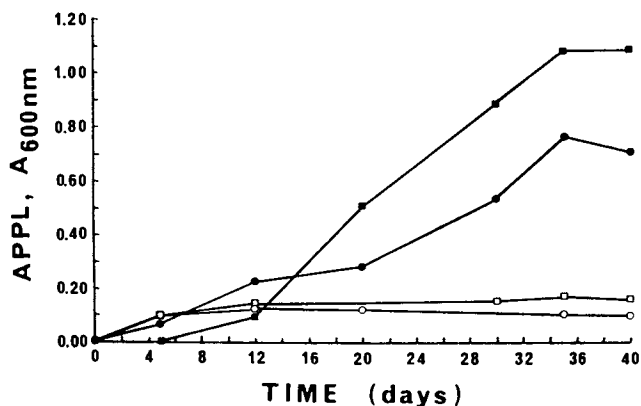


Figure 2. Influence of yeast extract on the production of APPL by cultures of *S. badius* and *S. viridosporus*. The bacteria were grown in minimal culture media with Indulin (0.5%) as source of carbon and either yeast extract (0.6%) or NH<sub>4</sub>Cl (0.02%) as nitrogen source. □ ; ■ = APPL produced by *S. badius* grown in the presence of either NH<sub>4</sub>Cl or yeast extract. (Reproduced with permission from Ref. 11, © 1989 ASM.) ○ ; ● = APPL produced by *S. viridosporus* grown in the presence of either NH<sub>4</sub>Cl or yeast extract.

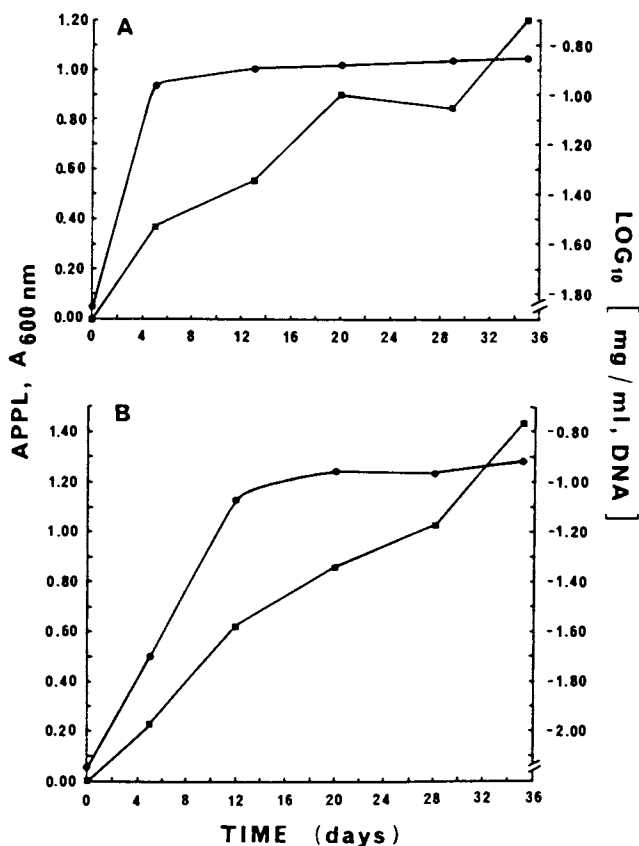


Figure 3. Bacterial growth and APPL production. The bacteria were grown in minimal culture media, adjusted at pH 7.5, with Indulin ATR (0.5%) as carbon source and yeast extract (0.6%) as nitrogen source. *S. badius* and *S. viridosporus* are shown in panels A and B, respectively. ■—■ = APPL; ●—● = DNA (Reproduced with permission from Ref. 11, © 1989 ASM).



and intracellular (membranous and cytosolic) proteins. Table I shows the location of the activity: only cell debris derived from *S. viridosporus* has no effect. Hydrogen peroxide increases activity only for the proteins derived from *S. badius* obtained at the end of the log phase (5 days) and is located in the cell debris or in the extracellular fraction. Ramachandra *et al.* (10) found extracellular peroxidase in *S. viridosporus* but identified an etherase in *S. badius*.

Table I. APPL Production by Secreted Proteins and Bacterial Extracts. Effect of Hydrogen Peroxide

		<i>S. badius</i>		<i>S. viridosporus</i>	
		H <sub>2</sub> O <sub>2</sub> (-)	H <sub>2</sub> O <sub>2</sub> (+)	H <sub>2</sub> O <sub>2</sub> (-)	H <sub>2</sub> O <sub>2</sub> (+)
Extracellular Enzymes	Early Proteins 5 or 12 days	++	+++ (+50%)	++	++
	Late Proteins 35 days	++	++	++	++
Intracellular Enzymes (5 or 12 days)	Cytosolic Proteins	++	++	++	++
	Cell Debris	++	+++ (+100%)	-	-

Evidence demonstrating that the degradation observed is catalyzed by enzyme(s) was obtained by typical denaturing treatments. Late extracellular protein fractions from both strains present the same characteristics: resistance to heat up to 100°C, partial resistance to acidity as low as pH 1.0 (samples being returned to pH 7.8 prior to assaying for activity), but are completely inactivated by proteolysis with a mixture of trypsin and chymotrypsin (Table II).

Table II. Denaturation of Stationary Phase Extracellular Enzymes

<i>S. badius</i>			<i>S. viridosporus</i>		
Heat 100°C	pH 1.0	Proteolysis	Heat 100°C	pH 1.0	Proteolysis
++	+	-	++	+	-
	(-50%)			(-75%)	

*Crude APPL Analysis.* The salient feature observed following the elemental analysis of the APPL's derived from cultures grown with yeast extract is

an unexpectedly high percentage of nitrogen (Table III). We first assume that this nitrogen originates from proteins and have therefore carried out an amino acid analysis. From the results (Table IV), we prove this assumption to be true.

Table III. Elemental analysis and methoxyl group quantification

Sample	%N	%C	%H	%O <sup>1</sup>	%OCH <sub>3</sub>
Indulin ATR	0.2	66.1	5.9	27.8	13.7
APPL <i>S. bad.</i>	6.1	51.6	5.6	36.7	6.8
APPL <i>S. vir.</i>	6.0	54.2	5.8	34.1	6.5

<sup>1</sup> Percentage of oxygen is calculated by difference.

Table IV. Amino acid compositions of the APPL associated proteins, of yeast extract and of the cellular soluble proteins obtained from *S. badius* and *S. viridosporus*. The APPL was obtained from 35 day culture media, the bacteria being grown with or without yeast extract. (Reprinted from ref. 11.)

Amino Acids	Amino Acids Concentration (picomoles) <sup>1</sup>						
	Yeast Extract	APPL (+) Yeast Ext.		APPL (-) Yeast Ext.		Cytosolic Extract	
		<i>S. bad.</i>	<i>S. vir.</i>	<i>S. bad.</i>	<i>S. vir.</i>	<i>S. bad.</i>	<i>S. vir.</i>
Asp	2.39	1.30	2.04	1.49	1.12	0.93	0.59
Glu	3.43	0.82	1.14	1.17	0.86	2.05	2.18
Ser	1.41	0.92	0.83	0.75	0.75	0.57	0.41
Gly	1.70	1.59	1.69	1.83	1.22	1.21	1.25
Arg	0.78	0.60	0.55	0.83	0.56	0.82	0.78
Thr	1.24	0.79	0.76	0.86	0.77	0.63	0.65
Ala	2.19	1.37	1.56	1.51	1.53	1.57	1.29
Pro	1.07	0.63	0.68	0.65	0.53	0.58	0.62
Tyr	0.29	0.29	0.29	0.29	0.29	0.29	0.29
Val	1.70	0.93	0.83	1.13	1.11	1.39	0.82
Ile	1.15	0.47	0.39	0.61	0.46	0.53	0.38
Leu	1.57	1.00	0.84	1.22	0.98	1.23	0.82
Phe	0.66	0.39	0.35	0.44	0.33	0.42	0.29
Lys	0.63	0.44	0.54	0.36	0.27	0.39	0.35

<sup>1</sup> All the data were calculated on the basis of a constant amount of tyrosine.

We can conclude that the yeast extract is not a source of contamination but, at the same time, cannot conclude whether these nitrogen fractions come from secreted proteins or from cytosolic proteins released



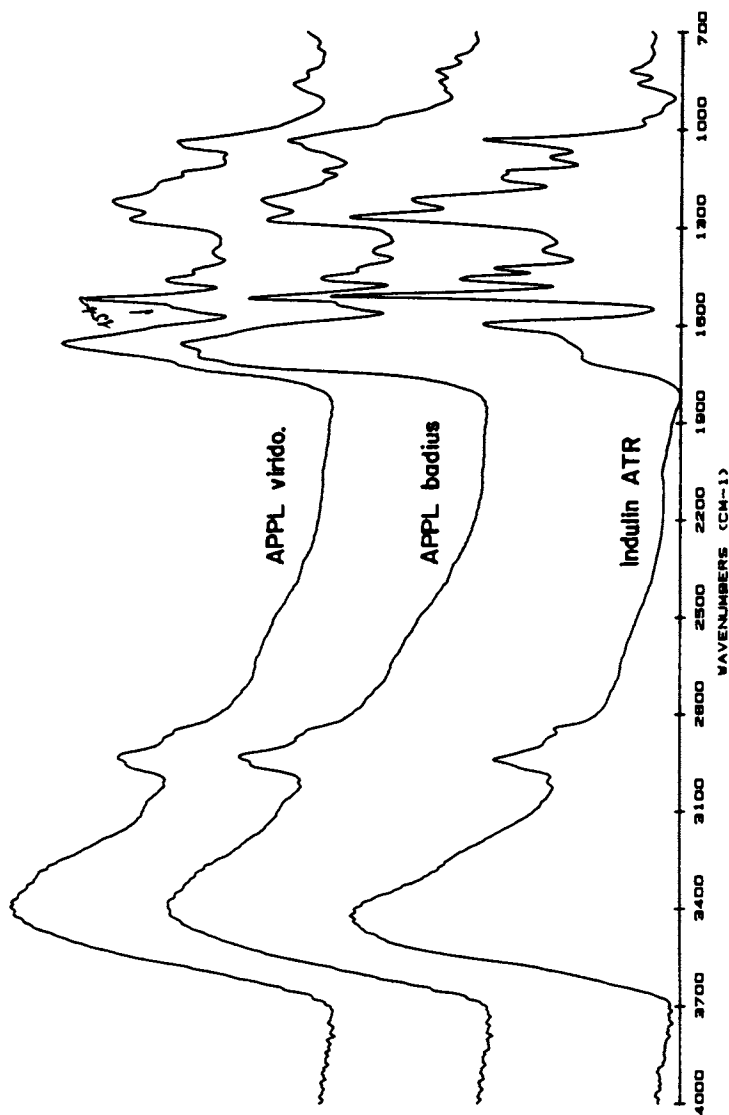


Figure 4. FTIR spectra of Indulin ATR and of the APPL's produced by *S. badius* and *S. viridosporus*. (Reproduced with permission from Ref. 12, © 1989 CNRC.)

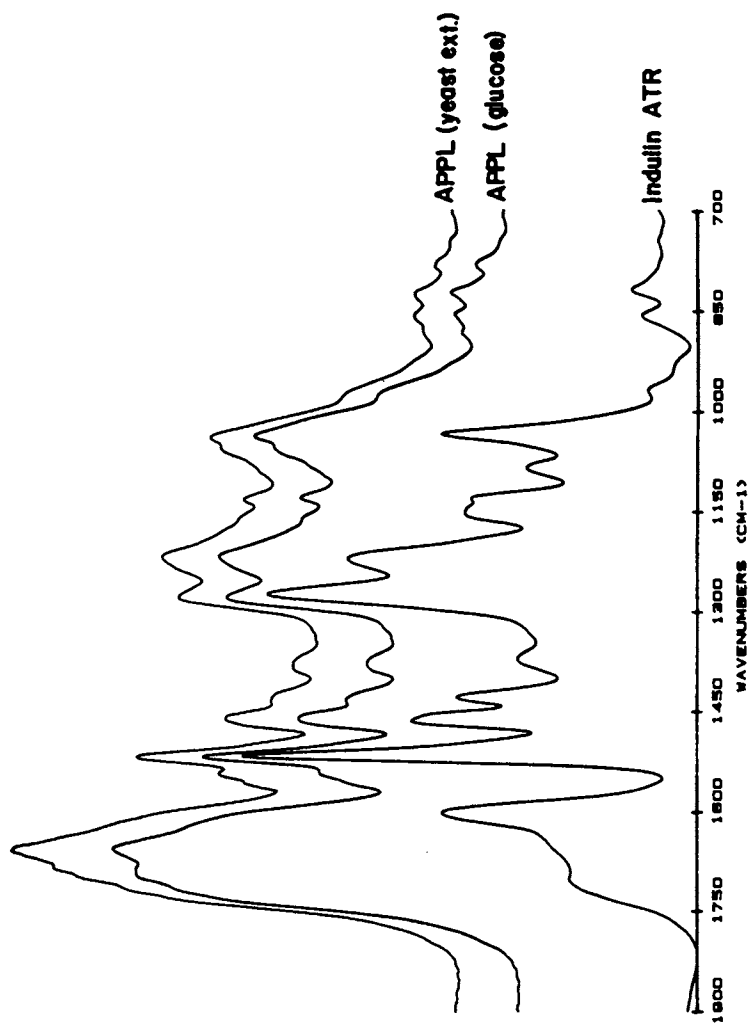


Figure 5. FTIR spectra ( $1900\text{-}700\text{ cm}^{-1}$ ) of Indulin ATR, and of the APPL's produced by *S. badtus* with and without yeast extract. (Reproduced with permission from Ref. 12, © 1989 CNRC.)

were similar for both APPL's (*S. badius* data shown in Figure 6). The presence of very high molecular weight components (MW > 300,000) is attributed to the protein fraction of the APPL, such large molecules never being found in Indulin ATR.

*Dissociation of the Protein-Polyphenolic Complex and Characterization of the Polyphenolic Fraction.* Since Indulin ATR is almost completely soluble in THF while the APPL's are quite insoluble in this solvent, but are soluble in DMF, a sequence of different percentage mixtures of these two solvents was used in order to dissociate the protein-lignin complexes for further analyses of the lignin part.

Despite the fact that crude APPL's are totally soluble in DMF, an important residue is obtained at the end of the solvent sequence (0:100, THF:DMF) indicating that the protein-rich fractions require association with the polyphenolic part for their solubilization in DMF (Table VI). Because each APPL has a different amino acid composition, its solubility distribution is also different, but in both cases, the THF fraction is the most lignin-like, with only 1% nitrogen. This is confirmed by FTIR analysis (Fig. 7). As the fractionation proceeds with increasing solvent polarity, the lignin characteristic bands at 1515, 1460, 1265, 1095, 1035, and 810  $\text{cm}^{-1}$  disappear, while the amide characteristic bands at 3290 and 3080  $\text{cm}^{-1}$  appear.

Table VI. Elemental Analysis of the Fractions Obtained by Sequential Solubilization

Sample	THF:DMF	% of Starting Material	%N	%C	%H	%O <sup>1</sup>
APPL	100:0	8.0	1.0	67.4	7.1	24.5
<i>S. bad.</i>	85:15	21.1	2.7	61.7	6.1	29.5
	50:50	19.0	4.8	58.6	6.4	30.2
	0:100	9.8	4.3	57.2	5.7	32.8
	Residue	42.1	8.7	49.6	6.5	35.2
APPL	100:0	2.3	not enough sample			
<i>S. vir.</i>	85:15	4.3	2.0	65.8	7.1	25.1
	50:50	36.3	3.3	61.7	6.6	28.4
	0:100	2.8	4.0	57.2	5.1	33.7
	Residue	54.3	9.9	49.6	6.9	33.6

<sup>1</sup> Percentage of oxygen is calculated by difference.

The molecular weight distribution obtained by size exclusion chromatography, for both APPL's THF soluble fraction and Indulin ATR, show similar profiles, the differences being that the ratio of high molecular weight (DP50) to the lower molecular weight (DP5) is inverted between Indulin ATR and both APPL fractions, the latter being richer in lower molecular weight (Fig. 8). Because the APPL's represent only 7% of the initial ma-

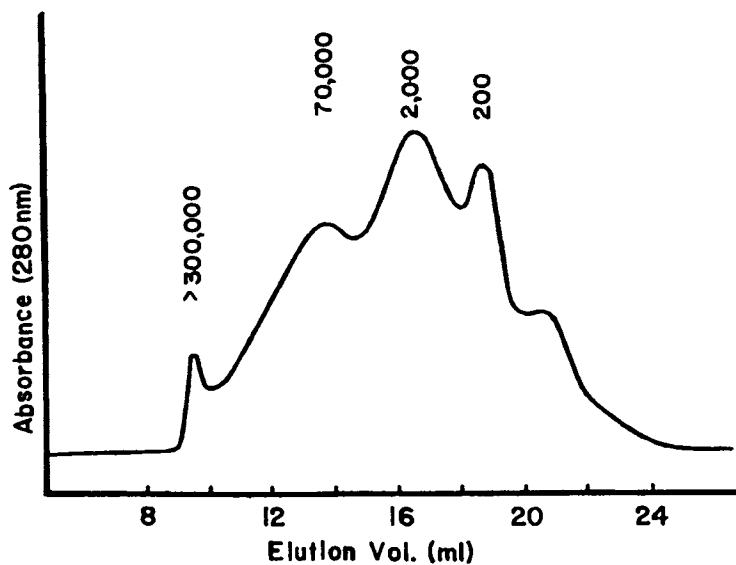


Figure 6. Aqueous size exclusion chromatography of the APPL derived from *S. badius*. Ferritin, aldolase, ovalbumin, chymotrypsinogen A and acetone were used as standards.

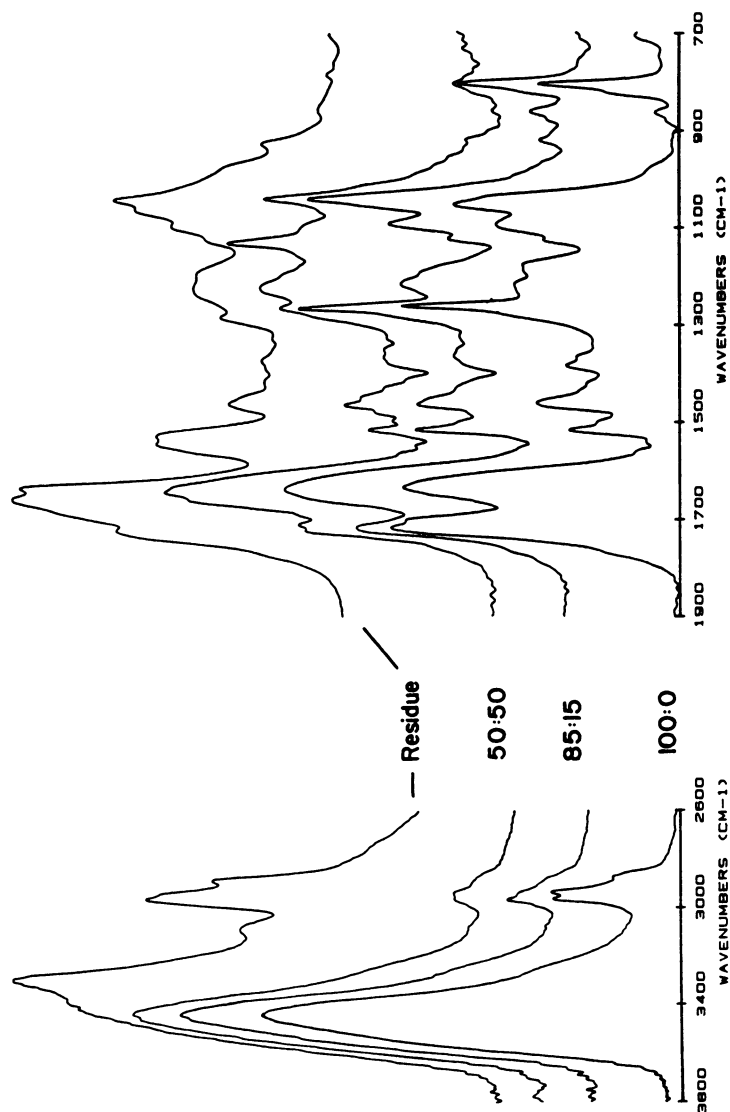


Figure 7. FTIR spectra of the fractions and of the insoluble residue obtained by sequential solvent solubilization. The fractions are identified by the THF:DMF ratio used. (Reproduced with permission from Ref. 12, © 1989, CNRC.)



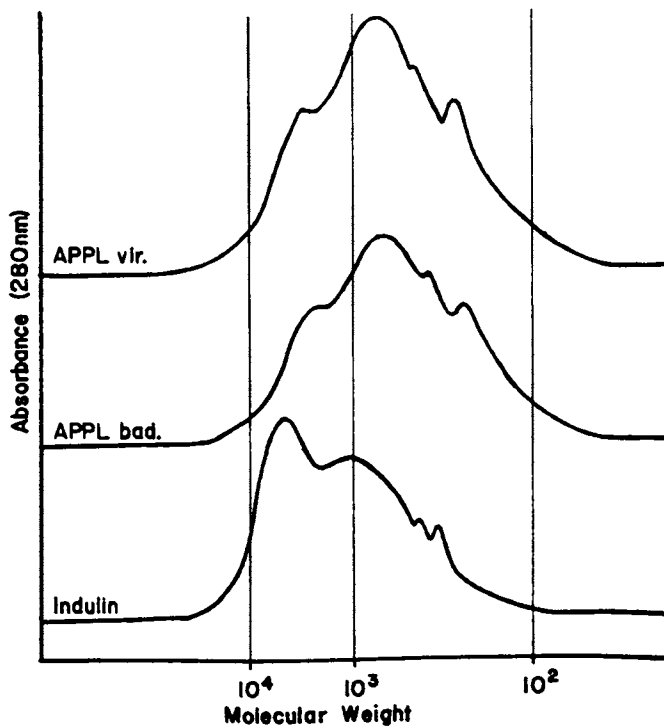


Figure 8. High performance size exclusion chromatography of Indulin ATR and of the THF soluble fraction of each APPL. (Reproduced with permission from Ref. 12, © 1989, CNRC.)

terial, this technique does not allow us to conclude whether or not APPL consists of Indulin ATR depolymerized fragments.

### Conclusions

The experiments reported were all conducted under the important assumption that enzymes present in the bacteria studied were responsible for the solubilization of the lignin. This assumption is supported by some, but not all of the results obtained, such as the H<sub>2</sub>O<sub>2</sub> activation of certain bacterial protein fractions. Another theory would be to suppose that the solubilizing proteins are, in fact, surfactants. This would explain, for example, the activity of these proteins at high temperatures. We do know, however, that proteins attach to APPL to form a soluble complex. Following the surfactant theory we would consider that Indulin ATR is a complex of lignin fragments insoluble only because of the medium's properties. The bacterial proteins would attach to the Indulin ATR increasing the hydrophilicity of the fragments, some able to become completely soluble in a neutral aqueous solution.

To prove that one theory, the other, or even a combination of both is correct, further studies of the purified secreted and cellular proteins from the bacteria will be part of the next series of experiments planned.

### Literature Cited

1. Antai, S. P.; Crawford, D. L. *Appl. Environ. Microbiol.* 1981, **42**, 378-80.
2. Barder, M. J.; Crawford, D. L. *Can. J. Microbiol.* 1981, **27**, 859-63.
3. Crawford, D. L. *Biotechnol. Bioeng. Symp.* 1981, **11**, 275-91.
4. Crawford, D. L.; Pometto, A. L., III; Crawford, R. L. *Appl. Environ. Microbiol.* 1983, **45**, 898-904.
5. Crawford, D. L.; Pettey, T. M.; Thede, B. M.; Deobald, L. A. *Biotechnol. Bioeng. Symp.* 1984, **14**, 241-56.
6. Pettey, T. M.; Crawford, D. L. *Appl. Environ. Microbiol.* 1984, **47**, 439-40.
7. Borgmeyer, J. R.; Crawford, D. L. *Appl. Environ. Microbiol.* 1985, **49**, 273-78.
8. Pometto, A. L., III; Crawford, D. L. *Appl. Environ. Microbiol.* 1986, **51**, 171-79.
9. Pometto, A. L., III; Crawford, D. L. *Appl. Environ. Microbiol.* 1986, **52**, 246-50.
10. Ramachandra, M.; Crawford, D. L.; Pometto, A. L., III. *Appl. Environ. Microbiol.* 1987, **53**, 2754-60.
11. Giroux, H.; Vidal, P. F.; Bouchard, J.; Lamy, F. *Appl. Environ. Microbiol.* 1989, **54**, 3064-70.
12. Vidal, P. F.; Bouchard, J.; Overend, R. P.; Chornet, E.; Giroux, H.; Lamy, F. *Can. J. Chem.* 1989, in press.
13. Burton, K. *Biochem. J.* 1955, **61**, 473-83.
14. Haluk, J. P.; Metche, M. *Cell. Chem. Technol.* 1986, **20**, 31-50.
15. Hergert, H. L. In *Lignins*; Sarkanen, K. V.; Ludwig, C. H., Eds.; Wiley: New York, 1971.

RECEIVED May 19, 1989

## Chapter 39

# Microbial Calorimetric Analysis

## Lignin-Related Compounds in Micromolar Concentrations

Rex E. Lovrien<sup>1</sup>, Mark L. Ferry<sup>1</sup>, Timothy S. Magnuson<sup>2</sup>,  
and Robert A. Blanchette<sup>2</sup>

<sup>1</sup>Biochemistry Department, Gortner Laboratory, University of Minnesota,  
St. Paul, MN 55108

<sup>2</sup>Plant Pathology and Forestry Department, University of Minnesota, St.  
Paul, MN 55108

Microbial combustion of lignin fragments and lignin model compounds produces heat which is measurable via heat conduction calorimetry, even with samples ranging in size from 5-200 nanomoles. The general method is called microbial calorimetric analysis (MCA). First, microbes (*Pseudomonas* or soil bacteria) are grown on lignin fragments or model compounds as a carbon source. The adapted bacteria, so obtained, then function as rapid-acting, specific reagents for metabolizing such compounds. The technique has the following advantages: (i) cells (1-2 mg) are capable of aerobically combusting many kinds of C<sub>1</sub>-C<sub>10</sub> compounds in 5-10 minutes; (ii) interfering compounds can be removed by stripping; (iii) detection limits are comparable to spectrophotometric methods (e.g., to micromolar levels for sugars and phenols); and (iv) chromogenic groups are not required for detection. The sensitivity of the technique is based on the large aerobic heats of such compounds, and the velocities with which adapted cells can drive metabolism.

Once common bacteria have been *adapted* to growing on lignin fragments, these compounds essentially undergo combustion producing heat. Current heat conduction calorimeters can easily measure such heats of aerobic metabolism, even in quantities ranging from 5-100 nanomoles (1,2). Bomb combustion calorimetry converts samples completely to carbon dioxide and water. Aerobic bacterial metabolism only produces half as much heat, e.g., sugars, phenols, alcohols and aliphatic acids liberate 100-600 Kcal/mol<sup>-1</sup>, and lignin and C<sub>8</sub>-<sub>12</sub> petroleum generate ~ 1000 Kcal/mol<sup>-1</sup>. The lower calorimetric measurement ( $\pm 3\%$  precision) is ~ 2-30 millicalories. Dividing such ranges by ca. 100-500 Kcal heat/mole gives ~ 5-200 nanomoles of

0097-6156/89/0399-0544\$06.00/0

© 1989 American Chemical Society

compound needed for microbial calorimetric analysis (MCA). Since sample volumes are 1-2 ml, micromolar concentrations can be used for this method. Besides the concentration ranges which any analytical method may be expected to cover, four further aspects are also important: namely, detectability of the analyte; whether a sample can be used "raw" or has to be isolated; interfering compounds and specificity; and cost.

Concerning detectability of lignin and cellulose derived fragments, MCA has considerable advantages. Such compounds are often poorly chromogenic; some have no chromogens at all, or are poorly prochromogenic, i.e., are difficult to attach a chromophore. But these sorts of compounds "burn" with large heats in MCA, so that a lack of chromophores for optical detection is not at all a hindrance. MCA can also utilize turbid, raw or pigmented samples, which are impossible for spectrophotometry. Microbial calorimetry was recently reviewed by Battley (3). Whereas earlier calorimeters required ca. 100 ml of microbial suspension, heat conduction calorimeters using the Seebeck effect and Peltier pump control require only 0.2 to 2 ml of substrate or analysis solution and of cell suspension. A 100-200 ml overnight culture provides enough cells for 10-20 measurements for MCA.

Microbial stripping adds much to MCA's scope, and simplifies it. Stripping uses induced bacteria for getting rid of interfering compounds. Figure 1 outlines direct calorimetry, and stripping, together with average parameters for lignin model compounds analysis. Stripping by *E. coli* was first used in cellulolysis, quantitating cellobiose vs. glucose (4). It was developed further for phenolic materials, using *Pseudomonas* and bacteria from soil isolates.

MCA takes advantage of bacterial ability to synthesize large amounts of enzymes necessary for carrying carbon sources through oxidative metabolism, thereby inducing the enzymes (5). They are analogous to the classic example, the *lac* operon of *E. coli*. (Grown on glucose, *E. coli* have 0.5 to 5  $\beta$ -galactosidase enzyme molecules per cell. But grown on lactose, *E. coli* can synthesize 1000 to 1,500  $\beta$ -galactosidase molecules/cell (6).) Thus, *M. trichosporium* produces almost 17% of its soluble protein as a methane monohydroxylase (7). A *Pseudomonas* synthesizes about 3% of its protein as protocatechuate monohydroxylase, when grown on *p*-hydroxybenzoate (8). Most of the pro-oxidative enzymes of bacteria are stabilized inside the cell, but are very fragile outside the cell. Therefore, the view that analysis may be carried out via isolated enzymes for aromatic processing, perhaps coupled to an electrode of some kind, appears quite impractical. MCA takes advantage of what bacterial cells can actually do, namely to stabilize and protect enzymes, besides the initial synthesis. Hence, MCA is likely to be far more practical than any "bioelectrode" method for analysis.

### Bacterial Growth and Adaptation

*Pseudomonas putida* ATCC 11172 was used for both microbial calorimetry and for stripping phenol and lower cresols. Several isolates from local soils, which were able to combust larger aromatics such as cinnamic and syringic

acids, were obtained by a circulating enrichment apparatus similar to that described by Audus (9). Lignin model compounds, 0.03%, plus 0.01% glucose were incubated with  $\sim 100$  g of soil for 2 days, with air circulation at room temperature. After 2 days, enricher inocula were transferred to plates with 0.5% yeast extract and the compound. (For cinnamic and hydroxycinnamic acid carbon sources, the yeast extract was left out.) Plate isolates were grown at room temperature for 12-48 h. Colonies from plates were used to inoculate shake-flask liquid cultures with Ashworth-Kornberg salts (10) containing 0.05% by weight of a carbon source and 0.03% yeast extract. Liquid culture growth usually occurred below 0.05% compound, but somewhat larger concentrations tended to kill even well adapted *Pseudomonas*. After growth (at 30°) the organisms were diluted with either minimal salts or isotonic saline and centrifugally washed twice. Cell concentrations were adjusted using the spectrophotometric turbidity factor  $2.0 \times 10^9 \times A_{660} \times \text{cm}^{-1}$  previously described (1) to measure numbers of cells/ml,  $\pm 10\%$  for *Pseudomonas*.

### Stripping

Adapted cells able to bind unwanted, interfering compounds were washed twice and adjusted in concentration. Approximately 1 ml of suspension containing  $5 \times 10^{10}$  cells was usually sufficient to strip 1 ml samples containing 50-100 nanomoles of interfering compound with over 90% removal effectiveness. After mixing the cells and samples by vortexing and incubating for a minute, the stripper cells were spun down in a microcentrifuge. An aliquot of the supernatant was taken for calorimetry or other means of analysis, e.g., Folin analysis.

### Spectrophotometric Analysis; Folin Phenol

Phenol and phenolic derivatives, cresol and related compounds were analyzed by Folin-Ciocalteu reagent at 700  $m\mu$ , standardizing each compound separately by its Folin response. Their slopes (molar absorption coefficients) were 8000-10,000  $M^{-1}\text{cm}^{-1}$ . Interestingly, methoxyl aromatics with no free hydroxyl groups were not reactive.

### Heat Conduction Calorimetry, Batch Mixing

Figure 2 illustrates the arrangement of a three-channel batch mixing calorimeter using Lipsett-Johnson-Maas vessels (11) for a 1 ml analysis sample, 2 ml microbial suspension, and 3 ml headspace. The fourth vessel in Figure 2, together with its Seebeck thermosensors, is a reference module. Usually it is loaded with 2 ml microbial suspension and 1 ml of solvent (minimal salts). The reference module voltage opposes all three sample modules so that each measurement is a difference or net power measurement. In effect, the heat of mixing the system, or the heat of residual microbial activity without carbon, is subtracted from the samples. The voltage signals of heat conduction calorimeters actually measure power. Power integrated over time equals heat, which is directly proportional to the area measured

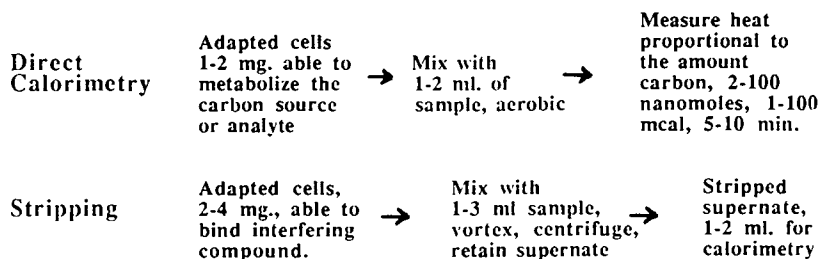


Figure 1. Methods of MCA: Direct calorimetry by microorganism metabolism of samples for analysis; stripping by microorganism binding of interfering compounds.

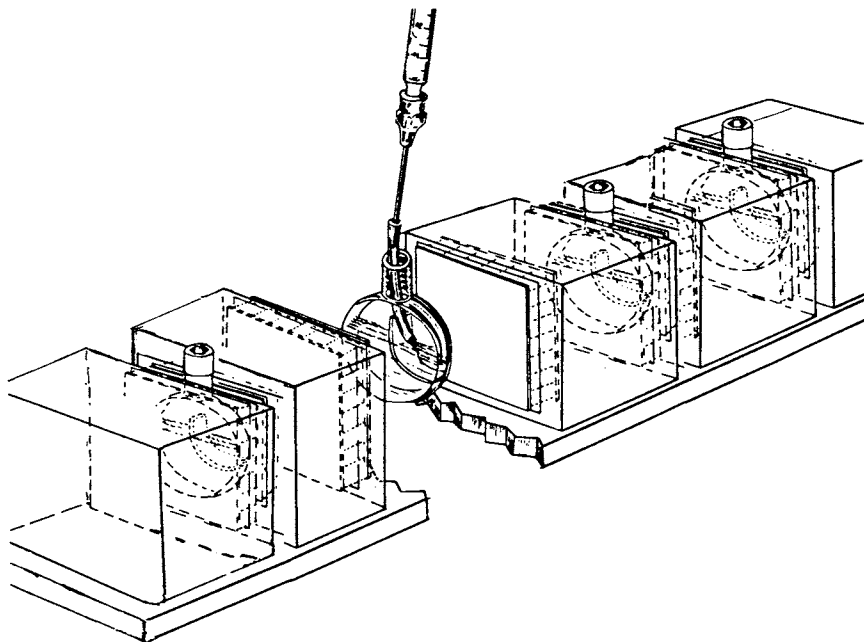


Figure 2. Heat conduction (Seebeck effect) batch mixing calorimeter for three samples and one reference channel. After loading and establishing baselines, the assembly is inverted to mix reactants and start heat production. (Reproduced with permission from Ref. 2. © 1983, Alan R. Liss, Inc.)

**American Chemical Society  
Library**

1155 16th St., N.W.

Washington, D.C. 20036

In Plant Calorimetry, Lewis et al.;  
ACS Symposium Series; American Chemical Society: Washington, DC, 1989.

under each thermogram as shown in Figure 3. Headspaces in each vessel contain 3-6 ml of air, that is, with approximately 50-100 fold excess oxygen for aerobic metabolism of 5-100 nanomoles of most substrates up to  $C_{12}$  sizes. More detailed parameters, response times, noise generation, figure of merit, etc., have been published (2) and incorporated in BRIC manufactured instruments. The unit shown in Figure 2 is inside a metal shell, surrounded by three metal boxes. The outer two boxes are Peltier pumped, for protecting against thermal fluctuations from outside. The system can be operated at any chosen temperature between 10-50°. The microbial calorimetric analyses were carried out at 25°. Heat conduction calorimeters derive their signals from heat flow, generated by the samples after mixing. They do not rely on measurement of small temperature changes. The heat conduction principle (12) is far easier and more sensitive, also less expensive, than nearly any means involving thermistors or thermometry. Calibration is carried out in two ways: electric resistance heating with a small probe inserted in each vessel; and "wet" calibration using Tris-HCl neutralization (2).

#### Microbial Calorimetric Analysis (MCA) of Compounds Using *Pseudomonas putida* ATCC 11172

*Pseudomonas* grown on phenol and various cresols combusts them at 25° in 300-600 sec if there are excess cells, ~ 1-2 mg dry weight, and limited carbon, ~ 5-30 nanomoles. Figure 3 shows that when *Pseudomonas* is adapted to *o*-cresol, it combusts *o*-cresol and phenol to completion in about 6 minutes. Grown on vanillic acid, *Pseudomonas* metabolizes limited amounts of vanillic acid, albeit somewhat more slowly than in the *o*-cresol or phenol utilizing system. Nevertheless, this occurs in far shorter times than can possibly be observed by a growth response. Ten to twenty nanomoles of vanillic acid metabolize ca. 30-50% as rapidly as *o*-cresol or phenol.

Growth on glucose allows the bacteria to combust glucose. But growth on glucose does not equip them to handle any of the lignin model compounds as indicated by the glucose grown cells mixed with *o*-cresol (lower trace of Figure 3). Such thermograms, besides measuring the nature of various organisms' responses to carbon sources, also measure metabolic rates. In the case of glucose and glucose-grown cells, when compared with data from Berka *et al.* who used *P. cepacia* and a spectrophotometric method to follow the disappearance of sugar (13), it was found that our rates of utilization agreed within a factor of less than two. Such rates from calorimetry are simply a division of the molar heat of aerobic glucose metabolism, 300 Kcal/mole glucose (1), by the power averaged over the time interval for combustion and the number of moles of glucose consumed. The quotient is a combined uptake and metabolic rate.

Standardization plots for MCA have the same nature as such plots for other analytic methods. They are plots of "readout" (in this case, heat) vs. concentration of standard. Figure 4 shows a standardization plot for MCA response to *o*-cresol, compared with a plot for Folin spectrophotometry which is also for *o*-cresol. The question that then arises is

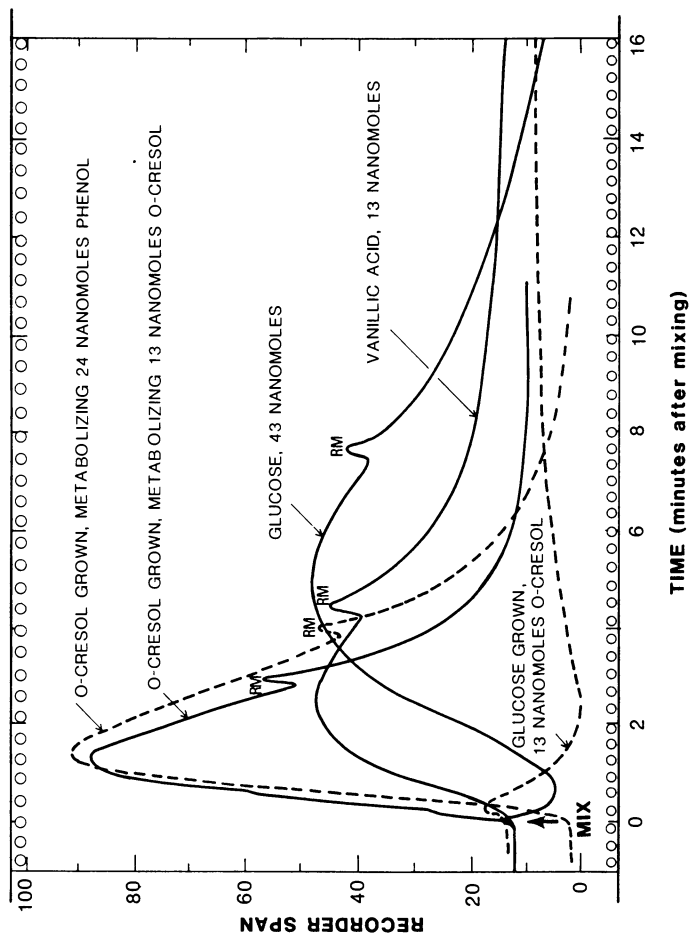


Figure 3. Microbial calorimetry of 10-40 nanomoles of compounds using *P. putida* adapted (upper four traces), and not adapted (lower trace) to the compounds, 25°C, minimal salts solvent. RM = remixing in mid-run to ensure aerobicity. Ordinate is proportional to power. Integrated areas are proportional to overall heat of consuming all metabolizable carbon.



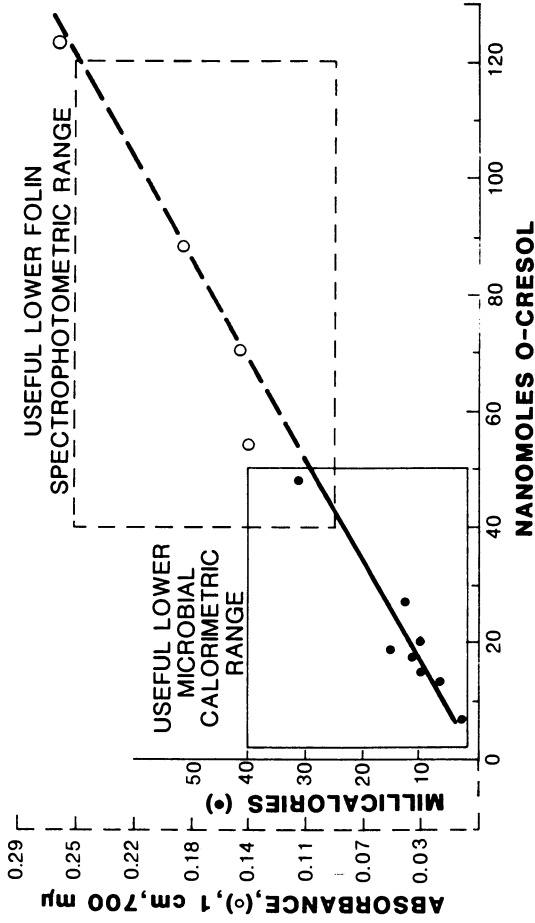


Figure 4. Comparison of MCA and Folin spectrophotometry for analysis of o-cresol spanning the lower practical ranges of instrumental readout.

the sensitivity of MCA compared with other methods in analysis of one lignin-related compound. Such a comparison depends largely on the lower heats suitable for Seebeck calorimetry, and the lower absorbancies suitable for spectrophotometry at optimum wavelength normally using a 1 cm cuvette. Absorbances of ca. 0.10-0.30 in spectrophotometry and heats of 3-40 millical in calorimetry were taken as reasonable criteria for Figure 4.

Important parameters which control such a comparison are the molar absorption coefficient for *o*-cresol-Folin color,  $\epsilon_{700} = 8140 M^{-1} \text{cm}^{-1}$ , and the molar heat of aerobic metabolism for *o*-cresol, 520 Kcal/mole *o*-cresol using aerobic *Pseudomonas*. The parameters are the slopes of the plots of Figure 4. Clearly the criteria for two completely different methods can be drawn closer together or further apart, depending on what instrumental "readouts" are taken as reasonable lower ranges. However, even when a rather intensely colored sample for analysis is compared, as Folin-cresol conjugates are, MCA is at least as sensitive as Folin spectrophotometry in the present case. The comparison accrues because of the large heat of aerobic metabolism, and use of excess cells, well adapted, and limited for carbon (limited analyte). If real samples are very turbid, or laden with Folin-reactive pigments as many lignin compounds are, microbial calorimetry has a further advantage. It is far less sensitive to such interference than spectrophotometry.

### Stripping Efficiency and Stripping Specificity

As with any other analytical method, MCA's capacity is enhanced if it is easy to remove interfering compounds. Microbial adaptation confers specificity in binding unwanted compounds so they can be swept out without losing the sample for analysis. Figures 5a and 5b show the data for phenol and vanillic acid stripping under convenient conditions, namely, with easily acquired amounts of stripper cells ( $5 \times 10^{10}$  cells), and conditions where interfering compound concentrations are relatively large, i.e., up to 10 times the amount of sample for analysis.

Phenol-grown cells nearly quantitatively bind and carry down phenol and some of the cresols in concentrations  $\sim 8 \times 10^{-3}$  mg/ml (ca.  $6 \times 10^{-5}$  M). Phenol and *o*-, *p*-, and *m*-cresol are stripped as shown in Figure 5a. In contrast, little vanillic acid is removed by phenol-grown *P. putida*, i.e., vanillate remains in the supernatant, whereas phenol and the cresols are bound and spun down with the stripper cells.

When the same *P. putida* are grown on vanillic acid, Figure 5b, vanillate efficiently binds and is stripped, whereas very little phenol is removed (see Figure 5a). Indeed, Figures 5a and 5b illustrate the efficiency and specificity with which *P. putida* ATCC 11172 binds phenols, and as can be seen is sharply dependent on the carbon source used for growth. Within cogeners, phenol itself and *o*-, *m*-, and *p*-cresol, there is not much discrimination in the ability of phenol-grown cells to strip them below levels of ca.  $8 \times 10^{-3}$  mg/ml. Above this concentration, differences between the individual compounds are seen but even these disappear when cell concentrations are made even larger. For  $50 \times 10^{10}$  phenol-grown *P. putida*/ml, up to

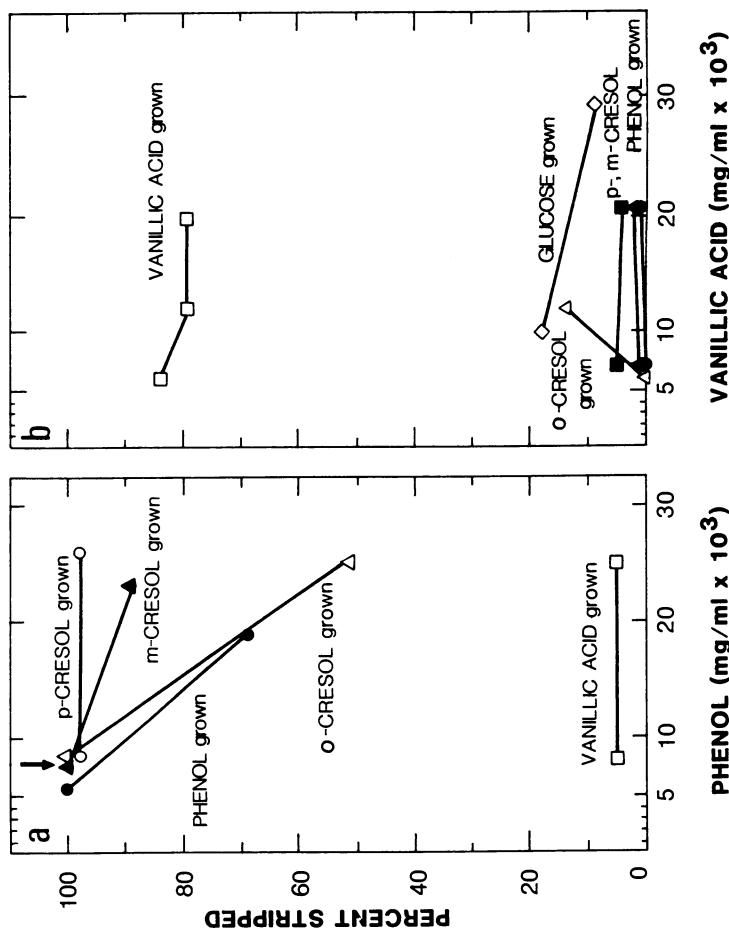


Figure 5. Stripping phenol, cresols and vanillic acid, dependent on *Pseudomonas* adaptation to compounds to be stripped;  $5 \times 10^{10}$  cells/ml during stripping. Arrow in Figure 5a: Concentration of compounds below which stripping is quantitative (see text).

$30 \times 10^{-3}$  mg/ml of these compounds all bind and therefore get stripped. However, for practical purposes, one prefers not to have to use such a large number of cells and ordinarily there is no need to. At least for this organism, usually  $5 \times 10^{10}$  cells/ml are enough to strip compounds of this kind in the  $10^{-6}$  to  $10^{-5}$  M range.

Glucose-grown *P. putida* strip glucose, but grown on the cresols they do not bind glucose efficiently in micromolar sugar concentrations nor metabolize it rapidly. From results of diverse experiments, we favor *E. coli* as strippers and metabolizers of carbohydrates in MCA (4). However, as might have been expected from Stanier, Palleroni and Doudoroff's research (14), *Pseudomonas* provides the best prospects for lignin model compound and petroleum compound binding and metabolism. An arrow in Figure 5a indicates an abscissal value, below which essentially 100% binding and stripping occurs. Calculations analogous to those carried out earlier (15) leads to the estimation that, given such an amount of phenol and such a number of cells ( $8 \times 10^{-3}$  mg/ml,  $5 \times 10^{10}$  cells/ml), only between 0.5 and 1.0% of membrane lipids are required to accommodate such an amount of phenol. That estimation does not indicate the mechanism of binding. But it does indicate that once the cells are adapted, they are adequately large "sponges" for such an amount of compound.

Stripping is simple, rapid, and greatly expands MCA for these kinds of compounds. Microbial stripping of this kind likely would be helpful in analytical methods other than calorimetry but oddly this has not been developed. Table I summarizes the main points from numbers of plots similar to Figures 5a and 5b. The conditions were:  $5 \times 10^{10}$  cells/ml, 6 to  $8 \times 10^{-3}$  mg compound to be stripped/ml, 30 second mixing. Glucose was stripped from  $15 \times 10^{-3}$  mg glucose/ml.

Table I. Efficiency of Stripping (Percent Removed) Compounds Dependent on the Carbon Source for Growth, *P. putida* ATCC 11172

Compound to be Stripped	Carbon Source on which Grown (adapted)					
	<i>o</i> -Cresol	<i>m</i> -Cresol	<i>p</i> -Cresol	Vanillic Acid	Phenol	Glc*
<i>o</i> -Cresol	97	100	93	73	100	6
<i>m</i> -Cresol	100	100	100	87	100	
<i>p</i> -Cresol	100	100	100	92	100	
Vanillic Acid	0	1	4	84	0	7
Phenol	100	100	99	5	100	
Glucose	0					56

\*Glc = Glucose.

### Calorimetric Combustion of *o*-Cresol and Vanillic Acid Mixtures in 5-100 Nanomoles Range

*P. putida* ATCC 11172 grown on *o*-cresol efficiently strips and also combusts *o*-cresol. Figure 6 shows MCA and stripping performance for *o*-cresol (lower abscissa) when considerable vanillic acid is present (upper abscissa). The data illustrates how adaptation confers specificity. First, using *o*-cresol grown cells for combusting an equimolar mixture of *o*-cresol and vanillic acid yields virtually the same plot as *o*-cresol alone, down to 8 nanomoles *o*-cresol. Secondly, after *o*-cresol stripping, nearly all the *o*-cresol is removed and vanillic acid interferes minimally (lower plot of Figure 6). Thirdly, adaptation to *o*-cresol enables the cells to combust and to strip *o*-cresol. But it disables them from using vanillic acid at any finite rate on MCA's time scale. However, vanillic acid-grown *P. putida* is fully capable of stripping and combusting vanillate in a few minutes. In short, adaptation confers reasonable specificity down to micromolar concentrations of *o*-cresol plus the ability to strip *o*-cresol.

### Lignin Model Compounds

In order to obtain rapid metabolism and rapid heat generation from aromatic compounds related to lignin, several soil isolates were used. *P. putida* ATCC 11172 did not grow easily on compounds such as syringic acid and certain other compounds more lignin-like. However, soils collected locally yielded bacteria, first from enrichment cultures and then grown on plates or defined liquid culture, were able to combust the compounds listed in Table II. The Table reports concentrations of the carbon source used in MCA, the time intervals needed for completely metabolizing 10-50 nanomoles of compound, and the apparent molar heats of metabolism in low carbon concentrations ( $\Delta^\circ\text{H}$ ). Cinnamic acid and 3,4-dimethoxycinnamate evolved rather extraordinary heats, over 800 Kcal/mole. Such heats were not expected in that 3,4-dimethoxycinnamate is already partly oxidized. Microbial combustion of naphthalene gave 810 Kcal/mole, 2-methylnaphthalene gave 652 Kcal/mole, using *P. putida* in earlier work (1). Plainly the relative state of oxidation or reduction of carbon sources does not predict how much heat compounds generate in microbial combustion, in contrast to conventional oxygen bomb calorimetric combustion. Rather, there is a dependence on how well, or how poorly, catabolites fit existing metabolic pathways of organisms (16). If there is poor fitting, more carbon has to be used in exothermic pathways emitting  $\text{CO}_2$  to generate needed intermediates such as NADH required to process whatever fragments that can be retained. Once cells (isolates) are adapted to these compounds they can drive metabolism through in 10-20 minutes, if carbon is limited and there are excess cells and oxygen. Thus, MCA does not need to complete a growth cycle as in growth assays, but simply takes up carbon and gets through the linear, early catabolic stages.

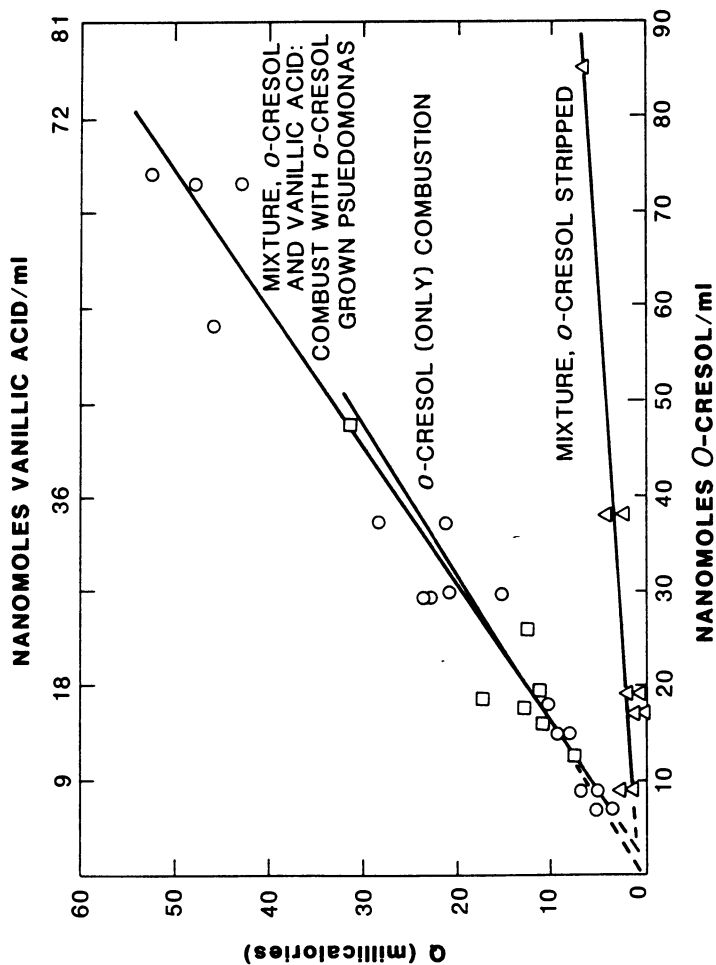


Figure 6. Calibration of heat generation from *o*-cresol by *Pseudomonas* metabolism as a standard plot for analysis of *o*-cresol alone and in *o*-cresol, vanillic acid mixtures, dependent on *Pseudomonas* adaptation in both calorimetry and stripping.

Table II. Lignin Model Compound Calorimetry with Soil Cultures

Compound	Sample Concentration (micromolar)	Time for Complete Combustion of 5-50 Nanomoles (min)	Molar Heat of Aerobic Metabolism, Kcal
<i>p</i> -Hydroxyphenyl-acetate	6-40	16	805
Syringic acid	21-42	18	470
Cinnamic acid	2-30	10	830
Hydrocinnamic acid	12-30	15	710
3,4-Dimethoxy-cinnamic acid	9-36	20	850

## Conclusions

MCA of oxidized lignin fragments (such as the hydroxycinnamic acids in Table II) appears to be as sensitive as spectrophotometric analyses from results seen so far, even comparing compounds that are brightly colored or which can be made so (chromogenic, prochromogenic compounds). MCA's specificities are determined by those compounds which bacteria can uptake and metabolize. Adapted bacteria are quite selective in this regard. Although MCA requires an excess of cells to drive analytical reactions rapidly, the required amounts usually are easily obtained once the inocula are available. About 1-5 mg of cells are needed for each combustion, and 2-10 mg for most stripping operations. Therefore, 50-300 ml of overnight culture is sufficient to produce cells for 10-30 combustions or strippings. Currently we are developing means for freezing cells so they may be stored.

Because MCA ranges down to 5-50  $\mu\text{M}$  analytes and air solubilities are  $\sim 1.3\text{mM}$  (dissolved  $\text{O}_2$ , 0.3 mM (1)), there is plenty of oxygen available at 25° to ensure aerobicity. Nevertheless, we use one or two remixings in mid-run (Fig. 3) to ensure aerobicity if sample concentrations are above ca. 50  $\mu\text{M}$ .

Oxygen respirometry has sometimes been used as a basis for analysis. Initially one might think the two methods, oxygen respirometry and microbial calorimetry, are equivalent. However, there are very large differences between them in practice when samples are micromolar in concentration. To analyze a few micromolar concentrations via disappearance of oxygen, the oxygen baseline concentrations have to be held in very narrow tolerances, i.e., in 0.1 to 5 or 10  $\mu\text{M}$  during analysis. Holding that against a background which (i) is sufficient to maintain full aerobicity, and (ii) likely to fluctuate for various reasons, is not easy in practice. MCA operates on very different grounds. Any roughly fluctuating oxygen concentration will do, as long as there is an oxygen surplus. MCA is carbon-limited, not oxygen difference-limited. The strength of MCA is that it uses a rough excess of cells, a rough excess of oxygen, and produces a signal directly

proportional to "carbon" (the sample). It is not dependent on detection of small changes in oxygen concentration against fluctuating, large, oxygen concentrations.

Lignin itself usually requires days, months, or years to biodegrade. However, oxidized lignin fragments can biodegrade rapidly if adapted bacteria are available. Over the years, dozens of microbial calorimetric studies of carbon utilization as a correlate of microbial growth have been carried out by Dermoun *et al.* (17). Many such papers leave the impression that heat generation commonly requires 8-24 hours to peak. In fact, however, any organism having a doubling time from 20-60 minutes must transport and metabolize carbon in 2-20 minutes. Therefore, oxidized fragments of lignin, and perhaps other lignin degradation products, whatever their source, can mostly be expected to "burn" rapidly, if cells are adapted and there are enough of them to bind all available carbon.

A disadvantage of MCA is that it is new and not familiar. However, MCA takes advantage of several ancient processes and is congruent with them, namely bacterial processing in soil, silage, sewage, and digestion. MCA simply measures their heats using organisms that propel these processes on a large scale.

### Acknowledgment

This work was supported by the University of Minnesota Agricultural Experiment Station and by the University Bioprocess Technology Institute.

### Literature Cited

1. Lovrien, R.; Jorgenson, G.; Ma, M.; Sund, W. *Biotech. Bioeng.* 1980, **22**, 1249-69.
2. Hammerstedt, R. H.; Lovrien, R. E. *J. Exp. Zool.* 1983, **228**, 459-69.
3. Battley, E. H. *Energetics of Microbial Growth*; Wiley-Interscience: New York, 1987; 322-51.
4. Lovrien, R.; Williams, K. K.; Ferry, M. L.; Ammend, D. A. *Appl. Environ. Microbiol.* 1987, **53**, 2935-41.
5. Parke, D. V. *Enzyme Induction*; Plenum Press: New York, 1975; Ch. 1-3.
6. Zubay, G. *Biochemistry*; Addison-Wesley Publ: Reading, MA, 1983; Ch. 26.
7. Fox, B. G.; Lipscomb, J. D. *Biochem. Biophys. Res. Comm.* 1988, **154**, 165-70.
8. Fujisawa, H.; Hayaishi, O. *J. Biol. Chem.* 1968, **243**, 2673-81.
9. Audus, L. J. *Nature* 1946, **158**, 149-50.
10. Ashworth, J. M.; Kornberg, H. L. *Proc. Roy. Soc. London Sec. B* 1966, **165**, 179-88.
11. Lipsett, S. G.; Johnson, F. M. G.; Maas, O. *J. Am. Chem. Soc.* 1927, **49**, 925-43.
12. Barisas, B. G.; Gill, S. J. *Ann. Rev. Phys. Chem.* 1978, **29**, 141-46.
13. Berka, T. R.; Allenza, P.; Lessie, T. G. *Curr. Microbiol.* 1984, **11**, 143-48.



14. Stanier, R. Y.; Palleroni, N. J.; Doudoroff, M. *J. Gen. Microbiol.* 1966, **43**, 159-79.
15. Lovrien, R.; Hart, G.; Anderson, K. J. *Microbios* 1977, **20**, 153-72.
16. Anderson, J. J.; Dagley, S. *J. Bacteriol.* 1980, **143**, 525-28.
17. Dermoun, Z.; Boussand, R.; Cotten, D.; Belaich, J. P. *Biotech. Bioeng.* 1985, 996-1004.

RECEIVED April 28, 1989

## Chapter 40

# Microbial Degradation of Tannins and Related Compounds

A. M. Deschamps

Laboratoire de Microbiologie Alimentaire et de Biotechnologie, Université de Bordeaux I, Avenue des Facultés, 33405 Talence, France

While tannins are usually described as antagonists of numerous microorganisms and being recalcitrant to biodegradation, they can nevertheless be degraded by a large variety of microorganisms. Because of their labile galloyl ester structures, hydrolysable tannins are more readily degraded than condensed tannins. This chapter reviews the limited progress made in understanding the potentially useful processes of the biodegradation of hydrolysable and condensed tannins.

Tannins are water-soluble phenolic compounds which are usually extracted from plant material by hot water. After lignins, they are the second most abundant group of plant phenolics. Their tanning property is due to their capacity to combine with proteins. However, they can also complex with other polymers such as alkaloids, cellulose, and pectins.

Tannins are usually concentrated in barks, galls or leaves of woody plants (1). Tannins are classified into two different groups, hydrolyzable or condensed, depending on the structure of the polymer (2). Hydrolyzable tannins are composed of esters of gallic acid (gallotannins) and/or ellagic acid (ellagitannins) with a sugar core, predominantly glucose (see Gross, this volume). Some of the most common structures are digalloyl 3,6 glucose or trigalloyl 1,3,6 glucose (Fig. 1); such structures have been discussed in detailed review papers by Haslam (1) and Metche and Girardin (2). The major commercial hydrolysable tannins are extracted from Chinese gall (*Rhus semialata*), sumach (*Rhus coriara*), Turkish gall (*Quercus infectoria*), tara (*Caesalpinia spinosa*), myrobolam (*Terminalia chebula*), and chestnut (*Castanea sativa*) (1).

The second group of tannins are the condensed tannins, or polymeric proanthocyanidins (2). These are composed of flavonoid units, and are more recalcitrant to biodegradation than hydrolysable tannins. Of these, the

0097-6156/89/0399-0559\$06.00/0  
© 1989 American Chemical Society

important commercial ones are extracted from wattle (*Acacia mollissima* and *A. mearnsii*), and quebracho (*Schinopsis lorentzii* and *S. balansae*). Condensed tannins are usually more abundant in tree barks and woods than their hydrolyzable counterparts (1).

Tannins have long been considered to be inhibitors of most microorganisms. For example, they are strong inhibitors of *Azotobacter* and nitrogen-fixing (3), nitrifying (4,5) and sulfate-reducing bacteria (6). Soil bacteria such as *Rhizobium* are also often sensitive to tannins. For this reason, tannins generally retard the rate of decomposition of vegetable matter (8) via inhibition of biodegradative enzymes of the attacking organism. (9,10). Fungi, such as *Fusarium*, *Verticillium*, *Aspergillus*, *Alternaria* (11,12), as well as yeasts (13) can also be inhibited by tannins. However, other related plant phenolics, such as anthocyanins, flavonoids, catechol, etc., can also inhibit these microorganisms (14). Tannins, when provided in very high concentrations over extended time periods, can also be toxic to higher organisms such as rats, rabbits, guinea-pigs (15) and man; hence their levels are regulated in many vegetable foods (16). Some authors have attributed the presence of tannins in barks or leaves to a defense system against predators or decomposing organisms (14,16). Nevertheless, many fungi or bacteria are quite resistant to tannins and can also degrade them.

### Microbial Degradation of Hydrolyzable Tannins

In 1913, Knudson (17) reported that tannic acid (the commercial name of the Chinese gall tannin) could be degraded by a strain of *Aspergillus niger*; previously the French scientist Pottevin (in 1900) had named this enzyme tannase (10). Since then, most of the progress on elucidating the mechanisms of hydrolysable tannin biodegradation has occurred since 1960.

*Tannase.* The enzyme tannase, or tannin-acyl hydrolase (EC 3:1:1:20), was described and purified from strains of *Aspergillus niger* by Haslam *et al.* (19) and Dhar and Bose (20). This enzyme splits the ester linkage of pendant galloyl groups from glucose in gallotannins. Surprisingly, the enzyme is not induced by tannic acid, and in *A. niger* it is mostly cell-wall bound or only slightly exocellular (20,21). The enzyme's optimal pH is 4-4.5 and its optimal temperature is 30°C. Tannase has been isolated from mycelial extracts (22) of other *Aspergillus* species, as well as from various *Penicillium* strains (Table I). Tannase has also been detected in a yeast culture, although its enzyme had different optima, i.e., the optimal pH was 6 and the temperature was 40°C (26). In *Candida* sp., tannase had a MW of 250,000 and was composed of two sub-units of glycoprotein structure (31); the tannase of *Aspergillus* was also of high molecular weight (24). Tannase has also been detected in bacterial cultures (29), where its optimum activity was pH 5.5 with different strains isolated from decayed barks.

*Degradation of Gallotannins.* Different investigations on tannase revealed that this enzyme was not equally efficient on all hydrolyzable tannins. This was particularly true for yeast, whose tannase was effective only on tannic

Table I. Microorganisms Producing Tannase (tannin-acyl hydrolase)

---

FUNGI:

- Aspergillus niger*: Haslam *et al.* (19); Pourrat *et al.* (21)  
*Aspergillus oryzae*: Iibuchi *et al.* (23)  
*Aspergillus flavus*: Adachi *et al.* (24)  
*Aspergillus japonicus*: Ganga *et al.* (22)  
*Penicillium chrysogenum*: Rajakumar and Nandy (25)  
*Penicillium notatum*: Ganga *et al.* (22)  
*Penicillium islandicum*: Ganga *et al.* (22)

## YEASTS:

- Candida* sp.: Aoki *et al.* (26)  
*Pichia*, several species: Jacob and Pignal (27)  
*Debaryomyces hansenii*: Jacob and Pignal (27)

## BACTERIA:

- Achromobacter* sp: Lewis and Starkey (28)  
*Bacillus pumilus*: Deschamps *et al.* (29)  
*Bacillus polymyxa*: Deschamps *et al.* (29)  
*Corynebacterium* sp: Deschamps *et al.* (29)  
*Klebsiella planticola*: Deschamps *et al.* (29)  
*Pseudomonas solanacearum*: Muthukumar and Mahadevan (30)
- 

acid, but not on natural tannins such as chestnut, oak, myrobolan or tara (27). Further, while Aoki *et al.* (26,31) were able to degrade tannic acid using *Rhodotorula rubra*, it was only weakly active on chestnut tannin (32).

On the other hand, fungal tannases efficiently degrade hydrolysable tannins. This has been shown by the degradation of amla (33) and myrobolan (34) tannins with enzymes from *Aspergillus niger*, and chestnut tannins with enzymes from different fungi (28). This property is currently used in the detoxification of tea tannin extracts using an industrially produced enzyme from *A. niger*.

Bacterial tannase literature is limited to the isolation of an *Achromobacter* capable of degrading gallotannin from chinese gall (Lewis and Starkey, 1969 (28)) and our own papers (29,30). In 1980 (35), we described a collection of tannic acid degrading bacteria, mostly from *Bacillus*, *Corynebacterium* and *Klebsiella* strains, which could degrade natural tannins such as those from chestnut and tara. Indeed, because of the simple structure of the gallotannin in tara species, this represents a potential source of gallic acid (36). The degradation of myrobolan tannin was also reported for *Pseudomonas solanacearum* (30).

*Degradation of Gallic Acid.* Gallic acid, an obligate intermediate in the degradation of gallotannins, is degraded by some bacteria such as *Pseudomonas* (37). In our laboratory, both *Klebsiella pneumoniae* (38) and *K. planticola* strains grew on tannins and utilized gallic acid as a carbon source (35). The same capacity was observed for *Citrobacter* species where pyro-

gallol accumulated as a metabolic end product. Koshida and Yamada (39) recently patented this method for pyrogallol production.

While gallic acid is probably utilized by fungi and yeasts as a carbon source, only a few papers have suggested this possibility (25,40,41), including one for *Aspergillus flavus* (42).

### Microbial Degradation of Condensed Tannins

Condensed tannins were considered to be highly recalcitrant to biodegradation until Basaraba (3) reported that some bacterial isolates could utilize wattle tannin as both a carbon and energy source. Later, Lewis and Starkey (28) isolated a strain of *Pseudomonas* which degraded catechin, and strains of *Aspergillus* and *Penicillium* which degraded wattle tannin.

*Fungal Degradation of Condensed Tannins.* Chandra *et al.* (43) first reported the isolation of fungi, such as *Aspergillus fumigatus*, *A. flavus*, *A. terreus* and various *Penicillium* sp., which were capable of degrading tannins extracted from apple wood. These observations were extended by Grant (44), using a strain of *P. adametzi* capable of degrading di- and tri-procyanidin structures, as well as (+) catechin and a crude tannin extract. Some unusual white-rot fungi, identified as *Bispora betulina* and *Isaria* sp., were also able to degrade condensed tannins extracted from Douglas-fir bark (45). Recently, Sivaswamy and Mahadevan (46) reported the degradation of wattle tannin by a strain of *Aspergillus niger*. Interestingly, it also produced tannase and could degrade the gallotannin, myrobolan. The edible puffball *Calvatia gigantea* can also degrade both hydrolyzable (chestnut) and condensed (wattle) tannins (47), as well as catechin. It has been proposed that this organism could be used for detoxification purposes, or for the valorization of high-tannin vegetable residues.

Yeasts have been described for the degradation of wattle tannin (48). This degradation was determined by the estimation of leucoanthocyanidin and flavan-3-ol groups (Fig. 2) in the remaining degraded tannin. Among the strains (*Candida guilliermondii*, *C. tropicalis*, *Torulopsis candida*) isolated and studied, the simultaneous degradation of both structures was not observed, suggesting different mechanisms of degradation. For example, a strain of *C. guilliermondii* degraded the flavan-3-ol structures but did not affect the leucoanthocyanidin components. Most yeasts were efficient degraders of quebracho tannins (32) and reduced the tannin content of pine and gaboon wood bark extracts by 70 to 80% in five days.

*Bacterial Degradation of Condensed Tannins.* Although Basaraba (5) proposed that bacteria could degrade condensed (wattle) tannin, this topic has only been investigated in our laboratory in Compiègne. In these studies, our objective was to control the rate of biodegradation of tannin-rich barks, such as those from pine and gaboon-wood (*Acoumea kleneana*). Consequently, we succeeded in isolating, by culture enrichment, bacteria capable of degrading and utilizing these barks (49), as well as quebracho (*Schinopsis lorentzii*) and wattle (*Acacia mollissima*) tannins. A collection of various genera and species was identified in these studies (50), with the genera

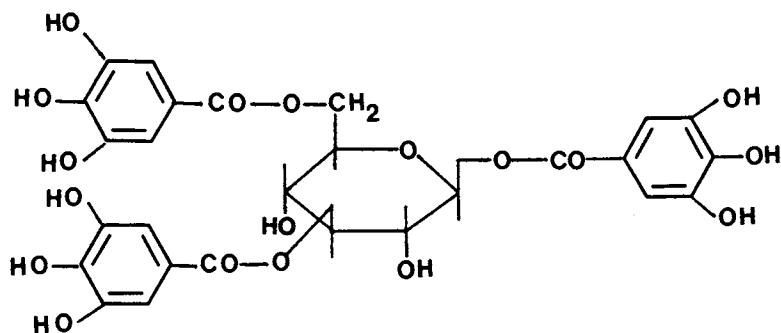


Figure 1. Structure of trigalloyl-1,3,6 glucose.

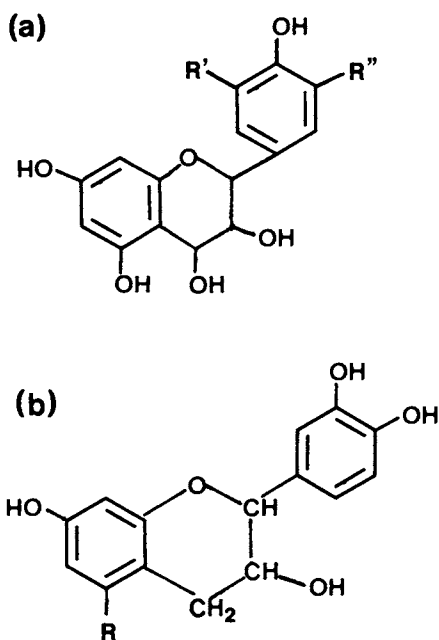


Figure 2. (a) Leucoanthocyanidin and (b) flavan-3-ol structures, where R, R' and R'' = H or OH.

*Bacillus*, *Klebsiella*, *Corynebacterium*, and *Pseudomonas* being the most frequently observed. The capacity of these bacteria to degrade tannins, and detoxify bark chips or barks extracts, was further demonstrated with pine (*Pinus maritima*) (51), oak (*Quercus pedunculata*) and gaboon wood (*Aucoumea kleneana*) barks (52). The degradation of quebracho and wattle tannins was also confirmed in pure cultures (53).

**Microbial Degradation of Catechin.** Since (+) catechin is a possible biodegradation product from condensed tannins, its utilization and bioconversion have been extensively examined by several research groups using fungi, bacteria and yeasts.

**Fungi.** Fungi-degrading catechin have been known for about twenty years, e.g., *Aspergillus niger*, *A. terreus*, *A. fumigatus*, *A. flavus* and *Penicillium* sp. (54) and *Penicillium adametzi* (44). In the latter case, the organism grew on catechin and anthocyanidin model compounds as sole carbon sources. Interestingly, the pathogenic fungus *Endothia parasitica* (55) also degraded catechin. To account for its biodegradation, Chandri *et al.* (54) first suggested that an extracellular enzyme must be involved, following which the enzyme catechin 2,3-dioxygenase was isolated from *Chaetomium cupreum* (56). The molecular weight (MW) of this glycoprotein was approximately 40,000 and catechin was cleaved via *meta*-ring fission.

**Bacteria.** Many bacteria degrade catechin and use it as a carbon source, as shown first by Lewis and Starkey (28). In 1982 Muthukumar *et al.* isolated several strains of *Rhizobium* and *Bradyrhizobium* (57), including *B. japonicum* which degraded catechin. This last species produced the same enzyme as *C. cupreum* (Waheeta and Mahadevan, personal communication). We also demonstrated that certain tannic-acid degrading bacteria can also degrade catechin (35). Recently, Baominathan and Mahadevan showed that catechin-degrading machinery was plasmid borne in *Pseudomonas solanacearum* (58), which also produces a catechin oxidase.

**Yeasts.** An interesting paper published in 1984 (59) claimed that rat-caecal microflora degraded catechin. To our knowledge no paper has dealt with yeasts, other than that some yeasts degrading wattle of quebracho tannins were able to grow weakly with catechin as a sole carbon source (32).

## Concluding Remarks

This review of literature on tannin degradation shows that our knowledge of this topic is only very slowly improving. Only a handful of laboratories are currently involved in this area. Of these, the Indian laboratories have made several interesting investigations recently, presumably because they are very active in leather manufacture and need to control the toxicity of their tannery effluents.

Some microorganisms degrading condensed tannins have been isolated and described, but no reports on the mechanism of the depolymerization process, or the enzymes involved in biodegradation, have appeared. It must be stressed that condensed tannin degradation may be associated with other

detoxification mechanisms, other than those operative for catechin. This assertion is made since many strains which grow on condensed tannins do not grow on catechin. This is unusual since this compound is often viewed as an intermediate of biodegradation. Consequently, catechin degradation should not be confused with condensed tannin degradation. More studies are needed, if we are to understand and elucidate the mechanism of the degradation of condensed tannins. Currently, there is insufficient data available for comparison of this degradation process to that of other polyphenols, such as lignin.

Further, while the degradation mechanisms of tannic and gallic acids are quite well understood for bacteria and fungi, few commercial applications have yet resulted, e.g., in the production of the enzyme tannase or the bioconversion of gallic acid (or tannins) to pyrogallol (60). In the case of the condensed tannins, however, their biodegradation has been much less thoroughly studied. Such studies are important since control and detoxification of tannins will continue to find application in the food industry (61), as well as in biotechnological processes using barks as lignocellulosic substrates (62). For these reasons, the isolation and identification of tannin-degrading enzymes, and the determination of their mechanism of action, are of great importance.

### Literature Cited

1. Haslam, E. In *Biochemistry of Plant Phenolics*; Plenum Press: New York, 1979, 475-523.
2. Metche, M.; Girardin, M. In *Les Polymeres Vegetaux*; Monties, B., Ed.; Gauthiers Villars: Paris, 1980.
3. Basabara, J. *Can. J. Microbiol.* 1966, **12**, 787-794.
4. Rice, E. L.; Pancholy, S. K.; *Am. J. Bot.* 1973, **60**, 691-702.
5. Basabara, J. *Plant Soil* 1964, **21**, 8-16.
6. Booth, G. H. *J. Appl. Bacteriol.* 1960, **23**, 125-129.
7. Muthukumar, G.; Mahadevan, A. *Leather Sci.* 1983, **30**, 263-269.
8. Benoit, R. E.; Starkey, R. L. *Soil Sci.* 1968, **105**, 203-208.
9. Goldstein, J. L.; Swain, T. *Phytochem.* 1965, **4**, 185-192.
10. Benoit, R. E.; Starkey, R. L. *Soil Sci.* 1968, **105**, 203-208.
11. Lewis, J. A.; Papavizas, G. C. *Can. J. Microbiol.* 1967, **13**, 1655-1661.
12. Mahadevan, A.; Muthukumar, G. *Hydrobiol.* 1980, **72**, 73-79.
13. Jacob, F. H.; Pignal, M. C. *Mycopathol. Mycol. Appl.* 1972, **48**, 121-142.
14. Mahadevan, A. *J. Sci. Indian Res.* 1974, **33**, 131-138.
15. Cameron, G. R.; Milton, R. F.; Allen, J. W. *Lancet* 1943, **14**, 179-186.
16. MacLeod, M. N. *Nutr. Abs. Rev.* 1974, **44**, 803-815.
17. Knudson, L. *J. Biol. Chem.* 1913, **14**, 159-184.
18. Pottevin, H. *Compt. rend.* 1900, **131**, 1215-1217.
19. Haslam, E.; Haworth, R. D.; Jones, K.; Rogers, H. J. *J. Chem. Soc.* 1961, 1821-1835.
20. Dhar, S. C.; Bose, S. M. *Leather Sci.* 1964, **11**, 27-38.



21. Pourrat, H. Regeat, F.; Pourrat, A.; Jean, D. *Biotechnol. Lett.* 1982, **4**, 583-588.
22. Ganga, P.S., Nandy, S. C.; Santappa, M. *Leather Sci.* 1977, **24**, 8-16.
23. Iibuchi, S.; Minoda, Y.; Yamada, K. *Agr. Biol. Chem.* 1972, **36**, 1553-1562.
24. Adachi, O.; Watanabe, M.; Yamada, H. *Agr. Biol. Chem.* 1968, **32**, 1079-1085.
25. Rajakumar, G. S.; Nandy, S. C. *Appl. Environ Microbiol.* 1983, **46**, 525-527.
26. Aoki, K.; Shinke, R.; Nishara, H. *Agr. Biol. Chem.* 1976, **40**, 79-85.
27. Jacob, F. H.; Pignal, M. C. *Mycopathol.* 1975, **57**, 139-148.
28. Lewis, J. A.; Starkey, R. L. *Soil Sci.* 1969, **107**, 235-241.
29. Deschamps, A. M.; Otuk, G.; Lebeault, J. M. *J. Ferment. Technol.* 1983, **61**, 55-59.
30. Muthukumar, G.; Mahadevan, A. *Indian J. Exp. Biol.* 1981, **19**, 1083-1085.
31. Aoki, K.; Shinke, R.; Nishara, H. *Agr. Biol. Chem.* 1976, **40**, 297-302.
32. Deschamps, A. M.; Leulliette, L. *Int. Biodeterior. Bull.* 1984, **20**, 237-240.
33. Srivastava, S. K.; Sharma, S. K. *Indian J. Plant Physiol.* **17**, 47-52.
34. Freudenberg, K.; Blummel, F.; Frank, T. *Z. Physiol. Chem.* 1927, **164**, 262.
35. Deschamps A. M.; Mahoudeau, G.; Conti, M.; Lebeault, J. M. *J. Ferment. Technol.* 1980, **58**, 93-97.
36. Deschamps, A. M.; Lebeault, J. M. *Biotechnol. Lett.* 1974, **6**, 237-242.
37. Trevors, J. T.; Basabara, J. *FEMS Microbiol. Lett.* 1980, **7**, 307-309.
38. Deschamps, A. M.; Richard, C.; Lebeault, J. M. *Ann. Microbiol.* 1983, **134A**, 189-196.
39. Yoshida, H.; Yamada, H. *Agr. Biol. Chem.* 1985, **49**, 659-663.
40. Rajakumar, G.; Nandy, S. C. *Leather Sci.* 1986, **33**, 220-227.
41. Dalvesco, G.; Fiusello, N.; Veittiranus, M. *Allonis* 1972, **17**, 25-40.
42. Gurujeyalakshmi, G.; Mahadevan, A. *Zentralbl. Mikrobiol.* 1987, **142**, 187-192.
43. Chandra, T.; Krishnamurthy, V.; Madhavakrishana, W.; Nayudamma, Y. *Leather Sci.* 1973, **20**, 269-273.
44. Grant, W. D. *Science* 1976, **193**, 1137-1139.
45. Ross, W. D.; Corden, M. E. *Wood Fibers* 1976, **6**, 2-12.
46. Sivaswamy, S. N.; Mahadevan, A. *J. Environ. Biol.* 1985, **6**, 271-278.
47. Galiotou-Panayotou, M.; Macris, B. J. *Appl. Microbiol. Biotechnol.* 1986, **23**, 502-506.
48. Otuk, G.; Deschamps, A. M. *Mycopathol.* 1983, **83**, 107-111.
49. Deschamps, A. M.; Mahoudeau, G.; Leulliette, L.; Lebeault, J. M. *Rev. Ecol. Biol. Sol.* 1980, **17**, 577-581.
50. Deschamps, A. M. *Eur. J. Forest Pathol.* 1982, **12**, 252-257.
51. Deschamps, A. M.; Gillie, J. P.; Lebeault, J. M. *Eur. J. Appl. Microbiol. Biotechnol.* 1981, **13**, 222-225.
52. Deschamps, A. M.; Leulliette, L. *Phytopathol. Z.* 1985, **113**, 304-310.

53. Deschamps, A. M. *Can. J. Microbiol.* 1985, **31**, 499-502.
54. Chandra, T.; Madhavakrishna, W. Nayudamma, Y. *Can. J. Microbiol.* 1969, **15**, 303-306.
55. Elkins, J. R.; Pate, W.; Lewis, J.; Porterfield, C. *III Int. Congr. Plant Path. (Abstract)*, 1978.
56. Sivaswamy, S. N., Mahadevan, A. *J. Indian Bot. Soc.* 1986, **65**, 95-100.
57. Muthukumar G.; Arunakumari, A.; Mahadevan, A. *Plant Soil* 1982, **69**, 163-169.
58. Boominathan, K.; Mahadevan, A. *FEMS Microbiol. Lett.* 1987, **40**, 147-150.
59. Groenewoud, G.; Hundt, H. K. L. *Xenobiotica* 1984, **14**, 711-717.
60. Kikuchi, M.; Katsumo, Y.; Mizusawa, K. Japanese patent JP 61, 108-393 (86,108,383), 1986. Kokai Tokkyo Koho.
61. Marakis, S. *Cryptog. Mycol.* 1986, **6**, 293-308.
62. Deschamps, A. M. *Biotechnological methods for valorization of bark wastes*. Int. Symp. Wood Pulp. Chem., Vancouver, 1985, 183-184.

RECEIVED May 19, 1989

## Chapter 41

# Specific Assays, Purification, and Study of Structure—Activity Relationships of Cellulolytic Enzymes

P. Tomme, V. Heriban<sup>1</sup>, H. Van Tilbeurgh, and M. Claeysens<sup>2</sup>

Laboratory for Biochemistry, Faculty of Sciences, State University of Ghent (RUG), K. L. Ledeganckstraat 35, B-9000 Ghent, Belgium

Differentiating activity assays of cellulase-components (all specific for  $\beta$ -1,4 glucosidic linkages) are described using chromogenic derivatives of lactose and the cellobioextrins. They proved to be valuable not only in specificity studies of these enzymes, but also as active site probes. An affinity chromatographic method for rapid isolation of some of these enzymes was also developed. New information on the domain structure of two cellobiohydrolases from *Trichoderma reesei* (CBH I and CBH II) resulted from structure-function investigations based on partial proteolysis and physical measurements. A cellulose-binding domain (C- or N-terminal) was separated from the core-enzymes, containing the active (hydrolytic) sites. In the "tadpole" structure of the intact enzymes—as deduced from small-angle X-ray scattering—the binding peptides protrude from their cores as flexible tails. Study of adsorption onto and hydrolysis of microcrystalline cellulose ("Avicel") led to new insights into the functional role of these domains and the synergism observed between CBH I and CBH II.

Native or processed cellulose (e.g., cotton, Avicel, filter paper) and its soluble derivatives (e.g., CMC, HEC<sup>3</sup>) are substrates most often used in the study of cellulases. The classification based on the use of these substrates (1,4- $\beta$ -D-glucan cellobiohydrolases (CBH), exo-cellulases, "Avicelases" and

---

NOTE: A list of abbreviations and symbols is given at the end of the text.

<sup>1</sup>On leave from the Technical University Bratislava, Chemical-Technological Faculty, Bratislava, Czechoslovakia

<sup>2</sup>Address correspondence to this author.

0097-6156/89/0399-0570\$06.00/0

© 1989 American Chemical Society

1,4- $\beta$ -D-glucan glucanohydrolases, endo-cellulases, "carboxymethylcellulases") is somewhat arbitrary.

Since the structure (crystallinity) and composition (degree of polymerization) of the cellulosic substrates is relatively unknown and the assays (reductometry, viscosimetry) are rather unspecific and sometimes lack sensitivity, we have introduced alternative chromophoric (fluorophoric) substrates containing ligands of known molecular properties (1), e.g., 2'-chloro, 4'-nitrophenyl and 4'-methyl-umbelliferyl  $\beta$ -D-glycosides, obtained via O-glycosidation (2). 1-Thioglycosides were prepared from the sugar mercaptans and the appropriate halogen derivatives (e.g., 1-chloro, 2,4-dinitrobenzene) (3).

### Materials and Methods

Enzymic hydrolysis (25-40°C) at the heterosidic bond of the chromogenic substrates was followed either continuously (via formation of 2'-chloro,4'-nitrophenol) at pH 5.5 (O.D. 405 nm) or discontinuously (4-methylumbelliferone fluorescence at pH 10, emission at  $\lambda > 435$ , excitation at  $\lambda 366$  nm). Reaction rates were calculated from the linear increase of O.D. ( $\epsilon_M = 9000 \text{ M}^{-1}\text{cm}^{-1}$ ) or fluorescence (standardization with 4-methylumbelliferone) versus time. Alternatively, an HPLC method was used to follow the formation of chromophoric reaction products, phenols and glycosides (1). Concentrations were calculated from peak heights after appropriate standardization.

Glucose was determined by the glucose oxidase-peroxidase method. Cellobiose (liberated enzymatically from methylcellotrioside) was determined in a coupled assay using cellobiose dehydrogenase from *Sporotrichum thermophile* (4).

Difference spectrophotometry or fluorescence quenching techniques were used to measure the binding of several chromophoric ligands to cellulolytic enzymes (5). A diafiltration technique (forced-flow dialysis) was adapted to measure binding isotherms and constants (6). Equilibrium binding parameters of non-chromophoric ligands (cellooligosaccharides) were determined by displacement (competition) experiments (5) or by measuring the protein UV-absorbance difference spectrum (7).

### Results

*Detection of Cellulolytic Activities in Gels.* Fluorogenic methylumbelliferyl derivatives of lactose and several cellodextrins were used to detect cellulases, after isoelectric focusing of crude or partially purified preparations from *Trichoderma sp.* (8), *Penicillium pinophilum* (9) and *Clostridium thermocellum* endoglucanases cloned in *E. coli* (10). The liberation of the strongly fluorescing 4-methylumbelliferone became readily visible after flooding the gel with a buffered solution of the appropriate substrate. The same technique was also applicable for development of SDS-PAGE chromatograms.

The results are summarized in Table I. Both the lactoside and the cellobioside were substrates of CBH I (*Tr. r.*, *P. p.*), EG I (*Tr. r.*) and of

EGC and EGD (*C. t.*). While CBH I and EG I from *Tr. r.*, showed very similar specificities, they could be differentiated by adding small amounts of cellobiose, a strongly competitive inhibitor of the cellobiohydrolase (Fig. 1). The cellotriose allowed detection of EG III activities in the culture filtrate of *Tr. r.* in spite of other activities being present; the addition of small amounts of gluconolactone effectively suppressed glucosidase activity.

Table I. Continuous Assays for Cellulolytic Enzymes

Glycosides	Enzyme							
	<i>Trichoderma</i>				<i>Clostridium</i>			
(Chromophore) (CNP/MeUmb)	CBH I	CBH II	EG I	EG III	EGA	EGB	EGC	EGD
Lactoside	+	-	+	-	-	-	+	+
Lactoside (+ G <sub>2</sub> )	-	-	+	-	-	-	-	-
Cellobioside	+	-	+	-	-	-	+	+
Cellotriose	-	-	-	+	-	+	+	-

**Activity Measurements in Solution.** The 2'-chloro, 4'-nitrophenyl  $\beta$ -D-glycosides offer an attractive alternative to classical reductometric methods. The substrate is sufficiently stable (pH 5.5, 50°C) and the favorable absorption characteristics of the liberated phenol ( $pK = 5.5$ ,  $\epsilon_M 9000 \text{ M}^{-1} \text{ cm}^{-1}$ , pH 5.5;  $\epsilon_M 16000$  at pH 6.5) allow sensitive, continuous measurements. Kinetic parameters for some of these substrates and enzymes were determined: K values were in the mM range for the lactoside (CBH I, EG I, EGD) and were at least 10 times lower for the cellobioside; turnover numbers ranged from 1 (CBH I, cellobioside) to  $300 \text{ min}^{-1}$  (EG D, cellobioside) (25°C).

Further differentiation was obtained using the chromophoric cellobiooligodextrins and a rapid and sensitive HPLC analysis of the reaction products (1). Specific degradation patterns were obtained for several enzymes such as those from *Clostridium* cloned in *E. coli* (Fig. 2).

A word of caution is appropriate, however. This was because unspecific cleavage at the heterosidic bond of these substrates was sometimes noticed, and the specificity was therefore not always exactly reflected.

**Binding Experiments.** Some of these chromophoric glycosides proved also to be valuable in cases where no hydrolysis by the cellulases occurred. This was shown in the case where the 4-methylumbelliferyl glucoside and cellobioside were not hydrolyzed by the CBH II from *Trichoderma* (see above) but could be used as reporter ligands in a series of binding experiments. Typically the fluorescence of the cellobioside was quenched in the presence of CBH II and was restored by the addition of excess amounts of non-chromophoric ligands, i.e., cellobiose (Fig. 3). Thus association constants

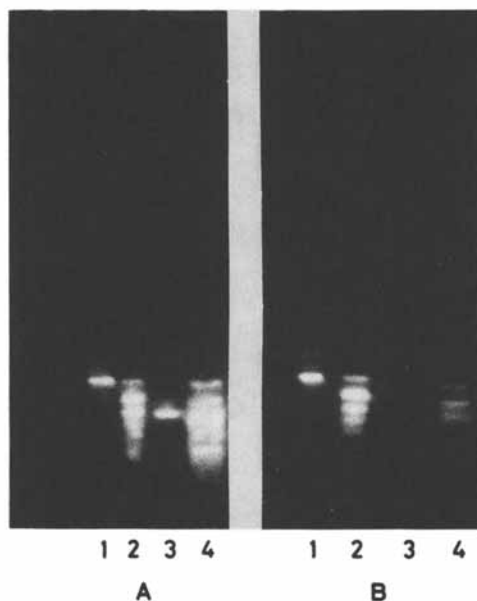


Figure 1. Analytical isoelectric focusing of cellulases from *Trichoderma reesei*. Detection of CBH I and EG I activities using MeUmbLac, in the absence (A) and presence (B) of 10 mM cellobiose. Lane 1, EG I; lane 2, EG I (iso-components); lane 3, CBH I (pI 3.9 component); lane 4, EG I-CBH I mixture). Gels were flooded with the fluorogenic substrate (pH 5.0) and after 5-10 min (room temperature) photographed (Polaroid 57, green filter) on a long wavelength UV-transilluminator (8).

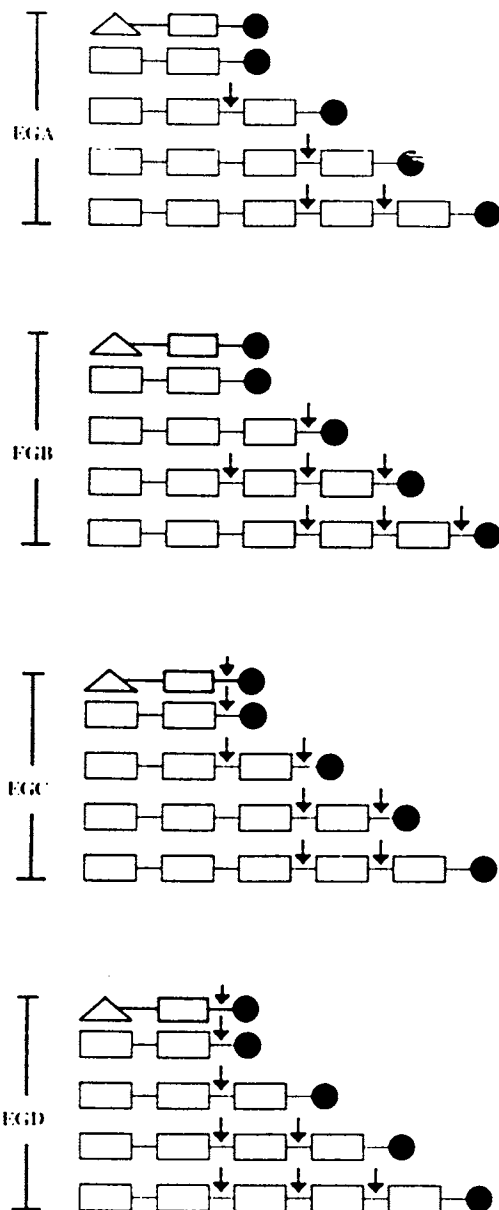


Figure 2. Specificities of Endoglucanases (EGA, EGB, EGC, EGD) from *Clostridium thermocellum* cloned in *E. coli* (10). The substrates (MeUmbGlc<sub>n</sub>, n = 2-5, MeUmbLac) are depicted (symbols:  $\Delta$ ,  $\beta$ -1,4 galactopyranosyl;  $\square$ ,  $\beta$ -1,4 glucopyranosyl;  $\bullet$ , 4-methylumbelliferyl) and the arrows indicate scission points as determined by HPLC (1).

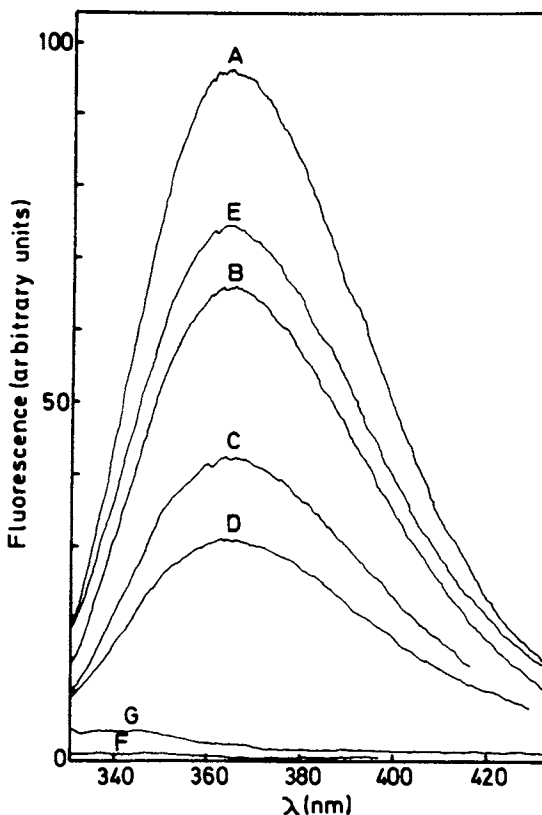


Figure 3. Quenching of the fluorescence spectrum of MeUmbG<sub>2</sub> by CBH II from *Trichoderma reesei* (5). Curve A represents the MeUmbG<sub>2</sub> (2 μM) spectrum in the absence of CBH II. Curves B, C and D show the spectra after the addition of several aliquots of 137.7 μM CBH II. Spectrum D changes to E when solid cellobiose (±2 mg) is added. When correction is made for dilution, spectrum E is equivalent to spectrum A. Curves F and G represent buffer and protein blanks, respectively. Spectra were measured at pH 5.0 and 6.6°C.



and thermodynamic binding parameters of non-chromophores were computed from displacement titrations, and a hypothetical binding scheme for CBH II was proposed (5).

The binding of chromophoric 1-thioglycosides from lactose or cellobiose to CBH I (*Tr. r.*) was followed by difference spectrophotometry of the ligand, or by the diafiltration technique (Fig. 4). Alternatively, perturbation of the protein spectrum could be used in the case of non-chromophoric ligands (Fig. 5).

### An Affinity Chromatographic Method for the Purification of Some Cellulolytic Enzymes

A considerable affinity of some cellulolytic enzymes (e.g., CBH I and CBH II from *Tr. r.* and the EG's from *C. t.*) for aryl 1-0- and 1-S-cellobiosides was evidenced by the  $K_m$  and  $K_i$  values (see above). This contrasted with the higher  $K_i$  values (typically, > mM) for some other enzymes (e.g., EGI from *Tr. r.*).

Coupling of an aryl 1-S-cellobioside to an affinity carrier was therefore expected to be useful in the chromatographic fractionation of "endo" and "exo" enzymes, e.g., from *Tr. r.* Preliminary tests indicated that CBH I and CBH II (prepurified by ion-exchange chromatography) were completely retained by the affinity support (4'-aminobenzyl 1-S-cellobioside coupled to Affigel-10 from Biorad). Desorption was achieved differentially by 0.1M lactose (elutes CBH I) and 0.01M cellobiose (elutes CBH I and CBH II). Attempts to elute the enzymes with 1M KCl, ethyleneglycol or glucose solutions were unsuccessful (11).

Thus a biospecific adsorbant was obtained; selective desorption should therefore permit successive elution of cellulolytic enzymes. It was thus found that the method was very useful in the purification of the cellobiohydrolases from *Tr. r.*, starting from very crude culture filtrates. Addition of glucose (0.1M) or gluconolactone suppressed the action of glucosidases present, preventing deterioration of the columns. The capacities exceeded 10 mg CBH I per ml gel (prepared with CNBr activated Sepharose).

Similar results were obtained with crude cellulase preparations from *Penicillium pinophilum* (12). The general applicability of this biospecific chromatography is illustrated by the isolation of the EGD from *C. t.*, cloned in *E. c.* (Fig. 6).

### Structural-Functional Investigations Based on Partial Proteolysis and Physical Measurements

The primary structure of several cellulolytic enzymes has been elucidated and this research has been further encouraged by the successful cloning and expression of heterologous genes in rapid growing host microorganisms, such as yeasts and some bacteria (e.g., 13, 14). Comparison of the known amino acid sequences of several cellobiohydrolases and endoglucanases of *Trichoderma reesei* showed that all these enzymes shared a homologous sequence of amino acids (A) separated from the cores of these enzymes by

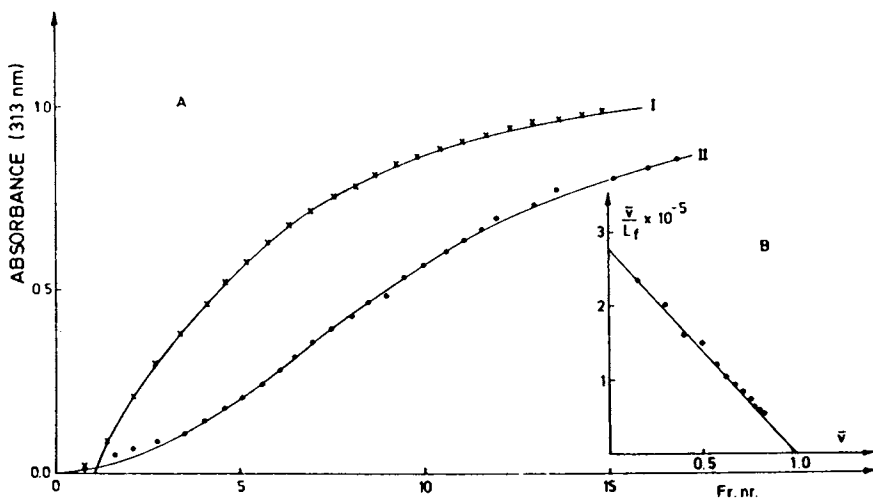


Figure 4. Determination of binding constants of 2',4'-dinitrophenyl 1-S- $\beta$ -cellobioside for CBH II by diafiltration (4°C).

- (A) The filtrate is collected in fractions and the concentration of free ligand ( $L_f$ ) is determined spectrophotometrically (313 nm,  $\epsilon_M = 12000 \text{ M}^{-1}\text{cm}^{-1}$ ). The ligand concentration in the stock solution is  $200 \mu\text{M}$ . The amount of bound ligand is computed from a blank (curve I) and a binding experiment (curve II) (6).
- (B) Scatchard plot:  $\frac{\bar{v}}{L_f} = nK - \bar{v}K$ ,  $\bar{v}$  is the degree of saturation as calculated from the amount of bound ligand and protein ( $170 \mu\text{M}$ ) in the dialysis cell;  $K$ , the association constant;  $n$ , the number of binding sites. In this case  $n = 0.97 \pm 0.06$  and  $K = 2.7 \pm 0.1 \times 10^5 \text{ M}^{-1}$ .

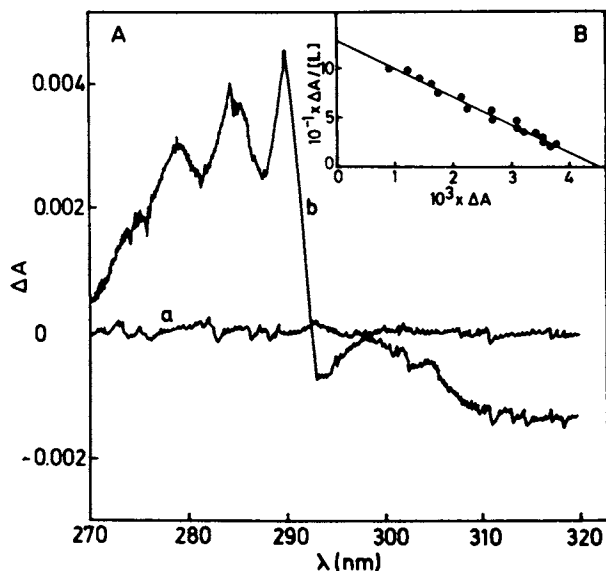


Figure 5. (A) Protein-difference spectrum for the binding of cellobiose onto CBH I (7.6°C). The baseline (a) was recorded (double beam spectrophotometer) with 0.720 mM cellobiose in the measuring cuvette and 0.720 mM sucrose in the reference cuvette. The difference spectrum (b) was recorded after addition of 9.3  $\mu\text{M}$  CBH I to both cuvettes.

(B) Linearized titration curve for the difference absorption spectrum occurring by binding of cellobiose onto CBH I (29°C) (see above). Each cuvette contained 12.4  $\mu\text{M}$  CBH I and was titrated (0-125  $\mu\text{l}$  5 mM sugar) with either cellobiose or sucrose. The sum of the signal changes at 290 nm and 294 nm (see A) are used in the calculation (5). The slope corresponds to  $K = (2.7 \pm 0.1)10^4 M^{-1}$  (association constant of cellobiose for CBH I).

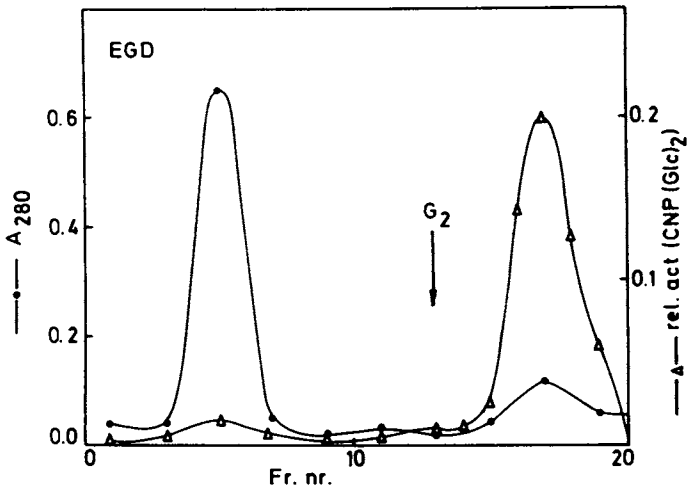


Figure 6. Affinity chromatography of EGD from *Clostridium thermocellum*. Nucleic acid preparation, heat treatment and ammonium sulfate precipitation (0-70%, 70-100%) were carried out as described (10). The final precipitate ( $\pm 50$  mg protein), dissolved in 50 mM sodium acetate, pH 5.0, was applied (after centrifugation) on the affinity column ( $2 \times 25$  cm) (4'-aminobenzyl 1-thio- $\beta$ -cellobioside coupled to Sepharose 4B) (11). Protein was monitored at 280 nm and the activity of the fractions (2 ml) determined using 2'-chloro-4'-nitrophenyl  $\beta$ -cellobioside (pH 6.5, 25°C) as described in the text. Elution with 10 mM G<sub>2</sub> was started as indicated.

heavily glycosylated, proline-serine rich domains (B). These domains were either at the N-terminus (CBH II and EG III) or at the C-terminus (CBH I and EG I); the B sequence was duplicated (BB') in the case of CBH II. These results led us to some structural work in an effort to elucidate the molecular organization of the cellobiohydrolases of *Tr. reesei*.

In an attempt to separate the domains from the cores, we used limited degradation with several proteases. CBH I (65 kda) and CBH II (58 kda) under native conditions could only be cleaved successfully with papain (15). The cores (56 and 45 kda) and terminal peptides (11 and 13 kda) were isolated by affinity chromatography (15,16) and the scission points were determined unequivocally. The effect on the activity of these enzymes was quite remarkable (Fig. 7). The cores remained perfectly active towards soluble substrates such as those described above. They exhibited, however, a considerably decreased activity towards native (microcrystalline) cellulose. These effects could be attributed to the loss of the terminal peptides, which were recognized as "binding domains," whose role is to raise the relative concentration of the intact enzymes on the cellulose surface. This aspect is discussed further below. The tertiary structures of the intact CBH I and its core in solution were examined by small angle X-ray scattering (SAXS) analysis (17, 18). The molecular parameters derived for the core ( $R_g = 2.09 \text{ nm}$ ,  $D_{max} = 6.5 \text{ nm}$ ) and for the intact CBH I ( $R_g = 4.27 \text{ nm}$ ,  $D_{max} = 18 \text{ nm}$ ) indicated very different shapes for both enzymes. Models constructed on the basis of these SAXS measurements showed a "tadpole structure" for the intact enzyme and an isotropic ellipsoid for the core (Fig. 8). The extended, flexible tail part of the "tadpole" should thus be identified with the C-terminal peptide of CBH I.

SAXS measurements with CBH II indicated a very similar tertiary structure for both CBH I and CBH II, in spite of a different domain arrangement (to be published). Discrete differences in the tail parts could, however, be noticed. The maximum diameter of CBH II (21.5 nm) was higher than in CBH I; this might be due to duplication of the glycosylated part in the former case. Thus, the functional differentiation of these cellulases can be reflected by structural differences.

The core-enzymes, prepared in our laboratory, and containing the active centers, were successfully crystallized (Dr. Jones, Uppsala, communicated) and tertiary structures will be described in the near future. Chemical modification studies on these enzymes are currently being undertaken in our laboratory; identification of important catalytic residues and location of the active centers will lead to more functional information on these enzymes. Other cellulases such as some endoglucanases from *Clostridium thermocellum* (EG A, EG B, EG D) (10) and EngA and Exg from *Cellulomonas fimi* (19) also contain sequences of conserved, terminally located and sometimes reiterated, amino acids. Some of these sequences are preceded by proline-serine rich domains. Thus, a bistructural-bifunctional organization seems to be a rather common feature among cellulases, at least for EngA and Exg from *C. fimi* and the enzymes from *Trichoderma reesei*.

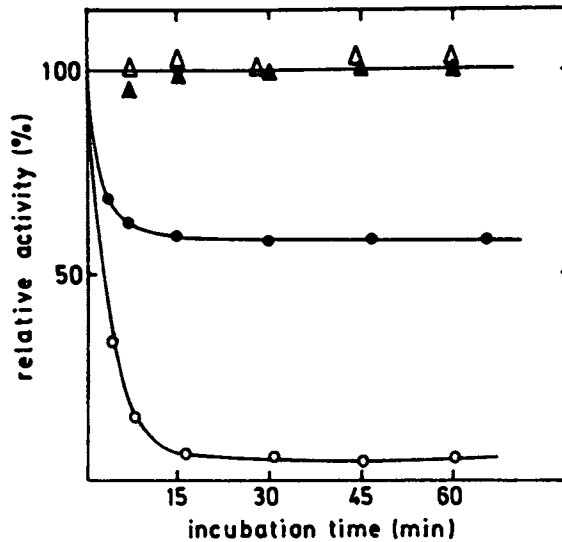


Figure 7. Residual activities of papain-digested CBH I (open symbols) and CBH II (closed symbols). The enzymes ( $\pm 180 \mu\text{M}$ ) were incubated (pH 5.0,  $25^\circ\text{C}$ ) with  $0.6 \mu\text{M}$  papain (300:1). Aliquots ( $50 \mu\text{l}$ ) were removed at times indicated to measure the Avicelase activities ( $\Delta$ ,  $\blacktriangle$ ) or to measure their activities against a small, chromophoric substrate as described in the text (CNPL in the case of CBH I,  $-\circ-$ ; MeUmbG<sub>3</sub> in the case of CBH II,  $-\bullet-$ ). Residual activities are given as percent of the original.

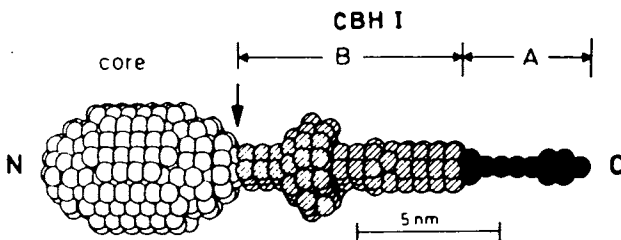


Figure 8. Model structure of intact CBH I as deduced from the results of small angle X-ray scattering experiments (17). The arrow indicates the proteolytic scission site (papain), dividing the core-protein (left) from the "binding domain" (right). A, A-domain; B, B-domain; N, N-terminus; C, C-terminus.

## Study of Binding and Synergism

Chromophoric substrates were also used as tools in the study of the binding of several cellulase components to their natural substrates (such as Avicel). This is illustrated here in the investigation of the synergy in binding of CBH I and CBH II from *Trichoderma reesei* onto Avicel. The enzymes were differentiated with CNPL (see above), which was a substrate only for CBH I (core I). Thus, the amount of CBH II adsorbed when a mixture of both enzymes was added, either simultaneously or sequentially, to Avicel was calculated from the amount of CBH I bound (activity measurements with CNPL) subtracted from the values for total protein binding (280 nm absorbance reading). The results obtained from these experiments are summarized as follows:

- CBH I and CBH II possessed their own, distinct adsorption sites on Avicel, as evident from our previous study (16).
- From adsorption-isotherms it was deduced that the total amount of CBH I bound (83 mg/g Avicel) was somewhat higher than for CBH II (64 mg/g Avicel).
- The core-enzymes (15,16) showed reduced adsorption capacities on Avicel of more than 50%, whereas the adsorptions on amorphous ( $H_3PO_4$ -swollen) cellulose were unaffected. This emphasized the role of the "binding domains" as described above.
- The active center of CBH I (or Core I) did not seem to be implicated in the adsorption on Avicel since no influence of small, soluble ligands (e.g., cellobiose) was observed (16). The importance of an adjacent site for the binding was, however, suspected because of inhibition of adsorption by large molecular weight ligands such as xylan (DP = 20-25).
- The active sites of CBH II (or Core II), on the other hand, participated in the adsorption phenomenon both onto (semi)crystalline (Avicel) and amorphous cellulose.
- The hydrolytic activities of the intact enzymes were comparable, but CBH I was much more sensitive to product (cellobiose) inhibition. Both core enzymes exhibited a strongly reduced activity (50-90%) which was correlated with the absence of the binding domain and their consequent lower binding capacity on Avicel. The activities of CBH I and Core I on amorphous cellulose were, however, comparable.
- The results of simultaneous and sequential adsorption experiments with CBH I, CBH II and their cores strongly indicated that the formation of a CBH I-CBH II complex in solution was a prerequisite for the observed exo-exo synergy. This complex presumably bound, at least partially, to sites normally occupied by CBH I. Although each component showed enhanced binding in the presence of the other (Fig. 9), the increased hydrolytic activities of the synergetic mixture were attributable to the CBH II component (Fig. 9). It was also observed that the combination of native CBH II with Core I gave the highest synergistic adsorption-hydrolysis effect.

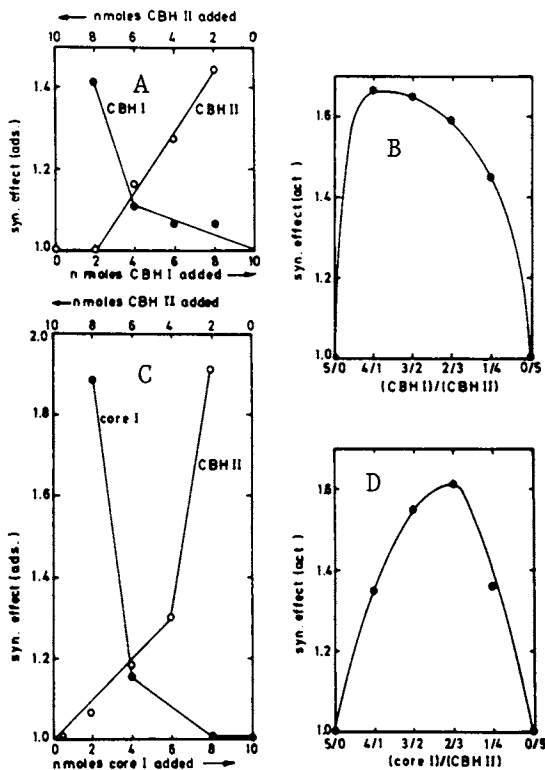


Figure 9. (A) Synergistic effect observed for the adsorption of CBH I/CBH II onto Avicel (pH 5.0, 25°C). In ordinate: the relative increase of adsorption (nmoles per mg Avicel) for each component ( $(enzyme)_{ads.}$ , S) in a mixture of CBH I and CBH II as compared to the adsorption of each enzyme present as single component ( $(enzyme)_{ads.}$ ).  $Syn. effect = \frac{(enzyme)_{ads., S}}{(enzyme)_{ads.}}$ . The amount of Avicel is 30 mg/ml and the amount of enzyme varies between 0-10 nmoles/ml for the experiments where only one component is added. In the synergistic mixtures, however, the total amount of enzyme is always 10 nmoles as shown in the figure (lower and upper abscis). In the absence of synergy curves should coincide with the abscis (ordinate value = 1).

(B) Synergistic effect on the hydrolysis of Avicel by CBH I/CBH II (pH 5.0, 37°C). CBH I and CBH II in different combinations (abscis) are mixed with Avicel (30 mg/ml). The total enzyme concentration is always 10  $\mu$ M and reducing sugars in the supernatant measured after 45 min incubation.

(C) Synergistic effect observed for the adsorption of core I/CBH II onto Avicel. Same conditions as in (A).

(D) Synergistic effect on the hydrolysis of Avicel by core I/CBH II. Same conditions as in (B).



- An attempt was made to correlate these results with a study of the mobility of these enzymes on the surface of the Avicel particles. CBH I (or its core) was labelled (FITC) and fluorescence recovery of the enzyme adsorbed was followed after photobleaching (Dr. Y. Engelborghs, Leuven, personal communication). No significant recovery was observed (10-12 sec). Additions of soluble ligands (cellobiose) or a second "synergistic" enzyme (CBH II) did not influence the signal. Thus, surface diffusion of these enzymes was not demonstrated and neither could exchange between bound and free enzyme in solution be detected, although the activity of the modified enzyme (FITC), both against Avicel and soluble substrates (e.g., CNPL), was unaffected.

### Conclusions

The study of cellulases has progressed considerably in the present decade. Recombinant DNA techniques have been applied and protein-chemical and structural studies have provided new insights. Crystallization of the first cellulases has succeeded recently and detailed structural information may be expected soon. It is hoped that this will give a further incentive to studying the intricate reaction mechanism of these enzymes and their substrate interactions (adsorptions). The important synergy phenomena certainly need a more systematic approach and new techniques should be applied in this area.

Our chromophoric substrates proved to be valuable in the study of several aspects of the enzymology of these cellulases. A rapid and specific method for purification (affinity chromatography) has been developed. Following our collaboration with several groups, new insights into the domain arrangement and tertiary structures of two cellulases were obtained. Contributions to the elucidation of the synergistic action (adsorption-hydrolysis) of these enzymes were achieved.

### Acknowledgments

Peter Tomme is an IWONL bursar (Belgium). Vladimir Heriban is indebted to the Ministerie van de Vlaamse Gemeenschap for a scholarship.

Marc Claeysens thanks the NFWO (Belgium) and NATO for grants. Herman van Tilbeurgh's present address is: Plant Genetic Systems, Plateaustraat, 9000 Gent, Belgium.

### Abbreviations and Symbols Used

A	: A-domain (peptide) in CBH I (CBH II)
Avicel	: microcrystalline cellulose (Am. Viscose Co.)
B(B')	: B-domain in CBH I (BB' in CBH II)
CBH I(II)	: cellobiohydrolase I(II) (EC 3.2.1.91)
( <i>Clostr. t.</i> )	: <i>Clostridium thermocellum</i>
CMC	: carboxymethylcellulose
CNPG <sub>2</sub>	: 2'-chloro, 4'-nitrophenyl $\beta$ -D-cellobioside
CNPG <sub>3</sub>	: 2'-chloro, 4'-nitrophenyl $\beta$ -D-cellotrioside

CNPL	:	2'-chloro, 4'-nitrophenyl $\beta$ -D-lactoside
$D_{max}$	:	maximum diameter
<i>E. coli</i> ( <i>E. c.</i> )	:	<i>Escherichia coli</i>
EG	:	endocellulase, endo 1, 4- $\beta$ -D-glucanase (EC 3.2.1.4)
FITC	:	fluoresceine-isothiocyanaat
(Glc) <sub>2</sub> , G <sub>2</sub>	:	cellobiose
(Glc) <sub>3</sub> , G <sub>3</sub>	:	cellotriose
HEC	:	hydroxyethylcellulose
MeUmbLac	:	4'-methylumbelliferyl $\beta$ -D-lactoside
MeUmb(Glc) <sub>2</sub>	:	4'-methylumbelliferyl $\beta$ -D-cellobioside
MeUmb(Glc) <sub>3</sub>	:	4'-methylumbelliferyl $\beta$ -D-cellotrioside
<i>P. p.</i>	:	<i>Penicillium pinophilum</i>
<i>R. g.</i>	:	radius of gyration
SAXS	:	small angle X-ray scattering
<i>Tr. r.</i>	:	<i>Trichoderma reesei</i>

### Literature Cited

1. van Tilbeurgh, H.; Loontjens, F. G.; De Bruyne, C. K.; Claeysens, M. In *Methods in Enzymology*; Academic Press: New York, 1988; Vol. 160, pp. 45-59.
2. Conchie, J.; Levy, G. A. In *Methods in Carbohydrate Chemistry*; Academic Press: New York, 1963; Vol. II, pp. 335-337.
3. Claeysens, M.; Saman, E.; De Bruyne, C. K.; Debruyne, A. *J. Carb. Nucleot. Nucleos.* 1978, 5, 33.
4. Canevascini, G. *Anal. Biochem.* 1958, 147, 419.
5. van Tilbeurgh, H.; Pettersson, L. G.; Bhikhabhai, R.; De Boeck, H.; Claeysens, M. *Eur. J. Biochem.* 1985, 148, 329.
6. Claeysens, M.; van Tilbeurgh, H.; De Bruyne, C. K. *Bull. Soc. Chim. Belg.* 1985, 94, 123.
7. van Tilbeurgh, H. Unpublished.
8. van Tilberugh, H.; Claeysens, M. *FEBS Lett.* 1985, 187, 283.
9. Wood, T. M.; McCrae, S. I.; Wilson, C. A.; Bhat, K. M.; Gow, L. A. In *Biochemistry and Genetics of Cellulose Degradation*; Academic Press: New York, 1988; pp. 31-52.
10. Béguin, P.; Millet, J.; Grépinet, O.; Navarro, A.; Juy, M.; Amit, A.; Poljak, R.; Aubert, J.-P. In *Biochemistry and Genetics of Cellulose Degradation*; Academic Press: New York; pp. 267-282.
11. Tomme, P.; McCrae, S. I.; Wood, T. M.; Claeysens, M. In *Methods in Enzymology*; Academic Press: New York, 1988; Vol. 160, p. 187-193.
12. Claeysens, M.; Wood, T. M. Unpublished.
13. Knowles, J.; Teeri, T.; Lehtovaara, P.; Penttilä, M.; Saloheimo, M. In *Biochemistry and Genetics of Cellulose Degradation*; Academic Press: New York, 1988; pp. 153-169.
14. Shoemaker, S.; Schweikart, V.; Ladner, M.; Gelfand, D.; Kwok, S.; Myambo, K.; Innis, M. *Bio/Technology* 1983, 1, 691.
15. van Tilbeurgh, H.; Tomme, P.; Claeysens, M.; Bhikhabhai, R.; Pettersson, L. B. *FEBS Lett.* 1986, 204, 223.

16. Tomme, P.; van Tilbeurgh, H.; Pettersson, L. G.; Van Damme, J.; Vandekerckhove, J.; Knowles, J.; Teeri, T.; Claeyssens, M. *Eur. J. Biochem.* 1988, **170**, 575.
17. Abuja, P. M.; Schmuck, M.; Pilz, I.; Tomme, P.; Claeyssens, M.; Esterbauer, H. *Eur. Biophys. J.* 1988, **15**, 339.
18. Abuja, P. M.; Pilz, I.; Claeyssens, M.; Tomme, P. *Biochem. Biophys. Res. Comm.* 1988, **156**, 180.
19. Miller, R. C.; Gilkes, N. R.; Greenberg, N. M.; Kilburn, D. G.; Langford, M. L.; Warren, R. A. J. In *Biochemistry and Genetics of Cellulose Degradation*; Academic Press: New York, 1988; pp. 235-248.

RECEIVED May 19, 1989

## Chapter 42

### Cellulases of *Cellulomonas fimi*

#### The Enzymes and Their Interactions with Substrate

D. G. Kilburn, N. R. Gilkes, R. C. Miller, Jr., and R. A. J. Warren

Department of Microbiology, University of British Columbia, 300-6174  
University Boulevard, Vancouver, British Columbia V6T 1W5, Canada

An exoglucanase and an endoglucanase of the bacterium *Cellulomonas fimi* are glycoproteins which bind strongly to microcrystalline cellulose. Each protein comprises two functionally independent domains joined by a sequence of proline and threonine residues: a catalytic domain which does not bind to cellulose; and a cellulose-binding domain which is not enzymatically active. The cellulose-binding domain is at the N-terminus of the endoglucanase but at the C-terminus of the exoglucanase. A *C. fimi* protease cleaves both enzymes to release the independently functioning domains. The glycosyl groups on the proteins protect them from cleavage by the protease when they are bound to cellulose.

Microorganisms use several types of extracellular enzymes to degrade cellulose to glucose: exoglucanases (1,4- $\beta$ -D-glucan cellobiohydrolases, E.C.3.2.91); endoglucanases (*endo*-1,4- $\beta$ -D-glucan glucanohydrolases, E.C.3.2.1.4); and, depending on the organism, cellobiases ( $\beta$ -D-glucoside glucosylhydrolases, E.C.3.2.1.21). In recent years, these enzymes have received considerable attention because of their possible use in the conversion of waste biomass, such as straw, sawdust and bagasse, to useful chemicals. An outcome of this work has been the realization that cellulases are of great interest in themselves, irrespective of their commercial potential (1).

A given microorganism may produce one or more enzymes of each type. An understanding of the role of each enzyme in cellulose biodegradation requires their purification and characterization, and an analysis of the ways in which they interact with the substrate and with each other. However, it is often quite difficult to determine the number and type of truly different enzymes produced by an organism. Many cellulolytic microorganisms secrete proteases, which may degrade some or all of the cellulases to smaller,

0097-6156/89/0399-0587\$06.00/0

© 1989 American Chemical Society

active species. Furthermore, cellulases from both procaryotic and eucaryotic microorganisms may be glycosylated, and deglycosylation *in vivo* can give rise to apparently different forms of an enzyme.

A widely used approach to resolve such problems is the cloning of the structural genes for cellulases (2). The nucleotide sequence of a gene can be used to predict the amino acid sequence of the cellulase it encodes, which in turn can be used to make predictions about the structure of the cellulase. All of this information can be used to make comparisons between cellulases from a single organism and from different organisms. Expression of a cloned gene in an appropriate host gives intact enzyme uncontaminated with other cellulases. If the native enzyme is glycosylated, expression of its gene in *Escherichia coli* gives the non-glycosylated form of the enzyme. Comparison of this with the intact, native enzyme will reveal the effects of glycosylation.

### Cellulases of *Cellulomonas fimi*

When grown on cellulosic substrates, the bacterium *Cellulomonas fimi* (3) produces a complex array of cellulases, some of which are glycosylated (4-6). Its cellulase profile varies with both the nature of the substrate and with culture age, possibly as a consequence of proteolysis and deglycosylation (6). An exoglucanase (Cex) and an endoglucanase (CenA) bind to the substrate in cultures grown with Avicel, a microcrystalline cellulose, and they can be recovered intact from the residual Avicel in such cultures (6). This facilitated their purification to homogeneity by subsequent fast-protein-liquid-chromatography (7). Both were glycoproteins (6). Both enzymes hydrolyzed carboxymethylcellulose (CMC), although with different kinetics (8); both released reducing sugar from Avicel; but only Cex hydrolyzed p-nitrophenylcellobioside (pNPC) and 4-methylumbelliferylcellobioside (MUC). Both proteins were monomers of very similar size: Cex contained 443 and CenA 418 amino acids.

Each protein was composed of three discrete segments: a sequence of 20 amino acids composed of only prolyl and threonyl residues, termed the Pro-Thr box, which was almost perfectly conserved; a sequence of about 100 amino acids which was rich in hydroxyamino acids, of low charge density, and 50% conserved; and a sequence of about 300 amino acids which had a relatively high charge density, but was not conserved (9). The order of the segments was reversed in the two enzymes (Fig. 1).

### Comparison of the Native and Recombinant Forms of *C. fimi* Cellulases

In structural terms, the only difference between native Cex and CenA and the recombinant forms of the enzymes produced in *E. coli* was that the former were glycosylated. For simplicity, the glycosylated forms are referred to as gCex and gCenA, and the non-glycosylated forms as ngCex and ngCenA.

Glycosylation did not affect the substrate specificities of Cex and CenA; it had very little effect on their catalytic activities; and it did not

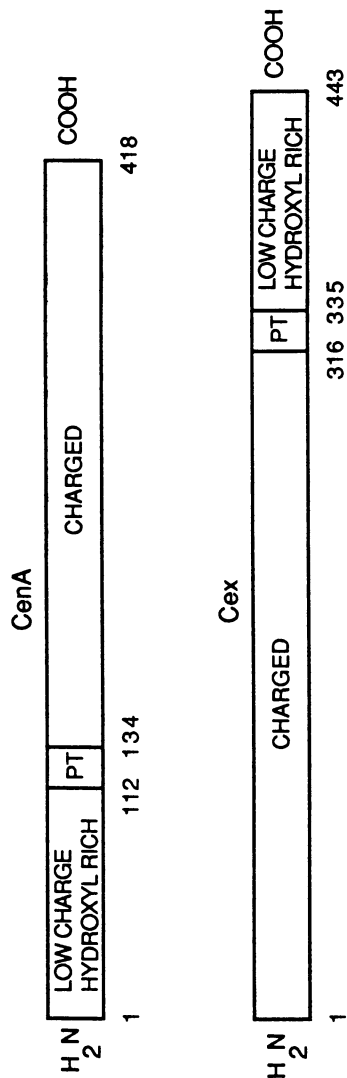


Figure 1. Overall structures of an exoglucanase (Cex) and an endoglucanase (CenA) from *C. fimi*. PT denotes a Pro-Thr box; the numbers refer to amino acid residues.

affect their stabilities to heat and pH (10). Both forms of the enzymes bound to Avicel, which facilitated their purification from *E. coli* (11, 12).

*C. fimi* secreted a serine protease which was active against the cellulases. In solution, the glycosylated forms of Cex and CenA were cleaved much more slowly than the non-glycosylated forms, and the cleavage sites appeared different in the two forms (N. R. Gilkes, unpublished observations). However, when the enzymes were bound to Avicel, the glycosylated forms of Cex and CenA were resistant to the protease, but the non-glycosylated forms remained sensitive (10) (Fig. 2). Therefore, one function of glycosylation was to protect Cex and CenA against proteolysis, especially when bound to cellulose.

### Interactions of *C. fimi* Cellulases with Cellulose

Cleavage of Avicel-bound ngCex and ngCenA released catalytically active fragments from the Avicel (Fig. 2), suggesting that Cex and CenA were organized into two independently functioning domains, a substrate-binding domain and a catalytic domain. This was confirmed by analysis of the cleavage products released by the action of the protease on ngCex and ngCenA in solution (12). Both enzymes were degraded to discrete fragments (Fig. 3). Analysis of the fragments showed that the primary cleavage of ngCex gave fragments of  $M_r$  30 kDa and 20 kDa (Fig. 4). In each case, the large fragment retained catalytic activity but did not bind to Avicel, whereas the smaller fragment was catalytically inactive but could bind to Avicel. The actual site of cleavage in both cases was at the carboxyl terminus of the Pro-Thr box (Fig. 4.)

It was quite clear that in Cex and CenA, the 50% conserved regions that had low charge density, and were rich in hydroxyamino acids, were the substrate-binding domains. In each enzyme, the binding domain was separated from the catalytic domain by a Pro-Thr box. Since the Pro-Thr box is quite similar to the hinge region of IgA<sub>1</sub> immunoglobulins (13), it is tempting to speculate that the Pro-Thr box functions as a hinge also, thereby allowing the catalytic domain to move over the surface of a cellulose fibril in spite of the enzyme being anchored at one end. Retention of their individual properties when separated by proteolysis showed quite clearly that the two domains functioned independently. This was emphasized for the catalytic domains by the properties of a fusion polypeptide in which the catalytic domain, Pro-Thr box, and the first 32 amino acids of the substrate-binding domain of Cex were fused to most of the catalytic domain of CenA (Fig. 5). The fusion polypeptide had both exoglucanase and endoglucanase activity (14).

Although its two domains could function independently, removal of the substrate-binding domain of ngCenA reduced enzymatic activity against microcrystalline cellulose but not against CMC or amorphous cellulose (12). This suggested that the substrate-binding domain played a critical role in the hydrolysis of crystalline cellulose.

The gene, *cenB*, for a second endoglucanase, CenB, of *C. fimi*, was also cloned in *E. coli* (11, 15). The polypeptide expressed from *cenB* in

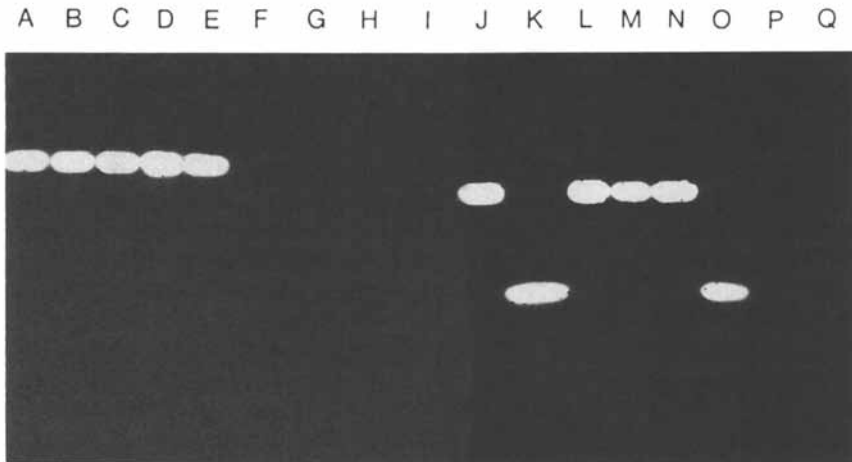


Figure 2. Zymogram of gCenA (A-I) and ngCenA (J-Q) after incubation with *C. fimi* protease. Cellulases, bound to Avicel, were incubated with protease or control buffer for 72 hr at 30°C, then centrifuged to give cellulose-bound (A-E, J-N) and supernatant (F-I, O-Q) fractions. Products were separated on a SDS gel, replicated onto CMC-agarose and developed with Congo red. A,J, buffer control (4°C incubation); B,F,K,O, protease; C,G,L,P, protease + PMSF control; D,H,M,Q, buffer control; E,I,N, buffer + PMSF control.



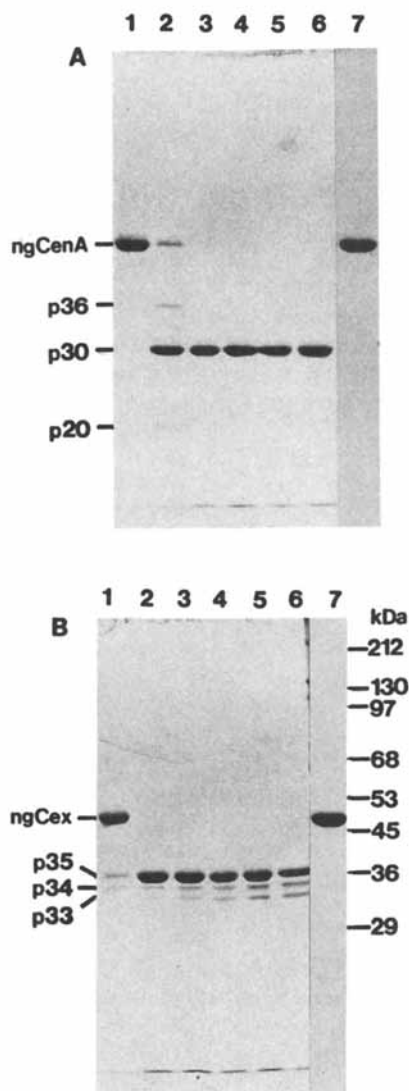


Figure 3. Time course of proteolysis of ngCenA and ngCex. 300  $\mu\text{g}$  of ngCenA (A) or ngCex (B) dissolved in 725  $\mu\text{l}$  of phosphate buffer containing 1.5 units of crude *C. fimi* protease were incubated at 37°C. Reactions were sampled at 0, 6, 24, 48, 96, and 144 h (lanes 1-6, respectively), treated with PMSF, and analyzed by SDS-PAGE (8% acrylamide). Control samples were incubated in the absence of protease for 144 h (lane 7). All lanes were loaded with sample equivalent to 2.8  $\mu\text{g}$  of initial protein.

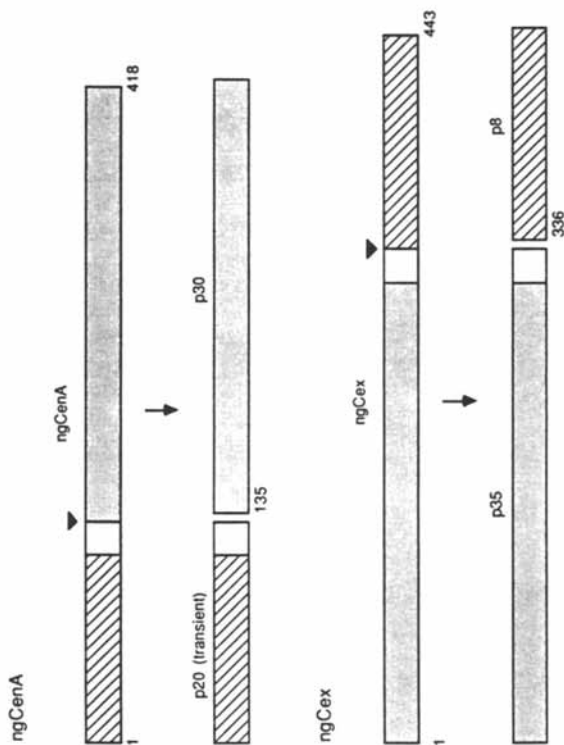


Figure 4. Schematic representation of cleavage of ngCenA and ngCex by *C. fimi* protease. The primary cleavage sites (solid triangles) were defined by amino-terminal sequence analyses, Western blot analyses, and the apparent molecular masses of appropriate fragments, in relation to the deduced amino acid sequences of ngCenA and ngCex. The proteins are drawn approximately to scale. Stippled areas represent catalytic domains: cross-hatched areas, cellulose binding domains; unshaded areas, Pro-Thr box hinge regions. Numbers refer to amino acid residues, beginning at the amino termini of the mature proteins from *C. fimi*.

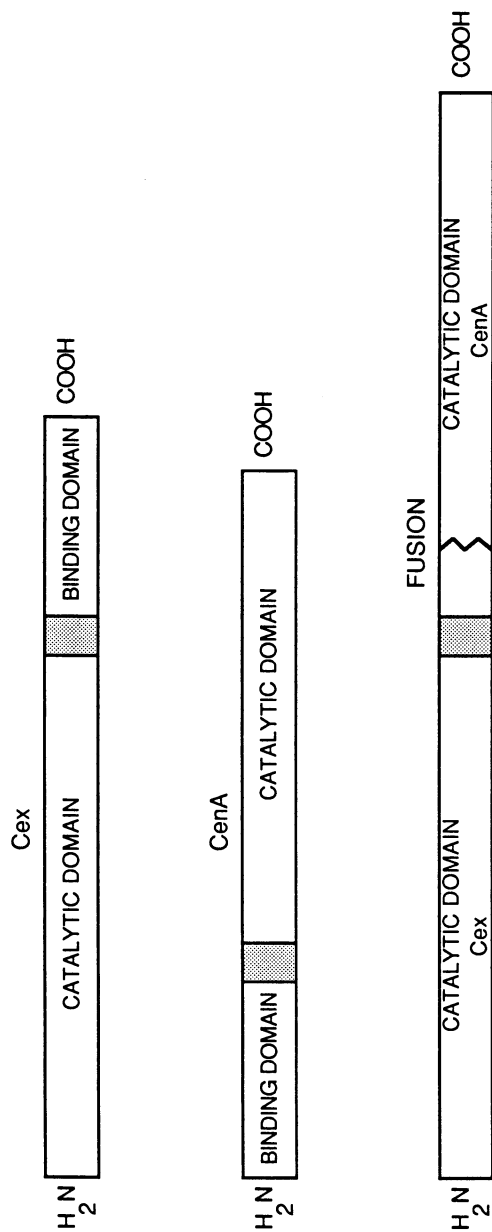


Figure 5. Schematic of the structure of the Cex-CenA fusion protein. The stippled areas are Pro-Thr boxes.

*E. coli* had a  $M_r$  of 110 kDa. It also could be bound to Avicel, but its structural relatedness to Cex and CenA has not yet been determined. A deletion mutant of *cenB* encoded a polypeptide of  $M_r$  70 kDa. The missing segment represented the carboxyl terminal 40 kDa or CenB. The 70 kDa fragment had enzymatic activity and it could still bind to substrate (11). The nature and function of the 40 kDa carboxyl terminus of CenB are being determined.

### Similarity of *C. fimi* Cellulases to *Trichoderma reesei* Cellulases

Analysis of the genes for four cellulases of the basidiomycete *T. reesei* showed that these proteins had a bifunctional organization remarkably similar to that of Cex and CenA of *C. fimi*, and again with reversal of domain order in pairs of the four enzymes (16).

The *T. reesei* enzymes could also be cleaved into separate domains by proteolysis, and this was discussed elsewhere (Claeyssens, M., and Tomme, P., this volume). Suffice it to emphasize here that the genes encoding cellulases in *C. fimi* and *T. reesei* appear to have arisen by domain shuffling and that the enzymes they encode appear to interact with cellulose in a comparable manner, i.e., a catalytic domain is held on the substrate by a binding domain. Cellulases from the bacterium *Clostridium thermocellum* also contained sequences analogous to Pro-Thr boxes as well as highly conserved carboxyl terminal sequences (2, 17, 18). It remains to be seen if they have functional organizations similar to those of the *C. fimi* and *T. reesei* enzymes.

### Acknowledgment

We thank the Natural Sciences and Engineering Research Council of Canada for financial support.

### Literature Cited

1. Aubert, J.-P.; Beguin, P.; Millet, J., Eds. *Biochemistry and Genetics of Cellulose Degradation*; FEMS Symp. No. 43; Academic Press: San Diego, 1988.
2. Beguin, P.; Gilkes, N. R.; Kilburn, D. G.; Miller, R. C., Jr.; O'Neill, G. P.; Warren, R. A. J. *CRC Crit. Rev. Biotechnol.* 1987, **6**, 129.
3. Stackenbrandt, E.; Kandler, O. *Int. J. Syst. Bacteriol.* 1979, **29**, 273.
4. Beguin, P.; Eisen, H.; Roupas, A. *J. Gen. Microbiol.* 1977, **101**, 191.
5. Beguin, P.; Eisen, H. *Eur. J. Biochem.* 1978, **87**, 525.
6. Langsford, M. L.; Gilkes, N. R.; Wakarchuk, W. W.; Kilburn, D. G.; Miller, R. C., Jr.; Warren, R. A. J. *J. Gen. Microbiol.* 1984, **130**, 1367.
7. Langsford, M. L. Ph.D. Thesis, University of British Columbia, 1988.
8. Gilkes, N. R.; Langsford, M. L.; Kilburn, D. G.; Miller, R. C., Jr.; Warren, R. A. J. *J. Biol. Chem.* 1984, **259**, 10455.
9. Warren, R. A. J.; Beck, C. F.; Gilkes, N. R.; Kilburn, D. G.; Langsford, M. L.; Miller, R. C., Jr.; O'Neill, G. P.; Scheufens, M.; Wong, W. K. R. *Proteins* 1986, **1**, 335.

10. Langsford, M. L.; Gilkes, N. R.; Singh, B.; Moser, B.; Miller, R. C., Jr.; Warren, R. A. J.; Kilburn, D. G. *FEBS Lett.* 1987, **225**, 163.
11. Owolabi, J.; Beguin, P.; Kilburn, D. G.; Miller, R. C., Jr.; Warren, R. A. *J. Appl. Environ. Microbiol.* 1988, **54**, 518.
12. Gilkes, N. R.; Warren, R. A. J.; Miller, R. C., Jr.; Kilburn, D. G. *J. Biol. Chem.* 1988, **263**, 10401.
13. Frangione, B.; Wolfenstein-Todel, C. *Proc. Nat. Acad. Sci. U.S.A.* 1972, **69**, 3673.
14. Warren, R. A. J.; Gerhard, B.; Gilkes, N. R.; Owolabi, J. B.; Kilburn, D. G.; Miller, R. C., Jr. *Gene* 1987, **61**, 421.
15. Gilkes, N. R.; Kilburn, D. G.; Langsford, M. L.; Miller, R. C., Jr.; Wakarchuk, W. W.; Warren, R. A. J.; Whittle, D. J.; Wong, W. K. R. *J. Gen. Microbiol.* 1984, **130**, 1377.
16. Knowles, J.; Lehtovaara, P.; Teeri, T. *Trends Biotechnol.* 1987, **5**, 255.
17. Beguin, P.; Cornet, P.; Aubert, J.-P. *J. Bacteriol* 1985, **162**, 102.
18. Grepinet, O.; Beguin, P. *Nucleic Acids Res.* 1986, **14**, 1791.

RECEIVED May 19, 1989

## Chapter 43

# $\beta$ -Glucosidases: Mechanism and Inhibition

Stephen G. Withers and Ian P. Street

Department of Chemistry, University of British Columbia, Vancouver,  
British Columbia V6T 1Y6, Canada

The generally accepted mechanism of action of glycosidases which hydrolyse glycosides with overall retention of configuration at the anomeric center involves a double displacement. Initial general acid-catalyzed generation of a glycosyl-enzyme intermediate is followed by its general base-catalyzed hydrolysis. Both the formation and the hydrolysis of the glycosyl-enzyme can be considered to proceed via oxocarbenium ion-like transition states. Destabilization of such transition states can be achieved by replacing the C-2 hydroxyl of the substrate by the more electronegative fluorine, thus slowing both steps. Simultaneous incorporation of an excellent leaving group (fluoride or dinitrophenolate) as the aglycone permits the accumulation of the intermediate which is sufficiently stable to be isolated. Investigation of such an intermediate generated on a  $\beta$ -glucosidase, by means of  $^{19}\text{F}$ -NMR, allowed its identification as an  $\alpha$ -D-glucopyranosyl-enzyme. Activated 2-deoxy-2-fluoroglycosides therefore act as mechanism-based inactivators, thereby representing a new class of "suicide" inactivators for glycosidases.

$\beta$ -Glucosidases play an important role in the degradation of cellulose by hydrolyzing cellobiose to glucose. In this way, not only is the key metabolite glucose produced, but also cellobiose, an inhibitor of exoglucanases, is removed. An understanding of the detailed chemical mechanism of action of this class of enzymes is therefore important both in terms of possible chemical, or genetic engineering approaches to generation of artificial enzymes and also in the design of specific inhibitors which could be valuable in preventing cellulose degradation.

0097-6156/89/0399-0597\$06.00/0

© 1989 American Chemical Society

All glycosidases studied to date have been found to effect hydrolysis of the glycosidic linkage by cleavage of the bond between the anomeric carbon and the glycosidic oxygen. However, two different stereochemical outcomes of such a hydrolytic mechanism are possible. The bond can be cleaved with retention of anomeric configuration (by a "retaining" glycosidase) (1-3), or with inversion of configuration (by an "invertin" glycosidase) (1-3). Many examples of each type have been found. Probably the most common class, and certainly the best defined mechanistically, is that of the "retaining" glycosidases. The most generally accepted mechanism of action for such enzymes is shown in Figure 1 for a "retaining"  $\beta$ -glucosidase, and involves an active site containing two mechanistically important residues; an acid catalyst whose identity in different systems is thought to be a carboxyl group or tyrosine, and a nucleophile considered to be a carboxylate residue in essentially all cases (see references 1-3 for reviews of glycosidase mechanisms). Binding of the glycoside substrate is thought to be followed by proton donation from the acid catalytic group to the glycosidic oxygen atom, thereby increasing the lability of the glycosidic bond. Bond heterolysis ensues, generating a free (aglyconic) alcohol which departs, and a glycosyl oxocarbenium ion species stabilized by interaction with the carboxylate group. The timing of this "attack" of the carboxylate group is probably such that the reaction has considerable  $S_N2$  character with no true oxocarbenium ion intermediate, but rather just a transition state with substantial oxocarbenium ion character. Such "pre-association" of the nucleophile has also been suggested to be very common in non-enzymic glycosyl transfer reactions (4). Thus the first step of the pathway involves the acid-catalyzed formation of a glycosyl-enzyme intermediate via an oxocarbenium ion-like transition state. Completion of the process involves attack of water at the anomeric center, with some general base catalytic assistance generating, in this case,  $\beta$ -D-glucopyranose as product. This second glycosyl transfer step, deglycosylation, will presumably also occur via a transition state with substantial oxocarbenium ion character.

Alternatives to this mechanism, which differ in some cases only relatively subtly, but in other cases quite dramatically, are not well supported, but include a possible mechanism involving an initial endocyclic C-O bond cleavage (5), and one involving a full oxocarbenium ion intermediate. The case against such mechanisms is discussed in some detail elsewhere (2).

The work described in this paper summarizes our recent attempts to provide substantial proof for the mechanism of Figure 1. This was achieved by trapping and isolating the glycosyl-enzyme intermediate, thus proving its existence, and also by directly determining the stereochemistry of the linkage of this sugar to the enzyme. Such studies, by their very nature, led to the generation of a new class of mechanism-based inactivators of glycosidases.

## Results and Discussion

Since both formation and hydrolysis of the glycosyl-enzyme proceed via oxocarbenium ion-like transition states, it seemed reasonable to assume,

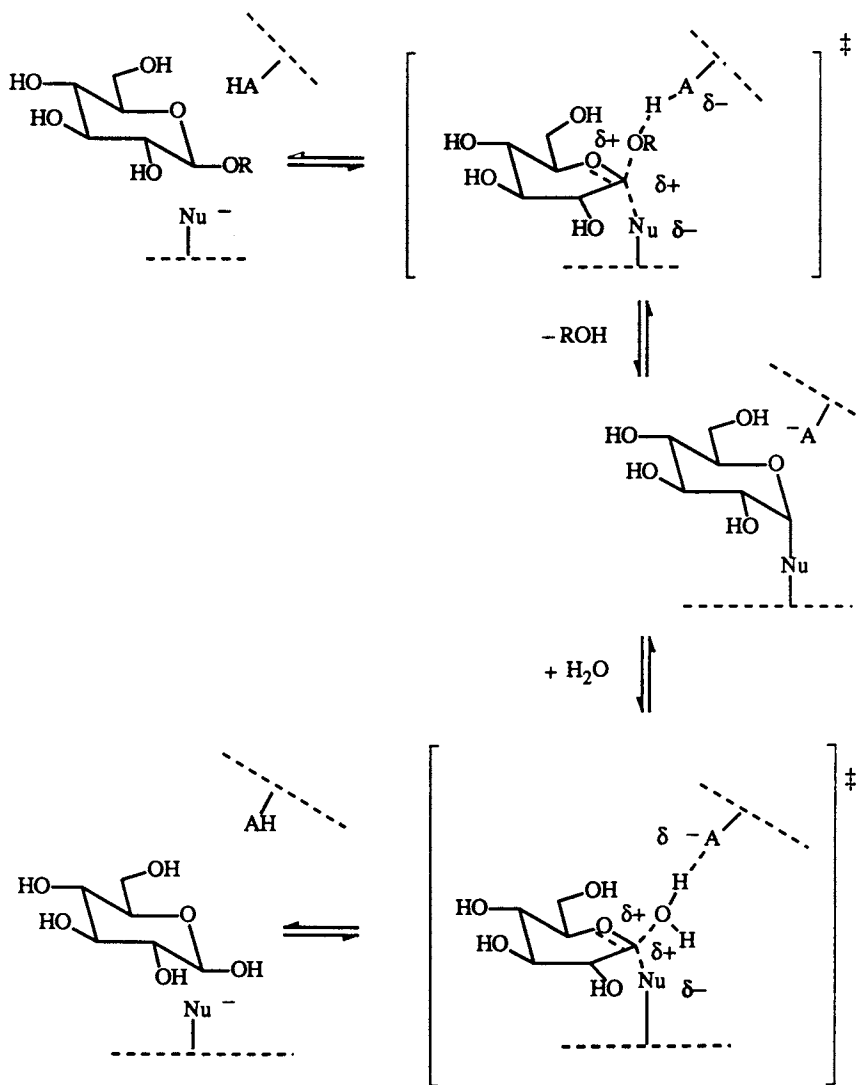


Figure 1. Mechanism of a "retaining"  $\beta$ -glucosidase. OR = the aglycone; Nu = the enzyme's nucleophile; HA = the enzyme's acid catalyst.



in line with our model non-enzymic studies (6), that substitution of the sugar hydroxyl at C-2 by the more electronegative fluorine would result in significant inductive destabilization of the adjacent positive charge at the transition state. This should result in decreased rates of glycosyl-enzyme formation *and* hydrolysis, thereby producing very slow substrates. Such indeed was observed to be the case. However, the incorporation of a relatively reactive leaving group (dinitrophenolate or fluoride) as the aglycone into such deactivated substrates might accelerate the rate of glycosyl-enzyme formation sufficiently, *without* affecting the rate of glycosyl-enzyme hydrolysis, to permit accumulation and trapping of the 2-deoxy-2-fluoro-glycosyl-enzyme intermediate. This could allow the structure and properties of such an intermediate to be investigated.

*Inactivation Studies.* This strategy was tested initially on a  $\beta$ -glucosidase isolated from *Alcaligenes faecalis* (7,8) and since cloned and expressed at high levels in *E. coli* (9), henceforward referred to as pABG5  $\beta$ -glucosidase. In the initial kinetic characterization (8), it had been noted that the best substrates (highest  $V_{max}$  and  $V_{max}/K_m$ ) included 2,4-dinitrophenyl  $\beta$ -D-glucopyranoside and  $\beta$ -D-glucosyl fluoride. Therefore the most promising candidates for trapping of a glycosyl-enzyme intermediate appeared to be 2,4-dinitrophenyl-2-deoxy-2-fluoro- $\beta$ -D-glucopyranoside (2F $\beta$ DNPGlu) and 2-deoxy-2-fluoro- $\beta$ -D-glucopyranosyl fluoride (2F $\beta$ GluF). These two compounds were synthesized as described previously (10,11,12,13) and tested with pABG5  $\beta$ -glucosidase for accumulation of an intermediate. Such testing was relatively facile, as the accumulation of the intermediate resulted in an apparent time-dependent inactivation of the enzyme. This occurred because the free enzyme, capable of interacting with substrate, was converted into the relatively inert 2-fluoroglucosyl-enzyme intermediate. Both compounds were indeed found to be excellent time-dependent inactivators (10,14), reacting according to the expected pseudo-first-order kinetics, as shown for 2F $\beta$ DNPGlu in Figure 2. The rate of inactivation was dependent upon the concentration of inactivator, showing saturation kinetics as expected for a simple inactivator binding non-covalently initially with a dissociation constant,  $K_i$ , and then inactivating the enzyme with a rate constant  $k_i$  according to the scheme below.



The following constants were determined: 2F $\beta$ DNPGlu,  $k_i = 25 \text{ min}^{-1}$ ,  $K_i = 0.05 \text{ mM}$ ; 2F $\beta$ GluF,  $k_i = 5.9 \text{ min}^{-1}$ ,  $K_i = 0.4 \text{ mM}$ .

*Evidence for the Proposed Mechanism.* A considerable effort was then expended in proving the mode of inactivation. Evidence that inactivation occurred by binding at the active site was given by the observation that the competitive inhibitor isopropylthio- $\beta$ -D-glucopyranoside (IPTG) ( $K_i = 4 \text{ mM}$ ) provided the expected protection against inactivation as shown in Figure 2c. Inactivation of the enzyme was accompanied by the release of a "burst" of aglycone (dinitrophenolate or fluoride) as required by such a

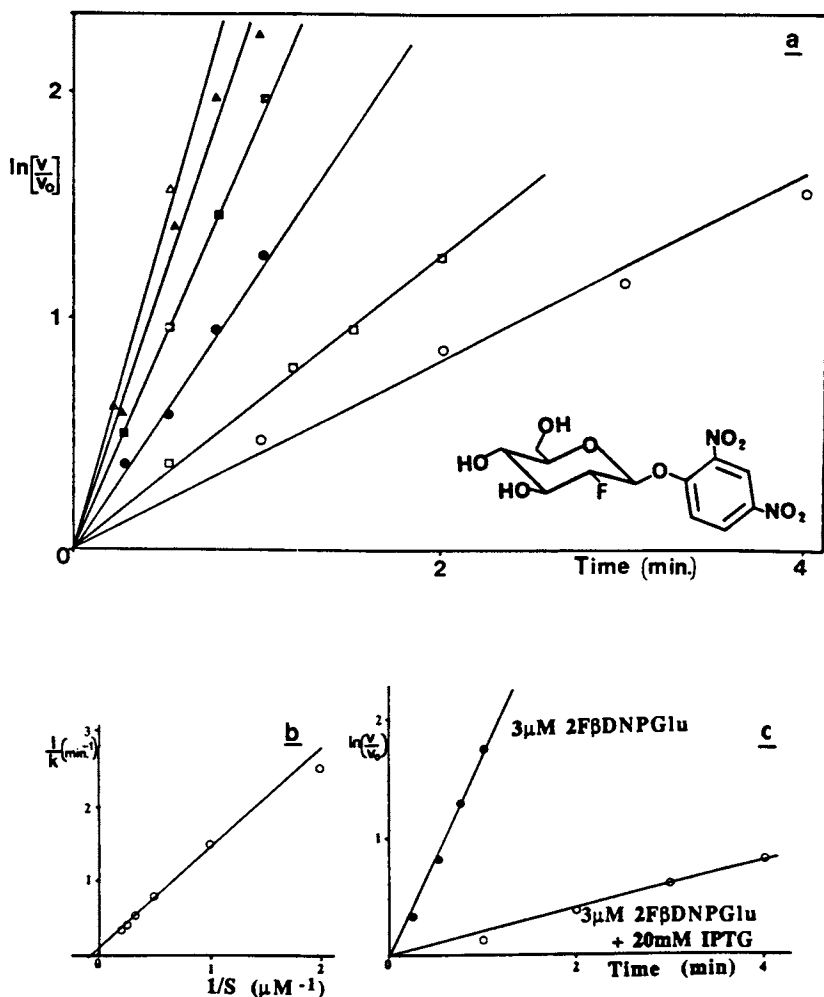


Figure 2. Inactivation of pABG5  $\beta$ -glucosidase with 2F $\beta$ DNPGlu (structure shown) (a)  $\beta$ -glucosidase incubated with the following concentrations of 2F $\beta$ DNPGlu and aliquots assayed against p-nitrophenyl  $\beta$ -glucopyranoside at the times shown:  $\circ$  = 0.5  $\mu$ M;  $\square$  = 1.0  $\mu$ M,  $\bullet$  = 2.0  $\mu$ M;  $\blacksquare$  = 3.0  $\mu$ M;  $\blacktriangle$  = 4.0  $\mu$ M;  $\triangle$  = 5.0  $\mu$ M). (b) Replot of first-order rate constants from 2a. (c) Protection against inhibition given by isopropylthio  $\beta$ -D-glucopyranoside (IPTG).

mechanism. The "burst" of dinitrophenolate was measured spectrophotometrically (Figure 3), while the "burst" of fluoride was measured by both  $^{19}\text{F}$ -NMR and by a dye-binding assay (15). In both cases an essentially stoichiometric (0.93-1.0:1) reaction was observed with release of one mole of aglycone per mole of enzyme inactivated. In addition to helping prove the mode of action of these inactivators this procedure provides a very convenient and accurate way of measuring the concentration of active enzyme present at any time, simply by performing an "active site titration" using  $2\text{F}\beta\text{DNPGlu}$ .

The formation of a 2-fluoroglucosyl-enzyme was demonstrated by means of  $^{19}\text{F}$ -NMR. Addition of  $2\text{F}\beta\text{GluF}$  (1.05mM) to a concentrated solution of pABG5  $\beta$ -glucosidase (0.73mM) in 50mM sodium phosphate buffer, pH 6.8 in a 5mm NMR tube, inactivated the enzyme very rapidly. The  $^{19}\text{F}$ -NMR spectrum of this sample is shown in Figure 4. Peaks were assigned as follows: The peak at 121.4 ppm was due to inorganic fluoride released upon inactivation of the enzyme. Peaks at 144.8 and 203.4 ppm were due to F-1 and F-2, respectively, of the small excess of unreacted  $2\text{F}\beta\text{GluF}$  remaining. The relatively broad peak at 197.3 ppm,  $\Delta\nu = 130\text{Hz}$ , was due to the 2-fluoroglucosyl-enzyme formed, both the chemical shift and the linewidth being consistent with this assignment. Dialysis of such a sample resulted in removal of all signals except the broad resonance at 197.3 ppm, demonstrating that the sugar was indeed covalently linked.

*Stereochemistry of the Intermediate.* These experiments therefore demonstrated that a 2-fluoroglucosyl-enzyme had been trapped. It was then of interest to prove the stereochemistry of the linkage of this sugar residue to the enzyme. Unfortunately, the  $^{19}\text{F}$ -NMR spectrum shown in Figure 4 was of no use in this regard, since the  $^{19}\text{F}$ -chemical shift of 2-deoxy-2-fluoro-glucose and its derivatives is relatively insensitive to the configuration of the anomeric substituent ( $\alpha$ - and  $\beta$ -2-deoxy-2-fluoro-D-glucose differ in  $^{19}\text{F}$  chemical shift by only 0.18 ppm and their tetra-*o*-acetates by only 1.4 ppm). Coupling constants are not much more sensitive and would, in any case, be lost in the large natural linewidth of the resonance. However, the chemical shifts of 2-deoxy-2-fluoro-D-mannose and its derivatives were shown previously to be very sensitive to anomeric configuration (16), e.g.,  $\alpha$ - and  $\beta$ -2-deoxy-2-fluoro-D-mannose differ in  $^{19}\text{F}$ -chemical shift by some 18.5 ppm. Since it had been shown previously (8) that pABG5  $\beta$ -glucosidase exhibits considerable  $\beta$ -mannosidase activity, it seemed that 2-deoxy-2-fluoro- $\beta$ -mannosyl fluoride ( $2\text{F}\beta\text{ManF}$ ) might be a good inactivator of the enzyme. If so, this would allow the generation of a 2-fluoro-mannosyl enzyme which could be investigated by  $^{19}\text{F}$ -NMR. Figure 5 shows the result of such an investigation where  $2\text{F}\beta\text{ManF}$  (1.52mM) has been added to pABG5  $\beta$ -glucosidase (0.74mM) in 50mM sodium phosphate buffer, pH 6.8, and placed in a 5mM NMR tube. The resonance at 121.0 ppm was due to inorganic fluoride released upon inactivation, whereas resonances at 149.5 and 224.4 ppm corresponded to F-1 and F-2, respectively, of the excess  $2\text{F}\beta\text{ManF}$  employed. The broad peak at 201.0 ppm was due to the 2-fluoro-mannosyl-enzyme adduct. The chemical shift ob-

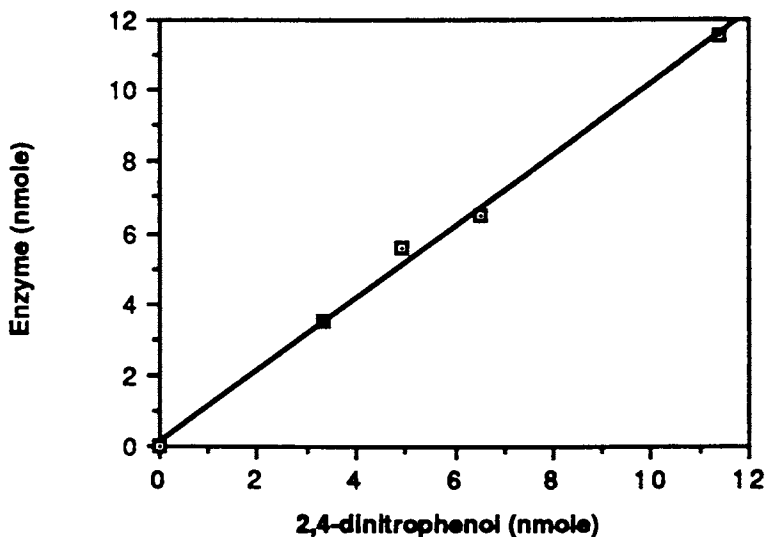


Figure 3. Measurement of the "burst" of dinitrophenolate released on reaction of  $2F\beta$ DNPGlu with pABG5  $\beta$ -glucosidase. Plot of quantity of 2,4-dinitrophenol released (from absorbance at 400nm) versus quantity of enzyme treated. Solutions of different concentrations of  $\beta$ -glucosidase in 50mM sodium phosphate buffer, pH 6.8 were incubated at 37°C in a 1cm pathlength glass cuvette in a spectrophotometer and the absorbance reading zeroed. A solution of  $2F\beta$ DNPGlu (sufficient to provide twice the estimated enzyme concentration) was added and the optical density at 400nm recorded. The quantity of dinitrophenol released was estimated using an extinction coefficient of  $11,300M^{-1}cm^{-1}$ . The quantity of enzyme was estimated using an extinction coefficient at 280nm of  $E^{0.1\%} = 2.20cm^{-1}$ , itself determined by a quantitative amino acid analysis.

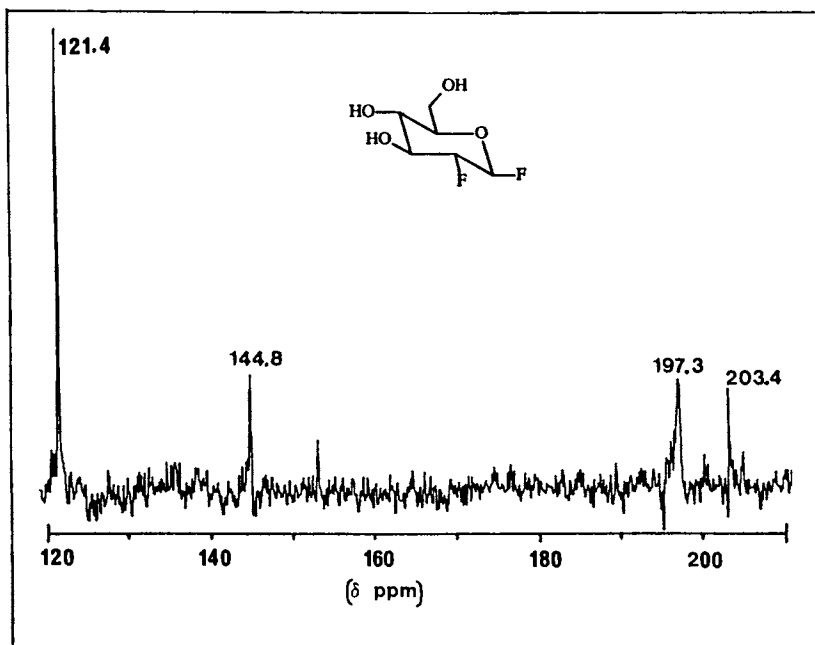


Figure 4. Proton decoupled  $^{19}\text{F}$ -NMR spectrum of pABG5  $\beta$ -glucosidase inactivated with 2F $\beta$ GluF (conditions as described in text). This spectrum was recorded on a 270 MHz Bruker/Nicolet instrument using gated proton decoupling (decoupler on during acquisition only) and a  $90^\circ$  pulse angle with a repetition delay of 2s. A spectral width of 40,000 Hz was employed and signal accumulated over 10,000 transients.

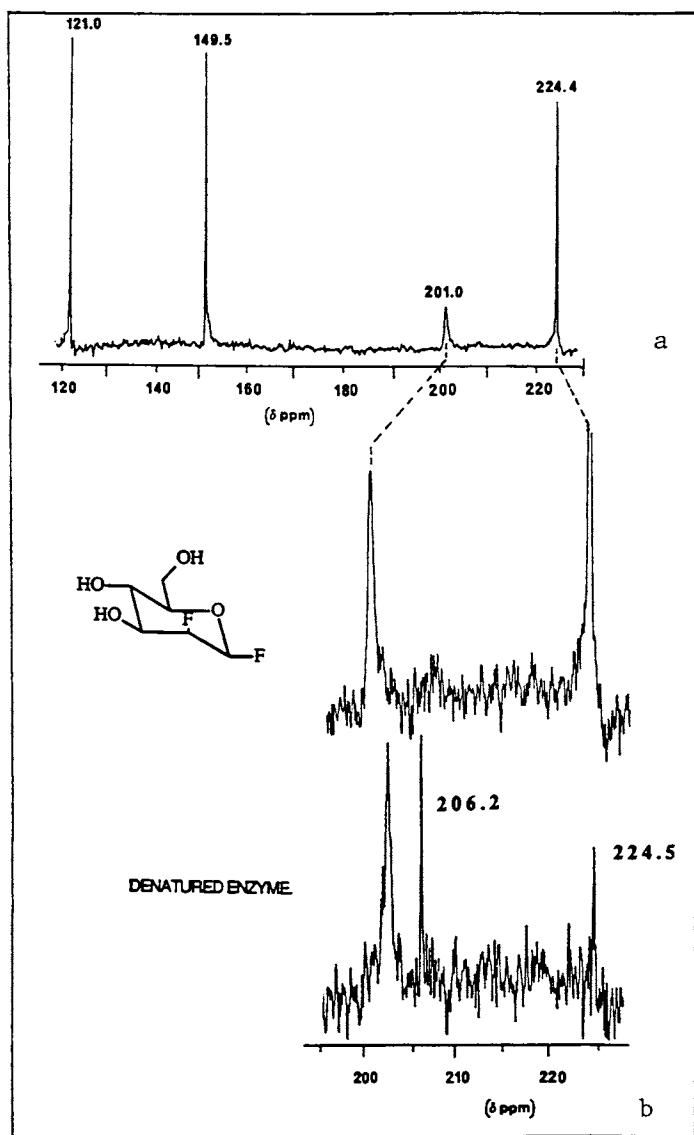


Figure 5. Proton decoupled  $^{19}\text{F}$ -NMR spectrum of pABG5  $\beta$ -glucosidase inactivated with 2F $\beta$ ManF (conditions as described in text). Spectra were recorded on a 270 MHz Bruker/Nicolet instrument using gated proton decoupling (decoupler on during acquisition only) and a  $90^\circ$  pulse angle with a repetition delay of 2s. A spectral width of 40,000 Hz was employed and signal accumulated over 10,000 transients for the native protein and 30,000 transients for the denatured protein in 8M urea. (a) Full spectrum with expansion below it; (b) Expansion of spectrum of denatured/dialyzed enzyme.

served was well within the range expected for an  $\alpha$ -linked 2-fluoro-mannose residue and some 16-20 ppm downfield of the region expected for a  $\beta$ -linkage. In light of the large chemical shift differences concerned, it was unlikely that other factors affected the chemical shift significantly. However, as described below, other factors were also considered. Since the  $^{19}\text{F}$ -NMR chemical shifts of 2-deoxy-2-fluoro-glycosides and -glycosyl esters are relatively insensitive to the chemical identities of the anomeric substituent, it was unlikely that a large chemical shift resulted from the replacement of the fluorine substituent at C-1 by the enzyme nucleophile so this was unlikely to be the source of the large shift, especially as no such large shift had been observed for the 2-fluoro-glucosyl enzyme. The binding of fluorinated ligands to macromolecules generally produces downfield shifts (17) which might confuse this interpretation. However, since such shifts are generally small, and because the chemical shift of the 2-deoxy-2-fluoro-glucosyl-enzyme was in the expected region, this seemed an unlikely cause for such a large shift. However, in order to be certain that this was not the case, the 2-fluoro-mannosyl-enzyme adduct was dialyzed overnight against 8M urea to denature it, and the  $^{19}\text{F}$ -NMR spectrum of the resultant unfolded protein, in which the fluoromannose residue would be exposed to solvent, was obtained (see Figure 5b). While a very small ( $\Delta\delta = 1.6$  ppm) upfield shift of the resonance was observed, the resonance remained well within the region anticipated for the  $\alpha$ -linked sugar. It is of interest to note that resonances arising from excess 2F $\beta$ ManF were removed by the dialysis, but the high molecular weight 2-fluoromannosyl-enzyme species was retained. Resonances at 206.2 and 224.5 ppm arose from  $\alpha$ - and  $\beta$ -2-deoxy-2-fluoro-D-mannose which had hydrolyzed after denaturation of the enzyme.

## Conclusion

By using 2-deoxy-2-fluoro-glycosides with good leaving groups at the anomeric center it was possible to trap the glycosyl-enzyme adduct long since postulated as an intermediate in glycosidase catalysis. Further, it was possible to unequivocally prove the stereochemistry of this species. This therefore provides very strong supportive evidence for the mechanism of enzyme-catalyzed glycoside hydrolysis shown in Figure 1. The mechanism involves a covalent glycosyl enzyme intermediate which is formed and hydrolyzed *via* oxocarbenium ion-like transition states. The 2-deoxy-2-fluoro-glycosides used in this work serve as good, specific mechanism-based inactivators of glycosidases, and may have future application in studies of oligosaccharide and polysaccharide degradation.

## Acknowledgments

We wish to thank D. Dolphin (Department of Chemistry, UBC) and R. A. J. Warren and W. W. Wakarchuk (Department of Microbiology, UBC) for their assistance in this work.

We also thank the Natural Sciences and Engineering Research Council of Canada and the British Columbia Health Care Research Foundation for financial support.

### Literature Cited

1. Sinnott, M. L. In *The Chemistry of Enzyme Action*; Elsevier: New York, 1984; p. 389.
2. Sinnott, M. L. In *Enzyme Mechanisms*; Royal Society of Chemistry, 1987; p. 259.
3. Lalegerie, P.; Legler, G.; Yon, J. M. *Biochimie* 1982, **64**, 977.
4. Jencks, W. P. *Chem. Soc. Rev.* 1981, **10**, 345.
5. Post, C. B.; Karplus, M. *J. Amer. Chem. Soc.* 1986, **108**, 1317.
6. Withers, S. G.; MacLennan, D. J.; Street, I. P. *Carbohydr. Res.* 1986, **154**, 127.
7. Han, Y. W.; Srinivasan, V. R. *J. Bacteriol.* 1969, **100**, 1355.
8. Day, A. G.; Withers, S. G. *Biochem. Cell Biol.* 1986, **64**, 914.
9. Wakarchuk, W. W.; Kilburn, D. G.; Miller, R. C.; Warren, R. A. J. *Mol. Gen. Genet.* 1986, **205**, 146.
10. Withers, S. G.; Street, I. P.; Bird, P.; Dolphin, D. H. *J. Amer. Chem. Soc.* 1987, **109**, 7530.
11. Adamson, J.; Foster, A. B.; Hall, L. D.; Johnson, R. N.; Hesse, R. M. *Carbohydr. Res.* 1970, **15**, 351.
12. Hall, L. D.; Johnson, R. N.; Adamson, J. B.; Foster, A. B. *Can. J. Chem.* 1971, **49**, 118.
13. Street, I. P.; Armstrong, C. R.; Withers, S. G. *Biochemistry* 1986, **25**, 6021.
14. Withers, S. G.; Rupitz, K.; Street, I. P. *J. Biol. Chem.* 1988, **263**, 7929.
15. Megregian, S. In *Colorimetric Determination of Non-Metals: Chemical Analysis*; Boltz, D. F.; Howell, J. A., Eds.; Wiley: New York, 1978; **8**, 109.
16. Phillips, L.; Wray, V. *J. Chem. Soc. (B)* 1971, 1618.
17. Gerig, J. T. In *Biological Magnetic Resonance*; Berliner, L. T.; Reuben, J., Eds.; 1978, **1**, 139.

RECEIVED April 11, 1989



## Chapter 44

# Environmental Potential of the *Trichoderma* Exocellular Enzyme System

J. M. Lynch

AFRC Institute of Horticultural Research, Littlehampton, West Sussex  
BN17 6LP, England

*Trichoderma* spp. produce enzymes in the cellulolytic (exo- and endo- $\beta$ -1-4- glucanase,  $\beta$ - glucosidase) and hemicellulolytic (especially xylanase and  $\beta$ -xylosidase) complexes which are effective in degrading natural lignocelluloses such as straw. Nitrogen can be provided to the fungus by cooperative nitrogen-fixing anaerobic bacteria (*Clostridium butyricum*). The fungus also produces a range of enzymes (chitinase, 1,3- $\beta$ -D glucanase and proteases) with the capacity to degrade the cell walls of a wide range of fungal plant pathogens. No correlation has been obtained between field biocontrol effectiveness and lytic enzyme production by different strains; this is possibly because antibiotic metabolites are also involved in the action. A target is to produce *Trichoderma* strains with elevated levels of degradative and lytic exocellular enzymes which also produce antibiotics and grow rapidly in the soil and rhizosphere environments.

Lignocelluloses are freely available in the environment as residues from crop plants and trees and there has been a great effort in recent years to develop effective and economic processes for their utilization. However, outside the mushroom industry, few cost-effective options have been identified. This led Wood (1) and Lynch (2) to echo the comments of Thaysen and Bunker (3) that the most effective route to utilize dead vegetation is in the natural processes of decay. There has been a tendency to develop cyclic arguments where the energy derived from lignocellulose utilization, to produce alcohol for example, is merely recycled in farm machinery to derive more lignocelluloses with no net energy gain.

*Trichoderma* species have a powerful set of well-characterized exoenzymes involved in the cellulolytic pathway: exo- $\beta$ -1,4-glucanase which hydrolyzes amorphous and microcrystalline cellulose; endo- $\beta$ -1,4-glucanase

0097-6156/89/0399-0608\$06.00/0

© 1989 American Chemical Society

which hydrolyzes cellulose derivatives; and  $\beta$ -glucosidase which hydrolyzes cellobiose derived from the glucanase action and cellodextrins to glucose (1). Xylanolytic activity can also be present to hydrolyze hemicelluloses (heterogeneous polymers of glucose, mannose, galactose, arabinose and xylose). Even though there is no ligninolytic activity in this genus, the preponderance of the polysaccharide components in lignocellulose and the indication that much of the polysaccharide is not tightly bound to the lignin and therefore relatively freely available in non-woody plants (4) make *Trichoderma* a good candidate for exploring lignocellulose utilization. Eveleigh (5) has reviewed the biology and biochemistry of the genus; but other than its utility in providing the source of commercial cellulases, there has been little industrial exploitation as yet. However, *Trichoderma* species, and the closely related *Gliocladium* species, have shown major potential as biological control agents of plant diseases (6) and a commercial preparation of *T. viride*, Binab T, is produced in Sweden as a biological control agent against the silver leaf disease of fruit trees caused by *Chondrostereum purpureum*. In this mode it is a mycoparasite, coiling around and penetrating the cell walls of plant pathogens, an action which, at least in part, must involve the release of lytic enzymes.

The purpose of this article is to outline the role of these enzyme systems in the soil/plant ecosystem and discuss how their useful characters might be elevated and exploited further.

### Lignocellulolysis

One of the favored organisms for study of cellulolysis by *Trichoderma* is *T. reesei*. Consequently, many mutant strains which hyperproduce cellulase have been obtained by treatment with ultraviolet light, gamma irradiation, the linear accelerator, diethyl sulphate and N-methyl-N'-nitro-N-nitrosoguanidine (7). Whereas much of the study of *T. reesei* has been with cellulose as substrate, it is relevant to consider the other fractions of natural lignocelluloses: hemicellulose and holocellulose (the combined cellulose and hemicellulose fraction).

When the hyper-cellulolytic mutant *T. reesei* QM9414 was grown on various substrates derived from wheat straw in stirred batch culture, the highest specific growth rates were on holocellulose and the hemicellulose-A defined by O'Dwyer (8); it grew poorly on lignocellulose. By contrast, *T. harzianum* IMI 275950 isolated from wheat straw grew better on lignocellulose (Table I). Despite these differences, the enzyme yields of the cellulase/xylanase complexes did not correlate with growth rate. These observations from this empirical study indicate that strains isolated or derived for growth on extracted substances may not necessarily be the most useful strains to exploit natural substrates.

When suitable strains to exploit natural substrates are available, their exploitation of cellulolytic substrates in pure culture could be restricted by the end-products of cellulolysis (cellobiose and glucose) repressing enzyme synthesis or inhibition/inactivation of further enzymic activity (Fig. 1). One of the simplest routes to relieve this difficulty was to use non-cellulolytic

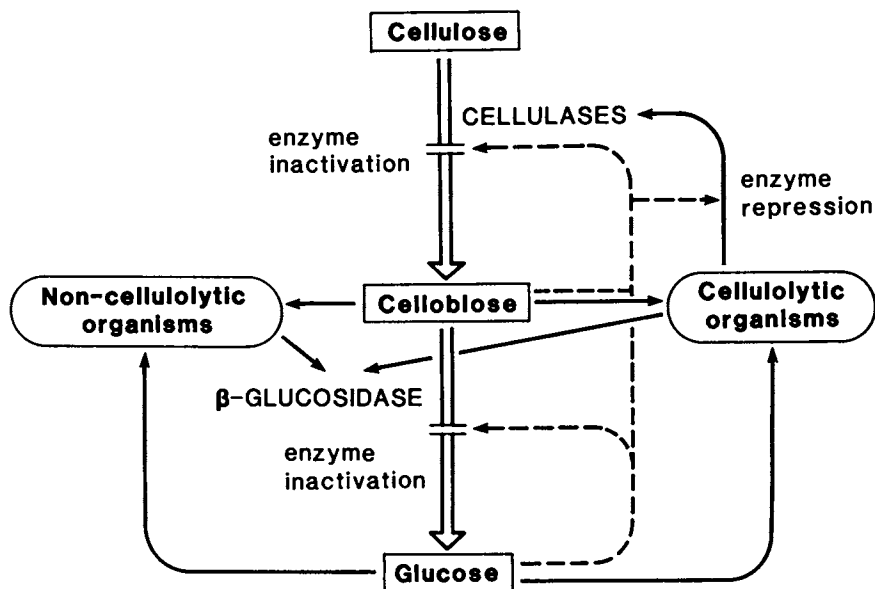


Figure 1. Possible interactions between micro-organisms during cellulose degradation. Source: Reproduced with permission from Ref. 11. © 1985, L. A. Harrison.

Table I. Growth of *Trichoderma reesei* QM9414 (Tr) and *T. harzianum* IMI275950 (Th) on wheat straw lignocellulose (lignocell.) or derived cellulosic materials from straw (cell., cellulose; hemicell-A, hemicellulose-A; holocell., holocellulose)

Organism	Tr	Tr	Tr	Tr	Th
Substrate	cell.	hemicell-A	holocell.	lignocell.	lignocell.
	<i>Enzyme Yield (units <math>\times 10^{-3}</math>/g cellulosic substrate)</i>				
CM <sup>1</sup> -cellulase	2.50	1.20	3.00	2.58	2.06
FP <sup>2</sup> -cellulase	0.26	0.08	0.40	0.30	0.20
$\beta$ -glucosidase	0.06	0.06	0.04	0.06	0.06
Xylanase	14.50	52.02	28.80	24.62	15.50
$\beta$ -xylosidase	0.20	0.38	0.48	0.16	0.22
	<i>Specific Growth Rate (h<sup>-1</sup>)</i>				
	0.029	0.085	0.086	0.016	0.025

Cultures were grown in a stirred batch fermenter, working volume 1 liter, using cellulose materials at 0.5% w/v as carbon substrates. Growth rate of cultures was determined by measuring the culture ATP concentration (aggregate of biomass and exocellular ATP) during exponential growth (9).

<sup>1</sup> Carboxymethylcellulose.

<sup>2</sup> Filter paper.

Source: Reproduced with permission from Ref. 10. © 1986, D. M. Gaunt.

or other cellulolytic species of fungi or bacteria to utilize the end-products, as presumably happens in the natural environment. However, rather than allowing the energy so generated in cellulolysis to go to waste, we have considered routes whereby that energy could be usefully diverted to other natural processes. One process in soil heavily restricted in nature by available energy is dinitrogen fixation, because about 15 moles ATP is required *in vitro* for nitrogenase to reduce one mole of N<sub>2</sub> to 2NH<sub>3</sub>. A conceptual scheme is outlined in Figure 2 where the cellulase comes from *T. harzianum* and *Clostridium butyricum* is the anaerobic bacterium providing the source of nitrogenase. In an open system without forced aeration, anaerobic microenvironments will occur such that there will be aerobic/anaerobic interfaces. The association between the organisms was promoted by the addition of small amounts of ammonium-N (13) and the species involved could co-exist in a range of oxygen atmospheres (14), possibly because the fungus was able to exclude oxygen from the anaerobe which is non-cellulolytic. When *C. butyricum* was provided with the cellulase enzyme from *T. viride* it indirectly metabolized cellulose as a carbon source in the absence of a source of fixed nitrogen under anaerobic conditions.

In searching for means to enhance this *in vitro* activity, a range of fungal isolates were screened for cellulolytic activity on straw. The tests used to assay activity included clearing of cellulose agar (zone size measured), loss of weight from straw, colony radial extension rate on a water-soluble extract

of straw and on internode sections of straw, and penetration rate into straw pieces (15). These *in vitro* tests identified useful activity and diffusibility of the cellulase/hemicellulase enzyme complexes. In all tests *Trichoderma* spp. performed most favorably, with *Sordaria alcina* and *Fusarium* spp. closely following. The latter group of species were pathogenic to plants and therefore should be excluded from agricultural environments, even though their cellulolytic activity was potentially useful for utilization of plant residues. The *Trichoderma* cellulase was active over a wide range of water potentials ( $-0.7$  to  $-7$  MPa) and its activity was greater at  $20^{\circ}\text{C}$  than at  $10^{\circ}\text{C}$  (16). These properties would again be useful if application in the environment was to be contemplated.

The *Trichoderma* spp. clearly formed an association with *C. butyricum*, as did the *Fusarium* spp. and *S. alcina*, indicated by the number of viable bacteria associating with straw and the rate of degradation of this substrate (17). By contrast, *Penicillium* spp. were generally less effective.

In order to further protect the anaerobe from oxygen, *E. cloacae*, which produces polysaccharides useful in stabilizing soil structures (18), was added to the *Trichoderma/Clostridium* consortium (19) (Fig. 3). When wheat straw contained in glass columns was treated with this consortium, and an N-free nutrient feed supplied at a steady rate, a maximum N gain of  $12\text{ mg N g}^{-1}$  straw was measured with about 50% of the substrate utilized. Added to  $3\text{ mg N g}^{-1}$  naturally present in the straw, the N input totals  $15\text{ mg N}$ . This rate is a little less than  $18\text{ mg N g}^{-1}$  original straw with about 25% substrate utilization which has been measured with studies using *Cellulomonas* sp. CS1-1 as the cellulase-producer and *Azospirillum brasilense* sp. as the (aerobic) nitrogenase-producer (20). Even so, if the figure could be extrapolated to field conditions, (e.g., straw from a wheat crop yielding about  $7\text{ t ha}^{-1}$  of grain) and a similar amount of straw, it would produce a total N gain to soil of  $105\text{ Kg N ha}^{-1}$ . The functioning of the associative cellulase/nitrogenase action will be dependent on soil and environmental conditions, and the potential for inoculation will depend on the level of natural associations already existing in soils. We successfully inoculated *T. harzianum* onto straw in soil but failed to elevate the populations of *C. butyricum/E. cloacae* and gains of N over those occurring naturally (21). Commercial opportunity usually depends on the effectiveness of inocula, even where useful natural processes are operating optimally. However, the environmental benefit of natural processes should be considered in more depth and farming processes reappraised where, for example, plant residues are destroyed by burning to simplify soil cultivation practices.

### Mycoparasitism

It has already been indicated that some *Trichoderma* and *Fusarium* spp. have comparable activities in natural substrate utilization. When inoculated onto plates of malt agar at  $20^{\circ}\text{C}$ , colonies of two species of *T. harzianum* had a radial extension rate of  $20.1$  and  $26.1\text{ mm d}^{-1}$ , whereas the maximum radial extension of the *Fusarium* spp. was  $12.8\text{ mm d}^{-1}$  (*F. culmorum*) (22). However, *Trichoderma* or *Fusarium* could become dom-

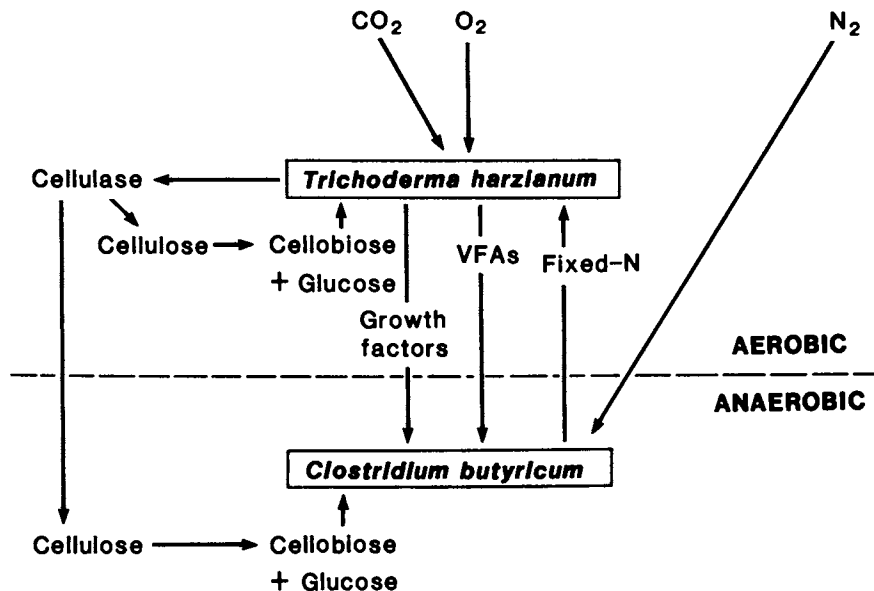


Figure 2. Interactions between *Clostridium butyricum* and *Trichoderma harzianum*. VFAs = volatile fatty acids. Source: Reproduced with permission from Ref. 12. © 1985, D. A. Veal.

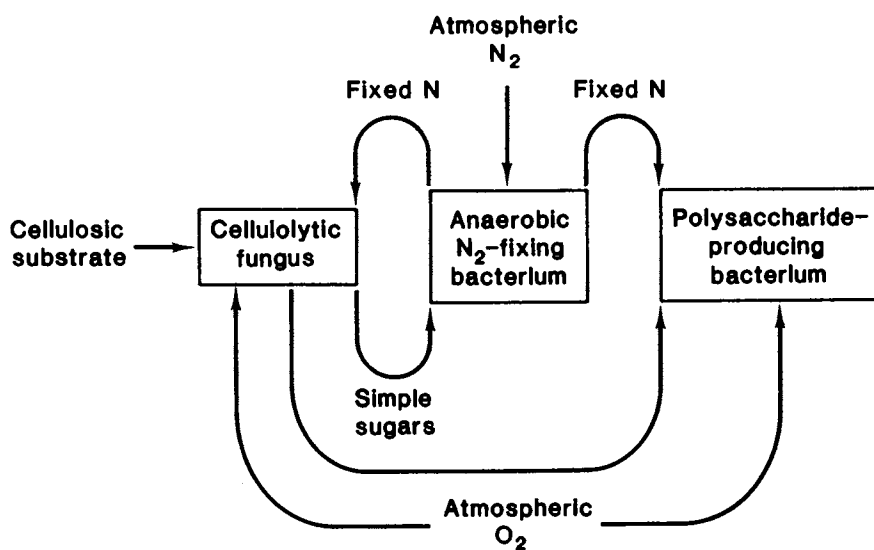


Figure 3. Schematic for the degradation of cellulosic substrates by a microbial consortium.

inant when spore suspensions of mixtures were inoculated together onto agar plates. Either fungus became dominant if its spore concentration in the mixture was greater by one order of magnitude than that of the other species. The potential therefore exists for these species to compete for natural substrates in the environment. This potential might be enhanced if one of the species had other useful attributes, in addition to a high capacity to degrade its substrates.

An "antibiotic" inhibition zone often appears around *Trichoderma* spp. interacting with other fungi. The genus contains many species which produce secondary metabolites. Claydon *et al.* (23) have identified an antibiotic from *T. harzianum* as a volatile, 6-n-pentyl-2H-pyran-2-one; this was recently shown to be an active antibiotic from *T. koningii* (24). The volatile appeared to be the factor responsible for the "coconut smell" of some biocontrol-effective strains of *T. harzianum* (25). However, in a Petriplate assay, it can be difficult to be certain that antibiosis is involved. As well as competitive growth, lytic enzymes could also contribute to the action and *Trichoderma* has been shown to produce  $\beta$ -1,3-glucanase and chitinase (26-29).

We observed the interaction between *T. harzianum* and the pathogen *Rhizoctonia solani* by use of scanning electron microscopy and noticed the hyphae of the antagonist coiling around the hyphae of the pathogen and penetrating some of them. When the antagonist was detached from the pathogen, scarring of the pathogen as well as hyphal penetration occurred. This phenomenon of mycoparasitism must at least in part be responsible for the biocontrol action. Mycoparasitism was only observed on tap water agar and not potato dextrose agar, indicating that more readily available carbon sources may repress the need to use the carbon substrates contained in cell walls. When *T. harzianum* IMI275950 was applied at various propagule numbers with *Pythium ultimum* at various doses in pots of peat/grit and lettuce grown in each pot, the effectiveness of the antagonist again depended on it being inoculated at a dominant concentration over the pathogen (Lumsden, R. D., USDA, Beltsville, MD; Lynch, J. M., AFRC Institute of Horticultural Research, Littlehampton, England; unpublished data).

When *T. harzianum* IMI298372 was grown on cell walls of *R. solani* as carbon source, electrophoresis showed that a much more complex mixture of extracellular proteins was formed when the antagonist was grown on glucose (28). While both 1,3- $\beta$ -D glucanase and chitinase were induced, irrespective of whether glucose or cell walls were used as the carbon substrate, the total activity and specific activity depended on the substrate (Table II).

The complex protein profiles from the fungus grown on the pathogen cell walls were resolved in part by using two-dimensional electrophoresis. This gave a more accurate picture of the number of proteins induced.

The profiles of major bands were similar when *T. harzianum* was grown on cell walls of *R. solani* strains from anastomosis groups AG2 and AG4, but for AG1 the profile was different; this may reflect differences in the composition or structure of cell walls between anastomosis groups (28, 29).

Table II. Enzyme Activity Induced in *T. harzianum* IMI298372

Growth Substrate at 5 g l <sup>-1</sup>	1,3- $\beta$ -D-glucanase Activity		Chitinase Activity	
	Total <sup>1</sup>	Specific <sup>2</sup>	Total <sup>3</sup>	Specific <sup>2</sup>
Glucose	36.7	0.573	0.412	0.0065
Cell walls of <i>Rhizoctonia solani</i>	26.7	0.111	1.132	0.0047

<sup>1</sup>  $\mu$ mol glucose released from laminarin min<sup>-1</sup>

<sup>2</sup>  $\mu$ mol products released min<sup>-1</sup> ( $\mu$ g protein)<sup>-1</sup>

<sup>3</sup>  $\mu$ mol N-acetylglucosamine released from chitin min<sup>-1</sup>

Source: Reproduced with permission from Ref. 28. © Society for General Microbiology.

In order to fractionate the extracellular protein fraction further, it was analyzed by isoelectric focusing, fast protein liquid chromatography and chromatofocusing in conjunction with gel filtration and polyacrylamide gel electrophoresis (29). Gel filtration revealed two peaks of protease activity at pH 4.0, corresponding to enzymes of molecular weights 65,000 and 23,000. With chromatofocusing in the ranges pH 7-4 and pH 9-6, a large number of proteases were separated, some of which could be "satellites" caused by alteration in charged amino acids. It should also be noted that some of the more prominent protein peaks did not correspond to any peaks of enzyme activity studied.

Elad *et al.* (26) suggested that strains of *Trichoderma* spp. may be selected for their biocontrol effectiveness by screening for 1,3- $\beta$ -D glucanase and chitinase activities, with chitin and glucan being perhaps the most obvious targets to attack in the fungal pathogen cell walls. Thus, total protein profiles were obtained from a range of *Trichoderma* spp. (28) and no correlation between those patterns and biocontrol effectiveness against *Rhizoctonia solani* was established (Ridout, C. J.; Coley-Smith, J. R.; Lynch, J. M., unpublished data). Chitinase activity could easily be detected by assaying the release of p-nitrophenyl-N-acetyl- $\beta$ -D-glucosamine (pNAG) as well as the standard method of assaying release of N-acetyl-glucosamine (NAG) from chitin (29). The assay using pNAG had the advantage of being simple, sensitive and reproducible. The ability of the chitinase enzyme to release NAG from chitin was considerably reduced after partially purifying this enzyme by gel filtration. This may be because other enzymes were also necessary to release NAG from chitin and these enzymes were removed by purification. The other enzymes could be proteases since these were induced in considerable quantities by cell walls of *R. solani*. Indeed, cell walls of many fungi contain proteins (32,33) and so protease activity could be important in the biocontrol action of fungi. There is a parallel for this with entomopathogenic fungi where *Beauveria bassiana* produces proteases which act in concert with chitinase in the penetration of insect



cuticles (34). Overall, however, it has to be concluded that the role of exoenzymes of *Trichoderma* in the biocontrol action against plant pathogenic fungi is quite unclear at present.

### Concluding Remarks

*Trichoderma* spp. produce a set of powerful diffusible exo-enzymes which can degrade the carbohydrate fractions of lignocelluloses. They also produce, in addition to antibiotics, a series of lytic enzymes which enable them to compete more readily for available substrates as well as destroying many plant pathogens. Another property ascribed to this genus recently is the ability to stimulate plant growth directly, possibly by the production of plant growth regulators (35-37). The following questions therefore arise: (1) How important is the natural action of *Trichoderma* spp. in inducing plant residue decomposition and suppressing pathogens? and (2) Is it possible to elevate this action by inoculation? The answer to the former question is unclear because a critical appraisal of the population biology of the fungus in soils is required. Most considerations have involved counting viable propagules and we found that this has little relationship to fungal biomass present (Lumsden, R. D., USDA, Beltsville, MD; Lynch, J. M., Whipps, J. M., Carter, J. P., AFRC Institute of Horticultural Research, Littlehampton, England; unpublished data). The second question has been answered more positively because we have shown that it has been possible to elevate the *Trichoderma* population size in soil at the expense of *Fusarium* by recovering straw from soil, chopping it into 1 cm lengths and determining the percentages of pieces giving rise to growth of each fungus when incubated on plates of malt and V-8 juice agars (21 and unpublished).

Thus, the environmental potential of *Trichoderma* may be considerable. However, much needs to be done yet to determine the relative role of its enzymes and metabolites in useful natural processes, and its natural population biology. It should then be possible to isolate from nature, or to clone, a strain which will be highly effective at colonizing crop residues and the rhizosphere, helping to regulate plant growth and nutrition while providing crop protection value. The prospects for this step appear quite good as knowledge on the molecular biology of *Trichoderma* is advancing rapidly, especially for *T. reesei* (7, 38). Genetic manipulation is likely to be by plasmid-mediated transformation. For example, the invertase of *Saccharomyces cerevisiae* has been cloned and expressed in *T. reesei* CL847 by protoplast transformation with plasmids (7).

### Acknowledgments

I am very grateful to my colleagues who have contributed to our studies on lignocellulolysis (J. P. Carter, S. J. Chapman, N. Curtis, D. M. Gaunt, P. Hand, S. H. T. Harper, L. A. Harrison, I. A. Kirkwood, N. Magan, A. P. J. Trinci, and D. A. Veal) and mycoparasitism (J. R. Coley-Smith, R. D. Lumsden, and C. J. Ridout) referred to in this paper. The financial aid of the Commission of the European Communities (Contract RUW-033-UK), the Agricultural Genetics Company, the Department of Trade

and Industry, and the Science and Engineering Research Council is also gratefully acknowledged.

### Literature Cited

1. Wood, D. A. *Ann. Proc. Phytochem. Soc. Eur.* 1985, **26**, 295-309.
2. Lynch, J. M. *J. Appl. Bacteriol. Symp. Supp.* 1987, 71S-83S.
3. Thaysen, A. C.; Bunker, H. J. *The Microbiology of Cellulose, Hemicellulose, Pectin and Gums*; Oxford Univ. Press: Oxford, 1927.
4. Harper, S. H. T.; Lynch, J. M. *J. Sci. Food Agric.* 1981, **32**, 1057-62.
5. Eveleigh, D. E. In *Biology of Industrial Micro-organisms*; Demain, A. L.; Solomon, N. A., Eds.; Benjamin Cummings Publishing Co.: Menlo Park, NJ, 1985; p. 489.
6. Papavizas, G. C. *Ann. Rev. Phytopath.* 1985, **23**, 23-54.
7. Durand, H. Baron, M.; Calmels, T.; Tiraby, G. In *Biochemistry and Genetics of Cellulose Degradation*; Aubert, J. P.; Beguin, P.; Millet, J., Eds.; Academic Press: London, 1988; p. 135.
8. O'Dwyer, M. H. *Biochem. J.* 1926, **20**, 656-64.
9. Gaunt, D. M.; Trinci, A. P. J.; Lynch, J. M. *Exp. Mycol.* 1985, **9**, 174-78.
10. Gaunt, D. M. Ph.D. Thesis, University of Manchester, 1986.
11. Harrison, L. A. Ph.D. Thesis, University of Warwick, 1985.
12. Veal, D. A. Ph.D. Thesis, University of Reading, 1985.
13. Veal, D. A.; Lynch, J. M. *J. Appl. Bacteriol.* 1987, **63**, 245-53.
14. Veal, D. A.; Lynch, J. M. *Nature, Lond.* 1984, **310**, 695-96.
15. Harper, S. H. T.; Lynch, J. M. *Trans. Brit. Mycol. Soc.* 1985, **85**, 655-61.
16. Magan, N.; Lynch, J. M. *J. Gen. Microbiol.* 1986, **132**, 1181-87.
17. Harper, S. H. T.; Lynch, J. M. *Curr. Microbiol.* 1986, **14**, 127-31.
18. Chapman, S. J.; Lynch, J. M. *Enzyme Microb. Technol.* 1985, **7**, 161-63.
19. Lynch, J. M.; Harper, S. H. T. *Phil. Trans. R. Soc. Lond.* 1985, **B310**, 221-26.
20. Halsall, D. M.; Goodchild, D. J. *Appl. Environ. Microbiol.* 1986, **51**, 849-54.
21. Magan, N.; Hand, P.; Kirkwood, I. A.; Lynch, J. M. *Soil Biol. Biochem.* 1989, **21**, 15-22.
22. Lynch, J. M. *Curr. Microbiol.* 1987, **16**, 49-53.
23. Claydon, N.; Allan, M.; Hanson, J. R.; Avent, A. G. *Trans. Brit. Mycol. Soc.* 1987, **20**, 263-64.
24. Simon, A.; Dunlop, R. W.; Chisalberti, E. L.; Sivasithamparan, K. *Soil Biol. Biochem.* 1988, **20**, 263-64.
25. Denis, C.; Webster, J. *Trans. Brit. Mycol. Soc.* 1971, **57**, 41-48.
26. Elad, Y.; Chet, I.; Henis, Y. *Can. J. Microbiol.* 1982, **28**, 719-25.
27. Elad, Y.; Barak, R.; Chet, I. *Can. J. Microbiol.* 1984, **16**, 381-86.
28. Ridout, C. J.; Coley-Smith, J. R.; Lynch, J. M. *J. Gen. Microbiol.* 1986, **132**, 2345-52.

29. Ridout, C. J.; Coley-Smith, J. R.; Lynch, J. M. *Enzyme Microb. Technol.* 1988, **10**, 180-87.
30. Reynolds, M.; Weinhold, A. R.; Morris, T. J. *Phytopathology* 1983, **73**, 903-06.
31. Kuninagen, S.; Yokosawa, R. *Ann. Phytopath. Soc. Japan* 1980, **46**, 150-58.
32. Bartnicki-Garcia, S. In *Handbook of Microbiology*; Laskin, A. I.; Lechevalier, H. A., Eds.; CRC Press: Cleveland, 1973; p. 201.
33. Rosenberger, P. *The Filamentous Fungi*; Edward Arnold: London, 1976; p. 328.
34. Ferron, P. *Ann. Rev. Entomol.* 1978, **23**, 409-42.
35. Baker, R.; Elad, Y.; Chet, I. *Phytopathology* 1984, **74**, 1019-21.
36. Chang, Y.; Chang, Y.; Baker, R. *Plant Disease* 1986, **70**, 145-48.
37. Windham, M. T.; Elad, Y.; Baker, R. *Phytopathology* 1986, **76**, 518-21.
38. Knowles, J.; Teeri, T. T.; Lehtovaara, P.; Penttilä, M.; Saloheimo, M. In *Biochemistry and Genetics of Cellulose Degradation*; Aubert, J. P.; Beguin, P.; Millet, J., Eds.; Academic Press: London, 1988; p. 153.

RECEIVED May 19, 1989

## Chapter 45

# Biodegradation of the Hetero-1,4-Linked Xylans

Robert F. H. Dekker

Commonwealth Scientific and Industrial Research Organisation, Division  
of Biotechnology, Private Bag 10, Clayton 3168, Victoria, Australia

The heteroxylans occur in the plant cell wall of terrestrial plants, and can be present to the extent of 35%, depending upon the plant species. They constitute a group of complex polysaccharides composed of a backbone chain of 1,4- $\beta$ -linked D-xylose residues to which are attached various appendages. These may be L-arabinose; D-glucuronic acid; various short oligosaccharide chains consisting of D-xylose, L-arabinose, galactose and D-glucuronic acid; *O*-acetyl groups; feruloyl and *p*-coumaroyl esters linked via L-arabinose residues; and benzyl ether groups as occur in lignin-carbohydrate complexes. The heteroxylans constitute a renewable feedstock from which many chemicals could be derived. This requires hydrolysis, and fermentation or transformation steps. While enzymes degrading the heteroxylan are known as xylanases, they also require the additional actions of  $\beta$ -xylosidases,  $\alpha$ -arabinosidases,  $\alpha$ -glucuronidases and certain esterases for total hydrolysis. This chapter is concerned with their specificity in degrading their substrate. The biodegradative pathways of the heteroxylans are also discussed.

The hetero-1,4-linked xylans (or heteroxylans) constitute a well-characterized group of polysaccharides which form the major components of the hemicellulosic fractions of terrestrial plants (1-4). Softwoods are an exception, where the heteroxylans can be present as a minor component of the total hemicelluloses. They have been isolated from grasses, legumes, ferns, softwoods and hardwoods, and collectively may constitute up to 35% of the total dry weight of higher land plants (4). As such the heteroxylans rank second to cellulose in abundance as naturally occurring organic chemicals in the biosphere. The heteroxylans are closely associated with other

0097-6156/89/0399-0619\$06.00/0

Published 1989 American Chemical Society

hemicellulosic polysaccharides, cellulose and lignin and are present in both primary and secondary layers of the plant cell wall. Certain heteroxylans are also found in the cell walls of the aleurone layer (5) and endosperm (6) of cereal grains. The pentosan content (as arabinoxylan) has been reported to range from 5-9% in wheat, 2-3% in wheat flour, 4-13% in germ and 20-35% in bran (7). Heteroxylans can therefore be botanically categorized as either non-endospermic, or endospermic (8). The heteroxylans from endospermic materials (caryopses) can be extracted under relatively mild conditions (e.g., water or dilute alkali) as these tissues are generally non-lignified. Lignified tissues (e.g., grasses and woody plants), however, require a delignification step (e.g., acidified chlorine dioxide (9)), and the heteroxylans are extracted from the resulting holocellulose using either dilute aqueous alkali (10) or DMSO (11). In their native state, i.e., within the plant cell wall, the heteroxylans are usually insoluble, but frequently show water solubility after isolation.

### Chemical Structure of the Heteroxylans

The classification of the heteroxylans is based upon chemical structure. Structurally, the heteroxylans are  $\beta$ -1,4-linked D-xylopyranosyl (Xylp) polymers to which are usually attached monosaccharide or short-chain oligosaccharides. These appendages consist mainly of 1,3-linked  $\alpha$ -L-arabinofuranosyl residues (Araf), (e.g., arabinoxylans, arabinoglucuronoxylans), or 1,2-linked  $\alpha$ -D-glucopyranosyl uronide residues (Glc pA, e.g., glucuronoxylans), where the glucuronic acid residue may contain an *O*-methyl group at carbon 4. *O*-Acetyl groups are also present as substituents on heteroxylans (2) and these are usually located on C-3 of the xylose residues but may also be present on C-2, or both (12-14). The degree of substitution is high, e.g., in some hardwood (e.g., birch) and grass (*Lolium* sp.) heteroxylans, every second xylose residue may be acetylated (2, 12, 15), while in beech leaves it has been reported (16) that every xylose residue may be substituted with an *O*-acetyl substituent. It should be emphasized that the *O*-acetyl groups are readily removed when the heteroxylans are extracted with alkali (saponified), and the isolated product can therefore be misleadingly low in *O*-acetyl content. Other chemical groups may also be linked to the heteroxylans. There is now evidence to suggest that lignin is covalently attached to heteroxylans and other plant cell wall polysaccharides (17). This evidence is derived from studies on the lignin-carbohydrate complex (LCC) of various grasses and hardwoods which were found to contain arabinose, xylose and glucuronic acid (and its 4-*O*-methyl derivative) as well as other sugars (18-20). There is still controversy, however, over the exact nature of the LCC bond despite evidence of the existence of ether (between arabinose and lignin (21)) and ester (between glucuronic acid and lignin (22)) linkages. More recently, feruloyl and *p*-coumaroyl esters have been shown to be covalently attached to arabinoxylobiosides (23, 24). The feruloyl esters of these compounds were isolated from crude cellulase digests of barley straw (23), wheat (25) and *Zea* shoot (26) cell walls, barley aleurone layers (27) and bagasse LCC (24). The identification of these com-

pounds provides further evidence that phenolic substituents such as those constituting lignin are attached to the xylan chain.

The detailed chemistry of the hemicelluloses including the heteroxylans has been reviewed by Aspinall (1, 28), Timell (2-4) and Wilkie (8). On the basis of their sugar composition the heteroxylans are classified as arabinoxylans (found mainly in endospermic tissue), arabinoglucuronoxylans (present in grasses and softwood species) and acetylated glucuronoxylans (in hardwoods). There are reports of a homoxylan occurring in esparto grass (29) while galactoarabinoglucuronoxylans have been found in bamboo (30). Endospermic heteroxylans including those derived from bran have been characterized as having highly branched structures (31, 32). Wheat and corn bran heteroxylans have been reported to carry at least one, and sometimes two, substituents per xylosyl residue of the xylan chain. These complex structures have been referred to as glucuronoarabinoxylans (31).

### Enzymes Degrading the Heteroxylans

Enzymes which attack the heteroxylans are of two types. Those that hydrolyze the glycan chain and its appendage groups are known as *hydrolases* [EC 3.2.1.], while those enzymes that remove the ester groups are known as *esterases* [EC 3.1.1.]. Although enzymes hydrolyzing the *O*-acetyl groups on heteroxylans have only been recently discovered (33), hydrolytic enzymes degrading the heteroxylans are well recognized, and have been the subject of several recent reviews (34-39). There are generally two kinds of hydrolases that degrade the heteroxylans. The first include the exo-glycosidases, which cleave monosaccharide and short side-chain oligosaccharide linkages, and are also involved in hydrolyzing the low MW end-products (e.g., oligosaccharides) released during depolymerization of the main backbone chain. The second group of enzymes include the glycanases, or polysaccharide hydrolases, and these are responsible for attack on the polymer backbone itself. They are classified according to the nature of the polysaccharide chain they act upon. In the case of the heteroxylans, they are known as the 1,4- $\beta$ -D-xylanases, or xylanases [EC 3.2.1.8.]. Only one type of xylanase, the endo-xylanase, has been identified which attack internal xylosidic linkages of the heteroxylan chain causing multiple scission that results in a decreased DP of the substrate. Exo-enzymes such as those that attack cellulose have not yet been unequivocally identified for the xylanases. This is in spite of the fact that there have been reports of  $\beta$ -xylosidases that can slowly attack xylan producing xylose (see (40)), and a novel exo-cellulase which also hydrolyzed xylan to xylobiose (Xyl<sub>2</sub>, (41)). However, even if exo-xylanases existed, they would only be expected to make a limited attack on heteroxylans as their actions would be terminated at each branch point encountered. The total hydrolysis of the heteroxylan chain requires the endo-xylanases acting in synergism with the exo-glycosidases, which include the  $\beta$ -xylosidases,  $\alpha$ -arabinosidases, galactosidases and  $\alpha$ -glucuronidases.

Enzymes attacking the non-glycosidic appendages of the heteroxylans include several recently discovered enzymes, i.e., acetyl-xylan esterase (42) and ferulic acid esterase (33), which are specific for the hydroly-

sis of *O*-acetyl and feruloyl groups, respectively. Another newly discovered enzyme is  $\alpha$ -glucuronidase (43) which specifically hydrolyzes the 4-*O*-methylglucuronic and glucuronic acid substituents from the xylan chain.

### Mode of Action of the Xylanases

In general, endo-1,4- $\beta$ -xylanases degrade heteroxylans by attacking internal  $\beta$ -xylosidic linkages of the xylan backbone chain resulting in multiple scission. The sites attacked along the xylan chain and the frequency of bond cleavage is governed by the structure of the heteroxylan (i.e., in the degree and frequency of side-chain substituents), and by the number of subsites in the active site of the enzyme which affects the free energy of binding to the glycosyl residues (44). The degradation products arising during the early course of hydrolysis are xylooligosaccharides, some of mixed constitution, i.e., usually containing arabinose and/or glucuronic acid or its 4-*O*-methyl derivative. The degree of polymerization (DP) of these products varies but is usually  $> 4$ . As hydrolysis proceeds these oligosaccharides are usually progressively converted to xylose and xylobiose; and in some cases, the final product may be xylobiose and xylotriose but no xylose may be formed. As is the case of most endo-xylanases, xylobiose is usually not further degraded (34, 37-40). The ultimate size of the final end-product is determined by the specificity of the enzyme, and this in turn, may be affected by the frequency and spacing of the monosaccharide, or side-chain substituents, on the xylan chain (40). Two types of endo-xylanases are generally recognized and are classified according to whether arabinose is cleaved during hydrolysis (40). In all of the cases reported, the xylanase preparation was highly purified as demonstrated by the usual criteria for homogeneity of proteins indicating that the hydrolysis of arabinose was not due to a contaminating enzyme. The debranching xylanases removed arabinose from arabinoxylans and arabinoglucuronoxylans by cleaving 1,3- $\alpha$ -L-arabinofuranosyl residues from the xylan backbone chain. Another feature of some highly purified endo-xylanases was that they showed transglycosylation activity, i.e., not only did these xylanases hydrolyze the xylan chain, but they were also capable of synthesizing oligosaccharides from the low MW hydrolysis products. An example is a xylanase preparation isolated from *Cryptococcus albidus* (45).

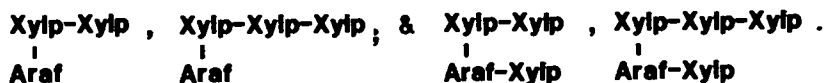
In discussing the mode of action of the xylanases only selected features will be discussed as there are numerous detailed reviews on this topic (34, 37, 38, 40). It is, however, important to emphasize that most of the xylanases reported in the literature display similar action patterns when attacking their substrates, whether they be xylan or xylooligosaccharides.

Two xylanases have been isolated (46) from the industrially important bacterium *Clostridium acetobutylicum*. This organism has the ability to ferment heteroxylans to acetone, *n*-butanol and ethanol. One of the xylanases isolated (i.e., of MW 65,000) hydrolyzed oat spelt xylan to oligosaccharides of DP 2-6 which were not further degraded (47). Xylohexaose (Xyl<sub>6</sub>) was only slowly degraded to xylotetraose (Xyl<sub>4</sub>) and Xyl<sub>2</sub>, while Xyl<sub>4</sub>, xylopentaose (Xyl<sub>5</sub>), xylotriose (Xyl<sub>3</sub>) and Xyl<sub>2</sub> were not degraded further. No

xylose was produced. The action pattern of this enzyme suggested that it required a substrate binding site of at least 6-7 xylose residues for bond cleavage to occur as Xyl<sub>6</sub> was the smallest xylooligosaccharide attacked. The other xylanase (MW 29,000) was more typical of endo-xylanases in that it degraded xylan into mainly Xyl<sub>2</sub> and Xyl<sub>3</sub> with some xylose appearing after 24 h hydrolysis (47). A thermophilic *Clostridium* sp., viz. *Cl. stercorearium*, which produces ethanol (48), produced three xylanases. These were optimally active at 65°C and degraded xylan (larchwood) yielding xylooligosaccharides of DP 2-3. Xyl<sub>2</sub> and Xyl<sub>3</sub> were not attacked, and arabinose was not detected in the xylan digests. This bacterium also produced a cell-wall bound enzyme(s) which acted preferentially on Xyl<sub>2</sub> and Xyl<sub>3</sub> to yield xylose, and which was reported to also attack xylan slowly liberating xylose (48). An alkalophilic *Bacillus* sp. has been isolated which produced xylanases when grown in alkaline medium (49). This bacterium produced two xylanases: one was active at neutral pH (xylanase N), while the other showed activity at alkaline pH (6-10) and was still active at pH 12.0 (xylanase A). Both xylanases were optimally active at 70°C, and degraded xylan to mainly Xyl<sub>2</sub> and Xyl<sub>3</sub>. Xylose was not produced in the course of hydrolysis, nor were Xyl<sub>2</sub> and Xyl<sub>3</sub> attacked. Xyl<sub>4</sub> was degraded to Xyl<sub>2</sub>, Xyl<sub>3</sub> and higher oligosaccharides, indicating transxylosylation activity. The alkaline stable xylanase is of industrial interest because of its stability at high pH. It could find application in removing xylan from wood cellulose pulps for use in the manufacture of rayon.

The xylanases of yeasts have been studied in detail by Biely and co-workers using *Cryptococcus albidus* as a model (35). The xylanase from *C. albidus* also possessed transglycosylation activity, and was capable of transferring xylose to cellobiose to form 6'-O-β-D-xylosyl compounds of cellobiose. These compounds could be degraded by the xylanase that was involved in their synthesis (50). In general, the action of yeast xylanases in attacking their substrates was similar to that produced by certain bacteria and fungi, and yielded mainly Xyl<sub>2</sub> and Xyl<sub>3</sub> as end-products (35).

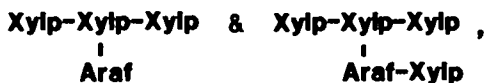
Xylanases produced by the actinomycete *Streptomyces* are well-characterized (51). A xylanase produced by *Streptomyces* sp. strain E-86 yielded some very interesting xylose oligosaccharides from corncob arabinoxylan which revealed the mode of action of the enzyme, and the nature of some of the side-group appendages to the xylan chain of corncob arabinoxylan. The main end-products of corncob arabinoxylan hydrolysis by the *Streptomyces* xylanase was Xyl<sub>2</sub> and Xyl<sub>3</sub> and some xylose, while the arabinoxylooligosaccharides consisted of two predominant types as shown below:



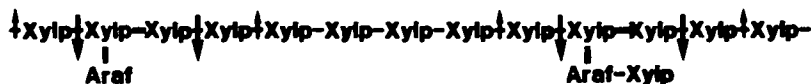
One series of xylooligosaccharide hydrolysis products contained an α-1,3-linked L-arabinofuranosyl group on the non-reducing xylose residue, while



the other series of xylooligosaccharides liberated contained an interposed L-arabinose residue attached to the non-reducing xylose unit. The interposed arabinose was linked to xylose via 1,3- and 2,1-bonds which were of the  $\alpha$ - and  $\beta$ -configuration, respectively. The production of these homologous series of arabinoxylooligosaccharides demonstrated that the  $\beta$ -1,4-D-xyloside linkage immediately to the *left* of the substituent group on the xylan chain was hydrolyzable by the xylanase, but the bond immediately to the *right* was resistant to hydrolysis (51). Two other arabinoxylooligosaccharides were also produced by the *Streptomyces* xylanase, viz.,



which are inconsistent with the predicted mode of action of this xylanase. However, the production of these oligosaccharides can be envisaged as occurring by the xylanase attacking the xylan chain where there are no substituent groups. During the early stages of hydrolysis Xyl<sub>4</sub> to Xyl<sub>6</sub> were produced which suggests that there were at least 7 contiguous xylose units unbranched. Cleavage as indicated below would result in the production of these branched arabinoxylooligosaccharides.



The isolation of the above oligosaccharides also revealed that corncob arabinoxylan contained side-chains of 2-O-D-xylopyranosyl-L-arabinofuranosides (51).

The best characterized and most studied of the xylanases have been those of fungal origin and especially those from *Aspergillus niger*, *Sporotrichum dimorphosporum*, *Ceratocystis paradoxa*, *Oxiporus* sp., *Trametes hirsuta* and some *Trichoderma* species (34,37). More recently, there has been interest in employing xylanolytic enzymes to remove xylans from wood cellulose pulps for use in the manufacture of rayon. Xylanases from *Trichoderma harzianum* (52), and the thermophilic fungus, *Thermoascus aurantiacus* (53) have been studied for this purpose. In general, multiple xylanases have been produced by the fungi, e.g., five from *A. niger* (54) and nine from *S. dimorphosporum* (55). While multiple xylanases are probably the result of proteolytic cleavage following their excretion into the extracellular medium, there are also reports of isozymes occurring (54).

Xylanases from *A. niger* with unusual hydrolysis specificities were recently reported (54), and five xylanases were isolated and purified. Xylanase 1 attacked soluble larchwood arabinoglucuronoxylan and xylose oligosaccharides of DP > 3, to mainly Xyl<sub>2</sub> and xylose, but was inactive towards an insoluble xylan fraction (larchwood) prepared by dissolving the aforementioned xylan in water and separating the undissolved fraction

(56). Xylanases 2 and 3, considered isoenzymes, degraded both soluble and insoluble xylans derived from larchwood at sites near arabinose substituents on the xylan chain, and yielded mainly Xyl<sub>3</sub> and Xyl<sub>5</sub> with lesser amounts of Xyl<sub>2</sub> but no xylose. Xylanase 4 showed none of the affinity of xylanases 2 and 3 for branch points, but was highly active towards linear xylooligosaccharides and more active on soluble than insoluble xylans. Finally, xylanase 5 attacked soluble xylan, but attacked insoluble xylan only if the arabinose branches were removed. No arabinose was liberated by any of the five *A. niger* xylanases. Insoluble xylan was also capable of being hydrolyzed by two xylanases of *T. harzianum* (57). A light scattering method was used to monitor hydrolysis, and both enzymes were found to completely solubilize the substrate within 0.5 h.

Enzymatic hydrolysis of a 4-*O*-methylglucuronoxylan from larchwood and oat spelt arabinoglucuronoxylan by a xylanase from *Polyporus tulipiferae* produced an array of xylooligosaccharides of mixed constitution containing either L-arabinose or 4-*O*-methyl-D-glucuronic acid substituent groups (58). The substituent groups were located on the non-reducing end of the xylooligosaccharide chain. Similar oligosaccharides were observed by others and these have been described in reference 34. Four oligosaccharides were identified as (4-*O*-Me)-GlcA-Xyl<sub>*n*</sub> (*n* being 3 and 4) for the acidic xylooligosaccharides, and Araf-Xyl<sub>*n*</sub> (*n* being 2 and 3) for the arabinoxylooligosaccharides. A new arabinoxylooligosaccharide was identified from enzymic digests of spear grass (*Heteropogon contortus*) hemicellulose B (branched xylan), and was produced by a xylanase from *Cephalosporium sacchari* (59). Its structure was confirmed by permethylation analysis and by specific enzymic hydrolysis to be 4<sup>3</sup>-α-L-Araf-β-D-Xyl<sub>4</sub>. The xylanase from *C. sacchari* which is an arabinose-debranching enzyme, hydrolyzed Araf-Xyl<sub>4</sub> to Araf-Xyl<sub>3</sub>, which was further hydrolyzed to arabinose, Xyl<sub>2</sub> and xylose. Finally, xylooligosaccharides containing *O*-acetyl groups have been isolated from *Schizophyllum commune* xylanase hydrolyzates of birch (steamed) acetylated xylan (42). Some of these oligosaccharides were identified as carrying several *O*-acetyl groups.

### Specificities of Xylanases

The specificity of a xylanase preparation may be determined from the isolation and characterization of oligosaccharides formed from xylan hydrolysis. While the oligosaccharides released were mainly dependent on the specificity of the xylanase, the complex structure of the heteroxylan also determines the extent of hydrolysis and the site of cleavage. Two types of xylooligosaccharides are usually produced: acidic (from glucuronoxylans) and neutral (from arabino- and arabinoglucurono-xylans). The specificity of the action of several purified xylanases on various heteroxylans is shown below:





opening, or exposing, the backbone xylan chain. This mode of action would allow the xylan chain to be more easily attacked by the xylanases, reducing steric hindrance by the side-chain groups. An exception to this would be the action of the debranching xylanases which are capable of removing the arabinose substituents. The ultimate end-products of the synergistic actions of these enzymes are xylose, arabinose, glucuronic acid and acetic acid, with some galactose and phenolic acids or benzyl compounds also being formed.

There is evidence that  $\beta$ -xylosidases enhance the rate and extent of hydrolysis of heteroxylans by xylanases (65,66). This synergism resembles that between cellulase and  $\beta$ -glucosidase in cellulose hydrolysis (67). Synergism was also observed between xylanase,  $\beta$ -xylosidase and  $\alpha$ -glucuronidase in degrading beechwood (*Fagus sylvatica*) xylan (43). Thus,  $\alpha$ -glucuronidase plays an important role in the complete hydrolysis of glucuronoxylans. Similarly, synergism was recently demonstrated in the hydrolysis of arabinoxylans by the actions of  $\alpha$ -L-arabinofuranosidase, xylanase and  $\beta$ -xylosidase (68). Likewise, acetylxylan esterases acted cooperatively with xylanases in degrading birch (*Betula verrucosa*) acetylated xylan (69). Xylanase alone released small quantities of xylooligosaccharides, some of which contained *O*-acetyl groups (69). When an acetylxylan esterase was added to a xylanase digest of acetylated xylan, the majority of the oligosaccharides produced were non-acetylated, and hydrolysis was accompanied by an increase in the rate and amount of xylose equivalents released. A similar increase in the rate and extent of acetic acid released was also observed. The esterase appeared to show preference for the low MW acetylated xylooligosaccharides rather than for the highly acetylated polysaccharide (69).

### Literature Cited

1. Aspinnall, G.O. *Adv. Carbohydr. Chem.* 1959, **14**, 429-468.
2. Timell, T.E. *Adv. Carbohydr. Chem.* 1964, **19**, 247-295.
3. Timell, T.E. *Adv. Carbohydr. Chem.* 1965, **20**, 409-483.
4. Timell, T.E. *Wood Sci. Technol.* 1967, **1**, 45-70.
5. McNeil, M.; Albersheim, P.; Taiz, L.; Jones, R.L. *Plant Physiol.* 1975, **55**, 64-68.
6. Mares, D.J.; Stone, B.A. *Aust. J. Biol. Sci.* 1973, **26**, 793-812.
7. Cerning, J., Guilbot, A. In *Wheat—Production and Utilization*; Inglett, G.E., Ed.; AVI: Westport, 1972, p.146-185.
8. Wilkie, K.C.B. *Adv. Carbohydr. Chem. Biochem.* 1979, **36**, 215-264.
9. Timell, T.E. *Meth. Carbohydr. Chem.* 1965, **5**, 144-145.
10. Whistler, R.L.; Feather, M.S. *Meth. Carbohydr. Chem.* 1965, **5**, 134-137.
11. Hagglund, E.; Lindberg, B.; McPherson, J. *Acta Chem. Scand.* 1956, **10**, 1160-1164.
12. Bouveng, H.O. *Acta Chem. Scand.* 1961, **15**, 96-100.
13. Lindberg, B.; Rosell, K.G.; Svensson, S. *Sven. Papperstidn.* 1973, **76**, 30-32.

14. Reicher, F.; Correa, J. B. C.; Gorin, P. A. J. *Carbohyd. Res.* 1984, **135**, 129-140.
15. Bacon, J. S. D.; Gordon, A. H.; Morris, E. J. *Biochem. J.* 1975, **149**, 485-487.
16. Wood, T. M.; McCrae, S. I. *Photochemistry* 1986, **25**, 1053-1055.
17. Richards, G. N. *Proc. Intl. Workshop on Plant Polysaccharides, Structure and Function*; Nantes, France, 9-11 July 1984, p.47-53.
18. Atsushi, K.; Azuma, J. I.; Kosijima, T. *Holzforschung* 1984, **38**, 141-149.
19. Neilson, M. J.; Richards, G. N. *Carbohyd. Res.* 1982, **104**, 121-138.
20. Eriksson, O.; Goring, D. A. I.; Lindgren, B. O. *Wood Sci. Technol.* 1980, 267-279.
21. Koshijima, T.; Watanabe, T.; Azuma, J. *Chem. Lett.* 1984, 1737-1740.
22. Das, N. N.; Das, S. C.; Sarkar, A. K.; Mukherjee, A. K. *Carbohyd. Res.* 1984, **129**, 197-207.
23. Mueller-Harvey, I.; Hartley, R. D.; Harris, P. J.; Curzon, E. H. *Carbohyd. Res.* 1986, **148**, 71-85.
24. Koshijima, T.; Kato, A.; Azuma, J. *Proc. Intl. Symp. Wood and Pulp Chem.* 1983, **1**, 159-163.
25. Smith, M. M.; Hartley, R. D. *Carbohyd. Res.* 1983, **118**, 65-80.
26. Kato, Y.; Nevins, D. J. *Carbohyd. Res.* 1985, **137**, 139-150.
27. Gubler, F.; Ashford, A. E.; Bacic, A.; Blakeney, A. B.; Stone, B. A. *Aust. J. Plant Physiol.* 1985, **12**, 307-317.
28. Aspinall, G. O. *Polysaccharides*; Pergamon Press: Oxford, 1970; 103-115.
29. Chanda, S. K.; Hirst, E. L.; Jones, J. K. N.; Percival, E. G. V. *J. Chem. Soc.* 1950, 1289-1297.
30. Wilkie, K. C. B.; Woo, S. L. *Carbohyd. Res.* 1977, **57**, 145-162.
31. Brillouet, J. M.; Joseleau, J. P. *Carbohyd. Res.* 1987, **159**, 109-126.
32. Bradbury, A. G. W.; Medcalf, D. G. *Abstr. Papers Ann. Mtg. Amer. Assoc. Cereal Chem.*, Denver, Colorado, 1981.
33. MacKenzie, C. R.; Bilous, D.; Schneider, H.; Johnson, K.G. *Appl. Environ. Microbiol.* 1987, **53**, 2835-2839.
34. Dekker, R. F. H. In *Biosynthesis and Biodegradation of Wood Components*; Higuchi, T., Ed.; Academic Press: New York, 1985; p. 505-533.
35. Biely, P. *Trends Biotech.* 1985, **3**, 286-290.
36. Woodward, J. *Top. Enzyme Ferment. Biotechnol.* 1984, **8**, 9-30.
37. Reilly, P. J. In *Trends in Biology of Fermentations for Fuels and Chemicals*; Hollaender, A., Ed.; Plenum Press: New York, 1981; p. 111-129.
38. Dekker, R. F. H. In *Polysaccharides in Food*; Blanchard, J. M. V.; Mitchell, J. R., Eds.; Butterworth's: London, 1979; p.93-108.
39. Wong, K. K. Y.; Tan, L. U. L.; Saddler, J. N. *Microbiol. Rev.* 1988, **52**, 305-317.
40. Dekker, R. F. H.; Richards, G. N. *Adv. Carbohyd. Chem. Biochem.* 1976, **32**, 277-352.
41. Shikata, S.; Nisizawa, K. *J. Biochem.* 1975, **78**, 499-512.
42. Biely, P.; Puls, J.; Schneider, H. *FEBS Lett.* 1985, **186**, 80-84.

43. Puls, J.; Schmidt, O.; Granzow, C. *Enzyme Microb. Technol.* 1987, **9**, 83-88.
44. Meagher, M. M.; Tao, B. Y.; Chow, J. M.; Reilly, P. J. *Carbohydr. Res.* 1988, **173**, 273-283.
45. Biely, P.; Vrsanska, M.; Kratky, Z. *Eur. J. Biochem.* 1981, **119**, 565-571.
46. Lee, S. F.; Forsberg, C. W.; Gibbins, L. N. *Appl. Environ. Microbiol.* 1985, **50**, 1068-1076.
47. Lee, S. F.; Forsberg, C. W.; Rattray, J. B. *Appl. Environ. Microbiol.* 1987, **53**, 644-650.
48. Berenger, J. F.; Frixon, C.; Bigliardi, J.; Creuzet, N. *Can. J. Microbiol.* 1985, **31**, 635-643.
49. Honda, H.; Kudo, T.; Ikura, Y.; Horikoshi, K. *Can. J. Microbiol.* 1985, **31**, 538-542.
50. Biely, P.; Vrsanska, M. *Carbohydr. Res.* 1983, **123**, 97-107.
51. Kusakabe, I.; Ohgushi, S.; Yasui, T.; Kobayashi, T. *Agric. Biol. Chem.* 1983, **47**, 2713-2723.
52. Tan, L. U. L.; Yu, E. K. C.; Louis-Seize, G. W.; Saddler, J. N. *Biotechnol. Bioeng.* 1987, **30**, 96-100.
53. Yu, E. K. C.; Tan, L. U. L.; Chan, M. K. H.; Deschatelets, L.; Saddler, J. N. *Enzyme Microb. Technol.* 1987, **9**, 16-24.
54. Fournier, R.; Frederick, M. M.; Frederick, J. R.; Reilly, P. J. *Biotechnol. Bioeng.* 1985, **27**, 539-546.
55. Comtat, J. *Carbohydr. Res.* 1983, **118**, 215-231.
56. Frederick, M. M.; Frederick, J. R.; Fratzke, A. R.; Reilly, P. J. *Carbohydr. Res.* 1981, **97**, 87-103.
57. Tan, L. U. L.; Wong, K. K. Y.; Saddler, J. N. *Enzyme Microb. Technol.* 1985, **7**, 431-436.
58. Brillouet, J. M. *Carbohydr. Res.* 1987, **159**, 165-170.
59. Shambe, T. *Carbohydr. Res.* 1983, **113**, 125-131.
60. Dekker, R. F. H.; Richards, G. N. *Carbohydr. Res.* 1975, **42**, 107-123.
61. Comtat, J.; Joseleau, J. P. *Carbohydr. Res.* 1981, **95**, 101-112.
62. Takenishi, S.; Tsujisaka, Y. *Agric. Biol. Ehc.* 1973, **37**, 1385-1391.
63. Sinner, M.; Dietrichs, H. H. *Holzforschung* 1976, **30**, 50-59.
64. Comtat, J.; Joseleau, J. P.; Bosso, C.; Barnoud, F. *Carbohydr. Res.* 1974, **38**, 217-224.
65. Dekker, R. F. H. *Biotechnol. Bioeng.* 1983, **25**, 1127-1146.
66. Deshpande, V.; Lachke, A.; Mishra, C.; Keskar, S.; Rao, M. *Biotechnol. Bioeng.* 1986, **28**, 1832-1837.
67. Sternberg, D.; Vijayakumar, P.; Reese, E. T. *Can. J. Microbiol.* 1977, **23**, 139-147.
68. Poutanen, K. J. *Biotechnol.* 1988, **7**, 271-282.
69. Biely, P.; MacKenzie, C. R.; Puls, J.; Schneider, H. *Bio/Technology* 1986, **4**, 731-733.

RECEIVED May 19, 1989

## Chapter 46

# The Xylanolytic Enzyme System of *Trichoderma reesei*

Kaisa Poutanen<sup>1</sup> and Jurgen Puls<sup>2</sup>

<sup>1</sup>VTT, Biotechnical Laboratory, Tietotie 2, SF-02150 Espoo, Finland

<sup>2</sup>BFH, Institute of Wood Chemistry, Leuchnerstrasse 91, D-2050 Hamburg, Federal Republic of Germany

The xylanolytic enzyme system of *Trichoderma reesei*, a well-known producer of cellulolytic enzymes, is versatile and well suited for the total hydrolysis of different xylans. It consists of two major, specific and several non-specific xylanases, at least one  $\beta$ -xylosidase,  $\alpha$ -arabinosidase and  $\alpha$ -glucuronidase and at least two acetyl esterases. The hydrolysis of polymeric xylans starts by the action of endoxylanases. The side-group-cleaving enzymes have their highest activities towards soluble, short xylo-oligosaccharides, and make the substituted oligosaccharides again accessible for xylanases and  $\beta$ -xylosidase.

Xylan is an essential constituent of hardwoods, softwoods, and annual plants. In enzymatic processing of lignocellulosic biomass, xylanolytic enzymes may be used either individually, in selected mixtures for specific effects on only the xylan component of the raw material, or in mixtures with cellulolytic, pectinolytic or amylolytic enzymes.

Xylans are heteropolysaccharides; accordingly, xylanolytic enzymes include different types of endo- and exo-glycosidases: 1,4- $\beta$ -D-xylanase (EC 3.2.1.8),  $\beta$ -xylosidase (EC 3.2.1.37),  $\alpha$ -arabinosidase (EC 3.2.1.55) and  $\alpha$ -glucuronidase. In addition to these, some acetyl esterases are considered xylanolytic because of their ability to deacetylate xylans. Of the xylanolytic enzymes, endo-1,4- $\beta$ -D-xylanases have been most extensively studied as reviewed recently (1-3). Endoxylanases are by definition depolymerizing enzymes, with highest activities towards long chain xylo-oligosaccharides or polysaccharides. The hydrolysis of the  $\beta$ -1,4-linkages of xylans is completed by the action of  $\beta$ -xylosidases, which generally have highest activities with xylobiose as substrate (4-6).

Multiple xylanases and  $\beta$ -xylosidases have been observed in different microorganisms, e.g., of the genera *Streptomyces* (7), *Aspergillus* (8), and

0097-6156/89/0399-0630\$06.00/0

© 1989 American Chemical Society

*Trichoderma* (9-10). Much less is known about the concurrent production of the enzymes which cleave substituent groups of the xylan polymer. The presence of acetyl xylan esterases (11,12) and  $\alpha$ -glucuronidases (13-15) in xylanolytic enzyme systems has only recently been pointed out. Although  $\alpha$ -arabinosidases have mainly been studied as arabinan-degrading enzymes (16), they have also been shown to release arabinose from xylans (17).

While *Trichoderma reesei* is best known as an efficient producer of cellulolytic enzymes, it has also been reported to produce xylanase and  $\beta$ -xylosidase (18-20). Two xylanases and a  $\beta$ -xylosidase have been purified from *T. reesei* (10), and two xylanases (21,22) and a  $\beta$ -xylosidase (5) from *T. viride*. We have previously shown that *T. reesei* produces all the enzymes needed for complete hydrolysis of native substituted xylans (23). One xylanase (24), a  $\beta$ -xylosidase (25), an  $\alpha$ -arabinosidase (26), and an acetyl esterase (27) of *T. reesei* have so far been purified. In this chapter, the mode of action of these enzymes in the hydrolysis of different xylans is discussed.

## Materials and Methods

*Source of Enzymes.* Culture filtrates of *T. reesei* strains VTT-D-79125 and Rut C-30 were used as starting material for purification of the individual enzymes and also as crude enzyme preparations in the hydrolysis experiments. Cultivations were carried out in a laboratory fermentor at 30°C for 4d on media containing Solka floc cellulose (James River Corp., New Hampshire, USA), or glucose and distiller's spent grain (Alko, Ltd., Koskenkorva, Finland).

*Enzyme Activity Assays.* Xylanase was assayed using 1% beechwood xylan (prepared according to the method of Ebringerova *et al.* (28)) as substrate as described previously (25).  $\beta$ -Xylosidase was assayed using 5 mM *p*-nitrophenyl- $\beta$ -D-xylopyranoside as substrate (25), and  $\alpha$ -arabinosidase was assayed using 10 mM *p*-nitrophenyl- $\alpha$ -L-arabinofuranoside (26).  $\alpha$ -Glucuronidase was assayed using 2% 4-*O*-methyl-glucuronosyl-xylobiose as substrate (13), and acetyl esterase was assayed using 1 mM  $\alpha$ -naphthyl acetate (27).

*Enzyme Purification.* The purification of the xylanolytic enzymes began with adsorption on a cation exchanger (CM-Sephrose FF) at pH 4.0. The final purification was accomplished by another ion exchange step as described previously for xylanase (24),  $\beta$ -xylosidase (25),  $\alpha$ -arabinosidase (26) and acetyl esterase (27).

*Hydrolysis Experiments.* The substrate in the hydrolysis experiments included alkali-extracted beechwood 4-*O*-methylglucuronoxylan, DMSO-extracted acetylated beechwood 4-*O*-methylglucuronoxylan, alkali-extracted wheat straw arabinoxylan and acetylated or deacetylated xylo-oligomers from steaming of birchwood (24). Deacetylation was carried out by incubating the freeze-dried xylo-oligomers in ammonia vapor overnight. Substrate concentration was 10 gl<sup>-1</sup>, temperature 45° and hydrolysis time 24 h.



**Analyses.** The mono- and disaccharides were analyzed by HPLC (26). Gel chromatographic analysis of the xylo-oligomers was performed in Fractogel TSK HW-50 (S) (Merck, FRG) and Biogel P4 minus 400 mesh (Bio-Rad, USA) columns (23). Acetic acid was analyzed enzymatically (Boehringer Test Combination 148 261).

## Results and Discussion

The culture filtrates of *T. reesei* contained a large number of both cellulolytic and hemicellulolytic enzymes, which could be partially separated by chromatofocussing (Fig. 1). Of the cellulolytic enzymes, several endoglucanases and two cellobiohydrolases have already been isolated and characterized (30). Some of the endoglucanases isolated are nonspecific and have xylanase activity (31). The two major xylanase (Xyl) peaks in Figure 1 corresponded to pI-values of above 7.5 and 5.5. When the former enzyme was further purified (24), its isoelectric point was found to be about pI 9 (Table I). Previously, the presence of at least three electrophoretically different xylanases in *T. reesei* culture filtrates was reported, with the most acidic one shown to have broad substrate specificity (10). This is in agreement with the reported occurrence of three xylanases (pI > 7, pI 5.1, pI 4.5) in *T. reesei* (32). The results of this study, together with those of others (10,20,31-33) suggest that the enzyme system of *T. reesei* contains two major, specific endoxylanases, with isoelectric points of 8.5-9 and 5-5.5, and many non-specific endoglycanases with more acidic pI-values and both 1,4- $\beta$ -glucanase and 1,4- $\beta$ -xylanase activities.

Table I. Xylanolytic Enzymes Isolated from *Trichoderma reesei*

Enzyme	MW <sup>a</sup> (kDa)	pI <sup>b</sup>	pH-Optimum	Reference
Xylanase	20	~ 9	5.3	24
$\beta$ -Xylosidase	100	4.7	4.0	25
$\alpha$ -Arabinosidase	53	7.5	4.0	26
Acetyl esterase	45	6.8	5.5	27

<sup>a</sup> From SDS-PAGE.

<sup>b</sup> From chromatofocussing.

The  $\beta$ -xylosidase of *T. reesei* was a rather large, probably dimeric enzyme and, like most other  $\beta$ -xylosidases, had an acidic pI-value (Table I). A  $\beta$ -xylosidase purified earlier from *T. viride* with a molecular weight of 101 kDa also had an isoelectric point pI 4.45 (5). In addition to *p*-nitrophenyl- $\beta$ -xylopyranoside and xylo-oligosaccharides, the  $\beta$ -xylosidase of *T. reesei* also showed activity with *p*-nitrophenyl- $\alpha$ -arabinofuranoside as substrate, but did not hydrolyze arabinan or release arabinose from arabinoxylan. The purified  $\alpha$ -arabinosidase, however, was capable of effecting both the latter hydrolyses (26, Table II). The isoelectric point of the  $\alpha$ -arabinosidase of *T. reesei* was pI 7.5 and its molecular weight 53 kDa (Table I).

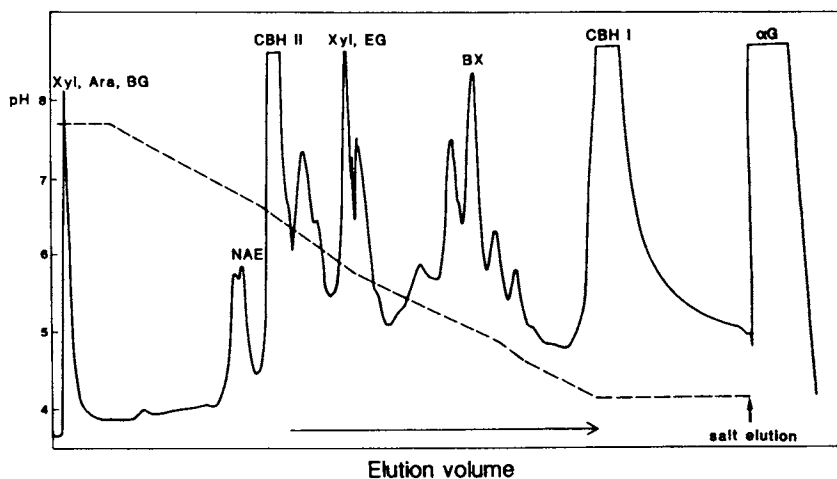


Figure 1. Fractionation of proteins in the culture filtrate of *Trichoderma reesei* according to their pI values: Xyl, xylanase; Ara, arabinosidase; AE, acetyl esterase;  $\beta$ X,  $\beta$ -xylosidase;  $\alpha$ G,  $\alpha$ -glucuronidase;  $\beta$ G,  $\beta$ -glucosidase; CBH, cellobiohydrolase; EG, endoglucanase. Chromatofocusing was performed in a PBE-94 anion exchange resin (Pharmacia) with a pH-gradient created by ampholyte buffers (Pharmacia). Solid line,  $A_{280}$ ; dotted line, pH. (Reproduced with permission from ref. 24. Copyright 1988.)

Table II. The effect of  $\alpha$ -arabinosidase on the hydrolysis of wheat straw arabinoxylan. Substrate concentration  $10 \text{ gl}^{-1}$ , initial pH 4, temperature  $45^\circ\text{C}$ , hydrolysis time 24 h

Xylanase <sup>a</sup>	Enzyme Activities (nkat/g substrate)			Hydrolysis Products (% of substrate)	
	$\beta$ -Xylosidase <sup>a</sup>	$\alpha$ -Arabinosidase <sup>a</sup>	Xylose	Arabinose	
25000	0	0	4	0	
25000	160	0	37	0	
25000	160	1400	43	4	
25000	160	14000	56	7	
25000 <sup>b</sup>	160 <sup>b</sup>	1300 <sup>b</sup>	56	7	

<sup>a</sup> Purified enzymes of *T. reesei*.

<sup>b</sup> Activities of crude *T. reesei* culture filtrate.

The hydrolysis products of three different xylans by the 20 kDa xylanase of *T. reesei* varied according to the nature and degree of substitution of the substrate (Fig. 2a-c). The role of acetyl groups in the accessibility of beechwood xylan was evident (Fig. 2a and 2b): The acetylated substrate was more soluble in water, more uniformly attacked by the enzyme and yielded a wider range of hydrolysis products (Fig. 2a). On the other hand, the hydrolyzate of the non-acetylated 4-*O*-methyl-glucuronosyl-substituted beech xylan contained some insoluble residue (not visible in the chromatogram) and large soluble oligomers, which were eluted in the void volume ( $X_n$ ) (Fig. 2b). Xylobiose and substituted oligomers were the main soluble hydrolysis products. The presence of 4-*O*-methylglucurono-substituted xylo-oligosaccharides was verified by anion exchange chromatography (14) (results not shown). The hydrolyzate of arabinoxylan resembled that of glucuronoxylan (Fig. 2c). The accumulation of 4-*O*-methyl-glucuronosyl- and arabinosyl substituted xylo-oligosaccharides has also been reported when using xylanases from other sources (34,35).

The role of arabinosyl substituents and the need for  $\alpha$ -arabinosidase in the production of xylose from arabinoxylan was also deduced from the results in Table II. When the purified 20 kDa xylanase and  $\beta$ -xylosidase were used in the hydrolysis, the xylose yield was only 66% of that produced by the whole culture filtrate at the same activity levels, and no arabinose was produced. Addition of  $\alpha$ -arabinosidase increased the yields of both xylose and arabinose.

The hydrolysis of acetylated xylo-oligomers from the steaming extract of birchwood using an enzyme mixture containing only xylanase and  $\beta$ -xylosidase was very limited (Table III). Chemical deacetylation showed that the substrate specificities of xylanase and  $\beta$ -xylosidase with respect to substrate DP overlapped, and that  $\beta$ -xylosidase also hydrolyzed longer oligosaccharides than xylobiose to xylose. The addition of acetyl esterase to the hydrolysis of acetylated xylo-oligomers enhanced xylose production (Table III), but deacetylation was still incomplete (the acetyl content of

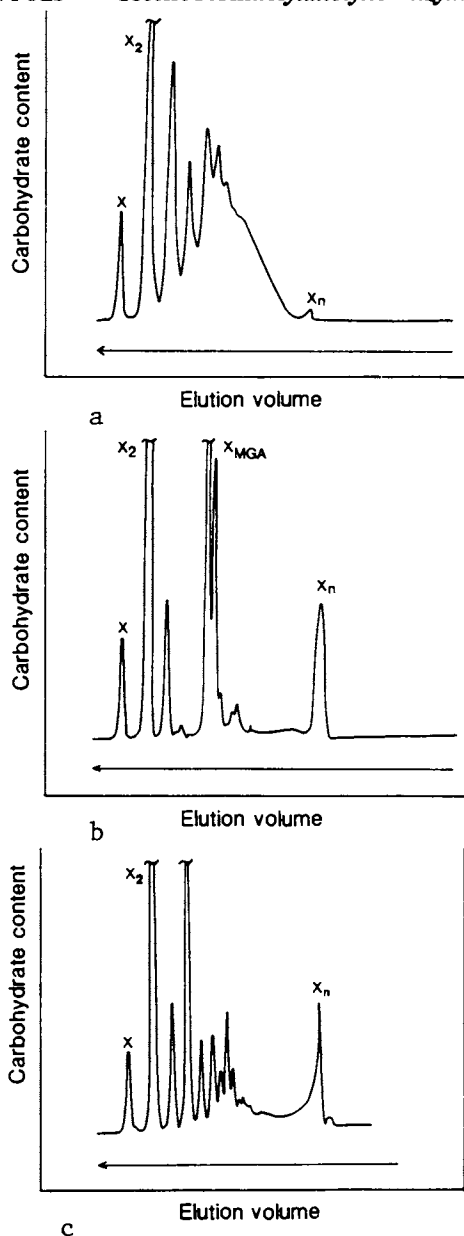


Figure 2. Hydrolysis products of beechwood *O*-acetylglucuronoxylan (Fig. 2a), beechwood glucuronoxylan (Fig. 2b), and wheat straw arabinoxylan (Fig. 2c), as analyzed by gel permeation chromatography. The hydrolysis was carried out at pH 5 at 45°C for 24 h using 10.000 nkat of the 20 kDa xylanase of *T. reesei*. X = xylose; X<sub>2</sub> = xylobiose; X<sub>MGA</sub> = 4-*O*-methylglucuronosyl substituted xylo-oligosaccharides; X<sub>n</sub> = xylo-oligosaccharides DP > 20.

substrate A was 10% of the dry weight). This phenomenon is being further studied. It is possible that the purified esterase specifically removed acetic acid from only one position on the xylopyranose ring (unpublished results).

Table III. Hydrolysis of acetylated (A) and chemically deacetylated (B) xylo-oligomers in the steaming extract of birchwood by purified enzymes of *T. reesei*. Substrate concentration 10 gl<sup>-1</sup>, initial pH 5, temperature 45°C, hydrolysis time 24 h

Substrate	Enzyme Activities (nkat g <sup>-1</sup> )			Hydrolysis Products (% of dry weight)		
	Xylanase	$\beta$ -Xylo- sidase	Acetyl Esterase	Xylose	Xylo- biose	Acetic Acid
A	5000	—	—	2	5	0.7
B	5000	—	—	3	25	—
A	—	500	—	7	< 1	0.7
B	—	500	—	21	< 1	—
A	5000	500	—	9	0	0.9
A	5000	500	500	18	< 1	3.3
B	5000	500	—	33	0	—

Synergism between the different xylanolytic enzymes was further demonstrated when a partially purified enzyme preparation was used as a source of xylanase activity (Table IV). This preparation, separated from *T. reesei* culture filtrate by gel chromatography (10), contained both the 20 kDa xylanase, another glycanase with high laminarinase and low xylanase activity, and a hitherto unidentified esterase. When supplemented with  $\beta$ -xylosidase, the xylanases and esterase of this preparation released about half of the xylose and acetic acid of the substrate (Table IV). When purified acetyl esterase was added, the yields of xylose and acetic acid increased further about 1.6-fold.

Because the  $\alpha$ -glucuronidase of *T. reesei* has not yet been purified, a culture filtrate of *Agaricus bisporus*, with high  $\alpha$ -glucuronidase activity (14) was used to complete the synergism. The addition of  $\alpha$ -glucuronidase cleaved off 4-O-methylglucuronic acid and made the oligomers accessible for  $\beta$ -xylosidase and esterases. Using this mixture, the xylose yield was increased to the same value as that obtained with the whole culture filtrate.

## Conclusions

The xylanolytic enzyme system of *T. reesei* consists of several endoxy-lanases, at least three different exoglycosidases and at least two acetyl esterases. These enzymes contribute to the hydrolysis of plant cell walls in many of the applications of cellulolytic *T. reesei* enzyme preparations. A schematic figure of the suggested hydrolysis mechanism of xylans by the

Table IV. Enzymatic Hydrolysis of the High-Molecular Fraction of Steamed Birchwood Xylan. The substrate was fractionated by ultrafiltration prior to hydrolysis to remove impurities and the 1-5 DP oligosaccharides. Substrate concentration 10 gl<sup>-1</sup>, initial pH 5, temperature 45°C, hydrolysis time 24 h

Xylanase <sup>a</sup>	Enzyme Activities (nkat/g substrate)			Hydrolysis Products (% of substrate)	
	$\beta$ -Xylo- sidase <sup>b</sup>	Acetyl Esterase <sup>b</sup>	$\alpha$ -Glucuro- nidase	Xylose	Acetic Acid
12000	0	0	0	6	4.5
0	500	0	0	6	0.5
0	0	500	0	0	1.2
0	0	0	30 <sup>c</sup>	1	0.5
12000	500	0	0	25	5.9
12000	500	500	0	42	9.4
12000	500	500	30 <sup>c</sup>	53	11.5
15000 <sup>d</sup>	500 <sup>d</sup>	500 <sup>d</sup>	20 <sup>d</sup>	53	12.1

<sup>a</sup> Partly purified preparation fractionated from *T. reesei* culture filtrate by gel chromatography (10).

<sup>b</sup> Pure enzymes of *T. reesei*.

<sup>c</sup> *Agaricus bisporus* culture filtrate.

<sup>d</sup> *T. reesei* culture filtrate.

enzymes of *T. reesei* is shown in Figure 3. The hydrolysis starts by the action of endoxylanases, which decreases the average DP of the substrate. The side-group-cleaving enzymes have their highest activity towards soluble, short xylo-oligosaccharides, and the hydrolysis is completed by the synergistic action of both side-group and backbone-cleaving enzymes.

In addition to cellulolytic and xylanolytic enzymes the hydrolases produced by *T. reesei* have also been reported to include mannanase, pectinase, amyloglucosidase and protease (36,37). The present and potential applications of *T. reesei* enzymes include total hydrolysis of lignocellulosic materials to glucose and/or xylose, stimulation of germination in malting, more complete saccharification of cereals in grain alcohol production and improvement of the storage properties and digestibility of silage feed. In these applications synergism is needed not only between the individual xylanolytic or cellulolytic enzymes to hydrolyze xylan or cellulose, but probably also between different enzyme groups for successive hydrolysis of the plant cell wall matrix. Due to its versatility, *T. reesei* is an excellent source of enzymes in these cases. In applications where selective hydrolysis is required, however, the enzyme spectrum should be tailored for a particular purpose. This could be achieved by adjusting enzyme production conditions, by fractionating the enzymes or by molecular cloning.

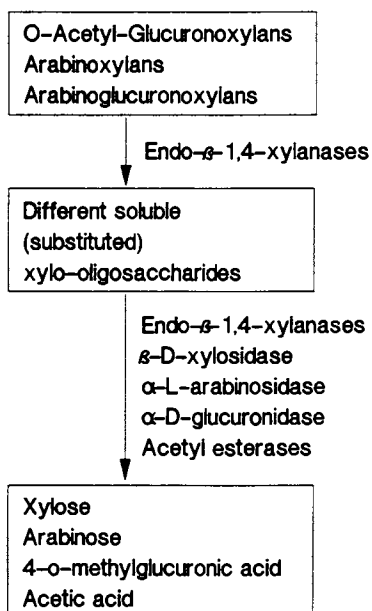


Figure 3. Tentative hydrolysis mechanism of different xylans by the xylanolytic enzymes of *T. reesei*.

## Literature Cited

1. Woodward, J. *Top. Enz. Ferment. Biotechnol.* 1984, **8**, 9-30.
2. Dekker, R. F. H. In *Biosynthesis and Biodegradation of Wood Components*; Higuchi, T., Ed.; Academic Press: Orlando, FL, 1985; p. 505.
3. Wong, K. K. Y.; Tan, L. U. L.; Saddler, J. N. *Microbiol. Rev.* 1988, **52**, 305-17.
4. Rodionova, N. A.; Tavobilov, I. M.; Bezborodov, A. M. *J. Appl. Biochem.* 1983, **5**, 300-12.
5. Matsuo, M.; Yasui, T. *Agric. Biol. Chem.* 1984, **48**, 1845-60.
6. Matsuo, M.; Fujie, A.; Win, M.; Yasui, T. *Agric. Biol. Chem.* 1987, **51**, 2367-79.
7. Marui, M.; Nakanishi, K.; Yasui, T. *Agric. Biol. Chem.* 1985, **49**, 3399-3407.
8. Fournier, R.; Frederick, M. M.; Frederick, J. R.; Reilly, P. J. *Biotechnol. Bioeng.* 1985, **27**, 539-46.
9. Wong, K. K. Y.; Tan, L. U. L.; Saddler, J. N. *Enz. Microb. Technol.* 1986, **8**, 617-22.
10. Lappalainen, A. *Biotechnol. Appl. Biochem.* 1986, **8**, 437-48.
11. Biely, P.; Puls, J.; Schneider, H. *FEBS Lett.* 1985, **186**, 80-84.
12. Biely, P.; MacKenzie, C. R.; Puls, J.; Schneider, H. *Bio/Technology* 1986, **4**, 731-33.
13. Puls, J.; Poutanen, K.; Schmidt, O.; Linko, M. *Proc. 3rd Intl. Conf. Biotechnol. in the Pulp and Paper Industry*; 1986, p. 93.
14. Puls, J.; Schmidt, O.; Granzow, C. *Enz. Microb. Technol.* 1987, **9**, 83-88.
15. Ishihara, M.; Shimizu, K. *Mokuzai Gakkaishi* 1988, **34**, 58-64.
16. Kaji, A. *Adv. Carbohydr. Chem. Biochem.* 1984, **42**, 383-94.
17. Andrewartha, K. A.; Phillips, D. R.; Stone, B. A. *Carbohydr. Res.* 1979, **77**, 191-204.
18. Tangnu, S. K.; Blanch, H. W.; Wilke, C. R. *Biotechnol. Bioeng.* 1981, **23**, 1837-49.
19. Dekker, R. F. H. *Biotechnol. Bioeng.* 1983, **25**, 1127-46.
20. Hrmova, M.; Biely, P.; Vrsanska, M. *Arch. Microbiol.* 1986, **144**, 307-11.
21. Sinner, M.; Dietrichs, H. H. *Holzforschung* 1975, **29**, 207-14.
22. Gibson, T. S.; McCleary, B. V. *Carbohydr. Polym.* 1987, **7**, 225-40.
23. Poutanen, K.; Rättö, M.; Puls, J.; Viikari, L. *J. Biotechnol.* 1987, **6**, 49-60.
24. Poutanen, K. Ph.D. Thesis, Technical Research Centre of Finland, Publications 47, Espoo, 1988.
25. Poutanen, K.; Puls, J. *Appl. Microbiol. Biotechnol.* 1988, **28**, 425-32.
26. Poutanen, K. *J. Biotechnol.* 1988, **7**, 271-82.
27. Poutanen, K.; Sundberg, M. *Appl. Microbiol. Biotechnol.* 1988, **28**, 419-24.
28. Ebringerova, A.; Kramav, A.; Rendos, F.; Domansky, R. *Holzforschung* 1967, **21**, 74-77.
29. Puls, J.; Poutanen, K.; Körner, H.-U.; Viikari, L. *Appl. Microbiol. Biotechnol.* 1985, **22**, 416-23.



30. Teeri, T. Ph.D. Thesis, Technical Research Centre of Finland, Publications 38, Espoo, 1987.
31. Biely, P.; Markovic, O. *Biotechnol. Appl. Biochem.* 1988, **10**, 99-106.
32. Esterbauer, H.; Hayn, M.; Tuisel, H.; Mahnert, W. *Holzforschung* 1983, **37**, 601-08.
33. Kolarova, N.; Farkas, V. *Biologia (Bratislava)* 1983, **38**, 721-25.
34. Sinner, M.; Dietrichs, H. H. *Holzforschung* 1976, **30**, 50-59.
35. Kusakabe, I.; Ohgushi, S.; Yasui, T.; Kobayashi, T. *Agric. Biol. Chem.* 1983, **47**, 2713-23.
36. Bailey, M. J.; Nevalainen, K. M. H. *Enzyme Microb. Technol.* 1981, **3**, 153-57.
37. Haltmeier, T.; Leisola, M.; Ulmer, D.; Waldner, R.; Fiechter, A. *Biotechnol. Bioeng.* 1983, **25**, 1685-90.

RECEIVED May 19, 1989

## Chapter 47

### Production and Purification of Xylanases

David J. Senior, Paul R. Mayers, and John N. Saddler

Biotechnology and Chemistry Department, Forintek Canada Corporation,  
800 Montreal Road, Ottawa, Ontario K1G 3Z5, Canada

Various groups have recently indicated that xylanase enzymes can be used to upgrade pulps. To be fully effective, it is essential that the enzymes are free of cellulase activity and have a high specific activity. Strategies followed to produce xylanases without contaminating cellulase activity include selective inactivation of the cellulase by heat and heavy metals and cloning of the xylanase gene into a cellulase-free host. We have shown that xylanase production by *Trichoderma harzanium* can be enhanced by selection of a suitable hemicellulase-rich growth substrate. A purified xylanase could be obtained by subsequent ultrafiltration and ion exchange treatment of the culture filtrate. Xylanase treatment of pulps could significantly decrease the xylan content while leaving the cellulose intact.

Xylanase production has been reported to occur in a wide spectrum of organisms. Although absent in vertebrate animals, xylanases are produced in many forms of bacteria, fungi and yeasts, crustaceans, algae and plant seeds. Current interest in xylanases has been focused primarily on the enzymes produced by fungi and bacteria and, to a lesser extent, yeasts. The high yields and relative ease of production have made these systems the most promising for future commercialization.

One of the major expenses incurred in the application of enzymes for bioconversion processes is the cost of enzyme production (1). The total cost of production includes the cost of fermentative production as well as downstream processing requirements. Both of these factors must be optimized and integrated for maximum cost-effectiveness.

Several different approaches have been followed to produce xylanases. Highest levels of extracellular xylanases have been produced in yeast and

0097-6156/89/0399-0641\$06.00/0

© 1989 American Chemical Society

fungal systems using xylan inducing growth substrates. In comparison, bacterial and cloned systems have produced moderate quantities of cellulase-free xylanases.

Two broad areas of application for xylanolytic enzymes have been identified (1). The first involves the use of xylanases with other hydrolytic enzymes in the bioconversion of wastes such as those from the forest and agricultural industries, and in the clarification and liquification of juices, vegetables and fruits. For these purposes, the enzyme preparations need only to be filtered and concentrated as essentially no further purification is required. Several specific examples of applications involving crude xylanase preparations include: bioconversion of cellulosic materials for subsequent fermentation (2); hydrolysis of pulp waste liquors; and wood extractives to monomeric sugars for subsequent production of single cell protein (3-5). Xylose produced by the action of xylanases can be used for subsequent production of higher value compounds such as ethanol (6), xylulose (7) and xylonic acid (8-9).

The second area of application involves the use of cellulase-free xylanases for removal of hemicellulose from pulps (10-20) and plant fibres (21). It is essential that these xylanase preparations are free of contaminating cellulase activity or damage to the cellulose fibres and consequently the product quality will result.

Here we examine the recent progress which has been made in the production and purification of xylanases.

### Xylanase Production by Yeasts

Biely *et al.* (22) have shown that xylanase production can be induced by use of appropriate substrates in the yeast *Cryptococcus albidus*. Wood xylans and xylan oligomers were found to increase extracellular xylanase production by two orders of magnitude when the yeast was grown on these materials rather than on a simple glucose medium. Xylobiose was identified as the only xylooligomer which was not degraded extracellularly and it was concluded that xylobiose is either a natural inducer of xylanase or its immediate precursor. Other xylopyranosides have also been investigated for their xylanase inducing potential in this yeast. Methyl- $\beta$ -D-xylopyranoside induced xylanase production at levels comparable to that obtained after growth on xylan (23). Morosoli *et al.* (24) demonstrated that the induction effect was manifested at the transcriptional level in this organism. Yasui *et al.* obtained a 15-20 fold greater increase in xylanase production using methyl- $\beta$ -D-xylopyranoside than when xylan was used as an inducer in *Cryptococcus flavus* (25). Leathers *et al.* (26) showed that xylose, xylobiose and arabinose were inducers of xylanases in *Aureobasidium pullulans*.

For xylanase applications which require xylanases of high selectivity (e.g., biopulping), any contaminating cellulases can be detrimental to the treatments. The constitutive levels of cellulases in yeasts is generally very low in relation to xylanase levels thus indicating yeast xylanase preparations are promising for the selective hydrolysis of xylans. However, extracellular yeast xylanases are typically produced in the order of 1 unit per millilitre

of culture filtrate, which is very low for cost-effective production. Recently, Leathers has reported the overproduction of a cellulase-free xylanase of very high specific activity from a colour variant strain of *A. pullulans* (27). The level of extracellular xylanase in the culture filtrate was 373 IU/mL which is comparable to the most prolific xylanase-producing fungal strains so far identified.

### Xylanase Production by Cloned Systems

Another alternative for production of cellulase-free xylanase preparations has been to clone the xylanase genes from xylanase producing bacteria. One xylanase producing strain, *Bacillus subtilis* PAP115, was chosen as a xylanase gene donor because of its relatively high level of extracellular xylanase production (0.9 IU/mL culture filtrate) and the thorough characterization of the enzyme (28). The gene was successfully inserted into *Escherichia coli* (WA802) and the xylanase produced was isolated and partially characterized. Only 25% of the original extracellular xylanase activity was recovered and this was localized within the cells (29). The same gene was inserted into *E. coli* JM105 and the new clones produced more xylanase than the original *Bacillus* (10). Unlike the first clone, about half of the xylanase activity was found extracellularly and yields were increased significantly.

Similar approaches to cloning of bacterial xylanases have been used for genes from *Clostridium acetobutylicum* (30), *Bacillus polymyxa* (31), *Bacteroides succinogenes* (32), *Clostridium thermocellum* (33) and *Pseudomonas fluorescens* subsp. *cellulosa* (34). In each case the xylanases were predominantly located intracellularly and the levels of xylanases produced from cloned systems were, in general, very low in comparison to yeast and fungal systems. A comparison of the production yields and extent of extracellular production for various cloned xylanase genes is found in Table I. Unlike most other cloned systems, the xylanase preparation from *B. succinogenes* was contaminated with cellulase activity.

Honda *et al.* have reported a xylanase gene from an alkalophilic *Bacillus* sp. C125 in *E. coli* (35-36). About 80% of the xylanase activity was secreted into the extracellular medium and the activity was slightly higher than that produced by the original *Bacillus* (approximately 0.6 IU/mL). A xylanase was produced from a xylanase gene cloned from alkalophilic *Aeromonas* sp. 212 at a level about 80 fold higher than in the original bacterium. Unfortunately, none of the enzyme was secreted extracellularly (37). Hammamoto and Horikoshi have recently succeeded in the construction of a secretion vector containing the xylanase gene from alkalophilic *Bacillus* sp. C125, which was then cloned into *E. coli* (38). Transformants which carried these genes secreted a significant amount of extracellular xylanase in comparison to clones which did not contain the secretion vector. It has been suggested that the secretion of the xylanase is directed by the characteristics of the protein itself. Future work may identify improvements to secretory sequences which will increase the extracellular quantities of xylanases from cloned systems.

Table I. Xylanases from Cloned Systems

Xylanase Gene Source	Enzyme Yield (IU/ml)	% Extracellular	Reference
<i>Aeromonas</i> sp. 212	1.63	0	(37)
<i>Bacillus polymyxa</i>	0.037	<10	(31)
<i>Bacillus subtilis</i>	0.5	0	(29)
<i>Bacillus subtilis</i>	2.2	50	(10)
<i>Bacillus</i> sp. C125	0.75	>70	(35-36)
<i>Bacillus</i> sp. C125 (secretion vector)	0.7	50	(38)
<i>Clostridium acetobutylicum</i>	64	0	(30)
<i>Clostridium thermocellum</i>	11.2	—	(33)
<i>Streptomyces lividans</i>	1200	100	(40)

Although most cloned xylanases are totally free from cellulase contamination, the recovery yields remain in general relatively low when compared to fungal systems. More effort in the areas of improved xylanase production yields and secretion may make the bacterial systems appear more promising for biotechnological applications. Recently an extracellular, cellulase-free xylanase enzyme was prepared by homologous cloning of a xylanase gene from *Streptomyces lividans* into a xylanase-cellulase-negative mutant of *S. lividans* (39). A considerable overproduction of this enzyme (up to 1200 IU/mL in the culture filtrate) has also been demonstrated when grown on xylan or hemicellulose-rich substrates (40).

### Fungal Xylanase Production

The use of filamentous fungi for production of xylanases was initially attractive because the enzymes are released extracellularly thus eliminating the need for cell lysis procedures. In addition, xylanase levels in fungal culture filtrates are typically in much higher concentrations than from yeasts and bacteria. Many examples of xylanases produced from fungi are listed in the review by Dekker (41).

It has been proposed that the production of xylanases and cellulases is under separate regulatory control in some filamentous fungi (1). Hrmova *et al.* (42) reached a similar conclusion after monitoring the daily production of these enzymes in *Trichoderma reesei* QM 9414. Xylanase and cellulase activities followed independent production profiles during fungal growth. The same effect has been observed in batch cultures of *T. harzianum*. We have observed peak xylanase activity on the third day of growth whereas the cellulase activity peaked after day five or six (unpublished).

There are many recent examples of xylanase induction in fungi grown on media containing xylan, hemicellulose-rich material and low molecular weight carbohydrates (42-66). It has generally been observed that higher

levels of xylanase are induced in systems containing higher xylan concentrations in the growth medium. A comparison of xylanase and cellulase production from various fungi is shown in Table II. Most cultures grown on xylan yielded higher levels of xylanase than when grown on similar concentrations of cellulose. With the exception of *Schizophyllum commune* (45), the highest production of xylanases by various species has been the result of growth on xylan. Although attempts have been made to standardize xylanase assays (67), some of the variation in enzyme activities reported must be attributed to variations in assay procedures among workers.

Using a xylan-free cellulose from *Acetobacter xylinum* as a growth substrate, Hrmova *et al.* demonstrated that small levels of constitutively produced xylanase could be attributed to cellulase activity in *T. reesei* QM9414 (42). As the concentration of xylan in the medium was increased, higher xylanase production resulted. Using a series of steam treated aspenwood samples, we have observed that the ratio of xylanase to cellulase activities produced on these materials increased directly with an increase in the ratio of xylan to cellulose in the medium (measured as xylan to glucan ratio) (Figure 1). Determination of these ratios for Avicel, Solka Floc and oat spelts xylan largely supported this relationship. Some deviation encountered between these growth substrates was likely due to variations in composition and accessibility of the substrate.

It is therefore apparent that with *Trichoderma* fungal systems, maximal levels of xylanases can be achieved by growing the cells in xylan containing media. The induction of xylanases in fungi grown on xylan medium, however, cannot be realized in all fungi with equivalent success. Unlike the level of xylanases induced in most fungi, the xylanase activity produced from *S. commune* grown on cellulose was unusually high (See Table II). Biely *et al.* (68) and Mackenzie and Bilous (69) have observed markedly higher production of xylanase in *S. commune* when grown on cellulose rather than on xylan.

The high cost of using purified xylans as substrates for xylanase induction are prohibitive for large-scale xylanase production. As an alternative, many groups have investigated the effectiveness of other hemicellulose-rich materials for this purpose. Examples of these include: agricultural wastes such as straws (2,45,47,50, 52,56,57,70,71), bran (47,56,57,60), sugar cane bagasse (57,61), corn cob and oak dust (70); pulp (2,45,52); pulp mill waste (3) and steam treated wood (53,59).

Alternative methods for more cost-effective xylanase production in fungi include the development of catabolite derepressed mutants, cellulase negative mutants, genetically engineered strains and high-xylanase-producing constitutive mutants. The latter case could afford high xylanase yields using soluble sugars as growth substrates which are both inexpensive and easy to handle in conventional fermentation equipment.

The vast majority of xylanases that have been produced are quite labile above 45-50°C. It would be of great advantage to employ xylanases which retain a high specific activity above this temperature range.

A number of thermostable xylanases have been prepared to varying

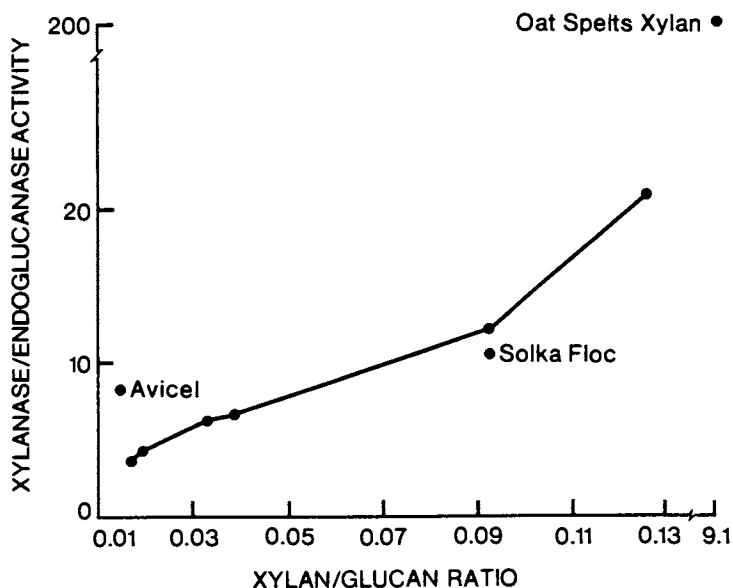


Figure 1. Induction of xylanases in *Trichoderma harzianum*. The ratios of xylanase to endocellulase activities were determined in the culture filtrates of *T. harzianum* grown on steam treated aspenwood. Aspen chips were steam treated from 20 to 240 s at 240°C to produce a series of samples with a variable content of xylan and cellulose. The specific content of these carbohydrates were expressed as the ratio of xylan to glucan. Enzyme activities were determined on culture filtrates of 300 mL batch cultures of *T. harzianum* grown on these wood samples at a loading of 1% (w/v) as described by Saddler and Mes-Hartree (66). Enzyme activities were also determined in culture filtrates of *T. harzianum* grown on Avicel, Solka Floc and oat spelts xylan.

Table II. Quantitative Comparison of Xylanase Activities<sup>a</sup> in Various Strains of Fungi

Source	Substrate	Incu- bation Time (Days)	Xylanase Activity (IU/ml)	Cellulase <sup>b</sup> Activity (IU/ml)	Ref.
<i>Agaricus bisporus</i>	Xylan(beechwood) 0.25%	14	0.22	— <sup>d</sup>	43
<i>Aspergillus awamori</i>	Wheat bran 3%	4	12	—	44
<i>Aspergillus niger</i>	Xylan(larchwood) 1%		4.8	—	60
<i>Aspergillus ochraceus</i>	Wheat bran 5% & xylan 0.2%	14	36.2	—	57
<i>Chaetomium cellulolyticum</i>	Xylan(larchwood) 1%	1	9.5	—	54
<i>Schizophyllum commune</i>	Avicel 4%	11	1244	65	45
	Xylan(larchwood) 1%	11	1.3	—	68
	Solka Floc 1%	11	44.6	—	68
<i>Thermonospora fusca</i>	Xylan(oat spelt) 1%	2-4	7.5	—	62
<i>T. curvata</i>	Xylan(oat spelt) 1%	2-4	8.8	—	62
<i>T. chromogena</i>	Xylan(oat spelt) 1%	2-4	1.3	—	62
<i>Trichoderma harzianum</i> E58	Xylan(larchwood) 1%	6	450	0.3	59
<i>Trichoderma longibrachiatum</i>	Solka Floc 1%	6	434	2.7	59
	Xylan 1%	12	17	—	49
<i>Trichoderma reesei</i> QM9414	Solka Floc 6%	4.6	130	—	44
	MCC <sup>c</sup> 1%	12	1.76	1.08	42
<i>T. reesei</i> QM9123	Xylan(beechwood) 1%	12	4.43	0.05	42
	Xylan(larchwood) 1%	5	22	0.12	51
	Xylan(larchwood) 1%	5	1.2-1.6	—	61
	Xylan(larchwood) 1%	6	3.1	—	68
	Solka Floc 1%	6	1.5	—	68
	Solka Floc 1%	7	2.7	10.3	50
<i>T. reesei</i> RUT30	Xylan 1%	7	6.7	9.7	50
	Xylan(larchwood) 1%	5	22	0.12	51
<i>T. reesei</i> C30	Solka Floc 1%	6	30	4.5	59
	Xylan 1%	6	230	0.4	59

<sup>a</sup> Activities determined in the culture filtrates.<sup>b</sup> Cellulase activity determined as activity on filter paper.<sup>c</sup> MCC = Microcrystalline cellulose.<sup>d</sup> Not determined.

American Chemical Society  
Library

1155 16th St., N.W.

Washington, D.C. 20036



degrees of purity using traditional purification techniques (72-81). A comparison of thermostable xylanase production in the culture filtrates from several sources is shown in Table III. One xylanase from *Clostridium stercorearium* demonstrated a half-life of 90 minutes at 81°C (73). The yields of thermostable xylanases in culture filtrates from various organisms have been generally quite low although levels up to 500 IU/mL have been observed with *Thermoascus aurantiacus* grown on xylan medium (74,75).

Table III. Comparison of Thermostable Xylanases from Various Sources

Xylanase Source	Half-Life at 80°C (min)	Xylanase Production (IU/ml)	Reference
<i>Bacillus stearothermophilus</i>	10-30	0.1	(72)
<i>Clostridium stercorearium</i> <sup>a</sup> A	90	56	(73)
<i>C. stercorearium</i> B	2.5	—	(73)
<i>C. stercorearium</i> C	8	—	(73)
<i>Thermoascus aurantiacus</i>	54	500	(74)
<i>Sporotrichum</i> sp.	8	0.92	(77)
<i>Humicola lanuginosa</i>	15	—	(78)
<i>Talaromyces byssochlamydoides</i>	—	1.7	(79)
<i>Thielavia terrestris</i>	—	18.5	(76)

<sup>a</sup> Half-life determined at 81°C.

### Purification of Xylanases: Focus on Application

The use of xylanases in the preparation of high-purity cellulosic materials requires that the enzyme preparations be free of any cellulase contamination. Treatments of pulps with xylanase preparations containing cellulases have resulted in damage to cellulose fibres as revealed by a drop in pulp viscosities (12,14,17). Similar pulp treatments in which cellulase-free xylanases were used resulted in increases in pulp viscosities (10,18,19). We have shown recently that an apparent increase in the degree of polymerization of cellulose treated with a cellulase-free xylanase is likely due to the selective removal of xylan, leaving an enriched cellulose residue (20).

Several methods to prepare high-purity xylanases for potential industrial applications have focused on eliminating the cellulase contamination instead of purifying the xylanase components. This appears to be a very effective approach as it precludes the need for very expensive biochemical procedures and focuses, rather, on a limited number of simple steps to eliminate cellulase activity. Since the remaining materials in the enzyme preparation are essentially inert with respect to the cellulose, their presence may often be ignored.

The preparation of xylanases from cloned systems has permitted production of cellulase-free xylanases. The xylanases produced from cloned

systems are largely intracellular and therefore must be released by disruption of the cellular membranes (10,29-31,33,34). In addition, enzyme yields in bacterial culture filtrates were generally much lower than those obtained using fungal systems. However, bacterial systems do offer the advantage that they require much shorter incubation periods for enzyme production. The recent development of a genetically engineered strain of *Streptomyces lividans* that produces an extremely high yield of extracellular, cellulase-free xylanase enzyme is likely to have a significant impact on the large-scale production of xylanases (40).

Using the high-xylanase producing filamentous fungus *Trichoderma harzianum* E58, Tan *et al.* have developed a procedure for the bulk purification of a cellulase-free endoxylanase of high specific activity (82,83). Typically  $7 \times 10^6$  units of xylanase activity can be obtained from a 17 L culture using a combination of ultrafiltration and ion exchange techniques. Gibson and McCleary have also described a more elaborate protocol for large-scale xylanase production from *Trichoderma viride* (84).

Selective inactivation of cellulase activities is another method which has been applied to fungal culture filtrates to produce cellulase-free xylanase preparations. Cellulase inactivation of a crude enzymatic complex was achieved by Barnoud *et al.* (15) using a 1 mM mercuric chloride solution. In the presence of this sulfhydryl binding metal, complete inactivation of endocellulases was observed whereas the xylanases retained 80% of their activity.

Many examples of the purification of xylanase enzymes to homogeneity can be found in the reviews of Dekker and Richards (85), Woodward (86) and Reilly (87). Other xylanases which have been prepared recently to very high purity using traditional biochemical techniques include xylanases from: *Sporotrichum dimorphosporum* (88); *Streptomyces* sp. (71); *Trichoderma harzianum* (5,55); *Clostridium acetobutylicum* (30,89); mesophilic fungal strain Y-94 (80); *Aspergillus niger* (90-92); and several thermostable xylanases discussed above.

Another method which may become a useful technique for selective inactivation of cellulases in enzyme mixtures is the use of selective heat inactivation. While establishing the thermostability properties of crude xylanases from a fungal strain Y-94, Mitsuishi *et al.* (80) observed differential heat labilities of the cellulase and xylanase activities in the culture filtrate. After an incubation period of 20 minutes at 65°C, the xylanase activity was reduced by 5-10% whereas the Avicelase and  $\beta$ -glucosidase activities were reduced by 100% and 60%, respectively. We have observed a similar temperature dependency of xylanase and cellulase activities in *T. aurantiacus*. As indicated in Figure 2, treatment of the culture filtrate at 70°C for 20 minutes resulted in less than a 5% loss in xylanase activity whereas cellulase activities were reduced by 40-50%. A similar effect has also been observed for the xylanases and cellulase enzymes produced in culture filtrates from *T. harzianum* (93). Further work in the area of heat treatments may improve the effectiveness of cellulase inactivation. Since the cellulase activities of some enzyme preparations can be more rapidly inactivated on

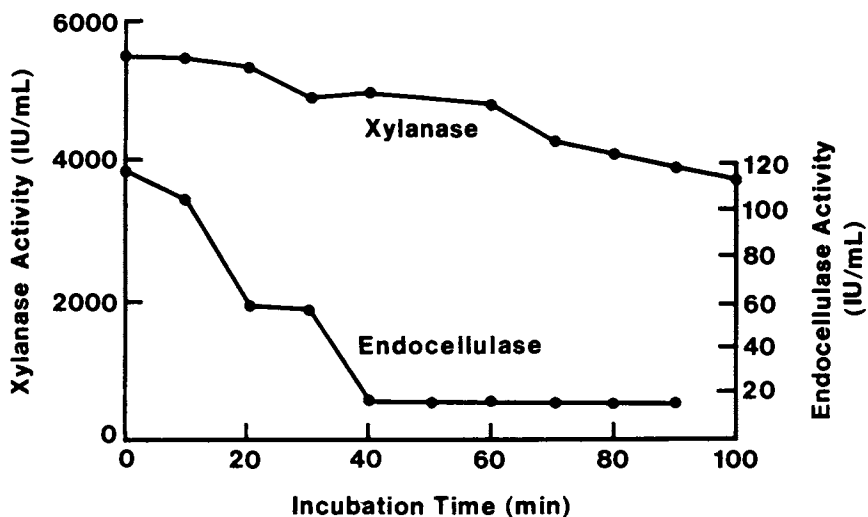


Figure 2. Heat inactivation profile of the xylanase in the culture filtrate from *Thermoascus aurantiacus*. Xylanase enzyme was prepared as described by Tan *et al.* (74). Xylanase and endocellulase activities were determined after the enzyme was incubated for the specified time at 70°C. Aliquots were removed and assayed at 50°C by the method described by Yu *et al.* (75). Activities were expressed as a percentage of the control stored at 4°C.

heating than the xylanase activities, it is possible that heat treatments may become a viable method for rapid and inexpensive purification of xylanases.

### Acknowledgments

The authors would like to thank C. M. Hogan for contributing to the xylanase induction work.

### Literature Cited

1. Biely, P. *Trends in Biotechnol.* 1985, **3**(11); 286-290.
2. Doppelbauer, R.; Esterbauer, H.; Steiner, W.; Lafferty, R. M.; Steinmuller, H. *Appl. Microbiol. Biotechnol.* 1987, **26**, 485-494.
3. Royer, J. C.; Nakas, J. P. *J. Ind. Microbiol.* 1987, **2**, 9-33.
4. Weckstrom, L.; Leisola, M. In *Fuels, Chemicals, Foods and Waste Treatment. Adv. in Biotechnology*; Moo-Young, M., Ed.; Pergamon Press: Toronto, 1981; **11**(4); 21-26.
5. Wong, K. K. Y.; Tan, L. U. L.; Saddler, J. N. *Can. J. Microbiol.* 1986, **32**, 570-576.
6. Skoog, K.; Hahn-Hagerdal, B. *Enz. Microbiol. Technol.* 1988, **10**, 66-80.
7. Pronk, J. T.; Bakker, A. W.; van Dam, H. H.; Straathof, A. J. J.; Scheffers, W. A.; van Dijken, J. P. *Enz. Microbiol. Technol.* 1988, **10**, 537-542.
8. Buchert, J.; Poutanen, K.; Puls, J.; Hukka, R.; Viikari, L. *Proceedings of the 4th European Congress on Biotechnology*; Neijssel, O. M.; van der Meer, R. R.; Luyben, K. Ch. A. M., Eds.; Elsevier Science Publ.: Amsterdam, 1987, p.281.
9. Buchert, J.; Puls, J.; Poutanen, K. *Appl. Microbiol. Biotechnol.* 1988, **28**, 367-372.
10. Paice, M. G.; Bernier, R., Jr.; Jurasek, L. *Biotechnol. Bioeng.* 1988, **32**, 235-239.
11. Joseleau, J.-P.; Gancet, C. *Svensk Papperstidn.* 1981, **84**, R123-127.
12. Paice, M. G.; Jurasek, L. *J. Wood Chem. Technol.* 1984, **4**(2), 187-198.
13. Mora, F.; Comtat, J.; Barnoud, F.; Pla, F.; Noe, P. *J. Wood Chem. Technol.* 1986, **6**, 147-165.
14. Noe, P.; Chevalier, J.; Mora, F.; Comtat, J. *J. Wood Chem. Technol.* 1986, **6**, 167-84.
15. Barnoud, F.; Comtat, J.; Joseleau, J. P.; Mora, F.; Ruel, K. *Biotechnology in the Pulp and Paper Industry*; Third International Conference, Stockholm, June 16-19, 1986; pp. 70-72.
16. Jurasek, L.; Paice, M. *Chemtech.* June 1986; 360-365.
17. Viikari, L.; Rauna, M.; Kantelinen, A.; Sundquist, J.; Linko, M. *Proceedings of the Third International Conference on Biotechnology in the Pulp and Paper Industry*; Stockholm, 1986; 67-69.
18. Chauvet, J.-M.; Comtat, J.; Noe, P. *Proceedings of the Paris Symposium on Wood and Pulping Chemistry*; May 1987; 325-327.
19. Jurasek, L.; Paice, M. G. *Biomass* 1988, **15**, 103-108.

20. Senior, D. J.; Mayers, P. R.; Miller, D.; Sutcliffe, R.; Tan, L. U. L.; Saddler, J. N. *Biotechnol. Lett.* 1988, **10**, 907-912.
21. Sharma, H. S. S. *Appl. Microbiol. Biotechnol.* 1987, **26**, 358-362.
22. Biely, P.; Kratky, Z.; Vrsanska, M.; Urmanicova, D. *Eur. J. Biochem.* 1980, **108**, 323-329.
23. Peciarova, A.; Biely, P. *Biochim. Biophys. Acta.* 1982, **716**, 391-399.
24. Morosoli, R.; Durand, S.; Letendre, E. D. *FEMS Microbiol. Lett.* 1987, **48**, 261-266.
25. Yasui, T.; Nguyen, B. T.; Nakanishi, K. *J. Ferment. Technol.* 1984, **62**(4), 353-359.
26. Leathers, T. D.; Detroy, R. W.; Bothast, R. J. *Biotechnol. Lett.* 1986, **8**(2), 867-872.
27. Leathers, T. D. *Appl. Env. Microbiol.* 1986, **52**, 1026-1030.
28. Bernier, R., Jr.; Desrochers, M.; Jurasek, L.; Paice, M. G. *Appl. Environ. Microbiol.* 1983, **46**(2), 511-514.
29. Bernier, R., Jr.; Driguez, H.; Desrochers, M. *Gene* 1983, **26**, 59-65.
30. Zappe, H.; Jones, D. T.; Woods, D. R. *Appl. Microbiol. Biotechnol.* 1987, **27**, 57-63.
31. Yang, R. C. A.; MacKenzie, R.; Bilous, D.; Seligy, V. L.; Narang, S. *Appl. Environ. Microbiol.* 1987, **54**(4), 477-481.
32. Sipat, A.; Taylor, K. A.; Lo, R. Y. C.; Forsberg, C. W.; Krell, P. J. *Appl. Environ. Microbiol.* 1987, **53**(3), 477-481.
33. Grepinet, O.; Cherbou, M.-C.; Beguin, P. *J. Bacteriol.* 1988; **170**, 4576-4581.
34. Gilbert, H. J.; Sullivan, D. A.; Jenkins, G.; Kellett, L. E.; Minton, N. P.; Hall, J. *J. Gen. Microbiol.* 1988, **134**, 3239-47.
35. Honda, H. T.; Kudo, T.; Horikoshi, K. *J. Bacteriol.* 1985, **161**, 784-785.
36. Honda, H. T.; Kudo, T.; Horikoshi, K. *Sys. Appl. Microbiol.* 1986, **8**, 152-157.
37. Kudo, T.; Ohkoshi, A.; Horikoshi, K. *J. Gen. Microbiol.* 1985, **131**, 2825-2830.
38. Hammamoto, T.; Horikoshi, K. *Agric. Biol. Chem.* 1987, **51**(11), 3133-3135.
39. Mondou, F.; Shareck, F.; Morosoli, F.; Kluepfel, D. *Gene* 1986, **49**, 323.
40. Bertrand, J.-L.; Morosoli, R.; Shareck, F.; Kluepfel, D. *Biotechnol. Bioeng.* 1989, **33**, 791-799.
41. Dekker, R. F. H. In *Biosynthesis and Biodegradation of Wood Components*; Higuchi, T., Ed.; Academic Press: Orlando, 1985; Ch. 18; p. 505-532.
42. Hrmova, M.; Biely, P.; Vrsanska, M. *Arch. Microbiol.* 1986, **144**, 307-311.
43. Puls, J.; Schmidt, O.; Granzow, C. *Enz. Microbiol. Technol.* 1987, **8**, 83-88.
44. Poutanen, K.; Ratto, M.; Puls, J.; Viikari, L. *J. Biotechnol.* 1987, **6**, 49-60.

45. Steiner, W.; Lafferty, R. M.; Gomes, I.; Esterbauer, I. G. H. *Biotechnol. Bioeng.* 1987, **XXX**, 169-178.
46. Vetter, J. *Acta Botanica Hungarica* 1986, **32**, 285-293.
47. Shamala, T. R.; Sreekantiah, K. R. *Enz. Micro. Technol.* 1986, **8**, 178-182.
48. Suh, D. H.; Becker, T. C.; Sands, J. A.; Montenecourt, B. S. *Biotechnol. Bioeng.* 1988, **32**, 821-825.
49. Thaker, A. J.; Ray, R. M.; Patel, H. C. *Ind. J. Exp. Biol.* 1986, **24**, 659-662.
50. Knapp, J. S.; Legg, M. *J. Appl. Bacteriol.* 1986, **61**, 319-329.
51. Chaudhary, K.; Tauro, P. *MIRCEN J.* 1986, **2**, 399-403.
52. Simionescu, CR. I.; Popa, V. I.; Rusan, M.; Vitalariu, C. *Bot. Soc. Brot.* 1986, **59**, 221-232.
53. Saddler, J. N.; Hogan, C. M.; Louis-Seize, G. *Appl. Microbiol. Biotechnol.* 1985, **22**, 139-145.
54. Dubeau, H.; Chahal, D. S.; Ishaque, M. *Biotechnol. Lett.* 1987, **9**(4), 275-280.
55. Tan, L. U. L.; Wong, K. K. Y.; Yu, E. K. C.; Saddler, J. N. *Enz. Microbiol. Technol.* 1985, **7**, 425-430.
56. Shamala, T. R.; Sreekantiah, K. R. *Enz. Microbiol. Technol.* 1987, **9**, 97-101.
57. Biswas, S. R.; Mishra, A. K.; Nanda, G. *Biotechnol. Bioeng.* 1988, **31**, 613-616.
58. Beldman, G.; Voragen, A. G. J.; Rombouts, F. M.; Searle-van Leeuwen, M. F.; Pilnik, W. *Biotechnol. Bioeng.* 1988, **31**, 160-167.
59. Saddler, J. N.; Chan, M. K. H.; Mes-Hartree, M.; Breuil, C. In *Biomass Conversion Technology, Principles and Practice*; Moo-Young, M., Ed.; Pergamon Press: Oxford, 1987; p.149-165.
60. Gokhale, D. V.; Puntambeker, V. S.; Deobagkar, D. N. *Biotechnol. Lett.* 1986, **8**(2), 137-138.
61. Dekker, R. F. H. *Biotechnol. Bioeng.* 1983, **XXV**, 1127-1146.
62. McCarthy, A. J.; Peace, E.; Broda, P. *Appl. Microbiol. Biotechnol.* 1985, **21**, 238-244.
63. MacKenzie, C. R.; Bilous, D.; Schneider, H.; Johnson, K. G. *Appl. Env. Microbiol.* 1987, **53**, 2835-2839.
64. Johnson, K. G.; Harrison, B. A.; Schneider, H.; MacKenzie, C. R.; Fontana, J. D. *Enz. Microbiol. Technol.* 1988, **10**, 403-409.
65. Rho, D.; Desrochers, M.; Jurasek, L.; Driguez, H.; Defaye, J. *J. Bacteriol.* 1982, **149**, 47-53.
66. Saddler, J. N.; Mes-Hartree, M. *Biotech. Adv.* 1984, **2**, 161.
67. Ghose, T. K.; Bisaria, U. S. *Pure Appl. Chem.* 1987, **59**, 1739-1752.
68. Biely, P.; MacKenzie, C. R.; Schneider, H. *Can. J. Microbiol.* 1988, **34**, 767-772.
69. MacKenzie, C. R.; Bilous, D. *Appl. Env. Microbiol.* 1988, **54**, 1170-1173.
70. Vetter, J. *Acta Bot. Hungarica* 1986, **32**, 285-293.

71. Nakajima, T.; Tsukamoto, K. I.; Watanabe, T.; Kainuma, K.; Matsuda, K. *J. Ferment. Technol.* 1984, **62**, 269-276.
72. Gruninger, H.; Fiechter, A. *Enz. Microbiol. Technol.* 1986, **8**, 309-314.
73. Berenger, J.-F.; Frixon, C.; Bigliardi, J.; Creuzet, N. *Can. J. Microbiol.* 1985, **31**, 635-643.
74. Tan, L. U. L.; Mayers, P.; Saddler, J. N. *Can. J. Microbiol.* 1987, **33**, 689-692.
75. Yu, E. K. C.; Tan, L. U. L.; Chan, M. K.-H.; Deschatelets, L.; Saddler, J. N. *Enz. Microbiol. Technol.* 1987, **9**, 16-24.
76. Merchant, R.; Merchant, F.; Margaritis, A. *Biotechnol. Lett.* 1988, **10**, 513-516.
77. Dubey, A. K.; Johri, B. N. *Proc. Ind. Acad. Sci. (Plant Sci.)* 1987, **97**(3), 247-258.
78. Kitpreechanavich, V.; Hayashi, M.; Nagai, S. *J. Ferment. Technol.* 1984, **62**(1), 63-69.
79. Yoshioka, H.; Nagato, N.; Chanavick, S.; Nilubol, N.; Hayashida, S. *Agric. Biol. Chem.* 1981, **45**, 2425-2432.
80. Mitsuishi, Y.; Yamanobe, T.; Yagisawa, M.; Takasaki, T. *Agric. Biol. Chem.* 1987, **51**(12), 3207-3213.
81. Grajek, W. *Biotechnol. Lett.* 1987, **9**(5), 353-356.
82. Tan, L. U. L.; Yu, E. K. C.; Louis-Seize, G. W.; Saddler, J. N. *Biotechnol. Bioeng.* 1987, **XXX**, 96-100.
83. Tan, L. U. L.; Saddler, J. N.; Yu, E. K. C. U.S. Patent Application Ser. No. 856,934, Granted February, 1988.
84. Gibson, T. S.; McCleary, B. V. *Carbohydr. Pol.* 1987, **7**, 225-240.
85. Dekker, R. F.; Richards, G. N. *Adv. Carb. Chem. Biochem.* 1976, **32**, 277-352.
86. Woodward, J. *Top. Enz. Ferment. Biotechnol.* 1984, **8**, 9-30.
87. Reilly, P. J. In *Trends in Biol. of Fermentations for Fuel and Chemistry*; Hoellaender, A., Ed.; Plenum Press: New York, 1981, p. 111-129.
88. Comtat, J. *Carbohydr. Res.* 1983, **118**, 215-231.
89. Lee, S. F.; Forsberg, C. W.; Rattray, J. B. *Appl. Env. Microbiol.* 1987, **53**(4), 644-650.
90. Fournier, R. A.; Fredrick, M. M.; Fredrick, J. R.; Reilly, P. J. *Biotechnol. Bioeng.* 1985, **XXVII**, 539-546.
91. Shei, J. C.; Fratzke, A. R.; Fredrick, M. M.; Fredrick, J. R.; Reilly, P. J. *Biotechnol. Bioeng.* 1985, **XXVII**, 533-538.
92. Frederick, M. M.; Kiang, C.-H.; Frederick, J. R.; Reilly, P. J. *Biotechnol. Bioeng.* 1985, **27**, 525-532.
93. Todorovic, R.; Matavulj, M.; Grujic, S.; Petrovic, J. *Mikrobiologija.* 1986, **23**(1), 33-38.

RECEIVED April 17, 1989

## Author Index

- Atkey, P. T., 426  
Barber, M. S., 361  
Bertram, R. E., 361  
Blanchette, Robert A., 544  
Bokelman, Gordon H., 68,169,278,300  
Bonner, Carol, 89  
Bouchard, J., 529  
Bourbonnais, R., 472  
Brisson, Louise, 122  
Brummell, David A., 18  
Catesson, Anne-Marie, 193  
Chornet, E., 529  
Claeyssens, M., 570  
Cowles, Joe R., 203  
Cui, Futong, 519  
Dantzig, Anne H., 399  
Dekker, Robert F. H., 619  
Deschamps, A. M., 619  
Devillers, Paulette, 312  
Dolphin, David, 519  
du Penhoat, Catherine Herve', 312  
Evans, C. S., 426  
Ferrantello, Lisa M., 214  
Ferry, Mark L., 544  
Ford, Clive W., 137  
Francesch, Charlette, 193  
Fraser, M. A., 426  
Frost, D. J., 248  
Fry, Stephen C., 33  
Fukazawa, Kazumi, 47  
Fukushima, K., 160  
Gallagher, I. M., 426  
Garbow, Joel R., 214  
Gaudillere, Monique, 182  
Gilkes, N. R., 587  
Giroux, H., 529  
Goldberg, Renée, 193, 312  
Gross, Georg G., 108  
Haemmerli, Stephan D., 454  
Harada, Hiroshi, 47  
Hartley, Roy D., 137  
Hattori, Takefumi, 412  
Heriban, V., 570  
Higuchi, Takayoshi, 412, 482, 503  
Hotchkiss, Jr., Arland T., 232  
Ibrahim, Ragai, 122  
Itoh, Takao, 257  
Jahn, G., 203  
Jensen, Roy A., 89  
Joseleau, Jean-Paul, 443  
Kilburn, D. G., 587  
Krakow, William, 278  
Kurosaka, Hiroshi, 412  
Lamy, F., 529  
Latchinian, Lilian, 122  
LeMay, R., 203  
Leisola, Matti S. A., 454  
Lewis, Norman G., 68, 169  
Lovrien, Rex E., 544  
Lynch, J. M., 608  
Maclachlan, Gordon A., 18  
Magnuson, Timothy S., 544  
Mason, T. L., 248  
Mayers, Paul R., 641  
Meijer, Emmo M., 454  
Midhon, Véronique, 312  
Miller, Jr., R. C., 587  
Miller, Janice G., 33  
Moerschbacher, Bruno M., 370  
Monties, Bernard, 182  
Morris, Paul, 89  
Morvan, Claudine, 312  
Northcote, D. H., 1  
Ohta, Akira, 412  
Overend, R. P., 529  
Paice, Michael G., 472  
Pang, An, 193  
Pearce, R. B., 346  
Peterson, C., 203  
Poutanen, Kaisa, 630  
Prat, Roger, 312  
Puls, Jurgen, 630  
Razal, Ramon A., 169  
Read, S. M., 248



- Ride, J. P., 361  
 Rinaudo, M., 324  
 Rolando, Christian, 193  
 Ruben, George C., 278, 300  
 Ruel, Katia, 443  
 Saddler, John N., 641  
 Sanglard, Dominique, 454  
 Scheld, W. H., 203  
 Schmidt, Harald W. H., 454  
 Schoemaker, Hans E., 454  
 Senior, David J., 641  
 Shibuya, Naoto, 333  
 Shimada, Mikio, 412  
 Slay, R. M., 248  
 Spencer, Paul A., 383  
 Stark, Ruth E., 214  
 Street, Ian P., 597  
 Takabe, Keiji, 47  
 Takahashi, Munezoh, 412  
 Terashima, Noritsugu, 148, 160  
 Tomme, P., 570  
 Towers, G. H. N., 383  
 Umezawa, Toshiaki, 503  
 Van Tilbeurgh, H., 570  
 Vidal, P. F., 529  
 Waldner, Roland, 454  
 Warren, R. A. J., 587  
 Wasserman, B. P., 248  
 Watada, A. E., 248  
 Withers, Stephen G., 597  
 Wood, D. A., 426  
 Wooten, Jan B., 169  
 Yamamoto, Etsuo, 68, 169  
 Zamir, Lolita O., 89  
 Zlotnik-Mazori, Tatyana, 214

## Affiliation Index

- AFRC Institute of Horticultural Research, 426,608  
 BFI, Institute of Wood Chemistry, 630  
 Biomembranes et Surfaces Cellulaires Végétales, ENS, 193,312  
 Centre de Recherches sur les Macromolécules Végétales, 443  
 Centre National de la Recherche Scientifique, 324  
 City University of New York, 214  
 Commonwealth Scientific and Industrial Research Organisation, 137,619  
 Concordia University, 122  
 Dartmouth College, 278,300  
 DSM Research, 454  
 Eli Lilly and Company, 399  
 Forintek Canada Corporation, 641  
 Givaudan Forschungsgesellschaft AG, 454  
 Hokkaido University, 47  
 IBM, 278  
 Institut National Agronomique Paris-Grignon, 182  
 Institut für Biologie III (Pflanzenphysiologie) der RWTH Aachen, 370  
 Kasetsart University, 47  
 Kyoto University, 257,412,482,503  
 Laboratoire de l'Activation Moléculaire, ENS, 193  
 McGill University, 18  
 Ministry of Agriculture, Forestry, and Fisheries, 333  
 Monsanto Company, 214  
 Nagoya University, 148,160  
 National Research Council of Canada, 529  
 New Jersey Agricultural Experiment Station, 248  
 Philip Morris USA, 68,169,278,300  
 Pulp and Paper Research Institute of Canada, 472  
 Rutgers University, 248  
 SCUEOR, Faculté des Sciences de Rouen, 312  
 Service RMN-ENS, 312  
 Shiga Forest Research Center, 412  
 State University of Ghent (RUG), 570  
 Swiss Federal Institute of Technology, 454  
 Thames Polytechnic, 426  
 U.S. Department of Agriculture, 137,232,248  
 Universität Ulm, 108  
 Université de Bordeaux I, 559  
 Université du Québec, 89  
 University Joseph Fourier of Grenoble, 324  
 University of Birmingham (England), 361  
 University of British Columbia, 383,519,587,597  
 University of Cambridge, 1  
 University of Edinburgh, 33  
 University of Florida, 89  
 University of Houston, 203  
 University of Minnesota, 544  
 University of Oxford, 346  
 University of Sherbrooke, 529  
 Virginia Polytechnic Institute and State University, 68,169  
 VTT, Biotechnical Laboratory, 630

## Subject Index

## A

## Acetate

- carbon source for fungi, 400
- effect on cutinase production, 400

*Acetobacter xylinum*

- cellulose formation, 278–279
- imaging of cellulose ribbon, 281
- sample preparation, 279

## Acetophenones, 386–388f

## Acetosyringone

- effect on transformation efficiency, 384–385
- signal compounds from tobacco tissues, 384

## Acetyl bromide lignin, contents in fescue, 184,185t

## Acetyl esterase, properties, 632t

*O*-Acetylglucuronoxylan,

- hydrolysis products, 634,635f

## Acid-precipitable polymeric lignin

- amino acid compositions of associated proteins, 535t,536
- characterization of polyphenolic fraction, 539t,542t,543
- crude analysis, 534–536
- effect of DNA growth on production, 530,533f
- effect of glucose on production, 530,531f
- effect of hydrogen peroxide on production, 534t
- effect of yeast extract on production, 530,532f
- elemental analysis, 534,535t
- formation, 529
- dissociation of the protein–polyphenolic complex, 539,541f
- FTIR spectra, 536,537–538f
- FTIR spectral analysis, 536t
- methoxyl group quantification, 534,535t
- molecular weight distributions, 536,539,540f
- production by secreted proteins and bacterial extracts, 530,534t

## Acidic polysaccharides, 34

## Affinity chromatographic method, purification of cellulolytic enzymes, 576,579f

*Agrobacterium tumefaciens*–plant interactions, signal compounds, 384Aminooxyacetic acid, inhibition of phenylalanine ammonia-lyase, 374  
(1-Amino-2-phenylethyl)phosphonic acid, inhibition of phenylalanine ammonia-lyase, 374

## Anisyl alcohol

- oxidation, 520
- oxidation in presence of 1,4-dimethoxybenzene, 523,525f
- oxidation in presence of veratryl alcohol, 523,525t

## Antimicrobial defense in plants, 346

## Arabinogalactoglucuronoxylan, possible structure of oligosaccharides obtained by partial acid hydrolysis, 343t

 $\alpha$ -Arabinosidase

- effect on hydrolysis of wheat straw arabinoxylan, 632,634t
- properties, 632t

## Arabinoxylan

- detailed structure of side chains, 340–343
- hydrolysis products, 634,635f

## L-Arogenate, synthesis, 89,90f,91

## Arogenate dehydrogenase

- activity, 96
- physiological manipulation, 104f,105

## Arogenate route, phenylalanine biosynthesis, 96

## Aromatic amino acid biosynthesis in higher plants

- alternative phenylpyruvate and arogenate routes to phenylalanine, 93
- demonstration approaches for intact cytosolic pathway, 93
- enzyme assays, 94
- existing case of intact cytosolic pathway, 91,92–93t
- maintenance of amino acid pool, 91

- Aromatic amino acid biosynthesis in higher plants—*Continued*  
 manipulation of isozyme expression by environmental treatments, 99,102f,103r,105  
 mechanism for shuttling of intermediates, 89,90f,91  
 pathway with triose—phosphate species, 99,101f  
 physiological manipulation by isozyme expression, 104f,105  
 protease removal, 94  
 reactions catalyzed by DAHP synthase—Co, 99,100f  
 solubilization of membrane proteins, 93–94  
 Aromatic monoacyl esters, biosynthesis by acyltransferases, 113,115r  
 Aromatic pathway enzymes, response to mechanical wounding, 103r,105  
 Aromatic ring cleavage by intact cells of white-rot basidiomycetes, product identification, 504,505f  
 Aromatic ring cleavage by laccase, phenolic  $\beta$ -O-4 substructure model compounds, 493,497–498f  
 Aromatic ring cleavage by lignin peroxidase artificial lignin, 493,499,500f  
 dehydrogenation  
 polymer, 511,513,514–516f  
 $^{18}\text{O}$  incorporation into enzymatic ring cleavage products, 506,509f  
 ( $\beta$ -O-4)—( $\beta$ -O-4) lignin substructure model trimer, 506,511,512f  
 $\beta$ -O-4 lignin substructure model dimers, 504,506–512  
 $\beta$ -O-4 model compounds, 493,494–495f  
 proposed mechanism, 506,510f  
 veratryl alcohol, 493,495–496f  
 Aromatic ring cleavage by white-rot basidiomycetes, monomeric aromatic compounds, 513  
 Assembly of cellulose, terminal complex hypothesis, 232–234  
 Auxin, effect on xyloglucan, 26–27
- B**
- Bacterial degradation, condensed tannins, 562,564  
 Bacterial degradation of kraft lignin acid-precipitable polymeric lignin production, 530,531–533f  
 bacterial growth, 530,531–533f  
 Bacterial degradation of kraft lignin—*Continued*  
 characterization of polyphenolic fraction, 539r,542r,543  
 crude acid-precipitable polymeric lignin analysis, 534–536  
 dissociation of protein—polyphenolic complex, 539,541f  
 experimental procedure, 529–530  
 separation of bacterial extracellular, membranous, and cytosolic proteins, 530,534r  
 Bacterial growth, effect on acid-precipitable polymeric lignin production, 530,533f  
 Bark tissue, defense, 350–355  
 Basidiomycete(s), preference for nitrogen-poor wood substrates, 413  
 Basidiomycete fungi, role in biodegradation of wood, 426  
 Binding, cellulolytic enzymes, 582  
 Binding of several chromophoric ligands to cellulolytic enzymes, measurement, 571  
 Binding protein—enzyme complex binding mechanism, 7–8  
 examples, 7  
 Biochemical significance, phenylalanine—cinnamate pathway in plants and fungi, 418–419  
 Biodegradability  
 phenolic acids, 140,142  
 phenolic aldehydes, 140,142  
 Biodegradation of hetero-1,4-linked xylans, 619–627  
 Biodegradation of heteroxylans enhancement by  $\beta$ -xylosidases, 627  
 pathways of microbial xylanases, 626–627  
 Biodegradation of lignocellulosic materials, role of secondary metabolism, 412–423  
 Biogenesis of *Chrysosplenium* flavonoids  
 electron microscopy, 132,133f  
 immunocytochemistry, 133f,134  
 immunofluorescence, 132,133f,134  
 localization studies, 132  
 mechanism, 124–127f  
 regulation, 131–132  
 Biomimetic studies in lignin degradation experimental procedures, 519  
 oxidation of anisyl alcohol, 523,525r  
 oxidation of veratryl alcohol, 522–523r  
 Biosynthesis of digalloylglucose, mechanism, 115,116r,117f  
 Biosynthesis of ellagitannins, mechanism, 118

- Biosynthesis of gallic acid,  
  pathways, 110–111,112f
- Biosynthesis of gallotannins, mechanism, 118
- Biosynthesis of  $\beta$ -glucogallin  
  formation, 113,114f  
  formation of pentagalloylglucose, 113–117  
  galloyl coenzyme A, 111,112f,113  
  mechanism, 113  
  phenolic acid esters formed, 111t
- Biosynthesis of lignin with cell organelle  
  identification of cell organelle  
    involved, 63  
  tracheid after S<sub>3</sub> stage, 63,64f  
  tracheid in S<sub>2</sub> stage, 63,64f
- Biosynthesis of *E*-monolignols,  
  pathways, 170–171,172f
- Biosynthesis of polysaccharides with cell  
  organelle  
  elucidation of pathway, 57  
  study by cytochemical staining  
    methods, 60,62f  
  tracheid in S<sub>3</sub> stage, 60,61f
- Boergeria forbesii*  
  immunofluorescence micrographs in  
    aplanospore, 271,273f  
  immunofluorescence micrographs of  
    microtubule orientation,  
    267,268–270f,272,272f
- Bomb combustion calorimetry,  
  description, 544–545
- Bran arabinoxylan  
  detailed structure of side chains, 340–343  
  proposed structure of trisaccharide and  
    fragmentation pattern, 340,342f,343  
  saccharide obtained by partial acid  
    hydrolysis, 340,341f
- Brown-rot fungi  
  phenylalanine–cinnamate pathway, 413,414f  
  production of secondary  
    metabolites, 413,416t  
  relationship among secondary metabolite  
    production, consumption of N and C  
    sources, and growth of  
    fungus, 413,415f,416
- Building units of lignin  
  formation, 10  
  polymerization, 10–11
- C
- Calcium interaction with pectins  
  degree of neutralization, 325–327  
  degree of pectin esterification, 326
- Calcium interaction with pectins—  
  *Continued*  
  degree of polymerization, 325–327  
  pectin carboxyl group distribution, 326  
  pectin chemical structure, 324–331
- Calcium content  
  effect on pectin intrinsic  
    viscosity, 329f,331  
  effect on pectin molecular  
    weight, 326,328f, 331
- Carbohydrates, effect on dehydrogenative  
  polymerization of monolignols, 155,156t
- Carbon types  
  composition in cutin, 220,223t  
  composition in suberin, 223,226t  
  quantitation, 217
- Carboxyl group distribution, effect on  
  calcium activity, 326
- Catechin, microbial degradation, 564
- Cell death  
  definition, 373  
  inhibition, 374–375  
  lignification as mechanism, 373–375  
  suicide inhibitors, 374
- Cell growth  
  requirement, 38  
  role of pectin, 300–301
- Cell organelle  
  biosynthesis of lignin, 63,64f  
  biosynthesis of poly-  
    saccharides, 57,60,61–62f
- Cell organelle during cell wall formation  
  changes in structure, 57,59f  
  semiquantitative measurements in  
    cytoplasm, 56–57,58f
- Cell wall  
  composition, 2  
  control of polysaccharide synthesis and  
    deposition during growth, 2–8  
  establishment of cross linkages, 11  
  factors influencing developmental  
    control, 2  
  formation, 2  
  isolation from different parts of rice  
    grains, 334,335f  
  phenylpropanoid metabolism, 68–85  
  proteins, 11–12
- Cell wall alterations  
  defense in gymnosperms, 350–354  
  defense in preexisting xylem, 356,358  
  defense in woody angiosperms, 353  
  effect on structural defense mechanisms in  
    plants, 348–349  
  histochemical responses, 350,351t

- Cell wall alterations—*Continued*  
 response to fungi invasion, 361  
 suitability to long-term defense in plants, 358–359
- Cell wall components in conifer tracheids, deposition, 47–64
- Cell wall extensibility, control by pectins, 312
- Cell wall formation, changes in cell organelle, 56–57,58–59f
- Cell wall isozymes, oxidative activities, 195,196f,197,198f
- Cell wall plasticity—pectin property relationship  
 cation-exchange capacity of cell walls vs. pH, 318,319f  
<sup>13</sup>C NMR spectra of pectin fractions, 316,317f, 318  
 composition of pectin fractions extracted from cell walls, 314,316f  
 experimental procedure, 313  
 growth gradient along mung bean hypocotyl, 314,315f  
 physicochemical properties of pectins, 318–321f,322z  
 selectivity coefficients of cell walls, 318,321f  
 water content of cell walls, 318,322z
- Cell wall polymer(s)  
 identification of changes, 333  
 summary of changes in rice grain, 344
- Cell wall polymer phenolic cross-linking, *See* Phenolic cross-linking in cell walls
- Cell wall preparations from rice grains  
 comparison of overall composition, 334,336z,337  
 detailed structure of side chains of bran arabinoxylan, 340,341–342f,343z  
 monosaccharide composition, 334,336z,337  
 scanning electron micrograph, 334,335f  
 structure of hemicellulosic polysaccharides, 337–340
- Cellobiose quinone oxidoreductase, lignin catabolism, 473
- Cellobioses, degradation of cellulose to glucose, 587
- Cellulase(s)  
 classification, 540–571  
 cloning of structural genes, 588  
*See also* Cellulolytic enzymes
- Cellulase(s) of *Cellulomonas fimi*  
 cellulase profile, 588  
 comparison of native and recombinant forms, 588,590,591f
- Cellulase(s) of *Cellulomonas fimi*—*Continued*  
 composition, 588  
 interactions with cellulose, 590,592–595  
 schematic representation of fusion protein structure, 590,594f  
 schematic representation of protease cleavage, 590,593f  
 similarity to *Trichoderma reesei* cellulases, 588  
 structures, 588,589f  
 time course of proteolysis, 590,592f
- Cellulase(s) of *Trichoderma reesei*, similarity to *Cellulomonas fimi* cellulases, 595
- Cellulase-free endoxylanase  
 bulk purification, 649  
 selective heat inactivation, 649,650f,651  
 selective inactivation of cellulase activities, 649
- Cellulase-free xylanases, production, 648–649
- Cellulolytic enzymes  
 activity measurements in solution, 572,574f  
 affinity chromatographic method for purification, 576,579f  
 analytical isoelectric focusing, 571–572,573f  
 binding, 582  
 binding constant  
 determination, 576,577–578f  
 binding experiments, 572,575f,576,577–578f  
 continuous assays, 571,572z  
 detection of activities in gels, 571,572z,573f  
 experimental procedures, 571  
 model structure, 580,581f  
 quenching of fluorescence spectrum, 572,575f,576  
 residual activities, 580,581f  
 structural–functional investigations based on partial proteolysis and physical measurements, 576  
 synergism, 582,583f,584  
*See also* Cellulase(s)
- Cellulomonas fimi*, cellulases, 588–595
- Cellulose  
 assembly, 232–234  
 description, 232  
 elucidation of biosynthetic pathway, 57  
 formation of *Acetobacter xylinum*, 278–279

- Cellulose—*Continued*  
interactions with *Cellulomonas fimi*  
cellulases, 590,592–595  
role of  $\beta$ -glucosidases in degradation, 597  
study of cellulases, 570
- Cellulose biodegradation, role of  
enzymes, 587–588
- Cellulose biosynthesis  
alteration, 240–242  
effects of noncellulosic cell wall  
polysaccharides, 241–242  
molecular genetics, 242–243  
role of terminal complexes, 232–243
- Cellulose microfibrils  
E-fracture face, 263,264f  
helical arrangement, 275  
methods for biogenesis studies, 257
- Cellulose ribbon from *Acetobacter xylinum*  
effect of Tinopal, 281  
gel deposited during normal  
growth, 281,282f  
imaging, 281
- Cellulose structure  
chain polarity, 238  
crystal structure, 237  
effect of source and developmental  
stage, 237  
forms of native polymorph, 238–239  
techniques for determination, 238
- Cellulose synthase, in vitro  
activity, 239–240
- Cereal grains, stages of differentiation in  
cell walls, 333–334
- Chalcone derivatives  
activity, 386,388f  
structure, 386,387f
- Chalcone synthase, description, 95
- Chemical structure, heteroxylans, 620–621
- Chemical structure of pectins, effect on  
interactions with calcium, 324–331
- Chitin  
elicitor of lignification, 364–365,375  
properties, 364
- Chitin oligomer  
signal for fungi  
recognition, 365,366f,367  
wheat germ agglutinin as receptor, 365
- Chitinase activity, detection, 615
- Chorismate mutase isozymes, differential  
properties, 92,93t
- Chrysosplenium* flavonoids  
biogenesis, 124,127f  
methylation–glucosylation  
sequence, 124–134
- Cinnamic acid, dimerization, 142
- Cinnamic acid 4-hydroxylase, activity during  
lignin biosynthesis, 372
- Cinnamyl alcohols, production, 10
- Citrus pectin  
micrograph of gel, 307,309f  
preparation, 304
- Cloned systems, xylanase  
production, 643,644t
- Commercial synthetic substrates, inhibition  
with salts from ferulic and  
 $\beta$ -fluoroferulic acids, 197,199
- Condensed tannins  
description, 108,559–560  
microbial degradation, 562,563f,564
- E-Coniferin, structure, 74–76
- Constitutive structural defenses of plants  
interxylary periderm, 349–350  
role of surface periderms, 349
- Cortical microtubules  
effect on orientation of  
microfibrils, 267  
immunofluorescence micrographs of  
microtubular orientation, 267–273  
orientation, 263,267–273
- 4-Coumarate:CoA ligase, activity  
during lignin biosynthesis, 372–373
- p-Coumaric acid  
chemical nature of ester linkages, 71  
structure, 71–72
- p-Coumaric acid–p-coumaric acid  
amounts in cell walls of tropical  
grasses, 142  
identification, 142  
structure, 142–143
- O-[5-O-(trans-p-Coumaroyl)- $\alpha$ -L-  
arabinofuranosyl]-(1–3)-O- $\beta$ -D-  
xylopyranosyl-(1–4)-D-xylopyranose,  
structure, 71–72
- Covalently linked hydroxycinnamic acids,  
function, 68
- Cross linkages in cell wall,  
establishment, 11
- Cross-polarization magic-angle spinning  
(CPMAS)  
determination of polymer dynamics, 217  
experimental procedure, 216–217  
isolation of biopolyesters, 216  
molecular structure studies, 228  
quantitation carbon types, 217  
spectra for suberin, 223,225f  
spectrum for cutin, 217,219f  
structural studies of solid polymers and  
biopolymers, 214

## Cutin

- chemical shifts, 217,218
- composition of carbon types, 220,223
- CPMAS spectrum, 217,219
- cross-polarization dynamics, 227-228
- cutin-wax interactions, 223,224
- depolymerization residue, 220,222f,223
- determination of dynamics, 214
- features of molecular structure, 227
- function, 399
- isolation, 216
- molecular model, 220,221f
- schematic representation, 214, 215f
- spin-relaxation times, 217,220
- structural characterization, 216

## Cutinase

- effect of acetate on production, 400
- effect of cutin addition on
  - induction, 402,405f
- effect of glucose on production, 400
- effect of growth conditions on synthesis
  - by *Fusarium solani*, 407
- function, 399-400
- kinetics of specific activity, 402,406f
- pathogenesis, 407
- regulation, 400
- separated <sup>35</sup>S-labeled extracellular
  - protein from cutin induction
    - medium, 402,407,408f
- specific activity vs. sole carbon source
  - in growth medium, 400,401f
- specific activity vs. two carbon
  - sources, 400,401f
- time course of production, 402,404f

Cutinase-defective mutant of *Fusarium solani*

- effect of cutin addition on
  - induction, 402,405f
- kinetics of specific activity, 402,406f
- pathogenesis, 407
- properties, 400-409
- selection procedure, 400,402,403f
- separated <sup>35</sup>S-labeled extracellular
  - protein from cutin induction
    - medium, 402,407,408f
- time course of production, 402,404f

## D

- DAHPh synthase isozyme, differential
  - properties, 92
- Defense in bark tissues
  - cell wall alterations in
    - gymnosperms, 350-354
  - cell wall alterations in woody
    - angiosperms, 353

Defense in bark tissues—*Continued*

- fungal hyphae in bark, 353,354f
  - necrophylactic periderm, 351-353,354f
  - responses in nonwoody perennial
    - plants, 353,355,357f
  - structural responses, 350-351,352f
- Defense in living wood
  - cell wall alterations in preexisting
    - xylem, 356,358
  - tissue barriers formed de
    - novo, 355-356,357f
- Degradation, xyloglucan, 24,26-27
- Degree of esterification, effect on calcium
  - activity, 326
- Degree of neutralization, effect on calcium
  - activity, 325-326,327f
- Degree of polymerization, effect on calcium
  - activity, 325-326,327f
- Dehydrodiferulic acid
  - amounts released from cell walls by
    - cellulose treatments, 138,140
  - covalent linkage to cell wall
    - polysaccharides, 140
  - formation, 140
- Dehydrogenation polymer
  - aromatic ring cleavage by lignin
    - peroxidase, 513,514-516f
  - degradation products, 514,516f
  - gel filtration, 513,515f
  - preparation of lignins, 513,514f
- Dehydrogenative polymerization,
  - description, 483,484f
- Dehydrogenative polymerization of
  - monolignols
    - effect of carbohydrate, 155,156
    - effect of pH, 156-157
- Depolymerization residue,
  - cutin, 220,222f,223
- Deposition, xyloglucan, 24,26
- Deposition of polysaccharides
  - composition of radioactivity in neutral
    - sugars, 49,53f
  - distribution through cell wall, 49,52f
  - effect of amount of sugars during tracheid
    - maturation, 49,50-51f
  - factors influencing control, 8
  - influencing factors, 48
  - pioneering work, 48
  - processes during cell wall formation, 49
- Dicots, composition of cell wall, 18
- Didehydrodiferulic acid
  - formation, 80-81
  - structure, 77-78
- Digalloylglucose, biosynthesis, 115-117

- Digestibility, influencing factors, 137
- 4,4'-Dihydroxytruxillic acid  
 identification, 142  
 structure, 77-78
- Dimeric lignin models  
 reduction, 456  
 structures, 456-457
- Dimeric phenolic acid constituents of cell walls  
 amount in plant cell wall, 142  
 asymmetrical splitting, 142,143f  
 effect of sunlight, 142  
 identification, 142  
 symmetrical splitting, 142,143f
- Dimeric phenylpropanoids, occurrence in plant cell wall, 77-78
- 3,4-Dimethoxypropen-2-ol, structure, 71,73
- Disease resistance, requirements for defense in perennial plant tissues, 347
- Dityrosine, structure, 42,43f
- DNA content, effect on acid-precipitable polymeric lignin production, 530,533f
- Double-labeling technique, analysis of structure and reactions of lignin, 151-158
- Driselase, activity, 39
- E
- Elicitation of lignification  
 chitin, 375  
 gene-specific effect of elicitor, 375-376  
 inhibition of polygalacturonic acid, 376  
 purification of elicitor, 375
- Elicitor  
 definition, 375  
 gene-specific effect, 375-376  
 lignification, 363-364  
 purification, 375  
 symptoms caused in leaves, 376
- Elicitor of lignification, chitin, 364-365
- Ellagitannins  
 biosynthesis, 118  
 structure, 108,109f
- Endoglucanase(s)  
 degradation of cellulose to glucose, 587  
 specific degradation patterns, 572,574f
- Endo-1,4- $\beta$ -glucanase  
 effects of xyloglucan oligosaccharides on activity, 29  
 function, 608-609  
 xyloglucan hydrolysis, 24-26
- Endomembrane theory, description, 69
- Endospermic heteroxylans, extraction, 620
- Endoxylanases, description, 630
- Environmental potential, *Trichoderma* exocellular enzyme system, 608
- Enzymatic glucosylation, mechanism, 124
- Enzymatic O-methylation, mechanism, 123-124
- Enzymatic reaction involving phenylpropanoids in plant cell walls  
 $\beta$ -glucosidases, 80  
 hydroxycinnamic acid transferases, 82-85  
 peroxidases, 80-83
- Enzyme(s)  
 analysis, 208  
 binding to proteins for polysaccharide synthesis, 7-8  
 degradation of heteroxylans, 621-622
- Enzyme excretion during wood cell wall degradation  
 action of hydroxyl radicals on wood cell walls, 448,451-452f  
 carbonyl group labeling, 445,451-452f  
 diffusion of fungal glycohydrolases, 446,447f,448,449  
 diffusion of lignin peroxidase, 448,450f  
 immunocytochemical controls, 446  
 immunocytochemical labeling, 445-446  
 labeling with anti-crude enzyme mixture, 446,447f,448,449f  
 labeling with anti-ligninase, 448,450f  
 plant material, 445  
 preparation of antisera, 445  
 tissue preparation for electron microscopy, 445
- Enzyme organization, problems with analysis in vivo, 95
- Enzymic hydrolysis, analysis, 571
- 4-O-Ethylguaiacylglycerol- $\beta$ -guaiacyl ether, reactions, 522,524f
- Exoglucanases, degradation of cellulose to glucose, 587
- Exo-1,4- $\beta$ -glucanase, function, 608
- Extensins, basic, description, 34
- Extracellular feruloylation, evidence, 41-42
- E/Z photoisomerization, phenylpropanoids, 79
- F
- Ferulic acid  
 inhibition of synthetic substrates, 197,199  
 oxidation of salts from tobacco plants, 194,195t  
 siting in wall polysaccharides, 39  
 structure, 71-72,194,196f



- [1-<sup>13</sup>C]Ferulic acid, incorporation into root tissue, 171,174f,175
- [2-<sup>13</sup>C]Ferulic acid, incorporation into root tissue, 175,176f,177
- [3-<sup>13</sup>C]Ferulic acid, incorporation into root tissue, 177,178f,179
- O*-[5-*O-trans*-Feruloyl- $\alpha$ -L-arabinofuranosyl]- (1-3)-*O*- $\beta$ -D-xylanopyranosyl- (1-4)-D-xylopyranose, structure, 71-72,140-141
- Feruloylation of the matrix polysaccharides, hypothetical mechanisms, 83-84,85f
- Fescue, lignification, 184,185f,186
- Flavan-3-ol groups, structure, 562,563f
- Flavonoid(s)
- biosynthetic origin, 123
  - detoxification of reactive hydroxyl groups, 123
  - distribution in plant kingdom, 123
  - enzymatic O-methylation, 123
  - polymethylated, *See* Polymethylated flavonoids
  - significance of accumulation, 134
- Flavonoid synthesis in *Chrysosplenium americanum*, regulation, 131-132
- $\beta$ -Fluoroferulic acid
- inhibition of commercial synthetic substrates, 197,199
  - oxidation of salts from tobacco plants, 194,195t
  - structure, 194,196f
- Folin phenol, spectrophotometric analysis, 546
- Forages of Gramineae
- effect of aromatic binding on animal nutrition, 182
  - production, 182
- Freeze-fracture studies, terminal complexes, 257
- Fucosyltransferase, fucosylation of xyloglucan, 23
- Fungal degradation, condensed tannins, 562,563f
- Fungal isolates, cellulolytic activity on straw, 611-612
- Fungal xylanase production
- activities in strains of fungi, 645,647t
  - advantages, 644
  - methods for cost-effective production, 645
  - ratio of xylanase to cellulase activities, 645,646f
  - thermostable enzyme preparation, 645,648t
- Fungi, model for recognition by wheat, 365,366f,367-368
- Fungi invasion, response by cell wall alterations, 361
- Fungi recognition
- model, 365,366f,367-368
  - signals, 367
- Fusarium solani*
- production of isozymes of cutinase, 400
  - properties of cutinase-defective mutant, 401-409
- G
- Galacturonic acid, occurrence in pectin, 301
- Gallic acid
- biosynthesis, 110-111,112f
  - degradation by tannase, 561-562
- Gallotannin(s)
- biosynthesis, 108-118
  - degradation by tannase, 560-561
  - structure, 108,109f
- Gallotannin biosynthesis, enzymology, 108-118
- Galloyl coenzyme A thioester
- chemical synthesis, 111,112f
  - UV spectrum, 111,114f
- Gels, detection of cellulolytic activities, 571,572t,573
- (1-4)- $\beta$ -D-Glucan chains, conformation in  $\alpha$ -ulose submicrofibrils, 293,296
- (1-3)- $\beta$ -Glucan synthase
- advantages of purification using 3-[(3-chloroamidopropyl)dimethylammonio]-1-propanesulfonate, 253,255
  - affinity labeling with UDP-pyridoxal, 252t
  - antibody generation, 250
  - chemical modification, 249-250
  - electrophoresis, 249
  - electrophoretic analysis, 250,251f,254f
  - immunoprecipitation, 250,252t
  - inhibition by UDP-pyridoxal, 252,253t
  - partial purification from red beet storage tissue, 248-249
  - phosphorylation, 250,253,254f
  - preparation of fractions, 249
  - problems with purification, 249
- $\beta$ -Glucogallin
- biosynthesis, 111-114
  - galloyl exchange with glucose, 115
- Glucomannan synthesis, influencing factors, 4,6t

- Glucose  
determination, 572  
effect on acid-precipitable polymeric lignin production, 530,531f  
effect on cutinase production, 400  
Glucose oxidase, lignin catabolism, 473  
 $\beta$ -Glucosidase(s)  
function, 609  
hydrolysis of glycosidic linkage, 598  
mechanism of action of retaining enzyme, 598,599f  
reactions involving phenylpropanoids in plant cell walls, 80  
role in cellulose degradation, 597  
 $\beta$ -Glucosidase mechanism  
effect of substitution of sugar hydroxyl at C-2, 598,600  
formation of 2-fluoroglucosyl enzyme, 602,604f  
inactivation studies, 600,601f  
measurement of burst of dinitrophenolate, 600,602,603f  
pathway, 598,599f  
stereochemistry of intermediate, 602,605f, 606  
Glycosylation  
kinetics, 129,131  
partially methylated flavonols, 128–134  
Glucosyltransferase  
function, 248  
properties, 129,131f  
2'-*O*-Glucosyltransferase, immunological evidence, 129t,130f  
2'-5'-*O*-Glucosyltransferase, purification, 128–129,130f  
Glucuroxylan, hydrolysis products, 634,635f  
Glycohydrolases,  
diffusion, 446,447f,448,449f  
Glycoproteins, examples in cell wall, 11–12  
Glyoxal oxidase, lignin catabolism, 473  
Graminaceous lignins  
experimental procedure, 183–184  
lignification of fescue, 184,185f,186  
lignification of maize internodes, 186–187t,188f,189  
variations, 183  
Gramineae, importance of lignification for induced resistance mechanisms, 371  
Grass cell walls, alkaline hydrolysis, 122  
Gravity, effect on lignin synthesis, 203–213  
Growing plant cell wall, working model, 33–44  
Growth measurements, mung bean hypocotyls, 313
- H
- Heat conduction calorimeters, measurement of heats of aerobic metabolism, 544  
Heat conduction calorimetry, batch mixing, 546,547f,548,549f  
Heteroxylans  
biodegradation, 626–627  
categories, 620  
chemical structure, 620–621  
mode of action of xylanases, 622–625  
occurrence of hemicellulosic fractions of terrestrial plants, 619–620  
specificities of xylanases, 625–626  
types of enzymes used in degradation, 621–622  
Hexokinases, protein binding, 7  
High-purity xylanases, preparation, 648  
Higher galloylated glucose derivatives, formation, 116  
Hydrogen peroxide generating system, secondary metabolic pathway, 421  
Hydrolyzable tannins  
description, 108,559  
microbial degradation, 560,561t,562  
structure, 559,563f  
 $\alpha$ -Hydroxyacetosyringone, signal compounds from tobacco tissues, 384  
Hydroxycinnamic acid(s)  
attachment to structural cell wall polymers, 81,82f  
binding to cell wall polymers, 70–71  
chemical nature of ester linkages, 71  
common acids in plant cell walls, 70t  
esterification, 122  
function, 68  
histochemical survey, 69  
phenyl ether bond linkages, 71,74  
structure, 386,387f  
visualization, 70  
Hydroxycinnamic acid transferases,  
evidence, 83–84,85f  
5-Hydroxyferulic acid, activity, 386,389  
*p*-Hydroxyphenyl–guaiaacyl-type dehydrogenative polymer, condensed structures, 157t,158f  
Hydroxyl radicals, action on wood cell walls, 448,451–452f
- I
- Immunogold labeling, poststaining procedure, 427

- Indulin ATR, *See* Kraft lignin
- Infection-induced lignification in wheat  
 chemical and physical evidence for  
 presence at wounds, 362  
 chitin as elicitor, 364–365  
 defense mechanism in unwounded leaves, 363  
 defense mechanism in wounded leaves, 362  
 elicitors, 363–364  
 importance as general resistance  
 mechanism, 362  
 inhibition, 368  
 model for fungi  
 recognition, 365,366f,367–368  
 specificity of induction, 363  
 wheat germ agglutinin as receptor, 365
- Inhibition of cell wall peroxidases  
 anion-exchange chromatogram of xylem  
 peroxidases, 197,198f  
 experimental procedures, 195  
 Lineweaver–Burk plots, 197,200–201f  
 oxidation of salts from ferulic and  
 $\beta$ -fluoroferulic acids, 194,195t  
 oxidative activities of cell wall  
 isozymes, 195,196f,197
- Intact cytosolic pathway  
 demonstration approaches, 93  
 evidence, 91–92,93t
- Intracellular feruloylation reactions,  
 evidence, 39,40f,41
- Iron *meso*-tetra-(2,6-dichloro-3-  
 sulfonatophenyl)porphyrin chloride  
 biomimetic catalysis of lignins, 520  
 catalyzed reactions, 522,524f  
 structure, 520–521
- Z-Isoconiferin, structure, 74,76
- Isodityrosine  
 factors influencing formation in cell  
 wall, 43–44  
 structure, 42,43f
- Z-Isosyringin, structure, 74–76
- Isozyme expression  
 manipulation by environmental  
 treatments, 99,102f,103t,105  
 physiological manipulation, 104f,105
- K
- Kraft lignin, bacterial degradation, 529–543
- L
- Laccase  
 activity determination, 473
- Laccase—*Continued*  
 aromatic ring cleavage of phenolic  $\beta$ -O-4  
 model compounds, 493,497–498f  
 catalysis of side-chain cleavage of  $\beta$ -1  
 and  $\beta$ -O-4 model compounds, 487  
 catalysis reactions, 482  
 depolymerization of lignin, 426  
 effect of antiserum on enzyme  
 activity, 428,429t  
 production and isolation, 473  
 production of antibodies, 428  
 specificity of antibodies, 441
- Laccase antiserum, effect on enzyme  
 activity, 428,429t
- Left-handed helical cellulose microfibril  
 bundled cellulose micro-  
 fibrils, 290,294–295f  
 comparison of submicrofibril model to TEM  
 image of submicrofibril, 286,287–288f  
 computer-generated optical diffraction  
 patterns, 280–281  
 effect of Tinopal, 281, 283–284f,286  
 evidence, 290,293,296  
 gel deposited during normal  
 growth, 281,282f  
 material preparation, 279–280  
 micrographs, 280  
 submicrofibril model, 281,285f,286
- Leucoanthocyanidin, structure, 562,563f
- Lignification  
 active induction as defense  
 mechanism, 370–371  
 causal factor in resistance, 373–375  
 effect on defense mechanisms in  
 plants, 348–349  
 elicitation, 375–376,377f  
 evidence for participation in resistance  
 reactions, 371–372  
 modes of action as resistance  
 mechanism, 371  
 response to disease, 361  
 wheat-stem rust system, 372  
*See also* Infection-induced lignification  
 in wheat
- Lignification of fescue  
 acetyl bromide lignin contents, 184,185t  
 differences from maize internode  
 lignification, 189–190  
 lignin monomer composition, 184,185t,186  
 sulfuric acid lignin contents, 184,185t
- Lignification of maize internodes  
 acetyl bromide lignin contents, 186t  
 differences from fescue  
 lignification, 189–190

- Lignification of maize internodes—*Continued*  
GC chromatogram of thioacidolysis products, 187,188f  
monomeric composition of lignin in parietal residue, 186,187t,189  
monomeric composition of lignin in saponification residue, 186,187t,189  
sulfuric acid lignin contents, 186t
- Lignification of tracheids  
densitometer traces of UV photonegatives, 54,55f  
incorporation of tritiated phenylalanine, 54,55f,56  
investigation methods, 49  
mechanism, 56  
transmission electron microscopy, 54  
types of lignin deposition processes, 49,54
- Lignification of young plant seedlings  
control experiments, 207  
effect of microgravity on lignin content, 212–213  
enzyme analysis, 208  
flight activities, 204,207  
flight hardware, 204,205–206f  
lignin analysis, 207–208  
lignin content vs. gravity environment, 208,209–210t  
lignin content vs. seedling type, 210t  
peroxidase activity, 211t  
phenylalanine ammonia-lyase activity, 211t  
postflight activities, 207  
preflight activities, 204  
protein analysis, 208  
schematic representation of plant growth chambers, 204,206f  
schematic representation of plant growth unit, 204,205f
- Lignin  
analysis, 207–208  
analysis of structure and reactions by double-labeling technique, 151–158  
approaches for structure elucidation, 148  
biosynthesis with cell organelle, 63,64f  
classification, 170  
constituent of cell wall, 2  
description, 77,503,519  
formation, 81,83,170,172  
mechanical barrier against pathogenic invasion, 370  
mechanisms of biodegradation, 519  
metabolism, 465  
problems with structure elucidation, 148–149,170
- Lignin—*Continued*  
roles in cell walls, 169  
specific labeling in plant tissue, 149  
structure, 77
- $\beta$ -O-4 Lignin substructure model dimers  
degradation by lignin peroxidase, 504,506,507–510f  
degradation by white-rot fungi, 504,505f  
derivation of methyl group of methyl oxalate, 506,508f
- ( $\beta$ -O-4)–( $\beta$ -O-4) Lignin substructure model trimer, aromatic ring cleavage by lignin peroxidase, 506,511,512f
- Lignin biodegradation  
cell disruption, 461  
cell growth, 461  
degradation of nonphenolic lignin models with Ca-carbonyl substituent, 458–459,460f  
effect of metabolism of aromatic fragments on degradation, 458,461  
history of research, 454–455  
hypothetical scheme by ligninolytic cultures, 467,468f  
metabolism of lignin, 465,467,468f,469  
metabolism of monomeric lignin models, 464–465,466f  
microbes, 482  
oxidation, 456  
oxidative process, 455  
partial purification of reductases, 461  
physiological and biochemical relationships with veratryl alcohol biosynthesis, 421–422  
problem with Ca-carbonyl compound formation, 467,469  
quinone reduction, 455,462,463f  
quinone–hydroquinone formation, 456,458  
reductase activity measurement, 462  
reduction, 455–457  
reduction experiments, 461  
relative absorbance of culture supernatant, 462,463f  
relative reduction rates, 462,464t  
research on lignin peroxidases, 455  
role of oxidative enzymes, 477,480f  
study approaches, 503
- Lignin biodegradation–veratryl alcohol biosynthesis, physiological and biochemical relationships, 421–422
- Lignin biosynthesis studies  
changes to macromolecules during delignification, 154,155t  
degree of ring substitution, 151–154

- Lignin biosynthesis studies—*Continued*  
 dehydrogenative polymerization of monolignols, 155,156*t*,157  
 factors influencing degree of substitution, 153,154*t*  
*p*-hydroxyphenyl—guaiacyl type dehydrogenative polymer, 157*t*,158*f*  
 retention of methoxyl groups during formation, 154  
 retention of propanoid side chains during formation, 153–154  
 use of double-labeled guaiacyl lignin precursors, 151*t*
- Lignin catabolism, enzymes, 472–473
- Lignin degradation  
 biomimetic studies, 519–527  
 mechanisms by lignin peroxidase and laccase of white-rot fungi, 482–501  
 reactions, 503
- Lignin formation  
 phenylalanine ammonia-lyase activity required, 9–10  
 polymerization of building units, 10–11  
 reduction of building units, 10  
 role of glucosides, 10
- Lignin formation in xylem cell walls, dehydrogenative polymerization, 483,484*f*
- Lignin model compounds, microbial calorimetric analysis, 554,556*t*
- Lignin monomer polymerization, role of peroxidases, 193
- Lignin peroxidase  
 aromatic ring cleavage of artificial lignin, 493,499,500*f*  
 aromatic ring cleavage of dehydrogenation polymer, 511,513,514–516*f*  
 aromatic ring cleavage of ( $\beta$ -O-4)-( $\beta$ -O-4) lignin substructure model trimer, 506,511,512*f*  
 aromatic ring cleavage of nonphenolic  $\beta$ -O-4 lignin substructure model compounds and veratryl alcohol, 493  
 catalysis of side-chain cleavage reactions of  $\beta$ -1 and  $\beta$ -O-4 lignin model compounds, 483–489  
 catalysis reactions, 482–483  
 degradation of lignin, 426  
 degradation of  $\beta$ -O-4 lignin substructure model dimers, 504,506–510*f*  
 diffusion, 448,450*f*  
 lignin catabolism, 472  
 reactions, 455  
 specificity of antibodies, 441
- Lignin precursors  
 control of synthesis by phenylalanine ammonia-lyase, 8–9  
 hydroxylation, 9  
 methylation, 9–10
- Lignin structure in situ in vascular plant cell walls  
 biosynthesis, 170–171  
 incorporation of [ $1$ - $^{13}$ C]ferulic acid, 171,174*f*,175  
 incorporation of [ $2$ - $^{13}$ C]ferulic acid, 175,176*f*,177  
 incorporation of [ $3$ - $^{13}$ C]ferulic acid, 177,178*f*,179  
 solid-state  $^{13}$ C NMR spectroscopy of intact plant tissue, 171,173
- Lignin synthesis, effect of gravity, 203–213
- Ligninase  
 role, 519  
 synthesis, 519
- Ligninolytic enzyme, discovery, 454–455
- Lignocellulolysis  
 growth of *Trichoderma* on lignocellulose, 609,611*t*  
 interactions between *Clostridium* and *Trichoderma*, 611,613*f*  
 interactions between microorganisms during cellulose degradation, 609,610*f*,611  
 schematic representation for degradation of cellulosic substrates by microbial consortium, 612,613*f*
- Lignocellulose(s), effective and economic utilization, 608
- Lignocellulose-degrading enzymes, ultrastructural localization, 426
- Lignocellulosic materials, role of secondary metabolism in biodegradation, 412–423
- Linear terminal complexes  
 development in selected green algae, 263,265–266*f*  
 elongated type, 263,266*f*  
 factors influencing movement in plasma membrane, 263  
 localization, 271,274*f*,275  
 nascent type, 263,266*f*  
 time course of length, 263,265*f*
- Lipid  
 formation, 12  
 transport to cell wall, 12
- Living wood, disease resistance, 355–358
- M
- Macromolecular lignin, 160–167

- Maize internodes, lignification, 186–187*i*,188*f*,189
- Major structural polymers of cell wall  
acidic polysaccharides, 34  
basic extensins, 34  
diagram of principal components, 34,35*f*,36  
microfibrillar cellulose, 34  
neutral hemicelluloses, 34
- Manganese peroxidase, lignin catabolism, 472
- Metabolism of xyloglucan  
degradation, 24,26–27  
deposition, 24,26*t*  
structural function, 24
- O-Methylation, kinetics, 128
- 4-O-Methylglucuronoxylan, enzymatic hydrolysis, 625
- O-Methyltransferases  
activity during lignin biosynthesis, 372  
properties, 126*t*,128  
purification, 126,127*f*  
substrate specificity, 126,128
- Microautoradiography  
differentiating xylem, 162–165  
distribution of silver grains, 163,166*f*  
experimental procedure, 161–162
- Microbial calorimetric analysis  
advantages, 545  
bacterial growth and adaptation, 545–546  
bacterial synthesis of enzymes, 545  
batch mixing, 546,547*f*,548,549*f*  
calibration of heat generation from *o*-cresol, 554,555*f*  
concentration ranges, 545  
controlling factors, 551  
detectability of lignin- and cellulose-derived fragments, 545  
lignin model compounds, 554,556*t*  
methods, 545,547*f*  
microbial stripping, 545  
spectrophotometric analysis, 546  
standardization plots, 548,550*f*,551  
stripping, 546  
stripping efficiency, 551,552*f*,553*t*  
stripping specificity, 551,552*f*,553  
use of *Pseudomonas putida* ATCC 11172, 548,550*f*,551
- Microbial degradation of catechin, 564
- Microbial degradation of condensed tannins 562–564
- Microbial degradation of hydrolyzable tannins, 560–561
- Microbial degradation of tannins, process, 559–564
- Microfibril orientation  
freeze–fracture replica, 274*f*,275  
in aplanospore, 271,274*f*,275  
microtubule-independent control, 271,274*f*,275
- Microfibrillar cellulose, description, 34
- Mode of action of xylanases  
degradation products, 622  
sites, 622
- Molecular genetics, cellulose biosynthesis, 242–243
- Molecular model, cutin, 220,221*f*
- Molecular weight of xyloglucan, influencing factors, 20
- Monocot(s), composition of cell wall, 18–19
- Monocot arabinoxylans, hydrolysis product, 122
- Monolignols  
activity, 386,388*f*  
structural features for activity, 389  
structure, 386,387*f*
- E*-Monolignols, biosynthesis, 170–171,172*f*
- Z*-Monolignols  
formation and role in beech bark, 74,77  
role in lignin formation, 83  
structures, 74–76
- Monolignols and monolignol glucosides  
formation and role in beech bark, 74,77  
proposed mechanism of monolignol transport into cell wall, 74,75*f*  
structures, 74,76
- Monomeric aromatic compounds, aromatic ring cleavage by white-rot basidiomycetes, 513
- Monomeric lignin models, metabolism, 464–465,466*f*
- Monomeric phenylpropanoids  
hydroxycinnamic acids, 69–74  
monolignols and monolignol glucosides, 74,75*f*,76–77
- Multiple-substituted phenolic acid esters, biosynthesis, 115,116*t*
- Mung bean hypocotyls  
composition of pectin fractions extracted from cell walls, 314,316*t*  
factors influencing cell growth potential, 318–322  
growth gradient, 314,315*f*  
growth measurements, 313
- Mycoparasitism  
antibiotic inhibition zone around *Trichoderma* species, 614  
enzyme activity induced in *Trichoderma*, 614,615*t*

Mycoparasitism—*Continued*

- fractionation of extracellular protein fraction, 615
- occurrence, 614
- protein profiles from fungus grown on pathogen cell walls, 614–615
- role of exoenzymes of *Trichoderma* in biocontrol action against plant pathogenic fungi, 612
- selection of *Trichoderma* for biocontrol effectiveness, 615
- Trichoderma* and *Fusarium* activities in natural substrate utilization, 612,614

## N

- Necrotrophic fungi, prevention by ring of lignified cells at wound margins, 371
- Neutral hemicelluloses, description, 34
- Nitrogen recycling, with phenylalanine ammonia-lyase, 419
- Nonendospermic heteroxylans, extraction, 620
- Nonwoody perennial plants, defense responses, 353,355,357f

## O

- Oligogalacturonates, preparation, 325
- Oxidation in lignin biodegradation, radical cation mechanism, 456
- Oxidative coupling of phenolic side chains in cell wall, evidence of specificity, 42–44
- Oxidative enzymes from lignin-degrading fungus *Pleurotus sajor-caju*
  - elution profile showing resolution of enzyme activity peaks, 474,476f
  - enzyme assays, 473–474
  - enzyme production and isolation, 473
  - enzyme properties, 474t
  - relative oxidation rates of aromatic alcohols, 477,478f
  - relative oxidation rates of methoxyl-substituted benzyl alcohols, 477f
  - role in lignin biodegradation, 477,480f
  - time course of ligninolytic activity, 474,475f

- Oxidative phenolic coupling in cell wall, consequences and requirements, 38

## P

- Partially methylated flavonols, 128–134
- Pea xyloglucan, structure, 19,22f
- Pectin(s)
  - commercial uses, 301
  - composition, 300
  - control of primary cell wall extensibility, 312
  - cross-linking mechanism in presence of calcium, 330f, 331
  - description, 324
  - effect of calcium content on intrinsic viscosity, 329f, 331
  - effect of calcium content on molecular weight, 326, 328f, 331
  - effect of calcium content on chemical structure, 324–331
  - effect of carboxyl group distribution on calcium activity, 326
  - effect of degree of esterification on calcium activity, 326
  - effect of enzymes and pH on behavior, 324
  - gel formation, 301
  - hydrolysis products, 122–123
  - methylation analysis, 301
  - model of chemical structure of tobacco compound, 301,302f,303
  - model of helical portions of pectin chain, 303
  - occurrence in tobacco lamina, 301
  - occurrence of rhamnogalacturonans, 301–303
  - role in cell growth, 300–301
  - prediction of electrostatic properties, 325
  - preparation, 325
  - procedure for obtaining images of epidermal cell surfaces, 304
  - role of degree of neutralization on calcium activity, 325–326,327f
  - role of degree of polymerization on calcium activity, 325–326,327f
  - structural characterization, 301
  - structural roles, 324
  - See also* Citrus pectin, Tobacco pectin
- Pentagalloylglucose, formation from  $\beta$ -glucogallin, 113–117
- Perennial plant tissues
  - constitutive structural defenses, 349–350
  - structural defense mechanisms, 347–349

- Periderms, definition, 349
- Peroxidase(s)  
activity determination, 208
- Peroxidase(s)—*Continued*  
activity in seedlings, 211*r*  
inhibition, 194–201  
reactions involving phenylpropanoids in plant cell walls, 80–83  
role in lignin monomer polymerization, 193  
pH, effect on dehydrogenative polymerization of monolignols, 156–157
- Phanerochaete chrysosporium*, wood cell wall degradation, 443–452
- Phenolic acids  
activity, 386,388*f*  
amounts released from graminaceous cell walls by treatment with NaOH, 138*r*  
relationships with  
biodegradability, 140,142  
structure of compounds released from graminaceous cell walls by NaOH treatment, 138,139*f*
- Phenolic aldehydes  
amounts released from graminaceous cell walls by treatment with NaOH, 138*r*  
covalent linkage to cell wall polysaccharides, 140  
relationships with  
biodegradability, 140,142  
structure of compounds released from graminaceous cell walls by NaOH treatment, 138,139*f*
- Phenolic cross-linking in cell walls  
biological effectiveness, 33–34  
specificity of reactions, 38–42
- Phenylalanine ammonia-lyase  
activity determination, 208  
activity during lignin biosynthesis, 372–373  
activity in seedlings, 211*r*  
activity in white-rot fungus, 418*r*  
control of lignin precursor synthesis, 8–9  
induction of activity of growth factors, 9  
inhibition by aminooxyacetic acid, 374  
inhibition by (1-amino-2-phenylethyl)-phosphonic acid, 372  
nitrogen recycling, 419  
role in phenylalanine conversion to secondary metabolites, 412–413,414*f*
- L-Phenylalanine biosynthesis,  
alternative enzymatic routing, 96,97–98*f*,99
- Phenylalanine–cinnamate pathway  
biochemical significance, 418–419
- Phenylalanine–cinnamate pathway—  
*Continued*  
comparison in brown-rot and white-rot fungi, 413–418
- Phenylpropanoid(s), reactions in plant cell walls, 79–85
- Phenylpropanoid biosynthesis, relationship with enzyme changes, 89
- Phenylpropanoid(s) in plant cell walls  
classification, 69–78  
function, 68  
metabolism, 68–85
- Phenylpyruvate route, phenylalanine biosynthesis, 96,97*f*,99
- Photochemical coupling, phenylpropanoids, 79
- Photochemical reactions of phenylpropanoids in cell wall  
E/Z photoisomerization, 79  
photochemical coupling, 79
- Plant–*Agrobacterium tumefaciens*  
interactions, signal compounds, 384
- Plant cell wall(s)  
components, 137  
factors influencing biodegradability, 137  
presence of phenolic side chains, 33  
principal structure components, 203
- Plant cell wall constituents, importance in understanding relationship with wall biodegradation, 137
- Plant polyesters, solid-state NMR studies of molecular structure and dynamics, 214–228
- Plastidic chorismate mutase, inhibition, 91
- Pleurotus sajor-caju*, properties, 473
- Poly B–411  
decolorization, 526*f*,527  
electrochemical oxidation, 525,526*f*  
structure, 520  
use as lignin model, 525
- Polygalacturonic acid  
preparation, 325  
suppression of elicitor-induced lignification response in wheat leaves, 376
- Polymeric phenylpropanoids, occurrence in plant cell wall, 77
- Polymethylated flavonoids  
detoxification of reactive hydroxyl groups, 123  
distribution in plant kingdom, 123  
pathway for enzymatic synthesis, 124,125*f*
- Polysaccharides  
binding protein and enzyme complex, 7–8  
biosynthesis with organelle, 57,60,61–62*f*



- Polysaccharides—*Continued*  
 composition in cell wall, 2–3  
 control of synthesis and deposition, 2–8  
 deposition, 48–53  
 deposition of wall polysaccharides, 8  
 glucomannan synthesis, 4,6,7  
 influence of side branch incorporation on  
 main chain synthesis, 3  
 meristematic cell, 4,5f  
 role of synthases, 3  
 secondary wall from bean cells, 4,5f  
 synthesis, 3–4,5f  
 Prephenate aminotransferase, activity, 95–96  
 Primary cell wall  
 assembly of xyloglucan–microfibril  
 framework, 36,37f,38  
 consequences and requirements of oxidative  
 phenolic coupling, 38  
 major structural polymers, 34,35f,36  
 requirement for growth, 38  
 Primary cell walls of growing tissues in  
 higher plants, composition, 18  
 Protein(s)  
 analysis, 208  
 binding to enzymes for polysaccharide  
 synthesis, 7–8  
 examples in cell wall, 11–12  
 Protohemin  
 biomimetic catalysis of lignins, 520  
 structure, 520–521  
 Protolignin  
 factors influencing properties, 160–161  
 selective labeling of specific structural  
 unit, 149–150  
 specific labeling, 150  
 Protolignin structure determination  
 administration of precursor, 161–162  
 biogenesis in woody  
 angiosperms, 162–165  
 biogenesis in woody gymnosperms, 163  
 causes of heterogeneity, 166,168  
 preparation of microautoradiogram, 162  
 radioactive precursors for  
 microautoradiography, 161  
 schematic representation of cell wall  
 component deposition, 166,167f  
 selectivity of labeling, 162
- Q
- Quinone(s)  
 reduction, 462,463f  
 relative reduction rates, 462,464t
- Quinone–hydroquinone formation, lignin  
 biodegradation, 456,458  
 Quinone reduction, step in lignin  
 biodegradation, 455
- R
- Reduction in lignin biodegradation  
 scheme, 455–456  
 structures, 456–457  
 Resistance reactions, evidence for  
 participation of lignification, 371–372  
 Rhizobiaceae  
 for microbial pathogen, 383  
 initial interaction with plants, 383  
 Rice grain  
 comparative studies on cell  
 wall polymers, 333–343  
 isolation of cell walls from  
 different parts, 334  
 Ruminant digestibility of plant material,  
 chemical treatments, 182–183
- S
- Salts from tobacco plants,  
 oxidation, 194,195t  
 Secondary metabolites  
 production by brown-rot fungus, 413,416t  
 role in biodegradation of lignocellulosic  
 materials, 412  
 Shikimate dehydrogenase, activity, 96  
 Shikimate route, phenylalanine  
 biosyntheses, 96,98f,99  
 Side-chain cleavage reactions of lignin  
 model compounds  
 catalyzed by laccase, 487,490–492  
 catalyzed by lignin peroxidase, 483,485–489  
 Solid-state <sup>13</sup>C NMR spectroscopy of  
 intact plant tissue  
 incorporation of [1-<sup>13</sup>C]ferulic  
 acid, 171,174f,175  
 incorporation of [2-<sup>13</sup>C]ferulic  
 acid, 175,176f,177  
 incorporation of [3-<sup>13</sup>C]ferulic  
 acid, 177,178f,179  
 lignin structure analysis, 171,173  
 Specific fusion efficiency,  
 2'-O-glucosyltransferase, 129t  
 Specific labeling, protolignin, 150  
 Specificities of xylanases  
 action on heteroxylans, 625–626

- Specificities of xylanases—*Continued*  
determination, 625
- Specificity in oxidative coupling of phenolic side chains in cell wall orientation of coupling in protein-bound tyrosine residues, 42,43  
role of isoperoxidase, 44  
role of neighboring polysaccharide molecules in orientation determination, 44  
role of pH, 44
- Specificity of phenolic cross-linking reactions in cell wall background, 38  
evidence for intracellular feruloylation reactions, 39,40f,41  
possible extracellular feruloylation, 41–42  
siting of ferulic acid in wall polysaccharides, 39
- Spin-relaxation times  
cutin, 217,220t  
suberin, 226,227t
- Streptomyces*  
action on lignocellulose, 529  
denaturation of stationary-phase extracellular enzymes, 534t
- Stripping, procedure, 546
- Stripping efficiency, microbial calorimetric analysis, 551,552f,553t
- Stripping specificity, microbial calorimetric analysis, 551,552f,553
- Structural defense mechanisms in plants effect of cell wall alterations, 348–349  
induced defenses, 348
- Structural function, xyloglucan, 24
- Structure, xyloglucan, 19–20,22f
- Structure–activity relationships, virulence-inducing phenolics, 389–390
- Suberins  
carbon types, 223,226t  
CPMAS spectra for suberized cell walls, 223,225f  
cross-polarization dynamics, 227–228  
description, 77  
features of molecular structure, 227  
formation, 81,83,170,172  
function, 68  
role, 169,214  
schematic representation, 214,215f  
spin-relaxation time, 226,227t  
structure, 77
- Substrate specificity, *O*-methyltransferases, 126,128
- Subunit identification studies,  
(1,3)- $\beta$ -glucan synthase, 248–255
- Sulfuric acid lignin, contents in fescue, 184,185t
- Synergism, cellulolytic enzymes, 582,583f,584
- Synthases, role in polysaccharide synthesis in cell wall, 3–4,5f
- Synthesis of polysaccharides, role of synthases, 3–4,5f
- Synthetic iron *meso*-tetraphenylporphyrin biomimetic catalysis of lignins, 519–520  
structure, 519,521
- E*-Syringin, structure, 74–76
- T
- Tannase  
degradation of gallic acid, 561–562  
degradation of gallotannins, 560–561  
microbial degradation of hydrolyzable tannins, 560,561t,562
- Tannins  
classifications, 559  
current investigations, 564–565  
description, 559  
inhibition of microorganisms, 560  
microbial degradation of condensed tannins, 562,563f,564  
microbial degradation of hydrolyzable tannins, 560,561t,562  
structure, 559,563f
- Terminal complex(es)  
consolidation of linear terminal complexes, 235  
consolidation of rosette/globule terminal complexes, 235  
definition, 257  
discoveries from freeze–fracture studies, 257  
evolutionary significance of types, 257–258  
evolutionary trend from algae to higher plants, 258,262–263,264f  
examples, 233  
factors controlling orientation, 258  
fixed vs. mobile sites of cellulose biosynthesis, 234  
in *Acetobacter xylinum*, 233–234  
linear, *See* Linear terminal complexes  
location in green algae, 258,262t  
plasma membrane insertion, 236  
role in cellulose synthesis, 233

- Terminal complex hypothesis,  
description, 232–233
- Thermostable xylanases, preparation from  
various sources, 645,648t
- Tobacco pectin  
gel formation, 303–304  
micrographs of gel, 307,308f  
preparation, 303  
samples for noncutinized lower epidermal  
cell surfaces, 304,305–306f,307  
*See also* Pectin(s)
- Tobacco primary cell wall  
bundled cellulose micro-  
fibrils, 290,294–295f  
sample preparation, 279–280
- Tracheids, lignification, 49,54,55f,56
- Transformation efficiency, effect on  
acetosyringone, 385
- Transmission electron microscopy (TEM)  
localization of proteins and molecules  
with tissue sections, 427–441  
structural characterization and  
visualization of pectin, 303–310  
tracheid lignification, 54
- Trichoderma*, environmental potential, 616
- Trichoderma* exocellular enzyme system,  
environmental potential, 606–616
- Trichoderma reesei*  
cellulases, 595  
production of xylanase and  
 $\beta$ -xylosidase, 631  
xylanolytic enzyme system, 631–638
- Trichoderma* species  
enzymes involved in cellulolytic  
pathway, 608–609  
ligninolytic activity, 609  
lignocellulolysis, 609–613  
mycoparasitism, 612,614–616  
use as biological control of agents of  
plant diseases, 609  
xylanolytic activity, 609
- 1,3,6-Trigalloylglucose,  
structure, 559,563f
- Triple-stranded left-handed helical  
cellulose microfibril  
bundled cellulose microfibrils of tobacco  
leaves, 290,294–295f  
model with three left-handed helical  
submicrofibrils, 290,292f  
negatively stained microfibril, 286,289f  
self-assembly of microfibril on cell  
exterior, 290,291f
- Tyrosine, structure, 42,43f
- U
- Ultrastructural localization of  
lignocellulose-degrading enzymes  
antibody production, 428  
detection of cross-reactive  
material, 429,434f  
effect of immunoglobulin G on  
labeling, 429,433f  
effect of laccase antisera on  
labeling, 436,440f  
effect of plant phytochrome antisera on  
labeling, 436,439f  
growth of *Coriolus versicolor* on wood, 426  
immunogold labeling, 427–428  
labeling in decayed beech  
heartwood, 436,437f  
labeling in undecayed beech  
heartwood, 436,438f  
labeling on hyphal wall, 429,435f,436  
laccase labeling site for beech  
heartwood, 429,432–433f  
laccase labeling site for malt  
agar, 429,430–431f  
location within cell wall and mucilage of  
hyphae of *Coriolus  
versicolor*, 436,441  
organism, 426  
TEM, 428
- V
- Valonia ventricosa*, immunofluorescence  
micrographs of  
microtubules, 271,272–273f
- Vegetable tannins, classifications, 108
- Veratraldehyde  
product of lignin peroxidase catalyzed  
oxidation of veratryl alcohol, 464–465  
relative reduction rates, 462,464t
- Veratryl alcohol  
oxidation in aqueous solution vs. pH, 520  
oxidation procedure, 520  
oxidation yields, 522t  
structure, 71,73
- Veratryl alcohol biosynthesis, physiological  
and biochemical relationships with  
lignin biodegradation, 421–422
- Veratryl alcohol metabolism,  
scheme, 465,466t
- Veratryl alcohol oxidases  
activity determination, 473–474  
enzyme properties, 474t

- Veratryl alcohol oxidation,  
products, 458,460f
- Veratryl alcohol synthesis—lignin  
degradation in white-rot fungi  
aromatic ring and  $\alpha$ - $\text{C}\beta$  bond  
cleavage, 419,420f,421  
hydrogen peroxide generating system, 421
- Vesicle fusion at membrane surface, factors  
influencing control, 8
- vir* gene expression, examination, 385–386
- vir* inducers, isolation, 394–395
- vir* induction assay, description, 395–396
- virA* gene product, location, 385
- Virulence genes, role in tumorigenesis, 384
- Virulence-inducing phenolics detected by  
*Agrobacterium tumefaciens*  
activity, 387,388f  
bacterial strains, 394  
chemical specificity, 383  
GC, 396  
induction assay, 395–396  
isolation of limited host range  
inducers, 394–395  
limitations of host range, 390  
limited host range signal  
compounds, 390–391  
plant materials, 394  
structural features required for  
activity, 389  
structure–activity relationships, 383  
structure of epicatechin–  
gallate, 392,393f  
structures, 386,387f  
wide host range signal compounds, 391
- W**
- Wall polysaccharides, deposition, 8
- Water, constituent of cell wall, 2
- Wheat, model for recognition of  
fungi, 365,366f,367–368
- Wheat germ agglutinin, receptor for chitin  
oligomers, 365
- Wheat-stem rust system  
effect of radioactive phenolic  
precursors, 373  
fungal growth inhibition, 373  
hypothetical scheme of events leading to  
race–cultivar specific resistance or  
susceptibility, 376,377f  
lignification, 372–373
- White-rot basidiomycetes  
aromatic ring cleavage, 513
- White-rot basidiomycetes—*Continued*  
identification of aromatic ring  
cleavage products of lignin  
substructure models, 503–504
- White-rot fungi  
correlation between veratryl alcohol  
synthesis and lignin degradation, 419  
degradation of  $\beta$ -O-4 lignin substructure  
model dimers, 504,505f  
phenylalanine ammonia-lyase activity, 418  
phenylalanine–cinnamate  
pathway, 416,417f,418  
role in biodegradation of woody  
materials, 472
- Wood cell wall degradation by *Phanerochaete*  
*chrysosporium*  
enzyme excretion, 445–452  
oxidative degradation by lignin  
peroxidases, 445  
patterns, 427  
types, 443,444f
- Woody perennials, importance of disease  
resistance, 346–347
- X**
- Xylan, occurrence, 630
- Xylanase(s)  
approaches for production, 641–642  
areas of application, 642  
bioconversion of wastes, 642  
biodegradation of heteroxylans, 626–627  
enzymatic hydrolysis, 625  
isolation from *Bacillus* species, 623  
isolation from *Clostridium*  
*acetobutylicum*, 622–623  
isolation from *Cryptococcus albidus*, 623  
isolation from fungi, 624–625  
isolation from *Streptomyces*, 623–624  
major expense in application, 641  
occurrence in microorganisms, 630–631  
production in organisms, 641  
properties, 632  
removal of hemicellulose from pulps and  
plant fibers, 642  
specificities, 625–626
- Xylanase enzymes  
examples of purification to  
homogeneity, 649  
heat inactivation profile, 649,650f,651
- Xylanase production by cloned systems, 643–644
- Xylanase production by fungi, 644–645,647t
- Xylanase production by yeasts, 642–643

- Xylanase purification, focus on application, 648–649,650f,651
- Xylanolytic enzyme(s), 630
- Xylanolytic enzyme system of *Trichoderma reesei*  
analyses, 632  
enzyme purification, 631  
enzymes activity assays, 631  
hydrolysis experiments, 631  
hydrolysis of arabinoxylan, 632,634t  
hydrolysis of high molecular weight fraction of steamed xylan, 636,637t  
hydrolysis of xylo oligomers, 634,636t  
hydrolysis products, 634,635f  
properties, 632t  
protein fractionation, 632,633f  
source of enzymes, 631  
tentative hydrolysis mechanism, 636–637,638f
- Xylem, cell wall alterations as defense, 356,358
- Xylo oligomers, hydrolysis, 634,636t
- Xyloglucan  
degradation, 24,26–27  
deposition, 24,26t  
elution profile, 21,22f  
factors influencing molecular weight, 20  
hydrogen bonding, 23  
hydrolysis, 19–20  
localization in cell walls, 23–24,25f  
metabolism, 24–27  
occurrence in dicot cell walls, 18  
occurrence in monocot cell walls, 18–19  
solubility, 23
- Xyloglucan—*Continued*  
structural function, 24  
structure, 19,22f  
synthesis by Golgi membranes, 20  
synthesis of glucose–xylose backbone, 20
- Xyloglucan backbone  
additions, 21,23,25f  
biosynthesis, 20–21,22f  
incorporation of fucose, 21,23,25f
- Xyloglucan—microfibril framework, assembly to cell wall, 36,37f,38
- Xyloglucan subunits as oligosaccharins  
effect on endo-1,4- $\beta$ -glucanase activity, 29  
growth-inhibitory action, 28t  
regulatory effects of plant cells, 27,28t,29
- $\beta$ -Xylosidase(s)  
enhancement of hydrolysis of heteroxylans by xylanases, 627  
hydrolysis of  $\beta$ -1,4 linkages, 630
- $\beta$ -Xylosidase(s)—*Continued*  
occurrence in microorganisms, 630–631  
properties, 632f
- Y
- Yeast, xylanase production, 642–643
- Yeast extract, effect on acid-precipitable polymeric lignin production, 530,532f